



HIGHWAY CAPACITY MANUAL

6TH EDITION | A GUIDE FOR MULTIMODAL MOBILITY ANALYSIS

VOLUME 4: APPLICATIONS GUIDE

The National Academies of
SCIENCES • ENGINEERING • MEDICINE

TRANSPORTATION RESEARCH BOARD
WASHINGTON, D.C. | WWW.TRB.ORG

TRANSPORTATION RESEARCH BOARD 2016 EXECUTIVE COMMITTEE *

Chair: James M. Crites, Executive Vice President of Operations,
Dallas–Fort Worth International Airport, Texas

Vice Chair: Paul Trombino III, Director, Iowa Department of
Transportation, Ames

Executive Director: Neil J. Pedersen, Transportation Research Board

Victoria A. Arroyo, Executive Director, Georgetown Climate Center;
Assistant Dean, Centers and Institutes; and Professor and Director,
Environmental Law Program, Georgetown University Law Center,
Washington, D.C.

Scott E. Bennett, Director, Arkansas State Highway and Transportation
Department, Little Rock

Jennifer Cohan, Secretary, Delaware Department of Transportation, Dover

Malcolm Dougherty, Director, California Department of
Transportation, Sacramento

A. Stewart Fotheringham, Professor, School of Geographical Sciences
and Urban Planning, Arizona State University, Tempe

John S. Halikowski, Director, Arizona Department of Transportation,
Phoenix

Susan Hanson, Distinguished University Professor Emerita, Graduate
School of Geography, Clark University, Worcester, Massachusetts

Steve Heminger, Executive Director, Metropolitan Transportation
Commission, Oakland, California

Chris T. Hendrickson, Hamerschlag Professor of Engineering, Carnegie
Mellon University, Pittsburgh, Pennsylvania

Jeffrey D. Holt, Managing Director, Power, Energy, and Infrastructure
Group, BMO Capital Markets Corporation, New York

S. Jack Hu, Vice President for Research and J. Reid and Polly Anderson
Professor of Manufacturing, University of Michigan, Ann Arbor

Roger B. Huff, President, HGLC, LLC, Farmington Hills, Michigan

Geraldine Knatz, Professor, Sol Price School of Public Policy, Viterbi
School of Engineering, University of Southern California, Los Angeles

Ysela Llort, Consultant, Miami, Florida

Melinda McGrath, Executive Director, Mississippi Department of
Transportation, Jackson

James P. Redeker, Commissioner, Connecticut Department of
Transportation, Newington

Mark L. Rosenberg, Executive Director, The Task Force for Global
Health, Inc., Decatur, Georgia

Kumares C. Sinha, Olson Distinguished Professor of Civil Engineering,
Purdue University, West Lafayette, Indiana

Daniel Sperling, Professor of Civil Engineering and Environmental
Science and Policy; Director, Institute of Transportation Studies,
University of California, Davis

Kirk T. Steudle, Director, Michigan Department of Transportation,
Lansing (Past Chair, 2014)

Gary C. Thomas, President and Executive Director, Dallas Area Rapid
Transit, Dallas, Texas

Pat Thomas, Senior Vice President of State Government Affairs, United
Parcel Service, Washington, D.C.

Katherine F. Turnbull, Executive Associate Director and Research
Scientist, Texas A&M Transportation Institute, College Station

Dean Wise, Vice President of Network Strategy, Burlington Northern
Santa Fe Railway, Fort Worth, Texas

Thomas P. Bostick (Lieutenant General, U.S. Army), Chief of Engineers
and Commanding General, U.S. Army Corps of Engineers, Washington,
D.C. (ex officio)

James C. Card (Vice Admiral, U.S. Coast Guard, retired), Maritime
Consultant, The Woodlands, Texas, and Chair, TRB Marine Board
(ex officio)

T. F. Scott Darling III, Acting Administrator and Chief Counsel, Federal
Motor Carrier Safety Administration, U.S. Department of Transportation
(ex officio)

Marie Therese Dominguez, Administrator, Pipeline and Hazardous
Materials Safety Administration, U.S. Department of Transportation
(ex officio)

Sarah Feinberg, Administrator, Federal Railroad Administration,
U.S. Department of Transportation (ex officio)

Carolyn Flowers, Acting Administrator, Federal Transit Administration,
U.S. Department of Transportation (ex officio)

LeRoy Gishi, Chief, Division of Transportation, Bureau of Indian
Affairs, U.S. Department of the Interior, Washington, D.C. (ex officio)

John T. Gray II, Senior Vice President, Policy and Economics,
Association of American Railroads, Washington, D.C. (ex officio)

Michael P. Huerta, Administrator, Federal Aviation Administration,
U.S. Department of Transportation (ex officio)

Paul N. Jaenichen, Sr., Administrator, Maritime Administration,
U.S. Department of Transportation (ex officio)

Bevan B. Kirley, Research Associate, University of North Carolina
Highway Safety Research Center, Chapel Hill, and Chair, TRB Young
Members Council (ex officio)

Gregory G. Nadeau, Administrator, Federal Highway Administration,
U.S. Department of Transportation (ex officio)

Wayne Nastri, Acting Executive Officer, South Coast Air Quality
Management District, Diamond Bar, California (ex officio)

Mark R. Rosekind, Administrator, National Highway Traffic Safety
Administration, U.S. Department of Transportation (ex officio)

Craig A. Rutland, U.S. Air Force Pavement Engineer, U.S. Air Force
Civil Engineer Center, Tyndall Air Force Base, Florida (ex officio)

Reuben Sarkar, Deputy Assistant Secretary for Transportation,
U.S. Department of Energy (ex officio)

Richard A. White, Acting President and CEO, American Public
Transportation Association, Washington, D.C. (ex officio)

Gregory D. Winfree, Assistant Secretary for Research and Technology,
Office of the Secretary, U.S. Department of Transportation (ex officio)

Frederick G. (Bud) Wright, Executive Director, American Association
of State Highway and Transportation Officials, Washington, D.C.
(ex officio)

Paul F. Zukunft (Admiral, U.S. Coast Guard), Commandant, U.S. Coast
Guard, U.S. Department of Homeland Security (ex officio)

Transportation Research Board publications are available by ordering
individual publications directly from the TRB Business Office, through
the Internet at www.TRB.org, or by annual subscription through
organizational or individual affiliation with TRB. Affiliates and library
subscribers are eligible for substantial discounts. For further information,
contact the Transportation Research Board Business Office, 500 Fifth
Street, NW, Washington, DC 20001 (telephone 202-334-3213;
fax 202-334-2519; or e-mail TRBsales@nas.edu).

Copyright 2016 by the National Academy of Sciences.

All rights reserved.

Printed in the United States of America.

ISBN 978-0-309-36997-8 [Slipcased set of three volumes]

ISBN 978-0-309-36998-5 [Volume 1]

ISBN 978-0-309-36999-2 [Volume 2]

ISBN 978-0-309-37000-4 [Volume 3]

ISBN 978-0-309-37001-1 [Volume 4, online only]

The National Academies of
SCIENCES • ENGINEERING • MEDICINE

The **National Academy of Sciences** was established in 1863 by an Act of Congress, signed by President Lincoln, as a private, nongovernmental institution to advise the nation on issues related to science and technology. Members are elected by their peers for outstanding contributions to research. Dr. Ralph J. Cicerone is president.

The **National Academy of Engineering** was established in 1964 under the charter of the National Academy of Sciences to bring the practices of engineering to advising the nation. Members are elected by their peers for extraordinary contributions to engineering. Dr. C. D. Mote, Jr., is president.

The **National Academy of Medicine** (formerly the Institute of Medicine) was established in 1970 under the charter of the National Academy of Sciences to advise the nation on medical and health issues. Members are elected by their peers for distinguished contributions to medicine and health. Dr. Victor J. Dzau is president.

The three Academies work together as the National Academies of Sciences, Engineering, and Medicine to provide independent, objective analysis and advice to the nation and conduct other activities to solve complex problems and inform public policy decisions. The Academies also encourage education and research, recognize outstanding contributions to knowledge, and increase public understanding in matters of science, engineering, and medicine.

Learn more about the National Academies of Sciences, Engineering, and Medicine at **www.national-academies.org**.

The **Transportation Research Board** is one of seven major programs of the National Academies of Sciences, Engineering, and Medicine. The mission of the Transportation Research Board is to increase the benefits that transportation contributes to society by providing leadership in transportation innovation and progress through research and information exchange, conducted within a setting that is objective, interdisciplinary, and multimodal. The Board's varied committees, task forces, and panels annually engage about 7,000 engineers, scientists, and other transportation researchers and practitioners from the public and private sectors and academia, all of whom contribute their expertise in the public interest. The program is supported by state transportation departments, federal agencies including the component administrations of the U.S. Department of Transportation, and other organizations and individuals interested in the development of transportation.

Learn more about the Transportation Research Board at **www.TRB.org**.

CHAPTER 25
FREEWAY FACILITIES: SUPPLEMENTAL

CONTENTS

1. INTRODUCTION 25-1

- Chapter Scope 25-1
- Chapter Organization 25-1
- Limitations of the Methodologies 25-1

2. GLOSSARY OF VARIABLE DEFINITIONS 25-3

- Overview 25-3
- Global Variables 25-3
- Segment Variables 25-4
- Node Variables 25-5
- On-Ramp Variables 25-6
- Off-Ramp Variables 25-6
- Facilitywide Variables 25-6
- Travel Time Reliability Variables 25-7

3. UNDERSATURATED SEGMENT EVALUATION 25-9

- Facility Speed Constraint 25-9
- Directional Facility Module 25-10

4. OVERSATURATED SEGMENT EVALUATION 25-11

- Procedure Parameters 25-11
- Flow Estimation 25-13
- Segment and Ramp Performance Measures 25-25
- Oversaturation Analysis within Managed Lanes 25-26

5. WORK ZONE ANALYSIS DETAILS 25-28

- Special Work Zone Configurations 25-28

6. PLANNING-LEVEL METHODOLOGY FOR FREEWAY FACILITIES 25-34

- Input Requirements 25-34
- Step 1: Demand-Level Calculations 25-36
- Step 2: Section Capacity Calculations and Adjustments 25-37
- Step 3: Delay Rate Estimation 25-38
- Step 4: Average Travel Time, Speed, and Density Calculations 25-39
- Step 5: Level of Service 25-40

7. MIXED-FLOW MODEL FOR COMPOSITE GRADES	25-41
Overview of the Methodology	25-41
Step 1: Input Data	25-41
Step 2: Capacity Assessment	25-41
Step 3: Specify Initial Conditions.....	25-44
Step 4: Compute Truck Spot and Space-based Travel Time Rates	25-44
Step 5: Compute Automobile Spot and Space-Based Travel Time Rates ..	25-50
Step 6: Compute Mixed-Flow Space-Based Travel Time Rate and Speed	25-51
Step 7: Overall Results.....	25-52
8. FREEWAY CALIBRATION METHODOLOGY	25-53
Calibration at the Core Freeway Facility Level	25-53
Calibration at the Travel Time Reliability Level	25-60
Calibration at the Reliability Strategy Assessment Level	25-65
9. FREEWAY SCENARIO GENERATION.....	25-68
Introduction	25-68
Methodology	25-71
10. COMPUTATIONAL ENGINE OVERVIEW.....	25-84
11. EXAMPLE PROBLEMS	25-85
Example Problem 1: Evaluation of an Undersaturated Facility.....	25-85
Example Problem 2: Evaluation of an Oversaturated Facility	25-92
Example Problem 3: Capacity Improvements to an Oversaturated Facility	25-97
Example Problem 4: Evaluation of an Undersaturated Facility with a Work zone.....	25-102
Example Problem 5: Evaluation of an Oversaturated Facility with a Managed Lane.....	25-108
Example Problem 6: Planning-Level Analysis of a Freeway Facility.....	25-113
Example Problem 7: Reliability Evaluation of an Existing Freeway Facility	25-118
Example Problem 8: Reliability Analysis with Geometric Improvements	25-122
Example Problem 9: Evaluation of Incident Management	25-123
Example Problem 10: Planning-Level Reliability Analysis	25-124
Example Problem 11: Estimating Freeway Composite Grade Operations with the Mixed-Flow Model.....	25-125
12. REFERENCES.....	25-135
APPENDIX A: TRUCK PERFORMANCE CURVES.....	25-137

LIST OF EXHIBITS

Exhibit 25-1 Node–Segment Representation of a Directional Freeway Facility..... 25-11

Exhibit 25-2 Segment Flow–Density Function 25-13

Exhibit 25-3 Oversaturated Analysis Procedure..... 25-14

Exhibit 25-4 Definitions of Mainline and Segment Flows 25-19

Exhibit 25-5 Flow–Density Function with a Shock Wave 25-21

Exhibit 25-6 Vertical Queuing from a Managed Lane Due to Queue Presence on the General Purpose Lanes 25-27

Exhibit 25-7 On-Ramp Merge Diagram for 2-to-1 Freeway Work Zone Configuration..... 25-28

Exhibit 25-8 Proportion of Work Zone Queue Discharge Rate (Relative to the Basic Work Zone Capacity) Available for Mainline Flow Upstream of Merge Area 25-29

Exhibit 25-9 Off-Ramp Diverge Diagram for a 2-to-1 Freeway Work Zone Configuration..... 25-30

Exhibit 25-10 Proportion of Work Zone Capacity Available for Mainline Flow Downstream of Diverge Area 25-31

Exhibit 25-11 Proportion of Off-Ramp Demand Served in Work Zone 25-31

Exhibit 25-12 Proportion of Available Work Zone Capacity for a Directional Crossover in the Work Zone..... 25-31

Exhibit 25-13 Model Coefficients for Estimating the Proportion of Work Zone Capacity in a Weaving Segment 25-33

Exhibit 25-14 Model Coefficients for Estimating the Proportion of Off-Ramp Volume Served in the Weaving Area 25-33

Exhibit 25-15 Schematics of Freeway Sections..... 25-34

Exhibit 25-16 Parameter Values for Undersaturated Model..... 25-39

Exhibit 25-17 LOS Criteria for Urban and Rural Freeway Facilities..... 25-40

Exhibit 25-18 Schematic of a Composite Grade 25-41

Exhibit 25-19 Mixed-Flow Methodology Overview 25-42

Exhibit 25-20 SUT Spot Rates Versus Distance with Initial Speeds of 75 and 30 mi/h 25-45

Exhibit 25-21 TT Spot Rates Versus Distance with Initial Speeds of 75 and 20 mi/h 25-45

Exhibit 25-22 SUT Travel Time Versus Distance Curves for 70-mi/h Initial Speed..... 25-47

Exhibit 25-23 SUT Travel Time Versus Distance Curves for 30-mi/h Initial Speed..... 25-47

Exhibit 25-24 δ Values for SUTs 25-48

Exhibit 25-25 δ Values for TTs.....	25-48
Exhibit 25-26 Calibration Steps for the Core Freeway Facility Level	25-54
Exhibit 25-27 Effect of Calibrating Free-Flow Speed on Capacity	25-55
Exhibit 25-28 Effects of Segment Capacity	25-56
Exhibit 25-29 Effects of Queue Discharge Rate Drop	25-56
Exhibit 25-30 Effects of Jam Density.....	25-57
Exhibit 25-31 Effect of Demand Level.....	25-58
Exhibit 25-32 Comprehensive Reliability Calibration Steps.....	25-60
Exhibit 25-33 High Demand Level on the Seed Day.....	25-62
Exhibit 25-34 Low Demand Level on the Seed Day.....	25-62
Exhibit 25-35 Overestimating the Impacts of Nonrecurring Sources of Congestion	25-63
Exhibit 25-36 Underestimating the Impacts of Nonrecurring Sources of Congestion	25-64
Exhibit 25-37 Process Flow Overview for Freeway Scenario Generation.....	25-69
Exhibit 25-38 Distribution of Number of Incidents in the Scenarios.....	25-70
Exhibit 25-39 Detailed Freeway Scenario Generation Flowchart.....	25-72
Exhibit 25-40 Listing of Weather Stations with Available Weather Data	25-76
Exhibit 25-41 Incident Duration Distribution Parameters in Minutes	25-81
Exhibit 25-42 List of Example Problems	25-85
Exhibit 25-43 Example Problem 1: Freeway Facility.....	25-85
Exhibit 25-44 Example Problem 1: Geometry of Directional Freeway Facility	25-85
Exhibit 25-45 Example Problem 1: Demand Inputs	25-87
Exhibit 25-46 Example Problem 1: Segment Capacities	25-88
Exhibit 25-47 Example Problem 1: Segment Demand-to-Capacity Ratios	25-89
Exhibit 25-48 Example Problem 1: Volume-Served Matrix	25-89
Exhibit 25-49 Example Problem 1: Speed Matrix	25-90
Exhibit 25-50 Example Problem 1: Density Matrix	25-90
Exhibit 25-51 Example Problem 1: LOS Matrix	25-90
Exhibit 25-52 Example Problem 1: Facility Performance Measure Summary	25-92
Exhibit 25-53 Example Problem 2: Demand Inputs	25-93
Exhibit 25-54 Example Problem 2: Segment Capacities	25-94
Exhibit 25-55 Example Problem 2: Segment Demand-to-Capacity Ratios	25-95
Exhibit 25-56 Example Problem 2: Volume-Served Matrix	25-96
Exhibit 25-57 Example Problem 2: Speed Matrix	25-96
Exhibit 25-58 Example Problem 2: Density Matrix	25-96

Exhibit 25-59 Example Problem 2: Expanded LOS Matrix.....	25-96
Exhibit 25-60 Example Problem 2: Facility Performance Measure Summary	25-97
Exhibit 25-61 Example Problem 3: Freeway Facility	25-98
Exhibit 25-62 Example Problem 3: Geometry of Directional Freeway Facility.....	25-98
Exhibit 25-63 Example Problem 3: Segment Capacities.....	25-100
Exhibit 25-64 Example Problem 3: Segment Demand-to-Capacity Ratios.....	25-100
Exhibit 25-65 Example Problem 3: Speed Matrix.....	25-101
Exhibit 25-66 Example Problem 3: Density Matrix.....	25-101
Exhibit 25-67 Example Problem 3: LOS Matrix.....	25-101
Exhibit 25-68 Example Problem 3: Facility Performance Measure Summary	25-102
Exhibit 25-69 Example Problem 4: Freeway Facility	25-102
Exhibit 25-70 Example Problem 4: Geometry of Directional Freeway Facility.....	25-102
Exhibit 25-71 Example Problem 4: Segment Capacities.....	25-104
Exhibit 25-72 Example Problem 4: Segment Demand-to-Capacity Ratios.....	25-105
Exhibit 25-73 Example Problem 4: Volume-Served Matrix.....	25-106
Exhibit 25-74 Example Problem 4: Speed Matrix.....	25-106
Exhibit 25-75 Example Problem 4: Density Matrix.....	25-107
Exhibit 25-76 Example Problem 4: LOS Matrix.....	25-107
Exhibit 25-77 Example Problem 4: Facility Performance Measure Summary	25-107
Exhibit 25-78 Example Problem 5: Freeway Facility	25-108
Exhibit 25-79 Example Problem 5: Geometry of Directional Freeway Facility.....	25-108
Exhibit 25-80 Example Problem 5: Demand Inputs on the Mainline.....	25-109
Exhibit 25-81 Example Problem 5: Segment Capacities.....	25-110
Exhibit 25-82 Example Problem 5: Segment Demand-to-Capacity Ratios.....	25-110
Exhibit 25-83 Example Problem 5: Speed Matrix.....	25-111
Exhibit 25-84 Example Problem 5: Density Matrix.....	25-111
Exhibit 25-85 Example Problem 5: LOS Matrix.....	25-111
Exhibit 25-86 Example Problem 5: Facility Performance Measure Summary for Lane Groups	25-112
Exhibit 25-87 Example Problem 5: Facility Performance Measure Summary	25-112
Exhibit 25-88 Example Problem 6: AADT Values for the Facility.....	25-113
Exhibit 25-89 Example Problem 6: Section Definition for the Facility.....	25-114

Exhibit 25-90 Example Problem 6: Demand Flow Rates (pc/h) on the Subject Facility..... 25-114

Exhibit 25-91 Example Problem 6: Demand-to-Capacity Ratios by Section and Analysis Period 25-115

Exhibit 25-92 Example Problem 6: Delay Rates by Section and Analysis Period..... 25-116

Exhibit 25-93 Example Problem 6: Travel Rates by Section and Analysis Period..... 25-117

Exhibit 25-94 Example Problem 6: Average Travel Times by Section and Analysis Period 25-117

Exhibit 25-95 Example Problem 6: Density by Section and Analysis Period..... 25-117

Exhibit 25-96 Example Problem 6: Facility Performance Summary 25-117

Exhibit 25-97 Example Problem 7: Freeway Facility..... 25-118

Exhibit 25-98 Example Problem 7: Geometry of Directional Freeway Facility 25-118

Exhibit 25-99 Example Problem 7: Demand Flow Rates (veh/h) by Analysis Period in the Base Data Set 25-119

Exhibit 25-100 Example Problem 7: Demand Ratios Relative to AADT 25-120

Exhibit 25-101 Example Problem 7: Weather Event Probabilities by Season 25-120

Exhibit 25-102 Example Problem 7: CAF, SAF, and Event Duration Values Associated with Weather Events..... 25-120

Exhibit 25-103 Example Problem 7: Incident Frequencies by Month..... 25-121

Exhibit 25-104 Example Problem 7: Summary Reliability Performance Measure Results 25-121

Exhibit 25-105 Example Problem 7: VMT-Weighted TTI Probability and Cumulative Distribution Functions 25-122

Exhibit 25-106 Example Problem 8: Freeway Facility..... 25-122

Exhibit 25-107 Example Problem 8: Summary Reliability Performance Measure Results 25-123

Exhibit 25-108 Example Problem 9: Summary Reliability Performance Measure Results 25-124

Exhibit 25-109 Example Problem 11: Spot Speeds of All Segments..... 25-134

Exhibit 25-110 Example Problem 11: Space Mean Speeds of All Segments ... 25-134

Exhibit 25-111 Example Problem 11: Overall Space Mean Speeds of All Segments 25-134

Exhibit 25-A1 SUT Travel Time Versus Distance Curves for 35-mi/h Initial Speed 25-137

Exhibit 25-A2 SUT Travel Time Versus Distance Curves for 40-mi/h Initial Speed 25-137

Exhibit 25-A3 SUT Travel Time Versus Distance Curves for 45-mi/h Initial Speed	25-138
Exhibit 25-A4 SUT Travel Time Versus Distance Curves for 50-mi/h Initial Speed	25-138
Exhibit 25-A5 SUT Travel Time Versus Distance Curves for 55-mi/h Initial Speed	25-139
Exhibit 25-A6 SUT Travel Time Versus Distance Curves for 60-mi/h Initial Speed	25-139
Exhibit 25-A7 SUT Travel Time Versus Distance Curves for 65-mi/h Initial Speed	25-140
Exhibit 25-A8 SUT Travel Time Versus Distance Curves for 75-mi/h Initial Speed	25-140
Exhibit 25-A9 TT Travel Time Versus Distance Curves for 20-mi/h Initial Speed.....	25-141
Exhibit 25-A10 TT Travel Time Versus Distance Curves for 25-mi/h Initial Speed	25-141
Exhibit 25-A11 TT Travel Time Versus Distance Curves for 30-mi/h Initial Speed	25-142
Exhibit 25-A12 TT Travel Time Versus Distance Curves for 35-mi/h Initial Speed	25-142
Exhibit 25-A13 TT Travel Time Versus Distance Curves for 40-mi/h Initial Speed	25-143
Exhibit 25-A14 TT Travel Time Versus Distance Curves for 45-mi/h Initial Speed	25-143
Exhibit 25-A15 TT Travel Time Versus Distance Curves for 50-mi/h Initial Speed	25-144
Exhibit 25-A16 TT Travel Time Versus Distance Curves for 55-mi/h Initial Speed	25-144
Exhibit 25-A17 TT Travel Time Versus Distance Curves for 60-mi/h Initial Speed	25-145
Exhibit 25-A18 TT Travel Time Versus Distance Curves for 65-mi/h Initial Speed	25-145
Exhibit 25-A19 TT Travel Time Versus Distance Curves for 70-mi/h Initial Speed	25-146
Exhibit 25-A20 TT Travel Time Versus Distance Curves for 75-mi/h Initial Speed	25-146

1. INTRODUCTION

CHAPTER SCOPE

Chapter 25 is the supplemental chapter for Chapter 10, which describes the core methodology for freeway facilities, and Chapter 11, which presents a methodology for evaluating freeway reliability and active traffic and demand management (ATDM) strategies. The computations used by these methodologies are detailed in this supplemental chapter. The documentation is closely tied to FREEVAL-2015E, the computational engine for Chapter 10 and Chapter 11.

The FREEVAL (FREeway EVALuation) tool was initially developed for the 2000 edition of the *Highway Capacity Manual (HCM)* (1, 2) and has been updated to reflect subsequent methodological changes in the HCM. All variable definitions and subroutine labels presented in this chapter are consistent with the computational code in FREEVAL-2015E. The Technical Reference Library in Volume 4 contains a FREEVAL-2015E user guide, which provides more details on how to use the computational engine. Other software implementations of this method are available and can be used instead of the computational engine.

CHAPTER ORGANIZATION

Section 2 presents a glossary of all relevant variables used in the procedures and the computational engine. Section 3 and Section 4, respectively, provide details of the undersaturated and oversaturated flow procedures. Section 5 describes details for work zone analysis. Section 6 develops the planning-level methodology for freeway facilities, and Section 7 discusses the mixed-flow model for composite grades. Section 8 develops the freeway calibration methodology at three levels. Section 9 discusses freeway scenario generation, and Section 10 presents an overview of the computational engine structure. Example problems are presented in Section 11, and Section 12 provides references for the chapter.

LIMITATIONS OF THE METHODOLOGIES

The completeness of the analysis will be limited if freeway segment cells in the first time interval, the final time interval, and the first freeway segment do not have demand-to-capacity ratios of 1.00 or less. The methodology can handle congestion in the first interval properly, although it will not quantify any congestion that could have occurred before the first time interval. To ensure a complete quantification of the effects of congestion, it is recommended that the analysis contain an initial undersaturated time interval. If all freeway segments in the final time interval do not exhibit demand-to-capacity ratios less than 1.00, congestion will continue beyond the final time interval, and additional time intervals should be added. This fact will be noted as a difference between the vehicle miles of travel desired at the end of the analysis (demand flow) and the corresponding vehicle miles of travel flow generated (volume served). If queues extend upstream of the first segment, the analysis will not account for the congestion outside the freeway facility but will store the vehicles vertically until

VOLUME 4: APPLICATIONS
GUIDE

25. Freeway Facilities: Supplemental

- 26. Freeway and Highway Segments: Supplemental
- 27. Freeway Weaving: Supplemental
- 28. Freeway Merges and Diverges: Supplemental
- 29. Urban Street Facilities: Supplemental
- 30. Urban Street Segments: Supplemental
- 31. Signalized Intersections: Supplemental
- 32. STOP-Controlled Intersections: Supplemental
- 33. Roundabouts: Supplemental
- 34. Interchange Ramp Terminals: Supplemental
- 35. Pedestrians and Bicycles: Supplemental
- 36. Concepts: Supplemental
- 37. ATDM: Supplemental

the congestion clears the first segment. The same process is followed for queues on on-ramp segments.

The methodology for oversaturated conditions described in this chapter is based on concepts of traffic flow theory and assumes a linear speed–flow relationship for densities greater than 45 passenger cars per mile per lane (pc/mi/ln). This relationship has not been extensively calibrated for field observations on U.S. freeways, and analysts should therefore perform their own validation from local data to obtain additional confidence in the results of this procedure. For an example of a validation exercise for this methodology, the reader is referred elsewhere (3).

The procedure described here becomes extremely complex when the queue from a downstream bottleneck extends into an upstream bottleneck, causing a queue interaction. When such cases arise, the reliability of the methodology is questionable, and the user is cautioned about the validity of the results. For heavily congested directional freeway facilities with interacting bottleneck queues, a traffic simulation model might be more applicable. Noninteracting bottlenecks are addressed by the methodology.

The procedure focuses on analyzing a directional series of freeway segments. It describes the performance of a facility but falls short of addressing the broader transportation network. The analyst is cautioned that severe congestion on a freeway—especially freeway on-ramps—is likely to affect the adjacent surface street network. Similarly, the procedure is limited in its ability to predict the impacts of an oversaturated off-ramp and the associated queues that may spill back onto the freeway. Alternative tools are suitable to evaluate these impacts.

2. GLOSSARY OF VARIABLE DEFINITIONS

OVERVIEW

This glossary defines internal variables used exclusively in the freeway facilities methodology. The variables are consistent with those used in the computational engine for the freeway facilities methodology.

If a managed lane facility is adjacent to the general purpose lanes, the oversaturated freeway facilities methodology will analyze each facility independently. As a result, the variables presented in this chapter will pertain to general purpose and managed lane facilities separately.

The glossary of variables is presented in seven parts: global variables, segment variables, node variables, on-ramp variables, off-ramp variables, facilitywide variables, and travel time reliability variables. Global variables are used across multiple aspects of the procedure. Segment variables represent conditions on segments. Node variables denote flows across a node connecting two segments. On- and off-ramp variables correspond to flow on ramps. Facilitywide variables pertain to aggregate traffic performance over the entire general purpose or managed lane facility. Reliability variables pertain to traffic performance over a period of up to one year.

In addition to the spatial categories listed above, there are temporal divisions that represent characteristics over a time step or a time interval. The first dimension associated with each variable specifies whether the variable refers to segment or node characteristics. The labeling scheme for nodes and segments is such that segment i is immediately downstream of node i . The distinction of nodes and segments is used primarily in the oversaturated flow regime as discussed in Section 4.

Thus, there is always one more node than the number of segments on a facility. The second and third dimensions denote a time step t and a time interval p . Facility variables are estimates of the average performance over the length of the facility. The units of flow are in vehicles per time step. The selection of the time step size is discussed later in this chapter.

The variable symbols used internally by the computational engine and replicated in this chapter frequently differ from the symbols used elsewhere in the HCM, particularly in Chapter 10, Freeway Facilities Core Methodology. For example, the HCM uses n to represent the number of segments forming a facility, whereas the computational engine and this chapter use NS .

GLOBAL VARIABLES

- i —index to segment or node number: $i = 1, 2, \dots, NS$ (for segments) and $i = 1, 2, \dots, NS + 1$ (for nodes). In the computational engine, i is represented as the index of the *GPSegments/MLSegments Array List* variable in the Seed class.
- KC —ideal density at capacity in vehicles per mile per lane (veh/mi/ln). The density at capacity is 45 pc/mi/ln, which must be converted to vehicles per mile per lane by using the heavy-vehicle adjustment factor

f_{HV} described in Chapter 12, Basic Freeway and Multilane Highway Segments.

- KJ —facilitywide jam density (veh/mi/ln).
- NS —number of segments on the facility. NS is represented as the size of the *GPSegments/MLSegments ArrayList* variable in the Seed class.
- P —number of (15-min) analysis periods in the study period. Represented as *Period* in the computational engine. For a 24-h analysis, the theoretical maximum is 96 analysis periods.
- p —analysis period index: $p = 1, 2, \dots, P$.
- S —number of computational time steps in an analysis period (integer). S is represented as *Step* in the computational engine. S is set as a constant of 60 in the computational engine, corresponding to a 15-s interval and allowing a minimum segment length of 300 ft.
- t —time step index in a single analysis period: $t = 1, 2, \dots, S$.
- T —number of time steps in 1 h (integer). T is set as a constant of 240 in the computational engine, or equal to four times the value of S .
- α —fraction of capacity drop in queue discharge conditions due to congestion on the facility. This variable is represented as *inCapacityDropPercentage* in the GPMLSegment class in the computational engine.

SEGMENT VARIABLES

- $ED(i, p)$ —expected demand (veh/h) that would arrive at segment i on the basis of upstream conditions over time interval p . The upstream queuing effects include the metering of traffic from an upstream queue but not the spillback of vehicles from a downstream queue.
- $K(i, p)$ —average traffic density (veh/mi/ln) of segment i over time interval p as estimated by the oversaturated procedure. This variable is represented as the *scenAllDensity_veh* variable in the GPMLSegment class in the computational engine.
- $KB(i, p)$ —background density: segment i density (veh/mi/ln) over time interval p assuming there is no queuing on the segment. This density is calculated by using the expected demand on the segment in the corresponding undersaturated procedure in Chapters 12, 13, and 14.
- $KQ(i, t, p)$ —queue density: vehicle density (veh/mi/ln) in the queue on segment i during time step t in time interval p . Queue density is calculated on the basis of a linear density–flow relationship in the congested regime.
- $L(i)$ —length of segment i (mi). This variable converts the *inSegLength_ft* variable (in feet) to miles when necessary in equations.
- $N(i, p)$ —number of lanes on segment i in time interval p . It could vary by time interval if a temporary lane closure is in effect. N is represented as

the *inMainlineNumLanes* variable in the GPMLSegment class in the computational engine.

- $NV(i, t, p)$ —number of vehicles present on segment i at the end of time step t during time interval p . The number of vehicles is initially based on the calculations of Chapters 12, 13, and 14, but, as queues grow and dissipate, input–output analysis updates these values in each time step.
- $Q(i, t, p)$ —total queue length on segment i at the end of time step t in time interval p (ft).
- $SC(i, p)$ —segment capacity: maximum number of vehicles (veh/h) that can pass through segment i in time interval p based strictly on traffic and geometric properties. These capacities are calculated by using Chapters 12, 13, and 14. Segment capacity is represented as the *scenMainlineCapacity_veh* variable in the GPMLSegment class in the computational engine.
- $SD(i, p)$ —segment demand: desired flow rate (veh/h) through segment i including on- and off-ramp demands in time interval p (veh). This segment demand is calculated without any capacity constraints. It is represented as the *scenMainlineDemand_veh* variable in the GPMLSegment class in the computational engine.
- $SF(i, t, p)$ —segment flow (veh/h) out of segment i during time step t in time interval p (veh).
- $U(i, p)$ —average space mean speed over the length of segment i during time interval p (mi/h). It is represented as the *scenSpeed* variable in the GPMLSegment class in the computational engine.
- $UV(i, t, p)$ —unserved vehicles: the additional number of vehicles stored on segment i at the end of time step t in time interval p due to a downstream bottleneck.
- $WS(i, p)$ —wave speed: speed at which a front-clearing queue shock wave travels through segment i during time interval p (ft/s).
- $WTT(i, p)$ —wave travel time: time taken by the shock wave traveling at wave speed WS to travel from the downstream end of segment i to the upstream end of the segment during time interval p , in time steps.

NODE VARIABLES

- $MF(i, t, p)$ —actual mainline flow rate that can cross node i during time step t in time interval p .
- $MI(i, t, p)$ —maximum mainline input: maximum flow desiring to enter node i during time step t in time interval p , based on flows from all upstream segments and taking into account all geometric and traffic constraints upstream of the node, including queues accumulated from previous time intervals.
- $MO1(i, t, p)$ —maximum Mainline Output 1: maximum allowable mainline flow rate across node i during time step t in time interval p , limited by the flow from an on-ramp at node i .

- $MO2(i, t, p)$ —maximum Mainline Output 2: maximum allowable mainline flow rate across node i during time step t in time interval p , limited by available storage on segment i due to a downstream queue.
- $MO3(i, t, p)$ —maximum Mainline Output 3: maximum allowable mainline flow rate across node i during time step t in time interval p , limited by the presence of queued vehicles at the upstream end of segment i while the queue clears from the downstream end of segment i .

ON-RAMP VARIABLES

- $ONRC(i, p)$ —geometric carrying capacity of on-ramp at node i during time interval p .
- $ONRD(i, p)$ —demand flow rate for on-ramp at node i in time interval p .
- $ONRF(i, t, p)$ —actual ramp flow rate that can cross on-ramp node i during time step t in time interval p ; it takes into account control constraints (e.g., ramp meters).
- $ONRI(i, t, p)$ —input flow rate desiring to enter the merge point at on-ramp i during time step t in time interval p , based on current ramp demand and ramp queues accumulated from previous time intervals.
- $ONRO(i, t, p)$ —maximum output flow rate that can enter the merge point from on-ramp i during time step t in time interval p ; it is constrained by Lane 1 (shoulder lane) flow on segment i and the segment i capacity or by a queue spillback filling the mainline segment from a bottleneck further downstream, whichever governs.
- $ONRQ(i, t, p)$ —unmet demand that is stored as a queue on the on-ramp roadway at node i during time step t in time interval p (veh).
- $RM(i, p)$ —maximum allowable rate of an on-ramp meter at the on-ramp at node i during time interval p (veh/h).

OFF-RAMP VARIABLES

- $DEF(i, t, p)$ —deficit: unmet demand from a previous time interval p that flows past node i during time step t ; it is used in off-ramp flow calculations downstream of a bottleneck.
- $OFRD(i, p)$ —desired off-ramp demand flow exiting at off-ramp i during time interval p .
- $OFRF(i, t, p)$ —actual flow that can exit at off-ramp i during time step t in time interval p .

FACILITYWIDE VARIABLES

- $K(NS, P)$ —average vehicle density over the entire facility during the entire analysis period P .
- $K(NS, p)$ —average vehicle density over the entire facility during time interval p .
- $SMS(NS, P)$ —average analysis period facility speed: average space mean speed over the entire facility during the entire analysis period P .

- $SMS(NS, p)$ —average time interval facility speed: average space mean speed over the entire facility during time interval p .

TRAVEL TIME RELIABILITY VARIABLES

- CR_j —crash rate per 100 million vehicle miles traveled (VMT) in month j .
- D_{SP} —duration of study period SP (h).
- $DAF_s(tp, seg)$ —demand adjustment factor for scenario s , period tp , and segment seg .
- DC_s —demand combination associated with scenario s .
- $DM(s)$ —demand multiplier associated with scenario s .
- $DM(\text{Seed})$ —demand multiplier associated with the seed file.
- \overline{DM}_j —weighted average demand multiplier for all days in month j relative to seed value.
- $E[n_w j]$ —expected frequency of weather event w in month j , rounded to the nearest integer.
- $E_{15min}[D_w]$ —expected duration of weather event w , rounded to the nearest 15-min increment.
- $\mathbb{G}(i)$ —distribution function for incident with severity type i .
- ICR —incident-to-crash ratio.
- Inc_{Dur} —incident duration (min).
- Inc_{Type} —incident severity type (1–5).
- n_{inc} —number of incidents.
- n_j —expected frequency of all incidents in the study period for month j , rounded to the nearest integer.
- $n_{Day,k}$ —number of days in the reliability reporting period associated with demand combination k .
- N_{DC} —number of demand-level combinations considered.
- N_{Scen} —number of scenarios in the analysis.
- $N_{Inc,i}$ —number of incidents associated with severity type i .
- $N_{Scen,Inc}$ —number of all incident events generated for all scenarios.
- $N_{Scen,j}$ —number of scenarios associated with month j of the reliability reporting period.
- $\bar{N}_{DC,WZ}$ —adjusted number of replications of a demand combination for which the work zone is active.
- $P\{s\}$ —probability of scenario s .
- $P_i\{w, j\}$ —time-wise probability of weather type w in month j .

- r_{DC} —ratio of weekday types with an active work zone in a given month to the total number of each weekday type occurring in a given month.
- $VM T_{seed}$ —vehicle miles of travel in the seed file.
- $VM T_{seg,u}$ —vehicle miles traveled on segment seg during analysis period u in the seed file.
- δ_x —adjustment parameters to satisfy equilibrium calibration equations.

3. UNDERSATURATED SEGMENT EVALUATION

FACILITY SPEED CONSTRAINT

This module begins with the first segment in the first time interval. For each cell, the flow (or volume) is equal to demand, the volume-to-capacity ratio is equal to the demand-to-capacity ratio, and undersaturated flow conditions prevail. Performance measures for the first segment during the first time interval are calculated by using the procedures for the corresponding segment type in Chapters 12, 13, and 14.

The analysis continues to the next downstream freeway segment in the same time interval, and the performance measures are calculated. The process is continued until the final downstream freeway segment cell in this time interval has been analyzed. For each cell, the volume-to-capacity ratio and performance measures are calculated for each freeway segment in the first time interval. The analysis continues in the second time interval beginning at the furthest upstream freeway segment and moving downstream until all freeway segments in that time interval have been analyzed. This pattern continues for the third time interval, fourth time interval, and so on until the methodology encounters a time interval that contains one or more segments with a demand-to-capacity ratio greater than 1.00 or when the final segment in the final time interval is analyzed. If no oversaturated segments are encountered, the segment performance measures are taken directly from Chapters 12, 13, and 14, and the facility performance measures are calculated as described next in the Directional Facility Module subsection.

When the analysis moves from isolated segments to a facility, an additional constraint is necessary that controls the relative speed between two segments. To limit the speeds downstream of a segment experiencing a low average speed, a maximum achievable speed is imposed on the downstream segments. This maximum speed is based on acceleration characteristics reported elsewhere (4) and is shown in Equation 25-1.

$$V_{max} = FFS - (FFS - V_{prev}) \times e^{-0.00162 \times L}$$

where

V_{max} = maximum achievable segment speed (mi/h),

FFS = segment free-flow speed (mi/h),

V_{prev} = average speed on immediate upstream segment (mi/h), and

L = distance from midpoints of the upstream segment and the subject segment (ft).

On the facility level, a speed constraint is introduced that limits the maximum achievable speed downstream of a segment experiencing a low average speed.

Equation 25-1

DIRECTIONAL FACILITY MODULE

The traffic performance measures can be aggregated over the length of the directional freeway facility, over the time duration of the study interval, or over the entire time–space domain. Each measure is discussed in the following paragraphs.

Aggregating the estimated traffic performance measures over the entire length of the freeway facility provides facilitywide estimates for each time interval. Facilitywide travel times, vehicle distance of travel, and vehicle hours of travel and delay can be computed, and patterns of their variation over the connected time intervals can be assessed. The computational engine is limited to 15-min time intervals and 1-min time steps.

Aggregating the estimated traffic performance measures over the time duration of the study interval provides an assessment of the performance of each segment along the freeway facility. Average and cumulative distributions of speed and density for each segment can be determined, and patterns of the variation over connected freeway segments can be compared. Average trip times, vehicle distance of travel, and vehicle hours of travel are easily assessed for each segment and compared.

Aggregating the estimated traffic performance measures over the entire time–space domain provides an overall assessment over the study interval time duration. Overall average speeds, average trip times, total vehicle distance traveled, and total vehicle hours of travel and delay are the most obvious overall traffic performance measures. Equation 25-2 through Equation 25-5 show how the facilitywide performance measures are calculated.

Facility space mean speed in time interval p is calculated with Equation 25-2:

Equation 25-2

$$SMS_p(NS) = \frac{\sum_{i=1}^{NS} SF(i, p) \times L(i)}{\sum_{i=1}^{NS} SF(i, p) \times \frac{L(i)}{U(i, p)}}$$

Average facility density in time interval p is calculated with Equation 25-3:

Equation 25-3

$$K_p(NS) = \frac{\sum_{i=1}^{NS} K(i, p) \times L(i)}{\sum_{i=1}^{NS} L(i) \times N(i, p)}$$

Overall space mean speed across all intervals is calculated with Equation 25-4:

Equation 25-4

$$SMS(NS, p) = \frac{\sum_{p=1}^P \sum_{i=1}^{NS} SF(i, p) \times L(i)}{\sum_{p=1}^P \sum_{i=1}^{NS} SF(i, p) \times \frac{L(i)}{U(i, p)}}$$

Overall average density across all intervals is calculated with Equation 25-5:

Equation 25-5

$$K(NS, p) = \frac{\sum_{p=1}^P \sum_{i=1}^{NS} K(i, p) \times L(i)}{\sum_{p=1}^P \sum_{i=1}^{NS} L(i) \times N(i, p)}$$

These performance measures can be compared for different alternatives to assess the impacts of different volume scenarios or the effects of geometric improvements to the facility.

4. OVERSATURATED SEGMENT EVALUATION

Oversaturated flow conditions occur when the demand on one or more freeway segment cells exceeds its capacity. The oversaturated segment evaluation procedure presented in this chapter is performed separately for general purpose and managed lanes. To evaluate the effect of interactions between the general purpose and managed lanes, additional delays are introduced and calculated in the form of vertical queueing, which is discussed at the end of this section.

Once oversaturation is encountered, the methodology changes its temporal and spatial units of analysis. The spatial units become nodes and segments, and the temporal unit moves from a time interval to smaller time steps. A node is defined as the junction of two segments. There is always one more node than there are segments, with a node added at the beginning and end of each segment. The numbering of nodes and segments begins at the upstream end and moves to the downstream end, with the segment upstream of node i numbered segment $i - 1$ and the downstream segment numbered i , as shown in Exhibit 25-1. The intermediate segments and node numbers represent the division of the section between Ramps 1 and 2 into three segments numbered 2 (ONR), 3 (BASIC), and 4 (OFR). The oversaturated analysis moves from the first node to each downstream node in the same time step. After completion of a time step, the same nodal analysis is performed for subsequent time steps.

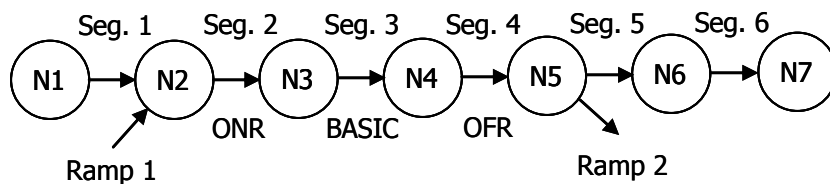


Exhibit 25-1
Node-Segment
Representation of a
Directional Freeway Facility

The oversaturated analysis focuses on the computation of segment average flows and densities in each time interval. These parameters are later aggregated to produce facilitywide estimates. Two key inputs into the flow estimation procedures are the time step duration for flow updates and a flow-density function. These two inputs are described in the next subsections.

PROCEDURE PARAMETERS

Time Step Duration

Segment flows are calculated in each time step and are used to calculate the number of vehicles on each segment at the end of every time step. The number of vehicles on each segment is used to track queue accumulation and discharge and to calculate the average segment density.

To provide accurate estimates of flows in oversaturated conditions, the time intervals are divided into smaller time steps. The conversion from time intervals to time steps occurs during the first oversaturated time interval and remains until the end of the analysis. The transition to time steps is essential because, at certain points in the methodology, future performance estimates are made on the basis of the past value of a variable.

The oversaturated methodology implemented in the computational engine assumes a time step of 15 s, which is adequate for segment lengths greater than 300 ft.

The computational engine assumes a time step of 15 s for oversaturated flow computations, which is adequate for most facilities with a minimum segment length greater than 300 ft. This time step is based on the assumption that a shockwave of (severe) congestion can travel at speeds up to 20 ft/s or 13.6 mi/h. A minimum segment length of 300 ft ensures that the congestion shockwave does not travel more than one segment length in one 15-s time step.

For shorter segments, two problem situations may arise. The first situation occurs when segments are short and the rate of queue growth (shockwave speed) is rapid. Under these conditions, a short segment may be completely undersaturated in one time step and completely queued in another. The methodology may store more vehicles in this segment during a time step than space allows. Fortunately, the next time step compensates for this error, and the procedure continues to track queues and store vehicles accurately after this correction.

The second situation in which small time steps are important occurs when two queues interact. There is a temporary inaccuracy due to the maximum output of a segment changing, thus causing the estimation of available storage to be slightly in error. This situation results in the storage of too many vehicles on a particular segment. This “supersaturation” is temporary and is compensated for in the next time step. Inadequate time step size will result in erroneous estimation of queue lengths and may affect other performance measures as well. Regardless, if queues interact, the results should be viewed with extreme caution.

Flow–Density Relationship

Analysis of freeway segments depends on the relationships between segment speed, flow, and density. Chapter 12, Basic Freeway and Multilane Highway Segments, defines a relationship between these variables and the calculation of performance measures in the undersaturated regime. The freeway facilities methodology presented here uses the same relationships for undersaturated segments. In other words, when a segment is undersaturated the computations of this methodology are identical to the results obtained from Chapters 12, 13, and 14 for basic freeway segments, weaving segments, and ramp segments, respectively.

The calculations for oversaturated segments assume a simplified linear flow–density diagram in the congested region. Exhibit 25-2 shows this flow–density diagram for a segment having a free-flow speed (FFS) of 75 mi/h. For other FFSs, the corresponding capacities in Chapters 12, 13, and 14 should be used.

The oversaturated regime curve in Exhibit 25-2 is constructed from a user-specified jam density (default is 190 pc/mi/ln) and the known value of capacity, defined as the flow at a density of 45 pc/mi/ln. The flow–density relationship is assumed to be linear between these two points. The slope of the resulting line describes the speed of the shock wave at which queues grow and dissipate, as discussed further below. The speed in a congested segment is obtained from the prevailing density in the segment, read along the linear flow–density relationship. Details on the theory of kinematic waves in highway traffic are given elsewhere (5–7).

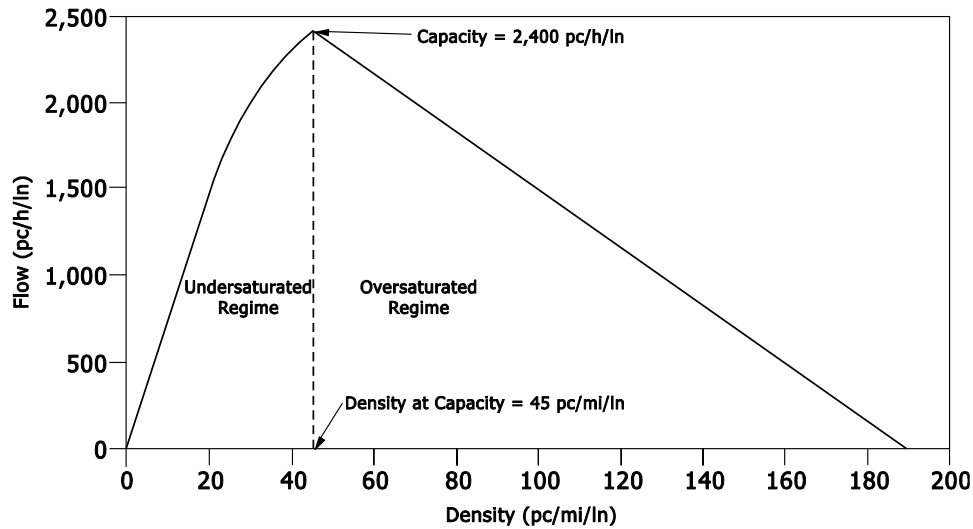


Exhibit 25-2
Segment Flow-Density
Function

Note: Assumed FFS = 75 mi/h.

FLOW ESTIMATION

The oversaturated portion of the methodology is detailed as a flowchart in Exhibit 25-3. The flowchart is divided into several sections over several pages. Processes that continue from one section of the flowchart to another are indicated by capital letters within parallelograms. Computations are detailed and labeled in the subsections that follow according to each step of the flowchart.

The procedure first calculates flow variables starting at the first node during the first time step of oversaturation and followed by each downstream node and segment in the same time step. After all computations in the first time step are completed, calculations are performed at each node and segment during subsequent time steps for all remaining time intervals until the analysis is completed.

Exhibit 25-3
Oversaturated Analysis
Procedure

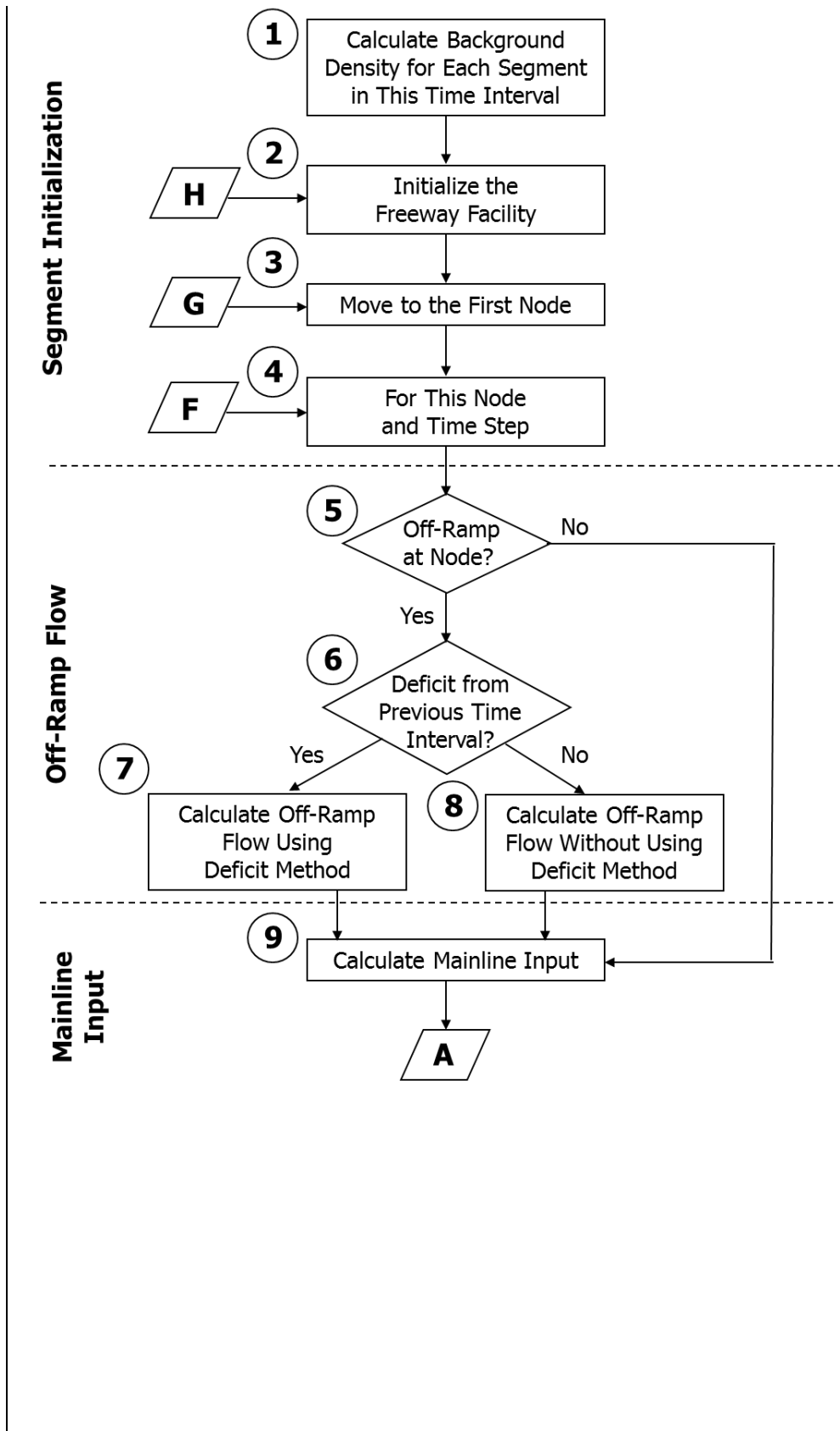


Exhibit 25-3 (cont'd.)
Oversaturated Analysis
Procedure

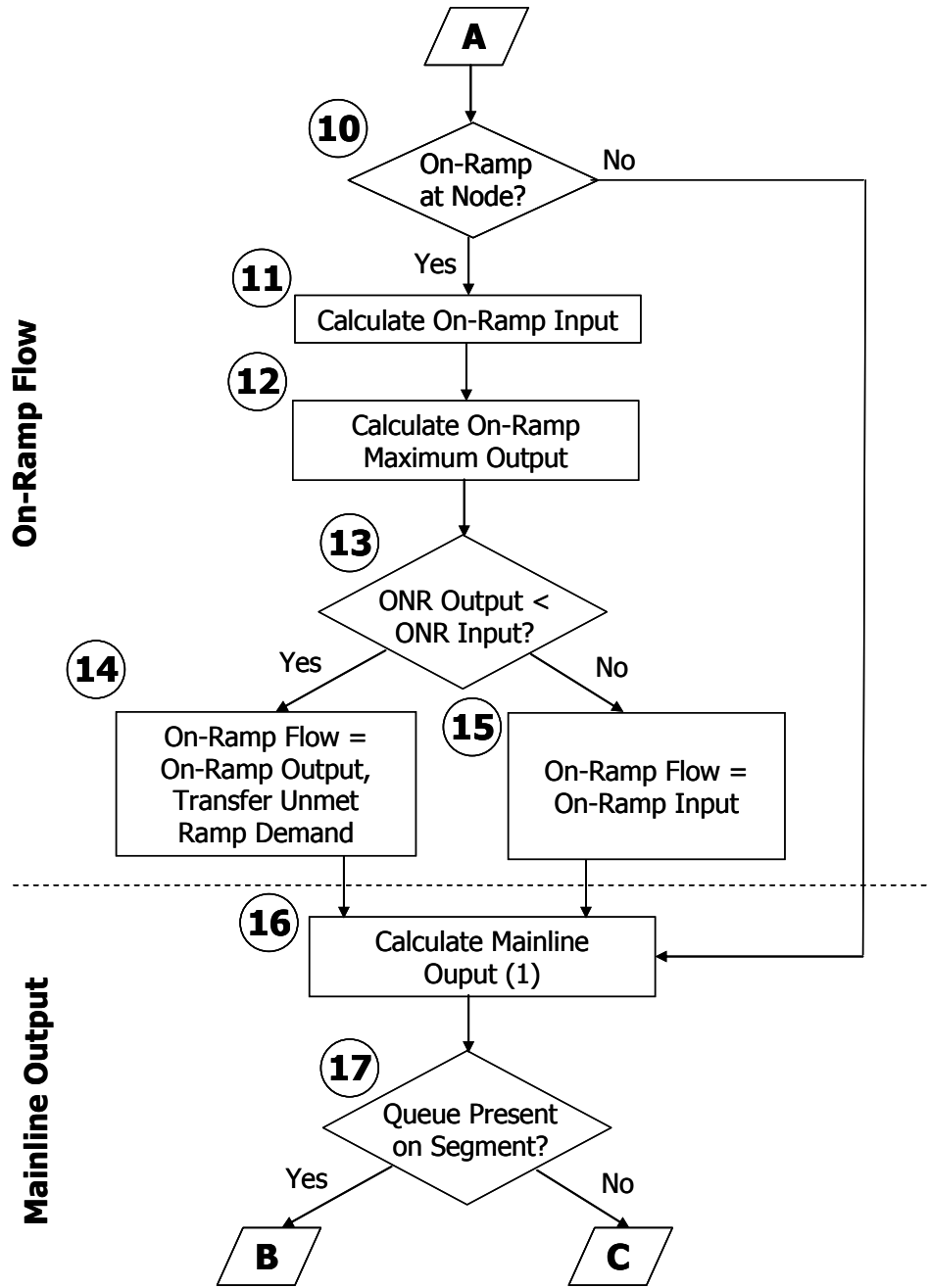


Exhibit 25-3 (cont'd.)
Oversaturated Analysis
Procedure

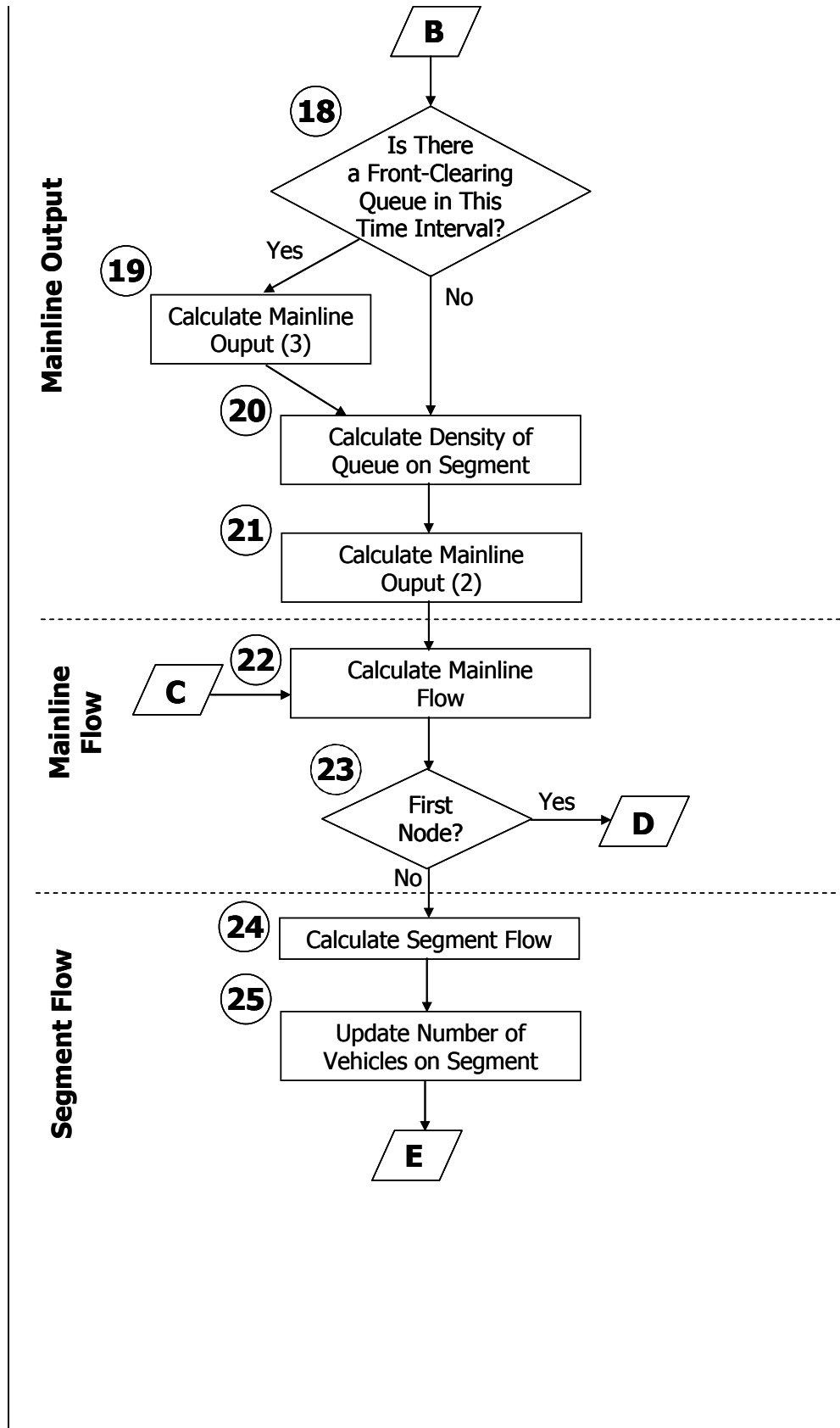
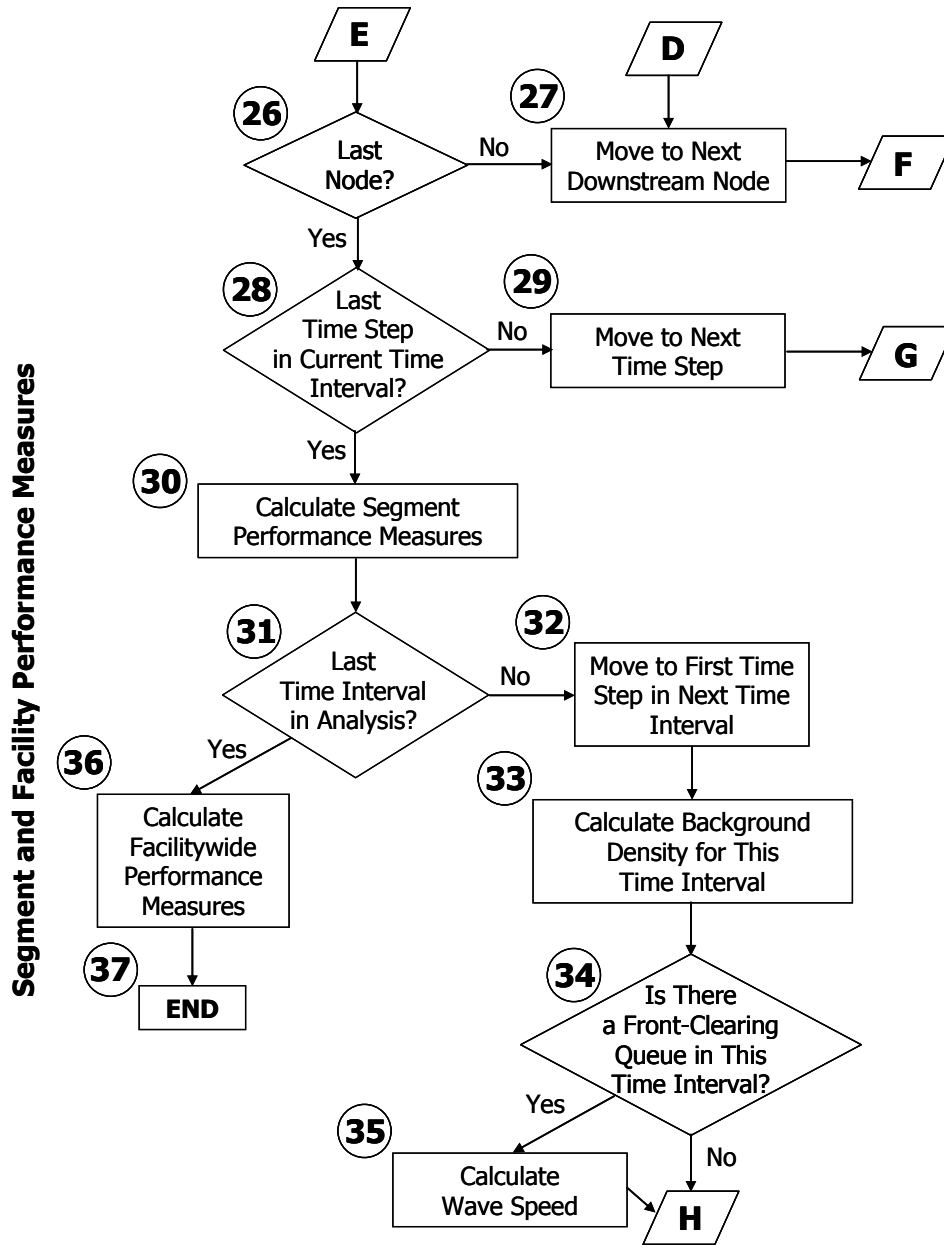


Exhibit 25-3 (cont'd.)
Oversaturated Analysis
Procedure



Segment Initialization: Exhibit 25-3, Steps 1–4

Steps 1–4 of the oversaturated procedure prepare the flow calculations for the first time step and specify return points for later time steps. To calculate the number of vehicles on each segment at the various time steps, the segments must contain the proper number of vehicles before the queuing analysis places unserved vehicles on segments. The initialization of each segment is described below. A simplified queuing analysis is initially performed to account for the effects of upstream bottlenecks. These bottlenecks meter traffic downstream of their location. The storage of unserved vehicles (those unable to enter the bottleneck) on upstream segments is performed in a later module. To obtain the proper number of vehicles on each segment, the expected demand *ED* is calculated. Expected demand is based on demands for and capacities of the

segment and includes the effects of all upstream segments. The expected demand is the flow of traffic expected to arrive at each segment if all queues were stacked vertically (i.e., no upstream effects of queues). In other words, all segments upstream of a bottleneck have expected demands equal to their actual demand. The expected demand of the bottleneck segment and all further downstream segments is calculated by assuming a capacity constraint at the bottleneck, which meters traffic to downstream segments. The expected demand ED is calculated for each segment with Equation 25-6:

Equation 25-6

$$ED(i, p) = \min[SC(i, p), ED(i - 1, p) + ONRD(i, p) - OFRD(i, p)]$$

The segment capacity SC applies to the length of the segment. With the expected demand calculated, the background density KB can be obtained for each segment by using the appropriate segment density estimation procedures in Chapters 12, 13, and 14. The background density is used to calculate the number of vehicles NV on each segment by using Equation 25-7. If there are unserved vehicles at the end of the preceding time interval, the unserved vehicles UV are transferred to the current time interval. Here, S refers to the final time step in the preceding time interval. The (0) term in NV represents the start of the first time step in time interval p . The corresponding term at the end of the time step is $NV(i, 1, p)$.

Equation 25-7

$$NV(i, 0, p) = KB(i, p) \times L(i) + UV(i, S, p - 1)$$

The number of vehicles calculated from the background density is the minimum number of vehicles that can be on the segment at any time. This constraint is a powerful check on the methodology because the existence of queues downstream cannot reduce this minimum. Rather, the segment can only store additional vehicles. The storage of unserved vehicles is determined in the segment flow calculation module later in this chapter.

Mainline Flow Calculations: Exhibit 25-3, Steps 9 and 16–23

The description of ramp flows follows the description of mainline flows. Thus, Steps 5–8 and 10–15 are skipped at this time to focus first on mainline flow computations. Because of skipping steps in the descriptions, some computations may include variables that have not been described but that have already been calculated in the flowchart.

Flows analyzed in oversaturated conditions are calculated for every time step and are expressed in terms of vehicles per time step. The procedure separately analyzes the flow across a node on the basis of the origin and destination of the flow across the node. The mainline flow is defined as the flow passing from upstream segment $i - 1$ to downstream segment i . It does not include the on-ramp flow. The flow to an off-ramp is the off-ramp flow. The flow from an on-ramp is the on-ramp flow. Each of these flows is shown in Exhibit 25-4 with the origin, destination, and relationship to segment i and node i .

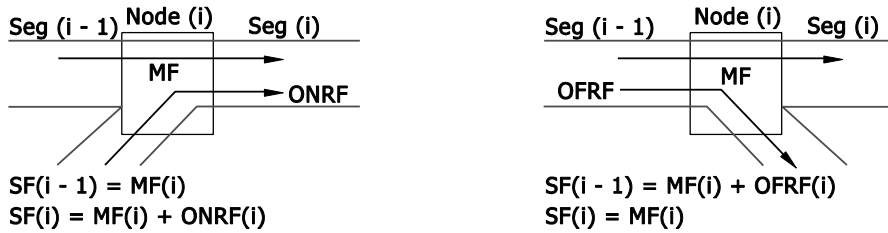


Exhibit 25-4
Definitions of Mainline and Segment Flows

The segment flow is the total output of a segment, as shown in Exhibit 25-4. Segment flows are calculated by determining the mainline and ramp flows. The mainline flow is calculated as the minimum of six constraints: mainline input (MI), $MO1$, $MO2$, $MO3$, upstream segment $i - 1$ capacity, and downstream segment i capacity, as explained next.

Mainline Input: Exhibit 25-3, Step 9

Mainline input MI is the number of vehicles that wish to travel through a node during the time step. The calculation includes (a) the effects of bottlenecks upstream of the analysis node, (b) the metering of traffic during queue accumulation, and (c) the presence of additional traffic during upstream queue discharge.

MI is calculated by taking the number of vehicles entering the node upstream of the analysis node, adding on-ramp flows or subtracting off-ramp flows, and adding the number of unserved vehicles on the upstream segment. Thus, MI is the maximum number of vehicles that wish to enter a node during a time step. MI is calculated by using Equation 25-8, where all values have units of vehicles per time step.

$$MI(i, t, o) = MF(i - 1, t, p) + ONRF(i - 1, t, p) - OFRF(i, t, p) + UV(i - 1, t - 1, p)$$

Equation 25-8

Mainline Output: Exhibit 25-3, Steps 16–21

The mainline output is the maximum number of vehicles that can exit a node, constrained by downstream bottlenecks or by merging on-ramp traffic. Different constraints on the output of a node result in three separate types of mainline outputs ($MO1$, $MO2$, and $MO3$).

Mainline Output 1, Ramp Flows: Exhibit 25-3, Step 16

$MO1$ is the constraint caused by the flow of vehicles from an on-ramp. The capacity of an on-ramp segment is shared by two competing flows. This on-ramp flow limits the flow from the mainline through this node. The total flow that can pass the node is estimated as the minimum of the segment i capacity and the mainline outputs from the preceding time step. The sharing of Lane 1 (shoulder lane) capacity is determined in the calculation of the on-ramp. $MO1$ is calculated by using Equation 25-9.

$$MO1 = \min \left\{ \begin{array}{l} SC(i, t, p) - ONRF(i, t, p) \\ MO2(i, t - 1, p) \\ MO3(i, t - 1, p) \end{array} \right.$$

Equation 25-9

Mainline Output 2, Segment Storage: Exhibit 25-3, Steps 20 and 21

The second constraint on the output of mainline flow through a node is caused by the growth of queues on a downstream segment. As a queue grows on a segment, it may eventually limit the flow into the current segment once the boundary of the queue reaches the upstream end of the segment. The boundary of the queue is treated as a shock wave. *MO2* is a limit on the flow exiting a node due to the presence of a queue on the downstream segment.

The *MO2* limitation is determined first by calculating the maximum number of vehicles allowed on a segment at a given queue density. The maximum flow that can enter a queued segment is the number of vehicles that leave the segment plus the difference between the maximum number of vehicles allowed on the segment and the number of vehicles already on the segment. The density of the queue is calculated by using Equation 25-10 for the linear density–flow relationship shown in Exhibit 25-2 earlier.

Equation 25-10

$$KQ(i, t, p) = KJ - [(KJ - KC) \times SF(i, t - 1, p)] / SC(i, p)$$

Once the queue density is computed, *MO2* can be computed by using Equation 25-11.

Equation 25-11

$$MO2(i, t, p) = SF(i, t - 1, p) - ONRF(i, t, p) + [KQ(i, t, p) \times L(i) - NV(i, t - 1, p)]$$

The performance of the downstream node is estimated by taking the performance during the preceding time step. This estimation remains valid when there are no interacting queues. When queues interact and the time steps are small enough, the error in the estimations is corrected in the next time step.

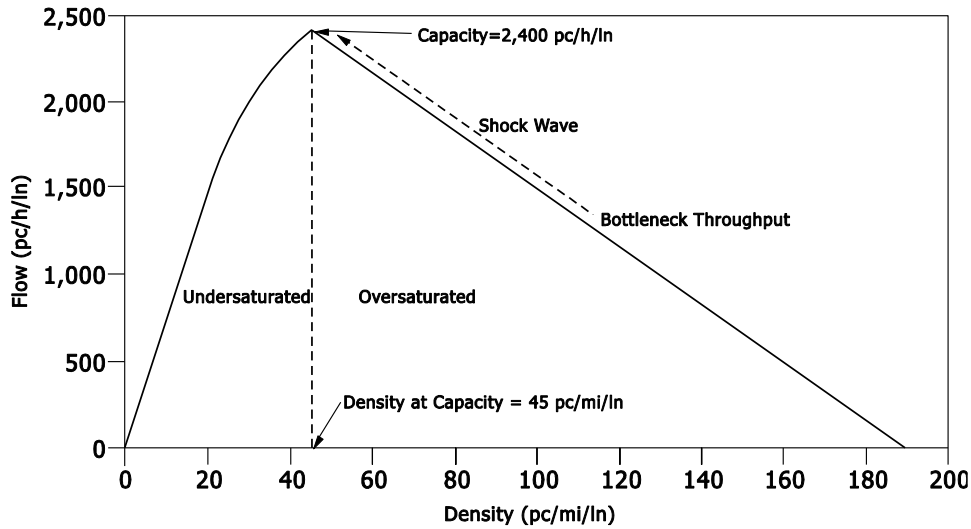
Mainline Output 3, Front-Clearing Queues: Exhibit 25-3, Steps 17–19

The final constraint on exiting mainline flows at a node is caused by downstream queues clearing from their downstream end. These front-clearing queues are typically caused by incidents in which there is a temporary reduction in capacity. A queue will clear from the front if two conditions are satisfied. First, the segment capacity (minus the on-ramp demand if present) for this time interval must be greater than the segment capacity (minus the ramp demand if present) in the preceding time interval. The second condition is that the segment capacity minus the ramp demand for this time interval must be greater than the segment demand for this time interval. A queue will clear from the front if both conditions in the following inequality (Equation 25-12) are met.

Equation 25-12

$$\begin{aligned} \text{If } [SC(i, p) - ONRD(i, p)] > [SC(i, p - 1) - ONRD(i, p - 1)] \\ \text{and } [SC(i, p) - ONRD(i, p)] > SD(i, p) \end{aligned}$$

A segment with a front-clearing queue will have the number of vehicles stored decrease during recovery, while the back of the queue position is unaffected. Thus, the clearing does not affect the segment throughput until the recovery wave has reached the upstream end of the front-clearing queue. The computational engine implementation is simplified by assuming the downstream segment is fully queued when the *MO3* constraint is applied. In the flow–density graph shown in Exhibit 25-5, the wave speed is estimated by the slope of the dashed line connecting the bottleneck throughput and the segment capacity points.



Note: Assumed FFS = 75 mi/h.

Exhibit 25-5
Flow-Density Function with a Shock Wave

The assumption of a linear flow-density function greatly simplifies the calculation of the wave speed. The bottleneck throughput value is not required to estimate the speed of the shock wave that travels along a known line. All that is required is the slope of the line, which is calculated with Equation 25-13.

$$WS(i, p) = SC(i, p) / [N(i, p) \times (KJ - KC)]$$

Equation 25-13

The wave speed is used to calculate the wave travel time *WTT*, which is the time it takes the front queue-clearing shock wave to traverse this segment. Dividing the wave speed *WS* by the segment length in miles gives *WTT*.

The recovery wave travel time is the time required for the conditions at the downstream end of the current segment to reach the upstream end of the current segment. To place a limit on the current node, the conditions at the downstream node are observed at a time in the past. This time is the wave travel time. This constraint on the current node is *MO3*. The calculation of *MO3* uses Equation 25-14 and Equation 25-15. If the wave travel time is not an integer number of time steps, then the weighted average performance of each variable is taken for the time steps nearest the wave travel time. This method is based on a process described elsewhere (5-7).

$$WTT = T \times L(i) / WS(i, p)$$

Equation 25-14

$$MO3(i, t, p) = \min \left\{ \begin{array}{l} MO1(i + 1, t - WTT, p) \\ MO2(i + 1, t - WTT, p) + OFRF(i + 1, t - WTT, p) \\ MO3(i + 1, t - WTT, p) + OFRF(i + 1, t - WTT, p) \\ SC(i, t - WTT, p) \\ SC(i + 1, t - WTT, p) + OFRF(i + 1, t - WTT, p) \\ - OFRF(i, t, p) \end{array} \right\}$$

Equation 25-15

Mainline Flow: Exhibit 25-3, Steps 22 and 23

The flow across a node is called the mainline flow *MF* and is the minimum of the following variables: *MI*, *MO1*, *MO2*, *MO3*, upstream segment *i - 1* capacity, and downstream segment *i* capacity, as shown in Equation 25-16.

Equation 25-16

$$MF(i, t, p) = \min \left\{ \begin{array}{l} MI(i, t, p) \\ MO1(i, t, p) \\ MO2(i, t, p) \\ MO3(i, t, p) \\ SC(i, t, p) \\ SC(i - 1, t, p) \end{array} \right\}$$

In addition to mainline flows, ramp flows must be analyzed. The presence of mainline queues also affects ramp flows.

On-Ramp Calculations: Exhibit 25-3, Steps 10–15

On-Ramp Input: Exhibit 25-3, Steps 10 and 11

The maximum on-ramp input *ONRI* is calculated by adding the on-ramp demand and the number of vehicles queued on the ramp. The queued vehicles are treated as unmet ramp demand that was not served in previous time steps. The on-ramp input is calculated with Equation 25-17.

Equation 25-17

$$ONRI(i, t, p) = ONRD(i, t, p) + ONRQ(i, t - 1, p)$$

On-Ramp Output: Exhibit 25-3, Step 12

The maximum on-ramp output *ONRO* is calculated on the basis of the mainline traffic through the node where the on-ramp is located. The on-ramp output is the minimum of two values. The first is segment *i* capacity minus *MI*, in the absence of downstream queues. Otherwise, the segment capacity is replaced by the throughput of the queue. This estimation implies that vehicles entering an on-ramp segment will fill Lanes 2 to *N* (where *N* is the number of lanes on the current segment) to capacity before entering Lane 1. This assumption is consistent with the estimation of *v*₁₂ from Chapter 14, Freeway Merge and Diverge Segments.

The second case occurs when the Lane 1 flow on segment *i* is greater than one-half of the Lane 1 capacity. At this point, the on-ramp maximum output is set to one-half of Lane 1 capacity. This output limitation implies that when the demands from the freeway and the on-ramp are very high, there will be forced one-to-one merging on the freeway from the freeway mainline and the on-ramp in Lane 1. An important characteristic of traffic behavior is that, in a forced merging situation, ramp and right-lane freeway vehicles will generally merge one on one, sharing the capacity of the rightmost freeway lane (8). In all cases, the on-ramp maximum output is also limited to the physical ramp road capacity and the ramp-metering rate, if present. The maximum on-ramp output is an important limitation on the ramp flow. Queuing occurs when the combined demand from the upstream segment and the on-ramp exceeds the throughput of the ramp segment. The queue can be located on the upstream segment, on the ramp, or on both and depends on the on-ramp maximum output. Equation 25-18 determines the value of the maximum on-ramp output.

$$\begin{aligned}
 & ONRO(i, t, p) \\
 = & \min \left\{ \max \left\{ \begin{array}{l} \min \left\{ \begin{array}{l} RM(i, t, p) \\ ONRC(i, t, p) \\ SC(i, t, p) \end{array} \right\} - MI(i, t, p) \\ \min \left\{ \begin{array}{l} MF(i + 1, t - 1, p) + ONRF(i, t - 1, p) \\ MO3(i, t - 1, p) + ONRF(i, t - 1, p) \end{array} \right\} \end{array} \right\} \right\}
 \end{aligned}$$

Equation 25-18

This model incorporates the maximum mainline output constraints from downstream queues, not just the segment capacity. This fact is significant because as a queue spills over an on-ramp segment, the flow through Lane 1 is constrained. This constraint, in turn, limits the flow that can enter Lane 1 from the on-ramp. The values of *MO2* and *MO3* for this time step are not yet known, so they are estimated from the preceding time step. This estimation is one rationale for using small time steps. If there is forced merging during the time step when the queue spills back over the current node, the on-ramp will discharge more than its share of vehicles (i.e., more than 50% of the Lane 1 flow). This situation will cause the mainline flow past node *i* to be underestimated. But during the next time step, the on-ramp flow will be at its correct flow rate, and a one-to-one sharing of Lane 1 will occur.

On-Ramp Flows, Queues, and Delays: Exhibit 25-3, Steps 13–15

Finally, the on-ramp flow is calculated on the basis of the on-ramp input and output values computed above. If the on-ramp input is less than the on-ramp output, then the on-ramp demand can be fully served in this time step and Equation 25-19 is used.

$$ONRF(i, t, p) = ONRI(i, t, p)$$

Equation 25-19

Otherwise, the ramp flow is constrained by the maximum on-ramp output, and Equation 25-20 is used.

$$ONRF(i, t, p) = ONRO(i, t, p)$$

Equation 25-20

In the latter case, the number of vehicles in the ramp queue is updated by using Equation 25-21.

$$ONRQ(i, t, p) = ONRI(i, t, p) - ONRO(i, t, p)$$

Equation 25-21

The total delay for on-ramp vehicles can be estimated by integrating the value of on-ramp queues over time. The methodology uses the discrete queue lengths estimated at the end of each interval $ONRQ(i, S, p)$ to produce overall ramp delays by time interval.

Off-Ramp Flow Calculation: Exhibit 25-3, Steps 5–8

The off-ramp flow is determined by calculating a diverge percentage on the basis of the segment and off-ramp demands. The diverge percentage varies only by time interval and remains constant for vehicles that are associated with a particular time interval. If there is an upstream queue, traffic may be metered to this off-ramp, which will cause a decrease in the off-ramp flow. When the vehicles that were metered arrive in the next time interval, they use the diverge

percentage associated with the preceding time interval. A deficit in flow, caused by traffic from an upstream queue meter, creates delays for vehicles destined to this off-ramp and other downstream destinations. The upstream segment flow is used because the procedure assumes a vehicle destined for an off-ramp is able to exit at the off-ramp once it enters the off-ramp segment. This deficit is calculated with Equation 25-22.

Equation 25-22

$$DEF(i, t, p) = \max \left\{ \left[\sum_{X=1}^{p-1} SD(i-1, X) - \sum_{X=1}^{p-1} \sum_{t=1}^T [MF(i-1, t, X) + ONRF(i-1, t, X)] \right], 0 \right\} + \sum_{t=1}^{t-1} [MF(i-1, t, p) + ONRF(i-1, t, p)]$$

If there is a deficit, then the off-ramp flow is calculated by using the deficit method. The deficit method is used differently in two specific situations. If the upstream mainline flow plus the flow from an on-ramp at the upstream node (if present) is less than the deficit for this time step, then the off-ramp flow is equal to the mainline and on-ramp flows times the off-ramp turning percentage in the preceding time interval, as indicated in Equation 25-23.

Equation 25-23

$$OFRF(i, t, p) = [MF(i-1, t, p) + ONRF(i-1, t, p)] \times \left[\frac{OFRD(i, p-1)}{SD(i-1, p-1)} \right]$$

However, if the deficit is less than the upstream mainline flow plus the on-ramp flow from an on-ramp at the upstream node (if present), then Equation 25-24 is used. This equation separates the flow into the remaining deficit flow and the balance of the arriving flow.

Equation 25-24

$$OFRF(i, t, p) = DEF(i, t, p) \times \left[\frac{OFRD(i, p-1)}{SD(i-1, p-1)} \right] + [MF(i-1, t, p) + ONRF(i-1, t, p) - DEF(i, t, p)] \times \left[\frac{OFRD(i, p)}{SD(i-1, p)} \right]$$

If there is no deficit, then the off-ramp flow is equal to the sum of the upstream mainline flow plus the on-ramp flow from an on-ramp at the upstream node (if present) multiplied by the off-ramp turning percentage for this time interval according to Equation 25-25.

Equation 25-25

$$OFRF(i, t, p) = [MF(i-1, t, p) + ONRF(i-1, t, p)] \times \left[\frac{OFRD(i, p)}{SD(i-1, p)} \right]$$

The procedure does not incorporate any delay or queue length computations for off-ramps.

Segment Flow Calculation: Exhibit 25-3, Steps 24 and 25

The segment flow is the number of vehicles that flow out of a segment during the current time step. These vehicles enter the current segment either to the mainline or to an off-ramp at the current node. The vehicles that entered the upstream segment may or may not have become queued within the segment. The segment flow *SF* is calculated with Equation 25-26.

Equation 25-26

$$SF(i-1, t, p) = MF(i, t, p) + OFRF(i, t, p)$$

The number of vehicles on each segment is calculated on the basis of the number of vehicles that were on the segment in the preceding time step, the number of vehicles that entered the segment in this time step, and the number of vehicles that leave the segment in this time step. Because the number of vehicles that leave a segment must be known, the number of vehicles on the current segment cannot be determined until the upstream segment is analyzed. The number of vehicles on each segment NV is calculated with Equation 25-27.

$$NV(i-1, t, p) = NV(i-1, t-1, p) + MF(i-1, t, p) + ONRF(i-1, t, p) - MF(i, t, p) - OFRF(i, t, p)$$

Equation 25-27

The number of unserved vehicles stored on a segment is calculated as the difference between the number of vehicles on the segment and the number of vehicles that would be on the segment at the background density. The number of unserved vehicles UV stored on a segment is calculated with Equation 25-28.

$$UV(i-1, t, p) = NV(i-1, t, p) - [KB(i-1, p) \times L(i-1)]$$

Equation 25-28

If the number of unserved vehicles is greater than zero, then a queue is present on the facility upstream of the node in question. The presence of a queue and congestion indicates that the node capacity is in queue discharge mode, which means the queue discharge capacity is reduced relative to the pre-breakdown capacity by a factor α . To account for this queue discharge effect, Equation 25-29 is applied to any active bottleneck along the facility if $UV(i-1, t, p) > 0.001$. This tolerance over an absolute value of zero is necessary to account for potential rounding errors in the procedure.

$$SC(i, t, p) = (1 - \alpha) \times SC(i, t, p)$$

Equation 25-29

SEGMENT AND RAMP PERFORMANCE MEASURES

In the final time step of a time interval, the segment flows are averaged over the time interval, and the performance measures for each segment are calculated. If there was no queue on a particular segment during the entire time interval, then the performance measures are calculated from the corresponding Chapter 12, 13, or 14 method for that segment. Because there are T time steps in an hour, the average segment flow rate in vehicles per hour in time interval p is calculated by using Equation 25-30.

$$SF(i, p) = \frac{T}{S} \sum_{t=1}^S SF(i, t, p)$$

Equation 25-30

If $T = 60$ (1-min time step) and $S = 15$ (interval = 15 min), then $T/S = 4$. If there was a queue on the current segment in any time step during the time interval, then the segment performance measures are calculated in three steps. First, the average number of vehicles NV over a time interval is calculated for each segment by using Equation 25-31.

$$NV(i, p) = \frac{1}{S} \sum_{t=1}^S NV(i, t, p)$$

Equation 25-31

Second, the average segment density K is calculated by taking the average number of vehicles NV for all time steps in the time interval and dividing it by the segment length, as shown by Equation 25-32.

Equation 25-32

$$K(i, p) = \frac{NV(i, p)}{L(i)}$$

Third, the average speed U on the current segment i during the current time interval p is calculated with Equation 25-33.

Equation 25-33

$$U(i, p) = \frac{SF(i, p)}{K(i, p)}$$

Additional segment performance measures can be derived from the basic measures shown in Equation 25-30 through Equation 25-33. Most prominent is segment delay, which can be computed as the difference in segment travel time at speed $U(i, p)$ and at the segment FFS.

The final segment performance measure is the length of the queue at the end of the time interval (i.e., step S in time interval p). The length of a queue Q on the segment, in feet, is calculated with Equation 25-34.

Equation 25-34

$$Q(i, p) = \frac{UV(i, S, p)}{\max[(KQ(i, S, p) - KB(i, p)), 1]} \times 5,280$$

OVERSATURATION ANALYSIS WITHIN MANAGED LANES

Whenever oversaturated conditions occur (as defined in Chapter 10) on freeway facilities that contain managed lanes, the freeway facilities methodology invokes the oversaturated analysis described in this chapter for both the general purpose and managed lane facilities. The analysis will be performed separately for each facility, meaning that the queues in either the general purpose or managed lanes do not interact with each other. For freeway facilities with managed lanes that do not have any access segments connecting the two lane groups, performing oversaturated analysis separately yields accurate performance measures for both the general purpose and managed lanes.

However, when access segments connect the two lane groups, no method currently exists to model the queue interaction between the two. In this situation, the queue spillback between the general purpose and managed lanes is modeled as a “vertical queue.” The vehicles that cannot enter the general purpose or managed lane facilities due to the presence of a queue do not translate into actual queuing on the origin lane group, as shown in Exhibit 25-6.

The freeway facilities methodology keeps track of vehicles that cannot enter the downstream segment (past the access point) in the form of a vertical queue, and it releases these vehicles as congestion dissipates. Note that there are two vertical queues for each access segment, one for vehicles traveling from the managed to the general purpose lanes, and the other for vehicles traveling from the general purpose to the managed lanes. Exhibit 25-6 shows an example of a vertical queue for the first situation. Note that the existence of a vertical queue does not lead to actual queuing on the managed lane.

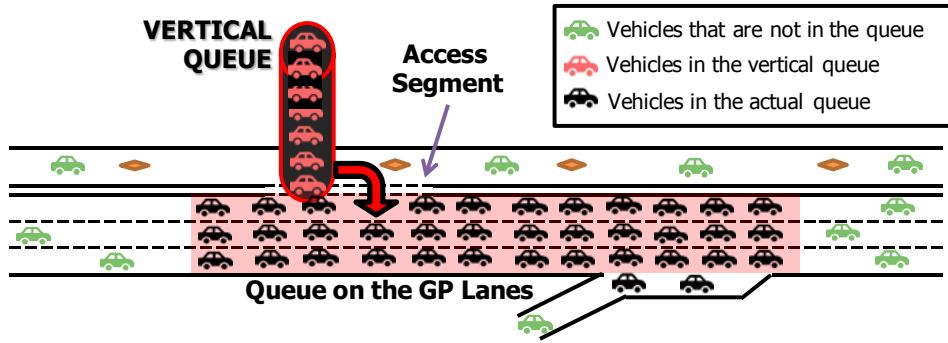


Exhibit 25-6
Vertical Queuing from a Managed Lane Due to Queue Presence on the General Purpose Lanes

Despite this simplification of queue spillback modeling, the methodology keeps track of the delays vehicles encounter in the vertical queues. The delay is computed as the number of vehicles stored in the vertical queue, multiplied by 15 min of delay in each analysis period. The delay of the vehicles originating from the managed lanes that are waiting in the vertical queue is estimated based on Equation 25-35.

$$D_{ML,vert} = N_{ML,vert} \times 0.25$$

Equation 25-35

where

$D_{ML,vert}$ = delay incurred by vehicles originating from the managed lanes waiting in the vertical queue for one 15-min analysis period (h) and

$N_{ML,vert}$ = average number of vehicles originating from the managed lanes that are waiting in the vertical queue in one analysis period (veh).

Similar to the vehicle delay in the managed lanes, the delay of vehicles originating from the general purpose lanes that are waiting in the vertical queue is estimated based on Equation 25-36.

$$D_{GP,vert} = N_{GP,vert} \times 0.25$$

Equation 25-36

where

$D_{GP,vert}$ = delay incurred by vehicles originating from the general purpose lanes waiting in the vertical queue for one 15-min analysis period (h) and

$N_{GP,vert}$ = average number of vehicles originating from the general purpose lanes that are waiting in the vertical queue in one analysis period (veh).

5. WORK ZONE ANALYSIS DETAILS

This section provides additional computational details for work zone analysis on freeway facilities. The analysis of work zones on basic segments on a facility is described in Chapter 10, Freeway Facilities Core Methodology; this section provides additional analysis details for work zones in merge, diverge, and weaving segments, as well as the analysis of directional crossover work zones. The information provided in this section is largely based on results from National Cooperative Highway Research Program Project 03-107 (9).

SPECIAL WORK ZONE CONFIGURATIONS

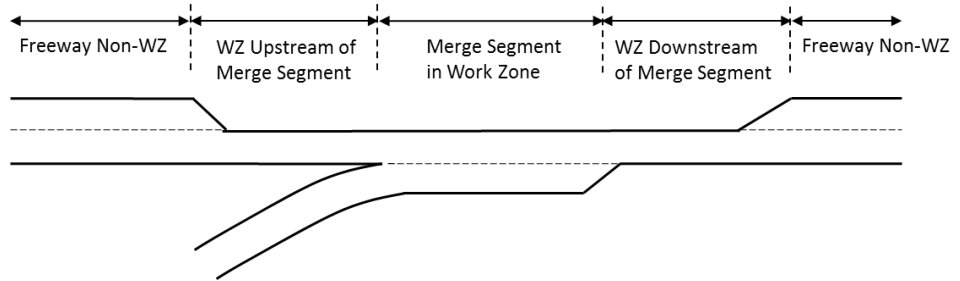
The queue discharge rate model predictions explained in Chapter 10 apply to basic freeway segments. These estimates should be adjusted for special freeway work zone configurations, such as merge segments, diverge segments, weaving segments, and work zones with directional crossovers. The relationships presented in this section were derived from field-calibrated microsimulation models for the special work zone configurations.

No data were available for the impacts of these work zone configurations on FFS, and so FFS estimates for these configurations should be used only when local data are not available. One exception is the FFS for a directional crossover, which should be estimated from the geometric design of the configuration, and is used as an input to the queue discharge rate estimation for that work zone configuration.

Work Zone Capacity Adjustments for Merge Segments

The proportion of work zone capacity (in reference to the basic work zone capacity calculated in Chapter 10) that is allocated to the mainline flow in a merge segment is presented separately for locations upstream and downstream of the special work zone activity segment. Exhibit 25-7 shows an example for a merge area within a construction zone.

Exhibit 25-7
On-Ramp Merge Diagram for 2-to-1 Freeway Work Zone Configuration



Note: WZ = work zone.

Exhibit 25-8 through Exhibit 25-12 give the proportion of work zone capacity allocated to mainline flow in merge, diverge, and directional crossover segments. For a weaving segment, a predictive model is presented following those exhibits. In the exhibits, only a subset of potential work zone configurations is presented,

as these are the only ones that were included in the simulation modeling effort in the original research.

Exhibit 25-8 presents the proportion of available capacity upstream of a merge area in a construction zone, as a function of work zone lane configurations, different levels of on-ramp input volumes, and lengths of the acceleration lane. Upstream of the work zone, the proportion of capacity available to the mainline movement decreases considerably as the on-ramp demand increases.

Work Zone Lane Configuration	On-Ramp Input Demand (pc/h)	Acceleration Lane Length (ft)							
		100	300	500	700	900	1,100	1,300	1,500
2 to 1	0	1.00	1.00	1.00	1.00	1.00	1.00	1.00	1.00
	250	1.00	0.86	0.86	0.86	0.86	0.86	0.86	0.86
	500	1.00	0.70	0.70	0.70	0.70	0.70	0.70	0.70
	750	1.00	0.53	0.53	0.53	0.53	0.53	0.53	0.53
	1,000	1.00	0.49	0.45	0.40	0.40	0.40	0.40	0.40
2 to 2	0	1.00	1.00	1.00	1.00	1.00	1.00	1.00	1.00
	250	1.00	0.92	0.92	0.92	0.92	0.92	0.92	0.92
	500	1.00	0.84	0.84	0.84	0.84	0.84	0.84	0.84
	750	1.00	0.75	0.75	0.75	0.75	0.75	0.75	0.75
	1,000	1.00	0.67	0.67	0.67	0.67	0.67	0.67	0.67
3 to 2	0	1.00	1.00	1.00	1.00	1.00	1.00	1.00	1.00
	250	1.00	0.95	0.95	0.95	0.95	0.95	0.95	0.95
	500	1.00	0.87	0.87	0.87	0.87	0.87	0.86	0.86
	750	1.00	0.78	0.78	0.78	0.78	0.78	0.78	0.78
	1,000	1.00	0.70	0.70	0.70	0.70	0.70	0.70	0.70
4 to 3	0	1.00	1.00	1.00	1.00	1.00	1.00	1.00	1.00
	250	1.00	0.97	0.97	0.98	0.98	0.98	0.98	0.98
	500	1.00	0.91	0.91	0.91	0.92	0.92	0.92	0.92
	750	1.00	0.85	0.85	0.85	0.86	0.86	0.86	0.86
	1,000	1.00	0.79	0.79	0.79	0.79	0.80	0.80	0.80

Exhibit 25-8
Proportion of Work Zone Queue Discharge Rate (Relative to the Basic Work Zone Capacity) Available for Mainline Flow Upstream of Merge Area

The capacity of the merge segment is the same as a basic work zone segment, with the caveat that the on-ramp flow consumes a portion of the mainline capacity. As a result, the available capacity upstream of the merge area leading into the work zone will be reduced once the queue spills back to the lane drop point. The proportions presented in Exhibit 25-8 approximate the conditions of a zipper merge configuration, with capacity divided approximately equally between the on-ramp and the right-most freeway mainline lane. In other words, the estimates correspond to a worst-case scenario for mainline flow in terms of available capacity, and a best-case scenario for the on-ramp movement. Note that the proportions for a 100-ft acceleration lane length are all 1.0 because on-ramp vehicles will experience difficulty entering the mainline lanes with the extremely short acceleration lane. These findings are based on results from microscopic simulation models of this configuration.

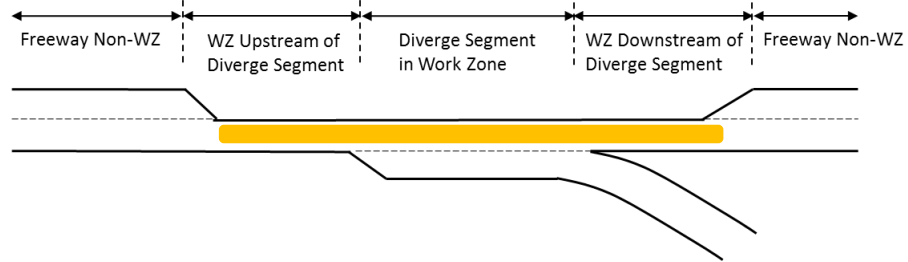
Research (9) shows that the throughput downstream of a merge area is approximately equal to the upstream queue discharge rate (before the merge) in most cases, with some configurations actually showing a marginal increase in flow. This slight increase occurs because additional demand from the on-ramp is able to more efficiently utilize gaps in the work zone queue discharge flow without the turbulence effects of the upstream lane drop. This effect was primarily observed for long acceleration lanes. However, for a more conservative

estimate of work zone operations, it is recommended not to consider this increase in flow downstream of the merge area regardless of lane configuration, on-ramp input volume, or acceleration lane length.

Work Zone Capacity Adjustments for Diverge Segments

Similar to merge segment analysis, the analysis of diverge segments distinguishes between the diverge segment portions of the work zone that are upstream and downstream of the diverge segment. Exhibit 25-9 shows an example for a diverge area within a construction zone.

Exhibit 25-9
Off-Ramp Diverge Diagram for a 2-to-1 Freeway Work Zone Configuration



Note: WZ = work zone.

Exhibit 25-10 presents the proportion of available capacity downstream of a diverge area for various freeway work zone lane configurations, different levels of off-ramp volume percentage, and deceleration lane lengths. Upstream of the diverge area, research (9) shows the available capacity is generally equivalent to that of a basic work zone segment. Therefore, it is recommended to apply a fixed adjustment of 1.00 upstream of the diverge area regardless of lane configuration, off-ramp volume percentage, or deceleration lane length.

At the downstream end, however, the proportion of available capacity for mainline volume decreases significantly as the off-ramp volume percentage increases. Analysts should expect work zone operations to improve downstream of a diverge segment (but still within the work zone) because some portion of traffic will exit the freeway, thereby decreasing the processed volume below the downstream capacity. However, if the deceleration lane lengths are shorter than 100 ft, exiting vehicles will need to slow down while still on the mainline to complete the exit maneuver. This speed reduction may drop mainline capacity by as much as 10% or more.

For a diverge area, the proportion of off-ramp demand that can be served in the work zone under congested conditions can be predicted as presented in Exhibit 25-11. This proportion is defined as the off-ramp observed volume divided by the off-ramp demand volume.

Work Zone Lane Configuration	Off-Ramp Volume Percentage	Deceleration Lane Length (ft)							
		100	300	500	700	900	1,100	1,300	1,500
2 to 1	0.0	1.00	1.00	1.00	1.00	1.00	1.00	1.00	1.00
	6.3	0.94	0.94	0.94	0.94	0.94	0.94	0.94	0.93
	12.5	0.87	0.88	0.88	0.88	0.88	0.88	0.87	0.87
	18.8	0.79	0.82	0.82	0.82	0.82	0.81	0.81	0.81
	25.0	0.72	0.76	0.76	0.75	0.75	0.75	0.75	0.75
2 to 2	0.0	1.00	1.00	1.00	1.00	1.00	1.00	1.00	1.00
	6.3	0.93	0.94	0.94	0.94	0.94	0.94	0.94	0.94
	12.5	0.84	0.87	0.87	0.87	0.87	0.87	0.87	0.87
	18.8	0.76	0.81	0.81	0.81	0.81	0.81	0.81	0.81
	25.0	0.68	0.75	0.75	0.75	0.75	0.75	0.75	0.75
3 to 2	0.0	1.00	1.00	1.00	1.00	1.00	1.00	1.00	1.00
	6.3	0.93	0.94	0.94	0.94	0.94	0.94	0.94	0.94
	12.5	0.86	0.87	0.87	0.87	0.87	0.87	0.87	0.87
	18.8	0.78	0.81	0.81	0.81	0.81	0.81	0.81	0.81
	25.0	0.69	0.74	0.74	0.74	0.74	0.74	0.74	0.74
4 to 3	0.0	1.00	1.00	1.00	1.00	1.00	1.00	1.00	1.00
	6.3	0.93	0.93	0.93	0.93	0.93	0.93	0.93	0.93
	12.5	0.86	0.87	0.87	0.87	0.87	0.87	0.87	0.87
	18.8	0.76	0.80	0.80	0.80	0.80	0.80	0.80	0.80
	25.0	0.64	0.73	0.73	0.73	0.73	0.73	0.73	0.73

Lane Configuration	Proportion of Off-Ramp Demand Served in Work Zone
2 to 1	0.39
2 to 2	0.82
3 to 2	0.53
4 to 3	0.60

Work Zone Capacity Adjustments for Crossover Segments

Exhibit 25-12 presents the proportion of work zone capacity available for a directional crossover for various crossover vehicle speeds. As shown in the exhibit, the crossover capacity is highly sensitive to average crossover speed. The variation in capacity for different work zone lane configurations was found to be negligible in crossovers. The estimates in Exhibit 25-12 should be applied as multipliers of the basic segment work zone capacity described above.

Lane Configuration	Crossover Average Speed (mi/h)		
	25	35	45
2 to 1			
3 to 2	0.83	0.90	0.94
4 to 3			

Work Zone Capacity Adjustments for Weaving Segments

In a weaving area, the proportion of work zone capacity available for mainline flow can be predicted by using a two-step model. In Step 1, the analyst estimates the maximum proportion of mainline flow that can be served through the work zone based on the work zone lane configuration and the volume ratio. This maximum becomes an upper bound on the actual estimated proportion, which is estimated in Step 2. In Step 2, the actual proportion of work zone capacity available for mainline flow is estimated based on the lane configuration, volume ratio, and auxiliary lane length. The final proportion of mainline flow that can be processed through the weaving segment is the lower of the two

Exhibit 25-10
Proportion of Work Zone Capacity Available for Mainline Flow Downstream of Diverge Area

Exhibit 25-11
Proportion of Off-Ramp Demand Served in Work Zone

Exhibit 25-12
Proportion of Available Work Zone Capacity for a Directional Crossover in the Work Zone

estimated proportions from Steps 1 and 2. The model intercept and coefficient values for Equation 25-37 and Equation 25-38 are presented in Exhibit 25-13.

Step 1: Estimate Maximum Mainline Allocation Proportion

Equation 25-37

$$MaxProportion = \text{Intercept} + \beta_1(2\text{-to-1}) + \beta_2(2\text{-to-2}) + \beta_3(3\text{-to-2}) + \beta_4(4\text{-to-3}) + \beta_5(VR)$$

where

MaxProportion = maximum proportion of work zone capacity available for mainline flow at the weave area (decimal),

Intercept = model intercept,

β_1 = model coefficient for 2-to-1 lane closures,

2-to-1 = indicator variable that is 1 when the work zone has a 2-to-1 configuration and 0 otherwise,

β_2 = model coefficient for 2-to-2 lane closures,

2-to-2 = indicator variable that is 1 when the work zone has a 2-to-2 configuration and 0 otherwise,

β_3 = model coefficient for 3-to-2 lane closures,

3-to-2 = indicator variable that is 1 when the work zone has a 3-to-2 configuration and 0 otherwise,

β_4 = model coefficient for 4-to-3 lane closures,

4-to-3 = indicator variable that is 1 when the work zone has a 4-to-3 configuration and 0 otherwise,

β_5 = model coefficient for volume ratio, and

VR = volume ratio = weave volume/total volume.

Step 2: Predict Mainline Proportion

Equation 25-38

$$\text{Proportion} = \text{Intercept} + \beta_1(2\text{-to-1}) + \beta_2(2\text{-to-2}) + \beta_3(3\text{-to-2}) + \beta_4(4\text{-to-3}) + \beta_5(VR) + \beta_6(AuxLength)$$

where

Proportion = proportion of work zone capacity available for mainline flow (decimal),

β_6 = model coefficient for auxiliary lane length,

AuxLength = auxiliary lane length (ft), and

all other variables are as defined previously.

The off-ramp demand volume proportion *Prop(off-ramp)* in the weaving area is estimated from Equation 25-39, with the intercept and model coefficients given in Exhibit 25-14, and all other variables as defined previously.

Equation 25-39

$$Prop(off-ramp) = \text{Intercept} + \beta_1(2\text{-to-1}) + \beta_2(2\text{-to-2}) + \beta_3(3\text{-to-2}) + \beta_4(4\text{-to-3}) + \beta_5(VR)$$

Model	Model Term	Coefficient	
Step 1: Maximum Proportion	Intercept	1.0023	
	Upstream	β_1	-0.1197
		β_2	0.0105
		β_3	0.0085
		β_4	0.0000
		β_5	-0.3048
	Downstream	Intercept	1.0573
		β_1	0.1307
		β_2	-0.0623
		β_3	0.0494
β_4		0.0000	
Step 2: Predicted Proportion	Upstream	Intercept	0.8491
		β_1	-0.0665
		β_2	0.0061
		β_3	0.0050
		β_4	0.0000
	β_5	-0.4687	
	β_6	9.0956×10^{-5}	
	Downstream	Intercept	0.8962
		β_1	0.2702
		β_2	0.0535
β_3		0.1073	
β_4		0.0000	
β_5	-0.9694		
β_6	30.5253×10^{-5}		

Model	Model Term	Coefficient
Off-Ramp Volume Proportion	Intercept	0.6162
	β_1	-0.2201
	β_2	0.2082
	β_3	-0.0551
	β_4	0.0000
β_5	0.0850	

Exhibit 25-13

Model Coefficients for Estimating the Proportion of Work Zone Capacity in a Weaving Segment

Exhibit 25-14

Model Coefficients for Estimating the Proportion of Off-Ramp Volume Served in the Weaving Area

6. PLANNING-LEVEL METHODOLOGY FOR FREEWAY FACILITIES

This section presents a planning-level approach for freeway facility analysis that is compatible with the operational method presented in Chapter 10, Freeway Facilities Core Methodology. The planning level-approach is specifically constructed to

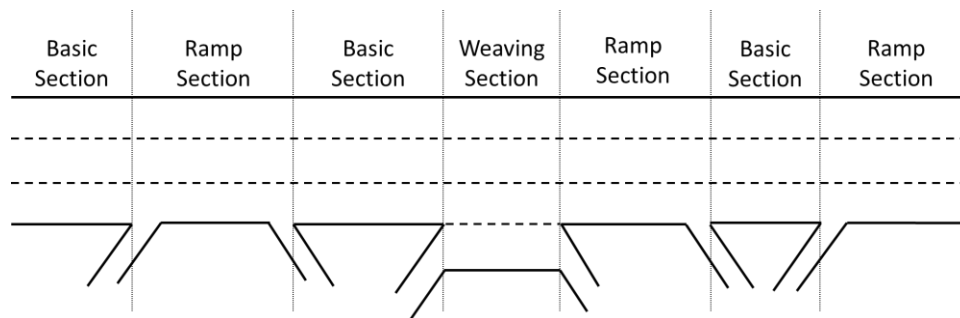
1. Use default values for as many of the operational parameters as practical;
2. Omit the need to enter detailed data about segment attributes (e.g., acceleration lane length and detailed weaving section geometry);
3. Aggregate the analysis to a coarser spatial representation, reporting at the freeway section level instead of the HCM segment level; and
4. Enable HCM users to manually carry out the analysis for a single peak hour without an extensive computational burden.

The method covers both undersaturated and oversaturated conditions and produces estimates of travel time, speed, density, and level of service (LOS). The underlying methodology relies on developing a relationship between *delay rate* per unit distance on a basic freeway segment, and the demand-to-capacity ratio. For weaving segments, capacity adjustment factors (CAFs) are developed based on the volume ratio and segment length. By using these factors, demand-to-capacity ratios on weaving segments can be adjusted, and the segment is subsequently treated similarly to a basic freeway segment. The capacities of merge and diverge segments are determined from the demand level, FFS, and space mean speed. CAFs are subsequently calculated for those segments, and their demand-to-capacity ratios are adjusted accordingly.

INPUT REQUIREMENTS

Input variables are characterized into global and section inputs. Sections are defined to occur between points where either demand or capacity changes, as shown in Exhibit 25-15.

Exhibit 25-15
Schematics of Freeway Sections



For instance, the first section in Exhibit 25-15 (starting from the left) is a basic freeway section. This section is followed by an on-ramp, and the demand level changes. Capacity and demand remain unchanged until the first off-ramp. Consequently, the second freeway section in Exhibit 25-15 is defined as a ramp section. The next section that follows is a basic freeway section. It is followed by

a weaving section (this section is a weaving section due to the presence of an auxiliary lane). The weaving section is followed by another ramp section (due to an off-ramp), a basic section, and finally a ramp section (due to an on-ramp). Introduction of freeway sections facilitates user input and is more compatible with links in travel demand models as well as modern digital data sources.

In the operational freeway facilities method, the influence area of an on-ramp or off-ramp is typically limited to a length of 1,500 ft. In the planning method, ramp sections can be longer. For cases where a ramp section length exceeds 2 mi, it is recommended to divide the section into multiple sections to avoid having the lower ramp section capacity apply for a very long distance.

Global inputs include information about the facility of interest and are applicable to all sections across all analysis periods. These inputs include

1. Free-flow speed (S_{FFS}),
2. Peak hour factor (PHF),
3. Percentage heavy vehicles ($\%HV$),
4. General terrain type for truck passenger-car equivalent (PCE) conversion,
5. K -factor [to convert directional annual average daily traffic (AADT) to peak hour flows], and
6. Traffic growth factor (f_{ig}).

The equation used to estimate section speeds in this planning method (Equation 25-45) is fully consistent with the basic freeway segment speed-flow models presented in Chapter 12, Basic Freeway and Multilane Highway Segments. Section inputs cover information that is applicable to a given section across all analysis periods and that may vary from one section to another as a function of

1. Section type (basic, weave, ramp),
2. Section length L (mi),
3. Section number of lanes, and
4. Section directional AADT.

This information, along with the global inputs, is used to calculate the free-flow travel rate (the inverse of FFS), CAFs for weave and ramp sections, adjusted lane capacity (the product of base capacity and CAF), and section capacity (the product of adjusted lane capacity and number of lanes). The planning methodology follows five basic steps:

1. Demand-level calculations;
2. Section capacity calculations and adjustments;
3. Delay rate estimation;
4. Average travel time, speed, and density calculations; and
5. Level of service.

All steps are described in detail below.

STEP 1: DEMAND-LEVEL CALCULATIONS

The demand level for each section is determined from the entering demand, exiting demand, and carryover demand from a previous analysis period (in the case of oversaturated conditions).

The methodology uses the directional average annual daily traffic on section i $AADT_i$, K -factor, traffic growth factor f_{tg} , and peak hour factor PHF during each 15-min analysis period t in the peak hour to compute the demand inflow and outflow $V_{i,t}$ as shown in Equation 25-40:

Equation 25-40

$$V_{i,t} = \begin{cases} AADT_i \times k \times f_{tg} & t = 1, 3 \\ AADT_i \times k \times \left(\frac{1}{PHF}\right) \times f_{tg} & t = 2 \\ AADT_i \times k \times \left(2 - \frac{1}{PHF}\right) \times f_{tg} & t = 4 \end{cases}$$

where all parameters were defined previously.

All demand inputs should be in units of passenger cars per hour per lane (pc/h/ln). If demands are given in units of vehicles per hour per lane (veh/h/ln), they need to be converted with Equation 25-41.

Equation 25-41

$$q_{i,t} = \frac{V_{i,t}}{f_{HV}}$$

where

$q_{i,t}$ = demand flow rate in PCEs (pc/h),

$V_{i,t}$ = demand flow rate in vehicles per hour (veh/h), and

f_{HV} = adjustment factor for presence of heavy vehicles in traffic stream.

Just as in the operational method, all heavy vehicles are classified as single-unit trucks (SUTs) or tractor-trailers (TTs). Recreational vehicles and buses are treated as SUTs. The heavy-vehicle adjustment factor f_{HV} is computed from the combination of the two heavy vehicle classes, which are added to get an overall truck percentage P_T , as shown by Equation 25-42.

Equation 25-42

$$f_{HV} = \frac{1}{1 + P_T(E_T - 1)}$$

where

f_{HV} = heavy-vehicle adjustment factor (decimal),

P_T = proportion of SUT and TTs in traffic stream (decimal), and

E_T = PCE of one heavy vehicle in the traffic stream (PCE).

The values for E_T are 2.0 for level terrain and 3.0 for rolling terrain. For specific grades, Chapter 12 provides other heavy-vehicle equivalency factors.

The converted demand flow rates $q_{i,t}$ can represent both inflow demand and outflow demand. For the first facility section and all on-ramps, $q_{i,t}$ represents inflow demand and is denoted by $(q_{i,z})_{in}$. For all off-ramps, $q_{i,t}$ represents outflow demand and is represented by $(q_{i,z})_{out}$.

Demand level $d_{i,t}$ (in passenger cars per hour) on section i in analysis period t is computed as the demand level in section $i - 1$, plus the inflow at section i during analysis period t , minus the outflow at the same section at analysis period t , plus any carryover demand $d'_{i,t-1}$ in section i from the previous analysis period $t - 1$. The relationship is as shown in Equation 25-43.

$$d_{i,t} = d_{i-1,t} + (q_{i,t})_{in} - (q_{i,t})_{out} + d'_{i,t-1}$$

Equation 25-43

where all variables are as defined previously.

The carryover demand $d'_{i,t-1}$ on section i at analysis period t is the difference between the section demand and capacity, as given by Equation 25-44.

$$d'_{i,t} = \max(d_{i,t} - c_i, 0)$$

Equation 25-44

The carryover demand is also used as an indication of a queue on the section. Note that in this approach, queues are stacked vertically and do not spill back into an upstream link. The section queue length is estimated by dividing the difference in lane demand and capacity by the density. Essentially, it provides an estimate for how long the queue would spill back at the given density, assuming a fixed number of lanes upstream of the bottleneck.

STEP 2: SECTION CAPACITY CALCULATIONS AND ADJUSTMENTS

The capacity of basic freeway sections is found by using the FFS and the percentage of heavy vehicles on the facility, as shown by Equation 25-45.

$$c_i = 2,200 + 10 \times [\min(70, S_{FFS}) - 50]$$

Equation 25-45

where c_i is the capacity of freeway section i (pc/h/ln) and S_{FFS} is the facility's free-flow speed (mi/h).

Equation 25-45 provides capacity values for basic freeway sections. This capacity must be adjusted for weaving, merge, diverge, and ramp sections, as described next.

Capacity Adjustments for Weaving Sections

As mentioned above, the planning method is derived from the basic freeway segment speed-flow model to estimate a section's delay rate and travel speed. When applied to weaving sections, an adjustment to capacity is required to account for the generally lower capacity in weaving segments. This capacity adjustment factor CAF_{weave} can be estimated with Equation 25-46.

$$CAF_{weave} = \min(0.884 - 0.0752V_r + 0.0000243L_s, 1)$$

Equation 25-46

where

CAF_{weave} = capacity adjustment factor used for a weaving segment
($0 \leq CAF_{weave} \leq 1.0$) (decimal),

V_r = ratio of weaving demand flow rate to total demand flow rate in the weaving segment (decimal), and

L_s = weaving segment length (mi).

Through this capacity adjustment, the basic section method can be extended to weaving sections, as described elsewhere (10). The process for estimating

CAF_{weave} is based on a representative weaving section with the following characteristics (see Chapter 13 for additional details):

- Minimum number of lane changes that must be made by a single weaving vehicle from the on-ramp to the freeway: $LC(RF) = 1$,
- Minimum number of lane changes that must be made by a single weaving vehicle from the freeway to the off-ramp: $LC(FR) = 1$,
- Minimum number of lane changes that must be made by a ramp-to-ramp vehicle to complete a weaving maneuver: $LC(RR) = 0$, and
- Number of lanes from which a weaving maneuver may be made with one or no lane changes: $N(WL) = 2$.

Adjustments for Ramp Sections

Research shows an average CAF of 0.9 can be used for ramp sections with an on-ramp or off-ramp (10, 11). It is recognized that known bottlenecks may have significantly reduced capacities that require a lower CAF. Further calibration of the CAF by the analyst is strongly encouraged when applying this method to on-ramp sections with known capacity constraints and congestion impacts. Analyst calibration of this factor is also possible for off-ramp sections.

STEP 3: DELAY RATE ESTIMATION

The planning-level approach estimates the delay rate per unit distance as a function of a section’s demand-to-capacity ratio. The delay rate is the difference between the actual and free-flow travel time per unit distance. For example, if a facility’s space mean speed is 60 mi/h relative to an FFS of 75 mi/h for a 0.5-mi segment, then the free-flow travel time is 0.4 min, and the actual travel time is 0.5 min. The delay rate per mile is the difference of those travel times divided by the segment length, which gives a delay rate of 0.2 min/mi. The calculation of the delay rate needs to be performed differently for undersaturated and oversaturated conditions, as described next.

Undersaturated Conditions

For undersaturated conditions, the basic freeway segment speed-flow model in Chapter 12 can be used to estimate delay rates. However, for a planning-level analysis, it is desirable to further simplify the estimation of delay rate to be a function of inputs readily available in a planning context. The delay rate $\Delta_{RU_{i,t}}$ (in minutes per mile) for segment i in time period t as a function of the demand-to-capacity ratio $d_{i,t}/c_i$ is given by Equation 25-47.

Equation 25-47

$$\Delta_{RU_{i,t}} = \begin{cases} 0 & \frac{d_{i,t}}{c_i} < E \\ A \left(\frac{d_{i,t}}{c_i}\right)^3 + B \left(\frac{d_{i,t}}{c_i}\right)^2 + C \left(\frac{d_{i,t}}{c_i}\right) + D & E \leq \frac{d_{i,t}}{c_i} \leq 1 \end{cases}$$

where A, B, C, D , and E are parameters given in Exhibit 25-16 and all other variables are as defined previously.

Free-Flow Speed (mi/h)	A	B	C	D	E
75	68.99	-77.97	34.04	-5.82	0.44
70	71.24	-85.48	35.58	-5.44	0.52
65	92.45	-127.33	56.34	-8.00	0.62
60	121.35	-184.84	83.21	-9.33	0.72
55	156.43	-248.99	99.20	-0.12	0.82

Exhibit 25-16
Parameter Values for
Undersaturated Model

Oversaturated Conditions

For oversaturated conditions, the additional delay rate is approximated assuming uniform arrival and departures at the bottleneck location. With the demand exceeding capacity, any demand that cannot be served through the bottleneck must be stored upstream of the bottleneck in a queue. The *additional* oversaturation delay rate $\Delta_{RO_{i,t}}$ (in minutes per mile) for segment *i* at analysis period *t*, over a 15-min (900-s) analysis period, is obtained by Equation 25-48.

$$\Delta_{RO_{i,t}} = \frac{450}{L} \left[\max \left(\frac{d_{i,t}}{c_i} - 1.0 \right) \right]$$

Equation 25-48

where all variables are as previously defined.

STEP 4: AVERAGE TRAVEL TIME, SPEED, AND DENSITY CALCULATIONS

After the delay rate is determined, the travel rate is computed by summing the delay rate and travel rate under free-flow conditions, as shown by Equation 25-49.

$$TR_{i,t} = \Delta_{RU_{i,t}} + \Delta_{RO_{i,t}} + TR_{FFS}$$

Equation 25-49

where $TR_{i,t}$ is the travel rate on segment *i* in analysis period *t* (min/mi), TR_{FFS} is the travel rate under free-flow conditions (min/mi), and all other parameters are as previously defined.

The section travel time is then computed by multiplying the travel rate and segment length, as shown by Equation 25-50.

$$T_{i,t} = TR_{i,t} \times L_i$$

Equation 25-50

where $T_{i,t}$ is the travel time on segment *i* in analysis period *t* (min/mi), $TR_{i,t}$ is the travel rate on segment *i* in analysis period *t* (min/mi), and L_i is the length of section *i* (mi).

The average speed $S_{i,t}$ (in miles per hour) on section *i* in analysis period *t* is computed by using Equation 25-51.

$$S_{i,t} = \frac{L_i}{T_{i,t}}$$

Equation 25-51

Finally, the density is calculated as shown by Equation 25-52.

$$D_{i,t} = \frac{d_{i,t}}{S_{i,t}}$$

Equation 25-52

where $D_{i,t}$ is density on section *i* in analysis period *t* (pc/mi), $d_{i,t}$ is section demand (pc/h), and $S_{i,t}$ is speed (mi/h).

Thus, the planning-level method provides a facility performance summary that includes whether the facility is undersaturated or oversaturated, the total facility travel time, the space mean speed, the average facility density, and the total queue length.

STEP 5: LEVEL OF SERVICE

With the density obtained in Step 4, LOS can be estimated for urban or rural facilities following the thresholds in Chapter 10.

The LOS criteria for urban and rural freeway facilities are repeated in Exhibit 25-17. Urban LOS thresholds are the same density-based criteria used for basic freeway segments. Studies on LOS perception by rural travelers indicate lower-density thresholds than those of their urban freeway counterparts. The average LOS applies to each 15-min time period.

Exhibit 25-17
LOS Criteria for Urban and Rural Freeway Facilities

LOS	Urban Freeway Facility Density (pc/mi/ln)	Rural Freeway Facility Density (pc/mi/ln)
A	≤11	≤6
B	>11–18	>6–14
C	>18–26	>14–22
D	>26–35	>22–29
E	>35–45	>29–39
F	>45 or any component section v_d/c ratio > 1.00	>39 or any component section v_d/c ratio >1.00

7. MIXED-FLOW MODEL FOR COMPOSITE GRADES

This section presents the application of the mixed-flow model in the case of composite grades. The procedure builds on the single-grade methodology described in Chapter 26, *Freeway and Highway Segments: Supplemental*, and uses the same basic set of equations. The procedure computes LOS, capacity, speed, and density for each segment and for the composite grade as a whole. Many of the equations in this section are identical to those presented in Chapter 26, although they have different equation numbers. The major difference with composite grades is that the analyst must compute the spot travel rates or spot speeds at the start and end of each segment on the composite grade as an input to the analysis of the next grade segment.

OVERVIEW OF THE METHODOLOGY

The methodology assumes the composite grade both begins and ends with a long, level segment. The example shown in Exhibit 25-18 has five segments.

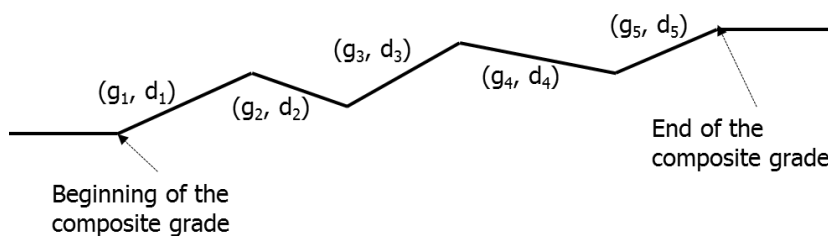


Exhibit 25-18
Schematic of a Composite Grade

Exhibit 25-19 presents the methodology flowchart. The remainder of this section provides the computational details for each step in the process.

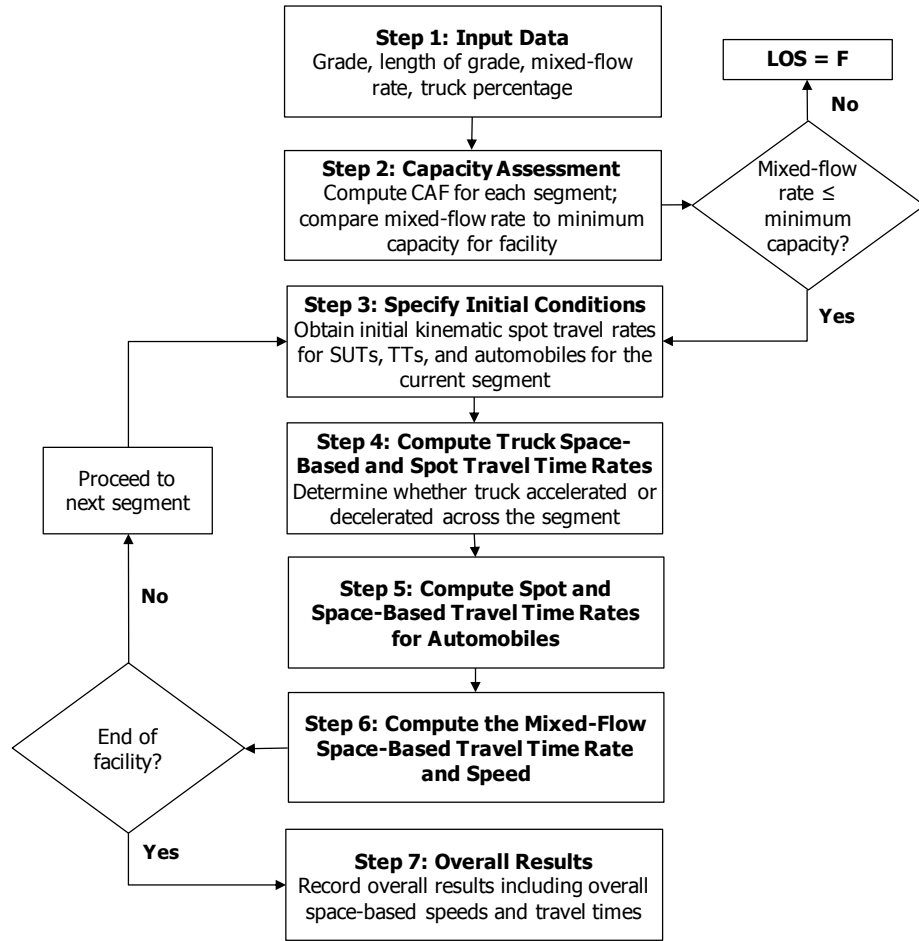
STEP 1: INPUT DATA

The user must supply the length d_j (mi) and the grade g_j (decimal) for each segment j , including the tangent segment immediately preceding the composite grade. In addition, the auto-only free-flow speed FFS (mi/h), peak hour factor PHF (decimal), the flow rate of mixed traffic v_{mix} (veh/h/ln), and the fraction of SUTs and TTs in the traffic stream must be specified for the facility as a whole.

STEP 2: CAPACITY ASSESSMENT

Before the composite grade is examined in detail, the capacity of the individual segments j is determined. A mixed-flow capacity adjustment factor $CAF_{mix,j}$ converts auto-only capacities into mixed-traffic-stream capacities. It is computed with Equation 25-53. The third term in this equation changes for each segment.

Exhibit 25-19
Mixed-Flow Methodology
Overview



Equation 25-53

$$CAF_{mix,j} = CAF_{ao} - CAF_{T,mix} - CAF_{g,mix,j}$$

where

$CAF_{mix,j}$ = mixed-flow capacity adjustment factor for segment j (decimal),

CAF_{ao} = capacity adjustment factor for the auto-only case (e.g., due to weather or incidents) (decimal),

$CAF_{T,mix}$ = capacity adjustment factor for the percentage of trucks in mixed-flow conditions (decimal), and

$CAF_{g,mix,j}$ = capacity adjustment factor for grade for segment j in mixed-flow conditions (decimal).

CAF for the Auto-Only Case

Because CAF_{ao} is used to convert auto-only capacities into mixed-traffic capacities, it defaults to a value of 1.0 unless other capacity adjustments are in effect (e.g., weather, incidents, driver population factor).

CAF for Truck Percentage

The CAF for truck percentage $CAF_{T,mix}$ is computed with Equation 25-54.

$$CAF_{T,mix} = 0.53 \times P_T^{0.72}$$

Equation 25-54

where P_T is the total percentage of SUTs and TTs in the traffic stream (decimal).

CAF for Grade Effect

The CAF for grade effect $CAF_{g,mix}$ accounts for the grade severity, grade length, and truck presence. It is computed by using Equation 25-55 with Equation 25-56.

$$CAF_{g,mix} = \rho_{g,mix} \times \max[0, 0.69 \times (e^{12.9g_j} - 1)] \times \max[0, 1.72 \times (1 - 1.71e^{-3.16d_j})]$$

Equation 25-55

with

$$\rho_{g,mix} = \begin{cases} 8 \times P_T & P_T < 0.01 \\ 0.126 - 0.03P_T & \text{otherwise} \end{cases}$$

Equation 25-56

where

$\rho_{g,mix}$ = coefficient for grade term in the mixed-flow CAF equation (decimal),

P_T = total truck percentage (decimal),

g_j = grade of segment j (decimal), and

d_j = length of segment j (mi).

Once $CAF_{mix,j}$ is computed, the mixed-flow capacity for each segment j is calculated with Equation 25-57.

$$C_{mix,j} = C_{ao} \times CAF_{mix,j}$$

Equation 25-57

where

$C_{mix,j}$ = mixed-flow capacity for segment j (veh/h/ln);

C_{ao} = auto-only capacity for the given FFS, from Exhibit 12-6 (pc/h/ln); and

$CAF_{mix,j}$ = mixed-flow capacity adjustment factor for segment j (decimal).

The procedure identifies the smallest of these capacities and designates it as C_{mix} . It also notes the segment that produces this capacity as j_c . The capacity C_{mix} is checked against the mixed-flow rate v_{mix} to check if $v_{mix} \geq C_{mix}$. If this condition occurs, the system is deemed to be oversaturated, LOS F is reported, and no further analysis is carried out. However, if $v_{mix} < C_{mix}$ the procedure continues.

STEP 3: SPECIFY INITIAL CONDITIONS

Starting with Step 3, the methodology analyzes each segment in sequence. Steps 3 through 6 are repeated for each segment until the final segment on the composite grade is reached. The main focus is on computing travel times and speeds for SUTs, TTs, and autos.

Step 3 specifies the initial kinematics-based spot speeds for SUTs and TTs. The effects of the traffic interaction terms are omitted for the time being. The focus is on the kinematic behavior of the trucks as they ascend and descend the individual grades. For the first segment, the initial kinematic spot speed is the speed for SUTs and TTs on the long, level segment that precedes the composite grade. For all subsequent segments, it is the kinematic spot speed at the end of the previous segment. The kinematic spot speeds are speeds without traffic interaction, which will be added to the final kinematic spot speeds to obtain final spot speeds of each segment.

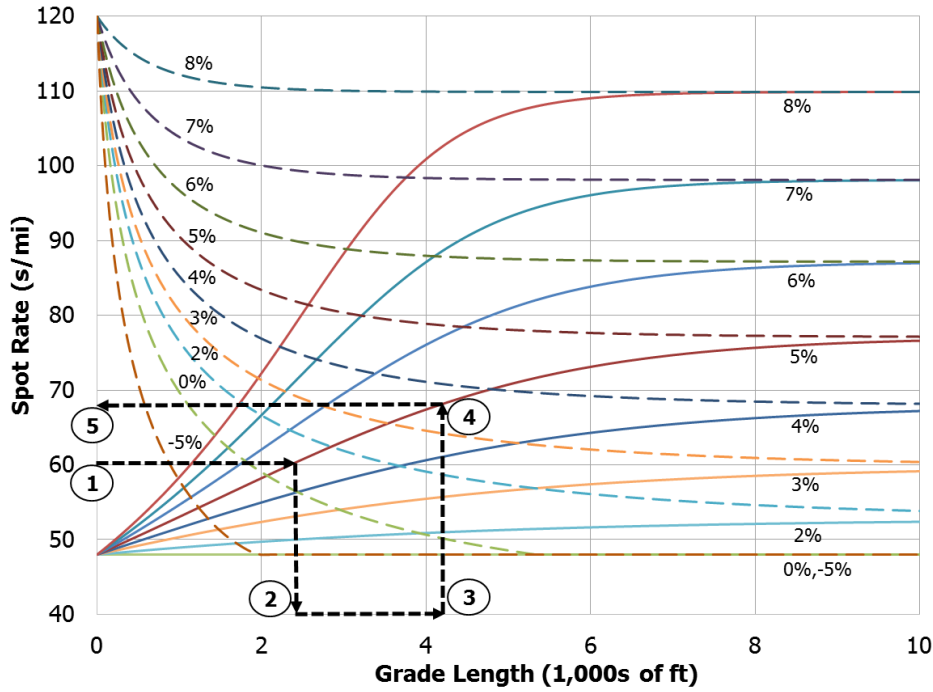
STEP 4: COMPUTE TRUCK SPOT AND SPACE-BASED TRAVEL TIME RATES

This step computes the SUT and TT space-based travel time rates for each of the segments and the spot rates at the end of each segment. The procedure follows a process similar to Step 5 of the mixed-flow model procedure described in Chapter 26.

The first substep involves analyzing the kinematic behavior of the trucks on the grade. The final spot rates are needed, as well as a determination of whether the trucks accelerated or decelerated on the grade.

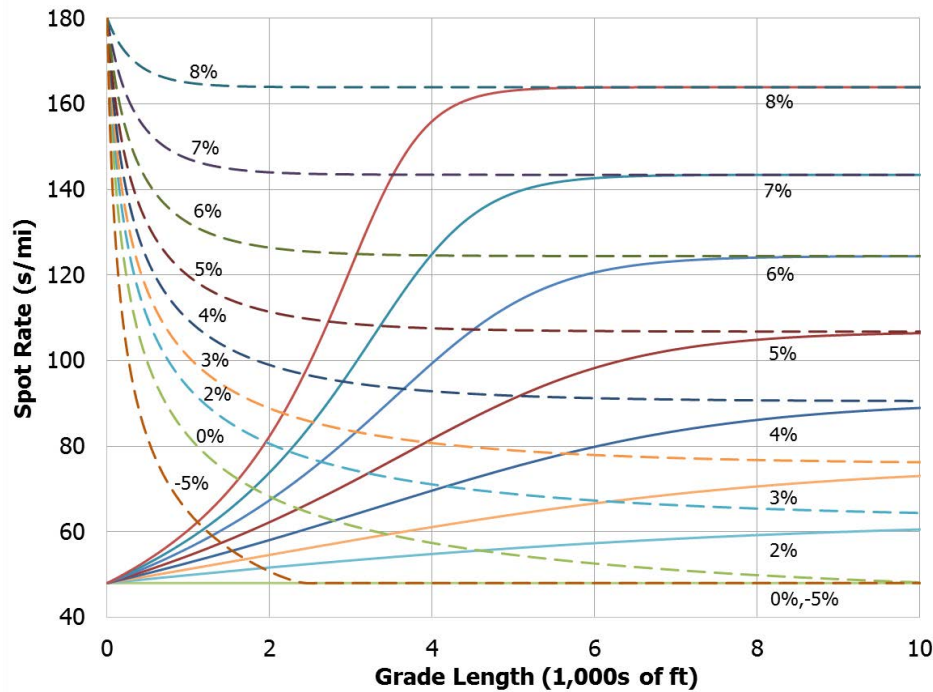
Exhibit 25-20 and Exhibit 25-21 can be used for these purposes. These graphs are based on kinematic relationships given elsewhere (12). Alternative models of propulsive and resistive forces, such as more complex ones that account for gear shifting (e.g., 13, 14), can produce longer travel times. Such considerations can be incorporated into the mixed-flow model by adjusting the parameter values that affect the tractive effort to account for the additional losses. The travel time rates presented here are based on a model that assumes constant peak-engine power. Other models (e.g., 13, 14) account for the power losses that occur for the time intervals prior to and after gear shifting when the engine speed is outside the range that produces peak power.

Exhibit 25-20 shows the trends in SUT spot rates for various grades starting from travel rates of 48 s/mi (75 mi/h) and 120 s/mi (30 mi/h). Exhibit 25-21 shows the same trends for a TT. Clearly, trucks decelerate as upgrades become steeper. For milder grades, trucks can often accelerate.



Notes: Curves in this graph assume a weight-to-horsepower ratio of 100. Solid curves are for an initial speed of 75 mi/h (48 s/mi) and dashed curves are for an initial speed of 30 mi/h (120 s/mi).

Exhibit 25-20
SUT Spot Rates Versus
Distance with Initial Speeds of
75 and 30 mi/h



Notes: Curves in this graph assume a weight-to-horsepower ratio of 100. Solid curves are for an initial speed of 75 mi/h (48 s/mi) and dashed curves are for an initial speed of 20 mi/h (180 s/mi).

Exhibit 25-21
TT Spot Rates Versus
Distance with Initial Speeds of
75 and 20 mi/h

In both Exhibit 25-20 and Exhibit 25-21, the x -axis gives the distance d traveled by the truck, and the y -axis gives the spot travel rate $\tau_{kin,j}$ at the end of that distance. The different curves are for various upgrades and downgrades.

To ascertain whether trucks accelerate or decelerate on segment j , consider the travel time rate trends shown in Exhibit 25-20 and Exhibit 25-21. If an SUT's final spot rate for segment j $\tau_{SUT,kin,fj}$ is greater than the SUT's initial spot rate for segment j $\tau_{SUT,kin,ij}$ and the TT's spot rate at the end of segment j $\tau_{TT,kin,fj}$ is greater than the TT's spot rate at the beginning of segment j $\tau_{TT,kin,ij}$ then both truck classes decelerate. If $\tau_{SUT,kin,fj} < \tau_{SUT,kin,ij}$ and $\tau_{TT,kin,fj} < \tau_{TT,kin,ij}$ then both truck classes accelerate.

To determine the end-of-grade spot travel time rates, start by finding the point on the applicable grade that corresponds to the initial kinematic rate. Treat that point as the zero distance location. Next, proceed along the grade length (x -axis) for a distance equal to the length d of the segment and read the spot rate at that distance. This reading is the final spot rate. For example, an SUT travels 2,000 ft starting from 60 mi/h (60 s/mi) on a 5% grade. Point 1 in Exhibit 25-20 is the 60-mi/h speed (60-s/mi rate) from which the SUT starts to travel on the 5% grade. Point 2 is the distance that is treated as the zero distance of the SUT. Point 3 represents the distance the SUT has traveled after 2,000 ft. The final spot rate can be read at Point 4. The initial kinematic SUT and TT spot rates for segment j $\tau_{SUT,kin,ij}$ and $\tau_{TT,kin,ij}$ are the kinematic spot rates at the end of the preceding segment. For remaining segments, $\tau_{SUT,kin,ij}$ and $\tau_{TT,kin,ij}$ are the kinematic spot rates at the end of the preceding segment $j - 1$, which are $\tau_{SUT,kin,fj-1}$ and $\tau_{TT,kin,fj-1}$.

The second substep involves determining the space-based travel time rates for SUTs and TTs. Exhibit 25-22 and Exhibit 25-23 provide examples. Exhibit 25-22 shows the time versus distance relationships for SUTs starting at 70 mi/h with a desired speed of 75 mi/h as they accelerate or decelerate on various grades. Exhibit 25-23 shows time versus distance relationships for SUTs starting at 30 mi/h as they ascend or descend grades. Relationships for a range of initial rates for both SUTs and TTs are provided in Appendix A.

In all exhibits, the x -axis is the distance d traveled by the truck, while the y -axis is the travel time T to cover the grade length d . The various curves in each exhibit represent different upgrades. All the truck profiles have a desired speed of 75 mi/h. For example, the 2% curve in Exhibit 25-23 shows travel time versus distance for SUTs starting from 30 mi/h with a desired speed of 75 mi/h.

When necessary, symbols are placed on the curves to indicate where a truck reaches 55, 60, 65, and 70 mi/h, for use when the speed limit is less than 75 mi/h, as indicated in the notes for Exhibit 25-23. For example, if the speed limit is 55 mi/h, it is assumed trucks will maintain a constant speed of 55 mi/h after reaching that speed. The analyst would use the graph to determine the travel time to accelerate to 55 mi/h and then perform the remainder of the travel time calculation using 55 mi/h as the truck speed. Not all curves have these symbols, as (a) the truck's crawl speed would be less than 55 mi/h for the particular grade, (b) the truck would take more than 10,000 ft to reach that speed, or (c) the graph being used starts from a relatively high speed (e.g., Exhibit 25-22).

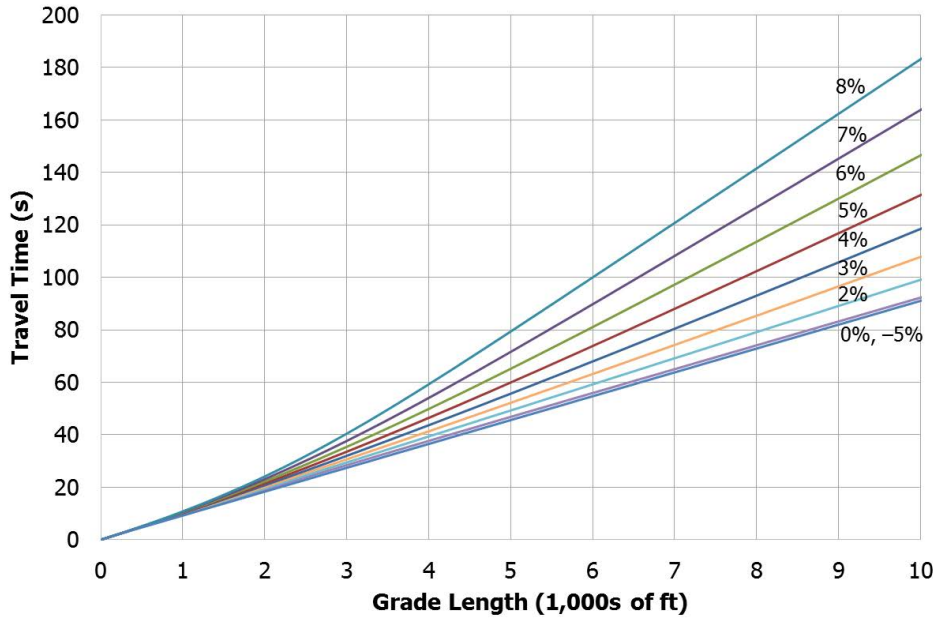


Exhibit 25-22
SUT Travel Time Versus
Distance Curves for 70-mi/h
Initial Speed

Note: Curves in this graph assume a weight-to-horsepower ratio of 100.

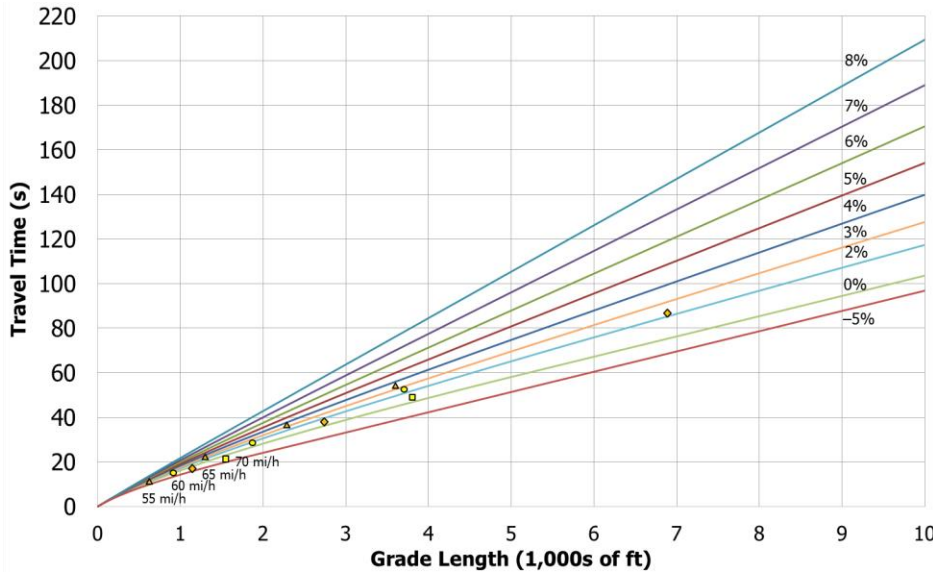


Exhibit 25-23
SUT Travel Time Versus
Distance Curves for 30-mi/h
Initial Speed

Notes: Curves in this graph assume a weight-to-horsepower ratio of 100.
Triangles indicate where a truck reaches 55 mi/h, circles indicate 60 mi/h, diamonds indicate 65 mi/h, and squares indicate 70 mi/h.

The analyst should use the Appendix A graph that has a starting spot speed closest to the value computed in the first substep. Because the graphs are provided in 5-mi/h increments, this choice means using the graph that is within 2.5 mi/h of the speed corresponding to the segment’s initial spot rate.

The kinematic space-based travel time rate τ_{kin} (in seconds per mile) can then be computed with Equation 25-58.

$$\tau_{kin} = T/d$$

Equation 25-58

where T is the segment travel time (s) and d is the grade length (mi).

The maximum grade length shown in the graphs is 10,000 ft. When the grade length exceeds 10,000 ft, the travel rate can be computed using Equation 25-59.

Equation 25-59

$$\tau_{kin} = \frac{T_{10000}}{d} + \delta \left(1 - \frac{10,000}{5,280d} \right) \times 5,280$$

where

τ_{kin} = kinematic travel rate (s/mi),

T_{10000} = travel time at 10,000 ft (s),

δ = slope of the travel time versus distance curve (s/ft),

d = grade length (mi), and

5,280 = number of feet in 1 mi.

The δ values for SUTs and TTs are shown in Exhibit 25-24 and Exhibit 25-25, respectively.

Exhibit 25-24
 δ Values for SUTs

Grade	Free-Flow Speed (mi/h)					
	50	55	60	65	70	75
-5%	0.0136	0.0124	0.0114	0.0105	0.0097	0.0091
0%	0.0136	0.0124	0.0114	0.0105	0.0097	0.0091
2%	0.0136	0.0124	0.0114	0.0105	0.0100	0.0099
3%	0.0136	0.0124	0.0114	0.0113	0.0112	0.0112
4%	0.0136	0.0129	0.0128	0.0128	0.0128	0.0127
5%	0.0146	0.0146	0.0146	0.0146	0.0145	0.0145
6%	0.0165	0.0165	0.0165	0.0165	0.0165	0.0165
7%	0.0186	0.0186	0.0186	0.0186	0.0186	0.0186
8%	0.0208	0.0208	0.0208	0.0208	0.0208	0.0208

Exhibit 25-25
 δ Values for TTs

Grade	Free-Flow Speed (mi/h)					
	50	55	60	65	70	75
-5%	0.0136	0.0124	0.0114	0.0105	0.0097	0.0091
0%	0.0136	0.0124	0.0114	0.0105	0.0097	0.0091
2%	0.0136	0.0124	0.0119	0.0118	0.0116	0.0115
3%	0.0143	0.0143	0.0142	0.0141	0.0140	0.0138
4%	0.0171	0.0171	0.0171	0.0170	0.0169	0.0168
5%	0.0202	0.0202	0.0202	0.0202	0.0202	0.0202
6%	0.0236	0.0236	0.0236	0.0236	0.0236	0.0236
7%	0.0272	0.0272	0.0272	0.0272	0.0272	0.0272
8%	0.0310	0.0310	0.0310	0.0310	0.0310	0.0310

Once the end-of-grade spot travel time rates and the space-based rates are obtained for the current segment, Equation 25-60 and Equation 25-61 are used to account for the traffic interaction term to obtain the actual truck spot and space-based travel time rates.

Equation 25-60

$$\tau_{*,SUT,j} = \tau_{*,SUT,kin,j} + \Delta\tau_{TI}$$

Equation 25-61

$$\tau_{*,TT,j} = \tau_{*,TT,kin,j} + \Delta\tau_{TI}$$

where

* = placeholder that can either be f to designate the spot travel time rate at the end of the segment or S to indicate the space-based rate across the segment,

- $\tau_{*,SUT,j}$ = spot travel time rate for SUTs at the end of segment j or the space-based rate (s/mi),
- $\tau_{*,SUT,kin,j}$ = kinematic final spot travel time rate or space-based rate for SUTs (s/mi),
- $\Delta\tau_{TI}$ = traffic interaction term (s/mi) from Equation 25-62,
- $\tau_{*,TT,j}$ = spot travel time rate for TTs at the end of segment j or the space-based rate (s/mi), and
- $\tau_{*,TT,kin,j}$ = kinematic final spot travel time rate or space-based rate for TTs (s/mi).

The traffic interaction term represents the contribution of other traffic to truck speeds or travel time rates in mixed flow. It is computed by Equation 25-62.

$$\Delta\tau_{TI} = \left(\frac{3,600}{S_{ao}} - \frac{3,600}{FFS} \right) \times \left[1 + 3 \left(\frac{1}{CAF_{mix}} - 1 \right) \right]$$

Equation 25-62

where

- $\Delta\tau_{TI}$ = traffic interaction term (s/mi),
- S_{ao} = auto-only speed for the given flow rate (mi/h) from Equation 25-63,
- FFS = base free-flow speed of the basic freeway segment (mi/h), and
- CAF_{mix} = mixed-flow capacity adjustment factor for the segment (decimal) from Equation 25-53.

The auto-only travel time rate for the given flow rate can be computed with Equation 25-63.

$$S_{ao} = \begin{cases} FFS & \frac{v_{mix}}{CAF_{mix}} \leq BP_{ao} \\ FFS - \frac{\left(FFS - \frac{C_{ao}}{D_c} \right) \left(\frac{v_{mix}}{CAF_{mix}} - BP_{ao} \right)^2}{(C_{ao} - BP_{ao})^2} & \frac{v_{mix}}{CAF_{mix}} > BP_{ao} \end{cases}$$

Equation 25-63

where

- S_{ao} = auto-only speed for the given flow rate (mi/h),
- FFS = base free-flow speed of the basic freeway segment (mi/h),
- C_{ao} = base segment capacity (pc/h/ln) from Exhibit 12-6,
- BP_{ao} = breakpoint in the auto-only flow condition (pc/h/ln) from Exhibit 12-6,
- D_c = density at capacity = 45 pc/mi/ln,
- v_{mix} = flow rate of mixed traffic (veh/h/ln), and
- CAF_{mix} = mixed-flow capacity adjustment factor for the basic freeway segment (decimal).

STEP 5: COMPUTE AUTOMOBILE SPOT AND SPACE-BASED TRAVEL TIME RATES

Whether trucks accelerate or decelerate, the automobile spot travel time rates at the end of the segment are computed with Equation 25-64. The analyst should check that the automobile spot rates are always less than or equal to the truck spot rates (i.e., automobile speeds are greater than or equal to truck speeds).

Equation 25-64

$$\tau_{f,a,j} = \frac{3,600}{FFS} + \Delta\tau_{TI} + \left[64.50 \times \left(\frac{v_{mix}}{1,000} \right)^{0.77} \times (P_{SUT})^{0.34} \times \max \left(0, \frac{\tau_{f,SUT,kin,j}}{100} - \frac{3,600}{FFS \times 100} \right)^{1.53} \right] + \left[79.50 \times \left(\frac{v_{mix}}{1,000} \right)^{0.81} \times (P_{TT})^{0.56} \times \max \left(0, \frac{\tau_{f,TT,kin,j}}{100} - \frac{3,600}{FFS \times 100} \right)^{1.32} \right]$$

where

$\tau_{f,a,j}$ = end-of-grade spot travel time rate for automobiles (s/mi),

$\tau_{f,SUT,kin,j}$ = spot kinematic travel time rate of SUTs at the end of segment j (s/mi),

$\tau_{f,TT,kin,j}$ = spot kinematic travel time rate of TTs at the end of segment j (s/mi),

$\Delta\tau_{TI}$ = traffic interaction term (s/mi),

v_{mix} = flow rate of mixed traffic (veh/h/ln),

FFS = base free-flow speed of the basic freeway segment (mi/h),

P_{SUT} = proportion of SUTs in the traffic stream (decimal), and

P_{TT} = proportion of TTs in the traffic stream (decimal).

In Step 4, it was determined whether trucks accelerate or decelerate across a segment. If they decelerate, Equation 25-65 is used to compute the auto space-based travel time rate. If trucks accelerate, Equation 25-66 is employed. The auto space mean rates are always less than or equal to the truck space mean rates.

Equation 25-65

$$\tau_{S,a,j} = \frac{3,600}{FFS} + \Delta\tau_{TI} + \left[100.42 \times \left(\frac{v_{mix}}{1,000} \right)^{0.46} \times (P_{SUT})^{0.68} \times \max \left(0, \frac{\tau_{S,SUT,kin,j}}{100} - \frac{3,600}{FFS \times 100} \right)^{2.76} \right] + \left[110.64 \times \left(\frac{v_{mix}}{1,000} \right)^{1.36} \times (P_{TT})^{0.62} \times \max \left(0, \frac{\tau_{S,TT,kin,j}}{100} - \frac{3,600}{FFS \times 100} \right)^{1.81} \right]$$

$$\tau_{S,a,j} = \frac{3,600}{FFS} + \Delta\tau_{TI} + \left[54.72 \times \left(\frac{v_{mix}}{1,000} \right)^{1.16} \times (P_{SUT})^{0.28} \times \max \left(0, \frac{\tau_{S,SUT,kin,j}}{100} - \frac{3,600}{FFS \times 100} \right)^{1.73} \right] + \left[69.72 \times \left(\frac{v_{mix}}{1,000} \right)^{1.32} \times (P_{TT})^{0.61} \times \max \left(0, \frac{\tau_{S,TT,kin,j}}{100} - \frac{3,600}{FFS \times 100} \right)^{1.33} \right]$$

Equation 25-66

where

$\tau_{S,a,j}$ = auto space-based travel time rate (s/mi),

$\tau_{S,SUT,kin,j}$ = kinematic space-based travel time rate of SUTs (s/mi),

$\tau_{S,TT,kin,j}$ = kinematic space-based travel time rate of TTs (s/mi),

$\Delta\tau_{TI}$ = traffic interaction term (s/mi),

v_{mix} = flow rate of mixed traffic (veh/h/ln),

FFS = base free-flow speed of the basic freeway segment (mi/h),

P_{SUT} = proportion of SUTs in the traffic stream (decimal), and

P_{TT} = proportion of TTs in the traffic stream (decimal).

The traffic interaction term is the same for all the travel time rate equations and can be computed with Equation 25-62.

STEP 6: COMPUTE MIXED-FLOW SPACE-BASED TRAVEL TIME RATE AND SPEED

The mixed-flow space-based travel time rate $\tau_{mix,j}$ and the space-based speed $S_{mix,j}$ are computed with Equation 25-67 and Equation 25-68, respectively.

$$\tau_{mix,j} = P_a \tau_{S,a,j} + P_{SUT} \tau_{S,SUT,j} + P_{TT} \tau_{S,TT,j}$$

Equation 25-67

$$S_{mix,j} = \frac{3,600}{\tau_{mix,j}}$$

Equation 25-68

where

$\tau_{mix,j}$ = mixed-flow space-based travel time rate for segment j (s/mi),

$\tau_{S,a,j}$ = automobile space-based travel time rate for segment j (s/mi),

$\tau_{S,SUT,j}$ = space-based travel time rate of SUTs (s/mi),

$\tau_{S,TT,j}$ = space-based travel time rate of TTs (s/mi),

P_{SUT} = proportion of SUTs in the traffic stream (decimal), and

P_{TT} = proportion of TTs in the traffic stream (decimal).

As indicated above, Steps 3 through 6 are repeated for each segment until the end of the composite grade is reached.

STEP 7: OVERALL RESULTS

Once spot and space mean speeds and travel time rates have been developed for all vehicle types on all segments, the overall performance of the composite grade can now be estimated. The mixed-flow travel time for each segment can be computed with Equation 25-69.

Equation 25-69

$$t_{\text{mix},j} = \frac{3,600d_j}{S_{\text{mix},j}}$$

where

$t_{\text{mix},j}$ = mixed-flow travel time segment j (s),

d_j = grade length of segment j (mi), and

$S_{\text{mix},j}$ = mixed-flow speed for segment j (mi/h).

The overall mixed-flow travel time $t_{\text{mix},oa}$ is the summation of mixed-flow travel times on all segments. The overall space-based travel speed can then be computed with Equation 25-70.

Equation 25-70

$$S_{\text{mix},oa} = \frac{3600d_{oa}}{t_{\text{mix},oa}}$$

where

$S_{\text{mix},oa}$ = overall mixed-flow speed (mi/h);

d_{oa} = overall distance, the summation of all the segment grade lengths on the composite grade (mi); and

$t_{\text{mix},oa}$ = overall mixed-flow travel time (s).

8. FREEWAY CALIBRATION METHODOLOGY

This section presents a calibration methodology for the procedures described in Chapter 10, Freeway Facilities Core Methodology, and Chapter 11, Freeway Reliability Analysis. The freeway calibration methodology is carried out at three main levels:

1. Calibration at the core freeway facility level,
2. Calibration at the reliability level, and
3. Calibration at the Active Traffic and Demand Management (ATDM) strategy assessment level.

The procedure uses *sequential calibration* to calibrate these three distinct methodological parts, meaning that the calibration is carried out sequentially for each level. After a level is fully calibrated, no further change is allowed from a different level. As a result, this approach requires that the calibration parameters of different levels be mutually exclusive.

The approach first calibrates the base scenario, then focuses on reliability-level calibration, and concludes with ATDM-level calibration. It is logical both that the base scenario (i.e., core freeway facility) should be fully calibrated before evaluating reliability or ATDM strategies and that the base scenario calibration should not be affected by any subsequent changes from the reliability or ATDM calibration levels. Consequently, it is critical to select a suitable base scenario with oversaturated flow conditions to ensure that the bottlenecks are calibrated appropriately. More information about the development of the methodology is provided in a paper (15) located in the Technical Reference Library section of online HCM Volume 4.

Calibration relies on field measurements of key input variables, including the segment capacity. Chapter 12, Basic Freeway and Multilane Highway Segments, provides definitions for prebreakdown and queue discharge capacity. Chapter 26, Freeway and Highway Segments: Supplemental, provides guidance for field measuring and estimating capacity from sensor data.

CALIBRATION AT THE CORE FREEWAY FACILITY LEVEL

The core freeway facility analysis is calibrated for a specific day, called the *seed day*. Exhibit 25-26 depicts five steps of the calibration process for a core facility analysis. After gathering input data, the actual calibration consists of three steps (Steps 2, 3, and 4), the order of which is somewhat flexible. Multiple iterations may be needed to achieve satisfactory performance. A detailed explanation of each step follows.

Step 1: Gather Input Data

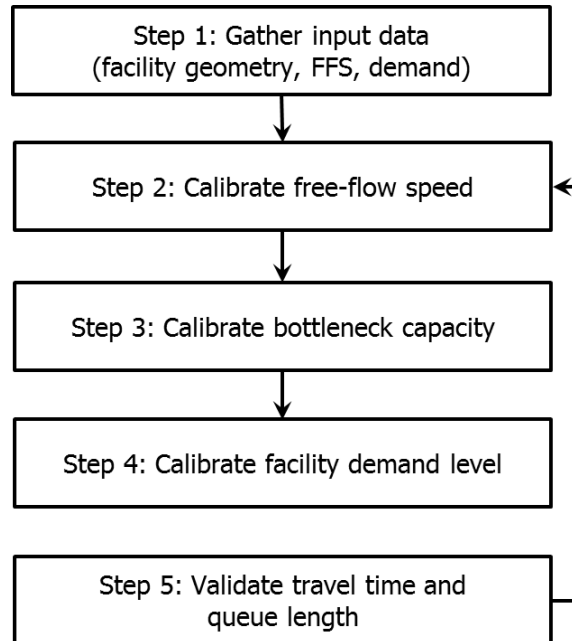
In this step, all input data required for a single freeway facility analysis (computational engine seed file) need to be gathered. These data include

1. Geometric information such as segment type, segment length, and number of lanes;

2. Facility free-flow speed (FFS);
3. Capacity estimate for bottleneck segment(s); and
4. Demand-level data for all segments in all time intervals.

Geometric data are model input parameters and will not be changed in the calibration process. The other three inputs (FFS, capacity, and demand) are used as calibration parameters.

Exhibit 25-26
Calibration Steps for the Core
Freeway Facility Level



Step 2: Calibrate Free-Flow Speed

FFS can be field measured or estimated by using the procedure given in Chapter 12. The FFS calibration procedure may be applied in either case; however, if accurate field measurements of FFS are available, great care should be taken before changing a field-measured input.

To start, the analyst should select a time interval with a low demand level and no active bottleneck. The analyst should then compare the estimated free-flow travel time of this interval with the field measurements. Because a later step requires the analyst to look at congested periods, the study period should be sufficiently long to include free-flow conditions before or after the onset of congestion.

The calibration process involves making a computational engine run for the seed day, recording the average travel time for a low-demand time interval, and comparing it to the observed travel time. The user needs to repeatedly perform one of the following actions until the predicted facility travel time is within a predefined threshold (e.g., 10% error tolerance) of the observed facility travel time:

- Reduce the FFS in 1- to 5-mi/h increments if the predicted travel time is less than the observed travel time, or

- Increase the FFS in 1- to 5-mi/h increments if the predicted travel time is more than the observed travel time.

This process should only be used for analysis periods with demand levels far less than oversaturation (i.e., free-flow conditions). The speed–flow diagram in Exhibit 25-27 illustrates the effect of different FFSs on the overall facility speed–flow–density relationship. A higher free-flow speed FFS_1 and a lower free-flow speed FFS_2 are shown. A 5-mi/h drop in FFS is associated with a drop in capacity equal to 50 pc/h/ln, except at very high FFSs.

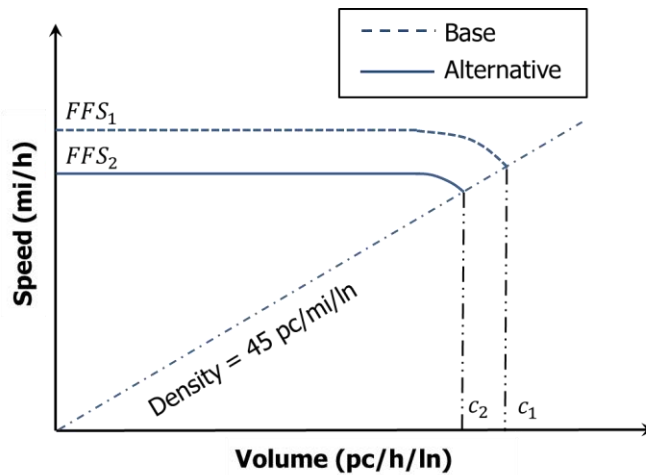


Exhibit 25-27
Effect of Calibrating Free-Flow Speed on Capacity

Step 3: Calibrate Bottleneck Capacity

In this step, the location and extent of bottlenecks are calibrated, which requires a freeway facility to feature at least some periods of oversaturated flow conditions. Guidance for selecting capacity measurement locations and for reducing the collected data is provided in Chapter 26.

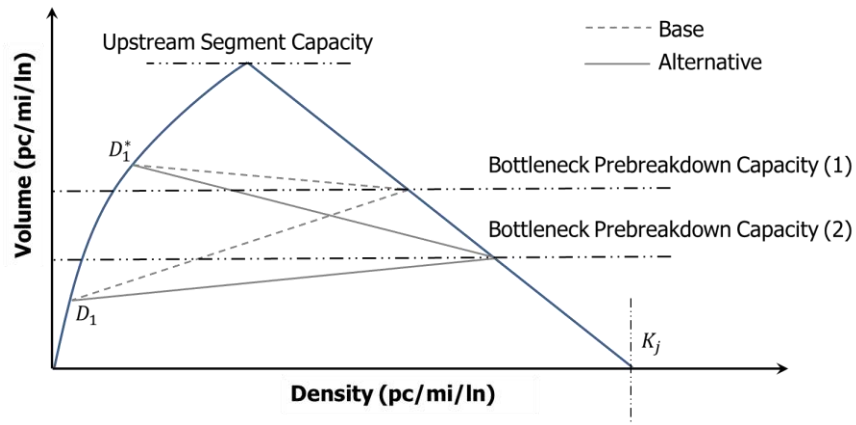
It is very important to calibrate for capacity, as research (11) shows the controlling capacity at the bottleneck is often significantly less than the HCM's base capacity. Three parameters are used to calibrate for the location and extent of bottlenecks:

1. *Prebreakdown capacity* at the bottleneck, implemented through a capacity adjustment factor (CAF) relative to the base capacity for a freeway segment. In the HCM, the prebreakdown flow rate is defined as the 15-min average flow rate immediately prior to the breakdown event. For the purposes of this chapter, the prebreakdown flow rate is equivalent to the segment capacity;
2. *Queue discharge rate* at the bottleneck following breakdown, as implemented through a percentage capacity drop α . In the HCM, the queue discharge rate is defined as the average flow rate during oversaturated conditions (i.e., during the time interval after breakdown and prior to recovery); and
3. *Jam density* of the queue forming upstream of the bottleneck, which describes the maximum density (minimum intervehicle spacing) in a queued condition.

The prebreakdown capacity and the queue-discharge capacity loss influence the actual throughput of the bottleneck, as well as the speed of shock waves describing the rate of change of the back of the queue. Jam density does not affect throughput; it only influences the formation and dissipation of queues at a bottleneck. The following exhibits illustrate the effects of these three calibration parameters in a shock wave diagram format.

In Exhibit 25-28, the number 1 denotes the base condition (dashed gray line) and the number 2 denotes the alternative condition (solid gray line). Two demand levels D are shown. Demand rates that are greater than the bottleneck capacity are noted with an asterisk.

Exhibit 25-28
Effects of Segment Capacity



Reducing the prebreakdown capacity increases the speed of the forming shock wave, but the speed of the recovery wave is decreased. As a result, a reduction in the segment's prebreakdown capacity is expected to increase congestion throughout the segment. Note that it is assumed a reduction in the segment capacity has no impact on the queue discharge rate at the bottleneck in the example above. The effects of a drop in queue discharge rate are shown in Exhibit 25-29.

Exhibit 25-29
Effects of Queue Discharge Rate Drop

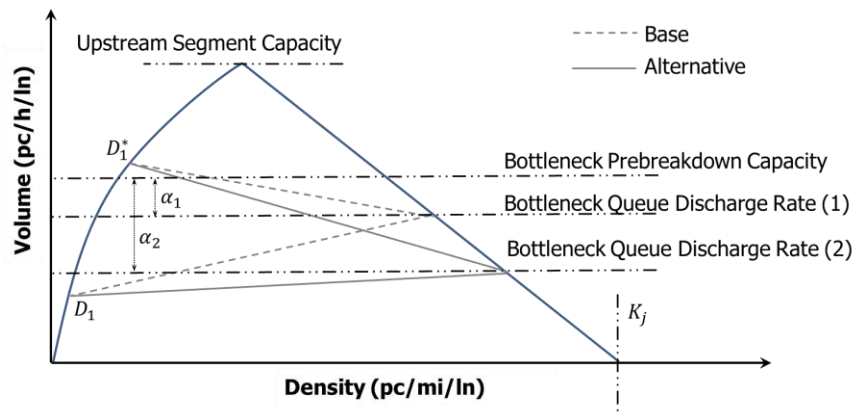


Exhibit 25-29 shows that including a queue discharge rate drop in the freeway model results in a reduction in bottleneck throughput after breakdown. The factor α describes the percentage reduction from prebreakdown capacity to

queue discharge rate. A larger α corresponds to a larger drop and lower throughput. Implementing this factor results in a drop in throughput, an increase in the speed of the forming shockwave, and a decrease in the speed of the recovery wave. The result is a threefold effect that leads to a higher level of congestion, which has been demonstrated in the literature (16). It is therefore expected that the capacity drop has a nonlinear effect on the overall facility performance.

Exhibit 25-30 shows the effect of an increase in the jam density on wave speeds. Interestingly, an increase in the jam density value reduces both the forming and recovery wave speeds, thus canceling each other's effects to some degree. The opposite situation occurs if jam density is decreased, in which case both the forming and recovery speeds will increase. Although jam density is likely to affect the queue size (a higher jam density results in a smaller queue size), it may not influence travel time values as much as the prebreakdown capacity and queue discharge rate do.

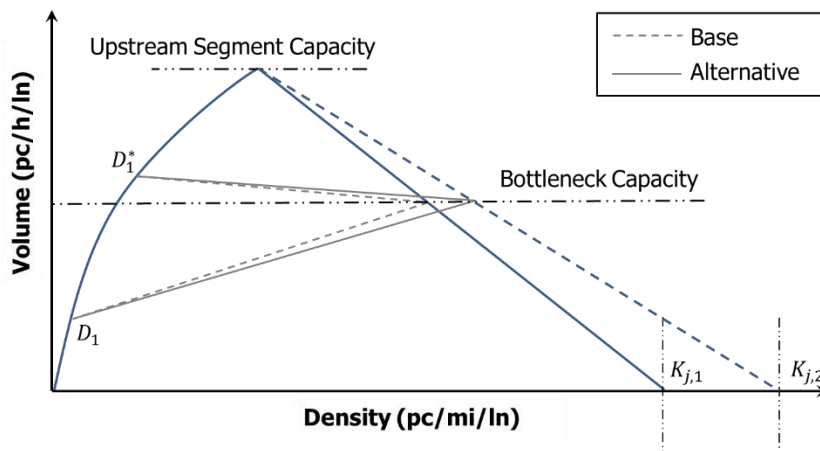


Exhibit 25-30
Effects of Jam Density

To calibrate for bottlenecks, the analyst needs to change the capacity and capacity drop values for different segments of the freeway facility to recreate the bottlenecks that are observed in the field. Therefore, the analyst must first identify recurring bottlenecks in the field.

Next, the calibration process begins with setting the segment capacity to the HCM value for the facility's FFS (e.g., 2,400 pc/h/ln for a 70-mi/h FFS). A value of 7% for capacity drop is recommended.

If these initial values predict the bottleneck location correctly, the analysis proceeds to the validation step. If the model fails to identify a bottleneck, the analyst should reduce capacity in increments of 50 pc/h/ln until a bottleneck occurs. However, if the HCM model identifies a bottleneck that does not exist in the field, the analyst should increase capacity in increments of 50 pc/h/ln until the bottleneck disappears.

It is recommended that analysts wait to adjust the capacity drop value until after the bottleneck locations have been fixed. This procedure is performed as part of validating the queue length and travel time, as explained in Step 5.

Step 4: Calibrate Facility Demand Level

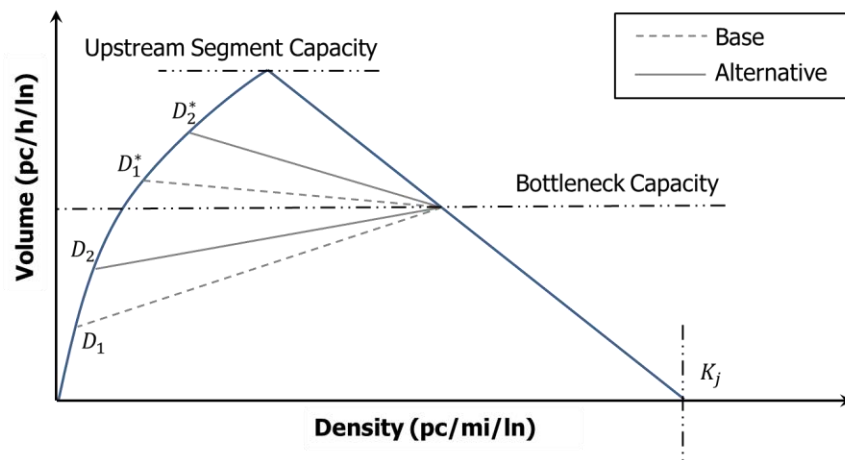
The demand level is a model input that can serve as a calibration parameter as a last resort. Presumably, demand has been measured based on field data, and therefore can be considered to be a fixed input. However, given the variability of demand (i.e., day-to-day fluctuation), as well as potential errors in volume and demand measurements, demand can become a calibration parameter after the FFS and capacity adjustment possibilities have been exhausted.

Two potential problems may be encountered with demand levels. First, in oversaturated conditions, it is not possible to measure the demand level downstream of a bottleneck or within a queued segment. The volume served is measured, rather than the demand level. Second, demand data vary from day to day, and the selected demand levels may not represent a “typical” day. This second problem is also true if AADT demand values are used to estimate peak period demands. As a result, although demand level is one of the inputs to the core freeway facility analysis, it may be subject to calibration.

To provide an example of the effect of the demand level on segment and facility travel time, a shockwave representation of the oversaturation model used in the core HCM freeway facilities methodology is presented. Although the HCM uses an adaptation of the cell-transmission model to estimate queue propagation and dissipation patterns at a bottleneck, the shockwave approach is useful to illustrate the calibration concepts here.

Exhibit 25-31 shows the flow–density relationship under high- and low-volume conditions for a segment that is just upstream of a bottleneck with a reduced capacity. As before, the number 1 denotes the base condition (dashed gray line), the number 2 denotes the alternative condition (solid gray line), and demand rates greater than the bottleneck capacity are denoted with an asterisk.

Exhibit 25-31
Effect of Demand Level



In Exhibit 25-31 it is evident that an overall increase in demand level (from D_1^* to D_2^* and from D_1 to D_2) would result in both an increase in the forming shock wave speed and a reduction in the recovery wave speed, assuming a fixed bottleneck capacity. In other words, an overall increase in demand level results in a higher level of congestion throughout. The greater the difference between upstream demand and downstream bottleneck capacity, the faster the resulting

shock wave either grows the queue (demand-to-capacity ratio > 1.0) or dissipates the queue (demand-to-capacity ratio ≤ 1.0).

The analyst should increase the demand level in increments of 50 pc/h/ln until all bottlenecks that are observed in the field are activated in the freeway facility core analysis. However, if the model predicts bottlenecks that do not exist in the field, the user should decrease the demand level in increments of 50 pc/h/ln until those bottlenecks are deactivated. This activity should be performed in conjunction with Step 3: Calibrate Bottleneck Capacity.

Step 5: Validate Travel Time and Queue Length

The validation step has two major components:

1. Validate facility travel time, and
2. Validate queue length at active bottlenecks.

Travel Time Validation

After fixing the FFS and the bottleneck locations, the analyst should adjust the calibration parameters further to match predicted and observed facility travel times within a defined range (a 10% or less difference is recommended). Note that FFS has already been fixed in Step 3 and will not be adjusted further in this step. This process can be done by adjusting

1. Demand level,
2. Prebreakdown capacity,
3. Capacity drop, and
4. Jam density.

The analyst is trying to match reasonably well the estimated and observed facility and segment travel times. If the model *underestimates* the travel time, the analyst should consider one of the following actions:

1. Increase the demand level (in increments of 100 pc/h/ln),
2. Reduce prebreakdown capacity (in increments of 100 pc/h/ln), or
3. Increase the capacity drop (in increments of 1%).

If the model *overestimates* travel time, the analyst should consider one of the following actions:

1. Reduce the demand level (in increments of 50 pc/h/ln),
2. Increase prebreakdown capacity (in increments of 50 pc/h/ln), or
3. Reduce the capacity drop (in increments of 1%).

Note that jam density is unlikely to have a significant impact on facility travel time and is therefore not included in the steps above.

Queue Length Validation

After the facility travel time is fixed, the queue lengths at the facility's active bottlenecks should be matched reasonably well (i.e., within 10%) through further adjustments to the capacity drop and jam density.

If the predicted queue length at an active bottleneck is *shorter* than observed in the field, the capacity drop should be *increased* and the jam density should be *decreased*.

However, if the predicted queue length is *longer* than that observed in the field, the capacity drop should be *decreased* and the jam density should be *increased*. It is recommended that the capacity drop be changed in increments of 1% and that the jam density be changed in increments of 10 pc/mi/ln.

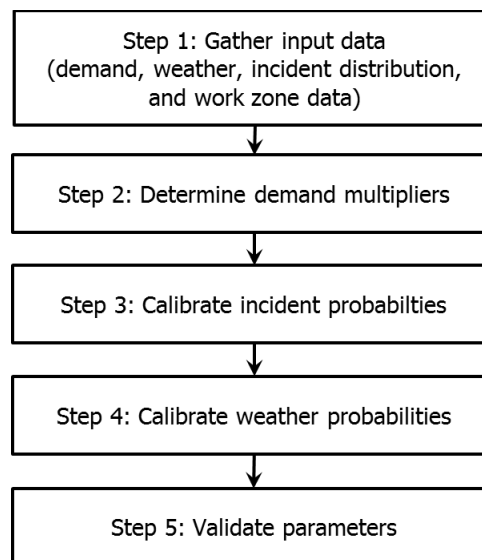
CALIBRATION AT THE TRAVEL TIME RELIABILITY LEVEL

After calibrating the core freeway facility methodology and fixing the value of its parameters, a comprehensive travel time reliability calibration is performed. Note that the process does not allow any change in the parameters that were calibrated in the previous step. The process requires a host of different input variables and calibration parameters. Comprehensive reliability-level calibration, as shown in Exhibit 25-32, starts with gathering the necessary input data. Some of these parameters, including facility geometry and FFS, are already known and fixed.

The process includes three major steps: whole-year demand calibration, incident calibration, and weather calibration. In the rest of this section, each step is presented in more detail.

To calibrate the methodology for a particular site, it is recommended that the analyst perform an initial comprehensive reliability run using default values for all input parameters and subsequently compare the predicted travel time index (TTI) cumulative distribution to the observed distribution. This section provides suggestions on how to change calibration parameters on the basis of the difference between the two TTI distributions.

Exhibit 25-32
Comprehensive Reliability
Calibration Steps



Step 1: Gather Input Data

In this step, all the input data required for a reliability analysis are gathered. These data include

1. Demand distribution over the reliability reporting period, converted to monthly and day-of-week demand multipliers;
2. Incident or crash rates and event durations, with the corresponding speed and capacity adjustment factors;
3. Weather probabilities, with the corresponding speed and capacity adjustment factors; and
4. Work zone and special event data, with the corresponding speed and capacity adjustment factors.

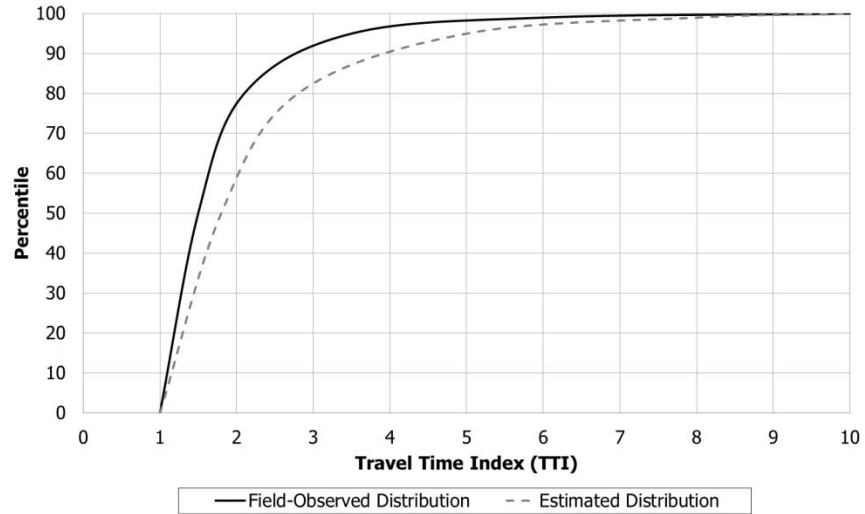
Specific details about these input data are provided in Chapter 11, Freeway Reliability Analysis.

Step 2: Determine Demand Multipliers

As mentioned above, the demand level for the seed day is either known or calibrated at the core freeway facility analysis level. However, in addition to the seed day, the reliability analysis requires the demand level for the other days included in the reliability reporting period. Because it is not feasible to measure demand level for all days, the methodology uses demand multipliers to convert the seed day demand to demand level for different days.

Although the demand level of the seed day may be accurately measured, the seed day may have experienced unusually low or high demand levels. In that event, the seed day demand either inflates or deflates the demand level for the other days of the reliability reporting period. In the example shown in Exhibit 25-33, a high demand level on the seed day causes the resulting TTI distribution to be consistently shifted to the right compared to the distribution observed in the field, across the full range of the distribution. Key reliability performance measures, such as TTI_{mean} or TTI_{95r} are also overestimated by the procedure in the case shown. To fix this problem (i.e., an inflated demand level for the seed day), the analyst needs to reduce the demand level in the seed file and make additional runs to determine whether the problem is resolved.

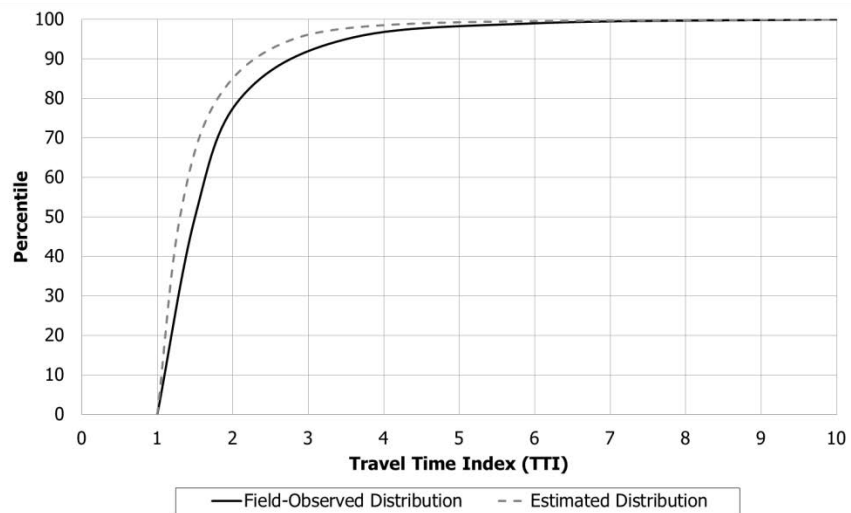
Exhibit 25-33
High Demand Level on the Seed Day



Note also in Exhibit 25-33 that the intercept with the x -axis is the same for both distributions, suggesting that the free-flow travel time at very low demands is the same in both cases. If the two distributions do not match at very low flow rates, this may be an indication that the free-flow speed calibration step for the core method was not performed correctly.

In contrast, in the example shown in Exhibit 25-34, the predicted TTI values are consistently lower than the observed values, suggesting that the seed day has an unusually low demand level. To resolve the problem, the demand level on the seed day should be increased and additional reliability runs performed.

Exhibit 25-34
Low Demand Level on the Seed Day



Another calibration lever is to change the distribution of the demand multipliers over the days of the reliability reporting period. This effort can improve the calibration of the methodology; however, its outcome is harder to predict. Users should change the distribution only when they have additional field information about seasonal and daily changes in the demand level that can bring it closer to reality.

When adjusting the demand level, users should try to bring the estimated 50th percentile TTI value to within 10% of the field-observed value. This is an iterative process that requires adjusting either the seed day demand level or the distribution of the demand multipliers, performing an additional comprehensive reliability run, and comparing the modeled and field-measured 50th percentile TTI values.

Step 3: Calibrate Incident Probabilities

When the demand level is calibrated, the predicted and observed TTI distributions are expected to closely follow each other up to the 50th to 60th TTI percentiles. However, nonrecurring sources of congestion usually influence the higher percentiles of the TTI distribution. They may cause a drift in distributions for higher percentiles, as shown in Exhibit 25-35. The figure shows a match between the predicted (red) and observed (blue) TTI distributions, but then suggests an overestimation of TTIs for higher percentiles with the red curve shifted to the right. As a result, to more accurately calibrate the comprehensive reliability analysis, the focus should be on incident and weather events. Incidents are known to have a more considerable impact on congestion level, and therefore the model is calibrated for incidents first, followed by weather events.

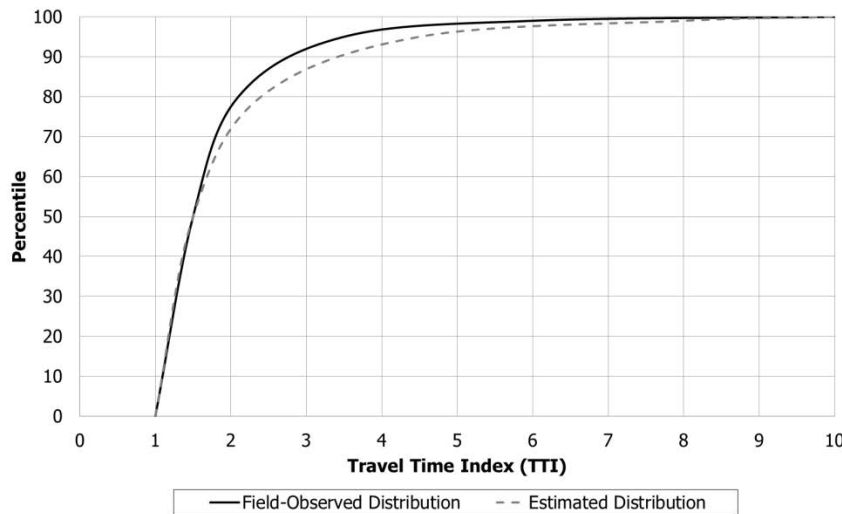


Exhibit 25-35
Overestimating the Impacts of
Nonrecurring Sources of
Congestion

Incidents can be calibrated by using a number of parameters as listed below:

1. Probability of incident severity for each month, or crash rate per 100 million vehicle-miles traveled for each month and crash-to-incident rate and incident severity distribution, depending on the approach used for scenario generation;
2. Incident duration attributes by severity type (mean, standard deviation, and distribution);
3. Capacity and speed adjustment factors by severity type; and
4. Demand adjustment factors by severity type.

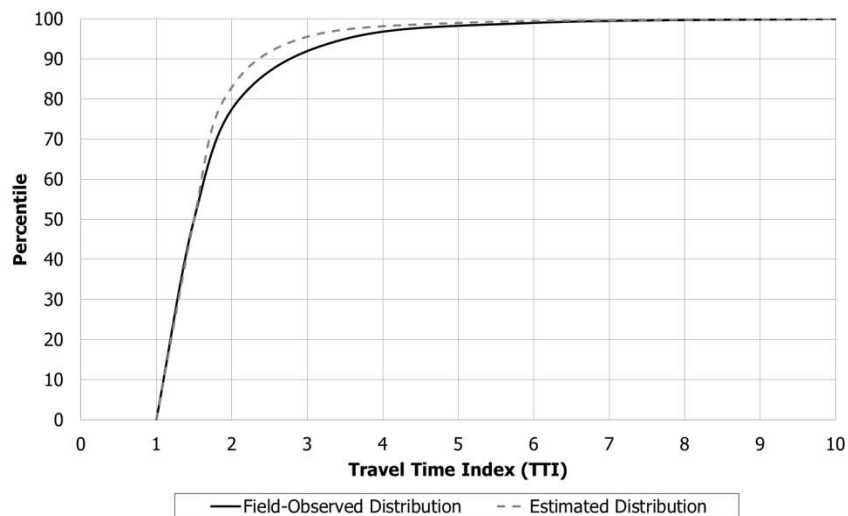
Incident attributes can be used to address overestimation in the tail of the predicted TTI distribution and to bring it closer to the observed distribution. For

the example shown in Exhibit 25-35, the predicted and observed TTI distributions almost match each other up to the 60th TTI percentile, indicating that the demand level and base congestion level (i.e., recurring congestion) are calibrated well. After the 60th percentile, the reliability methodology overestimated TTI values in this case.

To reduce TTI values, the analyst should start by reducing the crash rate or incident probability. The same effect is expected by reducing the demand adjustment factor (for incidents). Note that in the case of severe incidents, a significant reduction in the demand level is expected, as drivers start to reroute to avoid the congestion. Finally, increasing the capacity and speed adjustment factors are expected to reduce the impacts of incidents as well.

On the other hand, if the method underestimates TTI values at the tail of the distribution (see Exhibit 25-36), the user can increase the crash rate, incident probability, or demand adjustment factor. (Note that the maximum allowable value for the demand adjustment factor is 1.) In addition, reducing capacity and speed adjustment factors for incidents is expected to magnify the impacts of incidents on travel time and consequently increase TTI values.

Exhibit 25-36
Underestimating the Impacts of Nonrecurring Sources of Congestion



Step 4: Calibrate Weather Probabilities

Similar to incidents, weather events influence the tail of the TTI distribution, but to a lesser extent. The following calibration parameters are available:

1. Probability of different weather events by month,
2. Duration of each weather event,
3. Capacity and speed adjustment factors, and
4. Demand adjustment factor.

These calibration parameters are expected to impact the TTI distribution similarly to those parameters mentioned in Step 3 for incident calibration. Note that weather information is more likely to be accurate as it is based on 10 years of data, while incident data are more difficult to gather. In addition, incidents have a more considerable impact on the TTI distribution. Therefore, as mentioned

previously, it is recommended that the methodology be calibrated first through the demand and incident data, with the analyst turning to the weather-related parameters only if additional calibration is required.

For the example shown previously in Exhibit 25-35, the model overestimated TTI values in the tail of the distribution. The analyst can bring the two distributions closer to each other by reducing the probability of different weather events or by reducing their duration. The same effect is possible by increasing the capacity and speed adjustment factors or by reducing the demand adjustment factor. Note that in the case of extreme weather events, a significant reduction in the demand level is expected as travelers might decide to cancel their trips. However, data on such trends are very scarce and hard to collect. It is recommended that analysts adjust the demand adjustment factors only when there is evidence or knowledge of the trends on the study facility.

On the other hand, when the methodology underestimates TTI values in the tail of the distribution, as in Exhibit 25-36, the analyst can increase the probability of weather events or increase their durations. In addition, a reduction in capacity and speed adjustment factors is expected to move the distribution to the right.

Step 5: Validation

Changing all of the calibration parameters at the same time might lead to unexpected results. Therefore, the user is encouraged to change only one parameter at a time, run the comprehensive reliability methodology, plot and evaluate the new TTI distribution, and only then decide whether and how to change other parameters. The use of a computational engine makes running repeated reliability analyses with changing inputs a straightforward process.

The analyst should try to bring at least the predicted 80th and 95th percentile TTI values within 10% of the field-observed values. Preferably, additional percentiles should match the field data, although a perfect match may not be achievable. The collected field data should span the same reliability reporting period that was selected for the analysis, to ensure that results are comparable.

CALIBRATION AT THE RELIABILITY STRATEGY ASSESSMENT LEVEL

Calibration at the reliability strategy assessment level is only possible for strategies that have already been implemented in the field. For other strategies, calibration is not possible, other than based on expert judgment or comparison to an alternative tools analysis. However, the user can run a set of sensitivity analyses for each strategy to identify the trends and make sure that they match expectations. For example, a ramp-metering strategy is expected to shift the TTI distribution to the left, toward lower TTI values. The lower the metering rate, the larger the expected shift. If such a trend is observed, and if its extent is in a reasonable range, one can conclude that methodology works reasonably.

Similar to the calibration procedure at the comprehensive reliability level, the analyst must first gather all input data on facility geometry, free-flow speed, and demand level. Note that an important assumption is that the demand, incident, and weather calibration parameters are already fixed in the comprehensive

reliability calibration step. As a result, the analyst is left with the remaining calibration parameters that are specific to each scenario.

In general, different scenarios may change a facility's free-flow speed, capacity, demand, incident probability, and average incident duration. Therefore, "scenario-specific" calibration parameters are

1. Speed adjustment factor,
2. Capacity adjustment factor,
3. Metering rate,
4. Demand adjustment factor,
5. Incident probability, and
6. Average incident duration.

It is recommended that the analyst make a reliability strategy assessment run based on a combination of field measurements and default values, plot the predicted TTI distribution, and then compare the result to the field observation. Similar to the comprehensive reliability calibration procedure, the analyst can then make changes in the calibration parameters to bring the predicted distribution closer to the observed one.

Based on the modifications that each strategy makes in the freeway methodology, the user can adjust the corresponding calibration parameters. Similar to calibrating the comprehensive reliability methodology, increasing the speed adjustment factor is expected to reduce travel time across the facility, while reducing it has an opposite effect. Increasing the value of the capacity adjustment factor is expected to reduce the facility travel time. Increasing the metering rate will allow more vehicles to enter the mainline and is expected to increase the facility travel time and perhaps activate bottlenecks in merge areas. On the other hand, reducing the metering rate is likely to reduce travel time across the facility and eliminate bottlenecks at merge areas. Increasing the demand adjustment factor is expected to increase travel time throughout the facility and shift the TTI distribution toward larger TTI values, while reducing it has the opposite effect. Increasing the incident probability is expected to shift the tail of the TTI distribution toward higher TTI values, while reducing it shifts the tail toward lower values. Finally, changing the average incident duration is expected to influence the TTI distribution similarly to incident probability.

The analyst should avoid making several changes in calibration parameters at the same time, as this may result in changes in TTI distribution that are hard to explain and may make the calibration procedure more difficult. Instead, analysts should select one calibration parameter at a time, make changes, rerun the strategy assessment procedure, plot the TTI distribution, compare it to the field distribution, and make other changes as necessary.

The user needs to first identify the main source of difference between the predicted and field TTI distributions. If a difference between the two distributions is observed throughout all ranges of TTIs (similar to Exhibit 25-33 and Exhibit 25-34), changing parameters such as the speed adjustment factor, capacity adjustment factor, demand adjustment factor, and metering rate is

expected to bring the two distributions closer. The analyst should aim for a maximum of 10% difference between the 50th percentile of the predicted and observed TTI distributions at this stage.

On the other hand, if the difference between TTI distributions is observed mostly in the tail of the distribution (similar to Exhibit 25-35 and Exhibit 25-36), changing the incident probability and duration is expected to move the predicted distribution to the right. The analyst should aim for a maximum 10% difference between the 80th and 95th percentiles of the predicted and observed TTI distributions at this stage as well.

9. FREEWAY SCENARIO GENERATION

INTRODUCTION

This section provides details of the freeway scenario generation process. An overview of this process is provided in Chapter 11, Freeway Reliability Analysis, and elsewhere (17).

Freeway scenario generation utilizes a hybrid process, which includes deterministic and stochastic methods for modeling traffic demand, weather events, work zones, and incidents. The freeway reliability methodology uses a deterministic, calendar-based approach to model traffic demand levels and scheduled, significant work zone events. It uses a stochastic (Monte Carlo) approach to assign the occurrence of incident and weather events to scenarios. The method enumerates the different operational conditions on a freeway facility on the basis of varying combinations of factors affecting the facility travel time. Each unique set of operational conditions constitutes a *scenario*. A single replication of a scenario represents a unique combination of a day of week and month of year. The following seven principal stages, depicted in Exhibit 25-37, are involved in the scenario generation process:

- Stage 1, based on the user inputs, computes the number of different demand combinations and the resulting number of scenarios, along with their probabilities. These values also depend on the duration of the reliability reporting period.
- Stage 2 uses local traffic demand data to characterize the demand levels in the generated scenarios in a deterministic, calendar-based manner.
- Stage 3 incorporates scheduled work zones deterministically based on the calendar.
- Stage 4 incorporates published local weather event information, and generates the number and type of weather events, consistent with local data.
- Stage 5 randomly assigns the generated weather events in Stage 4 to the scenarios generated in Stage 1.
- Stage 6 utilizes the local crash or incident database to generate the number and severity of incident events, consistent with local data.
- Stage 7 randomly assigns incidents and their characteristics to each generated scenario in Stage 1.

The time frame within a given day when the reliability analysis is performed is called a *study period*. It consists of several contiguous 15-min *analysis periods*, which is the smallest temporal unit of analysis. The smallest spatial unit on the facility is an HCM analysis segment (see Chapters 12–14). The reliability reporting period is the time period over which the travel time distribution is generated (typically, but not necessarily, one year).

Each scenario representing a study period is characterized by a unique set of segment capacities, demands, free flow speeds, and number of lanes, for both

general purpose and managed lane segments on the freeway facility. Various scenarios are created by adjusting one or more of the above parameters. A probability value is associated with each scenario that represents its likelihood of occurrence. This probability is computed on the basis of the number of scenarios and replications.

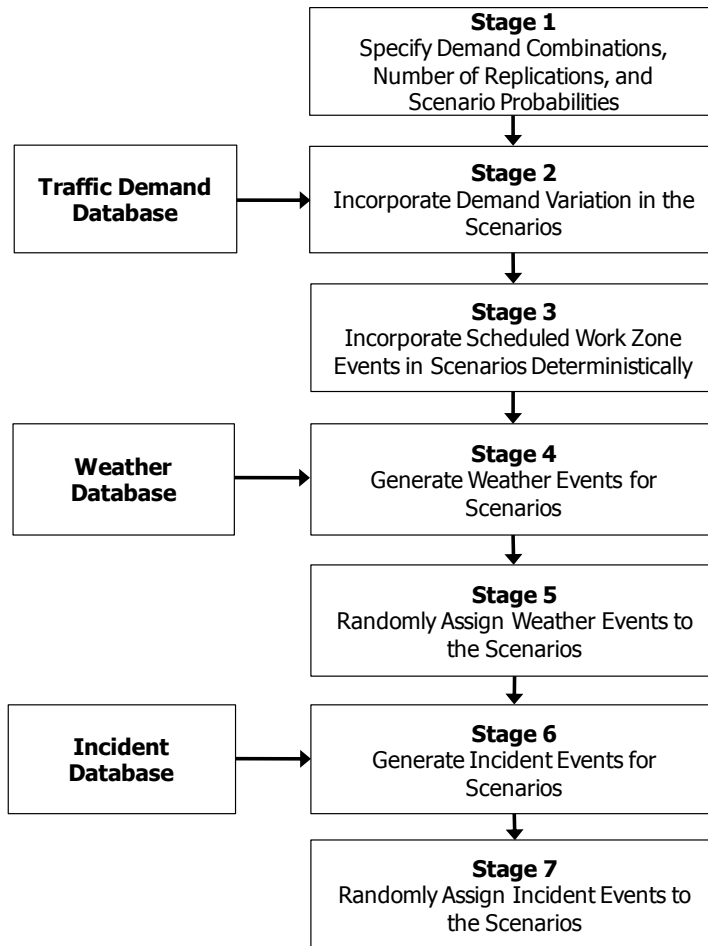
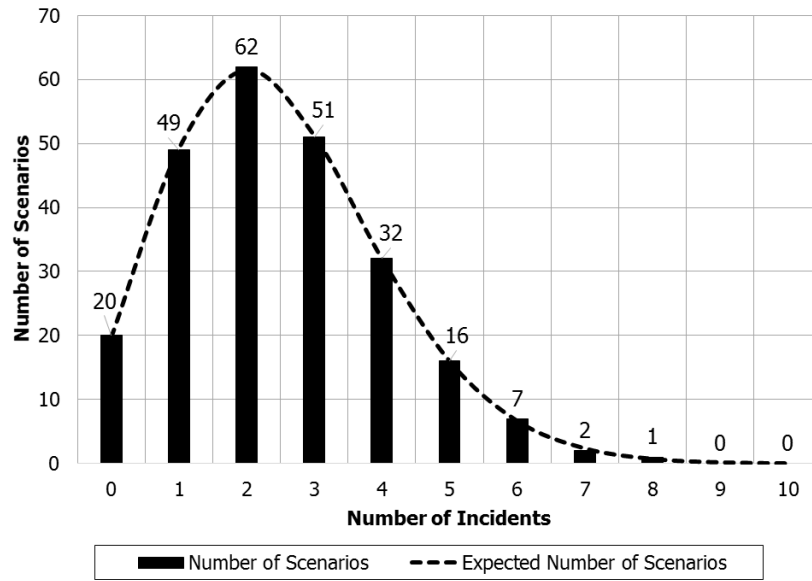


Exhibit 25-37
Process Flow Overview for
Freeway Scenario Generation

Scenarios are generated in such a manner that the characteristics of the factors affecting travel time within scenarios best match the input, field-observed conditions. For example, the distribution of the number of incidents generated in various scenarios should yield a distribution similar to that observed in the field. Exhibit 25-38 depicts such an example, in which the number of incidents modeled in all scenarios (histogram) is designed to match field-observed values (curve).

Exhibit 25-38
Distribution of Number of Incidents in the Scenarios



Therefore, the process of generating scenarios effectively turns into an optimization problem. The objective is to maximize the match (or minimize the difference) between the predicted and field-observed distributions by assigning appropriate traffic demand levels, weather events, work zones, and incidents within the different scenarios. Eight distributions are considered in the scenario generation procedure:

1. Temporal distribution of traffic demand level (typically expressed as a ratio of scenario demand to AADT),
2. Temporal distribution of weather event frequency (by calendar month, randomly assigned to scenarios),
3. Distribution of average weather event duration by weather event type (by calendar month),
4. Temporal distribution of incident event frequency (by calendar month, weighted in the facility by segment VMT),
5. Distribution of incident severity (user specified),
6. Distribution of incident duration by severity (user specified),
7. Distribution of incident event start time (random), and
8. Spatial distribution of incident events (random).

The scenario generation method attempts to generate scenarios such that all eight specified distributions match field observations, with consideration for the need to round to integer values and to the 15-min duration of the analysis period. Such rounding is not likely to generate any significant systematic bias in the analysis.

METHODOLOGY

The freeway reliability scenario generation methodology consists of 34 steps. Exhibit 25-39 shows the methodology's process flow. Note that when managed lanes are present on the facility, the reliability scenarios should also consider their varying operational characteristics. The methodology assumes traffic demand levels and weather events affect both general purpose and managed lane operations simultaneously. However, the methodology does not account for scheduled work zone events on the managed lanes. Analysts should repeat Steps 19–34 should they desire to model incident events on the managed lanes separately. An explanation of each step in the process flow follows. All variables used in this section are defined in Section 2.

Step 1: Prepare Necessary Data for the Reliability Analysis

In this step, the analyst provides all necessary data for executing the scenario generation method. The starting point is preparing a complete seed file describing the facility's demand and geometry for a single study period. Developing the seed file is akin to developing a data set for the core methodology, as described in Chapter 10. In addition, for scenario generation purposes, additional data must include (a) the start and end clock times of the study period, (b) the duration of the reliability reporting period, (c) the seed file date, (d) the series of demand multipliers (see Step 4) for each demand combination, (e) the nearest metropolitan area to the facility (for weather station data), (f) the crash or incident rates by month of year on the facility, and (g) other local inputs.

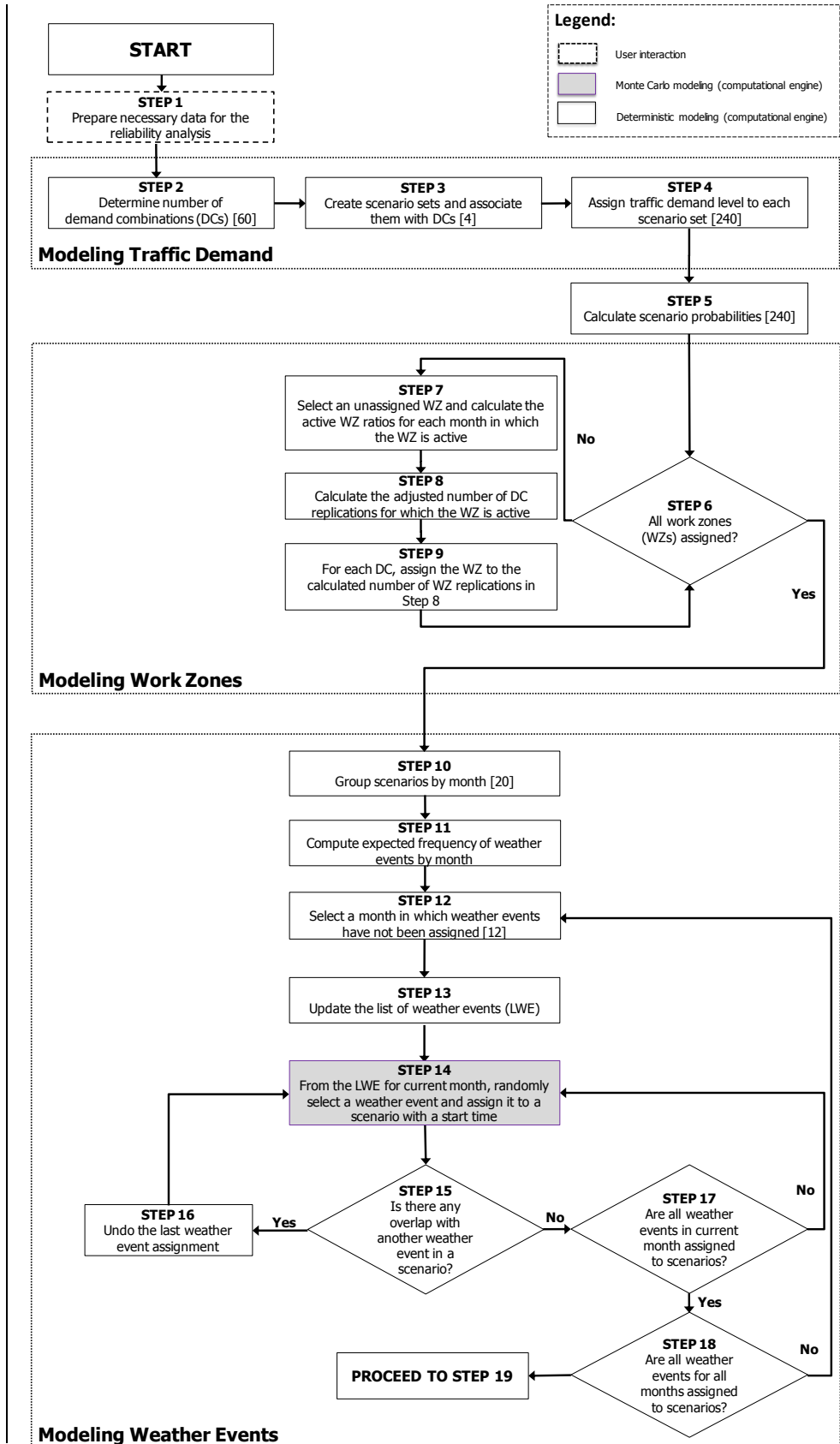
Step 2: Determine the Number of Demand Combinations

The freeway scenario generation method defines a demand combination as the combination of a specific weekday and month of year. Although demand levels in different demand combinations might be very similar (e.g., Tuesday and Wednesday afternoon volumes), the methodology handles them separately to keep the process simple. For a 1-year, weekday-only analysis, there are 60 such combinations (5×12). The number of demand combinations is defined by the variable N_{DC} .

Step 3: Create Scenario Sets and Associate Them with Demand Combinations

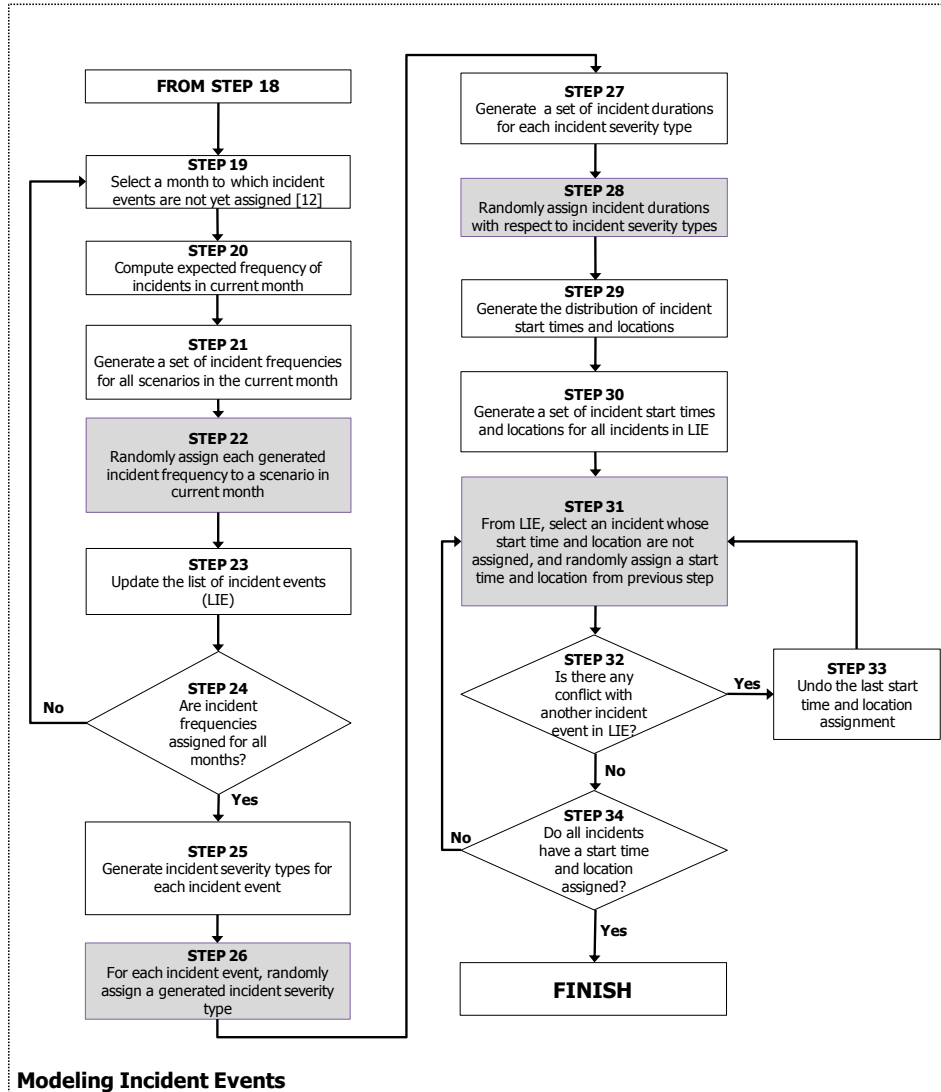
As a default, the methodology creates four scenario *replications* for each demand combination. The rationale behind four replications is that each demand combination usually consists of four or five calendar days. However, if a short-duration reliability reporting period is considered, the number of replications must be increased to capture sufficient variability in the travel time distribution. Typically, however, the default number of scenarios for a 1-year, weekday-only analysis would be $4 \times 60 = 240$ scenarios. The method allows the analyst to specify the number of replications per reliability analysis.

Exhibit 25-39
Detailed Freeway Scenario
Generation Flowchart



Note: Numbers in brackets are default values.

Exhibit 25-39 (cont'd.)
Detailed Freeway Scenario
Generation Flowchart



Modeling Incident Events

Note: Numbers in brackets are default values.

For each scenario, a set of adjustment factors is created for capacity, speed, demand, and number of lanes (CAF, SAF, DAF, and NLAF, respectively). At this point, each scenario contains default values for CAF, SAF, and DAF (all equal to 1) and NLAF (equal to 0), but the scenarios do not yet contain any demand, weather, or incident data. N_{scen} represents the total number of scenarios and is computed as:

$$N_{scen} = 4 \times N_{DC}$$

Equation 25-71

Step 4: Assign a Traffic Demand Level to Each Scenario Set

In this step, a traffic demand level is assigned to each scenario set (i.e., the number of replications used per scenario). For this purpose, demand multipliers, representing the ratio of the traffic demand level in each demand combination to the AADT are used to generate each scenario demand level. Because each scenario is associated with a unique demand combination, the ratio of the

Equation 25-72

$$DAF_s(tp, seg) = \frac{DM(s)}{DM(Seed_{tp})} \quad \forall tp \in SP \text{ and } seg \in Segments$$

where

$DAF_s(tp, seg)$ = demand adjustment factor for scenario s , period tp , and segment seg ;

$DM(Seed_{tp})$ = demand multiplier associated with the seed file; and

$DM(s)$ = demand multiplier associated with scenario s .

The process to calculate any demand value of any cell in a scenario is to multiply the cell demand value in the corresponding seed file (for the same HCM segment and analysis period) with the appropriate DAF, as shown in Equation 25-72. Note that if the facility contains managed lanes, the traffic demand level generated in this step will be effective for both the general purpose and managed lanes.

Step 5: Calculate Scenario Probabilities

The probability of a scenario occurrence is strictly a function of the number of days in the associated demand combination. Note that the probability of a scenario is fixed at this step and will not be altered in any subsequent steps. Simply stated, the probability of each scenario does not change by incorporating weather and incident events. The probability of each scenario is computed based on Equation 25-73.

Equation 25-73

$$P\{s\} = \frac{n_{Day,DC_s}}{4 \times \sum_{k=1}^{N_{DC}} n_{Day,k}}$$

where

$P\{s\}$ = probability of scenario s ,

DC_s = demand combination associated with scenario s ,

$n_{Day,k}$ = number of days in the reliability reporting period associated with demand combination k (typically four for a 1-year weekday analysis), and

N_{DC} = number of demand combinations.

After computing each scenario's probability, the probabilities are assigned to the scenarios created in Step 3. The probability of a scenario is a function of the number of days in the associated demand combination, which is typically four or five for a whole-year analysis. For a typical 1-year, weekday-only analysis, the probability of each scenario is approximately 1/240 or 4.33%.

Step 6: Determine Whether All Work Zones Have Been Assigned

If there are no scheduled work zones during the reliability reporting period, or if all scheduled work zones have been assigned to scenarios, the process flow proceeds to Step 10. Otherwise, the process moves to Step 7 and assigns the next

work zone. If there are no work zones considered in the reliability analysis, the process flow proceeds to Step 10.

Step 7: Calculate Active Work Zone Ratios

In this step, the parameter r_{DC} is calculated. This parameter is the ratio of each weekday type in which the work zone is active in a given month to the total number of each weekday type occurring in a given month. An unassigned work zone event is selected, and r_{DC} is calculated for each month in which the work zone is active.

Step 8: Calculate the Adjusted Number of Replications

For each affected demand combination in which a work zone is present, Equation 25-74 is used to calculate $\bar{N}_{DC,WZ}$, the adjusted number of replications of a demand combination for which the work zone is active.

$$\bar{N}_{DC,WZ} = \text{round}(r_{DC} \times N_r, 0)$$

Equation 25-74

Step 9: Assign the Work Zone to the Work Zone Replications

For each demand combination of each month in which the work zone is active, assign the work zone to the adjusted number of replications of each demand combination (equivalently scenarios) calculated in Step 8.

Step 10: Group Scenarios by Month

The attributes of inclement weather events are assumed to vary only by the month of the year. As such, in Step 10, all scenarios associated with a given month of year are grouped. Typically, this step involves grouping 20 scenarios (four replications of five weekdays each per month.)

Step 11: Compute the Expected Frequency of Weather Events by Month

The method uses the expected frequencies of weather events to create and characterize weather events. Historical data are used to estimate the probability, average duration, and standard deviation of duration of different weather conditions. Weather event likelihoods are reported in timewise probabilities that were computed for 103 metropolitan areas in the United States on the basis of 10 years of data. The resulting probability tables are provided as resource material in the Technical Reference Library in online HCM Volume 4. A listing of the 97 locations used to create the weather data is provided in Exhibit 25-40.

Only weather events that reduce capacity by more than 5% are included in the probability calculations. The average event duration and the standard deviation for each weather category are calculated by using the 10-year weather data set for each weather station. The probability of weather event type i in month j is found from Equation 25-75.

$$P_W\{i, j\} = \frac{\text{Sum of all SP durations in minutes in month } j \text{ that weather type } i \text{ is present}}{\text{Sum of all SP durations in minutes in month } j}$$

Equation 25-75

where SP indicates study period, and $P_w\{i, j\}$ is the probability of encountering weather type i in month j .

Exhibit 25-40
Listing of Weather Stations
with Available Weather Data

#	Airport Code	City, State	#	Airport Code	City, State
1	KBHM	Birmingham, AL	50	KGSO	Greensboro, NC
2	KLIT	Little Rock, AR	51	KRIC	Raleigh, NC
3	KPHX	Phoenix, AZ	52	KOMA	Omaha, NE
4	KTUS	Tucson, AZ	53	KABQ	Albuquerque, NM
5	KBFL	Bakersfield, CA	54	KLAS	Las Vegas, NV
6	KFAT	Fresno, CA	55	KALB	Albany, NY
7	KLAX	Los Angeles, CA	56	KBUF	Buffalo, NY
8	KMOD	Modesto, CA	57	KLGA	New York, NY
9	KCMA	Oxnard, CA	58	KPOU	Poughkeepsie, NY
10	KROC	Riverside, CA	59	KSAC	Rochester, NY
11	KSAN	Sacramento, CA	60	KSYR	Syracuse, NY
12	KSAT	San Diego, CA	61	KCAK	Akron, OH
13	KSJC	San Francisco, CA	62	KCVG	Cincinnati, OH
14	KSLC	San Jose, CA	63	KCLE	Cleveland, OH
15	KSDF	Stockton, CA	64	KCMH	Columbus, OH
16	KCOS	Colorado Springs, CO	65	KDAY	Dayton, OH
17	KDEN	Denver, CO	66	KTOL	Toledo, OH
18	KBDL	Hartford, CT	67	KYNG	Youngstown, OH
19	KDCA	Washington, DC	68	KOKC	Oklahoma City, OK
20	KFMY	Cape Coral, FL	69	KTUL	Tulsa, OK
21	KJAX	Jacksonville, FL	70	KPDX	Portland, OR
22	KTPA	Lakeland, FL	71	KABE	Allentown, PA
23	KMIA	Miami, FL	72	KMDT	Harrisburg, PA
24	KSRQ	North Port, FL	73	KLNS	Lancaster, PA
25	KMCO	Orlando, FL	74	KPHL	Philadelphia, PA
26	KMLB	Palm Bay, FL	75	KPIT	Pittsburgh, PA
27	KATL	Atlanta, GA	76	KAVP	Scranton, PA
28	KAGS	Augusta, GA	77	KPVD	Providence, RI
29	PHNL	Honolulu, HI	78	KCHS	Charleston, SC
30	KDSM	Des Moines, IA	79	KCAE	Columbia, SC
31	KBOI	Boise City, ID	80	KGSP	Greenville, SC
32	KORD	Chicago, IL	81	KCHA	Chattanooga, TN
33	KIND	Indianapolis, IN	82	KTYS	Knoxville, TN
34	KICT	Wichita, KS	83	KMEM	Memphis, TN
35	KSEA	Louisville, KY	84	KBNA	Nashville, TN
36	KBTR	Baton Rouge, LA	85	KAUS	Austin, TX
37	KMSY	New Orleans, LA	86	KDFW	Dallas, TX
38	KBOS	Boston, MA	87	KELP	El Paso, TX
39	KCEF	Springfield, MA	88	KIAH	Houston, TX
40	KORH	Worcester, MA	89	KMFE	McAllen, TX
41	KBWI	Baltimore, MD	90	KSCK	San Antonio, TX
42	KPWM	Portland, ME	91	KOGD	Ogden, UT
43	KDTW	Detroit, MI	92	KPVU	Provo, UT
44	KGRR	Grand Rapids, MI	93	KRIV	Richmond, VA
45	KMSP	Minneapolis, MN	94	KORF	Virginia Beach, VA
46	KMCI	Kansas City, MO	95	KSFO	Seattle, WA
47	KSTL	St. Louis, MO	96	KMSN	Madison, WI
48	KJAN	Jackson, MS	97	KMKE	Milwaukee, WI
49	KCLT	Charlotte, NC			

Source: Zegeer et al. (18).

Equation 25-76 is used to convert those reported probabilities into rounded expected monthly weather event frequencies.

Equation 25-76

$$E[n_w, j] = \text{round} \left(\frac{P_t\{w, j\} \times D_{SP} \times N_{Scen, j}}{E_{15min}[D_w]} \right)$$

where

$E[n_w, j]$ = expected frequency of weather event w in month j , rounded to the nearest integer;

$P_i\{w, j\}$ = timewise probability of weather type w in month j ;

D_{SP} = duration of study period SP (h);

$N_{Scen,j}$ = number of scenarios associated with month j of the reliability reporting period; and

$E_{15min}[D_w]$ = expected duration of weather event w rounded to the nearest 15-min increment.

In this step, the $E[n_w, j]$ values for each weather type w are computed in each month j of the reliability reporting period. Note that the unit of the expected frequency is *events per total scenario hours in each month*. Also note that the minimum value for $E_{15min}[D_w]$ is 0.25 h.

For example, if the study period is 5 h, if the probability of light rain during that month and time period (typically associated with about 20 scenarios) is 0.10, and if the average light rain event lasts 1 h, then the expected number of light rain events in that month is $(0.1 \times 5 \times 20)/1$, which rounds to 10 light rain weather events in that month, or 10 h of light rain in the month.

Step 12: Select a Month with Unassigned Weather Events

The process of assigning weather events in a month is independent of other months in the reliability reporting period. The process is carried out on a monthly basis. For this purpose, one month from the reliability reporting period without an assigned weather event is selected in the next steps.

Step 13: Update the List of Weather Events

In this step, the list of weather events is updated. That is, the weather events associated with the current month will have their characteristics (durations, CAFs, and SAFs) assigned.

Step 14: Assign Weather Events and Start Times to Scenarios

In this step, a weather event that was updated in the list of weather events in Step 13 is selected and randomly assigned to a scenario in the current month. The assignment of weather events to scenarios is carried out consistent with the relative scenario probabilities. In addition, a start time is randomly assigned to the selected weather event from the list of weather events. Because actual data on the start time of weather events are lacking, those are assigned randomly based on a uniform distribution.

Step 15: Identify Overlaps Between Weather Events in a Single Scenario

This step ensures there will be no temporal overlap between two weather events within a single scenario. Possible overlaps between weather events are checked, and if they exist, then Step 16 is executed. Otherwise, the process moves to Step 17.

Step 16: Undo the Most Recent Weather Event Assignment

If there is an overlap between weather events, the most recent weather assignment is undone. The process then goes back to Step 14 to reassign a scenario and a start time for the weather event.

Step 17: Check for Unassigned Weather Events in the Current Month

This step checks that all weather events present in the list of weather events have been assigned. If one or more unassigned weather events exist for the current month, the process returns to Step 14 to select another unassigned weather event.

Step 18: Check for Unassigned Weather Events in All Months

Once all weather events have been assigned to scenarios across all months in the reliability reporting period, the methodology proceeds to the incident modeling stage. Otherwise, the process returns to Step 12 to select another month from the reliability reporting period to have its weather events modeled in the associated scenarios.

Step 19: Select a Month with Unassigned Incidents

The methodology allows the user to directly enter monthly incident occurrences on a given facility during the study period into the procedure, should these values be available. Optimally, the distribution of incident durations, the start times, and the distribution of incidents by severity (e.g., number of lanes closed) could also be entered directly from a local incident database.

However, in most cases (including predictive reliability applications), these data will not be available, and incident events will need to be estimated from incident or crash rates (which vary by month and traffic demand levels). The methodology accounts for the correlation between incident and crash-only rates. Because the method attempts to generate the number of incident events based on their distributions, a high number of incidents could be assigned to a scenario that is associated with a low traffic demand level. The average traffic demand level for each month is therefore computed and used to characterize the incident events within scenarios in each month. Incident events are assigned to different months of the reliability reporting period independently. Therefore, a month from the reliability reporting period without any assigned incidents is first selected in the next steps.

Step 20: Compute the Expected Incident Frequency

The expected frequency of all incidents on the facility per study period in a given month j is computed with Equation 25-77.

$$n_j = IR_j \times VMT_j$$

where

n_j = expected frequency of all incidents in the study period for month j , rounded to the nearest integer;

IR_j = incident rate per 100 million VMT in month j ; and

Equation 25-77

VMT_j = average vehicle miles traveled for scenarios in month j , after adjusting the demand in the base scenario with the appropriate demand multipliers and multiplying by the facility length in miles.

If IR_j is not locally available, Equation 25-78 can be used to estimate it.

$$IR_j = CR_j \times ICR$$

Equation 25-78

where CR_j is the local facilitywide crash rate per 100 million VMT in month j and ICR is the local incident-to-crash ratio. In the absence of other data, a national default value for ICR is 4.9.

When the crash rate is not available locally, the Highway Economic Requirements System (HERS) model can be used to estimate it (19). Agencies may also use other predictive models such as the *Highway Safety Manual* (20). The crash or incident rate is estimated per 100 million VMT. The HERS model uses Equation 25-79 to estimate the crash rate.

$$CR = (154.0 - 1.203 \times ACR + 0.258 \times ACR^2 - 0.00000524 \times ACR^5) \times e^{0.0082 \times (12 - LW)}$$

Equation 25-79

where CR is the crash rate per 100 million VMT, ACR is the facility AADT divided by its two-way hourly capacity, and LW is the lane width in feet.

Step 21: Generate a Set of Incident Frequencies

The distribution of the number of incidents in a study period can be characterized by a Poisson distribution. Assume there are $N_{Scen,j}$ scenarios (typically 20) associated with the current month j . Then, on average, $n_j \times N_{Scen,j}$ incidents (rounded to the nearest integer) need be to generated and assigned to scenarios. Therefore, a set of $N_{Scen,j}$ numbers should be generated that best matches a Poisson distribution with a mean value of n_j , per Equation 25-80.

For this purpose, an adjustment parameter δ_1 is defined. By solving Equation 25-80, the frequency of incidents for a set of $N_{Scen,j}$ scenarios can be computed, following the Poisson distribution. The values of the adjustment parameter usually hover around 1 and are estimated from the equality.

$$\sum_{k=0}^{+\infty} (\text{round}[\delta_1 \times N_{Scen,j} \times \text{Prob}\{n_{inc} = k\}]) = N_{Scen,j}$$

Equation 25-80

where n_{inc} is the number of incidents and other variables are as defined previously. Subsequently, the number of scenarios that are assigned k incidents ($k = 0 \rightarrow \infty$) is determined by Equation 25-81.

$$\text{Number of Scenarios with } k \text{ incident events} = \text{round}[\delta_1 \times N_{Scen,j} \times \text{Prob}\{n_{inc} = k\}]$$

Equation 25-81

where all variables are as defined previously. By setting different k -values in the above equation, a set of monthly incident frequencies will be generated in this step.

Step 22: Assign Incidents to Scenarios

The incidents generated in Step 21 are randomly assigned to the scenarios associated with the current month. A random number is drawn with respect to scenario probabilities to determine the assigned scenario number.

Step 23: Update the List of Incident Events

The list of incident events is updated after the incident frequencies are generated. This list holds information for each incident event in the entire reliability analysis. The associated incident event information includes the assigned scenario number, calendar month, incident duration, incident impact factors (e.g., CAF, SAF), incident segment location, and incident start time.

Step 24: Check for Unassigned Incidents

This step ensures that incident event frequencies are generated and assigned to scenarios for all months in the reliability reporting period. Once incidents in all months have been processed in Steps 20–23, the scenario generation process continues to Step 25.

Step 25: Generate Incident Severities for Each Incident Event

A set of incident severities is generated for the entire set of incidents developed in Step 21. Note that this step is not carried out on a monthly basis. The distribution of incident severities must be known a priori for incorporation in the methodology. This distribution is defined by $\mathbb{G}(i)$, which is assumed to be homogeneous across the facility and different demand levels.

Agencies can estimate this distribution by analyzing their incident logs or they can use national default values. Equation 25-82 gives the definition of $\mathbb{G}(i)$ as a discrete distribution, where i denotes the incident severity type (e.g., $i = 1$ is a shoulder closure, and $i = 5$ is a four-lane closure).

Equation 25-82

$$\mathbb{G}(i) = \begin{cases} \mathcal{G}_1 & i = 1 \\ \mathcal{G}_2 & i = 2 \\ \mathcal{G}_3 & i = 3 \\ \mathcal{G}_4 & i = 4 \\ \mathcal{G}_5 & i = 5 \end{cases}$$

Suppose a total of $N_{Scen,Inc}$ incidents was generated in Steps 19–24. To generate incident severities, an adjustment parameter δ_2 is defined. By solving Equation 25-83, incident severities for all incidents in the list of incident events will be estimated that will follow the prespecified $\mathbb{G}(i)$ distribution.

Equation 25-83

$$\sum_i (\text{round}[\delta_2 \times N_{Scen,Inc} \times \mathbb{G}(i)]) = N_{Scen,Inc}$$

where all variables are as previously defined. The adjustment parameter is determined with Equation 25-83, and the number of scenarios that are assigned incident severity type i is determined by Equation 25-84.

Equation 25-84

Number of incidents with severity $i = (\text{round}[\delta_2 \times N_{Scen,Inc} \times \mathbb{G}(i)])$
 where all variables are as previously defined.

The distribution of incident severity $G(i)$ is shown in Equation 25-85. These values are based on national default values (18).

$$G(i) = \begin{cases} 0.754 & i = 1 \text{ (shoulder closed)} \\ 0.196 & i = 2 \text{ (one lane closed)} \\ 0.031 & i = 3 \text{ (two lanes closed)} \\ 0.019 & i = 4 \text{ (three lanes closed)} \\ 0 & i = 5 \text{ (four or more lanes closed)} \end{cases}$$

Equation 25-85

Step 26: Assign Incident Severity Type

The incident severities generated in Step 25 are randomly assigned to the incidents in the list of incident events.

Step 27: Generate Incident Durations by Incident Severity Type

The duration of each incident severity type is assumed to follow a lognormal distribution (15). Exhibit 25-41 shows default parameters for the incident duration distribution developed through research (18).

Statistics	Shoulder	No. of Lanes Closed		
		1	2	3 or more
Range	8.7–58	16–58.2	30.5–66.9	36–93.3
Average	34.0	34.6	53.6	69.6
Median	36.5	32.6	60.1	67.9
Standard deviation	15.1	13.8	13.9	21.9

Exhibit 25-41
Incident Duration Distribution Parameters in Minutes

Because $N_{Inc,i}$ incidents are associated with severity i , a set of $N_{Inc,i}$ numbers can be generated that best matches a lognormal distribution of incident durations. For this purpose, an adjustment parameter δ_3 is defined, as shown in Equation 25-86.

$$\sum_t (\text{round}[\delta_3 \times N_{Inc,i} \times \text{Prob}\{Inc_{Dur} = t, Inc_{Type} = i\}]) = N_{Inc,i}$$

Equation 25-86

where Inc_{Dur} is the incident duration in minutes, Inc_{Type} is the incident severity type (1–5, as listed in Equation 25-85), and other variables are as defined previously.

By solving Equation 25-86, the adjustment parameter is determined. The number of scenarios that are assigned an incident duration t are then determined by Equation 25-87.

$$\text{Number of scenarios assigned incident severity } i = \text{round}[\delta_3 \times N_{Inc,i} \times \text{Prob}\{Inc_{Dur} = t, Inc_{Type} = i\}]$$

Equation 25-87

where all variables are as defined previously.

By inserting different t -values in Equation 25-87, a set of incident durations for each incident severity type will be generated.

Step 28: Randomly Assign Incident Durations by Severity

The incident durations generated in Step 27 are randomly assigned to the incidents in the list of incident events on the basis of the incident severity.

Step 29: Generate the Distribution of Incident Start Times and Locations

In this step, the distribution of each incident start time and location is assigned based on Step 20, with the likelihood of having an incident on a segment in a given analysis period being correlated to the segment VMT. The distribution of incident start times will coincide with the distribution of facility VMT across all analysis periods. Further, the distribution of the location of an incident will be similarly tied to the distribution of VMT for each segment across the study period. Since $VMT_{seg,u}$ represents the VMT on segment seg during analysis period u in the seed file, the distribution of the incident locations will be determined by Equation 25-88.

Equation 25-88

$$\text{Prob}\{\text{Location} = \text{segment } x\} = \frac{\sum_u VMT_{x,u}}{\sum_{seg,u} VMT_{v,u}}$$

where $Location$ is the segment in which the incident occurs.

In a similar manner, the distribution of the incident start time will be determined by Equation 25-89.

Equation 25-89

$$\text{Prob}\{\text{StartTime} = \text{analysis period } y\} = \frac{\sum_v VMT_{v,y}}{\sum_{v,u} VMT_{v,u}}$$

where $StartTime$ is the analysis period in which the incident starts.

Step 30: Generate Incident Start Times and Locations for All Incidents

Assuming there are $N_{Scen,Inc}$ incidents in the list of incident events, two sets of $N_{Scen,Inc}$ numbers should be generated that best match the incident start time and location distributions. For this purpose, two adjustment variables, δ_4 and δ_5 , are defined by Equation 25-90 and Equation 25-91, respectively.

Equation 25-90

$$\sum_x (\text{round}[\delta_4 \times N_{Scen,Inc} \times \text{Prob}\{\text{Location} = x\}]) = N_{Scen,Inc}$$

Equation 25-91

$$\sum_y (\text{round}[\delta_5 \times N_{Scen,Inc} \times \text{Prob}\{\text{StartTime} = y\}]) = N_{Scen,Inc}$$

By solving Equation 25-90 and Equation 25-91, the adjustment parameters are determined. The number of incidents that are assigned to any segment seg are then determined from Equation 25-92.

Equation 25-92

$$\text{Number of incidents assigned to segment } seg = \text{round}[\delta_4 \times N_{Scen,Inc} \times \text{Prob}\{\text{Location} = seg\}]$$

Finally, the number of incidents that are assigned a starting time (analysis period tp) is determined from Equation 25-93.

Equation 25-93

$$\text{Number of incidents assigned a starting time in analysis period } tp = \text{round}[\delta_5 \times N_{Scen,Inc} \times \text{Prob}\{\text{StartTime} = tp\}]$$

By inserting different seg and tp values in the above equations, a set of incident locations and start times will be generated.

Step 31: Assign Start Times and Locations to Incidents

In this step, an incident from the list of incident events is selected whose start time and location have not been assigned. A start time and location already generated in Step 30 are randomly assigned to the selected incident.

Step 32: Check for Overlap with Previously Assigned Incidents

This step checks if there is any overlap between other incident events for which the start time and location have been assigned in the list of incident events. If there is an overlap, the process proceeds to Step 33. Otherwise, it proceeds to Step 34.

Step 33: Undo the Previous Start Time and Location Assignment

This step undoes the previous start time and location assignment from Step 31 that led to the identification of a conflict in the list of incident events in Step 32.

Step 34: Check Whether All Incident Start Times and Locations Have Been Assigned

If there are incidents in the list of incident events that have not been assigned a start time and location, the process returns to Step 31 for further assignment. Otherwise, all the incidents in the list of incident events have been fully described and are ready to be modeled in the scenarios.

10. COMPUTATIONAL ENGINE OVERVIEW

The FREEVAL-2015E computational engine is written in the Java programming language. Java is a free, open source, object-oriented programming language that is highly portable and will run on almost all platforms. Unlike procedural languages, which largely consist of code broken up into subroutines, object-oriented languages require that the code be expressed in terms of *objects*. These objects have functions that either operate on the data associated with them or on other objects. In Java, groups of objects are called *classes*. Classes are then grouped into *packages*, which seek to provide organization based on some shared purpose or similarity.

The computational engine consists of nine packages, each of which contains a group of classes specific to a certain aspect of the HCM analysis. The main package contains the two most important classes for the methodology. First, the Seed class contains all input data for the freeway facility (e.g., freeway geometry, demand) and is the backbone of the engine. Once the analysis has been run, the Seed class will also contain all output performance measures. Further, any reliability or ATDM analysis performed will use Seed as the basis for its analysis.

The second class in the main package is the GPMLSegment class. This class is used to represent the segments of the freeway facility (general purpose or managed lane), and contains the code for both the undersaturated and oversaturated computational modules. Much of this code is an exact translation of the HCM methodology, with differences only occurring when it was necessary to either improve the performance of the code, or to match Java programming conventions. An example of a difference is that some variable values may not be explicitly stored but rather are calculated only as needed.

The other eight packages build on these two main classes. Four of the packages consist of “helper” functions that are used throughout the code. These helper classes provide functionality ranging from general input-output actions, such as opening and saving files, to more specific purposes, such as creating facility output summaries and specifying parameters for ramp-metering methodologies. The final four packages relate to reliability and ATDM analysis. These packages contain the reliability scenario generator, as well as many additional data structures to facilitate data input for both reliability and ATDM analysis.

The Java programming language provides the integrated ability to generate its own documentation. Developers simply provide descriptions of classes, functions, and variables throughout the code, and Java compiles them into a set of documentation referred to as a “Javadoc.” This Javadoc follows the format of the official documentation of the language, thus allowing it to be easily understood and used by anyone familiar with the language. This documentation has been generated and is packaged with the computational engine. A user guide for the graphical user interface version of the engine is available to provide guidance on its use. These items can be found in the Technical Reference Library in online HCM Volume 4.

11. EXAMPLE PROBLEMS

This section presents eleven example problems illustrating the evaluation of freeway facilities using the core methodology, the reliability methodology, and the ATDM methodology. Exhibit 25-42 presents a list of these problems.

Example Problem	Description	Application
1	Evaluation of an undersaturated facility	Operational analysis
2	Evaluation of an oversaturated facility	Operational analysis
3	Capacity improvements to an oversaturated facility	Operational analysis
4	Evaluation of an undersaturated facility with a work zone	Operational analysis
5	Evaluation of an oversaturated facility with a managed lane	Operational analysis
6	Planning-level analysis of a freeway facility	Planning analysis
7	Reliability evaluation of an existing freeway facility	Reliability analysis
8	Reliability analysis with geometric improvements	Reliability analysis
9	Evaluation of incident management	ATDM analysis
10	Planning-level reliability analysis	Planning analysis
11	Estimating freeway composite grade operations with the mixed-flow model	Specialized truck analysis

Exhibit 25-42
List of Example Problems

EXAMPLE PROBLEM 1: EVALUATION OF AN UNDERSATURATED FACILITY

The Facility

The subject of this operational analysis is a 6-mi-long urban freeway facility that is composed of 11 individual analysis segments, as shown in Exhibit 25-43.

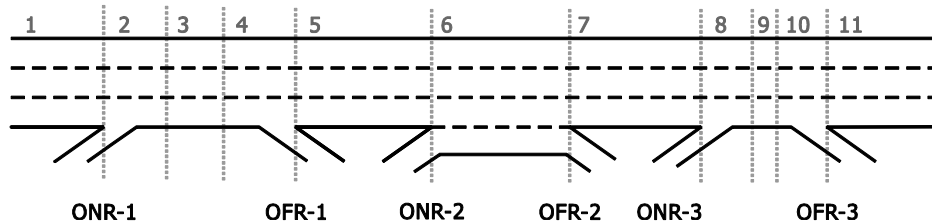


Exhibit 25-43
Example Problem 1:
Freeway Facility

The facility has three on-ramps and three off-ramps. Geometric details are given in Exhibit 25-44.

Segment No.	1	2	3	4	5	6	7	8	9	10	11
Segment type	B	ONR	B	OFR	B	B or W	B	ONR	R	OFR	B
Segment length (ft)	5,280	1,500	2,280	1,500	5,280	2,640	5,280	1,140	360	1,140	5,280
No. of lanes	3	3	3	3	3	4	3	3	3	3	3

Notes: B = basic freeway segment; W = weaving segment; ONR = on-ramp (merge) segment; OFR = off-ramp (diverge) segment; R = overlapping ramp segment.

Exhibit 25-44
Example Problem 1: Geometry
of Directional Freeway Facility

The on- and off-ramps in Segment 6 are connected by an auxiliary lane, and the segment may therefore operate as a weaving segment, depending on traffic patterns. The separation of the on-ramp in Segment 8 and the off-ramp in Segment 10 is less than 3,000 ft. Because the ramp influence area of on-ramps and off-ramps is 1,500 ft, according to Chapter 14, the segment affected by both ramps is analyzed as a separate overlapping ramp segment (Segment 9), labeled "R" in Exhibit 25-44.

The analysis question at hand is the following: What is the operational performance and LOS of the directional freeway facility shown in Exhibit 25-43?

The Facts

In addition to the information contained in Exhibit 25-43 and Exhibit 25-44, the following characteristics of the freeway facility are known:

SUTs and buses = 1.25% (all movements);

TTs = 1.00% (all movements);

Driver population = regular commuters;

FFS = 60 mi/h (all mainline segments);

Ramp FFS = 40 mi/h (all ramps);

Acceleration lane length = 500 ft (all ramps);

Deceleration lane length = 500 ft (all ramps);

D_{jam} = 190 pc/mi/ln;

c_{IFL} = 2,300 pc/h/ln (for FFS = 60 mi/h);

L_s = 1,640 ft (for Weaving Segment 6);

Total ramp density TRD = 1.0 ramp/mi;

Terrain = level; and

Analysis duration = 75 min (divided into five 15-min intervals).

A queue discharge capacity drop of 7% is assumed.

Comments

The facility was divided into analysis segments on the basis of the guidance given in Chapter 10, Freeway Facilities Core Methodology. The facility shown in Exhibit 25-43 depicts seven freeway *sections* (measured between ramps) that are divided into 11 analysis *segments*. The facility contains each of the possible segment types for illustrative purposes, including basic segment (B), weaving segment (W), merge segment (ONR), diverge segment (OFR), and overlapping ramp segment (R). The input data contain the required information needed for each of the segment methodologies.

The classification of the weave in Segment 6 is preliminary until it is determined whether the segment operates as a weave. For this purpose, the short length must be compared with the maximum length for weaving analysis to determine whether the Chapter 13, Freeway Weaving Segments, or the Chapter 12, Basic Freeway and Multilane Highway Segments, methodology is applicable. The short length of the weaving segment used for calculation is shorter than the weaving influence area over which the calculated speed and density measures are applied.

Chapter 12 must be consulted to find appropriate values for the heavy-vehicle adjustment factor f_{HV} . The computational engine automatically determines these adjustment factors for general terrain conditions, but user input is needed for specific upgrades and composite grades.

All input parameters have been specified, so default values are not needed. Fifteen-minute demand flow rates are given in vehicles per hour under prevailing conditions. These demands must be converted to passenger cars per hour under equivalent ideal conditions for use in the parts of the methodology related to segment LOS estimation. Details of the steps of the methodology follow.

Step A-1: Define Study Scope

In this initial step, the analyst defines the spatial extent of the facility (start and end points, total length) and the temporal extent of the analysis (number of 15-min analysis periods). The analyst should further decide which study extensions (if any) apply to the analysis (i.e., managed lanes, reliability, ATDM).

According to the inputs provided in the example, the number of time steps is five and the facility has 11 segments. The analysis does not involve a methodological extension.

Step A-2: Divide Facility into Sections and Segments

In this step, the analyst first defines the number of sections from gore point to gore point along the selected facility. These gore-to-gore sections are more consistent with modern freeway performance databases than HCM segments, and this consistency is critical for calibrating and validating the freeway facility. The analyst later divides sections into HCM segments (basic, merge, diverge, weave, overlapping ramp, or managed lane segment) as described in Chapter 10. The subject facility has already been segmented as shown in Exhibit 25-43.

Step A-3: Input Data

Data concerning demand, geometry, and other data are specified in this step. As the methodology builds on segment analysis, all data for each segment and each time period must be provided. Traffic demand inputs for all 11 segments and five analysis intervals are given in Exhibit 25-45.

Time Step (15 min)	Entering Flow Rate (veh/h)	Ramp Flow Rates by Time Period (veh/h)						Exiting Flow Rate (veh/h)
		ONR1	ONR2 ^a	ONR3	OFR1	OFR2	OFR3	
1	4,505	450	540 (50)	450	270	360	270	5,045
2	4,955	540	720 (100)	540	360	360	270	5,765
3	5,225	630	810 (150)	630	270	360	450	6,215
4	4,685	360	360 (80)	450	270	360	270	4,955
5	3,785	180	270 (50)	270	270	180	180	3,875

Note: ^a Numbers in parentheses indicate ONR-2 to OFR-2 demand flow rates in Weaving Segment 6.

The volumes in Exhibit 25-45 represent the 15-min demand flow rates on the facility as determined from field observations or other sources. The actual volume served in each segment will be determined by the methodology. The demand flows are given for the extended time-space domain, consistent with the recommendations in Chapter 10. Peaking occurs in the third 15-min period. Because inputs are in the form of 15-min flow rates, no peak hour factor adjustment is necessary. Additional geometric and traffic-related inputs are as specified in Exhibit 25-44 and the Facts section of the problem statement.

Exhibit 25-45
Example Problem 1:
Demand Inputs

Step A-4: Balance Demands

The traffic flows in Exhibit 25-45 are already given in the form of actual demands. Therefore, balancing demand is not necessary.

Step A-5: Identify Global Parameters

Global inputs are jam density and queue discharge capacity drop. Values for both parameters are given in the example problem’s Facts section.

Step A-6: Code Base Facility

Step 6 is the first step requiring the use of a computational engine or software. Data input needs for the computational engine include all items collected or estimated in the previous steps. These data generally need to be entered for each segment and each time period, making this one of the most time-consuming steps in the analysis.

Step A-7: Compute Segment Capacities

Segment capacities are determined by using the methodologies of Chapter 12 for basic freeway segments, Chapter 13 for weaving segments, and Chapter 14 for merge and diverge segments. The resulting capacities are shown in Exhibit 25-46. Because the capacity of a weaving segment depends on traffic patterns, including the weaving ratio, it varies by time period. The remaining segment capacities are constant in all five time intervals. The capacities for Segments 1–5 and 7–11 are the same because the segments have the same basic cross section. The units shown are in vehicles per hour.

Exhibit 25-46
Example Problem 1:
Segment Capacities

Time Step	Capacities (veh/h) by Segment										
	1	2	3	4	5	6	7	8	9	10	11
1						8,273					
2						8,281					
3	6,748	6,748	6,748	6,748	6,748	8,323	6,748	6,748	6,748	6,748	6,748
4						8,403					
5						8,463					

Step A-8: Calibrate with Adjustment Factors

This step allows the analyst to adjust demands, capacities, and FFSs for the purpose of calibration. The demand adjustment factor (DAF), capacity adjustment factor (CAF), and speed adjustment factor (SAF) can be modified for each segment and each time period. There is no adjustment needed for the subject facility according to the problem statement.

Step A-9: Adjust Managed Lane Cross Weave

This step is only required for facilities with managed lanes. The subject facility does not have a managed lane; therefore, this step is not required.

Step A-10: Compute Demand-to-Capacity Ratios

The demand-to-capacity ratios in Exhibit 25-47 are calculated from the demand flows in Exhibit 25-45 and the segment capacities in Exhibit 25-46.

Time Step	Demand-to-Capacity Ratios by Segment										
	1	2	3	4	5	6	7	8	9	10	11
1	0.67	0.73	0.73	0.73	0.69	0.63	0.72	0.79	0.79	0.79	0.75
2	0.73	0.81	0.81	0.81	0.76	0.71	0.81	0.89	0.89	0.89	0.85
3	0.77	0.87	0.87	0.87	0.83	0.77	0.89	0.99	0.99	0.99	0.92
4	0.69	0.75	0.75	0.75	0.71	0.61	0.71	0.77	0.77	0.77	0.73
5	0.56	0.59	0.59	0.59	0.55	0.47	0.56	0.60	0.60	0.60	0.57

Exhibit 25-47
Example Problem 1: Segment Demand-to-Capacity Ratios

The computed demand-to-capacity ratio matrix in Exhibit 25-47 shows no segments with a v_d/c ratio greater than 1.0 in any time interval. Consequently, the facility is categorized as *globally undersaturated*, and the analysis proceeds with computing the undersaturated service measures in Step A-11. Further, it is expected that no queuing will occur on the facility and that the volume served in each segment is identical to the input demand flows. Consequently, the matrix of volume-to-capacity ratios would be identical to the demand-to-capacity ratios in Exhibit 25-47. The resulting matrix of volumes served by segment and time interval is shown in Exhibit 25-48.

Time Step	Volumes Served (veh/h) by Segment										
	1	2	3	4	5	6	7	8	9	10	11
1	4,505	4,955	4,955	4,955	4,685	5,225	4,865	5,315	5,315	5,315	5,045
2	4,955	5,495	5,495	5,495	5,135	5,855	5,495	6,035	6,035	6,035	5,765
3	5,225	5,855	5,855	5,855	5,585	6,395	6,035	6,665	6,665	6,665	6,215
4	4,685	5,045	5,045	5,045	4,775	5,135	4,775	5,225	5,225	5,225	4,955
5	3,785	3,965	3,965	3,965	3,695	3,965	3,785	4,055	4,055	4,055	3,875

Exhibit 25-48
Example Problem 1: Volume-Served Matrix

Step A-11: Compute Undersaturated Segment Service Measures

Because the facility is globally undersaturated, the methodology proceeds to calculate service measures for each segment and each time period, starting with the first segment in Time Step 1. The computational details for each segment type are exactly as described in Chapters 12, 13, and 14. The weaving methodology in Chapter 13 checks whether the weaving short length L_s is less than or equal to the maximum weaving length L_{max} . It is assumed, for any time interval where L_s is longer than L_{max} , that the weaving segment will operate as a basic freeway segment.

The basic performance measures computed for each segment and each time step are the segment speed (Exhibit 25-49), density (Exhibit 25-50), and LOS (Exhibit 25-51).

Exhibit 25-49

Example Problem 1:
Speed Matrix

Time Step	Speed (mi/h) by Segment										
	1	2	3	4	5	6	7	8	9	10	11
1	60.0	53.9	59.7	56.1	60.0	48.0	59.9	53.4	53.4	56.0	59.7
2	59.9	53.2	58.6	55.8	59.6	46.8	58.6	52.3	52.3	55.7	57.6
3	59.4	52.6	57.2	55.7	58.3	46.2	56.2	50.6	50.6	51.8	55.1
4	60.0	53.8	59.7	56.1	60.0	49.7	60.0	53.6	53.6	56.0	59.9
5	60.0	54.9	59.8	56.3	60.0	52.5	60.0	54.8	54.8	56.5	60.0

Exhibit 25-50

Example Problem 1:
Density Matrix

Time Step	Density (veh/mi/ln) by Segment										
	1	2	3	4	5	6	7	8	9	10	11
1	25.0	30.6	27.6	29.4	26.0	27.2	27.1	33.2	33.2	31.6	28.1
2	27.6	34.5	31.2	32.8	28.7	31.3	31.2	38.5	38.5	36.1	33.4
3	29.3	37.1	34.1	35.0	31.9	34.6	35.8	43.9	43.9	42.9	37.6
4	26.0	31.3	28.1	30.0	26.5	25.8	26.5	32.5	32.5	31.1	27.6
5	21.0	24.1	22.0	23.5	20.5	18.9	21.0	24.7	24.7	23.9	21.5

Exhibit 25-51

Example Problem 1:
LOS Matrix

Time Step	LOS by Segment										
	1	2	3	4	5	6	7	8	9	10	11
1	C	C	D	C	D	C	D	D	D	D	D
2	D	D	D	D	D	D	D	D	E	D	D
3	D	D	D	D	D	D	E	E	E	D	E
4	D	C	D	C	D	C	D	C	D	D	D
5	C	C	C	C	C	B	C	C	C	C	C

Step A-13: Apply Managed Lane Adjacent Friction Factor

This step is only required for facilities with managed lanes.

Step A-14: Compute Lane Group Performance

This step is only required for facilities with managed lanes.

Step A-15: Compute Freeway Facility Service Performance Measures by Time Interval

In this analysis step, facilitywide performance measures are calculated for each time step. Example calculations are provided for the first time step only; summary results are shown for all five time steps.

First, the facility space mean speed S is calculated for time step $t = 1$ from the 11 individual segment flows $SF(i, t)$, segment lengths $L(i)$, and space mean speeds in each segment and time step $U(i, t)$.

$$S(t = 1) = \frac{\sum_{i=1}^{11} SF(i, 1) \times L(i)}{\sum_{i=1}^{11} SF(i, 1) \times \frac{L(i)}{U(i, 1)}}$$

$$\begin{aligned} \sum_{i=1}^{11} SF(i, 1) \times L(i) &= (4,505 \times 5,280) + (4,955 \times 1,500) + (4,955 \times 2,280) + \\ &\quad (4,955 \times 1,500) + (4,685 \times 5,280) + (5,225 \times 2,640) + \\ &\quad (4,865 \times 5,280) + (5,315 \times 1,140) + (5,315 \times 360) + \\ &\quad (5,315 \times 1,140) + (5,045 \times 5,280) \\ &= 154,836,000 \text{ veh-ft} \end{aligned}$$

$$\begin{aligned} \sum_{i=1}^{11} SF(i, 1) \times \frac{L(i)}{U(i, 1)} &= (4,505 \times 5,280 / 60.00) + (4,955 \times 1,500 / 53.90) \\ &+ (4,955 \times 2,280 / 59.70) + (4,955 \times 1,500 / 56.10) \\ &+ (4,685 \times 5,280 / 60.00) + (5,225 \times 2,640 / 48.00) \\ &+ (4,865 \times 5,280 / 59.90) + (5,315 \times 1,140 / 53.40) \\ &+ (5,315 \times 360 / 53.40) + (5,315 \times 1,140 / 56.00) \\ &+ (5,045 \times 5,280 / 59.70) \\ &= 2,688,024 \text{ veh-ft/mi/h} \end{aligned}$$

$$S(t = 1) = \frac{154,836,000}{2,688,024} = 57.6 \text{ mi/h}$$

Second, the average facility density is calculated for Time Step 1 from the individual segment densities D , segment lengths L , and number of vehicles in each segment N .

$$D(t = 1) = \frac{\sum_{i=1}^{11} D(i, 1) \times L(i) \times N(i, 1)}{\sum_{i=1}^{11} SL(i)N(i, 1)}$$

$$\begin{aligned} \sum_{i=1}^{11} D(i, 1) \times L(i) \times N(i, 1) &= (25.6 \times 5,280 \times 3) + (31.3 \times 1,500 \times 3) + (28.2 \times 2,280 \times 3) \\ &+ (30.1 \times 1,500 \times 3) + (26.6 \times 5,280 \times 3) + (27.8 \times 2,640 \times 4) \\ &+ (27.7 \times 5,280 \times 3) + (33.9 \times 1,140 \times 3) + (33.9 \times 360 \times 3) \\ &+ (32.4 \times 1,140 \times 3) + (28.8 \times 5,280 \times 3) \\ &= 2,687,957 \text{ (veh/mi/ln)(ln-ft)} \end{aligned}$$

$$\begin{aligned} \sum_{i=1}^{11} SL(i)N(i, 1) &= (5,280 \times 3) + (1,500 \times 3) + (2,280 \times 3) + (1,500 \times 3) \\ &+ (5,280 \times 3) + (2,640 \times 4) + (5,280 \times 3) + (1,140 \times 3) \\ &+ (360 \times 3) + (1,140 \times 3) + (5,280 \times 3) \\ &= 97,680 \text{ ln-ft} \end{aligned}$$

$$D(t = 1) = \frac{2,747,253}{97,680} = 28.1 \text{ veh/mi/ln}$$

These calculations are repeated for all five time steps. The overall space mean speed across all time steps is calculated as follows:

$$S(p = 5) = \frac{\sum_{p=1}^5 \sum_{i=1}^{11} SF(i, p) \times L(i)}{\sum_{p=1}^5 \sum_{i=1}^{11} SF(i, p) \times \frac{L(i)}{U(i, p)}}$$

The overall average density across all time steps is calculated as follows:

$$D(p = 5) = \frac{\sum_{p=1}^5 \sum_{i=1}^{11} D(i, p) \times L(i) \times N(i, p)}{\sum_{p=1}^5 \sum_{i=1}^{11} SL(i)N(i, p)}$$

The resulting performance and service measures for Time Steps 1–5 and the facility totals are shown in Exhibit 25-52.

Exhibit 25-52
 Example Problem 1: Facility
 Performance Measure
 Summary

Time Step	Performance Measure		LOS
	Space Mean Speed (mi/h)	Average Density (veh/mi/ln)	
1	57.6	27.5	D
2	56.6	31.3	D
3	55.0	34.8	E
4	57.9	27.5	D
5	58.4	21.4	C
Total	56.9	28.4	—

Step A-16: Aggregate to Section Level and Validate Against Field Data

This step is used to validate the analysis and is performed only when field data are available.

Step A-17: Estimate LOS and Report Performance Measures for Lane Groups and Facility

The LOS for each time interval is determined directly from the average density for each time interval by using Exhibit 10-7. No LOS is defined for the average across all time intervals.

Discussion

This facility turned out to be globally undersaturated. Consequently, the facility-aggregated performance measures could be calculated directly from the individual segment performance measures. An assessment of the segment service measures across the time-space domain can begin to highlight areas of potential congestion. Visually, this process can be facilitated by plotting the v_d/c , v_s/c , speed, or density matrices in contour plots.

EXAMPLE PROBLEM 2: EVALUATION OF AN OVERSATURATED FACILITY

The Facility

The facility used in Example Problem 2 is identical to the one in Example Problem 1, which is shown in Exhibit 25-43 and Exhibit 25-44.

The Facts

In addition to the information in Exhibit 25-43 and Exhibit 25-44, the following characteristics of the freeway facility are known:

- SUTs and buses = 1.25% (all movements);
- TTs = 1.00% (all movements);
- Driver population = regular commuters;
- FFS = 60 mi/h (all mainline segments);
- Ramp FFS = 40 mi/h (all ramps);
- Acceleration lane length = 500 ft (all ramps);
- Deceleration lane length = 500 ft (all ramps);
- D_{jam} = 190 pc/mi/ln;
- c_{IFL} = 2,300 pc/h/ln (for FFS = 60 mi/h);

$L_s = 1,640$ ft (for Weaving Segment 6);

$TRD = 1.0$ ramp/mi;

Terrain = level;

Analysis duration = 75 min (divided into five 15-min time steps); and

Demand adjustment = +11% increase in demand volumes across all segments and time steps relative to Example Problem 1.

As before, a queue discharge capacity drop of 7% is assumed.

Comments

The facility and all geometric inputs are identical to Example Problem 1. The same general comments apply. The results of Example Problem 1 suggested a globally undersaturated facility, but some segments were close to their capacity (v_d/c ratios approaching 1.0). In the second example, a facilitywide demand increase of 11% is applied to all segments and all time periods. Consequently, it is expected parts of the facility may become oversaturated and queues may form on the facility.

Step A-1: Define Study Scope

Similar to Example Problem 1, there are five time steps and the facility has 11 segments. The analysis does not include any extensions such as managed lanes, reliability, ATDM, or work zones.

Step A-2: Divide Facility into Sections and Segments

The subject facility segmentation is given in Exhibit 25-43. Therefore, there is no need to go through the segmentation process.

Step A-3: Input Data

The revised traffic demand inputs for all 11 segments and five analysis intervals are shown in Exhibit 25-53.

Time Step (15 min)	Entering Flow Rate (veh/h)	Ramp Flow Rates by Time Period (veh/h)						Exiting Flow Rate (veh/h)
		ONR1	ONR2 ^a	ONR3	OFR1	OFR2	OFR3	
1	5,001	500	599 (56)	500	300	400	300	5,600
2	5,500	599	799 (111)	599	400	400	300	6,399
3	5,800	699	899 (167)	699	300	400	500	6,899
4	5,200	400	400 (89)	500	300	400	300	5,500
5	4,201	200	300 (56)	300	300	200	200	4,301

Note: ^a Numbers in parentheses indicate ONR-2 to OFR-2 demand flow rates in Weaving Segment 6.

The values in Exhibit 25-53 represent the adjusted demand flows on the facility as determined from field observations or demand projections. The actual volume served in each segment will be determined during the application of the methodology and is expected to be less downstream of a congested segment. The demand flows are given for the extended time-space domain, consistent with the methodology presented in Chapter 10. Peaking occurs in the third 15-min period. Because inputs are in the form of 15-min observations, no peak hour factor

Exhibit 25-53
Example Problem 2:
Demand Inputs

adjustment is necessary. Additional geometric and traffic-related inputs are as specified in Exhibit 25-44 and the Facts section of the problem statement.

Step A-4: Balance Demands

The traffic flows in Exhibit 25-53 have already been given in the form of actual demands and no balancing is necessary.

Step A-5: Identify Global Parameters

Global inputs are jam density and queue discharge capacity drop. Values for both parameters are given in the Facts section of the problem statement.

Step A-6: Code Base Facility

In this step, all input data for the subject are coded in the computational engine. Note that this facility can be coded by increasing entry demand across the facility by 11% relative to the Example Problem 1 demands.

Step A-7: Compute Segment Capacities

Because no changes to segment geometry were made, the segment capacities for basic and ramp segments are consistent with Example Problem 1. Capacities for weaving segments are a function of weaving flow patterns, and the increased demand flows resulted in slight changes as shown in Exhibit 25-54.

Exhibit 25-54
Example Problem 2:
Segment Capacities

Time Step	Capacities (veh/h) by Segment										
	1	2	3	4	5	6	7	8	9	10	11
1						8,273					
2						8,281					
3	6,748	6,748	6,748	6,748	6,748	8,323	6,748	6,748	6,748	6,748	6,748
4						8,403					
5						8,463					

Step A-8: Calibrate with Adjustment Factors

This step allows the analyst to adjust demands, capacities, and FFSs for the purpose of calibration. There is no adjustment needed for the subject capacity according to the problem statement.

Step A-9: Adjust Managed Lane Cross Weave

This step is only required for facilities with managed lanes. The subject facility does not have a managed lane.

Step A-10: Compute Demand-to-Capacity Ratios

The demand-to-capacity ratios in Exhibit 25-55 are calculated from the demand flows in Exhibit 25-53 and the segment capacities in Exhibit 25-54.

Time Step	Demand-to-Capacity Ratios by Segment										
	1	2	3	4	5	6	7	8	9	10	11
1	0.74	0.82	0.82	0.82	0.77	0.70	0.80	0.87	0.87	0.87	0.83
2	0.82	0.90	0.90	0.90	0.84	0.78	0.90	0.99	0.99	0.99	0.95
3	0.86	0.96	0.96	0.96	0.92	0.85	0.99	1.10	1.10	1.10	1.02
4	0.77	0.83	0.83	0.83	0.79	0.68	0.79	0.86	0.86	0.86	0.82
5	0.62	0.65	0.65	0.65	0.61	0.52	0.62	0.67	0.67	0.67	0.64

Exhibit 25-55
Example Problem 2: Segment Demand-to-Capacity Ratios

The computed v_d/c matrix in Exhibit 25-55 shows Segments 8–11 have v_d/c ratios greater than 1.0 (bold values). Consequently, the facility is categorized as *oversaturated*, and the analysis proceeds with computing the oversaturated service measures in Step A-12. It is expected that queuing will occur on the facility upstream of the congested segments and that the volume served in each segment downstream of the congested segments will be less than its demand. This residual demand will be served in later time intervals, provided the upstream demand drops and queues are allowed to clear.

Step A-12: Compute Oversaturated Segment Service Measures

Computations for oversaturation apply to any segment with a v_d/c ratio greater than 1.0 as well as any segments upstream of those segments that experience queuing as a result of the bottleneck. All remaining segments are analyzed by using the individual segment methodologies of Chapters 12, 13, and 14, as applicable, with the caveat that volumes served may differ from demand flows.

Similar to Example Problem 1, in Example Problem 2 the methodology calculates performance measures for each segment and each time period, starting with the first segment in Time Step 1. The computations are repeated for all segments for Time Steps 1 and 2 without encountering a segment with $v_d/c > 1.0$. Once the methodology enters Time Period 3 and Segment 8, the oversaturated computational module is invoked.

At the first active bottleneck, the v_d/c ratio for Segment 8 will be exactly 1.0 and the segment will process traffic at its capacity. Consequently, demand for all downstream segments will be metered by that bottleneck. The unsatisfied demand is stored in upstream segments, which causes queuing in Segment 7 and perhaps segments further upstream depending on the level of excess demand. The rate of growth of the vehicle queue (wave speed) is estimated from shock wave theory. The performance measures (speed and density) of any segment with queuing are recomputed, and the newly calculated values override the results from the segment-specific procedures.

Any unsatisfied demand is served in later time periods. As a result, volumes served in later time periods may be higher than the period demand flows. The resulting matrix of volumes served for Example Problem 2 is shown in Exhibit 25-56.

Exhibit 25-56
Example Problem 2:
Volume-Served Matrix

Time Step	Volumes Served (veh/h) by Segment										
	1	2	3	4	5	6	7	8	9	10	11
1	5,001	5,500	5,500	5,500	5,200	5,800	5,400	5,900	5,900	5,900	5,600
2	5,500	6,099	6,099	6,099	5,700	6,499	6,099	6,699	6,699	6,699	6,399
3	5,800	6,499	6,499	6,499	5,831	6,281	5,584	6,284	6,284	6,284	5,859
4	5,200	5,600	5,600	5,600	5,668	6,311	5,776	6,276	6,276	6,276	5,934
5	4,201	4,401	4,401	4,401	4,102	4,608	4,840	5,140	5,140	5,140	4,912

As a result of the bottleneck activation in Segment 8 in Time Period 3, queues form in upstream Segments 7, 6, and 5. The queuing is associated with reduced speeds and increased densities in those segments. The results in this chapter were obtained from the computational engine. The resulting performance measures computed for each segment and time interval are speed (Exhibit 25-57), density (Exhibit 25-58), and LOS (Exhibit 25-59).

Exhibit 25-57
Example Problem 2:
Speed Matrix

Time Step	Speed (mi/h) by Segment										
	1	2	3	4	5	6	7	8	9	10	11
1	59.8	53.2	58.6	55.9	59.5	46.8	59.0	52.5	52.5	55.7	58.3
2	58.6	52.1	55.8	55.5	57.9	45.4	55.8	50.6	50.6	51.5	53.9
3	57.4	51.1	53.1	53.1	45.3	24.2	28.1	51.6	51.6	54.7	57.1
4	47.2	47.5	51.5	48.3	56.5	24.7	29.6	51.7	51.7	54.7	56.8
5	60.0	54.5	59.7	56.2	60.0	51.4	50.9	53.7	53.7	56.1	59.9

Exhibit 25-58
Example Problem 2:
Density Matrix

Time Step	Density (veh/mi/ln) by Segment										
	1	2	3	4	5	6	7	8	9	10	11
1	27.9	34.5	31.3	32.8	29.2	31.0	30.5	37.4	37.4	35.3	32.0
2	31.3	39.0	36.4	36.7	32.8	35.8	36.4	44.2	44.2	43.3	39.6
3	33.7	42.4	40.8	40.8	42.9	64.8	66.4	40.6	40.6	38.3	34.2
4	36.7	39.3	36.3	38.6	33.4	63.9	65.1	40.4	40.4	38.2	34.8
5	23.3	26.9	24.5	26.1	22.8	22.4	31.7	31.9	31.9	30.5	27.3

Exhibit 25-59
Example Problem 2:
Expanded LOS Matrix

Time Step	Density-Based LOS by Segment										
	1	2	3	4	5	6	7	8	9	10	11
1	D	D	D	D	D	D	D	D	E	D	D
2	D	D	E	D	D	E	E	E	E	D	E
3	D	D	E	D	E	F	F	D	E	D	D
4	E	E	E	E	D	F	F	D	E	D	E
5	C	C	C	C	C	C	D	C	D	C	D

Time Step	Demand-Based LOS by Segment										
	1	2	3	4	5	6	7	8	9	10	11
1											
2											
3								F	F	F	F
4											
5											

The LOS table for oversaturated facilities (Exhibit 25-59) distinguishes between the conventional density-based LOS and a segment demand-based LOS. The density-based stratification strictly depends on the prevailing average density on each segment. Segments downstream of the bottleneck, whose capacities are greater than or equal to the bottleneck capacity, operate at LOS E (or better), even though their v_d/c ratios are greater than 1.0. The demand-based LOS identifies those segments with demand-to-capacity ratios exceeding 1.0 as if they had been evaluated in isolation (i.e., using the methodologies of Chapters

12, 13, and 14). By contrasting the two parts of the LOS table, the analyst can develop an understanding of the metering effect of the bottleneck.

Step A-13: Apply Managed Lane Adjacent Friction Factor

This step is only required for facilities with managed lanes.

Step A-14: Compute Lane Group Performance

This step is only required for facilities with managed lanes.

Step A-15: Compute Freeway Facility Service Performance Measures by Time Interval

In the final analysis step, facilitywide performance measures are calculated for each time interval (Exhibit 25-60), consistent with Example Problem 1. Because the computations have already been shown, only summary results are shown here.

Time Interval	Performance Measure		LOS
	Space Mean Speed (mi/h)	Average Density (veh/mi/ln)	
1	56.8	31.0	D
2	54.4	36.2	E
3	42.5	45.6	F
4	42.5	43.8	E
5	56.4	26.2	D
Total	50.5	35.6	—

Exhibit 25-60
Example Problem 2: Facility Performance Measure Summary

Step A-16: Aggregate to Section Level and Validate Against Field Data

This step validates the analysis and is performed only when field data are available.

Step A-17: Estimate LOS and Report Performance Measures for Lane Groups and Facility

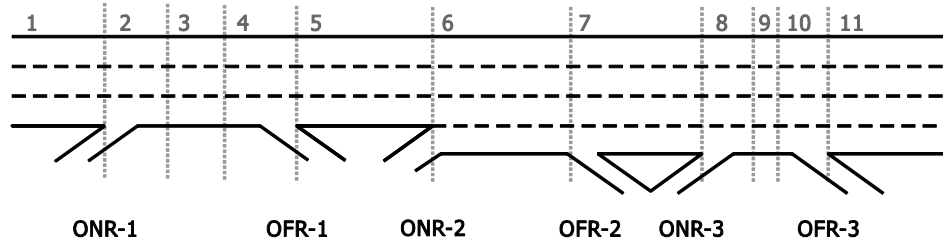
The LOS for each time interval is determined directly from the average density for each time interval. The facility operates at LOS F in Time Period 3 because one or more individual segments have demand-to-capacity ratios ≥ 1.0 , even though the average facility density is below the LOS F threshold.

EXAMPLE PROBLEM 3: CAPACITY IMPROVEMENTS TO AN OVERSATURATED FACILITY

The Facility

In this example, portions of the congested facility in Example Problem 2 are being improved in an attempt to alleviate the congestion resulting from the Segment 8 bottleneck. Exhibit 25-61 shows the upgraded facility geometry.

Exhibit 25-61
Example Problem 3:
Freeway Facility



The modified geometry of the 6-mi directional freeway facility is reflected in Exhibit 25-62.

Exhibit 25-62
Example Problem 3: Geometry
of Directional Freeway Facility

Segment No.	1	2	3	4	5	6	7	8	9	10	11
Segment type	B	ONR	B	OFR	B	B or W	B	ONR	R	OFR	B
Segment length (ft)	5,280	1,500	2,280	1,500	5,280	2,640	5,280	1,140	360	1,140	5,280
No. of lanes	3	3	3	3	3	4	4	4	4	4	4

Notes: B = basic freeway segment; W = weaving segment; ONR = on-ramp (merge) segment; OFR = off-ramp (diverge) segment; R = overlapping ramp segment.
Bold type indicates geometry changes from Example Problems 1 and 2.

The facility improvements consisted of adding a lane to Segments 7–11 to give the facility a continuous four-lane cross section starting in Segment 6. The active bottleneck in Example Problem 2 was in Segment 8, but prior analysis showed that other segments (Segments 9–11) showed similar demand-to-capacity ratios greater than 1.0. Consequently, any capacity improvements that are limited to Segment 8 would have merely moved the spatial location of the bottleneck farther downstream rather than improving the overall facility. Segments 9–11 may also be referred to as “hidden” or “inactive” bottlenecks, because their predicted congestion is mitigated by the upstream metering of traffic.

The Facts

In addition to the information contained in Exhibit 25-61 and Exhibit 25-62, the following characteristics of the freeway facility are known:

- SUTs and buses = 1.25% (all movements);
- Mainline TTs = 1.00% (all movements);
- Driver population = regular commuters;
- FFS = 60 mi/h (all mainline segments);
- Ramp FFS = 40 mi/h (all ramps);
- Acceleration lane length = 500 ft (all ramps);
- Deceleration lane length = 500 ft (all ramps);
- D_{jam} = 190 pc/mi/ln;
- c_{IFL} = 2,300 pc/h/ln (for FFS = 60 mi/h);
- L_s = 1,640 ft (for Weaving Segment 6);
- TRD = 1.0 ramp/mi;
- Terrain = level;
- Analysis duration = 75 min (divided into five 15-min intervals); and

Demand adjustment = +11% (all segments and all time intervals).

A queue discharge capacity drop of 7% is assumed.

Comments

The traffic demand flow inputs are identical to those in Example Problem 2, which reflected an 11% increase in traffic applied to all segments and all time periods relative to Example Problem 1. In an attempt to solve the congestion effect found in the earlier example, the facility was widened in Segments 7 through 11. This change directly affects the capacities of those segments.

In a more subtle way, the proposed modifications also change some of the defining parameters of Weaving Segment 6. With the added continuous lane downstream of the segment, the required number of lane changes from the ramp to the freeway is reduced from one to zero, following the guidelines in Chapter 13. These changes need to be considered when the undersaturated performance of that segment is evaluated. The weaving segment's capacity is unchanged relative to Example Problem 2 because, even with the proposed improvements, the number of weaving lanes remains two.

Step A-1: Define Study Scope

Similar to the previous example, the number of time steps is five and the facility has 11 segments. The analysis does not include any methodological extensions (i.e., managed lanes, reliability, ATDM, work zones).

Step A-2: Divide Facility into Sections and Segments

The segmentation of the subject facility is the same as in Example Problems 1 and 2 and is given in Exhibit 25-61. Therefore, the segmentation process is not repeated.

Step A-3: Input Data

Traffic demand inputs for all 11 segments and five analysis intervals are identical to those in Example Problem 2, as shown in Exhibit 25-53. The values represent the adjusted demand flows on the facility as determined from field observations or other sources. The actual volume served in each segment will be determined by using the methodologies and is expected to be less downstream of a congested segment. Additional geometric and traffic-related inputs are as specified in Exhibit 25-62 and the Facts section of the problem statement.

Step A-4: Balance Demands

The traffic flows in Exhibit 25-53 have already been given in the form of actual demands and no balancing is necessary.

Step A-5: Identify Global Parameters

Global inputs are jam density and queue discharge capacity drop. Values for both parameters are given in the Facts section of the problem statement.

Step A-6: Code Base Facility

In this step, all input data for the subject are coded in the computational engine.

Step A-7: Compute Segment Capacities

Segment capacities are determined by using the methodologies of Chapter 12 for basic freeway segments, Chapter 13 for weaving segments, and Chapter 14 for merge and diverge segments. The resulting capacities are shown in Exhibit 25-63. Because the capacity of a weaving segment depends on traffic patterns, it varies by time period. The remaining capacities are constant for all five time steps. The capacities for Segments 1–5 and Segments 7–11 are the same because the segments have the same basic cross section.

Exhibit 25-63
Example Problem 3:
Segment Capacities

Time Step	Capacities (veh/h) by Segment										
	1	2	3	4	5	6	7	8	9	10	11
1						8,273					
2						8,281					
3	6,748	6,748	6,748	6,748	6,748	8,323	8,998	8,998	8,998	8,998	8,998
4						8,403					
5						8,463					

Step A-8: Calibrate with Adjustment Factors

This step allows the user to adjust demands, capacities, and FFSs for the purpose of calibration. There is no adjustment needed for the subject capacity according to the problem statement.

Step A-9: Adjust Managed Lane Cross Weave

This step is only required for facilities with managed lanes. The subject facility does not have a managed lane.

Step A-10: Compute Demand-to-Capacity Ratios

The demand-to-capacity ratios in Exhibit 25-64 are calculated from the demand flows in Exhibit 25-53 and segment capacities in Exhibit 25-63.

Exhibit 25-64
Example Problem 3:
Segment Demand-to-Capacity Ratios

Time Step	Demand-to-Capacity Ratio by Segment										
	1	2	3	4	5	6	7	8	9	10	11
1	0.74	0.82	0.82	0.82	0.77	0.70	0.60	0.66	0.66	0.66	0.62
2	0.82	0.90	0.90	0.90	0.84	0.78	0.68	0.74	0.74	0.74	0.71
3	0.86	0.96	0.96	0.96	0.92	0.85	0.74	0.82	0.82	0.82	0.77
4	0.77	0.83	0.83	0.83	0.79	0.68	0.59	0.64	0.64	0.64	0.61
5	0.62	0.65	0.65	0.65	0.61	0.52	0.47	0.50	0.50	0.50	0.48

The demand-to-capacity ratio matrix for Example Problem 3 (Exhibit 25-64) shows the capacity improvements successfully reduced all the previously congested segments to $v_d/c < 1.0$. Therefore, it is expected that the facility will operate as *globally undersaturated* and that all segment performance measures can be directly computed by using the methodologies in Chapters 12, 13, and 14.

Step A-11: Compute Undersaturated Segment Service Measures

Because the facility is globally undersaturated, the methodology proceeds to calculate service measures for each segment and each time period, starting with the first segment in Time Step 1. The computational details for each segment type are exactly as described in Chapters 12, 13, and 14. The basic performance service measures computed for each segment and each time interval include segment speed (Exhibit 25-65), density (Exhibit 25-66), and LOS (Exhibit 25-67).

Time Step	Speed (mi/h) by Segment										
	1	2	3	4	5	6	7	8	9	10	11
1	59.8	53.2	58.6	55.9	59.5	50.5	60.0	54.9	54.9	58.1	60.0
2	58.6	52.1	55.8	55.5	57.9	50.1	60.0	54.3	54.3	57.7	60.0
3	57.4	51.1	53.1	53.1	55.2	49.7	59.8	53.6	53.6	57.2	59.5
4	59.5	53.0	58.3	55.8	59.2	50.8	60.0	55.0	55.0	58.1	60.0
5	60.0	54.5	59.7	56.2	60.0	53.4	60.0	55.9	55.9	58.8	60.0

Time Step	Density (veh/mi/ln) by Segment										
	1	2	3	4	5	6	7	8	9	10	11
1	27.9	34.5	31.3	32.8	29.2	28.7	22.5	26.8	26.8	25.4	23.3
2	31.3	39.0	36.4	36.7	32.8	32.5	25.4	30.9	30.9	29.0	26.7
3	33.7	42.4	40.8	40.8	37.4	35.7	28.0	34.5	34.5	32.4	29.0
4	29.2	35.2	32.0	33.4	29.8	28.1	22.1	26.4	26.4	24.9	22.9
5	23.3	26.9	24.5	26.1	22.8	20.6	17.5	20.1	20.1	19.1	17.9

Time Step	LOS by Segment										
	1	2	3	4	5	6	7	8	9	10	11
1	D	D	D	D	D	D	C	C	D	C	C
2	D	D	E	D	D	D	C	C	D	C	D
3	D	D	E	D	E	E	D	D	D	D	D
4	D	D	D	D	D	D	C	C	D	C	C
5	C	C	C	C	C	C	B	B	C	B	B

Step A-13: Apply Managed Lane Adjacent Friction Factor

This step is only required for facilities with managed lanes.

Step A-14: Compute Lane Group Performance

This step is only required for facilities with managed lanes.

Step A-15: Compute Freeway Facility Service Performance Measures by Time Interval

In this analysis step, facilitywide performance measures are calculated for each time step (Exhibit 25-68), consistent with Example Problem 2. Because the computations have already been shown, only summary results are shown here. The improvement restored the facility LOS to the values experienced in the original pregrowth scenario, as shown in Exhibit 25-68.

Exhibit 25-65
Example Problem 3:
Speed Matrix

Exhibit 25-66
Example Problem 3:
Density Matrix

Exhibit 25-67
Example Problem 3:
LOS Matrix

Exhibit 25-68

Example Problem 3: Facility Performance Measure Summary

Time Step	Performance Measure		LOS
	Space Mean Speed (mi/h)	Average Density (veh/mi/ln)	
1	57.9	26.8	D
2	57.1	30.3	D
3	55.9	33.5	D
4	57.8	26.9	D
5	58.6	20.8	C
Total	57.5	27.7	—

Step A-16: Aggregate to Section Level and Validate Against Field Data

This step validates the analysis and is performed only when field data are available.

Step A-17: Estimate LOS and Report Performance Measures for Lane Groups and Facility

The LOS for each time interval is determined directly from the average density for each time interval. The improvement restored the facility LOS to the values experienced in the original pregrowth (undersaturated) scenario shown in Exhibit 25-51.

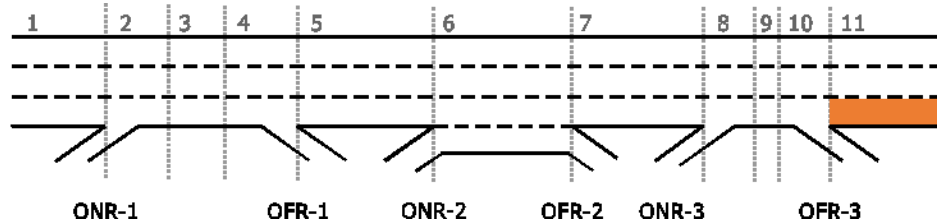
EXAMPLE PROBLEM 4: EVALUATION OF AN UNDERSATURATED FACILITY WITH A WORK ZONE

The Facility

In this example, a long-term work zone is placed on the final segment of Example Problem 1. Exhibit 25-69 shows the change to the facility.

Exhibit 25-69

Example Problem 4: Freeway Facility



The modified geometry of the 6-mi directional freeway facility is reflected in Exhibit 25-70.

Exhibit 25-70

Example Problem 4: Geometry of Directional Freeway Facility

Segment No.	1	2	3	4	5	6	7	8	9	10	11
Segment type	B	ONR	B	OFR	B	B or W	B	ONR	R	OFR	B
Segment length (ft)	5,280	1,500	2,280	1,500	5,280	2,640	5,280	1,140	360	1,140	5,280
No. of lanes	3	3	3	3	3	4	3	3	3	3	2

Notes: B = basic freeway segment; W = weaving segment; ONR = on-ramp (merge) segment; OFR = off-ramp (diverge) segment; R = overlapping ramp segment.

The Facts

In addition to the information contained in Exhibit 25-69 and Exhibit 25-70, the following characteristics of the freeway facility are known:

SUTs and buses = 1.25% (all movements);

Mainline TTs = 1.00% (all movements);

Driver population = regular commuters;

FFS = 60 mi/h (all mainline segments);

Ramp FFS = 40 mi/h (all ramps);

Acceleration lane length = 500 ft (all ramps);

Deceleration lane length = 500 ft (all ramps);

D_{jam} = 190 pc/mi/ln;

c_{IFL} = 2,300 pc/h/ln (for FFS = 60 mi/h);

L_s = 1,640 ft (for Weaving Segment 6);

TRD = 1.0 ramp/mi;

Terrain = level; and

Analysis duration = 75 min (divided into five 15-min intervals).

A queue discharge capacity drop of 7% is assumed for non-work zone conditions.

Comments

The traffic demand flow inputs are identical to those in Example Problem 1. The work zone has a single lane closure (in Segment 11), concrete barriers, and a lateral distance of 12 ft in an urban area. Daytime performance is of interest throughout the analysis.

Step A-1: Define Study Scope

Similar to the previous examples, there are five time steps and the facility has 11 segments. The work zone extension to the methodology will be included as part of the analysis.

Step A-2: Divide Facility into Sections and Segments

The segmentation of the subject facility is given in Exhibit 25-69. Therefore, there is no need to go through the segmentation process.

Step A-3: Input Data

Traffic demand inputs for all 11 segments and five analysis intervals are identical to those in Example Problem 1, as shown in Exhibit 25-45. The values represent the adjusted demand flows on the facility as determined from field observations or other sources. Additional geometric and traffic-related inputs are as specified in Exhibit 25-70 and the Facts section of the problem statement.

Step A-4: Balance Demands

The traffic flows in Exhibit 25-45 have already been given in the form of actual demands and no balancing is necessary.

Step A-5: Identify Global Parameters

Global inputs are jam density and queue discharge capacity drop. Values for both parameters are given in the Facts section of the problem statement.

Step A-6: Code Base Facility

In this step, all input data for the subject facility are coded in the computational engine.

Step A-7: Compute Segment Capacities

The resulting capacities are shown in Exhibit 25-71. Because the capacity of a weaving segment depends on traffic patterns, it varies by time period. The remaining capacities are constant for all five time steps. The capacities for Segments 1–5 and for Segments 7–10 are the same because the segments have the same basic cross section. The lane closure on Segment 11 reduces its base capacity by 33%. The impacts of work zone presence on further capacity reduction are assessed in the next step.

Exhibit 25-71
Example Problem 4:
Segment Capacities

Time Step	Capacities (veh/h) by Segment										
	1	2	3	4	5	6	7	8	9	10	11
1						8,273					
2						8,281					
3	6,748	6,748	6,748	6,748	6,748	8,323	6,748	6,748	6,748	6,748	4,499
4						8,403					
5						8,463					

Step A-8: Calibrate with Adjustment Factors

To calculate the CAF for the work zone (Segment 11), the queue discharge and prebreakdown capacities are required. As a result of the work zone, Segment 11 has two open lanes and one closed lane. Therefore, from Exhibit 10-15, its lane closure severity index *LCSI* value is equal to 0.75. Equation 10-8 gives the segment’s queue discharge capacity as follows:

$$QDR_{wz} = 2,093 - 154 \times LCSI - 194 \times f_{Br} - 179 \times f_{AT} + 9 \times f_{LAT} - 59 \times f_{DN}$$

$$\begin{aligned} QDR_{wz} &= 2,093 - 154 \times LCSI - 194 \times f_{Br} - 179 \times f_{AT} + 9 \times f_{LAT} - 59 \times f_{DN} \\ &= 2,093 - 154 \times 0.75 - 194 \times 0 - 179 \times 0 - 59 \times 0 + 9 \times 0 \\ &= 1,977.5 \text{ veh/h} \end{aligned}$$

Using Equation 10-9 and assuming a 13.1% queue discharge capacity drop in work zone conditions, prebreakdown capacity is calculated as follows:

$$c_{wz} = \frac{QDR_{wz}}{100 - \alpha_{wz}} \times 100$$

$$c_{wz} = \frac{1,977.5}{100 - 13.1} \times 100$$

$$c_{wz} = 2,275.6 \text{ veh/h}$$

Then, from Equation 10-11, the work zone CAF is equal to

$$CAF_{wz} = \frac{c_{wz}}{c} = \frac{2,275.6}{2,300} = 0.989$$

Using a similar approach, the work zone SAF can be found as follows from Equation 10-10 and Equation 10-12.

$$FFS_{wz} = 9.95 + 33.49 \times f_{Sr} + 0.53 \times SL_{wz} - 5.60 \times LCSl - 3.84 \times f_{Br} - 1.71 \times f_{DN} - 8.7 \times TRD$$

$$FFS_{wz} = 9.95 + 33.49 \times \left(\frac{60}{55}\right) + 0.53 \times 55 - 5.60 \times 0.75 - 3.84 \times 1 - 1.71 \times 0 - 8.7 \times 1$$

$$FFS_{wz} = 58.9 \text{ mi/h}$$

$$SAF_{wz} = \frac{FFS_{wz}}{FFS} = \frac{58.9}{60} = 0.982$$

These values will be used to update the capacity and FFS of Segment 11 in all time intervals. In addition, the number of lanes in the segment will be reduced to two.

Step A-9: Adjust Managed Lane Cross Weave

This step is only required for facilities with managed lanes. The subject facility does not have a managed lane.

Step A-10: Compute Demand-to-Capacity Ratios

The demand-to-capacity ratios shown in Exhibit 25-72 are calculated from the demand flows in Exhibit 25-45 and segment capacities in Exhibit 25-71.

Time Step	Demand-to-Capacity Ratio by Segment										
	1	2	3	4	5	6	7	8	9	10	11
1	0.67	0.73	0.73	0.73	0.69	0.63	0.72	0.79	0.79	0.79	1.26
2	0.73	0.81	0.81	0.81	0.76	0.71	0.81	0.89	0.89	0.89	1.44
3	0.77	0.87	0.87	0.87	0.83	0.77	0.89	0.99	0.99	0.99	1.56
4	0.69	0.75	0.75	0.75	0.71	0.61	0.71	0.77	0.77	0.77	1.24
5	0.56	0.59	0.59	0.59	0.55	0.47	0.56	0.60	0.60	0.60	0.97

Exhibit 25-72
Example Problem 4: Segment Demand-to-Capacity Ratios

The demand-to-capacity ratio matrix for Example Problem 4 (Exhibit 25-72) shows the presence of the work zone significantly increases the demand-to-capacity ratio on Segment 11. Queues are very likely to start to grow and spill back to upstream segments, and the facility is expected to operate in oversaturated conditions.

Step A-12: Compute Oversaturated Segment Service Measures

The computations for oversaturation apply to any segment with a v_d/c ratio greater than 1.0, as well as any segments upstream of those segments that experience queuing as a result of the bottleneck. All remaining segments are analyzed by using the individual segment methodologies of Chapters 12, 13, and 14, as applicable, with the caveat that the volumes served may differ from the demand flows.

Similar to Example Problem 1, in Example Problem 4, the methodology calculates performance measures for each segment and each time period, starting with the first segment in Time Step 1. The computations are repeated for the first 10 segments for Time Step 1 without encountering a segment with $v_a/c > 1.0$. Once the methodology enters Segment 11 in Time Step 1, the oversaturated computational module is invoked.

The v_a/c ratio for Segment 11, which has the first active bottleneck, will be more than 1.0 and the segment will process traffic at its capacity. Consequently, demand for all downstream segments will be metered by that bottleneck. The unsatisfied demand is stored in upstream segments, which causes queuing in Segment 10 and perhaps additional upstream segments, depending on the level of excess demand. The rate of growth of the vehicle queue (wave speed) is estimated from shock wave theory. The performance measures (speed and density) of any segment with queuing are recomputed, and the newly calculated values override the results from the segment-specific procedures.

Any unsatisfied demand is served in later time periods. As a result, volumes served in later time periods may be higher than the period demand flows. The resulting matrix of volumes served for Example Problem 4 is shown in Exhibit 25-73.

Exhibit 25-73
Example Problem 4:
Volume-Served Matrix

Time Step	Volumes Served (veh/h) by Segment										
	1	2	3	4	5	6	7	8	9	10	11
1	4,505	4,955	4,955	4,955	4,685	5,225	3,924	4,185	4,126	3,929	3,719
2	4,955	5,495	5,495	5,446	3,947	3,701	3,325	3,878	3,882	3,895	3,714
3	3,275	3,476	3,094	3,031	2,912	3,391	3,250	3,899	3,905	3,929	3,714
4	2,831	3,398	3,474	3,416	3,424	3,914	3,597	4,014	4,004	3,965	3,714
5	3,589	3,991	4,096	3,957	3,452	3,912	3,675	3,923	3,916	3,897	3,714

As a result of the bottleneck activation (due to the work zone's presence) in Segment 11 in Time Step 1, queues form in upstream Segments 10, 9, 8, 7, and 6. The queuing is associated with reduced speeds and increased densities in those segments. These and subsequent results were obtained from the computational engine. The resulting performance measures computed for each segment and time interval are speed (Exhibit 25-74), density (Exhibit 25-75), and LOS (Exhibit 25-76). Similar trends are observed in the following time intervals, with queuing reaching the beginning of the facility.

Exhibit 25-74
Example Problem 4:
Speed Matrix

Time Step	Speed (mi/h) by Segment										
	1	2	3	4	5	6	7	8	9	10	11
1	60.0	53.9	59.7	56.1	60.0	48.0	24.2	15.9	13.0	13.0	50.4
2	59.9	53.2	54.5	52.3	22.2	8.9	9.4	12.3	12.2	12.2	50.5
3	12.9	12.8	13.1	9.7	8.0	6.5	9.1	12.4	12.4	12.4	50.5
4	5.9	11.0	12.9	12.8	11.5	8.3	11.0	13.1	12.7	12.7	50.5
5	11.0	16.4	18.6	16.4	12.3	8.3	11.2	12.5	12.3	12.3	50.5

Time Step	Density (veh/mi/ln) by Segment										
	1	2	3	4	5	6	7	8	9	10	11
1	25.0	30.6	27.6	29.4	26.0	27.2	54.1	87.5	100.6	100.6	36.9
2	27.6	34.5	33.6	34.7	59.1	104.2	117.8	105.5	106.2	106.2	36.8
3	84.6	90.6	78.7	104.6	121.4	130.1	119.1	104.4	105.4	105.4	36.8
4	159.3	103.4	89.8	88.7	99.4	117.3	109.0	102.5	104.2	104.2	36.8
5	108.6	81.0	73.5	80.4	93.5	118.2	109.2	105.0	106.0	106.0	36.8

Time Step	LOS by Segment										
	1	2	3	4	5	6	7	8	9	10	11
1	C	C	D	C	D	C	F	F	F	F	E
2	D	D	D	D	F	F	F	F	F	F	E
3	F	F	F	F	F	F	F	F	F	F	E
4	F	F	F	F	F	F	F	F	F	F	E
5	F	F	F	F	F	F	F	F	F	F	E

Exhibit 25-75
Example Problem 4:
Density Matrix

Exhibit 25-76
Example Problem 4:
LOS Matrix

Step A-13: Apply Managed Lane Adjacent Friction Factor

This step is only required for facilities with managed lanes.

Step A-14: Compute Lane Group Performance

This step is only required for facilities with managed lanes.

Step A-15: Compute Freeway Facility Service Performance Measures by Time Interval

In the final analysis step, facilitywide performance measures are calculated for each time step (Exhibit 25-77). Because the computations have already been demonstrated in previous example problems, only summary results are shown. The work zone presence created significant congestion on the subject facility.

Time Step	Performance Measure		LOS
	Space Mean Speed (mi/h)	Average Density (veh/mi/ln)	
1	39.2	38.4	F
2	21.8	66.1	F
3	11.5	99.1	F
4	11.3	105.5	F
5	13.7	93.4	F
Total	19.5	80.5	—

Exhibit 25-77
Example Problem 4:
Facility Performance Measure Summary

Step A-16: Aggregate to Section Level and Validate Against Field Data

This step validates the analysis and is performed only when field data are available.

Step A-17: Estimate LOS and Report Performance Measures for Lane Groups and Facility

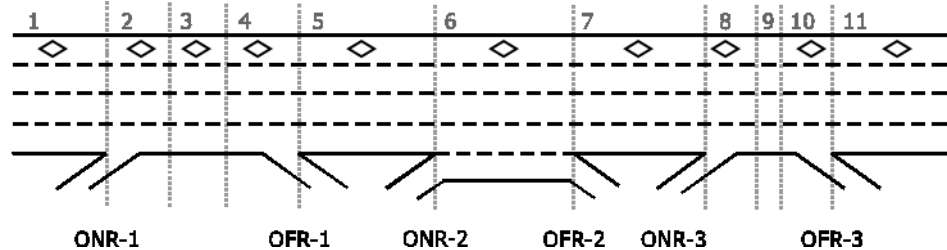
The LOS for each time interval is determined directly from the average density for each time interval. Work zone presence eroded the facility LOS to F in all time intervals.

EXAMPLE PROBLEM 5: EVALUATION OF AN OVERSATURATED FACILITY WITH A MANAGED LANE

The Facility

In this example, a managed lane will be added to the freeway facility described in Example Problem 2. Exhibit 25-78 shows the new facility geometry.

Exhibit 25-78
Example Problem 5:
Freeway Facility



Details of the modified geometry of the 6-mi directional freeway facility are provided in Exhibit 25-79.

Exhibit 25-79
Example Problem 5: Geometry
of Directional Freeway Facility

Segment No.	1	2	3	4	5	6	7	8	9	10	11
Segment type	B	ONR	B	OFR	B	B or W	B	ONR	R	OFR	B
Segment length (ft)	5,280	1,500	2,280	1,500	5,280	2,640	5,280	1,140	360	1,140	5,280
No. of GP lanes	3	3	3	3	3	4	3	3	3	3	3
No. of ML	1	1	1	1	1	1	1	1	1	1	1

Notes: B = basic freeway segment; W = weaving segment; ONR = on-ramp (merge) segment; OFR = off-ramp (diverge) segment; R = overlapping ramp segment; GP = general purpose; ML = managed lanes.

The Facts

In addition to the information contained in Exhibit 25-78 and Exhibit 25-79, the following characteristics of the freeway facility are known:

- SUTs and buses = 1.25% (all movements);
- Mainline TTs = 1.00% (all movements);
- Driver population = regular commuters;
- FFS = 60 mi/h (all mainline segments);
- Ramp FFS = 40 mi/h (all ramps);
- Acceleration lane length = 500 ft (all ramps);
- Deceleration lane length = 500 ft (all ramps);
- D_{jam} = 190 pc/mi/ln;
- c_{IFL} = 2,300 pc/h/ln (for FFS = 60 mi/h);
- L_s = 1,640 ft (for Weaving Segment 6);
- TRD = 1.0 ramp/mi;
- Terrain = level;
- Analysis duration = 75 min (divided into five 15-min intervals); and
- Demand adjustment = +11% (all segments and all time intervals).

A queue discharge capacity drop of 7% is assumed.

Comments

The traffic demand flow inputs are identical to those in Example Problem 2. The facility includes a single managed lane separated with marking with FFS equal to 60 mi/h. The lane is a basic managed lane with no intermediate access points. It is assumed 20% of entry traffic demand on the mainline will use the managed lane.

Step A-1: Define Study Scope

Similar to the previous examples, there are five time steps and the facility has 11 segments. The managed lane extension to the methodology will be used for this analysis.

Step A-2: Divide Facility into Sections and Segments

The segmentation of the subject facility is given in Exhibit 25-78. Therefore, the segmentation process is not repeated.

Step A-3: Input Data

On- and off-ramp demand flow rates are identical to those of Example Problem 2, shown in Exhibit 25-53. It is assumed total entry volume is identical to that of Example Problem 2; however, 20% of total demand is allocated to the managed lane, and the remaining 80% to the general purpose lanes, as shown in Exhibit 25-80.

Time Step	Entering Flow Rate on General Purpose Lanes (veh/h)	Entering Flow Rate on Managed Lane (veh/h)	Sum of Entering Flow Rate to the Facility (veh/h)
1	4,001	1,000	5,001
2	4,400	1,100	5,500
3	4,640	1,160	5,800
4	4,160	1,040	5,200
5	3,361	840	4,201

Exhibit 25-80
Example Problem 5: Demand Inputs on the Mainline

Step A-4: Balance Demands

The traffic flows in Exhibit 25-53 and Exhibit 25-80 have already been given in the form of actual demands and no balancing is necessary.

Step A-5: Identify Global Parameters

Global inputs are jam density and queue discharge capacity drop. Values for both parameters are given in the problem statement.

Step A-6: Code Base Facility

In this step, all input data for the subject facility are coded in the computational engine.

Step A-7: Compute Segment Capacities

Segment capacities are determined by using the methodologies of Chapter 12 for basic freeway segments (general purpose and managed lanes), Chapter 13 for weaving segments, and Chapter 14 for merge and diverge segments. The resulting capacities are shown in Exhibit 25-81.

Exhibit 25-81
Example Problem 5:
Segment Capacities

Time Step	Capacities (veh/h) by Segment for General Purpose Lanes										
	1	2	3	4	5	6	7	8	9	10	11
1						8,177					
2						8,189					
3	6,748	6,748	6,748	6,748	6,748	8,244	6,748	6,748	6,748	6,748	6,748
4						8,331					
5						8,403					

Time Step	Capacities (veh/h) by Segment for Managed Lane										
	1	2	3	4	5	6	7	8	9	10	11
1											
2											
3	1,614	1,614	1,614	1,614	1,614	1,614	1,614	1,614	1,614	1,614	1,614
4											
5											

Step A-8: Calibrate with Adjustment Factors

This step allows the analyst to adjust demands, capacities, and FFSs for the purpose of calibration. According to the problem statement, there is no adjustment needed for the subject facility’s capacity.

Step A-9: Adjust Managed Lane Cross Weave

This facility does not have a cross weave. Therefore, this step is skipped.

Step A-10: Compute Demand-to-Capacity Ratios

The demand-to-capacity ratios shown in Exhibit 25-82 are calculated from the demand flows in Exhibit 25-53 and Exhibit 25-80 and segment capacities in Exhibit 25-81.

Exhibit 25-82
Example Problem 5: Segment
Demand-to-Capacity Ratios

Time Step	Demand-to-Capacity Ratio by Segment (General Purpose Lanes)										
	1	2	3	4	5	6	7	8	9	10	11
1	0.59	0.67	0.67	0.67	0.62	0.59	0.65	0.73	0.73	0.73	0.68
2	0.65	0.74	0.74	0.74	0.68	0.66	0.74	0.83	0.83	0.83	0.79
3	0.69	0.79	0.79	0.79	0.75	0.72	0.82	0.92	0.92	0.92	0.85
4	0.62	0.68	0.68	0.68	0.63	0.56	0.63	0.71	0.71	0.71	0.66
5	0.50	0.53	0.53	0.53	0.48	0.42	0.50	0.54	0.54	0.54	0.51

Time Step	Demand-to-Capacity Ratio by Segment (Managed Lane)										
	1	2	3	4	5	6	7	8	9	10	11
1	0.62	0.62	0.62	0.62	0.62	0.62	0.62	0.62	0.62	0.62	0.62
2	0.68	0.68	0.68	0.68	0.68	0.68	0.68	0.68	0.68	0.68	0.68
3	0.72	0.72	0.72	0.72	0.72	0.72	0.72	0.72	0.72	0.72	0.72
4	0.64	0.64	0.64	0.64	0.64	0.64	0.64	0.64	0.64	0.64	0.64
5	0.52	0.52	0.52	0.52	0.52	0.52	0.52	0.52	0.52	0.52	0.52

The demand-to-capacity ratio matrix for Example Problem 5 (Exhibit 25-82) shows the addition of the managed lane improves traffic operations on the general purpose lanes. As such, it is expected the facility will operate in undersaturated conditions.

Step A-11: Compute Undersaturated Segment Service Measures

The computations for oversaturation apply to any segment with a v_d/c ratio greater than 1.0 as well as any segments upstream of those segments that experience queuing as a result of the bottleneck. All remaining segments are analyzed by using the individual segment methodologies of Chapters 12, 13, and

14, as applicable, with the caveat that volumes served may differ from demand flows.

The basic performance service measures computed for each segment and each time interval include segment speed (Exhibit 25-83), density (Exhibit 25-84), and LOS (Exhibit 25-85).

Time Step	Speed (mi/h) by Segment (General Purpose Lanes)										
	1	2	3	4	5	6	7	8	9	10	11
1	60.0	54.4	59.7	56.2	60.0	48.0	60.0	54.0	54.0	56.1	60.0
2	60.0	53.8	59.7	55.9	60.0	46.8	59.8	53.0	53.0	55.8	59.2
3	60.0	53.3	59.1	55.9	59.7	46.2	58.5	51.7	51.7	55.0	57.7
4	60.0	54.3	59.7	56.2	60.0	49.9	60.0	54.1	54.1	56.1	60.0
5	60.0	55.2	59.8	56.3	60.0	52.7	60.0	55.1	55.1	56.5	60.0

Time Step	Speed (mi/h) by Segment (Managed Lane)										
	1	2	3	4	5	6	7	8	9	10	11
1	59.3	59.3	59.3	59.3	59.3	59.3	59.3	59.3	59.3	59.3	59.3
2	58.9	58.9	58.9	58.9	58.9	58.9	58.9	53.5	53.5	58.1	58.9
3	58.6	58.6	58.6	58.6	58.6	58.6	58.6	52.1	52.1	52.1	58.6
4	59.2	59.2	59.2	59.2	59.2	59.2	59.2	59.2	59.2	59.2	59.2
5	59.7	59.7	59.7	59.7	59.7	59.7	59.7	59.7	59.7	59.7	59.7

Exhibit 25-83
Example Problem 5:
Speed Matrix

Time Step	Density (veh/mi/ln) by Segment (General Purpose Lanes)										
	1	2	3	4	5	6	7	8	9	10	11
1	22.2	27.6	25.0	26.7	23.3	25.0	24.4	30.3	30.3	29.1	25.6
2	24.4	31.0	27.9	29.8	25.6	28.9	27.9	35.2	35.2	33.4	29.8
3	25.8	33.4	30.1	31.8	28.1	32.2	31.6	40.2	40.2	37.8	33.2
4	23.1	28.0	25.3	27.1	23.7	23.4	23.7	29.3	29.3	28.3	24.8
5	18.7	21.5	19.8	21.1	18.1	16.9	18.7	22.1	22.1	21.6	19.2

Time Step	Density (veh/mi/ln) by Segment (Managed Lane)										
	1	2	3	4	5	6	7	8	9	10	11
1	16.9	16.9	16.9	16.9	16.9	16.9	16.9	16.9	16.9	16.9	16.9
2	18.7	18.7	18.7	18.7	18.7	18.7	18.7	20.6	20.6	18.7	18.7
3	19.8	19.8	19.8	19.8	19.8	19.8	19.8	22.3	22.3	22.3	19.8
4	17.6	17.6	17.6	17.6	17.6	17.6	17.6	17.6	17.6	17.6	17.6
5	14.1	14.1	14.1	14.1	14.1	14.1	14.1	14.1	14.1	14.1	14.1

Exhibit 25-84
Example Problem 5:
Density Matrix

Time Step	LOS by Segment (General Purpose Lanes)										
	1	2	3	4	5	6	7	8	9	10	11
1	C	C	C	C	C	C	C	C	D	C	C
2	C	C	D	C	C	D	D	D	E	D	D
3	C	D	D	D	D	D	D	D	E	D	D
4	C	C	C	C	C	C	C	C	D	C	C
5	C	B	C	C	C	B	C	B	C	C	C

Time Step	LOS by Segment (Managed Lane)										
	1	2	3	4	5	6	7	8	9	10	11
1	B	B	B	B	B	B	B	B	B	B	B
2	C	C	C	C	C	C	C	C	C	C	C
3	C	C	C	C	C	C	C	C	C	C	C
4	B	B	B	B	B	B	B	B	B	B	B
5	B	B	B	B	B	B	B	B	B	B	B

Exhibit 25-85
Example Problem 5:
LOS Matrix

Step A-13: Apply Managed Lane Adjacent Friction Factor

The subject facility has densities in excess of 35 pc/mi/ln. As a result, friction effects are applied according to the process described in Chapter 12. The indicator variable I_c in Equation 12-12 will have a nonzero value for the segments

and analysis periods during which the general purpose lane density is greater than 35 pc/mi/ln. Consequently, the S_3 term in Equation 12-12 will reduce the estimated general purpose lane speed as a result of the friction.

Step A-14: Compute Lane Group Performance

In this step, performance measures for all the facility’s lane groups are computed. The subject facility has two lane groups, one for general purpose lanes and one for the managed lane, as shown in Exhibit 25-86.

Exhibit 25-86
Example Problem 5: Facility Performance Measure Summary for Lane Groups

Time Step	General Purpose Lane Group Performance Measure		Managed Lane Group Performance Measure	
	Space Mean Speed (mi/h)	Average Density (veh/mi/ln)	Space Mean Speed (mi/h)	Average Density (veh/mi/ln)
1	57.7	24.9	59.3	16.9
2	57.3	28.1	58.6	18.8
3	56.5	31.0	58.0	20.0
4	58.0	24.6	59.2	17.6
5	58.5	19.1	59.7	14.1

Step A-15: Compute Freeway Facility Service Performance Measures by Time Interval

In the final analysis step, facilitywide performance measures are calculated for each time step (Exhibit 25-87). Because the computations have been demonstrated previously, only summary results are shown here. The addition of the managed lane reduced traffic congestion on the subject facility.

Exhibit 25-87
Example Problem 5: Facility Performance Measure Summary

Time Step	Performance Measure		LOS
	Space Mean Speed (mi/h)	Average Density (veh/mi/ln)	
1	58.0	23.4	C
2	57.5	26.4	D
3	56.7	29.1	D
4	58.2	23.3	C
5	58.7	18.1	C
Total	57.8	24.0	—

Step A-16: Aggregate to Section Level and Validate Against Field Data

This step validates the analysis and is performed only when field data are available.

Step A-17: Estimate LOS and Report Performance Measures for Lane Groups and Facility

The LOS for each time interval is determined directly from the average density for each time interval. The addition of the managed lane improved traffic conditions over the entire facility.

EXAMPLE PROBLEM 6: PLANNING-LEVEL ANALYSIS OF A FREEWAY FACILITY

The Facility

In this example, the planning-level methodology is used to analyze a freeway facility with geometric characteristics identical to the facility used in Example Problem 1. Exhibit 25-43 shows the facility geometry. Note that the planning methodology uses annual average daily traffic (AADT) values to calculate demand levels at the facility’s entry and exit points based on the hourly (K) and annual growth factors (f_g). As a result, although the AADTs have been manipulated in this example to create demand levels close to those of Example Problem 1, the results will not match precisely. Furthermore, because the planning-level methodology uses freeway sections rather than segments and is limited to four analysis periods, a direct comparison is not possible.

The Facts

In addition to the information given in Exhibit 25-43 and Exhibit 25-44, the following characteristics of the freeway facility are known:

- Heavy-vehicle percentage = 0%,
- Driver population = regular commuters on an urban facility,
- FFS = 60 mi/h (all mainline segments),
- Ramp FFS = 40 mi/h (all ramps),
- D_{jam} = 190 pc/mi/ln,
- K -factor = 0.09,
- Growth factor = 1,
- PHF = 0.9,
- Terrain = level, and
- Analysis duration = 60 min (divided into four 15-min analysis periods).

Average Annual Daily Traffic

The planning-level approach uses directional AADT values to approximate demand levels on different freeway sections. Exhibit 25-88 depicts AADT values on all entry points (i.e., the first basic freeway section and all on-ramps) and all exit points (all off-ramps).

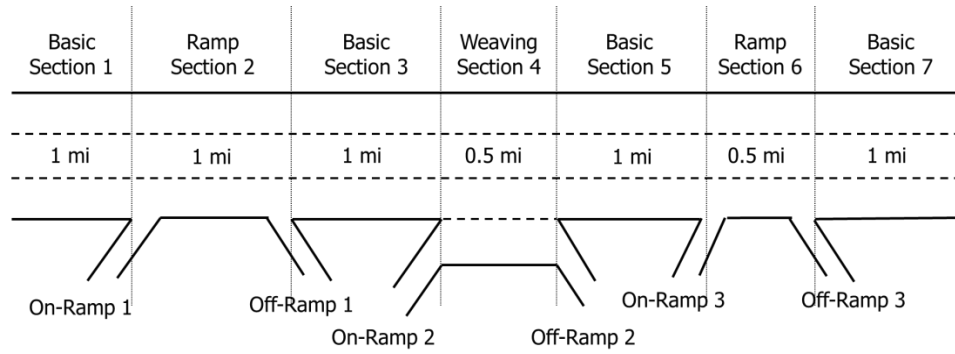
Entering AADT (veh/day)	Ramp AADT (veh/day)					
	ONR1	ONR2	ONR3	OFR1	OFR2	OFR3
55,000	4,500	5,400	4,500	2,700	3,600	2,700

Exhibit 25-88
Example Problem 6:
AADT Values for the Facility

Sections

The facility and all geometric inputs are identical to Example Problem 1. Exhibit 25-89 presents the different freeway sections for the facility of interest.

Exhibit 25-89
Example Problem 6: Section
Definition for the Facility



Section 1 is a basic section, identical to the HCM segmentation definition. An on-ramp roadway is located just downstream of Section 1 that results in changes in the demand level. As a result, a new section needs to be defined. The demand level on the new section remains fixed up to the first off-ramp roadway, at which point both the capacity and the demand change. As a result, Section 2 is defined as a ramp section. After the off-ramp roadway, the facility demand drops and remains fixed until the next on-ramp roadway. As a result, Section 3 is defined as a basic freeway section. Sections on the rest of the freeway facility are defined following a similar process. The result is that seven distinct sections are defined.

Step 1: Demand Level Calculations

The demand level on each section in each analysis period is determined by using the given AADT values, *PHF*, *K*-factor, heavy-vehicle factor, and growth factor.

$$q_{1,1} = AADT_1 \times K \times f_{tg} \times f_{HV} = 55,000 \times 0.09 \times 1 \times 1 = 4,950 \text{ pc/h}$$

$$q_{1,2} = AADT_1 \times K \times \left(\frac{1}{PHF}\right) \times f_{tg} \times f_{HV} = 55,000 \times 0.09 \times \left(\frac{1}{0.9}\right) \times 1 = 5,500 \text{ pc/h}$$

$$q_{1,3} = AADT_1 \times K \times f_{tg} = 55,000 \times 0.09 \times 1 \times f_{HV} = 4,950 \text{ pc/h}$$

$$q_{1,4} = AADT_1 \times K \times \left(2 - \frac{1}{PHF}\right) \times f_{tg} \times f_{HV} = 55,000 \times 0.09 \times \left(2 - \frac{1}{0.9}\right) \times 1 = 4,400 \text{ pc/h}$$

By following the same approach, the demand levels for all facility entry and exit points are found. The results are summarized in Exhibit 25-90.

Exhibit 25-90
Example Problem 6:
Demand Flow Rates (pc/h) on
the Subject Facility

Analysis Period	Entry	On-Ramp 1	Off-Ramp 1	On-Ramp 2	Off-Ramp 2	On-Ramp 3	Off-Ramp 3
1	4,950	405	243	486	324	405	243
2	5,500	450	270	540	360	450	270
3	4,950	405	243	486	324	405	243
4	4,400	360	216	432	288	360	216

After calculation of the entry and exit demand flow rates from the AADT values, the demand level in each section in each analysis period is found.

Step 2: Section Capacity Calculations and Adjustments

Equation 25-45 is used to determine the base capacity of each section. The base capacity of each section is then adjusted by using the appropriate adjustment factor for a weaving, ramp, merge, or diverge section. For instance, the capacity of Section 1 (a basic section) is determined as follows:

$$c_1 = (2,200 + 10 \times (\min(70, S_{FFS}) - 50)) = (2,200 + 10 \times (\min(70, 60) - 50))$$

$$c_1 = 2,300 \text{ pc/h/ln}$$

Because FFS and percentage heavy vehicles are global inputs, the capacity of each of the facility’s basic freeway sections is equal to 2,300 pc/h/ln. However, for all other sections, this base capacity needs to be adjusted.

Section 2 is a ramp section. The CAF for a ramp section is 0.9. Therefore, the capacity of Section 2 is computed as follows:

$$c_2 = 2300 \times 0.90 = 2,070 \text{ pc/h/ln}$$

Section 3 is a basic freeway section; therefore, its capacity remains at 2,300 pc/h/ln. However, Section 4 is a weaving section and its capacity will need to be adjusted. The CAF for a weaving section is determined by the volume ratio and section length.

The volume ratio (the ratio of weaving demand to total demand) is approximated by summing the weaving section’s ramp AADT values and dividing the result by the total AADT on the weaving section, as follows:

$$V_r = \frac{(5,400 + 3,600)}{55,000 + 4,500 - 2,700} = \frac{9,000}{56,800} = 0.158$$

The length of the weaving section is 0.5 mi. As a result, the CAF is calculated as follows:

$$CAF_{weave} = \min(0.884 - 0.0752V_r + 0.0000243L_s, 1)$$

$$CAF_{weave} = 0.884 - 0.0752 \times 0.164 + 0.0000243 \times 0.5 \times 5,280 = 0.94$$

Therefore, the capacity of Section 4 is

$$c_4 = 2,300 \times 0.94 = 2,162 \text{ pc/h/ln}$$

The capacities of Section 5 (basic), Section 6 (ramp), and Section 7 (basic) are 2,300, 2,070, and 2,300 pc/h/ln, respectively. At this stage, demand-to-capacity ratios for all sections in all analysis periods can be determined, as presented in Exhibit 25-91.

Analysis Period	Demand-to-Capacity Ratios by Section						
	1	2	3	4	5	6	7
1	0.72	0.86	0.74	0.65	0.76	0.91	0.79
2	0.80	0.96	0.82	0.72	0.85	1.02	0.88
3	0.72	0.86	0.74	0.65	0.76	0.93	0.80
4	0.64	0.77	0.66	0.58	0.68	0.81	0.70

As shown in Exhibit 25-91, the demand-to-capacity ratio in the sixth section in the second analysis period is greater than one. As a result, queue formation and low space mean speeds are expected on this section. The demand-to-capacity ratios on the remaining segments are below one across all analysis periods.

Exhibit 25-91
Example Problem 6:
Demand-to-Capacity Ratios by
Section and Analysis Period

Step 3: Delay Rate Estimation

In this step, demand-to-capacity ratios are used to determine delay rates for all sections of the facility across all analysis periods. FFS on the facility is 60 mi/h, and all demand-to-capacity ratios are below one. As a result, the delay rates for each section are found by using Equation 25-47.

$$\Delta_{RU_{i,t}} = \begin{cases} 0 & \frac{d_{i,t}}{c_i} < 0.72 \\ 121.35 \left(\frac{d_{i,t}}{c_i}\right)^3 + (-184.84) \left(\frac{d_{i,t}}{c_i}\right)^2 + 83.21 \left(\frac{d_{i,t}}{c_i}\right) + (-9.33) & 0.72 \leq \frac{d_{i,t}}{c_i} \leq 1 \end{cases}$$

For instance, the delay rate for Section 1 in the first analysis period is 0 s/mi, because its demand-to-capacity ratio of 0.717 is less than the 0.72 threshold used in Equation 25-47. Section 2’s demand-to-capacity ratio is 0.86, which is greater than the threshold. Therefore, its delay rate is calculated as follows:

$$\Delta_{RU_{2,1}} = 121.35(0.86)^3 + (-184.84)(0.86)^2 + 83.21(0.86) + (0.86) = 2.8 \text{ s/mi}$$

Delay rates for other sections of the facility are determined in the same way and are summarized in Exhibit 25-92.

Exhibit 25-92
Example Problem 6:
Delay Rates by Section and
Analysis Period

Analysis Period	Delay Rate by Section (s/mi)						
	1	2	3	4	5	6	7
1	0.0	2.8	0.2	0.0	0.5	5.0	0.8
2	1.0	7.4	1.6	0.1	2.3	11.7	3.3
3	0.0	2.8	0.2	0.0	0.5	5.8	1.1
4	0.0	0.5	0.0	0.0	0.0	1.3	0.0

Step 4: Average Travel Time, Speed, and Density Calculations

Delay rates are used to compute travel times and, consequently, speeds. To determine a section’s travel time, its travel rate is calculated by summing the section’s travel rate under free-flow conditions and its delay rates for undersaturated and oversaturated conditions. This calculation is repeated for each section across all analysis periods. The following equations demonstrate the calculation for the first two sections during the first analysis period:

$$TR_{1,1} = \Delta_{RU_{1,1}} + \Delta_{RO_{1,1}} + TR_{FFS} = 0.00 + 0.00 + \frac{3,600}{S_{FFS}} = \frac{3,600}{60} = 60 \text{ s/mi}$$

$$TR_{2,1} = \Delta_{RU_{2,1}} + \Delta_{RO_{2,1}} + TR_{FFS} = 0.00 + 0.00 + \frac{3,600}{S_{FFS}} = 2.8 + \frac{3,600}{60} = 62.8 \text{ s/mi}$$

Travel rates for all sections across all analysis periods are shown in Exhibit 25-93.

Analysis Period	Travel Rate by Section (s/mi)						
	1	2	3	4	5	6	7
1	60.0	62.8	60.2	60.0	60.5	65.0	60.8
2	61.0	67.4	61.6	60.1	62.3	71.7	63.3
3	60.0	62.8	60.2	60.0	60.5	65.8	61.1
4	60.0	60.5	60.0	60.0	60.0	61.3	60.0

Each section’s travel time is calculated by multiplying its travel rate by its length. The results are presented in Exhibit 25-94.

Analysis Period	Travel Time by Section (s)						
	1	2	3	4	5	6	7
1	60.0	62.8	60.2	30.0	60.5	32.5	60.8
2	61.0	67.4	61.6	30.0	62.3	35.8	63.3
3	60.0	62.8	60.2	30.0	60.5	32.9	61.1
4	60.0	60.5	60.0	30.0	60.0	30.7	60.0

Density is determined for each section across all analysis periods by dividing the section’s demand by its speed (section length divided by travel time). The results are shown in Exhibit 25-95.

Analysis Period	Density by Section (pc/mi/ln)						
	1	2	3	4	5	6	7
1	27.5	31.1	28.5	23.3	29.5	34.2	30.6
2	31.1	37.2	32.4	25.9	33.8	41.2	35.4
3	27.5	31.1	28.5	23.3	29.5	35.2	31.3
4	24.4	26.7	25.2	20.7	26.0	28.7	26.8

Finally, the approach provides a high-level summary that includes a capacity assessment, the aggregated travel time, the space mean speed, the average facility density, the total queue length, and the facility LOS by analysis period, as shown in Exhibit 25-96.

Analysis Period	High-Level Capacity Assessment	Travel Time (min)	Space Mean Speed (mi/h)	Average Facility Density (pc/mi/ln)	Total Queue Length (mi)	LOS
1	Undersaturated	6.1	58.9	29.2	0.0	D
2	Oversaturated	6.4	56.6	33.7	0.8	F
3	Undersaturated	6.1	58.8	29.4	0.0	D
4	Undersaturated	6.0	59.8	25.5	0.0	C

The average facility travel time in each time step is calculated by summing each section’s travel time and dividing the result by 60 to convert the units to minutes. Space mean speed in each analysis period is then calculated by dividing the total facility length by the facility travel time in each analysis period. The facility density is a length-weighted average of each section’s density, and the total queue length is the sum of each section’s queue length. Finally, LOS is calculated based on the urban freeway density thresholds if the demand-to-capacity ratio is less than 1; otherwise, LOS is set to F if any section operates at a demand-to-capacity ratio greater than 1.0.

The facility is oversaturated during the second analysis period, with one of the sections experiencing a demand-to-capacity ratio greater than 1.0. The

Exhibit 25-93

Example Problem 6:
Travel Rates by Section and Analysis Period

Exhibit 25-94

Example Problem 6:
Average Travel Times by Section and Analysis Period

Exhibit 25-95

Example Problem 6:
Density by Section and Analysis Period

Exhibit 25-96

Example Problem 6:
Facility Performance Summary

method estimates that a 0.8-mi queue will result from an active bottleneck. With at least one time interval operating at LOS F, it is recommended that a more detailed operational analysis of this facility be conducted to obtain a more accurate estimate of congestion patterns.

EXAMPLE PROBLEM 7: RELIABILITY EVALUATION OF AN EXISTING FREEWAY FACILITY

The Facility

This example problem uses the same 6-mi facility used in Example Problem 1. The facility consists of 11 segments with the properties indicated in Exhibit 25-97. Other facility characteristics are identical to those given in Example Problem 1, except that the study period in this example has been extended from 75 to 180 min. Exhibit 25-98 shows the facility geometry.

Exhibit 25-97
Example Problem 7:
Freeway Facility

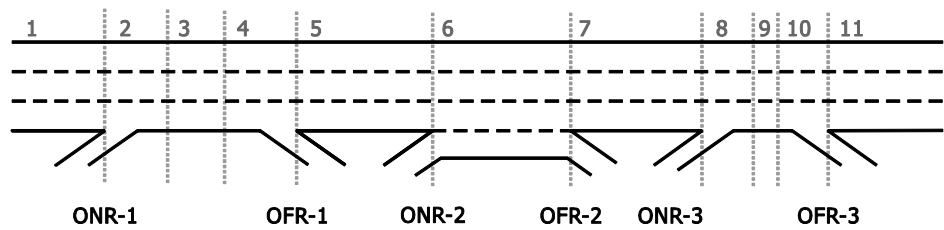


Exhibit 25-98
Example Problem 7: Geometry
of Directional Freeway Facility

Segment No.	1	2	3	4	5	6	7	8	9	10	11
Segment type	B	ONR	B	OFR	B	B or W	B	ONR	R	OFR	B
Segment length (ft)	5,280	1,500	2,280	1,500	5,280	2,640	5,280	1,140	360	1,140	5,280
No. of lanes	3	3	3	3	3	4	3	3	3	3	3

Notes: B = basic freeway segment; W = weaving segment; ONR = on-ramp (merge) segment; OFR = off-ramp (diverge) segment; R = overlapping ramp segment.

Input Data

This example illustrates the use of defaults and lookup tables to substitute for desirable but difficult to obtain data. Minimum facility inputs for the example problem include the following.

Facility Geometry

All the geometric information about the facility normally required for an HCM freeway facility analysis (Chapters 10–14) is also required for a reliability analysis. These data are supplied as part of the base scenario.

Study Parameters

These parameters specify the study period, the reliability reporting period, and the date represented by the traffic demand data used in the base scenario.

The study period in this example is from 4 to 7 p.m., which covers the afternoon and early evening peak hour and shoulder periods. Recurring congestion is typically present in the study direction of this facility during that period, which is why it has been selected for reliability analysis. The reliability reporting period is set as all weekdays in the calendar year. (For simplicity of presentation in this example, holidays have not been removed from the

reliability reporting period.) The demand data are reflective of AADT variations across the weekdays and months in a calendar year for the subject facility.

Base Demand

Demand flow rates in vehicles per hour are supplied for each 15-min analysis period in the base scenario. Care should be taken that demand data are measured upstream of any queued traffic. If necessary, demand can be estimated as the sum of departing volume and the change in the queue size at a recurring bottleneck.

Exhibit 25-99 provides the twelve 15-min demand flow rates required for the entire 3-h study period.

Analysis Period	Demand Entry	ONR1	ONR2	ONR3	OFR1	OFR2	OFR3
	Flow Rate						
1	3,095	270	270	270	180	270	180
2	3,595	360	360	360	270	360	270
3	4,175	360	450	450	270	360	270
4	4,505	450	540	450	270	360	270
5	4,955	540	720	540	360	360	270
6	5,225	630	810	630	270	360	450
7	4,685	360	360	450	270	360	270
8	3,785	180	270	270	270	180	180
9	3,305	180	270	270	270	180	180
10	2,805	180	270	270	270	180	180
11	2,455	180	180	180	270	180	180
12	2,405	180	180	180	180	180	180

Note: ONR = on-ramp; OFR = off-ramp.

Incident Data

Detailed incident logs are not available for this facility, but local data are available about the facility’s crash rate: 150 crashes per 100 million VMT. An earlier study conducted by the state in which the facility is located found that an average of seven incidents occur for every crash.

Computational Steps

Base Data Set Analysis

The Chapter 10 freeway facilities core methodology is applied to the base data set to ensure the specified facility boundaries and study period are sufficient to cover any bottlenecks and queues. In addition, because incident data are supplied in the form of a facility crash rate, the VMT associated with the base data set are calculated so that incident probabilities can be calculated in a subsequent step. In this case, 71,501 vehicle miles of travel occur on the facility over the 3-h base study period. The performance measures normally output by the Chapter 10 methodology are compiled for each combination of segment and analysis period during the study period and stored for later use. Of particular note, the facility operates just under capacity, with a maximum demand-to-capacity ratio of 0.99 in Segments 7–10.

Exhibit 25-99
 Example Problem 7: Demand Flow Rates (veh/h) by Analysis Period in the Base Data Set

Incorporating Demand Variability

Exhibit 25-100 provides demand ratios relative to AADT by month and day derived from a permanent traffic recorder on the facility. The demand values for the seed file were collected on a Tuesday in November.

Exhibit 25-100
Example Problem 7: Demand Ratios Relative to AADT

Month	Monday	Tuesday	Wednesday	Thursday	Friday
January	0.822	0.822	0.839	0.864	0.965
February	0.849	0.849	0.866	0.892	0.996
March	0.921	0.921	0.939	0.967	1.080
April	0.976	0.976	0.995	1.025	1.145
May	0.974	0.974	0.993	1.023	1.142
June	1.022	1.022	1.043	1.074	1.199
July	1.133	1.133	1.156	1.191	1.329
August	1.033	1.033	1.054	1.085	1.212
September	1.063	1.063	1.085	1.117	1.248
October	0.995	0.995	1.016	1.046	1.168
November	0.995	0.995	1.016	1.046	1.168
December	0.979	0.979	0.998	1.028	1.148

Incorporating Weather Variability

In the absence of facility-specific weather data, the default weather data for the metropolitan area closest to the facility are used.

In the absence of local data, the default CAF and SAF for an FFS of 60 mi/h are used for each weather event. These values are applied in a later step to each scenario involving a weather event. Exhibit 25-101 summarizes the probabilities of each weather event by season, and Exhibit 25-102 summarizes the CAF, SAF, and event duration values associated with each weather event.

Exhibit 25-101
Example Problem 7: Weather Event Probabilities by Season

Weather Event	Weather Event Probability by Season (%)			
	Winter	Spring	Summer	Fall
Medium rain	0.80	1.01	0.71	0.86
Heavy rain	0.47	0.81	1.33	0.68
Light snow	0.91	0.00	0.00	0.00
Light-medium snow	0.29	0.00	0.00	0.00
Medium-heavy snow	0.04	0.00	0.00	0.00
Heavy snow	0.00	0.00	0.00	0.00
Severe cold	0.00	0.00	0.00	0.00
Low visibility	0.97	0.12	0.16	0.34
Very low visibility	0.00	0.00	0.00	0.00
Minimal visibility	0.44	0.10	0.00	0.03
Nonsevere weather	96.09	97.95	97.80	98.08

Note: Winter = December, January, and February; spring = March, April, and May; summer = June, July, and August; fall = September, October, and November.

Exhibit 25-102
Example Problem 7: CAF, SAF, and Event Duration Values Associated with Weather Events

Weather Event	CAF	SAF	Average Duration (min)
Medium rain	0.93	0.95	40.2
Heavy rain	0.86	0.93	33.7
Light snow	0.96	0.92	93.1
Light-medium snow	0.94	0.90	33.4
Medium-heavy snow	0.91	0.88	21.7
Heavy snow	0.78	0.86	7.3
Severe cold	0.92	0.95	0.0
Low visibility	0.90	0.95	76.2
Very low visibility	0.88	0.94	0.0
Minimal visibility	0.90	0.94	145
Nonsevere weather	1.00	1.00	N/A

Note: N/A = not applicable.

Incorporating Incident Variability

For an existing freeway facility such as this one, detailed incident logs would be desirable so that facility-specific monthly or seasonal probabilities of various incident severities could be determined. However, in this case, incident logs of sufficient detail are not available.

Therefore, incident probabilities and severities are estimated by the alternative method of using local crash rates and ratios of incidents to crashes, in combination with default values, by using Equation 25-77 through Equation 25-79. The expected number of incidents during a study period under a specified demand pattern is the product of the crash rate, the local incident-to-crash ratio, the demand volume during the study period, and the facility length. The crash rate is 150 crashes per 100 million VMT; the ratio of incidents to crashes is given as 7. The resulting incident frequencies for different months of the reliability reporting period are determined as shown in Exhibit 25-103.

Month	Incident Frequency
January	0.65
February	0.67
March	0.72
April	0.77
May	0.77
June	0.80
July	0.89
August	0.82
September	0.83
October	0.83
November	0.79
December	0.77

Exhibit 25-103
Example Problem 7: Incident Frequencies by Month

Results and Discussion

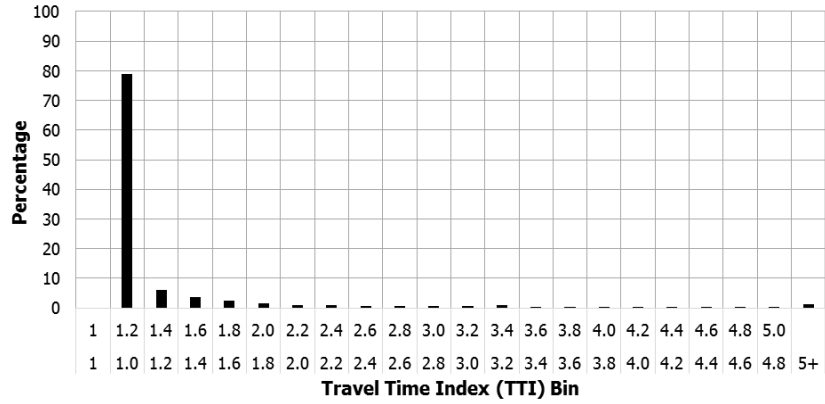
Exhibit 25-104 provides key reliability performance measure results for this example problem. The number of replications for each scenario was four, resulting in 240 scenarios. Exhibit 25-105 shows the generated probability and cumulative distributions of travel time index (TTI) for this example problem. A seed number of 1 was chosen to generate random numbers in the computational engine.

Reliability Performance Measure	Value from All Scenarios
TTI_{50}	1.03
TTI_{mean}	1.30
PTI (TTI_{95})	1.67
Maximum observed facility TTI (TTI_{max})	33.57
Misery index	5.76
Reliability rating	90.8%
Semi-standard deviation	2.05
Percentage VMT at TTI >2	2.95%

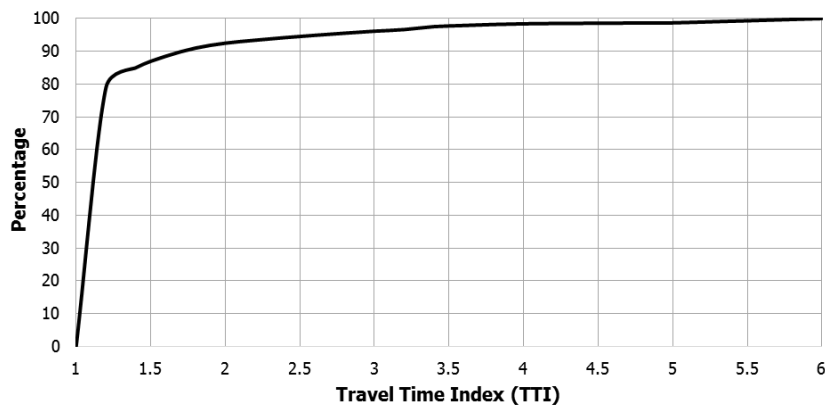
Note: PTI = planning time index; TTI = travel time index.

Exhibit 25-104
Example Problem 7: Summary Reliability Performance Measure Results

Exhibit 25-105
 Example Problem 7:
 VMT-Weighted TTI Probability
 and Cumulative Distribution
 Functions



(a) Probability Distribution Function



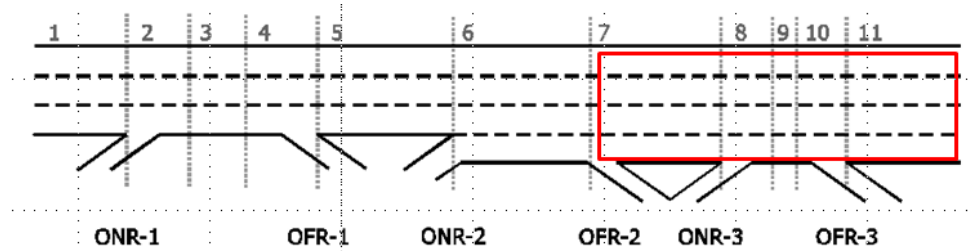
(b) Cumulative Distribution Function

EXAMPLE PROBLEM 8: RELIABILITY ANALYSIS WITH GEOMETRIC IMPROVEMENTS

The Facility

In this example, the freeway facility from Example Problem 6 is widened by a lane in Segments 7–11. These segments operated close to capacity in the base scenario and were definitely over capacity in scenarios with severe weather or incident conditions. The revised geometry also improves the operation of weaving Segment 6, because no lane changes are required of traffic entering at On-Ramp 2. Exhibit 25-106 provides a schematic of the freeway facility.

Exhibit 25-106
 Example Problem 8:
 Freeway Facility



Data Inputs

All the input data used in Example Problem 6 remain unchanged, except for the number of lanes on the facility. The extra lane creates the possibility of having a three-lane-closure incident scenario in the four-lane portion of the facility.

Results and Discussion

Exhibit 25-107 provides key reliability performance measure results for this example problem. The mean TTI across the reliability reporting period decreases from 1.54 to 1.18, corresponding to a speed improvement from 38.96 to 50.8 mi/h—more than a 10% increase and perhaps enough to justify the improvement, once non-reliability-related factors are taken into account. Similar results occur for most other performance measures.

Reliability Performance Measure	Value from All Scenarios
TTI_{50}	1.02
TTI_{mean}	1.18
PTI (TTI_{95})	1.17
Maximum observed facility TTI (TTI_{max})	33.5
Misery index	4.07
Reliability rating	97.56%
Semi-standard deviation	1.71
Percentage VMT at TTI >2	1.42%

Note: PTI = planning time index; TTI = travel time index.

Exhibit 25-107

Example Problem 8: Summary Reliability Performance Measure Results

EXAMPLE PROBLEM 9: EVALUATION OF INCIDENT MANAGEMENT

This example problem illustrates the analysis of a nonconstruction alternative that focuses on improved incident management strategies. In this example, the size of the motorist response fleet is increased and communication is improved between the various stakeholders (e.g., traffic management center, emergency responders, and motorist response fleet), allowing faster clearance of incidents than before.

Data Inputs

All the input data used in Example Problem 6 remain unchanged, except for the assumed incident durations and standard deviations. The default incident mean durations and standard deviations are reduced by 30% each for all incident severity types. Note that these values have been created for the purposes of this example problem and do not necessarily reflect results that would be obtained in an actual situation.

Results and Discussion

The key congestion and reliability statistics for this example problem are summarized in Exhibit 25-108. The mean TTI across the reliability reporting period decreases from 1.35 to 1.20, corresponding to a speed improvement from 44.4 to 50.0 mi/h—more than a 10% increase and perhaps enough to justify the improvement, once non-reliability-related factors are taken into account. Similar results occur for most other performance measures.

Exhibit 25-108
 Example Problem 9:
 Summary Reliability
 Performance Measure Results

Reliability Performance Measure	Value from All Scenarios
TTI_{50}	1.03
TTI_{mean}	1.25
PTI (TTI_{95})	1.59
Maximum observed facility TTI (TTI_{max})	30.7
Misery index	4.88
Reliability rating	91.36%
Semi-standard deviation	1.77
Percentage VMT at TTI >2	2.4%

Note: PTI = planning time index; TTI = travel time index.

EXAMPLE PROBLEM 10: PLANNING-LEVEL RELIABILITY ANALYSIS

This example illustrates the planning-level reliability analysis methodology described in Chapter 11. The method estimates the mean and 95th percentile TTI, as well as the percentage of trips occurring below a speed of 45 mi/h.

The Facts

The segment under study has three lanes in the analysis direction, an FFS of 75 mi/h, and a peak hour speed of 62 mi/h. The volume-to-capacity ratio during the peak hour is 0.95.

Solution

The value of TTI_{mean} is calculated from Equation 11-1, and is a function of the recurring delay rate RDR and the incident delay rate IDR . These rates are calculated from Equation 11-2 and Equation 11-3, respectively.

$$RDR = \frac{1}{S} - \frac{1}{FFS}$$

$$RDR = \frac{1}{62} - \frac{1}{75} = 0.00280$$

$$IDR = [0.020 - (N - 2) \times 0.003] \times X^{12}$$

$$IDR = [0.020 - (3 - 2) \times 0.003] \times (0.95)^{12} = 0.00919$$

TTI_{mean} can now be calculated as

$$TTI_{mean} = 1 + FFS \times (RDR + IDR)$$

$$TTI_{mean} = 1 + 75 \times (0.00280 + 0.00919)$$

$$TTI_{mean} = 1.899$$

TTI_{95} is calculated from Equation 11-4 as follows:

$$TTI_{95} = 1 + 3.67 \times \ln(TTI_{mean})$$

$$TTI_{95} = 1 + 3.67 \times \ln(1.899)$$

$$TTI_{95} = 3.353$$

Finally, the percentage of trips made at a speed below 45 mi/h is calculated with Equation 11-5.

$$PT_{45} = 1 - \exp(-1.5115 \times (TTI_{mean} - 1))$$

$$PT_{45} = 1 - \exp(-1.5115 \times (1.899 - 1))$$

$$PT_{45} = 74.3\%$$

EXAMPLE PROBLEM 11: ESTIMATING FREEWAY COMPOSITE GRADE OPERATIONS WITH THE MIXED-FLOW MODEL

This example problem addresses a composite grade section on a six-lane freeway. It illustrates how the mixed-flow model procedures can be applied to the case of composite grades.

The Facts

- Three segments with the following grades and lengths:
 - First segment: 1.5-mi basic segment on a 3% upgrade
 - Second segment: 2-mi basic segment on a 2% upgrade
 - Third segment: 1-mi basic segment on a 5% upgrade
- 5% SUTs and 10% TTs
- FFS of 65 mi/h
- 15-min mixed-traffic flow rate is 1,500 veh/h/ln (PHF = 1.0)

Comments

Chapter 26, Basic Freeway and Highway Segments: Supplemental, presents the procedure for estimating the speed on a single-grade basic freeway segment using the mixed-flow model. The task here is to estimate the speed by mode for each segment, along with the overall mixed-flow speed and travel time for the composite grade.

Step 1: Input Data

All input data are specified above.

Step 2: Capacity Assessment

The CAF for mixed flow allows for the conversion of auto-only capacities into mixed-traffic-stream capacities. It can be computed with Equation 25-53.

For the first segment,

$$CAF_{\text{mix},1} = CAF_{ao} - CAF_{T,\text{mix}} - CAF_{g,\text{mix},1}$$

There are four terms in the equation. The CAF for auto-only conditions CAF_{ao} is assumed to be 1, because no auto adjustments are necessary.

CAF for Truck Percentage

The truck effect term is computed from Equation 25-54.

$$CAF_{T,\text{mix}} = 0.53 \times P_T^{0.72} = 0.53 \times 0.15^{0.72} = 0.135$$

CAF for Grade Effect

The grade effect term is computed from Equation 25-55 and Equation 25-56. Given that the total truck percentage is 15%, the coefficient $\rho_{g,\text{mix}}$ is calculated as

$$\rho_{g,\text{mix}} = 0.126 - 0.03P_T = 0.126 - 0.03 \times 0.15 = 0.1215$$

and the CAF for grade effect for Segment 1 is calculated as

$$CAF_{g,mix,1} = \rho_{g,mix} \times \max[0, 0.69 \times (e^{12.9g_j} - 1)] \\ \times \max[0, 1.72 \times (1 - 1.71e^{-3.16d_j})]$$

$$CAF_{g,mix,1} = 0.1215 \times \max[0, 0.69 \times (e^{12.9 \times 0.03} - 1)] \\ \times \max[0, 1.72 \times (1 - 1.71e^{-3.16 \times 1.5})]$$

$$CAF_{g,mix,1} = 0.067$$

Mixed-Flow CAF

The mixed-flow CAF for Segment 1 can now be calculated from Equation 25-53.

$$CAF_{mix,j} = CAF_{ao} - CAF_{T,mix} - CAF_{g,mix,1} = 1.000 - 0.135 - 0.067 = 0.798$$

Segment Capacity

The mixed-flow capacity of segment 1 is computed from the segment's auto-only capacity and mixed-flow CAF. The auto-only capacity is determined from an equation in Exhibit 12-6.

$$C_{ao} = 2,200 + 10(FFS - 50) = 2,200 + 10 \times (65 - 50) = 2,350 \text{ pc/h/ln}$$

Segment 1's mixed-flow capacity is then determined with Equation 25-57.

$$C_{mix,1} = C_{ao} \times CAF_{mix,1} = 2,350 \times 0.798 = 1,875 \text{ veh/h/ln}$$

Because the mixed-flow CAFs and capacities for Segments 2 and 3 can be computed by following the same procedure, the results are presented directly without showing the computational details.

$$CAF_{mix,2} = CAF_{ao} - CAF_{T,mix} - CAF_{g,mix,2} = 1 - 0.135 - 0.042 = 0.823$$

$$C_{mix,2} = C_{ao} \times CAF_{mix,2} = 2,350 \times 0.823 = 1,934 \text{ veh/h/ln}$$

$$CAF_{mix,3} = CAF_{ao} - CAF_{T,mix} - CAF_{g,mix,3} = 1 - 0.135 - 0.122 = 0.743$$

$$C_{mix,3} = C_{ao} \times CAF_{mix,3} = 2,350 \times 0.743 = 1,746 \text{ veh/h/ln}$$

As the mixed-flow demand of 1,500 veh/h/ln is less than the smallest of the three segment capacities, 1,746 veh/h/ln, the analysis can proceed.

Steps 3 to 6

Steps 3 through 6 are repeated for each segment, as shown below.

Segment 1

Step 3: Specify Initial Conditions

Because this is the first segment, an FFS of 65 mi/h is used as the initial truck kinematic spot travel time rate. The effect of traffic interactions on truck speed is accounted for in Step 4.

Step 4: Compute Truck Space-Based and Spot Travel Time Rates

Kinematic Spot Rates. The initial truck kinematic spot travel time rates for both SUTs and TTs are 65 mi/h. These rates are located on the curves representing a 3% upgrade starting from 75 mi/h (48 s/mi) in Exhibit 25-20 (SUTs) and Exhibit 25-21 (TTs).

The SUT and TT spot rates versus distance curves starting from 65 mi/h will be applied to obtain $\tau_{f,SUT,kin,1}$ and $\tau_{f,TT,kin,1}$. In Exhibit 25-20, 65 mi/h (55.4 s/mi) occurs about 4,100 ft into the 3% grade. After an SUT travels for 1.5 mi (7,920 ft) starting at an initial speed of 65 mi/h, its spot rate can be read at 12,020 ft. That distance is outside the plot range, but Exhibit 25-20 shows SUTs reach a crawl speed of 59 s/mi (61 mi/h) at around 10,000 ft. Therefore, the kinematic spot rate for SUTs at the end of the first segment $\tau_{f,SUT,kin,1}$ is 59 s/mi.

In Exhibit 25-21, 65 mi/h (55.4 s/mi) is found at about 2,100 ft. After a TT travels for 1.5 mi (7,920 ft) from an initial speed of 65 mi/h, its spot rate can be read at 12,020 ft, which is outside the plot range in Exhibit 25-21. However, similar to SUTs, TTs approach their crawl speed at 10,000 ft, namely 73 s/mi (49.3 mi/h).

Because this is the first segment, the initial truck kinematic rates $\tau_{i,SUT,kin,1}$ and $\tau_{i,TT,kin,1}$ are equivalent to the free-flow rate of 55.4 s/mi. Because $\tau_{i,SUT,kin,1}$ is less than $\tau_{f,SUT,kin,1}$ and $\tau_{i,TT,kin,1}$ is less than $\tau_{f,TT,kin,1}$, both types of trucks decelerate on Segment 1, from 65 to 61 mi/h for SUTs and from 65 to 49.3 mi/h for TTs.

Kinematic Space-Based Rates. Because this is the first segment, the space-based speed at 0 ft is the FFS of 65 mi/h. Therefore, the 65-mi/h curve is applied to obtain $\tau_{S,SUT,kin,1}$ and $\tau_{S,TT,kin,1}$.

The time for an SUT to travel 7,920 feet starting from 65 mi/h on a 3% grade can be read from Exhibit 25-A7 and is 87 s. The corresponding travel time for a TT can be read from Exhibit 25-A18 and is 99 s. The space mean rate at 7,920 ft for an SUT $\tau_{S,SUT,kin,65,7920}$ and a TT $\tau_{S,TT,kin,65,7920}$ starting from a FFS of 65 mi/h on a 3% grade can then be computed by Equation 25-58:

$$\tau_{S,SUT,kin,65,7920} = \frac{T_{SUT,65,7920}}{d_1} = \frac{87}{7,920/5,280} = 58 \text{ s/mi}$$

$$\tau_{S,TT,kin,65,7920} = \frac{T_{TT,65,7920}}{d_1} = \frac{99}{7,920/5,280} = 66 \text{ s/mi}$$

Auto-Only Speed for the Given Flow Rate. The auto-only space mean speed for the given flow rate is computed with Equation 25-63.

$$S_{ao} = \left\{ \begin{array}{ll} FFS & \frac{v_{mix}}{CAF_{mix}} \leq BP_{ao} \\ FFS - \frac{(FFS - \frac{C_{ao}}{D_c}) (\frac{v_{mix}}{CAF_{mix}} - BP_{ao})^2}{(C_{ao} - BP_{ao})^2} & \frac{v_{mix}}{CAF_{mix}} > BP_{ao} \end{array} \right\}$$

The choice of equation depends on whether demand volumes are greater than or less than the breakpoint. An equation in Exhibit 12-6 is used to compute the breakpoint. For an auto-only condition, the CAF defaults to 1.0.

$$BP_{ao} = [1000 + 40 \times (75 - FFS)] \times CAF^2$$

$$BP_{ao} = [1000 + 40 \times (75 - 65)] \times 1^2 = 1,400 \text{ veh/h/ln}$$

As the demand volume of 1,500 veh/h/ln is greater than the breakpoint, the second of the two auto-only speed equations will be used. This equation requires knowing the auto-only capacity, which can be computed from Exhibit 12-6.

$$C_{ao} = 2,200 + 10 \times (65 - 50) = 2,350 \text{ pc/h/ln}$$

Then

$$S_{ao} = 65 - \frac{\left(65 - \frac{2,350}{45}\right) \left(\frac{1,500}{0.798} - 1,400\right)^2}{(2,350 - 1,400)^2} = 61.74 \text{ mi/h}$$

Traffic Interaction Term. The incremental traffic interaction term is computed with Equation 25-62.

$$\Delta\tau_{TI} = \left(\frac{3,600}{61.74} - \frac{3,600}{65}\right) \times \left(1 + 3 \left(\frac{1}{0.798} - 1\right)\right) = 5.15 \text{ s/mi}$$

Actual Spot Rates. The actual spot travel time rates of SUTs and TTs at the end of Segment 1 are computed from Equation 25-60 and Equation 25-61, respectively.

$$\tau_{f,SUT,1} = \tau_{f,SUT,kin,1} + \Delta\tau_{TI} = 59 + 5.15 = 64.15 \text{ s/mi}$$

$$\tau_{f,TT,1} = \tau_{f,TT,kin,1} + \Delta\tau_{TI} = 73 + 5.15 = 78.15 \text{ s/mi}$$

The initial spot rates of SUTs and TTs in Segment 1 can also be computed from Equation 25-60 and Equation 25-61.

$$\tau_{i,SUT,1} = \tau_{i,SUT,kin,1} + \Delta\tau_{TI} = (3,600/65) + 5.15 = 60.5 \text{ s/mi}$$

$$\tau_{i,TT,1} = \tau_{i,TT,kin,1} + \Delta\tau_{TI} = (3,600/65) + 5.15 = 60.5 \text{ s/mi}$$

Actual Space-Based Rates. Equation 25-60 and Equation 25-61 are also used to calculate the actual space-based travel time rates for SUTs and TTs. The traffic interaction term is the same as the term used for the spot rate calculations.

$$\tau_{s,SUT,1} = \tau_{s,SUT,kin,1} + \Delta\tau_{TI} = 58 + 5.15 = 63.15 \text{ s/mi}$$

$$\tau_{s,TT,1} = \tau_{s,TT,kin,1} + \Delta\tau_{TI} = 66 + 5.15 = 71.15 \text{ s/mi}$$

Step 5: Compute Spot and Space-Based Travel Time Rates for Autos

Equation 25-64 is used to compute the spot-based travel time rate for automobiles on the basis of the kinematic truck spot rate at the end of the segment.

$$\begin{aligned} \tau_{f,a,1} &= \frac{3,600}{65} + 5.15 \\ &+ \left[64.50 \times \left(\frac{1,500}{1,000}\right)^{0.77} \times 0.05^{0.34} \times \max\left(0, \frac{59}{100} - \frac{3,600}{65 \times 100}\right)^{1.53} \right] \\ &+ \left[79.5 \times \left(\frac{1,500}{1,000}\right)^{0.81} \times 0.10^{0.56} \times \max\left(0, \frac{73}{100} - \frac{3,600}{65 \times 100}\right)^{1.32} \right] \\ \tau_{f,a,1} &= 63.8 \text{ s/mi} \end{aligned}$$

When the initial auto spot travel time rate is computed, the trucks' kinematic spot rates are the same as the FFS, so the last two terms are 0. Therefore, Equation 25-64 can also be used to compute the initial auto spot rate, with the last two terms equal to 0.

$$\begin{aligned} \tau_{i,a,1} &= \frac{3,600}{65} + 5.15 + 0 + 0 \\ \tau_{i,a,1} &= 60.5 \text{ s/mi} \end{aligned}$$

It was determined in Step 4 that trucks decelerate in the first segment, so Equation 25-65 is used to compute the auto space-based rate on the basis of the kinematic truck space-based rates.

$$\begin{aligned} \tau_{S,a,1} &= \frac{3,600}{65} + 5.15 \\ &+ \left[100.42 \times \left(\frac{1,500}{1,000} \right)^{0.46} \times 0.05^{0.68} \times \max \left(0, \frac{58}{100} - \frac{3,600}{65 \times 100} \right)^{2.76} \right] \\ &+ \left[110.64 \times \left(\frac{1,500}{1,000} \right)^{1.36} \times 0.10^{0.62} \times \max \left(0, \frac{66}{100} - \frac{3,600}{65 \times 100} \right)^{1.81} \right] \\ \tau_{S,a,1} &= 61.3 \text{ s/mi} \end{aligned}$$

Step 6: Compute Mixed-Flow Space-Based Travel Time Rate and Speed

The mixed-flow travel rate $\tau_{\text{mix},1}$ and the mixed speed $S_{\text{mix},1}$ are computed with Equation 25-67 and Equation 25-68, respectively.

$$\tau_{\text{mix},1} = 0.85 \times 61.3 + 0.05 \times 63.15 + 0.10 \times 71.15 = 62.4 \text{ s/mi}$$

$$S_{\text{mix},1} = \frac{3,600}{62.4} = 57.7 \text{ mi/h}$$

Segment 2

Step 3: Specify Initial Conditions

For the second segment, the initial truck kinematic spot travel time rates are the final truck kinematic spot rates from the preceding segment. These are 59 s/mi (61.0 mi/h) for SUTs and 73 s/mi (49.3 mi/h) for TTs.

Step 4: Compute Truck Space-Based and Spot Travel Time Rates

Kinematic Spot Rates. The initial truck kinematic spot travel time rates for both SUTs and TTs were determined in Step 3.

In Exhibit 25-20, the initial SUT kinematic spot rate of 59 s/mi (61.0 mi/h) occurs on the curve for a 2% upgrade, starting from 30 mi/h (120 s/mi) at approximately 4,000 ft along the curve. After an SUT travels for 2 mi (10,560 ft), its spot rate can be read at 14,560 ft, which is outside the plot range. However, Exhibit 25-20 shows SUTs approach their crawl speed of 67.9 mi/h (53 s/mi) on a 2% grade. Because the specified FFS is 65 mi/h, SUTs will maintain a speed of 65 mi/h (55.4 s/mi) when the kinematic spot speeds exceed 65 mi/h. Therefore, the SUT spot rate at the end of Segment 2, $\tau_{f,SUT,kin,2}$ is 55.4 s/mi.

In Exhibit 25-21, the initial TT kinematic spot rate of 73 s/mi (49.3 mi/h) occurs on the curve for a 2% upgrade, starting from 20 mi/h (180 s/mi) at approximately 3,360 ft. After a TT travels for 2 mi (10,560 ft), its spot rate can be read at 13,920 ft, which is outside the plot range. However, Exhibit 25-21 shows TTs reach their crawl speed of 57.1 mi/h (63 s/mi) on a 2% grade. Thus, the TT spot rate at the end of Segment 2, $\tau_{f,TT,kin,2}$ is 63 s/mi.

On this segment, the final SUT and TT kinematic rates are greater than the initial rates, so both truck types accelerate on the second grade. The nomographs for the time versus distance relationships are applicable to both cases where

trucks are decelerating, and where they are accelerating. Acceleration is evident if the time required to cover a given distance is reducing as the distance increases.

Kinematic Space-Based Rates. The kinematic space-based speeds at 0 ft into Segment 2 equal the final kinematic spot speeds of Segment 1.

For SUTs, the final kinematic spot speed of Segment 1 was 61.0 mi/h (59 s/mi). As this speed is within 2.5 mi/h of 60 mi/h, Exhibit 25-A6 is used to obtain the SUT kinematic space-based travel time rate $\tau_{S,SUT,kin,2}$. The time for an SUT to travel 10,000 ft starting from an FFS of 60 mi/h on a 2% grade can be read from Exhibit 25-A6 and is 105 s.

For TTs, the final kinematic spot speed of Segment 1 was 49.3 mi/h (73 s/mi). As this speed is within 2.5 mi/h of 50 mi/h, Exhibit 25-A15 is applied to obtain the TT kinematic space-based rate $\tau_{S,TT,kin,2}$. The time for a TT to travel 10,000 ft starting from an FFS of 50 mi/h on a 2% grade can be read from Exhibit 25-A15 and is 125 s.

The space mean travel time rates for SUTs and TTs can now be computed by Equation 25-58.

$$\tau_{S,SUT,kin,60,10000} = \frac{T_{SUT,60,10000}}{d_2} = \frac{105}{10,000/5,280} = 55.4 \text{ s/mi}$$

$$\tau_{S,TT,kin,50,10000} = \frac{T_{TT,50,10000}}{d_2} = \frac{125}{10,000/5,280} = 66.0 \text{ s/mi}$$

The SUT and TT kinematic rates at a distance of 2 mi (10,560 ft) can be computed from Equation 25-59. The δ values for SUTs (0.0104) and TTs (0.0136) can be read from Exhibit 25-24 and Exhibit 25-25, respectively. The rates are computed as follows:

$$\tau_{S,SUT,kin,60,10560} = \frac{105}{2} + 0.0105 \times \left(1 - \frac{10,000}{2 \times 5,280}\right) \times 5,280 = 55.4 \text{ s/mi}$$

$$\tau_{S,TT,kin,60,10560} = \frac{125}{2} + 0.0118 \times \left(1 - \frac{10,000}{2 \times 5,280}\right) \times 5,280 = 65.8 \text{ s/mi}$$

Auto-Only Speed for the Given Flow Rate. The auto-only space mean speed for the given flow rate is computed with Equation 25-63. The breakpoint of the speed-flow curve was already determined to be 1,400 veh/h/ln, as part of the computations for the first segment. Thus,

$$S_{ao} = 65 - \frac{\left(65 - \frac{2,350}{45}\right) \left(\frac{1,500}{0.823} - 1,400\right)^2}{(2,350 - 1,400)^2} = 62.46 \text{ mi/h}$$

Traffic Interaction Term. The incremental traffic interaction term is computed by Equation 25-62.

$$\Delta\tau_{TI} = \left(\frac{3,600}{62.46} - \frac{3,600}{65}\right) \times \left(1 + 3 \left(\frac{1}{0.823} - 1\right)\right) = 3.71 \text{ s/mi}$$

Actual Spot Rates. The actual spot rates of SUTs and TTs at the end of Segment 2 are computed from Equation 25-60 and Equation 25-61, respectively.

$$\tau_{f,SUT,2} = \tau_{f,SUT,kin,2} + \Delta\tau_{TI} = 55.4 + 3.71 = 59.11 \text{ s/mi}$$

$$\tau_{f,TT,2} = \tau_{f,TT,kin,2} + \Delta\tau_{TI} = 63 + 3.71 = 66.71 \text{ s/mi}$$

Similarly, the space-based rates are

$$\tau_{S,SUT,2} = \tau_{S,SUT,kin,2} + \Delta\tau_{TI} = 55.4 + 3.71 = 59.11 \text{ s/mi}$$

$$\tau_{S,TT,2} = \tau_{S,TT,kin,2} + \Delta\tau_{TI} = 65.8 + 3.71 = 69.51 \text{ s/mi}$$

Step 5: Compute Spot and Space-Based Travel Time Rates for Autos

Equation 25-64 is used to compute the spot-based travel time rate for automobiles.

$$\begin{aligned} \tau_{f,a,2} &= \frac{3,600}{65} + 3.71 \\ &+ \left[64.50 \times \left(\frac{1,500}{1,000} \right)^{0.77} \times 0.05^{0.34} \times \max \left(0, \frac{55.4}{100} - \frac{3,600}{65 \times 100} \right)^{1.53} \right] \\ &+ \left[79.5 \times \left(\frac{1,500}{1,000} \right)^{0.81} \times 0.10^{0.56} \times \max \left(0, \frac{66.0}{100} - \frac{3,600}{65 \times 100} \right)^{1.32} \right] \\ \tau_{f,a,2} &= 60.1 \text{ s/mi} \end{aligned}$$

In this case, the auto spot rate of 60.1 s/mi is higher than the SUT spot rate of 59.1 s/mi. As the auto spot rate should always be less than or equal to the truck spot rate, the auto spot rate is set equal to 59.11 s/mi.

In Step 4, it was determined that trucks accelerate in Segment 2, so Equation 25-66 is used to compute the auto space-based rate.

$$\begin{aligned} \tau_{S,a,2} &= \frac{3,600}{65} + 3.71 \\ &+ \left[54.72 \times \left(\frac{1,500}{1,000} \right)^{1.16} \times 0.05^{0.28} \times \max \left(0, \frac{55.4}{100} - \frac{3,600}{65 \times 100} \right)^{1.73} \right] \\ &+ \left[69.72 \times \left(\frac{1,500}{1,000} \right)^{1.32} \times 0.10^{0.61} \times \max \left(0, \frac{65.8}{100} - \frac{3,600}{65 \times 100} \right)^{1.33} \right] \\ \tau_{S,a,2} &= 60.5 \text{ s/mi} \end{aligned}$$

Step 6: Compute Mixed-Flow Space-Based Travel Time Rate and Speed

The mixed-flow travel rate $\tau_{mix,2}$ and the mixed speed $S_{mix,2}$ are computed with Equation 25-67 and Equation 25-68, respectively.

$$\tau_{mix,2} = 0.85 \times 61.4 + 0.05 \times 62.01 + 0.10 \times 73.51 = 62.6 \text{ s/mi}$$

$$S_{mix,2} = \frac{3,600}{61.3} = 58.7 \text{ mi/h}$$

Segment 3

Step 3: Specify Initial Conditions

The initial truck kinematic spot travel time rates for Segment 3 are the final truck kinematic spot rates for Segment 2. These are 55.4 s/mi (65 mi/h) for SUTs and 63.0 s/mi (57.1 mi/h) for TTs.

Step 4: Compute Truck Space-Based and Spot Travel Time Rates

Kinematic Spot Rates. The initial truck kinematic spot travel time rates for both SUTs and TTs were determined in Step 3.

In Exhibit 25-20, the initial SUT kinematic spot rate of 55.4 s/mi (65 mi/h) occurs on the curve for a 5% upgrade, starting from 75 mi/h (48 s/mi) at approximately 1,500 ft along the curve. After an SUT travels 1 mi (5,280 ft), its spot rate can be read at 6,780 ft and is approximately 75 s/mi (48 mi/h). Thus, the SUT spot rate at the end of Segment 3 is 75 s/mi.

In Exhibit 25-21, the initial TT kinematic spot rate of 63 s/mi (57.1 mi/h) occurs on the curve for a 5% upgrade, starting from 75 mi/h (48 s/mi) at approximately 2,050 ft along the curve. After a TT travels 1 mi (5,280 ft), its spot rate can be read at 7,330 ft and is approximately 103 s/mi (35.0 mi/h). Thus, the TT spot rate at the end of Segment 3 is 103 s/mi.

In Segment 3, the initial kinematic rates for both truck types are less than the final kinematic rates. Therefore, both truck types decelerate in Segment 3.

Kinematic Space-Based Rates. The kinematic space-based speeds at 0 ft into Segment 3 equal the final kinematic spot speeds of Segment 2.

The final kinematic spot speed of SUTs in Segment 2 was 65 mi/h (55.4 s/mi). Exhibit 25-A7 is therefore used to obtain the SUT kinematic space-based rate $\tau_{S,SUT,kin,3}$. The travel time for SUTs at 5,280 ft, starting from 65 mi/h on a 5% grade, can be read from Exhibit 25-A7 and equals 67 s.

The final kinematic spot speed of TTs in Segment 2 was 57.2 mi/h (63.0 s/mi). As this value is within 2.5 mi/h of 55 mi/h, Exhibit 25-A16 is applied to obtain the TT kinematic space-based rate $\tau_{S,TT,kin,3}$. The travel time for TTs at 5,280 ft, starting from an FFS of 55 mi/h on a 5% grade, can be read from Exhibit 25-A16 and equals 89 s.

The space mean rate at 5,280 ft for SUTs and TTs can be computed by Equation 25-58.

$$\tau_{S,SUT,kin,65,5280} = \frac{T_{SUT,65,5280}}{d_3} = \frac{67}{5,280/5,280} = 67.0 \text{ s/mi}$$

$$\tau_{S,TT,kin,55,5280} = \frac{T_{TT,55,5280}}{d_3} = \frac{89}{5,280/5,280} = 89.0 \text{ s/mi}$$

Auto-Only Speed for the Given Flow Rate. The auto-only space mean speed for the given flow rate is computed with Equation 25-63. The breakpoint of the speed-flow curve was already determined to be 1,400 veh/h/ln as part of the computations for the first segment. Thus

$$S_{ao} = 65 - \frac{\left(65 - \frac{2,350}{45}\right) \left(\frac{1,500}{0.743} - 1,400\right)^2}{(2,350 - 1,400)^2} = 59.58 \text{ mi/h}$$

Traffic Interaction Term. The incremental traffic interaction term is computed by Equation 25-62.

$$\Delta\tau_{TI} = \left(\frac{3,600}{59.58} - \frac{3,600}{65}\right) \times \left(1 + 3\left(\frac{1}{0.743} - 1\right)\right) = 10.27 \text{ s/mi}$$

Actual Spot Rates. The actual spot rates of SUTs and TTs at the end of Segment 2 are computed from Equation 25-60 and Equation 25-61, respectively.

$$\tau_{f,SUT,3} = \tau_{f,SUT,kin,3} + \Delta\tau_{TI} = 75 + 10.27 = 85.27 \text{ s/mi}$$

$$\tau_{f,TT,3} = \tau_{f,TT,kin,3} + \Delta\tau_{TI} = 103 + 10.27 = 113.27 \text{ s/mi}$$

Similarly the space-based rates are:

$$\tau_{S,SUT,3} = \tau_{S,SUT,kin,3} + \Delta\tau_{TI} = 67.0 + 10.27 = 77.27 \text{ s/mi}$$

$$\tau_{S,TT,3} = \tau_{S,TT,kin,3} + \Delta\tau_{TI} = 89.0 + 10.27 = 99.27 \text{ s/mi}$$

Step 5: Compute Spot and Space-Based Travel Time Rates for Autos

Equation 25-64 is used to compute the spot-based travel time rate for automobiles.

$$\begin{aligned} \tau_{f,a,3} &= \frac{3,600}{65} + 10.27 \\ &+ \left[64.50 \times \left(\frac{1,500}{1,000} \right)^{0.77} \times 0.05^{0.34} \times \max \left(0, \frac{75}{100} - \frac{3,600}{65 \times 100} \right)^{1.53} \right] \\ &+ \left[79.5 \times \left(\frac{1,500}{1,000} \right)^{0.81} \times 0.10^{0.56} \times \max \left(0, \frac{103}{100} - \frac{3,600}{65 \times 100} \right)^{1.32} \right] \\ \tau_{f,a,3} &= 79.7 \text{ s/mi} \end{aligned}$$

In Step 4, it was determined that trucks decelerate in Segment 3, so Equation 25-65 is used to compute the auto space-based rate.

$$\begin{aligned} \tau_{S,a,3} &= \frac{3,600}{65} + 10.27 \\ &+ \left[100.42 \times \left(\frac{1,500}{1,000} \right)^{0.46} \times 0.05^{0.68} \times \max \left(0, \frac{67.0}{100} - \frac{3,600}{65 \times 100} \right)^{2.76} \right] \\ &+ \left[110.64 \times \left(\frac{1,500}{1,000} \right)^{1.36} \times 0.10^{0.62} \times \max \left(0, \frac{89.0}{100} - \frac{3,600}{65 \times 100} \right)^{1.81} \right] \\ \tau_{S,a,3} &= 72.1 \text{ s/mi} \end{aligned}$$

Step 6: Compute Mixed-Flow Space-Based Travel Time Rate and Speed

The mixed-flow travel rate $\tau_{mix,3}$ and the mixed speed $S_{mix,3}$ are computed using Equation 25-67 and Equation 25-68, respectively.

$$\tau_{mix,3} = 0.85 \times 72.1 + 0.05 \times 77.27 + 0.10 \times 99.27 = 75.1 \text{ s/mi}$$

$$S_{mix,3} = \frac{3,600}{75.1} = 47.9 \text{ mi/h}$$

Step 7: Overall Results

Now that results have been developed for all three segments, the overall performance of the composite grade can be computed. The mixed-flow travel time for each segment is computed with Equation 25-69.

$$t_{mix,1} = \frac{3,600d_1}{S_{mix,1}} = \frac{3,600 \times 1.5}{57.7} = 93.6 \text{ s}$$

$$t_{mix,2} = \frac{3,600d_2}{S_{mix,2}} = \frac{3,600 \times 2}{58.7} = 122.7 \text{ s}$$

$$t_{mix,3} = \frac{3,600d_3}{S_{mix,3}} = \frac{3,600 \times 1}{47.9} = 75.2 \text{ s}$$

The overall mixed-flow travel time $t_{mix,oa}$ is the sum of the mixed-flow travel times for all three segments and equals 294 s. Equation 25-70 can be used to compute the mixed-flow speed.

$$S_{mix,oa} = \frac{3,600d_{oa}}{t_{mix,oa}} = \frac{3600 \times 4.5}{291.5} = 55.6 \text{ mi/h}$$

Exhibit 25-109 shows the spot speeds of all the segments in the example.

Exhibit 25-109
Example Problem 11:
Spot Speeds of All Segments

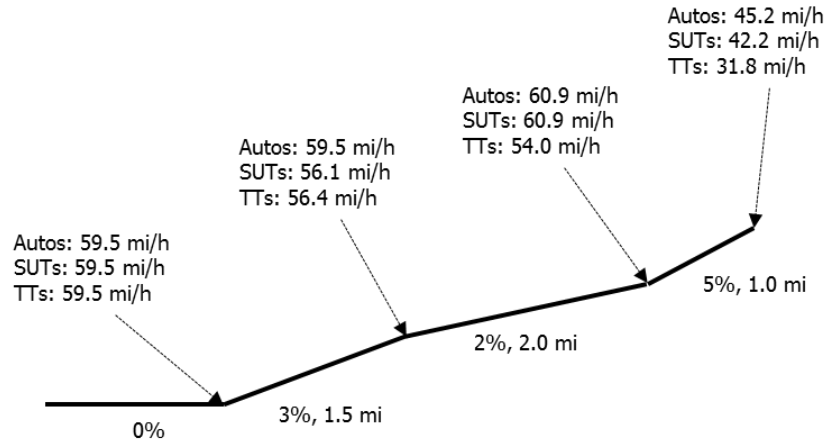


Exhibit 25-110 shows the space mean speeds of all the segments in the example.

Exhibit 25-110
Example Problem 11: Space
Mean Speeds of All Segments

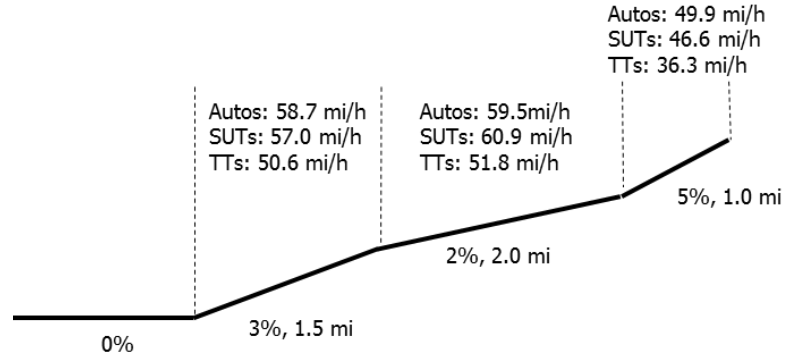
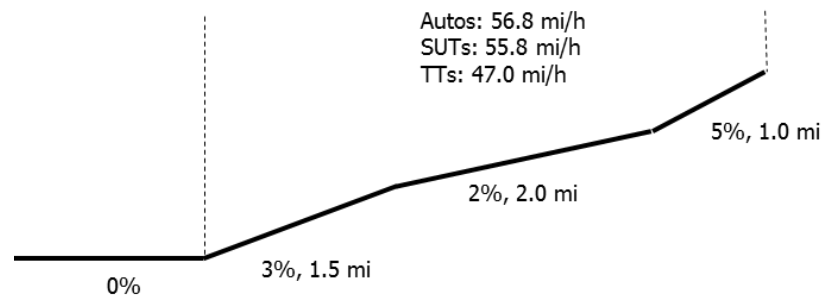


Exhibit 25-111 shows the overall space mean speeds of all the segments in the example.

Exhibit 25-111
Example Problem 11: Overall
Space Mean Speeds of All
Segments



12. REFERENCES

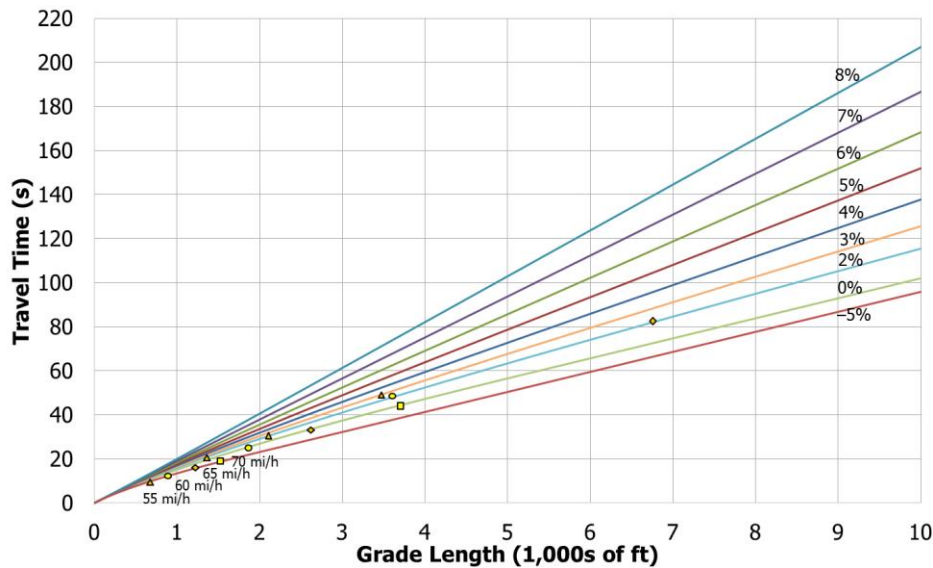
1. *Highway Capacity Manual*. Transportation Research Board, National Research Council, Washington, D.C., 2000.
2. Eads, B. S., N. M. Roupail, A. D. May, and F. Hall. Freeway Facilities Methodology in *Highway Capacity Manual 2000*. In *Transportation Research Record: Journal of the Transportation Research Board*, No. 1710, Transportation Research Board, National Research Council, Washington, D.C., 2000, pp. 171–180.
3. Hall, F. L., L. Bloomberg, N. M. Roupail, B. Eads, and A. D. May. Validation Results for Four Models of Oversaturated Freeway Facilities. In *Transportation Research Record: Journal of the Transportation Research Board*, No. 1710, Transportation Research Board, National Research Council, Washington, D.C., 2000, pp. 161–170.
4. *A Policy on Geometric Design of Highways and Streets*, 5th ed. American Association of State Highway and Transportation Officials, Washington, D.C., 2004.
5. Newell, G. F. A Simplified Theory of Kinematic Waves in Highway Traffic. Part I: General Theory. *Transportation Research*, Vol. 27B, No. 4, 1993, pp. 281–287.
6. Newell, G. F. A Simplified Theory of Kinematic Waves in Highway Traffic. Part II: Queuing at Freeway Bottlenecks. *Transportation Research*, Vol. 27B, No. 4, 1993, pp. 289–303.
7. Newell, G. F. A Simplified Theory of Kinematic Waves in Highway Traffic. Part III: Multidestination Flows. *Transportation Research*, Vol. 27B, No. 4, 1993, pp. 305–313.
8. Newman, L. *Freeway Operations Analysis*. Course Notes. University of California Institute of Transportation Studies University Extension, Berkeley, 1986.
9. Schoen, J. M., J. A. Bonneson, C. Safi, B. Schroeder, A. Hajbabaie, C. H. Yeom, N. Roupail, Y. Wang, W. Zhu, and Y. Zou. *Work Zone Capacity Methods for the Highway Capacity Manual*. National Cooperative Highway Research Program Project 3-107 final report, preliminary draft. Kittelson & Associates, Inc., Tucson, Ariz., April 2015.
10. Hajbabaie, A., N. M. Roupail, B. J. Schroeder, and R Dowling. Planning-Level Methodology for Freeway Facilities. In *Transportation Research Record: Journal of the Transportation Research Board*, No. 2483, Transportation Research Board of the National Academies, Washington, D.C., 2015, pp. 47–56.
11. Elefteriadou, L., A. Kondyli, and B. St. George. *Estimation of Capacities on Florida Freeways*. Final Report. Gainesville, Fla., Sept. 2014.

Some of these references can be found in the Technical Reference Library in Volume 4.

12. Dowling, R., G. F. List, B. Yang, E. Witzke, and A. Flannery. *NCFRP Report 31: Incorporating Truck Analysis into the Highway Capacity Manual*. Transportation Research Board of the National Academies, Washington, D.C., 2014.
13. Washburn, S. S., and S. Ozkul. *Heavy Vehicle Effects on Florida Freeways and Multilane Highways*. Report TRC-FDOT-93817-2013. Florida Department of Transportation, Tallahassee, Oct. 2013.
14. Ozkul, S., and S. S. Washburn. Updated Commercial Truck Speed Versus Distance-Grade Curves for the *Highway Capacity Manual*. In *Transportation Research Record: Journal of the Transportation Research Board*, No. 2483, Transportation Research Board of the National Academies, Washington, D.C., 2015, pp. 91–101.
15. Hajbabaie A., B. J. Schroeder, N. M. Rouphail, and S. Aghdashi. *Freeway Facility Calibration Procedure*. NCHRP 03-115 Working Paper U-8b. ITRE at North Carolina State University, Raleigh, Aug. 2014. (Available in the Technical Reference Library section of HCM Volume 4, <http://hcm.trb.org>.)
16. Hu, J., B. Schroeder, and N. Rouphail. Rationale for Incorporating Queue Discharge Flow into *Highway Capacity Manual* Procedure for Analysis of Freeway Facilities. In *Transportation Research Record: Journal of the Transportation Research Board*, No. 2286, Transportation Research Board of the National Academies, Washington, D.C., 2012, pp. 76–83.
17. Aghdashi, S., A. Hajbabaie, B. J. Schroeder, J. L. Trask, and N. M. Rouphail. Generating Scenarios of Freeway Reliability Analysis: Hybrid Approach. In *Transportation Research Record: Journal of the Transportation Research Board*, No. 2483, Transportation Research Board of the National Academies, Washington, D.C., 2015, pp. 148–159.
18. Zegeer, J., J. Bonneson, R. Dowling, P. Ryus, M. Vandehey, W. Kittelson, N. Rouphail, B. Schroeder, A. Hajbabaie, B. Aghdashi, T. Chase, S. Sajjadi, R. Margiotta, and L. Elefteriadou. *Incorporating Travel Time Reliability in the Highway Capacity Manual*. SHRP 2 Report S2-L08-RW-1. Transportation Research Board of the National Academies, Washington, D.C., 2014.
19. Federal Highway Administration. *Highway Economic Requirements System — State Version (HERS-ST)*. Technical Report. U.S. Department of Transportation, Washington, D.C., 2005.
20. *Highway Safety Manual*, 2014 Supplement to the *Highway Safety Manual*, 1st ed. American Association of State Highway and Transportation Officials, Washington, D.C., 2014.

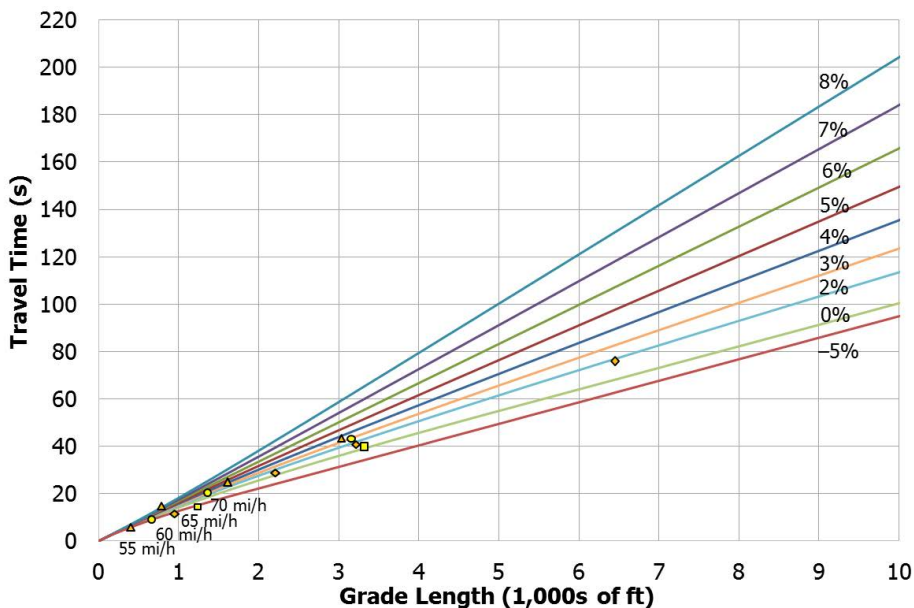
APPENDIX A: TRUCK PERFORMANCE CURVES

This appendix provides travel time versus distance curves for SUTs for initial speeds between 35 and 75 mi/h in 5-mi/h increments. Curves for SUTs for 30- and 70-mi/h initial speeds are presented in Section 7 as Exhibit 25-23 and Exhibit 25-22, respectively. The appendix also provides travel time versus distance curves for TTs for initial speeds between 20 and 75 mi/h in 5-mi/h increments.



Notes: Curves in this graph assume a weight-to-horsepower ratio of 100. Triangles indicate where a truck reaches 55 mi/h, circles indicate 60 mi/h, diamonds indicate 65 mi/h, and squares indicate 70 mi/h.

Exhibit 25-A1
SUT Travel Time Versus
Distance Curves for 35-mi/h
Initial Speed

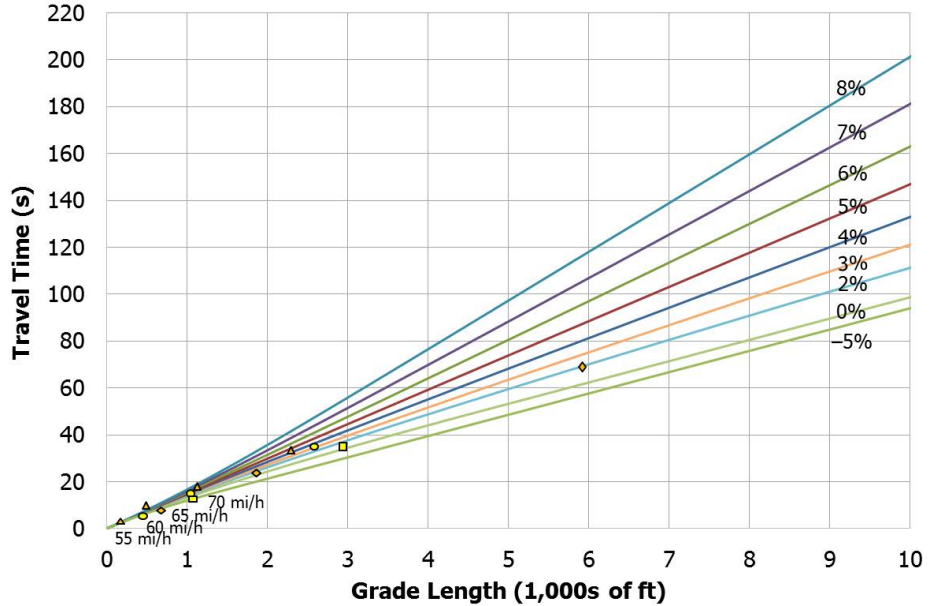


Notes: Curves in this graph assume a weight-to-horsepower ratio of 100. Triangles indicate where a truck reaches 55 mi/h, circles indicate 60 mi/h, diamonds indicate 65 mi/h, and squares indicate 70 mi/h.

Exhibit 25-A2
SUT Travel Time Versus
Distance Curves for 40-mi/h
Initial Speed

Exhibit 25-A3

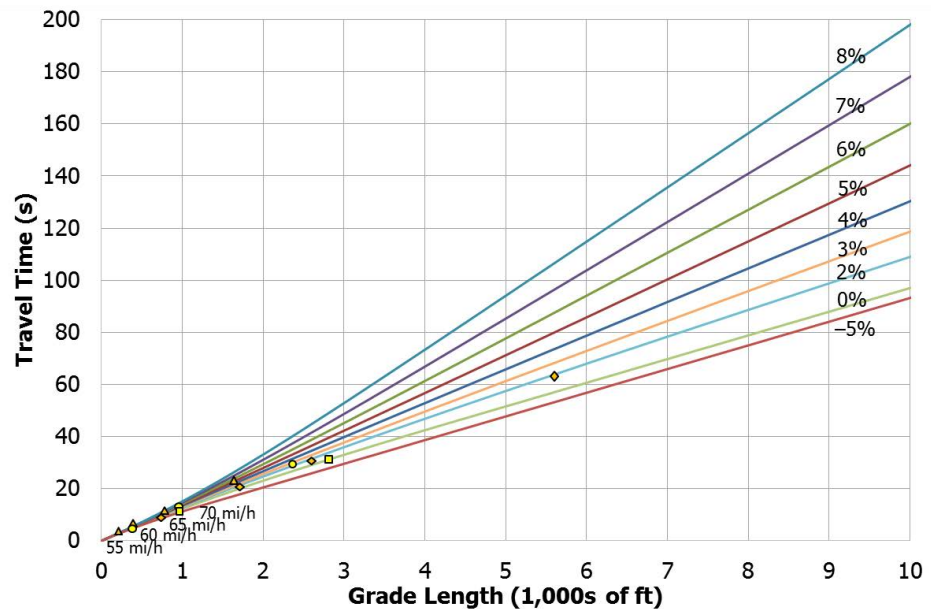
SUT Travel Time Versus Distance Curves for 45-mi/h Initial Speed



Notes: Curves in this graph assume a weight-to-horsepower ratio of 100. Triangles indicate where a truck reaches 55 mi/h, circles indicate 60 mi/h, diamonds indicate 65 mi/h, and squares indicate 70 mi/h.

Exhibit 25-A4

SUT Travel Time Versus Distance Curves for 50-mi/h Initial Speed



Notes: Curves in this graph assume a weight-to-horsepower ratio of 100. Triangles indicate where a truck reaches 55 mi/h, circles indicate 60 mi/h, diamonds indicate 65 mi/h, and squares indicate 70 mi/h.

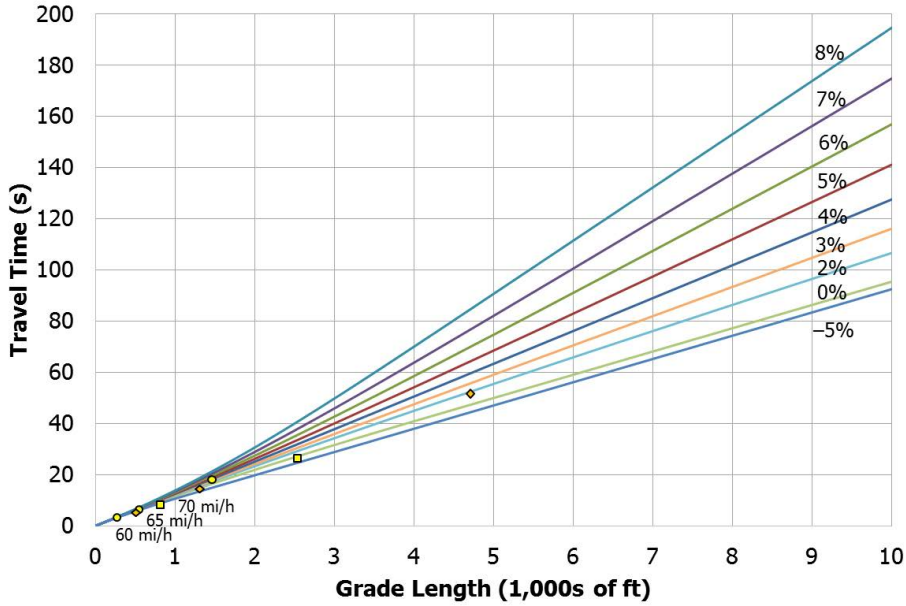


Exhibit 25-A5
SUT Travel Time Versus
Distance Curves for 55-mi/h
Initial Speed

Notes: Curves in this graph assume a weight-to-horsepower ratio of 100.
Circles indicate where a truck reaches 60 mi/h, diamonds indicate 65 mi/h, and squares indicate 70 mi/h.

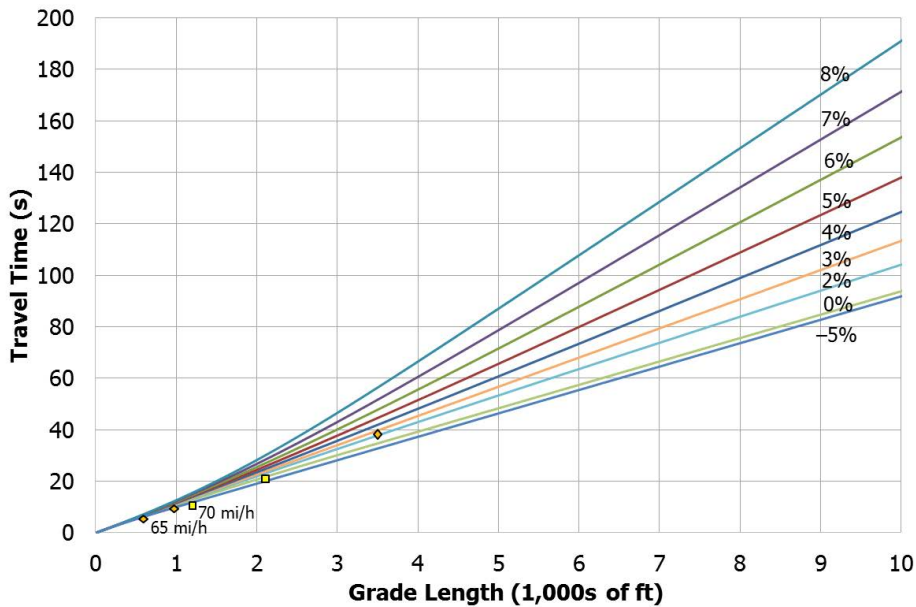
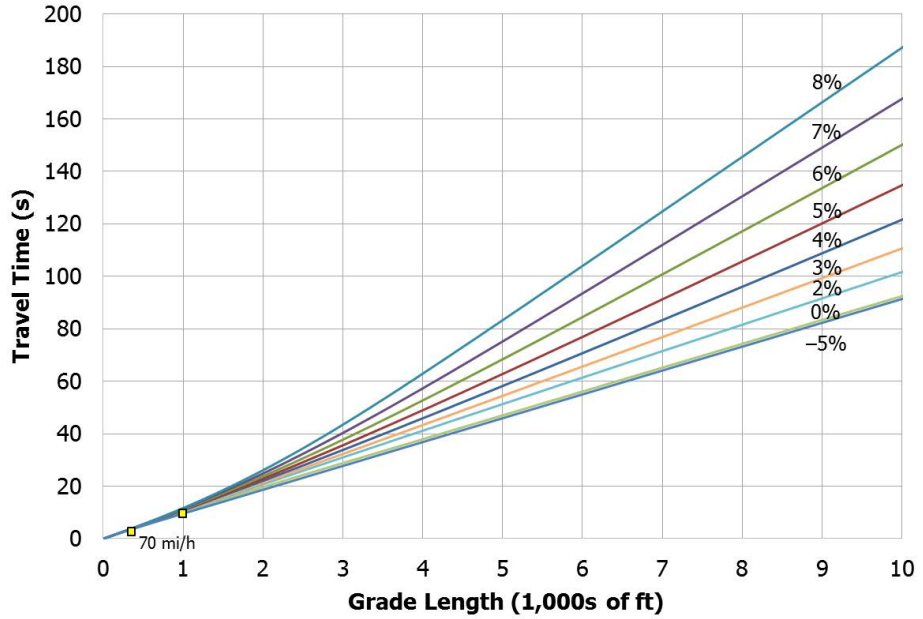


Exhibit 25-A6
SUT Travel Time Versus
Distance Curves for 60-mi/h
Initial Speed

Notes: Curves in this graph assume a weight-to-horsepower ratio of 100.
Diamonds indicate where a truck reaches 65 mi/h and squares indicate 70 mi/h.

Exhibit 25-A7

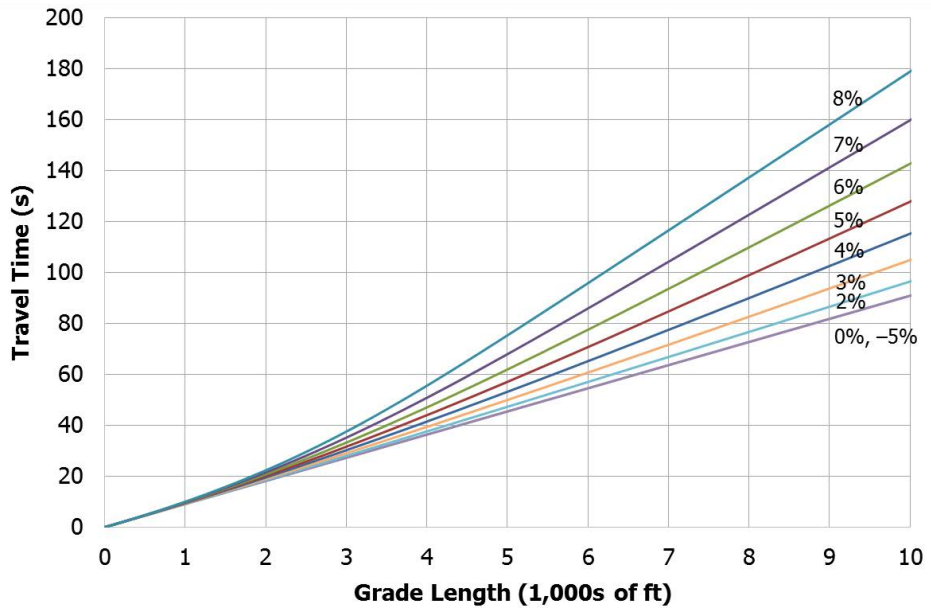
SUT Travel Time Versus
Distance Curves for 65-mi/h
Initial Speed



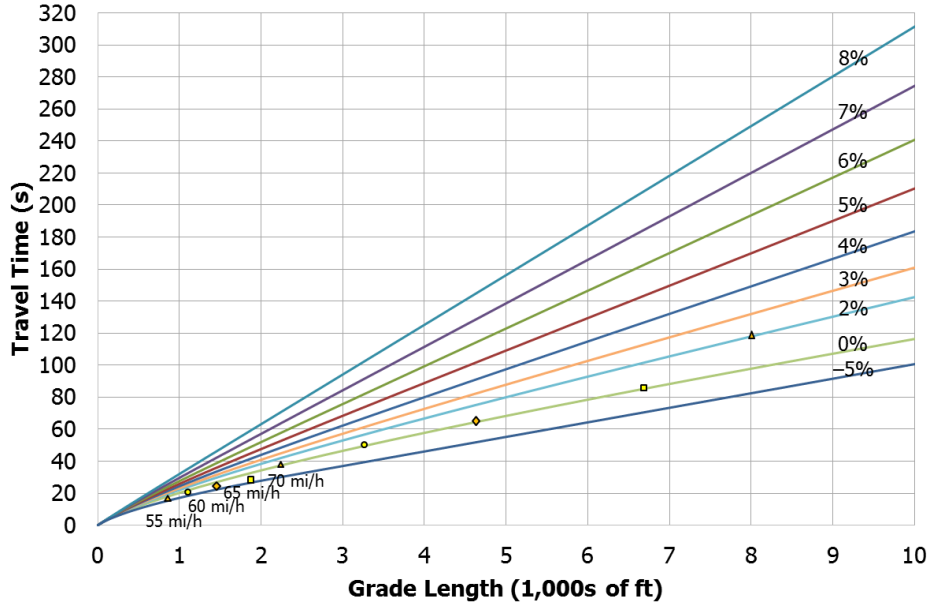
Notes: Curves in this graph assume a weight-to-horsepower ratio of 100.
Squares indicate where a truck reaches 70 mi/h.

Exhibit 25-A8

SUT Travel Time Versus
Distance Curves for 75-mi/h
Initial Speed

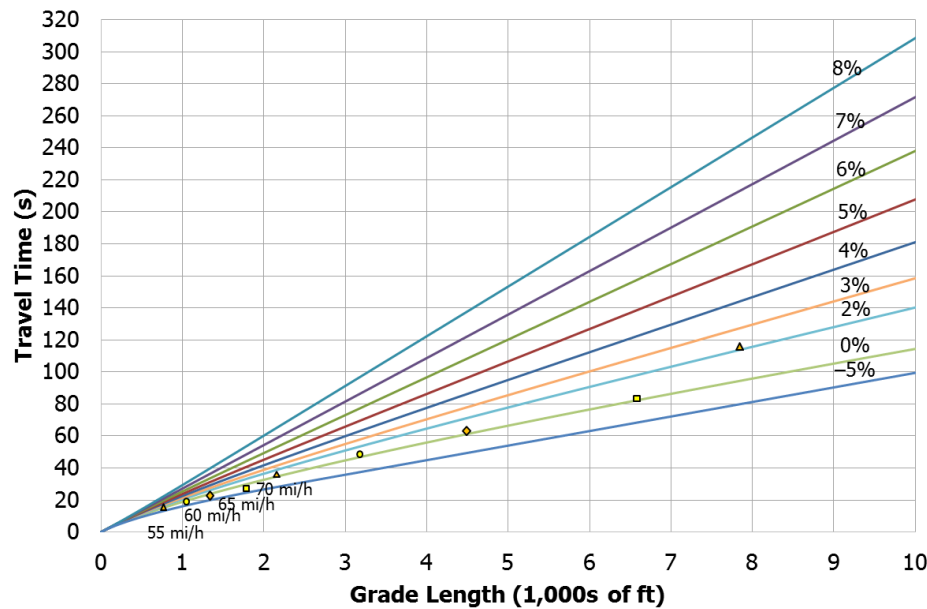


Note: Curves in this graph assume a weight-to-horsepower ratio of 100.



Notes: Curves in this graph assume a weight-to-horsepower ratio of 150. Triangles indicate where a truck reaches 55 mi/h, circles indicate 60 mi/h, diamonds indicate 65 mi/h, and squares indicate 70 mi/h.

Exhibit 25-A9
TT Travel Time Versus
Distance Curves for 20-mi/h
Initial Speed

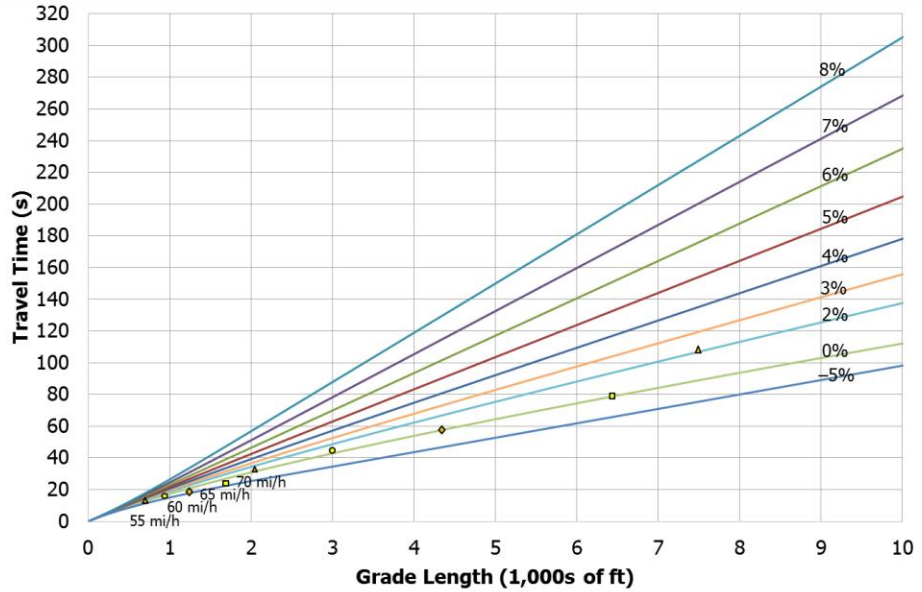


Notes: Curves in this graph assume a weight-to-horsepower ratio of 150. Triangles indicate where a truck reaches 55 mi/h, circles indicate 60 mi/h, diamonds indicate 65 mi/h, and squares indicate 70 mi/h.

Exhibit 25-A10
TT Travel Time Versus
Distance Curves for 25-mi/h
Initial Speed

Exhibit 25-A11

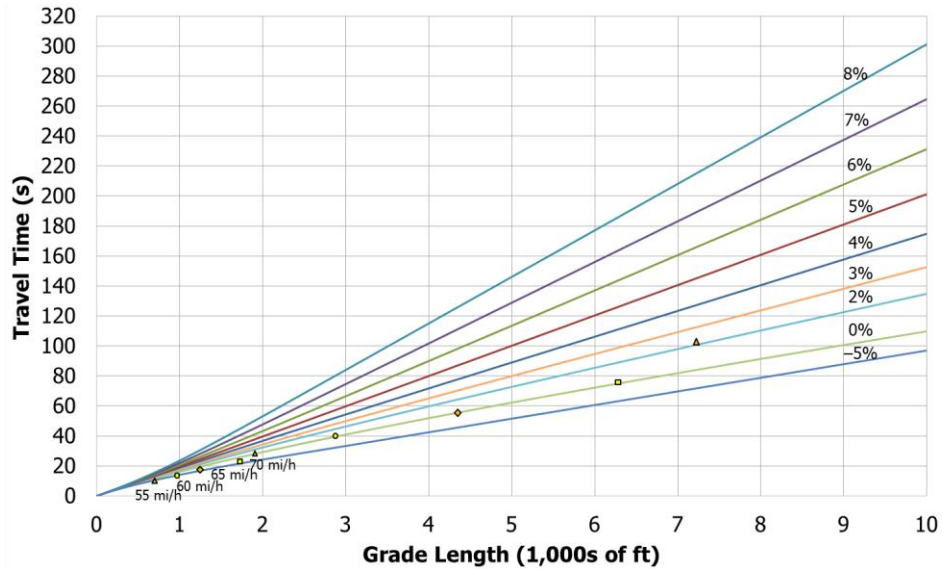
TT Travel Time Versus
Distance Curves for 30-mi/h
Initial Speed



Notes: Curves in this graph assume a weight-to-horsepower ratio of 150.
Triangles indicate where a truck reaches 55 mi/h, circles indicate 60 mi/h, diamonds indicate 65 mi/h, and squares indicate 70 mi/h.

Exhibit 25-A12

TT Travel Time Versus
Distance Curves for 35-mi/h
Initial Speed



Notes: Curves in this graph assume a weight-to-horsepower ratio of 150.
Triangles indicate where a truck reaches 55 mi/h, circles indicate 60 mi/h, diamonds indicate 65 mi/h, and squares indicate 70 mi/h.

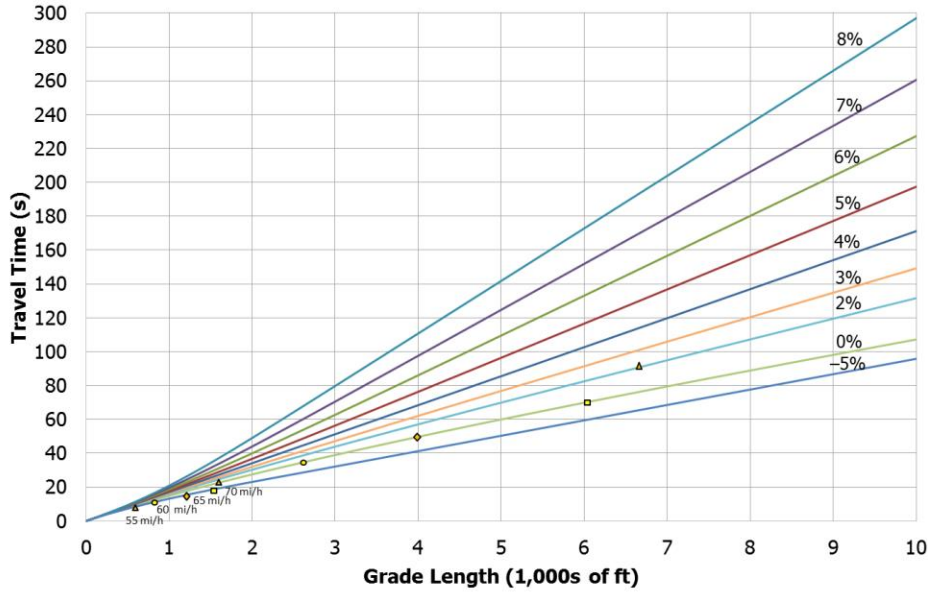


Exhibit 25-A13
TT Travel Time Versus
Distance Curves for 40-mi/h
Initial Speed

Notes: Curves in this graph assume a weight-to-horsepower ratio of 150.
Triangles indicate where a truck reaches 55 mi/h, circles indicate 60 mi/h, diamonds indicate 65 mi/h, and squares indicate 70 mi/h.

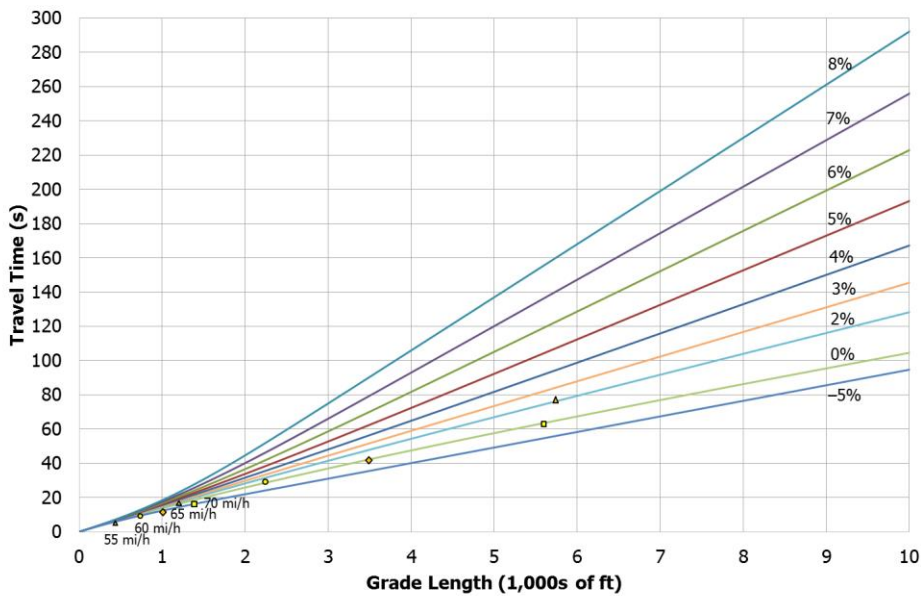
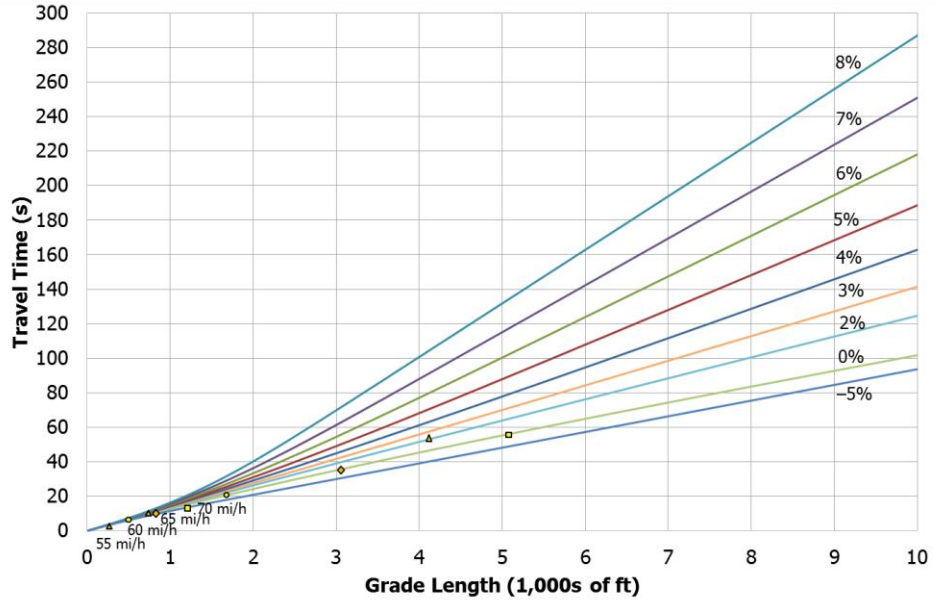


Exhibit 25-A14
TT Travel Time Versus
Distance Curves for 45-mi/h
Initial Speed

Notes: Curves in this graph assume a weight-to-horsepower ratio of 150.
Triangles indicate where a truck reaches 55 mi/h, circles indicate 60 mi/h, diamonds indicate 65 mi/h, and squares indicate 70 mi/h.

Exhibit 25-A15

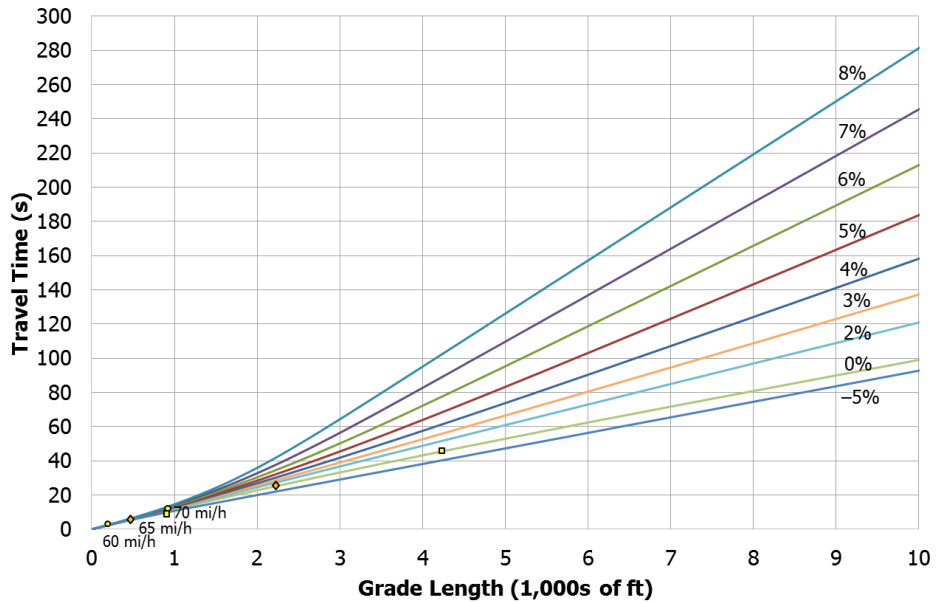
TT Travel Time Versus
Distance Curves for 50-mi/h
Initial Speed



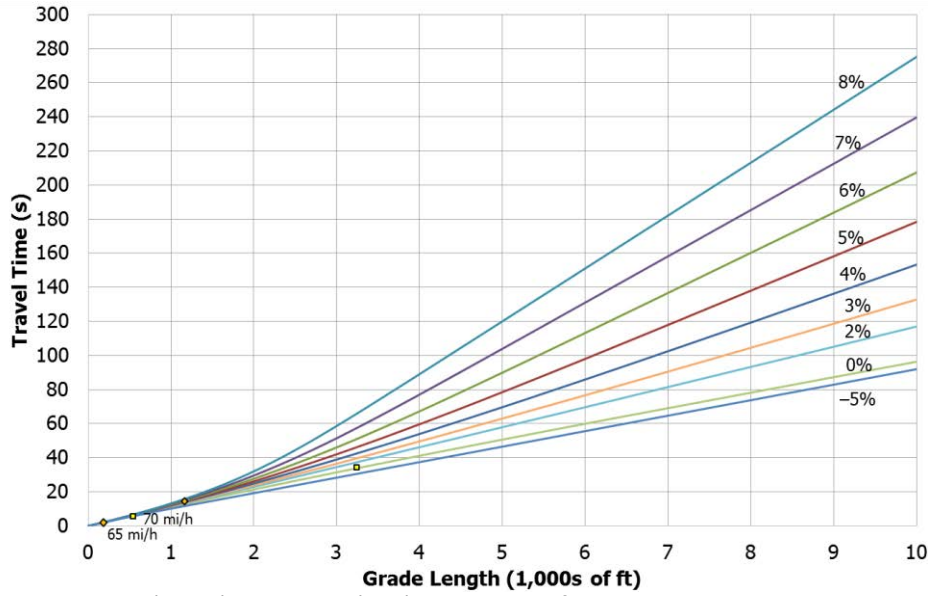
Notes: Curves in this graph assume a weight-to-horsepower ratio of 150.
Triangles indicate where a truck reaches 55 mi/h, circles indicate 60 mi/h, diamonds indicate 65 mi/h, and squares indicate 70 mi/h.

Exhibit 25-A16

TT Travel Time Versus
Distance Curves for 55-mi/h
Initial Speed

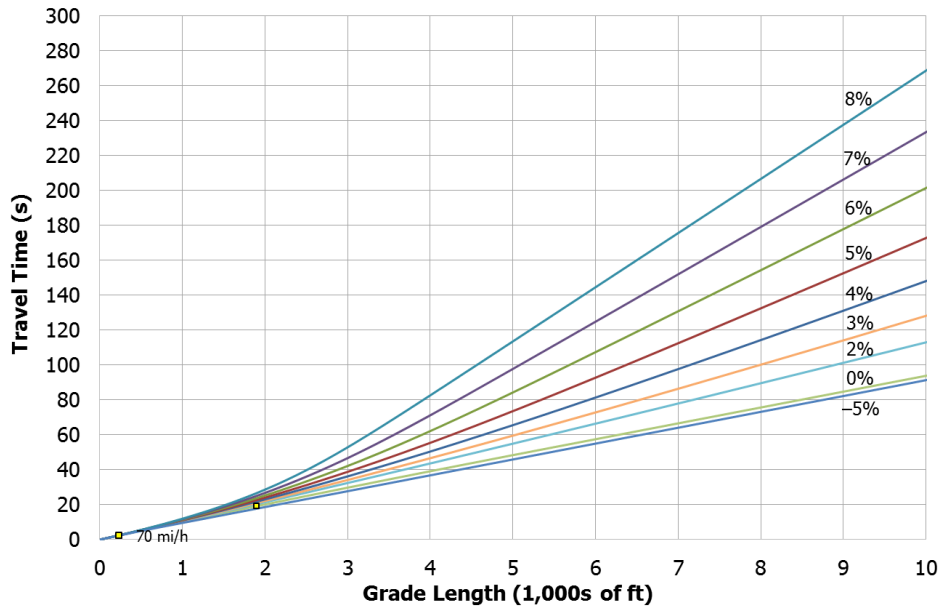


Notes: Curves in this graph assume a weight-to-horsepower ratio of 150.
Circles indicate where a truck reaches 60 mi/h, diamonds indicate 65 mi/h, and squares indicate 70 mi/h.



Notes: Curves in this graph assume a weight-to-horsepower ratio of 150.
Diamonds indicate where a truck reaches 65 mi/h and squares indicate 70 mi/h.

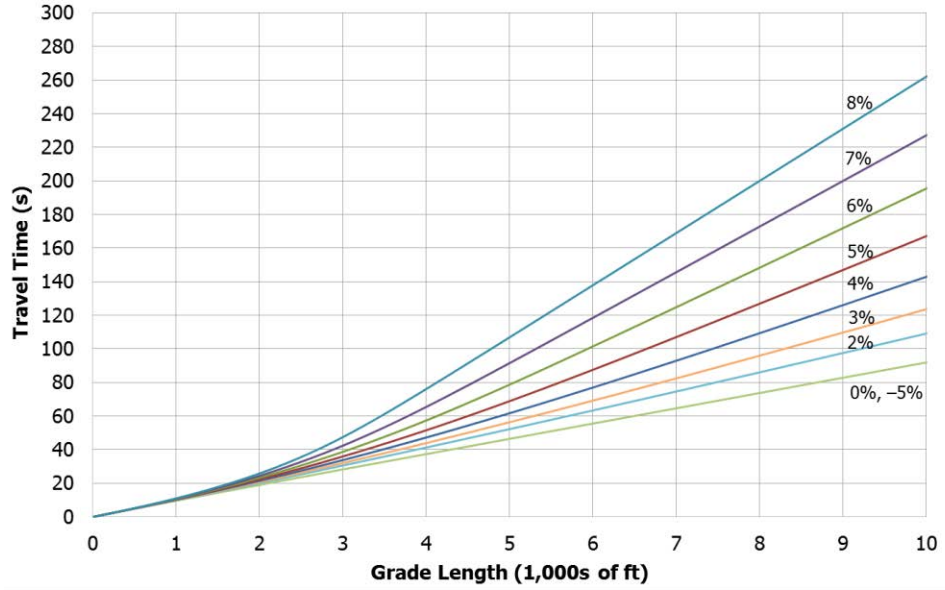
Exhibit 25-A17
TT Travel Time Versus
Distance Curves for 60-mi/h
Initial Speed



Notes: Curves in this graph assume a weight-to-horsepower ratio of 150.
Squares indicate where a truck reaches 70 mi/h.

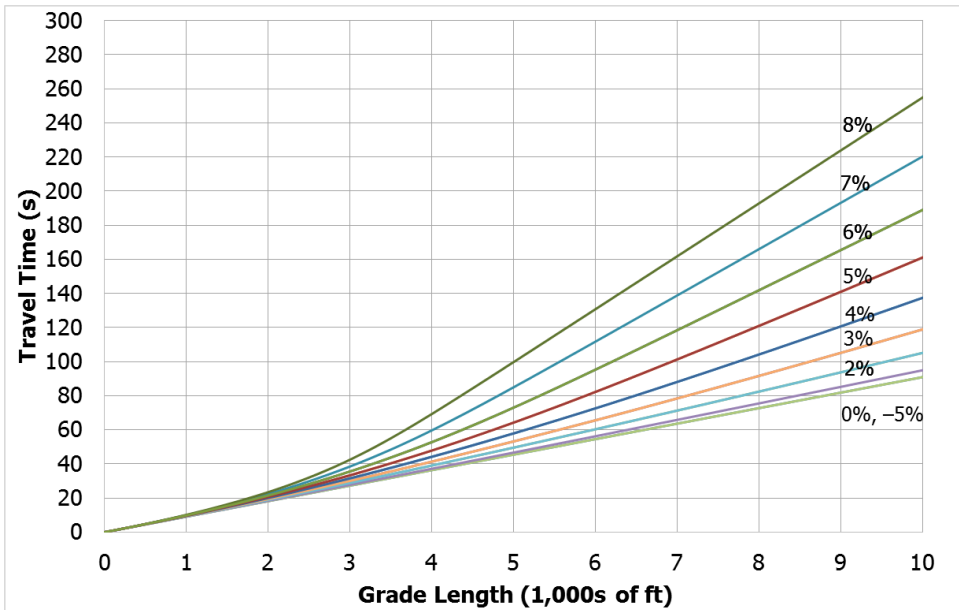
Exhibit 25-A18
TT Travel Time Versus
Distance Curves for 65-mi/h
Initial Speed

Exhibit 25-A19
 TT Travel Time Versus
 Distance Curves for 70-mi/h
 Initial Speed



Note: Curves in this graph assume a weight-to-horsepower ratio of 150.

Exhibit 25-A20
 TT Travel Time Versus
 Distance Curves for 75-mi/h
 Initial Speed



Note: Curves in this graph assume a weight-to-horsepower ratio of 150.



HIGHWAY CAPACITY MANUAL

6TH EDITION | A GUIDE FOR MULTIMODAL MOBILITY ANALYSIS

VOLUME 4: APPLICATIONS GUIDE

The National Academies of
SCIENCES • ENGINEERING • MEDICINE

TRANSPORTATION RESEARCH BOARD
WASHINGTON, D.C. | WWW.TRB.ORG

TRANSPORTATION RESEARCH BOARD 2016 EXECUTIVE COMMITTEE *

Chair: James M. Crites, Executive Vice President of Operations,
Dallas–Fort Worth International Airport, Texas

Vice Chair: Paul Trombino III, Director, Iowa Department of
Transportation, Ames

Executive Director: Neil J. Pedersen, Transportation Research Board

Victoria A. Arroyo, Executive Director, Georgetown Climate Center;
Assistant Dean, Centers and Institutes; and Professor and Director,
Environmental Law Program, Georgetown University Law Center,
Washington, D.C.

Scott E. Bennett, Director, Arkansas State Highway and Transportation
Department, Little Rock

Jennifer Cohan, Secretary, Delaware Department of Transportation, Dover

Malcolm Dougherty, Director, California Department of
Transportation, Sacramento

A. Stewart Fotheringham, Professor, School of Geographical Sciences
and Urban Planning, Arizona State University, Tempe

John S. Halikowski, Director, Arizona Department of Transportation,
Phoenix

Susan Hanson, Distinguished University Professor Emerita, Graduate
School of Geography, Clark University, Worcester, Massachusetts

Steve Heminger, Executive Director, Metropolitan Transportation
Commission, Oakland, California

Chris T. Hendrickson, Hamerschlag Professor of Engineering, Carnegie
Mellon University, Pittsburgh, Pennsylvania

Jeffrey D. Holt, Managing Director, Power, Energy, and Infrastructure
Group, BMO Capital Markets Corporation, New York

S. Jack Hu, Vice President for Research and J. Reid and Polly Anderson
Professor of Manufacturing, University of Michigan, Ann Arbor

Roger B. Huff, President, HGLC, LLC, Farmington Hills, Michigan

Geraldine Knatz, Professor, Sol Price School of Public Policy, Viterbi
School of Engineering, University of Southern California, Los Angeles

Ysela Llort, Consultant, Miami, Florida

Melinda McGrath, Executive Director, Mississippi Department of
Transportation, Jackson

James P. Redeker, Commissioner, Connecticut Department of
Transportation, Newington

Mark L. Rosenberg, Executive Director, The Task Force for Global
Health, Inc., Decatur, Georgia

Kumares C. Sinha, Olson Distinguished Professor of Civil Engineering,
Purdue University, West Lafayette, Indiana

Daniel Sperling, Professor of Civil Engineering and Environmental
Science and Policy; Director, Institute of Transportation Studies,
University of California, Davis

Kirk T. Steudle, Director, Michigan Department of Transportation,
Lansing (Past Chair, 2014)

Gary C. Thomas, President and Executive Director, Dallas Area Rapid
Transit, Dallas, Texas

Pat Thomas, Senior Vice President of State Government Affairs, United
Parcel Service, Washington, D.C.

Katherine F. Turnbull, Executive Associate Director and Research
Scientist, Texas A&M Transportation Institute, College Station

Dean Wise, Vice President of Network Strategy, Burlington Northern
Santa Fe Railway, Fort Worth, Texas

Thomas P. Bostick (Lieutenant General, U.S. Army), Chief of Engineers
and Commanding General, U.S. Army Corps of Engineers, Washington,
D.C. (ex officio)

James C. Card (Vice Admiral, U.S. Coast Guard, retired), Maritime
Consultant, The Woodlands, Texas, and Chair, TRB Marine Board
(ex officio)

T. F. Scott Darling III, Acting Administrator and Chief Counsel, Federal
Motor Carrier Safety Administration, U.S. Department of Transportation
(ex officio)

Marie Therese Dominguez, Administrator, Pipeline and Hazardous
Materials Safety Administration, U.S. Department of Transportation
(ex officio)

Sarah Feinberg, Administrator, Federal Railroad Administration,
U.S. Department of Transportation (ex officio)

Carolyn Flowers, Acting Administrator, Federal Transit Administration,
U.S. Department of Transportation (ex officio)

LeRoy Gishi, Chief, Division of Transportation, Bureau of Indian
Affairs, U.S. Department of the Interior, Washington, D.C. (ex officio)

John T. Gray II, Senior Vice President, Policy and Economics,
Association of American Railroads, Washington, D.C. (ex officio)

Michael P. Huerta, Administrator, Federal Aviation Administration,
U.S. Department of Transportation (ex officio)

Paul N. Jaenichen, Sr., Administrator, Maritime Administration,
U.S. Department of Transportation (ex officio)

Bevan B. Kirley, Research Associate, University of North Carolina
Highway Safety Research Center, Chapel Hill, and Chair, TRB Young
Members Council (ex officio)

Gregory G. Nadeau, Administrator, Federal Highway Administration,
U.S. Department of Transportation (ex officio)

Wayne Nastri, Acting Executive Officer, South Coast Air Quality
Management District, Diamond Bar, California (ex officio)

Mark R. Rosekind, Administrator, National Highway Traffic Safety
Administration, U.S. Department of Transportation (ex officio)

Craig A. Rutland, U.S. Air Force Pavement Engineer, U.S. Air Force
Civil Engineer Center, Tyndall Air Force Base, Florida (ex officio)

Reuben Sarkar, Deputy Assistant Secretary for Transportation,
U.S. Department of Energy (ex officio)

Richard A. White, Acting President and CEO, American Public
Transportation Association, Washington, D.C. (ex officio)

Gregory D. Winfree, Assistant Secretary for Research and Technology,
Office of the Secretary, U.S. Department of Transportation (ex officio)

Frederick G. (Bud) Wright, Executive Director, American Association
of State Highway and Transportation Officials, Washington, D.C.
(ex officio)

Paul F. Zukunft (Admiral, U.S. Coast Guard), Commandant, U.S. Coast
Guard, U.S. Department of Homeland Security (ex officio)

Transportation Research Board publications are available by ordering
individual publications directly from the TRB Business Office, through
the Internet at www.TRB.org, or by annual subscription through
organizational or individual affiliation with TRB. Affiliates and library
subscribers are eligible for substantial discounts. For further information,
contact the Transportation Research Board Business Office, 500 Fifth
Street, NW, Washington, DC 20001 (telephone 202-334-3213;
fax 202-334-2519; or e-mail TRBsales@nas.edu).

Copyright 2016 by the National Academy of Sciences.

All rights reserved.

Printed in the United States of America.

ISBN 978-0-309-36997-8 [Slipcased set of three volumes]

ISBN 978-0-309-36998-5 [Volume 1]

ISBN 978-0-309-36999-2 [Volume 2]

ISBN 978-0-309-37000-4 [Volume 3]

ISBN 978-0-309-37001-1 [Volume 4, online only]

The National Academies of
SCIENCES • ENGINEERING • MEDICINE

The **National Academy of Sciences** was established in 1863 by an Act of Congress, signed by President Lincoln, as a private, nongovernmental institution to advise the nation on issues related to science and technology. Members are elected by their peers for outstanding contributions to research. Dr. Ralph J. Cicerone is president.

The **National Academy of Engineering** was established in 1964 under the charter of the National Academy of Sciences to bring the practices of engineering to advising the nation. Members are elected by their peers for extraordinary contributions to engineering. Dr. C. D. Mote, Jr., is president.

The **National Academy of Medicine** (formerly the Institute of Medicine) was established in 1970 under the charter of the National Academy of Sciences to advise the nation on medical and health issues. Members are elected by their peers for distinguished contributions to medicine and health. Dr. Victor J. Dzau is president.

The three Academies work together as the National Academies of Sciences, Engineering, and Medicine to provide independent, objective analysis and advice to the nation and conduct other activities to solve complex problems and inform public policy decisions. The Academies also encourage education and research, recognize outstanding contributions to knowledge, and increase public understanding in matters of science, engineering, and medicine.

Learn more about the National Academies of Sciences, Engineering, and Medicine at **www.national-academies.org**.

The **Transportation Research Board** is one of seven major programs of the National Academies of Sciences, Engineering, and Medicine. The mission of the Transportation Research Board is to increase the benefits that transportation contributes to society by providing leadership in transportation innovation and progress through research and information exchange, conducted within a setting that is objective, interdisciplinary, and multimodal. The Board's varied committees, task forces, and panels annually engage about 7,000 engineers, scientists, and other transportation researchers and practitioners from the public and private sectors and academia, all of whom contribute their expertise in the public interest. The program is supported by state transportation departments, federal agencies including the component administrations of the U.S. Department of Transportation, and other organizations and individuals interested in the development of transportation.

Learn more about the Transportation Research Board at **www.TRB.org**.

CHAPTER 26
FREEWAY AND HIGHWAY SEGMENTS: SUPPLEMENTAL

CONTENTS

1. INTRODUCTION 26-1

2. STATE-SPECIFIC HEAVY-VEHICLE DEFAULT VALUES 26-2

3. TRUCK ANALYSIS USING THE MIXED-FLOW MODEL 26-4

 Introduction 26-4

 Overview of the Methodology 26-4

4. ADJUSTMENTS FOR DRIVER POPULATION EFFECTS 26-14

5. GUIDANCE FOR FREEWAY CAPACITY ESTIMATION 26-15

 Freeway Capacity Definitions 26-15

 Capacity Measurement Locations 26-16

 Capacity Estimation from Field Data 26-18

6. FREEWAY AND MULTILANE HIGHWAY EXAMPLE PROBLEMS 26-22

 Example Problem 1: Four-Lane Freeway LOS 26-22

 Example Problem 2: Number of Lanes Required for Target LOS 26-25

 Example Problem 3: Six-Lane Freeway LOS and Capacity 26-27

 Example Problem 4: LOS on a Five-Lane Highway with a Two-Way
 Left-Turn Lane 26-30

 Example Problem 5: Mixed-Flow Freeway Operations 26-32

 Example Problem 6: Severe Weather Effects on a Basic Freeway
 Segment 26-39

 Example Problem 7: Basic Managed Lane Segment 26-41

7. TWO-LANE HIGHWAY EXAMPLE PROBLEMS 26-46

 Example Problem 1: Class I Highway LOS 26-46

 Example Problem 2: Class II Highway LOS 26-50

 Example Problem 3: Class III Highway LOS 26-53

 Example Problem 4: LOS for a Class I Highway with a Passing Lane 26-55

 Example Problem 5: Two-Lane Highway Bicycle LOS 26-57

8. REFERENCES 26-59

APPENDIX A: TRUCK PERFORMANCE CURVES 26-60

APPENDIX B: WORK ZONES ON TWO-LANE HIGHWAYS 26-65

- Concepts 26-65
- Work Zone Capacity 26-66
- Queuing and Delay Analysis 26-69
- Example Calculation 26-71
- References 26-75

LIST OF EXHIBITS

Exhibit 26-1 State-Specific Default Values for Percentage of Heavy Vehicles on Freeways 26-2

Exhibit 26-2 State-Specific Default Values for Percentage of Heavy Vehicles on Multilane and Two-Lane Highways 26-3

Exhibit 26-3 Overview of Operational Analysis Methodology for Mixed-Flow Model 26-5

Exhibit 26-4 Speed–Flow Models for 70-mi/h Auto-Only Flow and a Representative Mixed Flow 26-5

Exhibit 26-5 SUT Travel Time Versus Distance Curves for 70-mi/h FFS 26-9

Exhibit 26-6 TT Travel Time Versus Distance Curves for 70-mi/h FFS 26-9

Exhibit 26-7 δ Values for SUTs 26-10

Exhibit 26-8 δ Values for TTs 26-10

Exhibit 26-9 Recommended CAF and SAF Adjustments for Driver Population Impacts 26-14

Exhibit 26-10 Recommended Capacity Measurement Location for Merge Bottlenecks 26-17

Exhibit 26-11 Recommended Capacity Measurement Location for Diverge Bottlenecks 26-17

Exhibit 26-12 Recommended Capacity Measurement Location for Weaving Bottlenecks 26-17

Exhibit 26-13 Illustrative Example of the Capacity Estimation Procedure 26-20

Exhibit 26-14 Capacity Estimation Using the 15% Acceptable Breakdown Rate Method 26-21

Exhibit 26-15 List of Freeway and Multilane Highway Example Problems 26-22

Exhibit 26-16 Example Problem 1: Graphical Solution 26-24

Exhibit 26-17 List of Two-Lane Highway Example Problems 26-46

Exhibit 26-18 Example Problem 1: Interpolation for ATS Adjustment Factor 26-48

Exhibit 26-19 Example Problem 1: Interpolation for Exponents a and b for Equation 15-10 26-49

Exhibit 26-20 Example Problem 1: Interpolation for $f_{np,PTSF}$ for Equation 15-9 26-49

Exhibit 26-21 Example Problem 4: Region Lengths 26-56

Exhibit 26-A1 SUT Travel Time Versus Distance Curves for 50-mi/h FFS 26-60

Exhibit 26-A2 SUT Travel Time Versus Distance Curves for 55-mi/h FFS 26-60

Exhibit 26-A3 SUT Travel Time Versus Distance Curves for 60-mi/h FFS 26-61

Exhibit 26-A4 SUT Travel Time Versus Distance Curves for 65-mi/h FFS 26-61

Exhibit 26-A5 SUT Travel Time Versus Distance Curves for 75-mi/h FFS 26-62

Exhibit 26-A6 TT Travel Time Versus Distance Curves for 50-mi/h FFS..... 26-62

Exhibit 26-A7 TT Travel Time Versus Distance Curves for 55-mi/h FFS..... 26-63

Exhibit 26-A8 TT Travel Time Versus Distance Curves for 60-mi/h FFS..... 26-63

Exhibit 26-A9 TT Travel Time Versus Distance Curves for 65-mi/h FFS..... 26-64

Exhibit 26-A10 TT Travel Time Versus Distance Curves for 75-mi/h FFS..... 26-64

Exhibit 26-B1 Traffic Control for a Two-Lane Highway Work Zone
 Involving a Lane Closure..... 26-66

Exhibit 26-B2 Directional Queueing Diagram for a Two-Lane Highway
 Lane-Closure Work Zone 26-70

Exhibit 26-B3 Example Calculation: Work Zone Roadway Parameters 26-71

Exhibit 26-B4 Example Calculation: Work Zone Traffic Parameters..... 26-71

1. INTRODUCTION

Chapter 26 is the supplemental chapter for Chapter 12, Basic Freeway and Multilane Highway Segments, and Chapter 15, Two-Lane Highways, which are found in Volume 2 of the *Highway Capacity Manual* (HCM).

Section 2 provides state-specific heavy-vehicle default values that can be applied to freeway, multilane highway, and two-lane highway analysis.

Section 3 presents a supplemental procedure for basic freeway segments that can be used to assess their operating performance under mixed-flow conditions when significant truck presence, a prolonged single upgrade, or both exist. Appendix A provides travel time versus distance curves for single-unit trucks (SUTs) and tractor-trailers (TTs) for a range of free-flow speeds (FFS) for use with this procedure. Chapter 25, Freeway Facilities: Supplemental, presents an extension of this method for composite grades on freeway facilities.

Section 4 provides suggested capacity and FFS adjustments to account for the effects of different proportions of motorists on a freeway or multilane highway who are not regular users of the facility.

Section 5 presents freeway capacity definitions, guidance on locating sensors for use in measuring freeway capacity, and guidance on estimating capacity from the collected sensor data.

Section 6 provides seven example problems demonstrating the basic freeway and multilane highway segment procedure presented in Chapter 12.

Section 7 provides five example problems demonstrating the motorized vehicle and bicycle methodologies for two-lane highways presented in Chapter 15.

Appendix B describes a methodology for calculating capacity and related performance measures for work zones along two-lane highways that involve the closure of a single lane.

VOLUME 4: APPLICATIONS
GUIDE

25. Freeway Facilities:
Supplemental

**26. Freeway and Highway
Segments:
Supplemental**

27. Freeway Weaving:
Supplemental

28. Freeway Merges and
Diverges: Supplemental

29. Urban Street Facilities:
Supplemental

30. Urban Street Segments:
Supplemental

31. Signalized Intersections:
Supplemental

32. STOP-Controlled
Intersections:
Supplemental

33. Roundabouts:
Supplemental

34. Interchange Ramp
Terminals: Supplemental

35. Pedestrians and Bicycles:
Supplemental

36. Concepts: Supplemental

37. ATDM: Supplemental

2. STATE-SPECIFIC HEAVY-VEHICLE DEFAULT VALUES

Research into the percentage of heavy vehicles on uninterrupted-flow facilities (1) found such a wide range of average values from state to state that not even regional default values could be developed. Exhibit 26-1 presents default values for the percentage of heavy vehicles on freeways by state and area population based on data from the 2004 Highway Performance Monitoring System. Exhibit 26-2 presents similar default values for multilane and two-lane highways. In cases in which states or local jurisdictions have developed their own default values, those values should be used in lieu of the values presented here. Analysts may also wish to develop their own default values based on local or more recent data.

Exhibit 26-1
State-Specific Default Values
for Percentage of Heavy
Vehicles on Freeways

State	Rural	Small Urban	Medium Urban	Large Urban	State	Rural	Small Urban	Medium Urban	Large Urban
AL*	14 ^a	7	7	7 ^a	MT	22 ^c	16 ^c	12 ^c	NA
AK	4	5 ^b	5	3 ^b	NC*	19 ^b	12 ^b	12	10 ^a
AR	30	24	13	14	ND	21 ^c	22 ^c	10 ^c	NA
AZ	21	19	18	11	NE	36	37	11	8
CA	16	10	7	6	NH	15 ^b	12 ^b	6 ^b	7 ^b
CO	12	10	8	7	NJ	8	6	6	9
CT	13	6	6	5	NM	26	12	21	12
DC	NA	NA	NA	4 ^b	NV	34 ^b	26	18 ^b	11 ^b
DE	—	—	9 ^b	8 ^b	NY	18	11	11	7
FL*	11	7	12	6	OH	24	13	10	8
GA*	19 ^b	7 ^b	12	8 ^b	OK	28	27	12	10
HI	5	19 ^b	2	3	OR	26	19	10	7
IA	20 ^c	24 ^c	11 ^c	10 ^c	PA	16	13	9	8
ID	29 ^c	28 ^b	12 ^b	7 ^b	PR*	6	7 ^b	7	4 ^b
IL	21	23	16	9	RI	3	—	NA	4
IN	26	25	23	14	SC*	19 ^b	7 ^b	7	8 ^b
KS	21 ^c	17 ^c	8 ^c	9 ^b	SD	20 ^c	14 ^c	9 ^c	NA
KY*	20 ^a	16	12	10 ^a	TN*	19	12	12	8
LA*	12 ^c	7 ^b	12	10 ^c	TX	16	28 ^c	8	5
MA	7 ^a	5	4 ^a	4	UT	34 ^c	—	18	13
MD	18	14	17	8	VA*	9	7	7	4
ME	5	5	5	NA	VT	15	12	6	NA
MI	18	12	13	8	WA	11	10	7	6
MN	11	10	6	4	WI	6	6	6	6
MO	29 ^b	23 ^b	13 ^b	10 ^b	WV	16 ^b	13 ^b	9 ^b	NA
MS*	9 ^b	7 ^b	7	6 ^b	WY	33 ^c	36 ^a	28 ^{c,d}	NA

Source: Zegeer et al. (1).

Notes: Populations are as follows: rural: <5,000; small urban: 5,000–50,000; medium urban: 50,000–250,000; large urban: >250,000.

Values shown represent mean values for the state for each population type except as otherwise noted.

NA = population group does not exist within the state; — = data not available.

* Because of limited data, small urban values were combined for two groups of states: AL, MS, PR, SC, and VA and FL, GA, KY, LA, NC, and TN. Medium urban values were combined for AL, FL, and VA.

^a Reported values appeared to be a mix of field observations and statewide values. The latter were discounted, such that the averages shown are based primarily on values deemed to be field observations, with some consideration given to nearby states and the value state personnel thought was statewide.

^b The default value was estimated from field observations from nearby states because of insufficient field data, a lack of data for this road type, or too-heavy reliance on statewide values.

^c The peak period percentage is identical to the daily average percentage for nearly all observations in the 2004 Highway Performance Monitoring System data set. Default values were estimated primarily from the daily average value but took into account the results from nearby states, particularly the difference between peak and daily values in those states.

^d This distribution was bimodal, with one group centered on 19% and the other on 44%.

State	Two-Lane Highways		Multilane Highways		State	Two-Lane Highways		Multilane Highways	
	Rural	Small Urban	Rural	Small Urban		Rural	Small Urban	Rural	Small Urban
AL	6 ^a	6 ^a	4 ^a	6 ^a	MT	10 ^c	4 ^c	6 ^c	3 ^c
AK	10	2	6	3	NC	8 ^b	4 ^b	6 ^b	6 ^b
AR	14	7	11	12	ND	14 ^c	3 ^c	12 ^c	7 ^c
AZ	9	11	9	9	NE	10	3	12	5
CA	9	5	9	6	NH	6 ^b	6 ^a	6 ^b	6 ^b
CO	11	4	5	5	NJ	8	7	8	6 ^b
CT	3	3	2	6 ^b	NM	17	7	23	12
DC	NA	NA	NA	NA	NV	17 ^b	5 ^c	10 ^c	6 ^c
DE	7	6	9	8	NY	8	5	8	5
FL	8	4	7	7	OH	11	4	14	9
GA	8 ^b	5 ^b	6 ^b	6 ^b	OK	14 ^a	5	17	11
HI	3	3	2	2	OR	12	5	6	9
IA	4 ^c	5 ^c	5 ^c	4 ^c	PA	6	3	5	4
ID	12 ^c	7 ^c	16 ^c	9 ^c	PR	5	5 ^b	5	6
IL	8	5	8	6	RI	2	1	2	6 ^b
IN	10	6 ^a	12	10	SC	8 ^b	5 ^b	6 ^b	6 ^b
KS	15 ^a	3	12 ^c	6 ^c	SD	13 ^c	4 ^c	12 ^c	7 ^c
KY	16 ^a	6 ^a	9 ^a	6 ^a	TN	5	4 ^a	6	4
LA	16 ^c	10 ^c	6 ^b	16	TX	13	9	12	9
MA	3 ^a	3 ^a	7 ^b	6 ^b	UT	20 ^c	9 ^c	22 ^c	14 ^c
MD	10	6	12	8	VA	4	2	5	2
ME	5	3	4	3	VT	8	5 ^a	7	6 ^b
MI	9	7 ^a	8	4	WA	15	8 ^a	10	7
MN	9	8 ^a	8	6	WI	4	5 ^a	4	5 ^a
MO	9 ^c	6 ^c	12 ^b	10 ^c	WV	6 ^b	6 ^b	5 ^b	6 ^b
MS	14 ^a	5 ^a	6 ^b	6 ^a	WY	15 ^c	6 ^c	10 ^c	9 ^c

Exhibit 26-2
State-Specific Default Values for Percentage of Heavy Vehicles on Multilane and Two-Lane Highways

Source: Zegeer et al. (1).

Notes: Populations are as follows: rural: <5,000; small urban: 5,000–50,000.

Values shown represent mean values for the state for each population type except as otherwise noted.

NA = population group does not exist within the state.

^a Reported values appeared to be a mix of field observations and statewide values. The latter were discounted, such that the averages shown are based primarily on values deemed to be field observations, with some consideration given to nearby states and the value state personnel thought was statewide.

^b Either there are insufficient field data, such that regional averages were used, or there are no usable field data, either because there are no data in the state for this road type or because there is a too-heavy reliance on statewide values for both the peak period and the daily average. In these cases, the default value was estimated from field observations for nearby states.

^c The peak period percentage is identical to the daily average percentage for all or almost all observations in the 2004 Highway Performance Monitoring System data set for this cell. Default values were estimated primarily from the daily average value for this cell, taking into account the results for other similar states in the same region, and in particular the difference between peak and daily average values in those states.

3. TRUCK ANALYSIS USING THE MIXED-FLOW MODEL

INTRODUCTION

This section presents a supplemental procedure that can be used to assess the operating performance of freeway segments under mixed-flow conditions when significant truck presence, a prolonged single upgrade, or both exist. This procedure *must* be used if the analyst is interested in estimating space mean speeds and densities for cars and trucks separately or for the mixed-traffic stream.

Chapter 12, Basic Freeway and Multilane Highway Segments, describes a methodology drawn from this procedure that can be used to assess a segment's level of service (LOS) by converting heavy vehicles into passenger cars by using passenger car equivalent (PCE) values. However, users are cautioned that the auto-only speeds and densities estimated by the PCE-based procedure are likely to be an approximation of reality at high truck percentages and on steep upgrades. For these situations, the mixed-flow model described here is recommended.

Analysts can also use the mixed-flow model for analyzing downgrades and both types of general terrain (level and rolling). When the truck percentage is low or the upgrade is not steep, both the mixed-flow model and the Chapter 12 PCE-based method provide similar results. Chapter 25, Freeway Facilities: Supplemental, extends the mixed-flow model to freeway facilities with multiple, composite grades. National research (2) shows that when the truck presence is low or the upgrade is not steep, both the mixed-flow model and the procedure applying PCE values provide similar results.

OVERVIEW OF THE METHODOLOGY

The process flow for applying the mixed-flow model is depicted in Exhibit 26-3. Selected parameters referenced in the methodology are indicated in Exhibit 26-4 for a 70-mi/h auto-only traffic stream and a representative mixed-traffic stream.

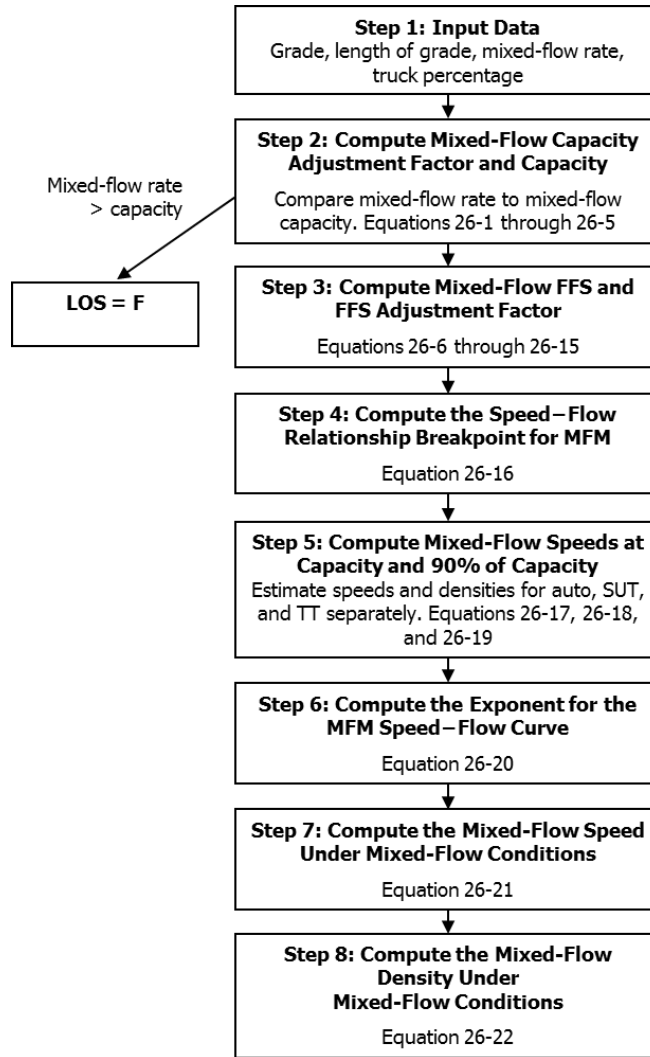


Exhibit 26-3
Overview of Operational
Analysis Methodology for
Mixed-Flow Model

Notes: SUT = single-unit truck; TT = tractor-trailer; FFS = free-flow speed; MFM = mixed-flow model.

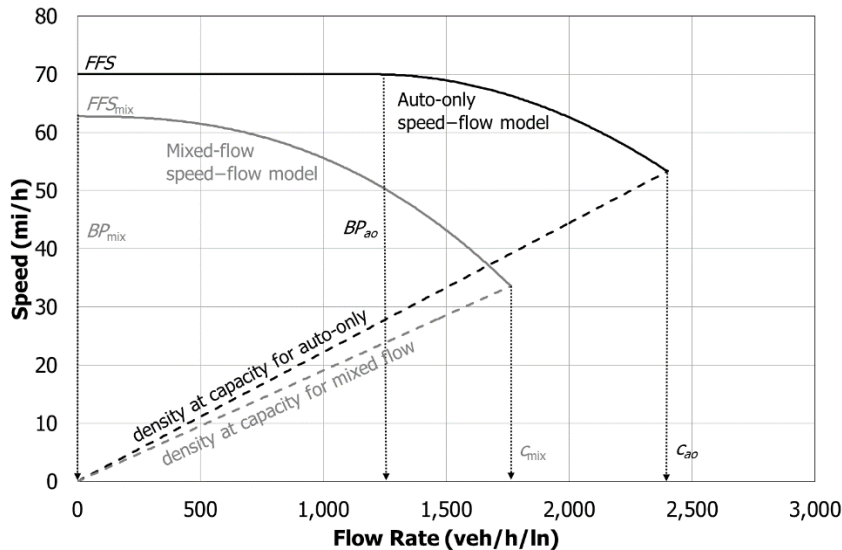


Exhibit 26-4
Speed-Flow Models for 70-
mi/h Auto-Only Flow and a
Representative Mixed Flow

Notes: BP = breakpoint; FFS = free-flow speed; c = capacity.

Step 1: Input Data

For a typical operational analysis, the analyst must specify the flow rate of the mixed-traffic stream v_{mix} , grade g , grade length d , SUT percentage P_{SUT} , and TT percentage P_{TT} for the traffic stream.

Step 2: Compute Mixed-Flow Capacity Adjustment Factor and Capacity

The capacity adjustment factor (CAF) for mixed-flow CAF_{mix} converts auto-only capacities into mixed-traffic capacities. It is computed with Equation 26-1.

Equation 26-1

$$CAF_{mix} = CAF_{ao} - CAF_{T,mix} - CAF_{g,mix}$$

where

CAF_{mix} = mixed-flow capacity adjustment factor for the basic freeway segment (decimal);

CAF_{ao} = capacity adjustment factor for the auto-only case (decimal);

$CAF_{T,mix}$ = capacity adjustment factor for percentage of trucks for the mixed-flow case (decimal); and

$CAF_{g,mix}$ = capacity adjustment factor for grade for the mixed-flow case (decimal).

CAF for the Auto-Only Case

Because CAF_{ao} is used to convert auto-only capacities into mixed-traffic capacities, it defaults to a value of 1.0 unless other capacity adjustments are in effect (e.g., weather, incidents, driver population factor).

CAF for Truck Percentage

The CAF for truck percentage $CAF_{T,mix}$ is computed with Equation 26-2.

Equation 26-2

$$CAF_{T,mix} = 0.53 \times P_T^{0.72}$$

where P_T is the total percentage of SUTs and TTs in the traffic stream (decimal).

CAF for Grade Effect

The CAF for grade effect $CAF_{g,mix}$ accounts for the grade severity, grade length, and truck presence. It is computed by using Equation 26-3 with Equation 26-3.

Equation 26-3

$$CAF_{g,mix} = \rho_{g,mix} \times \max[0, 0.69 \times (e^{12.9g} - 1)] \times \max[0, 1.72 \times (1 - 1.71e^{-3.16d})]$$

with

Equation 26-4

$$\rho_{g,mix} = \begin{cases} 8 \times P_T & P_T < 0.01 \\ 0.126 - 0.03P_T & \text{otherwise} \end{cases}$$

where

$\rho_{g,mix}$ = coefficient for grade term in the mixed-flow CAF equation (decimal),

P_T = total truck percentage (decimal),

g = grade (decimal), and

d = grade length (mi).

Once CAF_{mix} is computed, the mixed-flow capacity can be computed with Equation 26-5.

$$C_{mix} = C_{ao} \times CAF_{mix}$$

Equation 26-5

where

C_{mix} = mixed-flow capacity (veh/h/ln);

C_{ao} = auto-only capacity for the given FFS, from Exhibit 12-6 (pc/h/ln); and

CAF_{mix} = mixed-flow capacity adjustment factor for the basic freeway segment (decimal).

If the input flow rate of the mixed-traffic stream v_{mix} exceeds the mixed-flow capacity computed in Equation 26-5, then LOS F prevails, and the segment procedure stops. A facility analysis is recommended under these conditions.

Step 3: Compute Mixed-Flow FFS and FFS Adjustment Factor

Equation 26-6 through Equation 26-8 compute the free-flow travel rates (in seconds per mile) for SUTs, TTs, and automobiles, respectively, for a specific segment with a steep grade, high truck percentage, or both. For the purposes of calculating the automobile free-flow travel rate, the flow rate of the mixed-traffic stream v_{mix} is assumed to be 1 veh/h/ln when Equation 26-8 is used.

$$\tau_{SUT} = \tau_{SUT,kin} + \Delta\tau_{TI}$$

Equation 26-6

$$\tau_{TT} = \tau_{TT,kin} + \Delta\tau_{TI}$$

Equation 26-7

$$\tau_a = \frac{3,600}{FFS} + \Delta\tau_{TI}$$

Equation 26-8

$$+ 100.42 \times \left(\frac{v_{mix}}{1,000} \right)^{0.46} \times P_{SUT}^{0.68} \times \max \left[0, \frac{\tau_{SUT,kin}}{100} - \frac{3,600}{(FFS \times 100)} \right]^{2.76}$$

$$+ 110.64 \times \left(\frac{v_{mix}}{1,000} \right)^{1.36} \times P_{TT}^{0.62} \times \max \left[0, \frac{\tau_{TT,kin}}{100} - \frac{3,600}{(FFS \times 100)} \right]^{1.81}$$

where

τ_a = automobile free-flow travel rate (s/mi),

τ_{SUT} = SUT free-flow travel rate (s/mi),

τ_{TT} = TT free-flow travel rate (s/mi),

$\tau_{SUT,kin}$ = kinematic travel rate of SUTs (s/mi),

$\tau_{TT,kin}$ = kinematic travel rate of TTs (s/mi),

$\Delta\tau_{TI}$ = traffic interaction term (s/mi),

v_{mix} = flow rate of mixed traffic (veh/h/ln),

FFS = base free-flow speed of the basic freeway segment (mi/h),

P_{SUT} = SUT percentage (decimal),

P_{TT} = TT percentage (decimal), and

3,600 = number of seconds in 1 h.

Traffic Interaction Term

The traffic interaction term computed by Equation 26-9 is the contribution of traffic interactions to mixed-flow FFS. For the purposes of calculating the automobile free-flow travel rate, the traffic interaction term $\Delta\tau_{TI}$ is set to 0 when Equation 26-8 is used.

Equation 26-9

$$\Delta\tau_{TI} = \left(\frac{3,600}{S_{ao}} - \frac{3,600}{FFS} \right) \times \left(1 + 3 \left[\frac{1}{CAF_{mix}} - 1 \right] \right)$$

where

$\Delta\tau_{TI}$ = traffic interaction term (s/mi);

S_{ao} = auto-only speed for the given flow rate, from Equation 26-10 (mi/h);

FFS = base free-flow speed of the basic freeway segment (mi/h); and

CAF_{mix} = mixed-flow capacity adjustment factor for the basic freeway segment from Equation 26-1 (decimal).

Auto-Only Speed for the Given Flow Rate

The auto-only travel rate for the given flow rate is computed with Equation 26-10.

Equation 26-10

$$S_{ao} = \begin{cases} FFS & \frac{v_{mix}}{CAF_{mix}} \leq BP_{ao} \\ FFS - \frac{\left(FFS - \frac{c}{D_c} \right) \left(\frac{v_{mix}}{CAF_{mix}} - BP_{ao} \right)^2}{\left(c - BP_{ao} \right)^2} & \frac{v_{mix}}{CAF_{mix}} > BP_{ao} \end{cases}$$

where

FFS = base free-flow speed of the basic freeway segment (mi/h);

c = base segment capacity, from Exhibit 12-6 (pc/h/ln);

BP_{ao} = breakpoint for the auto-only flow condition, from Exhibit 12-6 (pc/h/ln);

D_c = density at capacity = 45 pc/mi/ln; and

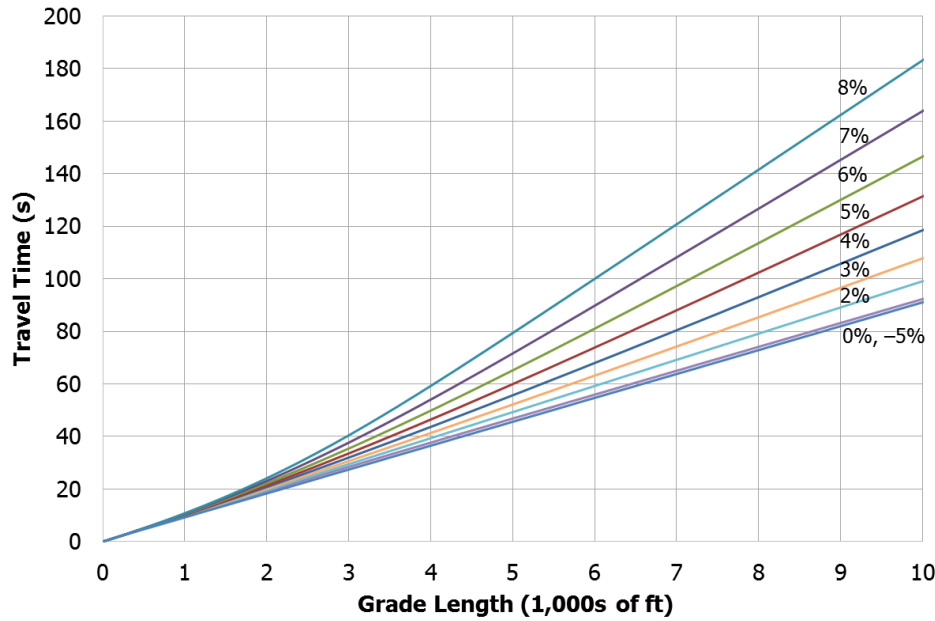
CAF_{mix} = mixed-flow capacity adjustment factor for the basic freeway segment, from Equation 26-1 (decimal).

Kinematic Travel Rates for SUTs and TTs

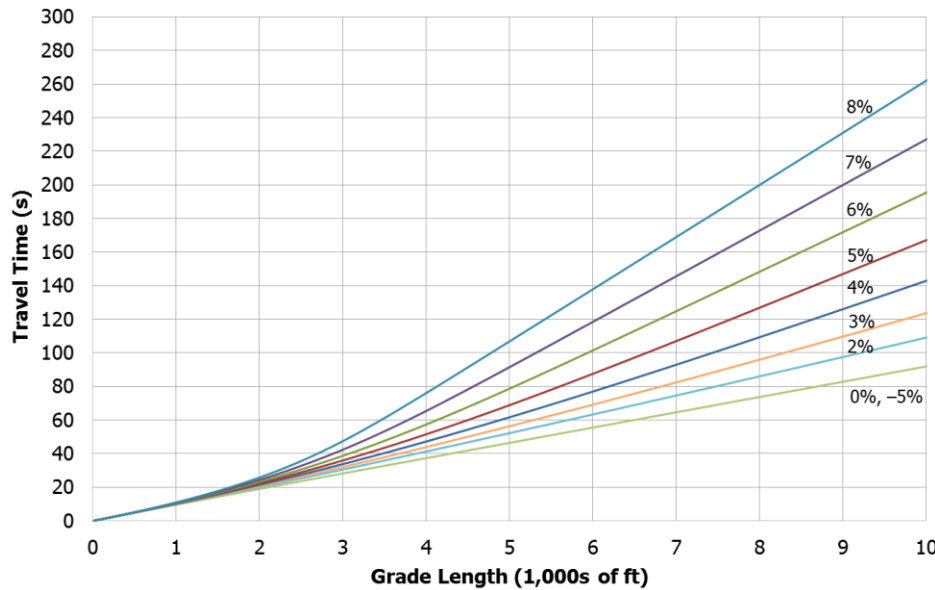
The kinematic travel rates for SUTs and TTs are obtained from truck travel time versus distance performance curves on the basis of the truck weight-to-horsepower ratio, grade, and grade length. Exhibit 26-5 shows truck travel time versus distance curves for a representative SUT starting from a speed of 70 mi/h. Alternate representations of how the propulsive and resistive forces vary with speed can produce slightly different results (e.g., 3, 4).

Exhibit 26-6 shows the corresponding curves for TTs for a base FFS of 70 mi/h. These curves can be used when the base FFS is within 2.5 mi/h of 70 mi/h. Appendix A provides additional curves for SUTs and TTs for FFS values of 50, 55, 60, 65, and 75 mi/h.

On downgrades, trucks are able to maintain their FFS, and their kinematic performance is the same as passenger cars. The analyst could use the Chapter 12 PCE-based method instead of the mixed-flow model in those cases.



Note: Curves in this graph assume a weight-to-horsepower ratio of 100.



Note: Curves in this graph assume a weight-to-horsepower ratio of 150.

The x -axis in Exhibit 26-5 and Exhibit 26-6 represents the distance d traveled by the truck, and the y -axis represents the travel time T to cover the grade length d . Different curves provide the travel times for different upgrades. The kinematic space mean travel rate can be computed with Equation 26-11.

$$\tau_{kin} = T/d$$

Exhibit 26-5
SUT Travel Time Versus Distance Curves for 70-mi/h FFS

Exhibit 26-6
TT Travel Time Versus Distance Curves for 70-mi/h FFS

Equation 26-11

where

- τ_{kin} = kinematic travel rate (s/mi),
- T = travel time (s), and
- d = grade length (mi).

The maximum grade length shown in Exhibit 26-5 and Exhibit 26-6 is 10,000 ft. When the grade is longer than 10,000 ft, the kinematic travel rate can be computed with Equation 26-12.

Equation 26-12

$$\tau_{kin} = \frac{T_{10000}}{d} + \delta \left(1 - \frac{10,000}{5,280d} \right) \times 5,280$$

where

- τ_{kin} = kinematic travel rate (s/mi),
- T_{10000} = travel time at 10,000 ft (s),
- δ = slope of the travel time versus distance curve (s/ft),
- d = grade length (mi), and
- 5,280 = number of feet in 1 mi.

The δ value for SUTs and TTs is shown in Exhibit 26-7 and Exhibit 26-8, respectively, for different combinations of grade and FFS.

Exhibit 26-7
 δ Values for SUTs

Grade	Free-Flow Speed (mi/h)					
	50	55	60	65	70	75
-5%	0.0136	0.0124	0.0114	0.0105	0.0097	0.0091
0%	0.0136	0.0124	0.0114	0.0105	0.0097	0.0091
2%	0.0136	0.0124	0.0114	0.0105	0.0100	0.0099
3%	0.0136	0.0124	0.0114	0.0113	0.0112	0.0112
4%	0.0136	0.0129	0.0128	0.0128	0.0128	0.0127
5%	0.0146	0.0146	0.0146	0.0146	0.0145	0.0145
6%	0.0165	0.0165	0.0165	0.0165	0.0165	0.0165
7%	0.0186	0.0186	0.0186	0.0186	0.0186	0.0186
8%	0.0208	0.0208	0.0208	0.0208	0.0208	0.0208

Exhibit 26-8
 δ Values for TTs

Grade	Free-Flow Speed (mi/h)					
	50	55	60	65	70	75
-5%	0.0136	0.0124	0.0114	0.0105	0.0097	0.0091
0%	0.0136	0.0124	0.0114	0.0105	0.0097	0.0091
2%	0.0136	0.0124	0.0119	0.0118	0.0116	0.0115
3%	0.0143	0.0143	0.0142	0.0141	0.0140	0.0138
4%	0.0171	0.0171	0.0171	0.0170	0.0169	0.0168
5%	0.0202	0.0202	0.0202	0.0202	0.0202	0.0202
6%	0.0236	0.0236	0.0236	0.0236	0.0236	0.0236
7%	0.0272	0.0272	0.0272	0.0272	0.0272	0.0272
8%	0.0310	0.0310	0.0310	0.0310	0.0310	0.0310

Once $\tau_{SUT,kin}$ and $\tau_{TT,kin}$ are obtained, Equation 26-6 and Equation 26-7 can be used to add the traffic interaction term to obtain the truck free-flow travel rates τ_{SUT} and τ_{TT} . Equation 26-8 can then be used to compute the automobile free-flow travel rate τ_a . Again, the mixed-flow rate v_{mix} is assumed to be 1 veh/h/ln when Equation 26-8 is used to estimate the automobile free-flow travel rate.

Mixed-Flow FFS

Equation 26-13 converts individual free-flow travel rates by mode into a mixed-flow free-flow travel rate, and Equation 26-14 then converts the mixed-flow free-flow travel rate into a mixed-flow FFS.

$$\tau = P_a \tau_a + P_{SUT} \tau_{SUT} + P_{TT} \tau_{TT}$$

$$FFS_{mix} = \frac{3,600}{\tau} = \frac{3,600}{P_a \tau_a + P_{SUT} \tau_{SUT} + P_{TT} \tau_{TT}}$$

Equation 26-13

Equation 26-14

where

- τ = mixed-flow free-flow travel rate (s/mi),
- τ_a = automobile free-flow travel rate (s/mi),
- τ_{SUT} = SUT free-flow travel rate (s/mi),
- τ_{TT} = TT free-flow travel rate (s/mi),
- P_a = automobile percentage (decimal),
- P_{SUT} = SUT percentage (decimal),
- P_{TT} = TT percentage (decimal), and
- FFS_{mix} = mixed-flow free-flow speed (mi/h).

FFS Adjustment Factor

The segment's speed adjustment factor (SAF) is estimated with Equation 26-15.

$$SAF_{mix} = FFS_{mix} / FFS$$

Equation 26-15

where

- SAF_{mix} = mixed-flow speed adjustment factor for the basic freeway segment (decimal),
- FFS_{mix} = mixed-flow free-flow speed (mi/h), and
- FFS = base free-flow speed of the basic freeway segment (mi/h).

Step 4: Compute the Speed–Flow Relationship Breakpoint for the Mixed-Flow Model

The breakpoint is the maximum flow rate up to which speed is maintained at the adjusted FFS level. It is computed by Equation 26-16 and is depicted in Exhibit 26-4.

$$BP_{mix} = \max[0, BP_{ao}(1 - 0.4P_T^{0.1} \times \max[0, e^{30g} + 1] \times d^{0.01})]$$

Equation 26-16

where

- BP_{mix} = breakpoint for mixed flow (veh/h/ln);
- BP_{ao} = breakpoint for the auto-only flow condition, from Exhibit 12-6 (pc/h/ln);
- P_T = total truck percentage (decimal);
- g = grade (decimal); and
- d = grade length (mi).

Step 5: Compute Mixed-Flow Speeds at Capacity and 90% of Capacity

To determine the mixed-flow speeds for the given mixed-flow rate, mixed-flow speeds at capacity and 90% of capacity are computed for calibration purposes. This computation, in turn, requires applying Equation 26-6 through Equation 26-8 to calculate individual speeds for SUTs, TTs, and automobiles, respectively. The equations are applied twice, first applying the value of C_{mix} as v_{mix} to calculate speed at capacity, and then applying the value of $0.9C_{mix}$ as v_{mix} to calculate speed at 90% of capacity.

The resulting modal travel time rates are converted to modal speeds S_m by using Equation 26-17.

Equation 26-17

$$S_m = \frac{3,600}{\tau_m}$$

where S_m is the speed (mi/h) for mode m (SUT, TT, or automobile), and τ_m is the travel time rate (s/mi) for mode m .

Next, densities for individual modes are computed with Equation 26-18.

Equation 26-18

$$D_m = v_m/S_m$$

where D_m is the density (SUT/mi, TT/mi, or pc/mi, depending on the mode) for mode m , v_m is the flow rate (SUT/h, TT/h, or pc/h) for mode m , and S_m is the speed (mi/h) for mode m .

Finally, the mixed-flow speed used for calibration S_{calib} is calculated with Equation 26-19.

Equation 26-19

$$S_{calib} = \frac{3,600}{P_a \tau_a + P_{SUT} \tau_{SUT} + P_{TT} \tau_{TT}}$$

Equation 26-19 is applied twice (i.e., two calibration points are needed), once using τ values at capacity and again using τ values for 90% of capacity.

Mixed-flow travel rates and mixed-flow speeds are calculated with Equations 26-13 and 26-14 twice (i.e., two calibration points are needed), once at capacity and once at 90% capacity.

Step 6: Compute the Exponent for the Mixed-Flow Model Speed–Flow Curve

The exponent for the speed–flow curve, which describes the rate at which speed drops as the flow rate increases in the nonlinear portion of the mixed-flow speed–flow curve (see Exhibit 26-4), is computed with Equation 26-20.

Equation 26-20

$$\phi_{mix} = 1.195 \times \frac{\ln\left(\frac{FFS_{mix} - S_{calib,90cap}}{FFS_{mix} - S_{calib,cap}}\right)}{\ln\left(\frac{0.9C_{mix} - BP_{mix}}{C_{mix} - BP_{mix}}\right)}$$

where

ϕ_{mix} = exponent for the speed–flow curve (decimal),

FFS_{mix} = mixed-flow free-flow speed (mi/h),

$S_{calib,90cap}$ = mixed-flow speed at 90% of capacity (mi/h),

$S_{calib, cap}$ = mixed-flow speed at capacity (mi/h),
 C_{mix} = mixed-flow capacity (veh/h/ln), and
 BP_{mix} = breakpoint for mixed flow (veh/h/ln).

Step 7: Compute the Mixed-Flow Speed Under Mixed-Flow Conditions

The mixed-flow speed for mixed-flow conditions is computed by using the generic form of the basic freeway segment speed–flow model, as shown in Equation 26-21.

$$S_{mix} = \begin{cases} FFS_{mix} & v_{mix} \leq BP_{mix} \\ FFS_{mix} - (FFS_{mix} - S_{calib, cap}) \left(\frac{v_{mix} - BP_{mix}}{C_{mix} - BP_{mix}} \right)^{\phi_{mix}} & v_{mix} > BP_{mix} \end{cases}$$

Equation 26-21

where

S_{mix} = mixed-flow speed (mi/h),
 FFS_{mix} = mixed-flow free-flow speed (mi/h),
 $S_{calib, cap}$ = mixed-flow speed at capacity (mi/h),
 v_{mix} = flow rate of mixed traffic (veh/h/ln),
 BP_{mix} = breakpoint for mixed flow (veh/h/ln),
 C_{mix} = mixed-flow capacity (veh/h/ln), and
 ϕ_{mix} = exponent for the speed–flow curve (decimal).

Step 8: Compute the Mixed-Flow Density Under Mixed-Flow Conditions

The mixed-flow density is computed by Equation 26-22.

$$D_{mix} = v_{mix} / S_{mix}$$

Equation 26-22

where

D_{mix} = mixed-flow density (veh/mi/ln),
 v_{mix} = flow rate of mixed traffic (veh/h/ln), and
 S_{mix} = mixed-flow speed (mi/h).

4. ADJUSTMENTS FOR DRIVER POPULATION EFFECTS

The base traffic stream characteristics for basic freeway and multilane highway segments are representative of traffic streams composed primarily of commuters or drivers who are familiar with the facility. It is generally accepted that traffic streams with different characteristics (e.g., recreational trips) use freeways less efficiently. Although data are sparse and reported results vary substantially, significantly lower capacities have been reported on weekends, particularly in recreational areas. Thus, it may generally be assumed the reduction in capacity extends to service flow rates and service volumes for other levels of service as well. In addition, it is expected that a reduction in FFS would be observed when large numbers of unfamiliar drivers are present in a freeway or multilane highway traffic stream.

The driver population adjustment factor f_p has previously been used in the HCM to reflect the effects of unfamiliar drivers in the traffic stream; it was applied as an increase in demand volume. The values of f_p ranged from 0.85 to 1.00 in most cases, although lower values have been observed in isolated cases. The HCM recommended the analyst use a value of 1.00 for this factor (reflecting a traffic stream composed of commuters or other regular drivers), unless there was sufficient evidence that a lower value should be used. When greater accuracy was needed, comparative field studies of commuter and noncommuter traffic flow and speeds were recommended.

With the addition of a unified speed-flow equation in Chapter 12, Basic Freeway and Multilane Highway Segments, and the ability to adjust both the base FFS and capacity in all freeway segment chapters (Chapters 12, 13, and 14) to account for incidents and weather events, the driver population factor is no longer used. Instead, FFS and capacity adjustment factors SAF_{pop} and CAF_{pop} are applied in combination with other applicable SAFs and CAFs.

In the absence of new research on driver population effects, recommended values of SAF_{pop} and CAF_{pop} have been developed that produce similar density results as those predicted using the former driver population factor approach. This conversion was performed by using the unified equation of Chapter 12 and therefore represents a slight approximation in the cases of weaving, merge, and diverge segments.

Judgment is still required when the analyst applies these adjustments and, in the absence of information to the contrary, the default value for SAF_{pop} and CAF_{pop} is always 1.0. Should the analyst expect a significant presence of unfamiliar drivers, the values shown in Exhibit 26-9 can serve as a guide for the analysis.

Exhibit 26-9
Recommended CAF and SAF
Adjustments for Driver
Population Impacts

Level of Driver Familiarity	CAF_{pop}	SAF_{pop}
All familiar drivers, regular commuters	1.000	1.000
Mostly familiar drivers	0.968	0.975
Balanced mix of familiar and unfamiliar drivers	0.939	0.950
Mostly unfamiliar drivers	0.898	0.913
All or overwhelmingly unfamiliar drivers	0.852	0.863

5. GUIDANCE FOR FREEWAY CAPACITY ESTIMATION

This section presents guidance for field measuring and estimating freeway capacity. The section is organized as follows: overall definitions of freeway capacity, guidance for field data collection using sensors, and guidance for estimating capacity from the collected data.

FREEWAY CAPACITY DEFINITIONS

Freeway segment capacity is commonly understood to be a maximum flow rate that is associated with the occurrence of some type of breakdown that in turn results in lower speeds and higher densities after the breakdown event. When oversaturation begins, queues develop and vehicles discharge from the bottleneck at a queue discharge rate that is usually lower than the throughput rate before the breakdown. This lower discharge rate after a breakdown is also known as the *capacity drop phenomenon*. Several key terms related to freeway capacity are defined below as they apply to this chapter.

Freeway Breakdown

A flow breakdown on a freeway represents the transition from uncongested to congested conditions, as evidenced by the formation of queues upstream of the bottleneck and reduced prevailing speeds.

In the HCM freeway methodology, the breakdown event on a freeway bottleneck is defined as a sudden drop in speed at least 25% below the FFS for a sustained period of at least 15 min that results in queuing upstream of the bottleneck.

Recovery

A freeway segment is considered to have recovered from the breakdown event and the resulting oversaturated conditions when the average speed (or density) reaches prebreakdown conditions for a minimum duration of 15 min. The definition of recovery is therefore the inverse of the definition of breakdown, requiring a recovery to be near prebreakdown conditions (operations above the speed threshold) for at least 15 min.

The HCM defines the breakdown recovery on a freeway bottleneck as a return of the prevailing speed to within 10% of the FFS for a sustained period of at least 15 min, without the presence of queuing upstream of the bottleneck.

Prebreakdown Flow Rate

The prebreakdown flow rate is the flow rate that immediately precedes the occurrence of a breakdown event. The literature suggests this flow rate does not have a fixed value, as evidence shows breakdowns are stochastic in nature and can occur following a range of flow rates. The prebreakdown flow rate is typically expressed in units of passenger cars per hour per lane. To achieve a uniform expression, trucks and other heavy vehicles are converted into an equivalent passenger car traffic stream.

In the HCM, the prebreakdown flow rate is defined as the 15-min average flow rate that occurs immediately prior to the breakdown event. For the purposes of this chapter, the prebreakdown flow rate is equivalent to the segment capacity.

Postbreakdown Flow Rate or Queue Discharge Flow Rate

The postbreakdown flow rate is also referred to as the *queue discharge flow rate* or the average discharge flow rate. This flow rate is usually lower than the prebreakdown flow rate, resulting in a significant loss of freeway throughput during congestion. Cases in which the postbreakdown flow rate exceeds the prebreakdown flow rate have been observed, mostly when the prebreakdown flow rate is low. Studies (5) have indicated the average difference between postbreakdown and prebreakdown flow rates varies widely, from as little as 2% to as much as 20%. In the absence of local information, a default value of 7% is recommended.

In the HCM, the queue discharge flow rate is defined as the average flow rate during oversaturated conditions (i.e., during the time interval after breakdown and prior to recovery).

CAPACITY MEASUREMENT LOCATIONS

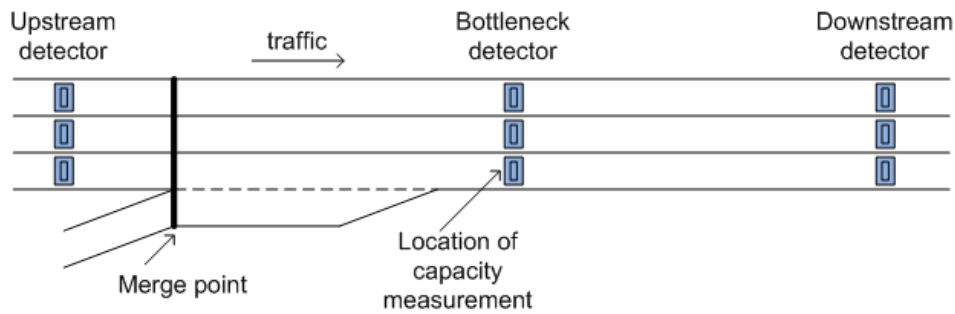
Research at freeway merging segments (6) has found a breakdown may first be observed either upstream or downstream of the actual bottleneck. Some research has indicated a breakdown may first be observed upstream of the bottleneck, slowly spreading downstream as vehicles accelerate past the start of the bottleneck. Other research has found the breakdown initially occurs downstream of the merge point and then moves upstream as a shock wave.

To identify the breakdown event from field data, the following process should be followed:

- Data are obtained at three sensors: (a) a bottleneck location (e.g., just downstream of the end of the acceleration lane), (b) at a nearby sensor location downstream of the bottleneck, and (c) at a nearby sensor location upstream of the bottleneck.
- Upstream and downstream sensors should be within 0.5 mi of the bottleneck, and the freeway ideally should have no entry or exit points between the three sensors (other than, for example, a bottleneck on-ramp).
- The bottleneck detector should be upstream of the beginning of the deceleration lane or downstream of the end of the acceleration lane to avoid missing flow in those lanes.
- The analyst evaluates data from the bottleneck sensor to identify a breakdown by using the definitions provided above.
- The analyst evaluates data from the downstream sensor for the same time period to ensure no breakdown exists, which indicates congestion at the bottleneck sensor is unlikely due to spillback from downstream congestion.

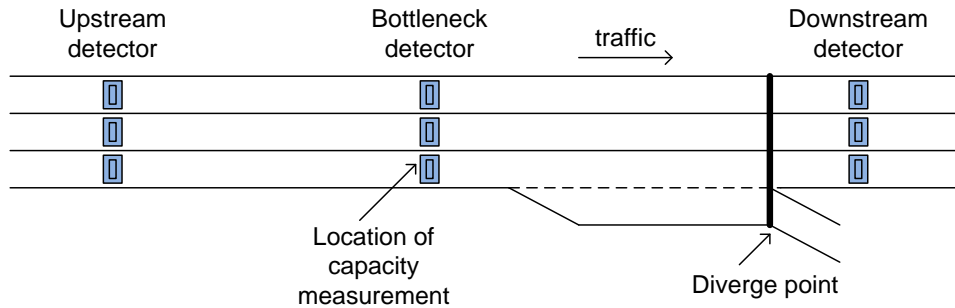
- The analyst evaluates data from the upstream sensor to verify queues are forming as a result of breakdown at the bottleneck. This check ensures observed drops in speeds and increases in density at the bottleneck sensor are indeed due to breakdown.

It is important that the measurements of flows, speeds, and densities used to estimate capacity are carried out at the correct locations, especially if the data will be generated from existing fixed freeway sensors, which may or may not be at the optimal locations to detect breakdown events. Capacity should always be measured at the bottleneck location. At merge bottlenecks or lane drops, this location is downstream of the merge point (Exhibit 26-10). At diverge bottlenecks, this location is upstream of the diverge point (Exhibit 26-11). At weaving bottlenecks, this location is within the weaving area (Exhibit 26-12).



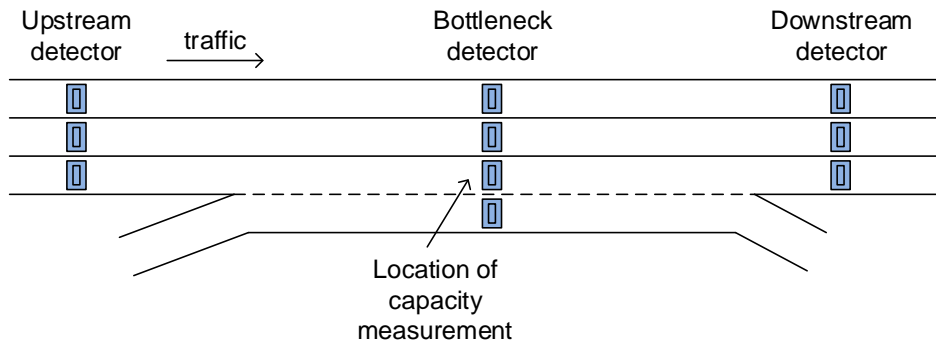
Source: Elefteriadou, Kondyli, and St. George (6).

Exhibit 26-10
Recommended Capacity
Measurement Location for
Merge Bottlenecks



Source: Elefteriadou, Kondyli, and St. George (6).

Exhibit 26-11
Recommended Capacity
Measurement Location for
Diverge Bottlenecks



Source: Elefteriadou, Kondyli, and St. George (6).

Exhibit 26-12
Recommended Capacity
Measurement Location for
Weaving Bottlenecks

Regardless of the bottleneck type, the analyst will be able to identify and measure capacity only if a breakdown occurs. As discussed below, the breakdown event is associated with the development of queues that form upstream of the bottleneck location (i.e., merge point, diverge point, weaving section) and propagate further upstream, but queues also propagate downstream as vehicles accelerate past the start of the bottleneck. Once breakdown events are identified, the analyst will be able to identify the prebreakdown and postbreakdown flow rates and estimate segment capacity based on the method discussed in the next section.

CAPACITY ESTIMATION FROM FIELD DATA

To estimate the capacity of the various freeway segments it is important to analyze data obtained under *recurring* congestion and under similar operational and weather conditions. Observations in which adverse weather, incidents, work zones, or special events were present must be analyzed separately to obtain capacities under various prevailing conditions. To obtain a reasonable capacity estimate, it is important to analyze a considerable amount of data over a period of several months to an entire year.

The recommended method for capacity estimation from sensor data takes into account that capacity is stochastic. That is, the same flow rate may or may not be followed by a breakdown. Therefore, during an observation period, both prebreakdown flow rates and flow rates that are not followed by breakdown events (uncongested flow rates) are considered. From these flow rates, the method develops a capacity distribution and then selects a capacity value based on an acceptable rate of breakdown. Two plausible (and equivalent) freeway segment capacity definitions are offered:

1. **Definition A:** Freeway segment capacity is the maximum 15-min flow rate (in passenger cars per hour per lane) that produces an acceptable ($\lambda\%$) rate of breakdown.
2. **Definition B:** Freeway segment capacity is the maximum 15-min flow rate (in passenger cars per hour per lane) that ensures stable flow ($100 - \lambda\%$) of the time.

The rate of breakdown λ is the ratio of the total number of periods observed under prebreakdown conditions, divided by the total number of 15-min uncongested observations under the same flow rate. A default acceptable rate of breakdown λ of 15% is recommended.

The capacity estimation process follows a series of eight steps and assumes sensors are placed at the appropriate locations (as discussed above) and are available to measure prebreakdown flows and ensure the absence of downstream congestion, which may bias the results described below.

1. Record the distribution of 15-min flow rates (in passenger cars per hour per lane) during the observation period (preferably a long period). For example, sampling from the sensor 24 h per day on weekdays over a year gives approximately $24 \times 4 \times 250 = 24,000$ flow rate observations.

2. Exclude the 15-min time periods when the freeway is in breakdown mode, as defined earlier, which will result in a distribution of uncongested 15-min flow rates. It is recommended to filter breakdowns due to nonrecurring sources of congestion, such as severe weather events or incidents, as the focus is on estimating the bottleneck's capacity under recurring congestion conditions.
3. Bin the uncongested flow rates into 100- or 200-pc/h/ln bins.
4. Compute the average flow rate in each bin.
5. For each bin, count the number of times the flow rates in the bin were immediately followed by the occurrence of a breakdown. In other words, bin the prebreakdown 15-min flow rates.
6. Calculate the actual probability of breakdown $P(B_F)$ in each bin, defined as the number of times a flow rate bin was in a prebreakdown condition $n(B)$, divided by the number of times that bin was observed to have occurred, or $n(F)$. The probability of breakdown $P(B_F)$ in each bin is simply $P(B_F) = n(B)/n(F)$.
7. Fit a Weibull distribution (7) to the empirical probability of breakdown computed in Step 6.
8. Based on the selected threshold breakdown (or stable flow) rate λ or $(1 - \lambda)$, determine the resulting capacity value from the Weibull distribution developed in Step 6 by using Equation 26-23. A value of λ of 15% is recommended.

$$\text{Capacity} = \beta \times \sqrt[\gamma]{-\ln(1 - \lambda)}$$

where β and γ , respectively, are the shape and scale parameters of the fitted Weibull distribution, and λ is as defined previously. When $\lambda = 0.15$, the equation simplifies to $c = \beta (0.163)^{1/\gamma}$.

The following example is based on actual data and involves estimating the capacity of a bottleneck on southbound I-440 in Raleigh, North Carolina. In this example, sensor data in the vicinity of an on-ramp bottleneck were collected for 260 weekdays from June 2014 to May 2015. The average percentage of trucks observed in the traffic stream was less than 1%; therefore, the conversion of trucks into PCEs is ignored for the purposes of this example.

The theoretical number of 15-min observations is 260 days \times 96 observations per day = 24,960 observations. After outliers were removed (observations from incident and weather events and congested-flow periods), there remained 22,984 periods when flow was deemed uncongested and that represented similar operational and weather conditions. Within these periods, 192 breakdowns were identified that met the criteria described above.

Exhibit 26-13 summarizes the computations for this example, using the eight steps given above. The example illustrates how the process yields a capacity value based on the recommended 15% breakdown rate.

Equation 26-23

Exhibit 26-13
Illustrative Example of the
Capacity Estimation Procedure

[1]	[2]	[3]	[4]	[5]	[6]	[7]
Flow Rate in Bins (pc/h/ln) From To		Average Flow Rate in Bin (pc/h/ln)	No. of Observed 15-min Uncongested Periods	No. of Observed 15-min Periods at a Prebreakdown Flow Rate	Probability of Breakdown in Bin	Cumulative Probability of Breakdown
0	99	50	4,570	0	0.0%	0.0%
100	199	150	1,657	1	0.1%	0.5%
200	299	250	1,009	3	0.3%	2.1%
300	399	350	765	2	0.3%	3.1%
400	499	450	889	2	0.2%	4.2%
500	599	550	913	0	0.0%	4.2%
600	699	650	746	0	0.0%	4.2%
700	799	750	657	0	0.0%	4.2%
800	899	850	534	0	0.0%	4.2%
900	999	950	458	0	0.0%	4.2%
1,000	1,099	1,050	798	0	0.0%	4.2%
1,100	1,199	1,150	1,801	1	0.1%	4.7%
1,200	1,299	1,250	2,171	2	0.1%	5.7%
1,300	1,399	1,350	1,662	5	0.3%	8.3%
1,400	1,499	1,450	1,185	8	0.7%	12.5%
1,500	1,599	1,550	866	10	1.2%	17.7%
1,600	1,699	1,650	618	13	2.1%	24.5%
1,700	1,799	1,750	495	22	4.4%	35.9%
1,800	1,899	1,850	322	6	1.9%	39.1%
1,900	1,999	1,950	258	16	6.2%	47.4%
2,000	2,099	2,050	301	45	15.0%	70.8%
2,100	2,199	2,150	227	37	16.3%	90.1%
2,200	2,299	2,250	79	18	22.8%	99.5%
2,300	2,399	2,350	3	1	33.3%	100.0%
2,400	2,499	2,450	0	0	NA	100.0%
Sum			22,984	192		

Notes: Numbers in brackets indicate column numbers. NA = not applicable.

The exhibit shows 22,984 15-min flow rate observations in Column 4, equivalent to 5,746 h of observations. Column 5 shows 192 breakdown events. The probability of breakdown in a bin is computed in Column 6, which is used to estimate capacity based on the defined λ threshold. Finally, Column 7 shows the cumulative distribution of prebreakdown flow rates, based on the data in Column 5.

The information in Exhibit 26-13 is shown graphically in Exhibit 26-14. The solid black curve to the right shows the Weibull distribution fitted to the data in Column 6; the actual data are also plotted. The distribution parameters were $\beta = 2,569$ and $\gamma = 9.13$. Substituting these values into Equation 26-23 and using $\lambda = 0.15$ yields a capacity value of 2,105 pc/h/ln. The gray dashed curve to the left in the exhibit represents the cumulative distribution of prebreakdown flow rates (i.e., Column 7). In this case, the calculated capacity value corresponded to approximately the 85th percentile of the prebreakdown flow rate distribution, as represented by the dotted lines.

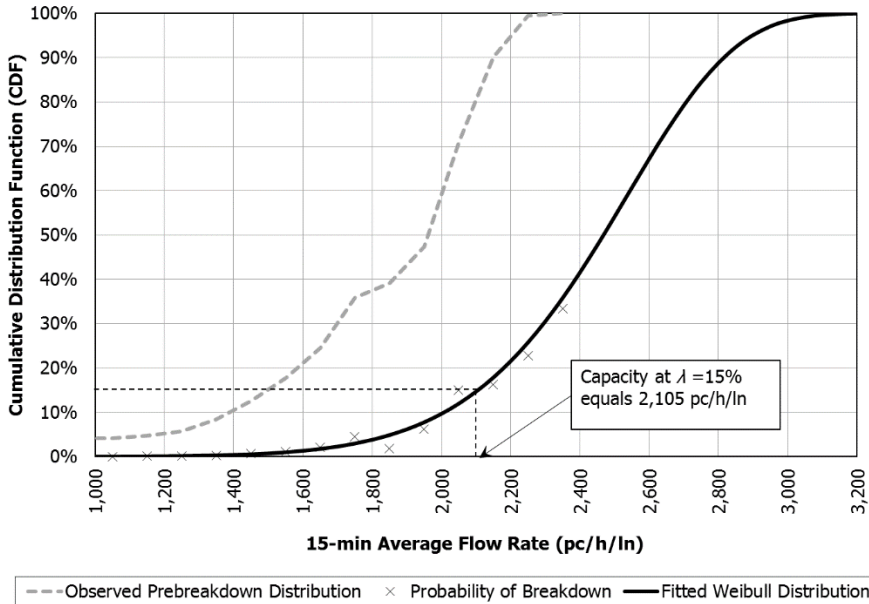


Exhibit 26-14
Capacity Estimation Using the
15% Acceptable Breakdown
Rate Method

In summary, the capacity estimation method considers the fact that flow rates preceding breakdown can also occur at other times without being followed by a breakdown. The definition of capacity is clear and unambiguous and can be explained to the HCM user or practitioner without much difficulty. However, the analyst needs to ensure there are a *sufficient number of breakdown observations* to be confident in the calculated capacity value.

6. FREEWAY AND MULTILANE HIGHWAY EXAMPLE PROBLEMS

Exhibit 26-15 lists the seven example problems provided in this section. The problems demonstrate the computational steps involved in applying the automobile methodology to basic freeway and multilane highway segments. All the freeway example problems address urban freeway situations.

Exhibit 26-15
List of Freeway and Multilane
Highway Example Problems

Example Problem	Description	Application
1	Four-lane freeway LOS	Operational analysis
2	Number of lanes required for target LOS	Design analysis
3	Six-lane freeway LOS and capacity	Operational and planning analysis
4	LOS on a five-lane highway with a two-way left-turn lane	Operational analysis
5	Mixed-flow operational performance	Operational analysis
6	Severe weather effects on a basic freeway segment	Operational analysis
7	Basic managed lane segment	Operational analysis

EXAMPLE PROBLEM 1: FOUR-LANE FREEWAY LOS

The Facts

- Four-lane freeway (two lanes in each direction)
- Lane width = 11 ft
- Right-side lateral clearance = 2 ft
- Commuter traffic (regular users)
- Peak hour, peak direction demand volume = 2,000 veh/h
- Traffic composition: 5% trucks
- Peak hour factor (PHF) = 0.92
- One cloverleaf interchange per mile
- Level terrain
- Facility operates under ideal conditions (no incidents, work zones, or weather events).

Comments

The task is to find the expected LOS for this freeway during the worst 15 min of the peak hour. With one cloverleaf interchange per mile, the total ramp density will be 4 ramps/mi.

Step 1: Input Data

All input data are specified above.

Step 2: Estimate and Adjust FFS

The FFS of the freeway is estimated from Equation 12-2 as follows:

$$FFS = 75.4 - f_{LW} - f_{RLC} - 3.22 \times TRD^{0.84}$$

The adjustment for lane width is selected from Exhibit 12-20 for 11-ft lanes (1.9 mi/h). The adjustment for right-side lateral clearance is selected from Exhibit 12-21 for a 2-ft clearance on a freeway with two lanes in one direction (2.4 mi/h). The total ramp density is 4 ramps/mi. Then

$$FFS = 75.4 - 1.9 - 2.4 - 3.22 \times 4^{0.84} = 60.8 \text{ mi/h}$$

Because the facility is operating under ideal conditions, the SAF used in Equation 12-5 is 1, and $FFS_{adj} = FFS$.

Step 3: Estimate and Adjust Capacity

The capacity of the freeway is estimated from Equation 12-6 as follows:

$$c = 2,200 + 10 \times (FFS_{adj} - 50)$$

$$c = 2,200 + 10 \times (60.8 - 50) = 2,308 \text{ pc/h/ln}$$

Because the facility is operating under ideal conditions, the CAF used in Equation 12-8 is 1, and $c_{adj} = c$.

Step 4: Adjust Demand Volume

The demand volume must be adjusted to a flow rate that reflects passenger cars per hour per lane under equivalent base conditions by using Equation 12-9.

$$v_p = \frac{V}{PHF \times N \times f_{HV}}$$

The demand volume is given as 2,000 veh/h. The PHF is specified to be 0.92, and there are two lanes in each direction. The driver population consists of regular users (commuters). Trucks make up 5% of the traffic stream, so a heavy-vehicle adjustment factor must be determined.

From Exhibit 12-25, the PCE for trucks is 2.0 for level terrain. The heavy-vehicle adjustment factor is then computed with Equation 12-10.

$$f_{HV} = \frac{1}{1 + P_T(E_T - 1)}$$

$$f_{HV} = \frac{1}{1 + 0.05(2.0 - 1)} = 0.952$$

then

$$v_f = \frac{2,000}{0.92 \times 2 \times 0.952 \times 1.00} = 1,142 \text{ pc/h/ln}$$

Because this value is less than the base capacity of 2,308 pc/h/ln for a freeway with FFS = 60.8 mi/h, LOS F does not exist, and the analysis continues to Step 5.

Step 5: Estimate Speed and Density

The FFS of the basic freeway segment is now estimated along with the demand flow rate (in passenger cars per hour per lane) under equivalent base

conditions. Using the equations provided in Exhibit 12-6, the breakpoint for a 60.8-mi/h FFS speed-flow curve is

$$BP_{adj} = [1,000 + 40 \times (75 - FFS_{adj})] \times CAF^2 = 1,568 \text{ pc/h/ln}$$

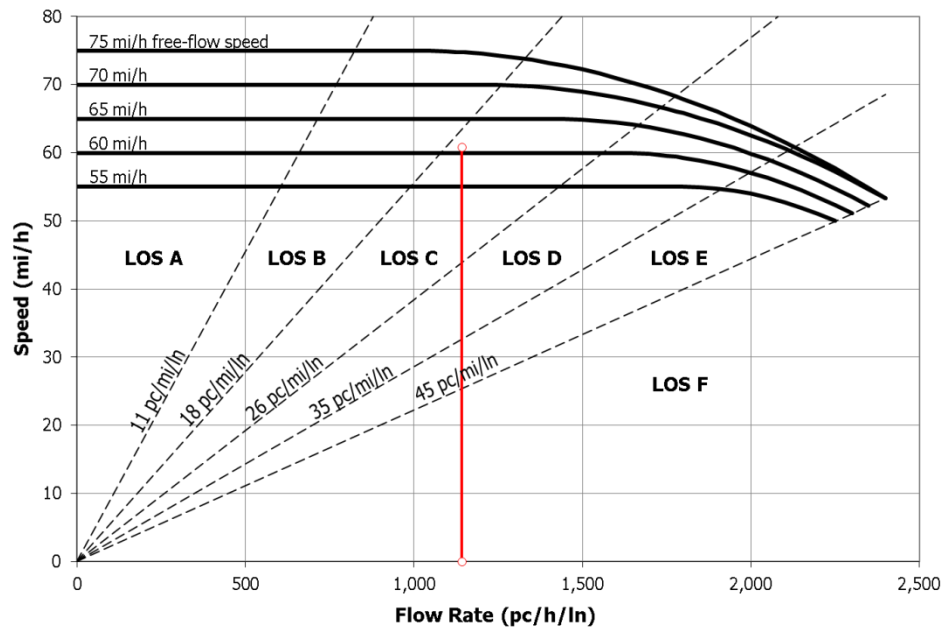
As the flow rate of 1,142 pc/h/ln is less than the breakpoint value of 1,568 pc/h/ln, the freeway operates within the constant-speed portion of the speed-flow curve, so $S = 60.8$ mi/h. The density of the traffic stream may now be computed from Equation 12-11.

$$D = \frac{v_p}{S} = \frac{1,142}{60.8} = 18.8 \text{ pc/mi/ln}$$

Step 6: Determine LOS

From Exhibit 12-15, a density of 18.8 pc/mi/ln corresponds to LOS C, but it is close to the boundary for LOS B, which is a maximum of 18 pc/mi/ln. This solution could also be calculated graphically from Exhibit 12-16, as illustrated in Exhibit 26-16.

Exhibit 26-16
Example Problem 1: Graphical Solution



Discussion

This basic freeway segment of a four-lane freeway is expected to operate at LOS C during the worst 15 min of the peak hour. It is important to note that the operation, although at LOS C, is close to the LOS B boundary. In most jurisdictions, this operation would be considered to be quite acceptable.

EXAMPLE PROBLEM 2: NUMBER OF LANES REQUIRED FOR TARGET LOS**The Facts**

- Demand volume = 4,000 veh/h (one direction)
- Level terrain
- Traffic composition: 8% SUTs and buses
- Provision of 12-ft lanes
- Provision of 6-ft right-side lateral clearance
- Commuter traffic (regular users)
- PHF = 0.85
- Ramp density = 3 ramps/mi
- Target LOS = D
- Facility operates under ideal conditions (no incidents, work zones, or weather events).

Comments

This example problem is a classic design application of the methodology. The number of lanes needed to provide LOS D during the worst 15 min of the peak hour is to be determined.

Step 1: Input Data

All input data are specified above.

Step 2: Estimate and Adjust FFS

FFS is estimated by using Equation 12-2. Because the lane width and lateral clearance to be provided on the new freeway will be 12 ft and 6 ft, respectively, there are no adjustments for these features from Exhibit 12-20 or Exhibit 12-21. The total ramp density is given as 3 ramps/mi. Then

$$FFS = 75.4 - f_{LW} - f_{RLC} - 3.22 \times TRD^{0.84}$$

$$FFS = 75.4 - 0 - 0 - 3.22 \times 3^{0.84} = 67.3 \text{ mi/h}$$

Because the facility is operating under ideal conditions, the SAF used in Equation 12-5 is 1, and $FFS_{adj} = FFS$.

Step 3: Estimate and Adjust Capacity

The capacity of the freeway is estimated from Equation 12-6.

$$c = 2,200 + 10 \times (FFS_{adj} - 50)$$

$$c = 2,200 + 10 \times (67.3 - 50) = 2,373 \text{ pc/h/ln}$$

Because the facility is operating under ideal conditions, the CAF used in Equation 12-8 is 1, and $c_{adj} = c$.

Step 4: Estimate Number of Lanes Needed

Because this is a design analysis, Step 4 of the operational analysis methodology is modified. Equation 12-23 may be used directly to determine the number of lanes needed to provide at least LOS D.

$$N = \frac{V}{MSF_i \times PHF \times f_{HV}}$$

A value of the maximum service flow rate must be selected from Exhibit 12-37 for an FFS of 65 mi/h and LOS D. Note that this exhibit only provides these values in 5-mi/h increments; therefore, FFS is rounded to 65 mi/h. The corresponding maximum service flow rate is 2,030 pc/h/ln.

The PHF is given as 0.85. A heavy-vehicle factor for 8% trucks must be determined by using Exhibit 12-25 for level terrain. The PCE of trucks on level terrain is 2.0, so the heavy-vehicle adjustment based on Equation 12-10 is

$$f_{HV} = \frac{1}{1 + P_T(E_T - 1)}$$

$$f_{HV} = \frac{1}{1 + 0.08(2 - 1)} = 0.926$$

and

$$N = \frac{4,000}{2,030 \times 0.85 \times 0.926 \times 1.00} = 2.5 \text{ ln}$$

It is not possible to build 2.5 lanes. To provide a minimum of LOS D, it will be necessary to provide three lanes in each direction, or a six-lane freeway.

At this point, the design application ends. It is possible, however, to consider what speed, density, and LOS will prevail when three lanes are actually provided. Therefore, the example problem continues with Steps 5 and 6.

Step 5: Estimate Speed and Density

In pursuing additional information, the problem now reverts to an operational analysis of a three-lane basic freeway segment with a demand volume of 4,000 pc/h.

Equation 12-9 is used to compute the actual demand flow rate per lane under equivalent base conditions.

$$v_p = \frac{V}{PHF \times N \times f_{HV}}$$

$$v_p = \frac{4,000}{0.85 \times 3 \times 0.926} = 1,694 \text{ pc/h/ln}$$

From Exhibit 12-6, the breakpoint for a speed-flow curve with FFS equal to 67.3 is

$$BP_{adj} = [1,000 + 40 \times (75 - FFS_{adj})] \times CAF^2 = 1,308 \text{ pc/h/ln}$$

In this case, the demand flow rate of 1,694 pc/h/ln exceeds the breakpoint value of 1,308 pc/h/ln, and the average speed will be less than the FFS.

The expected speed of the traffic stream may be estimated by using either Exhibit 12-7 (for a graphical solution) or Equation 12-1 as follows:

$$S = FFS_{adj} - \frac{\left(FFS_{adj} - \frac{c_{adj}}{D_c} \right) (v_p - BP)^a}{(c_{adj} - BP)^a}$$

$$S = 67.3 - \frac{\left(67.3 - \frac{2,373}{45}\right)(1,694 - 1,308)^2}{(2,373 - 1,308)^2} = 65.4 \text{ mi/h}$$

The density may now be computed from Equation 12-11.

$$D = \frac{v_p}{S} = \frac{1,694}{65.4} = 25.9 \text{ pc/mi/ln}$$

Step 6: Determine LOS

Entering Exhibit 12-15 with a density of 25.9 pc/mi/ln, the LOS is C, but that density is very close to the boundary of LOS D, which is 26 pc/mi/ln.

Discussion

The resulting LOS is C, which represents a better performance than the target design. Although the minimum number of lanes needed was 2.5, which would have produced a minimal LOS D, providing three lanes yields a density that is close to the LOS C boundary. In any event, the target LOS of the design will be met by providing a six-lane basic freeway segment.

EXAMPLE PROBLEM 3: SIX-LANE FREEWAY LOS AND CAPACITY

The Facts

- Volume of 5,000 veh/h (one direction, existing)
- Volume of 5,788 veh/h (one direction, in 3 years)
- Traffic composition: 4% trucks
- Rolling terrain
- Three lanes in each direction
- FFS = 70 mi/h (measured)
- PHF = 0.96
- Commuter traffic (regular users)
- Traffic growth = 5% per year
- Facility operates under ideal conditions (no incidents, work zones, or weather events).

Comments

This example consists of two operational analyses, one for the present demand volume of 5,000 pc/h and one for the demand volume of 5,788 pc/h expected in 3 years. In addition, a planning element is introduced: Assuming traffic grows as expected, when will the capacity of the roadway be exceeded? This analysis requires that capacity be determined in addition to the normal output of operational analyses.

Step 1: Input Data

All input data are specified above.

Step 2: Estimate and Adjust FFS

Step 2 is not needed, as the FFS was directly measured (70 mi/h). Because the facility is operating under ideal conditions, the SAF used in Equation 12-5 is 1, and $FFS_{adj} = FFS$.

Step 3: Estimate and Adjust Capacity

The capacity of the freeway is estimated from Equation 12-6.

$$c = 2,200 + 10 \times (FFS_{adj} - 50)$$

$$c = 2,200 + 10 \times (70 - 50) = 2,400 \text{ pc/h/ln}$$

Because the facility is operating under ideal conditions, the CAF used in Equation 12-8 is 1, and $c_{adj} = c$.

Step 4: Adjust Demand Volume

In this case, two demand volumes will be adjusted by using Equation 12-9.

$$v_p = \frac{V}{PHF \times N \times f_{HV}}$$

The PHF is given as 0.96, and there are three lanes in each direction. The heavy-vehicle factor will reflect 4% trucks in rolling terrain. From Exhibit 12-25, the PCE for trucks in rolling terrain is 3.0. Equation 12-10 then gives

$$f_{HV} = \frac{1}{1 + P_T(E_T - 1)}$$

$$f_{HV} = \frac{1}{1 + 0.04(3.0 - 1)} = 0.926$$

Two values of v_p are computed: one for present conditions and one for conditions in 3 years.

$$v_p(\text{present}) = \frac{5,000}{0.96 \times 3 \times 0.926} = 1,875 \text{ pc/h}$$

$$v_p(\text{future}) = \frac{5,788}{0.96 \times 3 \times 0.926} = 2,171 \text{ pc/h}$$

Step 5: Estimate Speed and Density

Two values of speed and density will be estimated, one each for the present and future conditions. Equation 12-1 will be used to estimate speeds. First, the breakpoint for the speed-flow curve is computed from Exhibit 12-6.

$$BP_{adj} = [1,000 + 40 \times (75 - FFS_{adj})] \times CAF^2 = 1,200 \text{ pc/h/ln}$$

One equation applies to both cases; a 70-mi/h FFS with a flow rate over 1,200 pc/h/ln is used.

$$S = FFS_{adj} - \frac{(FFS_{adj} - \frac{c_{adj}}{D_c})(v_p - BP)^a}{(c_{adj} - BP)^a}$$

$$S(\text{present}) = 70 - \frac{(70 - \frac{2,400}{45})(1,875 - 1,200)^2}{(2,400 - 1,200)^2} = 64.7 \text{ mi/h}$$

$$S(\text{future}) = 70 - \frac{\left(70 - \frac{2,400}{45}\right)(2,171 - 1,200)^2}{(2,400 - 1,200)^2} = 59.1 \text{ mi/h}$$

The corresponding densities may now be estimated from Equation 12-11.

$$D = \frac{v_P}{S}$$

$$D(\text{present}) = \frac{1,875}{64.7} = 29.0 \text{ pc/mi/ln}$$

$$D(\text{future}) = \frac{2,171}{59.1} = 36.7 \text{ pc/mi/ln}$$

Step 6: Determine LOS

From Exhibit 12-15, the LOS for the present situation is D, and the LOS for the future scenario (in 3 years) is E due to the increase in density.

Step 7: Determine When Capacity Will Be Reached

Step 7 is an additional step for this problem. To determine when capacity will be reached, the capacity of the basic freeway segment must be estimated. From Exhibit 12-37, the maximum service flow rate for LOS E on a basic freeway segment with a 70-mi/h FFS is 2,400 pc/h/ln. This flow rate is synonymous with capacity.

The analyst must be sure the capacity and demand flow rates compared in Step 7 are measured on the same basis. The 2,400 pc/h/ln is a flow rate under equivalent base conditions. The demand flow rate in 3 years was estimated to be 2,171 pc/h/ln on this basis. These two values, therefore, may be compared. As an alternative, the capacity could be computed for prevailing conditions with Equation 12-24.

$$SF_E = MSF_E \times N \times f_{HV}$$

$$SF_E = 2,400 \times 3 \times 0.926 = 6,667 \text{ veh/h}$$

This capacity, however, is stated as a *flow rate*. The demand volume is stated as an hourly volume. Thus, a *service volume* for LOS E is needed as estimated from Equation 12-25.

$$SV_E = SF_E \times PHF = 6,667 \times 0.96 = 6,400 \text{ veh/h}$$

The problem may be solved either by comparing the demand volume of 5,788 veh/h (in 3 years) with the hourly capacity of 6,400 veh/h or by comparing the demand flow rate under equivalent base conditions of 2,171 pc/h/ln with the base capacity of 2,400 pc/h/ln. With the hourly demand volume and capacity,

$$6,400 = 5,788 \times (1.05)^n$$

$$n = 2.06 \text{ years}$$

On the basis of the forecasts of traffic growth, the basic freeway segment described will reach capacity within 5 years. The demand value of 5,788 veh/h occurs 3 years from the present per the problem description, and the calculation above shows capacity is reached after an additional 2 years. If this result is added to the 3-year planning horizon, capacity will be reached within 5 years of the time of the analysis.

Discussion

The LOS on this segment will reach LOS E within 3 years due to the increase in density. The demand is expected to exceed capacity within 5 years. Given the normal lead times for planning, design, and approvals before the start of construction, it is probable that planning and preliminary design for an improvement should be started immediately.

EXAMPLE PROBLEM 4: LOS ON A FIVE-LANE HIGHWAY WITH A TWO-WAY LEFT-TURN LANE

The Facts

- Lane width: 12 ft
- Lateral clearance, both sides of the roadway: 12 ft
- Traffic composition: 6% trucks, with default truck mix (30% SUTs, 70% TTs)
- Access points per mile: eastbound = 10; westbound = 0
- PHF = 0.90
- Commuter traffic (regular users)
- Median type: two-way left-turn lane
- Peak hour demand: 1,500 veh/h
- The upgrade occurs in the westbound direction
- Posted speed limit = 45 mi/h

Comments

A 6,600-ft segment of a five-lane highway (two travel lanes in each direction plus a two-way left-turn lane) is on a 3.5% grade. At what LOS is the facility expected to operate in each direction?

There is one segment in each direction. The upgrade and downgrade segments on the 3.5% grade must be analyzed separately. This example is more complex than the previous examples because the segment characteristics are not all the same, particularly the number of access points. Because no base FFS is given, it will be estimated as the speed limit plus 7 mi/h, or $45 + 7 = 52$ mi/h.

Step 1: Input Data

All input data are given above.

Step 2: Estimate and Adjust FFS

FFS is estimated by using Equation 12-3.

$$FFS = BFFS - f_{LW} - f_{TLC} - f_M - f_A$$

In this case, the base FFS is estimated to be 52 mi/h. The lane width is 12 ft, which is the base condition; therefore, $f_{LW} = 0.0$ mi/h (Exhibit 12-20). The lateral clearance is 12 ft at each roadside, but a maximum value of 6 ft may be used. A two-way left-turn lane is considered to have a median lateral clearance of 6 ft. Thus, the total lateral clearance is $6 + 6 = 12$ ft, which is also a base condition.

Therefore, $f_{TLC} = 0.0$ mi/h (Exhibit 12-22). The median-type adjustment f_M is also 0.0 mi/h (Exhibit 12-23).

For this example problem, only the access-point density produces a nonzero adjustment to the base FFS. The eastbound (EB) segment (3.5% downgrade) has 10 access points/mi. From Exhibit 12-24, the corresponding FFS adjustment is 2.5 mi/h. The westbound (WB) segment (3.5% upgrade) has 0 access points/mi and a corresponding FFS adjustment of 0.0 mi/h. Therefore,

$$FFS_{EB} = 52.0 - 0.0 - 0.0 - 0.0 - 2.5 = 49.5 \text{ mi/h}$$

$$FFS_{WB} = 52.0 - 0.0 - 0.0 - 0.0 - 0.0 = 52.0 \text{ mi/h}$$

Step 3: Estimate and Adjust Capacity

The capacity of the multilane highway segment is estimated as follows from Equation 12-7.

$$c = 1,900 + 20 \times (FFS_{adj} - 45)$$

$$c_{EB} = 1,900 + 20 \times (49.5 - 45) = 1,990 \text{ pc/h/ln}$$

$$c_{WB} = 1,900 + 20 \times (52.0 - 45) = 2,040 \text{ pc/h/ln}$$

Step 4: Adjust Demand Volume

Demand volume is adjusted by using Equation 12-9.

$$v_p = \frac{V}{PHF \times N \times f_{HV}}$$

To compute the heavy-vehicle adjustment factor f_{HV} , PCEs for trucks are needed for (a) the 3.5%, 6,600-ft upgrade and (b) the 3.5%, 6,600-ft downgrade. The segment is 1.25 mi (6,600/5,280 ft) long. The following values are obtained from Exhibit 12-26:

- Eastbound: 2.24 (using 6% trucks, a 2% downgrade, and 1.25-mi grade length). Note that all downgrades exceeding 2% use the PCE values for a 2% downgrade.
- Westbound: 3.97 (using 6% trucks, a 3.5% upgrade, and a 1.25-mi grade length).

The heavy-vehicle adjustment factors f_{HV} for each segment are calculated from Equation 12-10.

$$f_{HV,EB} = \frac{1}{1 + 0.06 \times (2.24 - 1)} = 0.93$$

$$f_{HV,WB} = \frac{1}{1 + 0.06 \times (3.97 - 1)} = 0.85$$

The segments' flow rates are then calculated as

$$v_{p,EB} = \frac{1,500}{0.90 \times 2 \times 0.93} = 896 \text{ pc/h/ln}$$

$$v_{p,WB} = \frac{1,500}{0.90 \times 2 \times 0.85} = 980 \text{ pc/h/ln}$$

Step 5: Estimate Speed and Density

Speed is estimated with Equation 12-1 or the graph in Exhibit 12-7. With Equation 12-1, both demand flow rates are less than the multilane highway breakpoint value of 1,400 pc/h/ln. Therefore, the speeds *S* are equal to FFS. The densities are computed from Equation 12-11.

$$D_{EB} = \frac{v_{p,EB}}{S_{EB}} = \frac{896}{49.5} = 18.1 \text{ pc/mi/ln}$$

$$D_{WB} = \frac{v_{p,WB}}{S_{WB}} = \frac{980}{52} = 18.8 \text{ pc/mi/ln}$$

Step 6: Determine LOS

LOS is found by comparing the densities of the segments with the criteria in Exhibit 12-15. As both densities are greater than 18 pc/mi/ln, both upgrade and downgrade segments operate at LOS C.

Discussion

Even though the upgrade and downgrade segments operate at LOS C, they are very close to the LOS B boundary (18.0 pc/mi/ln). Both directions of the multilane highway on this grade operate well.

EXAMPLE PROBLEM 5: MIXED-FLOW FREEWAY OPERATIONS

This example illustrates the application of the mixed-flow model for an extended single grade on a six-lane rural freeway.

The Facts

- 2-mi basic segment on a 5% upgrade
- Traffic composition: 5% SUTs and 10% TTs
- FFS = 65 mi/h
- Mixed-traffic flow rate = 1,500 veh/h/ln

Comments

The task is to estimate the segment’s speed and density. Given the significant truck presence (15%) and the 5%, 2-mi grade, the mixed-flow model should be applied.

Step 1: Input Data

All input data are specified above.

Step 2: Compute Mixed-Flow Capacity Adjustment Factor

Capacity is computed with Equation 26-1.

$$CAF_{mix} = CAF_{ao} - CAF_{T,mix} - CAF_{g,mix}$$

There are three terms in the equation. The CAF for auto-only CAF_{ao} is 1.00, as no driver population, weather, incident, or work zone adjustments are specified in the problem statement.

The truck effect term is computed with Equation 26-2.

$$CAF_{T,mix} = 0.53 \times P_T^{0.72} = 0.53 \times 0.15^{0.72} = 0.135$$

The grade effect term is computed with Equation 26-3 and Equation 26-4.

$$CAF_{g,mix} = \rho_{g,mix} \times \max[0, 0.69 \times (e^{12.9g} - 1)] \\ \times \max[0, 1.72 \times (1 - 1.71e^{-3.16d})]$$

$$\rho_{g,mix} = 0.126 - 0.03P_T = 0.126 - (0.03)(0.15) = 0.1215$$

$$CAF_{g,mix} = 0.1215 \times \max[0, 0.69 \times (e^{(12.9)(0.05)} - 1)] \\ \times \max[0, 1.72 \times (1 - 1.71e^{(-3.16)(2)})] = 0.131$$

then

$$CAF_{mix} = 1 - 0.135 - 0.131 = 0.734$$

The mixed-flow capacity is then computed from Equation 26-5.

$$C_{mix} = C_{ao} \times CAF_{mix}$$

The auto-only capacity C_{ao} is computed from Exhibit 12-6.

$$C_{ao} = 2,200 + 10(FFS - 50) = 2,200 + 10 \times (65 - 50) = 2,350 \text{ pc/h/ln}$$

then

$$C_{mix} = 2,350 \times 0.734 = 1,725 \text{ veh/h/ln}$$

As the mixed-traffic flow rate of 1,500 veh/h/ln is less than the mixed-flow capacity of 1,725 veh/h/ln, the analysis can proceed.

Step 3: Compute Mixed-Flow FFS and FFS Adjustment Factor

Equation 26-6 through Equation 26-8 compute the free-flow travel rates for SUTs, TTs, and automobiles, respectively. The FFS of this basic freeway segment is 65 mi/h. Truck performance curves for free-flow speeds other than 70 ± 2.5 mi/h are provided in Appendix A. The 65-mi/h curves for SUTs and TTs are found in Exhibit 26-A4 and Exhibit 26-A9, respectively.

The travel time for a SUT T_{SUT} at a point 10,000 ft along the upgrade can be read directly from Exhibit 26-A4 by observing where the 5% upgrade curve intersects 10,000 ft: 134 s. Similarly, the travel time for a TT T_{TT} is 173 s.

As the grade is 2 mi (10,560 ft) long and the performance curves only provide values up to 10,000 ft, Equation 26-12 is used to determine the travel time rates for the upgrade as a whole. The slope of the travel time versus distance curve δ , which is used in Equation 26-12, can be determined from Exhibit 26-7 for SUTs and Exhibit 26-8 for TTs. The δ values are 0.0146 and 0.0202, respectively.

Then

$$\tau_{kin,SUT} = \frac{T_{SUT,10000ft}}{d} + \delta \left(1 - \frac{10,000}{5280d}\right) \times 5,280 \\ \tau_{kin,SUT} = \frac{134}{2} + 0.0146 \left(1 - \frac{10,000}{10,560}\right) \times 5,280 = 71.1 \text{ s/mi} \\ \tau_{kin,TT} = \frac{173}{2} + 0.0202 \left(1 - \frac{10,000}{10,560}\right) \times 5,280 = 92.2 \text{ s/mi}$$

As this step's objective is to compute the FFS of the mixed-traffic stream, the traffic interaction term $\Delta\tau_{TT}$ is zero, and the mixed-flow rate is set to 1 veh/h/ln.

The SUT, TT, and auto travel time rates are then computed using Equation 26-6 through Equation 26-8.

$$\tau_{SUT,FFS} = 71.1 + 0 = 71.1 \text{ s/mi}$$

$$\tau_{TT,FFS} = 92.2 + 0 = 92.2 \text{ s/mi}$$

$$\begin{aligned} \tau_{a,FFS} &= \frac{3,600}{FFS} + \Delta\tau_{TI} \\ &+ 100.42 \times \left(\frac{v_{mix}}{1,000}\right)^{0.46} \times P_{SUT}^{0.68} \times \max\left[0, \frac{\tau_{kin,SUT}}{100} - \frac{3,600}{(FFS \times 100)}\right]^{2.76} \\ &+ 110.64 \times \left(\frac{v_{mix}}{1,000}\right)^{1.36} \times P_{TT}^{0.62} \times \max\left[0, \frac{\tau_{kin,TT}}{100} - \frac{3,600}{(FFS \times 100)}\right]^{1.81} \end{aligned}$$

$$\begin{aligned} \tau_{a,FFS} &= \frac{3,600}{65} + 0 \\ &+ 100.42 \times \left(\frac{1}{1,000}\right)^{0.46} \times 0.05^{0.68} \times \max\left[0, \frac{71.1}{100} - \frac{3,600}{(65 \times 100)}\right]^{2.76} \\ &+ 110.64 \times \left(\frac{1}{1,000}\right)^{1.36} \times 0.1^{0.62} \times \max\left[0, \frac{92.2}{100} - \frac{3,600}{(65 \times 100)}\right]^{1.81} \end{aligned}$$

$$\tau_{a,FFS} = 55.4 \text{ s/mi}$$

Mixed-flow travel rates and speeds are computed with Equation 26-13 and Equation 26-14.

$$\begin{aligned} \tau_{mix,FFS} &= P_a \tau_{a,FFS} + P_{SUT} \tau_{SUT,FFS} + P_{TT} \tau_{TT,FFS} \\ \tau_{mix,FFS} &= (0.85)(55.4) + (0.05)(71.1) + (0.1)(92.2) = 59.87 \text{ s/mi} \end{aligned}$$

$$FFS_{mix} = \frac{3,600}{\tau_{mix,FFS}} = \frac{3,600}{59.87} = 60.1 \text{ mi/h}$$

Finally, the segment's SAF is estimated with Equation 26-15.

$$SAF_{mix} = \frac{FFS_{mix}}{FFS} = \frac{60.1}{65} = 0.92$$

Step 4: Compute the Mixed-Flow Rate at the Breakpoint

The breakpoint is calculated from Equation 26-16.

$$BP_{mix} = \max[0, BP_{ao}(1 - 0.4P_T^{0.1} \times \max[0, e^{30g} + 1] \times d^{0.01})]$$

where the auto-only breakpoint is calculated by using an equation given in Exhibit 12-6.

$$\begin{aligned} BP_{ao} &= [1,000 + 40 \times (75 - FFS)] \times CAF^2 \\ BP_{ao} &= [1,000 + 40 \times (75 - 65)] \times 1^2 = 1,400 \text{ veh/h/ln} \end{aligned}$$

then

$$\begin{aligned} BP_{mix} &= \max[0, (1,400)(1 - 0.4(0.15)^{0.1} \times \max[0, e^{30 \times 0.05} + 1] \times 2^{0.01})] \\ BP_{mix} &= 0 \text{ veh/h/ln} \end{aligned}$$

This result implies that speeds drop immediately at zero flow (i.e., the mixed-flow FFS cannot be sustained even at low flows).

Step 5: Compute Modal and Mixed-Flow Speeds at Capacity and 90% of Capacity

The speeds and densities for each mode at capacity and 90% of capacity are calculated in this step. Equation 26-6 through Equation 26-8 are applied twice more, once for a flow rate equal to the mixed-flow capacity of 1,725 veh/h/ln calculated in Step 2, and again for a flow rate equal to 90% of capacity. Applying these equations requires determining the traffic interaction term $\Delta\tau_{TI}$, which in turn requires determining the equivalent auto-only speed S_{ao} .

The calculation process will be demonstrated for conditions at capacity. The value of C_{mix} determined in Step 2 (1,725 veh/h/ln) will be used as v_{mix} in the calculations.

The auto-only speed at capacity is computed by Equation 26-10.

$$S_{ao} = \begin{cases} FFS & \frac{v_{mix}}{CAF_{mix}} \leq BP_{ao} \\ FFS - \frac{\left(FFS - \frac{c}{D_c}\right) \left(\frac{v_{mix}}{CAF_{mix}} - BP_{ao}\right)^2}{\left(c - BP_{ao}\right)^2} & \frac{v_{mix}}{CAF_{mix}} > BP_{ao} \end{cases}$$

The value of v_{mix}/CAF_{mix} is $1,725/0.734 = 2,350$ veh/h/ln, which is greater than the auto-only breakpoint of 1,400 veh/h/ln calculated in Step 4. Therefore, the second of the two equations is applied.

$$S_{ao, cap} = 65 - \frac{\left(65 - \frac{2,350}{45}\right) \left(\frac{1,725}{0.734} - 1,400\right)^2}{(2,350 - 1,400)^2} = 52.2 \text{ mi/h}$$

The traffic interaction term can now be computed with Equation 26-9.

$$\Delta\tau_{TI, cap} = \left(\frac{3,600}{S_{ao, cap}} - \frac{3,600}{FFS}\right) \times \left(1 + 3 \left[\frac{1}{CAF_{mix}} - 1\right]\right)$$

$$\Delta\tau_{TI, cap} = \left(\frac{3,600}{52.2} - \frac{3,600}{65}\right) \times \left(1 + 3 \left[\frac{1}{0.734} - 1\right]\right) = 28.3 \text{ s/mi}$$

Equation 26-6 through Equation 26-8 are now applied to find the modal travel time rates at capacity.

$$\tau_{SUT, cap} = \tau_{SUT, kin} + \Delta\tau_{TI} = 71.1 + 28.3 = 99.4 \text{ s/mi}$$

$$\tau_{TT, cap} = \tau_{TT, kin} + \Delta\tau_{TI} = 92.2 + 28.3 = 120.5 \text{ s/mi}$$

$$\tau_{a, cap} = \frac{3,600}{FFS} + \Delta\tau_{TI}$$

$$+ 100.42 \times \left(\frac{v_{mix}}{1,000}\right)^{0.46} \times P_{SUT}^{0.68} \times \max\left[0, \frac{\tau_{SUT, kin}}{100} - \frac{3,600}{(FFS \times 100)}\right]^{2.76}$$

$$+ 110.64 \times \left(\frac{v_{mix}}{1,000}\right)^{1.36} \times P_{TT}^{0.62} \times \max\left[0, \frac{\tau_{TT, kin}}{100} - \frac{3,600}{(FFS \times 100)}\right]^{1.81}$$

$$\begin{aligned}\tau_{a,cap} &= \frac{3,600}{65} + 28.3 \\ &+ 100.42 \times \left(\frac{1,725}{1,000}\right)^{0.46} \times 0.05^{0.68} \times \max\left[0, \frac{71.1}{100} - \frac{3,600}{(65 \times 100)}\right]^{2.76} \\ &+ 110.64 \times \left(\frac{1,725}{1,000}\right)^{1.36} \times 0.1^{0.62} \times \max\left[0, \frac{92.2}{100} - \frac{3,600}{(65 \times 100)}\right]^{1.81}\end{aligned}$$

$$\tau_{a,cap} = 92.9 \text{ s/mi}$$

Based on these travel rates, the overall mixed-traffic space mean speed at capacity can be calculated with Equation 26-19.

$$\begin{aligned}S_{calib,cap} &= \frac{3,600}{P_a \tau_a + P_{SUT} \tau_{SUT} + P_{TT} \tau_{TT}} \\ S_{calib,cap} &= \frac{3,600}{(0.85)(92.9) + (0.05)(99.4) + (0.1)(120.5)} = 37.5 \text{ mi/h}\end{aligned}$$

The same process is used to calculate the mixed-traffic speed at 90% of capacity ($v_{mix} = 0.9 \times 1,725 = 1,553 \text{ veh/h/ln}$). The resulting calculation results are

$$\begin{aligned}S_{ao,90cap} &= 65 - \frac{\left(65 - \frac{2,350}{45}\right) \left(\frac{1,553}{0.734} - 1,400\right)^2}{(2,350 - 1,400)^2} = 57.7 \text{ mi/h} \\ \Delta\tau_{TT,90cap} &= \left(\frac{3,600}{57.7} - \frac{3,600}{65}\right) \times \left(1 + 3 \left[\frac{1}{0.734} - 1\right]\right) = 14.6 \text{ s/mi} \\ \tau_{SUT,90cap} &= 71.1 + 14.6 = 85.7 \text{ s/mi} \\ \tau_{TT,90cap} &= 92.2 + 14.6 = 106.8 \text{ s/mi} \\ \tau_{a,90cap} &= \frac{3,600}{65} + 14.6 \\ &+ 100.42 \times \left(\frac{1,553}{1,000}\right)^{0.46} \times 0.05^{0.68} \times \max\left[0, \frac{71.1}{100} - \frac{3,600}{(65 \times 100)}\right]^{2.76} \\ &+ 110.64 \times \left(\frac{1,553}{1,000}\right)^{1.36} \times 0.1^{0.62} \times \max\left[0, \frac{92.2}{100} - \frac{3,600}{(65 \times 100)}\right]^{1.81}\end{aligned}$$

$$\tau_{a,90cap} = 78.0 \text{ s/mi}$$

$$S_{calib,90cap} = \frac{3,600}{(0.85)(78.0) + (0.05)(85.7) + (0.1)(106.8)} = 44.3 \text{ mi/h}$$

Step 6: Compute the Exponent for the Speed–Flow Curve

The exponent for the speed–flow curve is computed from Equation 26-20.

$$\begin{aligned}\phi_{mix} &= 1.195 \times \frac{\ln\left(\frac{FFS_{mix} - S_{calib,90cap}}{FFS_{mix} - S_{calib,cap}}\right)}{\ln\left(\frac{0.9C_{mix} - BP_{mix}}{C_{mix} - BP_{mix}}\right)} \\ \phi_{mix} &= 1.195 \times \frac{\ln\left(\frac{60.1 - 44.3}{60.1 - 37.5}\right)}{\ln\left(\frac{1,553 - 0}{1,725 - 0}\right)} = 4.07\end{aligned}$$

Step 7: Compute the Mixed-Flow Speed Under Mixed-Flow Conditions

The mixed-flow speed under mixed-flow conditions is computed by Equation 26-21.

$$S_{\text{mix}} = \begin{cases} FFS_{\text{mix}} & v_{\text{mix}} \leq BP_{\text{mix}} \\ FFS_{\text{mix}} - (FFS_{\text{mix}} - S_{\text{calib,cap}}) \left(\frac{v_{\text{mix}} - BP_{\text{mix}}}{C_{\text{mix}} - BP_{\text{mix}}} \right)^{\phi_{\text{mix}}} & v_{\text{mix}} > BP_{\text{mix}} \end{cases}$$

The mixed-flow rate is 1,500 veh/h/ln, which is greater than the breakpoint. Therefore,

$$S_{\text{mix}} = 60.1 - (60.1 - 37.5) \left(\frac{1,500 - 0}{1,725 - 0} \right)^{4.07} = 47.3 \text{ mi/h}$$

Step 8: Compute the Mixed-Flow Density Under Mixed-Flow Conditions

The final step is to compute the mixed-flow density by using Equation 26-22.

$$D_{\text{mix}} = \frac{v_{\text{mix}}}{S_{\text{mix}}} = \frac{1,500}{47.3} = 31.7 \text{ veh/mi/ln}$$

Comparison with the PCE-Based Approach

For comparison purposes, the following procedure show the results for this case if the PCE-based approach explained in Chapter 12 is applied.

Step 1: Input Data

All input data are specified above.

Step 2: Estimate and Adjust FFS

For basic freeway segments, Equation 12-2 can be used to estimate FFS.

$$FFS = BFFS - f_{LW} - f_{RLC} - 3.22 \times TRD^{0.84}$$

For the purposes of comparing the two methods with respect to truck effects on FFS, the lane width, lateral clearance, and ramp density adjustment factors can be neglected. Then,

$$FFS = 65 - 0 - 0 - 3.22 \times 0^{0.84} = 65 \text{ mi/h}$$

The adjusted FFS is computed from Equation 12-5, assuming no weather or incident effects.

$$\begin{aligned} FFS_{\text{adj}} &= FFS \times SAF \\ FFS_{\text{adj}} &= 65 \times 1 = 65 \text{ mi/h} \end{aligned}$$

Step 3: Estimate and Adjust Capacity

Equation 12-6 is used to compute the capacity of a basic freeway segment.

$$\begin{aligned} c &= 2,200 + 10 \times (FFS_{\text{adj}} - 50) \\ c &= 2,200 + 10 \times (65 - 50) = 2,350 \text{ pc/h/ln} \end{aligned}$$

Assuming no adverse weather conditions or incidents, the adjusted capacity from Equation 12-8 is then

$$c_{\text{adj}} = c \times CAF = 2,350 \times 1 = 2,350 \text{ pc/h/ln}$$

Step 4: Adjust Demand Volume

This basic freeway segment is in a rural area with more TTs than SUTs. Therefore, the PCE table for 30% SUTs and 70% TTs (Exhibit 12-26) will be used. As stated in the Facts section of the example problem, the grade is 5% for 2 mi. There are no values specifically for a 5% grade in Exhibit 12-26; therefore, PCE values will be interpolated from the values for 4.5% and 5.5%. As the maximum grade length provided in the exhibit is 1 mi for these two grades, values for a 1-mi grade will also apply to longer grades. For a 1-mi, 4.5% grade, the PCE value for 15% trucks is 3.11; and the PCE value for a 1-mi, 5.5% grade with 15% trucks is 3.51. Interpolating between these two values for a 5% grade results in a PCE of 3.31.

The heavy-vehicle factor can be computed with Equation 12-10.

$$f_{HV} = \frac{1}{1 + P_T(E_T - 1)} = \frac{1}{1 + 0.15 \times (3.31 - 1)} = 0.743$$

Equation 12-9 is used to adjust the demand volume to account for truck presence. The freeway is a three-lane facility and the driver population is assumed to be all local drivers.

$$v_p = \frac{V}{PHF \times N \times f_{HV}} = \frac{1,500 \times 3}{1 \times 3 \times 0.743} = 2,019 \text{ pc/h/ln}$$

Step 5: Estimate Speed and Density

The speed can be read directly from Exhibit 12-7 for a demand flow rate of 2,019 pc/h/ln. Under base conditions, the mean speed of the traffic stream is 59.6 mi/h as calculated from Equation 26-1.

Equation 12-11 is used to compute density.

$$D = \frac{v_p}{S} = \frac{2,019}{59.6} = 33.9 \text{ pc/mi/ln}$$

If the density above is multiplied by the heavy-vehicle factor, then the mixed-flow density D_{mix} can be estimated as follows:

$$D_{mix} = D \times f_{HV} = 33.9 \times 0.743 = 25.2 \text{ veh/mi/ln}$$

The PCE-based density of 25.2 veh/mi/ln is about 22% lower than 32.6 veh/mi/ln, which is the density predicted in Step 8 of the mixed-flow model. D_{mix} is the mixed-flow density, not an auto-only flow density. As such, it cannot be used to derive LOS.

EXAMPLE PROBLEM 6: SEVERE WEATHER EFFECTS ON A BASIC FREEWAY SEGMENT**The Facts**

- Four-lane freeway (two lanes in each direction)
- Lane width = 11 ft
- Right-side lateral clearance = 2 ft
- Commuter traffic (regular users)
- Peak hour, peak direction demand volume = 2,000 veh/h
- Traffic composition: 5% trucks
- PHF = 0.92
- One cloverleaf interchange per mile
- Rolling terrain
- Facility operates under heavy snow conditions ($CAF = 0.78$; $SAF = 0.86$).

Comments

The task is to find the expected LOS for this freeway during the worst 15 min of the peak hour under heavy snow conditions. With one cloverleaf interchange per mile, the total ramp density will be 4 ramps/mi. This example problem is similar to Example Problem 1, with the only change being the presence of heavy snow.

Step 1: Input Data

All input data are specified above.

Step 2: Estimate and Adjust FFS

The FFS of the freeway is estimated from Equation 12-2 as follows:

$$FFS = 75.4 - f_{LW} - f_{RLC} - 3.22 \times TRD^{0.84}$$

The adjustment for lane width is selected from Exhibit 12-20 for 11-ft lanes (1.9 mi/h). The adjustment for right-side lateral clearance is selected from Exhibit 12-21 for a 2-ft clearance on a freeway with two lanes in one direction (2.4 mi/h). The total ramp density is 4 ramps/mi. Then

$$FFS = 75.4 - 1.9 - 2.4 - 3.22 \times 4^{0.84} = 60.8 \text{ mi/h}$$

A free-flow speed adjustment factor (SAF) for heavy snow conditions can be obtained from Exhibit 11-5 in Chapter 11, Freeway Reliability Analysis, by interpolating between the values for 60 and 65 mi/h (0.86 and 0.85, respectively), resulting in a SAF of 0.86. No other speed adjustments are made, as no incidents were specified in the problem statement and because the driver population was specified to be commuters. The SAF is applied through Equation 12-5.

$$FFS_{adj} = FFS \times SAF = 60.8 \times 0.86 = 52.3 \text{ mi/h}$$

Step 3: Estimate and Adjust Capacity

Exhibit 11-5 also provides a CAF of 0.78 for heavy snow conditions, applicable to all FFS values. As with the SAF in Step 2, no other capacity adjustments apply in this situation. The freeway’s capacity is then estimated using Equation 12-6.

$$c = CAF(2,200 + 10 \times [FFS_{adj} - 50])$$

$$c = 0.78 \times (2,200 + 10 \times [52.3 - 50]) = 1,734 \text{ pc/h/ln}$$

Step 4: Adjust Demand Volume

The demand volume is adjusted by using Equation 12-9 to a flow rate that reflects passenger cars per hour per lane under equivalent base conditions.

$$v_p = \frac{V}{PHF \times N \times f_{HV}}$$

The demand volume is given as 2,000 veh/h. The PHF is specified to be 0.92, and there are two lanes in each direction. Trucks make up 5% of the traffic stream, so a heavy-vehicle adjustment factor must be determined.

From Exhibit 12-25, the PCE for trucks is 3.0 for rolling terrain. The heavy-vehicle adjustment factor is then computed by using Equation 12-10.

$$f_{HV} = \frac{1}{1 + P_T(E_T - 1)} = \frac{1}{1 + 0.05(3 - 1)} = 0.909$$

then

$$v_p = \frac{2,000}{0.92 \times 2 \times 0.91} = 1,195 \text{ pc/h/ln}$$

Because this value is less than the base capacity of 1,743 pc/h/ln for a freeway with an FFS of 52.3 mi/h, LOS F conditions do not exist, and the analysis continues to Step 5.

Step 5: Estimate Speed and Density

The FFS of the basic freeway segment is now estimated along with the demand flow rate (in passenger cars per hour per lane) under equivalent base conditions. Using the equations provided in Exhibit 12-6, the breakpoint for a 53.5-mi/h FFS speed–flow curve is

$$BP_{adj} = [1,000 + 40 \times (75 - FFS_{adj})] \times (CAF)^2$$

$$BP_{adj} = [1,000 + 40 \times (75 - 52.3)] \times (0.78)^2 = 1,161 \text{ pc/h/ln}$$

Because the flow rate is greater than the breakpoint value, the operating speed of the segment is estimated from Equation 12-1, by using a value of 2 for the exponent calibration parameter *a* from Exhibit 12-6.

$$S = FFS_{adj} - \frac{(FFS_{adj} - \frac{c_{adj}}{D_c})(v_p - BP)^a}{(c_{adj} - BP)^a}$$

$$S = 52.3 - \frac{(52.3 - \frac{1,734}{45})(1,195 - 1,161)^2}{(1,734 - 1,161)^2} = 52.3 \text{ mi/h}$$

The density may now be computed from Equation 12-11.

$$D = \frac{v_p}{S} = \frac{1,195}{52.3} = 22.8 \text{ pc/mi/ln}$$

Step 6: Determine LOS

From Exhibit 12-15, a density of 22.8 pc/mi/ln corresponds to LOS C.

Discussion

This basic freeway segment of a four-lane freeway is expected to operate at LOS C during the worst 15 min of the peak hour under heavy snow conditions, with an average speed of 52.3 mi/h and a density of 22.8 pc/mi/ln. By contrast, the same facility under no adverse weather conditions would be expected to operate at an FFS of 60.8 mi/h and a density of 19.7 pc/mi/ln, but still at LOS C. Although the segment's performance is affected by the snow, the overall LOS is unchanged.

However, the segment's capacity is reduced from 2,308 to 1,734 pc/h/ln, which means the snow effect would be more severe at elevated volume-to-capacity ratios, particularly as the segment approached capacity. For elevated flow rates, the snow condition is expected to result in further deterioration of speed and breakdown at lower flow rates.

EXAMPLE PROBLEM 7: BASIC MANAGED LANE SEGMENT

The Facts

- Six-lane freeway with two general purpose lanes and one managed lane in each direction
- Lane width = 11 ft
- Right-side lateral clearance = 2 ft
- Commuter traffic (regular users)
- Peak hour, peak direction demand volume in the general purpose lanes = 2,000 veh/h (Case 1) or 3,800 veh/h (Case 2)
- Peak hour, peak direction demand volume in the managed lane (both cases) = 1,300 veh/h
- Continuous access separation between the managed and general purpose lanes
- FFS = 60 mi/h for both the managed and general purpose lanes
- Traffic composition: 7.5% trucks, using the default truck mix for both the managed and general purpose lanes
- PHF = 0.92
- One cloverleaf interchange per mile
- Level terrain
- Facility operates under ideal conditions (no incidents, work zones, or weather events).

Comments

The task is to find the expected LOS for this freeway for both the managed and general purpose lanes during the worst 15 min of the peak hour for the two described cases. With one cloverleaf interchange per mile, the total ramp density will be 4 ramps/mi.

Step 1: Input Data

All input data are specified above.

Step 2: Estimate and Adjust FFS

The facility’s FFS is given as 60 mi/h for both the managed and general purpose lanes. Because the facility is operating under ideal conditions, the SAF used in Equation 12-5 is 1.

Step 3: Estimate and Adjust Capacity

The capacity of the freeway general purpose lanes is estimated from Equation 12-6 as follows:

$$c = 2,200 + 10 \times (FFS_{adj} - 50)$$

$$c = 2,200 + 10 \times (60 - 50) = 2,300 \text{ pc/h/ln}$$

As the freeway is operating under ideal conditions, no capacity adjustment is made for the general purpose lanes (i.e., CAF = 1 in Equation 12-8).

The capacity of the managed lane is calculated with Equation 12-14.

$$c_{adj} = CAF \times (c_{75} - \lambda_c \times [75 - FFS_{adj}])$$

As with the general purpose lanes, CAF = 1 for the managed lane. The values of the parameters C_{75} and λ_c are obtained from Exhibit 12-30, and are 1,800 and 10, respectively, for continuous access separation. Then

$$c_{adj} = 1.00 \times (1,800 - 10 \times [75 - 60]) = 1,650 \text{ pc/h/ln}$$

Step 4: Adjust Demand Volume

The demand volume is adjusted by using Equation 12-9 to a flow rate that reflects passenger cars per hour per lane under equivalent base conditions.

$$v_p = \frac{V}{PHF \times N \times f_{HV}}$$

The demand volume is given as 2,000 veh/h and 3,800 veh/h for Cases 1 and 2, respectively. The PHF is specified to be 0.92, and there are two lanes in each direction. Trucks make up 5% of the traffic stream, so a heavy-vehicle adjustment factor must be determined.

From Exhibit 12-25, the PCE for trucks is 2.0 for level terrain. The heavy-vehicle adjustment factor is then computed using Equation 12-10.

$$f_{HV} = \frac{1}{1 + P_T(E_T - 1)} \frac{1}{1 + 0.075(2.0 - 1)} = 0.93$$

Then for Case 1,

$$v_{p,GP,Case1} = \frac{2,000}{0.92 \times 2 \times 0.93} = 1,169 \text{ pc/h/ln}$$

and for Case 2,

$$v_{p,GP,Case2} = \frac{3,800}{0.92 \times 2 \times 0.93} = 2,221 \text{ pc/h/ln}$$

The flow rate on the managed lane is

$$v_{p,ML} = \frac{1,300}{0.92 \times 1 \times 0.93} = 1,519 \text{ pc/h/ln}$$

Because all the flow rates are less than their corresponding capacities, LOS F conditions do not exist, and the analysis continues to Step 5.

Step 5: Estimate Speed and Density

The FFS of the basic freeway segment is now estimated, along with the demand flow rate (in passenger cars per hour per lane) under equivalent base conditions. Based on the equations provided in Exhibit 12-6, the breakpoint for a 60-mi/h FFS speed-flow curve is

$$BP_{adj} = [1,000 + 40 \times (75 - FFS_{adj})] \times (CAF)^2$$

$$BP_{adj} = [1,000 + 40 \times (75 - 60)] \times (1.00)^2 = 1,600 \text{ pc/h/ln}$$

In Case 1, the flow rate is less than the breakpoint value of 1,600 pc/h/ln. As this flow rate is in the constant-speed portion of the curve, $S_{GP,Case1} = 60$ mi/h. The density of the traffic stream is computed from Equation 12-11.

$$D_{GP,Case1} = \frac{v_p}{S} = \frac{1,169}{60} = 19.5 \text{ pc/mi/ln}$$

In Case 2, the flow rate is higher than the breakpoint. Therefore, the speed is computed with Equation 12-1, by using a value of 2 for the exponent calibration parameter a from Exhibit 12-6, as follows:

$$S = FFS_{adj} - \frac{(FFS_{adj} - \frac{c_{adj}}{D_c})(v_p - BP)^a}{(c_{adj} - BP)^a}$$

$$S_{GP,Case2} = 60 - \frac{(60 - \frac{2,300}{45})(2,221 - 1,600)^2}{(2,300 - 1,600)^2} = 53.0 \text{ mi/h}$$

Density is computed with Equation 12-11.

$$D_{GP,Case2} = \frac{v_p}{S} = \frac{2,221}{53} = 41.9 \text{ pc/mi/ln}$$

To compute the managed lane speed, the breakpoint first needs to be computed by using Equation 12-13 and values for the parameters BP_{75} and λ_{BP} from Exhibit 12-30.

$$BP_{ML} = [BP_{75} + \lambda_{BP} \times (75 - FFS_{adj})] \times CAF^2$$

$$BP_{ML} = [500 + 0 \times (75 - 60)] \times (1.00)^2 = 500 \text{ pc/h/ln}$$

Because the managed lane flow rate is higher than the breakpoint, three speeds, S_1 , S_2 , and S_3 , need to be computed by using Equations 12-15, 12-17, and 12-19, respectively (with parameters from Exhibit 12-30), as follows:

$$S_1 = FFS_{adj} - A_1 \times \min(v_p, BP) = 60 - 0 \times \min(1,519, 500) = 60 \text{ mi/h}$$

$$S_2 = \frac{\left(S_{1,BP} - \frac{c_{adj}}{K_c^{n_f}}\right)}{(c_{adj} - BP)^{A_2}} (v_p - BP)^{A_2}$$

$$S_2 = \frac{\left(60 - \frac{1,650}{30}\right)}{(1,650 - 500)^{2.5}} (1,519 - 500)^{2.5} = 3.7 \text{ mi/h}$$

$$S_3 = \frac{\left(\frac{c_{adj}}{K_c^{n_f}}\right) - \left(\frac{c_{adj}}{K_c^f}\right)}{(c_{adj} - BP)^2} (v_p - BP)^2$$

$$S_3 = \frac{\left(\frac{1,650}{30}\right) - \left(\frac{1,650}{45}\right)}{(1,650 - 500)^2} (1,519 - 500)^2 = 14.4 \text{ mi/h}$$

The space mean speed of the managed lane is given by Equation 12-12.

$$S_{ML} = \begin{cases} S_1 & v_p \leq BP \\ S_1 - S_2 - I_c \times S_3 & BP < v_p \leq c \end{cases}$$

Because the managed lane's demand flow of 1,519 pc/h/ln is greater than the breakpoint value of 500 pc/h/ln calculated in Step 4, the second of the two equations applies. To apply this equation, the value of the indicator variable I_c must first be determined from Equation 12-18.

$$I_c = \begin{cases} 0 & K_{GP} \leq 35 \text{ pc/mi/ln} \\ & \text{or segment type is Buffer 2, Barrier 1, or Barrier 2} \\ 1 & \text{otherwise} \end{cases}$$

In Case 1, the density of the adjacent general purpose lane is less than 35 pc/mi/ln, as determined in Step 5. As a result, the indicator variable I_c will have a value of zero. Thus, the managed lane speed in Case 1 will be

$$S_{ML,Case1} = 60 - 3.7 - (0 \times 14.4) = 56.3 \text{ mi/h}$$

In Case 2, the density of the adjacent general purpose lane is greater than 35 pc/ln/mi, and therefore the indicator variable I_c will have a value of 1. The managed lane speed in Case 2 will be

$$S_{ML,Case2} = 60 - 3.7 - (1 \times 14.4) = 41.9 \text{ mi/h}$$

The managed lane density for the two cases is given by Equation 12-11.

$$D_{ML,Case1} = \frac{v_p}{S} = \frac{1,519}{56.3} = 27.0 \text{ pc/mi/ln}$$

$$D_{ML,Case2} = \frac{v_p}{S} = \frac{1,519}{41.9} = 36.3 \text{ pc/mi/ln}$$

Step 6: Determine LOS

The managed lane facility's density of 27.0 pc/mi/ln under Case 1 corresponds to LOS D, but it is close to the LOS C boundary, which has a maximum value of 26 pc/mi/ln. In Case 2, the density of 36.3 pc/mi/ln corresponds to LOS E.

Discussion

In this example, the managed lane's operating speed and density have been investigated for two operating conditions in the general purpose lanes. When high-density conditions exist in the general purpose lanes, the managed lane's operational speed is reduced and, as a consequence, the managed lane operates at a worse LOS than when lower-density conditions exist in the general purpose lanes.

7. TWO-LANE HIGHWAY EXAMPLE PROBLEMS

Exhibit 26-17 lists the five example problems provided in this section. The problems demonstrate the computational steps involved in applying the two-lane highway automobile and bicycle methodologies.

Exhibit 26-17
List of Two-Lane Highway
Example Problems

Problem Number	Description	Type of Analysis
1	Class I highway LOS	Operational analysis
2	Class II highway LOS	Operational analysis
3	Class III highway LOS	Operational analysis
4	LOS for a Class I highway with a passing lane	Operational analysis
5	Two-lane highway bicycle LOS	Planning analysis

The truck analysis methodology for two-lane highways is different from that for basic freeway segments and multilane highways. The methodology for two-lane highways is described in Chapter 15. Among other things, it distinguishes between trucks and recreational vehicles (RVs).

EXAMPLE PROBLEM 1: CLASS I HIGHWAY LOS

The Facts

A segment of Class I two-lane highway has the following known characteristics:

- Demand volume = 1,600 veh/h (total in both directions);
- Directional split (during analysis period) = 50/50;
- PHF = 0.95;
- 50% no-passing zones in the analysis segment (both directions);
- Rolling terrain;
- 14% trucks, 4% RVs;
- 11-ft lane widths;
- 4-ft usable shoulders;
- 20 access points/mi;
- 60-mi/h base FFS; and
- 10-mi segment length.

Find the expected LOS in each direction on the two-lane highway segment as described.

Comments

The problem statement calls for finding the LOS in each direction on a segment in rolling terrain. Because the directional split is 50/50, the solution in one direction will be the same as the solution in the other direction, so only one operational analysis needs to be conducted. The result will apply equally to each direction.

Because this is a Class I highway, both average travel speed (ATS) and percent time spent following (PTSF) must be estimated to determine the expected LOS.

Step 1: Input Data

All input data are specified above.

Step 2: Estimate the FFS

FFS is estimated with Equation 15-2 and adjustment factors found in Exhibit 15-7 (for lane and shoulder width) and Exhibit 15-8 (for access points in both directions). For 11-ft lane widths and 4-ft usable shoulders, the adjustment factor f_{LS} for these features is 1.7 mi/h; for 20 access points/mi, the adjustment factor f_A is 5.0 mi/h. Then

$$\begin{aligned} FFS &= BFFS - f_{LS} - f_A \\ FFS &= 60.0 - 1.7 - 5.0 = 53.3 \text{ mi/h} \end{aligned}$$

Step 3: Demand Adjustment for ATS

The demand volume must be adjusted to a flow rate (in passenger cars per hour) under equivalent base conditions. This adjustment is accomplished with Equation 15-3.

$$v_{i,ATS} = \frac{V_i}{PHF \times f_{g,ATS} \times f_{HV,ATS}}$$

Because the demand split is 50/50, both the analysis direction and opposing demand volumes are $1,600/2 = 800$ veh/h.

The grade adjustment factor $f_{g,ATS}$ is selected from Exhibit 15-9 for rolling terrain. The table is entered with a demand flow rate v_{vph} in vehicles per hour, or $800/0.95 = 842$ veh/h. By interpolation in Exhibit 15-9 between 800 and 900 veh/h, the factor is 0.99 to the nearest 0.01.

The PCE for trucks and RVs is obtained from Exhibit 15-11 for a demand flow rate of 842 veh/h. Again, by interpolation between 800 and 900 veh/h, the values obtained are $E_T = 1.4$ and $E_R = 1.1$. The heavy-vehicle adjustment is then computed with Equation 15-4.

$$\begin{aligned} f_{HV,ATS} &= \frac{1}{1 + P_T(E_T - 1) + P_R(E_R - 1)} \\ f_{HV,ATS} &= \frac{1}{1 + 0.14(1.4 - 1) + 0.04(1.1 - 1)} \\ f_{HV,ATS} &= 0.943 \end{aligned}$$

then

$$v_{d,ATS} = v_{o,ATS} = \frac{800}{0.95 \times 0.99 \times 0.943} = 902 \text{ pc/h}$$

Step 4: Estimate ATS

ATS is estimated with Equation 15-6. The adjustment factor $f_{np,ATS}$ is found in Exhibit 15-15 for an FFS of 53.3 mi/h, 50% no-passing zones, and an opposing demand flow of 902 veh/h. This selection must use interpolation on all three scales. Note that interpolation is only to the nearest 0.1 for this adjustment factor. Exhibit 26-18 illustrates the interpolation.

Exhibit 26-18

Example Problem 1:
Interpolation for ATS
Adjustment Factor

v_o (veh/h)	Factor for FFS = 55 mi/h			Factor for FFS = 50 mi/h		
	40% NPZ	50% NPZ	60% NPZ	40% NPZ	50% NPZ	60% NPZ
800	0.7	0.9	1.1	0.6	0.75	0.9
902		0.8			0.65	
1,000	0.6	0.7	0.8	0.4	0.55	0.7

Notes: $f_{np,ATS} = 0.65 + (0.8 - 0.65)(3.3/5.0) = 0.749 = \mathbf{0.7}$.
NPZ = no-passing zones.

Equation 15-6 gives the following:

$$ATS = FFS - 0.00776(v_{d,ATS} + v_{o,ATS}) - f_{np,ATS}$$

$$ATS = 53.3 - 0.00776(902 + 902) - 0.7$$

$$ATS = 53.3 - 14.0 - 0.7 = 38.6 \text{ mi/h}$$

Step 5: Demand Adjustment for PTSF

The adjusted demand used to estimate PTSF is found with Equation 15-7 and Equation 15-8. The grade adjustment factor is taken from Exhibit 15-16 for rolling terrain and a demand flow rate of $800/0.95 = 842$ pc/h. PCEs for trucks and RVs are taken from Exhibit 15-18. In both exhibits, the demand flow rate of 842 pc/h is interpolated between 800 pc/h and 900 pc/h to obtain the correct values. The following values are obtained:

$$f_{g,PTSF} = 1.00$$

$$E_T = 1.0$$

$$E_R = 1.0$$

Equation 15-8 gives the following:

$$f_{HV,PTSF} = \frac{1}{1 + P_T(E_T - 1) + P_R(E_R - 1)}$$

$$f_{HV,PTSF} = \frac{1}{1 + 0.14(1.0 - 1) + 0.04(1.0 - 1)}$$

$$f_{HV,PTSF} = 1.00$$

and Equation 15-7 gives

$$v_{i,PTSF} = \frac{V_i}{PHF \times f_{g,PTSF} \times f_{HV,PTSF}}$$

$$v_{i,PTSF} = \frac{800}{0.95 \times 1.00 \times 1.00}$$

$$v_{i,PTSF} = 842 \text{ pc/h}$$

Step 6: Estimate PTSF

PTSF is estimated with Equation 15-9 and Equation 15-10. Exhibit 15-20 is used to obtain exponents a and b for Equation 15-10, and Exhibit 15-21 is used to obtain the no-passing-zone adjustment for Equation 15-9. All three values require interpolation.

Exponents a and b are based on the opposing flow rate of 842 pc/h, which is interpolated between tabulated values of 800 and 1,000 pc/h. These values are illustrated in Exhibit 26-19.

Opposing Flow Rate (pc/h)	<i>a</i>	<i>b</i>
800	-0.0045	0.833
842	-0.0046	0.832
1,000	-0.0049	0.829

Equation 15-10 gives

$$BPTSF = 100[1 - \exp(av_d^b)]$$

$$BPTSF = 100[1 - \exp(0.0046 \times 842^{0.832})]$$

$$BPTSF = 71.3\%$$

The adjustment factor for no-passing zones must also be interpolated in two variables. Exhibit 15-21 is entered with 50% no-passing zones, a 50/50 directional split of traffic, and a total two-way demand flow rate of 842 + 842 = 1,684 pc/h. The interpolation is illustrated in Exhibit 26-20.

Total Flow Rate (pc/h)	Adjustment Factor for 40% NPZ	Adjustment Factor for 50% NPZ	Adjustment Factor for 60% NPZ
1,400	23.8	25.0	26.2
1,684		16.6 + (25.0 - 16.6) (316/600) = 21.0	
2,000	15.8	16.6	17.4

Note: NPZ = no-passing zone.

Equation 15-9 gives

$$PTSF = BPTSF + f_{np,PTSF} \left(\frac{v_{d,PTSF}}{v_{d,PTSF} + v_{o,PTSF}} \right)$$

$$PTSF = 71.3 + 21.0 \left(\frac{842}{842 + 842} \right)$$

$$PTSF = 81.8\%$$

Step 7: Estimate PFFS

This step, which estimates percent of FFS (PFFS), is only used for Class III highways.

Step 8: Determine LOS and Capacity

LOS is determined by comparing the estimated values of ATS and PTSF with the criteria of Exhibit 15-3. An ATS of 38.6 mi/h suggests LOS E will exist, and a PTSF of 81.8% also suggests LOS E will exist. Thus, both criteria lead to the conclusion that the segment will operate at LOS E.

Capacity is determined by either Equation 15-12 or Equation 15-13, whichever produces the lower estimate. Note, however, that all adjustment factors for use in these equations are based on a directional flow rate greater than 900 pc/h. Thus, the grade factor will be 1.00 for both ATS and PTSF. The PCE for trucks is 1.3 for ATS and 1.00 for PTSF; the PCE for RVs is 1.1 for ATS and 1.00 for PTSF.

The adjustment factors for heavy vehicles are as follows:

$$f_{HV,ATS} = \frac{1}{1 + 0.14(1.3 - 1) + 0.04(1.1 - 1)} = 0.96$$

$$f_{HV,PTSF} = \frac{1}{1 + 0.14(1.0 - 1) + 0.04(1.0 - 1)} = 1.00$$

Exhibit 26-19
Example Problem 1:
Interpolation for Exponents *a*
and *b* for Equation 15-10

Exhibit 26-20
Example Problem 1:
Interpolation for $f_{np,PTSF}$ for
Equation 15-9

and

$$c_{d,ATS} = 1,700f_{g,ATS}f_{HV,ATS} = 1,700 \times 1.00 \times 0.960 = 1,632 \text{ veh/h}$$

$$c_{d,PTSF} = 1,700f_{g,PTSF}f_{HV,PTSF} = 1,700 \times 1.00 \times 1.00 = 1,700 \text{ veh/h}$$

Obviously, the first value holds, and the directional capacity of this facility is 1,632 veh/h. Given the 50/50 directional distribution, the two-way capacity of the segment is $1,632 + 1,632 = 3,264$ veh/h. Because this capacity exceeds the limiting capacity of 3,200 pc/h, the directional capacity cannot be achieved with a 50/50 directional distribution. A total two-way capacity of 3,200 pc/h would prevail. In terms of prevailing conditions, the capacity would be $3,200 \times 1.00 \times 0.960 = 3,072$ veh/h. With a 50/50 directional split, this value implies a directional capacity of $3,072/2 = 1,536$ veh/h.

Discussion

The two-lane highway segment as described is expected to operate poorly, within LOS E. Although demand is only $842/1,536 = 0.55$ of capacity, the operation is poor. Both ATS and PTSF are at unacceptable levels (38.6 mi/h and 81.8%, respectively). This solution again highlights the characteristic of two-lane highways of having poor operations at relatively low volume-to-capacity ratios. This segment should clearly be examined for potential improvements.

Given the 50/50 directional split of traffic, results for the second direction would be identical.

EXAMPLE PROBLEM 2: CLASS II HIGHWAY LOS

The Facts

A segment of Class II highway is part of a scenic and recreational route and has the following known characteristics:

- 1,050 veh/h (both directions);
- 70/30 directional split;
- 5% trucks, 7% RVs;
- PHF = 0.85;
- 10-ft lanes and 2-ft shoulders;
- Base FFS = 55.0 mi/h;
- Rolling terrain;
- 10 access points/mi; and
- 60% no-passing zones.

Comments

Computational Steps 3 and 4, which relate to the estimation of average highway speed, will not be included. LOS for Class II highways depends solely on PTSF. The analysis will be conducted for both the 70% direction of flow and the 30% direction of flow. The necessary computations are accomplished by merely reversing the analysis direction and opposing flows.

Step 1: Input Data

All input data are summarized above.

Step 2: Estimate the FFS

FFS is estimated with Equation 15-2. Adjustment factors for lane and shoulder width (Exhibit 15-7) and access points per mile (Exhibit 15-8) are used.

Exhibit 15-7 is entered with 10-ft lanes and 2-ft shoulders. The resulting adjustment is 3.7 mi/h. Exhibit 15-8 is entered with 10 access points/mi. The resulting adjustment is 2.5 mi/h. FFS is then estimated as follows:

$$FFS = 55.0 - 3.7 - 2.5 = 48.8 \text{ mi/h}$$

Steps 3 and 4: Demand Adjustment for ATS and Estimate ATS

Steps 3 and 4 are not required for Class II highways.

Step 5: Demand Adjustment for PTSF

Equation 15-7 and Equation 15-8 are used to adjust analysis direction and opposing demands to flow rates under equivalent base conditions. With a 70/30 split of traffic, the two demands are as follows:

$$V_{70\%} = V_1 = 1,050 \times 0.70 = 735 \text{ veh/h}$$

$$V_{30\%} = V_2 = 1,050 \times 0.30 = 315 \text{ veh/h}$$

In this solution, directions will be referred to as 1 and 2. Because both directions are to be analyzed, their position as “analysis direction” and “opposing” will depend on which direction is under study.

Adjustment factors both for grades and for heavy vehicles are needed. Exhibit 15-16 (for grades) and Exhibit 15-18 (for heavy vehicles) are entered with a directional flow rate of $735/0.85 = 865 \text{ veh/h}$ (Direction 1) and $315/0.85 = 371 \text{ veh/h}$ (Direction 2). Interpolation is required in both cases. The following values are obtained:

$$f_{g,PTSF} = 1.00 \text{ (Direction 1), } 0.89 \text{ (Direction 2)}$$

$$E_T = 1.0 \text{ (Direction 1), } 1.6 \text{ (Direction 2)}$$

$$E_R = 1.0 \text{ (Direction 1), } 1.0 \text{ (Direction 2)}$$

The heavy-vehicle adjustment factor for both directions is computed with Equation 15-8.

$$f_{HV,PTSF,1} = \frac{1}{1 + 0.05(1.0 - 1) + 0.07(1.0 - 1)} = 1.00$$

$$f_{HV,PTSF,2} = \frac{1}{1 + 0.05(1.6 - 1) + 0.07(1.0 - 1)} = 0.97$$

The adjusted demand flow rates are computed with Equation 15-7.

$$v_{1,PTSF} = \frac{735}{0.85 \times 1.00 \times 1.00} = 865 \text{ pc/h}$$

$$v_{2,PTSF} = \frac{315}{0.85 \times 0.89 \times 0.97} = 429 \text{ pc/h}$$

Step 6: Estimate PTSF

PTSF is estimated with Equation 15-9 and Equation 15-10 with values a and b taken from Exhibit 15-20 and $f_{np,PTSF}$ taken from Exhibit 15-21.

Exhibit 15-20 is entered with opposing flow rates of 429 pc/h (for Direction 1) and 865 pc/h (for Direction 2). Both values must be interpolated. The resulting values are as follows:

$$\text{Direction 1: } a = -0.0024, b = 0.915$$

$$\text{Direction 2: } a = -0.0046, b = 0.832$$

Exhibit 15-21 is entered with the total demand flow rate of $865 + 429 = 1,294$ pc/h, a directional split of 70/30, and 60% no-passing zones. Interpolation is required. The factor is the same for both Directions 1 and 2.

$$f_{np,PTSF} = 23.0\%$$

The base PTSF is computed with Equation 15-10.

$$BPTSF_1 = 100[1 - \exp(-0.0024 \times 865^{0.915})] = 68.9\%$$

$$BPTSF_2 = 100[1 - \exp(-0.0046 \times 429^{0.832})] = 51.0\%$$

PTSF for each direction is computed with Equation 15-9.

$$PTSF_1 = 68.9 + 23.0 \left(\frac{865}{865 + 429} \right) = 84.3\%$$

$$PTSF_2 = 51.0 + 23.0 \left(\frac{429}{429 + 865} \right) = 58.6\%$$

Step 7: Estimate PFFS

Step 7 is only used for Class III highways.

Step 8: Determine LOS and Capacity

LOS is determined by comparing the PTSF values obtained with the criteria of Exhibit 15-3. Applying these criteria reveals that Direction 1 operates at LOS D and Direction 2 operates at LOS C.

By using the adjustment selected for ≥ 900 veh/h, capacity is computed with Equation 15-13.

$$c_{1,PTSF} = 1,700 \times 1.00 \times 1.00 = 1,700 \text{ veh/h}$$

$$c_{2,PTSF} = 1,700 \times 1.00 \times 1.00 = 1,700 \text{ veh/h}$$

Discussion

The LOS based solely on PTSF is, at best, somewhat marginal on this two-lane highway segment.

The value of capacity must be carefully considered. If the directional capacities were expanded to two-way capacities on the basis of the given demand split, the capacity in the 30% direction would imply a two-way capacity well in excess of the 3,200-pc/h limitation for both directions. Therefore, even though a capacity of 1,700 veh/h is possible in the 30% direction, it could not occur with a 70/30 demand split. In this case, the two-way capacity would be limited by the capacity in the 70% direction and would be $1,700/0.70 = 2,429$ veh/h. The practical capacity for

the 30% direction of flow is actually best estimated as 2,429 – 1,700 or 729 veh/h. Given that the 70/30 directional split holds, when the 30% direction reaches a demand flow rate of 729 veh/h, the opposing direction (the 70% side) would be at its capacity.

EXAMPLE PROBLEM 3: CLASS III HIGHWAY LOS

The Facts

A Class III two-lane highway runs through a rural community in level terrain. It has the following known characteristics:

- Demand volume = 900 veh/h (both directions);
- 10% trucks, no RVs;
- Measured FFS = 40 mi/h;
- 12-ft lanes, 6-ft shoulders;
- PHF = 0.88;
- 80% no-passing zones;
- 60/40 directional split;
- 40 access points/mi; and
- Level terrain.

Comments

Because this is a Class III highway, LOS will be based on PFFS. Thus, Steps 5 and 6, which relate to the estimation of PTSF, will not be used.

Step 1: Input Data

All input data are specified above.

Step 2: Estimate FFS

A measured FFS of 40 mi/h is specified.

Step 3: Demand Adjustment for ATS

The total demand volume of 900 veh/h must be separated into two directional flows. Because both directions will be evaluated, directions are labeled 1 and 2.

$$V_1 = 900 \times 0.60 = 540 \text{ veh/h}$$

$$V_2 = 900 \times 0.40 = 360 \text{ veh/h}$$

The adjusted demand flow rate (in passenger cars per hour) under equivalent base conditions is estimated with Equation 15-3. A grade adjustment factor is selected from Exhibit 15-9, and PCEs for trucks are selected from Exhibit 15-11. Both exhibits are entered with a demand flow rate in vehicles per hour.

$$v_1 = 540/0.88 = 614 \text{ veh/h}$$

$$v_2 = 360/0.88 = 409 \text{ veh/h}$$

The following values are selected from Exhibit 15-9 and Exhibit 15-11. In all cases, interpolation is required.

Value	Direction 1	Direction 2
$f_{g,ATS}$	1.00	1.00
E_T	1.1	1.3

Equation 15-4 gives

$$f_{HV,ATS,1} = \frac{1}{1 + 0.10(1.1 - 1)} = 0.99$$

$$f_{HV,ATS,2} = \frac{1}{1 + 0.10(1.3 - 1)} = 0.97$$

and use of Equation 15-3 gives

$$v_{1,ATS} = \frac{540}{0.88 \times 1.00 \times 0.97} = 620 \text{ pc/h}$$

$$v_{2,ATS} = \frac{360}{0.88 \times 1.00 \times 0.97} = 422 \text{ pc/h}$$

Step 4: Estimate ATS

ATS is estimated with Equation 15-6 with an adjustment factor for no-passing zones taken from Exhibit 15-15. The adjustment factor is based on a 40-mi/h FFS and 80% no-passing zones. Interpolating for an opposing demand flow rate of 422 pc/h (Direction 1) and 620 pc/h (Direction 2) gives the following:

$$f_{np,ATS,1} = 2.4 \text{ mi/h}$$

$$f_{np,ATS,2} = 1.6 \text{ mi/h}$$

Then, use of Equation 15-6 gives

$$ATS_1 = 40.0 - 0.00776(620 + 422) - 2.4 = 29.5 \text{ mi/h}$$

$$ATS_2 = 40.0 - 0.00776(422 + 620) - 1.6 = 30.3 \text{ mi/h}$$

Steps 5 and 6: Demand Adjustment for PTSF and Estimate PTSF

Steps 5 and 6 are not used for Class III highways.

Step 7: Estimate PFFS

The LOS for Class III facilities is based on PFFS achieved, or ATS/FFS. For this segment PFFS is as follows:

$$PFFS_1 = 29.5/40.0 = 73.8\%$$

$$PFFS_2 = 30.3/40.0 = 75.8\%$$

Step 8: Determine LOS and Capacity

From Exhibit 15-3, the LOS for Direction 1 is D, and the LOS for Direction 2 is C. The two values of PFFS are close, but the boundary condition between LOS C and D is 0.75. To be LOS C, PFFS must exceed 0.75, and it is just below the threshold in Direction 1 and just above the threshold in Direction 2.

Capacity is evaluated with adjustment factors for ≥ 900 pc/h in level terrain. This makes all adjustment factors 1.00 (for ATS). Thus, the capacity in either direction is as follows:

$$c_{1,ATS} = c_{2,ATS} = 1,700 \times 1.00 \times 1.00 = 1,700 \text{ veh/h}$$

The two-way capacity values implied are $1,700/0.60 = 2,833$ veh/h (Direction 1) and $1,700/0.40 = 4,250$ veh/h (Direction 2). Obviously, the implied two-way capacity is the 2,833 veh/h, which suggests the directional capacity in Direction 2 cannot be achieved with a 60/40 demand split. Rather, the directional capacity in Direction 2 occurs when the capacity in Direction 1 occurs, or $2,833 \times 0.40 = 1,133$ veh/h.

Discussion

This segment of a Class III two-lane highway operates just at the LOS C–D boundary. Depending on the length of the segment and local expectations, this LOS may or may not be acceptable.

EXAMPLE PROBLEM 4: LOS FOR A CLASS I HIGHWAY WITH A PASSING LANE

The Facts

The 10-mi segment of the two-lane highway analyzed in Example Problem 1 will be improved with 2-mi passing lanes (one in each direction), both installed at 1.00 mi from the segment's beginning. The segment without a passing lane has already been analyzed; the results of that analysis are listed below:

- Demand volume = 800 veh/h in each direction;
- Demand flow rate (ATS) = 902 pc/h in each direction;
- Demand flow rate (PTSF) = 842 pc/h in each direction;
- FFS = 53.3 mi/h;
- ATS = 38.6 mi/h;
- PTSF = 81.8%;
- Rolling terrain; and
- PHF = 0.95.

Comments

Because the directional distribution is 50/50, both directions will involve the same computations, and in both cases the passing lane will start 1.00 mi after the beginning of the 10-mi segment and will end 3.00 mi after the beginning of the segment.

Step 1: Conduct an Analysis Without the Passing Lane

Completed as Example Problem 1.

Step 2: Divide the Segment into Regions

Exhibit 26-21 shows the division of the 6-mi segment into regions. The effective downstream length of the passing lane is selected from Exhibit 15-23

Exhibit 26-21
Example Problem 4: Region Lengths

(value is different for ATS and PTSF) for a demand flow rate of $800/0.95 = 842$ veh/h.

To Determine	L_u (mi)	L_{pl} (mi)	L_{de} (mi) Exhibit 15-23	L_d (mi) Equation 15-19
ATS	1.00	2.00	1.7	5.3
PTSF	1.00	2.00	4.7	2.3

Step 3: Determine the PTSF

PTSF, as affected by the presence of a passing lane, is estimated with Equation 15-20 and an adjustment factor selected from Exhibit 15-26. The adjustment factor $f_{pl,PTSF}$ is 0.62. Then

$$PTSF_{pl} = \frac{PTSF_d \left[L_u + L_d + f_{pl,PTSF} L_{pl} + \left(\frac{1 + f_{pl,PTSF}}{2} \right) L_{de} \right]}{L_t}$$

$$PTSF_{pl} = \frac{81.8 \left[1.0 + 2.3 + (0.62 \times 2.00) + \left(\frac{1 + 0.62}{2} \right) 4.7 \right]}{10}$$

$$PTSF_{pl} = 68.3\%$$

Step 4: Determine the ATS

ATS as affected by the presence of a passing lane is found with Equation 15-22 and an adjustment factor selected from Exhibit 15-28. The adjustment factor selected is 1.11. Then

$$ATS_{pl} = \frac{ATS_d L_t}{L_u + L_d + \left(\frac{L_{pl}}{f_{pl,ATS}} \right) + \left(\frac{2L_{de}}{1 + f_{pl,ATS}} \right)}$$

$$ATS_{pl} = \frac{38.6 \times 10}{1.00 + 5.3 + \left(\frac{2.00}{1.11} \right) + \left(\frac{2 \times 11.7}{1 + 1.11} \right)}$$

$$ATS_{pl} = 39.7 \text{ mi/h}$$

Step 5: Determine the LOS

Exhibit 15-3 shows that the LOS, as determined by PTSF, has improved to D. The LOS determined by ATS remains E. Thus, although PTSF has improved significantly, the ATS has not improved enough to improve the overall LOS, which remains E.

Discussion

Adding a 2-mi passing lane to a 10-mi segment of Class I highway operating at LOS E was insufficient to improve the overall LOS, although the PTSF did improve from 81.8% to 68.3%. It is likely that a longer (or a second) passing lane would be needed to improve the ATS sufficiently to result in LOS C or LOS D.

EXAMPLE PROBLEM 5: TWO-LANE HIGHWAY BICYCLE LOS

A segment of two-lane highway (without passing lanes) is being evaluated for potential widening, realigning, and repaving. Analyze the impacts of the proposed project on the bicycle LOS (BLOS) in the peak direction.

The Facts

The roadway currently has the following characteristics:

- Lane width = 12 ft,
- Shoulder width = 2 ft,
- Pavement rating = 3 (fair),
- Posted speed limit = 50 mi/h,
- Hourly directional volume = 500 veh/h (no growth is expected),
- Percentage of heavy vehicles = 5%,
- PHF = 0.90, and
- No on-highway parking.

The proposed roadway design has the following characteristics:

- Lane width = 12 ft,
- Shoulder width = 6 ft,
- Pavement rating = 5 (very good),
- Posted speed limit = 55 mi/h, and
- No on-highway parking.

Step 1: Gather Input Data

All data needed to perform the analysis are listed above.

Step 2: Calculate the Directional Flow Rate in the Outside Lane

Using the hourly directional volume and the PHF, calculate the directional demand flow rate with Equation 15-24. Because this is a two-lane highway segment without a passing lane, the number of directional lanes N is 1. Because traffic volumes are not expected to grow over the period of the analysis, v_{OL} is the same for both current and future conditions.

$$v_{OL} = \frac{V}{PHF \times N} = \frac{500}{0.90 \times 1} = 556 \text{ veh/h}$$

Step 3: Calculate the Effective Width

For current conditions, the hourly directional demand V is greater than 160 veh/h and the paved shoulder width is 2 ft; therefore, Equation 15-27 and Equation 15-28 are used to determine the effective width of the outside lane. Under future conditions, the paved shoulder width will increase to 6 ft; therefore, Equation 15-26 and Equation 15-28 are used.

For current conditions,

$$W_v = W_{OL} + W_s = 12 + 2 = 14 \text{ ft}$$

$$W_e = W_v + (\%OHP[2 ft + W_s]) = 14 + (0 \times [2 + 2]) = 14 \text{ ft}$$

Under the proposed design,

$$W_v = W_{OL} + W_s = 12 + 6 = 18 \text{ ft}$$

$$W_e = W_v + W_s - 2 \times (\%OHP[2 ft + W_s]) = 18 + 6 - 2 \times (0 \times [2 + 6]) = 24 \text{ ft}$$

Step 4: Calculate the Effective Speed Factor

Equation 15-30 is used to calculate the effective speed factor. Under current conditions,

$$S_t = 1.1199 \ln(S_p - 20) + 0.8103 = 1.1199 \ln(50 - 20) + 0.8103 = 4.62$$

Under the proposed design,

$$S_t = 1.1199 \ln(55 - 20) + 0.8103 = 4.79$$

Step 5: Determine the LOS

Equation 15-31 is used to calculate the BLOS score, which is then used in Exhibit 15-4 to determine the LOS. Under existing conditions,

$$BLOS = 0.507 \ln(v_{OL}) + 0.1999 S_t (1 + 10.38 HV)^2 + 7.066 (1/P)^2 - 0.005 (W_e)^2 + 0.760$$

$$BLOS = 0.507 \ln(556) + 0.1999 (4.62) (1 + 10.38 \times 0.05)^2 + 7.066 (1/3)^2 - 0.005 (14)^2 + 0.760$$

$$BLOS = 3.205 + 2.131 + 0.785 - 0.980 + 0.760 = 5.90$$

Therefore, the BLOS for existing conditions is LOS F. Use of the same process for the proposed design results in the following:

$$BLOS = 0.507 \ln(556) + 0.1999 (4.79) (1 + 10.38 \times 0.05)^2 + 7.066 (1/5)^2 - 0.005 (24)^2 + 0.760$$

$$BLOS = 3.205 + 2.209 + 0.283 - 2.880 + 0.760 = 3.58$$

The corresponding LOS for the proposed design is LOS D, close to the boundary of LOS C ($BLOS = 3.50$).

Discussion

Although the posted speed would increase as a result of the proposed design, this negative impact on bicyclists would be more than offset by the proposed shoulder widening, as indicated by the improvement from LOS F to LOS D.

8. REFERENCES

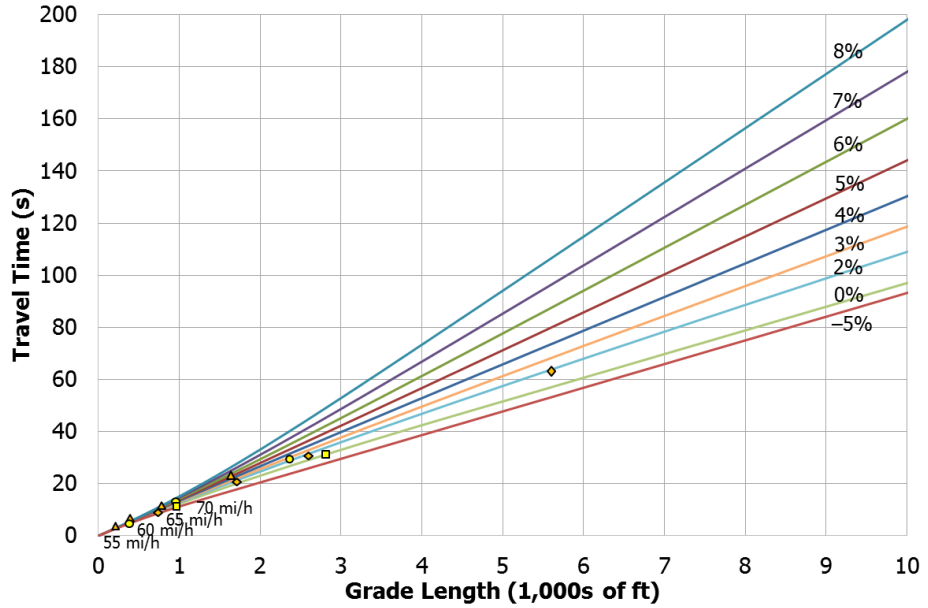
1. Zegeer, J. D., M. A. Vandehey, M. Blogg, K. Nguyen, and M. Ereti. *NCHRP Report 599: Default Values for Highway Capacity and Level of Service Analyses*. Transportation Research Board of the National Academies, Washington, D.C., 2008.
2. Dowling, R., G. F. List, B. Yang, E. Witzke, and A. Flannery. *NCFRP Report 41: Incorporating Truck Analysis into the Highway Capacity Manual*. Transportation Research Board of the National Academies, Washington, D.C., 2014.
3. Washburn, S. S., and S. Ozkul. *Heavy Vehicle Effects on Florida Freeways and Multilane Highways*. Report TRC-FDOT-93817-2013. Florida Department of Transportation, Tallahassee, 2013.
4. Ozkul, S., and Washburn, S. S. Updated Commercial Truck Speed versus Distance-Grade Curves for the *Highway Capacity Manual*. In *Transportation Research Record: Journal of the Transportation Research Board*, No. 2483, Transportation Research Board of the National Academies, Washington, D.C., 2015, pp. 91–101.
5. Hu, J., B. Schroeder, and N. Rouphail. Rationale for Incorporating Queue Discharge Flow into *Highway Capacity Manual* Procedure for Analysis of Freeway Facilities. In *Transportation Research Record: Journal of the Transportation Research Board*, No. 2286, Transportation Research Board of the National Academies, Washington, D.C., 2012, pp. 76–83.
6. Elefteriadou, L., A. Kondyli, and B. St. George. *Estimation of Capacities on Florida Freeways*. Final Report. Transportation Research Center, University of Florida, Gainesville, Sept. 2014.
7. Brilon, W., J. Geistefeldt, and M. Regler. Reliability of Freeway Traffic Flow: A Stochastic Concept of Capacity. In *Proceedings of the 16th International Symposium on Transportation and Traffic Theory*, College Park, Md., July 2005, pp. 125–144.

Some of these references can be found in the Technical Reference Library in Volume 4.

APPENDIX A: TRUCK PERFORMANCE CURVES

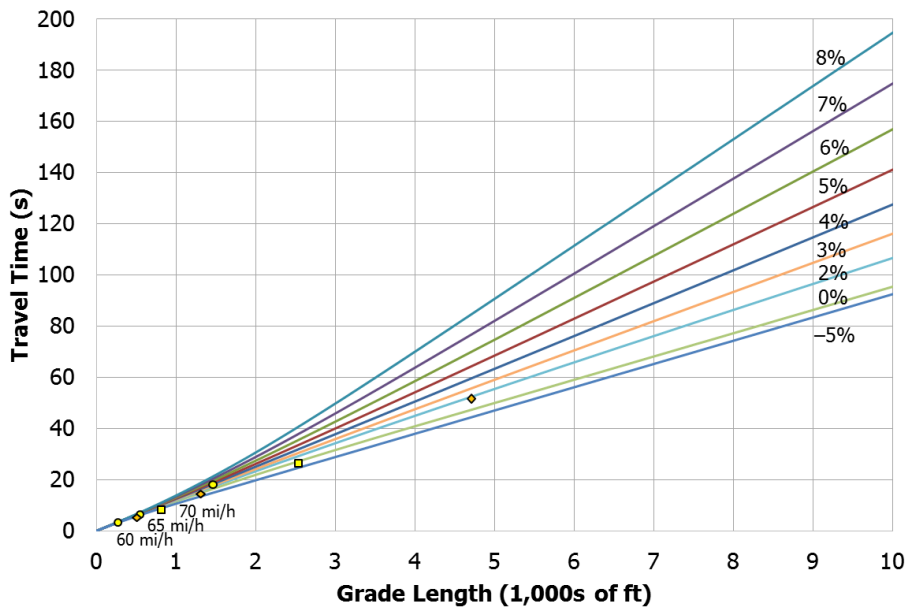
This appendix provides travel time versus distance curves for SUTs and TTs for 50-, 55-, 60-, 65-, and 75-mi/h free-flow speeds (FFS). Curves for SUTs and TTs for a 70-mi/h FFS are presented in Section 3 as Exhibit 26-5 and Exhibit 26-6, respectively.

Exhibit 26-A1
SUT Travel Time Versus Distance Curves for 50-mi/h FFS

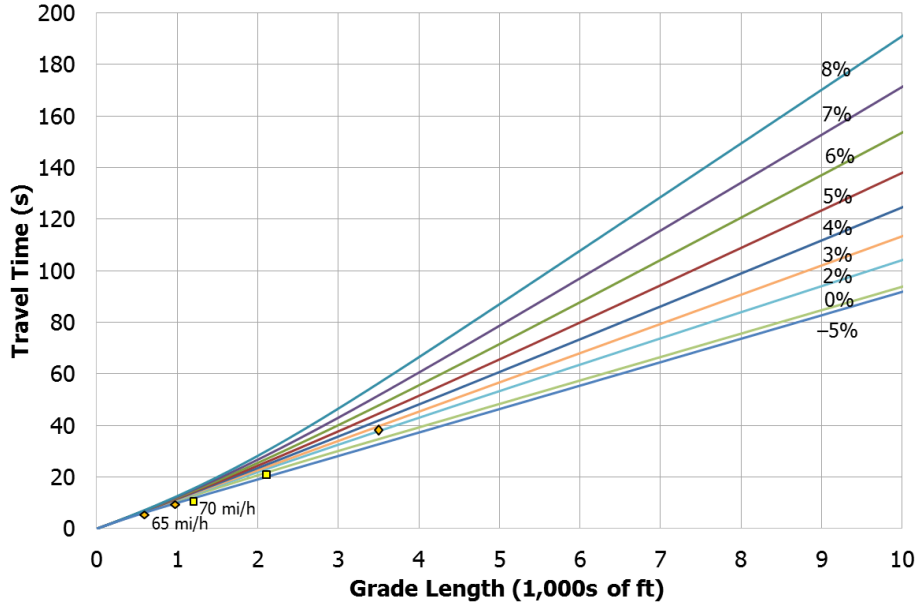


Notes: Curves in this graph assume a weight-to-horsepower ratio of 100. Triangles indicate where a truck reaches 55 mi/h, diamonds indicate 65 mi/h, and squares indicate 70 mi/h.

Exhibit 26-A2
SUT Travel Time Versus Distance Curves for 55-mi/h FFS

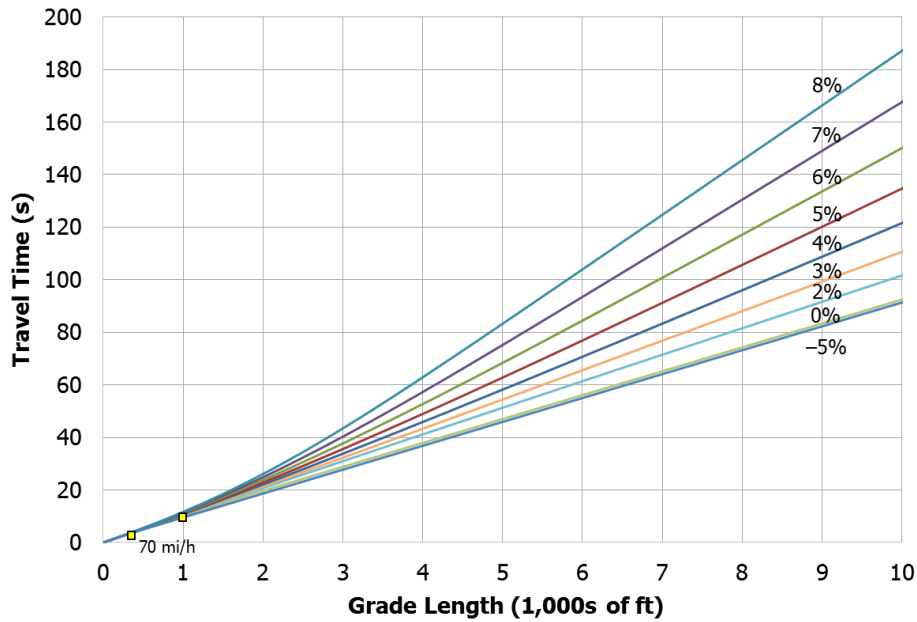


Notes: Curves in this graph assume a weight-to-horsepower ratio of 100. Circles indicate where a truck reaches 60 mi/h, diamonds indicate 65 mi/h, and squares indicate 70 mi/h.



Notes: Curves in this graph assume a weight-to-horsepower ratio of 100.
 Diamonds indicate where a truck reaches 65 mi/h and squares indicate 70 mi/h.

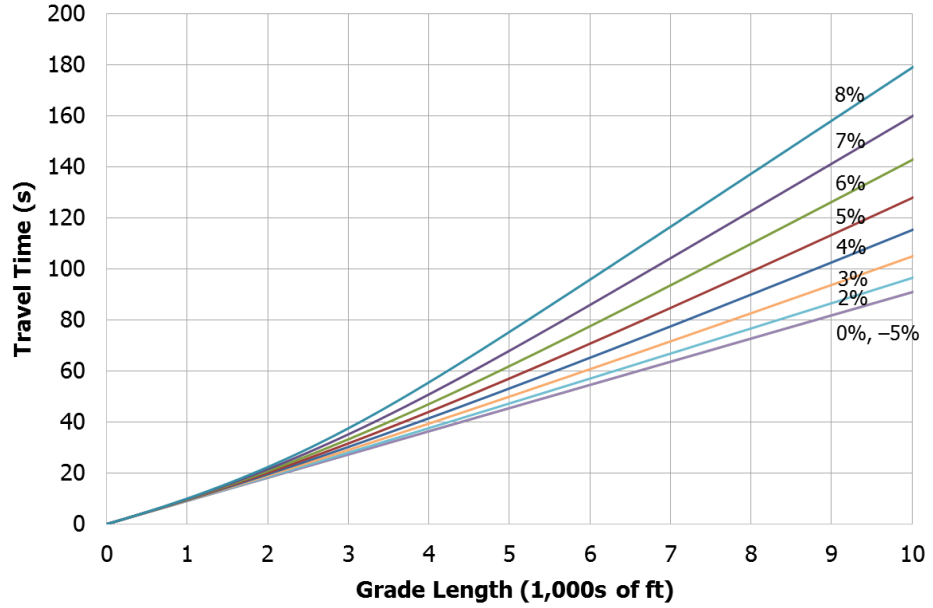
Exhibit 26-A3
 SUT Travel Time Versus
 Distance Curves for 60-mi/h
 FFS



Notes: Curves in this graph assume a weight-to-horsepower ratio of 100.
 Squares indicate where a truck reaches 70 mi/h.

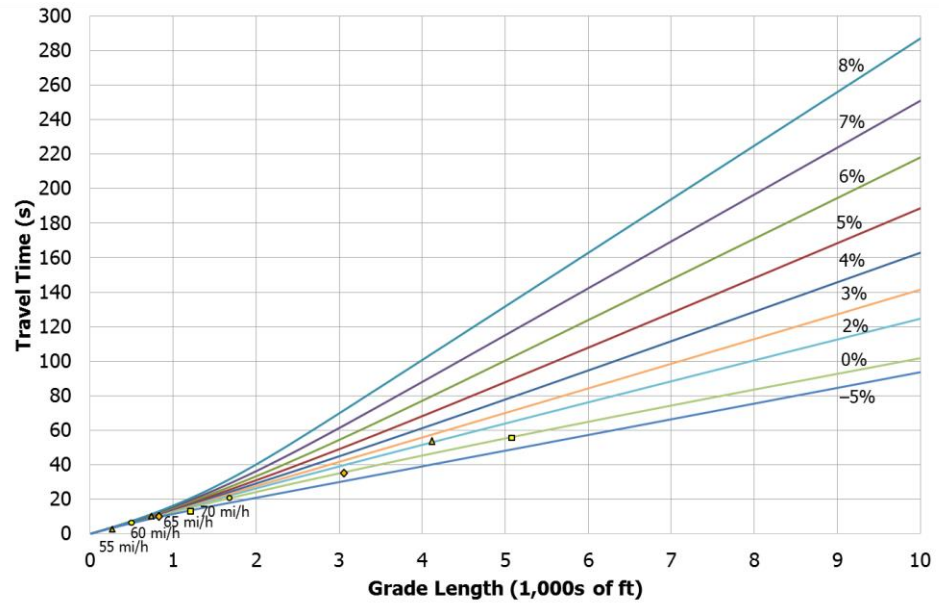
Exhibit 26-A4
 SUT Travel Time Versus
 Distance Curves for 65-mi/h
 FFS

Exhibit 26-A5
SUT Travel Time Versus
Distance Curves for 75-mi/h
FFS



Note: Curves in this graph assume a weight-to-horsepower ratio of 100.

Exhibit 26-A6
TT Travel Time Versus
Distance Curves for 50-mi/h
FFS



Notes: Curves in this graph assume a weight-to-horsepower ratio of 150.
Triangles indicate where a truck reaches 55 mi/h, circles indicate 60 mi/h, diamonds indicate 65 mi/h, and squares indicate 70 mi/h.

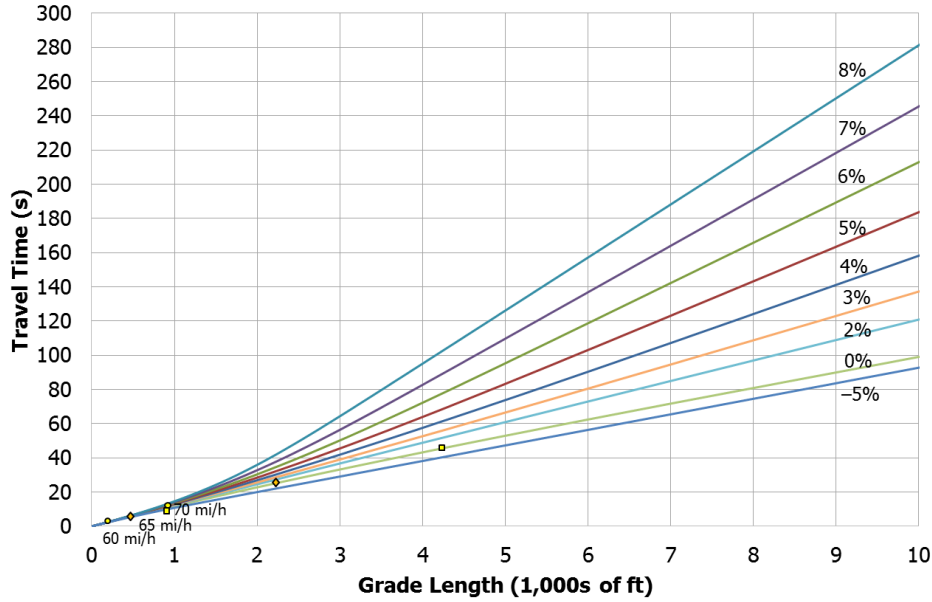


Exhibit 26-A7
TT Travel Time Versus
Distance Curves for 55-mi/h
FFS

Notes: Curves in this graph assume a weight-to-horsepower ratio of 150.
Circles indicate where a truck reaches 60 mi/h, diamonds indicate 65 mi/h, and squares indicate 70 mi/h.

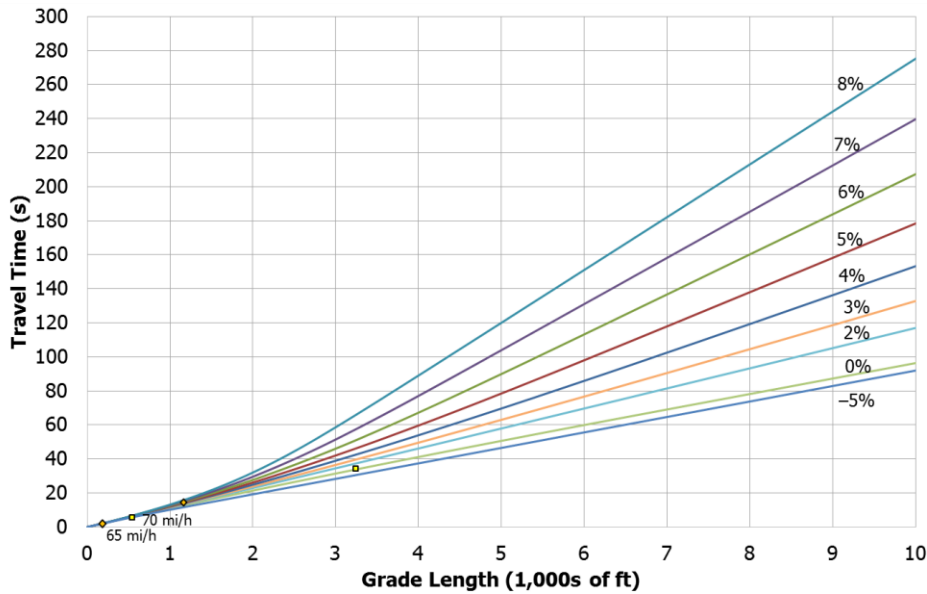
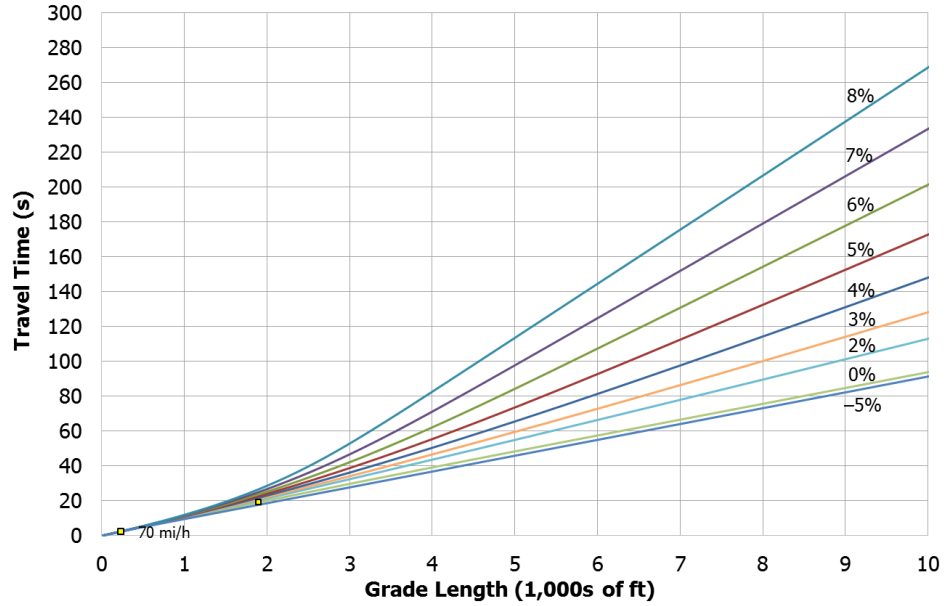


Exhibit 26-A8
TT Travel Time Versus
Distance Curves for 60-mi/h
FFS

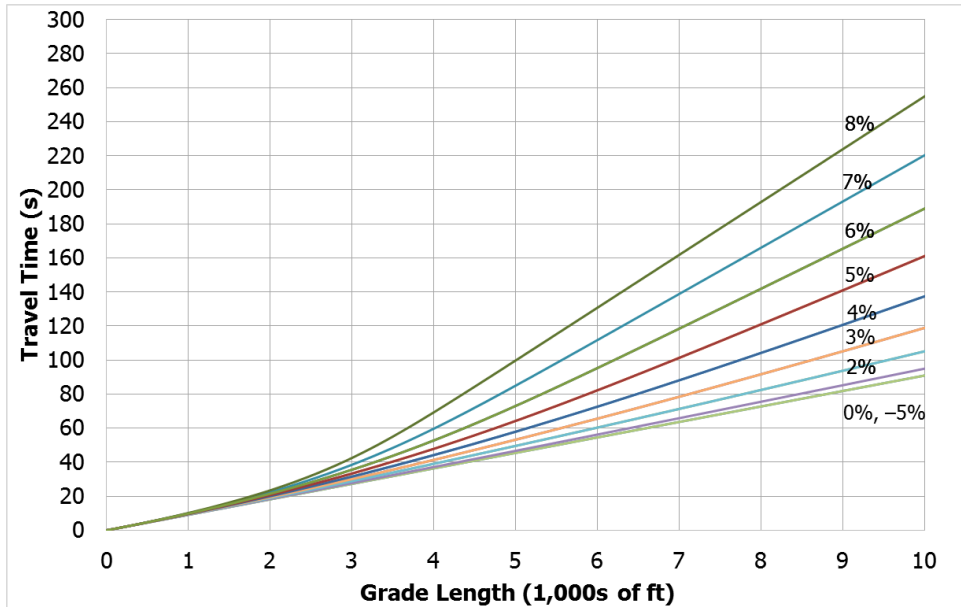
Notes: Curves in this graph assume a weight-to-horsepower ratio of 150.
Diamonds indicate where a truck reaches 65 mi/h and squares indicate 70 mi/h.

Exhibit 26-A9
 TT Travel Time Versus
 Distance Curves for 65-mi/h
 FFS



Notes: Curves in this graph assume a weight-to-horsepower ratio of 150.
 Squares indicate where a truck reaches 70 mi/h.

Exhibit 26-A10
 TT Travel Time Versus
 Distance Curves for 75-mi/h
 FFS



Note: Curves in this graph assume a weight-to-horsepower ratio of 150.

APPENDIX B: WORK ZONES ON TWO-LANE HIGHWAYS

This appendix presents a method for estimating the capacity and operation of work zones on two-lane highways when one of the two lanes is closed. This method is based on research conducted by National Cooperative Highway Research Program (NCHRP) Project 03-107 (B-1). At the time of writing, the HCM's two-lane highway methodology was being updated as part of NCHRP Project 17-65 (B-2), and it is anticipated that this work zone method will be integrated into the new two-lane highway methodology as part of that work.

Work zones along two-lane highways can take three forms:

1. *Shoulder closure.* Work activity is limited to the shoulder of one direction of travel and does not require lane reconfiguration. In this case, only the direction of travel adjacent to the work zone is slightly affected.
2. *Lane shift.* Work activity extends beyond the shoulder, but both directions of travel can be accommodated with a lane shift that utilizes the opposite paved shoulder.
3. *Lane closure.* Work activity requires the closure of one of the two lanes. Flaggers or temporary traffic signals are used to alternately serve one direction of travel at a time. Both directions of travel can be significantly affected.

The method presented in this appendix addresses the third scenario—lane closure—as it has the greatest impact on traffic operations.

CONCEPTS

A lane closure on a two-lane highway converts traffic flow from an uninterrupted to an interrupted condition. With traffic control devices (flaggers or signals) provided at each end, the operation of the lane closure can be described in terms similar to those used for a signalized intersection:

- *Capacity* is the number of vehicles that can be processed through the work zone per cycle or per hour. It can be determined based on the saturation flow rate at the control points and the traffic control “cycle length.”
- *Cycle length* is determined by the flagging operations or signal timing at each control point and the time required to travel through the work zone. Travel time is dependent on the average travel speed (ATS) of the platoons traveling through the work zone. Factors that may influence travel speed include posted speed limit, use of a pilot car, heavy-vehicle percentage, grade, intensity of construction activity, lane width, lateral distance to the work activity, and lighting conditions (day versus night).

Performance measures, including delay and queue length, can be calculated by using capacity and cycle length.

This method addresses a one-lane closure on a two-lane highway. Other types of work zones, such as shoulder closures or lane shifts, are not addressed.

The work zone capacity methodology is analogous to the capacity calculation for a two-phase traffic signal.

Exhibit 26-B1
Traffic Control for a Two-Lane Highway Work Zone Involving a Lane Closure

Measuring two-lane highway work zone saturation flow rates requires a longer data collection time than for a signalized intersection because of the longer cycle lengths involved.

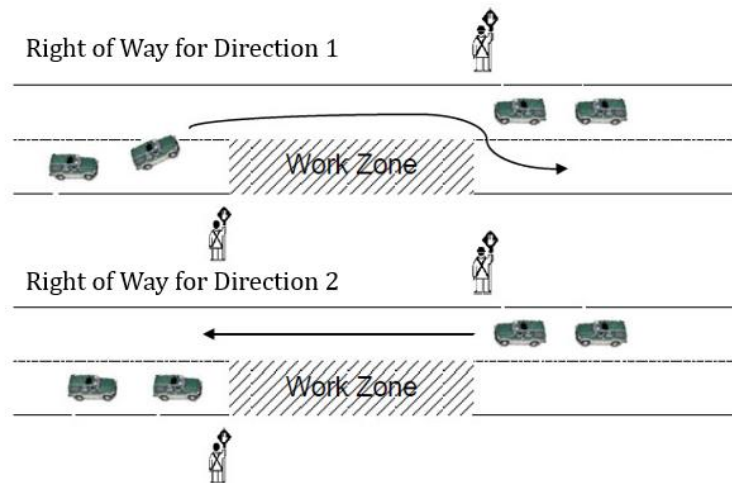
WORK ZONE CAPACITY

The methodology for estimating the capacity of a work zone on a two-lane highway with one lane closed is analogous to the capacity calculation for a two-phase signalized intersection. ATS is estimated from a regression model developed through observations of two directions of travel at three work zones (B-1).

Step 1: Collect Data

For a typical capacity calculation, the analyst must specify traffic information (including traffic demands, travel speed, and heavy-vehicle percentage), roadway geometric configuration (e.g., lane width, lateral clearance, speed limit), and work zone data (including work zone length, signal green time, and traffic control plan).

A basic traffic flagger control process for a two-lane highway work zone involving a lane closure is shown in Exhibit 26-B1. Direction 1 refers to the travel direction whose lane is blocked by the work zone; Direction 2 refers to the travel direction with the open lane.



Source: Schoen et al. (B-1).

Some data, such as ATS, saturation flow rate, and green interval length, may be difficult to collect in the field. In Steps 2–4, the mathematical models that can be used to estimate these data are presented. Analysts must note that, for capacity calculations, field data are always more desirable to use when available.

A procedure is given in Section 6 of Chapter 31, Signalized Intersections: Supplemental, for determining the saturation flow rate of a signalized intersection. This procedure involves counting and timing the number of queue discharge vehicles that pass through an intersection to determine the saturated vehicle headway. As two-lane highway work zone traffic control typically has a much longer cycle length than a typical signalized intersection, the time period for gathering saturation flow data is recommended to be 30–60 min. Of course, a longer time period is generally more desirable when possible. The work zone capacity can then be determined from the measured saturation flow rate and the effective green-to-cycle length ratio.

Step 2: Estimate ATS

A simple estimation of ATS can be obtained by following a procedure similar to the general procedure described in Chapter 15 for estimating two-lane highway ATS. Speeds for Directions 1 and 2 are calculated by Equation 26-B1 and Equation 26-B2, respectively. Research on two-lane highway work zones (B-1) found that Direction 2 (i.e., the direction whose lane is not closed) consistently had higher average speeds than Direction 1.

$$S_1 = 0.615 \times SL - f_{LS} - f_A - f_{np,ATS}$$

$$S_2 = 0.692 \times SL - f_{LS} - f_A - f_{np,ATS}$$

Equation 26-B1

Equation 26-B2

where

S_i = ATS in direction i (mi/h),

SL = speed limit for the two-lane highway segment (mi/h),

f_{LS} = adjustment for lane and shoulder width from Exhibit 15-7 (mi/h),

f_A = adjustment for access-point density from Exhibit 15-8 (mi/h), and

$f_{np,ATS}$ = adjustment factor for ATS determination for the percentage of no-passing zones in the analysis direction (mi/h) = 2.4 mi/h.

For two-lane highway work zones, $f_{np,ATS}$ provides a constant speed reduction of 2.4 mi/h in all conditions.

Step 3: Estimate Saturation Flow Rate

If the saturation flow rate is not measured in the field, a directional saturation flow rate can be estimated by using Equation 26-B3 with Equation 26-B4 and Equation 26-B5.

$$s_i = \frac{3,600}{\hat{h}_i}$$

Equation 26-B3

with

$$\hat{h}_i = h_0 \times f_{\text{speed},i}$$

$$f_{\text{speed},i} = 1 - 0.005(\min[S_i, 45] - 45)$$

Equation 26-B4

Equation 26-B5

where

s_i = saturation flow rate for direction i (pc/h);

\hat{h}_i = adjusted time headway for direction i (s);

h_0 = base saturation headway (s/pc) = 3,600/1,900 = 1.89 s/pc;

$f_{\text{speed},i}$ = ATS adjustment for direction i (decimal); and

S_i = ATS in direction i (mi/h).

Step 4: Estimate Green Time

The length of the green interval can be applied directly if a fixed-time signal is applied at the work zone site. However, most work zones apply flagger control, for which the green time in each cycle is not fixed. For flagger control under relatively balanced directional demand conditions, a simple estimation of optimal directional effective green time can be found by using Equation 26-B6.

Equation 26-B6

$$G_{opt} = \begin{cases} 20 & 0.0375l < 20 \\ 0.0375l & 20 \leq 0.0375l \leq 60 \\ 60 & 0.0375l > 60 \end{cases}$$

where

G_{opt} = optimal effective green time for one direction (s), and

l = work zone length (ft).

To ensure traffic can be fully discharged in two directions, directional effective green-time lengths must satisfy Equation 26-B6

Equation 26-B7

$$G_i \geq G_{i,min} = \frac{v_i}{s_i - v_i} (C - G_i)$$

with

Equation 26-B8

$$C = \frac{l}{S_{1,fps}} + \frac{l}{S_{2,fps}} + G_1 + G_2 + 2L_S$$

where

G_i = effective green time for direction i (s),

$G_{i,min}$ = minimum effective green time for direction i (s),

s_i = saturation flow rate for direction i (pc/h),

v_i = demand flow rate for direction i (pc/h),

C = cycle length (s),

$S_{i,fps}$ = ATS in direction i (ft/s) = $(S_i \times 5,280 \text{ ft/mi}) / (3,600 \text{ s/h})$,

S_i = ATS in direction i (mi/h), and

L_S = start-up lost time (s).

Step 5: Calculate Capacity

Directional capacity is calculated by Equation 26-B9.

Equation 26-B9

$$c_i = \frac{s_i G_i}{C}$$

where

c_i = capacity for direction i (pc/h),

s_i = saturation flow rate for direction i (pc/h),

G_i = effective green time for direction i (s), and

C = cycle length (s).

The *start-up lost time*, the elapsed time between the last vehicle in the opposing direction exiting the work zone and the entry of the first queued vehicle traveling in the subject direction, is assumed to be independent of traffic direction, as the two directions follow the same traffic control plan. A default value of 2 s for each direction is recommended.

The total capacity c_{total} (in passenger cars per hour) can be calculated by summing the two directional capacities, as shown in Equation 26-B6.

$$c_{total} = c_1 + c_2 = \frac{s_1 G_1 + s_2 G_2}{C}$$

Equation 26-B10

QUEUING AND DELAY ANALYSIS

The previous steps provide a simple procedure to check two-lane highway work zone capacity. In practice, it might also be useful to have performance data such as delay and queuing. Users can apply the model to determine the optimal control plan while minimizing the vehicle delay and queuing data.

A simple way to estimate vehicle delay and queue length is by assuming deterministic traffic flow for both directions. Exhibit 26-B2 shows the deterministic queuing diagram for a two-lane highway work zone. Although more accurate estimates can be calculated from microscopic simulations that incorporate random processes, these estimates might be difficult to accomplish in practice because of the extra time and resources required. Therefore, by a similar procedure to that used in Chapter 19 for signalized intersection control delay estimation, the incremental delay caused by random arrivals is added to the deterministic queuing delay associated with the work zone. The interval g_i shown in the exhibit is the portion of the green time with saturated departures.

The maximum queue length for each direction $Q_{i,max}$ (in passenger cars) is the height of the triangles in the queue length area of the exhibit. These lengths can be calculated by Equation 26-B11 and Equation 26-B12 for Directions 1 and 2, respectively.

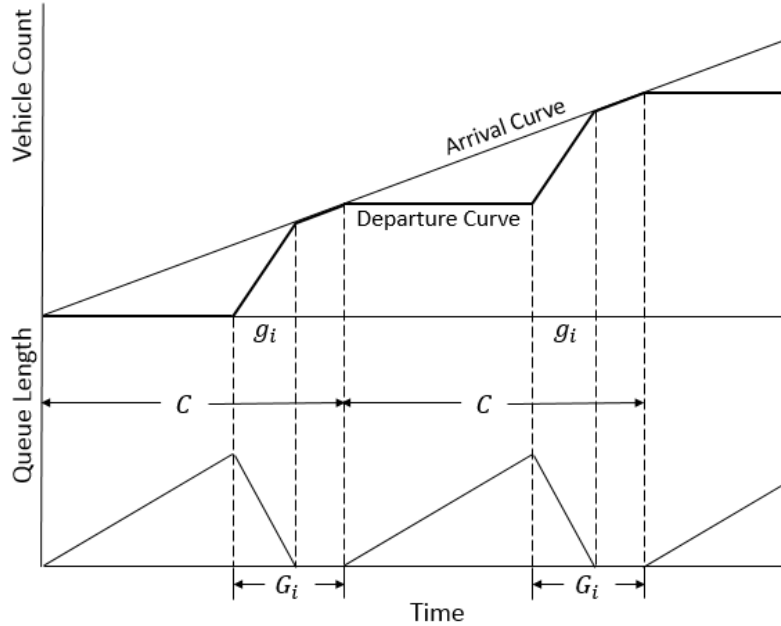
$$Q_{1,max} = \frac{v_1}{3,600} \left(\frac{l}{S_{1,fps}} + \frac{l}{S_{2,fps}} + G_2 + 2L_S \right)$$

Equation 26-B11

$$Q_{2,max} = \frac{v_2}{3,600} \left(\frac{l}{S_{1,fps}} + \frac{l}{S_{2,fps}} + G_1 + 2L_S \right)$$

Equation 26-B12

Exhibit 26-B2
Directional Queueing Diagram
for a Two-Lane Highway
Lane-Closure Work Zone



Source: Schoen et al. (**Error! Reference source not found.**).

For undersaturated conditions, directional vehicle delay caused by a two-lane highway work zone with one lane closed can be represented by Equation 26-B6

Equation 26-B13

$$d = d_1 + d_2$$

where

d = control delay per passenger car (s/pc),

d_1 = uniform control delay assuming uniform traffic arrivals (s/pc), and

d_2 = incremental delay resulting from random arrivals and oversaturation queues (s/pc).

For each direction i , the total directional uniform control delay per cycle $D_{1,i}$ (in seconds) is the triangle area in the queue length diagram (Exhibit 26-B2). It is calculated as one-half the queue length multiplied by the queueing duration. $D_{1,i}$ is given by Equation 26-B6.

Equation 26-B14

$$D_{1,i} = \frac{s_i v_i}{2(s_i - v_i)} (C - G_i)^2$$

The average uniform delay in direction i is given by Equation 26-B15.

Equation 26-B15

$$d_{1,i} = \frac{D_{1,i}}{v_i C} = \frac{s_i (C - G_i)^2}{2(s_i - v_i) C}$$

Finally, by following Equation 19-26 in Chapter 19, the average incremental delay in direction i is given by Equation 26-B16.

Equation 26-B16

$$d_{2,i} = 900 T \left[(X_i - 1) + \sqrt{(X_i - 1)^2 + \frac{8kIX_i}{c_i T}} \right]$$

where

- T = analysis period duration (h),
- k = incremental delay factor (decimal),
- I = upstream filtering adjustment factor (decimal),
- c_i = directional capacity (pc/h) from Equation 26-B9, and
- X_i = directional volume-to-capacity ratio or degree of saturation (unitless).

Values for k can be calculated with Equation 19-22 in Chapter 19. For fixed-time control, $k = 0.5$. Because the purpose of calculating delay in a work zone context is to identify the optimal effective green time, which is assumed to repeat every cycle, a value for k of 0.5 is recommended for use in Equation 26-B16. It incorporates the effects of metered arrivals from upstream signals or work zones. If the work zone is isolated, then $I = 1.0$.

The average delay per passenger car is the sum of the directional total delays, divided by the total number of passenger cars, as shown in Equation 26-B17. Note that the traffic flow rates used in the equation are in units of passenger cars per hour; therefore, vehicle delay is calculated in terms of seconds per passenger car.

$$d = \frac{(d_{1,1} + d_{2,1})v_1 + (d_{1,2} + d_{2,2})v_2}{v_1 + v_2}$$

Equation 26-B17

In equations calculating queue length and vehicle delay, all variables are given by roadway or traffic parameters, except that directional effective green time G_i should be determined by users. Thus users can change the traffic control plan to optimize the result. Users must note, however, that they should not arbitrarily choose an effective green-time value.

EXAMPLE CALCULATION

This subsection presents an example application of the methodology. An isolated 1,000-ft-long work zone will be located on a rural two-lane highway. Known peak hour roadway and traffic parameters are summarized in Exhibit 26-B3 and Exhibit 26-B4.

Direction	Lane Width (ft)	Shoulder Width (ft)	No. of Access Points per Mile	General Terrain Type
1	12	3	0	Rolling
2	12	3	0	Rolling

Exhibit 26-B3
Example Calculation: Work Zone Roadway Parameters

Direction	Speed Limit (mi/h)	Traffic Demand (veh/h)	Truck Percentage	RV Percentage
1	45	300	10.0	10.0
2	45	300	10.0	10.0

Exhibit 26-B4
Example Calculation: Work Zone Traffic Parameters

Step 1: Collect Data

Most of the necessary data are provided in the problem statement. However, for the purposes of calculating ATS, the traffic demand V_i (in vehicles per hour) must be converted into a traffic flow rate $v_{i,ATS}$ (in passenger cars per hour) by using Equation 15-3 in Chapter 15.

$$v_{i,ATS} = \frac{V_i}{PHF \times f_{g,ATS} \times f_{HV,ATS}}$$

This equation requires determining both an adjustment factor for grade (in this case, general terrain) and an adjustment factor for heavy vehicles (which also includes terrain effects). In addition, a peak hour factor (PHF) is applied.

As the PHF for this highway is not known, the default value of 0.88 given in Exhibit 15-5 will be used. From Exhibit 15-9, the ATS grade adjustment factor $f_{g,ATS}$ for rolling terrain is 0.83. Finally, from Exhibit 15-11, the truck PCE for ATS calculation purposes in rolling terrain is 2.1, and the RV PCE is 1.1. The ATS heavy vehicle adjustment factor $f_{HV,ATS}$ can then be calculated from Equation 15-4.

$$f_{HV,ATS} = \frac{1}{1 + P_T(E_T - 1) + P_R(E_R - 1)}$$

$$f_{HV,ATS} = \frac{1}{1 + (0.10)(2.1 - 1) + (0.10)(1.1 - 1)}$$

$$f_{HV,ATS} = 0.89$$

then

$$v_1 = v_2 = \frac{300}{0.88 \times 0.83 \times 0.89} = 461 \text{ pc/h}$$

Step 2: Estimate ATS

ATS through the work zone is calculated with Equation 26-B1 and Equation 26-B2 for Directions 1 and 2, respectively.

$$S_1 = 0.615 \times SL - f_{LS} - f_A - f_{np,ATS}$$

$$S_2 = 0.692 \times SL - f_{LS} - f_A - f_{np,ATS}$$

The speed limit SL is given, and the ATS adjustment factor for the percentage of no-passing zones in the analysis direction is a constant of 2.4 mi/h according to the text accompanying Equation 26-B2. From Exhibit 15-7, the adjustment for lane and shoulder width f_{LS} is 2.6 mi/h for 12-ft lane widths and 3-ft shoulder widths. Finally, from Exhibit 15-8, the adjustment for access point density is 0.0 mi/h when no access points are present. Then

$$S_1 = 0.615 \times 45 - 2.6 - 0 - 2.4 = 22.7 \text{ mi/h}$$

$$S_2 = 0.692 \times 45 - 2.6 - 0 - 2.4 = 26.1 \text{ mi/h}$$

Step 3: Estimate Saturation Flow Rate

Equation 26-B3 through Equation 26-B5 are used to estimate the saturation flow rate through the work zone.

First, the speed adjustment factor is calculated for each direction as follows:

$$f_{\text{speed},i} = 1 - 0.005(\min[S_i, 45] - 45)$$

$$f_{\text{speed},1} = 1 - 0.005(\min[22.7,45] - 45) = 1.11$$

$$f_{\text{speed},2} = 1 - 0.005(\min[26.1,45] - 45) = 1.09$$

Next, an adjusted time headway is calculated for each direction as follows:

$$\hat{h}_i = h_0 \times f_{\text{speed},i}$$

$$\hat{h}_1 = 1.89 \times 1.11 = 2.10 \text{ s}$$

$$\hat{h}_2 = 1.89 \times 1.09 = 2.06 \text{ s}$$

where the base saturation headway of 1.89 s/pc is as given in the text following Equation 26-B4.

Finally, the saturation flow rate for each direction is calculated as

$$s_i = \frac{3,600}{\hat{h}_i}$$

$$s_1 = \frac{3,600}{2.10} = 1,714 \text{ pc/h/ln}$$

$$s_2 = \frac{3,600}{2.06} = 1,748 \text{ pc/h/ln}$$

Step 4: Estimate Green Time

In Step 4, the effective green time length is determined. It may be difficult to choose a green time value without knowing the traffic performance parameters, but an estimate of the optimal value can be obtained with Equation 26-B6.

$$G_{opt} = \begin{cases} 20 & 0.0375l < 20 \\ 0.0375l & 20 \leq 0.0375l \leq 60 \\ 60 & 0.0375l > 60 \end{cases}$$

As the work zone will be 1,000 ft long, the value $0.0375l$ computes to 37.5 s. As 37.5 is between 20 and 60, it can be used directly; however, this value should be checked to make sure it is long enough to discharge the vehicle queues. Equation 26-B7 provides this check.

$$G_i \geq G_{i,min} = \frac{v_i}{s_i - v_i} (C - G_i)$$

The cycle length C is computed from Equation 26-B8, incorporating a default value of 2.0 s for the start-up lost time.

$$C = \frac{l}{S_{1,fps}} + \frac{l}{S_{2,fps}} + G_1 + G_2 + 2L_S$$

$$C = \frac{1,000}{22.7 \times 5,280/3,600} + \frac{1,000}{26.1 \times 5,280/3,600} + 37.5 + 37.5 + 2(2.0)$$

$$C = 135.2 \text{ s}$$

then

$$G_{1,min} = \frac{461}{1,714 - 461} (135.2 - 37.5) = 35.9 \text{ s}$$

$$G_{2,min} = \frac{461}{1,748 - 461} (135.2 - 37.5) = 35.0 \text{ s}$$

As the optimal effective green time of 37.5 s is greater than the minimum required time for each direction, it is accepted, and the process continues to Step 5.

Step 5: Calculate Capacity

Directional capacity is calculated with Equation 26-B9.

$$c_i = \frac{s_i G_i}{C}$$

$$c_1 = \frac{(1,714)(37.5)}{135.2} = 475 \text{ pc/h}$$

$$c_2 = \frac{(1,748)(37.5)}{135.2} = 485 \text{ pc/h}$$

As $v_1 < c_1$ and $v_2 < c_2$, this 1,000-ft work zone can serve the traffic demand without accumulating vehicle queues when the effective green time is 37.5 s for both directions.

Queuing and Delay

If desired, the maximum queue length and average vehicle delay can be calculated for both directions. The maximum queue length is calculated from Equation 26-B11 and Equation 26-B12 for Directions 1 and 2, respectively.

$$Q_{1,max} = \frac{v_1}{3,600} \left(\frac{l}{S_{1,fps}} + \frac{l}{S_{2,fps}} + G_2 + 2L_S \right)$$

$$Q_{1,max} = \frac{461}{3,600} (30.0 + 26.1 + 37.5 + 4.0) = 13 \text{ veh}$$

$$Q_{2,max} = \frac{v_2}{3,600} \left(\frac{l}{S_{1,fps}} + \frac{l}{S_{2,fps}} + G_1 + 2L_S \right)$$

$$Q_{2,max} = \frac{461}{3,600} (30.0 + 26.1 + 37.5 + 4.0) = 13 \text{ veh}$$

The average uniform delay by direction is calculated with Equation 26-B15.

$$d_{1,i} = \frac{s_i(C - G_i)^2}{2(s_i - v_i)C}$$

$$d_{1,1} = \frac{(1,714)(135.2 - 37.5)^2}{(2)(1,714 - 461)(135.2)} = 48.3 \text{ s/veh}$$

$$d_{1,2} = \frac{(1,748)(135.2 - 37.5)^2}{(2)(1,748 - 461)(135.2)} = 47.9 \text{ s/veh}$$

The average incremental delay by direction is calculated from Equation 26-B16. The recommended value of 0.5 is used for the incremental delay factor k , and as the work zone is isolated, a value of 1.0 is used for the upstream filtering adjustment factor I .

$$d_{2,i} = 900 T \left[(X_i - 1) + \sqrt{(X_i - 1)^2 + \frac{8kIX_i}{c_i T}} \right]$$

$$d_{2,1} = (900)(1) \left[\left(\frac{461}{475} - 1 \right) + \sqrt{\left(\frac{461}{475} - 1 \right)^2 + \frac{(8)(0.5)(1.0) \left(\frac{461}{475} \right)}{(475)(1)}} \right] = 59.1 \text{ s}$$

$$d_{2,2} = (900)(1) \left[\left(\frac{461}{485} - 1 \right) + \sqrt{\left(\frac{461}{485} - 1 \right)^2 + \frac{(8)(0.5)(1.0) \left(\frac{461}{485} \right)}{(485)(1)}} \right] = 46.8 \text{ s}$$

Finally, the average delay per passenger car is given by Equation 26-B17.

$$d = \frac{(48.3 + 59.1)(461) + (47.9 + 46.8)(461)}{461 + 461} = 101 \text{ s}$$

REFERENCES

- B-1. Schoen, J. M., J. A. Bonneson, C. Safi, B. Schroeder, A. Hajbabaie, C. H. Yeom, N. Rouphail, Y. Wang, W. Zhu, and Y. Zou. *Work Zone Capacity Methods for the Highway Capacity Manual*. National Cooperative Highway Research Program Project 3-107 final report, preliminary draft. Kittelson & Associates, Inc., Tucson, Ariz., April 2015.
- B-2. National Cooperative Highway Research Program Project 17-65 Website. <http://apps.trb.org/cmsfeed/TRBNetProjectDisplay.asp?ProjectID=3658>. Accessed May 28, 2015.



HIGHWAY CAPACITY MANUAL

6TH EDITION | A GUIDE FOR MULTIMODAL MOBILITY ANALYSIS

VOLUME 4: APPLICATIONS GUIDE

The National Academies of
SCIENCES • ENGINEERING • MEDICINE

TRANSPORTATION RESEARCH BOARD
WASHINGTON, D.C. | WWW.TRB.ORG

TRANSPORTATION RESEARCH BOARD 2016 EXECUTIVE COMMITTEE *

Chair: James M. Crites, Executive Vice President of Operations,
Dallas–Fort Worth International Airport, Texas

Vice Chair: Paul Trombino III, Director, Iowa Department of
Transportation, Ames

Executive Director: Neil J. Pedersen, Transportation Research Board

Victoria A. Arroyo, Executive Director, Georgetown Climate Center;
Assistant Dean, Centers and Institutes; and Professor and Director,
Environmental Law Program, Georgetown University Law Center,
Washington, D.C.

Scott E. Bennett, Director, Arkansas State Highway and Transportation
Department, Little Rock

Jennifer Cohan, Secretary, Delaware Department of Transportation, Dover

Malcolm Dougherty, Director, California Department of
Transportation, Sacramento

A. Stewart Fotheringham, Professor, School of Geographical Sciences
and Urban Planning, Arizona State University, Tempe

John S. Halikowski, Director, Arizona Department of Transportation,
Phoenix

Susan Hanson, Distinguished University Professor Emerita, Graduate
School of Geography, Clark University, Worcester, Massachusetts

Steve Heminger, Executive Director, Metropolitan Transportation
Commission, Oakland, California

Chris T. Hendrickson, Hamerschlag Professor of Engineering, Carnegie
Mellon University, Pittsburgh, Pennsylvania

Jeffrey D. Holt, Managing Director, Power, Energy, and Infrastructure
Group, BMO Capital Markets Corporation, New York

S. Jack Hu, Vice President for Research and J. Reid and Polly Anderson
Professor of Manufacturing, University of Michigan, Ann Arbor

Roger B. Huff, President, HGLC, LLC, Farmington Hills, Michigan

Geraldine Knatz, Professor, Sol Price School of Public Policy, Viterbi
School of Engineering, University of Southern California, Los Angeles

Ysela Llort, Consultant, Miami, Florida

Melinda McGrath, Executive Director, Mississippi Department of
Transportation, Jackson

James P. Redeker, Commissioner, Connecticut Department of
Transportation, Newington

Mark L. Rosenberg, Executive Director, The Task Force for Global
Health, Inc., Decatur, Georgia

Kumares C. Sinha, Olson Distinguished Professor of Civil Engineering,
Purdue University, West Lafayette, Indiana

Daniel Sperling, Professor of Civil Engineering and Environmental
Science and Policy; Director, Institute of Transportation Studies,
University of California, Davis

Kirk T. Steudle, Director, Michigan Department of Transportation,
Lansing (Past Chair, 2014)

Gary C. Thomas, President and Executive Director, Dallas Area Rapid
Transit, Dallas, Texas

Pat Thomas, Senior Vice President of State Government Affairs, United
Parcel Service, Washington, D.C.

Katherine F. Turnbull, Executive Associate Director and Research
Scientist, Texas A&M Transportation Institute, College Station

Dean Wise, Vice President of Network Strategy, Burlington Northern
Santa Fe Railway, Fort Worth, Texas

Thomas P. Bostick (Lieutenant General, U.S. Army), Chief of Engineers
and Commanding General, U.S. Army Corps of Engineers, Washington,
D.C. (ex officio)

James C. Card (Vice Admiral, U.S. Coast Guard, retired), Maritime
Consultant, The Woodlands, Texas, and Chair, TRB Marine Board
(ex officio)

T. F. Scott Darling III, Acting Administrator and Chief Counsel, Federal
Motor Carrier Safety Administration, U.S. Department of Transportation
(ex officio)

Marie Therese Dominguez, Administrator, Pipeline and Hazardous
Materials Safety Administration, U.S. Department of Transportation
(ex officio)

Sarah Feinberg, Administrator, Federal Railroad Administration,
U.S. Department of Transportation (ex officio)

Carolyn Flowers, Acting Administrator, Federal Transit Administration,
U.S. Department of Transportation (ex officio)

LeRoy Gishi, Chief, Division of Transportation, Bureau of Indian
Affairs, U.S. Department of the Interior, Washington, D.C. (ex officio)

John T. Gray II, Senior Vice President, Policy and Economics,
Association of American Railroads, Washington, D.C. (ex officio)

Michael P. Huerta, Administrator, Federal Aviation Administration,
U.S. Department of Transportation (ex officio)

Paul N. Jaenichen, Sr., Administrator, Maritime Administration,
U.S. Department of Transportation (ex officio)

Bevan B. Kirley, Research Associate, University of North Carolina
Highway Safety Research Center, Chapel Hill, and Chair, TRB Young
Members Council (ex officio)

Gregory G. Nadeau, Administrator, Federal Highway Administration,
U.S. Department of Transportation (ex officio)

Wayne Nastri, Acting Executive Officer, South Coast Air Quality
Management District, Diamond Bar, California (ex officio)

Mark R. Rosekind, Administrator, National Highway Traffic Safety
Administration, U.S. Department of Transportation (ex officio)

Craig A. Rutland, U.S. Air Force Pavement Engineer, U.S. Air Force
Civil Engineer Center, Tyndall Air Force Base, Florida (ex officio)

Reuben Sarkar, Deputy Assistant Secretary for Transportation,
U.S. Department of Energy (ex officio)

Richard A. White, Acting President and CEO, American Public
Transportation Association, Washington, D.C. (ex officio)

Gregory D. Winfree, Assistant Secretary for Research and Technology,
Office of the Secretary, U.S. Department of Transportation (ex officio)

Frederick G. (Bud) Wright, Executive Director, American Association
of State Highway and Transportation Officials, Washington, D.C.
(ex officio)

Paul F. Zukunft (Admiral, U.S. Coast Guard), Commandant, U.S. Coast
Guard, U.S. Department of Homeland Security (ex officio)

Transportation Research Board publications are available by ordering
individual publications directly from the TRB Business Office, through
the Internet at www.TRB.org, or by annual subscription through
organizational or individual affiliation with TRB. Affiliates and library
subscribers are eligible for substantial discounts. For further information,
contact the Transportation Research Board Business Office, 500 Fifth
Street, NW, Washington, DC 20001 (telephone 202-334-3213;
fax 202-334-2519; or e-mail TRBsales@nas.edu).

Copyright 2016 by the National Academy of Sciences.

All rights reserved.

Printed in the United States of America.

ISBN 978-0-309-36997-8 [Slipcased set of three volumes]

ISBN 978-0-309-36998-5 [Volume 1]

ISBN 978-0-309-36999-2 [Volume 2]

ISBN 978-0-309-37000-4 [Volume 3]

ISBN 978-0-309-37001-1 [Volume 4, online only]

The National Academies of
SCIENCES • ENGINEERING • MEDICINE

The **National Academy of Sciences** was established in 1863 by an Act of Congress, signed by President Lincoln, as a private, nongovernmental institution to advise the nation on issues related to science and technology. Members are elected by their peers for outstanding contributions to research. Dr. Ralph J. Cicerone is president.

The **National Academy of Engineering** was established in 1964 under the charter of the National Academy of Sciences to bring the practices of engineering to advising the nation. Members are elected by their peers for extraordinary contributions to engineering. Dr. C. D. Mote, Jr., is president.

The **National Academy of Medicine** (formerly the Institute of Medicine) was established in 1970 under the charter of the National Academy of Sciences to advise the nation on medical and health issues. Members are elected by their peers for distinguished contributions to medicine and health. Dr. Victor J. Dzau is president.

The three Academies work together as the National Academies of Sciences, Engineering, and Medicine to provide independent, objective analysis and advice to the nation and conduct other activities to solve complex problems and inform public policy decisions. The Academies also encourage education and research, recognize outstanding contributions to knowledge, and increase public understanding in matters of science, engineering, and medicine.

Learn more about the National Academies of Sciences, Engineering, and Medicine at **www.national-academies.org**.

The **Transportation Research Board** is one of seven major programs of the National Academies of Sciences, Engineering, and Medicine. The mission of the Transportation Research Board is to increase the benefits that transportation contributes to society by providing leadership in transportation innovation and progress through research and information exchange, conducted within a setting that is objective, interdisciplinary, and multimodal. The Board's varied committees, task forces, and panels annually engage about 7,000 engineers, scientists, and other transportation researchers and practitioners from the public and private sectors and academia, all of whom contribute their expertise in the public interest. The program is supported by state transportation departments, federal agencies including the component administrations of the U.S. Department of Transportation, and other organizations and individuals interested in the development of transportation.

Learn more about the Transportation Research Board at **www.TRB.org**.

CHAPTER 27
FREEWAY WEAVING: SUPPLEMENTAL

CONTENTS

1. INTRODUCTION 27-1

2. EXAMPLE PROBLEMS 27-2

 Example Problem 1: LOS of a Major Weaving Segment 27-2

 Example Problem 2: LOS for a Ramp Weave..... 27-7

 Example Problem 3: LOS of a Two-Sided Weaving Segment 27-11

 Example Problem 4: Design of a Major Weaving Segment for a
 Desired LOS..... 27-16

 Example Problem 5: Constructing a Service Volume Table for a
 Weaving Segment 27-22

 Example Problem 6: LOS of an ML Access Segment with Cross-
 Weaving 27-27

 Example Problem 7: ML Access Segment with Downstream Off-Ramp... 27-32

3. ALTERNATIVE TOOL EXAMPLES FOR WEAVING SEGMENTS 27-37

 Determining the Weaving Segment Capacity..... 27-38

 Effect of Demand on Performance..... 27-39

 Effect of Queue Backup from a Downstream Signal on the Exit Ramp..... 27-40

LIST OF EXHIBITS

Exhibit 27-1 List of Example Problems for Weaving Segment Analysis..... 27-2

Exhibit 27-2 Example Problem 1: Major Weaving Segment Data 27-2

Exhibit 27-3 Example Problem 1: Determination of Configuration Variables..... 27-4

Exhibit 27-4 Example Problem 1: Capacity of Entry and Exit Roadways..... 27-5

Exhibit 27-5 Example Problem 2: Ramp-Weave Segment Data 27-7

Exhibit 27-6 Example Problem 2: Configuration Characteristics 27-9

Exhibit 27-7 Example Problem 2: Capacity of Entry and Exit Legs 27-10

Exhibit 27-8 Example Problem 3: Two-Sided Weaving Segment Data 27-12

Exhibit 27-9 Example Problem 3: Configuration Characteristics 27-14

Exhibit 27-10 Example Problem 3: Capacity of Entry and Exit Legs 27-15

Exhibit 27-11 Example Problem 4: Major Weaving Segment Data 27-17

Exhibit 27-12 Example Problem 4: Trial Design 1 27-18

Exhibit 27-13 Example Problem 4: Trial Design 2 27-20

Exhibit 27-14 Example Problem 5: Maximum Density Thresholds for LOS A-D 27-23

Exhibit 27-15 Example Problem 5: Service Flow Rates (pc/h) Under Ideal Conditions (*SFI*) 27-25

Exhibit 27-16 Example Problem 5: Service Flow Rates (veh/h) Under Prevailing Conditions (*SF*) 27-25

Exhibit 27-17 Example Problem 5: Service Volumes (veh/h) Under Prevailing Conditions (*SV*) 27-26

Exhibit 27-18 Example Problem 5: Daily Service Volumes (veh/day) Under Prevailing Conditions (*DSV*) 27-26

Exhibit 27-19 Example Problem 6: ML Access Segment with Cross-Weaving 27-27

Exhibit 27-20 Example Problem 6: Hourly Flow Rates After PHF Is Applied..... 27-29

Exhibit 27-21 Example Problem 6: Configuration Characteristics 27-29

Exhibit 27-22 Example Problem 6: Capacity of Entry and Exit Legs..... 27-31

Exhibit 27-23 Example Problem 7: ML Access Segment Data 27-32

Exhibit 27-24 Example Problem 7: Weaving Flows for Managed Lane Segment 27-33

Exhibit 27-25 Link-Node Structure for the Simulated Weaving Segment 27-37

Exhibit 27-26 Input Data for Various Demand Levels (veh/h)..... 27-37

Exhibit 27-27 Determining the Capacity of a Weaving Segment by Simulation 27-38

Exhibit 27-28 Simulated Effect of Demand Volume on Weaving Segment Capacity and Speed	27-39
Exhibit 27-29 Exit Ramp Signal Operating Parameters	27-40
Exhibit 27-30 Deterioration of Weaving Segment Operation due to Queue Backup from a Traffic Signal	27-41
Exhibit 27-31 Effect of Demand on Weaving Segment Throughput with Exit Ramp Backup.....	27-41
Exhibit 27-32 Effect of Demand on Exit Ramp Throughput with Signal Queuing.....	27-42

1. INTRODUCTION

Chapter 27 is the supplemental chapter for Chapter 13, Freeway Weaving Segments, which is found in Volume 2 of the *Highway Capacity Manual* (HCM). Section 2 provides seven example problems demonstrating the application of the Chapter 13 core methodology and its extension to freeway managed lanes. Section 3 presents examples of applying alternative tools to the analysis of freeway weaving sections to address limitations of the Chapter 13 methodology.

VOLUME 4: APPLICATIONS
GUIDE

- 25. Freeway Facilities:
Supplemental
- 26. Freeway and Highway
Segments: Supplemental
- 27. Freeway Weaving:
Supplemental**
- 28. Freeway Merges and
Diverges: Supplemental
- 29. Urban Street Facilities:
Supplemental
- 30. Urban Street Segments:
Supplemental
- 31. Signalized Intersections:
Supplemental
- 32. STOP-Controlled
Intersections:
Supplemental
- 33. Roundabouts:
Supplemental
- 34. Interchange Ramp
Terminals: Supplemental
- 35. Pedestrians and Bicycles:
Supplemental
- 36. Concepts: Supplemental
- 37. ATDM: Supplemental

2. EXAMPLE PROBLEMS

The example problems in this section illustrate various applications of the freeway weaving segment methodology detailed in Chapter 13. Exhibit 27-1 lists the example problems included. Example problem results from intermediate and final calculations were derived by using a handheld scientific calculator with 12-digit precision. For displaying equation results in text, the results were appropriately rounded. Users may obtain slightly different results if rounded parameters are used in intermediate and final calculations.

Exhibit 27-1
List of Example Problems for Weaving Segment Analysis

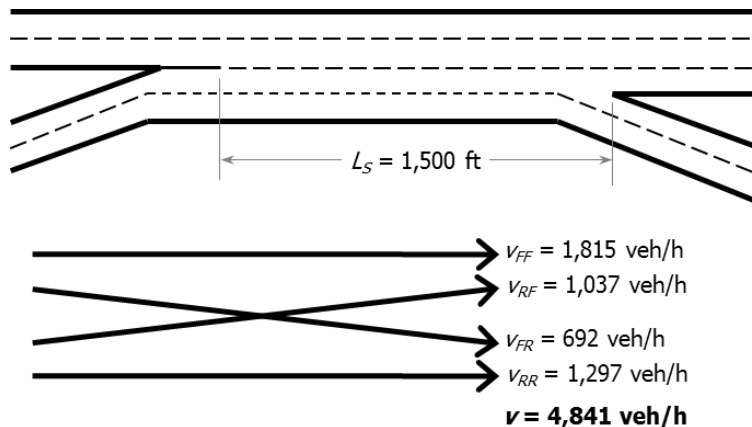
Example Problem	Description	Application
1	LOS of a major weaving segment	Operational analysis
2	LOS for a ramp weave	Operational analysis
3	LOS of a two-sided weaving segment	Operational analysis
4	Design of a major weaving segment for a desired LOS	Design analysis
5	Service volume table construction	Planning analysis
6	LOS of an ML access segment with cross-weaving	Operational analysis
7	ML access segment with downstream off-ramp	Operational analysis

EXAMPLE PROBLEM 1: LOS OF A MAJOR WEAVING SEGMENT

The Weaving Segment

The subject of this operational analysis is a major weaving segment on an urban freeway under nonsevere weather conditions and without incidents, as shown in Exhibit 27-2. The short length of the weaving segment L_s is 1,500 ft.

Exhibit 27-2
Example Problem 1: Major Weaving Segment Data



What is the level of service (LOS) and capacity of the weaving segment shown in Exhibit 27-2?

The Facts

In addition to the information contained in Exhibit 27-2, the following characteristics of the weaving segment are known:

PHF = 0.91 (for all movements);

Heavy vehicles = 5% trucks;

Driver population = regular commuters;

Free-flow speed (FFS) = 65 mi/h; ramp FFS = 50 mi/h;
 $c_{IFL} = 2,350$ pc/h/ln (for FFS = 65 mi/h);
 $ID = 0.8$ interchange/mi; and
 Terrain = level.

Note that the ideal freeway capacity per lane c_{IFL} is the capacity of a basic freeway segment, where the FFS is 65 mi/h. It is drawn from the methodology of Chapter 12, Basic Freeway and Multilane Highway Segments.

Comments

Chapter 12, Basic Freeway and Multilane Highway Segments, must be consulted to find appropriate values for the heavy-vehicle adjustment factor f_{HV} . Chapter 26, Section 2, should be consulted if the driver population includes a significant proportion of noncommuters.

All input parameters have been specified, so default values are not needed. Demand volumes are given in vehicles per hour under prevailing conditions. These must be converted to passenger cars per hour under equivalent ideal conditions for use with the weaving methodology. The weaving segment length must be compared with the maximum length for weaving analysis to determine whether the Chapter 13 methodology is applicable. The capacity of the weaving segment is estimated and compared with the total demand flow to determine whether LOS F exists. Lane-changing rates are calculated to allow estimations of speed for weaving and nonweaving flows. Average overall speed and density are computed and compared with the criteria of Exhibit 13-6 to determine LOS.

Without specific information to the contrary, it is assumed that good weather conditions prevail and that there are no incidents during the analysis period.

Step 1: Input Data

All inputs have been specified in Exhibit 27-2 and the Facts section of the problem statement.

Step 2: Adjust Volume

Equation 13-1 is used to convert the four component demand volumes to flow rates under equivalent ideal conditions. Chapter 12 is consulted to obtain a value of E_T (2.0 for level terrain). From Chapter 12, the heavy-vehicle adjustment factor is computed as

$$f_{HV} = \frac{1}{1 + P_T(E_T - 1)} = \frac{1}{1 + 0.05(2 - 1)} = 0.952$$

Equation 13-1 is now used to convert all demand volumes:

$$v_i = \frac{V_i}{PHF \times f_{HV}}$$

$$v_{FF} = \frac{1,815}{0.91 \times 0.952} = 2,094 \text{ pc/h}$$

$$v_{FR} = \frac{692}{0.91 \times 0.952} = 798 \text{ pc/h}$$

$$v_{RF} = \frac{1,037}{0.91 \times 0.952} = 1,197 \text{ pc/h}$$

$$v_{RR} = \frac{1,297}{0.91 \times 0.952} = 1,497 \text{ pc/h}$$

Then

$$v_W = 798 + 1,197 = 1,995 \text{ pc/h}$$

$$v_{NW} = 2,094 + 1,497 = 3,591 \text{ pc/h}$$

$$v = 1,995 + 3,591 = 5,586 \text{ pc/h}$$

$$VR = \frac{1,995}{5,586} = 0.357$$

Step 3: Determine Configuration Characteristics

The configuration is examined to determine the values of LC_{RF} , LC_{FR} , and N_{WL} . These determinations are illustrated in Exhibit 27-3. From these values, the minimum number of lane changes by weaving vehicles, LC_{MIN} , is then computed by using Equation 13-2.

Exhibit 27-3
Example Problem 1:
Determination of
Configuration Variables

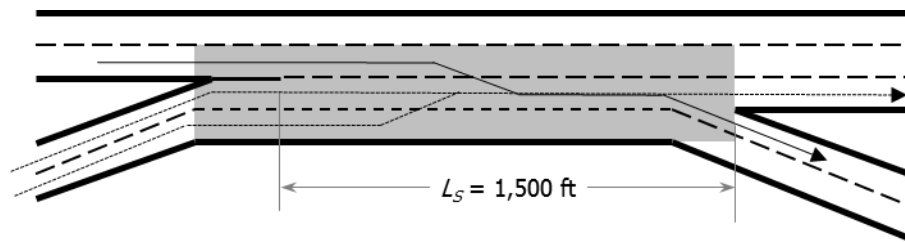


Exhibit 27-3 indicates that ramp-to-freeway vehicles can execute their weaving maneuver without making a lane change (if they so desire). Thus, $LC_{RF} = 0$. Freeway-to-ramp vehicles must make at least one lane change to complete their desired maneuver. Thus, $LC_{FR} = 1$. If optional lane changes are considered, weaving movements can be accomplished with one or no lane changes from both entering ramp lanes and from the rightmost freeway lane. Thus, $N_{WL} = 3$.

Equation 13-2 can now be applied:

$$LC_{MIN} = (LC_{RF} \times v_{RF}) + (LC_{FR} \times v_{FR})$$

$$LC_{MIN} = (0 \times 1,197) + (1 \times 798) = 798 \text{ lc/h}$$

Step 4: Determine Maximum Weaving Length

The maximum length over which weaving movements may exist is determined by Equation 13-4. The determination is case-specific, and the result is valid only for the case under consideration:

$$L_{MAX} = [5,728(1 + VR)^{1.6}] - (1,566N_{WL})$$

$$L_{MAX} = [5,728(1 + 0.357)^{1.6}] - (1,566 \times 3) = 4,639 \text{ ft}$$

Since the maximum length is significantly greater than the actual segment length of 1,500 ft, weaving operations do exist, and the analysis may continue with the weaving analysis methodology.

Step 5: Determine Weaving Segment Capacity

Capacity may be controlled by one of two factors: operations reaching a maximum density of 43 pc/mi/ln or by the weaving demand flow rate reaching 3,500 pc/h (for a weaving segment with $N_{WL} = 3$). Equations 13-5 through 13-10 are used to make these determinations.

Capacity Controlled by Density

$$c_{IWL} = c_{IFL} - [438.2(1 + VR)^{1.6}] + (0.0765L_S) + (119.8N_{WL})$$

$$c_{IWL} = 2,350 - [438.2(1 + 0.357)^{1.6}] + (0.0765 \times 1,500) + (119.8 \times 3)$$

$$c_{IWL} = 2,110 \text{ pc/h/ln}$$

$$c_W = c_{IWL} \times N \times f_{HV}$$

$$c_W = 2,110 \times 4 \times 0.952 = 8,038 \text{ veh/h}$$

Capacity Controlled by Maximum Weaving Flow Rate

$$c_{IW} = \frac{3,500}{VR} = \frac{3,500}{0.357} = 9,800 \text{ pc/h}$$

$$c_W = 9,800 \times 0.952 \times 1 = 9,333 \text{ veh/h}$$

Note that the methodology computes the capacity controlled by density in passenger cars per hour per lane, while the capacity controlled by maximum weaving flow rate is computed in passenger cars per hour. After conversion, however, both are in units of vehicles per hour.

The controlling value is the smaller of the two, or 8,038 veh/h. Since the total demand flow rate is only 5,320 veh/h, the capacity is clearly sufficient, and this situation will not result in LOS F.

Capacity of Input and Output Roadways

The capacity of the entry and exit roadways should also be checked, although this is rarely a factor in weaving segment operation. Basic capacities for the freeway entry and exit legs (with FFS = 65 mi/h) are taken from Chapter 12, while the capacity for the two-lane entry and exit ramps (with ramp FFS = 50 mi/h) is taken from Chapter 14. The comparisons are shown in Exhibit 27-4.

Leg	Demand Flow (pc/h)	Capacity (pc/h)
Freeway entry	2,094 + 798 = 2,892	2 × 2,350 = 4,700
Freeway exit	1,197 + 2,094 = 3,291	2 × 2,350 = 4,700
Ramp entry	1,197 + 1,497 = 2,694	4,100
Ramp exit	798 + 1,497 = 2,295	4,100

Exhibit 27-4
Example Problem 1: Capacity of Entry and Exit Roadways

As can be seen, capacity is sufficient on each of the entry and exit roadways and will therefore not affect operations within the weaving segment.

Step 6: Determine Lane-Changing Rates

Equations 13-11 through 13-17 are used to estimate the lane-changing rates of weaving and nonweaving vehicles in the weaving segment. In turn, these will be used to estimate weaving and nonweaving vehicle speeds.

Weaving Vehicle Lane-Changing Rate

$$LC_W = LC_{MIN} + 0.39[(L_S - 300)^{0.5} N^2 (1 + ID)^{0.8}]$$

$$LC_W = 798 + 0.39[(1,500 - 300)^{0.5} (4^2) (1 + 0.8)^{0.8}] = 1,144 \text{ lc/h}$$

Nonweaving Vehicle Lane-Changing Rate

$$I_{NW} = \frac{L_S \times ID \times v_{NW}}{10,000}$$

$$I_{NW} = \frac{1,500 \times 0.8 \times 3,591}{10,000} = 431 < 1,300$$

$$LC_{NW} = LC_{NW1} = (0.206v_{NW}) + (0.542L_S) - (192.6N)$$

$$LC_{NW} = (0.206 \times 3,591) + (0.542 \times 1,500) - (192.6 \times 4) = 782 \text{ lc/h}$$

Total Lane-Changing Rate

$$LC_{ALL} = LC_W + LC_{NW} = 1,144 + 782 = 1,926 \text{ lc/h}$$

Step 7: Determine Average Speeds of Weaving and Nonweaving Vehicles

The average speeds of weaving and nonweaving vehicles are computed from Equation 13-18 through Equation 13-21:

$$W = 0.226 \left(\frac{LC_{ALL}}{L_S} \right)^{0.789}$$

$$W = 0.226 \left(\frac{1,926}{1,500} \right)^{0.789} = 0.275$$

Then

$$S_W = 15 + \left(\frac{FFS \times SAF - 15}{1 + W} \right)$$

$$S_W = 15 + \left(\frac{FFS \times SAF - 15}{1 + W} \right) = 15 + \left(\frac{65 \times 1 - 15}{1 + 0.275} \right) = 54.2 \text{ mi/h}$$

and

$$S_{NW} = FFS \times SAF - (0.0072LC_{MIN}) - \left(0.0048 \frac{v}{N} \right)$$

$$S_{NW} = 65 \times 1 - (0.0072 \times 798) - \left(0.0048 \frac{5,586}{4} \right) = 52.5 \text{ mi/h}$$

Equation 13-22 is now used to compute the average speed of all vehicles in the segment:

$$S = \frac{v_W + v_{NW}}{\left(\frac{v_W}{S_W} \right) + \left(\frac{v_{NW}}{S_{NW}} \right)}$$

$$S = \frac{3,591 + 1,995}{\left(\frac{3,591}{52.5} \right) + \left(\frac{1,995}{54.2} \right)} = 53.1 \text{ mi/h}$$

Step 8: Determine LOS

Equation 13-23 is used to convert the average speed of all vehicles in the segment to an average density:

$$D = \frac{(v/N)}{S} = \frac{(5,586/4)}{53.1} = 26.3 \text{ pc/mi/ln}$$

The resulting density of 26.3 pc/mi/ln is compared with the LOS criteria of Exhibit 13-6. The LOS is C, since the density is within the specified range of 20 to 28 pc/h/ln for that level.

Discussion

As indicated by the results, this weaving segment operates at LOS C, with an average speed of 53.1 mi/h for all vehicles. Weaving vehicles travel a bit faster than nonweaving vehicles, primarily because the configuration favors weaving vehicles and many weaving maneuvers can be made without a lane change. In turn, the method estimates that nonweaving vehicles are affected by the weave turbulence, which results in a drop in speed of those movements. The demand flow rate of 4,841 veh/h is considerably less than the capacity of the segment, 8,038 veh/h. In other words, demand can grow significantly before reaching the capacity of the segment.

EXAMPLE PROBLEM 2: LOS FOR A RAMP WEAVE

The Weaving Segment

The weaving segment that is the subject of this operational analysis, under nonsevere weather conditions and without incidents, is shown in Exhibit 27-5. It is a typical ramp-weave segment.

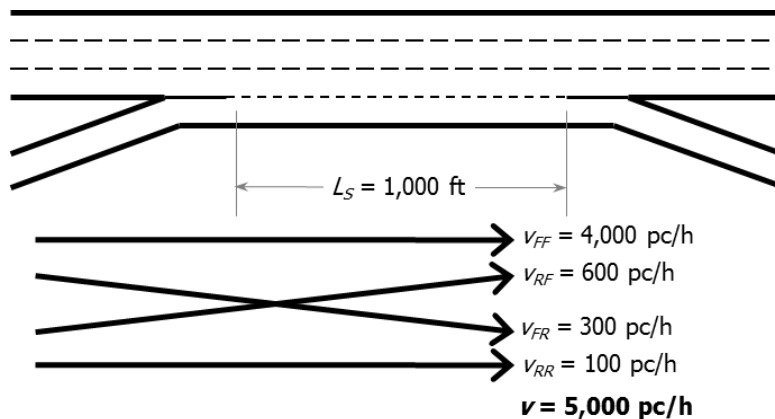


Exhibit 27-5
Example Problem 2: Ramp-Weave Segment Data

What is the capacity of the weaving segment of Exhibit 27-5, and at what LOS is it expected to operate with the demand flow rates as shown?

The Facts

In addition to the information given in Exhibit 27-5, the following facts are known about the subject weaving segment:

PHF = 1.00 (demands stated as flow rates);

Heavy vehicles = 0%; demand given in passenger car equivalents;

Driver population = regular commuters;
 FFS = 75 mi/h; RFFS = 40 mi/h;
 $c_{IFL} = 2,400$ pc/h/ln (for FFS = 75 mi/h);
 $ID = 1.0$ int/mi; and
 Terrain = level.

Comments

Because the demands have been specified as flow rates in passenger cars per hour under equivalent ideal conditions, Chapter 12 does not have to be consulted to obtain appropriate adjustment factors.

Several of the computational steps related to converting demand volumes to flow rates under equivalent ideal conditions are unnecessary, since demands are already specified in that form. Lane-changing characteristics will be estimated. The maximum length for weaving operations in this case will be estimated and compared with the actual length of the segment. The capacity of the segment will be estimated and compared with the demand to determine whether LOS F exists. If it does not, component flow speeds will be estimated and averaged. A density will be estimated and compared with the criteria of Exhibit 13-6 to determine the expected LOS.

Step 1: Input Data

All input data are stated in Exhibit 27-5 and the Facts section.

Step 2: Adjust Volume

Because all demands are stated as flow rates in passenger cars per hour under equivalent ideal conditions, no further conversions are necessary. Key volume parameters are as follows:

$$v_{FF} = 4,000 \text{ pc/h}$$

$$v_{FR} = 600 \text{ pc/h}$$

$$v_{RF} = 300 \text{ pc/h}$$

$$v_{RR} = 100 \text{ pc/h}$$

$$v_W = 600 + 300 = 900 \text{ pc/h}$$

$$v_{NW} = 4,000 + 100 = 4,100 \text{ pc/h}$$

$$v = 4,100 + 900 = 5,000 \text{ pc/h}$$

$$VR = \frac{900}{5,000} = 0.180$$

Step 3: Determine Configuration Characteristics

The configuration is examined to determine the values of LC_{RF} , LC_{FR} , and N_{WL} . These determinations are illustrated in Exhibit 27-6. From these values, the minimum number of lane changes by weaving vehicles LC_{MIN} is then computed by using Equation 13-2.

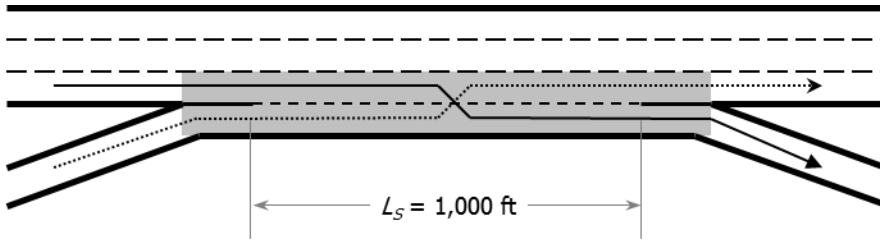


Exhibit 27-6
Example Problem 2:
Configuration Characteristics

From Exhibit 27-6, it is clear that all ramp-to-freeway vehicles must make at least one lane change ($LC_{RF} = 1$) and that all freeway-to-ramp vehicles must make at least one lane change ($LC_{FR} = 1$). It is also clear that a weaving maneuver can only be completed with a single lane change from the right lane of the freeway or the auxiliary lane ($N_{WL} = 2$). Then, by using Equation 13-2, LC_{MIN} is computed as

$$LC_{MIN} = (LC_{RF} \times v_{RF}) + (LC_{FR} \times v_{FR})$$

$$LC_{MIN} = (1 \times 600) + (1 \times 300) = 900 \text{ lc/h}$$

Step 4: Determine Maximum Weaving Length

The maximum length over which weaving operations may exist for the segment described is found by using Equation 13-4:

$$L_{MAX} = [5,728(1 + VR)^{1.6}] - (1,566N_{WL})$$

$$L_{MAX} = [5,728(1 + 0.180)^{1.6}] - (1,566 \times 2) = 4,333 \text{ ft} > 1,000 \text{ ft}$$

Since the maximum length for weaving operations significantly exceeds the actual length, this is a weaving segment, and the analysis continues.

Step 5: Determine Weaving Segment Capacity

The capacity of the weaving segment is controlled by one of two limiting factors: density reaches 43 pc/mi/ln or weaving demand reaches 2,400 pc/h for the configuration of Exhibit 27-5 (a ramp weave with $N_{WL} = 2$).

Capacity Limited by Density

The capacity limited by reaching a density of 43 pc/mi/ln is estimated by using Equation 13-5 and Equation 13-6:

$$c_{IWL} = c_{IFL} - [438.2(1 + VR)^{1.6}] + (0.0765L_S) + (119.8N_{WL})$$

$$c_{IWL} = 2,400 - [438.2(1 + 0.180)^{1.6}] + (0.0765 \times 1,000) + (119.8 \times 2)$$

$$c_{IWL} = 2,145 \text{ pc/h/ln}$$

$$c_W = c_{IWL} \times N \times f_{HV}$$

$$c_W = 2,145 \times 4 = 8,580 \text{ pc/h}$$

Capacity Limited by Weaving Demand Flow

The capacity limited by the weaving demand flow is estimated by using Equation 13-7 and Equation 13-8:

$$c_{IW} = \frac{2,400}{VR} = \frac{2,400}{0.180} = 13,333 \text{ pc/h}$$

$$c_W = c_{IW} \times f_{HV}$$

$$c_W = 13,333 \times 1 = 13,333 \text{ pc/h}$$

The controlling capacity is the smaller value, or 8,580 pc/h. At this point, the value is usually stated as vehicles per hour. In this case, because inputs were already adjusted and were stated in passenger cars per hour, conversions back to vehicles per hour are not possible.

Since the capacity of the weaving segment is larger than the demand flow rate of 5,000 pc/h, LOS F does not exist, and the analysis may continue.

Capacity of Input and Output Roadways

Although it is rarely a factor in weaving operations, the capacity of input and output roadways should be checked to ensure that no deficiencies exist. There are three input and output freeway lanes (with FFS = 75 mi/h) and one lane on the entrance and exit ramps (with ramp FFS = 35 mi/h). The criteria of Chapter 12 and Chapter 14, respectively, are used to determine the capacity of freeway legs and ramps. Demand flows and capacities are compared in Exhibit 27-7.

Exhibit 27-7
Example Problem 2: Capacity of Entry and Exit Legs

Leg	Demand Flow (pc/h)	Capacity (pc/h)
Freeway entry	4,000 + 300 = 4,300	3 × 2,400 = 7,200
Freeway exit	4,000 + 600 = 4,600	3 × 2,400 = 7,200
Ramp entry	600 + 100 = 700	2,000
Ramp exit	300 + 100 = 400	2,000

The capacity of all input and output roadways is sufficient to accommodate the demand flow rates.

Step 6: Determine Lane-Changing Rates

Equation 13-11 through Equation 13-17 are used to estimate the lane-changing rates of weaving and nonweaving vehicles in the weaving segment. In turn, these will be used to estimate weaving and nonweaving vehicle speeds.

Weaving Vehicle Lane-Changing Rate

$$LC_W = LC_{MIN} + 0.39[(L_S - 300)^{0.5} N^2 (1 + ID)^{0.8}]$$

$$LC_W = 900 + 0.39[(1,000 - 300)^{0.5} (4^2) (1 + 1)^{0.8}] = 1,187 \text{ lc/h}$$

Nonweaving Vehicle Lane-Changing Rate

$$I_{NW} = \frac{L_S \times ID \times v_{NW}}{10,000}$$

$$I_{NW} = \frac{1,000 \times 1 \times 4,100}{10,000} = 410 < 1,300$$

$$LC_{NW} = LC_{NW1} = (0.206v_{NW}) + (0.542L_S) - (192.6N)$$

$$LC_{NW} = (0.206 \times 4,100) + (0.542 \times 1,000) - (192.6 \times 4) = 616 \text{ lc/h}$$

Total Lane-Changing Rate

$$LC_{ALL} = LC_W + LC_{NW} = 1,187 + 616 = 1,803 \text{ lc/h}$$

Step 7: Determine Average Speeds of Weaving and Nonweaving Vehicles

The average speeds of weaving and nonweaving vehicles are computed from Equation 13-18 through Equation 13-21:

$$W = 0.226 \left(\frac{LC_{ALL}}{L_S} \right)^{0.789}$$

$$W = 0.226 \left(\frac{1,803}{1,000} \right)^{0.789} = 0.360$$

Then

$$S_W = 15 + \left(\frac{FFS \times SAF - 15}{1 + W} \right)$$

$$S_W = 15 + \left(\frac{75 \times 1 - 15}{1 + 0.360} \right) = 59.1 \text{ mi/h}$$

and

$$S_{NW} = FFS \times SAF - (0.0072LC_{MIN}) - \left(0.0048 \frac{v}{N} \right)$$

$$S_{NW} = 75 \times 1 - (0.0072 \times 900) - \left(0.0048 \frac{5,000}{4} \right) = 62.5 \text{ mi/h}$$

Equation 13-22 is now used to compute the average speed of all vehicles in the segment:

$$S = \frac{v_W + v_{NW}}{\left(\frac{v_W}{S_W} \right) + \left(\frac{v_{NW}}{S_{NW}} \right)}$$

$$S = \frac{4,100 + 900}{\left(\frac{4,100}{62.5} \right) + \left(\frac{900}{59.1} \right)} = 61.9 \text{ mi/h}$$

Step 8: Determine LOS

The average density in the weaving segment is estimated by using Equation 13-23.

$$D = \frac{(v/N)}{S} = \frac{(5,000/4)}{61.9} = 20.2 \text{ pc/mi/ln}$$

From Exhibit 13-6, this density is within the stated boundaries of LOS C (20 to 28 pc/mi/ln). However, it is very close to the LOS B boundary condition.

Discussion

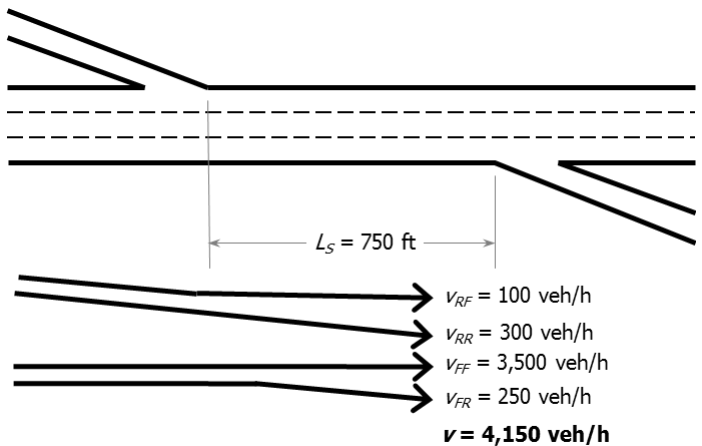
As noted, the segment is operating well (LOS C) and is close to the LOS B boundary. Weaving and nonweaving speeds are relatively high, suggesting a stable flow. The demand flow rate of 5,000 pc/h is well below the capacity of the segment (8,580 pc/h). Weaving vehicles travel somewhat more slowly than nonweaving vehicles, which is typical of ramp-weave segments, where the vast majority of nonweaving vehicles are running from freeway to freeway.

EXAMPLE PROBLEM 3: LOS OF A TWO-SIDED WEAVING SEGMENT

The Weaving Segment

The weaving segment that is the subject of this example problem is shown in Exhibit 27-8. The analysis assumes no adverse weather effects or incidents in the segment.

Exhibit 27-8
 Example Problem 3: Two-Sided Weaving Segment Data



What is the expected LOS and capacity for the weaving segment of Exhibit 27-8?

The Facts

In addition to the information contained in Exhibit 27-8, the following facts concerning the weaving segment are known:

- PHF = 0.94 (all movements);
- Heavy vehicles = 11% trucks;
- Driver population = regular commuters;
- FFS = 60 mi/h; ramp FFS = 30 mi/h;
- $c_{IFL} = 2,300 \text{ pc/h/ln}$ (for FFS = 60 mi/h);
- ID = 2 int/mi; and
- Terrain = rolling.

Comments

Because this example illustrates the analysis of a two-sided weaving segment, several key parameters are different from those for a more typical one-side weaving segment.

In a two-sided weaving segment, only the ramp-to-ramp flow is considered to be a weaving flow. While the freeway-to-freeway flow technically weaves with the ramp-to-ramp flow, the operation of freeway-to-freeway vehicles more closely resembles that of nonweaving vehicles. These vehicles generally make few lane changes as they move through the segment in a freeway lane. This segment is in a busy urban corridor with a high interchange density and a relatively low FFS for the freeway.

Solution steps are the same as in the first two example problems. However, since the segment is a two-sided weaving segment, some of the key values will be computed differently, as described in the methodology.

Component demand volumes will be converted to equivalent flow rates in passenger cars per hour under ideal conditions, and key demand parameters will be calculated. A maximum weaving length will be estimated to determine

whether a weaving analysis is appropriate. The capacity of the weaving segment will be estimated to determine whether LOS F exists. In addition, the segment density will be estimated to evaluate whether LOS F exists. If it does not, lane-changing parameters, speeds, density, and LOS will be estimated.

Step 1: Input Data

All information concerning this example problem is given in Exhibit 27-8 and the Facts section.

Step 2: Adjust Volume

To convert demand volumes to flow rates under equivalent ideal conditions, Chapter 12 must be consulted to obtain the following values:

$$E_T = 3.0 \text{ (for rolling terrain)}$$

Then

$$f_{HV} = \frac{1}{1 + P_T(E_T - 1)} = \frac{1}{1 + 0.11(3 - 1)} = 0.82$$

Component demand volumes may now be converted to flow rates under equivalent ideal conditions:

$$v_i = \frac{V_i}{PHF \times f_{HV}}$$

$$v_{FF} = \frac{3,500}{0.94 \times 0.82} = 4,541 \text{ pc/h}$$

$$v_{FR} = \frac{250}{0.94 \times 0.82} = 324 \text{ pc/h}$$

$$v_{RF} = \frac{100}{0.94 \times 0.82} = 130 \text{ pc/h}$$

$$v_{RR} = \frac{300}{0.94 \times 0.82} = 389 \text{ pc/h}$$

Because this is a two-sided weaving segment, the only weaving flow is the ramp-to-ramp flow. All other flows are treated as nonweaving. Then

$$v_W = 389 \text{ pc/h}$$

$$v_{NW} = 4,541 + 324 + 130 = 4,995 \text{ pc/h}$$

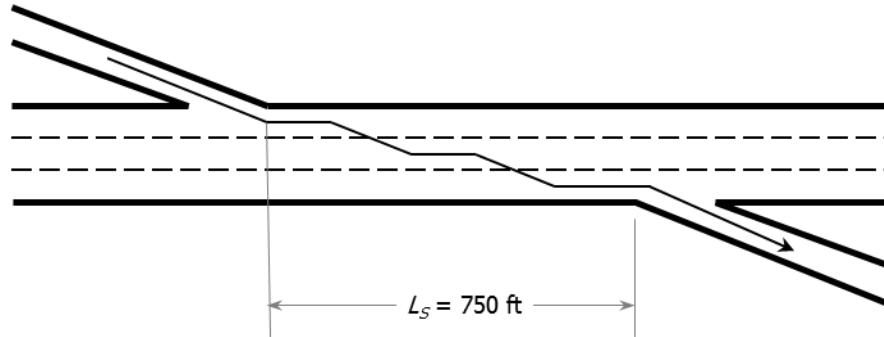
$$v = 4,995 + 389 = 5,384 \text{ pc/h}$$

$$VR = 389/5,384 = 0.072$$

Exhibit 27-9
Example Problem 3:
Configuration Characteristics

Step 3: Determine Configuration Characteristics

The determination of configuration characteristics is also affected by the existence of a two-sided weaving segment. Exhibit 27-9 illustrates the determination of LC_{RR} , the key variable for two-sided weaving segments. For such segments, $N_{WL} = 0$ by definition.



From Exhibit 27-9, ramp-to-ramp vehicles must make two lane changes to complete their desired weaving maneuver. Then

$$LC_{MIN} = (LC_{RR} \times v_{RR}) = 2 \times 389 = 778 \text{ lc/h}$$

Step 4: Determine Maximum Weaving Length

The maximum length of a weaving segment for this configuration and demand scenario is estimated by using Equation 13-4:

$$L_{MAX} = [5,728(1 + VR)^{1.6}] - (1,566N_{WL})$$

$$L_{MAX} = [5,728(1 + 0.072)^{1.6}] - (1,566 \times 0) = 6,405 \text{ ft} > 750 \text{ ft}$$

In this two-sided configuration, the impacts of weaving on operations could be felt at lengths as long as 6,405 ft. Since this is significantly greater than the actual length of 750 ft, the segment clearly operates as a weaving segment, and therefore the methodology of this chapter should be applied.

Step 5: Determine Weaving Segment Capacity

The capacity of a two-sided weaving segment can only be estimated when a density of 43 pc/h/ln is reached. This estimation is made by using Equation 13-5 and Equation 13-6:

$$c_{IWL} = c_{IFL} - [438.2(1 + VR)^{1.6}] + (0.0765L_S) + (119.8N_{WL})$$

$$c_{IWL} = 2,300 - [438.2(1 + 0.072)^{1.6}] + (0.0765 \times 750) + (119.8 \times 0)$$

$$c_{IWL} = 1,867 \text{ pc/h/ln}$$

$$c_W = c_{IWL} \times N \times f_{HV}$$

$$c_W = 1,867 \times 3 \times 0.816 = 4,573 \text{ veh/h} > 4,150 \text{ veh/h}$$

Because the capacity of the segment exceeds the demand volume (in vehicles per hour), LOS F is not expected, and the analysis may be continued.

The capacity of input and output roadways must also be checked. The freeway input and output roadways have three lanes and a capacity of $2,300 \times 3 = 6,900$ pc/h (Chapter 12). The one-lane ramps (with ramp FFS = 30 mi/h) have a capacity of 1,900 pc/h (Chapter 14). Exhibit 27-10 compares these capacities with the demand flow rates (in pc/h).

Leg	Demand Flow (pc/h)	Capacity (pc/h)
Freeway entry	$4,541 + 324 = 4,865$	6,900
Freeway exit	$4,541 + 130 = 4,671$	6,900
Ramp entry	$130 + 389 = 519$	1,900
Ramp exit	$324 + 389 = 713$	1,900

Exhibit 27-10
Example Problem 3: Capacity of Entry and Exit Legs

All demands are below their respective capacities.

Step 6: Determine Lane-Changing Rates

Equation 13-11 through Equation 13-17 are used to estimate the lane-changing rates of weaving and nonweaving vehicles in the weaving segment. In turn, these will be used to estimate weaving and nonweaving vehicle speeds.

Weaving Vehicle Lane-Changing Rate

$$LC_W = LC_{MIN} + 0.39[(L_S - 300)^{0.5} N^2 (1 + ID)^{0.8}]$$

$$LC_W = 778 + 0.39[(750 - 300)^{0.5} (3^2) (1 + 2)^{0.8}] = 960 \text{ lc/h}$$

Nonweaving Vehicle Lane-Changing Rate

$$I_{NW} = \frac{L_S \times ID \times v_{NW}}{10,000}$$

$$I_{NW} = \frac{750 \times 2 \times 5,015}{10,000} = 752 < 1,300$$

$$LC_{NW} = LC_{NW1} = (0.206v_{NW}) + (0.542L_S) - (192.6N)$$

$$LC_{NW} = (0.206 \times 5,015) + (0.542 \times 750) - (192.6 \times 3) = 861 \text{ lc/h}$$

Total Lane-Changing Rate

$$LC_{ALL} = LC_W + LC_{NW} = 960 + 861 = 1,821 \text{ lc/h}$$

Step 7: Determine Average Speeds of Weaving and Nonweaving Vehicles

The average speeds of weaving and nonweaving vehicles are computed from Equation 13-18 through Equation 13-21:

$$W = 0.226 \left(\frac{LC_{ALL}}{L_S} \right)^{0.789}$$

$$W = 0.226 \left(\frac{1,821}{750} \right)^{0.789} = 0.455$$

Then

$$S_W = 15 + \left(\frac{FFS \times SAF - 15}{1 + W} \right)$$

$$S_W = 15 + \left(\frac{60 \times 1 - 15}{1 + 0.455} \right) = 45.9 \text{ mi/h}$$

and

$$S_{NW} = FFS \times SAF - (0.0072LC_{MIN}) - \left(0.0048 \frac{v}{N}\right)$$

$$S_{NW} = 60 \times 1 - (0.0072 \times 778) - \left(0.0048 \frac{5,384}{3}\right) = 45.8 \text{ mi/h}$$

Equation 13-22 is now used to compute the average speed of all vehicles in the segment:

$$S = \frac{v_W + v_{NW}}{\left(\frac{v_W}{S_W}\right) + \left(\frac{v_{NW}}{S_{NW}}\right)}$$

$$S = \frac{389 + 4,995}{\left(\frac{389}{45.9}\right) + \left(\frac{4,995}{45.8}\right)} = 45.8 \text{ mi/h}$$

Step 8: Determine LOS

The average density in this two-sided weaving segment is estimated by using Equation 13-23:

$$D = \frac{(v/N)}{S} = \frac{(5,384/3)}{45.8} = 39.2 \text{ pc/mi/ln}$$

From Equation 13-12, this density is clearly in LOS E. It is not far from the 43 pc/h/ln that would likely cause a breakdown.

Discussion

This two-sided weaving segment operates at LOS E, not far from the LOS E/F boundary. The v/c ratio is $4,150/4,573 = 0.91$. The major problem is that 300 veh/h crossing the freeway from ramp to ramp creates a great deal of turbulence in the traffic stream and limits capacity. The speeds estimated for weaving and nonweaving vehicles are effectively the same in this example. Two-sided weaving segments do not operate well with such large numbers of ramp-to-ramp vehicles. If this were a basic freeway segment, the per lane flow rate of $5,405/3 = 1,802 \text{ pc/h/ln}$ would not be considered excessive and would be well within a basic freeway segment’s capacity of 2,300 pc/h/ln.

EXAMPLE PROBLEM 4: DESIGN OF A MAJOR WEAVING SEGMENT FOR A DESIRED LOS

The Weaving Segment

A weaving segment is to be designed between two major junctions in which two urban freeways join and then separate, as shown in Exhibit 27-11. The analysis assumes no adverse weather effects or incidents in the segment. Entry and exit legs have the numbers of lanes shown. The maximum length of the weaving segment is 1,000 ft, based on the location of the junctions. The FFS of all entry and exit legs is 75 mi/h. All demands are shown as flow rates under equivalent ideal conditions.

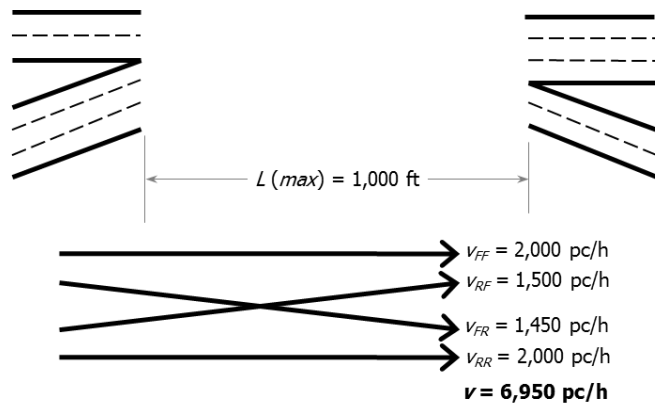


Exhibit 27-11
 Example Problem 4: Major
 Weaving Segment Data

What design would be appropriate to deliver LOS C for the demand flow rates shown?

The Facts

In addition to the information contained in Exhibit 27-11, the following facts are known concerning this weaving segment:

PHF = 1.00 (all demands stated as flow rates),

Heavy vehicles = 0% trucks (all demands in pc/h),

Driver population = regular commuters,

FFS = 75 mi/h (all legs and weaving segment),

$c_{IFL} = 2,400 \text{ pc/h/ln}$ (for FFS = 75 mi/h),

ID = 1 int/mi, and

Terrain = level.

Comments

As is the case in any weaving segment design, considerable constraints are imposed. The problem states that the maximum length is 1,000 ft, no doubt limited by locational issues for the merge and diverge junctions. Shorter lengths are probably not worth investigating, and the maximum should be assumed for all trial designs. The simplest design merely connects entering lanes with exit lanes in a straightforward manner, producing a section of five lanes. A section with four lanes could be considered by merging two lanes into one at the entry gore and separating it into two again at the exit gore. In any event, the design is limited to a section of four or five lanes. No other widths would work without major additions to input and output legs. The configuration cannot be changed without adding a lane to at least one of the entry or exit legs. Thus, the initial trial will be at a length of 1,000 ft, with the five entry lanes connected directly to the five exit lanes, with no changes to the exit or entry leg designs. If this does not produce an acceptable operation, changes will be considered.

While the problem clearly states that all legs are freeways, no feasible configuration produces a two-sided weaving section. Thus, to fit within the one-sided analysis methodology, the right-side entry and exit legs will be classified as ramps in the computational analysis. Note that by inspection, the capacity of all

entry and exit legs is more than sufficient to handle the demand flow rates indicated.

Step 1: Input Data—Trial 1

All input information is given in Exhibit 27-11 and in the accompanying Facts section for this example problem.

Step 2: Adjust Volume—Trial 1

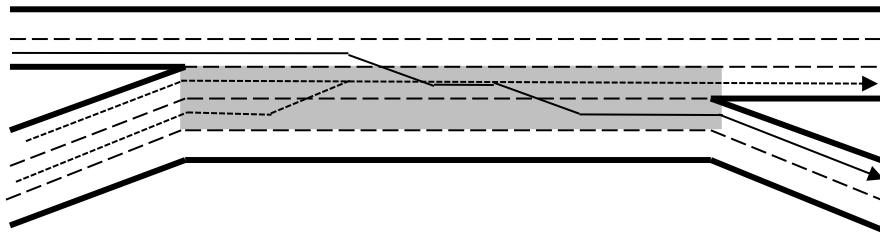
All demands are already stated as flow rates in passenger cars per hour under equivalent ideal conditions. No further adjustments are needed. Critical demand values are as follows:

$$\begin{aligned}
 v_{FF} &= 2,000 \text{ pc/h} \\
 v_{FR} &= 1,450 \text{ pc/h} \\
 v_{RF} &= 1,500 \text{ pc/h} \\
 v_{RR} &= 2,000 \text{ pc/h} \\
 v_W &= 1,500 + 1,450 = 2,950 \text{ pc/h} \\
 v_{NW} &= 2,000 + 2,000 = 4,000 \text{ pc/h} \\
 v &= 2,950 + 4,000 = 6,950 \text{ pc/h} \\
 VR &= 2,950/6,950 = 0.424
 \end{aligned}$$

Step 3: Determine Configuration Characteristics—Trial 1

Exhibit 27-12 illustrates the weaving segment formed under the assumed design discussed previously.

Exhibit 27-12
Example Problem 4: Trial Design 1



The direct connection of entry and exit legs produces a weaving segment in which the ramp-to-freeway movement can be made without a lane change ($LC_{RF} = 0$). However, freeway-to-ramp vehicles must make two lane changes ($LC_{FR} = 2$). With regard to the lane-changing pattern, there are no lanes on the entering freeway leg from which a weaving maneuver can be made with one or no lane changes. However, ramp drivers wishing to weave can enter on either of the two left ramp lanes and weave with one or no lane changes. Thus, $N_{WL} = 2$.

By using Equation 13-2, LC_{MIN} is computed as

$$\begin{aligned}
 LC_{MIN} &= (LC_{RF} \times v_{RF}) + (LC_{FR} \times v_{FR}) \\
 LC_{MIN} &= (0 \times 1,500) + (2 \times 1,450) = 2,900 \text{ lc/h}
 \end{aligned}$$

Step 4: Determine Maximum Weaving Length—Trial 1

The maximum length of a weaving segment for this configuration and demand scenario is estimated by using Equation 13-4:

$$L_{MAX} = [5,728(1 + VR)^{1.6}] - (1,566N_{WL})$$

$$L_{MAX} = [5,728(1 + 0.424)^{1.6}] - (1,566 \times 2) = 6,950 \text{ ft} > 1,000 \text{ ft}$$

Since the maximum length is much greater than the actual length of 1,000 ft, analysis of the segment with this chapter's methodology is appropriate.

Step 5: Determine Weaving Segment Capacity—Trial 1

The capacity of the weaving segment is controlled by one of two limiting factors: density reaches 43 pc/mi/ln or weaving demand reaches 2,400 pc/h for the configuration of Exhibit 27-12.

Capacity Limited by Density

The capacity limited by reaching a density of 43 pc/mi/ln is estimated by using Equation 13-5 and Equation 13-6:

$$c_{IWL} = c_{IFL} - [438.2(1 + VR)^{1.6}] + (0.0765L_S) + (119.8N_{WL})$$

$$c_{IWL} = 2,400 - [438.2(1 + 0.424)^{1.6}] + (0.0765 \times 1,000) + (119.8 \times 2)$$

$$c_{IWL} = 1,944 \text{ pc/h/ln}$$

$$c_W = c_{IWL} \times N \times f_{HV}$$

$$c_W = 1,944 \times 5 \times 1 = 9,721 \text{ pc/h}$$

Capacity Limited by Weaving Demand Flow

The capacity limited by the weaving demand flow is estimated by using Equation 13-7 and Equation 13-8:

$$c_{IW} = \frac{2,400}{VR} = \frac{2,400}{0.424} = 5,654 \text{ pc/h}$$

$$c_W = c_{IW} \times f_{HV} = 5,654 \times 1 = 5,654 \text{ pc/h}$$

In this case, the capacity of the segment is limited by the maximum weaving flow rate, which limits total capacity of the segment to 5,654 pc/h, which is smaller than the total demand flow rate of 6,950 pc/h. Thus, this section is expected to operate at LOS F. No further analysis is possible with this methodology.

Discussion: Trial 1

This weaving segment would be expected to fail under the proposed design. The critical feature appears to be the configuration. Note that the capacity is limited by the maximum weaving flows that can be sustained, not by a density expected to produce queuing. This is primarily due to the freeway-to-ramp flow, which must make two lane changes. The number of lane changes can be reduced to one by adding one lane to the "ramp" at the exit gore area. This not only reduces the number of lane changes made by 1,450 freeway-to-ramp vehicles but also increases the value of N_W from 2 to 3. In turn, the segment's capacity (as limited by weaving flow rate) is effectively increased to $3,500/VR = 3,500/0.424 =$

8,255 pc/h, which is well in excess of the demand flow rate of 6,950 pc/h. Another analysis (Trial 2) will be conducted by using this approach.

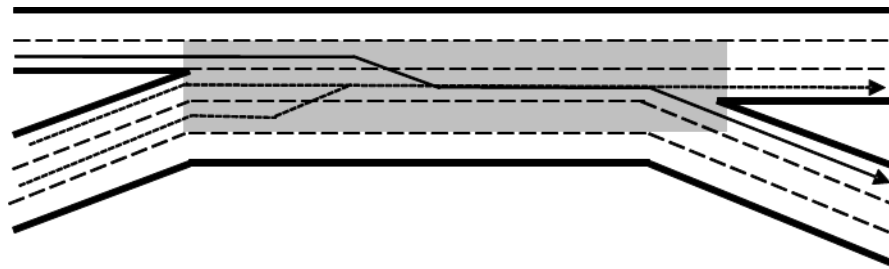
Steps 1 and 2: Input Data and Adjust Volume—Trial 2

Steps 1 and 2 are the same as for Trial 1. They are not repeated here. The new configuration affects the results beginning with Step 3.

Step 3: Determine Configuration Characteristics—Trial 2

Exhibit 27-13 illustrates the new configuration that will result from the changes discussed above. The addition of a lane to the exit-ramp leg allows the freeway-to-ramp movement to be completed with only one lane change ($LC_{FR} = 1$). The value of LC_{RF} is not affected and remains 0. The right lane of the freeway-entry leg can also be used by freeway-to-ramp drivers to make a weaving maneuver with a single lane change, increasing N_{WL} to 3.

Exhibit 27-13
Example Problem 4:
Trial Design 2



Then

$$LC_{MIN} = (LC_{RF} \times v_{RF}) + (LC_{FR} \times v_{FR})$$

$$LC_{MIN} = (0 \times 1,500) + (1 \times 1,450) = 1,450 \text{ lc/h}$$

Step 4: Determine Maximum Weaving Length—Trial 2

The maximum length of a weaving segment for this configuration and demand scenario is estimated by using Equation 13-4:

$$L_{MAX} = [5,728(1 + VR)^{1.6}] - (1,566N_{WL})$$

$$L_{MAX} = [5,728(1 + 0.424)^{1.6}] - (1,566 \times 3) = 5,391 \text{ ft} > 1,000 \text{ ft}$$

Since the maximum length is much greater than the actual length of 1,000 ft, analyzing the segment by using this chapter’s methodology is appropriate.

Step 5: Determine Weaving Segment Capacity—Trial 2

The capacity of the weaving segment is controlled by one of two limiting factors: density reaches 43 pc/mi/ln or weaving demand reaches 3,500 pc/h for the configuration of Exhibit 27-13.

Capacity Limited by Density

The capacity limited by reaching a density of 43 pc/mi/ln is estimated by using Equation 13-5 and Equation 13-6:

$$c_{IWL} = c_{IFL} - [438.2(1 + VR)^{1.6}] + (0.0765L_S) + (119.8N_{WL})$$

$$c_{IWL} = 2,400 - [438.2(1 + 0.424)^{1.6}] + (0.0765 \times 1,000) + (119.8 \times 3)$$

$$c_{IWL} = 2,064 \text{ pc/h/ln}$$

$$c_W = c_{IWL} \times N \times f_{HV}$$

$$c_W = 2,064 \times 5 \times 1 = 10,320 \text{ pc/h}$$

Capacity Limited by Weaving Demand Flow

The capacity limited by the weaving demand flow is estimated by using Equation 13-7 and Equation 13-8:

$$c_{IW} = \frac{3,500}{VR} = \frac{3,500}{0.424} = 8,255 \text{ pc/h}$$

$$c_W = c_{IW} \times f_{HV} \times f_p = 8,255 \times 1 \times 1 = 8,255 \text{ pc/h}$$

Once again, the capacity of the segment is limited by the maximum weaving flow rate: the difference is that now the capacity is 8,255 pc/h. This is larger than the total demand flow rate of 6,950 pc/h. Thus, this section is expected to operate without breakdown, and the analysis may continue.

Step 6: Determine Lane-Changing Rates—Trial 2

Equation 13-11 through Equation 13-17 are used to estimate the lane-changing rates of weaving and nonweaving vehicles in the weaving segment. In turn, these will be used to estimate weaving and nonweaving vehicle speeds.

Weaving Vehicle Lane-Changing Rate

$$LC_W = LC_{MIN} + 0.39[(L_S - 300)^{0.5} N^2 (1 + ID)^{0.8}]$$

$$LC_W = 1,450 + 0.39[(1,000 - 300)^{0.5} (5^2) (1 + 1)^{0.8}] = 1,899 \text{ lc/h}$$

Nonweaving Vehicle Lane-Changing Rate

$$I_{NW} = \frac{L_S \times ID \times v_{NW}}{10,000}$$

$$I_{NW} = \frac{1,000 \times 1 \times 4,000}{10,000} = 400 < 1,300$$

$$LC_{NW} = (0.206v_{NW}) + (0.542L_S) - (192.6N)$$

$$LC_{NW} = (0.206 \times 4,000) + (0.542 \times 1,000) - (192.6 \times 5) = 403 \text{ lc/h}$$

Total Lane-Changing Rate

$$LC_{ALL} = LC_W + LC_{NW} = 1,899 + 403 = 2,302 \text{ lc/h}$$

Step 7: Determine Average Speeds of Weaving and Nonweaving Vehicles—Trial 2

The average speeds of weaving and nonweaving vehicles are computed from Equation 13-18 through Equation 13-21.

$$W = 0.226 \left(\frac{LC_{ALL}}{L_S} \right)^{0.789}$$

$$W = 0.226 \left(\frac{2,302}{1,000} \right)^{0.789} = 0.436$$

Then

$$S_W = 15 + \left(\frac{FFS \times SAF - 15}{1 + W} \right)$$

$$S_W = 15 + \left(\frac{75 \times 1 - 15}{1 + 0.436} \right) = 56.8 \text{ mi/h}$$

and

$$S_{NW} = FFS \times SAF - (0.0072LC_{MIN}) - \left(0.0048 \frac{v}{N} \right)$$

$$S_{NW} = 75 \times 1 - (0.0072 \times 1,450) - \left(0.0048 \frac{6,950}{5} \right) = 57.9 \text{ mi/h}$$

Equation 13-22 is now used to compute the average speed of all vehicles in the segment:

$$S = \frac{v_W + v_{NW}}{\left(\frac{v_W}{S_W} \right) + \left(\frac{v_{NW}}{S_{NW}} \right)}$$

$$S = \frac{4,000 + 2,950}{\left(\frac{4,000}{57.9} \right) + \left(\frac{2,950}{56.8} \right)} = 57.4 \text{ mi/h}$$

Step 8: Determine the Level of Service—Trial 2

The average density in the weaving segment is estimated by using Equation 13-23:

$$D = \frac{(v/N)}{S} = \frac{(6,950/5)}{57.4} = 24.2 \text{ pc/mi/ln}$$

From Exhibit 13-12, this density is within the stated boundaries of LOS C (20 to 28 pc/mi/ln). Since the design target was LOS C, the second trial design is acceptable.

Discussion: Trial 2

The relatively small change in the configuration makes all the difference in this design. LOS C can be achieved by adding a lane to the right exit leg; without it, the section fails because of excessive weaving turbulence. If the extra lane is not needed on the departing freeway leg, it will be dropped somewhere downstream, perhaps as part of the next interchange. The extra lane would have to be carried for several thousand feet to be effective. An added lane generally will not be fully utilized by drivers if they are aware that it will be immediately dropped.

EXAMPLE PROBLEM 5: CONSTRUCTING A SERVICE VOLUME TABLE FOR A WEAVING SEGMENT

This example shows how a table of service flow rates or service volumes or both can be constructed for a weaving section with certain specified characteristics. The methodology of this chapter does not directly yield service flow rates or service volumes, but they can be developed by using spreadsheets or more sophisticated computer programs.

The key issue is the definition of the threshold values for the various levels of service. For weaving sections on freeways, levels of service are defined as limiting densities, as shown in Exhibit 27-14:

LOS	Maximum Density (pc/mi/ln)
A	10
B	20
C	28
D	35

Exhibit 27-14
Example Problem 5: Maximum Density Thresholds for LOS A-D

By definition, the service flow rate at LOS E is the capacity of the weaving section, which may or may not be keyed to a density.

Before the construction of such a table is illustrated, several key definitions should be reviewed:

- *Service flow rate (under ideal conditions)*: The maximum rate of flow under equivalent ideal conditions that can be sustained while maintaining the designated LOS (*SFI*, pc/h).
- *Service flow rate (under prevailing conditions)*: The maximum rate of flow under prevailing conditions that can be sustained while maintaining the designated LOS (*SF*, veh/h).
- *Service volume*: The maximum hourly volume under prevailing conditions that can be sustained while maintaining the designated LOS in the worst 15 min of the hour (*SV*, veh/h).
- *Daily service volume*: The maximum annual average daily traffic under prevailing conditions that can be sustained while maintaining the designated LOS in the worst 15 min of the peak hour (*DSV*, veh/day).

Note that flow rates are for a 15-min period, often a peak 15 min within the analysis hour, or the peak hour. These values are related as follows:

$$SF_i = SFI_i \times f_{HV}$$

$$SV_i = SF_i \times PHF$$

$$DSV_i = \frac{SV_i}{K \times D}$$

This chapter's methodology estimates both the capacity and the density expected in a weaving segment of given geometric and demand characteristics. Conceptually, the approach to generating values of *SFI* is straightforward: for any given situation, keep increasing the input flow rates until the boundary density for the LOS is reached; the input flow rate is the *SFI* for that situation and LOS. This obviously involves many iterations. A spreadsheet can be programmed to do this, either semiautomatically with manual input of demands, or fully automatically, with the spreadsheet automatically generating solutions until a density match is found. The latter method is not very efficient and involves a typical spreadsheet program running for several hours. A program could, of course, be written to automate the entire process.

An Example

While all of the computations cannot be shown, demonstration results for a specific case can be illustrated. A service volume table is desired for a weaving section with the following characteristics:

- One-sided major weaving section
- Demand splits as follows:
 - $v_{FF} = 65\%$ of v
 - $v_{RF} = 15\%$ of v
 - $v_{FR} = 12\%$ of v
 - $v_{RR} = 8\%$ of v
- Trucks = 5%
- Level terrain
- PHF = 0.93
- Regular commuters in the traffic stream
- $ID = 1$ interchange/mi
- FFS = 65 mi/h

For these characteristics, a service volume table can be constructed for a range of lengths and widths and for configurations in which N_w is 2 and 3. For illustrative purposes, lengths of 500, 1,000, 1,500, 2,000, and 2,500 ft and widths of three, four, or five lanes will be used. In a major weaving section, one weaving flow does not have to make a lane change. In this example, the ramp-to-freeway movement is assumed to have this characteristic. The freeway-to-ramp movement would require one or two lane changes, on the basis of the value of N_{WL} .

First Computations

Initial computations will be aimed at establishing values of SFI for the situations described. A spreadsheet will be constructed in which the first column is the flow rate to be tested (in passenger cars per hour under ideal conditions), and the last column produces a density. Each line will be iterated (manually in this case) until each threshold density value is reached. Intermediate columns will be programmed to produce the intermediate results needed to get to this result. Because maximum length and capacity are decided at intermediate points, the applicable results will be manually entered before continuing. Such a procedure is less difficult than it seems once the basic computations are programmed. Manual iteration using the input flow rate is efficient; the operator will observe how fast the results are converging to the desired threshold and will change the inputs accordingly.

The results of a first computation are shown in Exhibit 27-15. They represent service flow rates under ideal conditions, SFI . Consistent with the HCM's results presentation guidelines (Chapter 7, Interpreting HCM and Alternative Tool Results), all hourly service flow rates and volumes in these exhibits have been rounded down to the nearest 100 passenger cars or vehicles for presentation.

LOS	Length of Weaving Section (ft)									
	500	1,000	1,500	2,000	2,500	500	1,000	1,500	2,000	2,500
<i>N</i> = 3; <i>N_{WL}</i> = 2					<i>N</i> = 3; <i>N_{WL}</i> = 3					
A	1,700	1,700	1,700	1,700	1,700	1,800	1,800	1,800	1,800	1,800
B	3,200	3,200	3,200	3,200	3,200	3,300	3,300	3,400	3,400	3,400
C	4,200	4,200	4,300	4,300	4,300	4,400	4,500	4,500	4,500	4,500
D	5,000	5,100	5,100	5,100	5,100	5,300	5,400	5,400	5,500	5,500
E	5,900	6,000	6,100	6,300	6,400	6,300	6,400	6,500	6,600	6,700
<i>N</i> = 4; <i>N_{WL}</i> = 2					<i>N</i> = 4; <i>N_{WL}</i> = 3					
A	2,200	2,300	2,300	2,300	2,300	2,300	2,300	2,300	2,300	2,300
B	4,100	4,200	4,200	4,200	4,200	4,300	4,400	4,400	4,400	4,400
C	5,400	5,500	5,500	5,500	5,600	5,800	5,900	5,900	5,900	5,900
D	6,300	6,500	6,500	6,600	6,600	6,900	7,000	7,100	7,100	7,100
E	7,900	8,000	8,200	8,400	8,500	8,400	8,500	8,700	8,800	9,000
<i>N</i> = 5; <i>N_{WL}</i> = 2					<i>N</i> = 5; <i>N_{WL}</i> = 3					
A	2,800	2,800	2,800	2,800	2,800	2,900	2,900	2,900	2,900	2,900
B	5,000	5,100	5,100	5,100	5,100	5,400	5,400	5,400	5,500	5,500
C	6,500	6,600	6,700	6,700	6,700	7,100	7,200	7,200	7,300	7,300
D	7,600	7,800	7,900	7,900	7,900	8,400	8,600	8,700	8,700	8,700
E	8,800	8,800	8,800	8,800	8,800	10,500	10,700	10,900	11,100	11,200

Exhibit 27-15

Example Problem 5: Service Flow Rates (pc/h) Under Ideal Conditions (*SF*)

Exhibit 27-16 shows service flow rates under prevailing conditions, *SF*. Each value in Exhibit 27-15 (before rounding) is multiplied by

$$f_{HV} = \frac{1}{1 + P_T(E_T - 1)} = \frac{1}{1 + 0.05(2 - 1)} = 0.952$$

LOS	Length of Weaving Section (ft)									
	500	1,000	1,500	2,000	2,500	500	1,000	1,500	2,000	2,500
<i>N</i> = 3; <i>N_{WL}</i> = 2					<i>N</i> = 3; <i>N_{WL}</i> = 3					
A	1,600	1,600	1,600	1,600	1,600	1,700	1,700	1,700	1,700	1,700
B	3,000	3,000	3,100	3,100	3,100	3,100	3,200	3,200	3,200	3,200
C	4,000	4,000	4,100	4,100	4,100	4,200	4,300	4,300	4,300	4,300
D	4,700	4,800	4,900	4,900	4,900	5,100	5,100	5,200	5,200	5,200
E	5,600	5,700	5,800	5,900	6,100	6,000	6,100	6,200	6,200	6,400
<i>N</i> = 4; <i>N_{WL}</i> = 2					<i>N</i> = 4; <i>N_{WL}</i> = 3					
A	2,100	2,100	2,200	2,200	2,200	2,200	2,200	2,200	2,200	2,200
B	3,900	4,000	4,000	4,000	4,000	4,100	4,200	4,200	4,200	4,200
C	5,100	5,200	5,200	5,300	5,300	5,500	5,600	5,600	5,600	5,600
D	5,900	6,200	6,200	6,300	6,300	6,600	6,700	6,700	6,800	6,800
E	7,500	7,700	7,800	7,900	8,100	8,000	8,100	8,200	8,400	8,500
<i>N</i> = 5; <i>N_{WL}</i> = 2					<i>N</i> = 5; <i>N_{WL}</i> = 3					
A	2,600	2,700	2,700	2,700	2,700	2,700	2,700	2,800	2,800	2,800
B	4,700	4,800	4,900	4,900	4,900	5,100	5,100	5,200	5,200	5,200
C	6,200	6,300	6,300	6,400	6,400	6,700	6,800	6,900	6,900	6,900
D	7,300	7,400	7,500	7,500	7,500	8,000	8,200	8,200	8,300	8,300
E	8,400	8,400	8,400	8,400	8,400	10,000	10,200	10,300	10,500	10,700

Exhibit 27-16

Example Problem 5: Service Flow Rates (veh/h) Under Prevailing Conditions (*SF*)

Exhibit 27-17 shows service volumes, *SV*. Each value in Exhibit 27-16 (before rounding) is multiplied by a PHF of 0.93.

Exhibit 27-17

Example Problem 5: Service Volumes (veh/h) Under Prevailing Conditions (SV)

LOS	Length of Weaving Section (ft)													
	500	1,000	1,500	2,000	2,500	500	1,000	1,500	2,000	2,500				
<i>N</i> = 3; <i>N_{WL}</i> = 2					<i>N</i> = 3; <i>N_{WL}</i> = 3									
A	1,500	1,500	1,500	1,500	1,500	1,500	1,500	1,500	1,500	1,500	1,500	1,500	1,500	1,500
B	2,800	2,800	2,800	2,800	2,900	2,900	2,900	3,000	3,000	3,000	3,000	3,000	3,000	3,000
C	3,700	3,700	3,800	3,800	3,800	3,900	4,000	4,000	4,000	4,000	4,000	4,000	4,000	4,000
D	4,400	4,500	4,500	4,500	4,500	4,700	4,800	4,800	4,800	4,800	4,800	4,800	4,800	4,800
E	5,200	5,300	5,400	5,500	5,600	5,500	5,600	5,700	5,800	5,800	5,800	5,800	5,800	5,900
<i>N</i> = 4; <i>N_{WL}</i> = 2					<i>N</i> = 4; <i>N_{WL}</i> = 3									
A	2,000	2,000	2,000	2,000	2,000	2,000	2,100	2,100	2,100	2,100	2,100	2,100	2,100	2,100
B	3,600	3,700	3,700	3,700	3,700	3,800	3,900	3,900	3,900	3,900	3,900	3,900	3,900	3,900
C	4,700	4,800	4,900	4,900	4,900	5,100	5,200	5,200	5,200	5,200	5,200	5,200	5,200	5,200
D	5,500	5,700	5,800	5,800	5,800	6,100	6,200	6,300	6,300	6,300	6,300	6,300	6,300	6,300
E	7,000	7,100	7,300	7,400	7,500	7,400	7,500	7,700	7,800	7,800	7,800	7,800	7,800	7,900
<i>N</i> = 5; <i>N_{WL}</i> = 2					<i>N</i> = 5; <i>N_{WL}</i> = 3									
A	2,400	2,500	2,500	2,500	2,500	2,500	2,500	2,600	2,600	2,600	2,600	2,600	2,600	2,600
B	4,400	4,500	4,500	4,500	4,500	4,700	4,800	4,800	4,800	4,800	4,800	4,800	4,800	4,800
C	5,700	5,800	5,900	5,900	5,900	6,200	6,400	6,400	6,400	6,400	6,400	6,400	6,400	6,400
D	6,700	6,900	7,000	7,000	7,000	7,500	7,600	7,700	7,700	7,700	7,700	7,700	7,700	7,700
E	7,800	7,800	7,800	7,800	7,800	9,300	9,400	9,600	9,800	9,800	9,800	9,800	9,800	9,900

Exhibit 27-18 shows daily service volumes, *DSV*. An illustrative *K*-factor of 0.08 (typical of a large urban area) and an illustrative *D*-factor of 0.55 (typical of an urban route without strong peaking by direction) are used. Each nonrounded value used to generate Exhibit 27-17 was divided by both of these numbers.

Exhibit 27-18

Example Problem 5: Daily Service Volumes (veh/day) Under Prevailing Conditions (*DSV*)

LOS	Length of Weaving Section (ft)													
	500	1,000	1,500	2,000	2,500	500	1,000	1,500	2,000	2,500				
<i>N</i> = 3; <i>N_{WL}</i> = 2					<i>N</i> = 3; <i>N_{WL}</i> = 3									
A	35,200	35,200	35,400	35,500	35,600	36,200	36,300	36,300	36,300	36,300	36,300	36,300	36,300	36,300
B	64,300	65,300	65,500	65,700	66,100	67,600	68,000	68,400	68,400	68,400	68,400	68,400	68,400	68,400
C	84,700	86,100	86,700	87,200	87,500	89,700	90,900	91,500	91,700	91,700	91,700	91,700	91,700	91,900
D	100,800	102,800	103,600	104,000	104,400	107,800	109,600	110,200	110,600	110,600	110,600	110,600	110,800	110,800
E	119,800	122,100	124,400	126,700	129,100	127,000	129,400	131,600	132,800	132,800	132,800	132,800	133,000	136,300
<i>N</i> = 4; <i>N_{WL}</i> = 2					<i>N</i> = 4; <i>N_{WL}</i> = 3									
A	45,800	46,200	46,600	46,600	46,600	47,600	47,800	47,800	47,900	47,900	47,900	47,900	47,900	47,900
B	83,300	84,700	85,100	85,500	85,700	88,300	89,300	89,500	89,700	89,700	89,700	89,700	89,900	89,900
C	108,600	110,800	111,600	112,200	112,600	117,100	118,700	119,500	120,100	120,100	120,100	120,100	120,300	120,300
D	126,700	131,300	132,400	133,200	133,600	140,000	142,400	143,600	144,000	144,000	144,000	144,000	144,400	144,400
E	159,800	162,800	165,900	169,000	172,100	169,400	172,500	175,400	178,600	178,600	178,600	178,600	181,700	181,700
<i>N</i> = 5; <i>N_{WL}</i> = 2					<i>N</i> = 5; <i>N_{WL}</i> = 3									
A	56,300	57,100	57,300	57,500	57,500	58,700	58,900	59,300	59,400	59,400	59,400	59,400	59,400	59,400
B	101,400	103,000	103,600	104,200	104,400	108,600	109,600	110,000	110,600	110,600	110,600	110,600	110,800	110,800
C	131,300	133,800	135,000	135,800	136,200	142,800	145,400	146,200	146,800	146,800	146,800	146,800	147,400	147,400
D	154,500	157,700	159,100	159,900	160,300	170,600	173,600	175,000	175,800	175,800	175,800	175,800	175,800	175,800
E	178,800	178,800	178,800	178,800	178,800	211,800	215,600	219,500	223,300	223,300	223,300	223,300	227,200	227,200

This example problem illustrates how service volume tables may be created for a given set of weaving parameters. So many variables affect the operation of a weaving segment that “typical” service volume tables are not recommended. They may be significantly misleading when they are applied to segments with different parameters.

EXAMPLE PROBLEM 6: LOS OF AN ML ACCESS SEGMENT WITH CROSS-WEAVING

The ML Access Segment

Exhibit 27-19 shows a freeway facility that includes both general purpose and managed lanes. The analysis assumes no adverse weather effects or incidents in the segment. A freeway with an adjacent managed lane facility is evaluated as two parallel lane groups, as discussed in more detail in Chapter 10, Freeway Facilities Core Methodology. The example below shows two segments, each with two adjacent lane groups. Lane Group Pair 1 in the first segment includes a general purpose (GP) merge segment and a managed lane (ML) basic segment. Lane Group Pair 2 consists of GP and ML access segments.

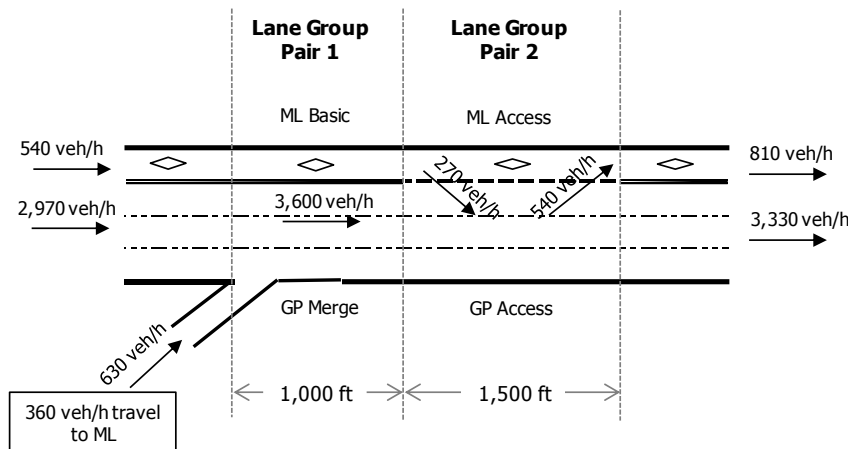


Exhibit 27-19
Example Problem 6:
ML Access Segment with
Cross-Weaving

Note: GP = general purpose, ML = managed lane.

What is the capacity reduction in the GP merge segment due to cross-weaving, and what is the expected LOS for the ML access segment with the demand flow rates shown?

The Facts

In addition to the information given in Exhibit 27-19, the following facts are known about the subject weaving segment:

PHF = 0.90;

Heavy vehicles = 0% single-unit trucks, 0% tractor-trailer;

Driver population = regular commuters;

FFS = 65 mi/h (for both managed and general purpose lanes);

c_{FL} = 2,350 pc/h/ln (for FFS = 65 mi/h);

ID = 1.0 interchange/mi; and

Terrain = level.

Comments

Lane-changing characteristics will be estimated for Lane Group Pair 2. The maximum length for weaving operations in the access segments will be

estimated and compared with the segment's actual length. The access segment's capacity will be estimated and compared with demand to determine whether LOS F exists. If it does not, component flow speeds will be estimated and averaged. Finally, the access segment density will be estimated and Exhibit 13-6 used to determine the expected LOS.

Capacity Reduction in GP Merge Segment (Lane Group Pair 1)

The capacity reduction due to the cross-weave effect is evaluated for Lane Group Pair 1. On the basis of the facility configuration provided in Exhibit 27-19, the L_{cw-min} and L_{cw-max} values are 1,000 ft and 2,500 ft, respectively. The cross-weave demand volume is $360/0.9 = 400$ veh/h. The number of general purpose lanes N_{GP} is 3. Thus the capacity reduction factor CRF will be

$$CRF = -0.0897 + 0.0252 \ln(CW) - 0.00001453L_{cw-min} + 0.002967N_{GP}$$

$$CRF = 0.056$$

Performance of ML Access Segment (Lane Group Pair 2)

The following steps illustrate the computations in the ML access segment, which is described above as Lane Group Pair 2.

Step 1: Input Data

All input data are stated in Exhibit 27-19 and the Facts section.

Step 2: Adjust Volume

The flow rates are computed on the basis of the hourly demand flow rates by using the specified PHF.

$$v_{FF} = \frac{3,060}{0.9} = 3,400 \text{ pc/h}$$

$$v_{FR} = \frac{540}{0.9} = 600 \text{ pc/h}$$

$$v_{RF} = \frac{270}{0.9} = 300 \text{ pc/h}$$

$$v_{RR} = \frac{270}{0.9} = 300 \text{ pc/h}$$

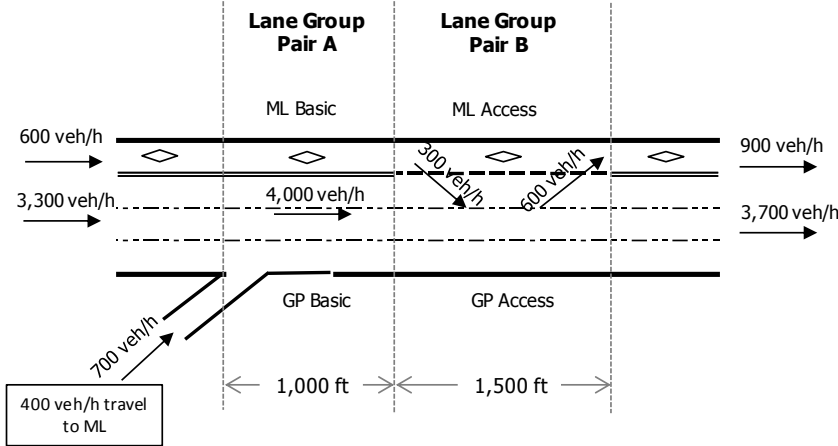
$$v_W = 600 + 300 = 900 \text{ pc/h}$$

$$v_{NW} = 3,400 + 300 = 3,700 \text{ pc/h}$$

$$v = 3,700 + 900 = 4,600 \text{ pc/h}$$

$$VR = \frac{900}{4,600} = 0.196$$

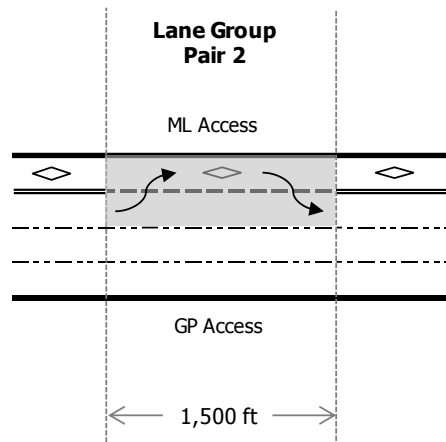
Exhibit 27-20 summarizes the hourly flow rates computed on the basis of hourly demand flow rates.



Note: GP = general purpose, ML = managed lane.

Step 3: Determine Configuration Characteristics

The configuration of the ML access segment is examined to determine the values of LC_{RF} , LC_{FR} and N_{WL} . The lane geometry is illustrated in Exhibit 27-21. From these values, the minimum number of lane changes by weaving vehicles LC_{MIN} is computed.



Note: GP = general purpose, ML = managed lane.

From Exhibit 27-21, it is clear that all ramp-to-freeway vehicles must make at least one lane change ($LC_{RF} = 1$). Similarly, all freeway-to-ramp vehicles must make at least one lane change ($LC_{FR} = 1$). In addition, a weaving maneuver can only be completed with a single lane change from the leftmost lane of the freeway or the auxiliary lane ($N_{WL} = 2$). Then, by using Equation 13-2, LC_{MIN} is computed as

$$LC_{MIN} = (LC_{RF} \times v_{RF}) + (LC_{FR} \times v_{FR})$$

$$LC_{MIN} = (1 \times 300) + (1 \times 600) = 900 \text{ lc/h}$$

Step 4: Determine Maximum Weaving Length

The maximum length over which weaving operations may exist for the segment described is found by using Equation 13-4:

Exhibit 27-20
Example Problem 6: Hourly Flow Rates After PHF Is Applied

Exhibit 27-21
Example Problem 6: Configuration Characteristics

$$L_{MAX} = [5,728(1 + VR)^{1.6}] - (1,566N_{WL})$$

$$L_{MAX} = [5,728(1 + 0.196)^{1.6}] - (1,566 \times 2) = 4,495 \text{ ft} > 1,500 \text{ ft}$$

Because the maximum length for weaving operations significantly exceeds the actual length, the segment qualifies as a weaving segment, and the analysis continues.

Step 5: Determine Weaving Segment Capacity

The capacity of the weaving segment is controlled by one of two limiting factors: density reaching 43 pc/mi/ln or weaving demand reaching 2,350 pc/h for the configuration of Exhibit 27-19 (a ramp-weave with $N_{WL} = 2$).

Capacity Limited by Density

The capacity limited by reaching a density of 43 pc/mi/ln is estimated by using Equation 13-5 and Equation 13-6:

$$c_{IWL} = c_{IFL} - [438.2(1 + VR)^{1.6}] + (0.0765L_S) + (119.8N_{WL})$$

$$c_{IWL} = 2,350 - [438.2(1 + 0.196)^{1.6}] + (0.0765 \times 1,500) + (119.8 \times 2)$$

$$c_{IWL} = 2,121 \text{ pc/h/ln}$$

$$c_W = c_{IWL} \times N \times f_{HV}$$

$$c_W = 2,121 \times 4 \times 1 = 8,483 \text{ pc/h}$$

Capacity Limited by Weaving Demand Flow

The capacity limited by the weaving demand flow is estimated by using Equation 13-7 and Equation 13-8:

$$c_{IW} = \frac{2,400}{VR} = \frac{2,400}{0.196} = 12,245 \text{ pc/h}$$

$$c_W = c_{IW} \times f_{HV}$$

$$c_W = 12,245 \times 1 = 12,245 \text{ pc/h}$$

The controlling capacity is the smaller of the two values, or 8,483 pc/h. At this point, the value is usually stated as vehicles per hour. In this case, because inputs were already adjusted and were stated in passenger cars per hour, conversions back to vehicles per hour are not possible.

Since the capacity of the weaving segment is larger than the demand flow rate of 4,600 pc/h, LOS F does not exist, and the analysis may continue.

Capacity of Input and Output Roadways

Although it is rarely a factor in weaving operations, the capacity of input and output roadways should be checked to ensure that no deficiencies exist. There are three input and output freeway lanes (with FFS = 65 mi/h). The capacities of the entry and exit ramps are determined for a basic managed lane segment with a free-flow speed of 65 mi/h, separated by markings. The criteria of Chapter 12 are used to determine the capacity of the freeway legs and the managed lane entry and exit lanes. Demand flows and capacities are compared in Exhibit 27-22.

Leg	Demand Flow (pc/h)	Capacity (pc/h)
Freeway entry	4,000	$3 \times 2,350 = 7,050$
Freeway exit	$4,000 + 300 - 600 = 3,700$	$3 \times 2,350 = 7,050$
Ramp entry	600	1,700
Ramp exit	$600 - 300 + 600 = 900$	1,700

Exhibit 27-22

Example Problem 6: Capacity of Entry and Exit Legs

The capacities of all input and output roadways are sufficient to accommodate the demand flow rates.

Step 6: Determine Lane-Changing Rates

Equation 13-11 through Equation 13-17 are used to estimate the lane-changing rates of weaving and nonweaving vehicles in the access segment. These rates will be used in Step 7 to estimate the weaving and nonweaving vehicle speeds.

Weaving Vehicle Lane-Changing Rate

$$LC_W = LC_{MIN} + 0.39[(L_S - 300)^{0.5} N^2 (1 + ID)^{0.8}]$$

$$LC_W = 900 + 0.39[(1,500 - 300)^{0.5} (4^2) (1 + 1)^{0.8}] = 1,276 \text{ lc/h}$$

Nonweaving Vehicle Lane-Changing Rate

$$I_{NW} = \frac{L_S \times ID \times v_{NW}}{10,000}$$

$$I_{NW} = \frac{1,500 \times 1 \times 3,700}{10,000} = 555 < 1,300$$

$$LC_{NW} = LC_{NW1} = (0.206v_{NW}) + (0.542L_S) - (192.6N)$$

$$LC_{NW} = (0.206 \times 3,700) + (0.542 \times 1,500) - (192.6 \times 4) = 805 \text{ lc/h}$$

Total Lane-Changing Rate

$$LC_{ALL} = LC_W + LC_{NW} = 1,276 + 805 = 2,081 \text{ lc/h}$$

Step 7: Determine Average Speeds of Weaving and Nonweaving Vehicles

The average speeds of weaving and nonweaving vehicles are computed from Equation 13-18 through Equation 13-21:

$$W = 0.226 \left(\frac{LC_{ALL}}{L_S} \right)^{0.789}$$

$$W = 0.226 \left(\frac{2,081}{1,500} \right)^{0.789} = 0.293$$

Then

$$S_W = 15 + \left(\frac{FFS \times SAF - 15}{1 + W} \right)$$

$$S_W = 15 + \left(\frac{65 \times 1 - 15}{1 + 0.293} \right) = 53.7 \text{ mi/h}$$

and

$$S_{NW} = FFS \times SAF - (0.0072LC_{MIN}) - \left(0.0048 \frac{v}{N} \right)$$

$$S_{NW} = 65 \times 1 - (0.0072 \times 900) - \left(0.0048 \frac{4,600}{4}\right) = 53.0 \text{ mi/h}$$

Equation 13-22 is now used to compute the average speed of all vehicles in the segment:

$$S = \frac{v_W + v_{NW}}{\left(\frac{v_W}{S_W}\right) + \left(\frac{v_{NW}}{S_{NW}}\right)}$$

$$S = \frac{900 + 3,700}{\left(\frac{900}{53.7}\right) + \left(\frac{3,700}{53.0}\right)} = 53.1 \text{ mi/h}$$

Step 8: Determine LOS

The average density in the weaving segment is estimated by using Equation 13-23.

$$D = \frac{(v/N)}{S} = \frac{(4,600/4)}{53.1} = 21.7 \text{ pc/mi/ln}$$

From Exhibit 13-6, this density is within the stated boundaries of LOS C (20 to 28 pc/mi/ln).

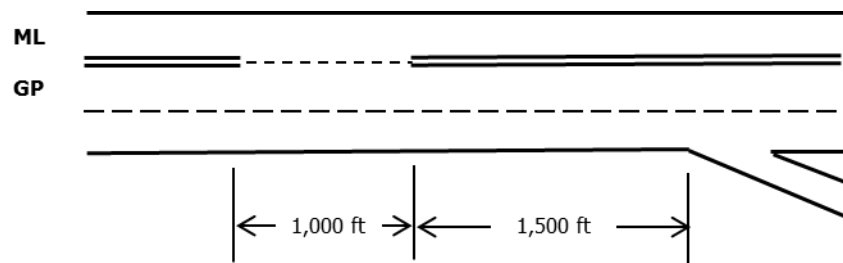
Discussion

As noted, the access segment is operating at LOS C. Weaving and nonweaving speeds are relatively high, suggesting a nearly stable flow. The demand flow rate of 4,600 pc/h is well below the access segment’s capacity of 8,483 pc/h.

EXAMPLE PROBLEM 7: ML ACCESS SEGMENT WITH DOWNSTREAM OFF-RAMP

An ML access segment is illustrated in Exhibit 27-23. The movements in and out of the managed lane may be considered to be analogous to a ramp-weave segment and analyzed accordingly. The impact of cross-weaving traffic between the managed lane and the nearby off-ramp must also be analyzed to determine its impact on capacity of the general purpose lanes.

Exhibit 27-23
Example Problem 7:
ML Access Segment Data



Note: GP = general purpose, ML = managed lane.

The FFS of the segment is 70 mi/h and the interchange density, ID , is 1 interchange per mile. Demand flow rates for this segment are shown in Exhibit 27-24. Note that all demand flows are stated in passenger car equivalents and represent the flow rate in the worst 15-min period of the hour.

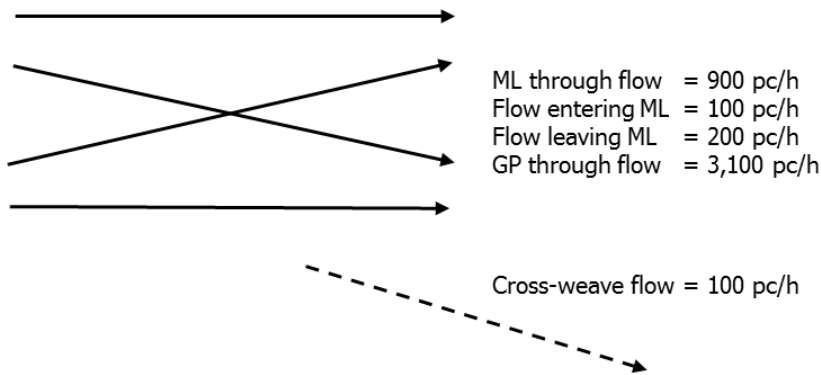


Exhibit 27-24
 Example Problem 7: Weaving
 Flows for Managed Lane
 Segment

Note: GP = general purpose, ML = managed lane.

Part 1: Analysis of the Weaving Between Managed Lanes and General Purpose Lanes

The first major issue to consider is the weaving segment created by movements into and out of the managed lane in the 1,000-ft access segment. This segment is treated as a ramp-weave configuration with a total of three lanes (including the managed lane). This is a bit of an approximation, given that the geometry of the managed lane is better than that of typical ramps in a ramp-weave segment. Speeds of weaving vehicles are likely to be underestimated, since approach speeds on the managed lane are considerably higher than what would be expected on a typical ramp.

Weaving Movements and Parameters

The primary weaving activity is between vehicles entering and leaving the managed lane in the 1,000-ft access segment. This may be treated as a three-lane ramp-weave segment and is analyzed with the basic methodology of this chapter.

Because of the simplicity of this case, certain parameters may be established by inspection:

$$N_{WL} = 2 \text{ lanes,}$$

$$LC_{MIN} = 100 + 200 = 300 \text{ lc/h, and}$$

$$VR = 300 / 4,300 = 0.07.$$

All ramp weaves have two weaving lanes, and each weaving vehicle in a ramp weave must execute one lane change.

Maximum Weaving Length

The maximum weaving length is determined with Equation 13-4.

$$L_{MAX} = [5,728(1 + VR)^{1.6}] - (1,566N_{WL})$$

$$L_{MAX} = [5,728(1 + 0.07)^{1.6}] - (1,566 \times 2) = 3,251 \text{ ft} > 1,000 \text{ ft}$$

The result is significantly longer than the actual weaving length of 1,000 ft. Thus, the access segment may be treated by using the weaving procedure.

Weaving Segment Capacity

The capacity of the ML access segment (a weaving segment) may be based on density limits (43 pc/mi/ln) or on the maximum weaving flow that can be accommodated by the ramp-weave configuration (2,400 pc/h).

The former is estimated by using Equations 13-5 and 13-6.

$$c_{IWL} = c_{IFL} - [438.2(1 + VR)^{1.6}] + (0.0765L_S) + (119.8N_{WL})$$

$$c_{IWL} = 2,400 - [438.2(1 + 0.07)^{1.6}] + (0.0765 \times 1,000) + (119.8 \times 2)$$

$$c_{IWL} = 2,228 \text{ pc/h/ln}$$

$$c_W = c_{IWL} \times N \times f_{HV}$$

$$c_W = 2,228 \times 3 \times 1 = 6,684 \text{ pc/h}$$

The capacity limited by maximum weaving flow is computed by using Equations 13-7 and 13-8.

$$c_{IW} = \frac{2,400}{VR} = \frac{2,400}{0.07} = 34,286 \text{ pc/h}$$

$$c_W = c_{IW} \times f_{HV} = 34,286 \times 1 = 34,286 \text{ pc/h}$$

Obviously, the capacity is controlled by maximum density and is established as 6,684 pc/h. Since the total flow in the segment is $900 + 100 + 200 + 3,100 = 4,300$ pc/h, failure (LOS F) is not expected, and the analysis of the weaving area continues. By inspection and comparison with Chapter 12 criteria, demand does not exceed capacity on any of the entry or exit roadways.

Estimate Lane-Changing Rates

To estimate total lane-changing rates, the total number of lane changes made by weaving and nonweaving vehicles (within the 1,000-ft access segment) must be estimated.

The total lane-changing rate for weaving vehicles is determined by using Equation 13-11.

$$LC_W = LC_{MIN} + 0.39[(L_S - 300)^{0.5} N^2 (1 + ID)^{0.8}]$$

$$LC_W = 300 + 0.39[(1,000 - 300)^{0.5} (3^2)(1 + 1)^{0.8}] = 462 \text{ lc/h}$$

The total lane-changing rate for nonweaving vehicles is found by using Equation 13-13 or 13-14, depending on the value of the nonweaving vehicle index computed with Equation 13-12.

$$I_{NW} = \frac{L_S \times ID \times v_{NW}}{10,000}$$

$$I_{NW} = \frac{1,000 \times 1 \times 4,000}{10,000} = 400 < 1,300$$

Since this value is less than 1,300, Equation 13-13 is applied.

$$LC_{NW} = LC_{NW1} = (0.206v_{NW}) + (0.542L_S) - (192.6N)$$

$$LC_{NW} = (0.206 \times 4,000) + (0.542 \times 1,000) - (192.6 \times 3) = 788 \text{ lc/h}$$

The total lane-changing rate for the ML access segment is

$$LC_{ALL} = LC_W + LC_{NW} = 462 + 788 = 1,250 \text{ lc/h}$$

Estimate Speed of Weaving and Nonweaving Vehicles

The speed of weaving vehicles in the ML access segment is estimated by using Equations 13-19 and 13-20.

$$W = 0.226 \left(\frac{LC_{ALL}}{L_S} \right)^{0.789}$$

$$W = 0.226 \left(\frac{1,250}{1,000} \right)^{0.789} = 0.2695$$

$$S_W = 15 + \left(\frac{FFS \times SAF - 15}{1 + W} \right)$$

$$S_W = 15 + \left(\frac{70 \times 1 - 15}{1 + 0.2695} \right) = 58.3 \text{ mi/h}$$

The speed of nonweaving vehicles is estimated by using Equation 13-21.

$$S_{NW} = FFS \times SAF - (0.0072LC_{MIN}) - \left(0.0048 \frac{v}{N} \right)$$

$$S_{NW} = 70 \times 1 - (0.0072 \times 300) - \left(0.0048 \frac{4,300}{3} \right) = 61.0 \text{ mi/h}$$

The average speed of all vehicles is found by using Equation 13-22.

$$S = \frac{v_W + v_{NW}}{\left(\frac{v_W}{S_W} \right) + \left(\frac{v_{NW}}{S_{NW}} \right)}$$

$$S = \frac{300 + 4,000}{\left(\frac{300}{58.3} \right) + \left(\frac{4,000}{61.0} \right)} = 60.8 \text{ mi/h}$$

Estimate the Density in the ML Access Segment and Determine the LOS

The density in the segment is found by using Equation 13-23.

$$D = \frac{(v/N)}{S} = \frac{(4,300/3)}{60.8} = 23.6 \text{ pc/mi/ln}$$

From Exhibit 13-12, this is LOS B but close to the LOS B/C boundary of 24 pc/mi/ln.

Part 2: Estimate the Impact of Cross-Weaving Vehicles on the Capacity of the General Purpose Lanes

The capacity of the two general purpose lanes (with FFS = 70 mi/h) is expected to be $2,400 \times 2 = 4,800$ pc/h. However, there are 100 pc/h executing cross-weaving movements to access the off-ramp that is 1,500 ft downstream of the ML access segment.

Equation 13-24 describes the impact that these cross-weaving vehicles are expected to have on general purpose lane capacity.

$$CRF = -0.0897 + 0.0252 \ln(CW) - 0.00001453L_{cw-min} + 0.002967N_{GP}$$

$$CRF = -0.0897 + 0.0252 \ln(100) - 0.00001453(1,500) + 0.002967(2)$$

$$CRF = 0.0105$$

$$CAF = 1 - CRF = 1 - 0.0105 = 0.9895$$

Therefore, the remaining capacity of the general purpose lanes is

$$c_{GPA} = c_{GP} \times CAF = 4,800 \times 0.9895 = 4,750 \text{ pc/h}$$

Discussion

In this case, the ML access segment is expected to work well. The actual weaving involving vehicles entering and leaving the segment results in an overall LOS B designation. The impact of cross-weaving vehicles using the off-ramp is negligible.

3. ALTERNATIVE TOOL EXAMPLES FOR WEAVING SEGMENTS

Chapter 13, Freeway Weaving Segments, described a methodology for analyzing freeway weaving segments to estimate their capacity, speed, and density as a function of traffic demand and geometric configuration. Supplemental problems involving the use of alternative tools for freeway weaving sections to address limitations of the Chapter 13 methodology are presented here. All of these examples are based on Example Problem 1 in this chapter, shown in Exhibit 27-2.

Three questions are addressed by using a typical microscopic traffic simulation tool that is based on the link-node structure:

1. Can weaving segment capacity be estimated realistically by simulation by varying the demand volumes up to and beyond capacity?
2. How does demand affect performance in terms of speed and density in the weaving segment, on the basis of the default model parameters for vehicle and behavioral characteristics?
3. How would the queue backup from a signal at the end of the off-ramp affect weaving operation?

The first step is to identify the link-node structure, as shown in Exhibit 27-25.

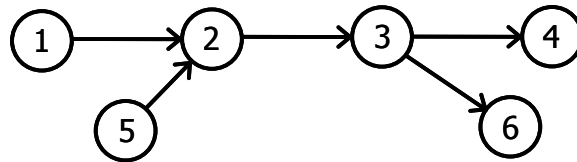


Exhibit 27-25
Link-Node Structure for the Simulated Weaving Segment

The next step is to develop input data for various demand levels. Several demand levels ranging from 80% to 180% of the original volumes were analyzed by simulation. The demand data, adjusted for a peak hour factor of 0.91, are given in Exhibit 27-26.

Type of Demand	Percent of Specified Demand					
	80	100	120	140	160	180
Freeway-to-freeway demand, V_{FF}	1,596	1,995	2,393	2,792	3,191	3,590
Ramp-to-freeway demand, V_{RF}	912	1,140	1,367	1,595	1,823	2,051
Freeway-to-ramp demand, V_{FR}	608	760	913	1,065	1,217	1,369
Ramp-to-ramp demand, V_{RR}	1,140	1,425	1,710	1,995	2,280	2,565
Total demand	4,256	5,320	6,384	7,448	8,512	9,576
Total freeway entry	2,204	2,755	3,306	3,857	4,408	4,959
Total freeway exit	2,507	3,134	3,761	4,388	5,015	5,641
Total ramp entry	2,052	2,565	3,078	3,591	4,104	4,617
Total ramp exit	1,749	2,186	2,623	3,060	3,497	3,934

Exhibit 27-26
Input Data for Various Demand Levels (veh/h)

Thirty simulation runs were made for each demand level. The results are discussed in the following sections. The need to determine performance measures from an analysis of vehicle trajectories was emphasized in Chapter 7, Interpreting HCM and Alternative Tool Results. Specific procedures for defining measures in terms of vehicle trajectories were proposed to guide the future

development of alternative tools. Pending further development, the examples presented in this chapter have applied existing versions of alternative tools and therefore do not reflect the trajectory-based measures described in Chapter 7.

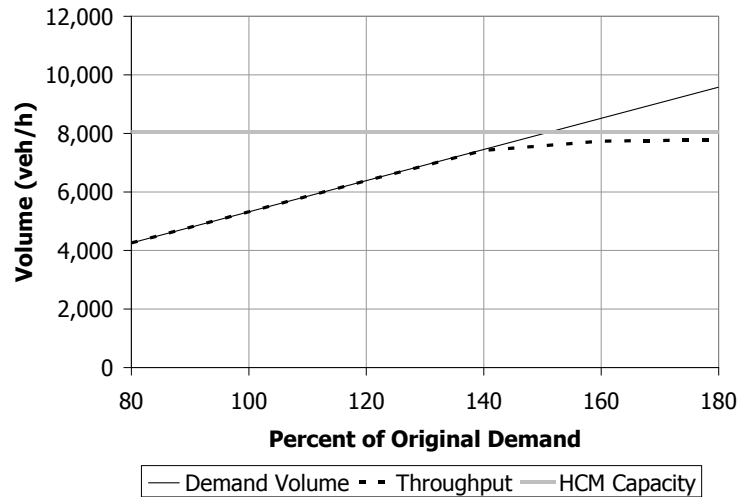
DETERMINING THE WEAVING SEGMENT CAPACITY

Simulation tools do not produce capacity estimates directly. The traditional way to estimate the capacity of a given system element is to overload it and determine the maximum throughput under the overloaded conditions. Care must be taken in this process because a severe overload can reduce the throughput by introducing self-aggravating phenomena upstream of the output point.

Exhibit 27-27 shows the relationship between demand volume and throughput, represented by the output of the weaving segment. As expected, throughput tracks demand precisely up to the point where no more vehicles can be accommodated. After that point it levels off and reaches a constant value that indicates the capacity of the segment. In this case, capacity was reached at approximately the same value as the HCM estimate. However, this degree of agreement between the two estimation techniques should not be expected as a general rule because of differences in the treatment of vehicle and geometric characteristics.

On the basis of observation, it is reasonable to conclude that the capacity of this weaving segment can be determined by overloading the facility and that the results are in general agreement with those of the HCM. In comparing capacity estimates, the analyst should remember that the HCM expresses results in passenger car equivalent vehicles, while simulation tools express results in actual vehicles. The results will diverge as the proportion of trucks increases.

Exhibit 27-27
Determining the Capacity of a Weaving Segment by Simulation



EFFECT OF DEMAND ON PERFORMANCE

Exhibit 27-28 shows the effect of demand on density and speed. Density increases with demand volume up to the segment capacity and then levels off at a constant value of approximately 75 veh/mi/ln, which represents very dense conditions. The speed remains close to the free-flow speed at lower demand volumes. It then drops in a more or less linear fashion and eventually levels off when capacity is reached. The minimum speed is approximately 26 mi/h.

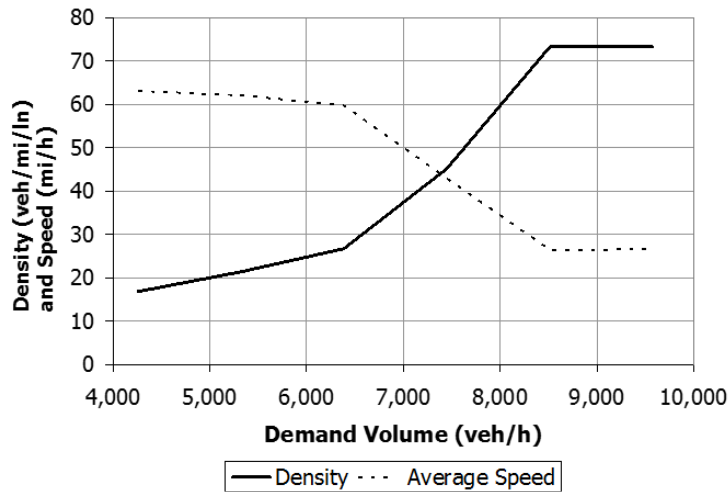


Exhibit 27-28
Simulated Effect of Demand Volume on Weaving Segment Capacity and Speed

At the originally specified demand volume level of 5,320 veh/h (peak hour adjusted), the estimated speed was 62.0 mi/h and the density was 21.4 veh/mi/ln. The corresponding values from simulation were 53.1 mi/h and 26.3 pc/ln/mi. Because of differences in definition, these results are not easy to compare. These differences illustrate the pitfalls of applying LOS thresholds to directly simulated density to determine the segment LOS.

The densities produced when demand exceeded capacity were greater than 70 veh/ln/mi. This level of density is usually associated with queues that back up from downstream bottlenecks; however, in this case, no such bottlenecks were present. Inspection of the animated graphics suggests that the increase in density within the weaving segment is caused by vehicles that are not able to get into the required lane for their chosen exit. Some vehicles were forced to stop and wait for a lane-changing opportunity, and the reduction in average speed produced a corresponding increase in the average density.

For purposes of illustration, this example focuses on a single link containing the weaving segment. The overloading of demand prevented all of the vehicles from entering the link and would have increased the delay substantially if the vehicles denied entry were considered. For this reason, the delay measures from the simulation were not included in this discussion.

EFFECT OF QUEUE BACKUP FROM A DOWNSTREAM SIGNAL ON THE EXIT RAMP

The operation of a weaving segment may be expected to deteriorate when congestion on the exit ramp causes a queue to back up into the weaving segment. This condition was one of the stated limitations of the methodology in Chapter 13, Freeway Weaving Segments.

Signal Operation

To create this condition, a pretimed signal with a slightly oversaturated operation is added 700 ft from the exit point. The operating parameters for the signal are given in Exhibit 27-29. Note that the right-turn capacity estimated by the Chapter 19, Signalized Intersections, procedure is slightly lower than the left-turn capacity because of the adjustment factors applied to turns by that procedure.

Exhibit 27-29
Exit Ramp Signal Operating Parameters

Cycle length	150 s
Green interval	95 s
Yellow interval	4 s
All-red clearance	1 s
Saturation flow rate	1,800 veh/hg/ln
<i>g/C</i> ratio	0.633
Left-turn movement	
• Lanes	1
• Capacity (by HCM Chapter 19)	1,083 veh/h
Right-turn movement	
• Lanes	1
• Capacity (by HCM Chapter 19)	969 veh/h
Link capacity (by HCM Chapter 19)	2,052 veh/h

Capacity Calibration

To ensure that the simulation model is properly calibrated to the HCM, the simulation tool’s operating parameters for the link were modified by trial and error to match the HCM estimate of the link capacity by overloading the link to determine its throughput. With a start-up lost time of 2.0 s and a steady-state headway of 1.8 s/veh, the simulated capacity for the link was 2,040 veh/h, which compares well with the HCM’s estimate of 2,052 veh/h.

Results with the Specified Demand

An initial run with the demand levels specified in the original example problem indicated severe problems on the freeway caused by the backup of vehicles from the signal. Two adverse conditions are observed in the graphics capture shown in Exhibit 27-30:

1. Some vehicles in the freeway mainline through lanes were unable to access the auxiliary lane for the exit ramp because of blockage in the lane.
2. The resulting use of the exit ramp lanes prevented the signal operation from reaching its full capacity. This caused a self-aggravating condition in which the queue backed up farther onto the freeway.

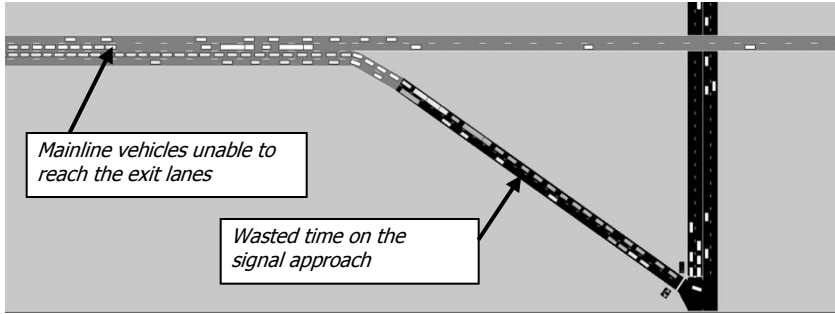


Exhibit 27-30
Deterioration of Weaving Segment Operation due to Queue Backup from a Traffic Signal

A reasonable conclusion is that the weaving segment would not operate properly at the specified demand levels. The logical solution to the problem would be to improve signal capacity. To support a recommendation for such an improvement, varying the demand levels to gain further insight into the operation might be desirable. Since it has already been discovered that the specified demand is too high, the original levels of 80% to 180% of the specified demand are clearly inappropriate. The new demand range will therefore be reduced to a level of 80% to 105%.

Effect of Reducing Demand on Throughput

Exhibit 27-31 illustrates the self-aggravating effect of too much demand. Throughput is generally expected to increase with demand up to the capacity of the facility and to level off at that point. Notice that the anticipated relationship was observed without the signal, as was shown in Exhibit 27-27.

When the signal was added, the situation changed significantly. The throughput peaked at about 95% of the specified demand and declined noticeably as more vehicles were allowed to enter the freeway. Another useful observation is that the peak throughput of approximately 4,560 veh/h is considerably below the estimated capacity of nearly 8,000 veh/h.

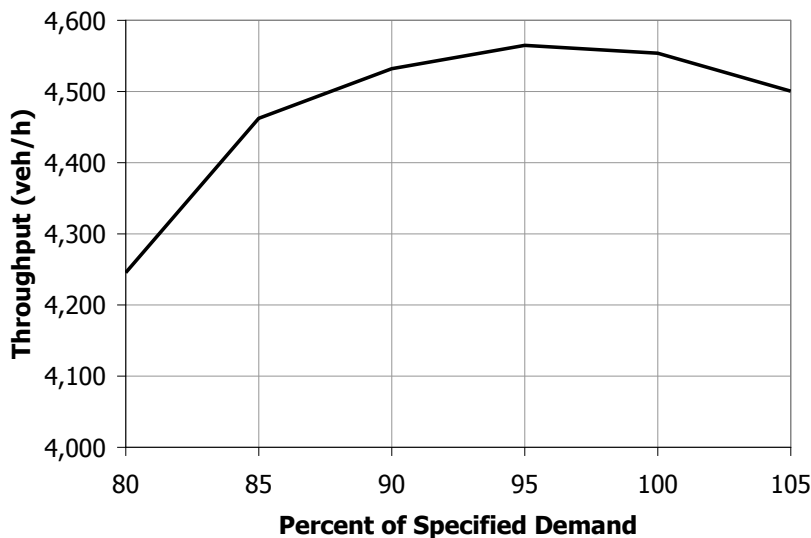
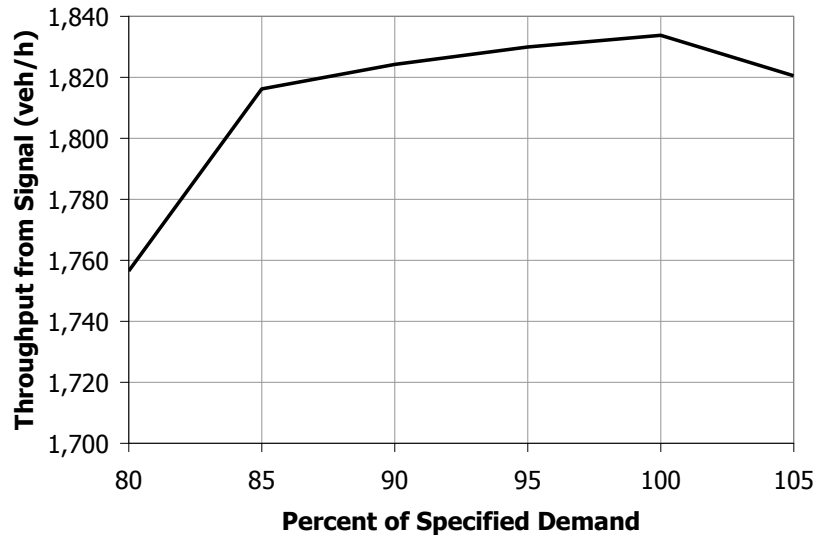


Exhibit 27-31
Effect of Demand on Weaving Segment Throughput with Exit Ramp Backup

The same phenomenon is observed on the exit ramp approach to the signal, as shown in Exhibit 27-32. The throughput declined with added demand after reaching its peak value of about 1,835 veh/h. Note that the peak throughput is also well below the capacity of 2,040 to 2,050 veh/h estimated by both the HCM and the simulation tool in the absence of upstream congestion.

Exhibit 27-32
Effect of Demand on Exit Ramp Throughput with Signal Queuing



This example illustrates the potential benefits of using simulation tools to address conditions that are beyond the scope of the HCM methodology. It also points out the need to consider conditions outside of the facility under study in making a performance assessment. Finally, it demonstrates that care must be taken in estimating the capacity of a facility through an arbitrary amount of demand overload.



HIGHWAY CAPACITY MANUAL

6TH EDITION | A GUIDE FOR MULTIMODAL MOBILITY ANALYSIS

VOLUME 4: APPLICATIONS GUIDE

The National Academies of
SCIENCES • ENGINEERING • MEDICINE

TRANSPORTATION RESEARCH BOARD
WASHINGTON, D.C. | WWW.TRB.ORG

TRANSPORTATION RESEARCH BOARD 2016 EXECUTIVE COMMITTEE *

Chair: James M. Crites, Executive Vice President of Operations,
Dallas–Fort Worth International Airport, Texas

Vice Chair: Paul Trombino III, Director, Iowa Department of
Transportation, Ames

Executive Director: Neil J. Pedersen, Transportation Research Board

Victoria A. Arroyo, Executive Director, Georgetown Climate Center;
Assistant Dean, Centers and Institutes; and Professor and Director,
Environmental Law Program, Georgetown University Law Center,
Washington, D.C.

Scott E. Bennett, Director, Arkansas State Highway and Transportation
Department, Little Rock

Jennifer Cohan, Secretary, Delaware Department of Transportation, Dover

Malcolm Dougherty, Director, California Department of
Transportation, Sacramento

A. Stewart Fotheringham, Professor, School of Geographical Sciences
and Urban Planning, Arizona State University, Tempe

John S. Halikowski, Director, Arizona Department of Transportation,
Phoenix

Susan Hanson, Distinguished University Professor Emerita, Graduate
School of Geography, Clark University, Worcester, Massachusetts

Steve Heminger, Executive Director, Metropolitan Transportation
Commission, Oakland, California

Chris T. Hendrickson, Hamerschlag Professor of Engineering, Carnegie
Mellon University, Pittsburgh, Pennsylvania

Jeffrey D. Holt, Managing Director, Power, Energy, and Infrastructure
Group, BMO Capital Markets Corporation, New York

S. Jack Hu, Vice President for Research and J. Reid and Polly Anderson
Professor of Manufacturing, University of Michigan, Ann Arbor

Roger B. Huff, President, HGLC, LLC, Farmington Hills, Michigan

Geraldine Knatz, Professor, Sol Price School of Public Policy, Viterbi
School of Engineering, University of Southern California, Los Angeles

Ysela Llort, Consultant, Miami, Florida

Melinda McGrath, Executive Director, Mississippi Department of
Transportation, Jackson

James P. Redeker, Commissioner, Connecticut Department of
Transportation, Newington

Mark L. Rosenberg, Executive Director, The Task Force for Global
Health, Inc., Decatur, Georgia

Kumares C. Sinha, Olson Distinguished Professor of Civil Engineering,
Purdue University, West Lafayette, Indiana

Daniel Sperling, Professor of Civil Engineering and Environmental
Science and Policy; Director, Institute of Transportation Studies,
University of California, Davis

Kirk T. Steudle, Director, Michigan Department of Transportation,
Lansing (Past Chair, 2014)

Gary C. Thomas, President and Executive Director, Dallas Area Rapid
Transit, Dallas, Texas

Pat Thomas, Senior Vice President of State Government Affairs, United
Parcel Service, Washington, D.C.

Katherine F. Turnbull, Executive Associate Director and Research
Scientist, Texas A&M Transportation Institute, College Station

Dean Wise, Vice President of Network Strategy, Burlington Northern
Santa Fe Railway, Fort Worth, Texas

Thomas P. Bostick (Lieutenant General, U.S. Army), Chief of Engineers
and Commanding General, U.S. Army Corps of Engineers, Washington,
D.C. (ex officio)

James C. Card (Vice Admiral, U.S. Coast Guard, retired), Maritime
Consultant, The Woodlands, Texas, and Chair, TRB Marine Board
(ex officio)

T. F. Scott Darling III, Acting Administrator and Chief Counsel, Federal
Motor Carrier Safety Administration, U.S. Department of Transportation
(ex officio)

Marie Therese Dominguez, Administrator, Pipeline and Hazardous
Materials Safety Administration, U.S. Department of Transportation
(ex officio)

Sarah Feinberg, Administrator, Federal Railroad Administration,
U.S. Department of Transportation (ex officio)

Carolyn Flowers, Acting Administrator, Federal Transit Administration,
U.S. Department of Transportation (ex officio)

LeRoy Gishi, Chief, Division of Transportation, Bureau of Indian
Affairs, U.S. Department of the Interior, Washington, D.C. (ex officio)

John T. Gray II, Senior Vice President, Policy and Economics,
Association of American Railroads, Washington, D.C. (ex officio)

Michael P. Huerta, Administrator, Federal Aviation Administration,
U.S. Department of Transportation (ex officio)

Paul N. Jaenichen, Sr., Administrator, Maritime Administration,
U.S. Department of Transportation (ex officio)

Bevan B. Kirley, Research Associate, University of North Carolina
Highway Safety Research Center, Chapel Hill, and Chair, TRB Young
Members Council (ex officio)

Gregory G. Nadeau, Administrator, Federal Highway Administration,
U.S. Department of Transportation (ex officio)

Wayne Nastri, Acting Executive Officer, South Coast Air Quality
Management District, Diamond Bar, California (ex officio)

Mark R. Rosekind, Administrator, National Highway Traffic Safety
Administration, U.S. Department of Transportation (ex officio)

Craig A. Rutland, U.S. Air Force Pavement Engineer, U.S. Air Force
Civil Engineer Center, Tyndall Air Force Base, Florida (ex officio)

Reuben Sarkar, Deputy Assistant Secretary for Transportation,
U.S. Department of Energy (ex officio)

Richard A. White, Acting President and CEO, American Public
Transportation Association, Washington, D.C. (ex officio)

Gregory D. Winfree, Assistant Secretary for Research and Technology,
Office of the Secretary, U.S. Department of Transportation (ex officio)

Frederick G. (Bud) Wright, Executive Director, American Association
of State Highway and Transportation Officials, Washington, D.C.
(ex officio)

Paul F. Zukunft (Admiral, U.S. Coast Guard), Commandant, U.S. Coast
Guard, U.S. Department of Homeland Security (ex officio)

Transportation Research Board publications are available by ordering
individual publications directly from the TRB Business Office, through
the Internet at www.TRB.org, or by annual subscription through
organizational or individual affiliation with TRB. Affiliates and library
subscribers are eligible for substantial discounts. For further information,
contact the Transportation Research Board Business Office, 500 Fifth
Street, NW, Washington, DC 20001 (telephone 202-334-3213;
fax 202-334-2519; or e-mail TRBsales@nas.edu).

Copyright 2016 by the National Academy of Sciences.

All rights reserved.

Printed in the United States of America.

ISBN 978-0-309-36997-8 [Slipcased set of three volumes]

ISBN 978-0-309-36998-5 [Volume 1]

ISBN 978-0-309-36999-2 [Volume 2]

ISBN 978-0-309-37000-4 [Volume 3]

ISBN 978-0-309-37001-1 [Volume 4, online only]

The National Academies of
SCIENCES • ENGINEERING • MEDICINE

The **National Academy of Sciences** was established in 1863 by an Act of Congress, signed by President Lincoln, as a private, nongovernmental institution to advise the nation on issues related to science and technology. Members are elected by their peers for outstanding contributions to research. Dr. Ralph J. Cicerone is president.

The **National Academy of Engineering** was established in 1964 under the charter of the National Academy of Sciences to bring the practices of engineering to advising the nation. Members are elected by their peers for extraordinary contributions to engineering. Dr. C. D. Mote, Jr., is president.

The **National Academy of Medicine** (formerly the Institute of Medicine) was established in 1970 under the charter of the National Academy of Sciences to advise the nation on medical and health issues. Members are elected by their peers for distinguished contributions to medicine and health. Dr. Victor J. Dzau is president.

The three Academies work together as the National Academies of Sciences, Engineering, and Medicine to provide independent, objective analysis and advice to the nation and conduct other activities to solve complex problems and inform public policy decisions. The Academies also encourage education and research, recognize outstanding contributions to knowledge, and increase public understanding in matters of science, engineering, and medicine.

Learn more about the National Academies of Sciences, Engineering, and Medicine at **www.national-academies.org**.

The **Transportation Research Board** is one of seven major programs of the National Academies of Sciences, Engineering, and Medicine. The mission of the Transportation Research Board is to increase the benefits that transportation contributes to society by providing leadership in transportation innovation and progress through research and information exchange, conducted within a setting that is objective, interdisciplinary, and multimodal. The Board's varied committees, task forces, and panels annually engage about 7,000 engineers, scientists, and other transportation researchers and practitioners from the public and private sectors and academia, all of whom contribute their expertise in the public interest. The program is supported by state transportation departments, federal agencies including the component administrations of the U.S. Department of Transportation, and other organizations and individuals interested in the development of transportation.

Learn more about the Transportation Research Board at **www.TRB.org**.

CHAPTER 28
FREEWAY MERGES AND DIVERGES: SUPPLEMENTAL

CONTENTS

1. INTRODUCTION 28-1

2. EXAMPLE PROBLEMS 28-2

 Example Problem 1: Isolated One-Lane, Right-Hand On-Ramp to a
 Four-Lane Freeway 28-2

 Example Problem 2: Two Adjacent Single-Lane, Right-Hand Off-
 Ramps on a Six-Lane Freeway 28-4

 Example Problem 3: One-Lane On-Ramp Followed by a One-Lane
 Off-Ramp on an Eight-Lane Freeway 28-9

 Example Problem 4: Single-Lane, Left-Hand On-Ramp on a Six-Lane
 Freeway 28-14

 Example Problem 5: Service Flow Rates and Service Volumes for an
 Isolated On-Ramp on a Six-Lane Freeway 28-17

3. ALTERNATIVE TOOL EXAMPLES FOR FREEWAY RAMPS 28-22

 Problem 1: Ramp-Metering Effects 28-22

 Problem 2: Conversion of Leftmost Lane to an HOV Lane 28-25

LIST OF EXHIBITS

Exhibit 28-1 List of Example Problems	28-2
Exhibit 28-2 Example Problem 2: Capacity Checks.....	28-7
Exhibit 28-3 Example Problem 3: Capacity Checks.....	28-12
Exhibit 28-4 Example Problem 5: Illustrative Service Flow Rates and Service Volumes Based on Approaching Freeway Demand.....	28-19
Exhibit 28-5 Example Problem 5: Illustrative Service Flow Rates and Service Volumes Based on a Fixed Freeway Demand.....	28-21
Exhibit 28-6 Graphics Capture of the Ramp Merge with Ramp Metering	28-23
Exhibit 28-7 Density as a Function of Ramp-Metering Headways.....	28-23
Exhibit 28-8 Capacity at a Ramp Junction as a Function of Ramp- Metering Headways	28-24
Exhibit 28-9 Queue Length on the Ramp as a Function of Ramp-Metering Headways	28-24
Exhibit 28-10 Graphics Capture of the Segment with an HOV Lane	28-25
Exhibit 28-11 Density of a Ramp Junction as a Function of the Carpool Percentage	28-25
Exhibit 28-12 Capacity of a Ramp Junction as a Function of the Carpool Percentage	28-26
Exhibit 28-13 Density of a Ramp Junction as a Function of the HOV Violation Percentage.....	28-26
Exhibit 28-14 Capacity of a Ramp Junction as a Function of the HOV Violation Percentage.....	28-27
Exhibit 28-15 Density of a Ramp Junction as a Function of the Distance at Which Drivers Begin to React	28-27
Exhibit 28-16 Capacity of a Ramp Junction as a Function of the Distance at Which Drivers Begin to React.....	28-28
Exhibit 28-17 Density of a Ramp Junction as a Function of the Percentage of HOV Usage.....	28-28
Exhibit 28-18 Capacity of a Ramp Junction as a Function of the Percentage of HOV Usage	28-29

1. INTRODUCTION

Chapter 28 is the supplemental chapter for Chapter 14, Freeway Merge and Diverge Segments, which is found in Volume 2 of the *Highway Capacity Manual* (HCM). Section 2 provides five example problems demonstrating the application of the Chapter 14 methodology and its extension to freeway managed lanes. Section 3 presents examples of applying alternative tools to the analysis of freeway merge and diverge segments to address limitations of the Chapter 14 methodology.

VOLUME 4: APPLICATIONS
GUIDE

- 25. Freeway Facilities:
Supplemental
- 26. Freeway and Highway
Segments: Supplemental
- 27. Freeway Weaving:
Supplemental
- 28. Freeway Merges and
Diverges: Supplemental**
- 29. Urban Street Facilities:
Supplemental
- 30. Urban Street Segments:
Supplemental
- 31. Signalized Intersections:
Supplemental
- 32. STOP-Controlled
Intersections:
Supplemental
- 33. Roundabouts:
Supplemental
- 34. Interchange Ramp
Terminals: Supplemental
- 35. Pedestrians and Bicycles:
Supplemental
- 36. Concepts: Supplemental
- 37. ATDM: Supplemental

2. EXAMPLE PROBLEMS

Exhibit 28-1 lists the example problems presented in this section.

Exhibit 28-1
List of Example Problems

Example Problem	Title	Type of Analysis
1	Isolated One-Lane, Right-Hand On-Ramp to a Four-Lane Freeway	Operational analysis
2	Two Adjacent Single-Lane, Right-Hand Off-Ramps on a Six-Lane Freeway	Operational analysis
3	One-Lane On-Ramp Followed by a One-Lane Off-Ramp on an Eight-Lane Freeway	Operational analysis
4	Single-Lane, Left-Hand On-Ramp on a Six-Lane Freeway	Special case
5	Service Flow Rates and Service Volumes for an Isolated On-Ramp on a Six-Lane Freeway	Service flow rates and service volumes

EXAMPLE PROBLEM 1: ISOLATED ONE-LANE, RIGHT-HAND ON-RAMP TO A FOUR-LANE FREEWAY

The Facts

The following data are available to describe the traffic and geometric characteristics of this location. The example assumes no impacts of inclement weather or incidents.

1. Isolated location (no adjacent ramps to consider);
2. One-lane ramp roadway and junction;
3. Four-lane freeway (two lanes in each direction);
4. Upstream freeway demand volume = 2,500 veh/h;
5. Ramp demand volume = 535 veh/h;
6. 5% trucks throughout;
7. Acceleration lane = 740 ft;
8. FFS, freeway = 60 mi/h;
9. FFS, ramp = 45 mi/h;
10. Level terrain for freeway and ramp;
11. Peak hour factor (PHF) = 0.90; and
12. Drivers are regular commuters.

Comments

All input parameters are known, so no default values are needed or used. Adjustment factors for heavy vehicles and driver population are found in Chapter 12, Basic Freeway and Multilane Highway Segments.

Step 1: Specify Inputs and Convert Demand Volumes to Demand Flow Rates

Input parameters were specified in the Facts section above. Equation 14-1 is used to convert demand volumes to flow rates under equivalent ideal conditions:

$$v_i = \frac{V_i}{PHF \times f_{HV}}$$

Demand volumes are given for the freeway and the ramp. The PHF is specified. The driver population adjustment factors for commuters are 1.00 (Chapter 12), while the heavy vehicle adjustment factor is computed as follows:

$$f_{HV} = \frac{1}{1 + P_T(E_T - 1)}$$

Truck presence is given. The value of E_T for level terrain is 2.0 (Chapter 12). On the basis of these values, the freeway and ramp demand volumes are converted as follows:

For the freeway,

$$f_{HV} = \frac{1}{1 + P_T(E_T - 1)} = \frac{1}{1 + 0.05(2.0 - 1)} = 0.952$$

$$v_F = \frac{2,500}{0.90 \times 0.952} = 2,918 \text{ pc/h}$$

For the ramp, the calculations are identical:

$$f_{HV} = \frac{1}{1 + 0.05(2.0 - 1)} = 0.952$$

$$v_R = \frac{535}{0.90 \times 0.952} = 625 \text{ pc/h}$$

Step 2: Estimate the Approaching Flow Rate in Lanes 1 and 2 of the Freeway Immediately Upstream of the Ramp Influence Area

The demand flow in Lanes 1 and 2 immediately upstream of the ramp influence area is computed by using Equation 14-2.

$$v_{12} = v_F \times P_{FM}$$

The freeway flow rate was computed in Step 1. The value of P_{FM} is found in Exhibit 14-8. For a four-lane freeway, the value is 1.00. Then

$$v_{12} = 2,918 \times 1.00 = 2,918 \text{ pc/h}$$

Because there are no outer lanes on a four-lane freeway, there is no need to check this result for reasonableness.

Step 3: Estimate the Capacity of the Ramp–Freeway Junction and Compare with Demand Flow Rates

The critical capacity checkpoint for a single-lane on-ramp is the downstream freeway segment:

$$v_{FO} = v_F + v_R = 2,918 + 625 = 3,543 \text{ pc/h}$$

The capacity of a four-lane freeway (two lanes in one direction) with an FFS of 60 mi/h is given in Exhibit 14-10. The capacity is 4,600 pc/h, which is more than the demand flow of 3,543 pc/h. The capacity of a one-lane ramp with an FFS of 45 mi/h is given in Exhibit 14-12 as 2,100 pc/h, which is well in excess of the ramp demand flow of 625 pc/h. The maximum desirable flow rate entering the ramp influence area is also 4,600 pc/h, again more than 3,543. Thus, the operation of the segment is expected to be stable. LOS F does not exist. Note that there were no adjustments to speed (SAF) or capacity (CAF) due to inclement weather, incidents, or other impacts for this case.

Step 4: Estimate Density in the Ramp Influence Area and Determine the Prevailing LOS

The estimated density in the ramp–freeway junction is estimated by using Equation 14-22:

$$D_R = 5.475 + 0.00734v_R + 0.0078v_{12} - 0.00627L_A$$

$$D_R = 5.475 + 0.00734(625) + 0.0078(2,918) - 0.00627(740)$$

$$D_R = 28.2 \text{ pc/mi/ln}$$

From Exhibit 14-3, this is LOS D, but the result is close to the LOS C boundary.

Step 5: Estimate Speeds in the Vicinity of Ramp–Freeway Junctions

Since there are no outer lanes on a four-lane freeway, only the speed within the ramp influence area should be computed, by using the equations given in Exhibit 14-13:

$$M_S = 0.321 + 0.0039e^{(v_{R12}/1,000)} - 0.002(L_A \times S_{FR} \times SAF/1,000)$$

$$M_S = 0.321 + 0.0039e^{(3,543/1,000)} - 0.002(740 \times 45 \times 1.00/1,000) = 0.389$$

$$S_R = FFS \times SAF - (FFS \times SAF - 42)M_S$$

$$S_R = 60 \times 1.00 - (60 \times 1.00 - 42)(0.389) = 53.0 \text{ mi/h}$$

Note that the speed adjustment factor, SAF, is 1.00, since this is not a case where inclement weather or other factors would necessitate a correction.

Discussion

The results indicate that the merge area operates in a stable fashion, with some deterioration in density and speed due to merging operations.

EXAMPLE PROBLEM 2: TWO ADJACENT SINGLE-LANE, RIGHT-HAND OFF-RAMPS ON A SIX-LANE FREEWAY

The Facts

The following information concerning demand volumes and geometries is available for this problem. The example assumes no impacts of inclement weather or incidents.

1. Two consecutive one-lane, right-hand off-ramps;
2. Six-lane freeway with FFS = 60 mi/h;
3. Level terrain for freeway and both ramps;

4. 7.5% trucks on freeway and both ramps;
5. First-ramp FFS = 40 mi/h;
6. Second-ramp FFS = 25 mi/h;
7. Drivers are regular commuters;
8. Freeway demand volume = 4,500 veh/h (immediately upstream of the first off-ramp);
9. First-ramp demand volume = 300 veh/h;
10. Second-ramp demand volume = 500 veh/h;
11. Distance between ramps = 750 ft;
12. First-ramp deceleration lane length = 500 ft;
13. Second-ramp deceleration lane length = 300 ft; and
14. Peak hour factor = 0.95.

Comments

The solution will use adjustment factors for heavy vehicle presence and driver population selected from Chapter 12, Basic Freeway and Multilane Highway Segments. All input parameters are specified, so no default values are needed or used.

Step 1: Specify Inputs and Convert Demand Volumes to Demand Flow Rates

Input parameters were specified in the Facts section above. Equation 14-1 is used to convert demand volumes to flow rates under equivalent ideal conditions:

$$v_i = \frac{V_i}{PHF \times f_{HV}}$$

In this case, three demand volumes must be converted: the freeway volume immediately upstream of the first ramp and the two ramp demand volumes. Since all demands include 7.5% trucks, only a single heavy vehicle adjustment factor will be needed. From Chapter 12, the appropriate value of E_T for level terrain is 2.0.

Then

$$f_{HV} = \frac{1}{1 + P_T(E_T - 1)} = \frac{1}{1 + 0.075(2 - 1)} = 0.930$$

and

$$v_F = \frac{4,500}{0.95 \times 0.930} = 5,093 \text{ pc/h}$$

$$v_{R1} = \frac{300}{0.95 \times 0.930} = 340 \text{ pc/h}$$

$$v_{R2} = \frac{500}{0.95 \times 0.930} = 566 \text{ pc/h}$$

Step 2: Estimate the Approaching Flow Rate in Lanes 1 and 2 of the Freeway Immediately Upstream of the Ramp Influence Area

Because two consecutive off-ramps are under consideration, the first will have to consider the impact of the second on its operations, and the second will have to consider the impact of the first.

First Off-Ramp

From Exhibit 14-9, flow in Lanes 1 and 2 of the freeway is estimated by using Equation 14-11 or Equation 14-9, depending on whether the impact of the downstream off-ramp is significant. This is determined by computing the equivalence distance by using Equation 14-13:

$$L_{EQ} = \frac{v_D}{1.15 - 0.000032v_F - 0.000369v_R}$$

$$L_{EQ} = \frac{566}{1.15 - 0.000032(5,093) - 0.000369(340)} = 657 \text{ ft}$$

Since the actual distance between ramps, 750 ft, is greater than the equivalence distance of 657 ft, the ramp may be treated as if it were isolated, with Equation 14-9:

$$P_{FD} = 0.760 - 0.000025v_F - 0.000046v_R$$

$$P_{FD} = 0.760 - 0.000025(5,093) - 0.000046(340) = 0.617$$

Then from Equation 14-8,

$$v_{12} = v_R + (v_F - v_R)P_{FD}$$

$$v_{12} = 340 + (5,093 - 340)(0.617) = 3,273 \text{ pc/h}$$

Because a six-lane freeway includes one lane in addition to the ramp influence areas (the innermost lane, Lane 3), the reasonableness of the predicted lane distribution of arriving freeway vehicles should be checked. The flow rate in Lane 3 is $5,093 - 3,273 = 1,820$ pc/h. The average flow per lane in Lanes 1 and 2 is $3,273/2 = 1,637$ pc/h (rounded to the nearest pc). Then:

Is $v_3 > 2,700$ pc/h/ln? **No**

Is $v_3 > 1.5 \times (1,637) = 2,456$ pc/h/ln? **No**

Since both checks for reasonable lane distribution are passed, the computed value of v_{12} for the first off-ramp is accepted as 3,273 pc/h.

Second Off-Ramp

From Exhibit 14-9, the second off-ramp should be analyzed by using Equation 14-9, which is for an isolated off-ramp. Adjacent upstream off-ramps do not affect the lane distribution of arriving vehicles at a downstream off-ramp.

The freeway flow approaching Ramp 2, however, includes the freeway flow approaching Ramp 1, less the flow rate of vehicles exiting the freeway at Ramp 1. Therefore, the freeway flow rate approaching Ramp 2 is as follows:

$$v_{F2} = 5,093 - 340 = 4,753 \text{ pc/h}$$

Then

$$P_{FD} = 0.760 - 0.000025v_F - 0.000046v_R$$

$$P_{FD} = 0.760 - 0.000025(4,753) - 0.000046(566) = 0.615$$

$$v_{12} = 566 + (4,753 - 566)(0.615) = 3,141 \text{ pc/h}$$

Again, because there is an outer lane on a six-lane freeway, the reasonableness of this estimate must be checked. The flow rate in the innermost lane v_3 is $4,753 - 3,141 = 1,612$ pc/h. The average flow rate in Lanes 1 and 2 is $3,141/2 = 1,571$ pc/h (rounded). Then:

$$\text{Is } v_3 > 2,700 \text{ pc/h/ln?} \quad \text{No}$$

$$\text{Is } v_3 > 1.5 \times 1,571 = 2,357 \text{ pc/h/ln?} \quad \text{No}$$

Once again, the predicted lane distribution of arriving vehicles is reasonable, and v_{12} is taken to be 3,141 pc/h.

Step 3: Estimate the Capacity of the Ramp–Freeway Junction and Compare with Demand Flow Rates

Because two off-ramps are involved in this segment, there are several capacity checkpoints:

1. Total freeway flow upstream of the first off-ramp (the point at which maximum freeway flow exists),
2. Capacity of both off-ramps, and
3. Maximum desirable flow rates entering each of the two off-ramp influence areas.

These comparisons are shown in Exhibit 28-2. Note that freeway capacity is based on a freeway with FFS = 60 mi/h. The first ramp capacity is based on a ramp FFS of 40 mi/h and the second on a ramp FFS of 25 mi/h.

Item	Capacity (pc/h) from Exhibit 14-10 or Exhibit 14-12	Demand Flow Rate (pc/h)	Problem?
Freeway flow rate	6,900	5,093	No
First off-ramp	2,000	340	No
Second off-ramp	1,900	566	No
Max. v_{12} first ramp	4,400	3,273	No
Max. v_{12} second ramp	4,400	3,141	No

Note: Max. = maximum.

None of the capacity values are exceeded, so operation of these ramp junctions will be stable, and LOS F does not occur. Again, there are no situations that would call for an adjustment to be made to speed (SAF) or capacity (CAF).

Step 4: Estimate Density in the Ramp Influence Area and Determine the Prevailing LOS

Because there are two off-ramps, two ramp influence areas are involved, and two ramp influence area densities will be computed with Equation 14-23.

$$D_R = 4.252 + 0.0086v_{12} - 0.009L_D$$

$$D_{R1} = 4.252 + 0.0086(3,273) - 0.009(500) = 27.9 \text{ pc/mi/ln}$$

$$D_{R2} = 4.252 + 0.0086(3,141) - 0.009(300) = 28.6 \text{ pc/mi/ln}$$

Exhibit 28-2
Example Problem 2:
Capacity Checks

From Exhibit 14-3, both of these ramp influence areas operate close to the boundary between LOS C and LOS D (28.0 pc/mi/ln). Ramp 1 operates in LOS C, while Ramp 2 operates in LOS D.

Although it makes virtually no difference in this case, note that the two ramp influence areas overlap. The influence area of the first off-ramp extends 1,500 ft upstream. The influence area of the second off-ramp also extends 1,500 ft upstream. Since the ramps are only 750 ft apart, the second ramp influence area overlaps the first for 750 ft (immediately upstream of the first diverge point). The worse of the two levels of service is applied to this 750-ft overlap. In this case, the levels of service are different, even though the predicted densities are similar. Thus, the overlapping influence area is assigned LOS D.

Step 5: Estimate Speeds in the Vicinity of Ramp–Freeway Junctions

Because these ramps are on a six-lane freeway with an outer lane, the speed within each ramp influence area, the speed in the outer lane adjacent to each ramp influence area, and the weighted average of the two can be estimated.

First Off-Ramp

The speed within the first ramp influence area is computed by using the equations given in Exhibit 14-14:

$$D_S = 0.883 + 0.00009v_R - 0.013S_{FR} \times SAF$$

$$D_S = 0.883 + 0.00009(340) - 0.013(40)(1.00) = 0.394$$

$$S_R = FFS \times SAF - (FFS \times SAF - 42)D_S$$

$$S_R = (60)(1.00) - (60 \times 1.00 - 42)(0.394) = 52.9 \text{ mi/h}$$

The flow rate in the outer lane v_{OA} is $5,093 - 3,273 = 1,820$ pc/h/ln. The average speed in this outer lane is computed as follows, by using the equation given in Exhibit 14-14:

$$S_O = 1.097 \times FFS \times SAF - 0.0039(v_{OA} - 1,000)$$

$$S_O = (1.097)(60)(1.00) - 0.0039(1,820 - 1,000) = 62.6 \text{ mi/h}$$

The average speed in Lane 3 is predicted to be slightly higher than the FFS of the freeway. This is not uncommon, since through vehicles at higher speeds use Lane 3 to avoid congestion in the ramp influence area. However, the average speed across all lanes should not be higher than the FFS. In this case, the average speed across all lanes is computed as follows, by using the appropriate equation from Exhibit 14-15:

$$S = \frac{v_{12} + v_{OA}N_O}{\left(\frac{v_{12}}{S_R}\right) + \left(\frac{V_{OA}N_O}{S_O}\right)} = \frac{3,273 + (1,820)(1)}{\left(\frac{3,273}{52.9}\right) + \left(\frac{1,820 \times 1}{62.6}\right)} = 56.0 \text{ mi/h}$$

This result is, as expected, less than the FFS of the freeway.

Note that once again the SAF is 1.00, since there are no conditions that would require an adjustment.

Second Off-Ramp

The speed in the second ramp influence area is computed as follows:

$$D_S = 0.883 + 0.00009(566) - 0.013(25)(1.00) = 0.609$$

$$S_R = (60)(1.00) - (60 \times 1.00 - 42)(0.609) = 49.0 \text{ mi/h}$$

Lane 3 has a demand flow rate of $4,753 - 3,141 = 1,612$ pc/h/ln. The average speed in this outer lane is computed as follows:

$$S_O = (1.097)(60)(1.00) - 0.0039(1,612 - 1,000) = 63.4 \text{ mi/h}$$

The average speed across all freeway lanes is

$$S = \frac{v_{12} + v_{OA}N_O}{\left(\frac{v_{12}}{S_R}\right) + \left(\frac{V_{OA}N_O}{S_O}\right)} = \frac{3,141 + (1,612)(1)}{\left(\frac{3,141}{49.0}\right) + \left(\frac{1,612 \times 1}{63.4}\right)} = 53.1 \text{ mi/h}$$

Discussion

The speed results in this case are interesting. While densities are similar for both ramps, the density is somewhat higher and the speed somewhat lower in the second influence area. This is primarily the result of a shorter deceleration lane and a lower ramp FFS (25 mi/h versus 40 mi/h). In both cases, the average speed in the outer lane is higher than the FFS, which applies as an average across all lanes.

Since the operation is stable, there is no special concern here, short of a significant increase in demand flows. LOS is technically D but falls just over the LOS C boundary. In this case the step-function LOS assigned may imply operation poorer than actually exists. It emphasizes the importance of knowing not only the LOS but also the value of the service measure that produces it.

EXAMPLE PROBLEM 3: ONE-LANE ON-RAMP FOLLOWED BY A ONE-LANE OFF-RAMP ON AN EIGHT-LANE FREEWAY**The Facts**

The following information is available concerning this pair of ramps to be analyzed. The example assumes no impacts of inclement weather or incidents.

1. Eight-lane freeway with an FFS of 65 mi/h;
2. One-lane, right-hand on-ramp with an FFS of 30 mi/h;
3. One-lane, right-hand off-ramp with an FFS of 25 mi/h;
4. Distance between ramps = 1,300 ft;
5. Acceleration lane on Ramp 1 = 260 ft;
6. Deceleration lane on Ramp 2 = 260 ft;
7. Level terrain on freeway and both ramps;
8. 10% trucks on freeway and off-ramp;
9. 5% trucks on on-ramp;
10. Freeway flow rate (upstream of first ramp) = 5,490 veh/h;
11. On-ramp flow rate = 410 veh/h;
12. Off-ramp flow rate = 600 veh/h;

- 13. PHF = 0.94; and
- 14. Drivers are regular commuters.

Comments

As with previous example problems, the conversion of demand volumes to flow rates requires adjustment factors selected from Chapter 12, Basic Freeway and Multilane Highway Segments. All pertinent information is given, and no default values will be applied.

Step 1: Specify Inputs and Convert Demand Volumes to Demand Flow Rates

Input parameters were specified in the Facts section above. Equation 14-1 is used to convert demand volumes to flow rates under equivalent ideal conditions:

$$v_i = \frac{V_i}{PHF \times f_{HV}}$$

Three demand volumes must be converted to flow rates under equivalent ideal conditions: the freeway volume immediately upstream of the first ramp junction, the first ramp volume, and the second ramp volume. Because the freeway segment under study has level terrain, the value of E_T will be 2.0 for all volumes.

Then, for the freeway demand volume,

$$f_{HV} = \frac{1}{1 + P_T(E_T - 1)} = \frac{1}{1 + 0.10(2 - 1)} = 0.91$$

$$v_F = \frac{5,490}{0.94 \times 0.91} = 6,418 \text{ pc/h}$$

For the on-ramp demand volume,

$$f_{HV} = \frac{1}{1 + 0.05(2 - 1)} = 0.952$$

$$v_{R1} = \frac{410}{0.94 \times 0.952} = 458 \text{ pc/h}$$

For the off-ramp demand volume,

$$f_{HV} = \frac{1}{1 + 0.10(2 - 1)} = 0.91$$

$$v_{R2} = \frac{600}{0.94 \times 0.91} = 701 \text{ pc/h}$$

In the remaining computations, these converted demand flow rates are used as input values.

Step 2: Estimate the Approaching Flow Rate in Lanes 1 and 2 of the Freeway Immediately Upstream of the Ramp Influence Area

Once again, the situation involves a pair of adjacent ramps. Analysis of each ramp must take into account the potential impact of the other on its operations. Because the ramps are on an eight-lane freeway (four lanes in each direction), Exhibit 14-8 and Exhibit 14-9 indicate that each ramp is considered as if it were isolated.

First Ramp: On-Ramp

Exhibit 14-8 applies to on-ramps. Exhibit 14-8 presents two possible equations for use in estimating v_{12} on the basis of the value of v_F/S_{FR} . In this case, the value is $6,418/30 = 213.9 > 72$. Therefore, the second equation for eight-lane freeways given in Exhibit 14-8 is used, giving the following:

$$v_{12} = v_F \times P_{FM}$$

$$P_{FM} = 0.2178 - 0.000125v_R = 0.2178 - 0.000125(458) = 0.16$$

$$v_{12} = (6,418)(0.16) = 1,027 \text{ pc/h}$$

Because the eight-lane freeway includes two outer lanes in each direction, the reasonableness of this prediction must be checked. The average flow per lane in Lanes 1 and 2 is $1,027/2 = 514 \text{ pc/h/ln}$ (rounded). The flow in the two outer lanes, Lanes 3 and 4, is $6,418 - 1,027 = 5,391 \text{ pc/h}$. The average flow per lane in Lanes 3 and 4 is, therefore, $5,391/2 \sim 2,696 \text{ pc/h/ln}$. Then:

$$\text{Is } v_{av34} > 2,700 \text{ pc/h/ln?} \quad \mathbf{No}$$

$$\text{Is } v_{av34} > 1.5 \times 514 = 771 \text{ pc/h/ln?} \quad \mathbf{Yes}$$

Therefore, the predicted lane distribution is not reasonable. Too many vehicles are placed in the two outer lanes compared with Lanes 1 and 2. Equation 14-19 is used to produce a more reasonable distribution:

$$v_{12a} = \left(\frac{v_F}{2.50} \right) = \left(\frac{6,418}{2.50} \right) = 2,567 \text{ pc/h}$$

On the basis of this adjusted value, the number of vehicles now assigned to the two outer lanes is $6,418 - 2,567 = 3,851 \text{ pc/h}$.

Second Ramp: Off-Ramp

Equation 14-8 and Exhibit 14-9 apply to off-ramps. Exhibit 14-9 shows that the value of P_{FD} for off-ramps on eight-lane freeways is a constant: 0.436. Since the methodology is based on regression analysis of a database, the recommendation of a constant reflects a small sample size in that database. Note also that the freeway flow approaching the second ramp is the sum of the freeway flow approaching the first ramp and the on-ramp flow that is now also on the freeway, or $6,418 + 458 = 6,876 \text{ pc/h}$. The flow rate in Lanes 1 and 2 is now easily computed by using Equation 14-8:

$$v_{12} = v_R + (v_F - v_R)P_{FD}$$

$$v_{12} = 701 + (6,876 - 701)(0.436) = 3,393 \text{ pc/h}$$

Because there are two outer lanes on this eight-lane freeway, the reasonableness of this estimate must be checked. The average flow per lane in Lanes 1 and 2 is $3,393/2 = 1,697 \text{ pc/h/ln}$. The total flow in Lanes 3 and 4 of the freeway is $6,876 - 3,393 = 3,483 \text{ pc/h}$, or an average flow rate per lane of $3,483/2 = 1,742 \text{ pc/h/ln}$.

$$\text{Is } v_{av34} > 2,700 \text{ pc/h/ln?} \quad \mathbf{No}$$

$$\text{Is } v_{av34} > 1.5 \times 1,697 = 2,545 \text{ pc/h/ln?} \quad \mathbf{No}$$

Therefore, the estimated value of v_{12} is deemed reasonable and is carried forward in the computations.

Step 3: Estimate the Capacity of the Ramp–Freeway Junction and Compare with Demand Flow Rates

Because there are two ramps in this segment, there are five capacity checkpoints to consider:

1. The freeway flow rate at its maximum point—which in this case is between the on- and off-ramp, since this is the only location where both on- and off-ramp vehicles are on the freeway.
2. The capacity of the on-ramp.
3. The capacity of the off-ramp.
4. The maximum desirable flow entering the on-ramp influence area.
5. The maximum desirable flow entering the off-ramp influence area.

These comparisons are shown in Exhibit 28-3. The capacity of the freeway is based on an eight-lane freeway with an FFS of 65 mi/h. The capacity of the on-ramp is based on an FFS of 30 mi/h, and the capacity of the off-ramp is based on an FFS of 25 mi/h.

Exhibit 28-3
Example Problem 3:
Capacity Checks

Item	Capacity (pc/h) from Exhibit 14-10 or Exhibit 14-12	Demand Flow Rate (pc/h)	Problem?
Freeway flow rate	9,400	6,876	No
First on-ramp	1,900	458	No
Second off-ramp	1,900	701	No
Max. v_{R12} first ramp	4,600	$2,567 + 458 = 3,025$	No
Max. v_{12} second ramp	4,400	3,393	No

There are no capacity concerns, since all demands are well below the associated capacities or maximum desirable values. No adjustments to capacity are required. LOS F is not present in any part of this segment, and operations are expected to be stable.

Step 4: Estimate Density in the Ramp Influence Area and Determine the Prevailing LOS

Equation 14-22 is used to find the density in the first on-ramp influence area:

$$D_R = 5.475 + 0.00734v_R + 0.0078v_{12} - 0.00627L_A$$

$$D_R = 5.475 + 0.00734(458) + 0.0078(2,567) - 0.00627(260)$$

$$D_R = 27.2 \text{ pc/mi/ln}$$

Equation 14-23 is used to find the density in the second off-ramp influence area:

$$D_R = 4.252 + 0.0086v_{12} - 0.009L_D$$

$$D_R = 4.252 + 0.0086(3,393) - 0.009(260) = 31.1 \text{ pc/mi/ln}$$

From Exhibit 14-3, both of these ramp influence areas operate close to the boundary between LOS C and LOS D (28 pc/mi/ln). Ramp 1 operates in LOS C, while Ramp 2 operates in LOS D.

Because the on-ramp influence area extends 1,500 ft downstream, the off-ramp influence area extends 1,500 ft upstream, and the two ramps are only 1,300 ft apart, the distance between the ramps is included in both. Therefore, the lower LOS D for the off-ramp governs the operation. Note that the additional 200 ft of

the off-ramp influence area is actually upstream of the on-ramp, and the additional 200 ft of the on-ramp influence area is downstream of the off-ramp.

Step 5: Estimate Speeds in the Vicinity of Ramp–Freeway Junctions

Because the facility is an eight-lane freeway, speeds should be estimated for the two ramp influence areas, for the outer lanes (Lanes 3 and 4) adjacent to the ramp influence areas, and for all vehicles—the weighted average of the other two speeds.

First Ramp (On-Ramp)

Equations for estimation of average speed in an on-ramp influence area and in outer lanes adjacent to it are taken from Exhibit 14-13.

$$M_S = 0.321 + 0.0039e^{(v_{R12}/1,000)} - 0.002(L_A \times S_{FR} \times SAF/1,000)$$

$$M_S = 0.321 + 0.0039e^{(3,025/1,000)} - 0.002(260 \times 30 \times 1.00/1,000) = 0.385$$

$$S_R = FFS \times SAF - (FFS \times SAF - 42)M_S$$

$$S_R = (65)(1.00) - (65 \times 1.00 - 42)(0.385) = 56.2 \text{ mi/h}$$

Since the average outer lane demand flow rate is $3,851/2 = 1,926$ pc/h/ln, which is greater than 500 pc/h/ln and less than 2,300 pc/h/ln, the outer speed is estimated as follows, by using the appropriate equation from Exhibit 14-13:

$$S_O = FFS \times SAF - 0.0036(v_{OA} - 500)$$

$$S_O = (65)(1.00) - 0.0036(1,926 - 500) = 59.9 \text{ mi/h}$$

Note that the speed adjustment factor (SAF) is 1.00.

The weighted average speed of all vehicles is

$$S = \frac{v_{12} + v_{OA}N_O}{\left(\frac{v_{12}}{S_R}\right) + \left(\frac{v_{OA}N_O}{S_O}\right)} = \frac{3,025 + (1,926)(2)}{\left(\frac{3,025}{56.2}\right) + \left(\frac{1,926 \times 2}{59.9}\right)} = 58.2 \text{ mi/h}$$

Second Ramp (Off-Ramp)

For off-ramps, equations for estimation of average speed are drawn from Exhibit 14-14. At the second ramp, the flow in Lanes 1 and 2 has been computed as 3,392 pc/h or 1,696 pc/h/ln, while the flow in Lanes 3 and 4 is 3,483 pc/h or 1,742 pc/h/ln. Then

$$D_S = 0.883 + 0.00009v_R - 0.013S_{FR} \times SAF$$

$$D_S = 0.883 + 0.00009(701) - 0.013(25)(1.00) = 0.621$$

$$S_R = FFS \times SAF - (FFS \times SAF - 42)D_S$$

$$S_R = (65)(1.00) - (65 \times 1.00 - 42)(0.621) = 50.7 \text{ mi/h}$$

Because the average flow in the outer lanes is greater than 1,000 pc/h/ln, the average speed of vehicles in the outer lanes (Lanes 3 and 4) is as follows:

$$S_O = 1.097 \times FFS \times SAF - 0.0039(v_{OA} - 1,000)$$

$$S_O = (1.097)(65)(1.00) - 0.0039(1,742 - 1,000) = 68.4 \text{ mi/h}$$

The weighted average speed of all vehicles is

$$S = \frac{v_{12} + v_{OA}N_O}{\left(\frac{v_{12}}{S_R}\right) + \left(\frac{V_{OA}N_O}{S_O}\right)} = \frac{3,393 + (1,742)(2)}{\left(\frac{3,393}{50.7}\right) + \left(\frac{1,742 \times 2}{68.4}\right)} = 58.3 \text{ mi/h}$$

Discussion

As noted previously, between the ramps, the influence areas of both ramps fully overlap. Since a higher density is predicted for the off-ramp influence area, and LOS D results, this density should be applied to the entire area between the two ramps.

The speed results are also interesting. The slower speeds within the off-ramp influence area will also control the overlap area. On the other hand, the speed results indicate a higher average speed for all vehicles associated with the off-ramp than for those associated with the on-ramp. This is primarily due to the much larger disparity between speeds within the ramp influence area and in outer lanes when the off-ramp is considered. The speed differential is more than 20 mi/h for the off-ramp, as opposed to a little more than 3 mi/h for the on-ramp. This is not entirely unexpected. At diverge junctions, vehicles in outer lanes tend to face less turbulence than those in outer lanes near merge junctions. All off-ramp vehicles must be in Lanes 1 and 2 for some distance before exiting the freeway. On-ramp vehicles, in contrast, can execute as many lane changes as they wish, and more of them may wind up in outer lanes within 1,500 ft of the junction point.

Thus, the total operation of this two-ramp segment is expected to be LOS D, with speeds of approximately 50 mi/h in Lanes 1 and 2 and approximately 70 mi/h in Lanes 3 and 4.

EXAMPLE PROBLEM 4: SINGLE-LANE, LEFT-HAND ON-RAMP ON A SIX-LANE FREEWAY

The Facts

The following information is available concerning this example problem. The example assumes no impacts of inclement weather or incidents.

1. One-lane, left-side on-ramp on a six-lane freeway (three lanes in each direction);
2. Freeway demand volume upstream of ramp = 4,000 veh/h;
3. On-ramp demand volume = 490 veh/h;
4. 7.5% trucks on freeway, 3% trucks on the on-ramp;
5. Freeway FFS = 65 mi/h;
6. Ramp FFS = 30 mi/h;
7. Acceleration lane = 820 ft;
8. Level terrain on freeway and ramp;
9. Drivers are regular commuters; and
10. PHF = 0.90.

Comments

This is a special application of the ramp analysis methodology presented in Chapter 14. For left-hand ramps, the flow rate in Lanes 1 and 2 (v_{12}) is initially computed as if it were a right-hand ramp. Exhibit 14-18 is then used to convert this result to an estimate of the flow in Lanes 2 and 3 (v_{23}), since these are the two leftmost lanes that will be involved in the merge. In effect, the ramp influence area is, in this case, Lanes 3 and 4 and the acceleration lane for a distance of 1,500 ft downstream of the merge point.

Step 1: Specify Inputs and Convert Demand Volumes to Demand Flow Rates

Input parameters were specified in the Facts section above. Equation 14-1 is used to convert demand volumes to flow rates under equivalent ideal conditions:

$$v_i = \frac{V_i}{PHF \times f_{HV}}$$

From Chapter 12, Basic Freeway and Multilane Highway Segments, the passenger car equivalent E_T for trucks in level terrain is 2.0.

For the freeway demand volume,

$$f_{HV} = \frac{1}{1 + P_T(E_T - 1)} = \frac{1}{1 + 0.075(2 - 1)} = 0.93$$

$$v_F = \frac{4,000}{0.90 \times 0.93} = 4,779 \text{ pc/h}$$

For the ramp demand volume,

$$f_{HV} = \frac{1}{1 + 0.03(2 - 1)} = 0.971$$

$$v_R = \frac{490}{0.90 \times 0.971} = 561 \text{ pc/h}$$

Step 2: Estimate the Approaching Flow Rate in Lanes 1 and 2 of the Freeway Immediately Upstream of the Ramp Influence Area

To estimate flow in the two left lanes, the flow normally expected in Lanes 1 and 2 for a similar right-hand ramp must first be computed. From Exhibit 14-8, for an isolated on-ramp on a six-lane freeway, Equation 14-4 is used:

$$v_{12} = v_F \times P_{FM}$$

$$P_{FM} = 0.5775 + 0.000028L_A = 0.5775 + 0.000028(820) = 0.600$$

$$v_{12} = (4,779)(0.600) = 2,867 \text{ pc/h}$$

From Exhibit 14-18, the adjustment factor applied to this result to find the estimated flow rate in Lanes 2 and 3 is 1.12. Therefore,

$$v_{23} = 2,867 \times 1.12 = 3,211 \text{ pc/h}$$

While, strictly speaking, the reasonableness criteria for lane distribution do not apply to left-hand ramps, they can be applied very approximately. In this case, the single "outer lane" (which is now Lane 1) would have a flow rate of $4,779 - 3,211 = 1,568$ pc/h. This is not greater than 2,700 pc/h/ln, nor is it greater than 1.5 times the average flow in Lanes 2 and 3 ($1.5 \times 3,211/2 = 2,408$ pc/h/ln).

Thus, even if the reasonableness criteria were approximately applied in this case, no violation would exist.

The remaining computations proceed for the left-hand ramp, with the substitution of v_{34} for v_{12} in all algorithms used.

Step 3: Estimate the Capacity of the Ramp–Freeway Junction and Compare with Demand Flow Rates

For this case, there are three simple checkpoints:

1. The principal capacity checkpoint is the total demand flow rate downstream of the merge, $4,779 + 561 = 5,340$ pc/h. From Exhibit 14-10, for a six-lane freeway with an FFS of 65 mi/h, the capacity is 7,050 pc/h, well over the demand flow rate.
2. The ramp roadway capacity should also be checked by using Exhibit 14-12. For a single-lane ramp with an FFS of 30 mi/h, the capacity is 1,900 pc/h, which is much greater than the demand flow rate of 561 pc/h.
3. Finally, the maximum flow entering the ramp influence area should be checked. In this case, a left-hand ramp, the total flow entering the ramp influence area is the freeway flow remaining in Lanes 2 and 3 plus the ramp flow rate. Thus, the total flow entering the ramp influence area is $3,211 + 561 = 3,772$ pc/h, which is lower than the maximum desirable flow rate of 4,600 pc/h, shown in Exhibit 14-10.

Thus, there are no capacity problems at this merge point, and stable operations are expected. LOS F will not result from the stated conditions.

Step 4: Estimate Density in the Ramp Influence Area and Determine the Prevailing LOS

The density in the ramp influence area is found by using Equation 14-22, except v_{23} replaces v_{12} because of the left-hand ramp placement:

$$D_S = 5.475 + 0.00734v_R + 0.0078v_{23} - 0.00627L_A$$

$$D_S = 5.475 + 0.00734(561) + 0.0078(3,211) - 0.00627(820)$$

$$D_S = 29.5 \text{ pc/mi/ln}$$

From Exhibit 14-3, this is LOS D.

Step 5: Estimate Speeds in the Vicinity of Ramp–Freeway Junctions

The speed estimation algorithms were calibrated for right-hand ramps, and the estimation algorithms for “outer lane(s)” assume that these are the leftmost lanes. Thus, for a left-hand ramp, these computations must be considered approximate at best.

By using the equations in Exhibit 14-13, the following results are obtained:

$$M_S = 0.321 + 0.0039e^{(v_{R23}/1,000)} - 0.002(L_A \times S_{FR} \times SAF/1,000)$$

$$M_S = 0.321 + 0.0039e^{(3,777/1,000)} - 0.002(820 \times 30 \times 1.00/1,000) = 0.443$$

$$S_R = FFS \times SAF - (FFS \times SAF - 42)M_S$$

$$S_R = (65)(1.00) - (65 \times 1.00 - 42)(0.443) = 54.8 \text{ mi/h}$$

$$S_o = FFS \times SAF - 0.0036(v_{oA} - 500)$$

$$S_o = (65)(1.00) - 0.0036(1,568 - 500) = 61.2 \text{ mi/h}$$

$$S = \frac{v_{23} + v_{oA}N_o}{\left(\frac{v_{23}}{S_R}\right) + \left(\frac{V_{oA}N_o}{S_o}\right)} = \frac{3,777 + (1,568)(1)}{\left(\frac{3,777}{54.8}\right) + \left(\frac{1,568 \times 1}{61.2}\right)} = 56.5 \text{ mi/h}$$

While traffic in the outer lane is predicted to travel somewhat faster than traffic in the lanes in the ramp influence area (which includes the acceleration lane), the approximate nature of the speed result for left-hand ramps makes it difficult to draw any firm conclusions concerning speed behavior.

Discussion

This example problem is typical of the way the situations in the Special Cases section of Chapter 14 are treated. Modifications as specified are applied to the standard algorithms used for single-lane, right-hand ramp junctions. In this case, operations are acceptable, but in LOS D—though not far from the LOS C boundary. Because the left-hand lanes are expected to carry freeway traffic flowing faster than right-hand lanes, right-hand ramps are normally preferable to left-hand ramps when they can be provided without great difficulty.

EXAMPLE PROBLEM 5: SERVICE FLOW RATES AND SERVICE VOLUMES FOR AN ISOLATED ON-RAMP ON A SIX-LANE FREEWAY

The Facts

The following information is available concerning this example problem. The example assumes no impacts of inclement weather or incidents.

1. Single-lane, right-hand on-ramp with an FFS of 40 mi/h;
2. Six-lane freeway (three lanes in each direction) with an FFS of 70 mi/h;
3. Level terrain for freeway and ramp;
4. 6.5% trucks on both freeway and ramp segments;
5. Peak hour factor = 0.87;
6. Drivers are regular users of the facility; and
7. Acceleration lane = 1,000 ft.

Comments

This example illustrates the computation of service flow rates and service volumes for a ramp–freeway junction. The case selected is relatively straightforward to avoid extraneous complications that have been addressed in other example problems.

Two approaches will be demonstrated:

1. The ramp demand flow rate will be stated as a fixed percentage of the arriving freeway flow rate. The service flow rates and service volumes are expressed as arriving freeway flow rates that result in the threshold densities within the ramp influence area that define the limits of the various levels of service. For this computation, the ramp flow is set at 10% of the approaching freeway flow rate.

2. A fixed freeway demand flow rate will be stated, with service flow rates and service volumes expressed as ramp demand flow rates that result in the threshold densities within the ramp influence area that define the limits of the various levels of service. For this computation, the approaching freeway flow rate is set at 4,000 veh/h.

For LOS E, density does not define the limiting value of service flow rate, which is analogous to capacity for ramp–freeway junctions. It is defined as the flow that results in capacity being reached on the downstream freeway segment or ramp roadway.

Since all algorithms in this methodology are calibrated for passenger cars per hour under equivalent ideal conditions, initial computations are made in those terms. Results are then converted to service flow rates by using the appropriate heavy vehicle and driver population adjustment factors. Service flow rates are then converted to service volumes by multiplying by the peak hour factor.

From Exhibit 14-3, the following densities define the limits of LOS A–D:

LOS A: 10 pc/mi/ln

LOS B: 20 pc/mi/ln

LOS C: 28 pc/mi/ln

LOS D: 35 pc/mi/ln

From Exhibit 14-10 and Exhibit 14-12, capacity (or the threshold for LOS E) occurs when the downstream freeway flow rate reaches 7,200 pc/h (FFS = 70 mi/h) or when the ramp flow rate reaches 2,000 pc/h (ramp FFS = 40 mi/h).

Case 1: Ramp Demand Flow Rate = 0.10 × Freeway Demand Flow Rate

Equation 14-22 defines the density in an on-ramp influence area as follows:

$$D_R = 5.475 + 0.00734v_R + 0.0078v_{12} - 0.00627L_A$$

In this case

$$v_R = 0.10 v_F$$

$$L_A = 1,000 \text{ ft}$$

Equation 14-22 and Exhibit 14-8 give the following:

$$v_{12} = v_F \times P_{FM}$$

$$P_{FM} = 0.5775 + 0.000028L_A = 0.5775 + 0.000028(1,000) = 0.6055$$

$$v_{12} = 0.6055v_F$$

Substitution of these values into Equation 14-22 gives

$$D_R = 5.475 + 0.00734(0.10v_F) + 0.0078(0.6055v_F) - 0.00627(1,000)$$

$$D_R = 5.475 + 0.000734v_F + 0.00472v_F - 6.27$$

$$D_R = 0.005454v_F - 0.795$$

$$v_F = \frac{D_R + 0.795}{0.005454}$$

This equation can now be solved for threshold values of v_F for LOS A through D by using the appropriate threshold values of density. The results will be in terms of service flow rates under equivalent ideal conditions:

$$v_F(\text{LOS A}) = \frac{10 + 0.795}{0.005454} = 1,979 \text{ pc/h}$$

$$v_F(\text{LOS B}) = \frac{20 + 0.795}{0.005454} = 3,813 \text{ pc/h}$$

$$v_F(\text{LOS C}) = \frac{28 + 0.795}{0.005454} = 5,280 \text{ pc/h}$$

$$v_F(\text{LOS D}) = \frac{35 + 0.795}{0.005454} = 6,563 \text{ pc/h}$$

At capacity, the limiting flow rate occurs when the downstream freeway segment is 7,200 pc/h. If the ramp flow rate is 0.10 of the approaching freeway flow rate, then

$$v_{FO} = 7,200 = v_F + 0.10v_F = 1.10v_F$$

$$v_F(\text{LOS E}) = \frac{7,200}{1.10} = 6,545 \text{ pc/h}$$

This must be checked to ensure that the ramp flow rate ($0.10 \times 6,545 = 655$ pc/h) does not exceed the ramp capacity of 2,000 pc/h. Since it does not, the computation stands.

However, the LOS E (capacity) threshold is lower than the LOS D threshold. This indicates that LOS D operation cannot be achieved at this location. Before densities reach the 35-pc/h/ln threshold for LOS D, the capacity of the merge junction has been reached. Thus, there is no service flow rate or service volume for LOS D.

The computed values are in terms of passenger cars per hour under equivalent ideal conditions. To convert them to service flow rates in vehicles per hour under prevailing conditions, they must be multiplied by the heavy vehicle adjustment factor and the driver population factor. The approaching freeway flow includes 6.5% trucks on both the ramp and the mainline. For level terrain (Chapter 12, Basic Freeway and Multilane Highway Segments), $E_T = 2.0$. Then

$$f_{HV} = \frac{1}{1 + P_T(E_T - 1)}$$

$$f_{HV} = \frac{1}{1 + 0.065(2 - 1)} = 0.939$$

Service volumes are obtained by multiplying service flow rates by the specified PHF, 0.87. These computations are illustrated in Exhibit 28-4.

LOS	Service Flow Rate, Ideal Conditions (pc/h)	Service Flow Rate, Prevailing Conditions (SF) (veh/h)	Service Volume (SV) (veh/h)
A	1,979	$1,979 \times 0.939 \times 1 = 1,858$	$1,858 \times 0.87 = 1,616$
B	3,813	$3,813 \times 0.939 \times 1 = 3,580$	$3,580 \times 0.87 = 3,115$
C	5,280	$5,280 \times 0.939 \times 1 = 4,958$	$4,958 \times 0.87 = 4,313$
D	NA	NA	NA
E	6,545	$6,545 \times 0.939 \times 1 = 6,146$	$6,146 \times 0.87 = 5,347$

The service flow rates and service volumes shown in Exhibit 28-4 are stated in terms of the approaching hourly freeway demand.

Exhibit 28-4
Example Problem 5:
Illustrative Service Flow Rates
and Service Volumes Based
on Approaching Freeway
Demand

Case 2: Approaching Freeway Demand Volume = 4,000 veh/h

In this case, the approaching freeway demand will be held constant, and service flow rates and service volumes will be stated in terms of the ramp demand that can be accommodated at each LOS.

Since the freeway demand is stated in terms of an hourly volume in mixed vehicles per hour, it will be converted to passenger cars per hour under equivalent ideal conditions for use in the algorithms of this methodology:

$$v_F = \frac{V_F}{PHF \times f_{HV}} = \frac{4,000}{0.87 \times 0.939} = 4,896 \text{ pc/h}$$

The density is estimated by using Equation 14-22, and the variable P_{FM} —which is not dependent on v_R —remains 0.6055 as in Case 1. With a fixed value of freeway demand,

$$v_{12} = 0.6055 \times 4,896 = 2,965 \text{ pc/h}$$

Then, by using Equation 14-22,

$$\begin{aligned} D_R &= 5.475 + 0.00734v_R + 0.0078v_{12} - 0.00627L_A \\ D_R &= 5.475 + 0.00734v_R + 0.0078(2,965) - 0.00627(1,000) \\ D_R &= 22.33 + 0.00734v_R \\ v_R &= \frac{D_R - 22.33}{0.00734} \end{aligned}$$

It is clear from this equation that neither LOS A ($D_R = 10$ pc/mi/ln) nor LOS B ($D_R = 20$ pc/mi/ln) can be achieved with a freeway demand flow of 4,896 pc/h.

For LOS C and D,

$$\begin{aligned} v_R(\text{LOS C}) &= \frac{28-22.33}{0.00734} = 772 \text{ pc/h} \\ v_R(\text{LOS D}) &= \frac{35-22.33}{0.00734} = 1,726 \text{ pc/h} \end{aligned}$$

Capacity, the limit of LOS E, occurs when the downstream freeway flow reaches 7,200 pc/h. With a fixed freeway demand,

$$\begin{aligned} v_{FO} &= 7,200 - 4,896 + v_R \\ v_R(\text{LOS E}) &= 7,900 - 4,896 = 3,004 \text{ pc/h} \end{aligned}$$

This, however, violates the capacity of the ramp roadway, which is 2,000 pc/h. Thus, the limiting ramp flow rate for LOS E is set at 2,000 pc/h.

As in Case 1, these values are all stated in terms of passenger cars per hour under equivalent ideal conditions. They are converted to service flow rates by multiplying by the appropriate heavy vehicle factor (0.939 from Case 1). Service flow rates are converted to service volumes by multiplying by the PHF. These computations for ramp service volumes are illustrated in Exhibit 28-5.

LOS	Service Flow Rate, Ideal Conditions (pc/h)	Service Flow Rate, Prevailing Conditions (veh/h)	Ramp Service Volume (veh/h)
A	NA	NA	NA
B	NA	NA	NA
C	769	$772 \times 0.939 \times 1 = 725$	$725 \times 0.87 = 631$
D	1,723	$1,726 \times 0.939 \times 1 = 1,621$	$1,621 \times 0.87 = 1,410$
E	2,000	$2,000 \times 0.939 \times 1 = 1,878$	$1,878 \times 0.87 = 1,633$

These service flow rates and service volumes are based on a constant upstream arriving freeway demand and are stated in terms of limiting on-ramp demands for that condition.

Discussion

As this illustration shows, many considerations are involved in estimating service flow rates and service volumes for ramp–freeway junctions, not the least of which is specifying how such values should be defined. The concept of service flow rates and service volumes at specific ramp–freeway junctions is of limited utility. Since many of the details that affect the estimates will not be determined until final designs are prepared, operational analysis of the proposed design may be more appropriate.

Case 2 could have applications in considering how to time ramp meters. Appropriate limiting ramp flows can be estimated by using the same approach as for service volumes and service flow rates.

Exhibit 28-5
Example Problem 5:
Illustrative Service Flow Rates
and Service Volumes Based
on a Fixed Freeway Demand

3. ALTERNATIVE TOOL EXAMPLES FOR FREEWAY RAMPS

Chapter 14, Freeway Merge and Diverge Segments, described a methodology for analyzing ramps and ramp junctions to estimate capacity, speed, and density as a function of traffic demand and geometric configuration. This chapter includes two supplemental problems that examine situations that are beyond the scope of the Chapter 14 methodology. A typical microsimulation-based tool is used for this purpose, and the simulation results are compared, where appropriate, with those of the HCM.

Both problems are based on this chapter's Example Problem 3, which analyzes an eight-lane freeway segment with an entrance and an exit ramp. The first problem evaluates the effects of the addition of ramp metering, while the second evaluates the impacts of converting the leftmost lane of the mainline into a high-occupancy vehicle (HOV) lane.

The need to determine performance measures based on the analysis of vehicle trajectories was emphasized in Chapter 7, Interpreting HCM and Alternative Tool Results. Specific procedures for defining measures in terms of vehicle trajectories were proposed to guide the future development of alternative tools. Pending further development, the examples presented in this chapter have applied existing versions of alternative tools and therefore do not reflect the trajectory-based measures described in Chapter 7.

For purposes of illustration, the default calibration parameters of the simulation tool (e.g., lane-changing behavioral characteristics) were applied to these examples. However, most simulation tools offer the ability to adjust these parameters. The parameter values can have a significant effect on the results, especially when the operation is close to full saturation.

PROBLEM 1: RAMP-METERING EFFECTS

This problem analyzes the impacts of ramp metering along the segment. The HCM procedure for ramp-merge junctions cannot estimate the impacts of ramp metering. These impacts can be approximated to some extent by not allowing the ramp demand to exceed the ramp-metering rate. To address ramp metering at a more detailed level, a typical microsimulation tool was used to evaluate the impacts of ramp metering on the density and capacity of the merge.

The subject segment consists of an on-ramp followed by an off-ramp, separated by 1,300 ft. The upstream segment is 1 mi long. Each simulation run was for 1 full hour. It was assumed that the mainline demand was 6,111 veh/h and that the ramp demand was 444 veh/h. The ramp metering is clock-time based (i.e., the metering rate does not change as a function of the mainline demand).

Experiments were conducted to obtain the density and capacity of the subject segment as a function of the ramp-metering rate. The queue length upstream of the ramp meter was also obtained as a function of the ramp-metering rate. Exhibit 28-6 provides a graphics capture of the simulated site.

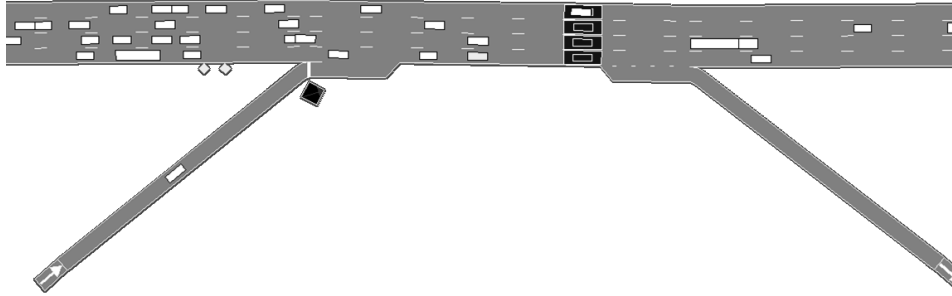


Exhibit 28-6
Graphics Capture of the Ramp Merge with Ramp Metering

Exhibit 28-7 provides the density of the segment between the on-ramp and the off-ramp as a function of the ramp-metering rate (or discharge headway from the on-ramp). As shown, the density is not much affected by the ramp-metering rate. As expected, the density of Lane 1 (the rightmost lane) is the highest, while the density in Lane 4 is the lowest.

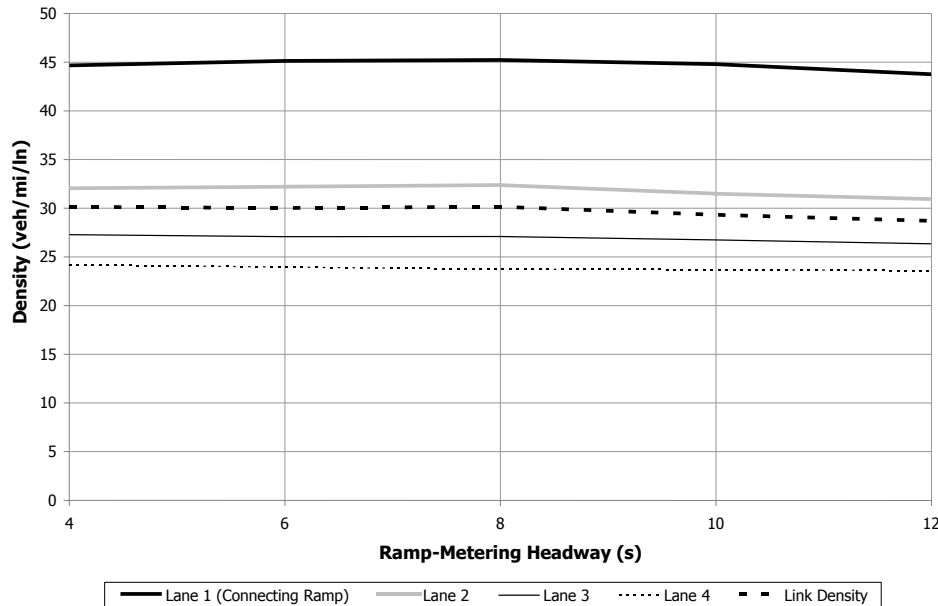


Exhibit 28-7
Density as a Function of Ramp-Metering Headways

Exhibit 28-8 provides capacity as a function of the ramp-metering headway and when no ramp metering is implemented. As shown, the simulation model predicts that capacity is higher when ramp metering is implemented. Capacity in simulation is typically measured in the form of maximum throughput downstream of a queued segment and is therefore one of the outputs of the simulation, as opposed to an input as in the HCM.

Exhibit 28-8
Capacity at a Ramp Junction
as a Function of Ramp-
Metering Headways

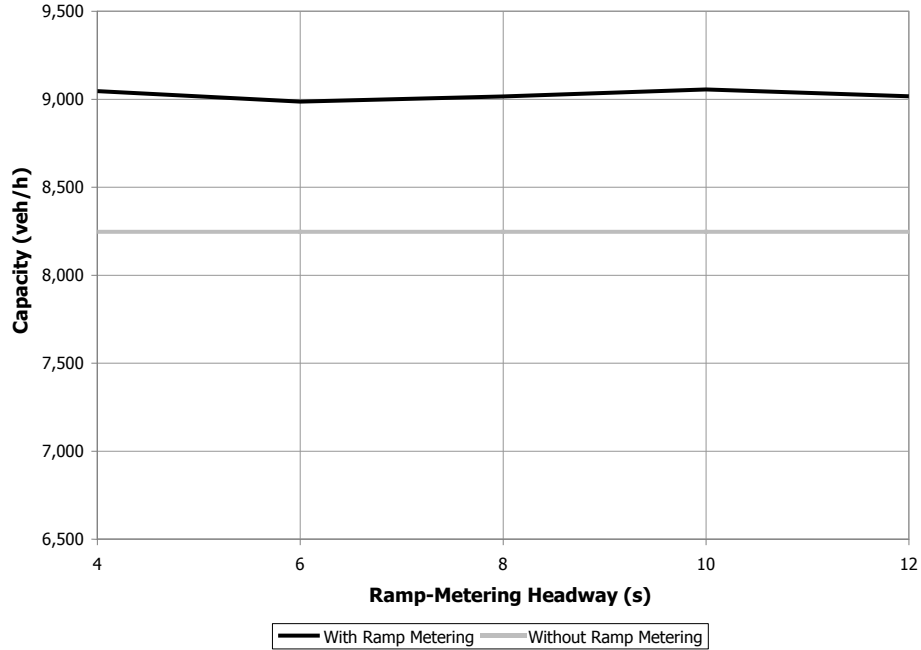
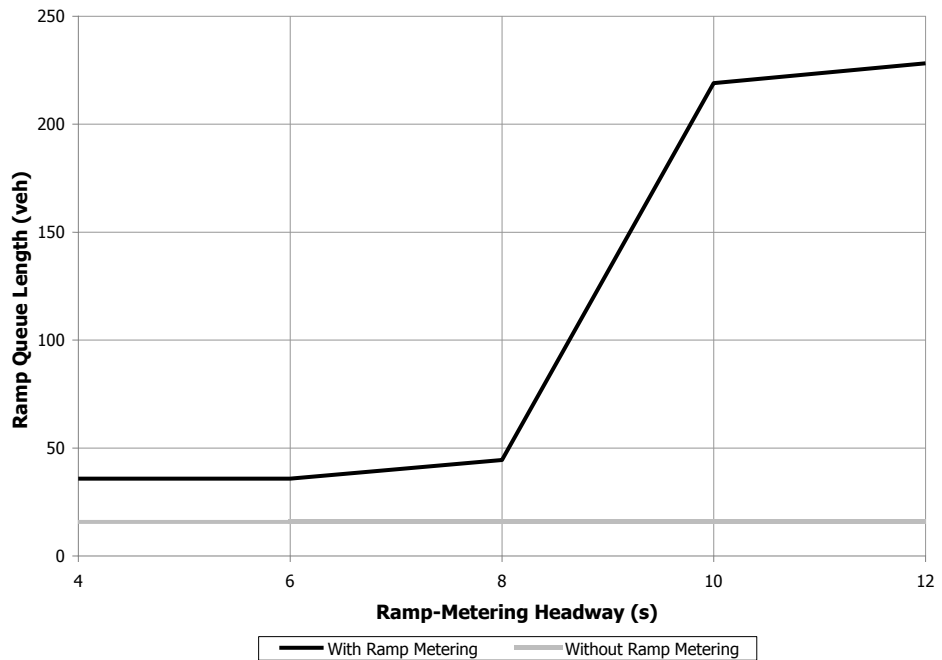


Exhibit 28-9 provides the queue length expected on the ramp as a function of the ramp-metering headway and when no ramp metering is implemented. As expected, the queue length is higher when ramp metering is implemented, and it increases dramatically when the ramp-metering rate exceeds 8 s/veh. The reason for this increase is that the demand on the ramp is approximately 8 s/veh (444 veh/h corresponds to an average headway of 8.1 s/veh).

Exhibit 28-9
Queue Length on the Ramp as
a Function of Ramp-Metering
Headways



As indicated above, the effects of ramp metering cannot be evaluated with the HCM. The freeway facilities methodology (HCM Chapter 10) can handle changes in segment capacity; however, other tools are required to estimate what the maximum throughput would be under various types of ramp-metering algorithms and rates. Also, the HCM cannot estimate the queue length on the on-ramp as a function of ramp metering. An analytical method could be developed to estimate queue length as a function of demand and service rate at the meter.

PROBLEM 2: CONVERSION OF LEFTMOST LANE TO AN HOV LANE

This problem is also based on this chapter’s Example Problem 3. It evaluates operating conditions when the leftmost lane of the mainline is converted into an HOV lane. Exhibit 28-10 provides a graphics capture of the segment.

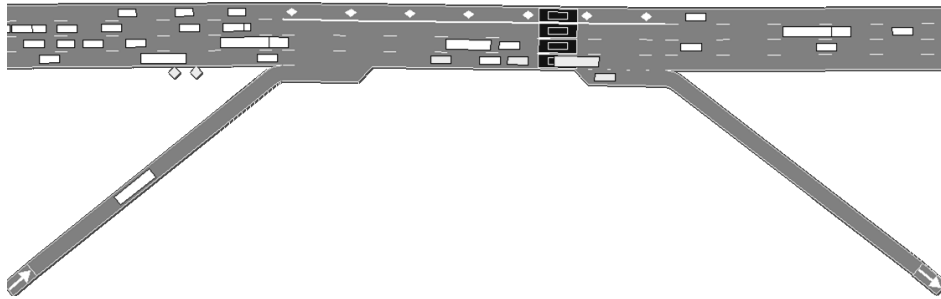


Exhibit 28-10
Graphics Capture of the Segment with an HOV Lane

Exhibit 28-11 and Exhibit 28-12 show the density and capacity of the ramp junction as a function of the percentage of carpools. As shown, when the percentage of carpools increases, the density of the HOV lane and the overall link capacity increase. This occurs because for the range of values tested here, the utilization of the HOV lane increases, which improves the overall link performance.

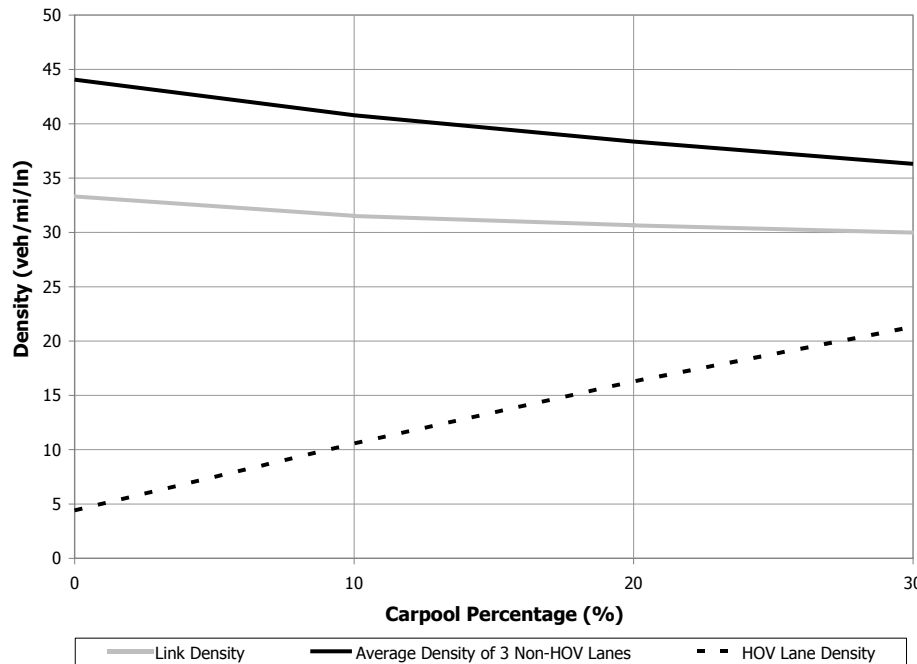


Exhibit 28-11
Density of a Ramp Junction as a Function of the Carpool Percentage

Exhibit 28-12
Capacity of a Ramp Junction
as a Function of the Carpool
Percentage

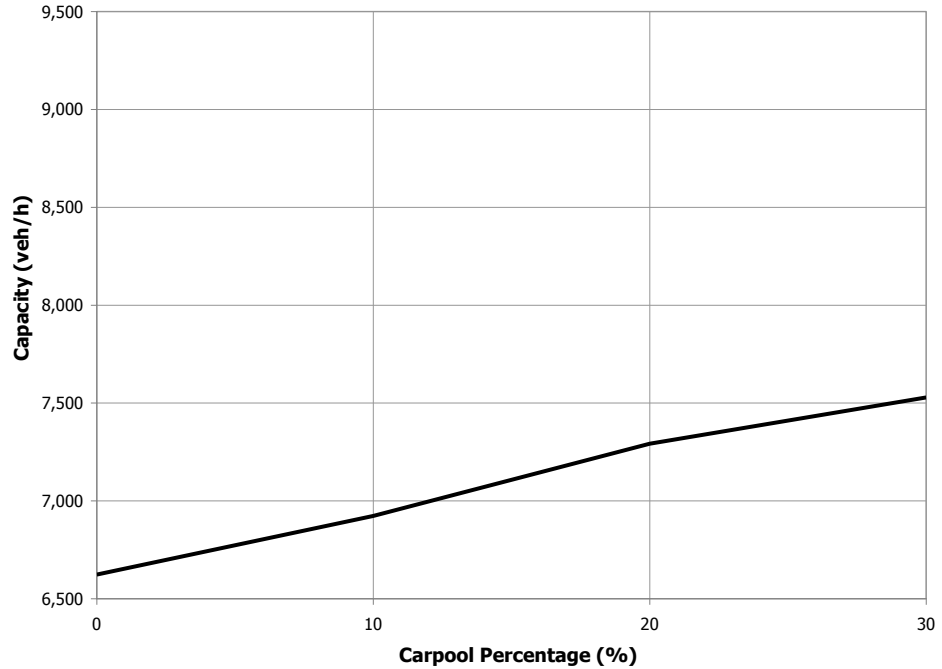
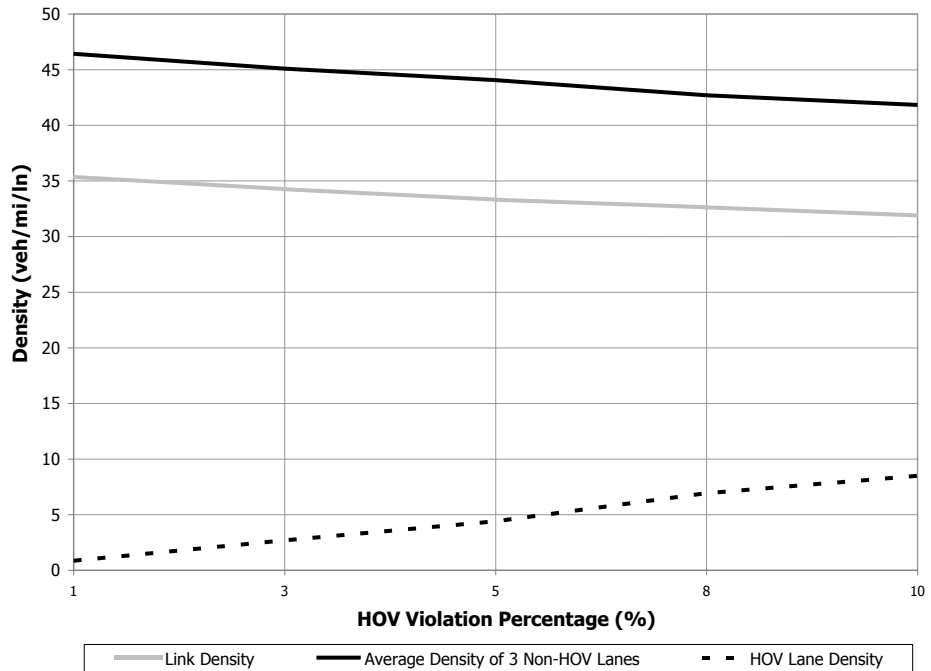


Exhibit 28-13 presents the density as a function of HOV violators, while Exhibit 28-14 presents the corresponding capacity. These two graphs assume that there are 10% carpools in the traffic stream. As shown, density generally decreases while capacity increases as the percentage of HOV violators increases. The reason is that under this scenario, the facility is more efficiently utilized as violations increase with general traffic using the HOV lane.

Exhibit 28-13
Density of a Ramp Junction as
a Function of the HOV
Violation Percentage



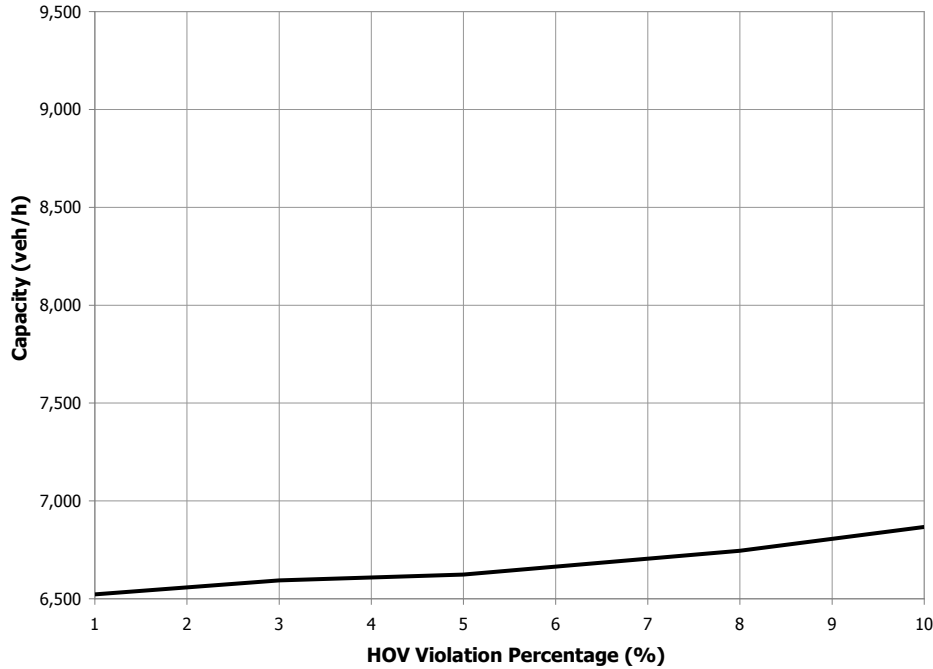


Exhibit 28-14
Capacity of a Ramp Junction
as a Function of the HOV
Violation Percentage

Exhibit 28-15 and Exhibit 28-16 present the density and capacity of the ramp junction as a function of the distance at which drivers begin to react to the presence of the HOV lane (i.e., the distance to the regulatory sign). As shown, the longer that distance, the lower the density of the HOV lane and the higher the density in the other lanes. The reason is that under this scenario the percentage of carpools is relatively low (10%). When the HOV lane begins, non-HOVs congregate in the remaining lanes. Capacity is reduced as the distance at which drivers begin to react increases, because the HOV lane is not utilized as much when drivers are given early warning to switch lanes.

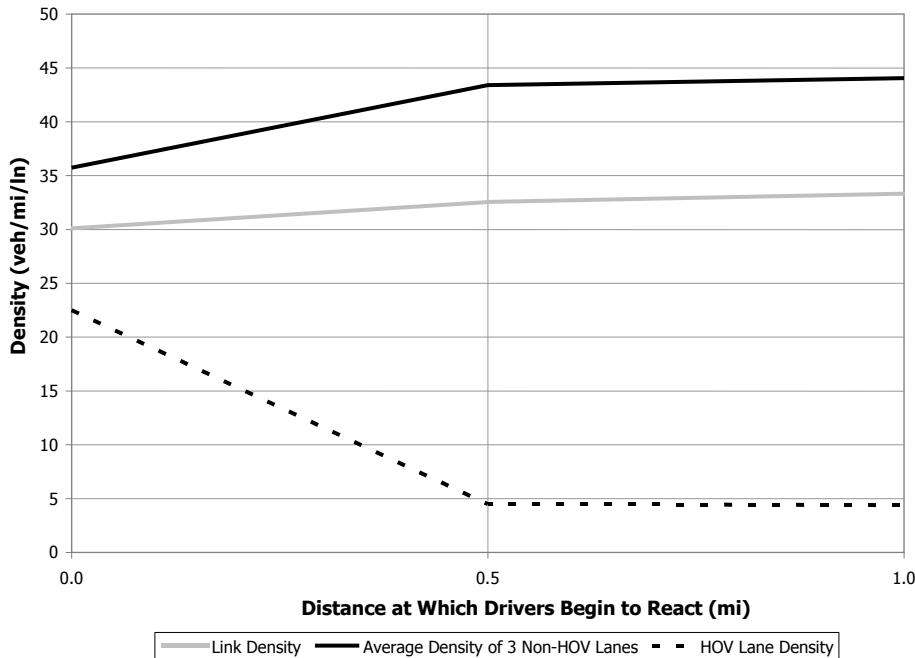


Exhibit 28-15
Density of a Ramp Junction as
a Function of the Distance at
Which Drivers Begin to React

Exhibit 28-16

Capacity of a Ramp Junction as a Function of the Distance at Which Drivers Begin to React

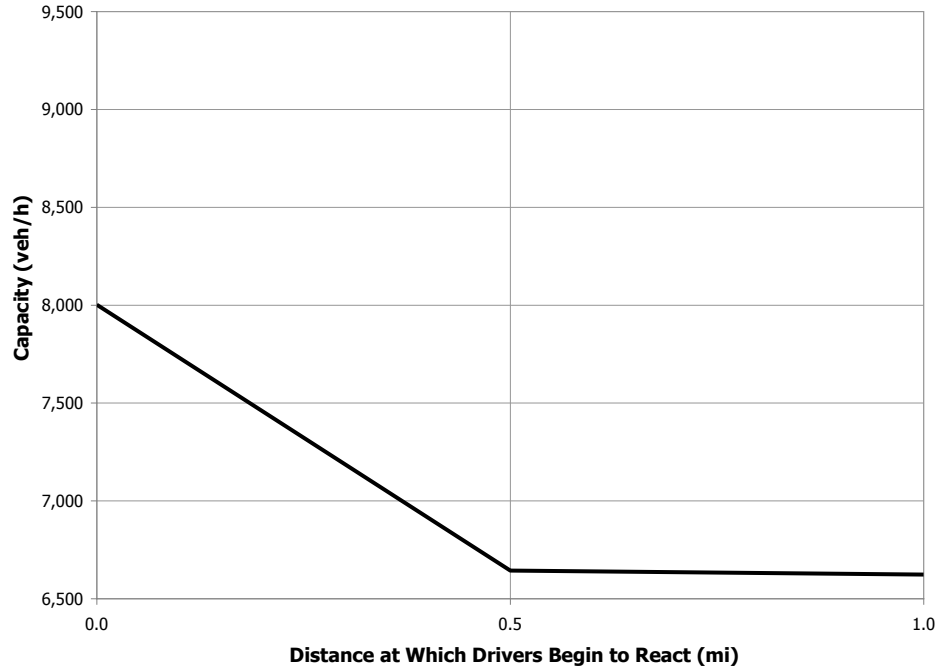
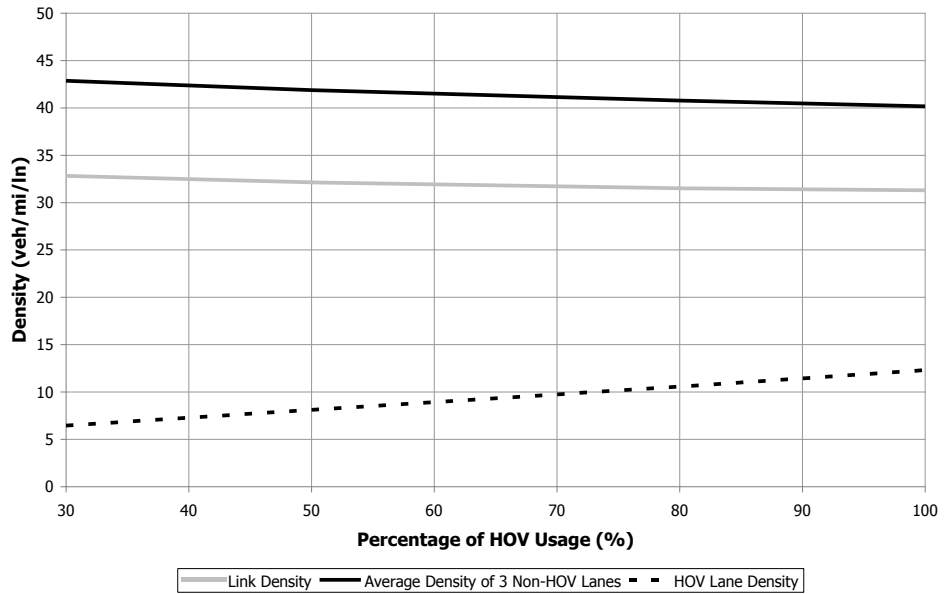


Exhibit 28-17 and Exhibit 28-18 present the density and capacity of the ramp junction as a function of the percentage of HOV usage. As expected, when usage of the HOV lane increases, the density of the HOV lane and the overall link capacity increase.

Exhibit 28-17

Density of a Ramp Junction as a Function of the Percentage of HOV Usage



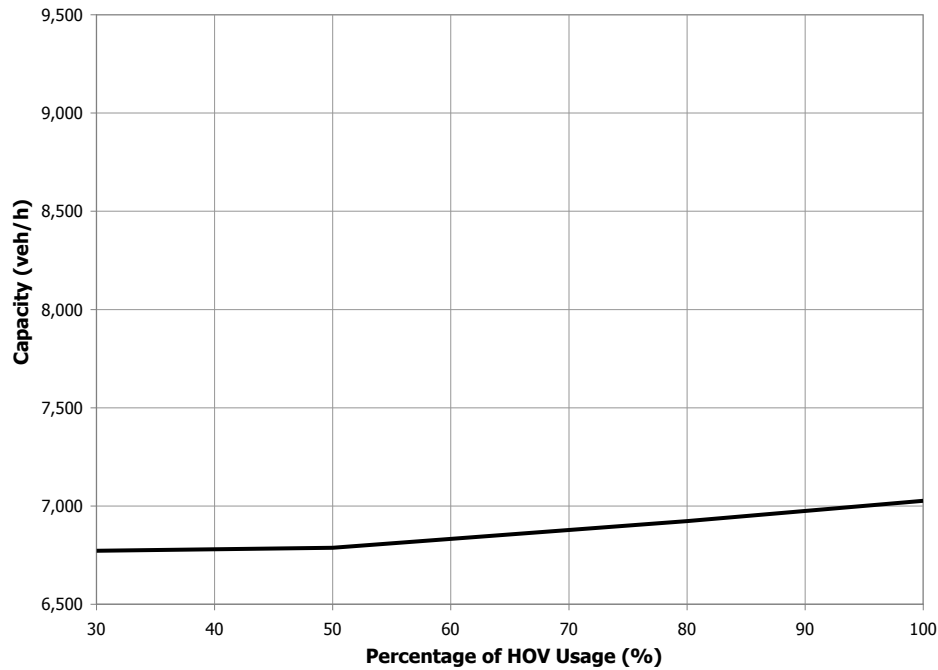


Exhibit 28-18
Capacity of a Ramp Junction
as a Function of the
Percentage of HOV Usage

The type of analysis presented in this example cannot be conducted with the HCM, since the method does not estimate the HOV lane density separately. Variables such as the impact of the distance of the HOV regulatory sign cannot be evaluated, since they pertain to driver behavior attributes and their impact on density and capacity. The impact of the percentage of carpools and the percentage of violators could perhaps be estimated with appropriate modifications of the existing HCM method.



HIGHWAY CAPACITY MANUAL

6TH EDITION | A GUIDE FOR MULTIMODAL MOBILITY ANALYSIS

VOLUME 4: APPLICATIONS GUIDE

The National Academies of
SCIENCES • ENGINEERING • MEDICINE

TRANSPORTATION RESEARCH BOARD
WASHINGTON, D.C. | WWW.TRB.ORG

TRANSPORTATION RESEARCH BOARD 2016 EXECUTIVE COMMITTEE *

Chair: James M. Crites, Executive Vice President of Operations,
Dallas–Fort Worth International Airport, Texas

Vice Chair: Paul Trombino III, Director, Iowa Department of
Transportation, Ames

Executive Director: Neil J. Pedersen, Transportation Research Board

Victoria A. Arroyo, Executive Director, Georgetown Climate Center;
Assistant Dean, Centers and Institutes; and Professor and Director,
Environmental Law Program, Georgetown University Law Center,
Washington, D.C.

Scott E. Bennett, Director, Arkansas State Highway and Transportation
Department, Little Rock

Jennifer Cohan, Secretary, Delaware Department of Transportation, Dover

Malcolm Dougherty, Director, California Department of
Transportation, Sacramento

A. Stewart Fotheringham, Professor, School of Geographical Sciences
and Urban Planning, Arizona State University, Tempe

John S. Halikowski, Director, Arizona Department of Transportation,
Phoenix

Susan Hanson, Distinguished University Professor Emerita, Graduate
School of Geography, Clark University, Worcester, Massachusetts

Steve Heminger, Executive Director, Metropolitan Transportation
Commission, Oakland, California

Chris T. Hendrickson, Hamerschlag Professor of Engineering, Carnegie
Mellon University, Pittsburgh, Pennsylvania

Jeffrey D. Holt, Managing Director, Power, Energy, and Infrastructure
Group, BMO Capital Markets Corporation, New York

S. Jack Hu, Vice President for Research and J. Reid and Polly Anderson
Professor of Manufacturing, University of Michigan, Ann Arbor

Roger B. Huff, President, HGLC, LLC, Farmington Hills, Michigan

Geraldine Knatz, Professor, Sol Price School of Public Policy, Viterbi
School of Engineering, University of Southern California, Los Angeles

Ysela Llort, Consultant, Miami, Florida

Melinda McGrath, Executive Director, Mississippi Department of
Transportation, Jackson

James P. Redeker, Commissioner, Connecticut Department of
Transportation, Newington

Mark L. Rosenberg, Executive Director, The Task Force for Global
Health, Inc., Decatur, Georgia

Kumares C. Sinha, Olson Distinguished Professor of Civil Engineering,
Purdue University, West Lafayette, Indiana

Daniel Sperling, Professor of Civil Engineering and Environmental
Science and Policy; Director, Institute of Transportation Studies,
University of California, Davis

Kirk T. Steudle, Director, Michigan Department of Transportation,
Lansing (Past Chair, 2014)

Gary C. Thomas, President and Executive Director, Dallas Area Rapid
Transit, Dallas, Texas

Pat Thomas, Senior Vice President of State Government Affairs, United
Parcel Service, Washington, D.C.

Katherine F. Turnbull, Executive Associate Director and Research
Scientist, Texas A&M Transportation Institute, College Station

Dean Wise, Vice President of Network Strategy, Burlington Northern
Santa Fe Railway, Fort Worth, Texas

Thomas P. Bostick (Lieutenant General, U.S. Army), Chief of Engineers
and Commanding General, U.S. Army Corps of Engineers, Washington,
D.C. (ex officio)

James C. Card (Vice Admiral, U.S. Coast Guard, retired), Maritime
Consultant, The Woodlands, Texas, and Chair, TRB Marine Board
(ex officio)

T. F. Scott Darling III, Acting Administrator and Chief Counsel, Federal
Motor Carrier Safety Administration, U.S. Department of Transportation
(ex officio)

Marie Therese Dominguez, Administrator, Pipeline and Hazardous
Materials Safety Administration, U.S. Department of Transportation
(ex officio)

Sarah Feinberg, Administrator, Federal Railroad Administration,
U.S. Department of Transportation (ex officio)

Carolyn Flowers, Acting Administrator, Federal Transit Administration,
U.S. Department of Transportation (ex officio)

LeRoy Gishi, Chief, Division of Transportation, Bureau of Indian
Affairs, U.S. Department of the Interior, Washington, D.C. (ex officio)

John T. Gray II, Senior Vice President, Policy and Economics,
Association of American Railroads, Washington, D.C. (ex officio)

Michael P. Huerta, Administrator, Federal Aviation Administration,
U.S. Department of Transportation (ex officio)

Paul N. Jaenichen, Sr., Administrator, Maritime Administration,
U.S. Department of Transportation (ex officio)

Bevan B. Kirley, Research Associate, University of North Carolina
Highway Safety Research Center, Chapel Hill, and Chair, TRB Young
Members Council (ex officio)

Gregory G. Nadeau, Administrator, Federal Highway Administration,
U.S. Department of Transportation (ex officio)

Wayne Nastri, Acting Executive Officer, South Coast Air Quality
Management District, Diamond Bar, California (ex officio)

Mark R. Rosekind, Administrator, National Highway Traffic Safety
Administration, U.S. Department of Transportation (ex officio)

Craig A. Rutland, U.S. Air Force Pavement Engineer, U.S. Air Force
Civil Engineer Center, Tyndall Air Force Base, Florida (ex officio)

Reuben Sarkar, Deputy Assistant Secretary for Transportation,
U.S. Department of Energy (ex officio)

Richard A. White, Acting President and CEO, American Public
Transportation Association, Washington, D.C. (ex officio)

Gregory D. Winfree, Assistant Secretary for Research and Technology,
Office of the Secretary, U.S. Department of Transportation (ex officio)

Frederick G. (Bud) Wright, Executive Director, American Association
of State Highway and Transportation Officials, Washington, D.C.
(ex officio)

Paul F. Zukunft (Admiral, U.S. Coast Guard), Commandant, U.S. Coast
Guard, U.S. Department of Homeland Security (ex officio)

Transportation Research Board publications are available by ordering
individual publications directly from the TRB Business Office, through
the Internet at www.TRB.org, or by annual subscription through
organizational or individual affiliation with TRB. Affiliates and library
subscribers are eligible for substantial discounts. For further information,
contact the Transportation Research Board Business Office, 500 Fifth
Street, NW, Washington, DC 20001 (telephone 202-334-3213;
fax 202-334-2519; or e-mail TRBsales@nas.edu).

Copyright 2016 by the National Academy of Sciences.

All rights reserved.

Printed in the United States of America.

ISBN 978-0-309-36997-8 [Slipcased set of three volumes]

ISBN 978-0-309-36998-5 [Volume 1]

ISBN 978-0-309-36999-2 [Volume 2]

ISBN 978-0-309-37000-4 [Volume 3]

ISBN 978-0-309-37001-1 [Volume 4, online only]

The National Academies of
SCIENCES • ENGINEERING • MEDICINE

The **National Academy of Sciences** was established in 1863 by an Act of Congress, signed by President Lincoln, as a private, nongovernmental institution to advise the nation on issues related to science and technology. Members are elected by their peers for outstanding contributions to research. Dr. Ralph J. Cicerone is president.

The **National Academy of Engineering** was established in 1964 under the charter of the National Academy of Sciences to bring the practices of engineering to advising the nation. Members are elected by their peers for extraordinary contributions to engineering. Dr. C. D. Mote, Jr., is president.

The **National Academy of Medicine** (formerly the Institute of Medicine) was established in 1970 under the charter of the National Academy of Sciences to advise the nation on medical and health issues. Members are elected by their peers for distinguished contributions to medicine and health. Dr. Victor J. Dzau is president.

The three Academies work together as the National Academies of Sciences, Engineering, and Medicine to provide independent, objective analysis and advice to the nation and conduct other activities to solve complex problems and inform public policy decisions. The Academies also encourage education and research, recognize outstanding contributions to knowledge, and increase public understanding in matters of science, engineering, and medicine.

Learn more about the National Academies of Sciences, Engineering, and Medicine at **www.national-academies.org**.

The **Transportation Research Board** is one of seven major programs of the National Academies of Sciences, Engineering, and Medicine. The mission of the Transportation Research Board is to increase the benefits that transportation contributes to society by providing leadership in transportation innovation and progress through research and information exchange, conducted within a setting that is objective, interdisciplinary, and multimodal. The Board's varied committees, task forces, and panels annually engage about 7,000 engineers, scientists, and other transportation researchers and practitioners from the public and private sectors and academia, all of whom contribute their expertise in the public interest. The program is supported by state transportation departments, federal agencies including the component administrations of the U.S. Department of Transportation, and other organizations and individuals interested in the development of transportation.

Learn more about the Transportation Research Board at **www.TRB.org**.

CHAPTER 29
URBAN STREET FACILITIES: SUPPLEMENTAL

CONTENTS

1. INTRODUCTION 29-1

2. SCENARIO GENERATION PROCEDURE 29-2

 Weather Event Generation 29-2

 Traffic Demand Variation Generation 29-7

 Traffic Incident Generation..... 29-8

 Scenario Dataset Generation 29-16

3. SUSTAINED SPILLBACK PROCEDURE 29-25

 Overview of the Procedure..... 29-25

 Computational Steps 29-26

 Procedure for Saving Performance Measures..... 29-31

 Computational Engine Documentation 29-33

4. USE OF ALTERNATIVE TOOLS..... 29-36

 Basic Example Problem Configuration 29-36

 Signal Timing Plan Design 29-38

 Demonstration of Alternative Tool Applications..... 29-50

5. EXAMPLE PROBLEMS 29-60

 Example Problem 1: Automobile-Oriented Urban Street 29-60

 Example Problem 2: Pedestrian and Bicycle Improvements 29-68

 Example Problem 3: Pedestrian and Parking Improvements..... 29-73

 Example Problem 4: Existing Urban Street Reliability 29-78

 Example Problem 5: Urban Street Strategy Evaluation..... 29-95

6. REFERENCES..... 29-100

LIST OF EXHIBITS

Exhibit 29-1 Weather Event Procedure 29-3

Exhibit 29-2 Traffic Demand Variation Procedure 29-8

Exhibit 29-3 Traffic Incident Procedure for Intersection Incidents 29-9

Exhibit 29-4 Scenario File Generation Procedure 29-17

Exhibit 29-5 Additional Critical Left-Turn Headway due to Weather 29-24

Exhibit 29-6 Spillback Procedure Flowchart 29-34

Exhibit 29-7 Sustained Spillback Module Routines 29-35

Exhibit 29-8 Base Configuration for the Examples 29-37

Exhibit 29-9 Demand Flow Rates and Phasing Plan for Each Intersection 29-37

Exhibit 29-10 Elements of a Typical Signal Timing Design Tool 29-39

Exhibit 29-11 Cycle Length Optimization Results 29-41

Exhibit 29-12 Timing Plan Developed by Split and Offset Optimization 29-42

Exhibit 29-13 Performance Measures for the Initial Timing Plan 29-42

Exhibit 29-14 Progression Quality Measures for the Initial Design 29-43

Exhibit 29-15 Progression Quality Measures for the Improved
Progression Design 29-43

Exhibit 29-16 Time–Space Diagram for the Initial Design 29-44

Exhibit 29-17 Time–Space Diagram for the Modified Progression Design 29-44

Exhibit 29-18 Offset Changes for the Modified Progression Design 29-44

Exhibit 29-19 Alternative Time–Space Diagram Format 29-45

Exhibit 29-20 Example Illustrating the Use of Flow Profiles 29-46

Exhibit 29-21 Composite Flow Profiles for the First Eastbound Segment 29-47

Exhibit 29-22 Variation of Queue Length Throughout the Signal Cycle for
the First Eastbound Segment 29-47

Exhibit 29-23 Time–Space Diagram with Flows and Queues 29-48

Exhibit 29-24 Optimized Phasing Modifications 29-49

Exhibit 29-25 Time–Space Diagram for the Optimized Phasing Plan 29-49

Exhibit 29-26 Time–Space Diagram Showing Ideal Eastbound
Progression 29-50

Exhibit 29-27 Parameters for the Parking Example 29-51

Exhibit 29-28 Effect of Parking Activity Level on Travel Time and Delay 29-51

Exhibit 29-29 Effect of Parking Activity Level on the Percentage of Stops 29-52

Exhibit 29-30 Roundabout Configuration for Intersection 3 29-53

Exhibit 29-31 Time–Space Diagrams Showing Simultaneous and
Alternating Platoon Arrivals at the Roundabout 29-53

Exhibit 29-32 Performance Comparison for Simultaneous and Alternating Platoon Arrivals at a Roundabout.....	29-54
Exhibit 29-33 Queuing Results for the Theoretical Example	29-56
Exhibit 29-34 Queuing Results for Simultaneous Platoons.....	29-56
Exhibit 29-35 Queuing Results for Alternating Platoons	29-57
Exhibit 29-36 Queuing Results for Isolated TWSC Operation.....	29-58
Exhibit 29-37 Effect of Cross-Street Demand Volume on Queue Backup Beyond 100 ft from the Stop Line	29-59
Exhibit 29-38 Example Problems.....	29-60
Exhibit 29-39 Example Problem 1: Urban Street Schematic.....	29-60
Exhibit 29-40 Example Problem 1: Segment Geometry	29-61
Exhibit 29-41 Example Problem 1: Intersection Turn Movement Counts.....	29-61
Exhibit 29-42 Example Problem 1: Signal Conditions for Intersection 1	29-62
Exhibit 29-43 Example Problem 1: Geometric Conditions and Traffic Characteristics for Signalized Intersection 1	29-63
Exhibit 29-44 Example Problem 1: Access Point Data	29-63
Exhibit 29-45 Example Problem 1: Intersection 1 Evaluation	29-64
Exhibit 29-46 Example Problem 1: Intersection 5 Evaluation	29-65
Exhibit 29-47 Example Problem 1: Segment 1 Evaluation.....	29-66
Exhibit 29-48 Example Problem 1: Segment 5 Evaluation.....	29-66
Exhibit 29-49 Example Problem 1: Facility Evaluation.....	29-67
Exhibit 29-50 Example Problem 2: Segment Geometry	29-68
Exhibit 29-51 Example Problem 2: Intersection 1 Evaluation	29-69
Exhibit 29-52 Example Problem 2: Intersection 5 Evaluation	29-69
Exhibit 29-53 Example Problem 2: Segment 1 Evaluation.....	29-71
Exhibit 29-54 Example Problem 2: Segment 5 Evaluation.....	29-71
Exhibit 29-55 Example Problem 2: Facility Evaluation.....	29-72
Exhibit 29-56 Example Problem 3: Segment Geometry	29-74
Exhibit 29-57 Example Problem 3: Intersection 1 Evaluation	29-74
Exhibit 29-58 Example Problem 3: Intersection 5 Evaluation	29-75
Exhibit 29-59 Example Problem 3: Segment 1 Evaluation.....	29-76
Exhibit 29-60 Example Problem 3: Segment 5 Evaluation.....	29-76
Exhibit 29-61 Example Problem 3: Facility Evaluation.....	29-78
Exhibit 29-62 Example Problem 4: Urban Street Facility.....	29-79
Exhibit 29-63 Example Problem 4: Input Data Needs and Sources	29-80
Exhibit 29-64 Example Problem 4: Intersection 1 Signal Timing Data	29-80
Exhibit 29-65 Example Problem 4: Sample Weather Data for Lincoln, Nebraska.....	29-83

Exhibit 29-66 Example Problem 4: Sample Generated Weather Events	29-84
Exhibit 29-67 Example Problem 4: Sample Demand Profile Calculations	29-86
Exhibit 29-68 Example Problem 4: Locally Available Crash Frequency Data	29-87
Exhibit 29-69 Example Problem 4: Computation of Crash Frequency by Weather Type	29-88
Exhibit 29-70 Example Problem 4: Incident Determination for April 6, 9:00 a.m., for Segment 1-2	29-90
Exhibit 29-71 Example Problem 4: Incident Determination for January 10, 7:00 a.m., for Segment 1-2	29-90
Exhibit 29-72 Example Problem 4: Sample Calculation of Incident Duration	29-91
Exhibit 29-73 Example Problem 4: Reliability Performance Measure Results	29-93
Exhibit 29-74 Example Problem 4: Eastbound Travel Time Distribution	29-94
Exhibit 29-75 Example Problem 4: Confidence Interval Calculation for Eastbound Direction	29-94
Exhibit 29-76 Example Problem 4: Annual VHD by Cause	29-95
Exhibit 29-77 Example Problem 4: Percentage of Annual VHD by Cause	29-95
Exhibit 29-78 Example Problem 5: Results for Strategy 1	29-98
Exhibit 29-79 Example Problem 5: Results for Strategy 2	29-98
Exhibit 29-80 Example Problem 5: Results for Strategy 3	29-99

1. INTRODUCTION

Chapter 29 is the supplemental chapter for Chapter 16: Urban Street Facilities and Chapter 17: Urban Street Reliability and ATDM, which are found in Volume 3 of the *Highway Capacity Manual* (HCM). This chapter presents detailed information about the following aspects of urban street facility evaluation:

- The process for generating the scenarios used to evaluate travel time reliability and
- The process for evaluating facilities with sustained spillback.

This chapter also provides details about the computational engine that implements the sustained spillback procedure and example applications of alternative tools. Finally, the chapter provides five example problems that demonstrate the application of the methodologies to a multimodal evaluation of urban street performance and to the evaluation of urban street reliability.

VOLUME 4: APPLICATIONS
GUIDE

25. Freeway Facilities: Supplemental
26. Freeway and Highway Segments: Supplemental
27. Freeway Weaving: Supplemental
28. Freeway Merges and Diverges: Supplemental
- 29. Urban Street Facilities: Supplemental**
30. Urban Street Segments: Supplemental
31. Signalized Intersections: Supplemental
32. STOP-Controlled Intersections: Supplemental
33. Roundabouts: Supplemental
34. Interchange Ramp Terminals: Supplemental
35. Pedestrians and Bicycles: Supplemental
36. Concepts: Supplemental
37. ATDM: Supplemental

2. SCENARIO GENERATION PROCEDURE

The methodology for evaluating reliability is described in Section 3 of Chapter 17, Urban Street Reliability and ATDM. It consists of three stages that are implemented in the sequence listed below:

- Scenario generation,
- Facility evaluation, and
- Performance summary.

The scenario generation stage is implemented through four sequential procedures: (a) weather event generation, (b) traffic demand variation generation, (c) traffic incident generation, and (d) scenario dataset generation. This stage generates the set of analysis periods that make up the reliability reporting period. The sequence of computations associated with each procedure is described in this section.

Details of the facility evaluation stage and the performance summary stage are provided in Section 3 of Chapter 17.

The combination of demand volume, speed, saturation flow rate, and signal timing established for each analysis period is assumed to be unique, relative to the other analysis periods. This assumption recognizes that it is extremely rare in the urban street environment for two or more analysis periods to have the same combination of demand volume, capacity, and traffic control for all segments and intersections making up the facility. Thus, each analysis period is considered to be one scenario.

WEATHER EVENT GENERATION

The weather event procedure is used to predict weather events that could occur during the reliability reporting period. The events predicted include rainfall and snowfall. The time following each event that the pavement remains wet or covered by snow or ice is also predicted. The presence of these conditions has been found to influence running speed and intersection saturation flow rate.

The sequence of calculations in the weather event procedure is shown in Exhibit 29-1. The calculations proceed on a day-by-day basis in chronological order. If a day is determined to have a weather event, its start time and duration are recorded for later use in the traffic incident procedure. Thereafter, each analysis period is evaluated in chronological order for any given day with a weather event. If the analysis period is associated with a weather event, the event type (i.e., rain or snow), precipitation rate (i.e., intensity), and pavement status (i.e., wet or snow covered) are recorded for later use in the scenario file generation procedure.

The weather event procedure consists of eight calculation steps. The calculations associated with each step are described in the following paragraphs. A random number is used in several of the steps. All random numbers have a real value that is uniformly distributed from 0.0 to 1.0.

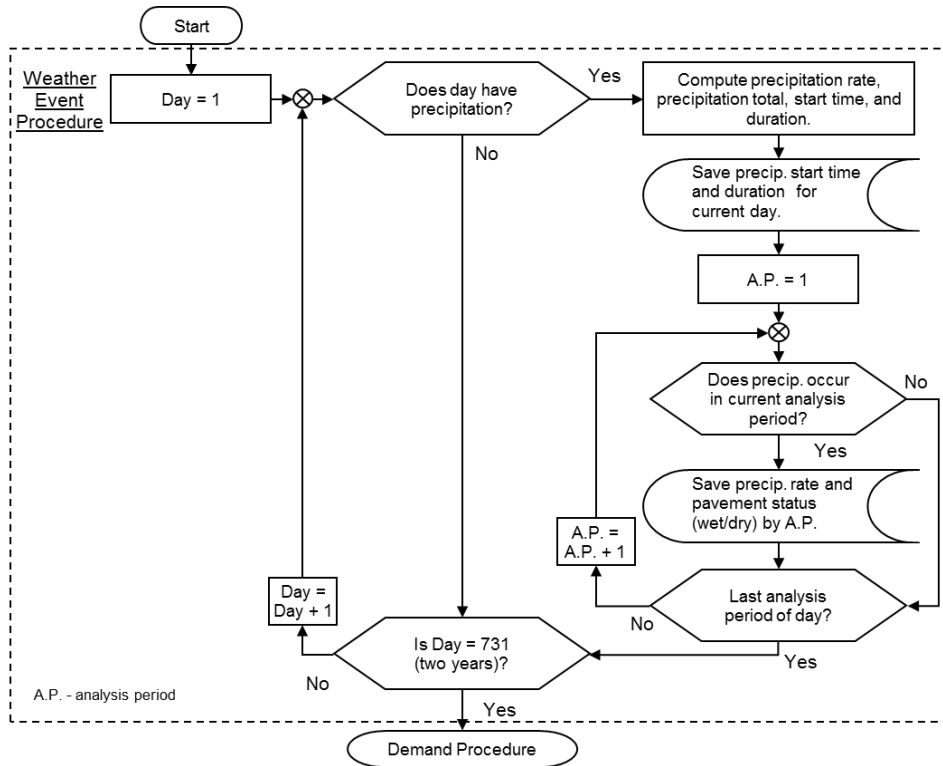


Exhibit 29-1
Weather Event Procedure

Step 1: Precipitation Prediction

The probability of precipitation for any given day is computed by using the following equation:

$$P(\text{precip})_m = \frac{Ndp_m}{Nd_m}$$

Equation 29-1

where

$P(\text{precip})_m$ = probability of precipitation in any given day of month m ,

Ndp_m = number of days with precipitation of 0.01 in. or more in month m (d),
and

Nd_m = total number of days in month m (d).

For each day considered in month m , the following rule is checked to determine whether precipitation occurs:

$$\text{No precipitation if } Rp_{d,m} \geq P(\text{precip})_m$$

$$\text{Precipitation if } Rp_{d,m} < P(\text{precip})_m$$

Equation 29-2

where $Rp_{d,m}$ is the random number for precipitation for day d of month m . The rule is applied to each day (on a monthly basis) in the reliability reporting period.

Step 2: Precipitation Type

If precipitation occurs, the following equation is used to estimate the average temperature during the weather event for the subject day (1):

$$T_{d,m} = \text{normal}^{-1}(p = Rg_d, \mu = \bar{T}_m, \sigma = s_T)$$

Equation 29-3

where

$T_{d,m}$ = average temperature for day d of month m (°F),

Rg_d = random number for temperature for day d ,

\bar{T}_m = normal daily mean temperature in month m (°F),

s_T = standard deviation of daily mean temperature in a month
(= 5.0) (°F), and

$\text{normal}^{-1}(p, \mu, \sigma)$ = value associated with probability p for a cumulative normal distribution with mean μ and standard deviation σ .

The average temperature for the day is used to determine whether the precipitation is in the form of rain or snow. The following rule is checked to determine the form of the precipitation for that day:

Equation 29-4

Rain if $T_{d,m} \geq 32^\circ\text{F}$

Snow if $T_{d,m} < 32^\circ\text{F}$

Step 3: Rain Intensity

The following equation is used to estimate the rainfall rate during a rain event:

Equation 29-5

$$rr_{d,m} = \text{gamma}^{-1}(p = Rr_d, \mu = \bar{r}r_m, \sigma = s_{\pi,m})$$

where

$rr_{d,m}$ = rainfall rate for the rain event occurring on day d of month m
(in./h),

Rr_d = random number for rainfall rate for day d ,

$\bar{r}r_m$ = precipitation rate in month m (in./h),

$s_{rr,m}$ = standard deviation of precipitation rate in month m (= 1.0 $\bar{r}r_m$)
(in./h), and

$\text{gamma}^{-1}(p, \mu, \sigma)$ = value associated with probability p for a cumulative gamma distribution with mean μ and standard deviation σ .

The average precipitation rate (and its standard deviation) is based on time periods when precipitation is falling. Thus, the average precipitation rate represents an average for all hours for which precipitation is falling (and excluding any hours when precipitation is not falling).

The following equation is used to estimate the total amount of rainfall for a rain event. Each day with precipitation is assumed to have one rain event.

Equation 29-6

$$tr_{d,m} = \text{gamma}^{-1}(p = Rt_d, \mu = \bar{t}r_m, \sigma = s_{tr,m})$$

with

Equation 29-7

$$\bar{t}r_m = \frac{tp_m}{Nd p_m}$$

Equation 29-8

$$s_{tr,m} = \min(2.5 \bar{t}r_m, 0.65)$$

where

$tr_{d,m}$ = total rainfall for the rain event occurring on day d of month m (in./event),

Rt_d = random number for rainfall total for day d ($= Rr_d$),

\bar{tr}_m = average total rainfall per event in month m (in./event),

$s_{tr,m}$ = standard deviation of total rainfall in month m (in./event),

tp_m = total normal precipitation for month m (in.), and

Ndp_m = number of days with precipitation of 0.01 in. or more in month m (d).

Total rainfall for a rain event is the product of rainfall rate and rain event duration. Thus, the total rainfall amount is highly correlated with the rainfall rate. For reliability evaluation, total rainfall is assumed to be perfectly correlated with rainfall rate such that they share the same random number. This approach may result in slightly less variability in the estimated total rainfall; however, it precludes the occasional calculation of unrealistically long or short rain events.

Step 4: Rainfall Duration

The following equation is used to estimate the rainfall duration for a rain event:

$$dr_{d,m} = \frac{tr_{d,m}}{rr_{d,m}}$$

Equation 29-9

where

$dr_{d,m}$ = rainfall duration for the rain event occurring on day d of month m (h/event),

$tr_{d,m}$ = total rainfall for the rain event occurring on day d of month m (in./event), and

$rr_{d,m}$ = rainfall rate for the rain event occurring on day d of month m (in./h).

The duration computed with Equation 29-9 is used in a subsequent step to determine whether an analysis period is associated with a rain event. To simplify the analytics in this subsequent step, it is assumed that no rain event extends beyond midnight. To ensure this outcome, the duration computed from Equation 29-9 is compared with the duration between the start of the study period and midnight. The rainfall duration is then set to equal the smaller of these two values.

Step 5: Start Time of Weather Event

The hour of the day that the rain event starts is determined randomly. The start hour is computed with the following equation:

$$ts_{d,m} = (24 - dr_{d,m})R_{s,d}$$

Equation 29-10

where

$ts_{d,m}$ = start of rain event on day d of month m (h),

24 = number of hours in a day (h/day),

$dr_{d,m}$ = rainfall duration for the rain event occurring on day d of month m (h/event), and

$R_{s,d}$ = random number for rain event start time for day d .

The start time from Equation 29-10 is rounded to the nearest hour for 1-h analysis periods or to the nearest quarter hour for 15-min analysis periods.

Step 6: Wet Pavement Duration

After a rain event, the pavement typically remains wet for some length of time. The presence of wet pavement can influence road safety by reducing surface-tire friction. Research (1) indicates that wet pavement time can be computed with the following equation:

Equation 29-11

$$dw_{d,m} = dr_{d,m} + do_{d,m} + dd_{d,m}$$

with

Equation 29-12

$$dd_{d,m} = 0.888 \exp(-0.0070 T_{d,m}) + 0.19 I_{\text{night}}$$

where

$dw_{d,m}$ = duration of wet pavement for rain event occurring on day d of month m (h/event),

$dr_{d,m}$ = rainfall duration for the rain event occurring on day d of month m (h/event),

$do_{d,m}$ = duration of pavement runoff for rain event occurring on day d of month m (= 0.083) (h/event),

$T_{d,m}$ = average temperature for day d of month m (°F),

I_{night} = indicator variable for night (= 0.0 if rain starts between 6:00 a.m. and 6:00 p.m., 1.0 otherwise), and

$dd_{d,m}$ = duration of drying time for rain event occurring on day d of month m (h/event).

The duration computed with Equation 29-11 is used in a subsequent step to determine whether an analysis period is associated with wet pavement conditions. To simplify the analytics in this subsequent step, it is assumed that no rain event extends beyond midnight. To ensure this outcome, the duration computed from Equation 29-11 is compared with the duration between the start of the rain event and midnight. The wet pavement duration is then set to equal the smaller of these two values.

Step 7: Snow Intensity and Duration

The snowfall rate (i.e., intensity) and duration are computed by using the calculation sequence in Steps 3 to 6. The equations are the same. The average snowfall rate and average snow total per event are computed by multiplying the average precipitation rate and average total rainfall per event, respectively, by the ratio of snow depth to rain depth. This ratio is estimated at 10 in./in on the basis of an analysis of weather data reported by the National Climatic Data Center (2).

In Step 6, the duration of pavement runoff is defined differently for snow events. Specifically, it is defined as the time after the snow stops falling that snowpack (or ice) covers the pavement. After this period elapses, the pavement is exposed and drying begins. A default value for this variable is provided in Exhibit 17-8 in Chapter 17.

Step 8: Identify Analysis Period Weather

Steps 1 through 7 are repeated for each day of a 2-year period, starting with the first day of the reliability reporting period. This 2-year record of weather events is used in the traffic incident procedure to estimate the weather-related incident frequency.

The days that have weather events are subsequently examined to determine whether the event occurs during the study period. Specifically, each analysis period is examined to determine whether it is associated with a weather event. If the pavement is wet during an analysis period, the precipitation type (i.e., rain or snow) is recorded for that period. If precipitation is falling, the precipitation rate is also recorded.

The duration of precipitation and wet pavement from Equation 29-9 and Equation 29-11, respectively, are rounded to the nearest hour for 1-h analysis periods or to the nearest quarter hour for 15-min analysis periods. The rounding ensures the most representative match between event duration and analysis period start and end times.

TRAFFIC DEMAND VARIATION GENERATION

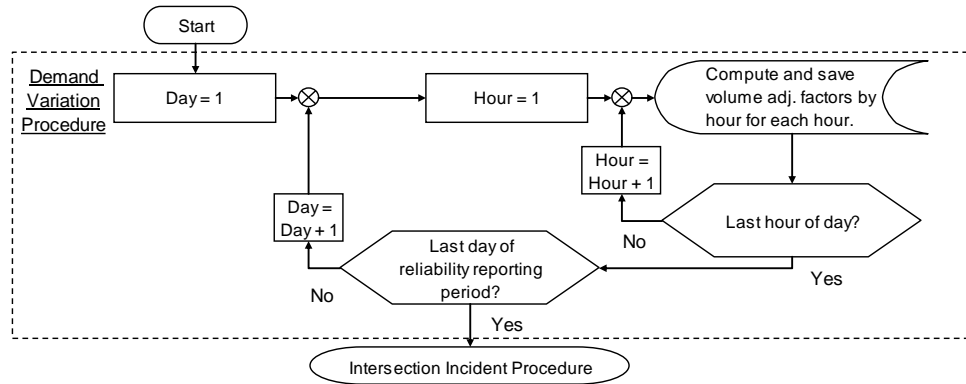
The traffic demand variation procedure is used to identify the appropriate traffic demand adjustment factors for each analysis period in the reliability reporting period. One set of factors accounts for systematic volume variation by hour of day, day of week, and month of year. Default values for these factors are provided in Exhibit 17-5 to Exhibit 17-7 in Chapter 17.

The sequence of calculations in the traffic demand variation procedure is shown in Exhibit 29-2. The calculations proceed on a day-by-day and hour-by-hour basis in chronological order. Within a given day, the procedure considers only the hours within the study period. The factors identified in this procedure are subsequently used in the scenario file generation procedure to compute the demand volume for the subject urban street facility.

A random variation adjustment factor is also available and can be included, if desired, by the analyst. It accounts for the random variation in volume that occurs among 15-min time periods. This factor is described in more detail in the Scenario Dataset Generation section.

The procedure includes two adjustment factors to account for a reduction in traffic demand during inclement weather. One factor addresses demand change during periods of rain. The second factor addresses demand change during periods of snow. Default values for these factors are provided in Exhibit 17-8 in Chapter 17.

Exhibit 29-2
Traffic Demand Variation Procedure



This procedure does not address traffic diversion due to the presence of work zones or special events. Their accommodation in a reliability evaluation is discussed in the Analysis Techniques subsection of Section 5 in Chapter 17.

If the traffic volumes provided in the base dataset and the alternative datasets are computed by using planning procedures, the volumes in the dataset are assumed to represent the average day of week and month of year. In this situation, the adjustment factors for day of week and month of year are set to a value of 1.0.

The factors identified in this procedure are subsequently used in the scenario dataset generation procedure to compute the demand volume for the subject urban street facility.

TRAFFIC INCIDENT GENERATION

The traffic incident procedure is used to predict incident date, time, and duration. It also determines incident event type (i.e., crash or noncrash), severity level, and location on the facility. Location is defined by the specific intersection or segment on which the incident occurs and whether the incident occurs on the shoulder, one lane, or multiple lanes. The procedure uses weather event and traffic demand variation information from the previous procedures in the incident prediction process.

The sequence of calculations in the traffic incident procedure is shown in Exhibit 29-3. The sequence shown is applicable to incidents occurring at signalized intersections. A similar sequence is followed for incidents occurring at locations along the urban street between the signalized intersections (i.e., midsignal segments).

The traffic incident procedure consists of six calculation steps. The calculations associated with each step are described in the following paragraphs. A random number is used in several of the steps. All random numbers have a real value that is uniformly distributed from 0.0 to 1.0.

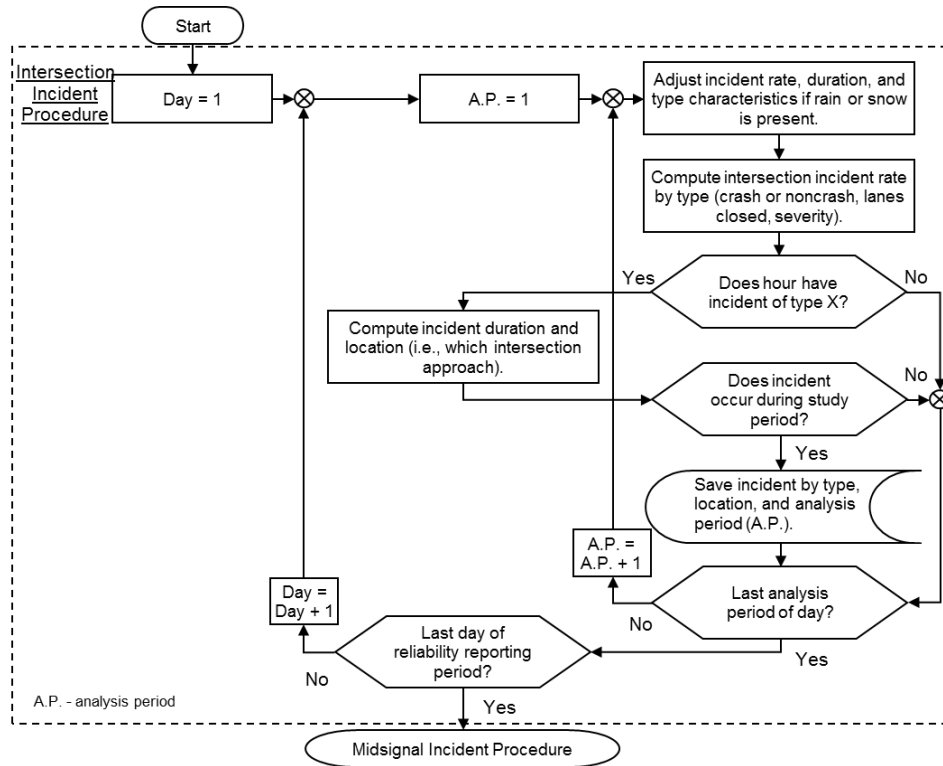


Exhibit 29-3
Traffic Incident Procedure for Intersection Incidents

Step 1: Compute the Equivalent Crash Frequency for Weather

Crash frequency increases when the road is wet, covered by snow, or covered by ice. The effect of weather on crash frequency is incorporated in the reliability methodology by converting the input crash frequency data into an equivalent crash frequency for each type of weather condition. The equivalent crash frequency for dry pavement conditions is defined with the following equation:

$$F_{C_{str(i),dry}} = \frac{F_{C_{str(i)}} 8,760 Ny}{Nh_{dry} + CFAF_{rf}Nh_{rf} + CFAF_{wp}Nh_{wp} + CFAF_{sf}Nh_{sf} + CFAF_{sp}Nh_{sp}}$$

Equation 29-13

where

$F_{C_{str(i),dry}}$ = equivalent crash frequency when every day is dry for street location i of type str ($str = int$: intersection, seg : segment) (crashes/year),

$F_{C_{str(i)}}$ = expected crash frequency for street location i of type str (crashes/year),

8,760 = number of hours in a year (h/year),

Ny = total number of years (years),

Nh_{dry} = total number of hours in Ny years with dry conditions (h),

Nh_{rf} = total number of hours in Ny years with rainfall conditions (h),

Nh_{wp} = total number of hours in Ny years with wet pavement and not raining (h),

Nh_{sf} = total number of hours in Ny years with snowfall conditions (h),

Nh_{sp} = total number of hours in Ny years with snow or ice on pavement and not snowing (h),

$CFAF_{rf}$ = crash frequency adjustment factor for rainfall,

$CFAF_{wp}$ = crash frequency adjustment factor for wet pavement (not raining),

$CFAF_{sf}$ = crash frequency adjustment factor for snowfall, and

$CFAF_{sp}$ = crash frequency adjustment factor for snow or ice on pavement (not snowing).

The equivalent crash frequency for nondry conditions is computed with the following equation. The crash frequency adjustment factor (CFAF) for dry weather $CFAF_{dry}$ is 1.0.

Equation 29-14

$$Fc_{str(i),wea} = Fc_{str(i),dry} CFAF_{wea}$$

where

$Fc_{str(i),wea}$ = equivalent crash frequency when every day has weather condition wea ($wea = dry$: no precipitation and dry pavement, rf : rainfall, wp : wet pavement but not raining, sf : snowfall, sp : snow or ice on pavement but not snowing) for street location i of type str (crashes/year);

$Fc_{str(i),dry}$ = equivalent crash frequency when every day is dry for street location i of type str (crashes/year); and

$CFAF_{wea}$ = crash frequency adjustment factor for weather condition wea .

Equation 29-14 requires the total number of hours for each weather condition in the vicinity of the subject facility. A weather history that extends for 2 or more years should be used to reduce the random variability in the data. These hours can be obtained from available weather records or estimated by using the weather event procedure.

This step is applied separately to each intersection and segment on the facility. The expected crash frequency Fc is provided by the analyst for the subject intersection or the subject segment, whichever is applicable.

The CFAF is the ratio of hourly crash frequency during the weather event to the hourly crash rate during clear, dry hours. It is computed by using one or more years of historical weather data and crash data for the region in which the subject facility is located. Default values for these factors are provided in Exhibit 17-9 in Chapter 17.

Step 2: Establish the CFAFs for Work Zones and Special Events

If the analysis period occurs during a work zone or special event, the CFAF variable for segments $CFAF_{str}$ and the CFAF variable for intersections $CFAF_{int}$ are set equal to the values provided by the analyst. Otherwise, $CFAF_{str}$ and $CFAF_{int}$ equal 1.0. This step is repeated for each analysis period of the reliability reporting period.

Step 3: Determine Whether an Incident Occurs

During this step, each of the 24 h in the subject day is examined to determine whether an incident occurs. The analysis considers each street location (i.e., intersection and segment) separately. At each street location, each of the following 12 incident types is separately addressed. Each of these types is separately considered for each hour of the day (whether the hour coincides with an analysis period is determined in a subsequent step).

- Crash, one lane blocked, fatal or injury;
- Crash, two or more lanes blocked, fatal or injury;
- Crash, shoulder location, fatal or injury;
- Crash, one lane blocked, property damage only;
- Crash, two or more lanes blocked, property damage only;
- Crash, shoulder location, property damage only;
- Noncrash, one lane blocked, breakdown;
- Noncrash, two or more lanes blocked, breakdown;
- Noncrash, shoulder location, breakdown;
- Noncrash, one lane blocked, other;
- Noncrash, two or more lanes blocked, other; and
- Noncrash, shoulder location, other.

Initially, the weather event data are checked to determine whether the subject day and hour are associated with rainfall, wet pavement and not raining, snowfall, or snow or ice on pavement and not snowing. For a given day, street location, and hour of day, the average incident frequency is computed with the following equation on the basis of the weather present at that hour and day.

$$F_{i_{str(i),wea}(h,d)} = CFAF_{str} \frac{F_{C_{str(i),wea}}}{p_{C_{str,wea}}}$$

"Other" refers to any kind of nonbreakdown incident (e.g., spill, dropped load).

Equation 29-15

where

$F_{i_{str(i),wea}(h,d)}$ = expected incident frequency for street location i of type str and weather condition $wea(h,d)$ during hour h and day d (incidents/year);

$CFAF_{str}$ = crash frequency adjustment factor for street location type str ;

$F_{C_{str(i),wea}}$ = equivalent crash frequency when every day has weather condition wea for street location i of type str (crashes/year); and

$p_{C_{str,wea}}$ = proportion of incidents that are crashes for street location type str and weather condition wea .

Default values for the proportion of incidents are provided in the third column of Exhibit 17-11 in Chapter 17.

The incident frequency is converted to an hourly frequency that is sensitive to traffic demand variation by hour of day, day of week, and month of year. The converted frequency is computed with the following equation:

Equation 29-16

$$f_{str(i),wea(h,d),h,d} = \frac{F_{str(i),wea(h,d)}}{8,760} (24 f_{hod,h,d}) f_{dow,d} f_{moy,d}$$

where

$f_{str(i),wea(h,d),h,d}$ = expected hourly incident frequency for street location i of type str and weather condition $wea(h, d)$ during hour h and day d (incidents/h),

$F_{str(i),wea(h,d)}$ = expected incident frequency for street location i of type str and weather condition $wea(h, d)$ during hour h and day d (incidents/year),

8,760 = number of hours in a year (h/year),

24 = number of hours in a day (h/day),

$f_{hod,h,d}$ = hour-of-day adjustment factor based on hour h and day d ,

$f_{dow,d}$ = day-of-week adjustment factor based on day d , and

$f_{moy,d}$ = month-of-year adjustment factor based on day d .

The hour-of-day adjustment factor includes a day subscript because its values depend on whether the day occurs during a weekday or weekend. The day subscript for the day-of-week factor is used to determine which of the 7 weekdays is associated with the subject day. Similarly, the month subscript is used to determine which of the 12 months is associated with the subject day for the month-of-year factor. Default values for these adjustment factors are provided in Exhibit 17-5 to Exhibit 17-7 in Chapter 17.

Incidents for a given day, street location, incident type, and hour of day are assumed to follow a Poisson distribution. For any given combination of conditions, the probability of more than one incident of a given type is negligible, which simplifies the mathematics so that the question of whether an incident occurs is reduced to whether there are zero incidents or one incident of a given type. Equation 29-17 is used to compute the probability of no incidents occurring. Default values for the proportion of incidents are provided in Exhibit 17-11 and Exhibit 17-12 in Chapter 17.

Equation 29-17

$$p0_{str(i),wea(h,d),con,lan,sev,h,d} = \exp(-f_{str(i),wea(h,d),h,d} \times p_{str,wea(h,d),con,lan,sev})$$

where

$p0_{str(i),wea(h,d),con,lan,sev,h,d}$ = probability of no incident for street location i of type str , weather condition $wea(h, d)$ during hour h and day d , event type con ($con = cr$: crash, nc : noncrash), lane location lan ($lan = 1L$: one lane, $2L$: two or more lanes, sh : shoulder), and severity sev ($sev = pdo$: property damage only, fi : fatal or injury, bkd : breakdown, oth : other);

$f_{str(i),wea(h,d),h,d}$ = expected hourly incident frequency for street location i of type str and weather condition $wea(h, d)$ during hour h and day d (incidents/h); and

$p_{str,wea(h,d),con,lan,sev}^i$ = proportion of incidents for street location type str , weather condition $wea(h, d)$ during hour h and day d , event type con , lane location lan , and severity sev .

The following rule is checked to determine whether the incident of a specific type occurs:

$$\begin{aligned} \text{No incident if } Ri_{str(i),wea(h,d),con,lan,sev,h,d} &\leq p0_{str(i),wea(h,d),con,lan,sev,h,d} \\ \text{Incident if } Ri_{str(i),wea(h,d),con,lan,sev,h,d} &> p0_{str(i),wea(h,d),con,lan,sev,h,d} \end{aligned}$$

Equation 29-18

where

$Ri_{str(i),wea(h,d),con,lan,sev,h,d}$ = random number for incident for street location i of type str , weather condition $wea(h, d)$ during hour h and day d , event type con , lane location lan , and severity sev ; and

$p0_{str(i),wea(h,d),con,lan,sev,h,d}$ = probability of no incident for street location i of type str , weather condition $wea(h, d)$ during hour h and day d , event type con , lane location lan , and severity sev .

Step 4: Determine Incident Duration

If the result of Step 3 indicates that an incident occurs for a given day, street location, incident type, and hour of day, the calculations in this step are used to determine the incident duration. Each hour of the day is considered separately in this step.

Incident duration includes the incident detection time, response time, and clearance time. Research (1) indicates that these values can vary by weather condition, event type, lane location, and severity. Default values for average incident duration are provided in the text associated with Exhibit 17-10 in Chapter 17.

The following equation is used to estimate the incident duration for a given incident:

$$di_{str(i),wea(h,d),con,lan,sev,h,d} = \text{gamma}^{-1} \left(\begin{array}{l} p = Rd_{str(i),con,lan,sev,h,d} \\ \mu = \bar{di}_{str,wea(h,d),con,lan,sev} \\ \sigma = S_{str,wea(h,d),con,lan,sev} \end{array} \right)$$

Equation 29-19

where

$di_{str(i),wea(h,d),con,lan,sev,h,d}$ = incident duration for street location i of type str , weather condition $wea(h, d)$ during hour h and day d , event type con , lane location lan , and severity sev (h);

$Rd_{str(i),con,lan,sev,h,d}$ = random number for incident duration for street location i of type str for hour h and day d , event type con , lane location lan , and severity sev ;

$\bar{di}_{str,wea(h,d),con,lan,sev}$ = average incident duration for street location type str , weather condition $wea(h, d)$ during hour h and day d , event type con , lane location lan , and severity sev (h);

$S_{str,wea(h,d),con,lan,sev}$ = standard deviation of incident duration for street location type str , weather condition $wea(h, d)$ during

hour h and day d , event type con , lane location lan , and severity sev ($= 0.8 \bar{d}i_{str,vea(h,d),con,lan,sev}$) (h); and

$\text{gamma}^{-1}(p, \mu, \sigma)$ = value associated with probability p for cumulative gamma distribution with mean μ and standard deviation σ .

The duration computed with Equation 29-19 is used in a subsequent step to determine whether an analysis period is associated with an incident. To simplify the analytics in this subsequent step, it is assumed that no incident extends beyond midnight. To ensure this outcome, the duration computed from Equation 29-19 is compared with the duration between the start of the study period and midnight. The incident duration is then set to equal the smaller of these two values.

Step 5: Determine Incident Location

If the result of Step 3 indicates that an incident occurs for a given day, street location, incident type, and hour of day, the calculations in this step are used to determine the incident location. For intersections, the location is determined to be one of the intersection legs. For segments, the location is determined to be one of the two travel directions. The location algorithm is volume-based so that the correct location determinations are made when three-leg intersections or one-way streets are addressed. Each hour of the day is considered separately in this step.

Intersection Location

When a specific intersection is associated with an incident, the location of the incident is based on consideration of each intersection leg volume lv . This volume represents the sum of all movements entering the intersection on the approach lanes and movements exiting the intersection on the adjacent departure lanes. In the field, this volume would be measured by establishing a reference line from outside curb to outside curb on the subject leg (near the crosswalk) and counting all vehicles that cross the line, regardless of travel direction.

The leg volumes are then summed, starting with the leg associated with National Electrical Manufacturers Association (NEMA) Phase 2, to produce a cumulative volume by leg. These volumes are then converted to a proportion by dividing by the sum of the leg volumes. The calculation of these proportions is described by the following equations. One set of proportions is determined for the base dataset and for each work zone and special event dataset.

Equation 29-20

$$\begin{aligned}
 pv_{int(i),2} &= lv_{int(i),2} / (2 tv_{int(i)}) \\
 pv_{int(i),4} &= pv_{int(i),2} + lv_{int(i),4} / (2 tv_{int(i)}) \\
 pv_{int(i),6} &= pv_{int(i),4} + lv_{int(i),6} / (2 tv_{int(i)}) \\
 pv_{int(i),8} &= 1.0
 \end{aligned}$$

with

$$tv_{int(i)} = \sum_{j=1}^{12} v_{input,int(i),j}$$

Equation 29-21

where

$pv_{int(i),n}$ = cumulative sum of volume proportions for leg associated with NEMA phase n ($n = 2, 4, 6, 8$) at intersection i ,

$lv_{int(i),n}$ = leg volume (two-way total) for leg associated with NEMA phase n at intersection i (veh/h),

$tv_{int(i)}$ = total volume entering intersection i (veh/h), and

$v_{input,int(i),j}$ = movement j volume at intersection i (from dataset) (veh/h).

The leg location of the incident is determined by comparing a random number with the cumulative volume proportions. With this technique, the likelihood of an incident being assigned to a leg is proportional to its volume relative to the other leg volumes. The location is determined for a given intersection i by the following rule:

- Incident on Phase 2 if $Rv_{int(i),con,lan,sev} \leq pv_{int(i),2}$
- Incident on Phase 4 if $pv_{int(i),2} < Rv_{int(i),con,lan,sev} \leq pv_{int(i),4}$
- Incident on Phase 6 if $pv_{int(i),4} < Rv_{int(i),con,lan,sev} \leq pv_{int(i),6}$
- Incident on Phase 8 if $pv_{int(i),6} < Rv_{int(i),con,lan,sev} \leq pv_{int(i),8}$

Equation 29-22

where

$Rv_{int(i),con,lan,sev}$ = random number for leg volume for intersection i , event type con , lane location lan , and severity sev ; and

$pv_{int(i),n}$ = cumulative sum of volume proportions for leg associated with NEMA phase n ($n = 2, 4, 6, 8$) at intersection i .

Segment Location

When a specific segment is associated with an incident, the location of the incident is based on consideration of the volume in each direction of travel dv . This volume is computed by using the movement volume at the boundary intersection that uses NEMA Phase 2 to serve exiting through vehicles. The volume in the Phase 2 direction is computed as the sum of the movements exiting the segment at the boundary intersection (i.e., it equals the approach lane volume). The volume in the Phase 6 direction is computed as the sum of the movements entering the segment at the boundary intersection (i.e., it equals the departure lane volume). The two directional volumes are referenced to NEMA Phases 2 and 6. The sum of these two volumes equals the Phase 2 leg volume described in the previous subsection.

A cumulative volume proportion by direction is used to determine incident location. The calculation of these proportions is described by the following equations. One set of proportions is determined for the base dataset and for each work zone and special event dataset.

Equation 29-23

$$pv_{seg(i),2} = dv_{seg(i),2} / (dv_{seg(i),2} + dv_{seg(i),6})$$

$$pv_{seg(i),6} = 1.0$$

where

$pv_{seg(i),n}$ = volume proportion for the direction of travel served by NEMA phase n ($n = 2, 6$) on segment i , and

$dv_{seg(i),n}$ = directional volume for the direction of travel served by NEMA phase n on segment i (veh/h).

The segment location of the incident is determined by comparing a random number with the cumulative volume proportions. With this technique, the likelihood of an incident being assigned to a direction of travel is proportional to its volume, relative to the volume in the other direction. The location is determined for a given segment i by the following rule:

Equation 29-24

$$\text{Incident in Phase 2 direction if } Rv_{seg(i),con,lan,sev} \leq pv_{seg(i),2}$$

$$\text{Incident in Phase 6 direction if } pv_{seg(i),2} < Rv_{seg(i),con,lan,sev} \leq pv_{seg(i),6}$$

where

$Rv_{seg(i),con,lan,sev}$ = random number for volume for segment i , event type con , lane location lan , and severity sev ; and

$pv_{seg(i),n}$ = volume proportion for the direction of travel served by NEMA phase n ($n = 2, 6$) on segment i .

Step 6: Identify Analysis Period Incidents

Steps 3 through 5 are repeated for each hour of the subject day. As implied by the discussion to this point, all incidents are assumed to occur at the start of a given hour.

During this step, the analysis periods associated with an incident are identified. Specifically, each hour of the study period is examined to determine whether it coincides with an incident. If an incident occurs, its event type, lane location, severity, and street location are identified and recorded. Each subsequent analysis period coincident with the incident is also recorded.

The incident duration from Equation 29-19 is rounded to the nearest hour for 1-h analysis periods or to the nearest quarter hour for 15-min analysis periods. This rounding is performed to ensure the most representative match between event duration and analysis period start and end times.

SCENARIO DATASET GENERATION

The scenario dataset generation procedure uses the results from the preceding three procedures to develop one HCM dataset for each analysis period in the reliability reporting period. As discussed previously, each analysis period is considered to be one scenario.

The sequence of calculations in the scenario file generation procedure is shown in Exhibit 29-4. The calculations and file generation proceed on a day-by-day and analysis-period-by-analysis-period basis in chronological order. If a day

is coincident with a work zone or special event, the appropriate alternative dataset is loaded. Otherwise, the base dataset is loaded.

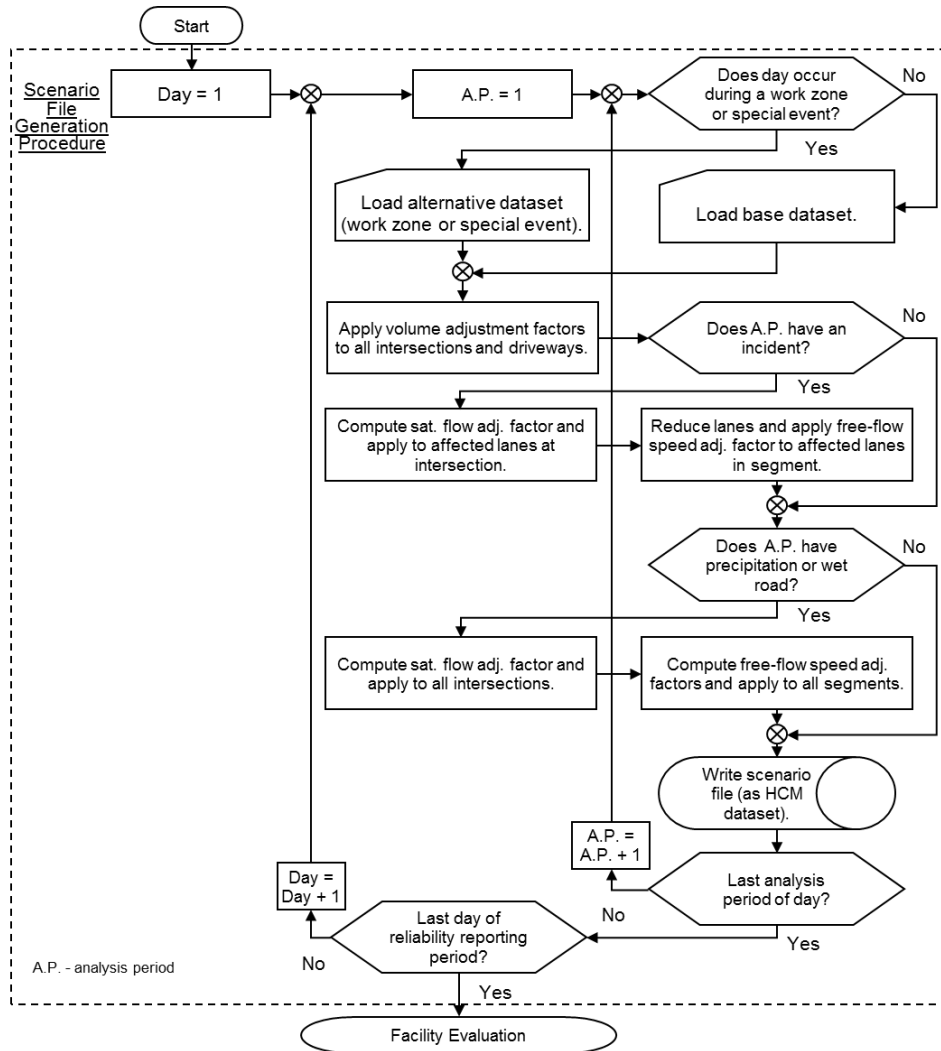


Exhibit 29-4
Scenario File Generation Procedure

This procedure creates a new HCM dataset for each analysis period. The dataset is modified to reflect conditions present during a given analysis period. Modifications are made to the traffic volumes at each intersection and driveway and to the saturation flow rate at intersections influenced by an incident or a weather event. The speed is also adjusted for segments influenced by an incident or a weather event.

The incident history developed by the traffic incident procedure is consulted during this procedure to determine whether an incident occurs at an intersection or on a segment. If an incident occurs at an intersection, the incident lane location data are consulted to determine which approach and movements are affected. If the incident occurs on the shoulder, the shoulder in question is assumed to be the outside shoulder (as opposed to the inside shoulder). If a one-lane incident occurs, the incident is assumed to occur in the outside lane. If a two-or-more-lane incident occurs, it is assumed to occur in the outside two lanes. The incident is also

assumed to occur on the intersection approach lanes as opposed to the departure lanes. These assumptions are consistent with typical intersection crash patterns.

The scenario dataset generation procedure consists of nine calculation steps. The calculations associated with each step are described in the following paragraphs.

Step 1: Acquire the Appropriate Dataset

During this step, the appropriate HCM dataset is acquired. This step proceeds day by day and analysis period by analysis period in chronological order. The date is used to determine whether a work zone or special event is present. If one is present, the appropriate alternative dataset is acquired. Otherwise, the base dataset is acquired. The hour-of-day, day-of-week, and month-of-year demand adjustment factors associated with each dataset are also acquired (as identified previously in the traffic demand variation procedure).

Step 2: Compute Weather Adjustment Factors

Signalized Intersections

The following equation is used to compute the saturation flow rate adjustment factor for analysis periods with poor weather conditions. It is used in Step 5 to estimate intersection saturation flow rate during weather events.

Equation 29-25

$$f_{rs,ap,d} = \frac{1.0}{1.0 + 0.48 R_{r,ap,d} + 0.39 R_{s,ap,d}}$$

where

$f_{rs,ap,d}$ = saturation flow adjustment factor for rainfall or snowfall during analysis period ap and day d ,

$R_{r,ap,d}$ = rainfall rate during analysis period ap and day d (in./h), and

$R_{s,ap,d}$ = precipitation rate when snow is falling during analysis period ap and day d (in./h).

If Equation 29-25 is used for analysis periods with falling rain, the variable R_s should equal 0.0. If it is used for analysis periods with falling snow, the variable R_r should equal 0.0. The variable R_s equals the precipitation rate in terms of equivalent inches of water per hour (i.e., it is not a snowfall rate).

The value obtained from Equation 29-25 applies when precipitation is falling. If the pavement is wet and there is no rainfall, the adjustment factor $f_{rs,ap,d}$ is 0.95. If snow or ice is on the pavement and snow is not falling, the adjustment factor $f_{rs,ap,d}$ is 0.90.

Segments

The following equation is used to compute the free-flow speed adjustment factor for analysis periods with poor weather conditions. It is used in Step 7 to estimate the additional running time during weather events.

Equation 29-26

$$f_{s,rs,ap,d} = \frac{1.0}{1.0 + 0.48 R_{r,ap,d} + 1.4 R_{s,ap,d}}$$

where

$f_{s,rs,ap,d}$ = free-flow speed adjustment factor for rainfall or snowfall during analysis period ap and day d ,

$R_{r,ap,d}$ = rainfall rate during analysis period ap and day d (in./h), and

$R_{s,ap,d}$ = precipitation rate when snow is falling during analysis period ap and day d (in./h).

If Equation 29-26 is used for analysis periods with falling rain, the variable R_s should equal 0.0. If it is used for analysis periods with falling snow, the variable R_r should equal 0.0. The variable R_s equals the precipitation rate in terms of equivalent inches of water per hour (i.e., it is not a snowfall rate).

The value obtained from Equation 29-26 applies when precipitation is falling. If the pavement is wet and there is no rainfall, the adjustment factor $f_{s,rs,ap,d}$ is 0.95. If snow or ice is on the pavement and snow is not falling, the adjustment factor $f_{s,rs,ap,d}$ is 0.90.

Step 3: Acquire Demand Adjustment Factors

During this step, the hour-of-day, day-of-week, and month-of-year demand adjustment factors associated with each analysis period are acquired (as identified previously in the traffic demand variation procedure). They are used in Step 6 to estimate the analysis period volumes.

Step 4: Compute Incident Adjustment Factors for Intersections

The following equation is used to compute the saturation flow rate adjustment factor for analysis periods associated with an incident. It is used in Step 5 to estimate intersection saturation flow rate during incidents.

$$f_{ic,int(i),n,m,ap,d} = \left(1 - \frac{N_{ic,int(i),n,m,ap,d}}{N_{n,int(i),n,m}}\right) \left(1 - \frac{b_{ic,int(i),n,ap,d}}{\sum_{m \in L,T,R} N_{n,int(i),n,m}}\right) \geq 0.10$$

Equation 29-27

with

$$b_{ic,int(i),n,ap,d} = 0.58 I_{fi,int(i),n,ap,d} + 0.42 I_{pdo,int(i),n,ap,d} + 0.17 I_{other,int(i),n,ap,d}$$

Equation 29-28

where

$f_{ic,int(i),n,m,ap,d}$ = saturation flow adjustment factor for incident presence for movement m ($m = L$: left, T : through, R : right) on leg associated with NEMA phase n ($n = 2, 4, 6, 8$) at intersection i during analysis period ap and day d ,

$N_{n,int(i),n,m}$ = number of lanes serving movement m under normal (i.e., nonincident) conditions on leg associated with NEMA phase n at intersection i (ln),

$N_{ic,int(i),n,m,ap,d}$ = number of lanes serving movement m blocked by the incident on leg associated with NEMA phase n at intersection i during analysis period ap and day d (ln),

$b_{ic,int(i),n,ap,d}$ = calibration coefficient based on incident severity on leg associated with NEMA phase n at intersection i during analysis period ap and day d ,

$I_{pdo,int(i),n,ap,d}$ = indicator variable for property-damage-only (PDO) crash on leg associated with NEMA phase n at intersection i during analysis period ap and day d (= 1.0 if PDO crash, 0.0 otherwise),

$I_{fi,int(i),n,ap,d}$ = indicator variable for fatal-or-injury crash on leg associated with NEMA phase n at intersection i during analysis period ap and day d (= 1.0 if fatal-or-injury crash, 0.0 otherwise), and

$I_{other,int(i),n,ap,d}$ = indicator variable for noncrash incident on leg associated with NEMA phase n at intersection i during analysis period ap and day d (= 1.0 if noncrash incident, 0.0 otherwise).

Equation 29-27 is applied to each approach traffic movement. For a given movement, the first term of Equation 29-27 adjusts the saturation flow rate on the basis of the number of lanes that are blocked by the incident. If the incident is located on the shoulder or in the lanes associated with another movement m (i.e., $N_{ic} = 0$), this term equals 1.0.

Equation 29-27 is used for each movement to estimate the saturation flow rate adjustment factor for incidents. If all lanes associated with a movement are closed because of the incident, an adjustment factor of 0.10 is used. This approach effectively closes the lane but does not remove it from the intersection, as described in the dataset.

Step 5: Compute Saturation Flow Rate for Intersections

During this step, the saturation flow rate for each intersection movement is adjusted by using the factors computed in Steps 2 and 4. The weather adjustment factor is applied to all movements at all intersections. The incident adjustment factor is applied only to the movements affected by an incident.

The weather and incident factors are multiplied by the saturation flow rate in the dataset to produce a revised estimate of the saturation flow rate.

Step 6: Compute Traffic Demand Volumes

Adjust Movement Volumes

During this step, the volume for each movement is adjusted by using the appropriate hour-of-day, day-of-week, and month-of-year factors to estimate the average hourly flow rate for the subject analysis period. The following equation is used for this purpose:

Equation 29-29

$$v_{int(i),j,h,d} = \frac{v_{input,int(i),j}}{f_{hod,input} f_{dow,input} f_{moy,input}} f_{hod,h,d} f_{dow,d} f_{moy,d}$$

where

$v_{int(i),j,h,d}$ = adjusted hourly flow rate for movement j at intersection i during hour h and day d (veh/h),

- $v_{input,int(i),j}$ = movement j volume at intersection i (from base dataset or alternative dataset) (veh/h),
- $f_{hod,h,d}$ = hour-of-day adjustment factor based on hour h and day d ,
- $f_{dow,d}$ = day-of-week adjustment factor based on day d ,
- $f_{moy,d}$ = month-of-year adjustment factor based on day d ,
- $f_{hod,input}$ = hour-of-day adjustment factor for hour and day associated with v_{input} ,
- $f_{dow,input}$ = day-of-week adjustment factor for day associated with v_{input} and
- $f_{moy,input}$ = month-of-year adjustment factor for day associated with v_{input} .

If a 15-min analysis period is used, the adjusted hourly flow rate is applied to all four analysis periods coincident with the subject hour h . Equation 29-29 is also used to adjust the volumes associated with each unsignalized access point on each segment.

Random Variation Among 15-min Periods

If a 15-min analysis period is used, the analyst has the option of adding a random element to the adjusted hourly volume for each movement and analysis period. Doing so provides a more realistic estimate of performance measure variability. However, it ensures that every analysis period is unique (thereby lessening the likelihood that similar scenarios can be found for the purpose of reducing the total number of scenarios to be evaluated). If this option is applied, the turn movement volumes at each signalized intersection are adjusted by using a random variability based on the peak hour factor. Similarly, the turn movement volumes at each unsignalized access point are adjusted by using a random variability based on a Poisson distribution.

If the analyst desires to add a random element to the adjusted hourly volume, the first step is to estimate the demand flow rate variability adjustment factor with the following equation:

$$f_{int(i),j,h,d} = \frac{1.0 - PHF_{int(i)}}{PHF_{int(i)}} \sqrt{0.25 v_{int(i),j,h,d} \times \exp(-0.00679 + 0.004 PHF_{int(i)}^{-4})}$$

Equation 29-30

where

- $f_{int(i),j,h,d}$ = adjustment factor used to estimate the standard deviation of demand flow rate for movement j at intersection i during hour h and day d ,
- $PHF_{int(i)}$ = peak hour factor for intersection i , and
- $v_{int(i),j,h,d}$ = adjusted hourly flow rate for movement j at intersection i during hour h and day d (veh/h).

The second step is to compute the randomized hourly flow rate for each movement at each signalized intersection with the following equation:

$$v_{int(i),j,ap,d}^* = 4.0 \times \text{gamma}^{-1} \left(\begin{matrix} p = R f_{ap,d}, \mu = 0.25 v_{int(i),j,h,d} \\ \sigma = f_{int(i),j,h,d} \sqrt{0.25 v_{int(i),j,h,d}} \end{matrix} \right)$$

Equation 29-31

where

$v_{int(i),j,ap,d}^*$ = randomized hourly flow rate for movement j at intersection i during analysis period ap and day d (veh/h),

$\text{gamma}^{-1}(p, \mu, \sigma)$ = value associated with probability p for cumulative gamma distribution with mean μ and standard deviation σ ,

$Rf_{ap,d}$ = random number for flow rate for analysis period ap and day d ,

$v_{int(i),j,h,d}$ = adjusted hourly flow rate for movement j at intersection i during hour h and day d (veh/h), and

$f_{int(i),j,h,d}$ = adjustment factor used to estimate the standard deviation of demand flow rate for movement j at intersection i during hour h and day d .

Similarly, the following equations are used to compute the randomized hourly flow rates for each unsignalized access point. The first equation is used if the adjusted hourly flow rate is 64 veh/h or less. The second equation is used if the flow rate exceeds 64 veh/h.

If $v_{int(i),j,h,d} \leq 64$ veh/h,

Equation 29-32

$$v_{int(i),j,ap,d}^* = 4.0 \times \text{Poisson}^{-1}(p = Rf_{ap,d}, \mu = 0.25 v_{int(i),j,h,d})$$

Otherwise,

Equation 29-33

$$v_{int(i),j,ap,d}^* = 4.0 \times \text{normal}^{-1} \left(\begin{array}{l} p = Rf_{ap,d}, \mu = 0.25 v_{int(i),j,h,d} \\ \sigma = \sqrt{0.25 v_{int(i),j,h,d}} \end{array} \right)$$

where

$v_{int(i),j,ap,d}^*$ = randomized hourly flow rate for movement j at intersection i during analysis period ap and day d (veh/h),

$\text{Poisson}^{-1}(p, \mu)$ = value associated with probability p for the cumulative Poisson distribution with mean μ ,

$Rf_{ap,d}$ = random number for flow rate for analysis period ap and day d ,

$v_{int(i),j,h,d}$ = adjusted hourly flow rate for movement j at intersection i during hour h and day d (veh/h), and

$\text{normal}^{-1}(p, \mu, \sigma)$ = value associated with probability p for a cumulative normal distribution with mean μ and standard deviation σ .

Step 7: Compute Speed for Segments

Additional Delay

During this step, the effect of incidents and weather on segment speed is determined. This effect is added to the HCM dataset as an additional delay incurred along the segment. The variable d_{other} in Equation 18-7 is used with this approach. This additional delay is computed with the following equations:

Equation 29-34

$$d_{\text{other},seg(i),n,ap,d} = L_{seg(i)} \left(\frac{1.0}{S_{fo,seg(i),n,ap,d}^*} - \frac{1.0}{S_{fo,seg(i),n}} \right)$$

with

$$S_{fo,seg(i),n,ap,d}^* = S_{fo,seg(i),n} \times f_{s,rs,ap,d} \times \left(1.0 - \frac{b_{ic,seg(i),n,ap,d}}{N_{o,seg(i),n}} \right)$$

Equation 29-35

$$b_{ic,seg(i),n,ap,d} = 0.58 I_{fi,seg(i),n,ap,d} + 0.42 I_{pdo,seg(i),n,ap,d} + 0.17 I_{other,seg(i),n,ap,d}$$

Equation 29-36

where

$d_{other,seg(i),n,ap,d}$ = additional delay for the direction of travel served by NEMA phase n ($n = 2, 6$) on segment i during analysis period ap and day d (s/veh),

$L_{seg(i)}$ = length of segment i (ft),

$S_{fo,seg(i),n}$ = base free-flow speed for the direction of travel served by NEMA phase n on segment i (ft/s),

$S_{fo,seg(i),n,ap,d}^*$ = adjusted base free-flow speed for the direction of travel served by NEMA phase n on segment i during analysis period ap and day d (ft/s),

$f_{s,rs,ap,d}$ = free-flow speed adjustment factor for rainfall or snowfall during analysis period ap and day d ,

$b_{ic,seg(i),n,ap,d}$ = calibration coefficient based on incident severity on leg associated with NEMA phase n at intersection i during analysis period ap and day d ,

$N_{o,seg(i),n}$ = number of lanes serving direction of travel served by NEMA phase n on segment i (ln),

$I_{pdo,seg(i),n,ap,d}$ = indicator variable for property-damage-only (PDO) crash in the direction of travel served by NEMA phase n on segment i during analysis period ap and day d (= 1.0 if PDO crash, 0.0 otherwise),

$I_{fi,seg(i),n,ap,d}$ = indicator variable for fatal-or-injury crash in the direction of travel served by NEMA phase n on segment i during analysis period ap and day d (= 1.0 if fatal-or-injury crash, 0.0 otherwise), and

$I_{other,seg(i),n,ap,d}$ = indicator variable for noncrash incident in the direction of travel served by NEMA phase n on segment i during analysis period ap and day d (= 1.0 if noncrash incident, 0.0 otherwise).

The delay estimated from Equation 29-34 is added to the value of the “other delay” variable in the dataset to produce a combined “other delay” value for segment running speed estimation.

Segment Lane Closure

If an incident is determined to be located in one or more lanes, the variable for the number of through lanes on the segment is reduced accordingly. This adjustment is made for the specific segment and direction of travel associated with the incident.

The variable indicating the number of major-street through lanes at each unsignalized access point is reduced in a similar manner when the incident occurs on a segment and closes one or more lanes. This adjustment is made for each access point on the specific segment affected by the incident.

Step 8: Adjust Critical Left-Turn Headway

Research (1) indicates that the critical headway for left-turn drivers increases by 0.7 to 1.2 s, depending on the type of weather event and the opposing lane associated with the conflicting vehicle. The recommended increase in the critical headway value for each weather condition is listed in Exhibit 29-5.

Exhibit 29-5
Additional Critical Left-Turn
Headway due to Weather

Weather Condition	Additional Critical Left-Turn Headway (s)
Clear, snow on pavement	0.9
Clear, ice on pavement	0.9
Clear, water on pavement	0.7
Snowing	1.2
Raining	0.7

Step 9: Save Scenario Dataset

During this step, the dataset with the updated values is saved for evaluation in the next stage of the reliability methodology. One dataset is saved for each analysis period (i.e., scenario).

3. SUSTAINED SPILLBACK PROCEDURE

This section describes a procedure for using the methodologies described in Chapter 16, Urban Street Facilities, and Chapter 18, Urban Street Segments, to evaluate a facility with spillback in one or more travel directions on one or more segments.

The discussion in this section addresses sustained spillback. Sustained spillback occurs as a result of oversaturation (i.e., more vehicles discharging from the upstream intersection than can be served at the subject downstream intersection). The spillback can exist at the start of the study period, or it can occur at some point during the study period. Spillback that first occurs after the study period is not addressed.

OVERVIEW OF THE PROCEDURE

The effect of spillback on traffic flow is modeled through an iterative process that applies the urban street segments methodology to each segment of the subject urban street facility. If spillback occurs on a segment, the discharge rate of each traffic movement entering the segment is reduced so that (a) the number of vehicles entering the segment equals the number of vehicles exiting the segment and (b) the residual queue length equals the available queue storage distance.

The approach used to model spillback effects is similar to the technique used for multiple time period analysis, as described in the subsection Multiple Time Period Analysis in Section 3 of Chapter 18. However, in this application, a single analysis period is divided into subperiods for separate evaluation. Each subperiod is defined by using the following rules:

- The first subperiod starts with the start of the analysis period.
- The current subperiod ends (and a new subperiod starts) with each new occurrence of spillback on the facility.
- The total of all subperiod durations must equal the original analysis period duration.

As with the multiple-time-period analysis technique, the residual queue from one subperiod becomes the initial queue for the next subperiod. When all subperiods have been evaluated by using the urban street segments methodology, the performance measures for each subperiod are aggregated for the analysis period with a weighted-average technique, where the weight is the volume associated with the subperiod.

Section 3 of Chapter 30, Urban Street Segments: Supplemental, describes a “spillback check” procedure for determining whether queue spillback occurs on a segment during a given analysis period. That procedure also predicts the *controlling time until spillback*. This time is used in the sustained spillback procedure to determine when the current subperiod ends.

Section 3 of Chapter 30 also describes a procedure for predicting the *effective average vehicle spacing*. This spacing is used in the sustained spillback procedure to determine the maximum queue storage in a turn bay and along a segment.

COMPUTATIONAL STEPS

This subsection describes the sequence of computational steps that culminate in the calculation of facility performance for a specified analysis period. The input data requirements for this procedure are the same as for the urban street segments methodology (hereafter referred to as the “methodology”).

Step 1: Initialize Variables

Set the original analysis period variable T_o equal to the analysis period T that is input by the analyst. Set the total time variable $T_{total,0}$ equal to zero and the subperiod counter k to 0.

Step 2: Implement the Methodology

The methodology is used in this step to evaluate each segment on the facility. The analysis period duration used in the methodology is computed as $T = T_o - T_{total,k}$. Increase the value of the subperiod counter k by 1. Hence, for the first subperiod ($k = 0$), the analysis period duration T equals T_o (i.e., $T = T_o - 0.0$).

Step 3: Check for Spillback

During this step, the results from Step 2 are examined to determine whether there is a new occurrence of spillback. One direction of travel on one segment is considered a “site.” Each site is checked in this step. Any site that has experienced spillback during a previous subperiod is not considered in this step.

The predicted controlling time until spillback is recorded in this step. If several sites experience spillback, the time of spillback that is recorded is based on the site experiencing spillback first. The site that experiences spillback first is flagged as having spilled back. The controlling time until spillback for the subperiod $T_{cs,k}$ is set equal to the time until spillback for this site. The total time variable is computed with the following equation. It represents a cumulative total time for the current and all previous subperiods.

Equation 29-37

$$T_{total,k} = T_{total,k-1} + T_{cs,k}$$

where

$T_{total,k}$ = total analysis time for subperiods 0 to k (h), and

$T_{cs,k}$ = controlling time until spillback for the subperiod k (h).

If spillback does not occur, the performance measures from Step 2 are saved by using the procedure described in a subsequent subsection. The analyst then proceeds to Step 10 to determine the aggregate performance measures for the analysis period.

Step 4: Implement the Methodology to Evaluate a Subperiod

At the start of this step, the analysis period is set equal to the controlling time determined in Step 3 (i.e., $T = T_{cs,k}$). All other input variables remain unchanged. Then, the methodology is implemented to evaluate the facility. The performance measures from this evaluation are saved by using the procedure described in a subsequent subsection.

Step 5: Prepare for the Next Subperiod by Determining the Initial Queue

During this step, the input data are modified by updating the initial queue values for all movement groups at each intersection. This modification is necessary to prepare for a new evaluation of the facility for the next subperiod. The initial queue for each movement group is set to the estimated residual queue from the previous evaluation.

The initial queue values for the movement groups at the downstream intersection that exit each segment are checked by comparing them with the available queue storage distance. The storage distance for the left-turn movement group is computed with the following equation. The storage distance for the right-turn movement group is computed with a variation of this equation.

$$N_{qx,lt,n,k} = \frac{L_{a,thru} + L_{a,lt}(N_{lt} - 1)}{L_{h,k}^*}$$

Equation 29-38

where

$N_{qx,lt,n,k}$ = maximum queue storage for left-turn movement group during subperiod k (veh),

$L_{a,thru}$ = available queue storage distance for the through movement (ft),

$L_{a,lt}$ = available queue storage distance for the left-turn movement (ft),

N_{lt} = number of lanes in the left-turn bay (ln), and

$L_{h,k}^*$ = effective average vehicle spacing in stationary queue during subperiod k (ft/veh).

The available queue storage distance for the through movement equals the segment length less the width of the upstream intersection. For turn movements served from a turn bay, this length equals the length of the turn bay. For turn movements served from a lane equal in length to that of the segment, the queue storage length equals the segment length less the width of the upstream intersection.

The maximum queue storage for the through movement group is computed with the following equation:

$$N_{qx,thru,n,k} = \frac{L_{a,thru} N_{th}}{L_{h,k}^*}$$

Equation 29-39

where

$N_{qx,thru,n,k}$ = maximum queue storage for through movement group during subperiod k (veh), and

N_{th} = number of through lanes (shared or exclusive) (ln).

The initial queue for each movement group exiting a segment is compared with the maximum queue storage values. Any initial queue that exceeds the maximum value is set to equal the maximum value.

Step 6: Prepare for the Next Subperiod by Determining the Saturation Flow Rate Adjustment

During this step, the saturation flow rate is recomputed for movement groups entering the site identified in Step 3 as having spillback. This modification is necessary to prepare for a new evaluation of the facility during the next subperiod.

The process of recomputing this saturation flow rate uses an iterative loop. The loop converges when the saturation flow rate computed for each upstream movement is sufficiently small that the number of vehicles entering the spillback segment just equals the number of vehicles that leave the segment. A “spillback” saturation flow rate adjustment factor f_{sp} is computed for each movement to produce this result. Its value is set to 1.0 at the start of the first loop (i.e., $f_{sp,0} = 1.0$).

The process begins by setting the analysis time to equal the time remaining in the original analysis period (i.e., $T = T_o - T_{total,k}$).

The next task is to compute the estimated volume arriving to each movement exiting the segment at the downstream signalized intersection (i.e., the adjusted destination volume). This calculation is based on the origin–destination matrix and discharge volume for each movement entering the segment. These quantities are obtained from the variables calculated by using the methodology, as described in Section 2 of Chapter 30. The adjusted destination volume is computed with the following equation:

Equation 29-40

$$D_{a,j,k} = \sum_{i=1}^4 v_{od,i,j,k}$$

where

$D_{a,j,k}$ = adjusted volume for destination j ($j = 1, 2, 3, 4$) for subperiod k (veh/h), and

$v_{od,i,j,k}$ = volume entering from origin i and exiting at destination j for subperiod k (veh/h).

The letters j and i in Equation 29-40 denote the following four movements: 1 = left turn, 2 = through, 3 = right turn, and 4 = combined midsegment access points.

The next task is to compute the proportion of $D_{a,j,k}$ coming from upstream origin i . These proportions are computed with the following equation:

Equation 29-41

$$b_{i,j,k} = \frac{v_{od,i,j,k}}{D_{a,j,k}}$$

where $b_{i,j,k}$ is the proportion of volume at destination j that came from origin i for subperiod k (veh/h).

The next task is to estimate the maximum discharge rate for each upstream movement. This estimate is based on consideration of the capacity of the downstream movements exiting the segment and their volume. When the segment has incurred spillback, the capacity of one or more of these exiting movements is inadequate relative to the discharge rates of the upstream movements entering the segment. The computed maximum discharge rate is

intended to indicate the amount by which each upstream movement's discharge needs to be limited so that there is a balance between the number of vehicles entering and exiting the segment. The following equation is used for this purpose. It is applied to each of the four upstream entry movements i .

$$\begin{aligned}
 dv_{u,i,k} &= b_{i,2,k} \times c_{d,2,k} \\
 &+ \min(b_{i,1,k} \times c_{d,1,k}, fx_{i,2,k} \times v_{od,i,1,k}) \\
 &+ \min(b_{i,3,k} \times c_{d,3,k}, fx_{i,2,k} \times v_{od,i,3,k}) \\
 &+ fx_{i,2,k} \times v_{od,4,k}
 \end{aligned}$$

Equation 29-42

with

$$fx_{i,2,k} = \frac{b_{i,2,k} \times c_{d,2,k}}{v_{od,i,2,k}}$$

Equation 29-43

where

$dv_{u,i,k}$ = maximum discharge rate for upstream movement i for subperiod k (veh/h),

$c_{d,j,k}$ = capacity at the downstream intersection for movement j for subperiod k (veh/h), and

$fx_{i,2,k}$ = volume adjustment factor for origin i for subperiod k .

The factor fx is the ratio of two quantities. The numerator is the downstream through capacity that is available to the upstream through movement. The denominator is the volume entering the segment as a through movement and exiting as a through movement. The ratio is used to adjust the exiting turn movement and access point volumes so that they are reduced by the same proportion as is the volume for the exiting through movement.

The product $b_{i,j,k} \times c_{d,j,k}$ represents the maximum discharge rate for entry movement i that can be destined for exit movement j such that the origin-destination volume balance is maintained and the exit movement's capacity is not exceeded. It represents the allocation of a downstream movement's capacity to each of the upstream movements that use that capacity, where the allocation is proportional to the upstream movement's volume contribution to the downstream movement volume.

The capacity for the combined set of access points is unknown and is unlikely to be the source of spillback. Hence, this capacity is not considered in Equation 29-42.

The next task is to estimate the saturation flow rate adjustment factor for the movements at the upstream signalized intersection. The movements of interest are those entering the subject segment. The following equation is used for this purpose:

$$f_{sp,i,k,l} = \left(\frac{dv_{u,i,k}}{c_{u,i,k}} \right)^{0.5} \times f_{ms,i,k} \times f_{sp,i,k,l-1}$$

Equation 29-44

where

$f_{sp,i,k,l}$ = adjustment factor for spillback for upstream movement i for iteration l in subperiod k ,

$c_{u,i,k}$ = capacity at the upstream intersection for movement i for subperiod k (veh/h), and

$f_{ms,i,k}$ = adjustment factor for downstream lane blockage for movement i for subperiod k .

The adjustment factor is shown to have a subscript l indicating that the factor value is refined through an iterative process where the factor computed in a previous iteration is updated by using Equation 29-44.

In theory, the exponent associated with the ratio in parentheses should be 1.0. However, an exponent of 0.5 was found to provide for a smoother convergence to the correct factor value.

The procedure for calculating the adjustment factor for downstream lane blockage f_{ms} is described in Section 3 of Chapter 30, Urban Street Segments: Supplemental. This adjustment factor is incorporated into the spillback factor (as shown in Equation 29-44) for segments with spillback.

The last task of this step is to adjust the access point entry volumes. The following equation is used for this purpose. One factor is computed for each access point movement that departs from the access point and enters the direction of travel with spillback.

Equation 29-45

$$f_{ap,m,n,i,k,p} = (f_{x_{i,A,k}})^{0.5} \times f_{ap,m,n,i,k,p-1}$$

where $f_{ap,m,n,i,k,p}$ is the access point volume adjustment factor for movement i at access point n of site m for iteration p in subperiod k . The access point volume adjustment factors are used to adjust the volume entering the segment at each access point.

Step 7: Implement the Methodology to Evaluate the Remaining Time

The methodology is implemented in this step to evaluate each segment on the facility. The analysis period was set in Step 6 to equal the time remaining in the original analysis period. The saturation flow rate of each movement influenced by spillback is adjusted by using the factors quantified in Step 6.

Step 8: Compute the Queue Prediction Error

During this step, the predicted residual queue for each movement group is compared with the maximum queue storage. This distance is computed with the equations described in Step 5. Any difference between the predicted and maximum queues is considered a prediction error. If the sum of the absolute errors for all movements is not equal to a small value, the analysis returns to Step 6.

Step 9: Check the Total Time of Analysis

During this step, the total time of analysis $T_{total,k}$ is compared with the original analysis period T_o . If they are equal, the analysis continues with Step 10.

If the two times are not in agreement, the access point volumes are restored to their original value and then multiplied by the most current access point volume adjustment factor. The analysis then returns to Step 2.

Step 10: Compute the Performance Measure Summary

During this step, the average value of each performance measure is computed. The value is a representation of the average condition for the analysis period. For uniform delay at one intersection, it is computed with the following equation:

$$d_{1,i,j} = \frac{d_{1,agg,i,j,all}}{T_o \times v_{i,j}}$$

Equation 29-46

where

- $d_{1,i,j}$ = uniform delay for lane group j at intersection i (s/veh),
- $d_{1,agg,i,j,all}$ = aggregated uniform delay for lane group j at intersection i for all subperiods (s/veh),
- T_o = analysis period duration for the first subperiod (h), and
- $v_{i,j}$ = demand flow rate for lane group j at intersection i (veh/h).

A variation of Equation 29-46 is used to compute the average value for the other intersection performance measures of interest. The equations for computing the aggregated uniform delay are provided in the next subsection.

The following equation is used to compute the average running time for one site, where a site is one direction of travel on one segment:

$$t_{R,m} = \frac{t_{R,agg,m,all}}{\sum_{k=0}^n w_{thru,m,k}}$$

Equation 29-47

where

- $t_{R,m}$ = segment running time for site m (s),
- $t_{R,agg,m,all}$ = aggregated segment running time for site m for all n subperiods (s), and
- $w_{thru,m,k}$ = weighting factor for site m for subperiod k (veh).

A variation of Equation 29-47 is used to compute the average value for the other intersection performance measures of interest. The term in the denominator of Equation 29-47 equals the total through volume during the analysis period. The equations for computing the aggregated segment running time and weighting factor are provided in the next subsection.

PROCEDURE FOR SAVING PERFORMANCE MEASURES

The performance measures computed by using the methodology are saved at selected points within the spillback procedure. These measures correspond to a specific subperiod of the analysis period. Each measure is “saved” by accumulating its value for each subperiod. This sum is then used to compute an average performance measure value during the last step of the procedure.

The following equation is used to save the computed uniform delay for one intersection lane group. The computed delay represents a cumulative total time for the current and all previous subperiods.

Equation 29-48

$$d_{1,agg,i,j,k} = d_{1,agg,i,j,k-1} + d_{1,i,j,k} \times w_{i,j,k}$$

with

Equation 29-49

$$w_{i,j,k} = T \times v_{i,j,k}$$

where

$d_{1,agg,i,j,k}$ = aggregated uniform delay for lane group j at intersection i for subperiods 0 to k (s/veh),

$d_{1,i,j,k}$ = uniform delay for lane group j at intersection i for subperiod k (s/veh),

$w_{i,j,k}$ = weighting factor for lane group j at intersection i for subperiod k (veh), and

$v_{i,j,k}$ = demand flow rate for lane group j at intersection i for subperiod k (veh/h).

The weighting factor represents the number of vehicles arriving during the analysis period for the specified lane group.

A variation of Equation 29-48 is also used to compute the aggregated values of the following performance measures at each intersection:

- Incremental delay,
- Initial queue delay,
- Uniform stop rate,
- Incremental stop rate based on second-term back-of-queue size, and
- Initial queue stop rate based on third-term back-of-queue size.

The following equation is used to save the computed running time for one site, where a site is one direction of travel on one segment:

Equation 29-50

$$t_{R,agg,m,k} = t_{R,agg,m,k-1} + t_{R,m,k} \times w_{thru,m,k}$$

with

Equation 29-51

$$w_{thru,m,k} = T \times [v_{t,i,j,k} N_{t,i,j} + v_{sl,i,j,k} (1 - P_{L,i,j,k}) + v_{sr,i,j,k} (1 - P_{R,i,j,k})]$$

where

$t_{R,agg,m,k}$ = aggregated segment running time for site m for subperiods 0 to k (s),

$t_{R,m,k}$ = segment running time for site m for subperiod k (s),

$w_{thru,m,k}$ = weighting factor for site m for subperiod k (veh),

$v_{t,i,j,k}$ = demand flow rate in exclusive through lane group j at intersection i for subperiod k (veh/h/ln),

$N_{t,i,j}$ = number of lanes in exclusive through lane group j at intersection i (ln),

$v_{sl,i,j,k}$ = demand flow rate in shared left-turn and through lane group j at intersection i for subperiod k (veh/h),

$v_{sr,i,j,k}$ = demand flow rate in shared right-turn and through lane group j at intersection i for subperiod k (veh/h),

$P_{L,i,j,k}$ = proportion of left-turning vehicles in the shared lane group j at intersection i for subperiod k , and

$P_{R,i,j,k}$ = proportion of right-turning vehicles in the shared lane group j at intersection i for subperiod k .

When Equation 29-50 and Equation 29-51 are applied, the lane groups j and intersection i are located at the downstream end of the subject site m . The weighting factor represents the number of through vehicles arriving at the downstream intersection as a through movement during the analysis period.

A variation of Equation 29-50 is also used to compute the aggregated values of the following performance measures at each intersection:

- Through movement delay,
- Through movement stop rate,
- Travel time at free-flow speed, and
- Travel time at base free-flow speed.

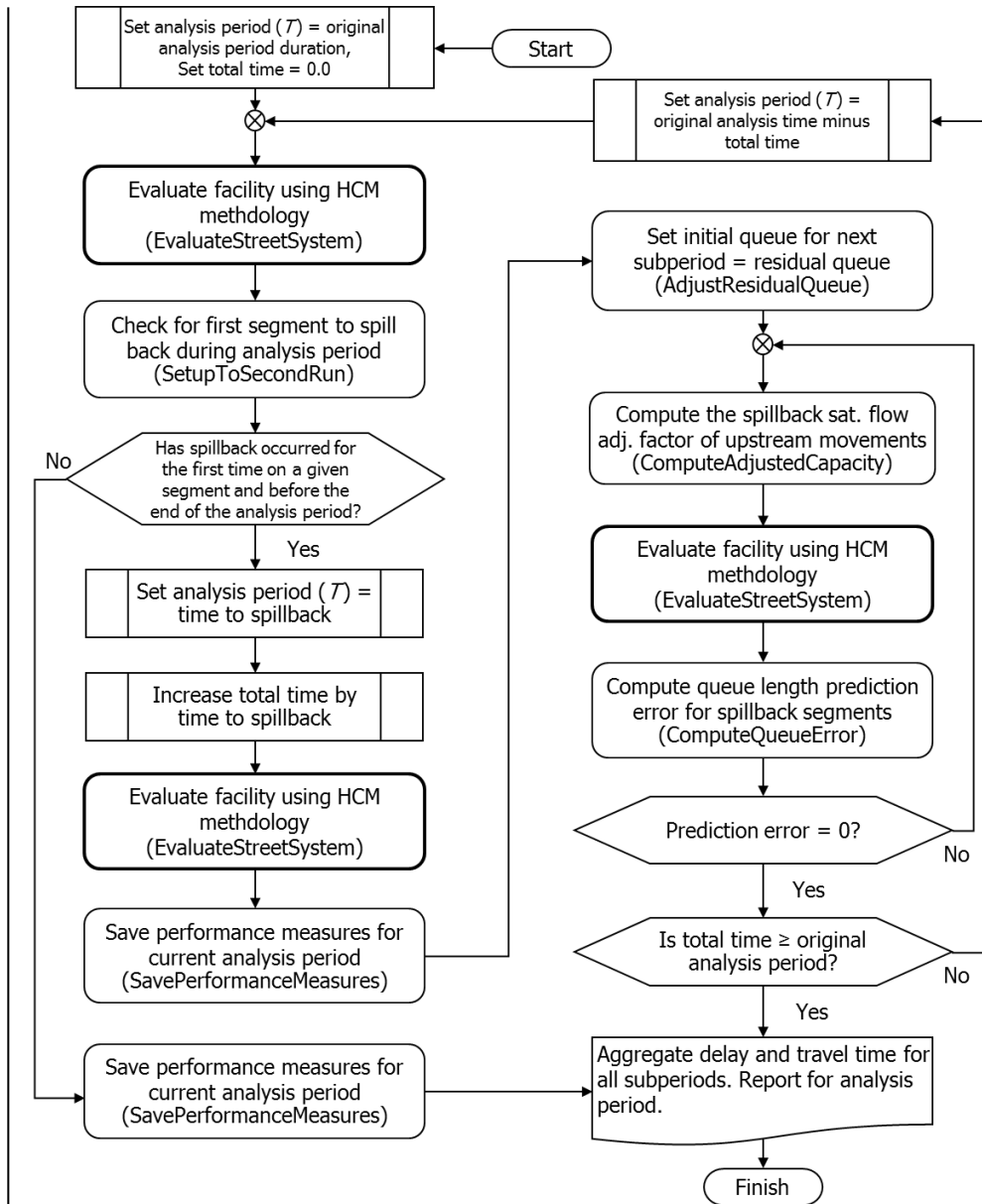
COMPUTATIONAL ENGINE DOCUMENTATION

This section describes the logic flow of the sustained spillback procedure. The description uses a flowchart and linkage list to document the procedure's implementation in the computational engine.

The sequence of calculations in the spillback methodology is shown in Exhibit 29-6. It consists of several routines and two loops, one of which is an iterative loop with a convergence criterion.

The urban street segments methodology is implemented at three separate points in the flowchart. Each point of implementation is indicated in the exhibit with a box that references the phrase "HCM methodology." The engine documentation of this methodology is provided in Section 7 of Chapter 30, Urban Street Segments: Supplemental.

Exhibit 29-6
Spillback Procedure Flowchart



A description of the logic flow is as follows. The urban street segments methodology is initially implemented and the presence of spillback is checked. If spillback does not occur, the results are reported and the process is concluded. If spillback occurs on a segment, a subperiod is defined and the urban street segments methodology is reimplemented by using an analysis period that is shortened to equal the time until spillback.

The iterative loop shown on the right side of the exhibit is called to quantify a saturation flow rate adjustment factor for each movement entering the segment with spillback. The value of this factor is determined to be that needed to limit the entry movement volume so that the residual queue on the segment does not exceed the available queue storage distance.

The main routines identified in Exhibit 29-6 are listed in Exhibit 29-7. The list provides more information about each routine’s function and the conditions for its use.

Routine	Description	Conditions for Use
SetupToSecondRun	Find first segment to spill back (that has not previously spilled back) and reset the analysis time to equal the controlling spillback time.	None
SavePerformanceMeasures	Save results from current evaluation with those from all prior subperiods (if any).	None
AdjustResidualQueue	Set initial queue of next subperiod to equal the residual queue from the current subperiod.	Apply to all intersections subjected to spillback in current subperiod.
ComputeAdjustedCapacity	Compute a saturation flow rate adjustment factor for all intersection and driveway movements subjected to spillback from a downstream intersection.	Apply to all intersections subjected to spillback in current subperiod.
ComputeQueueError	Compare predicted queue length with available storage length for each movement experiencing spillback. Compute queue error as the absolute value of the difference between the predicted and available lengths.	Apply to all segments experiencing spillback in current subperiod.

Exhibit 29-7
Sustained Spillback Module Routines

4. USE OF ALTERNATIVE TOOLS

This section presents examples using alternative traffic analysis tools that deal specifically with the limitations of the methodologies described in Chapters 16 to 22. Both deterministic and stochastic tools are used for this presentation. The focus is on the motorized vehicle mode because alternative tools are applied more frequently to deal with motorized vehicle traffic.

Several other chapters present examples covering the use of alternative tools to deal with the limitations of specific methodologies. These chapters are identified in the following list:

- Chapter 27, Freeway Weaving: Supplemental, presents a simulation example that demonstrates the detrimental effect of queue backup from an exit ramp signal on the operation of a freeway weaving section.
- Chapter 31, Signalized Intersections: Supplemental, presents simulation examples that demonstrate the effect of storage bay overflow, right-turn-on-red operation, short through lanes, and closely spaced intersections.
- Chapter 34, Interchange Ramp Terminals: Supplemental, presents a simulation example that demonstrates the effect of ramp-metering signals on the operation of a diamond interchange. Another simulation example examines the effect of the diamond interchange on the operation of a nearby intersection under two-way stop control.
- Chapter 36, Concepts: Supplemental, demonstrates the use of individual vehicle trajectory analysis to examine cyclical queuing characteristics and to assess queue spillover into an upstream segment.

The need to determine performance measures from an analysis of vehicle trajectories was emphasized in Chapter 7, Interpreting HCM and Alternative Tool Results, and Chapter 36, Concepts: Supplemental. Specific procedures for defining measures in terms of vehicle trajectories were proposed to guide the future development of alternative tools. Most of the examples presented in this section have applied existing versions of alternative tools and, therefore, do not reflect the proposed trajectory-based measures.

This section consists of three main subsections. The first describes the base urban street facility used in the examples presented in the other two subsections. The second describes the use of alternative tools for signal timing design and evaluation. The third demonstrates the use of alternative tools in addressing some of the limitations of the HCM methodologies.

BASIC EXAMPLE PROBLEM CONFIGURATION

The base configuration for the examples in this section is shown in Exhibit 29-8. Five signalized intersections are included with a spacing of 2,000 ft between the upstream stop lines of each intersection. Each intersection has the same layout, with two lanes for through and right-turn movements and one 150-ft-long left-turn bay.

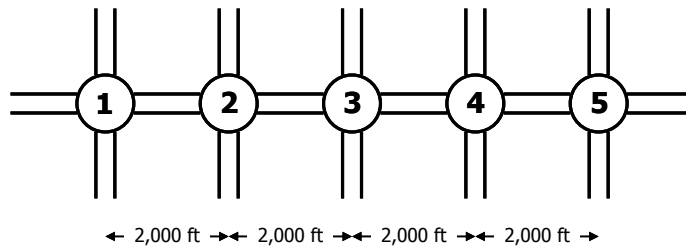


Exhibit 29-8
Base Configuration for the Examples

The phasing and demand flow rates for each intersection are shown in Exhibit 29-9. Leading protected phases are provided for all protected left turns. Intersections 1 and 5 have protected phases for all left turns. Intersections 2 and 4 have only permitted left turns. Intersection 3 has protected left turns on the major street and permitted left turns on the minor street.

Int. No.	Movement	Peak 15-min Adjusted Demand			Phasing Plan
		Left	Through	Right	
1	Major st.	120	800	80	
	Minor st.	120	600	80	
2	Major st.	80	800	120	
	Minor st.	80	600	120	
3	Major st.	120	800	80	
	Minor st.	80	600	120	
4	Major st.	80	800	120	
	Minor st.	80	600	120	
5	Major st.	120	800	80	
	Minor st.	120	600	80	

Exhibit 29-9
Demand Flow Rates and Phasing Plan for Each Intersection

To simplify the discussion, the examples will focus on design and analysis features that are beyond the stated limitations of the urban street analysis procedures contained in Chapters 16 through 22. For example, pretimed control will be assumed here because the ability to deal with traffic-actuated control is not a limitation of the Chapter 19 signalized intersection analysis methodology. For the same reason, the analysis of complex phasing schemes that fall within the scope of the Chapter 19 procedures (e.g., protected-permitted phasing) will be avoided. Parameters that influence the saturation flow rate (e.g., trucks, grade, lane width, parking) will not be considered here because they are accommodated in other chapters.

A symmetrical demand volume pattern will be used to facilitate interpretation of results. The demand volumes are assumed to be peak-hour adjusted. Fixed yellow-change and red-clearance intervals of 4 s and 1 s, respectively, will be assigned to all phases. Through-traffic phases and protected left-turn phases will be assigned minimum green times of 10 s and 8 s, respectively.

SIGNAL TIMING PLAN DESIGN

The methodologies in the HCM were developed to determine the performance of a roadway segment under specific conditions. In simple cases, the procedures may be applied in reverse for design purposes (e.g., determining the number of required lanes). In more complex situations requiring optimization of design parameters, the procedures must be applied iteratively within an external software structure. Some alternative tools provide this type of optimization structure and therefore offer a valuable extension of the HCM methodologies. The extent of HCM compatibility varies among tools.

Two deterministic optimization tools are applied in this section. Each tool is used to illustrate a different approach for producing the signal timing parameters required by the procedures of Chapters 18 and 19. This discussion is not intended as a comprehensive tutorial on signal timing plan design (STPD). A more detailed treatment of this subject is available (3), which serves as a comprehensive guide to traffic signal timing and includes a discussion of the use of deterministic optimization tools. It represents a synthesis of traffic signal timing concepts and their application and focuses on the use of detection, related timing parameters, and effects on users at the intersection.

Deterministic STPD Tools

Several deterministic plan design tools are available commercially. Each tool represents a comprehensive package with its own computational and interface features. A typical tool configuration is illustrated in Exhibit 29-10. The following elements are included in the configuration:

- The computational model, which performs the design, optimization, and analysis functions. Two components are included in the computational model. The first computes performance measures on the basis of specified input data and operating parameters. The second contains the optimization routines that seek a combination of operating parameters that will produce the best performance.
- The data input editor, which organizes and facilitates the entry of traffic data and operating parameters to be supplied to the computational model. The data input editor establishes the “look and feel” of each tool. The details vary considerably among tools. For example, some tools offer the ability to compute saturation flow rates internally by using procedures similar to those prescribed in Chapter 19, Signalized Intersections.

- Import/export features, which facilitate communication of datasets between other applications and devices. These features are intended to enhance the productivity of each tool.
- Direct links to other applications, such as microscopic simulation tools and fully HCM-compliant software.
- Graphic displays, which provide insight into time–space relationships, queuing, and platoon propagation.

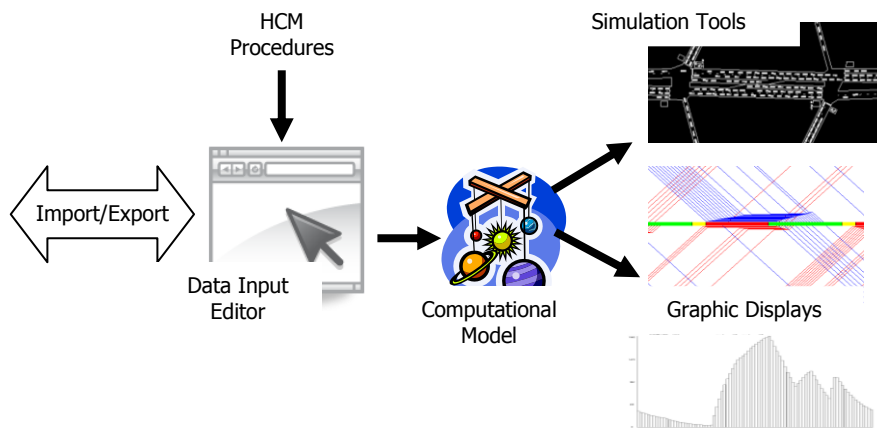


Exhibit 29-10
Elements of a Typical Signal
Timing Design Tool

The urban streets analysis procedures presented in the HCM deal with the operation of an urban street facility as a set of interconnected segments. Most of the commonly used STPD tools are configured to accommodate traffic control networks involving multiple intersecting routes. To simplify the discussion, the example presented here is limited to a single arterial route that will be analyzed as a system.

Two widely used STPD tools will be applied to this example to illustrate their features and to show how they can be used to supplement the urban street facilities analysis procedures prescribed in this manual. Both tools are commercially available software products. More information about these tools can be found elsewhere (4, 5). The discussion in this section deals with the combination of features available from both tools without reference to a specific tool.

Performance Measures

Both STPD tools deal with performance measures that are computed by the procedures prescribed in this manual in addition to performance measures that are beyond the scope of those procedures. The performance measures covered in Chapters 16 and 18 include delay, stops, average speed, and queue length. The discussion of those measures in this section will focus on their use in STPD and not on comparison of the values computed by different methods.

Several other measures beyond the scope of the HCM methodologies are commonly associated with signal timing plan design and evaluation. The following measures are derived from analysis of travel characteristics, including stops, delay, and queuing:

- *Fuel consumption* (gal/h), the amount of fuel consumed because of vehicle miles traveled, stops, and delay, as computed by a model specific to each tool;
- *Operating cost* (\$/h), the total cost of operation of all vehicles as computed by a model specific to each tool; and
- *Time jammed*, the percentage of time that the queue on a link has backed up beyond the link limit.

STPD tools also deal with a set of performance measures related to the quality of progression between intersections. These measures, all of which are outside of the HCM scope, have been defined in the literature or by developers of specific tools as follows:

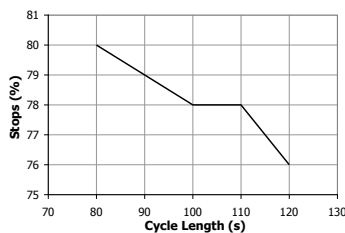
- *Bandwidth* is defined by the number of seconds during which vehicles traveling at the design speed will be able to progress through a set of intersections. *Link bandwidth* is the width of the progression band (in seconds) passing between adjacent intersections that define the link. *Arterial bandwidth* is the width of the progression band that travels the entire length of the arterial route.
- *Progression efficiency* is the ratio of the arterial bandwidth to the cycle length. It thus represents the proportion of the cycle that contains the arterial progression band. Suggested upper limits for “poor,” “fair,” and “good” progression are 0.12, 0.24, and 0.36, respectively (5). Values above 0.36 are characterized as “great” progression.
- *Progression attainability* is the ratio of the arterial bandwidth to the shortest green time for arterial through traffic on the route. By definition, the arterial progression band cannot be greater than the shortest green time. Therefore, an attainability of 100% indicates that further improvement is only possible through the provision of additional green time. The need for fine-tuning is suggested for attainability values between 70% and 99%, with major changes needed for values below 70% (5).
- *Progression opportunities (PROS)* are a measure of arterial progression quality that recognizes progression bands that are continuous between two or more consecutive links but do not travel the full length of the arterial. The number of PROS observed by a driver at any point in time and space is defined by the number of intersections that lie ahead within the progression band. The concept is based on the premise that driver perception of progression quality increases with the number of consecutive links that can be traversed within the progression band. The measure is accumulated in a manner similar to the score in a game of bowling, where success in one frame is passed on to the next frame to increase the total score if the success continues. More detailed information on the computation of PROS is available elsewhere (5).
- *Interference* is expressed as the percentage of time that an arterial through vehicle entering a link on the green signal and traveling at the design speed will be stopped at the next signal. This measure is arguably an indication of poor perceived progression quality (5).

- *Dilemma zone vehicles* indicates the number of vehicles arriving on the yellow interval. Thus, it offers a potential safety-related measure. The computational details are described elsewhere (4).
- The *coordinatability factor (CF)*, while it is not strictly a performance measure as defined in this manual, is a measure of the desirability of coordinating two intersections on the basis of several factors including intersection spacing, speeds, and platoon formation. It is expressed as a relative value between 0 and 100. This measure is described in more detail elsewhere (4), where it is suggested that values above 80 indicate a definite need for coordination.

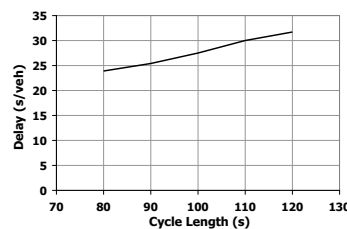
Initial Timing Plan Design

An initial timing plan design will first be performed by using one of the STPD tools. From the list of performance measures just discussed, fuel consumption will be chosen in this example as the performance measure for optimization. Other measures or combinations of measures could have been selected. No recommendation is implied in the selection of this particular measure. It serves this discussion because it supports an analysis of the trade-off between other measures such as stops and delay.

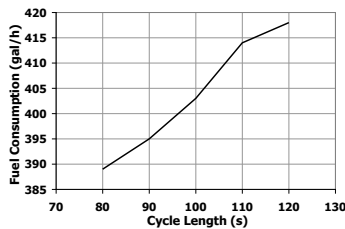
A cycle length within a specified range must be selected first. Minimum and maximum cycle lengths of 80 and 120 s, respectively, will be used. The cycle optimization results are presented in Exhibit 29-11, which shows the effect of the cycle length on delay, stops, and fuel consumption as computed by the STPD. While delay and stops move in opposite directions, their combined effect suggests that the minimum fuel consumption will be reached with an 80-s cycle. This is not surprising because it is generally recognized that the optimal cycle length for balanced progression is twice the link travel time at the design speed, which is $2 \times 34 = 68$ s for a 2,000-ft link at 40 mi/h. However, 68 s is below the minimum cycle length constraint. On the basis of these results, an 80-s cycle will be selected for optimization of the other timing plan parameters.



(a) Stops Optimization



(b) Delay Optimization



(c) Fuel Consumption Optimization

Exhibit 29-11
Cycle Length Optimization Results

The split and offset optimization was carried out next. The resulting timing plan is shown in Exhibit 29-12. This table represents the initial timing plan to be investigated and refined.

Exhibit 29-12
Timing Plan Developed by Split and Offset Optimization

Intersection	Offset	Phase 1	Phase 2	Phase 3	Phase 4	Total
1	0	13	29	13	25	80
2	34	45	35			80
3	3	13	33	34		80
4	31	45	35			80
5	78	13	29	13	25	80

Notes: All times are in seconds.
Offsets are referenced to the first arterial through-traffic phase.

Initial Timing Plan Performance

A summary of the performance measures for the initial timing plan is presented in Exhibit 29-13. Separate columns are included in this table for *route totals*, which include only the segments that make up the urban street facility as defined in Chapter 16, and *system totals*, which include the measures from the cross-street segments. Note that some of the performance measures reported in this table are also reported by the Chapter 16 methodology. While the STPD tool definitions and model structures are similar to the HCM (e.g., uniform and random components), no comparison of the values will be offered in this discussion because the focus is on the STPD and not on modeling differences.

Exhibit 29-13
Performance Measures for the Initial Timing Plan

Performance Measure	Units	System Totals	Route Totals
Total travel	veh-mi/h	4,927	3,063
Total travel time	veh-h/h	240	120
Uniform delay	veh-h/h	95	34
Random delay	veh-h/h	22	8
Total delay	veh-h/h	116	43
Average delay	s/veh	23.5	17.4
Passenger delay	p-h/h	140	51
Uniform stops	veh/h	12,893	5,576
Uniform stops	%	72	63
Random stops	veh/h	1,277	440
Random stops	%	7	5
Total stops	veh/h	14,171	6,016
Total stops	%	79	68
Links with $d/c > 1$		0	0
Links with queue overflow		0	0
Time jammed	%	0	0
Period length	s	900	900
System speed	mi/h	20.5	25.6
Fuel consumption	gal/h	387	195
Operating cost	\$/h	3,063	1,049

The initial timing plan design was based on minimizing fuel consumption as a performance measure. The signal progression characteristics of this design are also of interest. The progression characteristics will be examined in both numerical and graphics representations. The numbers are presented in Exhibit 29-14 and are based on the progression performance measures that were defined earlier. The interference values indicate the proportion of time that a vehicle entering a link in the progression band would be stopped at the next signal. The PROS are accumulated from progression bands that pass through some adjacent signals along the route. The low progression efficiency and attainability and

PROS values suggest that this design, while optimal in some respects, would not produce a very favorable motorist perception of progression quality.

Performance Measure	Westbound	Eastbound	Average
Bandwidth efficiency	10%	5%	8%
Progression attainability	28%	14%	21%
Interference	9%	10%	
PROS	30%	28%	29%

Adjustments to Improve Progression Quality

Because of the low quality of progression, it is logical to revisit the initial design with the objective of maximizing progression quality instead of minimizing fuel consumption. The same cycle length range (80 to 120 s) was used for this purpose, and the runs were repeated with the objective of maximizing PROS. The maximum value of PROS was obtained with the same cycle length and phase times as the initial design. The progression performance measures associated with this timing plan are shown in Exhibit 29-15. These measures do not differ substantially from the initial design, nor do the offsets. The total PROS value increased from 29% to 30%, but the performance was somewhat better balanced by direction. Thus, there is not a large trade-off between the objectives of maximizing performance and maximizing progression quality in this case.

A combination of factors peculiar to this example has led to the conclusion that the signal timing parameters for optimizing performance and progression are basically the same. The symmetry of the layout and phasing created a situation in which fuel consumption could be minimized by favoring either direction at the expense of the other. The balanced design was favored by the PROS optimization because it offered a minimal numerical advantage (30% versus 29%). One of the main reasons why both design approaches chose the lowest acceptable cycle length is that, as pointed out previously, the theoretical optimum cycle length was below the lowest acceptable cycle length.

Performance Measure	Westbound	Eastbound	Average
Bandwidth efficiency	8%	8%	8%
Attainability	21%	21%	21%
Interference	9%	9%	
PROS	30%	30%	30%

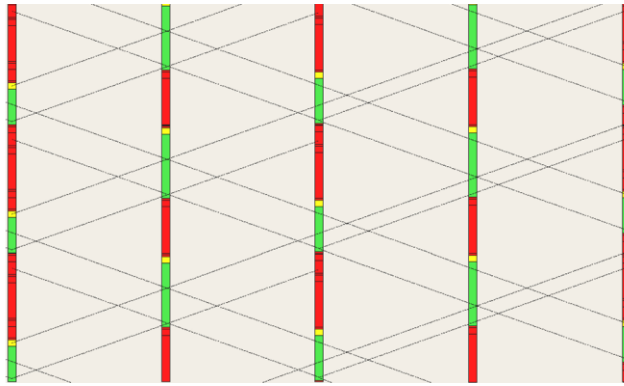
Time–Space Diagrams

STPD tools typically produce graphic displays depicting progression characteristics. The most common display is the time–space diagram, which is well documented in the literature and understood by all practitioners. The time–space diagram reflecting the initial design is shown in Exhibit 29-16. Note that, even though the traffic volumes are balanced in both directions, the design appears to favor the westbound (right-to-left) direction. Because of the symmetry of this example, a dual solution that yields the same performance but that favors the eastbound direction is likely to exist.

Exhibit 29-14
Progression Quality Measures for the Initial Design

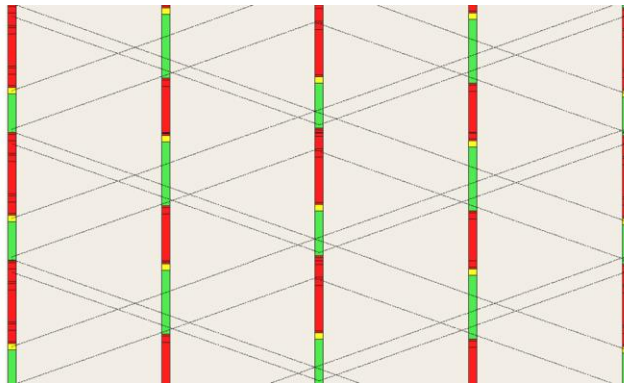
Exhibit 29-15
Progression Quality Measures for the Improved Progression Design

Exhibit 29-16
Time-Space Diagram for the Initial Design



The time-space diagram depicting the modified progression design is shown in Exhibit 29-17. This design shows a better balance between the eastbound and westbound directions. There is good progression into the system from both ends, but the band in both directions is halted at the center intersection. The PROS accumulation is evident in the bands that progress between some of the intersections.

Exhibit 29-17
Time-Space Diagram for the Modified Progression Design



The difference between the initial and modified designs appears to be minimal. The modified design will be chosen for further investigation because it offers a better balance between the two directions. The offset changes for this design are presented in Exhibit 29-18.

Exhibit 29-18
Offset Changes for the Modified Progression Design

Intersection	Initial Offsets	Revised Offsets
1	0	0
2	34	30
3	3	76
4	31	30
5	78	0

The time-space diagram for this operation from another STPD tool is shown in Exhibit 29-19. The timing plan is the same as the plan that was depicted in Exhibit 29-17, but the format of the display differs slightly. Both the link band and the arterial band as defined previously are shown on this display. The individual signal phases are also depicted. Both types of time-space diagrams offer a manual adjustment feature whereby the offsets may be changed by dragging the signal display back and forth on the monitor screen.

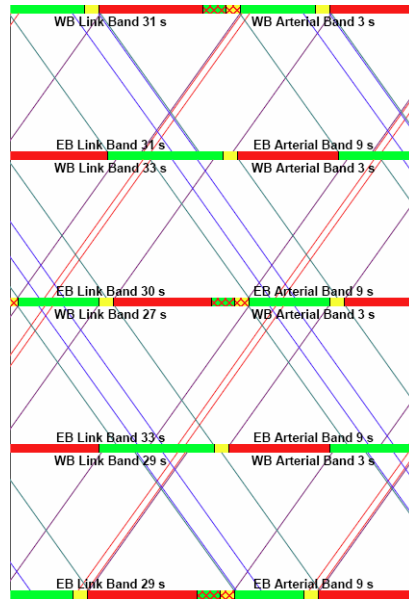


Exhibit 29-19
Alternative Time-Space
Diagram Format

Other Graphic Displays

Other graphics formats are not as ubiquitous as the time-space diagram but can provide useful insights into the operation at and between intersections.

Flow Profile Diagrams

One example is the flow profile diagram, which is simply a plot of the flow rate over one complete cycle. Flow profiles may be created to portray either the arrival or the departure flows at a stop line.

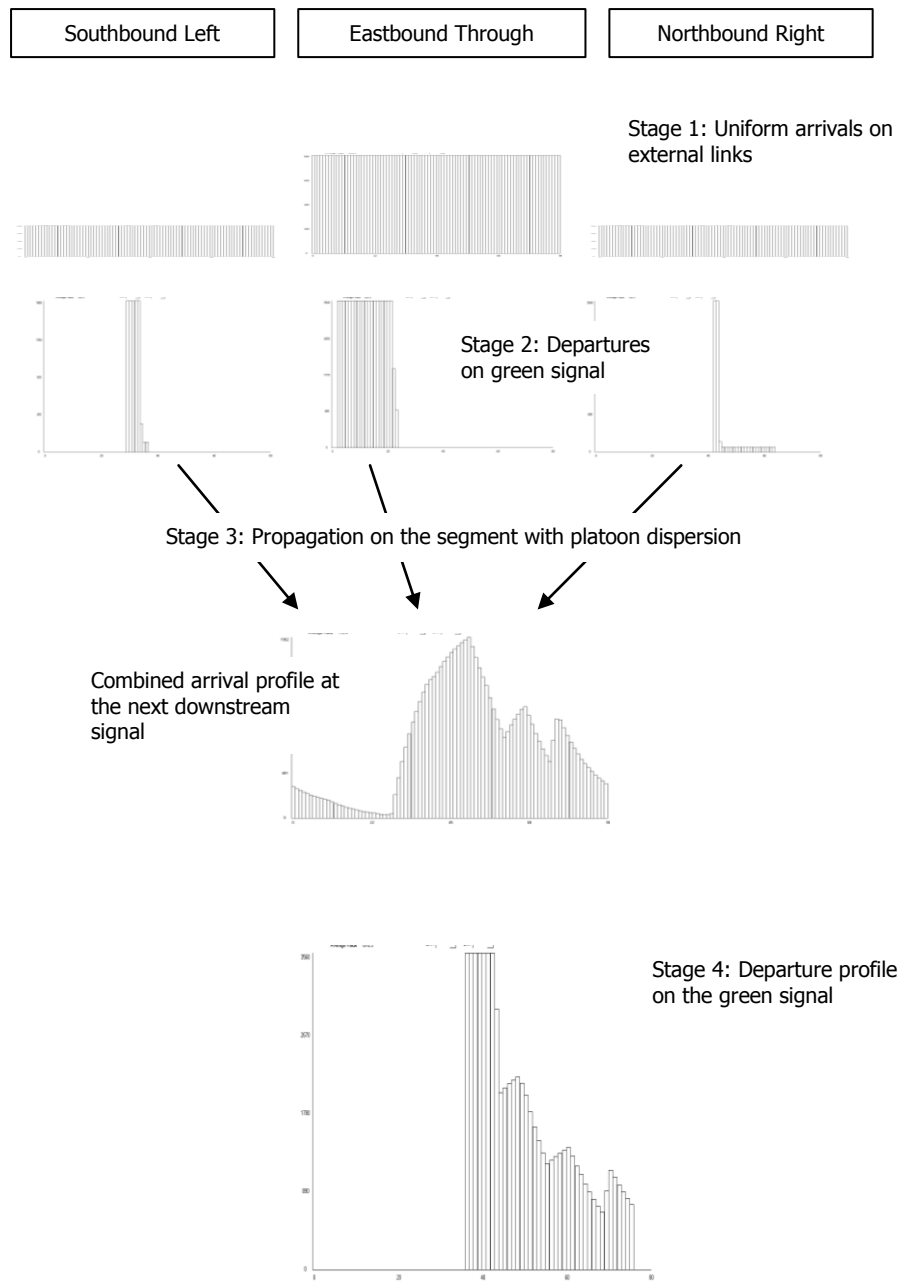
An example illustrating the use of flow profiles is presented in Exhibit 29-20. The eastbound segment between the first and second intersections is depicted in this example. The traffic inputs to this segment come from three independent movements at Intersection 1: southbound left, eastbound through, and northbound right.

Four stages of the progress of traffic into and out of this segment are depicted in the exhibit:

1. *Uniform arrivals on external links:* Each of the three movements entering the segment will arrive with a flow profile that is constant throughout the cycle because of the absence of platoon-forming phenomena on external links.
2. *Departures on the green signal:* Each movement proceeds on a different phase and therefore enters the link at a different time.
3. *Propagation on the segment with platoon dispersion:* Each of the three movements will be propagated downstream to the next signal by using a model that applies the design speed and incorporates platoon dispersion. Arrival of the platoons at the downstream end of the segment: The composite arrival profile is illustrated in the figure. The profile represents the sum of all of the movements entering the link.
4. *Departure on the green signal:* The platoons are regrouped at this point into a new flow profile because of the effect of the signal. The extent of

Exhibit 29-20
Example Illustrating the Use
of Flow Profiles

regrouping will depend on the proportion of time that the signal is green. If a continuous green signal were displayed, the output flow profile would match the input flow profile exactly.



The departure profile for this movement forms one input to the next link and is therefore equivalent to Stage 2 in the list above. The vehicles entering on different phases from the cross street must be added to this movement to form the input to the next segment as the process repeats itself throughout the facility.

The preceding description of the accumulation, discharge, and propagation characteristics of flow profiles is of special interest to this discussion because the same models used by the STPD tool have been adopted by the analysis

procedures given in Chapter 18, Urban Street Segments. These procedures are described by Exhibit 30-3 through Exhibit 30-5 in Chapter 30, Urban Street Segments: Supplemental. Therefore, the graphical representations given in Exhibit 29-20 should be useful in facilitating understanding of the procedures prescribed in Chapter 18.

Composite Flow Profiles

Another form of flow profile graphics is illustrated in Exhibit 29-21. This text-based display offers a composite view of the flow profiles by showing the arrival and departure graphics on the same figure represented by different characters. The uniform arrival pattern from the external link is evident at the upstream intersection, which corresponds to Stages 1 and 2 of Exhibit 29-20. The effect of the platooned arrivals is also evident at the downstream intersection, corresponding to Stages 4 and 5. More details on interpreting the composite flow profiles are given elsewhere (5).

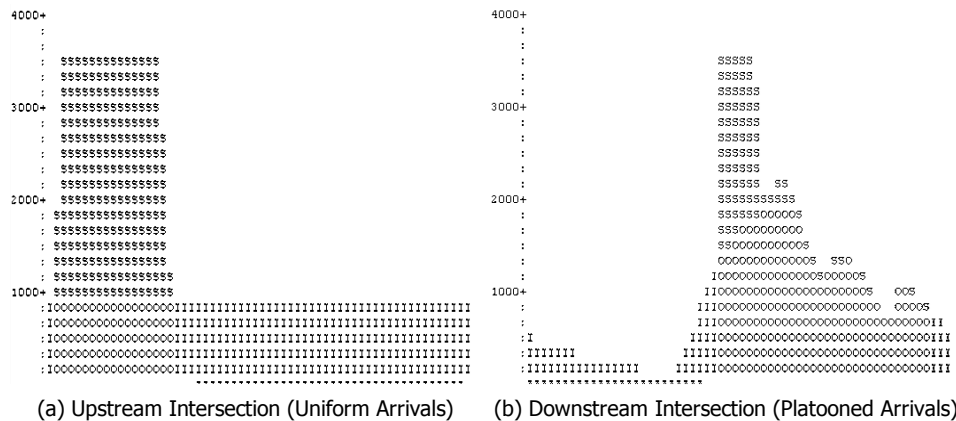


Exhibit 29-21
Composite Flow Profiles for the First Eastbound Segment

Queue Length Graphics

The accumulation and discharge of queues can also be represented graphically in a manner that is consistent with the analysis procedures of Chapters 16 through 19. An example of graphics depicting the queue length throughout the cycle is presented in Exhibit 29-22. The upstream signal shows the familiar triangular shape that is the basis of the uniform delay equation. The downstream signal shows the effect of platooned arrivals on the length of the queue.

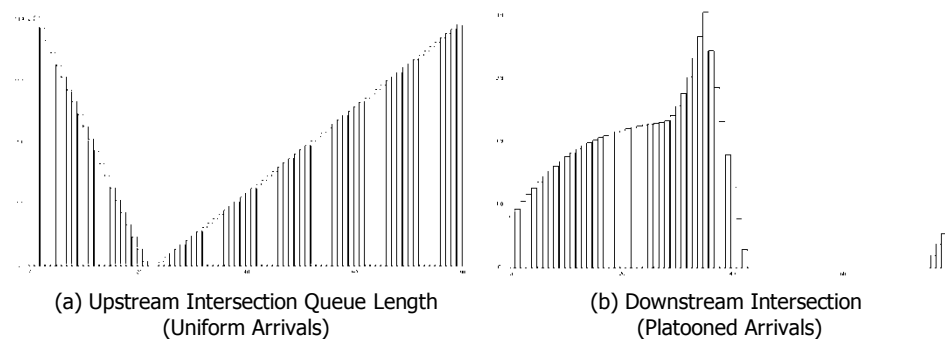
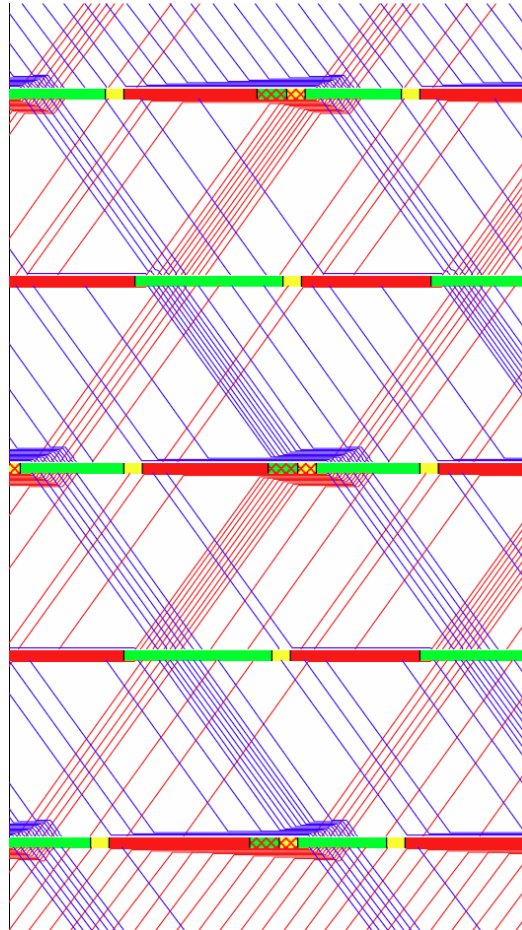


Exhibit 29-22
Variation of Queue Length Throughout the Signal Cycle for the First Eastbound Segment

Adding Flows and Queues to the Time–Space Diagram

One useful display superimposes the flow profiles and queuing characteristics on the time–space diagram to give a complete picture of the operation of the facility. An example of this display representing the improved progression design is presented in Exhibit 29-23. The flow rates are represented by the density of the lines progressing between intersections at the design speed. The queues are represented by horizontal lines upstream of each intersection. From this diagram, the effect of the design on queue accumulation and discharge and on the propagation of flows between intersections can be visualized.

Exhibit 29-23
Time–Space Diagram with
Flows and Queues



Potential Improvements from Phasing Optimization

The quality of progression in this example was improved from the initial design, but the results leave room for further improvement. For example, there are minimal arterial through bands. The current design was based on leading phases for all protected left turns. The operation might be improved by the application of lagging left-turn phases on some approaches. The procedures given in Chapter 18 are sensitive to the phase order. These procedures could be applied manually to seek a better operation. The use of STPD tools for this purpose will be demonstrated here because phasing optimization is internalized in the tools as a computational feature.

The phasing optimization process recommended changes at two of the five intersections. The phasing modifications are shown in Exhibit 29-24. Lead-lag phasing was applied at both intersections. As a result of the optimization, the arterial bandwidth increased from 6 to 16 s in both directions. The total signal delay decreased from 220 to 200 s/veh. The arterial speed increased from 22.1 to 23.0 mi/h. Thus, the phasing optimization would improve both the progression quality and the operational performance of the route. The progression quality improvement is evident in the time-space diagram presented in Exhibit 29-25.

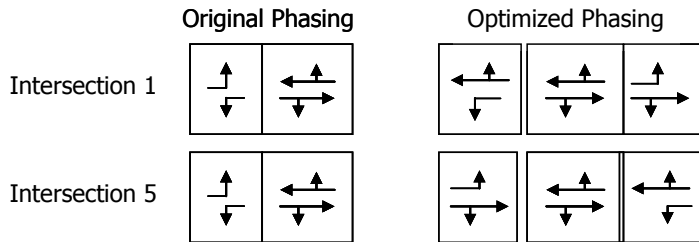


Exhibit 29-24
Optimized Phasing
Modifications

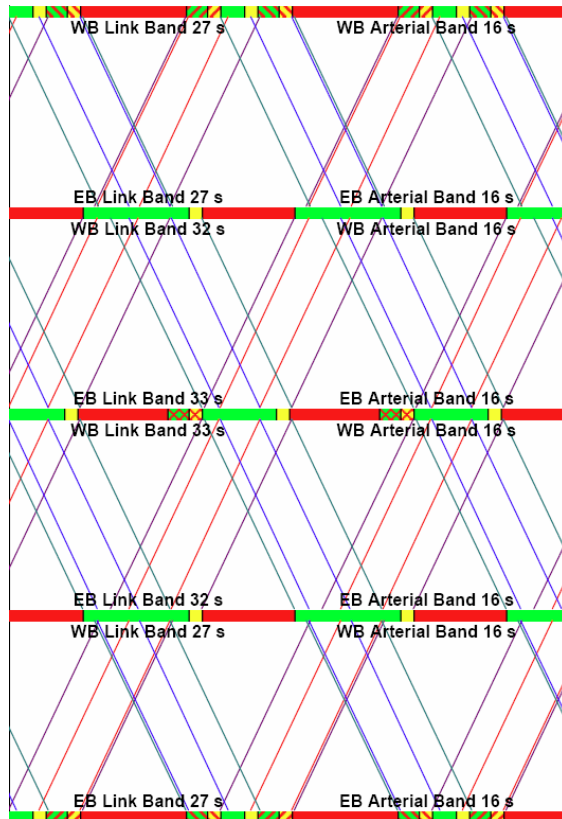


Exhibit 29-25
Time-Space Diagram for the
Optimized Phasing Plan

The decision to implement lead-lag phasing involves many factors including safety and local preferences. This discussion has been limited to a demonstration of how STPD tools can be used in the assessment of the operational effects of phasing optimization as one input to the decision process. The suggested modifications will not be implemented in the balance of the examples.

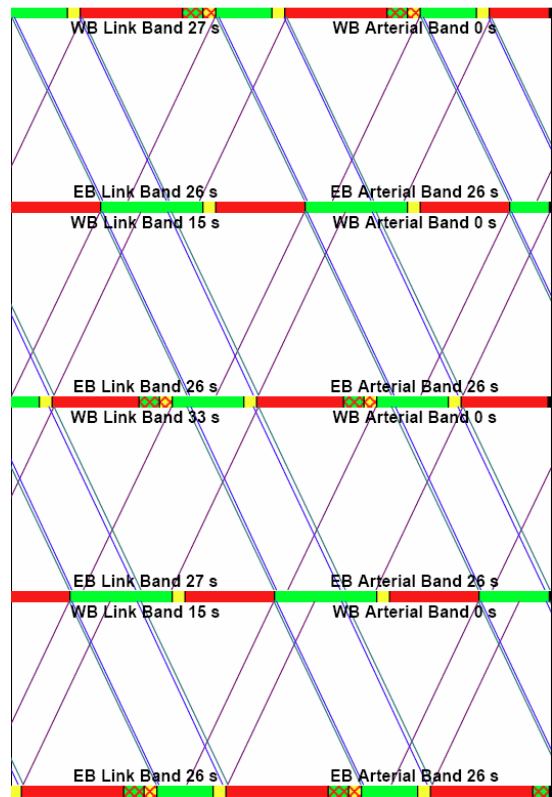
DEMONSTRATION OF ALTERNATIVE TOOL APPLICATIONS

Effect of Midsegment Parking Activities

The HCM methodology in Chapter 18 recognizes midsegment activities such as cross-street entry between signals and access point density. A procedure is provided in the methodology for estimating the delay due to vehicles turning left or right into an access point approach. However, no procedures are included for estimating the delay or stops due to other causes such as pedestrian interference and parking maneuvers. Alternative tools must be used to assess these effects.

This section will demonstrate the use of a typical microscopic simulation tool (6) to assess the effects of midsegment parking maneuvers on the performance of an urban street facility. The signal timing plan example from the previous section will be used for this purpose. The offsets will be modified first to create “ideal” progression in the eastbound direction at the expense of the westbound flow. The investigation will focus on the eastbound flow. The offsets and time–space diagram depicting this operation are shown in Exhibit 29-26. Offset 1 is referenced to the first phase for arterial through movements. Offset 2 is referenced to Phase 1. Their values will differ because of leading left-turn phases at some intersections. Different tools require different offset references.

Exhibit 29-26
Time–Space Diagram Showing
Ideal Eastbound Progression



Signal	Offset 1	Offset 2
1	0	0
2	35	47
3	63	68
4	23	35
5	57	56

The treatment of parking maneuvers by the selected simulation tool is described in the tool’s user guide (6). The following parameters must be supplied for each segment that contains on-street parking spaces:

- Beginning of the parking area with respect to the downstream end of the segment,

- Length of the parking area,
- Mean duration of a parking maneuver, and
- Mean frequency of parking maneuvers.

The occurrence and duration of parking maneuvers are randomized around their specified mean values. The parameters that will be used in this example are shown in Exhibit 29-27.

Parameter	Value
Beginning of the parking area	200 ft from the downstream intersection
Length of the parking area	1,600 ft (leaving 200 ft to the upstream intersection)
Mean duration of a parking maneuver	30 s
Mean frequency of parking maneuvers	0 veh/h (no parking maneuvers) 60 veh/h 120 veh/h 180 veh/h 240 veh/h Represents a range of approximately 15 min to 60 min average parking duration

Exhibit 29-27
Parameters for the Parking Example

The simulation runs covered 80 cycles of operation. Separate runs were made for each level of parking frequency. The default simulation parameters of the selected tool were used.

The effect of the parking activity on travel time and delay is presented in Exhibit 29-28, which shows the total travel time for the facility as well as the two delay components of travel time (total delay and control delay). Each of the values represents the sum of the individual segment values. The graphs demonstrate that all of the relationships were more or less linear with respect to the parking activity level.

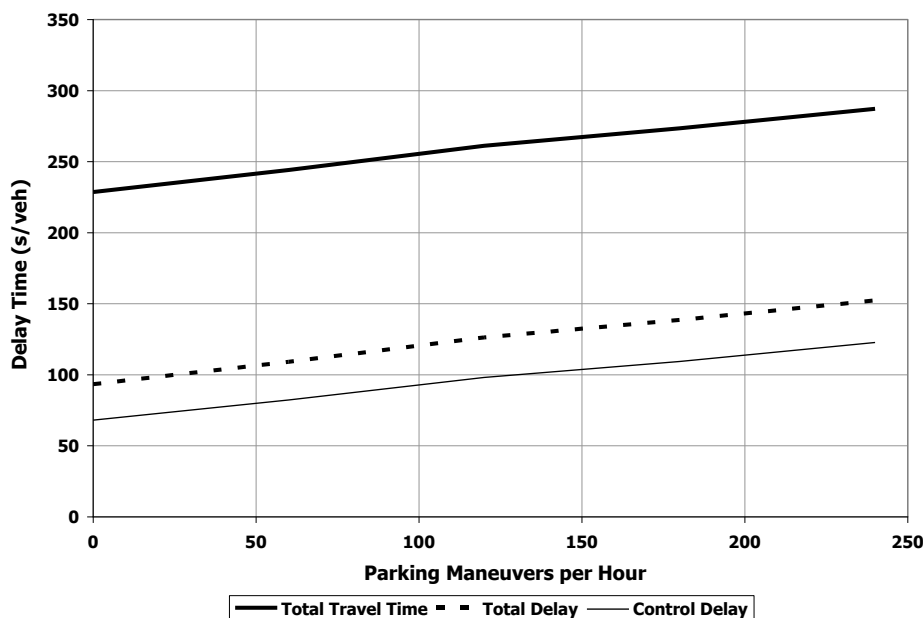
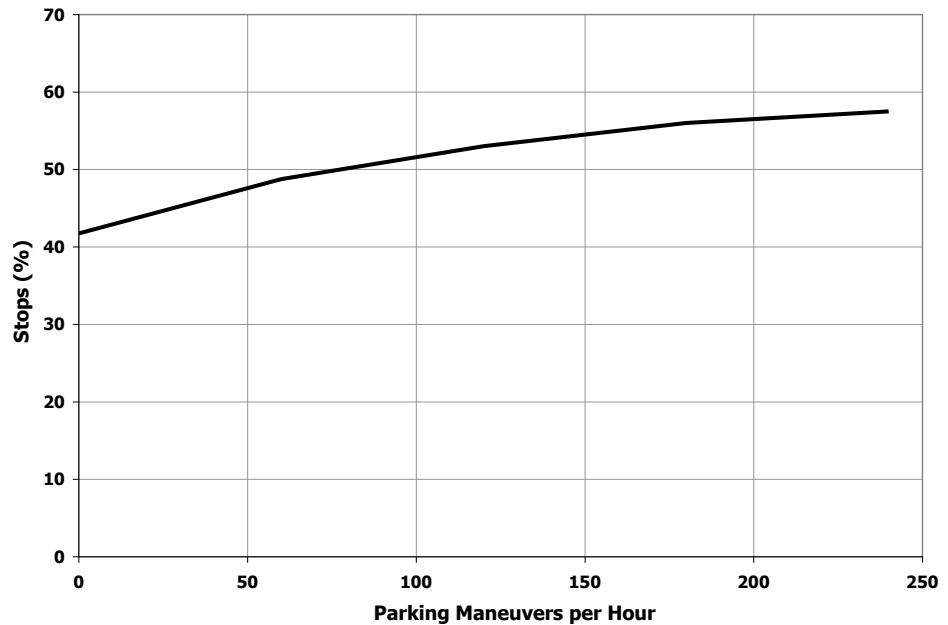


Exhibit 29-28
Effect of Parking Activity Level on Travel Time and Delay

Exhibit 29-29
Effect of Parking Activity Level
on the Percentage of Stops

The effect of the parking activity on stops is presented in Exhibit 29-29. For this example, the average percentage of stops for all eastbound vehicles increased from slightly more than 40% to slightly less than 60% throughout the range of parking activity levels. Both of these exhibits indicate that the simulation tool was able to extend the capability for analysis of urban street facilities beyond the stated limitations of the methodology presented in Chapter 16.



Effect of Platooned Arrivals at a Roundabout

Chapter 22, Roundabouts, describes a methodology for analyzing the operation of an isolated roundabout. Section 9 of Chapter 30, Urban Street Segments: Supplemental, describes a methodology for analyzing the operation of street segments bounded by roundabouts. Neither methodology explicitly accounts for the effect that platooned arrivals from a signal may have on roundabout operational performance. Therefore, the analysis of a roundabout as a part of a coordinated traffic control system is likely better accomplished with alternative tools. The alternative deterministic tools described earlier in this section do not deal explicitly with roundabouts in coordinated systems. Most simulation tools offer some roundabout modeling capability, although the level of modeling detail varies among tools.

This subsection describes the use of a typical simulation tool (7) in analyzing a roundabout within the arterial configuration of the previous example in this section. For this purpose, Intersection 3 at the center of the system will be converted to a roundabout with two lanes on each approach. To simplify the discussion, a basic symmetrical configuration will be used, because the discussion will be limited to the effect of platooned arrivals on the operation. The design aspects of roundabouts are covered in Chapter 22, Roundabouts, with more details provided in Chapter 33, Roundabouts: Supplemental, and elsewhere (8). The default traffic modeling parameters of the simulation tool will be applied. The roundabout configuration is shown schematically in Exhibit 29-30.

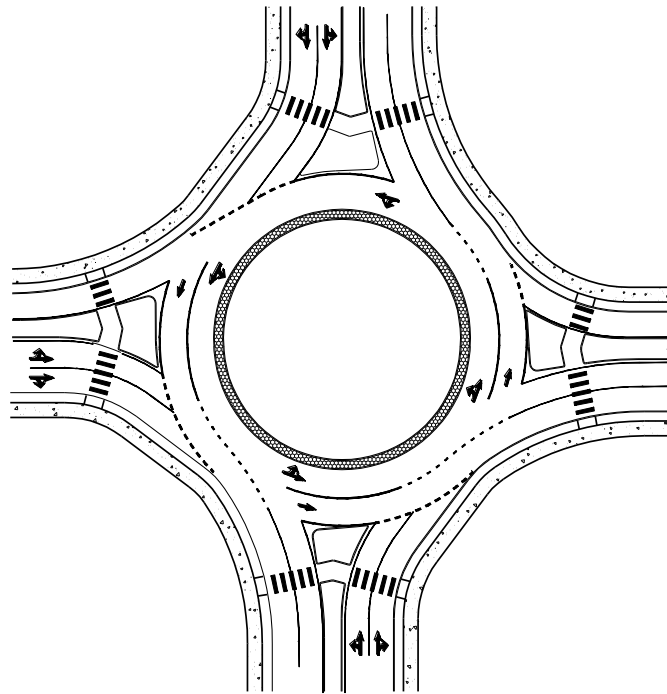


Exhibit 29-30
Roundabout Configuration for
Intersection 3

This example will examine two STPDs that create substantially different platoon arrival characteristics on the arterial approaches to the roundabout. The time-space diagrams representing the two designs are shown in Exhibit 29-31. The first design provides simultaneous arrival of the arterial platoons from both directions. The second creates a situation in which one platoon will arrive in the first half of the cycle and the other will arrive during the second half. The two cases will be described as “simultaneous” and “alternating” platoon arrivals.

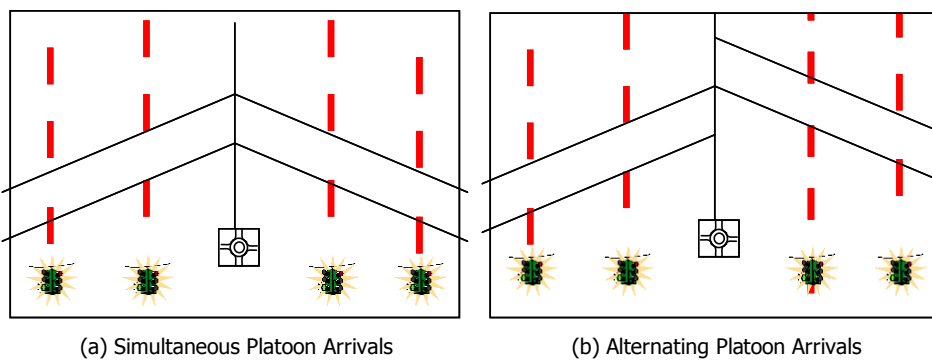


Exhibit 29-31
Time-Space Diagrams
Showing Simultaneous and
Alternating Platoon Arrivals at
the Roundabout

The platoon arrival characteristics can only be expected to influence the operation of a roundabout with relatively free-flowing traffic. While a two-lane roundabout could accommodate the demand volumes used in the previous examples in which the intersection was signalized, the initial simulation runs indicated enough queuing on all approaches to obscure the effect of the progression design. Since the focus of this example is on the effect of the adjacent signal timing plan, the demand volumes on the cross-street approaches to the roundabout will be reduced by 100 veh/h (approximately 17%) to provide a better demonstration of that effect.

Exhibit 29-32
Performance Comparison for Simultaneous and Alternating Platoon Arrivals at a Roundabout

Ten simulation runs were performed for both progression designs, and the average values of the performance measures were used to compare the two designs. The performance measures illustrated in Exhibit 29-32 include delay and stops on all approaches to the roundabout and travel times on individual link segments and on the route as a whole.

Movement	Alternating	Simultaneous	Difference	Percent
<i>Delay</i>				
Major-street approaches	15.81	14.18	1.64	10.34
Minor-street approaches	19.36	19.88	-0.52	-2.69
<i>Stops</i>				
Major-street approaches	0.59	0.52	0.08	12.71
Minor-street approaches	0.88	0.89	-0.01	-0.57
<i>Average Travel Times</i>				
Through vehicles traveling the full route	250.60	237.74	12.86	5.13
Approach links	58.06	56.30	1.76	3.03
Exit links	50.76	45.66	5.10	10.05

As a general observation, the simultaneous design performed noticeably better than did the alternating design on the major street, with a slight degradation to the cross-street performance. Travel times for vehicles traveling the full length of the facility were improved by about 5%. Travel times on the arterial segments entering and leaving the roundabout were improved by 3% and 10%, respectively.

This example has demonstrated that the simulation tool was able to describe the effect of two signal progression schemes on the performance of a roundabout within a coordinated arterial signal system. The next example will deal with the same basic arterial layout except that the roundabout will be replaced by a two-way STOP-controlled (TWSC) intersection. The platoon arrival types can be expected to have a greater influence on the TWSC operation than the roundabout because the effect is much more direct. Major-street vehicles always have the right-of-way over minor-street vehicles. Simultaneous platoons arriving from both directions will provide more opportunity for gaps in the major-street flow. Alternating platoons will keep major-street vehicles in the intersection for a greater proportion of time, thereby restricting cross-street access.

The effect at a roundabout is much more subtle because minor-street vehicles have the right-of-way over major-street vehicles once they have entered the roundabout. With simultaneous arrivals, platoons from opposite directions assist each other by keeping the minor-street vehicles from entering and seizing control of the roadway. When there is no traffic from the opposite direction, as in the case of alternating arrivals, a major-street movement is more likely to encounter minor-street vehicles within the roundabout. This phenomenon explains the 10% improvement in performance for simultaneous arrivals in the roundabout example as indicated in Exhibit 29-32.

Queue Length Analysis Based on Vehicle Trajectories

The HCM's segment-based chapters provide deterministic procedures for estimating the extent of queue backup on either signalized or unsignalized approaches. Most of the procedures are sensitive to some degree to platoon formation from adjacent signals. Most provide estimates of the average back of queue (BOQ) and the expected BOQ at some level of probability.

One additional queuing measure that can be derived from simulation is the proportion of time that the BOQ might be expected to extend beyond a specified point. This measure can be obtained directly from the analysis of individual vehicle trajectories by using the procedures set forth in Chapter 7, Interpreting HCM and Alternative Tool Results, and Chapter 36, Concepts: Supplemental. Those procedures will be applied in this example to examine the queuing characteristics on the minor-street approach to a TWSC intersection operating within a signalized arterial system. The criteria and procedures prescribed in Chapter 36 for identifying the onset and release from the queued state will be used.

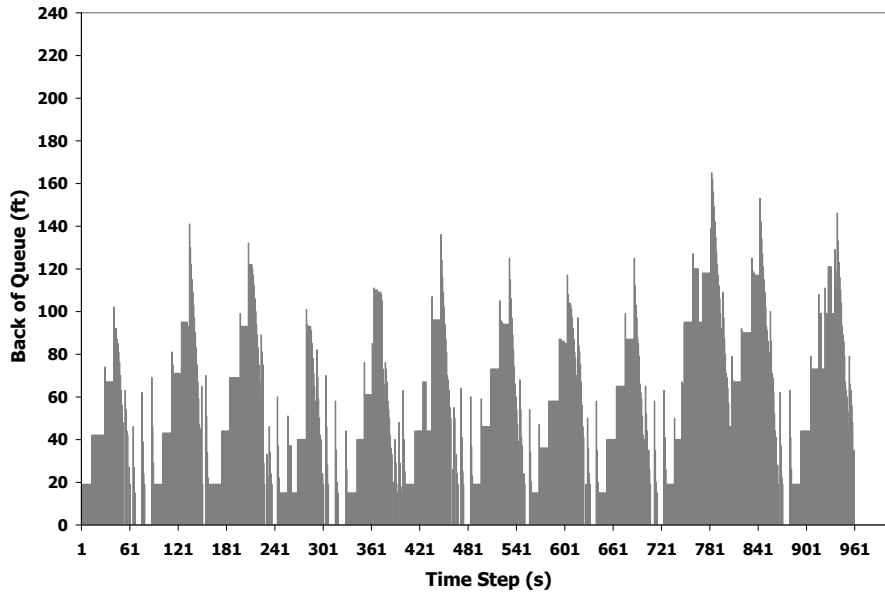
The same urban street configuration will be used for this purpose. The center intersection that was converted to a roundabout in the previous example will now be converted to TWSC. Because of the unique characteristics of TWSC, a few changes will have to be made to the configuration. TWSC capacities are lower than those of signals or roundabouts, so the minor-street demand volumes will have to be reduced. The two-lane approaches will be preserved, but the additional left-turn bay will be eliminated. The same two platoon arrival configurations (simultaneous and alternating) will be examined to determine their effect on the minor-street queuing characteristics. The signal timing plans from the roundabout example, as illustrated in Exhibit 29-31, will also be used here. Twelve cycles covering 960 s will be simulated for each case to be examined, and the individual vehicle trajectories will be recorded.

Queuing Characteristics

The first part of this example will demonstrate TWSC operation with an idealized scenario to provide a starting point for more practical examples. Two intersecting streams of through movements with completely uniform characteristics will be simulated. As many of the stochastic features of the simulation model as possible will be disabled. This is a highly theoretical situation with no real practical applications in the field. Its purpose is to provide a baseline for comparison.

The formation of queues under these conditions is illustrated in Exhibit 29-33, which shows the instantaneous BOQ for all time steps in the simulation. The cross-street entry volume was 600 veh/h in each direction, representing approximately the capacity of the approach. The cyclical operation is evident here, with 12 discernible cycles observed. Each cycle has a similar appearance. The differences among cycles are due to embedded stochastic features that could not be disabled.

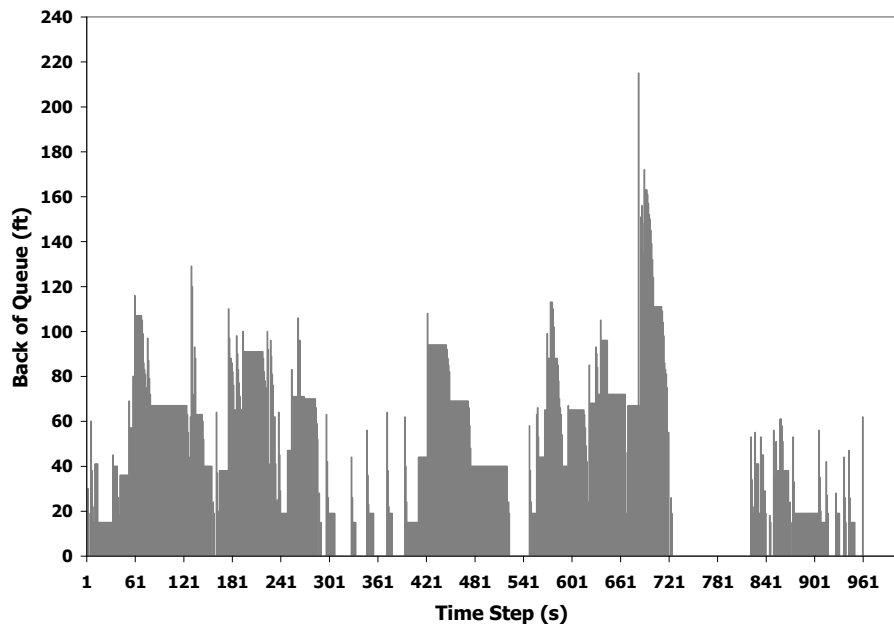
Exhibit 29-33
Queuing Results for the
Theoretical Example



The signal timing plan with simultaneous platoon arrivals should produce the most cyclical operation that could actually be observed in the field. This configuration was simulated by loading the minor street to near capacity levels as determined experimentally. The entry volume was 350 veh/h.

The queuing results are shown in Exhibit 29-34. Some cyclical characteristics are still evident here, but they are considerably diminished from the idealized case. The loss of cyclical characteristics results from cross-street turning movements entering the segments at their upstream intersections and from the general stochastic nature of simulation modeling.

Exhibit 29-34
Queuing Results for
Simultaneous Platoons



The operation was simulated next with alternating platoon arrivals. Again the demand volumes were set to the experimentally determined approach capacity, which was 270 veh/h, or about 25% lower than the capacity with simultaneous platoons. The results are presented in Exhibit 29-35. Some further loss of cyclical properties due to the spreading of entry opportunities across a greater proportion of the cycle is observed here.

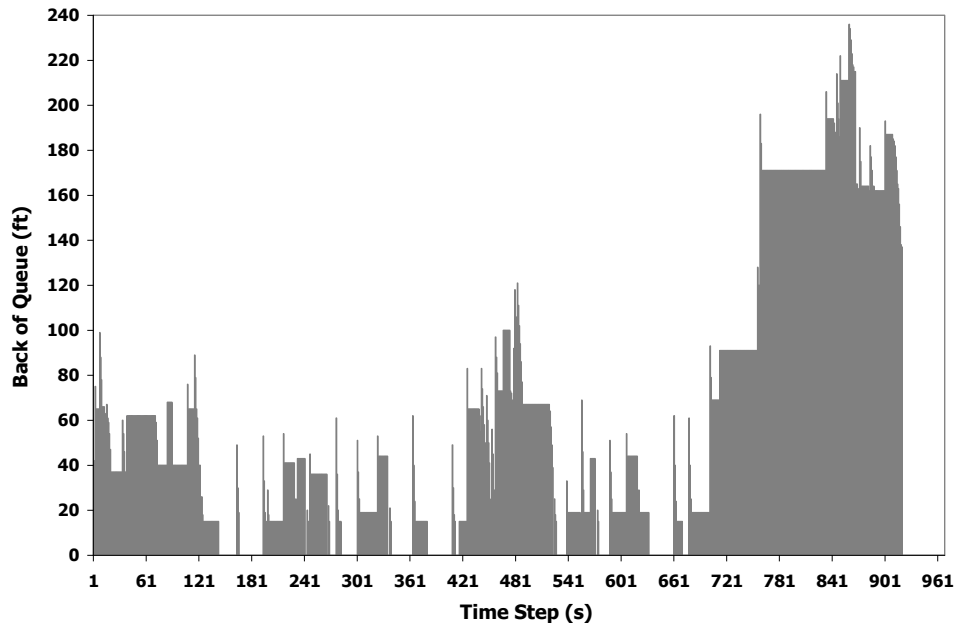
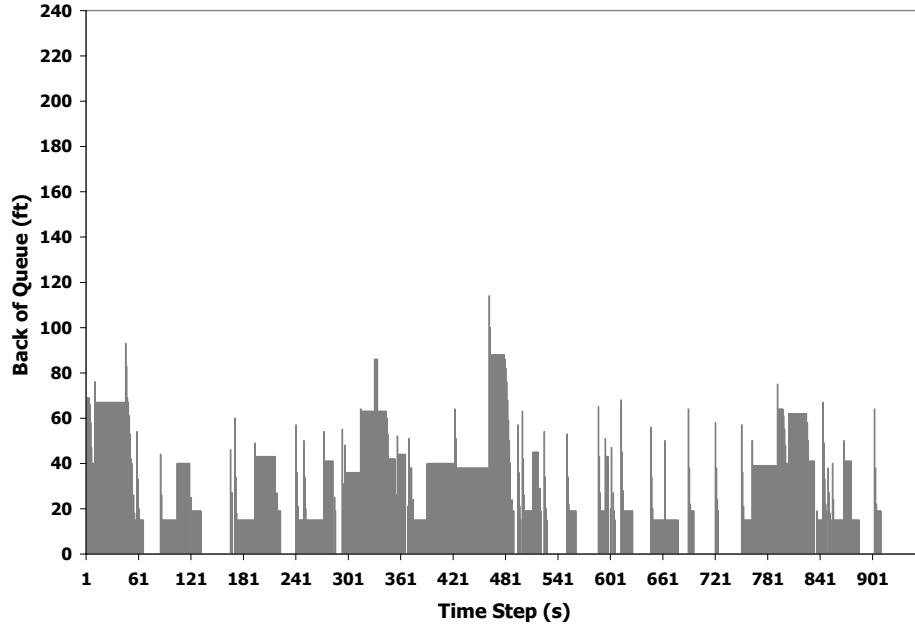


Exhibit 29-35
Queuing Results for
Alternating Platoons

The least cyclical characteristics would be expected from simulation of a completely isolated operation. The 2,000-ft link lengths were retained for this case, but no adjacent intersections existed. All other parameters remained the same, including the entry volume because the entry capacity for isolated operation was found to be the same as the case with alternating platoons.

The results are presented in Exhibit 29-36. There are no cyclical characteristics here because there is no underlying cycle in the operation. Also, even with the same entry volume as the alternating platoon case, the peak BOQs are much lower. This is because the entry opportunities are distributed randomly in time instead of being concentrated at specific points in the cycle.

Exhibit 29-36
 Queuing Results for Isolated
 TWSC Operation



Back-of-Queue Assessment

The discussion to this point has focused on instantaneous BOQs in an effort to understand the general nature of queuing under the conditions that were examined. With knowledge of the instantaneous BOQ values available from simulation, useful performance measures related to queuing can be produced from simulation. One such measure is the proportion of time that a queue would be expected to back up beyond a specified point. This concept is different from the probability of backup to that point normally associated with deterministic tools. The balance of the discussion will deal with the proportion of time with queue backup (PTQB) beyond a specified point.

The three cases examined in this example were simulated with cross-street demand volumes of 80, 160, 240, 320, and 400 veh/h, and the PTQB characteristics were determined by simulation for each case. The results were plotted for a specified distance of 100 ft from the stop line as shown in Exhibit 29-37. Each case is represented by a separate line that shows the percentage of time that the queue would be expected to back up beyond 100 ft from the stop line for each cross-street entry volume level. The simultaneous platoon case showed the lowest BOQ levels, starting with no time with BOQ beyond 100 ft below 240 veh/h, and reached a value of nearly 90% of the time at the maximum volume of 400 veh/h. Predictably, the isolated case was the most susceptible to queue backup, and the alternating platoon case fell somewhere in between.

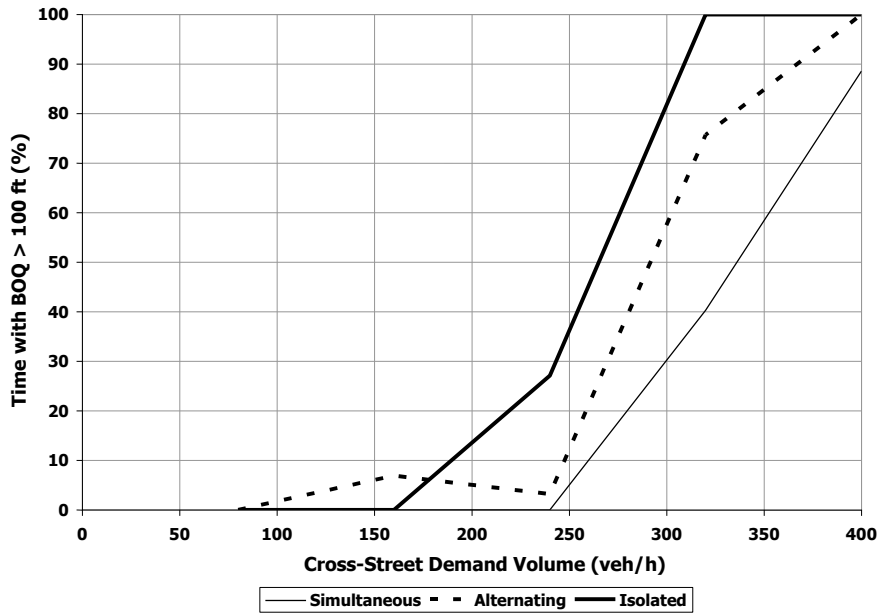


Exhibit 29-37
 Effect of Cross-Street Demand Volume on Queue Backup Beyond 100 ft from the Stop Line

This example has demonstrated the use of simulation to produce potentially useful queuing measures based on the analysis of individual vehicle trajectories. It has also demonstrated how simulation can be used to assess the queuing characteristics of a minor-street approach to a TWSC intersection operating in a coordinated signal environment.

5. EXAMPLE PROBLEMS

This section describes the application of the motorized vehicle, pedestrian, bicycle, and transit methodologies through a series of example problems. Exhibit 29-38 provides an overview of these problems. The focus of the examples is to illustrate the multimodal facility evaluation process. An operational analysis level is used for all examples. The planning and preliminary engineering analysis level is identical to the operational analysis level in terms of the calculations except that default values are used when field-measured values are not available.

Exhibit 29-38
Example Problems

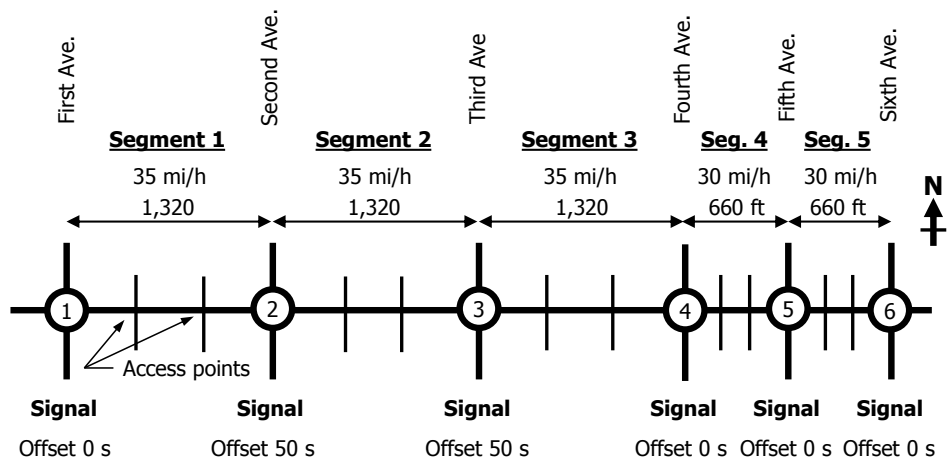
Problem Number	Description	Analysis Level
1	Automobile-oriented urban street	Operational
2	Widen the sidewalks and add bicycle lanes on both sides of facility	Operational
3	Widen the sidewalks and add parking on both sides of facility	Operational
4	Urban street reliability under existing conditions	Operational
5	Urban street reliability strategy evaluation	Planning

EXAMPLE PROBLEM 1: AUTOMOBILE-ORIENTED URBAN STREET

The Urban Street Facility

A 1-mi urban street facility is shown in Exhibit 29-39. It is located in a downtown area and oriented in an east–west travel direction. The facility consists of five segments with a signalized boundary intersection for each segment. Segments 1, 2, and 3 are 1,320 ft long and have a speed limit of 35 mi/h. Segments 4 and 5 are 660 ft long and have a speed limit of 30 mi/h. Each segment has two active access point intersections.

Exhibit 29-39
Example Problem 1: Urban Street Schematic



Segments 1, 2, and 3 pass through a mixture of office and strip commercial. Segments 4 and 5 are in a built-up shopping area.

The geometry of the typical street segment is shown in Exhibit 29-40. It is the same for each segment. The street has a curbed, four-lane cross section with two lanes in each direction. There is a 1.5-ft curb-and-gutter section on each side of the street. There are 200-ft left-turn bays on each approach to each signalized intersection. Right-turn vehicles share the outside lane with through vehicles on each intersection approach. A 6-ft sidewalk is provided on each side of the street

adjacent to the curb. No fixed objects are located along the outside of the sidewalk. Midsegment pedestrian crossings are legal. No bicycle lanes are provided on the facility or its cross streets. No parking is allowed along the street.

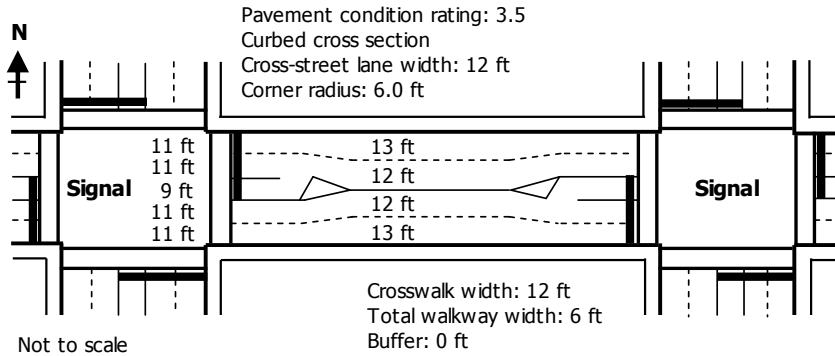


Exhibit 29-40
 Example Problem 1: Segment Geometry

The Question

What are the travel speed and level of service (LOS) of the motorized vehicle, pedestrian, bicycle, and transit modes in both directions of travel along the facility?

The Facts

The traffic counts for one segment are shown in Exhibit 29-41. The counts are the same for all of the other segments. The counts were taken during the 15-min analysis period of interest. However, they have been converted to hourly flow rates.

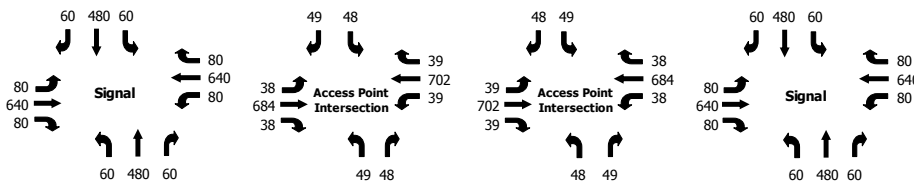


Exhibit 29-41
 Example Problem 1:
 Intersection Turn Movement Counts

The signalization conditions are shown in Exhibit 29-42. The conditions shown are identified as belonging to Signalized Intersection 1; however, they are the same for the other signalized intersections (with the exception of offset). The signals operate with coordinated-actuated control. The left-turn movements on the northbound and southbound approaches operate under permitted control. The left-turn movements on the major street operate as protected-permitted in a lead-lead sequence.

Exhibit 29-42 indicates that the passage time for each phase is 2.0 s. The minimum green setting is 5 s for the major-street left-turn phases and 18 s for the cross-street phases. The offset to Phase 2 (the reference phase) end-of-green interval is 0.0 s. The offset for each of the other intersections is shown in Exhibit 29-39. A fixed-force mode is used to ensure that coordination is maintained. The cycle length is 100 s.

Exhibit 29-42

Example Problem 1: Signal Conditions for Intersection 1

Controller Data Worksheet							
General Information							
Cross street: First Avenue				Analysis period: 7:15 am to 7:30 am			
Phase Sequence							
Phases 1 and 2				Phases 3 and 8			
Enter choice	2	1. WB left (1) with WB thru (6) 2. WB left (1) before EB thru (2) 3. EB thru (2) before WB left (1)		Enter choice	1	1. NB left (3) with NB thru (8) 2. NB left (3) before SB thru (4) 3. SB thru (4) before NB left (3)	
Phases 5 and 6				Phases 4 and 7			
Enter choice	2	1. EB left (5) with EB thru (2) 2. EB left (5) before WB thru (6) 3. WB thru (6) before EB left (5)		Enter choice	1	1. SB left (7) with SB thru (4) 2. SB left (7) before NB thru (8) 3. NB thru (8) before SB left (7)	
Left-Turn Mode							
Phase 1 or 2				Phase 3 or 8			
Enter choice	2	2. WB left (1) prot-perm 3. WB left (1) protected		Enter choice	1	1. NB left permitted 4. NB left & thru (split)	
Phase 5 or 6				Phase 4 or 7			
Enter choice	2	2. EB left (5) prot-perm 3. EB left (5) protected		Enter choice	1	1. SB left permitted 4. SB left & thru (split)	
Phase Settings							
Approach	Eastbound		Westbound		Northbound		Southbound
Phase number	5	2	1	6	8		4
Movement	L	T+R	L	T+R	L+T+R		L+T+R
Lead/lag left-turn phase	Lead	--	Lead	--	--		--
Left-turn mode	Pr/Pm	--	Pr/Pm	--	Perm.		Perm.
Passage time, s	2.0		2.0		2.0		2.0
Phase split, s	20	45	20	45	35		35
Minimum green, s	5		5		18		18
Yellow change, s	3.0	3.0	3.0	3.0	3.0		3.0
Red clearance, s	1.0	1.0	1.0	1.0	1.0		1.0
Walk+ ped. clear, s		17.1		17.1	17.1		17.1
Recall?	No		No		No		No
Dual entry?	No	Yes	No	Yes	Yes		Yes
Simultaneous gap-out?	Yes			Yes			
Dallas left-turn phasing?	No						
Coordination settings	Offset, s:	0	Offset Ref.:	End of Green	Force Mode:	Fixed	
	Cycle, s:	100			Reference phase:	2	
Protected right turn with left-turn phase?	n.a.		n.a.		n.a.		n.a.

Geometric conditions and traffic characteristics for Signalized Intersection 1 are shown in Exhibit 29-43. They are the same for the other signalized intersections. The movement numbers follow the numbering convention shown in Exhibit 19-1 of Chapter 19.

All intersection movements include 3% heavy vehicles. The segment and intersection approaches are effectively level. No parking is allowed along the facility or its cross-street approaches. With a few exceptions (discussed below), local buses stop on the eastbound and westbound approaches to each signalized intersection at a rate of 3 buses/h.

Arrivals for all cross-street movements are effectively random, so a platoon ratio of 1.00 is used. The through movement arriving to the eastbound approach at Intersection 1 exhibits favorable progression from an upstream signal, so a platoon ratio of 1.33 is used. For similar reasons, a ratio of 1.33 is also used for the through movement arriving to the westbound approach at Intersection 6. Right-turn-on-red volume is estimated at 5.0% of the right-turn volume.

Intersection Data Worksheet												
Approach	Eastbound			Westbound			Northbound			Southbound		
Movement	L	T	R	L	T	R	L	T	R	L	T	R
Movement number	5	2	12	1	6	16	3	8	18	7	4	14
Intersection Geometry												
Number of lanes	1	2	0	1	2	0	1	2	0	1	2	0
Lane assignment	L	TR	n.a.	L	TR	n.a.	L	TR	n.a.	L	TR	n.a.
Average lane width, ft	9.0	11.0		9.0	11.0		12.0	12.0		12.0	12.0	
Number of receiving lanes	2			2			2			2		
Turn bay or segment length, ft	200	0		200	1320		200	999		200	999	
Traffic Characteristics												
Volume, veh/h	80	640	80	80	640	80	60	480	60	60	480	60
Right-turn-on-red volume, veh/h			4			4			3			3
Percent heavy vehicles, %	3	3		3	3		3	3		3	3	
Lane utilization adjustment factor												
Peak hour factor	1.00	1.00	1.00	1.00	1.00	1.00	1.00	1.00	1.00	1.00	1.00	1.00
Start-up lost time, s	2.0	2.0		2.0	2.0		2.0	2.0		2.0	2.0	
Extension of eff. green time, s	2.0	2.0		2.0	2.0		2.0	2.0		2.0	2.0	
Platoon ratio	1.000	1.333					1.000	1.000		1.000	1.000	
Upstream filtering factor	1.00	1.00					1.00	1.00		1.00	1.00	
Pedestrian volume, p/h		100			100			100			100	
Bicycle volume, bicycles/h		1			1			1			1	
Opposing right-turn lane influence												
Initial queue, veh	0	0		0	0		0	0		0	0	
Speed limit, mi/h	35	35		35	35		35	35		35	35	
Unsignalized movement volume, veh/h	0	0	0	0	0	0	0	0	0	0	0	0
Unsignalized movement delay, s/veh	0	0	0	0	0	0	0	0	0	0	0	0
Unsignalized mvt. stop rate, stops/veh	0.0	0.0	0.0	0.0	0.0	0.0	0.0	0.0	0.0	0.0	0.0	0.0
Approach Data												
	Left Side		Right Side	Left Side		Right Side	Left Side		Right Side	Left Side		Right Side
Parking present?	No		No	No		No	No		No	No		No
Parking maneuvers, maneuvers/h												
Bus stopping rate, buses/h			3			3			0			0
Approach grade, %	0	0	0	0	0	0	0	0	0	0	0	0
Detection Data												
Stop line detector presence	Presence			Presence			Presence	Presence		Presence	Presence	
Stop line detector length, ft	40			40			40	40		40	40	

Exhibit 29-43
Example Problem 1:
Geometric Conditions and
Traffic Characteristics for
Signalized Intersection 1

Each segment has a barrier curb along the outside of the street in each direction of travel. With allowance for the upstream signal width, the percentage of the segment length with curb is estimated at 94% for Segments 1, 2, and 3. It is estimated as 88% for Segments 4 and 5.

The traffic and lane assignment data for the two access point intersections for Segment 1 are shown in Exhibit 29-44. These data are the same for the other segments; however, the access point locations (shown in the first column) are reduced by one-half for Segments 4 and 5. The movement numbers follow the numbering convention shown in Exhibit 20-1 of Chapter 20, Two-Way STOP-Controlled Intersections. There are no turn bays on the segment at the two access point intersections.

Access Point Input Data													
Access Point	Approach	Eastbound			Westbound			Northbound			Southbound		
Location, ft	Movement	L	T	R	L	T	R	L	T	R	L	T	R
440	Movement number	1	2	3	4	5	6	7	8	9	10	11	12
	Volume, veh/h	38	684	38	39	702	39	49	0	48	48	0	49
West end	Lanes	0	2	0	0	2	0	1	0	1	1	0	1
880	Volume, veh/h	39	702	39	38	684	38	48	0	49	49	0	48
	Lanes	0	2	0	0	2	0	1	0	1	1	0	1

Exhibit 29-44
Example Problem 1: Access
Point Data

A low wall is located along about 25% of the sidewalk in Segments 1, 2, and 3. In contrast, 10% of the sidewalk along Segments 4 and 5 is adjacent to a low wall, 35% to a building face, and 15% to a window display.

Office and strip commercial activity along Segments 1, 2, and 3 generates a pedestrian volume of 100 p/h on the adjacent sidewalks and crosswalks. Shopping activity along Segments 4 and 5 generates a pedestrian volume of 300 p/h on the adjacent sidewalks and crosswalks. A lack of bicycle lanes has discouraged bicycle traffic on the facility and its cross streets; however, a bicycle volume of 1.0 bicycle/h is entered for each intersection approach.

Local buses stop on the eastbound and westbound approaches to each signalized intersection, with the exception of Intersection 5. There are no stops on either approach to Intersection 5. However, transit stops are provided along the facility at 0.25-mi intervals, so the service is considered to be local. As a result,

the westbound transit frequency on Segment 5 and the eastbound transit frequency on Segment 4 are considered to be the same as for the adjacent segments (i.e., 3 buses/h). The bus dwell time at each stop averages 20 s. Buses arrive within 5 min of their scheduled time about 75% of the time and have a load factor of 0.80 passengers/seat. Each bus stop has a bench but no shelter.

Outline of Solution

This section outlines the results of the facility evaluation. To complete this evaluation, the motorized vehicle, pedestrian, and bicycle methodologies in Chapter 19 were used to evaluate each of the signalized intersections on the facility. The procedure in Chapter 20 was used to estimate delay for pedestrians crossing at a midsegment location. The motorized vehicle, pedestrian, bicycle, and transit methodologies in Chapter 18 were then used to evaluate both directions of travel on each segment. Finally, the methodologies described in Chapter 16 were used to evaluate all four travel modes in both directions of travel on the facility. The findings from each evaluation are summarized in the following three subparts.

Intersection Evaluation

The results of the evaluation of Intersection 1 (i.e., First Avenue) are shown in Exhibit 29-45. The results for Intersections 2, 3, and eastbound Intersection 4 are similar. In contrast, Intersections 5 and 6 are associated with a shorter segment length, lower speed limit, and higher pedestrian volume, so their operation is different from that of the other intersections. The results for Intersection 5 (i.e., Fifth Avenue) are shown in Exhibit 29-46. Intersection 6 and westbound Intersection 4 have similar results.

Exhibit 29-45
Example Problem 1:
Intersection 1 Evaluation

Intersection	Approach	Intersection Evaluation Summary											
		Eastbound			Westbound			Northbound			Southbound		
First Avenue	Basic Description	L	TR	n.a.	L	TR	n.a.	L	TR	n.a.	L	TR	n.a.
	Applicable lane assignments	5	2	12	1	6	16	3	8	18	7	4	14
	Primary movement number	80	640	80	80	640	80	60	480	60	60	480	60
	Vehicle volume, veh/h	100			100			100			100		
	Conflicting crosswalk volume, p/h	1			1			1			1		
	Bicycle volume, bicycle/h	1			1			1			1		
	Approach lanes, ln	1	2	0	1	2	0	1	2	0	1	2	0
	Vehicle Level of Service												
	Int. delay, s/veh	0.17	0.33	0.33	0.15	0.33	0.33	0.37	0.62	0.62	0.37	0.62	0.62
	20.4	7.78	5.75	5.78	7.06	13.43	13.78	43.24	34.18	34.26	43.24	34.18	34.26
	Int. level of service	0.27	0.20	0.20	0.26	0.48	0.50	0.85	0.77	0.77	0.85	0.77	0.77
	C	A	A	A	A	B	B	D	C	C	D	C	C
	Pedestrian Level of Service												
Corner location	Adjacent to Eastbound			Adjacent to Westbound			Adjacent to Northbound			Adjacent to Southbound			
Corner circulation area, ft ² /p	93.7			93.7			93.7			93.7			
Crosswalk location	Crossing major			Crossing major			Crossing minor			Crossing minor			
Crosswalk circulation area, ft ² /p	75.9			75.9			82.4			82.4			
Pedestrian delay, s/p	42.3			42.3			42.3			42.3			
Pedestrian LOS score	2.75			2.75			2.66			2.66			
Level of service	C			C			B			B			
Bicycle Level of Service													
Bicycle delay, s/bicycle	5.8			13.8			34.3			34.3			
Bicycle LOS score	3.72			3.72			2.87			2.87			
Level of service	D			D			C			C			

Exhibit 29-46
Example Problem 1:
Intersection 5 Evaluation

Intersection	Intersection Evaluation Summary												
	Approach	Eastbound			Westbound			Northbound			Southbound		
Fifth Avenue	Basic Description												
	Applicable lane assignments	L	TR	n.a.	L	TR	n.a.	L	TR	n.a.	L	TR	n.a.
	Primary movement number	5	2	12	1	6	16	3	8	18	7	4	14
	Vehicle volume, veh/h	80	640	80	80	640	80	60	480	60	60	480	60
	Conflicting crosswalk volume, p/h	300			300			300			300		
	Bicycle volume, bicycle/h	1			1			1			1		
	Approach lanes, ln	1	2	0	1	2	0	1	2	0	1	2	0
	Vehicle Level of Service												
	Int. delay, s/veh	0.16	0.34	0.34	0.16	0.34	0.34	0.36	0.62	0.62	0.36	0.62	0.62
	20.0 Control delay, s/veh	7.89	8.39	7.99	7.79	9.71	9.38	43.12	33.87	34.01	43.12	33.87	34.01
Int. level of service	0.29	0.30	0.28	0.29	0.34	0.33	0.86	0.77	0.78	0.86	0.77	0.78	
B Level of service	A	A	A	A	A	A	D	C	C	D	C	C	
Pedestrian Level of Service													
Corner location	Adjacent to Eastbound			Adjacent to Westbound			Adjacent to Northbound			Adjacent to Southbound			
Corner circulation area, ft ² /p	14.8			14.8			14.8			14.8			
Crosswalk location	Crossing major			Crossing major			Crossing minor			Crossing minor			
Crosswalk circulation area, ft ² /p	24.5			24.5			26.7			26.7			
Pedestrian delay, s/p	42.3			42.3			42.3			42.3			
Pedestrian LOS score	2.70			2.70			2.62			2.62			
Level of service	B			B			B			B			
Bicycle Level of Service													
Bicycle delay, s/bicycle	8.7			10.0			34.0			34.0			
Bicycle LOS score	3.72			3.72			2.87			2.87			
Level of service	D			D			C			C			

Both exhibits indicate that the major-street vehicular through movements (i.e., eastbound Movement 2 and westbound Movement 6) operate with very low delay and few stops. The LOS is A and B for the eastbound and westbound through movements, respectively.

Pedestrian circulation area on the corners of Intersection 1 is generous, with pedestrians able to move in their desired path without conflict. Corner circulation area at Intersection 5 is restricted, with pedestrians having limited ability to pass slower pedestrians.

At Intersection 1, the low pedestrian volume results in generous crosswalk circulation area. Pedestrians rarely need to adjust their path to avoid conflicts. In contrast, the high pedestrian volume at Intersection 5 results in a constrained crosswalk circulation area. Pedestrians frequently adjust their path to avoid conflict. At each intersection, pedestrians experience an average wait of about 42 s at the corner to cross the street in any direction. This delay is lengthy, and some pedestrians may not comply with the signal indications. At Intersection 1, the pedestrian LOS is C for the major-street crossing and B for the minor-street crossing. At Intersection 5, the pedestrian LOS is B for the major-street and minor-street crossings.

The lack of a bicycle lane combined with a moderately high traffic volume results in a bicycle LOS D on the eastbound and westbound approaches of Intersection 1 and Intersection 5.

Segment Evaluation

The results of the evaluation of Segment 1 (i.e., First Avenue to Second Avenue) are shown in Exhibit 29-47. The results for Segments 2 and 3 are similar. In contrast, Segments 4 and 5 are associated with a shorter segment length, lower speed limit, and higher pedestrian volume, so their operation is different from that of the other intersections. The results for Segment 5 (i.e., Fifth Avenue to Sixth Avenue) are shown in Exhibit 29-48. Segment 4 has similar results.

Exhibit 29-47

Example Problem 1:
Segment 1 Evaluation

Segment	Segment Evaluation Summary		
	Travel Direction	Eastbound	Westbound
First Avenue to Second Avenue	Basic Description		
	Speed limit, mi/h	35	35
	Vehicle volume, veh/h	800	800
	Through lanes, ln	2	2
Segment length, ft 1,320	Vehicle Level of Service		
	Base free-flow speed, mi/h	40.9	40.9
	Travel speed, mi/h	24.2	23.4
	Spatial stop rate, stops/mi	1.72	1.93
	Level of service	C	C
	Pedestrian Level of Service		
	Pedestrian space, ft ² /p	593.9	593.9
	Pedestrian travel speed, ft/s	3.54	3.54
	Pedestrian LOS score	3.48	3.48
	Level of service	C	C
	Bicycle Level of Service		
	Bicycle travel speed, mi/h	12.44	12.20
	Bicycle LOS score	3.67	3.67
	Level of service	D	D
	Transit Level of Service		
	Transit travel speed, mi/h	12.8	12.4
	Transit LOS score	3.17	3.20
	Level of service	C	C

Exhibit 29-48

Example Problem 1:
Segment 5 Evaluation

Segment	Segment Evaluation Summary		
	Travel Direction	Eastbound	Westbound
Fifth Avenue to Sixth Avenue	Basic Description		
	Speed limit, mi/h	30	30
	Vehicle volume, veh/h	800	800
	Through lanes, ln	2	2
Segment length, ft 660	Vehicle Level of Service		
	Base free-flow speed, mi/h	37.9	37.9
	Travel speed, mi/h	17.6	17.4
	Spatial stop rate, stops/mi	2.63	2.75
	Level of service	D	D
	Pedestrian Level of Service		
	Pedestrian space, ft ² /p	153.3	153.3
	Pedestrian travel speed, ft/s	3.18	3.18
	Pedestrian LOS score	3.27	3.27
	Level of service	C	C
	Bicycle Level of Service		
	Bicycle travel speed, mi/h	11.37	11.26
	Bicycle LOS score	3.67	3.67
	Level of service	D	D
	Transit Level of Service		
	Transit travel speed, mi/h	7.7	17.4
	Transit LOS score	3.63	2.78
	Level of service	D	C

Exhibit 29-47 indicates that the vehicular through movements on Segment 1 in the eastbound and westbound travel directions have a travel speed of 24 and 23 mi/h, respectively (i.e., about 58% of the base free-flow speed). The LOS of each movement is C. In contrast, Exhibit 29-48 indicates that the through movements have a travel speed of only about 17 mi/h on Segment 5 (or 46% of the base free-flow speed), which is LOS D. Vehicles stop at a rate of about 1.8 stops/mi on Segment 1 and about 2.7 stops/mi on Segment 5.

Pedestrian space on the sidewalk along the segment is generous on Segment 1 and adequate on Segment 5. These characterizations are based on Exhibit 16-9 and an assumed dominance of platoon flow for Segments 4 and 5. Pedestrians on these sidewalks can walk freely without having to alter their path to accommodate other pedestrians. The segment travel speed (3.54 ft/s for Segment 1 and 3.18 ft/s for Segment 5) is adequate but would desirably exceed 4.0 ft/s. Nevertheless, the sidewalk is near the traffic lanes, and crossing the street

at a midsegment location can be difficult. As a result, the pedestrian LOS is C on all segments.

The lack of a bicycle lane, combined with a moderately high traffic volume, results in a bicycle LOS D for both directions of travel on all segments.

Transit travel speed is about 12 mi/h on Segment 1 and corresponds to LOS C. On Segment 5, the travel speed is about 8 mi/h and 17 mi/h in the eastbound and westbound directions, respectively. The low speed for the eastbound direction results in LOS D. The higher speed for the westbound direction is due to the lack of a westbound transit stop on Segment 5. It results in LOS C for this direction.

Facility Evaluation

The methodologies described in Chapter 16 were used to compute the aggregate performance measures for each travel direction along the facility. The results are shown in Exhibit 29-49. This exhibit indicates that the vehicle travel speed is about 22 mi/h in each travel direction (or 56% of the base free-flow speed). An overall LOS C applies to both vehicular movements on the facility; however, it is noted that LOS D applies to Segments 4 and 5. Vehicles incur stops along the facility at a rate of about 1.9 stops/mi.

		Facility Evaluation Summary	
Travel Direction		Eastbound	Westbound
Facility length, ft 5,280	Vehicle Level of Service		
	Base free-flow speed, mi/h	40.1	40.1
	Travel speed, mi/h	22.6	22.2
	Spatial stop rate, stops/mi	1.83	1.93
	Level of service	C	C
	Poorest perf. segment LOS	D	D
	Pedestrian Level of Service		
	Pedestrian space, ft ² /p	298.6	298.6
	Pedestrian travel speed, ft/s	3.4	3.4
	Pedestrian LOS score	3.42	3.42
	Level of service	C	C
	Poorest perf. segment LOS	C	C
	Bicycle Level of Service		
	Bicycle travel speed, mi/h	12.3	12.2
	Bicycle LOS score	3.67	3.67
	Level of service	D	D
	Poorest perf. segment LOS	D	D
	Transit Level of Service		
	Transit travel speed, mi/h	12.4	12.3
	Transit LOS score	3.15	3.17
	Level of service	C	C
	Poorest perf. segment LOS	D	D

Exhibit 29-49
Example Problem 1:
Facility Evaluation

Pedestrian space on the sidewalk along the facility is generous. Pedestrians on the sidewalks can walk freely without having to alter their path to accommodate other pedestrians. The facility travel speed of about 3.4 ft/s is adequate but would desirably exceed 4.0 ft/s. Nevertheless, the sidewalk is near the traffic lanes, and crossing the street at a midsegment location can be difficult. As a result, the pedestrian LOS is C for both directions of travel.

The lack of a bicycle lane, combined with a moderately high traffic volume, results in an overall bicycle LOS D for both directions of travel.

Transit travel speed is about 12 mi/h on the facility in each direction of travel. An overall LOS C is assigned to each direction. The lower speed on westbound

Segment 4 and eastbound Segment 5 is noted to result in LOS D for those segments.

EXAMPLE PROBLEM 2: PEDESTRIAN AND BICYCLE IMPROVEMENTS

The Urban Street Facility

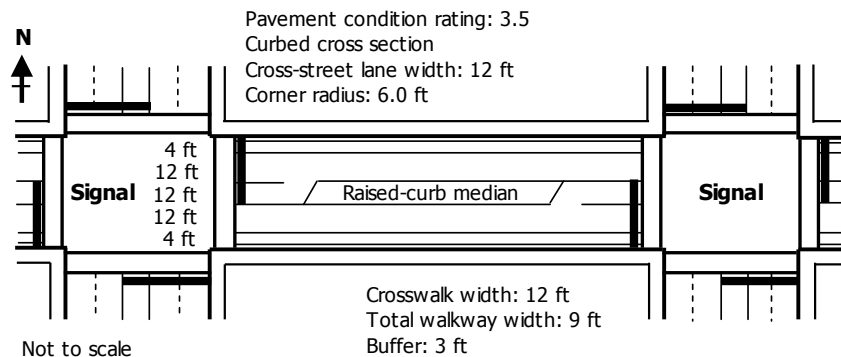
The 1-mi urban street facility shown in Exhibit 29-39 is being considered for geometric design modifications to improve pedestrian and bicycle service. The following changes to the facility are proposed:

- Eliminate one vehicle lane in each direction,
- Add a 12-ft raised-curb median,
- Add a 4-ft bicycle lane in each direction,
- Increase the total walkway width to 9 ft,
- Add a 3-ft buffer between the sidewalk and the curb, and
- Add bushes to the buffer with a 10-ft spacing.

No fixed objects are located along the outside of the sidewalk. The analysis for Example Problem 1 represents the existing condition, against which this alternative will be evaluated.

The geometry of the typical street segment is shown in Exhibit 29-50. It is the same for each segment. Additional segment details are provided in the discussion for Example Problem 1.

Exhibit 29-50
Example Problem 2:
Segment Geometry



The Question

What are the travel speed and LOS of the motorized vehicle, pedestrian, bicycle, and transit modes in both directions of travel along the facility?

The Facts

The traffic counts, signalization, and intersection geometry are listed in Exhibit 29-41 to Exhibit 29-44. They are unchanged from Example Problem 1.

Outline of Solution

This section outlines the results of the facility evaluation. The motorized vehicle, pedestrian, and bicycle methodologies in Chapter 19 were used to evaluate each of the signalized intersections on the facility. The procedure in Chapter 20 was used to estimate delay for pedestrians crossing at a midsegment

location. The motorized vehicle, pedestrian, bicycle, and transit methodologies in Chapter 18 were then used to evaluate both directions of travel on each segment. Finally, the methodologies described in Chapter 16 were used to evaluate all four travel modes in both directions of travel on the facility. The findings from each evaluation are summarized in the following three subparts.

Intersection Evaluation

The results of the evaluation of Intersection 1 (i.e., First Avenue) are shown in Exhibit 29-51. The results for Intersections 2, 3, and eastbound Intersection 4 are similar. In contrast, Intersections 5 and 6 are associated with a shorter segment length, lower speed limit, and higher pedestrian volume, so their operation is different from that of the other intersections. The results for Intersection 5 (i.e., Fifth Avenue) are shown in Exhibit 29-52. Intersection 6 and westbound Intersection 4 have similar results.

Intersection	Approach	Intersection Evaluation Summary											
		Eastbound			Westbound			Northbound			Southbound		
First Avenue	Basic Description												
	Applicable lane assignments	L	TR	n.a.	L	TR	n.a.	L	TR	n.a.	L	TR	n.a.
	Primary movement number	5	2	12	1	6	16	3	8	18	7	4	14
	Vehicle volume, veh/h	80	640	80	80	640	80	60	480	60	60	480	60
	Conflicting crosswalk volume, p/h	100			100			100			100		
	Bicycle volume, bicycle/h	1			1			1			1		
	Approach lanes, ln	1	1	0	1	1	0	1	2	0	1	2	0
	Vehicle Level of Service												
	Volume-to-capacity ratio	0.20	0.67	0.67	0.18	0.67	0.67	0.36	0.63	0.63	0.36	0.63	0.63
	Control delay, s/veh	10.67	9.73	9.73	8.75	14.48	14.48	43.28	34.14	34.26	43.28	34.14	34.26
	Stop rate, stops/veh	0.43	0.25	0.25	0.34	0.46	0.46	0.85	0.77	0.77	0.85	0.77	0.77
	Level of service	B	A	A	A	B	B	D	C	C	D	C	C
	Pedestrian Level of Service												
Corner location	Adjacent to Eastbound			Adjacent to Westbound			Adjacent to Northbound			Adjacent to Southbound			
Corner circulation area, ft ² /p	282.1			282.1			282.1			282.1			
Crosswalk location	Crossing major			Crossing major			Crossing minor			Crossing minor			
Crosswalk circulation area, ft ² /p	69.7			69.7			82.5			82.4			
Pedestrian delay, s/p	42.3			42.3			42.3			42.3			
Pedestrian LOS score	2.63			2.63			2.66			2.66			
Level of service	B			B			B			B			
Bicycle Level of Service													
Bicycle delay, s/bicycle	8.4			8.4			34.3			34.3			
Bicycle LOS score	2.99			2.99			2.77			2.77			
Level of service	C			C			C			C			

Exhibit 29-51
Example Problem 2:
Intersection 1 Evaluation

Intersection	Approach	Intersection Evaluation Summary											
		Eastbound			Westbound			Northbound			Southbound		
Fifth Avenue	Basic Description												
	Applicable lane assignments	L	TR	n.a.	L	TR	n.a.	L	TR	n.a.	L	TR	n.a.
	Primary movement number	5	2	12	1	6	16	3	8	18	7	4	14
	Vehicle volume, veh/h	80	640	80	80	640	80	60	480	60	60	480	60
	Conflicting crosswalk volume, p/h	300			300			300			300		
	Bicycle volume, bicycle/h	1			1			1			1		
	Approach lanes, ln	1	1	0	1	1	0	1	2	0	1	2	0
	Vehicle Level of Service												
	Volume-to-capacity ratio	0.21	0.67	0.67	0.21	0.67	0.67	0.36	0.63	0.63	0.36	0.63	0.63
	Control delay, s/veh	11.49	16.90	16.90	11.66	16.41	16.41	43.20	33.97	34.20	43.20	33.97	34.20
	Stop rate, stops/veh	0.47	0.56	0.56	0.48	0.54	0.54	0.86	0.78	0.78	0.86	0.78	0.78
	Level of service	B	B	B	B	B	B	D	C	C	D	C	C
	Pedestrian Level of Service												
Corner location	Adjacent to Eastbound			Adjacent to Westbound			Adjacent to Northbound			Adjacent to Southbound			
Corner circulation area, ft ² /p	77.6			77.6			77.6			77.6			
Crosswalk location	Crossing major			Crossing major			Crossing minor			Crossing minor			
Crosswalk circulation area, ft ² /p	22.4			22.4			26.6			26.7			
Pedestrian delay, s/p	42.3			42.3			42.3			42.3			
Pedestrian LOS score	2.55			2.55			2.62			2.62			
Level of service	B			B			B			B			
Bicycle Level of Service													
Bicycle delay, s/bicycle	8.6			8.6			34.2			34.2			
Bicycle LOS score	2.99			2.99			2.77			2.77			
Level of service	C			C			C			C			

Exhibit 29-52
Example Problem 2:
Intersection 5 Evaluation

Both exhibits indicate that the vehicular through movements on the facility (i.e., eastbound Movement 2 and westbound Movement 6) operate with low delay and few stops. For the eastbound through movement, the LOS is A at Intersection 1 and B at Intersection 5. The LOS is B for the westbound through movement at both intersections. Relative to Example Problem 1, the delay for the through movements has increased by 1 to 3 s at Intersection 1 and by 6 to 8 s at Intersection 5. This increase is sufficient to lower the LOS designation for the through movements at Intersection 5 (i.e., from A to B).

Pedestrian circulation area on the corners of Intersections 1 and 5 is generous, with few instances of conflict. This condition is improved from Example Problem 1 and reflects the provision of wider sidewalks.

Relative to Example Problem 1, the reduction in through lanes has reduced the time provided to pedestrians to cross the major street. This reduction resulted in larger pedestrian groups using the crosswalk and a small reduction in crosswalk pedestrian space. At Intersection 1, pedestrian space is still generous, with few instances of conflict. At Intersection 5, the problem is amplified by a higher pedestrian demand. Pedestrian space in the crosswalks is constrained, and pedestrians are likely to find that their ability to pass slower pedestrians is limited.

At each intersection, pedestrians experience an average wait of about 42 s at the corner to cross the street in any direction. This condition has not changed from Example Problem 1.

At both intersections, the pedestrian LOS is B for the major-street and minor-street crossings. Relative to Example Problem 1, the pedestrian LOS score for the major-street crossings has improved a small amount at all intersections. At Intersection 1, this change is sufficient to result in a change in service level (i.e., from C to B) for the major-street crossings.

Bicyclists using the bicycle lanes are expected to be delayed about 8 s/bicycle on the eastbound and westbound approaches at each intersection. This level of delay is desirably low. However, the bicycle lane is relatively narrow at 4 ft, which leads to LOS C on the eastbound and westbound approaches of both intersections. This LOS is an improvement over the LOS D identified in Example Problem 1.

Segment Evaluation

The results of the evaluation of Segment 1 (i.e., First Avenue to Second Avenue) are shown in Exhibit 29-53. The results for Segments 2 and 3 are similar. In contrast, Segments 4 and 5 are associated with a shorter segment length, lower speed limit, and higher pedestrian volume, so their operation is different from the other intersections. The results for Segment 5 (i.e., Fifth Avenue to Sixth Avenue) are shown in Exhibit 29-54. Segment 4 has similar results.

The results reported in this section reflect the segment geometry shown in Exhibit 29-50. These results are compared with those from Example Problem 1. The differences in performance are a result of the changes identified in the bullet list that precedes Exhibit 29-50. Most notable in this list is the reduction in lanes for motorized vehicles, which results in a doubling of vehicles in the remaining lanes. The vehicle volume in these lanes has a significant influence on bicycle and pedestrian performance.

Segment	Segment Evaluation Summary		
	Travel Direction	Eastbound	Westbound
First Avenue to Second Avenue	Basic Description		
	Speed limit, mi/h	35	35
Segment length, ft 1,320	Vehicle volume, veh/h	800	800
	Through lanes, ln	1	1
Vehicle Level of Service			
Base free-flow speed, mi/h	38.7	38.7	
Travel speed, mi/h	21.5	21.6	
Spatial stop rate, stops/mi	1.86	1.84	
Level of service	C	C	
Pedestrian Level of Service			
Pedestrian space, ft ² /p	809.9	809.9	
Pedestrian travel speed, ft/s	3.55	3.55	
Pedestrian LOS score	2.93	2.93	
Level of service	C	C	
Bicycle Level of Service			
Bicycle travel speed, mi/h	13.16	13.16	
Bicycle LOS score	3.02	3.02	
Level of service	C	C	
Transit Level of Service			
Transit travel speed, mi/h	10.3	10.3	
Transit LOS score	3.43	3.43	
Level of service	C	C	

Exhibit 29-53
Example Problem 2:
Segment 1 Evaluation

Segment	Segment Evaluation Summary		
	Travel Direction	Eastbound	Westbound
Fifth Avenue to Sixth Avenue	Basic Description		
	Speed limit, mi/h	30	30
Segment length, ft 660	Vehicle volume, veh/h	800	800
	Through lanes, ln	1	1
Vehicle Level of Service			
Base free-flow speed, mi/h	35.3	35.3	
Travel speed, mi/h	12.9	13.2	
Spatial stop rate, stops/mi	4.59	4.35	
Level of service	E	E	
Pedestrian Level of Service			
Pedestrian space, ft ² /p	225.4	225.4	
Pedestrian travel speed, ft/s	3.18	3.18	
Pedestrian LOS score	2.85	2.85	
Level of service	C	C	
Bicycle Level of Service			
Bicycle travel speed, mi/h	11.67	11.67	
Bicycle LOS score	3.01	3.01	
Level of service	C	C	
Transit Level of Service			
Transit travel speed, mi/h	5.3	13.2	
Transit LOS score	3.99	3.14	
Level of service	D	C	

Exhibit 29-54
Example Problem 2:
Segment 5 Evaluation

Exhibit 29-53 indicates that the vehicular through movements on Segment 1 in the eastbound and westbound travel directions have a travel speed of about 22 mi/h (i.e., about 56% of the base free-flow speed). LOS C applies to both movements. In contrast, Exhibit 29-54 indicates that the through movements have a travel speed of only about 13 mi/h on Segment 5 (or 37% of the base free-flow speed), which is LOS E. Vehicles stop at a rate of about 1.8 stops/mi on Segment 1 and about 4.6 stops/mi on Segment 5. Relative to Example Problem 1, the quality of service has been degraded for vehicles traveling along Segment 5.

Pedestrian space on the sidewalk along the segment is generous on Segment 1. Pedestrians can walk freely without having to alter their path to accommodate other pedestrians. Pedestrian space is adequate on Segment 5, with pedestrians in platoons occasionally needing to adjust their path to avoid conflict. These characterizations are based on Exhibit 16-9 and on an assumed dominance of platoon flow for Segments 4 and 5. Relative to Example Problem 1,

the sidewalks are more distant from the traffic lanes and crossing the street at a midsegment location is easier because of the raised curb median. The LOS score indicates improved pedestrian service; however, the pedestrian LOS remains at C on all segments.

Bicyclists using the bicycle lanes experience a travel speed of 13 mi/h on Segment 1 and 12 mi/h on Segment 5. This travel speed is considered desirable. However, the bicycle lane is relatively narrow at 4 ft, so a bicycle LOS C results for both directions of travel on each segment. The bicycle LOS scores, while still poor, indicate that bicycle service has improved on both segments relative to that found in Example Problem 1. In fact, the bicycle LOS for each segment has improved by one letter designation.

Transit travel speed is 10 mi/h on Segment 1 and corresponds to LOS C. On Segment 5, the travel speed is about 5 mi/h and 13 mi/h in the eastbound and westbound directions, respectively. The low speed for the eastbound direction results in LOS D. The higher speed for the westbound direction is due to the lack of a westbound transit stop on Segment 5. It results in LOS C. Relative to Example Problem 1, the slower vehicular travel speed has increased the transit LOS scores, which indicates a lower quality of service.

Facility Evaluation

The methodologies described in Chapter 16 were used to compute the aggregate performance measures for each travel direction along the facility. The results are shown in Exhibit 29-55. This exhibit indicates that the vehicle travel speed is about 18 mi/h in each travel direction (or 48% of the base free-flow speed). An overall LOS D applies to vehicle travel in each direction on the facility. It is noted that LOS E applies to Segments 4 and 5. Vehicles incur stops along the facility at a rate of about 2.6 stops/mi. Relative to Example Problem 1, vehicular travel speed has dropped about 4 mi/h, and motorized vehicle LOS has degraded one level for this scenario.

Exhibit 29-55
Example Problem 2:
Facility Evaluation

		Facility Evaluation Summary	
		Travel Direction	Eastbound
Facility length, ft 5,280	Vehicle Level of Service		
	Base free-flow speed, mi/h	37.8	37.8
	Travel speed, mi/h	18.3	18.3
	Spatial stop rate, stops/mi	2.61	2.59
	Level of service	D	D
	Poorest perf. segment LOS	E	E
	Pedestrian Level of Service		
	Pedestrian space, ft ² /p	422.2	422.2
	Pedestrian travel speed, ft/s	3.4	3.4
	Pedestrian LOS score	2.91	2.91
	Level of service	C	C
	Poorest perf. segment LOS	C	C
	Bicycle Level of Service		
	Bicycle travel speed, mi/h	12.7	12.8
	Bicycle LOS score	3.02	3.02
	Level of service	C	C
	Poorest perf. segment LOS	C	C
	Transit Level of Service		
	Transit travel speed, mi/h	9.3	9.3
	Transit LOS score	3.48	3.48
Level of service	C	C	
Poorest perf. segment LOS	D	D	

Pedestrian space on the sidewalk along the facility is generous. Pedestrians on the sidewalks can walk freely without having to alter their path to accommodate other pedestrians. Increasing the separation between the sidewalk and traffic lanes and improving pedestrians' ability to cross the street at midsegment locations (by adding a raised-curb median) have resulted in a lower LOS score, which indicates improved service relative to Example Problem 1. However, the pedestrian LOS letter (C) is unchanged.

Bicyclists in the bicycle lanes are estimated to experience an average travel speed of about 13 mi/h. This travel speed is considered desirable. However, the 4-ft bicycle lane is relatively narrow and produces LOS C. This level is one level improved over that found for Example Problem 1.

Transit travel speed is about 9 mi/h on the facility in each direction of travel. An overall LOS C is assigned to each direction. Relative to Example Problem 1, the LOS designation is unchanged; however, the transit speed is slower, and the transit LOS score higher, which indicates a reduction in the quality of service.

EXAMPLE PROBLEM 3: PEDESTRIAN AND PARKING IMPROVEMENTS

The Urban Street Facility

The 1-mi urban street facility shown in Exhibit 29-39 is being considered for geometric design modifications to improve parking and pedestrian service. The following changes to the facility are proposed:

- Eliminate one vehicle lane in each direction,
- Add a 12-ft raised-curb median,
- Add a 9.5-ft parking lane in each direction, and
- Increase the total walkway width to 7 ft.

No fixed objects will be located along the outside of the sidewalk. The on-street parking is expected to be occupied 50% of the time. Parking maneuvers are estimated to cause 1.8 s/veh additional delay on Segments 1, 2, and 3. On Segments 4 and 5, these maneuvers are estimated to cause 0.3 s/veh additional delay. The analysis for Example Problem 1 represents the existing condition, against which this alternative will be evaluated.

The geometry of the typical street segment is shown in Exhibit 29-56. It is the same for each segment. Additional segment details are provided in the discussion for Example Problem 1.

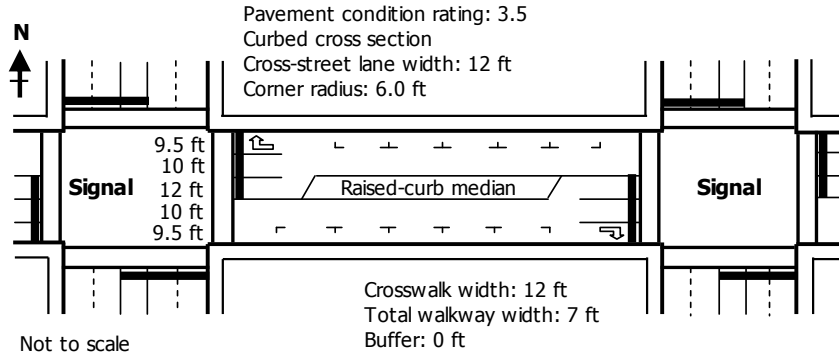
The Question

What are the travel speed and LOS of the motorized vehicle, pedestrian, bicycle, and transit modes in both directions of travel along the facility?

The Facts

The traffic counts, signalization, and intersection geometry are listed in Exhibit 29-41 to Exhibit 29-44. They are unchanged from Example Problem 1.

Exhibit 29-56
Example Problem 3:
Segment Geometry



Outline of Solution

This section outlines the results of the facility evaluation. To complete this evaluation, the motorized vehicle, pedestrian, and bicycle methodologies in Chapter 19 were used to evaluate each of the signalized intersections on the facility. The procedure in Chapter 20 was used to estimate pedestrian delay when crossing at a midsegment location. The motorized vehicle, pedestrian, bicycle, and transit methodologies in Chapter 18 were then used to evaluate both directions of travel on each segment. Finally, the methodologies described in Chapter 16 were used to evaluate all four travel modes in both directions of travel on the facility. The findings from each evaluation are summarized in the following three subparts.

Intersection Evaluation

The results of the evaluation of Intersection 1 (i.e., First Avenue) are shown in Exhibit 29-57. The results for Intersections 2, 3, and eastbound Intersection 4 are similar. In contrast, Intersections 5 and 6 are associated with a shorter segment length, lower speed limit, and higher pedestrian volume, so their operation is different from that of the other intersections. The results for Intersection 5 (i.e., Fifth Avenue) are shown in Exhibit 29-58. Intersection 6 and westbound Intersection 4 have similar results.

Exhibit 29-57
Example Problem 3:
Intersection 1 Evaluation

Intersection	Intersection Evaluation Summary												
	Approach	Eastbound			Westbound			Northbound		Southbound			
First Avenue	Basic Description	L	T	R	L	T	R	L	TR	n.a.	L	TR	n.a.
	Applicable lane assignments	5	2	12	1	6	16	3	8	18	7	4	14
	Primary movement number	80	640	80	80	640	80	60	480	60	60	480	60
	Vehicle volume, veh/h	100			100			100		100			
	Conflicting crosswalk volume, p/h	1	1	1	1	1	1	1	2	0	1	2	0
	Bicycle volume, bicycle/h	1	1	1	1	1	1	1	2	0	1	2	0
	Approach lanes, ln	1			1			1		1			
	Vehicle Level of Service	0.19			0.17			0.36		0.63			
	Volume-to-capacity ratio	0.19	0.58	0.09	0.17	0.58	0.09	0.36	0.63	0.63	0.36	0.63	0.63
	Int. delay, s/veh	10.12	8.11	9.04	7.66	16.71	11.29	43.28	34.14	34.26	43.28	34.14	34.26
21.8	0.40	0.23	0.34	0.28	0.56	0.41	0.85	0.77	0.77	0.85	0.77	0.77	
Int. level of service	B			A			B		C				
C	B			A			D		C				
Level of service	B			A			B		C				
Pedestrian Level of Service	Adjacent to Eastbound			Adjacent to Westbound			Adjacent to Northbound		Adjacent to Southbound				
Corner location	148.1			148.1			148.1		148.1				
Corner circulation area, ft ² /p	Crossing major			Crossing major			Crossing minor		Crossing minor				
Crosswalk location	74.0			74.0			82.6		82.4				
Crosswalk circulation area, ft ² /p	42.3			42.3			42.3		42.3				
Pedestrian delay, s/p	2.67			2.67			2.66		2.66				
Pedestrian LOS score	B			B			B		B				
Level of service	B			B			B		B				
Bicycle Level of Service	8.1			16.7			34.3		34.3				
Bicycle delay, s/bicycle	4.27			4.27			2.83		2.83				
Bicycle LOS score	E			E			C		C				
Level of service	E			E			C		C				

Exhibit 29-58
Example Problem 3:
Intersection 5 Evaluation

Intersection	Approach	Intersection Evaluation Summary											
		Eastbound			Westbound			Northbound			Southbound		
Fifth Avenue	Basic Description												
	Applicable lane assignments	L	T	R	L	T	R	L	TR	n.a.	L	TR	n.a.
	Primary movement number	5	2	12	1	6	16	3	8	18	7	4	14
	Vehicle volume, veh/h	80	640	80	80	640	80	60	480	60	60	480	60
	Conflicting crosswalk volume, p/h	300			300			300			300		
	Bicycle volume, bicycle/h	1			1			1			1		
	Approach lanes, ln	1			1			1			2		
	Vehicle Level of Service												
	Int. delay, s/veh	0.19	0.59	0.09	0.18	0.59	0.09	0.36	0.64	0.64	0.36	0.64	0.64
	21.7	9.95	12.04	4.87	9.57	13.71	6.48	43.20	33.91	34.25	43.20	33.91	34.25
	Int. level of service	0.41	0.39	0.19	0.39	0.46	0.25	0.86	0.77	0.78	0.86	0.77	0.78
	C	A	B	A	A	B	A	D	C	C	D	C	C
	Pedestrian Level of Service												
Corner location	Adjacent to Eastbound			Adjacent to Westbound			Adjacent to Northbound			Adjacent to Southbound			
Corner circulation area, ft ² /p	33.0			33.0			33.0			33.0			
Crosswalk location	Crossing major			Crossing major			Crossing minor			Crossing minor			
Crosswalk circulation area, ft ² /p	23.8			23.8			26.7			26.7			
Pedestrian delay, s/p	42.3			42.3			42.3			42.3			
Pedestrian LOS score	2.61			2.61			2.62			2.62			
Level of service	B			B			B			B			
Bicycle Level of Service													
Bicycle delay, s/bicycle	12.0			13.7			34.2			34.2			
Bicycle LOS score	4.27			4.27			2.83			2.83			
Level of service	E			E			C			C			

Both exhibits indicate that the vehicular through movements on the facility (i.e., eastbound Movement 2 and westbound Movement 6) operate with very low delay and few stops. For the eastbound through movement, the LOS is A at Intersection 1 and B at Intersection 5. The LOS is B for the westbound through movement at both intersections. Relative to Example Problem 1, the delay for the through movements has increased by a few seconds at both intersections. However, this increase is sufficient to lower the LOS designation for only the eastbound through movement at Intersection 5.

Pedestrian circulation area on the corners of Intersection 1 is generous. However, corner circulation area at Intersection 5 is constrained, with pedestrians frequently needing to adjust their path to avoid slower pedestrians. Regardless, this condition is improved from Example Problem 1 and reflects the provision of wider sidewalks.

Relative to Example Problem 1, the reduction in lanes has reduced the time provided to pedestrians to cross the major street. This reduction resulted in larger pedestrian groups using the crosswalk and a slight reduction in crosswalk pedestrian space. At Intersection 1, pedestrian space is generous. However, pedestrian space is constrained at Intersection 5, with pedestrians having limited ability to pass slower pedestrians as they cross the street.

At each intersection, pedestrians experience an average wait of about 42 s at the corner to cross the street in any direction. At both intersections, the pedestrian LOS is B for the major-street crossing and the minor-street crossing. The LOS designation has improved for the major-street crossing at Intersection 1 by one letter, relative to Example Problem 1, and remains unchanged at Intersection 5.

The lack of a bicycle lane combined with a high traffic volume results in a bicycle LOS E on the eastbound and westbound approaches of Intersection 1 and Intersection 5. This level is worse than the LOS D identified in Example Problem 1 because the traffic volume per lane has doubled.

Segment Evaluation

The results of the evaluation of Segment 1 (i.e., First Avenue to Second Avenue) are shown in Exhibit 29-59. The results for Segments 2 and 3 are similar. In contrast, Segments 4 and 5 are associated with a shorter segment length, lower

speed limit, and higher pedestrian volume, so their operation is different from that of the other intersections. The results for Segment 5 (i.e., Fifth Avenue to Sixth Avenue) are shown in Exhibit 29-60. Segment 4 has similar results.

The results reported in this section reflect the segment geometry shown in Exhibit 29-56. These results are compared with those from Example Problem 1. The differences in performance are a result of the changes identified in the bullet list that precedes Exhibit 29-56. Most notable in this list is the reduction in lanes for motorized vehicles, which results in a doubling of vehicles in the remaining lanes. The vehicle volume in these lanes has a significant influence on bicycle and pedestrian performance.

Exhibit 29-59
Example Problem 3:
Segment 1 Evaluation

Segment	Segment Evaluation Summary		
	Travel Direction	Eastbound	Westbound
First Avenue to Second Avenue	Basic Description		
	Speed limit, mi/h	35	35
Segment length, ft 1,320	Vehicle volume, veh/h	800	800
	Through lanes, ln	1	1
Vehicle Level of Service			
Base free-flow speed, mi/h	36.2	36.2	
Travel speed, mi/h	19.6	19.1	
Spatial stop rate, stops/mi	2.08	2.23	
Level of service	C	C	
Pedestrian Level of Service			
Pedestrian space, ft ² /p	737.9	737.9	
Pedestrian travel speed, ft/s	3.55	3.55	
Pedestrian LOS score	2.93	2.93	
Level of service	C	C	
Bicycle Level of Service			
Bicycle travel speed, mi/h	11.91	11.73	
Bicycle LOS score	4.16	4.16	
Level of service	D	D	
Transit Level of Service			
Transit travel speed, mi/h	10.3	10.1	
Transit LOS score	3.40	3.42	
Level of service	C	C	

Exhibit 29-60
Example Problem 3:
Segment 5 Evaluation

Segment	Segment Evaluation Summary		
	Travel Direction	Eastbound	Westbound
Fifth Avenue to Sixth Avenue	Basic Description		
	Speed limit, mi/h	30	30
Segment length, ft 660	Vehicle volume, veh/h	800	800
	Through lanes, ln	1	1
Vehicle Level of Service			
Base free-flow speed, mi/h	33.3	33.3	
Travel speed, mi/h	14.3	13.9	
Spatial stop rate, stops/mi	3.40	3.66	
Level of service	D	D	
Pedestrian Level of Service			
Pedestrian space, ft ² /p	201.4	201.4	
Pedestrian travel speed, ft/s	3.18	3.18	
Pedestrian LOS score	2.87	2.87	
Level of service	C	C	
Bicycle Level of Service			
Bicycle travel speed, mi/h	10.49	10.29	
Bicycle LOS score	4.13	4.13	
Level of service	D	D	
Transit Level of Service			
Transit travel speed, mi/h	6.2	13.9	
Transit LOS score	3.84	3.05	
Level of service	D	C	

Exhibit 29-59 indicates that the vehicular through movements on Segment 1 in the eastbound and westbound travel directions have a travel speed of about 19 mi/h (i.e., about 53% of the base free-flow speed). LOS C applies to both

movements. In contrast, Exhibit 29-60 indicates that the through movements have a travel speed of only about 14 mi/h on Segment 5 (or 42% of the base free-flow speed), which is LOS D. Vehicles stop at a rate of about 2.1 stops/mi on Segment 1 and about 3.5 stops/mi on Segment 5. Relative to Example Problem 1, conditions have degraded for vehicles traveling along these segments, but not enough to drop the LOS designation.

Pedestrian space on the sidewalk along the segment is generous on Segment 1 and adequate on Segment 5. These characterizations are based on Exhibit 16-9 and on an assumed dominance of platoon flow for Segments 4 and 5. Pedestrians on these sidewalks can walk freely without having to alter their path to accommodate other pedestrians. Relative to Example Problem 1, the sidewalks are more distant from the traffic lanes, and crossing the street at a midsegment location is easier because of the raised-curb median. The LOS score indicates improved pedestrian service; however, the pedestrian LOS remains at C on all segments.

The lack of a bicycle lane combined with a high traffic volume results in a bicycle LOS D for both directions of travel on Segment 1 and Segment 5. Relative to Example Problem 1, the quality of service has degraded for bicyclists on all segments. This reduction in service is due largely to the increased density of vehicles in the mixed traffic lanes.

Transit travel speed is about 10 mi/h on Segment 1 and corresponds to LOS C. On Segment 5, the travel speed is about 6 mi/h and 14 mi/h in the eastbound and westbound directions, respectively. The low speed for the eastbound direction results in LOS D. The higher speed for the westbound direction is due to the lack of a westbound transit stop on Segment 5. It results in LOS C. Relative to Example Problem 1, the slower vehicular travel speed has increased the transit LOS scores, which indicates a lower quality of service.

Facility Evaluation

The methodology described in Section 2 is used to compute the aggregate performance measures for each travel direction along the facility. The results are shown in Exhibit 29-61. This exhibit indicates that the vehicle travel speed is about 18 mi/h in each travel direction (or 51% of the base free-flow speed). An overall LOS C applies to both vehicular movements on the facility; however, it is noted that LOS D applies to Segments 4 and 5. Vehicles incur stops along the facility at a rate of about 2.3 stops/mi. Relative to Example Problem 1, the quality of vehicular service has degraded, but not enough to drop the LOS designation.

Pedestrian space on the sidewalk along the facility is generous. Pedestrians on the sidewalks can walk freely without having to alter their path to accommodate other pedestrians. Increasing the separation between the sidewalk and traffic lanes and improving pedestrians' ability to cross the street at midsegment locations (by adding a raised-curb median) have resulted in a lower LOS score, which indicates improved service relative to Example Problem 1. However, the pedestrian LOS letter (C) is unchanged.

Exhibit 29-61
 Example Problem 3:
 Facility Evaluation

		Facility Evaluation Summary	
Travel Direction		Eastbound	Westbound
Facility length, ft 5,280	Vehicle Level of Service		
	Base free-flow speed, mi/h	35.4	35.4
	Travel speed, mi/h	18.2	18.1
	Spatial stop rate, stops/mi	2.27	2.34
	Level of service	C	C
	Poorest perf. segment LOS	D	D
	Pedestrian Level of Service		
	Pedestrian space, ft ² /p	381.1	381.1
	Pedestrian travel speed, ft/s	3.4	3.4
	Pedestrian LOS score	2.92	2.92
	Level of service	C	C
	Poorest perf. segment LOS	C	C
	Bicycle Level of Service		
	Bicycle travel speed, mi/h	11.6	11.6
	Bicycle LOS score	4.15	4.15
	Level of service	D	D
	Poorest perf. segment LOS	D	D
	Transit Level of Service		
	Transit travel speed, mi/h	10.0	9.9
	Transit LOS score	3.39	3.39
Level of service	C	C	
Poorest perf. segment LOS	D	D	

The lack of a bicycle lane combined with a high traffic volume results in an overall bicycle LOS D for both directions of travel. The quality of service has degraded slightly, relative to Example Problem 1, but not enough to drop the LOS designation.

Transit travel speed is about 10 mi/h on the facility in each direction of travel. An overall LOS C is assigned to each direction. Conditions have degraded slightly, relative to Example Problem 1, but not enough to drop the transit LOS designation.

EXAMPLE PROBLEM 4: EXISTING URBAN STREET RELIABILITY

Objective

This example problem illustrates

- The steps involved in calculating reliability statistics for an urban street facility using the minimum required data for the analysis,
- Identification of the key reliability problems on the facility, and
- Diagnosis of the causes (e.g., demand, weather, incidents) of reliability problems on the facility.

Site

The selected site for this example problem is an idealized 3-mi-long principal arterial street located in Lincoln, Nebraska. The street is a two-way, four-lane, divided roadway with shoulders. There are seven signalized intersections that are spaced uniformly at 0.5-mi intervals along the street. The posted speed limit on the major street and the minor streets is 35 mi/h. A portion of this street is shown in Exhibit 29-62. The distances shown are the same for the other segments of the facility.

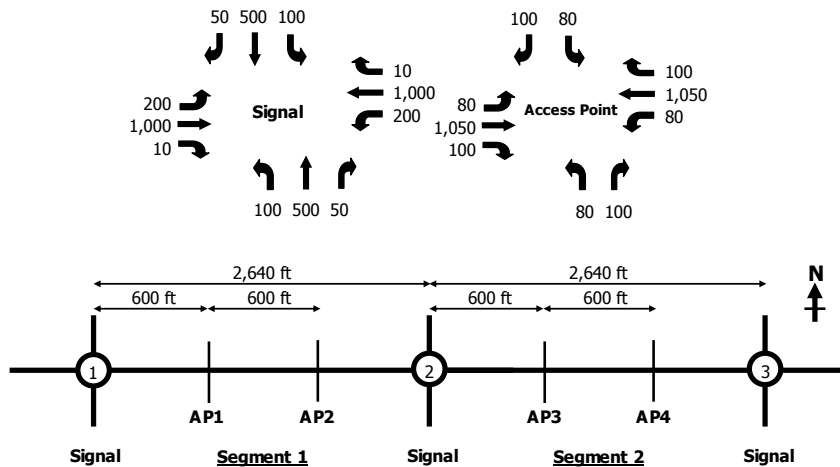


Exhibit 29-62
Example Problem 4:
Urban Street Facility

Also shown in Exhibit 29-62 are the traffic movement volumes for each intersection and access point on the facility. Each intersection has the same volume, and each access point has the same volume. Intersection geometry and signal timing are described in a subsequent section.

Required Input Data

This section describes the input data needed for both the reliability methodology and the core HCM urban streets methodology. The dataset that describes conditions under which no work zones or special events are present is known as the *base dataset*. Other datasets used to describe work zones or special events are called *alternative datasets*.

Reliability Methodology Input Data

Exhibit 29-63 lists the input data needed for an urban street reliability evaluation. The agency does not collect traffic volume data on a continual basis, so the factors and ratios that describe demand patterns will be defaulted. Traffic counts for one representative day are provided by the analysis and used as the basis for estimating volume during other hours of the year. Lincoln, Nebraska, is one of the communities for which a 10-year summary of weather data is provided, so the default weather data will be used. Incident data are available locally as annual crash frequencies by intersection and street segment. It was determined that the effect of work zones or special events on reliability would not be considered in the evaluation.

HCM Urban Street Methodology Input Data

This subsection describes the data gathered to develop the base dataset. The base dataset contains all of the input data required to conduct an urban street facility analysis with the methodologies described in HCM Chapters 16 through 19. Alternative datasets are not needed because the effects of work zones and special events are not being considered in the evaluation.

Exhibit 29-63

Example Problem 4: Input Data Needs and Sources

Data Category	Input Data Need	Data Value
Functional class	Urban street functional class	Urban principal arterial
Nearest city	Required when defaulted weather data used	Lincoln, Nebraska
Geometrics	Presence of shoulder	Yes
Time periods	Analysis period	15 min
	Study period	7-10 a.m.
	Reliability reporting period	Weekdays for 1 year
Demand patterns	Hour-of-day factors	Will be defaulted
	Day-of-week demand ratio	
	Month-of year demand ratio	
	Demand change due to rain, snow	
Weather	Rain, snow, and temperature data by month	Will be defaulted
	Pavement runoff duration	
Incidents	Segment and intersection crash frequencies	Available locally (See Step 5)
	Crash frequency adjustment factors for work zones or special events	Not required (no work zones)
	Factors influencing incident duration	Will be defaulted
Work zones and special events	Changes to base conditions (alternative dataset) and schedule	Not required (no work zones)
Traffic counts	Day and time of traffic counts used in base and alternative datasets	Tuesday, January 4, 7-8 a.m. No alternative datasets required (no work zones)

Traffic count data for the hour beginning at 7:00 a.m. are available from a recent traffic count taken on a Tuesday, January 4. Weather conditions were clear and the pavement was dry. The traffic volumes are shown in Exhibit 29-62. They are the same at all seven intersections for this idealized example.

Exhibit 29-64 provides the signal timing data for Intersection 1. The other signalized intersections have the same signal timing.

Exhibit 29-64

Example Problem 4: Intersection 1 Signal Timing Data

Approach Movement	Eastbound			Westbound			Northbound			Southbound		
	L	T	R	L	T	R	L	T	R	L	T	R
NEMA movement no.	5	2	12	1	6	16	3	8	18	7	4	14
Volume (veh/h)	200	1000	10	200	1000	10	100	500	50	100	500	50
Lanes	1	2	1	1	2	1	1	2	0	1	2	0
Turn bay length (ft)	200	0	200	200	0	200	200	0	0	200	0	0
Saturation flow rate (veh/h/ln)	1,800	1,800	1,800	1,800	1,800	1,800	1,800	1,800	1,800	1,800	1,800	1,800
Platoon ratio	1.000	1.333	1.000	1.000	1.333	1.000	1.000	1.000	1.000	1.000	1.000	1.000
Initial queue (veh)	0	0	0	0	0	0	0	0	0	0	0	0
Speed limit (mi/h)	--	35	--	--	35	--	--	35	--	--	35	--
Detector length (ft)	40			40	--	--	40	40	--	40	40	--
Lead/lag left-turn phase	Lead	--		Lead	--		Lead	--		Lead	--	
Left-turn mode	Prot.	--		Prot.	--		Pr/Pm	--		Pr/Pm	--	
Passage time (s)	2.0	--		2.0	--		2.0	2.0		2.0	2.0	
Minimum green (s)	5	--		5	--		5	5		5	5	
Change period (Y+Rc) (s)	3.0	4.0		3.0	4.0		3.0	4.0		3.0	4.0	
Phase splits (s)	20.0	35.0		20.0	35.0		20.0	25.0		20.0	25.0	
Max. recall	Off	--		Off	--		Off	Off		Off	Off	
Min. recall	Off	--		Off	--		Off	Off		Off	Off	
Dual entry	No	Yes		No	Yes		No	Yes		No	Yes	
Simultaneous gap out	Yes	Yes		Yes	Yes		Yes	Yes		Yes	Yes	
Dallas phasing	No	No		No	No		No	No		No	No	
Reference phase	2											
Offset (s)	0 or 50											

Notes: L = left turn, T = through, R = right turn, Prot. = protected, Pr/Pm = permissive-protected. See Chapter 18 for definitions of signal timing variables.

At each signalized intersection, there are left- and right-turn bays on each of the two major-street approaches, left-turn bays on each of the minor-street approaches, and two through lanes on each approach. Two unsignalized access points exist between each signal.

The posted speed limit for the major street and the minor streets is 35 mi/h. The traffic signals operate in coordinated-actuated mode at a 100-s cycle. The offset for the eastbound through phase alternates between 0 and 50 s at successive intersections to provide good two-way progression.

The peak hour factor is 0.99, 0.92, 0.93, 0.94, 0.95, 0.96, and 0.97 at Intersections 1 through 7, respectively.

Analysis Replications

The urban street reliability method uses a Monte Carlo approach to generate variables describing weather events, incidents, and random demand fluctuations for each scenario in the reliability reporting period. One variation of this approach is to use an initial random number seed. The use of a seed number ensures that the same random number sequence is used each time a set of scenarios is generated for a given reliability reporting period. Any positive integer can be used as a seed value. Each set of scenarios is called a replication.

Because events (e.g., a storm, a crash) are generated randomly in the urban street method, the possibility exists that highly unlikely events could be overrepresented or underrepresented in a given set of scenarios. To minimize any bias these rare events may cause, the set of scenarios should be replicated and evaluated two or more times. Each time the set of scenarios is created, the inputs should be identical, except that a different set of random number seeds is used. Then, the performance measures of interest from the evaluation of each set of scenarios are averaged to produce the final performance results.

Five replications were found to provide sufficient precision in the predicted reliability measures for this example problem. The seed numbers in the following list were selected by the analyst for this example problem. The first replication used seed numbers 82, 11, and 63. The second replication used numbers 83, 12, and 64. This pattern continues for the other three replications.

- Weather event generator: 82, 83, 85, 87, 89
- Demand event generator: 11, 12, 14, 16, 18
- Incident event generator: 63, 64, 66, 68, 70

The random number sequence created by a specific seed number may be specific to the software implementation and computer platform used in the analysis. As a result, evaluating the same dataset and seed number in different software or on a different platform may produce results different from those shown here. Each result, though different, will be equally valid.

Computational Steps

This example problem proceeds through the following steps:

1. Establish the purpose, scope, and approach.
2. Code datasets.

A Monte Carlo approach is used when there is some randomness in the value of a variable due to unknown influences (and known influences by other variables that also have some randomness) such that it is difficult to determine the frequency (or probability) of the subject variable's value accurately.

Multiple analysis replications are needed to determine the confidence interval for the final performance results.

3. Estimate weather events.
4. Estimate demand volumes.
5. Estimate incident events.
6. Generate scenarios.
7. Apply the Chapter 16 motorized vehicle methodology.
8. Conduct quality control and error checking.
9. Interpret results.

Step 1: Establish the Purpose, Scope, and Approach

Define the Purpose

The agency responsible for this urban street wishes to perform a reliability analysis of existing conditions to determine whether the facility is experiencing significant reliability problems. It also wants to diagnose the primary causes of any identified reliability problems on the facility so that an improvement strategy can be developed.

Define the Reliability Analysis Box

The results from a preliminary evaluation of the facility were used to define the general spatial and temporal boundaries of congestion on the facility under fair weather, nonincident conditions. A study period consisting of the weekday morning peak period (7–10 a.m.) and a study area consisting of the 3-mi length of facility between Intersections 1 and 7 encompass all of the recurring congestion.

The reliability reporting period is to include all weekdays during the course of a year. The duration of the analysis period will be 15 min.

Select Reliability Performance Measures

Reliability will be reported by using the following performance measures: mean travel time index (TTI), 80th percentile TTI, 95th percentile TTI (PTI), reliability rating, and total delay (in vehicle hours) for the reliability reporting period.

Step 2: Code Datasets

Select Reliability Factors for Evaluation

The major causes of travel time reliability problems are demand surges, weather, and incidents. Reliability problems associated with work zones and special events were determined not to be key elements of the evaluation of this specific facility.

Code the Base Dataset

The base dataset was developed for the selected study section and study period. This dataset describes the traffic demand, geometry, and signal timing conditions for the intersections and segments on the subject urban street facility during the study period when no work zones are present and no special events occur. The data included in this dataset are described in Chapters 16 through 19.

Code the Alternative Datasets

Only the base dataset will be required because no work zones are planned in the next year and no special events affect the facility on weekdays.

Step 3: Estimate Weather Events

This step predicts weather event date, time, type (i.e., rain or snow), and duration for each study period day in the reliability reporting period.

Identify Input Data

The default weather data for Lincoln, Nebraska, are a compilation of 10 years of historical data from the National Climatic Data Center (2, 9) and include the following statistics:

- Total normal precipitation,
- Total normal snowfall,
- Number of days with precipitation of 0.01 in. or more,
- Normal daily mean temperature, and
- Precipitation rate.

One inch of snowfall is estimated to have the water content of 0.1 in. of rain. Exhibit 29-65 shows the historical weather data for 2 months of the year.

Weather Data	January	April
Normal precipitation ^a (in.)	0.67	2.90
Normal snowfall (in.)	6.60	1.50
Days with precipitation (days)	5	9
Daily mean temperature (°F)	22.40	51.20
Precipitation rate (in./h)	0.030	0.062

Note: ^a Rainfall plus water content of snow.

Determine Weather Events for Each Day

At this point in the analysis, weather is estimated for all days during a 2-year period. The analysis is not yet confined to the days within the reliability reporting period or the hours within the study period. The purpose of the extra calculations is to define the expected weather pattern for the study facility, which will be used in a later step to estimate incident frequencies.

A Monte Carlo approach is used to decide whether precipitation will occur in a given day. If it does, a Monte Carlo approach is also used to determine the type of precipitation (i.e., rain or snow), precipitation rate, total precipitation, and start time for the current day. The details of the scenario generation process are described in Section 2.

Exhibit 29-66 illustrates the results of the calculations for 2 weeks in January and 2 weeks in April. These results are based on the historical weather data for Lincoln, Nebraska, as shown in Exhibit 29-65. The random number values shown in the exhibit are intended to illustrate the computations within this specific table. Different values are obtained if the random number seed is changed. Only dates falling within the reliability reporting period are shown.

Exhibit 29-65

Example Problem 4: Sample Weather Data for Lincoln, Nebraska

Exhibit 29-66
Example Problem 4: Sample
Generated Weather Events

For reliability evaluation, total precipitation is assumed to be perfectly correlated with the precipitation rate such that storms producing a large total precipitation are associated with a high precipitation rate. This relationship is replicated by estimating both values by using the same random number.

As can be seen from Exhibit 29-66, the computed event durations may exceed 24 h, but when the end times are set for the event, any event that ends beyond 24:00 is truncated to 24:00.

Date	Precipitation RN R_p	Precipitation? (Yes/No)	Temperature RN RT_d	Mean Temperature (° F)	Snow/Rain?	Precipitation Rate RN RP_d	Precipitation Rate (in./h)	Total Precipitation RN RTP_d	Total Precipitation (in.)	Precipitation Start RN $RS_{d,m}$	Start of Precipitation Event	Precipitation Duration (h)	Time Wet After Precip. (h)	Day/Night?	Total Event Duration (h)	End of Precipitation	End of Wet Pavement
Jan 10	0.03	Yes	0.94	30	Snow	0.83	0.54	0.83	2.08	0.23	4:30	3.88	1.22	Night	5.10	8:23	9:36
Jan 11	0.00	Yes	0.22	19	Snow	0.62	0.29	0.62	0.27	0.21	4:45	0.95	1.28	Night	2.23	5:42	6:59
Jan 12	0.30	No															
Jan 13	0.90	No															
Jan 14	0.20	No															
Jan 24	0.00	Yes	0.89	28	Snow	0.09	0.03	0.09	0.01	0.12	3:00	0.01	1.23	Night	1.23	3:00	4:14
Jan 25	0.53	No															
Jan 26	0.45	No															
Jan 27	0.21	No															
Jan 28	0.60	No															
Apr 4	0.64	No															
Apr 5	0.24	Yes	0.11	45	Rain	0.40	0.03	0.40	0.02	1.00	23:15	0.68	0.07	Night	0.75	23:56	24:00
Apr 6	0.22	Yes	0.19	47	Rain	0.31	0.02	0.31	0.01	0.08	1:45	0.34	0.92	Night	1.26	2:05	3:00
Apr 7	0.78	No															
Apr 8	0.39	No															
Apr 11	0.55	No															
Apr 12	0.37	No															
Apr 13	0.10	Yes	0.28	48	Rain	0.82	0.11	0.82	0.54	0.39	7:15	5.05	0.72	Day	5.76	12:18	13:01
Apr 14	0.78	No															
Apr 15	0.27	Yes	0.98	61	Rain	0.73	0.08	0.73	0.30	0.57	11:30	3.62	0.66	Day	4.28	15:07	15:47

Note: RN = random number.

Determine Weather Events for Each Analysis Period

The days that have weather events are subsequently examined to determine whether the event occurs during the study period. Specifically, each analysis period is examined to determine whether it is associated with a weather event. An examination of the start and end times in Exhibit 29-66 indicates that the snow on January 10 and the rain on April 13 occur during the 7:00 to 10:00 a.m. study period.

Step 4: Estimate Demand Volumes

This step identifies the appropriate traffic volume adjustment factors (demand ratios) for each date and time during the reliability reporting period. These factors are used during the scenario file generation procedure to estimate the volume associated with each analysis period. If the analyst does not provide demand ratios based on local data, the default ratios provided in Section 5, Applications, of Chapter 17 are used.

Identify Input Data

The input data needed for this step are identified in the following list:

- Hour-of-day demand ratio,

- Day-of-week demand ratio,
- Month-of-year demand ratio,
- Demand change factor for rain event, and
- Demand change factor for snow event.

The default values for these factors are obtained from Exhibit 17-5 to Exhibit 17-8. Their selection is based on the functional class of the subject facility, which is “urban principal arterial.”

Determine Base Demand Ratio

First, the demand ratios for the day of the traffic count are determined. The count was taken on Tuesday, January 4, during the 7:00 a.m. hour. By using the default demand ratio data from Exhibit 17-5 through Exhibit 17-7, the following can be seen:

- The hour-of-day ratio for the 7:00 a.m. hour for principal arterials is 0.071,
- The day-of-week ratio for Tuesdays is 0.98, and
- The month-of-year ratio for principal arterials in January is 0.831.

Multiplying these three factors together yields the base demand ratio of 0.0578. This ratio indicates that counted traffic volumes represent 5.78% of annual average daily traffic (AADT), if this urban street’s demand pattern is similar to that of the default demand data.

Determine Analysis Period Demand Ratio

A similar process is used to determine the demand ratio represented by each analysis period, except that an additional adjustment is made for weather. From Exhibit 17-8, a default 1.00 demand adjustment factor is applied to analysis periods with rain and a 0.80 adjustment factor is applied to analysis periods with snow.

As an example, the weather generator produced snow conditions for Monday, January 10, at 7:00 a.m. Default demand ratio data are obtained again from Exhibit 17-5 through Exhibit 17-7. The text accompanying Exhibit 17-8 states that a demand change factor of 0.80 is appropriate for snowing conditions. Therefore, the factor values in the following list are established for the evaluation:

- The hour-of-day ratio for the 7:00 a.m. hour for principal arterials is 0.071,
- The day-of-week ratio for Mondays is 0.98,
- The month-of-year ratio for principal arterials in January is 0.831, and
- The demand change factor is 0.80.

Multiplying these factors together yields the demand ratio of 0.0463. This ratio indicates that the analysis period volumes represent 4.63% of AADT. Therefore, the traffic counts are multiplied by $(0.0463 / 0.0578) = 0.800$ to produce equivalent volumes for the hour starting at 7:00 a.m. on Monday, January 10.

Exhibit 29-67 shows a selection of demand profile computations for different hours, days, months, and weather events. Each row in this exhibit corresponds to

one analysis period (i.e., scenario). The ratio shown in the last column of this exhibit is multiplied by the traffic counts for each signalized intersection to estimate the equivalent hourly flow rate for the associated analysis period.

Exhibit 29-67
Example Problem 4: Sample Demand Profile Calculations

Date	Weekday	Time	Weather	Weather Factor	Hour Factor	Day Factor	Month Factor	Total Factor	Total/Base
Jan 10	Mon	7:00	Snow	0.80	0.071	0.980	0.831	0.0463	0.800
Jan 10	Mon	7:15	Snow	0.80	0.071	0.980	0.831	0.0463	0.800
Jan 10	Mon	7:30	Snow	0.80	0.071	0.980	0.831	0.0463	0.800
Jan 10	Mon	7:45	Snow	0.80	0.071	0.980	0.831	0.0463	0.800
Jan 10	Mon	8:00	Snow	0.80	0.058	0.980	0.831	0.0378	0.654
Jan 10	Mon	8:15	Snow	0.80	0.058	0.980	0.831	0.0378	0.654
Jan 10	Mon	8:30	Dry	1.00	0.058	0.980	0.831	0.0472	0.817
Jan 10	Mon	8:45	Dry	1.00	0.058	0.980	0.831	0.0472	0.817
Jan 10	Mon	9:00	Dry	1.00	0.047	0.980	0.831	0.0383	0.662
Jan 10	Mon	9:15	Dry	1.00	0.047	0.980	0.831	0.0383	0.662
Jan 10	Mon	9:30	Dry	1.00	0.047	0.980	0.831	0.0383	0.662
Jan 10	Mon	9:45	Dry	1.00	0.047	0.980	0.831	0.0383	0.662
Apr 6	Wed	7:00	Dry	1.00	0.071	1.000	0.987	0.0701	1.212
Apr 6	Wed	7:15	Dry	1.00	0.071	1.000	0.987	0.0701	1.212
Apr 6	Wed	7:30	Dry	1.00	0.071	1.000	0.987	0.0701	1.212
Apr 6	Wed	7:45	Dry	1.00	0.071	1.000	0.987	0.0701	1.212
Apr 6	Wed	8:00	Dry	1.00	0.058	1.000	0.987	0.0572	0.990
Apr 6	Wed	8:15	Dry	1.00	0.058	1.000	0.987	0.0572	0.990
Apr 6	Wed	8:30	Dry	1.00	0.058	1.000	0.987	0.0572	0.990
Apr 6	Wed	8:45	Dry	1.00	0.058	1.000	0.987	0.0572	0.990
Apr 6	Wed	9:00	Dry	1.00	0.047	1.000	0.987	0.0464	0.802
Apr 6	Wed	9:15	Dry	1.00	0.047	1.000	0.987	0.0464	0.802
Apr 6	Wed	9:30	Dry	1.00	0.047	1.000	0.987	0.0464	0.802
Apr 6	Wed	9:45	Dry	1.00	0.047	1.000	0.987	0.0464	0.802

Step 5: Estimate Incident Events

The procedure described in this step is used to predict incident event dates, times, and durations. It also determines each incident event’s type (i.e., crash or noncrash), severity level, and location on the facility. The procedure uses weather event and demand variation information from the two previous steps as part of the incident prediction process. Crash frequency data are used to estimate the frequency of both crash-related incidents and non-crash-related incidents.

For an urban street reliability evaluation, incidents are categorized as being

- Segment-related or
- Intersection-related.

These two categories are mutually exclusive.

Identify Input Data

Incident frequency data. Three-year average crash frequencies are determined from locally available crash records for each segment and intersection along the facility. These averages are shown in Exhibit 29-68. The frequency of noncrash incidents is estimated from the crash frequency data in a subsequent step. Noncrash incident frequency is not an input quantity due to the difficulty agencies have in acquiring noncrash incident data.

Location	Crash Frequency (crashes/year)
Segment 1-2 (Intersections 1 to 2)	15
Segment 2-3 (Intersections 2 to 3)	16
Segment 3-4 (Intersections 3 to 4)	17
Segment 4-5 (Intersections 4 to 5)	18
Segment 5-6 (Intersections 5 to 6)	19
Segment 6-7 (Intersections 6 to 7)	20
Intersection 1	32
Intersection 2	33
Intersection 3	34
Intersection 4	35
Intersection 5	36
Intersection 6	37
Intersection 7	38

Exhibit 29-68

Example Problem 4: Locally Available Crash Frequency Data

Work zone/special event crash frequency adjustment factors. Work zones and special events are not being considered in this example; therefore, these crash frequency adjustment factors do not need to be provided.

Weather event crash frequency adjustment factors. The default crash frequency adjustment factors given in Exhibit 17-9 are used.

Incident duration factors. The default incident detection and response times given in Exhibit 17-9 and the default clearance times given in Exhibit 17-10 are used.

Incident distribution. The default incident distribution given in Exhibit 17-11 for urban street facilities with shoulders is used.

Compute Equivalent Crash Frequency for Weather

This step converts the average crash frequencies (supplied as input data) into the equivalent crash frequencies for each weather type.

First, the input crash frequency data for segments and intersections are converted into an equivalent crash frequency for each of the following weather conditions: clear and dry, rainfall, wet pavement (not raining), and snow or ice on pavement (not snowing). This conversion is based on the number of hours during a 2-year period that a particular weather condition occurs and the crash adjustment factor corresponding to each weather condition. For this example problem, the number of hours in a year with a particular weather condition is determined from the default weather data for Lincoln, Nebraska.

The equivalent crash frequency when every day is dry for street location *i* is computed with Equation 29-13 and Equation 29-14.

Exhibit 29-69 illustrates the computations of the equivalent crash frequencies by weather type for two segments and three intersections. The calculations are similar for the other segments and intersections.

Exhibit 29-69

Example Problem 4:
Computation of Crash
Frequency by Weather Type

Variable	Definition	Segments		Intersections		
		1-2	2-3	1	2	3
$FC_{str(i)}$	Observed average crash frequency	15	16	65	66	67
N_y	Number of years	2	2	2	2	2
Nh_{dry}	Hours of dry weather	17026.98	17026.98	17026.98	17026.98	17026.98
Nh_{rf}	Hours of rainfall	278.22	278.22	278.22	278.22	278.22
Nh_{wp}	Hours of wet pavement	104.33	104.33	104.33	104.33	104.33
Nh_{sf}	Hours of snowfall	64.61	64.61	64.61	64.61	64.61
Nh_{sp}	Hours of snow or ice on pavement	45.86	45.86	45.86	45.86	45.86
Crash frequency adjustment factors for...						
$CFAF_{rf}$	Rainfall	2.0	2.0	2.0	2.0	2.0
$CFAF_{wp}$	Wet pavement	3.0	3.0	3.0	3.0	3.0
$CFAF_{sf}$	Snowfall	1.5	1.5	1.5	1.5	1.5
$CFAF_{sp}$	Snow or ice on pavement	2.75	2.75	2.75	2.75	2.75
Calculated crash frequencies for...						
$FC_{str(i),dry}$	Dry weather	14.50	15.47	30.94	31.91	32.88
$FC_{str(i),rf}$	Rainfall	29.01	30.94	61.89	63.82	65.75
$FC_{str(i),wp}$	Wet pavement	43.51	46.41	92.83	95.73	98.63
$FC_{str(i),sf}$	Snowfall	21.76	23.21	46.41	47.86	49.32
$FC_{str(i),sp}$	Snow or ice on pavement	39.89	42.54	85.09	87.75	90.41

Note: Total hours of dry, rainfall, wet pavement, snowfall, and snow or ice on pavement = 17,520 h (2 years).

Establish Crash Frequency Adjustment Factors for Work Zones or Special Events

This step is skipped because work zones and special events are not being considered for this evaluation.

Determine Whether an Incident Occurs

This step goes through each of the 24 h of each day that is represented in the reliability reporting period. For each hour, whether an incident occurs is determined. If an incident occurs, its duration is also determined. Finally, for each incident identified in this manner, whether some portion (or all) of the incident occurs during a portion of the study period is determined.

Weather-adjusted incident frequencies. First, for a given hour in a given day, the weather event data are checked to see which weather condition (dry, rainfall, snowfall, wet pavement and not raining, or snow or ice on pavement and not snowing) was generated for that hour. The expected incident frequencies for street locations (i.e., segments and intersections) $Fi_{str(i),wea(h,d)}$ are determined from (a) the corresponding crash frequency for the given weather condition $FC_{str(i),wea}$ (from a previous step) and (b) a factor $pc_{str,wea}$ relating total crashes to total incidents for the given weather condition (from the default values in the third column of Exhibit 17-11). If a special event or work zone was present on the given hour and day, the expected incident frequency is multiplied by the segment or intersection (as appropriate) crash frequency adjustment factor $CFAF_{str}$ specified by the analyst for special events and work zones. Equation 29-15 is used to compute the expected incident frequency:

$$Fi_{str(i),wea(h,d)} = CFAF_{str} \frac{FC_{str(i),wea}}{pc_{str,wea}}$$

For example, weather was dry on Wednesday, April 6, at 9:00 a.m. For Segment 1-2, the equivalent crash frequency for dry weather is 14.50 crashes/year (from Exhibit 29-69). The ratio of crashes to incidents for segments in dry weather is 0.358. There is no work zone or special event, so the crash adjustment factor is 1.0. Then

$$F_{i_{seg1-2,dry}} = (1.0) \frac{(14.50)}{(0.358)} = 40.5 \text{ incidents/year}$$

Similarly, snow was falling on Monday, January 10, at 7:00 a.m. The equivalent crash frequency for snowfall on Segment 1-2 is 21.76 crashes/year. The ratio of crashes to incidents for segments in snowy weather is 0.358. Therefore,

$$F_{i_{seg1-2,sf}} = (1.0) \frac{(21.76)}{(0.358)} = 60.8 \text{ incidents/year}$$

Conversion to hourly frequencies. Next, the incident frequency $F_{i_{str(i),wea(h,d)}}$ is converted to an hourly frequency $f_{i_{str(i),wea(h,d),h,d}}$ by multiplying it by the percent of annual demand represented by the hour and by dividing by the number of days in a year (expressed as a ratio of hours). The same hour-of-day $f_{hod,h,d}$, day-of-week $f_{dow,d}$, and month-of-year $f_{moy,d}$ demand ratios used in Step 4 are used here. Equation 29-16 is used, where “8,760” represents the number of hours in a year and “24” represents the number of hours in a day.

$$f_{i_{str(i),wea(h,d),h,d}} = \frac{F_{i_{str(i),wea(h,d)}}}{8,760} (24 f_{hod,h,d}) f_{dow,d} f_{moy,d}$$

The month-of-year demand ratio for April is 0.987, the day-of-week demand ratio for Wednesday is 1.00, and the hour-of-day demand ratio for 9:00 a.m. is 0.047. The incident frequency for this day and time is calculated above as 40.5 incidents per year. Therefore, the equivalent hourly incident frequency for Segment 1-2 on Wednesday, April 6, at 9:00 a.m. is

$$f_{i_{seg1-2,dry,0900,Apr06}} = \frac{(40.5)}{8,760} (24 \times 0.047)(1.00)(0.987) = 0.00515 \text{ incidents/h}$$

Similarly, the equivalent hourly incident frequency for Segment 1-2 on Monday, January 10, at 7:00 a.m. is

$$f_{i_{seg1-2,sf,0700,Jan10}} = \frac{(60.8)}{8,760} (24 \times 0.071)(0.98)(0.831) = 0.00963 \text{ incidents/h}$$

Probability of no incidents. Incidents for a given day, street location, incident type, and hour of day are assumed to follow a Poisson distribution, as given in Equation 29-17.

Exhibit 29-70 demonstrates the determination of incidents for Segment 1-2 on April 6 for the 9:00 a.m. hour. Exhibit 29-71 does the same for January 10 for the 7:00 a.m. hour.

If more than one incident occurs at the same time and location, the more serious incident is considered in the methodology. During an incident, the methodology requires that at least one lane remain open in each direction of travel on a segment and on each intersection approach. If the number of lanes blocked by an incident is predicted to equal the number of lanes available on the segment or intersection approach, one lane is maintained open and the remaining lanes are blocked. For example, if the segment has two lanes in the subject travel direction and an incident occurs and is predicted to block two lanes, the incident is modeled as blocking only one lane.

Exhibit 29-70

Example Problem 4: Incident Determination for April 6, 9:00 a.m., for Segment 1-2

Incident Type			Incident Proportion	Hourly Incident Frequency	exp (-fi x pi)	Random Number	Incident ?
Crash	1 lane	Fatal/injury	0.036	0.00515	0.99981	0.90019	No
Crash	1 lane	PDO	0.083	0.00515	0.99957	0.38078	No
Crash	2 lane	Fatal/injury	0.028	0.00515	0.99986	0.90860	No
Crash	2 lane	PDO	0.030	0.00515	0.99984	0.06081	No
Crash	Shoulder	Fatal/injury	0.021	0.00515	0.99990	0.82183	No
Crash	Shoulder	PDO	0.016	0.00515	0.99918	0.34916	No
Noncrash	1 lane	Breakdown	0.456	0.00515	0.99766	0.99900	Yes
Noncrash	1 lane	Other	0.089	0.00515	0.99954	0.59842	No
Noncrash	2 lane	Breakdown	0.059	0.00515	0.99970	0.69323	No
Noncrash	2 lane	Other	0.017	0.00515	0.99991	0.08131	No
Noncrash	Shoulder	Breakdown	0.014	0.00515	0.99993	0.13012	No
Noncrash	Shoulder	Other	0.007	0.00515	0.99996	0.44620	No

Notes: Incident proportions total 100%. PDO = property damage only.
Random numbers have been selected to illustrate this particular step of the computations. They are not necessarily the same results that would be achieved in a full run of the procedure.

Exhibit 29-71

Example Problem 4: Incident Determination for January 10, 7:00 a.m., for Segment 1-2

Incident Type			Incident Proportion	Hourly Incident Frequency	exp (-fi x pi)	Random Number	Incident ?
Crash	1 lane	Fatal/injury	0.036	0.00963	0.99965	0.21041	No
Crash	1 lane	PDO	0.083	0.00963	0.99920	0.83017	No
Crash	2 lane	Fatal/injury	0.028	0.00963	0.99973	0.58437	No
Crash	2 lane	PDO	0.030	0.00963	0.99971	0.80487	No
Crash	Shoulder	Fatal/injury	0.021	0.00963	0.99981	0.35441	No
Crash	Shoulder	PDO	0.016	0.00963	0.99846	0.64888	No
Noncrash	1 lane	Breakdown	0.456	0.00963	0.99562	0.40513	No
Noncrash	1 lane	Other	0.089	0.00963	0.99914	0.98428	No
Noncrash	2 lane	Breakdown	0.059	0.00963	0.99943	0.61918	No
Noncrash	2 lane	Other	0.017	0.00963	0.99983	0.13712	No
Noncrash	Shoulder	Breakdown	0.014	0.00963	0.99987	0.30502	No
Noncrash	Shoulder	Other	0.007	0.00963	0.99993	0.33279	No

Note: Incident proportions total 100%. PDO = property damage only.
Random numbers have been selected to illustrate this particular step of the computations. They are not necessarily the same results that would be achieved in a full run of the procedure.

Determine Incident Duration

If the result of the previous step indicates that an incident occurs in a given segment or intersection during a given hour and day, the incident duration is then determined randomly from a gamma distribution by using the average incident duration and the standard deviation of incident duration as inputs. These values are supplied as input data.

The duration is used in a subsequent step to determine which analysis periods are associated with an incident. The incident duration is rounded to the nearest quarter hour for 15-min analysis periods. This rounding is performed to ensure the most representative match between event duration and analysis period start and end times. This approach causes events that are shorter than one-half the analysis period duration to be ignored (i.e., they are not recognized in the scenario generation process).

Exhibit 29-70 shows that a noncrash, one-lane, breakdown incident was generated for Segment 1-2 on April 6 starting at the 9:00 a.m. hour. Exhibit 29-72 shows the inputs into the incident duration calculation and the result. As with other computations in this example problem involving random numbers, different values are obtained if the random number seed is changed.

Variable	Value
Location	Segment 1-2
Incident type	Noncrash
Number of lanes involved	1-lane
Incident severity	Breakdown
Weather	Dry
Incident detection time (min)	2.0
Incident response time, dry weather (min)	15.0
Incident clearance time (min)	10.8
Average incident duration (min)	27.8
Standard deviation of incident duration (min)	22.2
Average incident duration (h)	0.463
Standard deviation of incident duration (h)	0.371
Random number	0.57455
Gamma function alpha parameter (mean ² /variance)	1.5625
Gamma function beta parameter (variance/mean)	0.2965
Duration (h)	0.433
Rounded duration (nearest 15 min) (h)	0.50
Incident start time	9:00
Incident end time	9:30

Exhibit 29-72

Example Problem 4: Sample Calculation of Incident Duration

Determine Incident Location

If an incident occurs at a segment or intersection during a given hour and day, its location is determined in this step. For intersections, the location is one of the intersection legs. For segments, the location is one of the two segment travel directions.

In the case of the incident identified on Segment 1-2 at 9:00 a.m. on April 6, the two directions of the segment have equal traffic volumes (see Exhibit 29-62) and therefore have equal probability of having the incident occur. This time, the scenario generator randomly assigned the incident to the westbound direction (identified as being associated with NEMA Phase 6 at the intersection).

Identify Analysis Period Incidents

The preceding steps of the incident estimation procedure are repeated for each hour of each day in the reliability reporting period. During this step, the analysis periods associated with an incident are identified. Specifically, each hour of the study period is examined to determine whether it coincides with an incident. If an incident occurs, its event type, lane location, severity, and street location are identified and recorded. Each subsequent analysis period coincident with the incident is also recorded.

Step 6: Generate Scenarios

This step uses the results from Steps 3 to 5 to create one scenario for each analysis period in the reliability reporting period. The base dataset coded in Step 2 represents the “seed” file from which the new scenarios are created.

As discussed previously, each analysis period is considered to be one scenario. There are 3,120 analysis periods in the reliability reporting period (= 4 analysis periods/hour × 3 hours/day × 5 days/week × 52 weeks/year × 1 year/reporting period). Thus, there are 3,120 scenarios.

Each scenario created in this step includes the appropriate adjustments to segment running speed and intersection saturation flow rate associated with the weather events or incidents that are predicted to occur during the corresponding

analysis period. If an analysis period has an incident, the number of lanes is reduced, the saturation flow rate is adjusted for affected intersection lanes, and a free-flow speed adjustment factor is applied to the affected lanes in the segment. If an analysis period has rainfall, snowfall, wet pavement, or snow or ice on the pavement, the saturation flow rate is adjusted for all intersections, the free-flow speed is adjusted for all segments, and the left-turn critical headways are adjusted for all intersections.

The traffic demand volumes in each dataset are adjusted for monthly, weekly, and hourly variations.

Step 7: Apply the Chapter 16 Motorized Vehicle Methodology

The analysis methodology for urban street facility evaluation is applied to each scenario generated in the previous step. At the conclusion of this step, the delay and queue length for each intersection, as well as the speed and travel time for each segment, are computed for each scenario.

Step 8: Conduct Quality Control and Error Checking

The quality control of thousands of scenarios is difficult, so it is recommended that the analyst focus on error checking and quality control on the base dataset. The results should be error-checked to the analyst's satisfaction to ensure that they accurately represent real-world congestion on the facility under recurring demand conditions with no incidents and under dry weather conditions. The same criteria for error checking should be used as for a conventional HCM analysis, but with the recognition that any error in the base dataset will be crucial, because it will be reproduced thousands of times by the scenario generator.

The total delay for each scenario should be scanned to identify the study periods likely to be associated with exceptionally long queues. For a given study period, the final queue on each entry intersection approach for the last analysis period should not be longer than the corresponding initial queue for the first analysis period. The study period duration should be increased (i.e., started earlier, ended later) such that this condition is satisfied. Ideally, the study period is sufficiently long that these reference initial and final queues both equal zero. An efficient approach for making this check is to start by evaluating the scenario with the largest total delay.

Step 9: Interpret Results

This step examines the reliability results for the existing facility. These results are listed in Exhibit 29-73. Although both travel directions have the same volume and capacity, several of the values in this exhibit vary slightly by travel direction because of the use of Monte Carlo methods.

The vehicle miles traveled (VMT) is computed for each scenario and added for all scenarios in the reliability reporting period. This statistic describes overall facility utilization for the reliability reporting period.

Measure	Eastbound	Westbound
Vehicle miles traveled ^a	2,260	2,257
Number of scenarios ^a	3,120	3,120
Base free-flow travel time ^b (s)	262.9	262.9
Mean TTI ^b	1.69	1.64
80th percentile TTI	1.57	1.56
95th percentile TTI (PTI)	2.98	2.61
Reliability rating	93.2	94.1
Total delay ^b (veh-h)		72.0

Notes: ^aThis statistic represents a total for the reliability reporting period.
^bThis statistic represents an average of the value for each scenario (i.e., an average value for all scenarios).

Exhibit 29-73
 Example Problem 4: Reliability
 Performance Measure Results

The travel time indices shown in Exhibit 29-73 were computed by finding the average (i.e., mean), 80th, and 95th percentile travel times for a given direction of travel across all scenarios and dividing by the facility’s base free-flow speed. Since hourly demands, geometry, weather, and signal timings are identical in both directions, the differences between the indices illustrate the effects of random variation in incidents and 15-min demands for the two directions.

The reliability rating describes the percent of VMT on the facility associated with a TTI less than 2.5. A facility that satisfies this criterion during a given scenario is likely to provide LOS D or better for that scenario. The reliability ratings shown in the exhibit indicate that more than 90% of the vehicle miles of travel on the facility are associated with LOS D or better.

The total delay (in vehicle hours) combines the delay per vehicle and volume of all intersection lane groups at each intersection during a scenario. This statistic increases with an increase in volume or delay. It is the only statistic of those listed in Exhibit 29-73 that considers the performance of all traffic movements (i.e., the other measures consider just the major-street through movement). Hence, it is useful for quantifying the overall change in operation associated with a strategy. When considered on a scenario-by-scenario basis, this statistic can be used to identify those scenarios with extensive queuing on one or more “entry” approaches (i.e., the cross-street intersection approaches and the major-street approaches that are external to the facility).

Exhibit 29-74 shows the travel time distribution for the facility’s eastbound travel direction. That for the westbound direction has a similar shape. The longer travel times tend to be associated with poor weather. The longest travel times coincide with one or more incidents and poor weather.

The reliability methodology was repeated several times to examine the variability in the reliability performance measures. Each replication used the same input data, with the exception that the three random numbers were changed for each replication. Exhibit 29-75 shows the predicted average and 95th percentile travel times for the eastbound travel direction based on five replications.

Exhibit 29-74
 Example Problem 4:
 Eastbound Travel Time
 Distribution

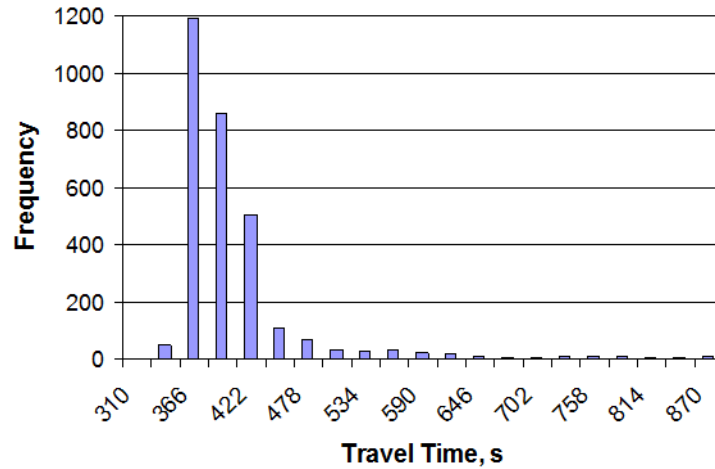


Exhibit 29-75
 Example Problem 4:
 Confidence Interval
 Calculation for Eastbound
 Direction

Replication	Average Travel Time (s)	95th Percentile Travel Time (s)
1	443.7	783.8
2	441.4	787.5
3	432.8	758.4
4	439.3	740.0
5	433.7	772.9
Average	438.2	768.5
Standard deviation	4.79	19.6
95th% confidence interval	432.2–444.1 (±1.36%)	744.4–792.8 (±3.16%)

The last three rows of Exhibit 29-75 show the statistics for the sample of five observations. The 95th percentile confidence interval was computed by using Equation 17-3. The confidence interval for the average travel time is 432.2 to 441.1 s, which equates to ±1.36% of the overall average travel time. Similarly, the confidence interval for the 95th percentile travel time is ±3.16% of the average of the 95th percentile travel times. This confidence interval is larger than that of the average travel time because the 95th percentile travel time tends to be influenced more by the occurrence of incidents and poor weather. As suggested by the formulation of Equation 17-3, the confidence interval can be reduced in width by increasing the number of replications.

The contribution of demand, incidents, and weather to total vehicle hours of delay (VHD) during the reliability reporting period is used to determine the relative contributions of each factor to the facility’s reliability. The annual VHD takes into account both the severity of the event and its likelihood of occurrence. VHD is computed by identifying the appropriate category for each scenario and adding the estimated VHD for each scenario in this category. The results are summed for all scenarios in each category in the reliability reporting period. They are presented in Exhibit 29-76 and Exhibit 29-77. The categories have been condensed to facilitate the diagnosis of the primary causes of reliability problems on the urban street. Demand has been grouped into two levels. All foul weather and incident scenarios have been grouped into a single category each.

An examination of the cell values in Exhibit 29-77 yields the conclusion that the single most significant cause of annual delay on the urban street example is high demand, which accounts for 53.6% of annual delay during fair weather with

no incidents. Incidents or bad weather collectively account for 22.9% of annual delay on the facility (17.8% + 7.3% + 2.8% – 5.1% – 0.0%).

	Total Delay by Demand and Weather (veh-h)				
	Low Demand		High Demand		Total
	Fair Weather	Foul Weather	Fair Weather	Foul Weather	
No incidents	52,957	6,337	120,393	5,025	184,712
Incidents	5,865	23	22,714	11,437	40,039
Total	58,822	6,360	143,107	16,462	224,751

	Low Demand		High Demand		Total
	Fair Weather	Foul Weather	Fair Weather	Foul Weather	
No incidents	23.6%	2.8%	53.6%	2.2%	82.2%
Incidents	2.6%	0.0%	10.1%	5.1%	17.8%
Total	26.2%	2.8%	63.7%	7.3%	100.0%

Exhibit 29-76

Example Problem 4: Annual VHD by Cause

Exhibit 29-77

Example Problem 4: Percentage of Annual VHD by Cause

EXAMPLE PROBLEM 5: URBAN STREET STRATEGY EVALUATION

Objective

This example problem illustrates an application of the reliability methodology for alternatives analysis. The objective is to demonstrate the utility of reliability information in evaluating improvement strategies. The strategies considered in this example involve changes in the urban street’s geometric design or its signal operation. These changes are shown to affect traffic operation and safety, both of which can influence reliability.

Site

The same urban street described in Example Problem 4 is used in this example problem.

Required Input Data

The same types of required input data described in Example Problem 4 are used here. The conditions described in Example Problem 4 are used as the starting point for evaluating each of three strategies that have been identified as having the potential to improve facility reliability. One base dataset is used to describe the “existing” facility of Example Problem 4, while one base dataset is associated with each strategy, resulting in a total of four base datasets. Specific changes to the Example Problem 4 base dataset required to represent each strategy are described later. The three strategies are as follows:

1. Shift 5 s from the cross-street left-turn phase to the major-street through phase.
2. Change the major-street left-turn mode from protected-only to protected-permitted.
3. Eliminate major-street right-turn bays and add a second lane to major-street left-turn bays.

These strategies were formulated to address a capacity deficiency for the major-street through movements at each intersection. This deficiency was noted as part of the analysis described in Example Problem 4. The change associated with each strategy was implemented at each of the seven intersections on the street.

For this example problem, the changes needed to implement the strategies require changes only to the base datasets. However, some strategies may require changes to the reliability methodology input data, the base datasets, or the alternative datasets.

Computational Steps

This example problem proceeds through the following steps:

1. Establish the purpose, scope, and approach.
2. Code datasets.
3. Generate scenarios.
4. Apply the Chapter 16 motorized vehicle methodology.
5. Interpret results.

Step 1: Establish the Purpose, Scope, and Approach

Define the Purpose

The agency responsible for this urban street wishes to perform a reliability analysis of existing conditions to determine which of the three strategies offers the greatest potential for improvement in facility reliability.

Define the Reliability Analysis Box

The results from a preliminary evaluation of the facility were used to define the general spatial and temporal boundaries of congestion on the facility under fair weather, nonincident conditions. A study period consisting of the weekday morning peak period (7–10 a.m.) and a study area consisting of the 3-mi length of facility between Intersections 1 and 7 encompass all of the recurring congestion.

The reliability reporting period is desired to include all weekdays during the course of a year. The duration of the analysis period will be 15 min.

Select Reliability Performance Measures

Reliability will be reported by using the following performance measures: mean TTI, 80th percentile TTI, 95th percentile TTI (PTI), reliability rating, and total delay (in vehicle hours) for the reliability reporting period.

Step 2: Code Datasets

Code the Base Dataset

The first base dataset represents existing conditions and is identical to the base dataset described in Example Problem 4. This base dataset was modified as follows to create a new base dataset (three in all) for each strategy being evaluated:

- The signal timing parameters for the Strategy 1 base dataset were modified at each intersection to reduce the phase splits for the minor-street left-turn movements by 5 s and to increase the phase splits for the major-street through movements by 5 s.
- The signal timing parameters for the Strategy 2 base dataset were modified at each intersection to change the major-street left-turn mode

from protected-only to protected-permitted. Furthermore, Chapter 12 of the *Highway Safety Manual (10)* indicates that intersection crash frequency increases by 11% on average when this change is made. Therefore, the crash frequency input data for each intersection were increased to reflect this change.

- The geometric parameters for the Strategy 3 base dataset were modified at each intersection to eliminate the major-street right-turn bays and to add a second lane to the major-street left-turn bays. Furthermore, Chapter 12 of the *Highway Safety Manual (10)* indicates that intersection crash frequency increases by 9% for this change. Therefore, the crash frequency input data for each intersection were increased to reflect this change.

Code the Alternative Datasets

Since no work zones are planned in the next year and no special events affect the facility on weekdays, only the base datasets will be required.

Step 3: Generate Scenarios

During this step, the reliability methodology is used to create one scenario for each analysis period in the reliability reporting period. The base datasets coded in Step 2 represent the “seed” files from which the scenarios associated with each strategy are created. As in Example Problem 4, one set of 3,120 scenarios is created for the existing facility. Additional sets of 3,120 scenarios are created for each of the three strategies.

Step 4: Apply the Chapter 16 Motorized Vehicle Methodology

The analysis methodology for urban street facility evaluation is applied to each scenario generated in the previous step, as described in Example Problem 4.

Step 5: Interpret Results

This step examines the reliability results for the facility. Initially, the results for the existing facility are described. Then, the results for each of the three strategies are summarized and compared with those of the existing facility. The formulation of these strategies was motivated by an examination of the results for the existing facility. The examination indicated that the major-street through movements had inadequate capacity during the morning peak traffic hour for several high-volume months of the year.

Results for the Existing Facility

The results for the existing facility are the same as for Example Problem 4, given previously in Exhibit 29-73 through Exhibit 29-77.

Results for Strategy 1

In Strategy 1, 5 s are taken from the cross-street left-turn phase split. This change increases the time available to the major-street through (i.e., coordinated) phase and increases the through movement capacity. The results for this strategy are listed in Exhibit 29-78. The first two rows list the average values obtained

Exhibit 29-78
Example Problem 5: Results
for Strategy 1

from five replications. The third row lists the change in the performance measure value. The last row indicates whether the change is statistically significant.

Case	Travel Time (s)		Total Delay (veh-h)	Reliability Rating
	Average	95th Percentile		
Existing	438.2	768.5	70.7	93.2
Strategy 1	400.7	542.2	66.2	96.8
Change	-37.5	-226.3	-4.5	3.6
Significant?	Yes	Yes	Yes	Yes

Note: Results based on five replications.

The statistics in Exhibit 29-78 indicate that the strategy produces a relatively large improvement in travel time, particularly in the 95th percentile travel time. The strategy improves reliability during the peak hour for the high-volume months, which is reflected by the increase in the reliability rating. It forecasts an increase of 3.6% in the VMT for which LOS D or better is provided. On the other hand, delay to the cross-street left-turn movements increases. This increase partially offsets the decrease in delay to the major-street through movements. This trade-off is reflected by a small reduction of 4.5 veh-h total delay.

Results for Strategy 2

In Strategy 2, the major-street left-turn mode is changed from protected-only to protected-permitted. This change reduces the time required by the major-street left-turn phase, which increases the time available to the coordinated phase and increases the through movement capacity. The results of the evaluation of this strategy are given in Exhibit 29-79.

Exhibit 29-79
Example Problem 5: Results
for Strategy 2

Case	Travel Time (s)		Total Delay (veh-h)	Reliability Rating
	Average	95th Percentile		
Existing	438.2	768.5	70.7	93.2
Strategy 2	382.9	473.5	49.6	97.3
Change	-55.3	-295.0	-21.1	4.1
Significant?	Yes	Yes	Yes	Yes

Note: Results based on five replications.

The statistics in Exhibit 29-79 indicate that Strategy 2 produces a relatively large improvement in travel time, particularly in the average travel time, relative to Strategy 1. The strategy improves reliability during the peak hour for the high-volume months, reflected by the increase in the reliability rating. It forecasts an increase of 4.1 percent in the VMT for which LOS D or better is provided. The delay to the major-street through movements decreases without a significant increase in the delay to the other movements. This trend is reflected by the notable reduction of 21.1 veh-h total delay.

Results for Strategy 3

In Strategy 3, the major-street right-turn bays are eliminated and second lanes are added to the major-street left-turn bays. This change reduced the time required by the major-street left-turn phase, which increased the time available to the coordinated phase and increased the through movement capacity. The results for this strategy are listed in Exhibit 29-80.

Case	Travel Time (s)		Total Delay (veh-h)	Reliability Rating
	Average	95th Percentile		
Existing	438.2	768.5	70.7	93.2
Strategy 3	410.0	460.2	59.0	98.5
Change Significant?	-28.2 No	-308.3 Yes	-11.7 Yes	5.3 Yes

Note: Results based on five replications.

Exhibit 29-80
Example Problem 5: Results for Strategy 3

The statistics in Exhibit 29-80 indicate that the strategy produces a relatively large improvement in travel time, particularly in the 95th percentile travel time. The strategy improves reliability during the peak hour for the high-volume months, reflected by the increase in the reliability rating. It forecasts an increase of 5.3% in the VMT for which LOS D or better is provided. Delay to the major-street through movements decreases, as reflected by the reduction of 11.7 veh-h total delay. The change in average travel time is not statistically significant because the loss of the right-turn bays shifts the location of many incidents from the bays to the through lanes. This shift causes the average travel time for Strategy 3 to vary more widely among scenarios.

Summary of Findings

All three strategies improved the facility’s reliability and overall operation. Strategy 1 (shift 5 s to the coordinated phase) provides some improvement in reliability of travel through the facility and some reduction in total delay in the system.

Strategy 2 (protected-only to protected-permitted) provides the *lowest average travel time* and the *lowest total delay*. It also provides a notable improvement in travel reliability.

Strategy 3 (eliminate right-turn lanes, increase left-turn lanes) provides the *biggest improvement in reliability* of travel. It also provides some overall benefit in terms of lower travel time and total delay.

The selection of the best strategy should include consideration of the change in road user costs, as measured in terms of reliability, total delay, and crash frequency. Viable strategies are those for which the reduction in road user costs exceeds the construction costs associated with strategy installation and maintenance.

Some of these references can be found in the Technical Reference Library in Volume 4.

6. REFERENCES

1. Zegeer, J., J. Bonneson, R. Dowling, P. Ryus, M. Vandehey, W. Kittelson, N. Roupail, B. Schroeder, A. Hajbabaie, B. Aghdashi, T. Chase, S. Sajjadi, R. Margiotta, and L. Elefteriadou. *Incorporating Travel Time Reliability into the Highway Capacity Manual*. SHRP 2 Report S2-L08-RW-1. Transportation Research Board of the National Academies, Washington, D.C., 2014.
2. *Comparative Climatic Data for the United States Through 2010*. National Climatic Data Center, National Oceanic and Atmospheric Administration, Asheville, N.C., 2011. <http://www.ncdc.noaa.gov>. Accessed Sept. 21, 2011.
3. Urbanik, T., A. Tanaka, B. Lozner, E. Lindstrom, K. Lee, S. Quayle, S. Beard, S. Tsoi, P. Ryus, D. Gettman, S. Sunkari, K. Balke, and D. Bullock. *NCHRP Report 812: Signal Timing Manual*, 2nd ed. Transportation Research Board, Washington, D.C., 2015.
4. Husch, D., and J. Albeck. *Synchro Studio 7 User's Guide*. Trafficware, Ltd., 2006.
5. Wallace, C., K. Courage, M. Hadi, and A. Gan. *TRANSYT-7F User's Guide, Vol. 4 in a Series: Methodology for Optimizing Signal Timing*. University of Florida, Gainesville, March 1998.
6. *Corridor-Microscopic Simulation Program (CORSIM) Version 6.1 User's Guide*. University of Florida, Gainesville, 2008.
7. *VISSIM 5.10 User Manual*. PTV Vision, Karlsruhe, Germany, 2008.
8. Rodegerdts, L., J. Bansen, C. Tiesler, J. Knudsen, E. Myers, M. Johnson, M. Moule, B. Persaud, C. Lyon, S. Hallmark, H. Isebrands, R. B. Crown, B. Guichet, and A. O'Brien. *NCHRP Report 672: Roundabouts: An Informational Guide*, 2nd ed. Transportation Research Board of the National Academies, Washington, D.C., 2010.
9. *Rainfall Frequency Atlas of the U.S.: Rainfall Event Statistics*. National Climatic Data Center, National Oceanic and Atmospheric Administration, Asheville, N.C., 2011. <http://www.ncdc.noaa.gov/oa/documentlibrary/rainfall.html>. Accessed Sept. 21, 2011.
10. *Highway Safety Manual*, 1st ed. American Association of State Highway and Transportation Officials, Washington, D.C., 2010.



HIGHWAY CAPACITY MANUAL

6TH EDITION | A GUIDE FOR MULTIMODAL MOBILITY ANALYSIS

VOLUME 4: APPLICATIONS GUIDE

The National Academies of
SCIENCES • ENGINEERING • MEDICINE

TRANSPORTATION RESEARCH BOARD
WASHINGTON, D.C. | WWW.TRB.ORG

TRANSPORTATION RESEARCH BOARD 2016 EXECUTIVE COMMITTEE *

Chair: James M. Crites, Executive Vice President of Operations,
Dallas–Fort Worth International Airport, Texas

Vice Chair: Paul Trombino III, Director, Iowa Department of
Transportation, Ames

Executive Director: Neil J. Pedersen, Transportation Research Board

Victoria A. Arroyo, Executive Director, Georgetown Climate Center;
Assistant Dean, Centers and Institutes; and Professor and Director,
Environmental Law Program, Georgetown University Law Center,
Washington, D.C.

Scott E. Bennett, Director, Arkansas State Highway and Transportation
Department, Little Rock

Jennifer Cohan, Secretary, Delaware Department of Transportation, Dover

Malcolm Dougherty, Director, California Department of
Transportation, Sacramento

A. Stewart Fotheringham, Professor, School of Geographical Sciences
and Urban Planning, Arizona State University, Tempe

John S. Halikowski, Director, Arizona Department of Transportation,
Phoenix

Susan Hanson, Distinguished University Professor Emerita, Graduate
School of Geography, Clark University, Worcester, Massachusetts

Steve Heminger, Executive Director, Metropolitan Transportation
Commission, Oakland, California

Chris T. Hendrickson, Hamerschlag Professor of Engineering, Carnegie
Mellon University, Pittsburgh, Pennsylvania

Jeffrey D. Holt, Managing Director, Power, Energy, and Infrastructure
Group, BMO Capital Markets Corporation, New York

S. Jack Hu, Vice President for Research and J. Reid and Polly Anderson
Professor of Manufacturing, University of Michigan, Ann Arbor

Roger B. Huff, President, HGLC, LLC, Farmington Hills, Michigan

Geraldine Knatz, Professor, Sol Price School of Public Policy, Viterbi
School of Engineering, University of Southern California, Los Angeles

Ysela Llort, Consultant, Miami, Florida

Melinda McGrath, Executive Director, Mississippi Department of
Transportation, Jackson

James P. Redeker, Commissioner, Connecticut Department of
Transportation, Newington

Mark L. Rosenberg, Executive Director, The Task Force for Global
Health, Inc., Decatur, Georgia

Kumares C. Sinha, Olson Distinguished Professor of Civil Engineering,
Purdue University, West Lafayette, Indiana

Daniel Sperling, Professor of Civil Engineering and Environmental
Science and Policy; Director, Institute of Transportation Studies,
University of California, Davis

Kirk T. Steudle, Director, Michigan Department of Transportation,
Lansing (Past Chair, 2014)

Gary C. Thomas, President and Executive Director, Dallas Area Rapid
Transit, Dallas, Texas

Pat Thomas, Senior Vice President of State Government Affairs, United
Parcel Service, Washington, D.C.

Katherine F. Turnbull, Executive Associate Director and Research
Scientist, Texas A&M Transportation Institute, College Station

Dean Wise, Vice President of Network Strategy, Burlington Northern
Santa Fe Railway, Fort Worth, Texas

Thomas P. Bostick (Lieutenant General, U.S. Army), Chief of Engineers
and Commanding General, U.S. Army Corps of Engineers, Washington,
D.C. (ex officio)

James C. Card (Vice Admiral, U.S. Coast Guard, retired), Maritime
Consultant, The Woodlands, Texas, and Chair, TRB Marine Board
(ex officio)

T. F. Scott Darling III, Acting Administrator and Chief Counsel, Federal
Motor Carrier Safety Administration, U.S. Department of Transportation
(ex officio)

Marie Therese Dominguez, Administrator, Pipeline and Hazardous
Materials Safety Administration, U.S. Department of Transportation
(ex officio)

Sarah Feinberg, Administrator, Federal Railroad Administration,
U.S. Department of Transportation (ex officio)

Carolyn Flowers, Acting Administrator, Federal Transit Administration,
U.S. Department of Transportation (ex officio)

LeRoy Gishi, Chief, Division of Transportation, Bureau of Indian
Affairs, U.S. Department of the Interior, Washington, D.C. (ex officio)

John T. Gray II, Senior Vice President, Policy and Economics,
Association of American Railroads, Washington, D.C. (ex officio)

Michael P. Huerta, Administrator, Federal Aviation Administration,
U.S. Department of Transportation (ex officio)

Paul N. Jaenichen, Sr., Administrator, Maritime Administration,
U.S. Department of Transportation (ex officio)

Bevan B. Kirley, Research Associate, University of North Carolina
Highway Safety Research Center, Chapel Hill, and Chair, TRB Young
Members Council (ex officio)

Gregory G. Nadeau, Administrator, Federal Highway Administration,
U.S. Department of Transportation (ex officio)

Wayne Nastri, Acting Executive Officer, South Coast Air Quality
Management District, Diamond Bar, California (ex officio)

Mark R. Rosekind, Administrator, National Highway Traffic Safety
Administration, U.S. Department of Transportation (ex officio)

Craig A. Rutland, U.S. Air Force Pavement Engineer, U.S. Air Force
Civil Engineer Center, Tyndall Air Force Base, Florida (ex officio)

Reuben Sarkar, Deputy Assistant Secretary for Transportation,
U.S. Department of Energy (ex officio)

Richard A. White, Acting President and CEO, American Public
Transportation Association, Washington, D.C. (ex officio)

Gregory D. Winfree, Assistant Secretary for Research and Technology,
Office of the Secretary, U.S. Department of Transportation (ex officio)

Frederick G. (Bud) Wright, Executive Director, American Association
of State Highway and Transportation Officials, Washington, D.C.
(ex officio)

Paul F. Zukunft (Admiral, U.S. Coast Guard), Commandant, U.S. Coast
Guard, U.S. Department of Homeland Security (ex officio)

Transportation Research Board publications are available by ordering
individual publications directly from the TRB Business Office, through
the Internet at www.TRB.org, or by annual subscription through
organizational or individual affiliation with TRB. Affiliates and library
subscribers are eligible for substantial discounts. For further information,
contact the Transportation Research Board Business Office, 500 Fifth
Street, NW, Washington, DC 20001 (telephone 202-334-3213;
fax 202-334-2519; or e-mail TRBsales@nas.edu).

Copyright 2016 by the National Academy of Sciences.

All rights reserved.

Printed in the United States of America.

ISBN 978-0-309-36997-8 [Slipcased set of three volumes]

ISBN 978-0-309-36998-5 [Volume 1]

ISBN 978-0-309-36999-2 [Volume 2]

ISBN 978-0-309-37000-4 [Volume 3]

ISBN 978-0-309-37001-1 [Volume 4, online only]

The National Academies of
SCIENCES • ENGINEERING • MEDICINE

The **National Academy of Sciences** was established in 1863 by an Act of Congress, signed by President Lincoln, as a private, nongovernmental institution to advise the nation on issues related to science and technology. Members are elected by their peers for outstanding contributions to research. Dr. Ralph J. Cicerone is president.

The **National Academy of Engineering** was established in 1964 under the charter of the National Academy of Sciences to bring the practices of engineering to advising the nation. Members are elected by their peers for extraordinary contributions to engineering. Dr. C. D. Mote, Jr., is president.

The **National Academy of Medicine** (formerly the Institute of Medicine) was established in 1970 under the charter of the National Academy of Sciences to advise the nation on medical and health issues. Members are elected by their peers for distinguished contributions to medicine and health. Dr. Victor J. Dzau is president.

The three Academies work together as the National Academies of Sciences, Engineering, and Medicine to provide independent, objective analysis and advice to the nation and conduct other activities to solve complex problems and inform public policy decisions. The Academies also encourage education and research, recognize outstanding contributions to knowledge, and increase public understanding in matters of science, engineering, and medicine.

Learn more about the National Academies of Sciences, Engineering, and Medicine at **www.national-academies.org**.

The **Transportation Research Board** is one of seven major programs of the National Academies of Sciences, Engineering, and Medicine. The mission of the Transportation Research Board is to increase the benefits that transportation contributes to society by providing leadership in transportation innovation and progress through research and information exchange, conducted within a setting that is objective, interdisciplinary, and multimodal. The Board's varied committees, task forces, and panels annually engage about 7,000 engineers, scientists, and other transportation researchers and practitioners from the public and private sectors and academia, all of whom contribute their expertise in the public interest. The program is supported by state transportation departments, federal agencies including the component administrations of the U.S. Department of Transportation, and other organizations and individuals interested in the development of transportation.

Learn more about the Transportation Research Board at **www.TRB.org**.

CHAPTER 30
URBAN STREET SEGMENTS: SUPPLEMENTAL

CONTENTS

1. INTRODUCTION.....	30-1
2. TRAFFIC DEMAND ADJUSTMENTS	30-2
Capacity Constraint and Volume Balance.....	30-2
Origin–Destination Distribution.....	30-4
3. SIGNALIZED SEGMENT ANALYSIS.....	30-7
Discharge Flow Profile.....	30-7
Running Time	30-8
Projected Arrival Flow Profile.....	30-8
Proportion of Time Blocked	30-11
Sustained Spillback.....	30-12
Midsegment Lane Restriction	30-19
4. DELAY DUE TO TURNS	30-21
Delay due to Left Turns	30-21
Delay due to Right Turns.....	30-26
5. PLANNING-LEVEL ANALYSIS APPLICATION.....	30-30
Overview of the Application.....	30-30
Required Data and Sources	30-30
Methodology.....	30-30
Example Problem.....	30-37
6. FIELD MEASUREMENT TECHNIQUES	30-39
Free-Flow Speed.....	30-39
Average Travel Speed	30-40
7. COMPUTATIONAL ENGINE DOCUMENTATION	30-43
Flowcharts.....	30-43
Linkage Lists.....	30-46

8. EXAMPLE PROBLEMS	30-49
Example Problem 1: Motorized Vehicle LOS	30-49
Example Problem 2: Pedestrian LOS	30-57
Example Problem 3: Bicycle LOS.....	30-63
Example Problem 4: Transit LOS.....	30-67
9. ROUNDABOUT SEGMENT METHODOLOGY	30-73
Scope of the Methodology	30-73
Limitations of the Methodology	30-73
Required Input Data and Sources	30-73
Geometric Design Data	30-74
Computational Steps	30-75
10. REFERENCES	30-84

LIST OF EXHIBITS

Exhibit 30-1 Entry and Exit Movements on the Typical Street Segment 30-2

Exhibit 30-2 Default Seed Proportions for Origin–Destination Matrix 30-5

Exhibit 30-3 Platoon Dispersion Model 30-9

Exhibit 30-4 Arrival Flow Profile Estimation Procedure 30-10

Exhibit 30-5 Estimation of Blocked Period Duration 30-12

Exhibit 30-6 Vehicle Trajectories During Spillback Conditions 30-13

Exhibit 30-7 Required Input Data for the Planning-Level Analysis
Application..... 30-30

Exhibit 30-8 Planning-Level Analysis Application for Urban Street
Segments..... 30-31

Exhibit 30-9 Planning-Level Analysis: Running Time Worksheet..... 30-32

Exhibit 30-10 Planning-Level Analysis: Proportion Arriving During
Green Worksheet..... 30-33

Exhibit 30-11 Planning-Level Analysis: Control Delay Worksheet 30-34

Exhibit 30-12 Planning-Level Analysis: Stop Rate Worksheet 30-35

Exhibit 30-13 Planning-Level Analysis: Travel Speed and Spatial Stop
Rate Worksheet..... 30-36

Exhibit 30-14 Planning-Level Analysis: Example Problem..... 30-37

Exhibit 30-15 Travel Time Field Worksheet 30-42

Exhibit 30-16 Methodology Flowchart..... 30-43

Exhibit 30-17 Setup Module..... 30-44

Exhibit 30-18 Segment Evaluation Module 30-44

Exhibit 30-19 Segment Analysis Module 30-45

Exhibit 30-20 Delay due to Turns Module..... 30-45

Exhibit 30-21 Performance Measures Module 30-46

Exhibit 30-22 Segment Evaluation Module Routines..... 30-47

Exhibit 30-23 Segment Analysis Module Routines 30-47

Exhibit 30-24 Delay due to Turns Module Routines 30-48

Exhibit 30-25 Example Problems..... 30-49

Exhibit 30-26 Example Problem 1: Urban Street Segment Schematic..... 30-49

Exhibit 30-27 Example Problem 1: Intersection Turn Movement Counts..... 30-50

Exhibit 30-28 Example Problem 1: Signal Conditions for Intersection 1 30-50

Exhibit 30-29 Example Problem 1: Geometric Conditions and Traffic
Characteristics for Signalized Intersection 1 30-51

Exhibit 30-30 Example Problem 1: Segment Data 30-52

Exhibit 30-31 Example Problem 1: Access Point Data 30-52

Exhibit 30-32 Example Problem 1: Movement-Based Output Data.....	30-52
Exhibit 30-33 Example Problem 1: Timer-Based Phase Output Data.....	30-54
Exhibit 30-34 Example Problem 1: Timer-Based Movement Output Data	30-55
Exhibit 30-35 Example Problem 1: Movement-Based Access Point Output Data.....	30-55
Exhibit 30-36 Example Problem 1: Performance Measure Summary	30-57
Exhibit 30-37 Example Problem 2: Segment Geometry	30-58
Exhibit 30-38 Example Problem 3: Segment Geometry	30-63
Exhibit 30-39 Example Problem 4: Segment Geometry	30-67
Exhibit 30-40 Validity Range of Inputs and Calculated Values for Analysis of Motor Vehicles on an Urban Street Roundabout Segment	30-73
Exhibit 30-41 Additional Required Input Data, Potential Data Sources, and Default Values for Analysis of Motor Vehicles on an Urban Street Roundabout Segment.....	30-74
Exhibit 30-42 Illustration of Geometric Design Data	30-74
Exhibit 30-43 Base Free-Flow Speed Adjustment Factors	30-76
Exhibit 30-44 Illustration of Subsegment Dimensions.....	30-78

1. INTRODUCTION

Chapter 30 is the supplemental chapter for Chapter 18, Urban Street Segments, which is found in Volume 3 of the *Highway Capacity Manual* (HCM). This chapter presents detailed information about the following aspects of the Chapter 18 motorized vehicle methodology:

- The adjustments made to the input vehicular demand flow rates at signalized boundary intersections so that they reasonably reflect actual operating conditions during the analysis period,
- The process for analyzing vehicular traffic flow on a segment bounded by signalized intersections, and
- The process for estimating through-vehicle delay due to vehicle turning movements at unsignalized midsegment access points.

This chapter provides a simplified version of the Chapter 18 motorized vehicle methodology that is suitable for planning applications. It describes techniques for measuring free-flow speed and average travel speed in the field and provides details about the computational engine that implements the Chapter 18 motorized vehicle methodology. Chapter 30 provides four example problems that demonstrate the application of the motorized vehicle, pedestrian, bicycle, and transit methodologies to an urban street segment. Finally, the chapter provides an overview of the methodology for evaluating the performance of the motor vehicle mode on an urban street segment bounded by one or more roundabouts.

VOLUME 4: APPLICATIONS GUIDE

25. Freeway Facilities: Supplemental
26. Freeway and Highway Segments: Supplemental
27. Freeway Weaving: Supplemental
28. Freeway Merges and Diverges: Supplemental
29. Urban Street Facilities: Supplemental
- 30. Urban Street Segments: Supplemental**
31. Signalized Intersections: Supplemental
32. STOP-Controlled Intersections: Supplemental
33. Roundabouts: Supplemental
34. Interchange Ramp Terminals: Supplemental
35. Pedestrians and Bicycles: Supplemental
36. Concepts: Supplemental
37. ATDM: Supplemental

2. TRAFFIC DEMAND ADJUSTMENTS

This section describes adjustments made to the input vehicular demand flow rates at signalized boundary intersections so that they reasonably reflect actual operating conditions during the analysis period. These adjustments have no effect if existing vehicular flow rates are accurately quantified for the subject segment and all movements operate below their capacity. However, if the demand flow rate for any movement exceeds its capacity or if there is disagreement between the count of vehicles entering and the count exiting the segment, some movement flow rates will need to be adjusted for accurate evaluation of segment operation.

This section describes two procedures that check the input flow rates and make adjustments if necessary. These procedures are

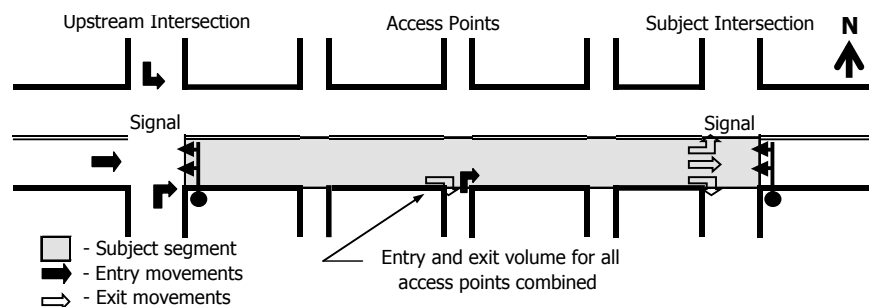
- Capacity constraint and volume balance and
- Origin–destination distribution.

These procedures can be extended to the analysis of unsignalized boundary intersections; however, the mechanics of this extension are not described.

CAPACITY CONSTRAINT AND VOLUME BALANCE

This subsection describes the procedure for determining the turn movement flow rates at each intersection along the subject urban street segment. The analysis is separately applied to each travel direction and proceeds in the direction of travel. The procedure consists of a series of steps that are completed in sequence for the entry and exit movements associated with each segment. These movements are shown in Exhibit 30-1.

Exhibit 30-1
Entry and Exit Movements on the Typical Street Segment



As indicated in Exhibit 30-1, three entry movements are associated with the upstream signalized intersection and three exit movements are associated with the downstream signalized intersection. Entry and exit movements also exist at each access point intersection. However, these movements are aggregated into one entry and one exit movement for simplicity.

The analysis procedure is described in the following steps. Frequent reference is made to “volume” in these steps. In this application, volume is considered to be equivalent to average flow rate for the analysis period and to have units of vehicles per hour (veh/h).

Step 1: Identify Entry and Exit Volumes

The volume for each entry and exit movement is identified during this step. The volume entering the segment from each access point intersection should be identified and added to obtain a total for the segment. Similarly, the volume exiting the segment from each access point intersection should be identified and added for the segment.

A maximum of eight entry volumes are identified in this step. The seven volumes at the upstream boundary intersection include signalized left-turn volume, signalized through volume, signalized right-turn volume, unsignalized left-turn volume, unsignalized through volume, unsignalized right-turn volume, and right-turn-on-red (RTOR) volume. The eighth entry volume is the total access point entry volume.

A maximum of eight exit volumes are identified in this step. The seven volumes at the downstream boundary intersection include signalized left-turn volume, signalized through volume, signalized right-turn volume, unsignalized left-turn volume, unsignalized through volume, unsignalized right-turn volume, and RTOR volume. The eighth exit volume is the total access point exit volume.

Step 2: Estimate Movement Capacity

During this step, the capacity of each signalized entry movement is estimated. This estimate should be a reasonable approximation based on estimates of the saturation flow rate for the corresponding movement and the phase splits established for signal coordination. The capacity of the RTOR movements is not calculated during this step.

If the right-turn movement at the upstream intersection shares a lane with its adjacent through movement, the discharge flow rate for the turn movement can be estimated by using Equation 30-1.

$$s_{q|r} = s_{sr} P_R$$

Equation 30-1

where

- $s_{q|r}$ = shared lane discharge flow rate for upstream right-turn traffic movement in vehicles per hour per lane (veh/h/lane),
- s_{sr} = saturation flow rate in shared right-turn and through-lane group with permitted operation (veh/h/lane), and
- P_R = proportion of right-turning vehicles in the shared lane (decimal).

The procedure described in Section 2 of Chapter 31, Signalized Intersections: Supplemental, is used to estimate the two variables shown in Equation 30-1. A similar equation can be constructed to estimate the shared lane discharge flow rate for an upstream left-turn movement in a shared lane.

The capacity for the right-turn movement in the shared-lane lane group is then computed with Equation 30-2.

$$c_{q|r} = s_{q|r} g/C$$

Equation 30-2

where

- $c_{q|r}$ = shared lane capacity for upstream right-turn traffic movement (veh/h),

$s_{q|_r}$ = shared lane discharge flow rate for upstream right-turn traffic movement (veh/h/ln),

g = effective green time (s), and

C = cycle length (s).

The procedure described in Section 2 of Chapter 31 is used to estimate the signal timing variables shown in Equation 30-2. A similar equation can be constructed for an upstream left-turn movement in a shared lane.

Step 3: Compute Volume-to-Capacity Ratio

During this step, the volume-to-capacity ratio is computed for each signalized entry movement. This ratio is computed by dividing the arrival volume from Step 1 by the capacity estimated in Step 2. Any movements with a volume-to-capacity ratio in excess of 1.0 will meter the volume arriving to the downstream intersection. This ratio is not computed for the RTOR movements.

Step 4: Compute Discharge Volume

The discharge volume from each of the three signalized entry movements is equal to the smaller of its entry volume or its associated movement capacity. The total discharge volume for the combined access point approach is assumed to be equal to the total access point entry volume. Similarly, the discharge volume for each unsignalized and RTOR movement is assumed to equal its corresponding entry volume. As a last calculation, the eight discharge volumes are added to obtain the total discharge volume.

Step 5: Compute Adjusted Exit Volume

The total discharge volume from Step 4 should be compared with the total exit volume. The total exit volume is the sum of the eight exit volumes identified in Step 1. If the two totals do not agree, the eight exit volumes must be adjusted so that their sum equals the total discharge volume. The adjusted exit volume for a movement equals its exit volume multiplied by the "volume ratio." The volume ratio equals the total discharge volume divided by the total exit volume.

Step 6: Repeat Steps 1 Through 5 for Each Segment

The preceding steps should be completed for each segment in the facility in the subject direction of travel. The procedure should then be repeated for the opposing direction of travel.

ORIGIN–DESTINATION DISTRIBUTION

The volume of traffic that arrives at a downstream intersection for a given downstream movement represents the combined volume from each upstream point of entry weighted by its percentage contribution to the downstream exit movement. The distribution of these contribution percentages between each upstream and downstream pair is represented as an origin–destination distribution matrix.

The origin–destination matrix is important for estimating the arrival pattern of vehicles at the downstream intersection. Hence, the focus here is on upstream

entry movements that are signalized, because (a) they are typically the higher-volume movements and (b) the signal timing influences their time of arrival downstream. For these reasons, the origin–destination distribution is focused on the three upstream signalized movements. All other movements (i.e., unsignalized movements at the boundary intersections, access point movements, RTOR movements) are combined into one equivalent movement—referred to hereafter as the “access point” movement—that is assumed to arrive uniformly throughout the signal cycle.

Ideally, an origin–destination survey would be conducted for an existing segment, or the origin–destination data would be available from traffic forecasts by planning models. One matrix would be available for each direction of travel on the segment. In the absence of such information, origin–destination volumes can be estimated from the entry and exit volumes for a segment, where the exit volumes equal the adjusted arrival volumes from the procedure described in the previous subsection, Capacity Constraint and Volume Balance.

Each of the four entry movements to the segment shown in Exhibit 30-1 is considered an origin. Each of the four exit movements is a destination. The problem then becomes one of estimating the origin–destination table given the entering and exiting volumes.

This procedure is derived from research (1). It is based on the principle that total entry volume is equal to total exit volume. It uses seed proportions to represent the best estimate of the volume distribution. These proportions are refined through implementation of the procedure. It is derived to estimate the most probable origin–destination volumes by minimizing the deviation from the seed percentages while ensuring the equivalence of entry and exit volumes.

The use of seed percentages allows the procedure to adapt the origin–destination volume estimates to factors or geometric situations that induce greater preference for some entry–exit combinations than is suggested by simple volume proportion (e.g., a downstream freeway on-ramp). The default seed proportions are listed in Exhibit 30-2.

Seed Proportion by Origin Movement				Destination Movement
Left	Through	Right	Access Point	
0.02	0.10	0.05	0.02	Left
0.91	0.78	0.92	0.97	Through
0.05	0.10	0.02	0.01	Right
0.02	0.02	0.01	0.00	Access point
1.00	1.00	1.00	1.00	

Exhibit 30-2
Default Seed Proportions for Origin–Destination Matrix

Step 1: Set Adjusted Origin Volume

$$O_{a,i} = O_i$$

where

$O_{a,i}$ = adjusted volume for origin i ($i = 1, 2, 3, 4$) (veh/h), and

O_i = volume for origin i ($i = 1, 2, 3, 4$) (veh/h).

The letter i denotes the four movements entering the segment. This volume is computed for each of the four origins.

Equation 30-3

Step 2: Compute Adjusted Destination Volume

Equation 30-4

$$D_{a,j} = \sum_{i=1}^4 O_{a,i} p_{i,j}$$

where

$D_{a,j}$ = adjusted volume for destination j ($j = 1, 2, 3, 4$) (veh/h),

$O_{a,i}$ = adjusted volume for origin i ($i = 1, 2, 3, 4$) (veh/h), and

$p_{i,j}$ = seed proportion of volume from origin i to destination j (decimal).

The letter j denotes the four movements exiting the segment. This volume is computed for each of the four destinations.

Step 3: Compute Destination Adjustment Factor

Equation 30-5

$$b_{d,j} = \frac{D_j}{D_{a,j}}$$

where

$b_{d,j}$ = destination adjustment factor j ($j = 1, 2, 3, 4$),

D_j = volume for destination j ($j = 1, 2, 3, 4$) (veh/h), and

$D_{a,j}$ = adjusted volume for destination j ($j = 1, 2, 3, 4$) (veh/h).

This factor is computed for each of the four destinations.

Step 4: Compute Origin Adjustment Factor

Equation 30-6

$$b_{o,i} = \sum_{j=1}^4 b_{d,j} p_{i,j}$$

where $b_{o,i}$ is the origin adjustment factor i ($i = 1, 2, 3, 4$). This factor is computed for each of the four origins.

Step 5: Compute Adjusted Origin Volume

Equation 30-7

$$O_{a,i} = \frac{O_i}{b_{o,i}}$$

where $O_{a,i}$ is the adjusted volume for origin i ($i = 1, 2, 3, 4$) (veh/h). This volume is computed for each of the four origins. It replaces the value previously determined for this variable.

For each origin, compute the absolute difference between the adjusted origin volume from Equation 30-7 and the previous estimate of the adjusted origin volume. If the sum of these four differences is less than 0.01, proceed to Step 6; otherwise, set the adjusted origin volume for each origin equal to the value from Equation 30-7, go to Step 2, and repeat the calculation sequence.

Step 6: Compute Origin–Destination Volume

Equation 30-8

$$v_{i,j} = O_{a,i} b_{d,j} p_{i,j}$$

where $v_{i,j}$ is the volume entering from origin i and exiting at destination j (veh/h). This volume is computed for all 16 origin–destination pairs.

3. SIGNALIZED SEGMENT ANALYSIS

This section describes the process for analyzing vehicular traffic flow on a segment bounded by signalized intersections. Initially, this process computes the flow profile of discharging vehicles at the upstream intersection as influenced by the signal timing and phase sequence. It uses this profile to compute the arrival flow profile at a downstream junction. The arrival flow profile is then compared with the downstream signal timing and phase sequence to compute the proportion of vehicles arriving during green. The arrival flow profile is also used to compute the proportion of time that a platoon blocks one or more traffic movements at a downstream access point intersection. These two platoon descriptors are used in subsequent procedures to compute delay and other performance measures.

This section describes six procedures that are used to define the arrival flow profile and compute the related platoon descriptors. These procedures are

- Discharge flow profile,
- Running time,
- Projected arrival flow profile,
- Proportion of time blocked,
- Sustained spillback, and
- Midsegment lane restriction.

Each procedure is described in the following subsections.

DISCHARGE FLOW PROFILE

A flow profile is a macroscopic representation of steady traffic flow conditions for the average signal cycle during the specified analysis period. The cycle is represented as a series of 1-s time intervals (hereafter referred to as “time steps”). The start time of the cycle is 0.0 s, relative to the system reference time. The time steps are numbered from 1 to C' , where C' is the cycle length in units of time steps. The flow rate for step i represents an average of the flows that occur during the time period corresponding to step i for all cycles in the analysis period. This approach is conceptually the same as that used in the TRANSYT-7F model (2).

A discharge flow profile is computed for each of the upstream signalized left-turn, through, and right-turn movements. Each profile is defined by the time that the signal is effectively green and by the time that the queue service time ends. During the queue service time, the discharge flow rate is equal to the saturation flow rate. After the queue service time is reached, the discharge rate is set equal to the “adjusted discharge volume.” The adjusted discharge volume is equal to the discharge volume computed by using the procedures described in Section 2, but it is adjusted to reflect the “proportion of arrivals during green.” The latter adjustment adapts the discharge flow pattern to reflect platoon arrivals on the upstream segment.

The discharge flow profile is dependent on movement saturation flow rate, queue service time, phase duration, and proportion of arrivals during green for the discharging movements. The movement saturation flow rate is computed by using the procedure described in Section 3 of Chapter 19, Signalized Intersections. Procedures for calculating the remaining variables are described in subsequent subsections. This relationship introduces a circularity in the computations that requires an iterative sequence of calculations to converge on the steady-state solution.

RUNNING TIME

The running time procedure describes the calculation of running time between the upstream intersection and a downstream intersection. This procedure is described as Step 2 of the motorized vehicle methodology in Chapter 18, Urban Street Segments.

One component of running time is the delay due to various midsegment sources. One notable source of delay is left or right turns from the segment at an access point intersection. This delay is computed by using the procedure described in Section 4. Other sources of delay include on-street parking maneuvers and pedestrian crosswalks. Delay from these sources represents an input variable to the methodology.

PROJECTED ARRIVAL FLOW PROFILE

This subsection describes the procedure for predicting the arrival flow profile at a downstream intersection (i.e., access point or boundary intersection). This flow profile is based on the discharge flow profile and running time computed previously. The discharge flow profile is used with a platoon dispersion model to compute the arrival flow profile. The platoon dispersion model is summarized in the next part of this subsection. The procedure for using this model to estimate the arrival flow profile is described in the second part.

Platoon Dispersion Model

The platoon dispersion model was originally developed for use in the TRANSYT model (3). Input to the model is the discharge flow profile for a specified traffic movement. Output statistics from the model include (a) the arrival time of the leading vehicles in the platoon to a specified downstream intersection and (b) the flow rate during each subsequent time step.

In general, the arrival flow profile has a lower peak flow rate than the discharge flow profile owing to the dispersion of the platoon as it travels down the street. For similar reasons, the arrival flow profile is spread out over a longer period of time than the discharge flow profile. The rate of dispersion increases with increasing segment running time, which may be caused by access point activity, on-street parking maneuvers, and other midsegment delay sources.

The platoon dispersion model is described by Equation 30-9.

Equation 30-9

$$q'_{a|u,j} = F q'_{u,i} + (1 - F) q'_{a|u,j-1}$$

with

Equation 30-10

$$j = i + t'$$

where

- $q'_{a|u,j}$ = arrival flow rate in time step j at a downstream intersection from upstream source u (veh/step),
- $q'_{u,i}$ = departure flow rate in time step i at upstream source u (veh/step),
- F = smoothing factor,
- j = time step associated with platoon arrival time t' , and
- t' = platoon arrival time (steps).

The upstream flow source u can be the left-turn, through, or right-turn movement at the upstream boundary intersection. It can also be the collective set of left-turn or right-turn movements at access point intersections between the upstream boundary intersection and the subject intersection.

Exhibit 30-3 illustrates an arrival flow profile obtained from Equation 30-9. In this figure, the discharge flow profile is input to the model as variable $q'_{u,i}$. The dashed rectangles that form the discharge flow profile indicate the flow rate during each of nine time steps ($i = 1, 2, 3, \dots, 9$) that are each d_t seconds in duration. The vehicles that depart in the first time step ($i = 1$) arrive at the downstream intersection after traveling an amount of time equal to t' steps. The arrival flow at any time step $j (= i + t')$ is computed with Equation 30-9.

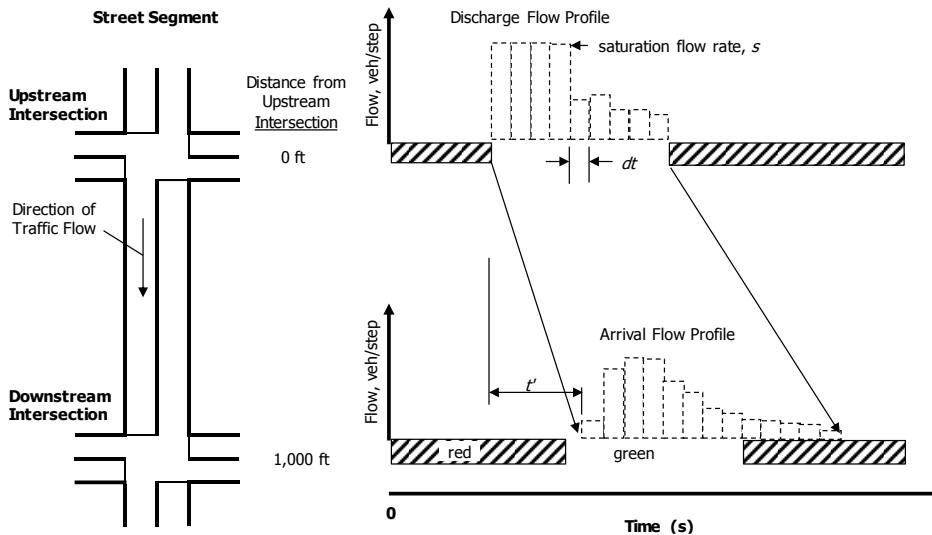


Exhibit 30-3
Platoon Dispersion Model

Research (4) indicates that Equation 30-11 describes the relationship between the smoothing factor and running time.

$$F = \frac{1}{1 + 0.138 t'_R + 0.315/d_t}$$

Equation 30-11

where

- t'_R = segment running time = t_R/d_t (steps),
- t_R = segment running time (s), and
- d_t = time step duration (s/step).

The recommended time step duration for this procedure is 1.0 s/step. Shorter values can be rationalized to provide a more accurate representation of the profile, but they also increase the time required for the computations. Experience indicates that 1.0 s/step provides a good balance between accuracy and computation time.

Equation 30-12 is used to compute platoon arrival time to the subject downstream intersection.

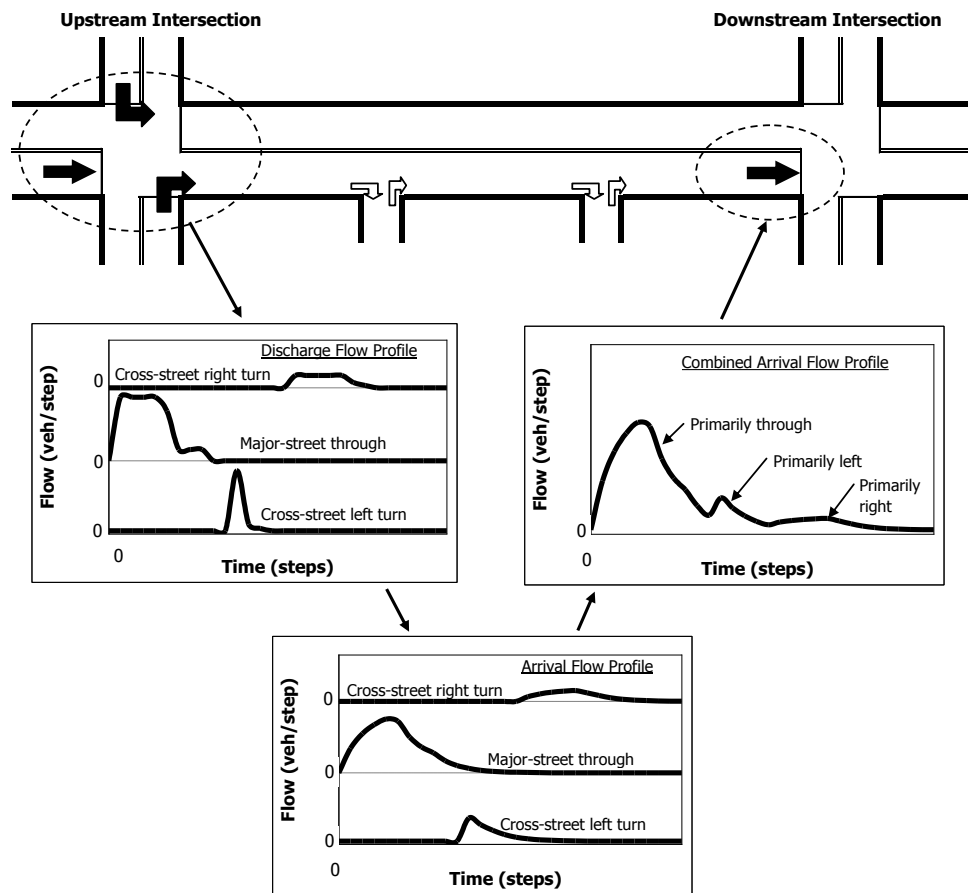
Equation 30-12

$$t' = t'_R - \frac{1}{F} + 1.25$$

Arrival Flow Profile

This subsection describes the procedure for computing the arrival flow profile. Typically, there are three upstream signalized traffic movements that depart at different times during the signal cycle; they are the minor-street right turn, major-street through, and minor-street left turn. Traffic may also enter the segment at various midblock access points or as an unsignalized movement at the boundary intersection. Exhibit 30-4 illustrates how these movements join to form the arrival flow profile for the subject downstream intersection.

Exhibit 30-4
Arrival Flow Profile Estimation Procedure



In application, the discharge flow profile for each of the departing movements is obtained from the discharge flow profile procedure described previously. These profiles are shown in the first of the three x-y plots in Exhibit

30-4. The platoon dispersion model is then used to estimate the arrival flows for each movement at a downstream intersection. These arrival flow profiles are shown in the second x - y plot in the exhibit. Arrivals from midsegment access points, which are not shown, are assumed to have a uniform arrival flow profile (i.e., a constant flow rate for all time steps).

Finally, the origin–destination distribution procedure is used to distribute each arrival flow profile to each of the downstream exit movements. The four arrival flow profiles associated with the subject exit movement are added together to produce the combined arrival flow profile. This profile is shown in the third x - y plot. The upstream movement contributions to this profile are indicated by arrows.

Comparison of the profiles in the first and second x - y plots of Exhibit 30-4 illustrates the platoon dispersion process. In the first x - y plot, the major-street through movement has formed a dense platoon as it departs the upstream intersection. However, by the time this platoon reaches the downstream intersection it has spread out and has a lower peak flow rate. In general, the amount of platoon dispersion increases with increasing segment length. For very long segments, the platoon structure degrades and arrivals become uniform throughout the cycle.

Platoon structure can also degrade as a result of significant access point activity along the segment. Streets with frequent active access point intersections tend to have more vehicles leave the platoon (i.e., turn from the segment at an access point) and enter the segment after the platoon passes (i.e., turn in to the segment at an access point). Both activities result in significant platoon decay.

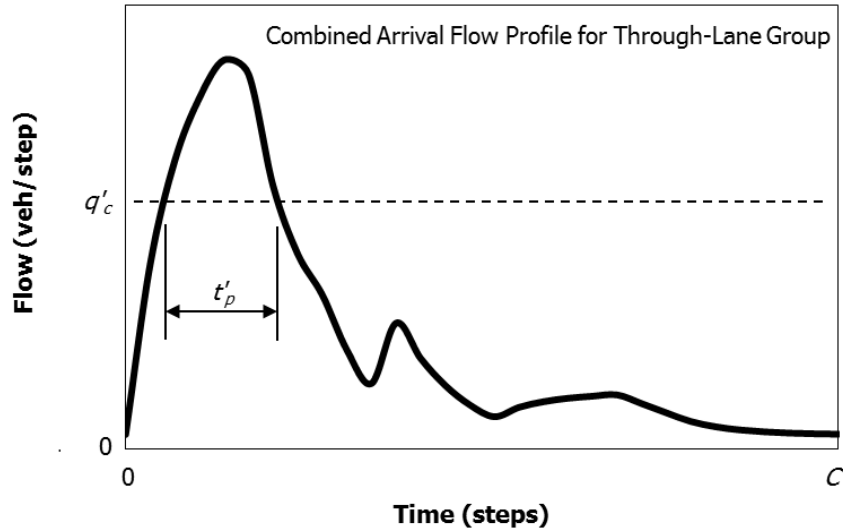
The effect of platoon decay is modeled by using the origin–destination matrix, in which the combined access point activity is represented as one volume assigned to midsegment origins and destinations. A large access point volume corresponds to a smaller volume that enters at the upstream boundary intersection as a defined platoon. This results in a larger portion of the combined arrival flow profile defined by uniform (rather than platoon) arrivals. When a street has busy access points, platoon decay tends to be a more dominant cause of platoon degradation than platoon dispersion.

PROPORTION OF TIME BLOCKED

The combined arrival flow profile can be used to estimate the time that a platoon passes through a downstream access point intersection. During this time period, the platoon can be dense enough to preclude a minor movement driver from finding an acceptable gap.

The use of the arrival flow profile to estimate the blocked period duration is shown in Exhibit 30-5. The profile shown represents the combined arrival flow profile for the through-lane group at a downstream access point intersection. The dashed line represents the critical platoon flow rate. Flow rates in excess of this threshold are rationalized to be associated with platoon headways that are too short to be entered (or crossed) by minor movements. The critical platoon flow rate q_c is equal to the inverse of the critical headway t_c associated with the minor

Exhibit 30-5
 Estimation of Blocked Period
 Duration



movement (i.e., $q_c = 3,600/t_c$). The appropriate critical headway values for various movements are identified in Chapter 20, Two-Way STOP-Controlled Intersections.

In the situation of a driver desiring to complete a left turn from the major street across the traffic stream represented by Exhibit 30-5, the proportion of time blocked is computed by using Equation 30-13. For this maneuver, the blocked period duration is based on the flow profile of the opposing through-lane group.

Equation 30-13

$$p_b = \frac{t'_p d_t}{C}$$

where

- p_b = proportion of time blocked (decimal),
- t'_p = blocked period duration (steps),
- d_t = time step duration (s/step), and
- C = cycle length (s).

Equation 30-13 is also used for the minor-street right-turn movement. However, in this situation, the blocked period duration is computed for the through-lane group approaching from the left. For the minor-street left-turn and through movements, the arrival flow profiles from both directions are evaluated. In this instance, the blocked period duration represents the time when a platoon from either direction is present in the intersection.

SUSTAINED SPILLBACK

This subsection describes two procedures that were developed for the evaluation of segments that experience sustained spillback. Sustained spillback occurs as a result of oversaturation (i.e., more vehicles discharging from the upstream intersection than can be served at the subject downstream intersection). The spillback can exist at the start of the study period, or it can occur at some point during the study period. Spillback that first occurs after the study period is not addressed.

Effective Average Vehicle Spacing

One piece of information needed to evaluate segments experiencing sustained spillback is the effective average vehicle spacing (5). A simple estimate of this spacing is computed as the sum of the average vehicle length and the average distance between two queued vehicles (as measured from the back bumper of the lead vehicle to the front bumper of the trailing vehicle).

Presumably, this estimate of average spacing could be divided into the segment length to determine the maximum number of queued vehicles on the segment during spillback. However, this result is biased because it is based on the assumption that all vehicles on the segment will always be stationary during spillback. This is a weak assumption because the downstream signal operation creates backward-traveling waves of starting and stopping. Between the starting wave and the stopping wave, vehicles are moving at the saturation headway and its associated speed. Their spacing exceeds that of the aforementioned “simple” estimate.

The procedure described in this subsection is used to estimate the effective average vehicle spacing L_h^* on a segment with spillback. The derivation of this new variable is based on the vehicle trajectories shown in Exhibit 30-6. The segment of interest is shown on the left side of the figure. Spillback is present for all of the cycles shown; however, trajectories are shown only for two cycles. The solid trajectories coincide with vehicles that enter the segment as a through movement at the upstream intersection. The dashed lines coincide with vehicles that enter the segment as a turn movement. A vehicle that enters the segment traveling north as a through vehicle is shown to experience four cycles before exiting the segment. The trajectories show that the vehicles move forward at a saturation headway of 3,600/s seconds per vehicle and a speed of V_a feet per second.

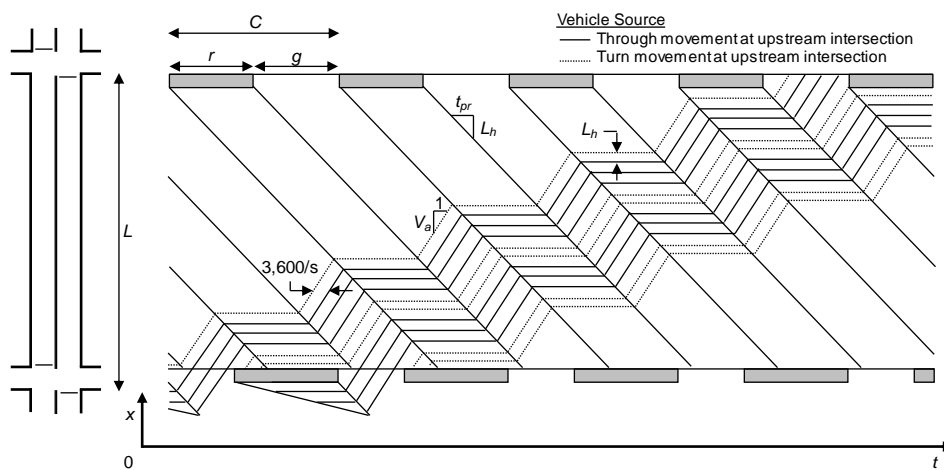


Exhibit 30-6
Vehicle Trajectories During Spillback Conditions

The lines that slope downward from the upper left to lower right represent the waves of reaction time. They have a slope of t_{pr} seconds per vehicle. The starting wave originates at the onset of the green indication, and the stopping wave originates at the onset of the red indication. The average vehicle spacing when vehicles are stopped is L_h feet per vehicle.

On the basis of the relationships shown in Exhibit 30-6, the following procedure can be used to estimate the effective average vehicle spacing.

Step 1. Compute Wave Travel Time

The time required for the driver reaction wave to propagate backward to the upstream intersection is computed with the following equation:

Equation 30-14

$$t_{max} = \frac{(L - W_i) t_{pr}}{L_h}$$

with

Equation 30-15

$$L_h = L_{pc}(1 - 0.01 P_{HV}) + 0.01 L_{HV} P_{HV}$$

where

- t_{max} = wave travel time (s);
- L = segment length (ft);
- W_i = width of upstream signalized intersection, as measured along the segment centerline (ft);
- t_{pr} = driver starting response time (= 1.3) (s/veh);
- L_h = average vehicle spacing in stationary queue (ft/veh);
- L_{pc} = stored passenger car lane length = 25 (ft);
- L_{HV} = stored heavy vehicle lane length = 45 (ft); and
- P_{HV} = percent heavy vehicles in the corresponding movement group (%).

Step 2. Compute Speed of Moving Queue

The average speed of the moving queue is computed with Equation 30-16:

Equation 30-16

$$V_a = \frac{L_h}{2.0 - t_{pr}}$$

where V_a is the average speed of moving queue (ft/s).

Step 3. Compute Effective Average Vehicle Spacing

The relationship between the trajectories of the moving vehicles defines the following association between speed, saturation flow rate, signal timing, and vehicle spacing.

Equation 30-17

$$\begin{aligned} &\text{If } 0.0 \leq t_{max} < r, \text{ then } L_h^* = L_h \\ &\text{If } r \leq t_{max} < C, \text{ then } L_h^* = 2.0 \left(\frac{r}{L - W_i} + \frac{1}{V_a} \right)^{-1} \geq L_h \\ &\text{If } C \leq t_{max}, \text{ then } L_h^* = \frac{L_h}{1.0 - 0.5 t_{pr} g / C} \end{aligned}$$

where

- L_h^* = effective average vehicle spacing in stationary queue (ft/veh),
- r = effective red time (= $C - g$) (s),
- g = effective green time (s), and
- C = cycle length (s).

Equation 30-17 has three component equations. The component equation used for a given segment and analysis period will be based on the value of t_{max} , r , and C . The value of average vehicle spacing from the first component equation is the smallest that can be obtained from Equation 30-17. The value from the last equation is the largest that can be obtained. The value obtained from the equation in the middle varies between these two extreme values, depending on the value of t_{max} .

Spillback Check

This subsection describes the procedure for determining whether queue spillback occurs on a segment during a given analysis period (4). The analysis is applied separately to each travel direction and proceeds in the direction of travel. The procedure consists of a series of steps that are completed in sequence for the signalized exit movements associated with each segment. These movements were shown in Exhibit 30-1. Spillback due to the movements associated with the access points is not specifically addressed.

Step 1: Identify Initial Queue

During this step, the initial queue for each signalized exit movement is identified. This value represents the queue present at the start of the analysis period (the total of all vehicles in all lanes serving the movement). The initial queue estimate would likely be available for the evaluation of an existing condition for which field observations indicate the presence of a queue at the start of the analysis period. For planning or preliminary design applications, it can be assumed to equal 0.0 vehicles.

Step 2: Identify Queue Storage Length

The length of queue storage for each exit movement is identified during this step. For turn movements served from a turn bay, this length equals the length of the turn bay. For through movements, this length equals the segment length less the width of the upstream intersection. For turn movements served from a lane equal in length to that of the segment, the queue storage length equals the segment length less the width of the upstream intersection.

Step 3: Compute Maximum Queue Storage

The maximum queue storage for the exiting through movement is computed with Equation 30-18:

$$N_{qx,thru} = \frac{(N_{th} - P_L - P_R) L_{a,thru}}{L_h^*}$$

where

$N_{qx,thru}$ = maximum queue storage for the through movement (veh),

N_{th} = number of through lanes (shared or exclusive) (ln),

P_L = proportion of left-turning vehicles in the shared lane (decimal),

P_R = proportion of right-turning vehicles in the shared lane (decimal),

Equation 30-18

$L_{a,thru}$ = available queue storage distance for the through movement (ft/ln), and
 L_h^* = effective average vehicle spacing in stationary queue (ft/veh).

The procedure described in Section 2 of Chapter 31, Signalized Intersections: Supplemental, is used to estimate P_L and P_R . If there are no shared lanes, $P_L = 0.0$ and $P_R = 0.0$.

The maximum queue storage for a turn movement is computed with Equation 30-19:

Equation 30-19

$$N_{qx,turn} = \frac{N_{turn} L_{a,turn} + P_{turn} L_{a,thru}}{L_h}$$

where

$N_{qx,turn}$ = maximum queue storage for a turn movement (veh),

N_{turn} = number of lanes in the turn bay (ln),

$L_{a,turn}$ = available queue storage distance for the turn movement (ft/ln),

P_{turn} = proportion of turning vehicles in the shared lane = P_L or P_R (decimal),
and

L_h = average vehicle spacing in stationary queue (ft/veh).

This equation is applicable to turn movements in exclusive lanes (i.e., $P_{turn} = 0.0$) and to turn movements that share a through lane.

Step 4: Compute Available Storage Length

The available storage length is computed for each signalized exit movement by using Equation 30-20.

Equation 30-20

$$N_{qa} = N_{qx} - Q_b \geq 0.0$$

where

N_{qa} = available queue storage (veh),

N_{qx} = maximum queue storage for the movement (veh), and

Q_b = initial queue at the start of the analysis period (veh).

The analysis thus far has treated the three signalized exit movements as if they were independent. At this point, the analysis must be extended to include the combined through and left-turn movement when the left-turn movement has a bay (i.e., it does not have a lane that extends the length of the segment). The analysis must also be extended to include the combined through and right-turn movement when the right-turn movement has a bay (but not a full-length lane).

The analysis of these newly formed “combined movements” is separated into two parts. The first part is the analysis of just the bay. This analysis is a continuation of the exit movement analysis using the subsequent steps of this procedure. The second part is the analysis of the length of the segment shared by the turn movement and the adjacent through movement. The following rules are used to evaluate the combined movements for the shared segment length:

1. The volume for each combined movement equals the sum of the adjusted arrival volumes for the two contributing movements. These volumes are

obtained from the procedure described in a previous subsection, Origin-Destination Distribution.

2. The initial queue for each combined movement is computed with Equation 30-21.

$$Q_{b,comb} = \max\left(0.0, Q_{b,turn} - \frac{L_{a,turn} N_{turn}}{L_h^*}, Q_{b,thru} - \frac{L_{a,turn} N_{th}}{L_h^*}\right)$$

Equation 30-21

where $Q_{b,comb}$ is the initial queue for the combined movement (veh). The other variables were defined previously and are evaluated for the movement indicated by the variable subscript.

3. The queue storage length for a combined movement $L_{a,comb}$ equals the queue storage length for the through movement less the queue storage length of the turn movement (i.e., $L_{a,comb} = L_{a,thru} - L_{a,turn}$).
4. The number of lanes available to the combined movement N_{comb} equals the number of lanes available to the through movement.
5. The maximum queue storage for the combined movement $N_{qx,comb}$ is computed with the following equation:

$$N_{qx,comb} = \frac{N_{th} L_{a,thru}}{L_h^*}$$

Equation 30-22

6. The available storage length for the combined movement $N_{qa,comb}$ is computed with the following equation:

$$N_{qa,comb} = N_{qx,comb} - Q_{b,comb} \geq 0.0$$

Equation 30-23

Step 5: Compute Capacity

The capacity for both the exit movements and the combined movements is established in this step. The capacity for each exit movement was computed in Step 2 in the subsection titled Capacity Constraint and Volume Balance. The capacity of the combined movements is computed by using Equation 30-24.

$$c = \frac{v_{a,1}}{X_1} + \frac{c_{thru}(N_{th} - 1)}{N_{th}}$$

Equation 30-24

with

$$v_{a,1} = \max\left(v_{a,turn}, \frac{v_{a,turn} + v_{a,thru}}{N_{th}}\right)$$

Equation 30-25

$$X_1 = \frac{v_{a,turn}}{c_{turn}} + \frac{v_{a,1} - v_{a,turn}}{c_{thru}/N_{th}}$$

Equation 30-26

where

- c = capacity of the combined movements (veh/h),
- $v_{a,1}$ = adjusted arrival volume in the shared lane (veh/h),
- X_1 = volume-to-capacity ratio in the shared lane,
- c_{thru} = capacity for the exiting through movement (veh/h),
- c_{turn} = capacity for the exiting turn movement (veh/h),
- $v_{a,turn}$ = adjusted arrival volume for the subject turn movement (veh/h),

$v_{a,thru}$ = adjusted arrival volume for the subject through movement (veh/h), and
 N_{th} = number of through lanes (shared or exclusive) (ln).

The two adjusted arrival volumes $v_{a,turn}$ and $v_{a,thru}$ are obtained from the procedure described in the Origin–Destination Distribution subsection.

Step 6: Compute Queue Growth Rate

During this step, the queue growth rate is computed for each signalized exit movement for which the storage extends the length of the segment. Typically, the through movement satisfies this requirement. A turn movement may also satisfy this requirement if it is served by an exclusive lane that extends the length of the segment. The queue growth rate is computed as the difference between the adjusted arrival volume v_a and the capacity c for the subject exit movement.

Equation 30-27 is used to compute this rate.

Equation 30-27

$$r_{qg} = v_a - c \geq 0.0$$

where r_{qg} is the queue growth rate (veh/h).

The queue growth rate is also computed for the combined movements formulated in Step 4. The adjusted volume used in Equation 30-27 represents the sum of the through and turn movement volumes in the combined group. The capacity for the group was computed in Step 5.

Step 7: Compute Time Until Spillback

During this step, the time until spillback is computed for each signalized exit movement for which the storage extends the length of the segment. This time is computed with Equation 30-28 for any movement with a nonzero queue growth rate.

Equation 30-28

$$T_c = \frac{N_{qa}}{r_{qg}}$$

where T_c is the time until spillback (h).

For turn movements served by a bay, the computed spillback time is the time required for the bay to overflow. It does not represent the time at which the turn-related queue reaches the upstream intersection.

Equation 30-28 is also used to compute the spillback time for the combined movements formulated in Step 4. However, this spillback time is the additional time required for the queue to grow along the length of segment shared by the turn movement and the adjacent through movement. This time must be added to the time required for the corresponding turn movement to overflow its bay to obtain the actual spillback time for the combined movement.

Step 8: Repeat Steps 1 Through 7 for Each Segment

The preceding steps should be completed for each segment in the facility in the subject direction of travel. The procedure should then be repeated for the opposing direction of travel.

Step 9: Determine Controlling Spillback Time

During this step, the shortest time until spillback for each of the exit movements (or movement groups) for each segment and direction of travel is identified. If the segment supports two travel directions, two values are identified (one value for each direction). The smaller of the two values is the controlling spillback time for the segment. If a movement (or movement group) does not spill back, it is not considered in this process for determining the controlling spillback time.

Next, the controlling segment times are compared for all segments that make up the facility. The shortest time found is the controlling spillback time for the facility.

If the controlling spillback time exceeds the analysis period, the results from the motorized vehicle methodology are considered to reflect the operation of the facility accurately. If spillback occurs before the end of the desired analysis period, the analyst should consider either (a) reducing the analysis period so that it ends before spillback occurs or (b) using the sustained spillback evaluation procedure in Chapter 29, Urban Street Facilities: Supplemental.

MIDSEGMENT LANE RESTRICTION

When one or more lanes on an urban street segment are temporarily closed, the flow in the lanes that remain open can be adversely affected. The closure can be due to a work zone, an incident, or a similar event. Occasionally, the lane closure can adversely affect the performance of traffic movements that are entering or exiting the segment at the boundary signalized intersection. Logically, the magnitude of the effect will increase as the distance between the intersection and lane closure decreases. The impact on the intersection that has a downstream lane closure is the subject of discussion in this subsection.

The procedure described in this subsection is used to adjust the saturation flow rate of the movements entering a segment when one or more downstream lanes are blocked. The procedure is developed for incorporation within the motorized vehicle methodology described in Chapters 18 and 19 (5). Specifically, the procedure is inserted into the motorized vehicle methodology in Chapter 18, Urban Street Segments, and used to compute a saturation flow rate adjustment factor for the movements entering the segment at the intersection. This adjustment factor is then implemented in the motorized vehicle methodology in Chapter 19, Signalized Intersections, to compute the adjusted saturation flow rate of the affected movements.

This procedure is added to the end of Step 4 of the motorized vehicle methodology described in Chapter 18. It occurs after the saturation flow rate and phase duration have been determined. It is implemented as part of the iterative convergence loop identified in the motorized vehicle methodology framework shown in Exhibit 18-8.

The calculation sequence begins with an estimate of the capacity for each traffic movement discharged to the downstream segment. This estimate is obtained by using the motorized vehicle methodology in Chapter 19. The next step is to compute the capacity of the downstream segment as influenced by the

midsegment lane restriction. The estimate of movement capacity is then compared with the downstream segment capacity. If the movement capacity exceeds the downstream segment capacity, the movement saturation flow rate is reduced proportionally by using an adjustment factor for downstream lane blockage.

The lane blockage saturation flow rate adjustment factor is computed for each movement entering the subject segment. The following equations are used to compute the factor value.

Equation 30-29

$$\text{If } c_{ms} < c_i \text{ or } f_{ms,i-1} < 1.0, \text{ then } f_{ms,i} = f_{ms,i-1} \frac{c_{ms}}{c_i} \geq 0.1$$

$$\text{Otherwise, } f_{ms,i} = 1.0$$

with

Equation 30-30

$$c_{ms} = 0.25 k_j N_{unblk} S_f \leq 1,800 N_{unblk}$$

where

$f_{ms,i}$ = adjustment factor for downstream lane blockage during iteration i ,

c_{ms} = midsegment capacity (veh/h),

c_i = movement capacity during iteration i (veh/h),

k_j = jam density (= 5,280 / L_h) (veh/mi/ln),

L_h = average vehicle spacing in stationary queue (ft/veh),

S_f = free-flow speed (mi/h), and

N_{unblk} = number of open lanes when blockage is present (ln).

The number of lanes used in Equation 30-30 equals the number of unblocked lanes (i.e., the open lanes) while the blockage is present.

The variable i in the adjustment factor subscript indicates that the factor's value is incrementally revised during each iteration of the convergence loop associated with the motorized vehicle methodology. Ultimately, the factor converges to a value that results in a movement capacity matching the available midsegment capacity. For the first iteration, the factor value is set to 1.0 for all movements. The factor value is also set to 1.0 if the segment is experiencing spillback. In this situation, a saturation flow rate adjustment factor for spillback (which incorporates the downstream lane blockage effect) is computed for the movement. The calculation of the factor for spillback is described in Chapter 29, Urban Street Facilities: Supplemental.

Equation 30-29 indicates that the factor is less than 1.0 when the midsegment capacity is smaller than the movement capacity. If the factor has been set to a value less than 1.0 in a previous iteration, it continues to be adjusted during each subsequent iteration until convergence is achieved. A minimum factor value of 0.1 is imposed as a practical lower limit.

4. DELAY DUE TO TURNS

This section describes a process for estimating the delay to through vehicles that follow vehicles turning from the major street into an unsignalized access point intersection. This delay can be incurred at any access point intersection along the street. For right-turn vehicles, the delay results when the following vehicles' speed is reduced to accommodate the turning vehicle. For left-turn vehicles, the delay results when the following vehicles must wait in queue while a vehicle ahead executes a left-turn maneuver at the access point. This delay occurs primarily on undivided streets; however, it can occur on divided streets when the left-turn queue exceeds the available storage and spills back into the inside through lane.

The delay estimation process consists of the following two procedures:

- Delay due to left turns and
- Delay due to right turns.

Each procedure is described in the following subsections. These procedures are based on the assumption that the segment traffic flows are random. While this assumption may not be strictly correct for urban streets, it is conservative in that it will yield slightly larger estimates of delay. Moreover, expansion of the models to accommodate platooned flows would not likely be cost-effective given the small amount of delay caused by turning vehicles.

DELAY DUE TO LEFT TURNS

Through vehicles on the major-street approach to an unsignalized intersection can incur delay when the left-turn queue exceeds the available storage and blocks the adjacent through lane (in this context, the undivided cross section is considered a major-street approach having no left-turn storage). The through vehicles that follow are delayed when they stop behind the queue of turning vehicles. This delay ends when the left-turn vehicle departs or the through vehicle merges into the adjacent through lane. By merging into the adjacent lane, drivers reduce their delay relative to the delay they would have incurred had they waited for the left-turn queue to clear. This delay is computed by using Equation 30-31.

$$d_{ap,l} = p_{ov} d_{t,1} \left(\frac{1}{P_L} - 1 \right) \frac{P_{lt}}{1 - P_{lt} - P_{rt}}$$

Equation 30-31

where

$d_{ap,l}$ = through-vehicle delay due to left turns (s/veh),

p_{ov} = probability of left-turn bay overflow (decimal),

$d_{t,1}$ = average delay to through vehicles in the inside lane (s/veh),

P_L = proportion of left-turning vehicles in the shared lane (decimal),

P_{lt} = proportion of left-turning vehicles on the subject approach (decimal), and

P_{rt} = proportion of right-turning vehicles on the subject approach (decimal).

As indicated by Equation 30-31, the delay due to left turns is based on the value of several variables. The following sequence of computations can be used to estimate these values (6).

Step 1: Compute the Probability of a Lane Change

Equation 30-32

$$P_{lc} = 1 - \left[\left(2 \frac{v_{app}}{s_{lc}} \right) - 1 \right]^2 \geq 0.0$$

with

Equation 30-33

$$v_{app} = \frac{v_{lt} + v_{th} + v_{rt}}{N_{sl} + N_t + N_{sr}}$$

where

P_{lc} = probability of a lane change among the approach through lanes,

v_{app} = average demand flow rate per through lane (upstream of any turn bays on the approach) (veh/h/ln),

s_{lc} = maximum flow rate in which a lane change can occur = 3,600/ t_{lc} (veh/h/ln),

t_{lc} = critical merge headway = 3.7 (s),

v_{lt} = left-turn demand flow rate (veh/h),

v_{th} = through demand flow rate (veh/h),

v_{rt} = right-turn demand flow rate (veh/h),

N_{sl} = number of lanes in shared left-turn and through-lane group (ln),

N_t = number of lanes in exclusive through-lane group (ln), and

N_{sr} = number of lanes in shared right-turn and through-lane group (ln).

If the ratio v_{app}/s_{lc} in Equation 30-32 exceeds 1.0, then it should be set to 1.0.

Step 2: Compute Through-Vehicle Equivalent for Left-Turn Vehicle

If there is a left-turn bay on the major street at the access point, the through-vehicle equivalent E_{L1} is 1.0. However, if there is no left-turn bay, the following equation is used to compute the through-vehicle equivalent.

Equation 30-34

$$E_{L1} = \frac{1,800}{c_l}$$

with

Equation 30-35

$$c_l = \frac{v_o e^{-v_o t_{cg}/3,600}}{1 - e^{-v_o t_{fh}/3,600}}$$

where

E_{L1} = equivalent number of through cars for a permitted left-turning vehicle,

c_l = capacity of a left-turn movement with permitted left-turn operation (veh/h),

v_o = opposing demand flow rate (veh/h),

t_{fh} = follow-up headway = 2.2 (s), and

t_{cg} = critical headway = 4.1 (s).

Step 3: Compute Modified Through-Vehicle Equivalent

$$E_{L1,m} = (E_{L1} - 1)P_{lc} + 1$$

$$E_{R,m} = (E_{R,ap} - 1)P_{lc} + 1$$

Equation 30-36

Equation 30-37

where

$E_{L1,m}$ = modified through-car equivalent for a permitted left-turning vehicle,

$E_{R,m}$ = modified through-car equivalent for a protected right-turning vehicle,
and

$E_{R,ap}$ = equivalent number of through cars for a protected right-turning vehicle at an access point (2.20 if there is no right-turn bay on the major street at the access point; 1.0 if there is a right-turn bay).

Step 4: Compute Proportion of Left Turns in Inside Through Lane

$$P_L = \frac{-b + \sqrt{b^2 - 4 I_t R c}}{2 I_t R} \leq 1.0$$

Equation 30-38

with

$$b = R - I_{lt} P_{lt} \{I_t + (N_{sl} + N_t + N_{sr} - 1)[(1 + I_t)E_{L1,m} - 1]\}$$

Equation 30-39

$$c = -I_{lt} P_{lt} (N_{sl} + N_t + N_{sr})$$

Equation 30-40

$$R = 1 + I_{rt} P_{rt} (E_{R,m} - 1)$$

Equation 30-41

where

R, b, c = intermediate calculation variables;

I_{lt} = indicator variable (1.0 when there is no left-turn bay on the major street at the access point, 0.0 when there is a left-turn bay);

I_{rt} = indicator variable (1.0 when there is no right-turn bay on the major street at the access point, 0.0 when there is a right-turn bay); and

I_t = indicator variable (1.0 when equations are used to evaluate delay due to left turns, 0.00001 when equations are used to evaluate delay due to right turns).

If the number of through lanes on the subject intersection approach ($= N_{sl} + N_t + N_{sr}$) is equal to 1.0, then $P_L = P_{lt}$.

The indicator variable I_t is used to adapt the equations to the analysis of lane volume for both left-turn- and right-turn-related delays. The variable has a value of 1.0 in the evaluation of left-turn-related delays. In this situation, it models the condition in which one or more left-turning vehicles are blocking the inside lane. In contrast, the variable has a negligibly small value when it is applied to right-turn-related delays. It models flow conditions in which all lanes are unblocked.

Step 5: Compute Proportion of Right Turns in Outside Through Lane

Equation 30-42
$$P_R = I_{rt} P_{rt} \frac{\frac{s_1}{1,800} + N_{sl} + N_t + N_{sr} - 1}{1 - I_{rt} P_{rt} \left(\frac{s_1}{1,800} + N_{sl} + N_t + N_{sr} - 2 \right) (E_{R,m} - 1)} \leq 1.0$$

with

Equation 30-43
$$s_1 = \frac{1,800 (1 + P_L I_t)}{1 + P_L (E_{L1,m} - 1) + (P_L E_{L1,m} I_t)}$$

where s_1 is the saturation flow rate for the inside lane (veh/h/ln). If the number of through lanes on the subject intersection approach ($= N_{sl} + N_t + N_{sr}$) is equal to 1.0, then $P_R = P_{rt}$.

Step 6: Compute Inside Lane and Outside Lane Flow Rates

Equation 30-44
$$v_1 = \frac{v_{lt}}{P_L}$$

Equation 30-45
$$v_n = \begin{cases} \frac{v_{rt}}{P_R} & \text{if } P_R > 0.0 \\ \frac{v_{lt} + v_{th} + v_{rt} - v_1}{N_{sl} + N_t + N_{sr} - 1} & \text{if } P_R = 0.0 \end{cases}$$

where

v_1 = flow rate for the inside lane (veh/h/ln) and

v_n = flow rate for the outside lane (veh/h/ln).

Step 7: Compute Intermediate Lane Flow Rate

If there are more than two lanes on the subject intersection approach, Equation 30-46 can be used to estimate the flow rate in the intermediate lanes.

Equation 30-46
$$v_i = \frac{v_{lt} + v_{th} + v_{rt} - v_1 - v_n}{N_{sl} + N_t + N_{sr} - 2}$$

where v_i is the flow rate for lane i (veh/h/ln). The flow rates in lanes 2, 3, . . . , $n - 1$ are identical and equal to the value obtained from Equation 30-46.

Step 8: Compute Merge Capacity

Equation 30-47 is used to compute the merge capacity available to through drivers waiting in the inside lane of a multilane approach.

Equation 30-47
$$c_{mg} = \frac{v_2 e^{-v_2 t_{lc}/3,600}}{1 - e^{-v_2 t_{lc}/3,600}}$$

where

c_{mg} = merge capacity (veh/h),

v_2 = flow rate in the adjacent through lane (veh/h/ln), and

t_{lc} = critical merge headway = 3.7 (s).

Step 9: Compute Delay to Through Vehicles That Merge

$$d_{mg} = 3,600 \left(\frac{1}{c_{mg}} - \frac{1}{1,800} \right) + 900 T \left[\frac{v_{mg}}{c_{mg}} - 1 + \sqrt{\left(\frac{v_{mg}}{c_{mg}} - 1 \right)^2 + \frac{8 v_{mg}}{c_{mg}^2 T}} \right]$$

Equation 30-48

with

$$v_{mg} = v_1 - v_{lt} \geq 0.0$$

Equation 30-49

where

d_{mg} = merge delay (s/veh),

v_{mg} = merge flow rate (veh/h/ln), and

T = analysis period duration (h).

This delay is incurred by through vehicles that stop in the inside lane and eventually merge into the adjacent through lane. The “1/1,800” term included in Equation 30-48 extracts the service time for the through vehicle from the delay estimate, so that the delay estimate represents the increase in travel time resulting from the left-turn queue.

Step 10: Compute Inside Lane Capacity

Equation 30-50 is used to compute the capacity of the inside lane for vehicles that do not merge.

$$c_{nm} = \frac{1,800(1 + P_L)}{1 + P_L(E_{L1} - 1) + (P_L E_{L1})}$$

Equation 30-50

where c_{nm} is the nonmerge capacity for the inside lane (veh/h). The unadjusted through-vehicle equivalent for a left-turn vehicle E_{L1} is used in this equation to estimate the nonmerge capacity.

Step 11: Compute Delay to Through Vehicles That Do Not Merge

$$d_{nm} = 3,600 \left(\frac{1}{c_{nm}} - \frac{1}{1,800} \right) + 900 T \left[\frac{v_1}{c_{nm}} - 1 + \sqrt{\left(\frac{v_1}{c_{nm}} - 1 \right)^2 + \frac{8 v_1}{c_{nm}^2 T}} \right]$$

Equation 30-51

where d_{nm} is the nonmerge delay for the inside lane (s/veh). This delay is incurred by through vehicles that stop in the inside lane and wait for the queue to clear. These vehicles do not merge into the adjacent lane.

Step 12: Compute Delay to Through Vehicles in the Inside Lane

This delay is estimated as the smaller of the delay relating to the merge and nonmerge maneuvers. It is computed with Equation 30-52.

$$d_{t,1} = \min(d_{nm}, d_{mg})$$

Equation 30-52

Step 13: Compute the Probability of Left-Turn Bay Overflow

The probability of left-turn bay overflow is computed by using the following equation:

$$p_{ov} = \left(\frac{v_{lt}}{c_l} \right)^{N_{qx,lt}+1}$$

Equation 30-53

Equation 30-54

with

$$N_{qx,lt} = \frac{N_{lt} L_{a,lt}}{L_h}$$

where

p_{ov} = probability of left-turn bay overflow (decimal),

$N_{qx,lt}$ = maximum queue storage for the left-turn movement (veh),

N_{lt} = number of lanes in the left-turn bay (ln),

$L_{a,lt}$ = available queue storage distance for the left-turn movement (ft/ln), and

L_h = average vehicle spacing in the stationary queue (see Equation 30-15) (ft/veh).

For an undivided cross section, the number of left-turn vehicles that can be stored, $N_{qx,lt}$ is equal to 0.0.

Step 14: Compute Through-Vehicle Delay due to Left Turns

The through-vehicle delay due to left turns $d_{ap,l}$ is computed with Equation 30-31.

DELAY DUE TO RIGHT TURNS

A vehicle turning right from the major street into an access point often delays the through vehicles that follow it. Through vehicles are delayed because they have to reduce speed to avoid a collision with the vehicle ahead, the first of which has reduced speed to avoid a collision with the right-turning vehicle. This delay can be several seconds in duration for the first few through vehicles but will always decrease to negligible values for subsequent vehicles as the need to reduce speed diminishes. For purposes of running time calculation, this delay must be averaged over all through vehicles traveling in the subject direction. The resulting average delay is computed with Equation 30-55.

Equation 30-55

$$d_{ap,r} = 0.67 d_{t|r} \frac{P_{rt}}{1 - P_{lt} - P_{rt}}$$

where

$d_{ap,r}$ = through-vehicle delay due to right turns (s/veh) and

$d_{t|r}$ = through-vehicle delay per right-turn maneuver (s/veh).

The variable $d_{t|r}$ in Equation 30-55 converges to 0.0 as the proportion of turning vehicles approaches 1.0. The constant 0.67 is a calibration factor based on field data. The steps undertaken to quantify this factor are described in the remainder of this subsection. Equation 30-55 can also be used to estimate the delay due to left-turn vehicles on a one-way street. In this case, variables associated with the right-turn movement would be redefined as applicable to the left-turn movement and vice versa.

As indicated by Equation 30-55, the delay due to right turns is based on the value of several variables. The following sequence of computations can be used to estimate these values (7).

Step 1: Compute Minimum Speed for the First Through Vehicle

$$u_m = 1.47 S_f - r_d(H_1 - h_{|\Delta < h < H_1}) \geq u_{rt}$$

Equation 30-56

with

$$h_{|\Delta < h < H_1} = \frac{1}{\lambda} + \frac{\Delta - H_1 e^{-\lambda(H_1 - \Delta)}}{1 - e^{-\lambda(H_1 - \Delta)}}$$

Equation 30-57

$$H_1 = \frac{1.47 S_f - u_{rt}}{r_d} + t_{cl} + \frac{L_h}{1.47 S_f} \geq \Delta$$

Equation 30-58

$$\lambda = \frac{1}{\frac{1}{q_n} - \Delta}$$

Equation 30-59

where

 u_m = minimum speed of the first through vehicle given that it is delayed (ft/s),

 u_{rt} = right-turn speed = 20 (ft/s),

 S_f = free-flow speed (mi/h),

 $h_{|\Delta < h < H_1}$ = average headway of those headways between Δ and H_1 (s/veh),

 Δ = headway of bunched vehicle stream = 1.5 (s/veh),

 H_1 = maximum headway that the first through vehicle can have and still incur delay (s/veh),

 r_d = deceleration rate = 6.7 (ft/s²),

 t_{cl} = clearance time of the right-turn vehicle = 0.6 (s),

 L_h = average vehicle spacing in stationary queue (see Equation 30-15) (ft/veh),

 λ = flow rate parameter (veh/s),

 q_n = outside lane flow rate = $v_n/3,600$ (veh/s), and

 v_n = flow rate for the outside lane (veh/h/ln).

The right-turn speed u_{rt} used in Equation 30-56 and Equation 30-58 is likely to be sensitive to access point design, including the approach profile, throat width, and curb radius. For level profiles and nominal throat widths, the speed can vary from 15 to 25 ft/s for radii varying from 20 to 60 ft, respectively. A default turn speed of 20 ft/s is recommended when information is not available to make a more accurate estimate.

The flow rate for the outside lane v_n is computed by using Steps 3, 4, 5, and 6 from the procedure described in the previous subsection, Delay due to Left Turns. However, the probability of a lane change P_{lc} is set equal to 1.0 when the calculations in Step 3 are made. In Steps 4 and 5, the variable I_i is set equal to 0.00001. The proportion of right-turning vehicles in the shared lane P_R is also computed at this point and used in a later step.

Step 2: Compute Delay to the First Through Vehicle

Equation 30-60

$$d_1 = \frac{(1.47 S_f - u_m)^2}{2 (1.47 S_f)} \left(\frac{1}{r_d} + \frac{1}{r_a} \right)$$

where d_1 is the conditional delay to the first through vehicle (s/veh), and r_a is the acceleration rate = 3.5 (ft/s²).

Step 3: Compute Delay to the Second Through Vehicle

Equation 30-61

$$d_2 = d_1 - (h_{|\Delta < h < H_2} - \Delta)$$

with

Equation 30-62

$$h_{|\Delta < h < H_2} = \frac{1}{\lambda} + \frac{\Delta - H_2 e^{-\lambda(H_2 - \Delta)}}{1 - e^{-\lambda(H_2 - \Delta)}}$$

Equation 30-63

$$H_2 = d_1 + \Delta$$

where d_2 is the conditional delay to Vehicle 2 (s/veh).

Step 4: Compute Delay to the Third and Subsequent Through Vehicles

Equation 30-64

$$d_i = d_{i-1} - (h_{|\Delta < h < H_i} - \Delta)$$

with

Equation 30-65

$$h_{|\Delta < h < H_i} = \frac{1}{\lambda} + \frac{\Delta - H_i e^{-\lambda(H_i - \Delta)}}{1 - e^{-\lambda(H_i - \Delta)}}$$

Equation 30-66

$$H_i = d_{i-1} + \Delta$$

where d_i is the conditional delay to vehicle i ($i = 3, 4, \dots$) (s/veh). As shown by Equation 30-61 and Equation 30-64, the delay to each subsequent through vehicle is less than or equal to that of the preceding vehicle. In fact, the sequence of delays always converges to zero when the average flow rate in the outside lane is less than $1/\Delta$.

Step 4 should be repeated for the third and subsequent through vehicles until the delay computed for vehicle i is less than 0.1 s. In general, this criterion results in delay being computed for only the first two or three vehicles.

Step 5: Compute Through-Vehicle Delay per Right-Turn Maneuver

The through-vehicle delay for the first two vehicles is computed with Equation 30-67.

Equation 30-67

$$d_{t|r} = d_1(1 - e^{-\lambda(H_1 - \Delta)})(1 - P_R) + d_2(1 - e^{-\lambda(H_1 - \Delta)})(1 - e^{-\lambda(H_2 - \Delta)})(1 - P_R)^2$$

where $d_{t|r}$ is the through-vehicle delay per right-turn maneuver (s/veh). If three or more vehicles are delayed, an additional term needs to be added to Equation 30-67 for each subsequent vehicle. In this situation, Equation 30-68 can be used to compute the delay for any number of vehicles.

Equation 30-68

$$d_{t|r} = \sum_{i=1}^{\infty} \left[d_i \times \prod_{j=1}^i (1 - e^{-\lambda(H_j - \Delta)}) \times (1 - P_R)^i \right]$$

Step 6: Compute Through-Vehicle Delay due to Right Turns

The through-vehicle delay due to right turns $d_{ap,r}$ is computed with Equation 30-55.

5. PLANNING-LEVEL ANALYSIS APPLICATION

OVERVIEW OF THE APPLICATION

This section describes a simplified method for evaluating the operation of a coordinated street segment with signalized boundary intersections. The application addresses motorized vehicle operation. It is focused on the analysis of the through movement at the boundary intersections. This method can be used when minimal data are available for the analysis and only approximate results are desired.

REQUIRED DATA AND SOURCES

The overall data requirements are summarized in Exhibit 30-7. Some of the input requirements may be met by assumed values or default values. Other data items are site-specific and must be obtained in the field. The objective of using the planning-level analysis application is to minimize the need for the collection of detailed field data.

Exhibit 30-7
Required Input Data for the
Planning-Level Analysis
Application

Data Category	Location	Input Data Element
Traffic characteristics	Boundary intersection	Through-demand flow rate Through-saturation flow rate Volume-to-capacity ratio of the upstream movements
	Segment	Platoon ratio Midsegment flow rate Midsegment delay
Geometric design	Boundary intersection	Number of through lanes Upstream intersection width
	Segment	Number of through lanes Segment length Restrictive median length Nonrestrictive median length Proportion of segment with curb Number of access point approaches Proportion of segment with on-street parking
Signal control	Boundary intersection	Effective green-to-cycle-length ratio Cycle length
Other	Segment	Analysis period duration Speed limit

At a minimum, the analyst must provide traffic volumes and the approach-lane configuration for the subject intersection. Default values for several variables are specifically identified in the methodology and integrated into the method. These values have been selected to be generally representative of typical conditions. Additional default values are identified in Section 3 of Chapter 18, Urban Street Segments.

METHODOLOGY

The methodology consists of five computational steps. These steps are

- Determine running time;
- Determine proportion arriving during green;
- Determine through control delay;

- Determine through stop rate; and
- Determine travel speed, spatial stop rate, and level of service (LOS).

Each step is executed in the sequence presented in the preceding list. This sequence is illustrated by the flowchart in Exhibit 30-8. The rectangles with rounded corners indicate the computational steps. The parallelograms indicate where input data are needed.

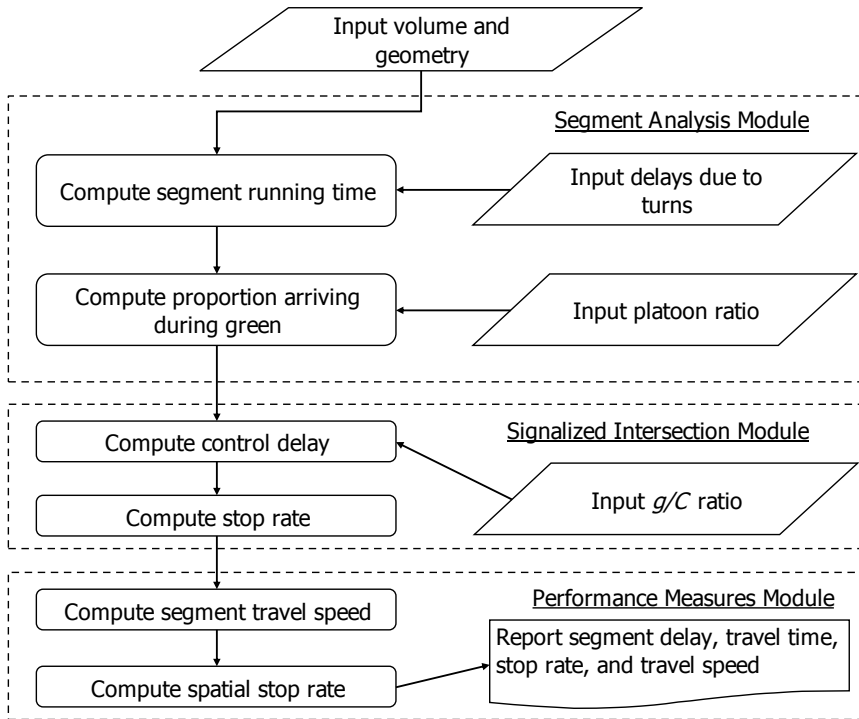


Exhibit 30-8
 Planning-Level Analysis
 Application for Urban Street
 Segments

The computations associated with each step identified in Exhibit 30-8 are described in Section 3 of Chapter 18. These computations are conveniently illustrated here in a series of worksheets; each worksheet corresponds to one or two of the calculation steps.

The first of the computational worksheets is the Running Time worksheet. It is shown as Exhibit 30-9 (values shown apply to the Example Problem, as discussed in a subsequent section).

Exhibit 30-9
 Planning-Level Analysis:
 Running Time Worksheet

RUNNING TIME WORKSHEET					
General Information		Site Information			
Analyst	JME	Street	Texas Avenue		
Agency or Company	ACME Engr.	Jurisdiction			
Date Performed	9/30/15	Analysis Year	2015		
Analysis Time Period	5:30 p.m. to 5:45 p.m.	Analysis Level	planning		
Base free-flow speed calibration factor (S_{calib}), mi/h: 0.0					
Input Data					
		Segment 1		Segment 2	
Direction of travel		EB/NB	WB/SB	EB/NB	WB/SB
Segment Data					
Number of through lanes for length of segment N_{th} (ln)		2	2		
Speed limit S_{pl} (mi/h)		35	35		
Midsegment volume v_m (veh/h)		1,150	1,150		
Total delay due to turns into access points $\sum d_{ap}$ (s/veh)		0.52	0.52		
Delay due to other midsegment sources d_{other} (s/veh)		0	0		
Length of segment L (ft)		1,800	1,800		
Width of upstream boundary intersection W_i (ft)		50	50		
Length of segment with restrictive median L_{rm} (ft)		0	0		
Length of segment with nonrestrictive median L_{nr} (ft)		0	0		
Start-up lost time l_1 (s)		2.0	2.0		
Access Data					
Proportion of segment with curb on right-hand side ρ_{curb}		0.70	0.70		
Number of access points on right-hand side N_{ap}		4	4		
Proportion of segment with on-street parking ρ_{pk}		0.00	0.00		
Running Time Computation					
Adjusted segment length L_{adj} (ft) $L_{adj} = L - W_i$		1,750	1,750		
Proportion of segment length with restrictive median ρ_{rm} $\rho_{rm} = L_{rm} / L_{adj}$		0.0	0.0		
Speed constant S_0 (mi/h), $S_0 = 25.6 + 0.47 S_{pl}$		42.1	42.1		
Adjustment for cross section f_{CS} (mi/h), $f_{CS} = 1.5 \rho_{rm} - 0.47 \rho_{curb} - 3.7 \rho_{curb} \rho_{rm}$		-0.3	-0.3		
Access point density D_a (access points/mi), $D_a = 5,280 (N_{ap,EB/NB} + N_{ap,WB/SB}) / L_{adj}$		24.1	24.1		
Adjustment for access points f_A (mi/h), $f_A = -0.078 D_a / N_{th}$		-0.9	-0.9		
Adjustment for on-street parking f_{pk} (mi/h), $f_{pk} = -3 \rho_{pk}$		0.0	0.0		
Base free-flow speed S_{f0} (mi/h), $S_{f0} = S_{calib} + S_0 + f_{CS} + f_A + f_{pk}$		40.8	40.8		
Segment length adjustment factor f_L , $f_L = 1.02 - 4.7 (S_{f0} - 19.5) / \max(L, 400) \leq 1.0$		0.96	0.96		
Free-flow speed S_f (mi/h), $S_f = S_{f0} f_L \geq S_{pl}$		39.3	39.3		
Proximity adjustment factor f_v , $f_v = \frac{2}{1 + \left(1 - \frac{v_m}{52.8 N_{th} S_f}\right)^{0.21}}$		1.03	1.03		
Running time t_R (s) $t_R = \frac{6.0 - l_1}{0.0025 L} + \frac{3,600 L}{5,280 S_f} f_v + \sum d_{ap} + d_{other}$		33.7	33.7		

Note: The first term in the running time equation is only applicable to segments with signal-controlled, STOP-controlled, or YIELD-controlled through movement at the boundary intersection.

The Running Time worksheet combines input data describing the segment geometric design, speed limit, volume, and access point frequency to estimate the base free-flow speed. This speed is then adjusted for segment length effects to obtain the expected free-flow speed. The free-flow speed is then used to estimate a free-flow travel time, which is adjusted for the proximity of other vehicles. Delay that is caused by turns into access points or other sources is added to the adjusted travel time. Default values for the delay due to turns at midsegment access points are listed in Exhibit 18-13 in Chapter 18. These defaults can be used when more accurate estimates of this delay are not available. The result of these adjustments is an estimate of the expected segment running time.

The second of the computational worksheets is the Proportion Arriving During Green worksheet. It is shown as Exhibit 30-10. This worksheet is designed for the analysis of the segment through-lane group. It documents the calculation of the proportion of vehicles that arrive during the green indication. Input data include the effective green-to-cycle-length ratio and platoon ratio.

PROPORTION ARRIVING DURING GREEN WORKSHEET				
General Information				
Project Description	Texas Avenue, 5:30 p.m. to 5:45 p.m.			
Input Data				
	Segment 1		Segment 2	
Direction of travel	EB/NB	WB/SB	EB/NB	WB/SB
Signal Timing Data				
Effective green-to-cycle-length ratio g/C	0.47	0.47		
Traffic Data				
Platoon ratio R_p	1.43	0.67		
Proportion Arriving During Green Computation				
Proportion arriving during green $P, P = R_p (g/C)$	0.67	0.31		

Exhibit 30-10
 Planning-Level Analysis:
 Proportion Arriving During
 Green Worksheet

The third computational worksheet is the Control Delay worksheet. It is shown as Exhibit 30-11. This worksheet is designed for the analysis of the segment through-lane group. Input variables include the analysis period duration, cycle length, effective green-to-cycle-length ratio, volume, saturation flow rate, and lanes. The proportion of arrivals during green is obtained from the previous worksheet.

The equation for computing the progression adjustment factor PF^* that is provided in Exhibit 30-11 is a simplified version of the exact equation (as provided in Section 3 of Chapter 19). The simplified equation, in combination with the supplemental adjustment factor f_{PAV} is sufficiently accurate for purposes of the planning-level analysis application.

The control delay is computed as the sum of two components. The first component to be computed is the uniform delay. The notation “min(1, X)” is shown in the equation used to compute this delay. It means that the value to be substituted for this text is the smaller of 1.0 and the volume-to-capacity ratio.

Exhibit 30-11
 Planning-Level Analysis:
 Control Delay Worksheet

CONTROL DELAY WORKSHEET				
General Information				
Project Description	Texas Avenue, 5:30 p.m. to 5:45 p.m.			
Input Data				
Analysis period T (h): 0.25	Segment 1		Segment 2	
Direction of travel	EB/NB	WB/SB	EB/NB	WB/SB
Signal Timing Data				
Cycle length C (s)	100	100		
Effective green-to-cycle-length ratio g/C	0.47	0.47		
Traffic Data				
Through-lane group volume v_{th} (veh/h)	968	950		
Lane group saturation flow rate s (veh/h/ln)	1,800	1,800		
Proportion of arrivals during green P	0.67	0.31		
Volume-to-capacity ratio X_u of the upstream movements	0.57	0.57		
Geometric Design Data				
Number of through lanes N_{th} (ln)	2	2		
Delay Computation				
Capacity c (veh/h), $c = N_{th} s g/C$	1,692	1,692		
Volume-to-capacity ratio X , $X = v_{th}/c$	0.57	0.56		
Supplemental adjustment factor for platoons arriving during green f_{PA} , $f_{PA} = 1.00$ except as noted below: If $0.50 < R_p \leq 0.85$, then $f_{PA} = 0.93$ If $1.15 < R_p \leq 1.50$, then $f_{PA} = 1.15$	1.15	0.93		
Progression adjustment factor PF^* , $PF^* = f_{PA} (1 - P)/(1 - g/C)$	0.71	1.20		
Uniform delay d_1 (s/veh), $d_1 = (PF^*) \frac{0.5 C (1 - g/C)^2}{1 - [\min(1, X)g/C]}$	13.6	23.0		
Upstream filtering adjustment factor I , $I = 1.0 - 0.91 X_u^{2.68} \geq 0.090$	0.80	0.80		
Incremental delay d_2 (s/veh), $d_2 = 900 T \left[(X - 1) + \sqrt{(X - 1)^2 + \frac{4 I X}{c T}} \right]$	1.13	1.08		
Control delay d (s/veh), $d = d_1 + d_2$	14.7	24.1		

The second delay component is the incremental delay, which is based on the upstream filtering adjustment factor. This factor requires the variable X_u , which can be estimated as the volume-to-capacity ratio of the segment through-lane group at the upstream signalized intersection. Additional detail on the calculation of this ratio is provided in Section 3 of Chapter 19, Signalized Intersections.

The fourth computational worksheet is the Stop Rate worksheet. It is shown as Exhibit 30-12. This worksheet is designed for the analysis of the segment through-lane group. The input variables are the same as those needed for the Control Delay worksheet with the addition of speed limit. The average speed

during the analysis period is estimated by using the equation provided. If the average speed is known, it should be substituted for the estimated value.

STOP RATE WORKSHEET				
General Information				
Project Description		Texas Avenue, 5:30 p.m. to 5:45 p.m.		
Input Data				
Analysis period T (h): 0.25	Segment 1		Segment 2	
Direction of travel	EB/NB	WB/SB	EB/NB	WB/SB
Signal Timing Data				
Cycle length C (s)	100	100		
Effective green-to-cycle-length ratio g/C	0.47	0.47		
Traffic Data				
Through-lane group volume v_{th} (veh/h)	968	950		
Lane group saturation flow rate s (veh/h/ln)	1,800	1,800		
Proportion of arrivals during green P	0.67	0.31		
Speed limit S_{pl} (mi/h)	35	35		
Incremental delay d_2 (s/veh)	1.13	1.08		
Geometric Design Data				
Number of through lanes N_{th} (ln)	2	2		
Stop Rate Computation				
Effective green time g (s), $g = C(g/C)$	47	47		
Effective red time r (s), $r = C - g$	53	53		
Capacity c (veh/h), $c = N_{th} s g/C$	1,692	1,692		
Volume-to-capacity ratio X , $X = v_{th}/c$	0.57	0.56		
Average speed S_a (mi/h), $S_a = 0.90 (25.6 + 0.47 S_{pl})$	37.8	37.8		
Threshold acceleration-deceleration delay (s), $(1 - P) g X$	8.8	18.1		
Acceleration-deceleration delay d_a (s), $d_a = 0.393 (S_a - 5.0)^2 / S_a$	11.2	11.2		
Deterministic stop rate h_1 (stops/veh), $h_1 = \frac{1 - P(1 + d_a/g)}{1 - P X}$ if $d_a \leq (1 - P) g X$ $h_1 = \frac{(1 - P)(r - d_a)}{r - (1 - P) g X}$ if $d_a > (1 - P) g X$	0.31	0.74		
Second-term back-of-queue size Q_2 (veh/ln), $Q_2 = c d_2 / (3,600 N_{th})$	0.26	0.25		
Full stop rate h (stops/veh), $h = h_1 + 3,600 N_{th} Q_2 / (v_{th} C)$	0.33	0.76		

Exhibit 30-12
Planning-Level Analysis: Stop Rate Worksheet

The stop rate is computed as the sum of two components. The first component to be computed is the deterministic stop rate. Two equations are available for this computation. The correct equation to use is based on a check of the acceleration-deceleration delay relative to the computed threshold value.

The second stop rate component is based on the second-term back-of-queue size. This queue represents the average number of vehicles that are unserved at the end of the green interval. It is based on the incremental delay computed for the Control Delay worksheet.

The fifth computational worksheet is the Travel Speed and Spatial Stop Rate worksheet. It is shown as Exhibit 30-13. This worksheet is designed for the analysis of the segment through-lane group. The input values include segment length and the full stop rate associated with other midsegment events (e.g., turns at access points). The other input data listed represent computed values and are obtained from the previous worksheets.

Exhibit 30-13
 Planning-Level Analysis:
 Travel Speed and Spatial Stop
 Rate Worksheet

TRAVEL SPEED AND SPATIAL STOP RATE WORKSHEET				
General Information				
Project Description	Texas Avenue, 5:30 p.m. to 5:45 p.m.			
Input Data				
	Segment 1		Segment 2	
Direction of travel	EB/NB	WB/SB	EB/NB	WB/SB
Length of segment L (ft)	1,800	1,800		
Base free-flow speed S_{f0} (mi/h)	40.8	40.8		
Running time t_R (s)	33.7	33.7		
Control delay d (s/veh)	14.7	24.1		
Full stop rate h (stops/veh)	0.33	0.76		
Full stop rate due to other midsegment sources h_{other} (stops/veh)	0	0		
Travel Speed Computation				
Travel time T_T (s), $T_T = t_R + d$	48.4	57.7		
Travel speed $S_{T,seg}$ (mi/h), $S_{T,seg} = \frac{3,600 L}{5,280 T_T}$	25.4	21.3		
Spatial Stop Rate Computation				
Total stop rate h_T (stops/veh), $h_T = h + h_{other}$	0.33	0.76		
Spatial stop rate H_{seg} (stops/mi), $H_{seg} = \frac{5,280 h_T}{L}$	0.96	2.23		
Level-of-Service Computation				
Volume-to-capacity ratio X , $X = v_{th}/C$	0.57	0.56		
Travel speed thresholds for base free-flow speed (S_{f0}) by interpolation of values in Exhibit 18-1 (mi/h)	A: >32.6 B: >27.3 C: >20.4 D: >16.3 E: >12.2	A: >32.6 B: >27.3 C: >20.4 D: >16.3 E: >12.2		
Level of service	C	C		

EXAMPLE PROBLEM

The Urban Street Segment

The total length of an undivided urban street segment is 1,800 ft. It is shown in Exhibit 30-14. Both of the boundary intersections are signalized. The street has a four-lane cross section with two lanes in each direction. There are left-turn bays on the subject segment at each signalized intersection.

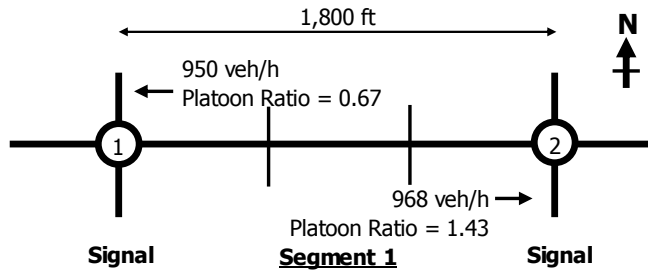


Exhibit 30-14
Planning-Level Analysis:
Example Problem

The segment has two access point intersections. Each intersection has two STOP-controlled side-street approaches, and each approach has sufficient traffic volume during the analysis period to be considered active. The segment also has two driveways on each side of the street; however, their turn movement volumes are too low for them to be considered active.

The Question

What are the travel speed, spatial stop rate, and LOS during the analysis hour for through-vehicle traffic in both directions of travel along the segment?

The Facts

Some details of the segment are shown in Exhibit 30-14. Both boundary intersections are signalized. The following additional information is known about the street segment:

- Through saturation flow rate: 1,800 veh/h/ln
- Midsegment volume: 1,150 veh/h
- Midsegment delay: 0.52 s/veh
- Number of through lanes at boundary intersection: 2
- Upstream intersection width: 50 ft
- Number of through lanes on segment: 2
- Proportion of street with curb: 0.70
- Proportion of street with on-street parking: 0.0
- g/C ratio: 0.47
- Cycle length: 100 s
- Analysis period: 0.25 h
- Speed limit: 35 mi/h
- Percent left turns at active access points: 6%
- Percent right turns at active access points: 8%

Selected Calculations

1. Compute total delay due to turns into access points	Midsegment lanes = 2 lanes Midsegment lane volume = 575 veh/h/ln Interpolate in Exhibit 18-13 to obtain 0.37 s/veh/pt through-vehicle delay. Number of active access points = 2 Percent turns = 7% [= (6 + 8)/2] Total delay per access pt. = $7/10 \times 0.37$ = 0.26 s/veh/pt Total delay per segment = 2×0.26 = 0.52 s/veh
2. Compute upstream filtering factor	No information was available about the volume-to-capacity ratio for the upstream movements, so this ratio was estimated to equal the volume-to-capacity ratio for the subject movement.

Results

The calculations are shown in Exhibit 30-9 to Exhibit 30-13. The travel speed for the eastbound direction is 25.4 mi/h. The travel speed for the westbound direction is 21.3 mi/h. The eastbound and westbound spatial stop rates are 0.96 and 2.23 stops/mi, respectively.

The base free-flow speed is 40.8 mi/h. By interpolating this value between those in Exhibit 18-1, the threshold travel speeds for LOS A, B, C, D, and E are >32.6, >27.3, >20.4, >16.3, and >12.2 mi/h, respectively. Thus, the travel speed for the eastbound direction of 26.3 mi/h corresponds to LOS C. The westbound LOS is similarly determined to be C.

6. FIELD MEASUREMENT TECHNIQUES

This section describes two techniques for estimating key vehicular traffic characteristics by using field data. The first technique is used to estimate free-flow speed. The second technique is used to estimate average travel speed.

The field measurements for both techniques should occur during a time period that is representative of the analysis period. This approach recognizes a possible difference in driver speed choice during different times of day (and, possibly, days of week and months of year).

FREE-FLOW SPEED

The following steps can be used to determine the free-flow speed for vehicular traffic on an urban street segment. The definition of “urban street segment” is provided in Section 2 of Chapter 18.

The speed measured with the technique described in this section describes the free-flow speed for the subject segment. It is not necessarily an accurate measurement of the free-flow speed on an adjacent segment because of possible differences in geometry, access point spacing, or speed limit.

Some urban streets have characteristics that can influence free-flow speed but that are not considered in the predictive procedure. If free-flow speed is measured for these segments, the results should be qualified to acknowledge the possible influence of these characteristics on the measured speed. These characteristics include a change in the posted speed limit along the segment, the display of an advisory speed sign that has an advisory speed lower than the speed limit, a change in the number of through lanes along the segment, significant grade, or a midsegment capacity constraint (e.g., narrow bridge).

Step 1. Conduct a spot-speed study at a midsegment location during low-volume conditions. Record the speed of 100 or more free-flowing passenger cars. A car is free-flowing when it has a headway of 8 s or more to the vehicle ahead and 5 s or more to the vehicle behind in the same traffic lane. In addition, a free-flow vehicle is not influenced (i.e., slowed) by the following factors: (a) vehicles turning onto (or off of) the subject segment at the boundary intersection or at a midsegment access point, (b) traffic control devices at the boundary intersections, or (c) traffic control devices deployed along the segment.

In view of the aforementioned definition of “free-flow vehicle,” vehicles turning into (or out of) an access point should not be included in the database. Vehicles that are accelerating or decelerating as a result of driver response to a traffic control signal should not be included in the database. Vehicles should not be included if they are influenced by signs that require a lower speed limit during school hours or signs that identify a railroad crossing.

Step 2. Compute the average of the spot speeds S_{spot} and their standard deviation σ_{spot} .

Step 3. Compute the segment free-flow speed S_f as a space mean speed by using Equation 30-69.

Equation 30-69

$$S_f = S_{\text{spot}} - \frac{\sigma_{\text{spot}}^2}{S_{\text{spot}}}$$

where

S_f = free-flow speed (mi/h),

S_{spot} = average spot speed (mi/h), and

σ_{spot} = standard deviation of spot speeds (mi/h).

Step 4. If the base free-flow speed S_{f_0} is also desired, it can be computed by using Equation 30-70.

Equation 30-70

$$S_{f_0} = \frac{S_f}{f_L}$$

with

Equation 30-71

$$f_L = 1.02 - 4.7 \frac{S_f - 19.5}{\max(L_s, 400)} \leq 1.0$$

where

S_{f_0} = base free-flow speed (mi/h),

S_f = free-flow speed (mi/h),

L_s = distance between adjacent signalized intersections (ft), and

f_L = signal spacing adjustment factor.

Equation 30-71 was originally derived with the intent of using the base free-flow speed S_{f_0} in the numerator of the second term. However, use of the free-flow speed S_f in its place is sufficient for this application.

Equation 30-71 was derived by using signalized boundary intersections. For more general applications, the definition of distance L_s is broadened so that it equals the distance between the two intersections that (a) bracket the subject segment and (b) each have a type of control that can impose on the subject through movement a legal requirement to stop or yield.

AVERAGE TRAVEL SPEED

The following steps can be used to determine the average travel speed for vehicular traffic on an urban street segment.

Step 1. Identify the time of the day (e.g., morning peak, evening peak, off-peak) during which the study will be conducted. Identify the segments to be evaluated.

Step 2. Conduct the test car travel time study for the identified segments during the identified study period. The following factors should be considered before or during the field study:

- The number of travel time runs will depend on the range of speeds found on the street. Six to 12 runs for each traffic volume condition are typically adequate. The analyst should determine the minimum number of runs on the basis of guidance provided elsewhere (8).

- The objective of the data collection is to obtain the information identified in the Travel Time Field Worksheet (i.e., vehicle location and arrival and departure times at each boundary intersection). This worksheet is shown in Exhibit 30-15. In general, each row of this worksheet represents the data for one direction of travel on one segment. If the street serves traffic in two travel directions, separate worksheets are typically used to record the data for each direction of travel.
- The equipment used to record the data may include a Global Positioning System–equipped laptop computer or simply a pair of stopwatches. If available, an instrumented test car should be used to reduce labor requirements and to facilitate recording and analysis.
- During the test run, the average-car technique is typically used and requires that the test car travel at the average speed of the traffic stream, as judged by its driver (8).
- The cumulative travel time is recorded as the vehicle passes the center of each boundary intersection. Whenever the test car stops or slows (i.e., 5 mi/h or less), the observer uses a second stopwatch to measure the duration of time the vehicle is stopped or slowed. This duration (and the cause of the delay) is recorded on the worksheet on the same row that is associated with the next boundary intersection to be reached. The rows are intentionally tall so that a midsegment delay and the signal delay can both be recorded in the same cell.
- Test car runs should begin at different time points in the signal cycle to avoid having all runs start from a “first in platoon” position.
- Some midsegment speedometer readings should also be recorded to check on unimpeded travel speeds and to see how they relate to the estimated free-flow speed.

Step 3. The cumulative travel time observations between adjacent boundary intersections are subtracted to obtain the travel time for the corresponding segment. This travel time can be averaged for all test runs to obtain an average segment travel time. The average is then divided into the segment length to obtain an estimate of the average travel speed. This speed should be computed for each direction of travel for the segment.

The data should be summarized to provide the following statistics for each segment travel direction: average travel speed, average delay time for the boundary intersection, and average delay time for other sources (pedestrian, parking maneuver, etc.).

The average segment travel time for each of several consecutive segments in a common direction of travel can be added to obtain the total travel time for the facility. This total travel time can then be divided into the facility length (i.e., the total length of all segments) to obtain the average travel speed for the facility. This calculation should be repeated to obtain the average travel speed for the other direction of travel.

7. COMPUTATIONAL ENGINE DOCUMENTATION

This section uses a series of flowcharts and linkage lists to document the logic flow for the computational engine.

FLOWCHARTS

The methodology flowchart is shown in Exhibit 30-16. The methodology consists of five main modules:

- Setup Module,
- Segment Evaluation Module,
- Segment Analysis Module,
- Delay due to Turns Module, and
- Performance Measures Module.

This subsection provides a separate flowchart for each of these modules.

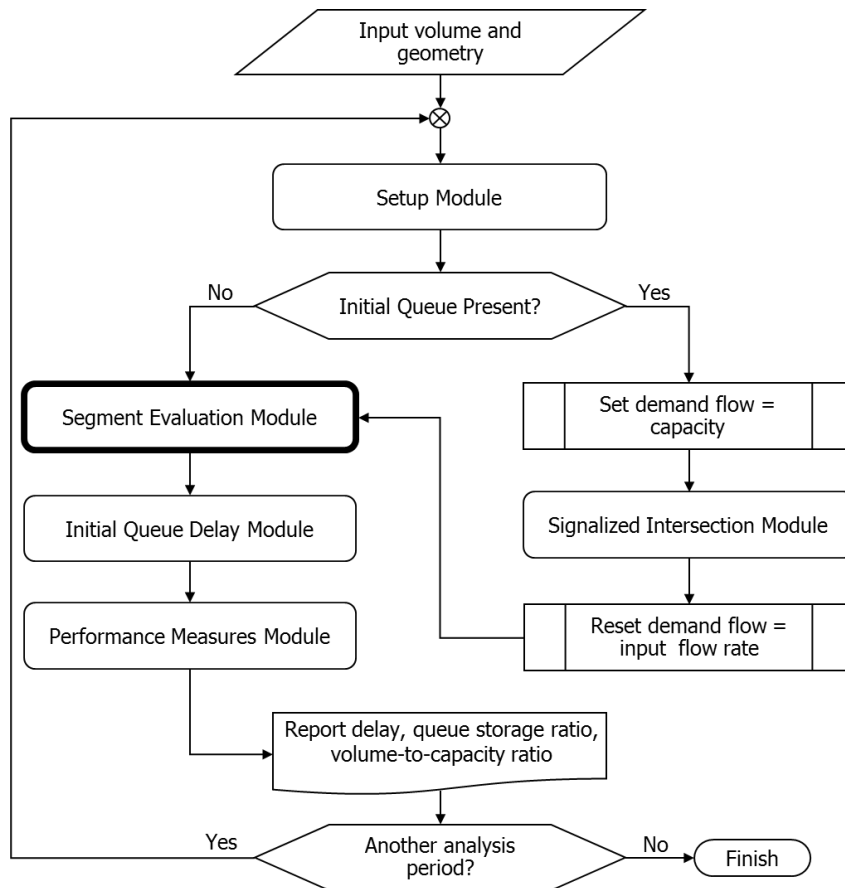
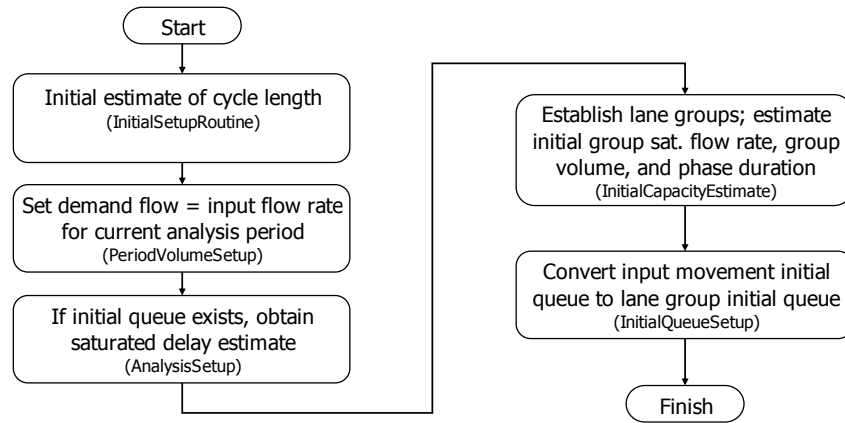


Exhibit 30-16
Methodology Flowchart

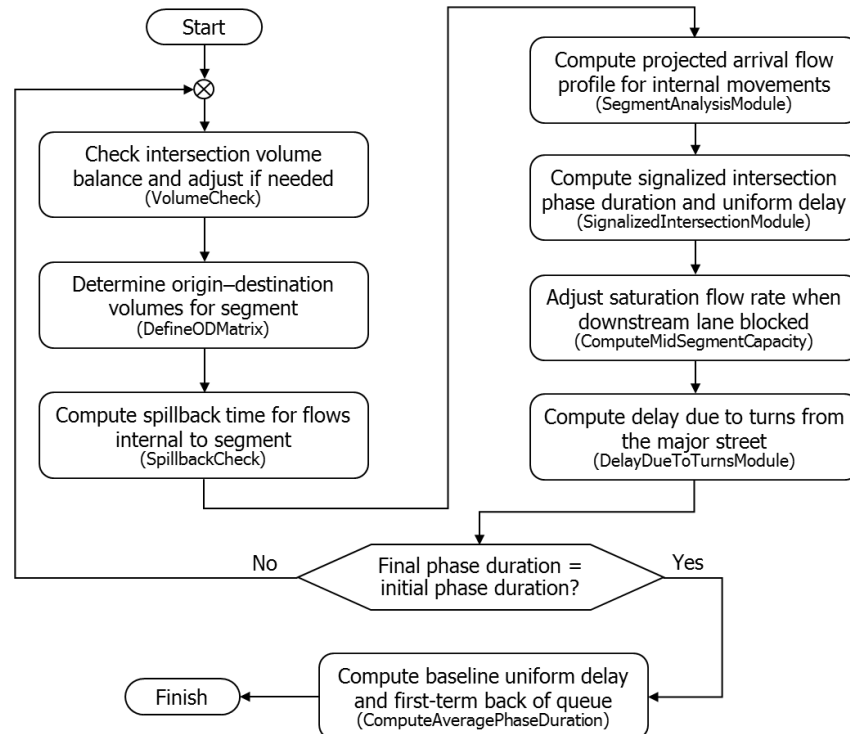
The Setup Module is shown in Exhibit 30-17. This module consists of five main routines, as shown in the large rectangles of the exhibit. The main function of each routine, as well as the name given to it in the computational engine, is also shown in the exhibit. These routines and the Initial Queue Delay Module are described in Chapter 31, Signalized Intersections: Supplemental.

Exhibit 30-17
Setup Module



The Segment Evaluation Module is shown in Exhibit 30-18. This module consists of eight main routines. The main function of each routine, as well as the name given to it in the computational engine, is also shown in the exhibit. The Segment Analysis Module and the Delay due to Turns Module are outlined in the next two exhibits. The Signalized Intersection Module and the Compute Average Phase Duration routine are described in Chapter 31. The Volume Check, Define Origin–Destination Matrix, Spillback Check, and Midsegment Capacity routines are described further in the next subsection.

Exhibit 30-18
Segment Evaluation Module



The Segment Analysis Module is shown in Exhibit 30-19. This module consists of seven main routines, six of which are implemented for both segment travel directions. The main function of each routine, as well as the name given to it in the computational engine, is also shown in the exhibit. These routines are described further in the next subsection.

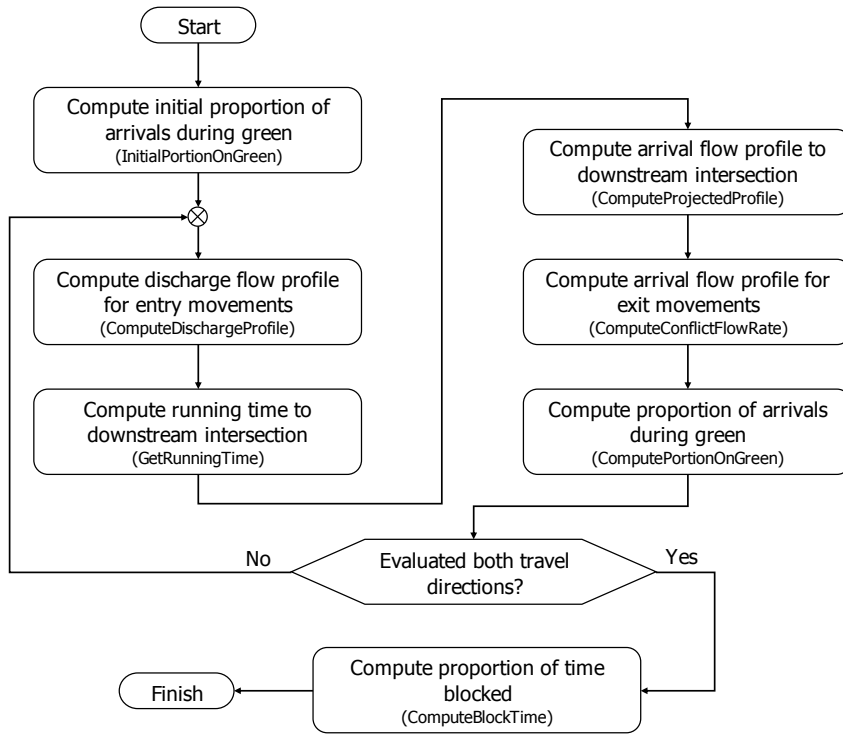


Exhibit 30-19
Segment Analysis Module

The Delay due to Turns Module is shown in Exhibit 30-20. This module consists of two main routines, each of which is implemented for both segment travel directions. The main function of each routine, as well as the name given to it in the computational engine, is also shown in the exhibit. These routines are described further in the next subsection.

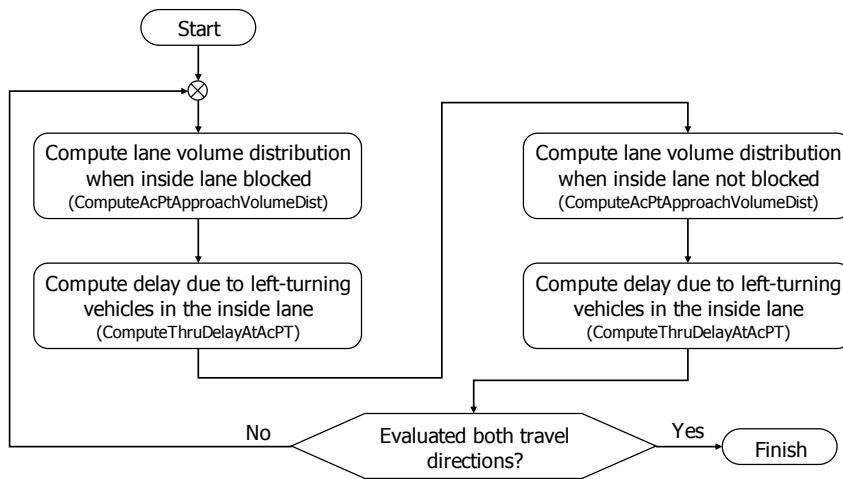
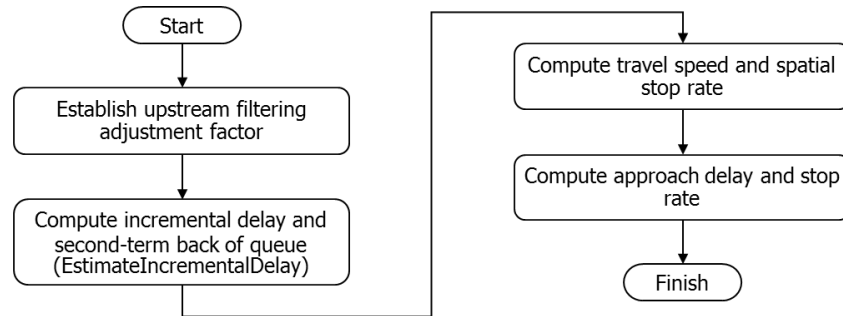


Exhibit 30-20
Delay due to Turns Module

Exhibit 30-21
Performance Measures
Module

The Performance Measures Module is shown in Exhibit 30-21. This module consists of four routines. The main function of each routine is also shown in the exhibit. One of the routines (i.e., EstimateIncrementalDelay) is complicated enough to justify its development as a separate entity in the computational engine. This routine is described in Chapter 31, Signalized Intersections: Supplemental.



LINKAGE LISTS

This subsection uses linkage lists to describe the main routines that make up the computational engine. Each list is provided in a table that identifies the routine and the various subroutines that it references. Conditions for which the subroutine is used are also provided.

The lists are organized by module, as described in the previous subsection. A total of three tables are provided to address the following three modules:

- Segment Evaluation Module,
- Segment Analysis Module, and
- Delay due to Turns Module.

The linkage list for the Segment Evaluation Module is provided in Exhibit 30-22. The main routines are listed in Column 1 and were previously identified in Exhibit 30-18.

The linkage list for the Segment Analysis Module is provided in Exhibit 30-23. The main routines are listed in Column 1 and were previously identified in Exhibit 30-19.

Finally, the linkage list for the Delay due to Turns Module is provided in Exhibit 30-24. The main routines are listed in Column 1 and were previously identified in Exhibit 30-20.

Routine	Subroutine	Conditions for Use
VolumeCheck	Ensure that discharge volume for each entry movement does not exceed its capacity.	Apply for both segment travel directions.
DefineODMatrix	ComputeODs (compute origin–destination volume for movements that enter and exit segment)	Apply to all intersections on segment and for both segment travel directions.
SpillbackCheck	ComputeSpillbackTime (compute spillback time for each exit movement at the downstream boundary intersection)	Apply for both segment travel directions.
SegmentAnalysisModule	See Exhibit 30-23.	
SignalizedIntersectionModule	See Chapter 31.	
ComputeMidSegmentCapacity	Compute midsegment capacity when restricted and reduce saturation flow rate of upstream movements so upstream discharge is less than or equal to the midsegment capacity.	Apply to each upstream signalized intersection traffic movement that enters segment.
DelayDueToTurnsModule	See Exhibit 30-24.	
ComputeAveragePhaseDuration	See Chapter 31.	

Exhibit 30-22
Segment Evaluation Module Routines

Routine	Subroutine	Conditions for Use
InitialPortionOnGreen	Compute proportion of arrivals during green (P) based on current signal timing.	None
ComputeDischargeProfile	Compute discharge flow rate for each 1-s interval of signal cycle at upstream boundary intersection.	Apply to each upstream boundary intersection movement that enters segment.
GetRunningTime	Compute running time on length of street between upstream boundary intersection and subject downstream intersection.	Apply to all intersections on the segment and for both segment travel directions.
ComputeProjectedProfile	Compute arrival flow profile reflecting dispersion of platoons formed at upstream boundary intersection.	Apply to each upstream boundary intersection movement that enters segment.
ComputeConflictFlowRate	Use arrival flow profile and origin–destination matrix to compute arrival flow rate for movements at subject intersection.	Apply to all intersections on the segment and for both segment travel directions.
	Compute conflicting flow rate at access point intersections on basis of the projected arrivals at each intersection.	Apply to all access point intersections and for both segment travel directions.
ComputePortionOnGreen	For each exit movement, compute count of vehicles arriving at downstream boundary intersection during green.	Apply to each downstream boundary intersection.
ComputeBlockTime	Use computed conflicting flow rates at each access point intersection to compute the proportion of time blocked for each nonpriority movement.	Apply to all access point intersections and for both travel segment travel directions.

Exhibit 30-23
Segment Analysis Module Routines

Exhibit 30-24

Delay due to Turns Module
Routines

Routine	Subroutine	Conditions for Use
ComputeAcPtApproach- VolumeDist	Compute the volume for each lane on the approach to the access point intersection when blocked by a left-turning vehicle.	Apply lane volume routine for case in which inside lane is blocked by a turning vehicle. Apply to all access point intersections and for both segment travel directions.
	Compute the volume for each lane on the approach to the access point intersection when <i>not</i> blocked by a left-turning vehicle.	Apply lane volume routine for case in which inside lane is <i>not</i> blocked by a turning vehicle. Apply to all access point intersections and for both segment travel directions.
ComputeThruDelayAtAcPT	Compute the probability of left-turn bay overflow at access point intersection.	If segment is undivided, the probability of bay overflow is 1.0.
	Compute the delay to through movements due to a left turn at an access point.	Apply to all access point intersections and for both segment travel directions.
	Based on lane volume estimate for case in which inside lane is blocked by a turning vehicle.	
	Compute the delay to through movements due to a right turn at an access point.	Apply to all access point intersections and for both segment travel directions.
	Based on lane volume estimate for case in which inside lane is <i>not</i> blocked by a turning vehicle.	

8. EXAMPLE PROBLEMS

This section describes the application of each of the motorized vehicle, pedestrian, bicycle, and transit methodologies through the use of example problems. Exhibit 30-25 provides an overview of these problems. The focus of the examples is on an operational analysis. A planning and preliminary engineering analysis is identical to the operational analysis in terms of the calculations, except that default values are used when field-measured values are not available.

Problem Number	Description	Analysis Type
1	Motorized Vehicle LOS	Operational
2	Pedestrian LOS	Operational
3	Bicycle LOS	Operational
4	Transit LOS	Operational

Exhibit 30-25
Example Problems

EXAMPLE PROBLEM 1: MOTORIZED VEHICLE LOS

The Urban Street Segment

The total length of an undivided urban street segment is 1,800 ft. The segment is shown in Exhibit 30-26. Both of the boundary intersections are signalized. The street has a four-lane cross section with two lanes in each direction. There are left-turn bays on the subject segment at each signalized intersection.

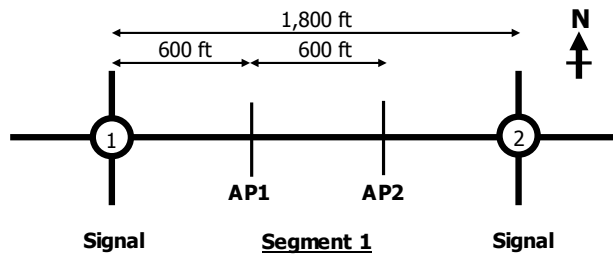


Exhibit 30-26
Example Problem 1: Urban Street Segment Schematic

The segment has two active access point intersections, shown in the exhibit as AP1 and AP2. Each intersection has two STOP-controlled side-street approaches. The segment has some additional driveways on each side of the street; however, their turn movement volumes are too low during the analysis period for them to be considered active. The few vehicles that do turn at these locations during the analysis period have been added to the corresponding volumes at the two active access point intersections.

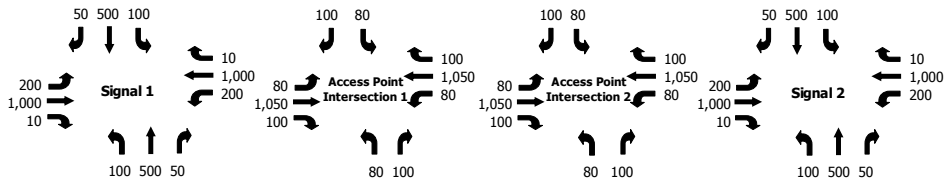
The Question

What are the travel speed, spatial stop rate, and LOS during the analysis period for the segment through movement in both directions of travel?

The Facts

The segment's traffic counts are listed in Exhibit 30-27. The counts were taken during the 15-min analysis period of interest. However, they have been converted to hourly flow rates. Note that the volumes leaving the signalized intersections do not add up to the volume arriving at the downstream access point intersection.

Exhibit 30-27
Example Problem 1:
Intersection Turn Movement
Counts



The signalization conditions are shown in Exhibit 30-28. The conditions shown are identified as belonging to Signalized Intersection 1; however, they are the same for Signalized Intersection 2. The signals operate with coordinated-actuated control. The left-turn movements on the northbound and southbound approaches operate under protected-permitted control and lead the opposing through movements (i.e., a lead-lead phase sequence). The left-turn movements on the major street operate as protected-only in a lead-lead sequence.

Exhibit 30-28
Example Problem 1: Signal
Conditions for Intersection 1

Controller Data Worksheet											
General Information											
Cross street: First Avenue					Analysis period: 7:15 am to 7:30 am						
Phase Sequence											
Phases 1 and 2					Phases 3 and 8						
Enter choice		2			1. WB left (1) with WB thru (6)		2		1. NB left (3) with NB thru (8)		
					2. WB left (1) before EB thru (2)				2. NB left (3) before SB thru (4)		
					3. EB thru (2) before WB left (1)				3. SB thru (4) before NB left (3)		
Phases 5 and 6					Phases 4 and 7						
Enter choice		2			1. EB left (5) with EB thru (2)		2		1. SB left (7) with SB thru (4)		
					2. EB left (5) before WB thru (6)				2. SB left (7) before NB thru (8)		
					3. WB thru (6) before EB left (5)				3. NB thru (8) before SB left (7)		
Left-Turn Mode											
Phase 1 or 2					Phase 3 or 8						
Enter choice		3			2. WB left (1) prot-perm		2		2. NB left (3) prot-perm		
					3. WB left (1) protected				3. NB left (3) protected		
Phase 5 or 6					Phase 4 or 7						
Enter choice		3			2. EB left (5) prot-perm		2		2. SB left (7) prot-perm		
					3. EB left (5) protected				3. SB left (7) protected		
Phase Settings											
Approach	Eastbound		Westbound		Northbound		Southbound				
Phase number	5	2	1	6	3	8	7	4			
Movement	L	T+R	L	T+R	L	T+R	L	T+R			
Lead/lag left-turn phase	Lead	--	Lead	--	Lead	--	Lead	--			
Left-turn mode	Prot.	--	Prot.	--	Pr/Pm	--	Pr/Pm	--			
Passage time, s	2.0		2.0		2.0	2.0	2.0	2.0			
Phase split, s	20	35	20	35	20	25	20	25			
Minimum green, s	5		5		5	5	5	5			
Yellow change, s	3.0	4.0	3.0	4.0	3.0	4.0	3.0	4.0			
Red clearance, s	0.0	0.0	0.0	0.0	0.0	0.0	0.0	0.0			
Walk+ ped. clear, s		0		0		0		0			
Recall?	No		No		No	No	No	No			
Dual entry ?	No	Yes	No	Yes	No	Yes	No	Yes			
Simultaneous gap-out?	Yes					Yes					
Dallas left-turn phasing?	No					No					
Coordination settings											
Offset, s:		0		Offset Ref.:		End of Green		Force Mode:		Fixed	
Cycle, s:		100						Reference phase:		2	

Exhibit 30-28 indicates that the passage time for each actuated phase is 2.0 s. The minimum green setting for each actuated phase is 5 s. The offset to Phase 2 (the reference phase) end-of-green interval is 0.0 s. A fixed-force mode is used to ensure that good coordination is maintained. The cycle length is 100 s.

Geometric conditions and traffic characteristics for Signalized Intersection 1 are shown in Exhibit 30-29. They are the same for Signalized Intersection 2. The movement numbers follow the numbering convention shown in Exhibit 19-1 of Chapter 19.

Intersection Data Worksheet												
Approach	Eastbound			Westbound			Northbound			Southbound		
Movement	L	T	R	L	T	R	L	T	R	L	T	R
Movement number	5	2	12	1	6	16	3	8	18	7	4	14
Intersection Geometry												
Number of lanes	1	2	1	1	2	1	1	2	0	1	2	0
Lane assignment	L	T	R	L	T	R	L	TR	n.a.	L	TR	n.a.
Average lane width, ft	12.0	12.0	12.0	12.0	12.0	12.0	12.0	12.0		12.0	12.0	
Number of receiving lanes	2			2						2		
Turn bay or segment length, ft	200	999	200	200	1800	200	200	999		200	999	
Traffic Characteristics												
Volume, veh/h	200	1000	10	200	1000	10	100	500	50	100	500	50
Right-turn-on-red volume, veh/h			0			0			0			0
Percent heavy vehicles, %	0	0	0	0	0	0	0	0	0	0	0	0
Lane utilization adjustment factor		1.000			1.000							
Peak hour factor	1.00	1.00	1.00	1.00	1.00	1.00	1.00	1.00	1.00	1.00	1.00	1.00
Start-up lost time, s	2.0	2.0	2.0	2.0	2.0	2.0	2.0	2.0		2.0	2.0	
Extension of eff. green time, s	2.0	2.0	2.0	2.0	2.0	2.0	2.0	2.0		2.0	2.0	
Platoon ratio	1.000	1.333	1.000				1.000	1.000		1.000	1.000	
Upstream filtering factor	1.00	1.00	1.00				1.00	1.00		1.00	1.00	
Pedestrian volume, p/h		0			0			0			0	
Bicycle volume, bicycles/h		0			0			0			0	
Opposing right-turn lane influence	Yes			Yes								
Initial queue, veh	0	0	0	0	0	0	0	0		0	0	
Speed limit, mi/h	35	35	35	35	35	35	35	35		35	35	
Unsignalized movement volume, veh/h	0	0	0	0	0	0	0	0		0	0	
Unsignalized movement delay, s/veh	0	0	0	0	0	0	0	0		0	0	
Unsignalized mvmt. stop rate, stops/veh	0.0	0.0	0.0	0.0	0.0	0.0	0.0	0.0		0.0	0.0	
Approach Data												
Parking present?	No		No	No		No	No		No	No		No
Parking maneuvers, maneuvers/h												
Bus stopping rate, buses/h			0			0				0		0
Approach grade, %	0	0	0	0	0	0	0	0		0	0	
Detection Data												
Stop line detector presence	Presence			Presence			Presence	Presence		Presence	Presence	
Stop line detector length, ft	40			40			40	40		40	40	

Exhibit 30-29
Example Problem 1:
Geometric Conditions and
Traffic Characteristics for
Signalized Intersection 1

All signalized intersection approaches have a 200-ft left-turn bay and two through lanes. The east–west approaches have a 200-ft right-turn lane. The north–south approaches have a shared through and right-turn lane. Many of the geometric and traffic characteristics shown in the exhibit are needed to compute the saturation flow rate with the procedure described in Section 3 of Chapter 19.

The platoon ratio is entered for all movements associated with an external approach to the segment. The eastbound through movement at Signalized Intersection 1 is known to be coordinated with the upstream intersection so that favorable progression occurs, as described by a platoon ratio of 1.333. The westbound through movement at Signalized Intersection 2 is also coordinated with its upstream intersection, and arrivals are described by a platoon ratio of 1.33. Arrivals to all other movements are characterized as “random” and are described with a platoon ratio of 1.00. The movements for the westbound approach at Signalized Intersection 1 (and eastbound approach at Signalized Intersection 2) are internal movements, so a platoon ratio (and upstream filtering factor) is not entered for them. More accurate values are computed during subsequent iterations by using a procedure provided in the methodology.

The speed limit on the segment and on the cross-street approaches is 35 mi/h. With a couple of exceptions, detection is located just upstream of the stop line in each traffic lane at the two signalized intersections. A 40-ft detection zone is used in each instance. The exceptions are the traffic lanes serving the major-street

through movement at each intersection. There is no detection for these movements because they are not actuated.

The geometric conditions that describe the segment are shown in Exhibit 30-30. These data are used to compute the free-flow speed for the segment.

Exhibit 30-30
Example Problem 1: Segment Data

Segment Data Worksheet		
Input Data	EB	WB
Basic Segment Data		
Number of through lanes that extend the length of the segment:	2	2
Speed limit, mph	35	35
Segment Length Data		
Length of segment (measured stopline to stopline), ft	1800	1800
Width of upstream signalized intersection, ft	50	50
Adjusted segment length, ft	1750	1750
Length of segment with a restrictive median (e.g. raised-curb), ft	0	0
Length of segment with a non-restrictive median (e.g. two-way left-turn lane), ft	0	0
Length of segment with no median, ft	1750	1750
Percentage of segment length with restrictive median, %	0	0
Access Data		
Percentage of street with curb on right-hand side (in direction of travel), %	70	70
Number of access points on right-hand side of street (in direction of travel)	4	4
Percentage of street with on-street parking on right-hand side (in direction of travel), %	0	0
Other Delay Data		
Mid-segment delay, s/veh	0	0

The traffic and lane assignment data for the two access point intersections are shown in Exhibit 30-31. The movement numbers follow the numbering convention shown in Exhibit 20-1 of Chapter 20, Two-Way STOP-Controlled Intersections. There are no turn bays on the segment at the two access point intersections.

Exhibit 30-31
Example Problem 1: Access Point Data

Access Point Input Data																	
Access	Approach	Eastbound				Westbound				Northbound				Southbound			
Point	Movement	L	T	R	L	T	R	L	T	R	L	T	R	L	T	R	
Location,ft	Movement number	1	2	3	4	5	6	7	8	9	10	11	12				
600	Volume, veh/h	80	1,050	100	80	1,050	100	80	0	100	80	0	100				
West end	Lanes	0	2	0	0	2	0	1	0	1	1	0	1				
1200	Volume, veh/h	80	1,050	100	80	1,050	100	80	0	100	80	0	100				
	Lanes	0	2	0	0	2	0	1	0	1	1	0	1				

Outline of Solution

Movement-Based Data

Exhibit 30-32 provides a summary of the analysis of the individual traffic movements at Signalized Intersection 1.

Exhibit 30-32
Example Problem 1:
Movement-Based Output Data

INTERSECTION 1	EB		EB		WB		WB		NB		NB		SB		SB	
	L	T	R	T	L	T	R	T	L	T	R	T	L	T	R	
Volume, veh/h	200	1,000	10	194	968	10	100	500	50	100	500	50	100	500	50	
Initial Queue, veh	0	0	0	0	0	0	0	0	0	0	0	0	0	0	0	
Ped-Bike Adj. Factor (A_pbT)	1.000		1.000	1.000	1.000	1.000	1.000	1.000	1.000	1.000	1.000	1.000	1.000	1.000	1.000	
Parking, Bus Adj. Factors (f_bb x f_p)	1.000	1.000	1.000	1.000	1.000	1.000	1.000	1.000	1.000	1.000	1.000	1.000	1.000	1.000	1.000	
Downstream Lane Blockage Factor (f_ms)	1.000	1.000	1.000	1.000	1.000	1.000	1.000	1.000	1.000	1.000	1.000	1.000	1.000	1.000	1.000	
Spillback Factor (f_sp)	1.000	1.000	1.000	1.000	1.000	1.000	1.000	1.000	1.000	1.000	1.000	1.000	1.000	1.000	1.000	
Adjusted Sat. Flow Rate, veh/h/ln	1,900	1,900	1,900	1,900	1,900	1,900	1,900	1,900	1,900	1,900	1,900	1,900	1,900	1,900	1,900	
Lanes	1	2	1	1	2	1	1	2	0	1	2	0	1	2	0	
Lane Assignment	L	T	R	L	T	R	L	TR	n.a.	L	TR	n.a.	L	TR	n.a.	
Capacity, veh/h	236	1,856	789	233	1,848	785	217	617	61	217	617	61	217	617	61	
Discharge Volume, veh/h	0	1,000	0	0	0	0	0	0	50	100	0	0	50	100	0	
Proportion Arriving On Green	0.131	0.651	0.488	0.045	0.493	0.501	0.061	0.181	0.181	0.061	0.181	0.181	0.061	0.181	0.181	
Approach Volume, veh/h		1,210			1,172			650			650			650		
Approach Delay, s/veh		18.0			23.4			39.7			39.7			39.7		
Approach Stop Rate, stops/veh		0.442			0.617			0.831			0.831			0.831		

With the exception of Initial Queue, Lanes, and Lane Assignment, the variables listed in Exhibit 30-32 have computed values. The volumes shown for the eastbound (EB), northbound (NB), and southbound (SB) movements are identical to the input volumes. The westbound (WB) volumes were computed from the input volumes during Step 1: Determine Traffic Demand Adjustments.

Specifically, they were reduced because the input westbound volume for this intersection exceeded the volume departing the upstream access point intersection (i.e., AP1).

Four factors are listed in the top half of Exhibit 30-32. These factors represent saturation flow rate adjustment factors. Their values are dependent on signal timing or lane volume, quantities that are computed during the iterative convergence loop (identified in the motorized vehicle methodology framework shown in Exhibit 18-8). As a result, the value of each factor also converges within this loop. The procedure for calculating the pedestrian–bicycle adjustment factor is described in Section 2 of Chapter 31. The procedure for calculating the parking–bus adjustment factor is described in Section 3 of Chapter 19. The procedure for calculating the downstream lane blockage (due to midsegment lane restriction) factor is described in Section 3 of this chapter. The methodology for calculating the spillback factor is described in Chapter 29.

Capacity for a movement is computed by using the movement volume proportion in each approach lane group, lane group saturation flow rate, and corresponding phase duration. This variable represents the capacity of the movement, regardless of whether it is served in an exclusive lane or a shared lane. If the movement is served in a shared lane, the movement capacity represents the portion of the lane group capacity available to the movement, as distributed in proportion to the volume of the movements served by the associated lane group.

Discharge volume is computed for movements that enter a segment during Step 1: Determine Traffic Demand Adjustments. At Signalized Intersection 1, the movements entering the segment are the eastbound through movement, the northbound right-turn movement, and the southbound left-turn movement. A value of 0.0 veh/h is shown for all other movements, which indicates that they are not relevant to this calculation. If volume exceeds capacity for any given movement, the discharge volume is set equal to the capacity. Otherwise, the discharge volume is equal to the movement volume.

The proportion arriving during green P is computed for internal movements during Step 3: Determine the Proportion Arriving During Green. In contrast, it is computed from the input platoon ratio for external movements.

The last three rows in Exhibit 30-32 represent summary statistics for the approach. The approach volume is the sum of the three movement volumes. Approach delay and approach stop rate are computed as volume-weighted averages for the lane groups served on an intersection approach.

Timer-Based Phase Data

Exhibit 30-33 provides a summary of the output data for Signalized Intersection 1 from a signal controller perspective. The controller has eight timing functions (or timers), with Timers 1 to 4 representing Ring 1 and Timers 5 to 8 representing Ring 2. The ring structure and phase assignments are described in Section 2 of Chapter 19. Timers 1, 2, 5, and 6 are used to control the east–west traffic movements on the segment. Timers 3, 4, 7, and 8 are used to control the north–south movements that cross the segment.

Exhibit 30-33

Example Problem 1: Timer-Based Phase Output Data

Timer Data	Timer:							
	1 WB L	2 EB T.R	3 NB L	4 SB T.T+R	5 EB L	6 WB T.R	7 SB L	8 NB T.T+R
Assigned Phase	1	2	3	4	5	6	7	8
Phase Duration (G+Y+Rc), s	15.90	52.84	9.13	22.13	16.10	52.63	9.13	22.13
Change Period (Y+Rc), s	3.00	4.00	3.00	4.00	3.00	4.00	3.00	4.00
Phase Start Time, s	35.27	51.16	4.00	13.14	35.27	51.37	4.00	13.14
Phase End Time, s	51.16	4.00	13.13	35.27	51.37	4.00	13.13	35.27
Max. Allowable Headway (MAH), s	3.13	0.00	3.13	3.06	3.13	0.00	3.13	3.06
Equivalent Maximum Green (Gmax), s	30.73	0.00	17.00	31.87	30.73	0.00	17.00	31.87
Max. Queue Clearance Time (g_c+I1), s	12.646	0.000	6.442	16.165	12.829	0.000	6.442	16.165
Green Extension Time (g_e), s	0.311	0.000	0.099	1.968	0.322	0.000	0.099	1.968
Probability of Phase Call (p_c)	0.995	0.000	0.938	1.000	0.996	0.000	0.938	1.000
Probability of Max Out (p_x)	0.000	0.000	0.000	0.016	0.000	0.000	0.000	0.016
Cycle Length, s: 100								

The timing function construct is essential to the modeling of a ring-based signal controller. *Timers* always occur in the same numeric sequence (i.e., 1 then 2 then 3 then 4 in Ring 1; 5 then 6 then 7 then 8 in Ring 2). The practice of associating movements with phases (e.g., the major-street through movement with Phase 2), coupled with the occasional need for lagging left-turn phases and split phasing, creates the situation in which *phases* do not always time in sequence. For example, with a lagging left-turn phase sequence, major-street through Phase 2 times first and then major-street left-turn Phase 1 times second.

The modern controller accommodates the assignment of phases to timing functions by allowing the ring structure to be redefined manually or by time-of-day settings. Specification of this structure is automated in the computational engine by the assignment of phases to timers.

The methodology is based on modeling *timers*, not on directly modeling movements or phases. The methodology converts movement and phase input data into timer input data. It then models controller response to these inputs and computes timer duration and related performance measures.

The two signalized intersections in this example problem have lead-lead left-turn sequences. Hence, the timer number is equal to the phase number (e.g., the westbound movement is associated with Phase 1, which is assigned to Timer 1).

The phase duration shown in Exhibit 30-33 is the estimated average phase duration during the analysis period. It represents the sum of the green, yellow change, and red clearance intervals. For Timer 2 (i.e., Phase 2), the average green interval duration can be computed as 48.84 s (= 52.84 – 4.00).

The phase start time is the time the timer (and phase) starts, relative to system time 0.0. For Phase 2, the start time is 51.16 s. The end of the green interval associated with this phase is 100.0 s (= 51.16 + 48.84). This time is equal to the cycle length, so the end of green actually occurs at 0.0 s. This result is expected because Phase 2 is the coordinated phase and the offset to the end of Phase 2 (relative to system time 0.0) was input as 0.0 s.

The phase end time is the time the timer (and phase) ends relative to system time 0.0. For Phase 2, the end of the green interval occurs at 0.0 s and the end of the phase occurs 4.0 s later (i.e., the change period duration).

The remaining variables in Exhibit 30-33 apply to the noncoordinated phases (i.e., the actuated phases). These variables describe the phase timing and operation. They are described in more detail in Section 2 of Chapter 19 and Section 2 of Chapter 31.

Timer-Based Movement Data

Exhibit 30-34 summarizes the output for Signalized Intersection 1 as it relates to the movements assigned to each timer. Separate sections of output are shown in the exhibit for the left-turn, through, and right-turn movements. The assigned movement row identifies the movement (previously identified in Exhibit 30-32) assigned to each timer.

The saturation flow rate shown in Exhibit 30-34 is the saturation flow rate for the movement. The procedure for calculating these rates is described in Section 3 of Chapter 19 and Section 3 of Chapter 31. In general, the rate for a movement is the same as for a lane group when the lane group serves one movement. The rate is split between the movements when the lane group is shared by two or more movements.

Timer Data	Timer:	1	2	3	4	5	6	7	8
		WB	EB	NB	SB	EB	WB	SB	NB
		L	T.R	L	T.T+R	L	T.R	L	T.T+R
Left-Turn Movement Data									
Assigned Movement		1		3		5		7	
Mvmt. Sat Flow, veh/h		1,805.00		1,805.00		1,805.00		1,805.00	
Through Movement Data									
Assigned Movement			2		4		6		8
Mvmt. Sat Flow, veh/h			3,800.00		3,401.19		3,800.00		3,401.19
Right-Turn Movement Data									
Assigned Movement				12		14		16	
Mvmt. Sat Flow, veh/h				1,615.00		338.99		1,615.00	

Exhibit 30-34
Example Problem 1: Timer-Based Movement Output Data

Timer-Based Lane Group Data

The motorized vehicle methodology described in Chapter 19 computes a variety of output statistics that portray the operation of each intersection lane group. The example problem in Chapter 19 illustrates these statistics and discusses their interpretation. The output data for the individual lane groups are not repeated in this chapter. Instead, the focus of the remaining discussion is on the access point output and the performance measures computed for the two through movements on the segment (i.e., eastbound through and westbound through).

Access Point Data

Exhibit 30-35 illustrates the output statistics for the two access point intersections located on the segment. The first six rows listed in the exhibit correspond to Access Point Intersection 1 (AP1), and the second six rows correspond to Access Point Intersection 2 (AP2). Additional sets of six rows would be provided in this table if additional access point intersections were evaluated.

Access Point Data	EB	EB	EB	WB	WB	WB	NB	NB	NB	SB	SB	SB
Segment 1	L	T	R	L	T	R	L	T	R	L	T	R
Movement:	1	2	3	4	5	6	7	8	9	10	11	12
Access Point Intersection No. 1												
1: Volume, veh/h	74.80	981.71	93.50	75.56	991.70	94.45	80.00	0.00	100.00	80.00	0.00	100.00
1: Lanes	0	2	0	0	2	0	1	0	1	1	0	1
1: Proportion time blocked	0.150			0.160			0.250	0.250	0.160	0.250	0.250	0.150
1: Delay to through vehicles, s/veh		0.193			0.194							
1: Prob. inside lane blocked by left		0.115			0.115							
1: Dist. from West/South signal, ft	600											
Access Point Intersection No. 2												
2: Volume, veh/h	75.56	991.70	94.45	74.80	981.71	93.50	80.00	0.00	100.00	80.00	0.00	100.00
2: Lanes	0	2	0	0	2	0	1	0	1	1	0	1
2: Proportion time blocked	0.160			0.150			0.250	0.250	0.150	0.250	0.250	0.160
2: Delay to through vehicles, s/veh		0.194			0.193							
2: Prob. inside lane blocked by left		0.115			0.115							
2: Dist. from West/South signal, ft	1,200											

Exhibit 30-35
Example Problem 1: Movement-Based Access Point Output Data

The eastbound and westbound volumes listed in Exhibit 30-35 are not equal to the input volumes. These volumes were adjusted during Step 1: Determine Traffic Demand Adjustments so that they equal the volume discharging from the upstream intersection. This routine achieves balance between all junction pairs (e.g., between Signalized Intersection 1 and Access Point Intersection 1, between Access Point Intersection 1 and Access Point Intersection 2, and so forth).

The “proportion of time blocked” is computed during Step 3: Determine the Proportion Arriving During Green. It represents the proportion of time during the cycle that the associated access point movement is blocked by the presence of a platoon passing through the intersection. For major-street left turns, the platoon of concern approaches from the opposing direction. For the minor-street left turn, platoons can approach from either direction and can combine to block this left turn for extended time periods. This trend can be seen by comparing the proportion of time blocked for the eastbound (major-street) left turn (i.e., 0.15) with that for the northbound (minor-street) left turn (i.e., 0.25) at Access Point Intersection 1.

The “delay to through vehicles” is computed during Step 2: Determine Running Time. It represents the sum of the delay due to vehicles turning left from the major street and the delay due to vehicles turning right from the major street. This delay tends to be small compared with typical signalized intersection delay values. But it can reduce overall travel speed if there are several high-volume access points on a street and only one or two through lanes in each direction of travel.

The “probability of the inside through lane being blocked” is also computed during Step 2: Determine Running Time as part of the delay-to-through-vehicles procedure. This variable indicates the probability that the left-turn bay at an access point will overflow into the inside through lane on the street segment. Hence, it indicates the potential for a through vehicle to be delayed by a left-turn maneuver. The segment being evaluated has an undivided cross section, and no left-turn bays are provided at the access point intersections. In this situation, the probability of overflow is 0.115, indicating that the inside lane is blocked about 11.5% of the time.

Results

Exhibit 30-36 summarizes the performance measures for the segment. Also shown are the results from the spillback check conducted during Step 1: Determine Traffic Demand Adjustments. The movements indicated in the column heading are those exiting the segment at a boundary intersection. Thus, the westbound movements on Segment 1 are those occurring at Signalized Intersection 1. Similarly, the eastbound movements on Segment 1 are those occurring at Signalized Intersection 2.

Segment Summary		EB	EB	EB	WB	WB	WB
Seg.No.	Movement:	L	T	R	L	T	R
		5	2	12	1	6	16
	1 Bay/Lane Spillback Time, h	never	never	never	never	never	never
	1 ShrdLane Spillback Time, h	never	never	never	never	never	never
	1 Base Free-Flow Speed, mph					40.78	
	1 Running Time, s					33.54	
	1 Running Speed, mph					36.59	
	1 Through Delay, s/veh					18.310	
	1 Travel Speed, mph					23.67	
	1 Stop Rate, stops/veh					0.547	
	1 Spatial Stop Rate, stops/mi					1.61	
	1 Through vol/cap ratio					0.52	
	1 Level of Service		C			C	
	1 Proportion Left Lanes		0.33			0.33	
	1 Auto. Traveler Perception Score		2.53			2.53	

SPILLBACK TIME, h: never

Exhibit 30-36
 Example Problem 1:
 Performance Measure
 Summary

The spillback check procedure computes the time of spillback for each of the internal movements. For turn movements, the bay/lane spillback time is the time before the turn bay overflows. For through movements, the bay/lane spillback time is the time before the through lane overflows due only to through demand. If a turn bay exists and it overflows, the turn volume will queue in the adjacent through lane. For this scenario, the shared lane spillback time is computed and used instead of the bay/lane spillback time. If several movements experience spillback, the time of first spillback is reported at the bottom of Exhibit 30-36.

The output data for the two through movements are listed in Exhibit 30-36, starting with the third row. The base free-flow speed (FFS) and running time statistics are computed during Step 2: Determine Running Time. The through delay listed is computed during Step 5: Determine Through Control Delay. It is a weighted average delay for the lane groups serving through movements at the downstream boundary intersection. The weight used in this average is the volume of through vehicles served by the lane group.

The base free-flow speed is 40.78 mi/h. By interpolating this value between those in Exhibit 18-1, the threshold travel speeds for LOS A, B, C, D, and E are as follows: >32.6, >27.5, >20.5, >16.3, and >12.3 mi/h, respectively. Thus, the travel speed for the eastbound direction of 23.67 mi/h corresponds to LOS C. The same conclusion is reached for the westbound travel direction.

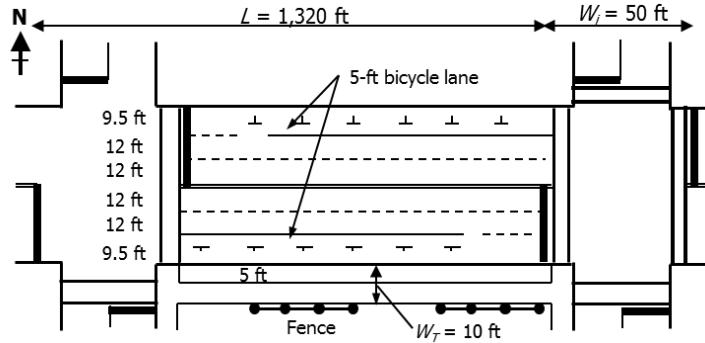
Each travel direction has one left-turn bay and three intersections. Thus, the proportion of intersections with left-turn lanes is 0.33. This proportion is used in Step 10: Determine Automobile Traveler Perception Score to compute the score of 2.53, which suggests that most automobile travelers would find segment service to be very good.

EXAMPLE PROBLEM 2: PEDESTRIAN LOS

The Segment

The sidewalk of interest is located along a 1,320-ft urban street segment. The segment is part of a collector street located near a community college. It is shown in Exhibit 30-37. Sidewalk is only shown for the south side of the segment for the convenience of illustration. It also exists on the north side of the segment.

Exhibit 30-37
 Example Problem 2: Segment
 Geometry



The Question

What is the pedestrian LOS for the sidewalk on the south side of the segment?

The Facts

The geometric details of the sidewalk and street cross section are shown in Exhibit 30-37. Both boundary intersections are signalized. Crossing the segment at uncontrolled midsegment locations is legal. The following additional information is known about the sidewalk and street segment:

Traffic characteristics:

- Midsegment flow rate in eastbound direction: 940 veh/h
- Pedestrian flow rate in south sidewalk (walking in both directions): 2,000 p/h
- Proportion of on-street parking occupied during analysis period: 0.20

Geometric characteristics:

- Outside shoulder width: none
- Parking lane width: 9.5 ft
- Cross section has raised curb along outside edge of roadway
- Effective width of fixed objects on sidewalk: 0.0 ft (no objects present)
- Presence of trees, bushes, or other vertical objects in buffer: No

Other data:

- Pedestrians can cross the segment legally and do so somewhat uniformly along its length
- Proportion of sidewalk adjacent to window display: 0.0
- Proportion of sidewalk adjacent to building face: 0.0
- Proportion of sidewalk adjacent to fence: 0.50

Performance measures obtained from supporting methodologies:

- Motorized vehicle running speed: 33 mi/h
- Pedestrian delay when walking parallel to the segment: 40 s/p
- Pedestrian delay when crossing the segment at the nearest signal-controlled crossing: 80 s/p
- Pedestrian waiting delay: 740 s/p
- Pedestrian LOS score for the downstream intersection: 3.6

Outline of Solution

First, the pedestrian space will be calculated for the sidewalk. This measure will then be compared with the qualitative descriptions of pedestrian space listed in Exhibit 18-15. Next, the pedestrian travel speed along the sidewalk will be calculated. Finally, LOS for the segment will be determined by using the computed pedestrian LOS score and the pedestrian space variables.

Computational Steps

Step 1: Determine Free-Flow Walking Speed

The average free-flow walking speed is estimated to be 4.4 ft/s on the basis of the guidance provided.

Step 2: Determine Average Pedestrian Space

The shy distance on the inside of the sidewalk is computed with Equation 18-24.

$$W_{s,i} = \max(W_{buf}, 1.5)$$

$$W_{s,i} = \max(5.0, 1.5)$$

$$W_{s,i} = 5.0 \text{ ft}$$

The shy distance on the outside of the sidewalk is computed with Equation 18-25.

$$W_{s,o} = 3.0 p_{\text{window}} + 2.0 p_{\text{building}} + 1.5 p_{\text{fence}}$$

$$W_{s,o} = 3.0(0.0) + 2.0(0.0) + 1.5(0.50)$$

$$W_{s,o} = 0.75 \text{ ft}$$

There are no fixed objects present on the sidewalk, so the adjusted fixed-object effective widths for the inside and outside of the sidewalk are both equal to 0.0 ft. The effective sidewalk width is computed with Equation 18-23.

$$W_E = W_T - W_{O,i} - W_{O,o} - W_{s,i} - W_{s,o} \geq 0.0$$

$$W_E = 10 - 0.0 - 0.0 - 5.0 - 0.75$$

$$W_E = 4.25 \text{ ft}$$

The pedestrian flow per unit width of sidewalk is computed with Equation 18-28 for the subject sidewalk.

$$v_p = \frac{v_{ped}}{60 W_E}$$

$$v_p = \frac{2,000}{60(4.25)}$$

$$v_p = 7.84 \text{ p/ft/min}$$

The average walking speed S_p is computed with Equation 18-29.

$$S_p = (1 - 0.00078 v_p^2) S_{pf} \geq 0.5 S_{pf}$$

$$S_p = [1 - 0.00078(7.84)^2](4.4)$$

$$S_p = 4.19 \text{ ft/s}$$

Finally, Equation 18-30 is used to compute average pedestrian space.

$$A_p = 60 \frac{S_p}{v_p}$$

$$A_p = 60 \frac{4.19}{7.84}$$

$$A_p = 32.0 \text{ ft}^2/\text{p}$$

The pedestrian space can be compared with the ranges provided in Exhibit 18-15 to make some judgments about the performance of the subject intersection corner. The criteria for platoon flow are considered applicable given the influence of the signalized intersections. According to the qualitative descriptions provided in this exhibit, walking speed will be restricted, as will the ability to pass slower pedestrians.

Step 3: Determine Pedestrian Delay at Intersection

The pedestrian methodology in Chapter 19, Signalized Intersections, was used to estimate two pedestrian delay values. One is the delay at the boundary intersection experienced by a pedestrian walking parallel to segment d_{pp} . This delay was computed to be 40 s/p. The second is the delay experienced by a pedestrian crossing the segment at the nearest signal-controlled crossing d_{pc} . This delay was computed to be 80 s/p.

The pedestrian methodology in Chapter 20, Two-Way STOP-Controlled Intersections, was used to estimate the delay incurred while waiting for an acceptable gap in traffic d_{pw} . This delay was computed to be 740 s/p.

Step 4: Determine Pedestrian Travel Speed

The pedestrian travel speed is computed with Equation 18-31.

$$S_{Tp,seg} = \frac{L}{\frac{L}{S_p} + d_{pp}}$$

$$S_{Tp,seg} = \frac{1,320}{\frac{1,320}{4.19} + 40}$$

$$S_{Tp,seg} = 3.72 \text{ ft/s}$$

This walking speed is slightly less than 4.0 ft/s and is considered acceptable, but a higher speed is desirable.

Step 5: Determine Pedestrian LOS Score for Intersection

The pedestrian methodology in Chapter 19 was used to determine the pedestrian LOS score for the downstream boundary intersection $I_{p,int}$. It was computed to be 3.60.

Step 6: Determine Pedestrian LOS Score for Link

The pedestrian LOS score for the link is computed from three factors. However, before these factors can be calculated, several cross-section variables

need to be adjusted and several coefficients need to be calculated. These variables and coefficients are calculated first. Then, the three factors are computed. Finally, they are combined to determine the desired score.

The midsegment demand flow rate is greater than 160 veh/h. The street cross section is curbed but there is no shoulder, so the adjusted width of paved outside shoulder W_{os}^* is 0.0 ft. Therefore, the effective total width of the outside through lane, bicycle lane, and shoulder W_v is computed as

$$\begin{aligned} W_v &= W_{ol} + W_{bl} + W_{os}^* + W_{pk} \\ W_v &= 12 + 5 + 0 + 9.5 \\ W_v &= 26.5 \text{ ft} \end{aligned}$$

Because the proportion of occupied on-street parking is less than 0.25 and the sum of the bicycle lane and parking lane widths exceeds 10.0 ft, the effective width of the combined bicycle lane and parking lane W_l is set to 10.0 ft.

The adjusted available sidewalk width W_{aA} is computed as

$$\begin{aligned} W_{aA} &= \min(W_T - W_{buf}, 10) \\ W_{aA} &= \min(10 - 5, 10) \\ W_{aA} &= 5 \text{ ft} \end{aligned}$$

The sidewalk width coefficient f_{sw} is computed as

$$\begin{aligned} f_{sw} &= 6.0 - 0.3 W_{aA} \\ f_{sw} &= 6.0 - 0.3(5.0) \\ f_{sw} &= 4.5 \text{ ft} \end{aligned}$$

The buffer area coefficient f_b is equal to 1.0 because there is no continuous barrier at least 3.0 ft high located in the buffer area.

The motorized vehicle methodology described in Section 3 of Chapter 18 was used to determine the motorized vehicle running speed S_R for the subject segment. This speed was computed to be 33.0 mi/h.

The cross-section adjustment factor is computed with Equation 18-33.

$$\begin{aligned} F_w &= -1.2276 \ln(W_v + 0.5 W_l + 50 p_{pk} + W_{buf} f_b + W_{aA} f_{sw}) \\ F_w &= -1.2276 \ln[26.5 + 0.5(10) + 50(0.20) + 5.0(1.0) + 5.0(4.5)] \\ F_w &= -5.20 \end{aligned}$$

The motorized vehicle volume adjustment factor is computed with Equation 18-34.

$$\begin{aligned} F_v &= 0.0091 \frac{v_m}{4 N_{th}} \\ F_v &= 0.0091 \frac{940}{4(2)} \\ F_v &= 1.07 \end{aligned}$$

The motorized vehicle speed adjustment factor is computed with Equation 18-35.

$$F_s = 4 \left(\frac{S_R}{100} \right)^2$$

$$F_s = 4 \left(\frac{33.0}{100} \right)^2$$

$$F_s = 0.44$$

Finally, the pedestrian LOS score for the link $I_{p,link}$ is calculated with Equation 18-32.

$$I_{p,link} = 6.0468 + F_w + F_v + F_s$$

$$I_{p,link} = 6.0468 + (-5.20) + 1.07 + 0.44$$

$$I_{p,link} = 2.35$$

Step 7: Determine Link LOS

The pedestrian LOS for the link is determined by using the pedestrian LOS score from Step 6. This score is compared with the link-based pedestrian LOS thresholds on the right side of Exhibit 18-2 to determine that the LOS for the specified direction of travel along the subject link is B.

Step 8: Determine Roadway Crossing Difficulty Factor

Crossings occur somewhat uniformly along the length of the segment, and the segment is bounded by two signalized intersections. Thus, the distance D_c is assumed to equal one-third of the segment length, or 440 ft (= 1,320/3), and the diversion distance D_d is computed as 880 ft (= 2 × 440 ft).

The delay incurred due to diversion is calculated by using Equation 18-37.

$$d_{pd} = \frac{D_d}{S_p} + d_{pc}$$

$$d_{pd} = \frac{880}{4.19} + 80$$

$$d_{pd} = 290 \text{ s/p}$$

The crossing delay used to estimate the roadway crossing difficulty factor is computed with the following equation.

$$d_{px} = \min(d_{pd}, d_{pw}, 60)$$

$$d_{px} = \min(290, 740, 60)$$

$$d_{px} = 60 \text{ s/p}$$

The roadway crossing difficulty factor is computed with Equation 18-38.

$$F_{cd} = 1.0 + \frac{0.10 d_{px} - (0.318 I_{p,link} + 0.220 I_{p,int} + 1.606)}{7.5} \leq 1.20$$

$$F_{cd} = 1.0 + \frac{0.10(60) - [0.318(2.35) + 0.220(3.60) + 1.606]}{7.5}$$

$$F_{cd} = 1.20$$

Step 9: Determine Pedestrian LOS Score for Segment

The pedestrian LOS score for the segment is computed with Equation 18-39.

$$I_{p,seg} = 0.75 \left[\frac{(F_{cd} I_{p,link} + 1)^3 \frac{L}{S_p} + (I_{p,int} + 1)^3 d_{pp}}{\frac{L}{S_p} + d_{pp}} \right]^{\frac{1}{3}} + 0.125$$

$$I_{p,seg} = 0.75 \left[\frac{[1.20(2.35) + 1]^3 \left(\frac{1,320}{4.19}\right) + (3.60 + 1)^3 (40)}{\frac{1,320}{4.19} + 40} \right]^{\frac{1}{3}} + 0.125$$

$$I_{p,seg} = 3.07$$

Step 10: Determine Segment LOS

The pedestrian LOS for the segment is determined by using the pedestrian LOS score from Step 9 and the average pedestrian space from Step 2. These two performance measures are compared with their respective thresholds on the left side of Exhibit 18-2 to determine that the LOS for the specified direction of travel along the subject segment is C.

EXAMPLE PROBLEM 3: BICYCLE LOS

The Segment

The bicycle lane of interest is located along a 1,320-ft urban street segment. The segment is part of a collector street located near a community college. The bicycle lane is provided for the eastbound direction of travel, as shown in Exhibit 30-38.

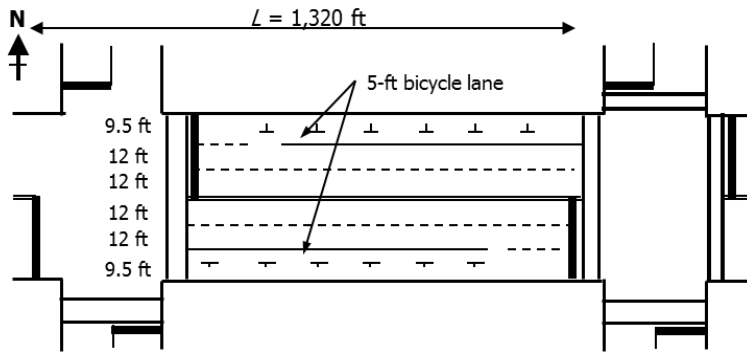


Exhibit 30-38
Example Problem 3: Segment Geometry

The Question

What is the bicycle LOS for the eastbound bicycle lane?

The Facts

The geometric details of the street cross section are shown in Exhibit 30-38. Both boundary intersections are signalized. The following additional information is known about the street segment:

Traffic characteristics:

Midsegment flow rate in eastbound direction: 940 veh/h

Percent heavy vehicles: 8.0%

Proportion of on-street parking occupied during analysis period: 0.20

Geometric characteristics:

Outside shoulder width: none

Parking lane width: 9.5 ft

Median type: undivided

Cross section has raised curb along the outside edge of the roadway

Number of access point approaches on right side of segment in subject travel direction: 3

Other data:

Pavement condition rating: 2.0

Performance measures obtained from supporting methodologies:

Motorized vehicle running speed: 33 mi/h

Bicycle control delay: 40 s/bicycle

Bicycle LOS score for the downstream intersection: 0.08

Outline of Solution

First, the bicycle delay at the boundary intersection will be computed. This delay will then be used to compute the bicycle travel speed. Next, a bicycle LOS score will be computed for the link. It will then be combined with a similar score for the boundary intersection and used to compute the bicycle LOS score for the segment. Finally, LOS for the segment will be determined by using the computed score and the thresholds in Exhibit 18-3.

Computational Steps

Step 1: Determine Bicycle Running Speed

The average bicycle running speed S_b could not be determined from field data. Therefore, it was estimated to be 15 mi/h on the basis of the guidance provided.

Step 2: Determine Bicycle Delay at Intersection

The motorized vehicle methodology in Chapter 19, Signalized Intersections, was used to estimate the bicycle delay at the boundary intersection d_b . This delay was computed to be 40.0 s/bicycle.

Step 3: Determine Bicycle Travel Speed

The segment running time of through bicycles is computed as

$$t_{Rb} = \frac{3,600 L}{5,280 S_b}$$
$$t_{Rb} = \frac{3,600(1,320)}{5,280(15)}$$
$$t_{Rb} = 60.0 \text{ s}$$

The average bicycle travel speed is computed with Equation 18-40.

$$S_{Tb,seg} = \frac{3,600 L}{5,280 (t_{Rb} + d_b)}$$

$$S_{Tb,seg} = \frac{3,600(1,320)}{5,280 (60.0 + 40.0)}$$

$$S_{Tb,seg} = 9.0 \text{ mi/h}$$

This travel speed is adequate, but a speed of 10 mi/h or more is considered desirable.

Step 4: Determine Bicycle LOS Score for Intersection

The bicycle methodology in Chapter 19 was used to determine the bicycle LOS score for the boundary intersection $I_{b,int}$. It was computed to be 0.08.

Step 5: Determine Bicycle LOS Score for Link

The bicycle LOS score is computed from four factors. However, before these factors can be calculated, several cross-section variables need to be adjusted. These variables are calculated first, and then the four factors are computed. Finally, they are combined to determine the desired score.

The street cross section is curbed but there is no shoulder, so the adjusted width of the paved outside shoulder W_{os}^* is 0.0 ft. Therefore, the total width of the outside through lane, bicycle lane, and paved shoulder W_t is computed as

$$W_t = W_{ol} + W_{bl} + W_{os}^*$$

$$W_t = 12 + 5 + 0$$

$$W_t = 17 \text{ ft}$$

The variable W_t does not include the width of the parking lane in this instance because the proportion of occupied on-street parking exceeds 0.0.

The total width of shoulder, bicycle lane, and parking lane W_l is computed as

$$W_l = W_{bl} + W_{os}^* + W_{pk}$$

$$W_l = 5 + 0 + 9.5$$

$$W_l = 14.5 \text{ ft}$$

The midsegment demand flow rate is greater than 160 veh/h. Therefore, the effective total width of the outside through lane, bicycle lane, and shoulder as a function of traffic volume W_v is equal to W_t .

The total width of shoulder, bicycle lane, and parking lane W_l exceeds 4.0 ft. Therefore, the effective width of the outside through lane is computed as

$$W_e = W_v + W_l - 20 p_{pk} \geq 0.0$$

$$W_e = 17 + 14.5 - 20(0.20) \geq 0.0$$

$$W_e = 27.5 \text{ ft}$$

The percent heavy vehicles is less than 50%, so the adjusted percent heavy vehicles P_{HVa} is equal to the input percent heavy vehicles P_{HV} of 8.0%.

The motorized vehicle methodology described in Section 3 of Chapter 18 was used to determine the motorized vehicle running speed S_R for the subject segment. This speed was computed to be 33.0 mi/h, which exceeds 21 mi/h. Therefore, the adjusted motorized vehicle speed S_{Ra} is also equal to 33.0 mi/h.

The midsegment demand flow rate is greater than 8 veh/h ($= 4 N_{th}$), so the adjusted midsegment demand flow rate v_{ma} is equal to the input demand flow rate of 940 veh/h.

The cross-section adjustment factor is computed with Equation 18-42.

$$F_w = -0.005 W_e^2$$

$$F_w = -0.005(27.5)^2$$

$$F_w = -3.78$$

The motorized vehicle volume adjustment factor comes from Equation 18-43.

$$F_v = 0.507 \ln\left(\frac{v_{ma}}{4 N_{th}}\right)$$

$$F_v = 0.507 \ln\left(\frac{940}{4(2)}\right)$$

$$F_v = 2.42$$

The motorized vehicle speed adjustment factor is computed with Equation 18-44.

$$F_S = 0.199[1.1199 \ln(S_{Ra} - 20) + 0.8103](1 + 0.1038 P_{HVa})^2$$

$$F_S = 0.199[1.1199 \ln(33.0 - 20) + 0.8103][1 + 0.1038(8.0)]^2$$

$$F_S = 2.46$$

The pavement condition adjustment factor is computed with Equation 18-45.

$$F_p = \frac{7.066}{P_c^2}$$

$$F_p = \frac{7.066}{(2.0)^2}$$

$$F_p = 1.77$$

Finally, the bicycle LOS score for the link $I_{b,link}$ is calculated with Equation 18-41.

$$I_{b,link} = 0.760 + F_w + F_v + F_S + F_p$$

$$I_{b,link} = 0.760 - 3.78 + 2.42 + 2.46 + 1.77$$

$$I_{b,link} = 3.62$$

Step 6: Determine Link LOS

The bicycle LOS for the link is determined by using the bicycle LOS score from Step 5. This score is compared with the link-based bicycle LOS thresholds in Exhibit 18-3 to determine that the LOS for the specified direction of travel along the subject link is D.

Step 7: Determine Bicycle LOS Score for Segment

The unsignalized conflicts factor is computed with Equation 18-47.

$$F_c = 0.035 \left(\frac{5,280 N_{ap,s}}{L} - 20 \right)$$

$$F_c = 0.035 \left[\frac{5,280 (3)}{1,320} - 20 \right]$$

$$F_c = -0.28$$

The bicycle LOS score for the segment is computed with Equation 18-46.

$$I_{b,seg} = 0.75 \left[\frac{(F_c + I_{b,link} + 1)^3 t_{R,b} + (I_{b,int} + 1)^3 d_b}{t_{R,b} + d_b} \right]^{\frac{1}{3}} + 0.125$$

$$I_{b,seg} = 0.75 \left[\frac{[(-0.28) + 3.62 + 1]^3 (60) + (0.08 + 1)^3 (40)}{60 + 40} \right]^{\frac{1}{3}} + 0.125$$

$$I_{b,seg} = 2.88$$

Step 8: Determine Segment LOS

The bicycle LOS for the segment is determined by using the bicycle LOS score from Step 7. This score is compared with the segment-based bicycle LOS thresholds in Exhibit 18-3 to determine that the LOS for the specified direction of travel along the subject segment is C.

EXAMPLE PROBLEM 4: TRANSIT LOS

The Segment

The transit route of interest travels east along a 1,320-ft urban street segment. The segment is part of a collector street located near a community college. It is shown in Exhibit 30-39. A bus stop is provided on the south side of the segment for the subject route.

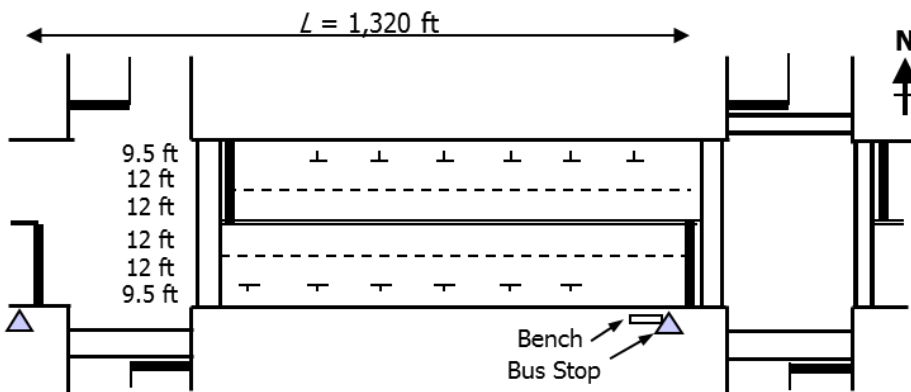


Exhibit 30-39
Example Problem 4: Segment Geometry

The Question

What is the transit LOS for the eastbound bus route on the subject segment?

The Facts

The geometric details of the segment are shown in Exhibit 30-39. Both boundary intersections are signalized. There is one stop in the segment for the eastbound route. The following additional information is known about the bus stop and street segment:

Transit characteristics:

Dwell time: 20.0 s

Transit frequency: 4 veh/h

Excess wait time data are not available for the stop, but the on-time performance of the route (based on a standard of up to 5 min late being considered "on time") at the previous time point is known (92%)

Passenger load factor: 0.83 passengers/seat

Other data:

Area type: not in a central business district

g/C ratio at downstream boundary intersection: 0.4729

Cycle length: 140 s

The bus stop in the segment has a bench, but no shelter

Number of routes serving the segment: 1

The bus stop is accessed from the right-turn lane (i.e., the stop is off-line).

Buses are exempt from the requirement to turn right but have no other traffic priority

Performance measures obtained from supporting methodologies:

Motorized vehicle running speed: 33 mi/h

Pedestrian LOS score for the link: 3.53

Through vehicle control delay at the downstream boundary intersection:
19.4 s/veh

Reentry delay: 16.17 s

Outline of Solution

First, the transit vehicle segment running time will be computed. Next, the control delay at the boundary intersection will be obtained and used to compute the transit vehicle segment travel speed. Then the transit wait-ride score will be computed. This score will be combined with the pedestrian LOS score for the link to compute the transit LOS score for the segment. Finally, LOS for the segment will be determined by comparing the computed score with the thresholds identified in Exhibit 18-3.

Computational Steps

Step 1: Determine Transit Vehicle Running Time

The transit vehicle running time is based on the segment running speed and delay due to a transit vehicle stop. These components are calculated first, and then running time is calculated.

Transit vehicle segment running speed can be computed with Equation 18-48.

$$S_{Rt} = \min \left(S_{Rt}, \frac{61}{1 + e^{-1.00 + (1,185 N_{ts}/L)}} \right)$$

$$S_{Rt} = \min \left(33.0, \frac{61}{1 + e^{-1.00 + (1,185(1)/1,320)}} \right)$$

$$S_{Rt} = 32.1 \text{ mi/h}$$

The acceleration and deceleration rates are unknown, so they are assumed to be 3.3 ft/s² and 4.0 ft/s², respectively, on the basis of data given in the *Transit Capacity and Quality of Service Manual* (9).

The bus stop is located on the near side of a signalized intersection. From Equation 18-50, the average proportion of bus stop acceleration–deceleration delay not due to the intersection’s traffic control f_{ad} is equal to the g/C ratio for the through movement in the bus’s direction of travel (in this case, eastbound). The effective green time g is 66.21 s (calculated as the phase duration minus the change period), and the cycle length is 140 s. Therefore, f_{ad} is 0.4729.

Equation 18-49 can now be used to compute the portion of bus stop delay due to acceleration and deceleration.

$$d_{ad} = \frac{5,280}{3,600} \left(\frac{S_{Rt}}{2} \right) \left(\frac{1}{r_{at}} + \frac{1}{r_{dt}} \right) f_{ad}$$

$$d_{ad} = \frac{5,280}{3,600} \left(\frac{32.1}{2} \right) \left(\frac{1}{3.3} + \frac{1}{4.0} \right) (0.4729)$$

$$d_{ad} = 6.15 \text{ s}$$

Equation 18-51 is used to compute the portion of bus stop delay due to serving passengers. The input average dwell time of 20.0 s and an f_{dt} value of 0.4729 are used in the equation, on the basis of the stop’s near-side location at a traffic signal and the g/C ratio computed in a previous step. The f_{dt} factor is used to avoid double-counting the portion of passenger service time that occurs during the signal’s red indication and is therefore included as part of control delay.

$$d_{ps} = t_d f_{dt}$$

$$d_{ps} = (20.0)(0.4729)$$

$$d_{ps} = 9.46 \text{ s}$$

The bus stop is located in the right-turn lane; therefore, the bus is subject to reentry delay on leaving the stop. On the basis of the guidance for reentry delay for a near-side stop at a traffic signal, the reentry delay d_{re} is equal to the queue service time g_s . This time is calculated to be 16.17 s by following the procedures in Section 3 of Chapter 31, Signalized Intersections: Supplemental.

Equation 18-52 is used to compute the total delay due to the transit stop.

$$d_{ts} = d_{ad} + d_{ps} + d_{re}$$

$$d_{ts} = 6.15 + 9.46 + 16.17$$

$$d_{ts} = 31.78 \text{ s}$$

Equation 18-53 is used to compute transit vehicle running time on the basis of the previously computed components.

$$t_{Rt} = \frac{3,600 L}{5,280 S_{Rt}} + \sum_{i=1}^{N_{ts}} d_{ts,i}$$

$$t_{Rt} = \frac{3,600(1,320)}{5,280(32.1)} + 31.78$$

$$t_{Rt} = 59.9 \text{ s}$$

Step 2: Determine Delay at Intersection

The through delay d_i at the boundary intersection is set equal to the through vehicle control delay exiting the segment at this intersection. The latter delay is 19.4 s/veh. Thus, the through delay d_i is equal to 19.4 s/veh.

Step 3: Determine Travel Speed

The average transit travel speed is computed with Equation 18-55.

$$S_{Tt,seg} = \frac{3,600 L}{5,280 (t_{Rt} + d)}$$

$$S_{Tt,seg} = \frac{3,600(1,320)}{5,280(59.9 + 19.4)}$$

$$S_{Tt,seg} = 11.3 \text{ mi/h}$$

Step 4: Determine Transit Wait-Ride Score

The wait-ride score is based on the headway factor and the perceived travel time factor. Each of these components is calculated separately. The wait-ride score is then calculated.

The input data indicate that there is one route on the segment, and its frequency is 4 veh/h. The headway factor is computed with Equation 18-56.

$$F_h = 4.00e^{-1.434/(v_s+0.001)}$$

$$F_h = 4.00e^{-1.434/(4+0.001)}$$

$$F_h = 2.80$$

The perceived travel time factor is based on several intermediate variables that need to be calculated first. The first of these calculations is the amenity time rate. It is calculated by using Equation 18-60. A default passenger trip length of 3.7 mi is used in the absence of other information.

$$T_{at} = \frac{1.3 p_{sh} + 0.2 p_{be}}{L_{pt}}$$

$$T_{at} = \frac{1.3(0.0) + 0.2(1.0)}{3.7}$$

$$T_{at} = 0.054 \text{ min/mi}$$

Since no information is available for actual excess wait time but on-time performance information is available for the route, Equation 18-61 is used to estimate excess wait time.

$$t_{ex} = [t_{late}(1 - p_{ot})]^2$$

$$t_{ex} = [5.0(1 - 0.92)]^2$$

$$t_{ex} = 0.16 \text{ min}$$

The excess wait time rate T_{ex} is then the excess wait time t_{ex} divided by the average passenger trip length L_{pt} : $0.16/3.7 = 0.043 \text{ min/mi}$.

The passenger load waiting factor is computed with Equation 18-59.

$$a_1 = 1 + \frac{4(F_l - 0.80)}{4.2}$$

$$a_1 = 1 + \frac{4(0.83 - 0.80)}{4.2}$$

$$a_1 = 1.03$$

The perceived travel time rate is computed with Equation 18-58.

$$T_{ptt} = \left(a_1 \frac{60}{S_{Tt,seg}} \right) + (2 T_{ex}) - T_{at}$$

$$T_{ptt} = \left(1.03 \frac{60}{11.3} \right) + [2(0.043)] - 0.054$$

$$T_{ptt} = 5.50 \text{ min/mi}$$

The segment is not located in a central business district of a metropolitan area with a population of 5 million or more, so the base travel time rate T_{btt} is equal to 4.0 min/mi. The perceived travel time factor is computed with Equation 18-57.

$$F_{tt} = \frac{(e - 1) T_{btt} - (e + 1) T_{ptt}}{(e - 1) T_{ptt} - (e + 1) T_{btt}}$$

$$F_{tt} = \frac{(-0.40 - 1)(4.0) - (-0.40 + 1)(5.50)}{(-0.40 - 1)(5.50) - (-0.40 + 1)(4.0)}$$

$$F_{tt} = 0.881$$

Finally, the transit wait-ride score is computed with Equation 18-62.

$$s_{w-r} = F_h F_{tt}$$

$$s_{w-r} = (2.80)(0.883)$$

$$s_{w-r} = 2.47$$

Step 5: Determine Pedestrian LOS Score for Link

The pedestrian methodology described in Chapter 18 was used to determine the pedestrian LOS score for the link $I_{p,link}$. This score was computed to be 3.53.

Step 6: Determine Transit LOS Score for Segment

The transit LOS score for the segment is computed with Equation 18-63.

$$I_{t,seg} = 6.0 - 1.50 s_{w-r} + 0.15 I_{p,link}$$

$$I_{t,seg} = 6.0 - 1.50(2.47) + 0.15(3.53)$$

$$I_{t,seg} = 2.83$$

Step 7: Determine LOS

The transit LOS is determined by using the transit LOS score from Step 6. This performance measure is compared with the thresholds in Exhibit 18-3 to determine that the LOS for the specified bus route is C.

9. ROUNDABOUT SEGMENT METHODOLOGY

SCOPE OF THE METHODOLOGY

This subsection provides an overview of the methodology for evaluating the performance of the motor vehicle mode on an urban street segment bounded by one or more roundabouts. The methodology is based on national research that measured the travel time performance of nine facilities containing three or more roundabouts in series (10). The methodology is designed to be integrated into the general motorized vehicle methodology for urban street segments described in Chapter 18. Only the relevant deviations from the general methodology are provided in this subsection.

LIMITATIONS OF THE METHODOLOGY

The methodologies in this subsection are based on regression analyses of field-measured data. The limits of these field data are provided in Exhibit 30-40. The analyst is cautioned with regard to the validity of the results when an input or intermediate calculated value is outside the range of the research data. In addition, the methodology does not account for capacity constraint caused by oversaturated conditions or the possible effects of an upstream signal on a downstream roundabout.

Input or Calculated Value	Minimum	Maximum
<i>Input Data</i>		
Inscribed circle diameter (ft)	84	245
Number of circulating lanes	1	2
Segment length (ft)	540	7,900
Posted speed limit (mi/h)	25	50
<i>Intermediate Calculations</i>		
Central island diameter (ft)	48	187
Length of first portion of segment (ft)	270	3,953
Length of second portion of segment (ft)	244	3,993
Free-flow speed (mi/h)	26	53
Roundabout influence area for first portion of segment (ft)	235	1,446
Roundabout influence area for second portion of segment (ft)	73	897
Geometric delay for first portion of segment (s)	0.1	9.5
Geometric delay for second portion of segment (s)	0.1	6.6

Exhibit 30-40

Validity Range of Inputs and Calculated Values for Analysis of Motor Vehicles on an Urban Street Roundabout Segment

REQUIRED INPUT DATA AND SOURCES

Exhibit 30-41 lists the additional required input data, potential data sources, and suggested default values for applying the methodology in this subsection. The reader should refer to Chapter 18 for a complete list of required input data. Guidance on selecting values for inscribed circle diameter and width of circulating lanes can be obtained elsewhere (11).

Exhibit 30-41

Additional Required Input Data, Potential Data Sources, and Default Values for Analysis of Motor Vehicles on an Urban Street Roundabout Segment

Required Data and Units	Potential Data Source(s)	Suggested Default Value
<i>Geometric Design Data</i>		
Inscribed circle diameter of upstream and downstream roundabout (ft)	Field data, aerial photo, preliminary design	130 ft for one-lane roundabout 180 ft for two-lane roundabout
Number of circulating lanes of upstream and downstream roundabout (ft)	Field data, aerial photo, preliminary design	Must be provided
Average width of circulating lanes of upstream and downstream roundabout (ft)	Field data, aerial photo, preliminary design	20 ft for one-lane roundabout 15 ft for two-lane roundabout
<i>Performance Measure Data</i>		
Control delay by lane at boundary roundabout (s/veh)	HCM method output	Must be provided
Capacity by lane at boundary roundabout (veh/h)	HCM method output	Must be provided

GEOMETRIC DESIGN DATA

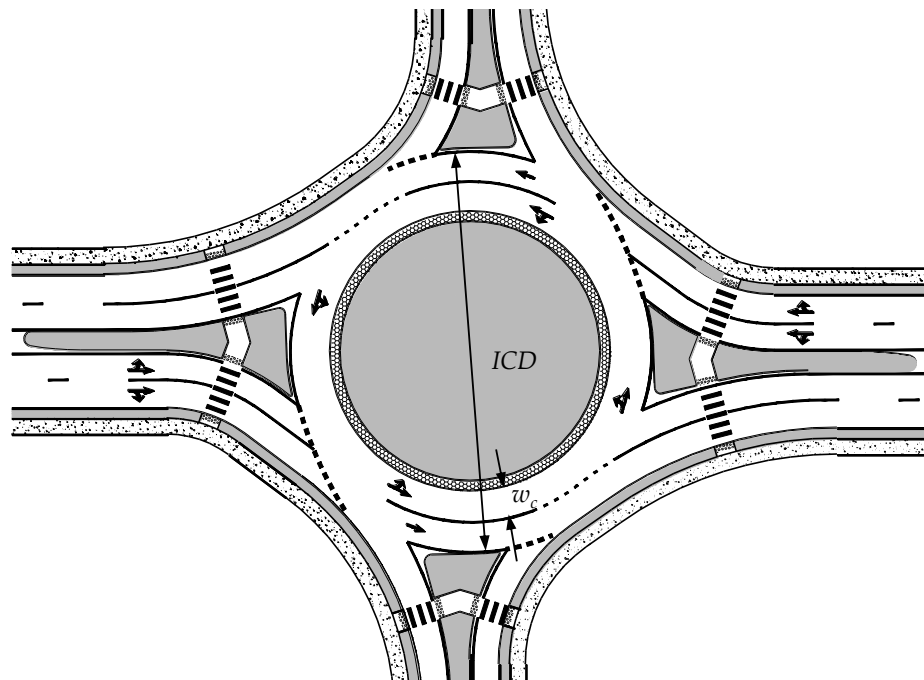
This subsection describes the geometric design data listed in Exhibit 30-41. These data describe the additional geometric elements of the roundabouts beyond the geometric elements of the intersections and segments described in Exhibit 18-5.

Inscribed Circle Diameter

The inscribed circle diameter, *ICD*, is the diameter of the largest circle that can be inscribed within the outer edges of the circulatory roadway. The ICD serves as the width of the roundabout. This is illustrated in Exhibit 30-42.

Exhibit 30-42

Illustration of Geometric Design Data



For the purposes of this methodology, if the ICD is variable throughout the roundabout (e.g., to accommodate a variable number of circulating lanes, as illustrated in Exhibit 30-42), the larger dimension should be used.

Number of Circulating Lanes

The number of circulating lanes N_c is the count of circulating lanes immediately downstream of the entry that forms the end of the segment under study.

Average Width of Circulating Lanes

The average width of circulating lanes w_c is measured in the section of circulatory roadway immediately downstream of the entry, that is, the same location where the number of circulating lanes is counted. This is illustrated in Exhibit 30-42.

COMPUTATIONAL STEPS

The computational steps described below are illustrated in the flowchart provided in Exhibit 18-8. The path followed is that of a noncoordinated system with YIELD control.

Step 1: Determine Traffic Demand Adjustments

The models developed for estimating travel speed through a series of roundabouts were calibrated by using roundabouts that were operating below capacity. Neither the capacity estimation procedures for roundabouts in Chapter 22 nor the procedures in this subsection explicitly account for capacity constraint that restricts (or meters) discharge volume from the intersection when the demand volume for an intersection traffic movement exceeds its capacity. Similarly, the methodology does not account for the effect on roundabout operations or travel time that may be created by queue spillback between two roundabouts. The occurrence of any of these conditions should be flagged, and an alternative tool should be considered.

Step 2: Determine Running Time

A procedure for determining running time for a segment bounded by one or more roundabouts is described in this step. It builds on the procedure described in Chapter 18. Each calculation is discussed in the following subparts, which culminate with the calculation of segment running time.

A. Determine Free-Flow Speed

Free-flow speed represents the average running speed of through vehicles traveling along a segment under low-volume conditions and not delayed by traffic control devices or other vehicles. It reflects the effect of the street environment on driver speed choice. Elements of the street environment that influence this choice under free-flow conditions include speed limit, access point density, median type, curb presence, and segment length. Further discussion on free-flow speed can be found in Section 3 of Chapter 18.

Free-flow speed (when the influence of roundabouts at one or both ends of the segment is considered) is calculated by separately determining the free-flow speed influenced by the roundabout at each end of the segment and then comparing these two free-flow speed estimates with the free-flow speed that would be estimated without the presence of roundabouts.

Base Free-Flow Speed

The base free-flow speed is defined to be the free-flow speed on longer segments and is computed the same for segments bounded by roundabouts as for segments bounded by signals. It includes the influence of speed limit, access point density, median type, curb presence, and on-street parking presence. It is computed with Equation 30-72.

Equation 30-72

$$S_{fo} = S_{calib} + S_0 + f_{cs} + f_A + f_{pk}$$

where

- S_{fo} = base free-flow speed (mi/h),
- S_{calib} = base free-flow speed calibration factor (mi/h),
- S_0 = speed constant (mi/h),
- f_{cs} = adjustment for cross section (mi/h),
- f_A = adjustment for access points (mi/h), and
- f_{pk} = adjustment for on-street parking (mi/h).

The speed constant and adjustment factors used in Equation 30-72 are listed in Exhibit 30-43. The exhibit is the same as Exhibit 18-11, except that the width of the signalized intersection used in the calculation for the adjustment for access points f_A has been replaced with the inscribed circle diameter of the roundabout, and the range of speed limits is restricted to the validity range for this method. Equations provided in the table footnote can also be used to compute these adjustment factors for conditions not shown in the exhibit. Further discussion of this equation and adjustment factors can be found in Chapter 18.

Exhibit 30-43
Base Free-Flow Speed
Adjustment Factors

Speed Limit (mi/h)	Speed Constant S_0 (mi/h) ^a	Percent with Restrictive Median (%)		Adjustment for Cross Section f_{cs} (mi/h) ^b	
		Median Type	Median (%)	No Curb	Curb
25	37.4	Restrictive	20	0.3	-0.9
30	39.7		40	0.6	-1.4
35	42.1		60	0.9	-1.8
40	44.4		80	1.2	-2.2
45	46.8		100	1.5	-2.7
50	49.1	Nonrestrictive	Not applicable	0.0	-0.5
		No median	Not applicable	0.0	-0.5

Access Density D_a (points/mi)	Adjustment for Access Points f_A by Lanes N_{th} (mi/h) ^c			Percent with On-Street Parking (%)	Adjustment for Parking (mi/h) ^d
	1 Lane	2 Lanes	3 Lanes		
0	0.0	0.0	0.0	0	0.0
2	-0.2	-0.1	-0.1	20	-0.6
4	-0.3	-0.2	-0.1	40	-1.2
10	-0.8	-0.4	-0.3	60	-1.8
20	-1.6	-0.8	-0.5	80	-2.4
40	-3.1	-1.6	-1.0	100	-3.0
60	-4.7	-2.3	-1.6		

Notes: ^a $S_0 = 25.6 + 0.47S_{pl}$, where S_{pl} = posted speed limit (mi/h).
^b $f_{cs} = 1.5 p_{mm} - 0.47 p_{curb} - 3.7 p_{curb} p_{mm}$, where p_{mm} = proportion of link length with restrictive median (decimal) and p_{curb} = proportion of segment with curb on the right-hand side (decimal).
^c $f_A = -0.078 D_a / N_{th}$ with $D_a = 5,280 (N_{ap,s} + N_{ap,o}) / (L - ICD)$, where D_a = access point density on segment (points/mi); N_{th} = number of through lanes on the segment in the subject direction of travel (ln); $N_{ap,s}$ = number of access point approaches on the right side in the subject direction of travel (points); $N_{ap,o}$ = number of access point approaches on the right side in the opposing direction of travel (points); L = segment length (ft); and ICD = inscribed circle diameter of roundabout (ft).
^d $f_{pk} = -3.0 \times$ proportion of link length with on-street parking available on the right-hand side (decimal).

Equation 30-72 has been calibrated by using data for many urban street segments collectively located throughout the United States, so the default value of 0.0 mi/h for S_{calib} is believed to yield results that are reasonably representative of driver behavior in most urban areas. However, if desired, a locally representative value can be determined from field-measured estimates of the base free-flow speed for several street segments. The local default value can be established for typical street segments or for specific street types. This calibration factor is determined as the one value that provides a statistically based best fit between the prediction from Equation 30-72 and the field-measured estimates. A procedure for estimating the base free-flow speed from field data is described in Section 6.

Roundabout Geometry and Speed Parameters

The computation of free-flow speed, roundabout influence area, and geometric delay requires measurement or estimation of a series of geometric parameters associated with the roundabout at one or both ends of the segment. These computations are performed separately for each roundabout.

The central island diameter is equal to the inscribed circle diameter minus the width of the circulatory roadway on each side of the central island. The circulatory roadway width is equal to the average width of each circulating lane times the number of circulating lanes. These calculations are combined into a single equation as given in Equation 30-73.

$$CID = ICD - 2N_c w_c$$

Equation 30-73

where

CID = central island diameter (ft),

ICD = inscribed circle diameter (ft),

N_c = number of circulating lane(s), and

w_c = average width of circulating lane(s) (ft).

The circulating speed, S_c , can be approximated by assuming that the circulating path occupies the centerline of the circulatory roadway with a radius equal to half the central island diameter plus half the total width of the circulatory roadway. This radius can be computed with Equation 30-74.

$$r_{c,th} = \frac{ICD}{2} + \frac{N_c w_c}{2}$$

Equation 30-74

where

$r_{c,th}$ = average radius of circulating path of through movement (ft),

ICD = inscribed circle diameter (ft),

N_c = number of circulating lane(s), and

w_c = average width of circulating lane(s) (ft).

The speed associated with this radius can be estimated with Equation 30-75 (12), which assumes a negative cross slope of the circulatory roadway of -0.02 , typical of many roundabouts.

Equation 30-75

$$S_c = 3.4614r_{c,th}^{0.3673}$$

where

S_c = circulating speed (mi/h), and

$r_{c,th}$ = average radius of circulating path of through movement (ft).

For the purposes of calculating free-flow speed, roundabout influence area, and geometric delay, the segment length is divided into two subsegments. Subsegment 1 consists of the portion of the segment from the yield line of the upstream roundabout to the midpoint between the two roundabouts, defined as halfway between the cross-street centerlines of the two roundabouts.

Subsegment 2 consists of the portion of the segment from this midpoint to the yield line of the downstream roundabout. The lengths of these subsegments are calculated with Equation 30-76 and Equation 30-77. These dimensions are illustrated in Exhibit 30-44.

Equation 30-76

$$L_1 = \frac{1}{2} \left(L - \frac{ICD_1}{2} + \frac{ICD_2}{2} \right) + \frac{ICD_1}{2}$$

Equation 30-77

$$L_2 = L - L_1$$

where

L_1 = length of Subsegment 1 (ft),

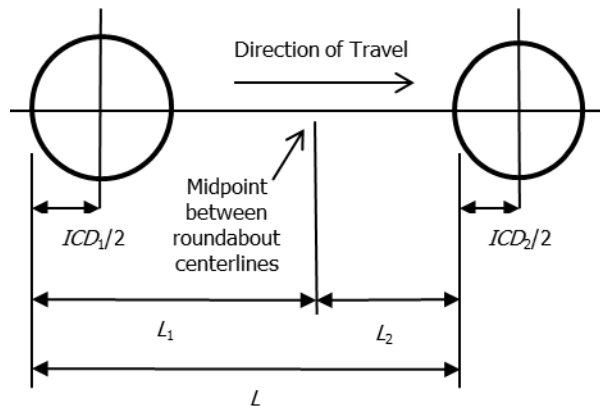
L_2 = length of Subsegment 2 (ft),

L = length of segment (ft),

ICD_1 = inscribed circle diameter of Roundabout 1 (ft), and

ICD_2 = inscribed circle diameter of Roundabout 2 (ft).

Exhibit 30-44
Illustration of Subsegment Dimensions



Free-Flow Speed for Upstream Subsegment (Subsegment 1)

Free-flow speed for Subsegment 1 (the upstream subsegment) is computed in a three-step process by first determining an initial free-flow speed. A roundabout influence area is then computed as the distance over which the geometric features of the roundabout influence travel speed. The initial free-flow speed is then adjusted downward if the roundabout influence area meets or exceeds the length of the subsegment.

The initial free-flow speed for Subsegment 1 is estimated from the subsegment length, posted speed limit, and central island diameter of the roundabout at the upstream end of the segment by using Equation 30-78.

$$S_{f,1,initial} = 14.6 + 0.0039L_1 + 0.48S_{PL} + 0.02CID_1$$

Equation 30-78

where

$S_{f,1,initial}$ = initial free-flow speed for Subsegment 1 (mi/h),

L_1 = length of Subsegment 1 (ft),

S_{PL} = posted speed limit (mi/h), and

CID_1 = central island diameter for roundabout at upstream end of Subsegment 1 (ft).

The roundabout influence area for Subsegment 1, RIA_1 , is estimated from the free-flow speed and circulating speed with Equation 30-79. This equation yields positive values for inputs within the range limits.

$$RIA_1 = -149.8 + 31.4S_{f,1,initial} - 22.5S_{c,1}$$

Equation 30-79

where

RIA_1 = roundabout influence area for Subsegment 1 (ft),

$S_{f,1,initial}$ = initial free-flow speed for Subsegment 1 (mi/h), and

$S_{c,1}$ = through movement circulating speed for roundabout at upstream end of segment (mi/h).

The roundabout influence area is then compared with the length of the subsegment, as shown in Equation 30-80. If the roundabout influence area is equal to or exceeds the length of the subsegment, the subsegment free-flow speed is reduced.

$$S_{f,1} = S_{f,1,initial} - 4.43 \text{ if } RIA_1 \geq L_1, \text{ else}$$

$$S_{f,1} = S_{f,1,initial}$$

Equation 30-80

where $S_{f,1}$ is the free-flow speed for Subsegment 1 (mi/h).

Free-Flow Speed for Downstream Subsegment (Subsegment 2)

The initial free-flow speed for Subsegment 2, $S_{f,2,initial}$, is estimated with Equation 30-81.

$$S_{f,2,initial} = 15.1 + 0.0037L_2 + 0.43S_{PL} + 0.05CID_2$$

Equation 30-81

where

$S_{f,2,initial}$ = initial free-flow speed for Subsegment 2 (mi/h),

L_2 = length of Subsegment 2 (ft),

S_{PL} = posted speed limit (mi/h), and

CID_2 = central island diameter for roundabout at downstream end of Subsegment 2 (ft).

The roundabout influence area for the subsegment RIA_2 is estimated from the free-flow speed and downstream circulating speed with Equation 30-82.

Equation 30-82

$$RIA_2 = 165.9 + 13.8S_{f,2,initial} - 21.1S_{c,2}$$

where

- RIA_2 = roundabout influence area for Subsegment 2 (ft),
- $S_{f,2,initial}$ = initial free-flow speed for Subsegment 2 (mi/h), and
- $S_{c,2}$ = through movement circulating speed for roundabout at downstream end of subsegment (mi/h).

The roundabout influence area is then compared with the length of the subsegment, as shown in Equation 30-83. If the roundabout influence area is equal to or exceeds the length of the subsegment, the subsegment free-flow speed is reduced to account for the overlap.

Equation 30-83

$$S_{f,2} = S_{f,2,initial} - 4.73 \text{ if } RIA_2 \geq L_2, \text{ else}$$

$$S_{f,2} = S_{f,2,initial}$$

where $S_{f,2}$ is the free-flow speed for Subsegment 2 (mi/h).

Free-Flow Speed Without Influence of Roundabouts

The calculation for free-flow speed without the geometric influence of roundabouts is the same as for segments bounded by signalized intersections, as provided in Chapter 18. Equation 30-84 is used to compute the value of an adjustment factor that accounts for the influence of short spacing of boundary intersections.

Equation 30-84

$$f_L = 1.02 - 4.7 \frac{S_{fo} - 19.5}{\max(L_s, 400)} \leq 1.0$$

where

- f_L = boundary intersection spacing adjustment factor;
- S_{fo} = base free-flow speed (mi/h); and
- L_s = distance between adjacent boundary intersections that (a) bracket the subject segment and (b) each have a type of control that can impose on the subject through movement a legal requirement to stop or yield, such as a roundabout (ft).

The predicted free-flow speed without the geometric influence of roundabouts is computed with Equation 30-85 on the basis of estimates of base free-flow speed and the signal spacing adjustment factor.

Equation 30-85

$$S_{f,non-rbt} = S_{fo} f_L \geq S_{pl}$$

where $S_{f,non-rbt}$ is the free-flow speed for nonroundabout segments (mi/h) and S_{pl} is the posted speed limit. If the speed obtained from Equation 30-85 is less than the speed limit, the speed limit is used.

Free-Flow Speed

The free-flow speeds for each subsegment are then compared with each other and with the nonroundabout free-flow speed with Equation 30-86. The lowest of these speeds is the governing free-flow speed for the segment. The analyst is cautioned that if the result of this calculation is outside the validity

range presented in Exhibit 30-40, the calculation is an extrapolation of the model. Note that the resulting free-flow speed for a segment bounded by one or more roundabouts may be lower than the posted speed, even though the nonroundabout free-flow speed is constrained by the posted speed in accordance with the motorized vehicle methodology in Chapter 18.

$$S_f = \min(S_{f,1}, S_{f,2}, S_{f,non-rbt})$$

Equation 30-86

B. Compute Adjustment for Vehicle Proximity

This step is the same as in Chapter 18.

C. Compute Delay due to Turning Vehicles

This step is the same as in Chapter 18.

D. Estimate Delay due to Other Sources

This step is the same as in Chapter 18.

E. Compute Segment Running Time

Equation 30-87 is used to compute the segment running time, which is based on Equation 18-7. It incorporates the conditions specified in Chapter 18 for a yield-controlled boundary exiting the segment: a start-up lost time of 2.5 s and the influence of the volume-to-capacity ratio of the roundabout entry.

$$t_R = \frac{3.5}{0.0025 L} \times \min\left(\frac{v_{th}}{c_{th}}, 1.00\right) + \frac{3,600 L}{5,280 S_f} f_v + \sum_{i=1}^{N_{ap}} d_{ap,i} + d_{other}$$

Equation 30-87

where

t_R = segment running time (s),

L = segment length (ft),

v_{th} = through-demand flow rate (veh/h),

c_{th} = through-movement capacity (veh/h),

f_v = proximity adjustment factor,

$d_{ap,i}$ = delay due to left and right turns from the street into access point intersection i (s/veh),

N_{ap} = number of influential access point approaches along the segment = $N_{ap,s} + p_{ap,lt} N_{ap,o}$ (points),

$N_{ap,s}$ = number of access point approaches on the right side in the subject direction of travel (points),

$N_{ap,o}$ = number of access point approaches on the right side in the opposing direction of travel (points),

$p_{ap,lt}$ = proportion of $N_{ap,o}$ that can be accessed by a left turn from the subject direction of travel, and

d_{other} = delay due to other sources along the segment (e.g., curb parking or pedestrians) (s/veh).

The variables v_{th} and c_{th} used in Equation 30-87 apply to the through movement exiting the segment at the boundary roundabout.

Step 3: Determine the Proportion Arriving During Green

This step does not apply to a segment with a downstream roundabout. The methodology does not account for the possible effects of an upstream signal on a downstream roundabout.

Step 4: Determine Signal Phase Duration

This step does not apply to a segment with a downstream roundabout.

Step 5: Determine Through Delay

The through delay for a segment with a roundabout at one or both ends is computed as a combination of control delay and geometric delay.

The procedure for computing the control delay at a roundabout at the downstream end of a segment is provided in Chapter 22, which determines the control delay for a roundabout on a lane-by-lane basis. For an approach with one lane, the through control delay is equal to the control delay of the lane. For an approach with two lanes, the through control delay is computed by allocating the control delay in each lane in proportion to the through traffic in each lane by using Equation 30-88.

Equation 30-88

$$d_{control,t} = \frac{d_{LL} v_{LL} P_{LL,T} + d_{RL} v_{RL} P_{RL,T}}{v_{th}}$$

where

$d_{control,t}$ = through control delay (s/veh),

v_{th} = through-demand flow rate (veh/h),

d_{LL} = control delay in left lane (s/veh),

v_{LL} = demand flow rate in left lane (veh/h),

d_{RL} = control delay in right lane (s/veh),

v_{RL} = demand flow rate in right lane (veh/h),

$P_{LL,T}$ = proportion of through-movement vehicles in the left lane (decimal), and

$P_{RL,T}$ = proportion of through-movement vehicles in the right lane (decimal).

Geometric delay is calculated separately for the presence of a roundabout on the two subsegments. If a roundabout is present on the upstream end of Subsegment 1 (regardless of the control present at the downstream end of Subsegment 2), the geometric delay for the upstream portion of the segment $d_{geom,1}$ is calculated with Equation 30-89. If the upstream end of the segment is controlled by a signalized or stop-controlled intersection or is uncontrolled, $d_{geom,1} = 0$.

Equation 30-89

$$d_{geom,1} = \max \left[-2.63 + 0.09S_f + 0.625ICD_1 \left(\frac{1}{S_{c,1}} - \frac{1}{S_f} \right), 0 \right]$$

where $d_{geom,1}$ is the geometric delay for Subsegment 1 (s/veh).

If a roundabout is present on the downstream end of the segment (regardless of the control present at the upstream end), the geometric delay for the downstream portion of the segment $d_{geom,2}$ is calculated with Equation 30-90. If the upstream end of the segment is controlled by a signalized or stop-controlled intersection or is uncontrolled, $d_{geom,2} = 0$.

$$d_{geom,2} = \max(1.57 + 0.11S_f - 0.21S_{c,2}, 0)$$

Equation 30-90

where $d_{geom,2}$ is the geometric delay for Subsegment 2 (s/veh).

The analyst is cautioned that if these calculations result in one or more geometric delay estimates outside the validity range presented in Exhibit 30-40, the calculation is an extrapolation of the model.

The through delay d_t is computed as the sum of control and geometric delays, as given in Equation 30-91.

$$d_t = d_{control,t} + d_{geom,1} + d_{geom,2}$$

Equation 30-91

Step 6: Determine Through Stop Rate

As noted in Chapter 18, the stop rate at a YIELD-controlled approach will vary with conflicting demand. It can be estimated (in stops per vehicle) as equal to the volume-to-capacity ratio of the through movement at the boundary intersection. This approach recognizes that YIELD control does not require drivers to come to a complete stop when there is no conflicting traffic. The through stop rate h is computed as given in Equation 30-92. The methodology does not apply for volume-to-capacity ratios exceeding 1.0.

$$h = \min\left(\frac{v_{th}}{c_{th}}, 1.00\right)$$

Equation 30-92

Step 7: Determine Travel Speed

This step is the same as for Chapter 18.

Step 8: Determine Spatial Stop Rate

This step is the same as for Chapter 18.

Step 9: Determine LOS

This step is the same as for Chapter 18. The base free-flow speed for the estimation of LOS is the same base free-flow speed as determined in Chapter 18.

Step 10: Determine Motor Vehicle Traveler Perception Score

Research has not been conducted on the traveler's perception of service quality for roundabouts in a manner that can be integrated into this methodology. As a result, the motor vehicle traveler perception score for a segment bounded by a roundabout is undefined and this step is not applicable for the evaluation of roundabout segments.

10. REFERENCES

1. Van Zuylen, H. The Estimation of Turning Flows on a Junction. *Traffic Engineering and Control*, Vol. 20, No. 11, 1979, pp. 539–541.
2. Wallace, C., K. Courage, M. Hadi, and A. Gan. *TRANSYT-7F User's Guide, Vol. 4 in a Series: Methodology for Optimizing Signal Timing*. University of Florida, Gainesville, March 1998.
3. Robertson, D. *TRANSYT: A Traffic Network Study Tool*. RRL Report LR 253. Road Research Laboratory, Crowthorne, Berkshire, United Kingdom, 1969.
4. Bonneson, J., M. Pratt, and M. Vandehey. *Predicting the Performance of Automobile Traffic on Urban Streets: Final Report*. NCHRP Project 3-79. Texas Transportation Institute, Texas A&M University, College Station, Jan. 2008.
5. Zegeer, J., J. Bonneson, R. Dowling, P. Ryus, M. Vandehey, W. Kittelson, N. Roupail, B. Schroeder, A. Hajbabaie, B. Aghdashi, T. Chase, S. Sajjadi, R. Margiotta, and L. Elefteriadou. *Incorporating Travel Time Reliability into the Highway Capacity Manual*. SHRP 2 Report S2-L08-RW-1. Transportation Research Board of the National Academies, Washington, D.C., 2014.
6. Bonneson, J., and J. Fitts. Delay to Major Street Through Vehicles at Two-Way Stop-Controlled Intersections. *Transportation Research Part A: Policy and Practice*, Vol. 33, Nos. 3–4, 1999, pp. 237–254.
7. Bonneson, J. Delay to Major Street Through Vehicles due to Right-Turn Activity. *Transportation Research Part A: Policy and Practice*, Vol. 32, No. 2, 1998, pp. 139–148.
8. Robertson, H., J. Hummer, and D. Nelson. *Manual of Transportation Engineering Studies*. Institute of Transportation Engineers, Washington, D.C., 2000.
9. Kittelson & Associates, Inc.; Parsons Brinckerhoff; KFH Group, Inc.; Texas A&M Transportation Institute; and Arup. *TCRP Report 165: Transit Capacity and Quality of Service Manual*, 3rd Edition. Transportation Research Board of the National Academies, Washington, D.C., 2013.
10. Rodegerdts, L. A., P. M. Jenior, Z. H. Bugg, B. L. Ray, B. J. Schroeder, and M. A. Brewer. *NCHRP Report 772: Evaluating the Performance of Corridors with Roundabouts*. Transportation Research Board of the National Academies, Washington, D. C., 2014.
11. Rodegerdts, L., J. Bansen, C. Tiesler, J. Knudsen, E. Myers, M. Johnson, M. Moule, B. Persaud, C. Lyon, S. Hallmark, H. Isebrands, R. B. Crown, B. Guichet, and A. O'Brien. *NCHRP Report 672: Roundabouts: An Informational Guide*, 2nd ed. Transportation Research Board of the National Academies, Washington, D.C., 2010.
12. Rodegerdts, L., M. Blogg, E. Wemple, E. Myers, M. Kyte, M. P. Dixon, G. F. List, A. Flannery, R. Troutbeck, W. Brilon, N. Wu, B. N. Persaud, C. Lyon, D. L. Harkey, and D. Carter. *NCHRP Report 572: Roundabouts in the United States*. Transportation Research Board of the National Academies, Washington, D.C., 2007.



HIGHWAY CAPACITY MANUAL

6TH EDITION | A GUIDE FOR MULTIMODAL MOBILITY ANALYSIS

VOLUME 4: APPLICATIONS GUIDE

The National Academies of
SCIENCES • ENGINEERING • MEDICINE

TRANSPORTATION RESEARCH BOARD
WASHINGTON, D.C. | WWW.TRB.ORG

TRANSPORTATION RESEARCH BOARD 2016 EXECUTIVE COMMITTEE *

Chair: James M. Crites, Executive Vice President of Operations,
Dallas–Fort Worth International Airport, Texas

Vice Chair: Paul Trombino III, Director, Iowa Department of
Transportation, Ames

Executive Director: Neil J. Pedersen, Transportation Research Board

Victoria A. Arroyo, Executive Director, Georgetown Climate Center;
Assistant Dean, Centers and Institutes; and Professor and Director,
Environmental Law Program, Georgetown University Law Center,
Washington, D.C.

Scott E. Bennett, Director, Arkansas State Highway and Transportation
Department, Little Rock

Jennifer Cohan, Secretary, Delaware Department of Transportation, Dover

Malcolm Dougherty, Director, California Department of
Transportation, Sacramento

A. Stewart Fotheringham, Professor, School of Geographical Sciences
and Urban Planning, Arizona State University, Tempe

John S. Halikowski, Director, Arizona Department of Transportation,
Phoenix

Susan Hanson, Distinguished University Professor Emerita, Graduate
School of Geography, Clark University, Worcester, Massachusetts

Steve Heminger, Executive Director, Metropolitan Transportation
Commission, Oakland, California

Chris T. Hendrickson, Hamerschlag Professor of Engineering, Carnegie
Mellon University, Pittsburgh, Pennsylvania

Jeffrey D. Holt, Managing Director, Power, Energy, and Infrastructure
Group, BMO Capital Markets Corporation, New York

S. Jack Hu, Vice President for Research and J. Reid and Polly Anderson
Professor of Manufacturing, University of Michigan, Ann Arbor

Roger B. Huff, President, HGLC, LLC, Farmington Hills, Michigan

Geraldine Knatz, Professor, Sol Price School of Public Policy, Viterbi
School of Engineering, University of Southern California, Los Angeles

Ysela Llort, Consultant, Miami, Florida

Melinda McGrath, Executive Director, Mississippi Department of
Transportation, Jackson

James P. Redeker, Commissioner, Connecticut Department of
Transportation, Newington

Mark L. Rosenberg, Executive Director, The Task Force for Global
Health, Inc., Decatur, Georgia

Kumares C. Sinha, Olson Distinguished Professor of Civil Engineering,
Purdue University, West Lafayette, Indiana

Daniel Sperling, Professor of Civil Engineering and Environmental
Science and Policy; Director, Institute of Transportation Studies,
University of California, Davis

Kirk T. Steudle, Director, Michigan Department of Transportation,
Lansing (Past Chair, 2014)

Gary C. Thomas, President and Executive Director, Dallas Area Rapid
Transit, Dallas, Texas

Pat Thomas, Senior Vice President of State Government Affairs, United
Parcel Service, Washington, D.C.

Katherine F. Turnbull, Executive Associate Director and Research
Scientist, Texas A&M Transportation Institute, College Station

Dean Wise, Vice President of Network Strategy, Burlington Northern
Santa Fe Railway, Fort Worth, Texas

Thomas P. Bostick (Lieutenant General, U.S. Army), Chief of Engineers
and Commanding General, U.S. Army Corps of Engineers, Washington,
D.C. (ex officio)

James C. Card (Vice Admiral, U.S. Coast Guard, retired), Maritime
Consultant, The Woodlands, Texas, and Chair, TRB Marine Board
(ex officio)

T. F. Scott Darling III, Acting Administrator and Chief Counsel, Federal
Motor Carrier Safety Administration, U.S. Department of Transportation
(ex officio)

Marie Therese Dominguez, Administrator, Pipeline and Hazardous
Materials Safety Administration, U.S. Department of Transportation
(ex officio)

Sarah Feinberg, Administrator, Federal Railroad Administration,
U.S. Department of Transportation (ex officio)

Carolyn Flowers, Acting Administrator, Federal Transit Administration,
U.S. Department of Transportation (ex officio)

LeRoy Gishi, Chief, Division of Transportation, Bureau of Indian
Affairs, U.S. Department of the Interior, Washington, D.C. (ex officio)

John T. Gray II, Senior Vice President, Policy and Economics,
Association of American Railroads, Washington, D.C. (ex officio)

Michael P. Huerta, Administrator, Federal Aviation Administration,
U.S. Department of Transportation (ex officio)

Paul N. Jaenichen, Sr., Administrator, Maritime Administration,
U.S. Department of Transportation (ex officio)

Bevan B. Kirley, Research Associate, University of North Carolina
Highway Safety Research Center, Chapel Hill, and Chair, TRB Young
Members Council (ex officio)

Gregory G. Nadeau, Administrator, Federal Highway Administration,
U.S. Department of Transportation (ex officio)

Wayne Nastri, Acting Executive Officer, South Coast Air Quality
Management District, Diamond Bar, California (ex officio)

Mark R. Rosekind, Administrator, National Highway Traffic Safety
Administration, U.S. Department of Transportation (ex officio)

Craig A. Rutland, U.S. Air Force Pavement Engineer, U.S. Air Force
Civil Engineer Center, Tyndall Air Force Base, Florida (ex officio)

Reuben Sarkar, Deputy Assistant Secretary for Transportation,
U.S. Department of Energy (ex officio)

Richard A. White, Acting President and CEO, American Public
Transportation Association, Washington, D.C. (ex officio)

Gregory D. Winfree, Assistant Secretary for Research and Technology,
Office of the Secretary, U.S. Department of Transportation (ex officio)

Frederick G. (Bud) Wright, Executive Director, American Association
of State Highway and Transportation Officials, Washington, D.C.
(ex officio)

Paul F. Zukunft (Admiral, U.S. Coast Guard), Commandant, U.S. Coast
Guard, U.S. Department of Homeland Security (ex officio)

Transportation Research Board publications are available by ordering
individual publications directly from the TRB Business Office, through
the Internet at www.TRB.org, or by annual subscription through
organizational or individual affiliation with TRB. Affiliates and library
subscribers are eligible for substantial discounts. For further information,
contact the Transportation Research Board Business Office, 500 Fifth
Street, NW, Washington, DC 20001 (telephone 202-334-3213;
fax 202-334-2519; or e-mail TRBsales@nas.edu).

Copyright 2016 by the National Academy of Sciences.

All rights reserved.

Printed in the United States of America.

ISBN 978-0-309-36997-8 [Slipcased set of three volumes]

ISBN 978-0-309-36998-5 [Volume 1]

ISBN 978-0-309-36999-2 [Volume 2]

ISBN 978-0-309-37000-4 [Volume 3]

ISBN 978-0-309-37001-1 [Volume 4, online only]

The National Academies of
SCIENCES • ENGINEERING • MEDICINE

The **National Academy of Sciences** was established in 1863 by an Act of Congress, signed by President Lincoln, as a private, nongovernmental institution to advise the nation on issues related to science and technology. Members are elected by their peers for outstanding contributions to research. Dr. Ralph J. Cicerone is president.

The **National Academy of Engineering** was established in 1964 under the charter of the National Academy of Sciences to bring the practices of engineering to advising the nation. Members are elected by their peers for extraordinary contributions to engineering. Dr. C. D. Mote, Jr., is president.

The **National Academy of Medicine** (formerly the Institute of Medicine) was established in 1970 under the charter of the National Academy of Sciences to advise the nation on medical and health issues. Members are elected by their peers for distinguished contributions to medicine and health. Dr. Victor J. Dzau is president.

The three Academies work together as the National Academies of Sciences, Engineering, and Medicine to provide independent, objective analysis and advice to the nation and conduct other activities to solve complex problems and inform public policy decisions. The Academies also encourage education and research, recognize outstanding contributions to knowledge, and increase public understanding in matters of science, engineering, and medicine.

Learn more about the National Academies of Sciences, Engineering, and Medicine at **www.national-academies.org**.

The **Transportation Research Board** is one of seven major programs of the National Academies of Sciences, Engineering, and Medicine. The mission of the Transportation Research Board is to increase the benefits that transportation contributes to society by providing leadership in transportation innovation and progress through research and information exchange, conducted within a setting that is objective, interdisciplinary, and multimodal. The Board's varied committees, task forces, and panels annually engage about 7,000 engineers, scientists, and other transportation researchers and practitioners from the public and private sectors and academia, all of whom contribute their expertise in the public interest. The program is supported by state transportation departments, federal agencies including the component administrations of the U.S. Department of Transportation, and other organizations and individuals interested in the development of transportation.

Learn more about the Transportation Research Board at **www.TRB.org**.

CHAPTER 31
SIGNALIZED INTERSECTIONS: SUPPLEMENTAL

CONTENTS

1. INTRODUCTION 31-1

2. CAPACITY AND PHASE DURATION 31-2

 Actuated Phase Duration 31-2

 Lane Group Flow Rate on Multiple-Lane Approaches 31-22

 Pretimed Phase Duration 31-30

 Pedestrian and Bicycle Adjustment Factors 31-34

 Work Zone Presence Adjustment Factor 31-40

3. QUEUE ACCUMULATION POLYGON 31-42

 Concepts 31-42

 General QAP Construction Procedure 31-43

 QAP Construction Procedure for Selected Lane Groups 31-45

4. QUEUE STORAGE RATIO 31-63

 Concepts 31-63

 Procedure for Estimating Back of Queue for Selected Lane Groups 31-70

5. PLANNING-LEVEL ANALYSIS APPLICATION 31-78

 Overview of the Application 31-78

 Required Data and Sources 31-80

 Methodology 31-80

 Worksheets 31-94

6. FIELD MEASUREMENT TECHNIQUES 31-99

 Field Measurement of Intersection Control Delay 31-99

 Field Measurement of Saturation Flow Rate 31-105

7. COMPUTATIONAL ENGINE DOCUMENTATION 31-111

 Flowcharts 31-111

 Linkage Lists 31-113

8. USE OF ALTERNATIVE TOOLS 31-119

 Effect of Storage Bay Overflow 31-119

 Effect of Right-Turn-on-Red Operation 31-121

Effect of Short Through Lanes	31-124
Effect of Closely Spaced Intersections	31-125
9. EXAMPLE PROBLEMS.....	31-127
Example Problem 1: Motorized Vehicle LOS	31-127
Example Problem 2: Pedestrian LOS	31-135
Example Problem 3: Bicycle LOS.....	31-141
10. REFERENCES.....	31-144

LIST OF EXHIBITS

Exhibit 31-1 Time Elements Influencing Actuated Phase Duration 31-3

Exhibit 31-2 Detection Design and Maximum Allowable Headway 31-8

Exhibit 31-3 Force-Off Points, Yield Point, and Phase Splits 31-14

Exhibit 31-4 Example Equivalent Maximum Green for Fixed Force Mode 31-16

Exhibit 31-5 Probability of a Lane Change 31-24

Exhibit 31-6 Input Variables for Lane Group Flow Rate Procedure 31-25

Exhibit 31-7 Example Intersection 31-32

Exhibit 31-8 Conflict Zone Locations 31-35

Exhibit 31-9 Work Zone on an Intersection Approach 31-40

Exhibit 31-10 Geometric Design Input Data Requirements for Work
Zones 31-40

Exhibit 31-11 Queue Accumulation Polygon for Protected Movements 31-43

Exhibit 31-12 Unblocked Permitted Green Time 31-46

Exhibit 31-13 QAP for Permitted Left-Turn Operation in an Exclusive
Lane 31-56

Exhibit 31-14 QAP for Permitted Left-Turn Operation in a Shared Lane 31-56

Exhibit 31-15 QAP for Leading, Protected-Permitted Left-Turn Operation
in an Exclusive Lane 31-56

Exhibit 31-16 QAP for Lagging, Protected-Permitted Left-Turn Operation
in an Exclusive Lane 31-57

Exhibit 31-17 QAP for Leading, Protected-Permitted Left-Turn Operation
in a Shared Lane 31-57

Exhibit 31-18 QAP for Lagging, Protected-Permitted Left-Turn Operation
in a Shared Lane 31-57

Exhibit 31-19 Polygon for Uniform Delay Calculation 31-59

Exhibit 31-20 Time–Space Diagram of Vehicle Trajectory on an
Intersection Approach 31-64

Exhibit 31-21 Cumulative Arrivals and Departures During an
Oversaturated Analysis Period 31-65

Exhibit 31-22 Third-Term Back-of-Queue Size with Increasing Queue 31-66

Exhibit 31-23 Third-Term Back-of-Queue Size with Decreasing Queue 31-66

Exhibit 31-24 Third-Term Back-of-Queue Size with Queue Clearing 31-66

Exhibit 31-25 Arrival–Departure Polygon 31-69

Exhibit 31-26 ADP for Permitted Left-Turn Operation in an Exclusive
Lane 31-71

Exhibit 31-27 ADP for Permitted Left-Turn Operation in a Shared Lane 31-72

Exhibit 31-28 ADP for Leading, Protected-Permitted Left-Turn Operation
in an Exclusive Lane 31-72

Exhibit 31-29 ADP for Lagging, Protected-Permitted Left-Turn Operation in an Exclusive Lane	31-72
Exhibit 31-30 ADP for Leading, Protected-Permitted Left-Turn Operation in a Shared Lane	31-73
Exhibit 31-31 ADP for Lagging, Protected-Permitted Left-Turn Operation in a Shared Lane	31-73
Exhibit 31-32 Required Input Data for the Planning-Level Analysis Application	31-80
Exhibit 31-33 Planning-Level Analysis: Equivalency Factor for Left Turns.....	31-83
Exhibit 31-34 Planning-Level Analysis: Equivalency Factor for Right Turns.....	31-83
Exhibit 31-35 Planning-Level Analysis: Equivalency Factor for Parking Activity	31-83
Exhibit 31-36 Planning-Level Analysis: Equivalency Factor for Lane Utilization	31-84
Exhibit 31-37 Planning-Level Analysis: Intersection Volume-to-Capacity Ratio Assessment Levels.....	31-90
Exhibit 31-38 Planning-Level Analysis: Progression Adjustment Factor	31-92
Exhibit 31-39 Planning-Level Analysis: Input Worksheet	31-95
Exhibit 31-40 Planning-Level Analysis: Left-Turn Treatment Worksheet.....	31-96
Exhibit 31-41 Planning Level Analysis: Intersection Sufficiency Worksheet	31-97
Exhibit 31-42 Planning-Level Analysis: Delay and LOS Worksheet	31-98
Exhibit 31-43 Control Delay Field Study Worksheet	31-101
Exhibit 31-44 Acceleration–Deceleration Correction Factor	31-103
Exhibit 31-45 Example Control Delay Field Study Worksheet.....	31-104
Exhibit 31-46 Example Worksheet with Residual Queue at End	31-105
Exhibit 31-47 Saturation Flow Rate Field Study Worksheet	31-107
Exhibit 31-48 Methodology Flowchart.....	31-111
Exhibit 31-49 Setup Module	31-112
Exhibit 31-50 Signalized Intersection Module	31-112
Exhibit 31-51 Initial Queue Delay Module	31-113
Exhibit 31-52 Performance Measures Module	31-113
Exhibit 31-53 Setup Module Routines.....	31-114
Exhibit 31-54 Signalized Intersection Module: Main Routines	31-115
Exhibit 31-55 Signalized Intersection Module: ComputeQAPolygon Routines.....	31-117
Exhibit 31-56 Performance Measures Module Routines	31-118
Exhibit 31-57 Effect of Storage Bay Length on Throughput and Delay	31-120

Exhibit 31-58 Effect of Storage Bay Length on Capacity	31-121
Exhibit 31-59 Effect of Right-Turn-on-Red and Lane Allocation on Delay	31-122
Exhibit 31-60 Effect of Right-Turn-on-Red and Right-Turn Volume on Delay	31-123
Exhibit 31-61 Effect of Right-Turn-on-Red and Right-Turn Protection on Delay	31-124
Exhibit 31-62 Closely Spaced Intersections	31-125
Exhibit 31-63 Effect of Closely Spaced Intersections on Capacity and Delay	31-126
Exhibit 31-64 Example Problems.....	31-127
Exhibit 31-65 Example Problem 1: Intersection Plan View	31-127
Exhibit 31-66 Example Problem 1: Traffic Characteristics Data	31-128
Exhibit 31-67 Example Problem 1: Geometric Design Data	31-128
Exhibit 31-68 Example Problem 1: Signal Control Data	31-128
Exhibit 31-69 Example Problem 1: Other Data.....	31-129
Exhibit 31-70 Example Problem 1: Movement Groups and Lane Groups.....	31-130
Exhibit 31-71 Example Problem 1: Movement Group Flow Rates.....	31-130
Exhibit 31-72 Example Problem 1: Lane Group Flow Rates	31-130
Exhibit 31-73 Example Problem 1: Adjusted Saturation Flow Rate.....	31-131
Exhibit 31-74 Example Problem 1: Proportion Arriving During Green.....	31-132
Exhibit 31-75 Example Problem 1: Signal Phase Duration.....	31-133
Exhibit 31-76 Example Problem 1: Capacity and Volume-to-Capacity Ratio	31-133
Exhibit 31-77 Example Problem 1: Control Delay	31-134
Exhibit 31-78 Example Problem 1: Back of Queue and Queue Storage Ratio	31-134
Exhibit 31-79 Example Problem 1: Queue Accumulation Polygon.....	31-135
Exhibit 31-80 Example Problem 2: Pedestrian Flow Rates.....	31-135
Exhibit 31-81 Example Problem 2: Vehicular Demand Flow Rates	31-136
Exhibit 31-82 Example Problem 3: Vehicular Demand Flow Rates and Cross-Section Element Widths.....	31-141

1. INTRODUCTION

Chapter 31 is the supplemental chapter for Chapter 19, Signalized Intersections, which is found in Volume 3 of the *Highway Capacity Manual* (HCM). This chapter presents detailed information about the following aspects of the Chapter 19 motorized vehicle methodology:

- Procedures are described for computing actuated phase duration and pretimed phase duration.
- Procedures are described for computing saturation flow rate adjustment factors to account for the presence of pedestrians, bicycles, and work zones.
- A procedure is described for computing uniform delay by using the queue accumulation polygon (QAP) concept. The procedure is extended to shared-lane lane groups and lane groups with permitted turn movements.
- A procedure is described for computing queue length and queue storage ratio.

This chapter provides a simplified version of the Chapter 19 motorized vehicle methodology that is suitable for planning applications. The chapter also describes techniques for measuring control delay and saturation flow rate in the field and provides details about the computational engine that implements the Chapter 19 motorized vehicle methodology. Finally, this chapter provides three example problems that demonstrate the application of the motorized vehicle, pedestrian, and bicycle methodologies to a signalized intersection.

VOLUME 4: APPLICATIONS
GUIDE

- 25. Freeway Facilities: Supplemental
- 26. Freeway and Highway Segments: Supplemental
- 27. Freeway Weaving: Supplemental
- 28. Freeway Merges and Diverges: Supplemental
- 29. Urban Street Facilities: Supplemental
- 30. Urban Street Segments: Supplemental
- 31. Signalized Intersections: Supplemental**
- 32. STOP-Controlled Intersections: Supplemental
- 33. Roundabouts: Supplemental
- 34. Interchange Ramp Terminals: Supplemental
- 35. Pedestrians and Bicycles: Supplemental
- 36. Concepts: Supplemental
- 37. ATDM: Supplemental

2. CAPACITY AND PHASE DURATION

This section describes five procedures related to the calculation of capacity and phase duration. The first procedure is used to calculate the average duration of an actuated phase, and the second is used to calculate the lane volume distribution on multilane intersection approaches. The third procedure focuses on the calculation of phase duration for pretimed intersection operation. The fourth procedure is used to compute the pedestrian and bicycle saturation flow rate adjustment factors, and the fifth computes the work zone saturation flow rate adjustment factor. Each procedure is described in a separate subsection.

ACTUATED PHASE DURATION

This subsection describes a procedure for estimating the average phase duration for an intersection that is operating with actuated control. When appropriate, the description is extended to include techniques for estimating the duration of noncoordinated and coordinated phases. Unless stated otherwise, a noncoordinated phase is modeled as an actuated phase in this methodology.

This subsection consists of the following seven parts:

- Concepts,
- Volume computations,
- Queue accumulation polygon,
- Maximum allowable headway,
- Equivalent maximum green,
- Average phase duration, and
- Probability of max-out.

The last six parts in the list above describe a series of calculations that are completed in the sequence shown to obtain estimates of average phase duration and the probability of phase termination by extension to its maximum green limit (i.e., max-out).

Concepts

The duration of an actuated phase is composed of five time periods, as shown in Equation 31-1. The first period represents the time lost while the queue reacts to the signal indication changing to green. The second interval represents the effective green time associated with queue clearance. The third period represents the time the green indication is extended by randomly arriving vehicles. It ends when there is a gap in traffic (i.e., gap-out) or a max-out. The fourth period represents the yellow change interval, and the last period represents the red clearance interval.

Equation 31-1

$$D_p = l_1 + g_s + g_e + Y + R_c$$

where

$$D_p = \text{phase duration (s),}$$

- l_1 = start-up lost time = 2.0 (s),
- Y = yellow change interval (s),
- R_c = red clearance interval (s),
- g_s = queue service time (s),
- g_e = green extension time (s).

The relationship between the variables in Equation 31-1 is shown in Exhibit 31-1 with a QAP. Key variables shown in the exhibit are defined for Equation 31-1 and in the following list:

- q_r = arrival flow rate during the effective red time = $(1 - P) q C/r$ (veh/s),
- P = proportion of vehicles arriving during the green indication (decimal),
- r = effective red time = $C - g$ (s),
- g = effective green time (s),
- s = adjusted saturation flow rate (veh/h/ln),
- q_g = arrival flow rate during the effective green time = $P q C/g$ (veh/s),
- q = arrival flow rate (veh/s),
- Q_r = queue size at the end of the effective red time = $q_r r$ (veh),
- l_2 = clearance lost time = $Y + R_c - e$ (s), and
- e = extension of effective green = 2.0 (s).

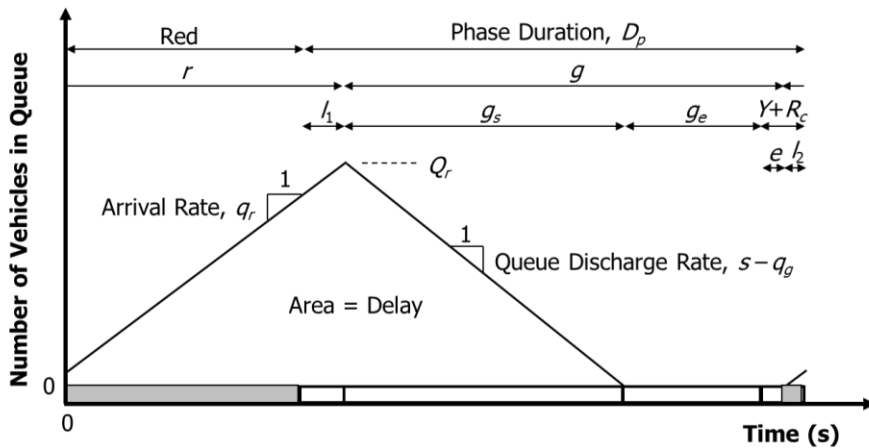


Exhibit 31-1
Time Elements Influencing
Actuated Phase Duration

Exhibit 31-1 shows the relationship between phase duration and queue size for the average signal cycle. During the red interval, vehicles arrive at a rate of q_r and form a queue. The queue reaches its maximum size l_1 seconds after the green interval starts. At this time, the queue begins to discharge at a rate equal to the saturation flow rate s less the arrival rate during green q_g . The queue clears g_s seconds after it first begins to discharge. Thereafter, random vehicle arrivals are detected and cause the green interval to be extended. Eventually, a gap occurs in traffic (or the maximum green limit is reached), and the green interval ends. The end of the green interval coincides with the end of the extension time g_e .

Equation 31-2

The effective green time for the phase is computed with Equation 31-2.

$$\begin{aligned} g &= D_p - l_1 - l_2 \\ &= g_s + g_e + e \end{aligned}$$

where all variables are as previously defined.

Coordinated Phase Duration

The duration of a coordinated phase is dictated by the cycle length and the force-off settings for the noncoordinated phases. These settings define the points in the signal cycle at which each noncoordinated phase must end. The force-off settings are used to ensure the coordinated phases receive a green indication at a specific time in the cycle. Presumably, this time is synchronized with the coordinated phase time at the adjacent intersections so that traffic progresses along the street segment. In general, the duration of a coordinated phase is equal to the cycle length less the time allocated to the conflicting phase in the same ring and less the time allocated to the minor-street phases. Detectors are not typically assigned to the coordinated phase, and this phase is not typically extended by the vehicles it serves.

Noncoordinated Phase Duration

The duration of a noncoordinated phase is dictated by traffic demand in much the same manner as for an actuated phase. However, the noncoordinated phase duration is typically constrained by its force-off setting (rather than a maximum green setting). A noncoordinated phase is referred to here and modeled as an *actuated* phase.

Right-Turn Overlap Duration

If a right-turn lane group is operated in a protected or protected-permitted mode, then the protected indication is assumed to be provided as a right-turn overlap with the complementary left-turn phase on the intersecting roadway. In this manner, the right-turn protected interval duration is dictated by the duration of the complementary left-turn phase (which is determined by the left-turn phase settings, left-turn detection, and left-turn volume). The procedures described in this subsection are used to determine the average duration of the complementary left-turn lane phase (and thus the protected right-turn interval duration).

The right-turn permitted interval duration is dictated by the phase settings, detection, and volume associated with the right-turn movement and its adjacent through movement. The procedures described in this subsection are used to determine the average duration of the phase serving the right-turn movement in a permitted manner.

Volume Computations

This subsection describes the calculations needed to quantify the time rate of calls submitted to the controller by the detectors. Two call rates are computed for each signal phase. The first rate represents the flow rate of calls for green extension that arrive during the green interval. The second call rate represents the flow rate of calls for phase activation that arrive during the red indication.

A. Call Rate to Extend Green

The call rate to extend the green indication for a given phase is based on the flow rate of the lane groups served by the phase. The call rate is represented in the analysis by the flow rate parameter. This parameter represents an adjusted flow rate that accounts for the tendency of drivers to form “bunches” (i.e., randomly formed platoons). The flow rate parameter for the phase is computed as shown by Equation 31-3 with Equation 31-4 and Equation 31-5.

$$\lambda^* = \sum_{i=1}^m \lambda_i$$

Equation 31-3

with

$$\lambda_i = \frac{\phi_i q_i}{1 - \Delta_i q_i}$$

Equation 31-4

$$\phi_i = e^{-b_i \Delta_i q_i}$$

Equation 31-5

where

- λ^* = flow rate parameter for the phase (veh/s);
- λ_i = flow rate parameter for lane group i ($i = 1, 2, \dots, m$) (veh/s);
- ϕ_i = proportion of free (unbunched) vehicles in lane group i (decimal);
- q_i = arrival flow rate for lane group $i = v_i/3,600$ (veh/s);
- v_i = demand flow rate for lane group i (veh/h);
- Δ_i = headway of bunched vehicle stream in lane group i ; = 1.5 s for single-lane lane group, 0.5 s otherwise (s/veh);
- m = number of lane groups served during the phase; and
- b_i = bunching factor for lane group i (0.6, 0.5, and 0.8 for lane groups with 1, 2, and 3 or more lanes, respectively).

Using Equation 31-6, Equation 31-7, and Equation 31-8, it is also useful to compute the following three variables for each phase. These variables are used in a later step to compute green extension time.

$$\phi^* = e^{-\sum_{i=1}^m b_i \Delta_i q_i}$$

Equation 31-6

$$\Delta^* = \frac{\sum_{i=1}^m \lambda_i \Delta_i}{\lambda^*}$$

Equation 31-7

$$q^* = \sum_{i=1}^m q_i$$

Equation 31-8

where

- ϕ^* = combined proportion of free (unbunched) vehicles for the phase (decimal),
- Δ^* = equivalent headway of bunched vehicle stream served by the phase (s/veh), and
- q^* = arrival flow rate for the phase (veh/s), and

all other variables are as previously defined.

The call rate for green extension for a phase that does not end at a barrier is equal to the flow rate parameter λ^* . If two phases terminate at a common barrier (i.e., one phase in each ring) and simultaneous gap-out is enabled, then the call rate for either phase is based on the combined set of lane groups being served by the two phases. To model this behavior, the lane group parameters for each phase are combined to estimate the call rate for green extension. Specifically, the variable m in the preceding six equations is modified to represent the combined number of lane groups served by both phases.

The following rules are evaluated to determine the number of lane groups served m if simultaneous gap-out is enabled. They are described for the case in which Phases 2, 6, 4, and 8 end at the barrier (as shown in Exhibit 19-2). The rules should be modified if other phase pairs end at the barrier.

1. If Phases 2 and 6 have simultaneous gap-out enabled, then the lane groups associated with Phase 2 are combined with the lane groups associated with Phase 6 in applying Equation 31-3 through Equation 31-8 for Phase 6. Similarly, the lane groups associated with Phase 6 are combined with the lane groups associated with Phase 2 in applying these equations for Phase 2.
2. If Phases 4 and 8 have simultaneous gap-out enabled, then the lane groups associated with Phase 4 are combined with the lane groups associated with Phase 8 in evaluating Phase 8. Similarly, the lane groups associated with Phase 8 are combined with the lane groups associated with Phase 4 in evaluating Phase 4.

B. Call Rate to Activate a Phase

The call rate to activate a phase is used to determine the probability that the phase is activated in the forthcoming cycle sequence. This rate is based on the arrival flow rate of the traffic movements served by the phase and whether the phase is associated with dual entry. Vehicles or pedestrians can call a phase, so a separate call rate is computed for each traffic movement.

i. Determine Phase Vehicular Flow Rate. The vehicular flow rate associated with a phase depends on the type of movements it serves as well as the approach lane allocation. The following rules apply in determining the phase vehicular flow rate:

1. If the phase exclusively serves a left-turn movement, then the phase vehicular flow rate is equal to the left-turn movement flow rate.
2. If the phase serves a through or right-turn movement and there is no exclusive left-turn phase for the adjacent left-turn movement, then the phase vehicular flow rate equals the approach flow rate.
3. If the phase serves a through or right-turn movement and there is an exclusive left-turn phase for the adjacent left-turn movement, then
 - a. If there is a left-turn bay, then the phase vehicular flow rate equals the sum of the through and right-turn movement flow rates.
 - b. If there is no left-turn bay, then the phase vehicular flow rate equals the approach flow rate.

- c. If split phasing is used, then the phase vehicular flow rate equals the approach flow rate.

ii. *Determine Activating Vehicular Call Rate.* The activating vehicular call rate q_v^* is equal to the phase vehicular flow rate divided by 3,600 to convert it to units of vehicles per second. If dual entry is activated for a phase, then the activation call rate must be modified by adding its original rate to that of both concurrent phases. For example, if Phase 2 is set for dual entry, then the modified Phase 2 activation call rate equals the original Phase 2 activation call rate plus the activation rate of Phase 5 and the activation rate of Phase 6. In this manner, Phase 2 is activated when demand is present for Phase 2, 5, or 6.

iii. *Determine Activating Pedestrian Call Rate.* The activating pedestrian call rate q_p^* is equal to the pedestrian flow rate associated with the subject approach divided by 3,600 to convert it to units of pedestrians per second. If dual entry is activated for a phase, then the activation call rate must be modified by adding its original rate to that of the opposing through phase. For example, if Phase 2 is set for dual entry, then the modified Phase 2 activation call rate equals the original Phase 2 activation call rate plus the activation rate of Phase 6. In this manner, Phase 2 is activated when pedestrian demand is present for Phase 2 or 6.

Queue Accumulation Polygon

This subsection summarizes the procedure used to construct the QAP associated with a lane group. This polygon defines the queue size for a traffic movement as a function of time during the cycle. The procedure is described more fully in Section 3; it is discussed here to illustrate its use in calculating queue service time.

For polygon construction, all flow rate variables are converted to common units of vehicles per second per lane. The presentation in this subsection is based on these units for q and s . If the flow rate q exceeds the lane capacity, then it is set to equal this capacity.

A polygon is shown in Exhibit 31-1 for a through movement in an exclusive lane. At the start of the effective red, vehicles arrive at a rate of q_r and accumulate to a length of Q_r vehicles at the time the effective green begins. Thereafter, the queue begins to discharge at a rate of $s - q_g$ until it clears after g_s seconds. The queue service time g_s represents the time required to serve the queue present at the end of effective red Q_r , plus any additional arrivals that join the queue before it fully clears. Queue service time is computed as $Q_r / (s - q_g)$. Substituting the variable relationships in the previous variable list into this equation yields Equation 31-9 for estimating queue service time.

$$g_s = \frac{q C (1 - P)}{\frac{s}{3,600} - q C (P/g)}$$

Equation 31-9

where P is the proportion of vehicles arriving during the green indication (decimal), s is the adjusted saturation flow rate (veh/h/ln), and all other variables are as previously defined.

The polygon in Exhibit 31-1 applies to some types of lane groups. Other polygon shapes are possible. A detailed procedure for constructing polygons is described in Section 3.

Maximum Allowable Headway

This subsection describes a procedure for calculating the maximum allowable headway (MAH) for the detection associated with a phase. It consists of two steps. Step A computes MAH for each lane group served by the subject phase. Step B combines MAH into an equivalent MAH for the phase. The latter step is used when a phase serves two or more lane groups or when simultaneous gap-out is enabled.

The procedure addresses the situation in which there is one zone of detection per lane. This type of detection is referred to here as *stop-line detection* because the detection zone is typically located at the stop line. However, some agencies prefer to locate the detection zone at a specified distance upstream from the stop line. This procedure can be used to evaluate any single-detector-per-lane design, provided the detector is located so that only the subject traffic movement travels over this detector during normal operation.

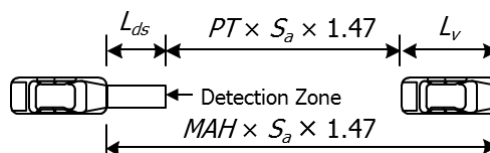
The detector length and detection mode input data are specified by movement group. When these data describe a through movement group, it is reasonable to assume they also describe the detection in any shared-lane lane groups that serve the through movement. This assumption allows the movement group inputs to describe the associated lane group values, and the analysis can proceed on a lane-group basis. However, if this assumption is not valid or if information about the detection design for each lane is known, then the procedure can be extended to the calculation of MAH for each lane. The lane-specific MAHs would then be combined for the phase that serves these lanes.

Concepts

MAH represents the maximum time that can elapse between successive calls for service without terminating the phase by gap-out. It is useful for describing the detection design and signal settings associated with a phase. MAH depends on the number of detectors serving the lane group, the length of these detectors, and the average vehicle speed in the lane group.

The relationship between passage time PT , detection zone length L_{ds} , vehicle length L_v , average speed S_a , and MAH is shown in Exhibit 31-2. The two vehicles shown are traveling from left to right and have a headway equal to MAH so that the second vehicle arrives at the detector the instant the passage time is set to time out.

Exhibit 31-2
Detection Design and
Maximum Allowable Headway



According to Exhibit 31-2, Equation 31-10 with Equation 31-11 can be derived for estimating MAH for stop-line detection operating in the presence mode.

$$MAH = PT + \frac{L_{ds} + L_v}{1.47 S_a}$$

Equation 31-10

with

$$L_v = L_{pc}(1 - 0.01 P_{HV}) + 0.01 L_{HV}P_{HV} - D_{sv}$$

Equation 31-11

where

MAH = maximum allowable headway (s/veh),

PT = passage time setting (s),

L_{ds} = length of the stop-line detection zone (ft),

L_v = detected length of the vehicle (ft),

S_a = average speed on the intersection approach (mi/h),

L_{pc} = stored passenger car lane length = 25 (ft),

P_{HV} = percentage heavy vehicles in the corresponding movement group (%),

L_{HV} = stored heavy-vehicle lane length = 45 (ft), and

D_{sv} = distance between stored vehicles = 8 (ft).

The average speed on the intersection approach can be estimated with Equation 31-12.

$$S_a = 0.90 (25.6 + 0.47 S_{pl})$$

Equation 31-12

where S_{pl} is the posted speed limit (mi/h).

Equation 31-10 is derived for the typical case in which the detection unit is operating in the presence mode. If it is operating in the pulse mode, then MAH equals the passage time setting PT .

A. Determine Maximum Allowable Headway

Equation 31-10 has been modified to adapt it to various combinations of lane use and left-turn operation. A family of equations is presented in this step. The appropriate equation is selected for the subject lane group and then used to compute the corresponding MAH.

The equations presented in this step are derived for the typical case in which the detection unit is operating in the presence mode. If a detector is operating in the pulse mode, then MAH equals the passage time setting PT .

MAH for lane groups serving through vehicles is calculated with Equation 31-13.

$$MAH_{th} = PT_{th} + \frac{L_{ds,th} + L_v}{1.47 S_a}$$

Equation 31-13

where

MAH_{th} = maximum allowable headway for through vehicles (s/veh),

PT_{th} = passage time setting for phase serving through vehicles (s),

$L_{ds,th}$ = length of the stop-line detection zone in the through lanes (ft), and

S_a = average speed on the intersection approach (mi/h).

MAH for a left-turn movement served in exclusive lanes with the protected mode (or protected-permitted mode) is based on Equation 31-13, but the equation is adjusted as shown in Equation 31-14 to account for the slower speed of the left-turn movement.

Equation 31-14

$$MAH_{lt,e,p} = PT_{lt} + \frac{L_{ds,lt} + L_v}{1.47 S_a} + \frac{E_L - 1}{s_o/3,600}$$

where

$MAH_{lt,e,p}$ = maximum allowable headway for protected left-turning vehicles in exclusive lane (s/veh),

PT_{lt} = passage time setting for phase serving the left-turning vehicles (s),

$L_{ds,lt}$ = length of the stop-line detection zone in the left-turn lanes (ft),

E_L = equivalent number of through cars for a protected left-turning vehicle = 1.05, and

s_o = base saturation flow rate (pc/h/ln).

MAH for left-turning vehicles served in a shared lane with the protected-permitted mode is calculated as shown in Equation 31-15.

Equation 31-15

$$MAH_{lt,s,p} = MAH_{th} + \frac{E_L - 1}{s_o/3,600}$$

where $MAH_{lt,s,p}$ is the maximum allowable headway for protected left-turning vehicles in a shared lane (s/veh).

MAH for left-turning vehicles served in an exclusive lane with the permitted mode is adjusted to account for the longer headway of the turning vehicle. In this case, the longer headway includes the time spent waiting for an acceptable gap in the opposing traffic stream. Equation 31-16 addresses these adjustments.

Equation 31-16

$$MAH_{lt,e} = PT_{th} + \frac{L_{ds,lt} + L_v}{1.47 S_a} + \frac{3,600}{s_l} - t_{fh}$$

where

$MAH_{lt,e}$ = maximum allowable headway for permitted left-turning vehicles in exclusive lane (s/veh),

s_l = saturation flow rate in exclusive left-turn lane group with permitted operation (veh/h/ln), and

t_{fh} = follow-up headway = 2.5 (s).

MAH for right-turning vehicles served in an exclusive lane with the protected mode is computed with Equation 31-17.

Equation 31-17

$$MAH_{rt,e,p} = PT_{rt} + \frac{L_{ds,rt} + L_v}{1.47 S_a} + \frac{E_R - 1}{s_o/3,600}$$

where

$MAH_{rt,e,p}$ = maximum allowable headway for protected right-turning vehicles in exclusive lane (s/veh),

PT_{rt} = passage time setting for phase serving right-turning vehicles (s),

E_R = equivalent number of through cars for a protected right-turning vehicle = 1.18, and

$L_{ds,rt}$ = length of the stop-line detection zone in the right-turn lanes (ft).

If the variable E_R in Equation 31-17 is divided by the pedestrian-bicycle saturation flow rate adjustment factor f_{Rpb} and PT_{th} is substituted for PT_{rt} , then the equation can be used to estimate $MAH_{rt,e}$ for permitted right-turning vehicles in an exclusive lane.

Equation 31-18 and Equation 31-19, respectively, are used to estimate MAH for left- and right-turning vehicles that are served in a shared lane with the permitted mode.

$$MAH_{lt,s} = MAH_{th} + \frac{3,600}{s_l} - t_{fh}$$

Equation 31-18

$$MAH_{rt,s} = MAH_{th} + \frac{(E_R/f_{Rpb}) - 1}{s_o/3,600}$$

Equation 31-19

where $MAH_{lt,s}$ is the maximum allowable headway for permitted left-turning vehicles in a shared lane (s/veh), and $MAH_{rt,s}$ is the maximum allowable headway for permitted right-turning vehicles in a shared lane (s/veh).

B. Determine Equivalent Maximum Allowable Headway

The equivalent MAH (i.e., MAH^*) is calculated for cases in which more than one lane group is served by a phase. It is also calculated for phases that end at a barrier and that are specified in the controller as needing to gap out at the same time as a phase in the other ring. The following rules are used to compute the equivalent MAH:

1. If simultaneous gap-out is not enabled, or the phase does not end at the barrier, then
 - a. If the phase serves only one movement, then MAH^* for the phase equals the MAH computed for the corresponding lane group.
 - b. This rule subset applies when the phase serves all movements and there is no exclusive left-turn phase for the approach (i.e., it operates with the permitted mode). The equations shown apply to the most general case in which a left-turn, through, and right-turn movement exist and a through lane group exists. If any of these movements or lane groups do not exist, then their corresponding flow rate parameter equals 0.0 veh/s.
 - i. If there is no left-turn lane group or right-turn lane group (i.e., shared lanes), then MAH^* for the phase is computed from Equation 31-20.

Equation 31-20

$$MAH^* = \frac{P_L \lambda_{sl} MAH_{lt,s} + [(1 - P_L) \lambda_{sl} + \lambda_t + (1 - P_R) \lambda_{sr}] MAH_{th} + P_R \lambda_{sr} MAH_{rt,s}}{\lambda_{sl} + \lambda_t + \lambda_{sr}}$$

where

λ_{sl} = flow rate parameter for shared left-turn and through lane group (veh/s),

λ_t = flow rate parameter for exclusive through lane group (veh/s),

λ_{sr} = flow rate parameter for shared right-turn and through lane group (veh/s),

P_L = proportion of left-turning vehicles in the shared lane (decimal), and

P_R = proportion of right-turning vehicles in the shared lane (decimal).

- ii. If there is a right-turn lane group but no left-turn lane group, then Equation 31-21 is applicable.

Equation 31-21

$$MAH^* = \frac{P_L \lambda_{sl} MAH_{lt,s} + [(1 - P_L) \lambda_{sl} + \lambda_t] MAH_{th} + \lambda_r MAH_{rt,e}}{\lambda_{sl} + \lambda_t + \lambda_r}$$

where λ_r is the flow rate parameter for the exclusive right-turn lane group (veh/s).

- iii. If there is a left-turn lane group but no right-turn lane group, then MAH^* for the phase is computed with Equation 31-22.

Equation 31-22

$$MAH^* = \frac{\lambda_l MAH_{lt,e} + [\lambda_t + (1 - P_R) \lambda_{sr}] MAH_{th} + P_R \lambda_{sr} MAH_{rt,s}}{\lambda_l + \lambda_t + \lambda_{sr}}$$

where λ_l is the flow rate parameter for the exclusive left-turn lane group (veh/s).

- iv. If there is a left-turn lane group and a right-turn lane group, then MAH^* for the phase is computed with Equation 31-23.

Equation 31-23

$$MAH^* = \frac{\lambda_l MAH_{lt,e} + \lambda_t MAH_{th} + \lambda_r MAH_{rt,e}}{\lambda_l + \lambda_t + \lambda_r}$$

- c. If the phase serves only a through lane group, right-turn lane group, or both, then

- i. If there is a right-turn lane group and a through lane group, then MAH^* for the phase is computed with Equation 31-24.

Equation 31-24

$$MAH^* = \frac{\lambda_t MAH_{th} + \lambda_r MAH_{rt,e}}{\lambda_t + \lambda_r}$$

- ii. If there is a shared right-turn and through lane group, then MAH^* for the phase is computed with Equation 31-25.

Equation 31-25

$$MAH^* = \frac{[\lambda_t + (1 - P_R) \lambda_{sr}] MAH_{th} + P_R \lambda_{sr} MAH_{rt,s}}{\lambda_t + \lambda_{sr}}$$

- d. If the phase serves all approach movements using split phasing, then

- i. If there is one lane group (i.e., a shared lane), then MAH^* for the phase equals the MAH computed for the lane group.

- ii. If there is more than one lane group, then MAH^* is computed with the equations in previous Rule 1.b, but $MAH_{lt,e,p}$ is substituted for $MAH_{lt,e}$, and $MAH_{lt,s,p}$ is substituted for $MAH_{lt,s}$.
 - e. If the phase has protected-permitted operation with a shared left-turn and through lane, then the equations in previous Rule 1.b (i.e., 1.b.i and 1.b.ii) apply. The detection for this operation does not influence the duration of the left-turn phase. The left-turn phase will be set to minimum recall and will extend to its minimum value before terminating.
2. If simultaneous gap-out is enabled and the phase ends at the barrier, then MAH^* for the phase is computed with Equation 31-26, where the summations shown are for all lane groups served by the subject (or concurrent) phase.

$$MAH^* = \frac{MAH \sum \lambda_i + MAH_c \sum \lambda_{c,i}}{\sum \lambda_i + \sum \lambda_{c,i}}$$

Equation 31-26

where

MAH^* = equivalent maximum allowable headway for the phase (s/veh),

MAH_c = maximum allowable headway for the concurrent phase that also ends at the barrier (s/veh), and

$\lambda_{c,i}$ = flow rate parameter for lane group i served in the concurrent phase that also ends at the barrier (veh/s).

When there is split phasing, there are no concurrent phases, and Equation 31-26 does not apply.

Equivalent Maximum Green

In coordinated-actuated operation, the force-off points are used to constrain the duration of the noncoordinated phases. Although the maximum green setting is also available to provide additional constraint, it is not commonly used. In fact, the default mode in most modern controllers is to inhibit the maximum green timer when the controller is used in a coordinated signal system.

The relationship between the force-off points, yield point, and phase splits is shown in Exhibit 31-3. The yield point is associated with the coordinated phases (i.e., Phases 2 and 6). It coincides with the start of the yellow change interval. If a call for service by one of the noncoordinated phases arrives after the yield point is reached, then the coordinated phases begin the termination process by presenting the yellow indication. Calls that arrive before the yield point are not served until the yield point is reached.

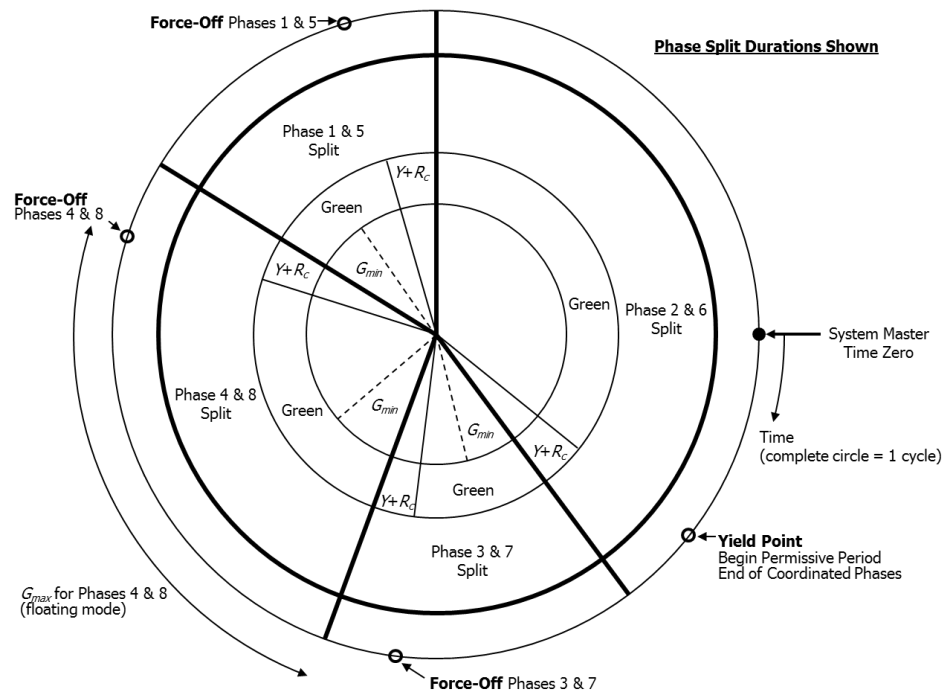
The force-off and yield points for common phase pairs are shown in Exhibit 31-3 to occur at the same time. This approach is shown for convenience of illustration. In practice, the two phases may have different force-off or yield points.

A permissive period typically follows the yield point. If a conflicting call arrives during the permissive period, then the phase termination process begins immediately, and all phases associated with conflicting calls are served in sequence. Permissive periods are typically long enough to ensure that all calls for

service are met during the signal cycle. This methodology does not explicitly model permissive periods. It is assumed the permissive period begins at the yield point and is sufficiently long that all conflicting calls are served in sequence each cycle.

One force-off point is associated with each of Phases 1, 3, 4, 5, 7, and 8. If a phase is extended to its force-off point, the phase begins the termination process by presenting the yellow indication (phases that terminate at a barrier must be in agreement to terminate before the yellow indication will be presented). Modern controllers compute the force-off points and yield point by using the entered phase splits and change periods. These computations are based on the relationships shown in Exhibit 31-3.

Exhibit 31-3
Force-Off Points, Yield Point,
and Phase Splits



The concept of equivalent maximum green is useful for modeling noncoordinated phase operation. This maximum green replicates the effect of a force-off or yield point on phase duration. The procedure described in this subsection is used to compute the equivalent maximum green for coordinated-actuated operation. Separate procedures are described for the fixed force mode and the floating force mode.

A. Determine Equivalent Maximum Green for Floating Force Mode

This step is applicable if the controller is set to operate in the floating force mode. With this mode, each noncoordinated phase has its force-off point set at the split time after the phase first becomes active. The force-off point for a phase is established when the phase is first activated. Thus, the force-off point “floats,” or changes, each time the phase is activated. This operation allows unused split time to revert to the coordinated phase via an early return to green. The equivalent maximum green for this mode is computed as being equal to the

phase split less the change period. This relationship is shown in Exhibit 31-3 for Phases 4 and 8.

B. Determine Equivalent Maximum Green for Fixed Force Mode

This step is applicable if the controller is set to operate in the fixed force mode. With this mode, each noncoordinated phase has its force-off point set at a fixed time in the cycle relative to time zero on the system master. The force-off points are established whenever a new timing plan is selected (e.g., by time of day) and remains “fixed” until a new plan is selected. This operation allows unused split time to revert to the following phase.

The equivalent maximum green for this mode is computed for each phase by first establishing the fixed force-off points (as shown in Exhibit 31-3) and then computing the average duration of each noncoordinated phase. The calculation process is iterative. For the first iteration, the equivalent maximum green is set equal to the phase split less the change period. Thereafter, the equivalent maximum green for a specific phase is computed as the difference between its force-off point and the sum of the previous phase durations, starting with the first noncoordinated phase. Equation 31-27 illustrates this computation for Phase 4, using the ring structure shown in Exhibit 19-2. A similar calculation is performed for the other phases.

$$G_{max,4} = FO_4 - (YP_2 + CP_2 + G_3 + CP_3)$$

Equation 31-27

where

$G_{max,4}$ = equivalent maximum green for Phase 4 (s),

FO_4 = force-off point for Phase 4 (s),

YP_2 = yield point for Phase 2 (s),

G_3 = green interval duration for Phase 3 (s), and

CP_3 = change period (yellow change interval plus red clearance interval) for Phase 3 (s).

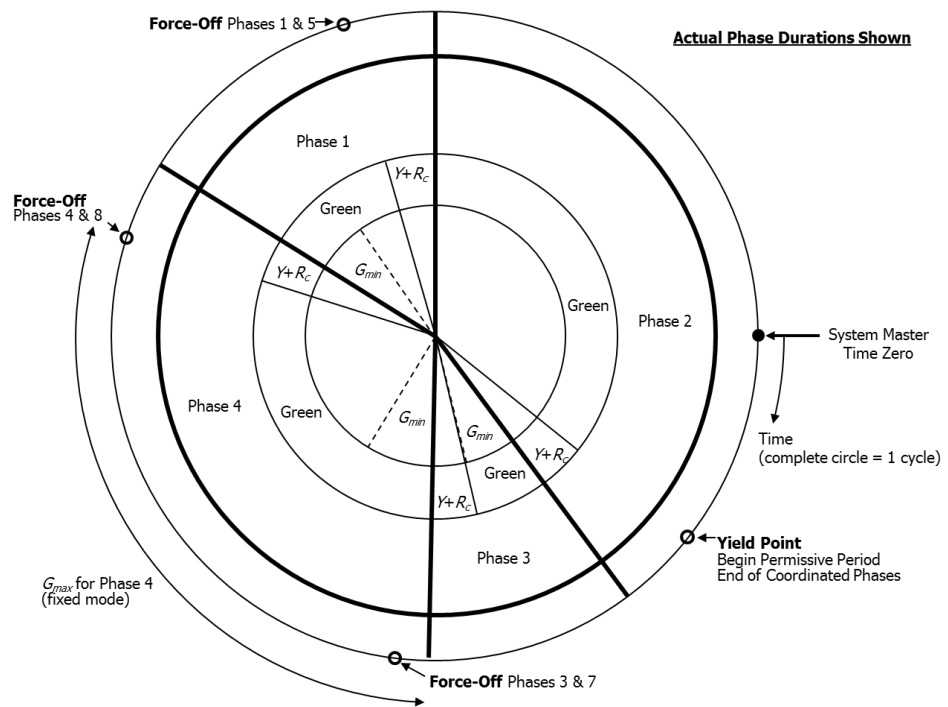
The maximum green obtained from Equation 31-27 is shown in Exhibit 31-4 for the ring that serves Phases 1, 2, 3, and 4. Unlike Exhibit 31-3, Exhibit 31-4 illustrates the *actual* average phase durations for a given cycle. In this example, Phase 3 timed to its minimum green and terminated. It never reached its force-off point. The unused time from Phase 3 was made available to Phase 4, which resulted in a larger maximum green than was obtained with the floating mode (see Exhibit 31-3). If every noncoordinated phase extends to its force-off point, then the maximum green from the fixed force mode equals that obtained from the floating force mode.

Average Phase Duration

This subsection describes the sequence of calculations needed to estimate the average duration of a phase. In fact, the process requires the combined calculation of the duration of all phases together because of the constraints imposed by the controller ring structure and associated barriers.

The calculation process is iterative because several intermediate equations require knowledge of the green interval duration. Specifically, the green interval duration is required in calculating lane group flow rate, queue service time, permitted green time, left-turn volume served during the permitted portion of a protected-permitted mode, and equivalent maximum green. To overcome this circular dependency, the green interval for each phase is initially estimated, and then the procedure is implemented by using this estimate. When completed, the procedure provides a new initial estimate of the green interval duration. The calculations are repeated until the initial estimate and computed green interval duration are effectively equal.

Exhibit 31-4
Example Equivalent Maximum Green for Fixed Force Mode



The calculation steps that constitute the procedure are described in the following paragraphs.

A. Compute Effective Change Period

The change period is computed for each phase. It is equal to the sum of the yellow change interval and the red clearance interval (i.e., $Y + R_c$). For phases that end at a barrier, the longer change period of the two phases that terminate at a barrier is used to define the effective change period for both phases.

B. Estimate Green Interval

An initial estimate of the green interval duration is provided for each phase. For the first iteration with fully actuated control, the initial estimate is equal to the maximum green setting. For the first iteration with coordinated-actuated control, the initial estimate is equal to the input phase split less the change period.

C. Compute Equivalent Maximum Green (Coordinated-Actuated)

If the controller is operating as coordinated-actuated, then the equivalent maximum green is computed for each phase. It is based on the estimated green interval duration, phase splits, and change periods. The previous subsection titled Equivalent Maximum Green describes how to compute this value.

D. Construct Queue Accumulation Polygon

The QAP is constructed for each lane group and corresponding phase by using the known flow rates and signal timing. The procedure for constructing this polygon is summarized in the previous subsection titled Queue Accumulation Polygon. It is described in more detail in Section 3.

E. Compute Queue Service Time

The queue service time g_s is computed for each QAP constructed in the previous step. For through movements or left-turn movements served during a left-turn phase, the polygon in Exhibit 31-1 applies and Equation 31-9 can be used. The procedure described in Section 3 is applicable to more complicated polygon shapes.

F. Compute Call Rate to Extend Green

The extending call rate is represented as the flow rate parameter λ . This parameter is computed for each lane group served by an actuated phase and is then aggregated to a phase-specific value. The procedure for computing this parameter is described in the previous subsection titled Volume Computations.

G. Compute Equivalent Maximum Allowable Headway

The equivalent maximum allowable headway MAH^* is computed for each actuated phase. The procedure for computing MAH^* is described in the previous subsection titled Maximum Allowable Headway.

H. Compute Number of Extensions Before Max-Out

The average number of extensions before the phase terminates by max-out is computed for each actuated phase with Equation 31-28.

$$n = q^* [G_{max} - (g_s + l_1)] \geq 0.0$$

Equation 31-28

where n is the number of extensions before the green interval reaches its maximum limit, G_{max} is the maximum green setting (s), and all other variables are as previously defined.

I. Compute Probability of Green Extension

The probability of the green interval being extended by randomly arriving vehicles is computed for each actuated phase with Equation 31-29.

$$p = 1 - \varphi^* e^{-\lambda^* (MAH^* - \Delta^*)}$$

Equation 31-29

where p is the probability of a call headway being less than the maximum allowable headway.

J. Compute Green Extension Time

The average green extension time is computed for each actuated phase with Equation 31-30.

Equation 31-30

$$g_e = \frac{p^2(1 - p^n)}{q^*(1 - p)}$$

K. Compute Activating Call Rate

The call rate to activate a phase is computed for each actuated phase. A separate rate is computed for vehicular traffic and for pedestrian traffic. The rate for each travel mode is based on its flow rate and the use of dual entry. The procedure for computing this rate is described in the previous subsection titled Volume Computations.

L. Compute Probability of Phase Call

The probability that an actuated phase is called depends on whether it is set on recall in the controller. If it is on recall, then the probability that the phase is called equals 1.0. If the phase is not on recall, then the probability that it is called can be estimated by using Equation 31-31 with Equation 31-32 and Equation 31-33.

Equation 31-31

$$p_c = p_v(1 - p_p) + p_p(1 - p_v) + p_v p_p$$

with

Equation 31-32

$$p_v = 1 - e^{-q_v^* C}$$

Equation 31-33

$$p_p = 1 - e^{-q_p^* P_p C}$$

where

p_c = probability that the subject phase is called,

p_v = probability that the subject phase is called by a vehicle detection,

p_p = probability that the subject phase is called by a pedestrian detection,

q_v^* = activating vehicular call rate for the phase (veh/s),

q_p^* = activating pedestrian call rate for the phase (p/s), and

P_p = probability of a pedestrian pressing the detector button = 0.51.

The probability of a pedestrian pressing the detector button reflects the tendency of some pedestrians to decline from using the detector button before crossing a street. Research indicates about 51% of all crossing pedestrians will push the button to place a call for pedestrian service (1).

M. Compute Unbalanced Green Duration

The unbalanced average green interval duration is computed for each actuated phase by using Equation 31-34 with Equation 31-35 and Equation 31-36.

Equation 31-34

$$G_u = G_{|veh,call} p_v(1 - p_p) + G_{|ped,call} p_p(1 - p_v) + \max(G_{|veh,call}, G_{|ped,call}) p_v p_p \leq G_{max}$$

with

Equation 31-35

$$G_{|veh,call} = \max(l_1 + g_s + g_e, G_{min})$$

$$G_{|ped,call} = Walk + PC$$

Equation 31-36

where

G_u = unbalanced green interval duration for a phase (s),

$G_{|veh,call}$ = average green interval given that the phase is called by a vehicle detection (s),

G_{min} = minimum green setting (s),

$G_{|ped,call}$ = average green interval given that the phase is called by a pedestrian detection (s),

Walk = pedestrian walk setting (s), and

PC = pedestrian clear setting (s).

If maximum recall is set for the phase, then G_u is equal to G_{max} . If the phase serves a left-turn movement that operates in the protected mode, then the probability that it is called by pedestrian detection p_p is equal to 0.0.

If the phase serves a left-turn movement that operates in the protected-permitted mode and the left-turn movement shares a lane with through vehicles, then the green interval duration is equal to the phase's minimum green setting.

The green interval duration obtained from this step is "unbalanced" because it does not reflect the constraints imposed by the controller ring structure and associated barriers. These constraints are imposed in Step O or Step P, depending on the type of control used at the intersection.

It is assumed the rest-in-walk mode is not enabled.

N. Compute Unbalanced Phase Duration

The unbalanced average phase duration is computed for each actuated phase by adding the unbalanced green interval duration and the corresponding change period components. This calculation is completed with Equation 31-37.

$$D_{up} = G_u + Y + R_c$$

Equation 31-37

where D_{up} is the unbalanced phase duration (s).

If simultaneous gap-out is enabled, the phase ends at a barrier, and the subject phase experiences green extension when the concurrent phase has reached its maximum green limit, then both phases are extended, but only due to the call flow rate of the subject phase. Hence, the green extension time computed in Step J is too long. The effect is accounted for in the current step by multiplying the green extension time from Step J by a "flow rate ratio." This ratio represents the sum of the flow rate parameter for each lane group served by the subject phase divided by the sum of the flow rate parameter for each group served by the subject phase and served by the concurrent phase (the latter sum equals the call rate from Step F).

O. Compute Average Phase Duration—Fully Actuated Control

For this discussion, it is assumed Phases 2 and 6 are serving Movements 2 and 6, respectively, on the major street (see Exhibit 19-2). If the left-turn

movements on the major street operate in the protected mode or the protected-permitted mode, then Movements 1 and 5 are served during Phases 1 and 5, respectively. Similarly, Phases 4 and 8 are serving Movements 4 and 8, respectively, on the minor street. If the left-turn movements on the minor street are protected or protected-permitted, then Phases 3 and 7 are serving Movements 3 and 7, respectively. If a through movement phase occurs first in a phase pair, then the other phase (i.e., the one serving the opposing left-turn movement) is a lagging left-turn phase.

The following rules are used to estimate the average duration of each phase:

1. Given two phases that occur in sequence between barriers (i.e., phase a followed by phase b), the duration of $D_{p,a}$ is equal to the unbalanced phase duration of the first phase to occur (i.e., $D_{p,a} = D_{up,a}$). The duration of $D_{p,b}$ is based on Equation 31-38 for the major-street phases.

Equation 31-38

$$D_{p,b} = \max(D_{up,1} + D_{up,2}, D_{up,5} + D_{up,6}) - D_{p,a}$$

where

- $D_{p,b}$ = phase duration for phase b , which occurs just after phase a (s);
- $D_{p,a}$ = phase duration for phase a , which occurs just before phase b (s); and
- $D_{up,i}$ = unbalanced phase duration for phase i ; $i = 1, 2, 5,$ and 6 for major street, and $i = 3, 4, 7,$ and 8 for minor street (s).

Equation 31-39 applies for the minor-street phases.

Equation 31-39

$$D_{p,b} = \max(D_{up,3} + D_{up,4}, D_{up,7} + D_{up,8}) - D_{p,a}$$

For example, if the phase pair consists of Phase 3 followed by Phase 4 (i.e., a leading left-turn arrangement), then $D_{p,3}$ is set to equal $D_{up,3}$ and $D_{p,4}$ is computed from Equation 31-39. In contrast, if the pair consists of Phase 8 followed by Phase 7 (i.e., a lagging left-turn arrangement), then $D_{p,8}$ is set to equal $D_{up,8}$ and $D_{p,7}$ is computed from Equation 31-39.

2. If an approach is served with one phase operating in the permitted mode (but not split phasing), then $D_{p,a}$ equals 0.0, and the equations above are used to estimate the duration of the phase (i.e., $D_{p,b}$).
3. If split phasing is used, then $D_{p,a}$ equals the unbalanced phase duration for one approach and $D_{p,b}$ equals the unbalanced phase duration for the other approach.

P. Compute Average Phase Duration—Coordinated-Actuated Control

For this discussion, it is assumed Phases 2 and 6 are the coordinated phases serving Movements 2 and 6, respectively (see Exhibit 19-2). If the left-turn movements operate in the protected mode or the protected-permitted mode, then the opposing left-turn movements are served during Phases 1 and 5. If a coordinated phase occurs first in the phase pair, then the other phase (i.e., the one serving the opposing left-turn movement) is a lagging left-turn phase.

The following rules are used to estimate the average duration of each phase:

1. If the phase is associated with the street serving the coordinated movements, then
 - a. If a left-turn phase exists for the subject approach, then its duration $D_{p,l}$ equals $D_{up,l}$ and the opposing through phase has a duration $D_{p,t}$ which is calculated by using Equation 31-40.

$$D_{p,t} = C - \max(D_{up,3} + D_{up,4}, D_{up,7} + D_{up,8}) - D_{p,l}$$

Equation 31-40

where $D_{p,t}$ is the phase duration for coordinated phase t ($t = 2$ or 6) (s), $D_{p,l}$ is the phase duration for left-turn phase l ($l = 1$ or 5) (s), and all other variables are as previously defined.

If Equation 31-40 is applied to Phase 2, then t equals 2 and l equals 1. If it is applied to Phase 6, then t equals 6 and l equals 5.

- b. If a left-turn phase does not exist for the subject approach, then $D_{p,l}$ equals 0.0, and Equation 31-40 is used to estimate the duration of the coordinated phase.

This procedure for determining average phase duration accommodates split phasing only on the street that does not serve the coordinated movements.

If $D_{p,t}$ obtained from Equation 31-40 is less than the minimum phase duration ($= G_{min} + Y + R_c$), then the phase splits are too generous and do not leave adequate time for the coordinated phases.

2. If the phase is associated with the street serving the noncoordinated movements, then the rules described in Step O are used to determine the phase's average duration.

Q. Compute Green Interval Duration

The average green interval duration is computed for each phase by subtracting the yellow change and red clearance intervals from the average phase duration.

$$G = D_p - Y - R_c$$

Equation 31-41

where G is the green interval duration (s).

R. Compare Computed and Estimated Green Interval Durations

The green interval duration from the previous step is compared with the value estimated in Step B. If the two values differ by 0.1 s or more, then the computed green interval becomes the new initial estimate, and the sequence of calculations is repeated starting with Step C. This process is repeated until the two green intervals differ by less than 0.1 s.

If the intersection is semiactuated or fully actuated, then the equilibrium cycle length is computed with Equation 31-42.

$$C_e = \sum_{i=1}^4 D_{p,i}$$

Equation 31-42

where C_e is the equilibrium cycle length (s) and i is the phase number. The sum in this equation includes all phases in Ring 1. The equilibrium cycle length is used in all subsequent calculations in which cycle length C is an input variable.

Probability of Max-Out

When the green indication is extended to its maximum green limit, the associated phase is considered to have terminated by max-out. The probability of max-out provides useful information about phase performance. When max-out occurs, the phase ends without consideration of whether the queue is served or vehicles are in the dilemma zone. Hence, a phase that frequently terminates by max-out may have inadequate capacity and may be associated with more frequent rear-end crashes.

The probability of max-out can be equated to the joint probability of there being a sequence of calls to the phase in service, each call having a headway that is shorter than the equivalent maximum allowable headway for the phase. This probability can be stated mathematically by using Equation 31-43 with Equation 31-44 and Equation 31-45.

Equation 31-43

$$p_x = p^{n_x}$$

with

Equation 31-44

$$n_x = \frac{G_{max} - MAH^* - (g_s + l_1)}{h} \geq 0.0$$

Equation 31-45

$$h = \frac{\Delta^* + (\varphi^*/\lambda^*) - (MAH^* + [1/\lambda^*]\varphi^*e^{-\lambda^*(MAH^*-\Delta^*)})}{1 - \varphi^*e^{-\lambda^*(MAH^*-\Delta^*)}}$$

where

p_x = probability of phase termination by extension to the maximum green limit,

h = average call headway for all calls with headways less than MAH^* (s), and

n_x = number of calls necessary to extend the green to max-out.

LANE GROUP FLOW RATE ON MULTIPLE-LANE APPROACHES

Introduction

When drivers approach an intersection, their primary criterion for lane choice is movement accommodation (i.e., left, through, or right). If multiple exclusive lanes are available to accommodate their movement, they tend to choose the lane that minimizes their service time (i.e., the time required to reach the stop line, as influenced by the number and type of vehicles between them and the stop line). This criterion tends to result in relatively equal lane use under most circumstances.

If one of the lanes being considered is a shared lane, then service time is influenced by the distribution of turning vehicles in the shared lane. Turning vehicles tend to have a longer service time because of the turn maneuver. Moreover, when turning vehicles operate in the permitted mode, their service time can be lengthy because of the gap search process.

Observation of driver lane-choice behavior indicates there is an equilibrium lane flow rate that characterizes the collective choices of the population of drivers. Research indicates the equilibrium flow rate can be estimated from the lane volume distribution that yields the minimum service time for the population of drivers having a choice of lanes (2).

A model for predicting the equilibrium lane flow rate on an intersection approach is described in this subsection. The model is based on the principle that through drivers will choose the lane that minimizes their perceived service time. As a result of this lane selection process, each lane will have the same minimum service time. The principle is represented mathematically by (a) defining service time for each lane as the product of lane flow rate and saturation headway, (b) representing this product as the lane demand-to-saturation flow rate ratio (i.e., v/s ratio), and (c) making the v/s ratios equal among alternative approach lanes. Equation 31-46 is derived from this representation.

$$\frac{v_i}{s_i} = \frac{\sum_{i=1}^{N_{th}} v_i}{\sum_{i=1}^{N_{th}} s_i}$$

Equation 31-46

where

v_i = demand flow rate in lane i (veh/h/ln),

s_i = saturation flow rate in lane i (veh/h/ln), and

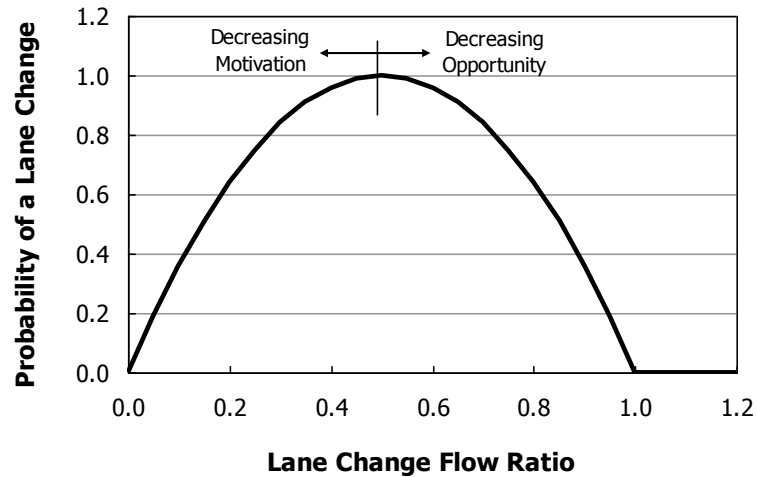
N_{th} = number of through lanes (shared or exclusive) (ln).

The “equalization of flow ratios” principle has been embodied in the HCM since the 1985 edition. Specifically, it has been used to derive the equation for estimating the proportion of left-turning vehicles in a shared lane P_L .

During field observations of various intersection approaches, it was noted that the principle overestimated the effect of turning vehicles in shared lanes for very low and for very high approach flow-rate conditions (3). Under low flow-rate conditions, it was rationalized that through drivers are not motivated to change lanes because the frequency of turns is very low and the threat of delay is negligible. Under high flow-rate conditions, it was rationalized that through drivers do not have an opportunity to change lanes because of the lack of adequate gaps in the outside lane. The field observations also indicated that most lane choice decisions (and related lane changes) for through drivers tended to occur upstream of the intersection, before deceleration occurs.

As a result of these field observations (3), the model was extended to include the probability of a lane change. The probability of a lane change represents the joint probability of there being motivation (i.e., moderate to high flow rates) and opportunity (i.e., adequate lane-change gaps). A variable that is common to each probability distribution is the ratio of the approach flow rate to the maximum flow rate that would allow any lane changes. This maximum flow rate is the rate corresponding to the minimum headway considered acceptable for a lane change (i.e., about 3.7 s) (4). Exhibit 31-5 illustrates the modeled relationship between lane change probability and the flow ratio in the traffic lanes upstream of the intersection, before deceleration occurs (3).

Exhibit 31-5
Probability of a Lane Change



Procedure

The procedure described in this subsection is generalized so it can be applied to any signalized intersection approach with any combination of exclusive turn lanes, shared lanes, and exclusive through lanes. At least one shared lane must be present, and the approach must have two or more lanes (or bays) serving two or more traffic movements. This type of generalized formulation is attractive because of its flexibility; however, the trade-off is that the calculation process is iterative. If a closed-form solution is desired, then one would likely have to be uniquely derived for each lane assignment combination.

The procedure is described in the following steps. Input variables used in the procedure are identified in the following list and are shown in Exhibit 31-6:

- N_l = number of lanes in exclusive left-turn lane group (ln),
- N_{sl} = number of lanes in shared left-turn and through lane group (ln),
- N_t = number of lanes in exclusive through lane group (ln),
- N_{sr} = number of lanes in shared right-turn and through lane group (ln),
- N_r = number of lanes in exclusive right-turn lane group (ln),
- N_{lr} = number of lanes in shared left- and right-turn lane group (ln),
- v_{lt} = left-turn demand flow rate (veh/h),
- v_{th} = through demand flow rate (veh/h),
- v_{rt} = right-turn demand flow rate (veh/h),
- v_l = demand flow rate in exclusive left-turn lane group (veh/h/ln),
- v_{sl} = demand flow rate in shared left-turn and through lane group (veh/h),
- v_t = demand flow rate in exclusive through lane group (veh/h/ln),
- v_{sr} = demand flow rate in shared right-turn and through lane group (veh/h),
- v_r = demand flow rate in exclusive right-turn lane group (veh/h/ln),
- v_{lr} = demand flow rate in shared left- and right-turn lane group (veh/h),

- $v_{sl,lt}$ = left-turn flow rate in shared lane group (veh/h/ln),
- $v_{sr,rt}$ = right-turn flow rate in shared lane group (veh/h/ln),
- s_l = saturation flow rate in exclusive left-turn lane group with permitted operation (veh/h/ln),
- s_{sl} = saturation flow rate in shared left-turn and through lane group with permitted operation (veh/h/ln),
- s_t = saturation flow rate in exclusive through lane group (veh/h/ln),
- s_{sr} = saturation flow rate in shared right-turn and through lane group with permitted operation (veh/h/ln),
- s_r = saturation flow rate in exclusive right-turn lane group with permitted operation (veh/h/ln),
- s_{lr} = saturation flow rate in shared left- and right-turn lane group (veh/h/ln),
- s_{th} = saturation flow rate of an exclusive through lane (= base saturation flow rate adjusted for lane width, heavy vehicles, grade, parking, buses, area type, work zone presence, downstream lane blockage, and spillback) (veh/h/ln),
- g_p = effective green time for permitted left-turn operation (s),
- g_f = time before the first left-turning vehicle arrives and blocks the shared lane (s), and
- g_u = duration of permitted left-turn green time that is not blocked by an opposing queue (s).

Each shared-lane lane group has one lane (i.e., $N_{sl} = 1$, $N_{sr} = 1$, and $N_{lr} = 1$). Procedures for calculating g_p , g_f , and g_u are provided in Section 3.

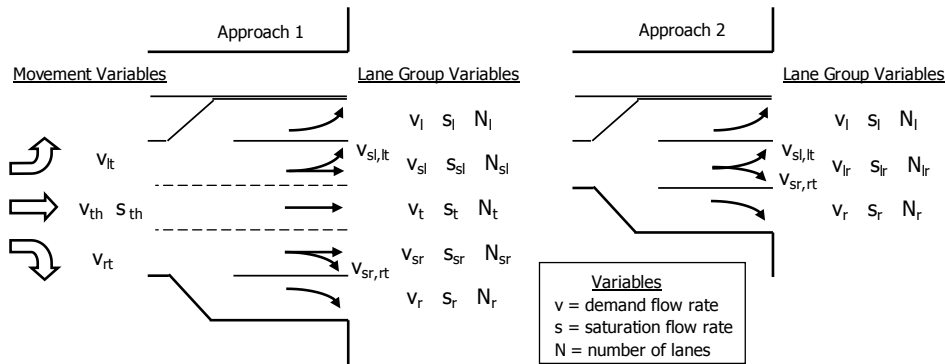


Exhibit 31-6
Input Variables for Lane Group Flow Rate Procedure

A. Compute Modified Through-Car Equivalent

Three modified through-car equivalent factors are computed for the left-turn movement. These factors are computed with Equation 31-47 through Equation 31-51.

$$E_{L,m} = (E_L - 1)P_{tc} + 1$$

Equation 31-47

Equation 31-48

$$E_{L1,m} = \left(\frac{E_{L1}}{f_{Lpb}} - 1 \right) P_{lc} + 1$$

Equation 31-49

$$E_{L2,m} = \left(\frac{E_{L2}}{f_{Lpb}} - 1 \right) P_{lc} + 1$$

with

Equation 31-50

$$P_{lc} = 1 - \left(\left[2 \frac{v_{app}}{s_{lc}} \right] - 1 \right)^2 \geq 0.0$$

Equation 31-51

$$v_{app} = \frac{v_{lt} + v_{th} + v_{rt}}{N_{sl} + N_t + N_{sr}}$$

where

$E_{L,m}$ = modified through-car equivalent for a protected left-turning vehicle,

$E_{L1,m}$ = modified through-car equivalent for a permitted left-turning vehicle,

E_L = equivalent number of through cars for a protected left-turning vehicle (= 1.05),

E_{L1} = equivalent number of through cars for a permitted left-turning vehicle,

$E_{L2,m}$ = modified through-car equivalent for a permitted left-turning vehicle when opposed by a queue on a single-lane approach,

E_{L2} = equivalent number of through cars for a permitted left-turning vehicle when opposed by a queue on a single-lane approach,

f_{Lpb} = pedestrian adjustment factor for left-turn groups,

P_{lc} = probability of a lane change among the approach through lanes,

v_{app} = average demand flow rate per through lane (upstream of any turn bays on the approach) (veh/h/ln),

s_{lc} = maximum flow rate at which a lane change can occur = 3,600/ t_{lc} (veh/h/ln), and

t_{lc} = critical merge headway = 3.7 (s).

The factor obtained from Equation 31-49 is applicable when permitted left-turning vehicles are opposed by a queue on a single-lane approach. Equations for calculating E_{L1} and E_{L2} are provided in Section 3. A procedure for calculating f_{Lpb} is provided later in this section.

If the approach has a shared left- and right-turn lane (as shown in Approach 2 in Exhibit 31-6), then Equation 31-52 is used to compute the average demand flow rate per lane (with $N_{lr} = 1.0$).

Equation 31-52

$$v_{app} = (v_{lt} + v_{rt})/N_{lr}$$

The modified through-car equivalent for permitted right-turning vehicles is computed with Equation 31-53.

Equation 31-53

$$E_{R,m} = \left(\frac{E_R}{f_{Rpb}} - 1 \right) P_{lc} + 1$$

where $E_{R,m}$ is the modified through-car equivalent for a protected right-turning vehicle, f_{Rpb} is the pedestrian-bicycle adjustment factor for right-turn groups, E_R is the equivalent number of through cars for a protected right-turning vehicle (= 1.18), and all other variables are as previously defined.

A procedure for calculating f_{Rpb} is provided later in this section.

If the opposing approach has two lanes serving through vehicles and the inside lane serves through and left-turn vehicles, then Equation 31-54 is used to compute the adjusted duration of permitted left-turn green time that is not blocked by an opposing queue g_u^* . This variable is then used in Equation 31-59 in replacement of the variable g_u . This adjustment is intended to reflect the occasional hesitancy of drivers to shift from the inside lane to the outside lane during higher-volume conditions for this approach-lane geometry. In all other cases of opposing approach-lane geometry, the variable g_u^* is not computed and Equation 31-59 is used as described in the text.

$$g_u^* = g_u + (g_{diff} \times P_{lc})$$

Equation 31-54

where

g_u^* = adjusted duration of permitted left-turn green time that is not blocked by an opposing queue (s), and

g_{diff} = supplemental service time (s).

Equation 31-107 in Section 3 can be used to calculate g_{diff} .

B. Estimate Shared-Lane Lane Group Flow Rate

The procedure to estimate the shared-lane lane group flow rate requires an initial estimate of the demand flow rate for each traffic movement in each shared-lane lane group on the subject approach. For the shared lane serving left-turn and through vehicles, the left-turn flow rate in the shared lane $v_{sl,lt}$ is initially estimated as 0.0 veh/h, and the total lane group flow rate v_{sl} is estimated as equal to the average flow rate per through lane v_{app} . For the shared lane serving right-turn vehicles, the right-turn flow rate in the shared lane $v_{sr,rt}$ is estimated as 0.0 veh/h, and the total lane group flow rate v_{sr} is estimated as equal to the average flow rate per through lane v_{app} . These estimates are updated in a subsequent step.

C. Compute Exclusive Lane-Group Flow Rate

The demand flow rate in the exclusive left-turn lane group v_l is computed with Equation 31-55, where all variables are as previously defined.

$$v_l = \frac{v_{lt} - v_{sl,lt}}{N_l} \geq 0.0$$

Equation 31-55

A similar calculation is completed to estimate the demand flow rate in the exclusive right-turn lane group v_r . The flow rate in the exclusive through lane group is then computed with Equation 31-56.

$$v_t = \frac{v_{th} - (v_{sl} - v_{sl,lt}) - (v_{sr} - v_{sr,rt})}{N_t} \geq 0.0$$

Equation 31-56

D. Compute Proportion of Turns in Shared-Lane Lane Groups

The proportion of left-turning vehicles in the shared left-turn and through lane is computed with Equation 31-57.

Equation 31-57

$$P_L = \frac{v_{sl,lt}}{v_{sl}} \leq 1.0$$

where P_L is the proportion of left-turning vehicles in the shared lane. Substitution of $v_{sr,rt}$ for $v_{sl,lt}$ and v_{sr} for v_{sl} in Equation 31-57 yields an estimate of the proportion of right-turning vehicles in the shared lane P_R .

The proportion of left-turning vehicles in the shared left- and right-turn lane is computed with Equation 31-58.

Equation 31-58

$$P_L = \frac{v_{sl,lt}}{v_{lr}} \leq 1.0$$

Substituting $v_{sr,rt}$ for $v_{sl,lt}$ in Equation 31-58 yields an estimate of the proportion of right-turning vehicles in the shared lane P_R .

E. Compute Lane Group Saturation Flow Rate

The saturation flow rate for the lane group shared by the left-turn and through movements is computed by using Equation 31-59 with Equation 31-60.

Equation 31-59

$$s_{sl} = \frac{s_{th}}{g_p} \left(g_f + \frac{g_{diff}}{1 + P_L[E_{L2,m} - 1]} + \frac{\min[g_p - g_f, g_u]}{1 + P_L[E_{L1,m} - 1]} + \frac{3,600 n_s^* f_{ms} f_{sp}}{s_{th}} \right)$$

with

Equation 31-60

$$n_s^* = \begin{cases} \frac{P_L}{1 - P_L} (1 - P_L^{n_s}) & \text{if } P_L < 0.999 \\ n_s P_L & \text{if } P_L \geq 0.999 \end{cases}$$

where g_{diff} is the supplemental service time (s), n_s^* is the expected number of sneakers per cycle in a shared left-turn lane, f_{ms} is the adjustment factor for downstream lane blockage, f_{sp} is the adjustment factor for sustained spillback, and all other variables are as previously defined.

Equation 31-107 in Section 3 can be used to calculate g_{diff} .

Equation 31-61 is used to compute the saturation flow rate in a shared right-turn and through lane group s_{sr} .

Equation 31-61

$$s_{sr} = \frac{s_{th}}{1 + P_R(E_{R,m} - 1)}$$

where P_R is the proportion of right-turning vehicles in the shared lane (decimal).

The saturation flow rate for the lane group serving left-turning vehicles in an exclusive lane s_l is computed with Equation 31-59, with $P_L = 1.0$, $g_{diff} = 0.0$, $g_f = 0.0$, and s_{th} replaced by s_{lt} (see Equation 31-112). Similarly, the saturation flow rate in an exclusive right-turn lane group s_r is computed with Equation 31-61, with $P_R = 1.0$.

The saturation flow rate for the lane group serving through vehicles in an exclusive lane is computed with Equation 31-62.

$$s_t = s_{th} f_s$$

where f_s is the adjustment factor for all lanes serving through vehicles on an approach with a shared left-turn and through lane group (= 1.0 if $N_{sl} = 0$; 0.91 otherwise).

The saturation flow rate for the shared left- and right-turn lane is computed with Equation 31-63.

$$s_{lr} = \frac{s_{th}}{1 + P_L(E_{L,m} - 1) + P_R(E_{R,m} - 1)}$$

Equation 31-62

Equation 31-63

F. Compute Flow Ratio

The flow ratio for the subject intersection approach is computed with Equation 31-64.

$$y^* = \frac{v_l N_l + v_{sl} N_{sl} + v_t N_t + v_{sr} N_{sr} + v_r N_r + v_{lr} N_{lr}}{s_l N_l + s_{sl} N_{sl} + s_t N_t + s_{sr} N_{sr} + s_r N_r + s_{lr} N_{lr}}$$

Equation 31-64

where y^* is the flow ratio for the approach. If a shared left- and right-turn lane exists on the subject approach, then $N_{sl} = 0$, $N_t = 0$, $N_{sr} = 0$, and $N_{lr} = 1$; otherwise, $N_{sl} = 1$, $N_t \geq 0$, $N_{sr} = 1$, and $N_{lr} = 0$.

G. Compute Revised Lane Group Flow Rate

The flow ratio from Step F is used to compute the demand flow rate in the exclusive left-turn lane group with Equation 31-65.

$$v_l = s_l y^*$$

Equation 31-65

In a similar manner, the demand flow rate for the other lane groups is estimated by multiplying the flow ratio y^* by the corresponding lane group saturation flow rate.

H. Compute Turn Movement Flow Rate in Shared-Lane Lane Groups

The left-turn demand flow rate in the shared lane group is computed with Equation 31-66.

$$v_{sl,lt} = v_{lt} - v_l \geq 0.0$$

Equation 31-66

Equation 31-66 can be used to compute the right-turn demand flow rate in the shared lane group by substituting $v_{sr,rt}$ for $v_{sl,lt}$, v_{rt} for v_{lt} , and v_r for v_l .

The demand flow rate in each shared-lane lane group is now compared with the rate estimated in Step B. If they differ by less than 0.1 veh/h, then the procedure is complete and the flow rates estimated in Steps G and H represent the best estimate of the flow rate for each lane group.

If there is disagreement between the lane group demand flow rates, then the calculations are repeated, starting with Step C. However, for this iteration, the flow rates computed in Steps G and H are used in the new calculation sequence. The calculations are complete when the flow rates used at the start of Step C differ from those obtained in Step H by less than 0.1 veh/h.

PRETIMED PHASE DURATION

The design of a pretimed timing plan can be a complex and iterative process that is generally carried out with the assistance of software. Several software products are available for this purpose. This subsection describes various strategies for pretimed signal-timing design and provides a procedure for implementing one of these strategies.

Design Strategies

Several aspects of signal-timing design, such as the choice of the timing strategy, are beyond the scope of this manual. Three basic strategies are commonly used for pretimed signals.

One strategy is to equalize the volume-to-capacity ratios for critical lane groups. It is the simplest strategy and the only one that can be calculated without excessive iteration. Under this strategy, the green time is allocated among the various signal phases in proportion to the flow ratio of the critical lane group for each phase. This strategy is described briefly in the next subsection. It is also used in the planning-level analysis application described in Section 5.

A second strategy is to minimize the total delay to all vehicles. This strategy is generally proposed as the optimal solution to the signal-timing problem. Variations of this strategy often combine other performance measures (e.g., stop rate, fuel consumption) in the optimization function. Many signal-timing software products offer this optimization feature. Some products use a delay estimation procedure identical to that in the motorized vehicle methodology in Chapter 19, but other products use minor departures from it.

A third strategy is to equalize the level of service (LOS) for all critical lane groups. This strategy promotes a LOS on all approaches that is consistent with the overall intersection LOS. It improves on the first and second strategies because they tend to produce a higher delay per vehicle for the minor movements at the intersection (and therefore a less favorable LOS).

Determining Phase Duration on the Basis of Vehicle Demand

Signal timing based on equalization of the volume-to-capacity ratio is described in this subsection. Equation 31-67, Equation 31-68, and Equation 31-69 are used to estimate the cycle length and effective green time for each critical phase. Conversion to green interval duration follows by applying the appropriate lost-time increments.

Equation 31-67

$$X_c = \left(\frac{C}{C - L} \right) \sum_{i \in ci} y_{c,i}$$

Equation 31-68

$$C = \frac{L X_c}{X_c - \sum_{i \in ci} y_{c,i}}$$

Equation 31-69

$$g_i = \frac{v_i C}{N_i s_i X_i} = \left(\frac{v}{N s} \right)_i \left(\frac{C}{X_i} \right)$$

where

C = cycle length (s),

L = cycle lost time (s),

X_c = critical intersection volume-to-capacity ratio,

$y_{c,i}$ = critical flow ratio for phase $i = v_i/(N s_i)$,

ci = set of critical phases on the critical path,

X_i = volume-to-capacity ratio for lane group i ,

v_i = demand flow rate for lane group i (veh/h),

N_i = number of lanes in lane group i (ln),

s_i = saturation flow rate for lane group i (veh/h/ln), and

g_i = effective green time for lane group i (s).

The summation term in each of these equations represents the summation of a specific variable for the set of critical phases. A critical phase is one phase of a set of phases that occurs in sequence whose combined flow ratio is the largest for the signal cycle.

Procedure

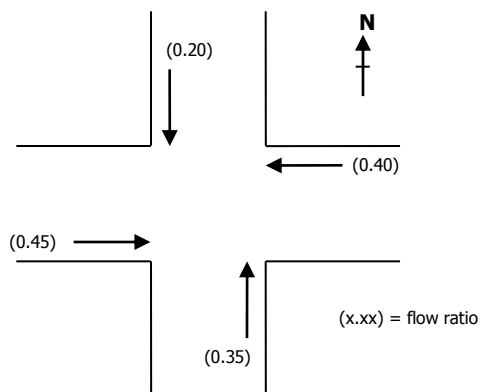
The following steps summarize the procedure for estimating the cycle length and effective green time for the critical phases:

1. Compute the flow ratio $[= v_i/(N s_i)]$ for each lane group and identify the critical flow ratio for each phase. When there are several lane groups on the approach and they are served during a common phase, then the lane group with the largest flow ratio represents the critical flow ratio for the phase. A procedure for identifying the critical phases and associated flow ratios is described in Section 4 of Chapter 19, Signalized Intersections.
2. If signal-system constraints do not dictate the cycle length, then estimate the minimum cycle length with Equation 31-68 by setting X_c equal to 1.0.
3. If signal-system constraints do not dictate the cycle length, then estimate the desired cycle length with Equation 31-68 by substituting a target volume-to-capacity ratio X_t for the critical ratio X_c . A value of X_t in the range of 0.80 to 0.90 is recommended for this purpose.
4. If signal-system constraints do not dictate the cycle length, then use the results of Steps 2 and 3 to select an appropriate cycle length for the signal. Otherwise, the cycle length is that dictated by the signal system.
5. Estimate the effective green time for each phase with Equation 31-69 and the target volume-to-capacity ratio.
6. Check the timing to ensure the effective green time and the lost time for each phase in a common ring sum to the cycle length.

Example Application

The procedure is illustrated by a sample calculation. Consider the intersection shown in Exhibit 31-7.

Exhibit 31-7
Example Intersection



Phases 2 and 6 serve the eastbound and westbound approaches, respectively. Phases 4 and 8 serve the southbound and northbound approaches, respectively. One phase from each pair will represent the critical phase and dictate the duration of both phases. It is assumed the lost time for each phase equals the change period (i.e., the yellow change interval plus the red clearance interval). Thus, the lost time for each critical phase is 4 s, or 8 s for the cycle.

In this simple example, only one lane group is served on each approach, so the critical flow ratios can be identified by inspection of Exhibit 31-7. Specifically, the critical flow ratio for the east–west phases is that associated with the eastbound approach (i.e., Phase 2) at a value of 0.45. Similarly, the critical flow ratio for the north–south phases is that associated with the northbound approach (i.e., Phase 8).

The minimum cycle length that will avoid oversaturation is computed by Equation 31-68 with $X_c = 1.00$.

$$C(\text{minimum}) = \frac{8(1.0)}{1.0 - (0.45 + 0.35)} = \frac{8}{0.2} = 40 \text{ s}$$

A target volume-to-capacity ratio of 0.80 is used to estimate the target cycle length.

$$C = \frac{8(0.8)}{0.8 - (0.45 + 0.35)} = \frac{6.4}{0} = \text{infinity}$$

This computation indicates a critical volume-to-capacity ratio of 0.8 cannot be provided with the present demand levels at the intersection.

As a second trial estimate, a target volume-to-capacity ratio of 0.92 is selected and used to estimate the target cycle length.

$$C = \frac{8(0.92)}{0.92 - (0.45 + 0.35)} = 61 \text{ s}$$

The estimate is rounded to 60 s for practical application. Equation 31-67 is then used to estimate the critical volume-to-capacity ratio of 0.923 for the selected cycle length of 60 s.

With Equation 31-69, the effective green time is allocated so the volume-to-capacity ratio for each critical lane group is equal to the target volume-to-capacity ratio. Thus, for the example problem, the target volume-to-capacity ratio

for each phase is 0.923. The effective green times are computed with Equation 31-69. The results of the calculations are listed below:

$$\begin{aligned} g_2 &= 0.45(60/0.923) = 29.3 \text{ s} \\ g_8 &= 0.35(60/0.923) = 22.7 \text{ s} \\ g_2 + g_8 + L &= 29.3 + 22.7 + 8.0 = 60.0 \text{ s} \end{aligned}$$

The duration of the effective green interval for Phase 6 is the same as for Phase 2, given that they have the same phase lost time. Similarly, the effective green interval for Phase 4 is the same as for Phase 8.

Determining Phase Duration on the Basis of Pedestrian Considerations

Two pedestrian considerations are addressed in this subsection as they relate to pretimed phase duration. One consideration addresses the time a pedestrian needs to perceive the signal indication and traverse the crosswalk. A second consideration addresses the time needed to serve cyclic pedestrian demand. When available, local guidelines or practice should be used to establish phase duration on the basis of pedestrian considerations.

A minimum green interval duration that allows a pedestrian to perceive the indication and traverse the crosswalk can be computed with Equation 31-70.

$$G_{p,min} = t_{pr} + \frac{L_{cc}}{S_p} - Y - R_c$$

Equation 31-70

where

$G_{p,min}$ = minimum green interval duration based on pedestrian crossing time (s),

t_{pr} = pedestrian perception of signal indication and curb departure time = 7.0 (s),

L_{cc} = curb-to-curb crossing distance (ft),

S_p = pedestrian walking speed = 3.5 (ft/s),

Y = yellow change interval (s), and

R_c = red clearance interval (s).

The variable t_{pr} in this equation represents the time pedestrians need to perceive the start of the phase and depart from the curb. A value of 7.0 s represents a conservatively long value that is adequate for most pedestrian crossing conditions. The variable S_p represents the pedestrian walking speed in a crosswalk. A value of 3.5 ft/s represents a conservatively slow value that most pedestrians will exceed.

If a permitted or protected-permitted left-turn operation is used for the left-turn movement that crosses the subject crosswalk, then the subtraction of the yellow change interval and the red clearance interval in Equation 31-70 may cause some conflict between pedestrians and left-turning vehicles. If this conflict can occur, then the minimum green interval duration should be computed as $G_{p,min} = t_{pr} + (L_{cc}/S_p)$.

The second pedestrian consideration in timing design is the time required to serve pedestrian demand. The green interval duration should equal or exceed this time to ensure pedestrian demand is served each cycle. The time needed to serve this demand is computed with either Equation 31-71 or Equation 31-72, along with Equation 31-73.

If the crosswalk width W is greater than 10 ft, then

Equation 31-71

$$t_{ps} = 3.2 + \frac{L_{cc}}{S_p} + 2.7 \frac{N_{ped}}{W}$$

If the crosswalk width W is less than or equal to 10 ft, then

Equation 31-72

$$t_{ps} = 3.2 + \frac{L_{cc}}{S_p} + 0.27 N_{ped}$$

with

Equation 31-73

$$N_{ped} = \frac{v_{ped,i}}{3,600} C$$

where

t_{ps} = pedestrian service time (s),

W = effective width of crosswalk (ft),

$v_{ped,i}$ = pedestrian flow rate in the subject crossing for travel direction i (p/h),
and

N_{ped} = number of pedestrians crossing during an interval (p).

Equation 31-73 assumes pedestrians always cross at the start of the phase. Thus, it yields a conservatively large estimate of N_{ped} because some pedestrians arrive and cross during the green indication.

Equation 31-73 is specific to the pedestrian flow rate in one direction of travel along the subject crosswalk. If the pedestrian flow rate varies significantly during the analysis period for the crosswalk's two travel directions, then t_{ps} should be calculated for both travel directions, and the larger value should be used to estimate the green interval duration needed to serve pedestrian demand.

PEDESTRIAN AND BICYCLE ADJUSTMENT FACTORS

Exhibit 31-8 shows sample conflict zones where intersection users compete for space. This competition reduces the saturation flow rate of the turning vehicles. Its effect is quantified in the pedestrian and bicycle adjustment factors. This subsection describes a procedure for calculating these factors, which are used in the procedure for calculating the adjusted saturation flow rate that is described in Section 3 of Chapter 19.

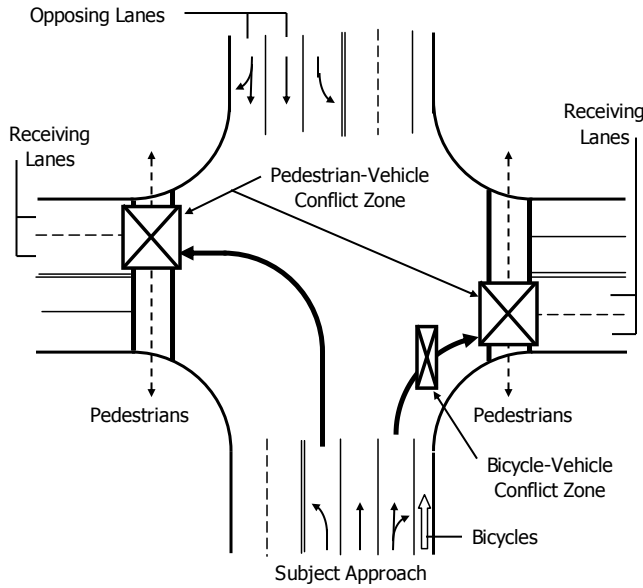


Exhibit 31-8
Conflict Zone Locations

This subsection consists of two subsections. The first subsection describes the procedure for computing (a) the pedestrian–bicycle adjustment factor for right-turn lane groups and (b) the pedestrian adjustment factor for left-turn lane groups from a one-way street. The second subsection describes the procedure for computing the pedestrian adjustment factor for left-turn groups served by permitted or protected-permitted operation.

The following guidance is used to determine the pedestrian adjustment factor for lane groups serving left-turn movements f_{Lpb} :

- If there are no conflicting pedestrians, then f_{Lpb} is equal to 1.0.
- If the lane group is on a two-way street and the protected mode or split phasing is used, then f_{Lpb} is equal to 1.0.
- If the lane group is on a one-way street, then the procedure described in the first subsection below is used to compute f_{Lpb} .
- If the lane group is on a two-way street and either the permitted mode or the protected-permitted mode is used, then the procedure described in the second subsection below is used to calculate f_{Lpb} .

The following guidance is used to determine the pedestrian–bicycle adjustment factor for lane groups serving right-turn movements f_{Rpb} :

- If there are no conflicting pedestrians or bicycles, then f_{Rpb} is equal to 1.0.
- If the protected mode is used, then f_{Rpb} is equal to 1.0.
- If the permitted mode or the protected-permitted mode is used, then the procedure described in the first subsection below is used to compute f_{Rpb} .

Right-Turn Movements and Left-Turn Movements from One-Way Street

A. Determine Pedestrian Flow Rate During Service

This procedure requires knowledge of the phase duration and cycle length. If these variables are not known and the intersection is pretimed, then they can be estimated by using the procedure described in the previous subsection titled Pretimed Phase Duration. If the intersection is actuated, then the average phase duration and cycle length can be computed by using the procedure described in the previous subsection titled Actuated Phase Duration.

The pedestrian flow rate during the pedestrian service time is computed with Equation 31-74.

Equation 31-74

$$v_{pedg} = v_{ped} \frac{C}{g_{ped}} \leq 5,000$$

where

v_{pedg} = pedestrian flow rate during the pedestrian service time (p/h),

v_{ped} = pedestrian flow rate in the subject crossing (walking in both directions) (p/h),

C = cycle length (s), and

g_{ped} = pedestrian service time (s).

If the phase providing service to pedestrians is actuated, has a pedestrian signal head, and rest-in-walk is not enabled, then the pedestrian service time is equal to the smaller of (a) the effective green time for the phase or (b) the sum of the walk and pedestrian clear settings [i.e., $g_{ped} = \min(g, \text{Walk} + PC)$]. Otherwise, the pedestrian service time can be assumed to equal the effective green time for the phase (i.e., $g_{ped} = g$).

B. Determine Average Pedestrian Occupancy

If the pedestrian flow rate during the pedestrian service time is 1,000 p/h or less, then the pedestrian occupancy is computed with Equation 31-75.

Equation 31-75

$$OCC_{pedg} = \frac{v_{pedg}}{2,000}$$

where OCC_{pedg} is the pedestrian occupancy.

If the pedestrian flow rate during the pedestrian service time exceeds 1,000 p/h, then Equation 31-76 is used.

Equation 31-76

$$OCC_{pedg} = 0.4 + \frac{v_{pedg}}{10,000} \leq 0.90$$

A practical upper limit on v_{pedg} of 5,000 p/h should be maintained when Equation 31-76 is used.

C. Determine Bicycle Flow Rate During Green

The bicycle flow rate during the green indication is computed with Equation 31-77.

Equation 31-77

$$v_{bicg} = v_{bic} \frac{C}{g} \leq 1,900$$

where

v_{bicg} = bicycle flow rate during the green indication (bicycles/h),

v_{bic} = bicycle flow rate (bicycles/h),

C = cycle length (s), and

g = effective green time (s).

D. Determine Average Bicycle Occupancy

The average bicycle occupancy is computed with Equation 31-78.

$$OCC_{bicg} = 0.02 + \frac{v_{bicg}}{2,700}$$

Equation 31-78

where OCC_{bicg} is the bicycle occupancy, and v_{bicg} is the bicycle flow rate during the green indication (bicycles/h).

A practical upper limit on v_{bicg} of 1,900 bicycles/h should be maintained when Equation 31-78 is used.

E. Determine Relevant Conflict Zone Occupancy

Equation 31-79 is used for right-turn movements with no bicycle interference or for left-turn movements from a one-way street. This equation is based on the assumptions that (a) pedestrian crossing activity takes place during the time period associated with g_{pedr} and (b) no crossing occurs during the green time period $g - g_{pedr}$ when this time period exists.

$$OCC_r = \frac{g_{ped}}{g} OCC_{pedg}$$

Equation 31-79

where OCC_r is the relevant conflict zone occupancy.

Alternatively, Equation 31-80 is used for right-turn movements with pedestrian and bicycle interference, with all variables as previously defined.

$$OCC_r = \left(\frac{g_{ped}}{g} OCC_{pedg} \right) + OCC_{bicg} - \left(\frac{g_{ped}}{g} OCC_{pedg} OCC_{bicg} \right)$$

Equation 31-80

F. Determine Unoccupied Time

If the number of cross-street receiving lanes is equal to the number of turn lanes, then turning vehicles will not be able to maneuver around pedestrians or bicycles. In this situation, the time the conflict zone is unoccupied is computed with Equation 31-81.

$$A_{pbT} = 1 - OCC_r$$

Equation 31-81

where A_{pbT} is the unoccupied time, and OCC_r is the relevant conflict zone occupancy.

Alternatively, if the number of cross-street receiving lanes exceeds the number of turn lanes, turning vehicles will more likely maneuver around pedestrians or bicycles. In this situation, the effect of pedestrians and bicycles on saturation flow is lower, and the time the conflict zone is unoccupied is computed with Equation 31-82.

$$A_{pbT} = 1 - 0.6 OCC_r$$

Equation 31-82

Either Equation 31-81 or Equation 31-82 is used to compute A_{pbT} . The choice of which equation to use should be based on careful consideration of the number of turn lanes and the number of receiving lanes. At some intersections, drivers may consistently and deliberately make illegal turns from an exclusive through lane. At other intersections, proper turning cannot be executed because the receiving lane is blocked by double-parked vehicles. For these reasons, the number of turn lanes and receiving lanes should be determined from field observation.

G. Determine Saturation Flow Rate Adjustment Factor

For permitted right-turn operation in an exclusive lane, Equation 31-83 is used to compute the pedestrian–bicycle adjustment factor.

Equation 31-83

$$f_{Rpb} = A_{pbT}$$

where f_{Rpb} is the pedestrian–bicycle adjustment factor for right-turn groups, and A_{pbT} is the unoccupied time.

For protected-permitted operation in an exclusive lane, the factor from Equation 31-83 is used to compute the adjusted saturation flow rate during the permitted period. The factor has a value of 1.0 when used to compute the adjusted saturation flow rate for the protected period.

For left-turn movements from a one-way street, Equation 31-84 is used to compute the pedestrian adjustment factor.

Equation 31-84

$$f_{Lpb} = A_{pbT}$$

where f_{Lpb} is the pedestrian adjustment factor for left-turn groups, and A_{pbT} is the unoccupied time.

Permitted and Protected-Permitted Left-Turn Movements

This subsection describes a procedure for computing the adjustment factor for left-turn movements on a two-way street that are operating in either the permitted mode or the protected-permitted mode. The calculations in this subsection supplement the procedure described in the previous subsection. The calculations described in Steps A and B in the previous subsection must be completed first (substitute the effective permitted green time g_p for g in Step A), after which the calculations described in this subsection are completed.

This procedure does not account for vehicle–bicycle conflict during the left-turn maneuver.

A. Compute Pedestrian Occupancy After Queue Clears

The pedestrian occupancy after the opposing queue clears is computed with Equation 31-85 or Equation 31-86. The opposing-queue service time g_q is computed as the effective permitted green time g_p less the duration of permitted left-turn green time that is not blocked by an opposing queue g_u (i.e., $g_q = g_p - g_u$).

If $g_q < g_{ped}$, then

Equation 31-85

$$OCC_{pedu} = OCC_{pedg} \left(1 - \frac{0.5 g_q}{g_{ped}} \right)$$

otherwise

$$OCC_{pedu} = 0.0$$

where OCC_{pedu} is the pedestrian occupancy after the opposing queue clears, g_q is the opposing-queue service time ($= g_s$ for the opposing movement) (s), and all other variables are as previously defined.

If the opposing-queue service time g_q equals or exceeds the pedestrian service time g_{ped} , then the opposing queue consumes the entire pedestrian service time.

B. Determine Relevant Conflict Zone Occupancy

After the opposing queue clears, left-turning vehicles complete their maneuvers on the basis of accepted gap availability in the opposing traffic stream. Relevant conflict zone occupancy is a function of the probability of accepted gap availability and pedestrian occupancy. It is computed with Equation 31-87.

$$OCC_r = \frac{g_{ped} - g_q}{g_p - g_q} (OCC_{pedu}) e^{-5.00 v_o / 3,600}$$

where v_o is the opposing demand flow rate (veh/h), g_p is the effective green time for permitted left-turn operation (s), and all other variables are as previously defined.

The opposing demand flow rate v_o is determined to be one of two cases. In Case 1, v_o equals the sum of the opposing through and right-turn volumes. In Case 2, v_o equals the opposing through volume. Case 2 applies when there is a through movement on the opposing approach and one of the following conditions applies: (a) there is an exclusive right-turn lane on the opposing approach and the analyst optionally indicates that this lane does not influence the left-turn drivers' gap acceptance, or (b) there is no right-turn movement on the opposing approach. Case 1 applies whenever Case 2 does not apply.

When an exclusive right-turn lane exists on the opposing approach, the default condition is to assume this lane influences the subject left-turn drivers' gap acceptance. The determination that the exclusive right-turn lane does not influence gap acceptance should be based on knowledge of local driver behavior, traffic conditions, and intersection geometry.

C. Determine Unoccupied Time

Either Equation 31-81 or Equation 31-82 from the previous subsection (i.e., Step F above) is used to compute A_{pbT} . The choice of which equation to use should be based on a consideration of the number of left-turn lanes and the number of receiving lanes.

D. Determine Saturation Flow Rate Adjustment Factor

Equation 31-88 is used to compute the pedestrian adjustment factor f_{Lpb} from A_{pbT} , the unoccupied time.

$$f_{Lpb} = A_{pbT}$$

Equation 31-86

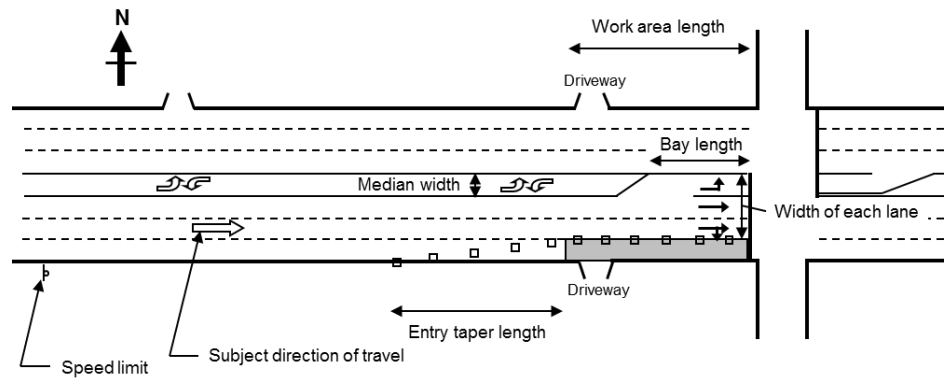
Equation 31-87

Equation 31-88

WORK ZONE PRESENCE ADJUSTMENT FACTOR

The procedure described in this subsection can be used to evaluate signalized intersection operation when a work zone is present on the intersection approach. The work zone is considered to be on the intersection approach if some (or all) of the work zone is located between the stop line and a point 250 ft upstream of the stop line. The work zone may be located on the shoulder, or it may include the closure of one or more lanes. An intersection with a work zone located on the eastbound approach is shown in Exhibit 31-9.

Exhibit 31-9
Work Zone on an Intersection Approach



Required Input Data

The input data that are needed to estimate the effect of work zone presence on saturation flow rate are listed in Exhibit 31-10. The two data elements listed are described in this subsection. The contents of Exhibit 31-10 are in addition to those listed in Exhibit 19-11.

Exhibit 31-10
Geometric Design Input Data Requirements for Work Zones

Input Data Element and Units	Basis
Number of lanes open on the approach in the work zone (ln)	Approach
Approach lane width during work zone (ft)	Approach

Note: Approach = one value or condition for the intersection approach.

Number of Lanes Open on the Approach in the Work Zone

The number of lanes open on the approach in the work zone represents the count of left-turn and through lanes that are open during work zone presence. The count does not include any exclusive right-turn lanes that may exist. The count is taken in the work zone (not upstream or downstream of the work zone). If the number of lanes in the work zone varies, then the smallest number of lanes provided to motorists is used for this input variable.

Approach Lane Width During Work Zone

The approach lane width represents the total width of all open left-turn, through, and right-turn lanes on the intersection approach when the work zone is present.

Computational Steps

The saturation flow rate adjustment factor for the case in which a work zone is located at the intersection can be computed by using Equation 31-89 with Equation 31-90 and Equation 31-91.

$$f_{wz} = 0.858 \times f_{wid} \times f_{reduce} \leq 1.0$$

Equation 31-89

with

$$f_{wid} = \frac{1}{1 - 0.0057 (a_w - 12)}$$

Equation 31-90

$$f_{reduce} = \frac{1}{1 + 0.0402 (n_o - n_{wz})}$$

Equation 31-91

where

f_{wz} = adjustment factor for work zone presence at the intersection,

f_{wid} = adjustment factor for approach width,

f_{reduce} = adjustment factor for reducing lanes during work zone presence,

a_w = approach lane width during work zone (= total width of all open left-turn, through, and right-turn lanes) (ft),

n_o = number of left-turn and through lanes open during normal operation (ln), and

n_{wz} = number of left-turn and through lanes open during work zone presence (ln).

This factor is computed during Step 4, Determine Adjusted Saturation Flow Rate, of the motorized vehicle methodology in Chapter 19, Signalized Intersections. One value is computed for (and is applicable to) all lane groups on the subject intersection approach.

3. QUEUE ACCUMULATION POLYGON

This section describes a procedure for using the queue accumulation polygon (QAP) to estimate delay. The section consists of three subsections. The first subsection provides a review of concepts related to the QAP. The second subsection describes a general procedure for developing the QAP, and the third subsection extends the general procedure to the evaluation of left-turn lane groups.

The discussion in this section describes basic principles for developing polygons for selected types of lane assignment, lane grouping, left-turn operation, and phase sequence. The analyst is referred to the computational engine for specific calculation details, especially as they relate to assignments, groupings, left-turn operations, and phase sequences not addressed in this section. This engine is described in Section 7.

CONCEPTS

The QAP is a graphic tool for describing the deterministic relationship between vehicle arrivals, departures, queue service time, and delay. The QAP defines the queue size for a traffic movement as a function of time during the cycle. The shape of the polygon is defined by the following factors: arrival flow rate during the effective red and green intervals, saturation flow rate associated with each movement in the lane group, signal indication status, left-turn operation mode, and phase sequence. Once constructed, the polygon can be used to compute the queue service time, capacity, and uniform delay for the corresponding lane group.

A QAP is shown in Exhibit 31-11. The variables shown in the exhibit are defined in the following list:

$$r = \text{effective red time} = C - g \text{ (s)},$$

$$g = \text{effective green time (s)},$$

$$C = \text{cycle length (s)},$$

$$g_s = \text{queue service time} = Q_r / (s - q_g) \text{ (s)},$$

$$g_e = \text{green extension time (s)},$$

$$q = \text{arrival flow rate} = v / 3,600 \text{ (veh/s)},$$

$$v = \text{demand flow rate (veh/h)},$$

$$q_r = \text{arrival flow rate during the effective red time} = (1 - P) q C / r \text{ (veh/s)},$$

$$q_g = \text{arrival flow rate during the effective green time} = P q C / g \text{ (veh/s)},$$

$$Q_r = \text{queue size at the end of the effective red time} = q_r r \text{ (veh)},$$

$$P = \text{proportion of vehicles arriving during the green indication (decimal)},$$

and

$$s = \text{adjusted saturation flow rate (veh/h/ln)}.$$

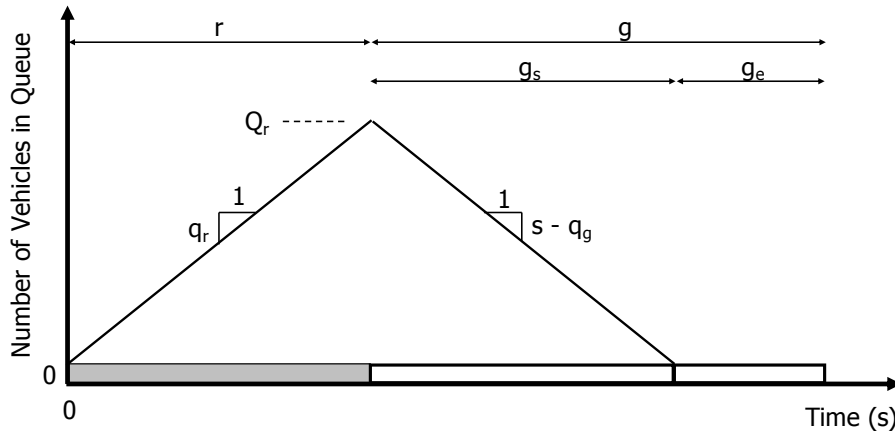


Exhibit 31-11
Queue Accumulation Polygon
for Protected Movements

In application, all flow rate variables are converted to common units of vehicles per second per lane. The presentation in this section is based on these units for q and s .

The polygon in Exhibit 31-11 applies to either a through lane group or a left- or right-turn lane group with exclusive lanes operating with the protected mode. Other polygon shapes are possible, depending on whether the lane group includes a shared lane and whether the lane group serves a permitted (or protected-permitted) left-turn movement. In general, a unique polygon shape will be dictated by each combination of left-turn operational mode (i.e., permitted, protected, or protected-permitted) and phase sequence (i.e., lead, lag, or split). A general procedure for constructing these polygons is described in the next subsection.

GENERAL QAP CONSTRUCTION PROCEDURE

This subsection describes a general procedure for constructing a QAP for a lane group at a signalized intersection. It is directly applicable to left-turn lane groups that have exclusive lanes and protected operation, through lane groups with exclusive lanes, and right-turn lane groups with exclusive lanes. Variations that extend this procedure to turn lane groups with shared lanes, permitted operation, or protected-permitted operation are described in the next subsection.

The construction of a QAP is based on identification of flow rates and service times during the average signal cycle. These rates and times define periods of queue growth, queue service, and service upon arrival. As shown in Exhibit 31-11, the rates and times define queue size as it varies during the cycle. The resulting polygon formed by the queue size profile can be decomposed into a series of trapezoid or triangle shapes, with each shape having a known time interval. Collectively, the areas of the individual shapes can be added to equal the area of the polygon, and the time intervals can be added to equal the cycle length.

The QAP calculation sequence follows the order of interval occurrence over time, and the results can be recorded graphically (as in Exhibit 31-11) or in a tabular manner (i.e., row by row, where each row represents one time interval). A time interval is defined to begin and end at points when either the departure rate or the arrival rate changes. For the duration of the interval, these rates are assumed to be constant.

The following text outlines the calculation sequence used to construct a QAP for a specified lane group. The sequence is repeated for each lane group at the intersection, with the through lane groups evaluated first so the saturation flow rate of permitted left-turn lane groups can be based on the known queue service time for the opposing traffic movements.

1. The QAP calculations for a given lane group start with the end of the effective green period for the phase serving the subject lane group in a protected manner. The initial queue Q_i is assumed to equal 0.0 vehicles.
2. Determine the points in the cycle when the arrival flow rate or the discharge rate changes. The arrival rate may change because of platoons formed in response to an upstream signal, so it is expressed in terms of the arrival rate during green q_g and during red q_r . The discharge rate may change because of the start or end of effective green, a change in the saturation flow rate, the depletion of the subject queue, the depletion of the opposing queue, or the departure of left-turn vehicles as sneakers.
3. For the time interval between the points identified in Step 2, number each interval and compute its duration. Next, identify the arrival rate and discharge rate associated with the interval. Finally, confirm that the sum of all interval durations equals the cycle length.
4. Calculate the capacity of each interval for which there is some discharge, including sneakers when applicable. The sum of these capacities equals the total lane group capacity. Calculate the demand volume for each interval for which there are some arrivals. The sum of these volumes equals the total lane group volume.
5. Calculate the volume-to-capacity ratio X for the lane group by dividing the lane group's total volume by its total capacity. If the volume-to-capacity ratio exceeds 1.0, then calculate the adjusted arrival flow rate q' for each interval by dividing the original flow rate q by X (i.e., $q' = q/X$).
6. Calculate the queue at the end of interval i with Equation 31-92.

Equation 31-92

$$Q_i = Q_{i-1} - \left(\frac{s}{3,600} - \frac{q}{N} \right) t_{d,i} \geq 0.0$$

where Q_i is the queue size at the end of interval i (veh), $t_{d,i}$ is the duration of time interval i during which the arrival flow rate and saturation flow rate are constant (s), and all other variables are as previously defined.

7. If the queue at the end of interval i equals 0.0 vehicles, then compute the duration of the trapezoid or triangle with Equation 31-93. The subject interval should be divided into two intervals, with the first interval having a duration of $t_{t,i}$ and the second interval having a duration of $t_{d,i} - t_{t,i}$. The second interval has starting and ending queues equal to 0.0 vehicles.

Equation 31-93

$$t_{t,i} = \min(t_{d,i}, Q_{i-1}/w_q)$$

where $t_{t,i}$ is the duration of trapezoid or triangle in interval i (s), w_q is the queue change rate (= discharge rate minus arrival rate) (veh/s), and all other variables are as previously defined.

8. Steps 6 and 7 are repeated for each interval in the cycle.

9. When all intervals are completed, the assumption of a zero starting queue (made in Step 1) is checked. The queue size computed for the last interval should always equal the initially assumed value. If this is not the case, then Steps 6 through 8 are repeated by using the ending queue size of the last interval as the starting queue size for the first interval.
10. When all intervals have been evaluated and the starting and ending queue sizes are equal, then the uniform delay can be calculated. This calculation starts with computing the area of each trapezoid or triangle. These areas are then added to determine the total delay. Finally, the total delay is divided by the number of arrivals per cycle to produce uniform delay. Equations for calculating uniform delay by using the QAP are described in Step 7 of the next subsection.

QAP CONSTRUCTION PROCEDURE FOR SELECTED LANE GROUPS

This subsection describes a seven-step procedure for constructing a QAP for selected lane groups. The focus is on left-turn movements in lane groups with shared lanes, permitted operation, or protected-permitted operation. However, there is some discussion of other lane groups, lane assignments, and operation. The procedure described in this subsection represents an extension of the general procedure described in the previous subsection.

Step 1. Determine Permitted Green Time

This step applies when the subject left-turn movement is served by using the permitted mode or the protected-permitted mode. Two effective green times are computed. One is the effective green time for permitted left-turn operation g_p . This green time occurs during the period when the adjacent and opposing through movements both have a circular green indication (after adjustment for lost time).

The other effective green time represents the duration of permitted left-turn green time that is not blocked by an opposing queue g_u . This green time represents the time during the effective green time for permitted left-turn operation g_p that is not used to serve the opposing queue. This time is available to the subject left-turn movement to filter through the conflicting traffic stream.

Exhibit 31-12 provides equations for computing the unblocked permitted green time for left-turn Movement 1 (see Exhibit 19-1) when Dallas left-turn phasing is *not* used. Similar equations can be derived for the other left-turn movements or when Dallas phasing is used. The variables defined in this exhibit are provided in the following list:

- g_u = duration of permitted left-turn green time that is not blocked by an opposing queue (s),
- G_U = displayed green interval corresponding to g_u (s),
- e = extension of effective green = 2.0 (s),
- l_1 = start-up lost time = 2.0 (s),
- G_q = displayed green interval corresponding to g_q (s),

Exhibit 31-12
Unblocked Permitted Green Time

D_p = phase duration (s),
 R_c = red clearance interval (s),
 Y = yellow change interval (s), and
 g_q = opposing-queue service time (= g_s for the opposing movement) (s).

Phase Sequence (phase numbers shown in boxes)	Displayed Unblocked Permitted Green Time $G_{U1}(s)^a$	Permitted Start-Up Lost Time $I_{1,p}(s)^b$	Permitted Extension Time $e_p(s)^c$				
Lead- Lead <table border="1" style="display: inline-table; vertical-align: middle;"><tr><td>1</td><td>2</td></tr><tr><td>5</td><td>6</td></tr></table>	1	2	5	6	$G_{U1} = \min[D_{p1} + D_{p2} - D_{p5} - Y_6 - R_{c6}, G_{U1}^*]$ with $G_{U1}^* = D_{p2} - Y_6 - R_{c6} - G_{q2}$	$I_{1,1}^*$	e_1
1	2						
5	6						
<table border="1" style="display: inline-table; vertical-align: middle;"><tr><td>1</td><td>2</td></tr><tr><td>5</td><td>6</td></tr></table>	1	2	5	6	$G_{U1} = D_{p2} - Y_6 - R_{c6} - G_{q2}$	$I_{1,1}^*$	e_1
1	2						
5	6						
Lead- Lag or Lead- Perm <table border="1" style="display: inline-table; vertical-align: middle;"><tr><td>1</td><td>2</td></tr><tr><td>6</td><td>5</td></tr></table>	1	2	6	5	$G_{U1} = D_{p6} - Y_6 - R_{c6} - D_{p1} - G_{q2}$	0.0	e_1
1	2						
6	5						
<table border="1" style="display: inline-table; vertical-align: middle;"><tr><td>1</td><td>2</td></tr><tr><td>6</td><td>5</td></tr></table>	1	2	6	5	No permitted period	Not applicable	Not applicable
1	2						
6	5						
<table border="1" style="display: inline-table; vertical-align: middle;"><tr><td>1</td><td>2</td></tr><tr><td colspan="2">6</td></tr></table>	1	2	6		$G_{U1} = D_{p6} - Y_6 - R_{c6} - D_{p1} - G_{q2}$	0.0	e_1
1	2						
6							
Lag- Lead or Lag- Perm <table border="1" style="display: inline-table; vertical-align: middle;"><tr><td>2</td><td>1</td></tr><tr><td>5</td><td>6</td></tr></table>	2	1	5	6	No permitted period	Not applicable	Not applicable
2	1						
5	6						
<table border="1" style="display: inline-table; vertical-align: middle;"><tr><td>2</td><td>1</td></tr><tr><td>5</td><td>6</td></tr></table>	2	1	5	6	$G_{U1} = D_{p2} - Y_2 - R_{c2} - \max[D_{p5}, G_{q2}]$	$I_{1,1}$	0.0
2	1						
5	6						
<table border="1" style="display: inline-table; vertical-align: middle;"><tr><td>2</td><td>1</td></tr><tr><td colspan="2">6</td></tr></table>	2	1	6		$G_{U1} = \min[D_{p2} - Y_2 - R_{c2}, D_{p6} - Y_6 - R_{c6}] - G_{q2}$	$I_{1,1}$	0.0
2	1						
6							
Perm- Lead <table border="1" style="display: inline-table; vertical-align: middle;"><tr><td colspan="2">2</td></tr><tr><td>5</td><td>6</td></tr></table>	2		5	6	$G_{U1} = D_{p2} - Y_2 - R_{c2} - \max[D_{p5}, G_{q2}]$	$I_{1,1}$	e_1
2							
5	6						
Perm- Lag <table border="1" style="display: inline-table; vertical-align: middle;"><tr><td colspan="2">2</td></tr><tr><td>6</td><td>5</td></tr></table>	2		6	5	$G_{U1} = \min[D_{p2} - Y_2 - R_{c2}, D_{p6} - Y_6 - R_{c6}] - G_{q2}$	$I_{1,1}$	e_1
2							
6	5						
Perm- Perm <table border="1" style="display: inline-table; vertical-align: middle;"><tr><td colspan="2">2</td></tr><tr><td colspan="2">6</td></tr></table>	2		6		$G_{U1} = D_{p2} - Y_6 - R_{c6} - G_{q2}$	$I_{1,1}$	e_1
2							
6							
Lag- Lag <table border="1" style="display: inline-table; vertical-align: middle;"><tr><td>2</td><td>1</td></tr><tr><td>6</td><td>5</td></tr></table>	2	1	6	5	$G_{U1} = \min[D_{p2} - Y_2 - R_{c2}, D_{p6} - Y_6 - R_{c6}] - G_{q2}$	$I_{1,1}$	e_1^*
2	1						
6	5						
<table border="1" style="display: inline-table; vertical-align: middle;"><tr><td>2</td><td>1</td></tr><tr><td>6</td><td>5</td></tr></table>	2	1	6	5	$G_{U1} = \min[D_{p2} - Y_2 - R_{c2}, D_{p6} - Y_6 - R_{c6}] - G_{q2}$	$I_{1,1}$	e_1^*
2	1						
6	5						

Notes: ^a G_{q2} is computed for each opposing lane (excluding any opposing shared left-turn lane), and the value used corresponds to the lane requiring the longest time to clear. In general, if the opposing lanes serve through movements exclusively, then $G_{q2} = g_q + I_1$. If an opposing lane is shared, then $G_{q2} = g_p - g_e + I_1$, where g_p is the effective green time for permitted operation (s), g_e is the green extension time (s), and I_1 is the start-up lost time (s).
^b If $D_{p5} > (D_{p1} - Y_1 - R_{c1})$, then $I_1^* = D_{p5} - (D_{p1} - Y_1 - R_{c1}) + I_1 - e_1$; otherwise, $I_1^* = 0.0$. Regardless, the result should not be less than 0.0 or more than I_1 .
^c $e_1^* = D_{p2} - (D_{p6} - Y_6 - R_{c6})$, provided the result is not less than 0.0 or more than e_1 .
 Perm = permitted.

For the first four variables in the preceding list, the subscript "1" is added to the variable when it is used in an Exhibit 31-12 equation. This subscript denotes Movement 1. For the next four variables in the list, a numeric subscript is added to the variable when it is used in an equation from the exhibit. This subscript denotes the phase number associated with the variable. Exhibit 31-12 applies only to left-turn Movement 1. The subscripts need to be changed to apply the equations to other left-turn movements.

The equations shown in Exhibit 31-12 indicate that the effective green time for the permitted operation of Phase 1 depends on the duration of Phase 2 and

sometimes the duration of Phase 5. In all instances, Movement 1 has permitted operation during all, or a portion of, Phase 6.

For a given left-turn lane group, one of the equations in the second column (Displayed Unblocked Permitted Green Time) of Exhibit 31-12 will apply. It is used to compute the displayed green interval corresponding to g_u (i.e., G_U). The computed G_U is required to have a nonnegative value. If the calculation yields a negative value, then G_U is set to 0.0.

The same equation can be used to compute the displayed green interval corresponding to g_p (i.e., G_p) by substituting G_p for G_U and 0.0 for G_q . Again, the computed G_p is required to have a nonnegative value. If the calculation yields a negative value, then G_p is set to 0.0.

Equation 31-94 is used to compute the effective green time for permitted left-turn operation.

$$g_p = G_p - l_{1,p} + e_p \geq 0.0$$

Equation 31-94

where

- g_p = effective green time for permitted left-turn operation (s),
- G_p = displayed green interval corresponding to g_p (s),
- $l_{1,p}$ = permitted start-up lost time (s), and
- e_p = permitted extension of effective green (s).

The values of $l_{1,p}$ and e_p used in Equation 31-94 are obtained from the two right-hand columns (Permitted Start-Up Lost Time and Permitted Extension Time, respectively) of Exhibit 31-12.

The start-up lost time for g_u is considered to occur coincident with the start-up lost time associated with g_p . Hence, if the opposing-queue service time consumes an initial portion of g_p , then there is no start-up lost time associated with g_u . The rationale for this approach is that left-turn drivers waiting for the opposing queue to clear will be anticipating queue clearance and may be moving forward slowly (perhaps already beyond the stop line) so that there is negligible start-up lost time at this point. This approach also accommodates the consideration of multiple effective green-time terms when there is a shared lane (e.g., g_j), and it avoids inclusion of multiple start-up lost times during g_p . In accordance with this rationale, Equation 31-95 is used to compute the permitted left-turn green time that is not blocked by an opposing queue g_u , where all other variables are as previously defined.

$$g_u = G_u + e_p \leq g_p$$

Equation 31-95

If protected-permitted operation exists and Dallas phasing is used, then the displayed green interval corresponding to g_u (i.e., G_U) is equal to the opposing through phase duration minus the queue service time and change period of the opposing through phase (i.e., $G_{U1} = D_{p2} - Y_2 - R_{c2} - G_{q2}$). The permitted start-up lost time $l_{1,p}$ and permitted extension of effective green e_p are equal to l_1 and e , respectively. Otherwise, all the calculations described previously apply.

Step 2. Determine Time Before First Left-Turn Vehicle Arrives

This step applies when the left-turn movement is served by using the permitted mode on a shared-lane approach. The variable of interest represents the time that elapses from the start of the permitted green to the arrival of the first left-turning vehicle at the stop line. During this time, through vehicles in the shared lane are served at the saturation flow rate of an exclusive through lane.

Considerations of vehicle distribution impose an upper limit on the time before the first left-turn vehicle arrives when it is used to define a period of saturation flow. This limit is computed with Equation 31-96.

Equation 31-96

$$g_{f,max} = \frac{(1 - P_L)}{0.5 P_L} (1 - [1 - P_L]^{0.5 g_p}) - l_{1,p} \geq 0.0$$

where $g_{f,max}$ is the maximum time before the first left-turning vehicle arrives and within which there are sufficient through vehicles to depart at saturation (s), P_L is the proportion of left-turning vehicles in the shared lane (decimal), and all other variables are as previously defined.

The value of 0.5 in two locations in Equation 31-96 represents the approximate saturation flow rate (in vehicles per second) of through vehicles in an exclusive lane. This approximation simplifies the calculation and provides sufficient accuracy in the estimate of $g_{f,max}$.

The time before the first left-turning vehicle arrives and blocks the shared lane is computed with Equation 31-97 or Equation 31-98, along with Equation 31-99.

If the approach has one lane, then

Equation 31-97

$$g_f = \max (G_p e^{-0.860 LTC^{0.629}} - l_{1,p}, 0.0) \leq g_{f,max}$$

otherwise

Equation 31-98

$$g_f = \max (G_p e^{-0.882 LTC^{0.717}} - l_{1,p}, 0.0) \leq g_{f,max}$$

with

Equation 31-99

$$LTC = \frac{v_{lt} C}{3,600}$$

where

g_f = time before the first left-turning vehicle arrives and blocks the shared lane (s),

LTC = left-turn flow rate per cycle (veh/cycle), and

v_{lt} = left-turn demand flow rate (veh/h).

The approach is considered to have one lane for this step if (a) there is one lane serving all vehicles on the approach and (b) the left-turn movement on this approach shares the one lane.

Step 3. Determine Permitted Left-Turn Saturation Flow Rate

This step applies when left-turning vehicles are served by using the permitted mode or the protected-permitted mode from an exclusive lane. The saturation flow rate for permitted left-turn operation is calculated with Equation 31-100.

$$s_p = \frac{v_o e^{-v_o t_{cg}/3,600}}{1 - e^{-v_o t_{fh}/3,600}}$$

Equation 31-100

where

s_p = saturation flow rate of a permitted left-turn movement (veh/h/ln),

v_o = opposing demand flow rate (veh/h),

t_{cg} = critical headway = 4.5 (s), and

t_{fh} = follow-up headway = 2.5 (s).

The opposing demand flow rate v_o is determined to be one of two cases. In Case 1, v_o equals the sum of the opposing through and right-turn volumes. In Case 2, v_o equals the opposing through volume. Case 2 applies when there is a through movement on the opposing approach and one of the following conditions applies: (a) there is an exclusive right-turn lane on the opposing approach and the analyst optionally indicates that this lane does not influence the left-turn drivers' gap acceptance, or (b) there is no right-turn movement on the opposing approach. Case 1 applies whenever Case 2 does not apply.

When an exclusive right-turn lane exists on the opposing approach, the default condition is to assume this lane influences the subject left-turn drivers' gap acceptance. The determination that the exclusive right-turn lane does not influence gap acceptance should be based on knowledge of local driver behavior, traffic conditions, and intersection geometry.

In those instances in which the opposing volume equals 0.0 veh/h during the analysis period, the opposing volume is set to a value of 0.1 veh/h.

The opposing demand flow rate is not adjusted for unequal lane use in this equation. Increasing this flow rate to account for unequal lane use would misrepresent the frequency and size of headways in the opposing traffic stream. Thus, this adjustment would result in the left-turn saturation flow rate being underestimated.

Step 4. Determine Through-Car Equivalent

This step applies when left-turning vehicles are served by using the permitted mode or the protected-permitted mode. Two variables are computed to quantify the relationship between left-turn saturation flow rate and the base saturation flow rate. The first variable represents the more common case in which left-turning vehicles filter through an oncoming traffic stream. It is computed from Equation 31-101.

$$E_{L1} = \frac{s_o}{s_p}$$

Equation 31-101

where

E_{L1} = equivalent number of through cars for a permitted left-turning vehicle,

s_o = base saturation flow rate (pc/h/ln), and

s_p = saturation flow rate of a permitted left-turn movement (veh/h/ln).

The second variable to be computed represents the case in which the opposing approach has one lane. It describes the saturation flow rate during the time interval coincident with the queue service time of the opposing queue. For this case, the saturation flow rate during the period after the arrival of the first blocking left-turning vehicle and before the end of the opposing-queue service time is influenced by the proportion of left-turning vehicles in the opposing traffic stream. These vehicles create artificial gaps in the opposing traffic stream through which the blocking left-turning vehicles on the subject approach can turn. This effect is considered through calculation of the following through-car equivalency factor by using Equation 31-102 with Equation 31-103.

Equation 31-102

$$E_{L2} = \frac{1 - (1 - P_{lto})^{n_q}}{P_{lto}} \geq E_L$$

with

Equation 31-103

$$n_q = 0.278(g_p - g_u - g_f) \geq 0.0$$

where

E_{L2} = equivalent number of through cars for a permitted left-turning vehicle when opposed by a queue on a single-lane approach,

P_{lto} = proportion of left-turning vehicles in the opposing traffic stream (decimal),

n_q = maximum number of opposing vehicles that could arrive after g_f and before g_u (veh), and

all other variables are as previously defined.

The value of 0.278 in Equation 31-103 represents the approximate saturation flow rate (in vehicles per second) of vehicles in the opposing shared lane. This approximation simplifies the calculation and provides sufficient accuracy in the estimation of n_q .

There is one lane on the opposing approach when this approach has one lane serving through vehicles, a left-turn movement that shares the through lane, and one of the following conditions applies: (a) there is an exclusive right-turn lane on the opposing approach and the analyst optionally indicates that this lane does not influence the left-turn drivers' gap acceptance, (b) there is a right-turn movement on the opposing approach and it shares the through lane, or (c) there is no right-turn movement on the opposing approach.

When an exclusive right-turn lane exists on the opposing approach, the default condition is to assume this lane influences the subject left-turn drivers' gap acceptance. The determination that the exclusive right-turn lane does not influence gap acceptance should be based on knowledge of local driver behavior, traffic conditions, and intersection geometry.

Step 5. Determine Proportion of Turns in a Shared Lane

This step applies when turning vehicles share a lane with through vehicles and the approach has two or more lanes. The proportion of turning vehicles in the shared lane is used in the next step to determine the saturation flow rate for the shared lane.

The proportion of left-turning vehicles in the shared lane P_L is computed if the shared lane includes left-turning vehicles. The proportion of right-turning vehicles in the shared lane P_R is computed if the shared lane includes right-turning vehicles. Guidance for computing these two variables is provided in Section 2.

If the approach has one traffic lane, then P_L equals the proportion of left-turning vehicles on the subject approach P_{lv} and P_R equals the proportion of right-turning vehicles on the subject approach P_{rt} .

Step 6. Determine Lane Group Saturation Flow Rate

The saturation flow rate for the lane group is computed during this step. When the lane group consists of an exclusive lane operating in the protected mode, then it has one saturation flow rate. This rate equals the adjusted saturation flow rate computed by the procedure described in the motorized vehicle methodology in Section 3 of Chapter 19.

The focus of discussion in this step is the calculation of saturation flow rate for lane groups that are *not* in an exclusive lane or operating in the protected mode. Thus, the discussion in this step focuses on shared-lane lane groups and lane groups for which the permitted or protected-permitted mode is used. As the discussion indicates, these lane groups often have two or more saturation flow rates, depending on the phase sequence and operational mode of the turn movements.

Permitted Right-Turn Operation in Exclusive Lane

The saturation flow rate for a permitted right-turn operation in an exclusive lane is computed with Equation 31-104.

$$s_r = s_o f_w f_{HVg} f_p f_{bb} f_a f_{LU} f_{RT} f_{Rpb} f_{wz} f_{ms} f_{sp}$$

where s_r is the saturation flow rate in an exclusive right-turn lane group with permitted operation (veh/h/ln), and the other variables are defined following Equation 19-8 in Chapter 19.

Permitted Right-Turn Operation in Shared Lane

The saturation flow rate for permitted right-turn operation in a shared lane is computed with Equation 31-105.

$$s_{sr} = \frac{s_{th}}{1 + P_R \left(\frac{E_R}{f_{Rpb}} - 1 \right)}$$

Equation 31-104

Equation 31-105

where

s_{sr} = saturation flow rate in shared right-turn and through lane group with permitted operation (veh/h/ln),

s_{th} = saturation flow rate of an exclusive through lane (= base saturation flow rate adjusted for lane width, heavy vehicles, grade, parking, buses, area type, work zone presence, downstream lane blockage, and spillback) (veh/h/ln),

P_R = proportion of right-turning vehicles in the shared lane (decimal),

E_R = equivalent number of through cars for a protected right-turning vehicle = 1.18, and

f_{Rpb} = pedestrian-bicycle adjustment factor for right-turn groups.

The value of f_{Rpb} is obtained by the procedure described in Section 2.

Protected-Permitted Right-Turn Operation in Exclusive Lane

Two saturation flow rates are associated with protected-permitted operation. The saturation flow rate during the protected period s_{rt} is computed with Equation 31-106.

Equation 31-106

$$s_{rt} = s_o f_w f_{HVg} f_p f_{bb} f_a f_{LU} f_{RT} f_{wz} f_{ms} f_{sp}$$

where s_{rt} is the saturation flow rate of an exclusive right-turn lane with protected operation (veh/h/ln), and the other variables are defined following Equation 19-8 in Chapter 19.

The saturation flow rate during the permitted period is computed with Equation 31-104.

Permitted Left-Turn Operation in Shared Lane

There are three possible saturation flow periods during the effective green time associated with permitted left-turn operation in a shared lane. The first period occurs before the arrival of the first left-turning vehicle in the shared lane. This left-turning vehicle will block the shared lane until the opposing queue clears and a gap is available in the opposing traffic stream. The duration of this flow period is g_f . The saturation flow during this period is equal to s_{th} .

The second period of flow begins after g_f and ends with clearance of the opposing queue. It is computed with Equation 31-107.

Equation 31-107

$$g_{diff} = g_p - g_u - g_f \geq 0.0$$

where g_{diff} is the supplemental service time (s), and all other variables are as previously defined. This period may or may not exist, depending on the values of g_u and g_f .

If there are two or more opposing traffic lanes, then the saturation flow during the second period $s_{s/2}$ equals 0.0 veh/h/ln. However, if the opposing approach has only one traffic lane, then the flow during this period occurs at a reduced rate that reflects the blocking effect of left-turning vehicles as they await an opposing left-turning vehicle. Left-turning vehicles during this period are

assigned a through-car equivalent E_{L2} . The saturation flow rate for the shared lane is computed with Equation 31-108.

$$s_{sl2} = \frac{s_{th}}{1 + P_L \left(\frac{E_{L2}}{f_{Lpb}} - 1 \right)}$$

Equation 31-108

where s_{sl2} is the saturation flow rate in the shared left-turn and through lane group during Period 2 (veh/h/ln), P_L is the proportion of left-turning vehicles in the shared lane (decimal), and all other variables are as previously defined.

There is one lane on the opposing approach when this approach has one lane serving through vehicles, a left-turn movement that shares the through lane, and one of the following conditions applies: (a) there is an exclusive right-turn lane on the opposing approach and the analyst optionally indicates that this lane does not influence the left-turn drivers' gap acceptance, (b) there is a right-turn movement on the opposing approach and it shares the through lane, or (c) there is no right-turn movement on the opposing approach.

When an exclusive right-turn lane exists on the opposing approach, the default condition is to assume this lane influences the subject left-turn drivers' gap acceptance. The determination that the exclusive right-turn lane does not influence gap acceptance should be based on knowledge of local driver behavior, traffic conditions, and intersection geometry.

The third period of flow begins after clearance of the opposing queue or arrival of the first blocking left-turn vehicle, whichever occurs last. Its duration equals the smaller of $g_p - g_f$ or g_u . The saturation flow rate for this period is computed with Equation 31-109.

$$s_{sl3} = \frac{s_{th}}{1 + P_L \left(\frac{E_{L1}}{f_{Lpb}} - 1 \right)}$$

Equation 31-109

where s_{sl3} is the saturation flow rate in the shared left-turn and through lane group during Period 3 (veh/h/ln).

For multiple-lane approaches, the impact of the shared lane is extended to include the adjacent through traffic lanes. Specifically, queued drivers are observed to maneuver from lane to lane on the approach to avoid delay associated with the left-turning vehicles in the shared lane. The effect of this impact is accounted for by multiplying the saturation flow rate of the adjacent lanes by a factor of 0.91.

Permitted Left-Turn Operation in Exclusive Lane

There are two possible saturation flow periods during the effective green time associated with permitted left-turn operation in an exclusive lane. The two flow periods are discussed in reverse order, with the second period of flow discussed first.

The second period of flow begins after clearance of the opposing queue. Its duration is g_u . The saturation flow rate for this period is computed with Equation 31-110.

Equation 31-110

$$s_l = s_p f_w f_{HVg} f_p f_{bb} f_a f_{LU} f_{Lpb} f_{wz} f_{ms} f_{sp}$$

where s_l is the saturation flow rate in an exclusive left-turn lane group with permitted operation (veh/h/ln), and all other variables are defined following Equation 19-8 in Chapter 19.

The first period of flow begins with the start of the effective green period and ends with the clearance of the opposing queue. It is computed by using Equation 31-107 with the variable g_f equal to 0.0.

If there are two or more opposing traffic lanes, then the saturation flow during the first period s_{l1} equals 0.0 veh/h/ln. However, if the opposing approach has only one traffic lane, then the saturation flow rate is computed with Equation 31-111.

Equation 31-111

$$s_{l1} = \frac{s_l}{\left(\frac{E_{L2}}{f_{Lpb}}\right)}$$

where s_{l1} is the saturation flow rate in the exclusive left-turn lane group during Period 1 (veh/h/ln). The discussion following Equation 31-108 provides guidance for determining whether the opposing approach has only one traffic lane.

Protected-Permitted Left-Turn Operation in Exclusive Lane

Two saturation flow rates are associated with protected-permitted operation. The saturation flow rate during the protected period s_{lt} is computed with Equation 31-112.

Equation 31-112

$$s_{lt} = s_o f_w f_{HVg} f_p f_{bb} f_a f_{LU} f_{LT} f_{wz} f_{ms} f_{sp}$$

where s_{lt} is the saturation flow rate of an exclusive left-turn lane with protected operation (veh/h/ln), and all other variables are defined following Equation 19-8 in Chapter 19.

The saturation flow rate during the permitted period is computed with Equation 31-110. The duration of the permitted period is equal to g_u .

Protected-Permitted Left-Turn Operation in Shared Lane

The use of a protected-permitted operation in a shared lane has some special requirements to ensure safe and efficient operation. This operational mode requires display of the green ball when the left-turn green arrow is displayed (i.e., the green arrow is not displayed without also displaying the circular green). The following conditions are applied for actuated, protected-permitted operation in a shared lane:

- The left-turn phase is set to minimum recall.
- The maximum green setting for the left-turn phase must be less than or equal to the minimum green for the adjacent through phase.
- If both opposing approaches have protected-permitted operation in a shared lane, then the phase sequence must be lead-lag.
- No vehicle detection is assigned to the left-turn phase.
- Vehicle detection in the shared lane is assigned to the adjacent through movement phase.

There are four possible saturation flow periods during the effective green time associated with protected-permitted left-turn operation in a shared lane. The first three periods are the same as those for permitted left-turn operation in a shared lane (as described above).

The fourth period of flow coincides with the left-turn phase (i.e., the protected period). Its duration is equal to the effective green time for the left-turn phase g_l . The flow rate during this period is computed with Equation 31-113.

$$s_{sl4} = \frac{s_{th}}{1 + P_L(E_L - 1)}$$

Equation 31-113

where s_{sl4} is the saturation flow rate in the shared left-turn and through lane group during Period 4 (veh/h/ln).

For multiple-lane approaches, the impact of the shared lane is extended to include the adjacent through lanes. This impact is accounted for by multiplying the saturation flow rate of the adjacent lanes by a factor of 0.91.

Protected Left- and Right-Turn Operation in a Shared Lane

The saturation flow rate in a shared left- and right-turn lane group with protected operation is computed with Equation 31-114.

$$s_{lr} = \frac{s_{th}}{1 + P_L(E_L - 1) + P_R(E_R - 1)}$$

Equation 31-114

where s_{lr} is the saturation flow rate in the shared left- and right-turn lane group (veh/h/ln).

Step 7. Define Queue Accumulation Polygon

During this step, the green times and saturation flow rates are used to construct the QAP associated with each lane group. The polygon is then used to estimate uniform delay and queue service time. The lane group with the longest queue service time dictates the queue service time for the phase.

The QAP in Exhibit 31-11 applies to either a through lane group or a left- or right-turn lane group with exclusive lanes operating with the protected mode. This polygon also applies to split phasing and to shared lane groups serving through and right-turning vehicles operating with the permitted mode. For split phasing, each approach is evaluated separately to determine its queue service time and uniform delay. If the approach has left- or right-turn lanes, then a separate polygon is constructed for each turn lane group.

More complicated combinations of lane assignment, phase sequence, and left-turn operational mode dictate more complicated polygons. A polygon (or its tabular equivalent) must be derived for each combination. The most common combinations are illustrated in Exhibit 31-13 through Exhibit 31-16.

Exhibit 31-13
QAP for Permitted Left-Turn
Operation in an Exclusive
Lane

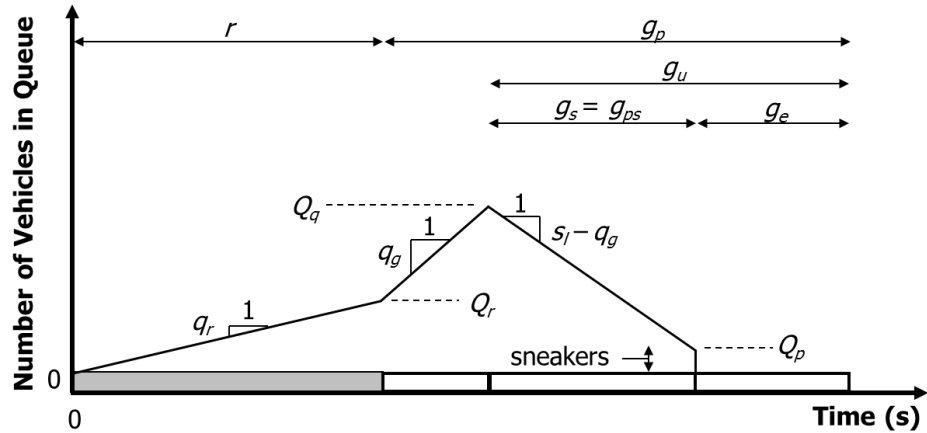


Exhibit 31-14
QAP for Permitted Left-Turn
Operation in a Shared Lane

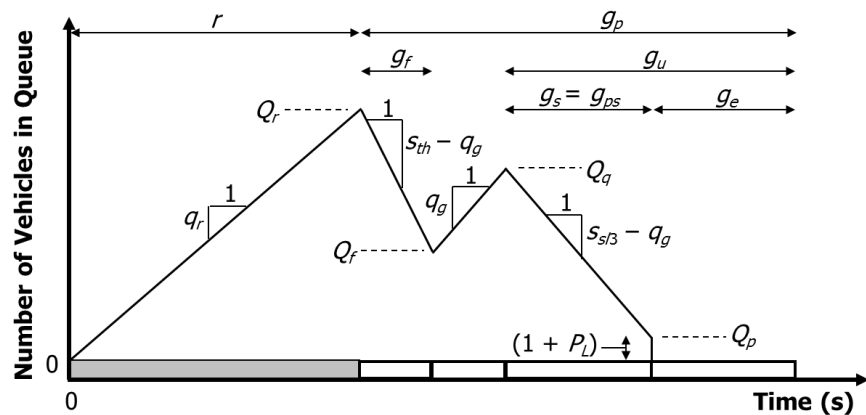
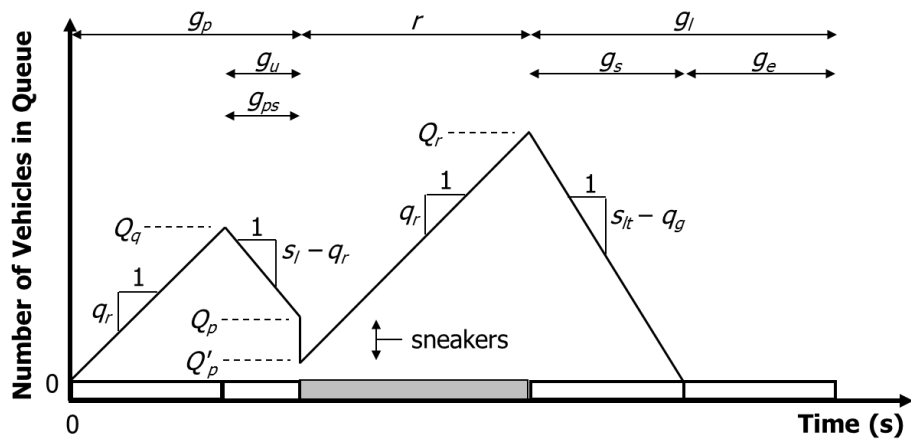


Exhibit 31-15
QAP for Leading, Protected-
Permitted Left-Turn Operation
in an Exclusive Lane



The concept is extended to shared left-turn and through lane groups with protected-permitted operation in Exhibit 31-17 and Exhibit 31-18. Other polygon shapes exist, depending on traffic flow rates, phase sequence, lane use, and left-turn operational mode. The concept of polygon construction must be extended to these other combinations to accurately estimate queue service time and uniform delay.

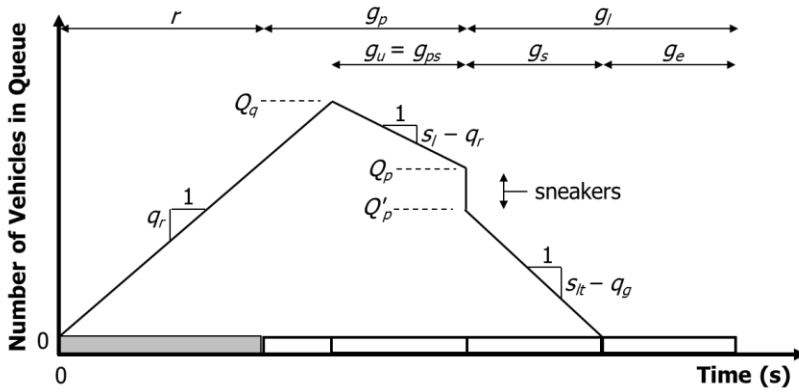


Exhibit 31-16
QAP for Lagging, Protected-Permitted Left-Turn Operation in an Exclusive Lane

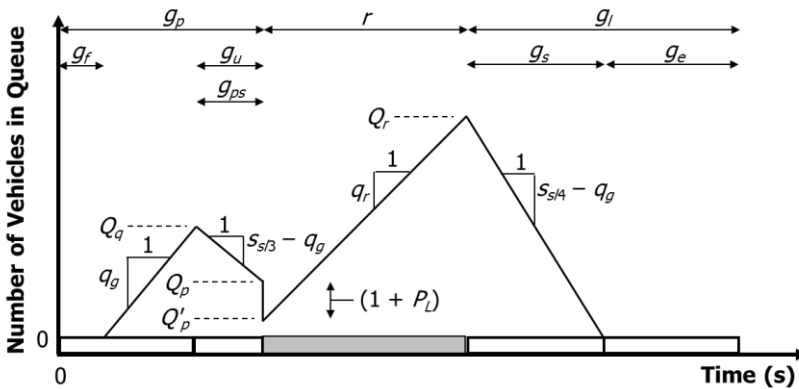


Exhibit 31-17
QAP for Leading, Protected-Permitted Left-Turn Operation in a Shared Lane

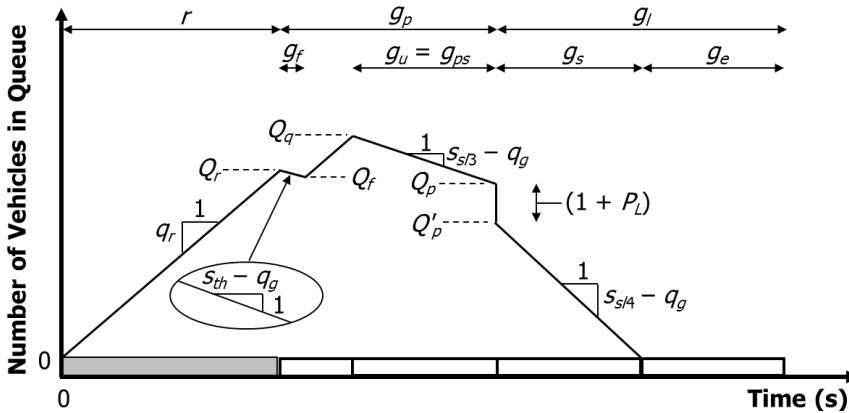


Exhibit 31-18
QAP for Lagging, Protected-Permitted Left-Turn Operation in a Shared Lane

Most of the variables shown in the following exhibits are defined in a previous subsection. Other variables are defined as follows:

- g_l = effective green time for left-turn phase (s);
- g_{ps} = queue service time during permitted left-turn operation (s);
- Q_q = queue size at the start of g_u (veh);
- Q_p = queue size at the end of permitted service time (veh);
- Q'_p = queue size at the end of permitted service time, adjusted for sneakers (veh); and

Q_f = queue size at the end of g_f (veh).

The polygon in Exhibit 31-13 applies to the left-turn lane group with an exclusive lane that operates in the permitted mode during the adjacent through phase. If the phase extends to max-out, then some left-turning vehicles will be served as sneakers. The expected number of sneakers for this mode is reduced if downstream lane blockage or spillback is present [i.e., sneakers = $n_s f_{ms} f_{sp}$ where n_s is the number of sneakers per cycle = 2.0 (veh), f_{ms} is the adjustment factor for downstream lane blockage, and f_{sp} is the adjustment factor for sustained spillback].

The polygon in Exhibit 31-14 applies to the left-turn and through lane group on a shared lane approach with permitted operation. If the phase extends to max-out, then some left-turning vehicles will be served as sneakers. The expected number of sneakers (shown as $1 + P_L$) is computed as $(1 + P_L) f_{ms} f_{sp}$ where P_L is the proportion of left-turning vehicles in the shared lane.

The polygon in Exhibit 31-15 applies to left-turn movements that have protected-permitted operation with a leading left-turn phase and an exclusive lane. The polygon in Exhibit 31-16 applies to left-turn movements that have protected-permitted operation with a lagging left-turn phase and an exclusive lane. If a queue exists at the end of the permitted period for either polygon, then the queue is reduced by the number of sneakers (where sneakers = $n_s f_{ms} f_{sp}$).

The polygon in Exhibit 31-17 applies to left-turn movements that have protected-permitted operation with a leading left-turn phase and a shared left-turn and through lane group. The polygon in Exhibit 31-18 applies to the same movements and operation but with a lagging left-turn phase. If a queue exists at the end of the permitted period for either polygon, then the queue is reduced by the expected number of sneakers [which is computed as $(1 + P_L) f_{ms} f_{sp}$].

As noted above, all polygons are based on the requirement that lane volume cannot exceed lane capacity for the purpose of estimating the queue service time. This requirement is met in the polygons shown because the queue size equals 0.0 vehicles at some point during the cycle.

Exhibit 31-14 through Exhibit 31-18 are shown to indicate that queue size equals 0.0 vehicles at the start of the cycle (i.e., time = 0.0 s). In fact, the queue may not equal 0.0 vehicles at the start of the cycle for some signal timing and traffic conditions. Rather, there may be a nonzero queue at the start of the cycle, and a queue of 0.0 vehicles may not be reached until a different time in the cycle. Thus, in modeling any of the polygons in Exhibit 31-14 through Exhibit 31-18, an iterative process is required. For the first iteration, the queue is assumed to equal 0.0 vehicles at the start of the cycle. The polygon is then constructed, and the queue status is checked at the end of the cycle. If the queue at the end of the cycle is not 0.0 vehicles, then this value is used as a starting point in a second polygon construction. The second polygon will result in a queue at the end of the cycle that equals the queue used at the start of the cycle. Moreover, a queue value of 0.0 vehicles will occur at some point in the cycle.

A. Compute Uniform Delay and Queue Service Time

The procedure for calculating uniform delay and queue service time is described in this step. Exhibit 31-19 is used for this purpose.

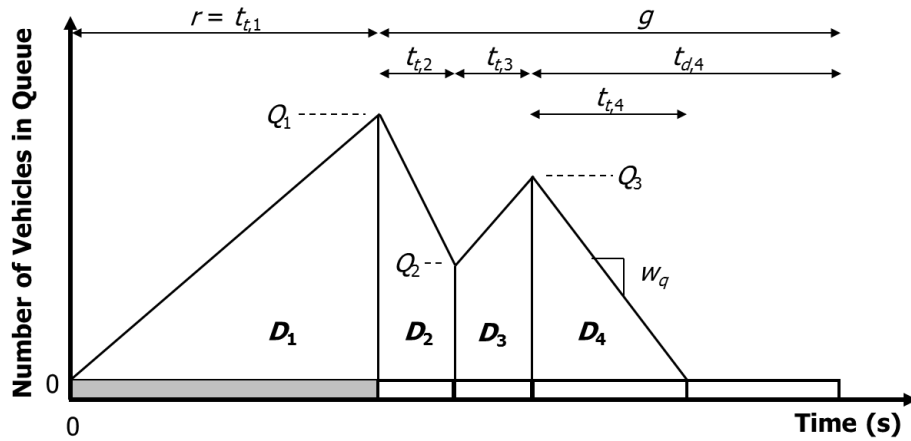


Exhibit 31-19
Polygon for Uniform Delay Calculation

The area bounded by the polygon represents the total delay incurred during the average cycle. The total delay is then divided by the number of arrivals per cycle to estimate the average uniform delay. These calculations are summarized in Equation 31-115 with Equation 31-116.

$$d_1 = \frac{0.5 \sum_{i=1} (Q_{i-1} + Q_i) t_{t,i}}{q C}$$

Equation 31-115

with

$$t_{t,i} = \min(t_{d,i}, Q_{i-1}/w_q)$$

Equation 31-116

where d_1 is the uniform delay (s/veh), $t_{t,i}$ is the duration of trapezoid or triangle in interval i (s), w_q is the queue change rate (i.e., slope of the upper boundary of the trapezoid or triangle) (veh/s), and all other variables are as previously defined.

The summation term in Equation 31-115 includes all intervals for which there is a nonzero queue. In general, $t_{t,i}$ will equal the duration of the corresponding interval. However, during some intervals, the queue will decrease to 0.0 vehicles and $t_{t,i}$ will be only as long as the time required for the queue to dissipate ($= Q_{i-1}/w_q$). This condition is shown to occur during Time Interval 4 in Exhibit 31-19.

The time required for the queue to dissipate represents the queue service time. The queue can dissipate during one or more intervals for turn movements that operate in the protected-permitted mode and for shared-lane lane groups.

For lane groups with exclusive lanes and protected operation, there is one queue service time. It is followed by the green extension time.

For permitted left-turn operation in an exclusive lane, there is one queue service time. It is followed by the green extension time.

For permitted left-turn operation in a shared lane, there can be two queue service times. The green extension time follows the last service time to occur.

For protected-permitted left-turn operation in an exclusive lane, there can be two queue service times. The service time that ends during the protected period is followed by the green extension time.

For protected-permitted left-turn operation in a shared lane, there can be three queue service times. The green extension time can follow the service time that ends during the protected period, but it is more likely to follow the last service time to occur during the permitted period.

For phases serving through or right-turning vehicles in two or more lane groups, the queue service time is measured from the start of the phase to the time when the queue in each lane group has been serviced (i.e., the longest queue service time controls). This consideration is extended to lane groups with shared through and left-turning vehicles.

B. Calculate Lane Group Capacity

This step describes the procedure used to calculate lane group capacity. It is based on the QAP and considers all opportunities for service during the cycle. The equations vary, depending on the left-turn operational mode, phase sequence, and lane assignments for the subject lane group.

Protected Left-Turn Operation in Exclusive Lane

The capacity for a protected left-turn operation in an exclusive-lane lane group is computed with Equation 31-117.

Equation 31-117

$$c_{l,e,p} = \frac{g_l s_{lt}}{C} N_l$$

where $c_{l,e,p}$ is the capacity of an exclusive-lane lane group with protected left-turn operation (veh/h), g_l is the effective green time for the left-turn phase (s), N_l is the number of lanes in the exclusive left-turn lane group (ln), and all other variables are as previously defined.

The available capacity for the lane group is computed with Equation 31-118.

Equation 31-118

$$c_{a,l,e,p} = \frac{G_{max} s_{lt}}{C} N_l$$

where $c_{a,l,e,p}$ is the available capacity of an exclusive-lane lane group with protected left-turn operation (veh/h), G_{max} is the maximum green setting (s), and all other variables are as previously defined.

Equation 31-117 and Equation 31-118 can also be used to calculate the capacity of lane groups composed of through lanes and lane groups composed of right-turn lanes with proper substitution of saturation flow rate, number of lanes, and maximum green variables.

Permitted Left-Turn Operation in Exclusive Lane

The capacity for a permitted left-turn operation in an exclusive-lane lane group is computed with Equation 31-119.

Equation 31-119

$$c_{l,e} = \frac{g_u s_l + 3,600 n_s f_{ms} f_{sp}}{C} N_l$$

where $c_{l,e}$ is the capacity of an exclusive-lane lane group with permitted left-turn operation (veh/h), n_s is the number of sneakers per cycle = 2.0 (veh), and all other variables are as previously defined.

The available capacity for the lane group is computed with Equation 31-120.

$$c_{a,l,e} = c_{l,e} + \frac{(G_{max} - g) s_l}{C} N_l$$

Equation 31-120

where $c_{a,l,e}$ is the available capacity of an exclusive-lane lane group with permitted left-turn operation (veh/h), and all other variables are as previously defined.

The saturation flow rate s_l is specifically included in the term with the maximum green setting G_{max} in Equation 31-120 because this rate represents the saturation flow rate present at the end of the green interval. That is, it is the saturation flow rate that would occur when the green is extended to its maximum green limit as a result of cycle-by-cycle fluctuations in the demand flow rate.

Permitted Left-Turn Operation in Shared Lane

The capacity for a permitted left-turn operation in a shared-lane lane group is computed with Equation 31-121.

$$c_{sl} = \frac{g_p s_{sl} + 3,600(1 + P_L) f_{ms} f_{sp}}{C}$$

Equation 31-121

where c_{sl} is the capacity of a shared-lane lane group with permitted left-turn operation (veh/h), s_{sl} is the saturation flow rate in a shared left-turn and through lane group with permitted operation (veh/h/ln), and all other variables are as previously defined.

The saturation flow rate in Equation 31-121 is computed with Equation 31-122 (all variables are as previously defined).

$$s_{sl} = \frac{s_{th}}{g_p} \left(g_f + \frac{g_{diff}}{1 + P_L \left[\frac{E_{L2}}{f_{Lpb}} - 1 \right]} + \frac{\min(g_p - g_f, g_u)}{1 + P_L \left[\frac{E_{L1}}{f_{Lpb}} - 1 \right]} \right)$$

Equation 31-122

The available capacity for the lane group is computed with Equation 31-123.

$$c_{a,sl} = c_{sl} + \frac{(G_{max} - g_p) s_{sl3}}{C}$$

Equation 31-123

where $c_{a,sl}$ is the available capacity of a shared-lane lane group with permitted left-turn operation (veh/h).

The saturation flow rate s_{sl3} is specifically included in the term with the maximum green setting G_{max} in Equation 31-123 because this rate represents the saturation flow rate present at the end of the green interval.

Protected-Permitted Left-Turn Operation in Exclusive Lane

The capacity for a protected-permitted left-turn operation in an exclusive-lane lane group is computed with Equation 31-124.

$$c_{l,e,pp} = \left(\frac{g_l s_{lt}}{C} + \frac{g_u s_l + 3,600 n_s f_{ms} f_{sp}}{C} \right) N_l$$

Equation 31-124

where $c_{l,e,pp}$ is the capacity of an exclusive-lane lane group with protected-permitted left-turn operation (veh/h).

The available capacity for the lane group is computed with Equation 31-125.

Equation 31-125

$$c_{a,l,e,pp} = \left(\frac{G_{max} s_{lt}}{C} + \frac{g_u s_l + 3,600 n_s f_{ms} f_{sp}}{C} \right) N_l$$

where $c_{a,l,e,pp}$ is the available capacity of an exclusive-lane lane group with protected-permitted left-turn operation (veh/h) and all other variables are as previously defined.

Protected-Permitted Left-Turn Operation in Shared Lane

The capacity for a protected-permitted left-turn operation in a shared-lane lane group is computed with Equation 31-126.

Equation 31-126

$$c_{sl,pp} = \frac{g_l s_{sl4}}{C} + \frac{g_p s_{sl} + 3,600(1 + P_L) f_{ms} f_{sp}}{C}$$

where $c_{sl,pp}$ is the capacity of a shared-lane lane group with protected-permitted left-turn operation (veh/h).

If the lane group is associated with a leading left-turn phase, then the available capacity for the lane group is computed with Equation 31-127.

Equation 31-127

$$c_{a,sl,pp} = c_{sl,pp} + \frac{(G_{max} - g_p) s_{sl3}}{C}$$

where $c_{a,sl,pp}$ is the available capacity of a shared-lane lane group with protected-permitted left-turn operation (veh/h).

When the lane group is associated with a lagging left-turn phase, then the variable s_{sl3} in Equation 31-127 is replaced by s_{sl4} .

Protected-Permitted Right-Turn Operation in Exclusive Lane

The capacity for a protected-permitted right-turn operation in an exclusive-lane lane group is computed with Equation 31-128.

Equation 31-128

$$c_{r,e,pp} = \left(\frac{g_l s_{rt}}{C} + \frac{g_r s_r}{C} \right) N_r$$

where $c_{r,e,pp}$ is the capacity of an exclusive-lane lane group with protected-permitted right-turn operation (veh/h), g_l is the effective green time for the complementary left-turn phase (s), g_r is the effective green time for the phase serving the subject right-turn movement during its permitted period, and all other variables are as previously defined.

The available capacity for the lane group is computed with Equation 31-129.

Equation 31-129

$$c_{a,r,e,pp} = \left(\frac{G_{max,r} s_{rt}}{C} + \frac{g_r s_r}{C} \right) N_r$$

where $c_{a,r,e,pp}$ is the available capacity of an exclusive-lane lane group with protected-permitted right-turn operation (veh/h), and $G_{max,r}$ is the maximum green setting for the phase serving the subject right-turn movement during its permitted period (s).

4. QUEUE STORAGE RATIO

This section discusses queue storage ratio as a performance measure at a signalized intersection. This measure represents the ratio of the back-of-queue size to the available vehicle storage length. The first subsection reviews concepts related to back-of-queue estimation. The second subsection describes a procedure for estimating the back-of-queue size and queue storage ratio.

The discussion in this section describes basic principles for quantifying the back of queue for selected types of lane assignment, lane grouping, left-turn operation, and phase sequence. The analyst is referred to the computational engine for specific calculation details, especially as they relate to assignments, groupings, left-turn operation, and phase sequences not addressed in this section. This engine is described in Section 7.

CONCEPTS

The *back of queue* represents the maximum backward extent of queued vehicles during a typical cycle, as measured from the stop line to the last queued vehicle. The back-of-queue size is typically reached after the onset of the green indication. The point when it is reached occurs just before the most distant queued vehicle begins forward motion as a consequence of the green indication and in response to the forward motion of the vehicle ahead.

A *queued vehicle* is defined as a vehicle that is fully stopped as a consequence of the signal. A *full stop* is defined to occur when a vehicle slows to zero (or a crawl speed, if in queue) as a consequence of the change in signal indication from green to red, but not necessarily in direct response to an observed red indication.

The back-of-queue size that is estimated by the equations described here represents an overall average for the analysis period. It is represented in units of vehicles.

Background

Queue size is defined here to include only fully stopped vehicles. Vehicles that slow as they approach the back of the queue are considered to incur a *partial stop* but are not considered to be part of the queue. The distinction between a full and a partial stop is shown in Exhibit 31-20. This exhibit illustrates the trajectory of several vehicles as they traverse an intersection approach during one signal cycle. There is no residual queue at the end of the cycle.

Each thin line in Exhibit 31-20 that slopes upward from left to right represents the trajectory of one vehicle. The average time between trajectories represents the headway between vehicles (i.e., the inverse of flow rate q). The slope of the trajectory represents the vehicle's speed. The curved portion of a trajectory indicates deceleration or acceleration. The horizontal portion of a trajectory indicates a stopped condition. The effective red r and effective green g times are shown at the top of the exhibit. The other variables shown are defined in the discussion below.

Exhibit 31-20
Time-Space Diagram of Vehicle Trajectory on an Intersection Approach

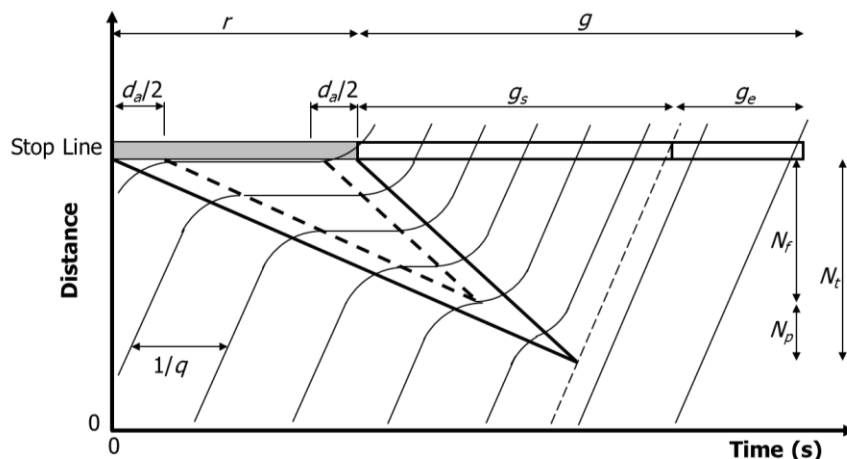


Exhibit 31-20 shows the trajectories of eight vehicles. The first five trajectories (counting from left to right) have a horizontal component to their trajectory that indicates they have reached a full stop as a result of the red indication. The sixth trajectory has some deceleration and acceleration but the vehicle does not stop. This trajectory indicates a partial stop was incurred for the associated vehicle. The last two trajectories do not incur deceleration or acceleration, and the associated vehicles do not slow or stop. Thus, the number of full stops N_f is 5 and the number of partial stops N_p is 1. The total number of stops N_t is 6. The back-of-queue size is equal to the number of full stops.

The back-of-queue size (computed by the procedure described in the next subsection) represents the average back-of-queue size for the analysis period. It is based only on those vehicles that arrive during the analysis period and join the queue. It includes the vehicles that are still in queue after the analysis period ends. The back-of-queue size for a given lane group is computed with Equation 31-130.

Equation 31-130

$$Q = Q_1 + Q_2 + Q_3$$

where

- Q = back-of-queue size (veh/ln),
- Q_1 = first-term back-of-queue size (veh/ln),
- Q_2 = second-term back-of-queue size (veh/ln), and
- Q_3 = third-term back-of-queue size (veh/ln).

The first-term back-of-queue estimate quantifies the queue size described in Exhibit 31-20. It represents the queue caused by the signal cycling through its phase sequence.

The second-term back-of-queue estimate consists of two queue components. One component accounts for the effect of random, cycle-by-cycle fluctuations in demand that occasionally exceed capacity. This fluctuation results in the occasional overflow queue at the end of the green interval (i.e., cycle failure). The second component accounts for queuing due to a sustained oversaturation during the analysis period. This queuing occurs when aggregate demand during the analysis period exceeds aggregate capacity. It is sometimes referred to as the deterministic queue component and is shown as variable $Q_{2,d}$ in Exhibit 31-21.

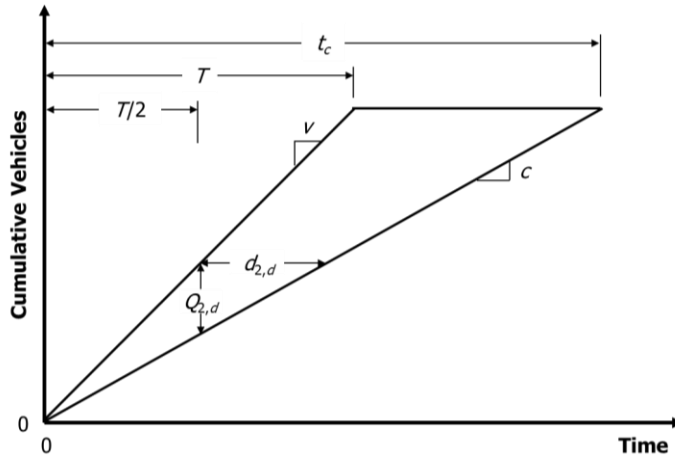


Exhibit 31-21
Cumulative Arrivals and
Departures During an
Oversaturated Analysis Period

Exhibit 31-21 illustrates the queue growth that occurs as vehicles arrive at a demand flow rate v during the analysis period T , which has capacity c . The deterministic delay component is represented by the triangular area bounded by the thick line and is associated with an average delay per vehicle represented by the variable $d_{2,d}$. The average queue size associated with this delay is shown in the exhibit as $Q_{2,d}$. The queue present at the end of the analysis period [$= T(v - c)$] is referred to as the *residual queue*.

The equation used to estimate the second-term queue is based on the assumption that no initial queue is present at the start of the analysis period. The third-term back-of-queue estimate is used to account for the additional queuing that occurs during the analysis period because of an initial queue. This queue is a result of unmet demand in the previous time period. It does *not* include any vehicles that may be in queue due to random, cycle-by-cycle fluctuations in demand that occasionally exceed capacity. When a multiple-period analysis is undertaken, the initial queue for the second and subsequent analysis periods is equal to the residual queue from the previous analysis period.

Exhibit 31-22 illustrates the queue due to an initial queue as a trapezoid shape bounded by thick lines. The average queue is represented by the variable Q_3 . The initial queue size is shown as consisting of Q_b vehicles. The duration of time during the analysis period for which the effect of the initial queue is still present is represented by the variable t . This duration is shown to equal the analysis period in Exhibit 31-22. However, it can be less than the analysis period duration for some lower-volume conditions.

Exhibit 31-22
Third-Term Back-of-Queue
Size with Increasing Queue

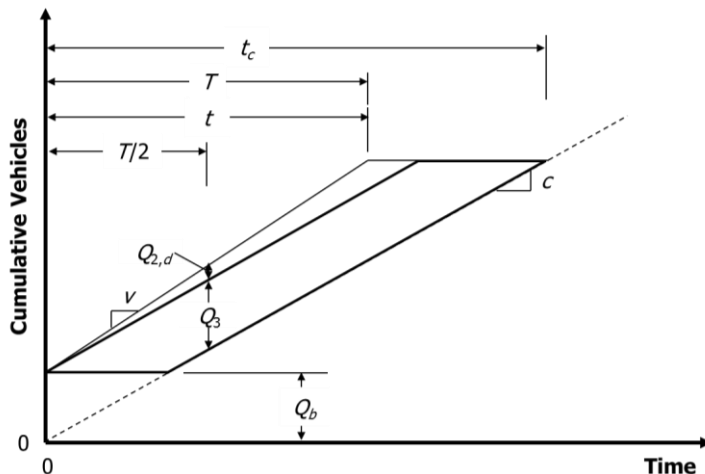


Exhibit 31-22 illustrates the case in which the demand flow rate v exceeds the capacity c during the analysis period. In contrast, Exhibit 31-23 and Exhibit 31-24 illustrate alternative cases in which the demand flow rate is less than the capacity.

Exhibit 31-23
Third-Term Back-of-Queue
Size with Decreasing Queue

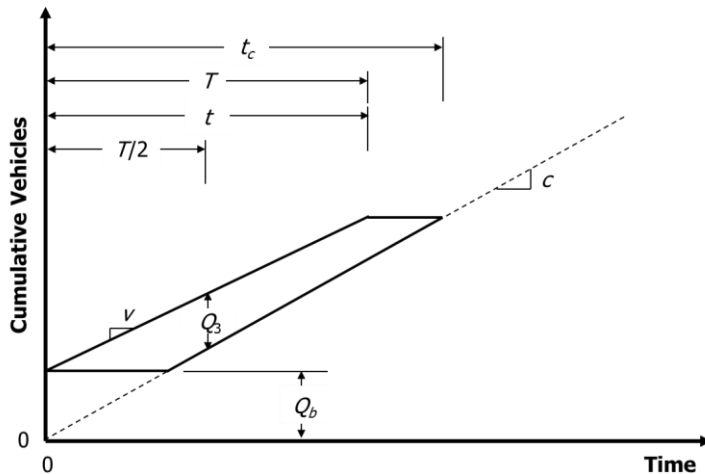
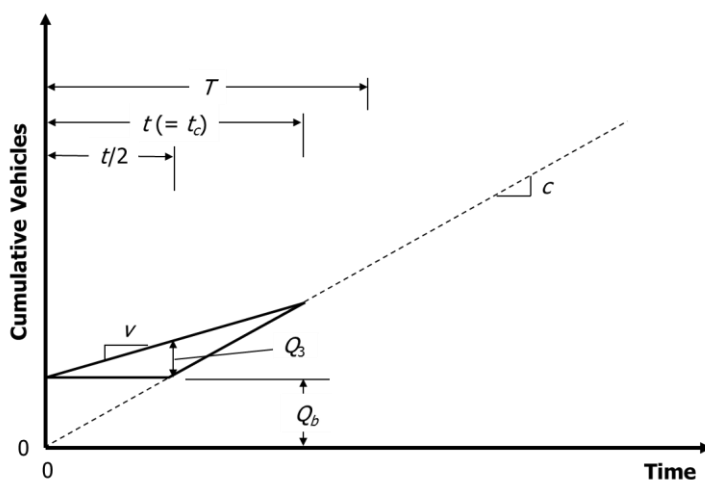


Exhibit 31-24
Third-Term Back-of-Queue
Size with Queue Clearing



In this chapter, *initial queue* is always used in reference to the initial queue due to unmet demand in the previous time period. It *never* refers to vehicles in queue due to random, cycle-by-cycle fluctuations in demand.

Acceleration–Deceleration Delay

The acceleration–deceleration delay d_a term shown in Exhibit 31-20 is used to distinguish between a fully and a partially stopped vehicle. This delay term represents the time required to decelerate to a stop and then accelerate back to the initial speed, less the time it would have taken to traverse the equivalent distance at the initial speed.

Various definitions are used to describe when a vehicle is stopped for the purpose of field measurement. These definitions typically allow the observed vehicle to be called “stopped” even if it has a slow speed (e.g., 2 to 5 mi/h) while moving up in the queue. Many stochastic simulation programs also have a similar allowance. These practical considerations in the count of stopped vehicles require the specification of a threshold speed that can be used to identify when a vehicle is effectively stopped. The acceleration–deceleration delay for a specified threshold speed is estimated with Equation 31-131.

$$d_a = \frac{[1.47 (S_a - S_s)]^2}{2 (1.47 S_a)} \left(\frac{1}{r_a} + \frac{1}{r_d} \right)$$

Equation 31-131

where

- d_a = acceleration–deceleration delay (s),
- S_a = average speed on the intersection approach (mi/h),
- S_s = threshold speed defining a stopped vehicle = 5.0 (mi/h),
- r_a = acceleration rate = 3.5 (ft/s²), and
- r_d = deceleration rate = 4.0 (ft/s²).

The average speed on the intersection approach S_a is representative of vehicles that would pass unimpeded through the intersection if the signal were green for an extended period. It can be estimated with Equation 31-132.

$$S_a = 0.90 (25.6 + 0.47 S_{pl})$$

Equation 31-132

where S_{pl} is the posted speed limit (mi/h).

The threshold speed S_s represents the speed at or below which a vehicle is said to be effectively stopped while in queue or when joining a queue. The strictest definition of this speed is 0.0 mi/h, which coincides with a complete stop. However, vehicles sometimes move up in the queue while drivers wait for the green indication. A vehicle that moves up in the queue and then stops again does not incur an additional full stop. The threshold speed that is judged to differentiate between vehicles that truly stop and those that are just moving up in the queue is 5 mi/h.

Acceleration–deceleration delay values from Equation 31-131 typically range from 8 to 14 s, with larger values in this range corresponding to higher speeds.

Arrival–Departure Polygon

The arrival–departure polygon (ADP) associated with a lane is a graphic tool for computing the number of full stops N_f . The number of full stops has been shown to be equivalent to the first-term back-of-queue size (5).

The ADP separately portrays the cumulative number of arrivals and departures associated with a traffic movement as a function of time during the average cycle. It is related but not identical to the QAP. The main difference is that the polygon sides in the ADP represent an arrival rate or a discharge rate but not both. In contrast, the polygon sides in the QAP represent the combined arrival and discharge rates that may occur during a common time interval.

The ADP is useful for estimating the stop rate and back-of-queue size, and the QAP is useful for estimating delay and queue service time.

The ADP for a through movement is presented in Exhibit 31-25, which shows the polygon for a typical cycle. The red and green intervals are ordered from left to right in the sequence of presentation so that the last two time periods correspond to the queue service time g_s and green extension time g_e of the subject phase. The variables shown in the exhibit are defined in the following list:

t_f = service time for fully stopped vehicles (s),

N_f = number of fully stopped vehicles (veh/ln),

g_s = queue service time (s),

g_e = green extension time (s),

q_r = arrival flow rate during the effective red time = $(1 - P) q C/r$ (veh/s),

P = proportion of vehicles arriving during the green indication (decimal),

q = arrival flow rate = $v/3,600$ (veh/s),

v = demand flow rate (veh/h),

r = effective red time = $C - g$ (s),

g = effective green time (s),

C = cycle length (s),

q_g = arrival flow rate during the effective green time = $P q C/g$ (veh/s), and

Q_r = queue size at the end of the effective red time = $q_r r$ (veh).

In application, all flow rate variables are converted to common units of vehicles per second per lane. The presentation in this section is based on these units for q and s . If the flow rate q exceeds the lane capacity, then it is set to equal this capacity.

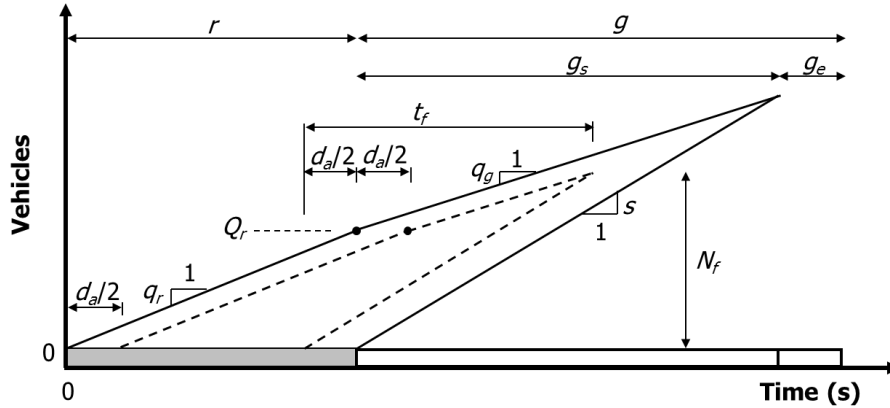


Exhibit 31-25
Arrival-Departure Polygon

The upper solid trend line in Exhibit 31-25 corresponds to vehicles arriving at the intersection. The lower solid trend line corresponds to queued vehicles departing the stop line. The lower trend line is horizontal during the effective red, denoting no departures. The vertical distance between these two lines at any instant in time represents the number of vehicles in the queue.

At the start of the effective red, vehicles begin to queue at a rate of q_r and accumulate to a length of Q_r vehicles at the time the effective green begins. Thereafter, the rate of arrival is q_g until the end of the effective green period. The queue service time g_s represents the time required to serve the queue present at the end of the effective red Q_r plus any additional arrivals that join the queue before it fully clears. The dashed line in this exhibit represents only those vehicles that complete a full stop. The dashed line lags behind the solid arrival line by one-half the value of d_a (i.e., $d_a/2$). In contrast, the dashed line corresponding to initiation of the departure process leads the solid departure line by $d_a/2$.

One-half the acceleration-deceleration delay d_a (i.e., $d_a/2$) occurs at both the end of the arrival process and the start of the discharge process. This assumption is made for convenience in developing the polygon. The derivation of the stop rate and queue length equations indicates that the two components are always combined as d_a . Thus, the assumed distribution of this delay to each of the two occurrences does not influence the accuracy of the estimated back-of-queue size.

The number of fully stopped vehicles N_f represents the number of vehicles that arrive before the queue of stopped vehicles has departed. Equation 31-133 is used for computing this variable (all other variables are as previously defined).

$$N_f = q_r r + q_g (t_f - d_a)$$

Equation 31-133

Equation 31-134 can also be used for estimating N_f .

$$N_f = \frac{s t_f}{3,600}$$

Equation 31-134

Combining Equation 31-133 and Equation 31-134 to eliminate N_f and solve for t_f yields Equation 31-135.

$$t_f = \frac{q_r r - q_g d_a}{s - q_g}$$

Equation 31-135

Equation 31-136

Equation 31-135 can be used with Equation 31-133 to obtain an estimate of N_f . The first-term back-of-queue size is then computed with Equation 31-136.

$$Q_1 = N_f$$

The polygon in Exhibit 31-25 applies to either a through lane group or a left- or right-turn lane group with exclusive lanes operating with the protected mode. Other shapes are possible, depending on whether the lane group includes a shared lane and whether the lane group serves a permitted (or protected-permitted) left-turn movement. In general, a unique shape is dictated by each combination of left-turn operational mode (i.e., permitted, protected, or protected-permitted) and phase sequence (i.e., lead, lag, or split). A general procedure for constructing these polygons is described in the next subsection.

PROCEDURE FOR ESTIMATING BACK OF QUEUE FOR SELECTED LANE GROUPS

This subsection describes a procedure for estimating the back-of-queue size for a lane group at a signalized intersection. The procedure is described in a narrative format and does not define every equation needed to develop a polygon for every combination of lane allocation, left-turn operational mode, and phase sequence. This approach is taken because of the large number of equations required to address the full range of combinations found at intersections in most cities. However, all these equations have been developed and are automated in the computational engine that is described in Section 7. Some of the equations presented in the previous section are repeated in this subsection for reader convenience.

The procedure requires the previous construction of the QAP. The construction of the QAP is described in Section 3.

Step 1. Determine Acceleration–Deceleration Delay

The acceleration–deceleration delay term is used to distinguish between fully and partially stopped vehicles. It is computed with Equation 31-131.

Step 2. Define Arrival–Departure Polygon

During this step, the green times and flow rates used previously to construct the QAP are now used to construct the ADP associated with each lane group served during a phase.

The ADP in Exhibit 31-25 applies to either a through lane group or a left- or right-turn lane group with exclusive lanes operating with the protected mode. This polygon is also applicable to split phasing and to shared lane groups serving through and right-turning vehicles operating with the permitted mode. For split phasing, each approach is evaluated separately to determine its overall stop rate. If the approach has a turn lane, then a separate polygon is constructed for both the turn and the through lane groups.

More complicated combinations of phase sequence and left-turn operational mode dictate more complicated polygons. A polygon must be derived for each combination. The most common combinations are illustrated in Exhibit 31-26 through Exhibit 31-29.

Exhibit 31-27

ADP for Permitted Left-Turn Operation in a Shared Lane

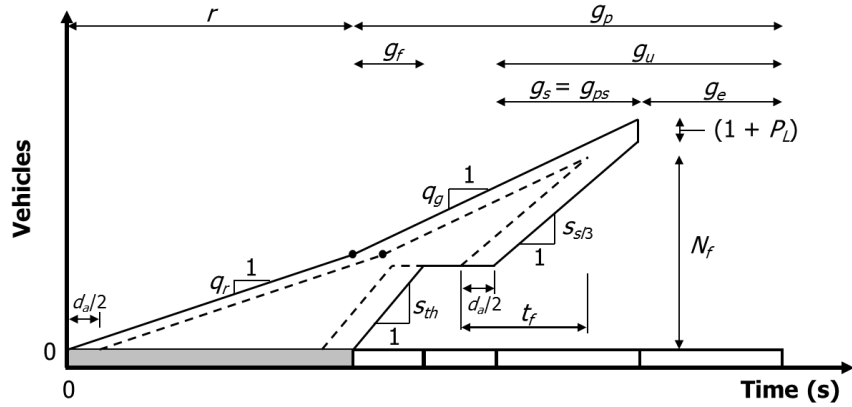


Exhibit 31-28

ADP for Leading, Protected-Permitted Left-Turn Operation in an Exclusive Lane

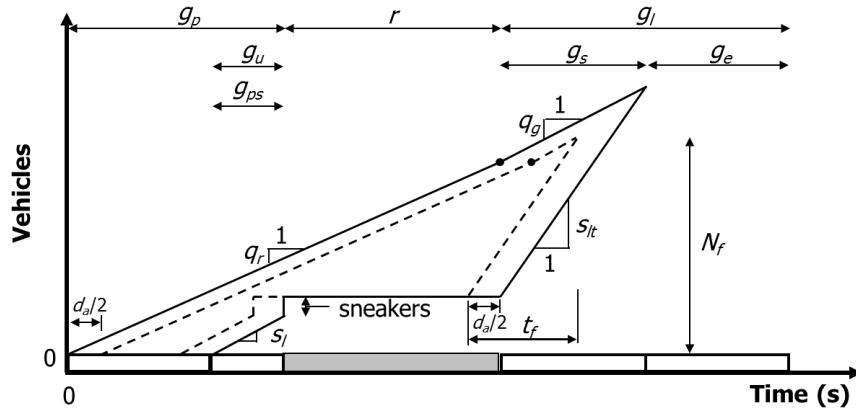
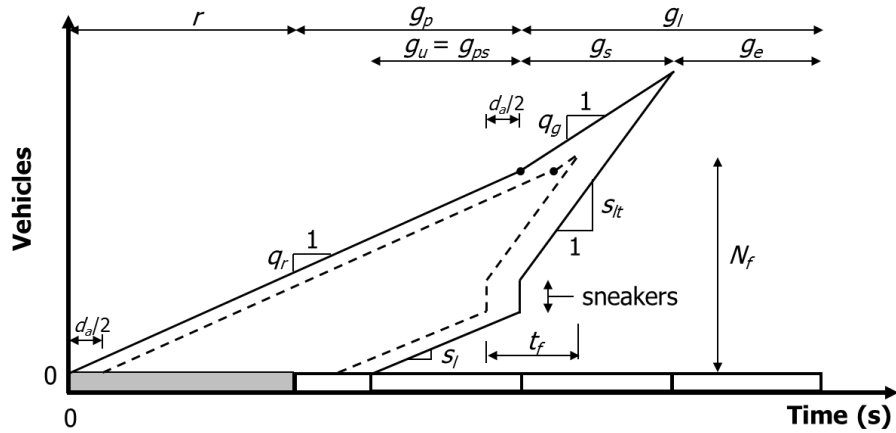


Exhibit 31-29

ADP for Lagging, Protected-Permitted Left-Turn Operation in an Exclusive Lane



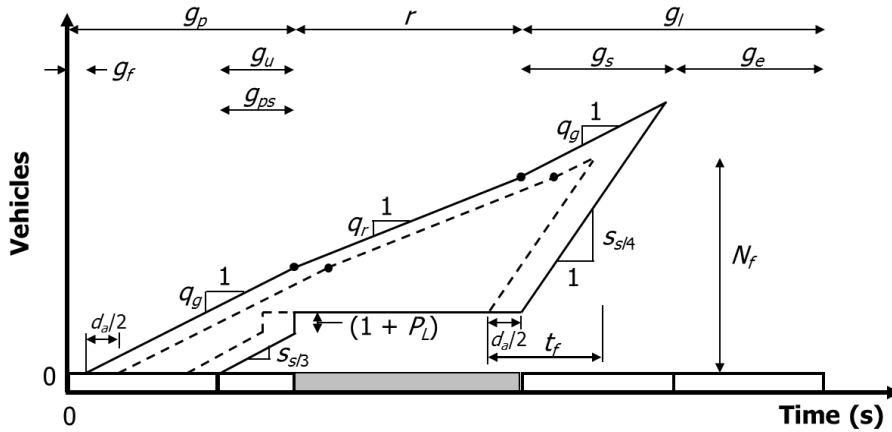


Exhibit 31-30
ADP for Leading, Protected-Permitted Left-Turn Operation in a Shared Lane

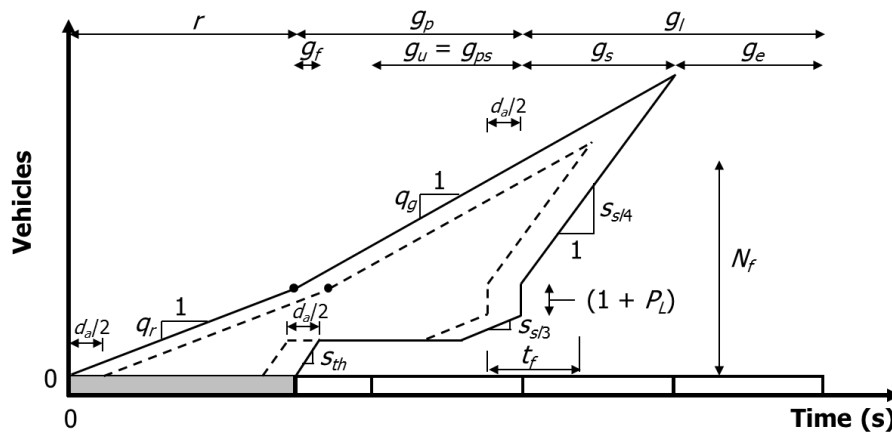


Exhibit 31-31
ADP for Lagging, Protected-Permitted Left-Turn Operation in a Shared Lane

The polygon in Exhibit 31-26 applies to the left-turn lane group served by an exclusive lane that operates in the permitted mode during the adjacent through phase. If the phase extends to max-out, then some left-turning vehicles will be served as sneakers. The expected number of sneakers for this mode is reduced if downstream lane blockage or spillback is present [i.e., sneakers = $n_s f_{ms} f_{sp}$ where n_s is the number of sneakers per cycle = 2.0 (veh), f_{ms} is the adjustment factor for downstream lane blockage, and f_{sp} is the adjustment factor for sustained spillback].

The polygon in Exhibit 31-27 applies to the left-turn and through lane group on a shared-lane approach with permitted operation. If the phase extends to max-out, then some left-turning vehicles will be served as sneakers. The expected number of sneakers (shown as $1 + P_L$) is computed as $(1 + P_L) f_{ms} f_{sp}$, where P_L is the proportion of left-turning vehicles in the shared lane, and all other variables are as previously defined.

The polygon in Exhibit 31-28 applies to left-turn movements that have protected-permitted operation with a leading left-turn phase and an exclusive left-turn lane. The polygon in Exhibit 31-29 applies to the same movements and operation but with a lagging left-turn phase. If a queue exists at the end of the permitted period for either polygon, then the queue is reduced by the number of sneakers (where sneakers = $n_s f_{ms} f_{sp}$).

The polygon in Exhibit 31-30 applies to left-turn movements that have protected-permitted operation with a leading left-turn phase and a shared left-turn and through lane group. The polygon in Exhibit 31-31 applies to the same movements and operation but with a lagging left-turn phase. If a queue exists at the end of the permitted period for either polygon, then the queue is reduced by the expected number of sneakers [which is computed as $(1 + P_L) f_{ms} f_{sp}$].

As noted above, all polygons are based on the requirement that lane volume cannot exceed lane capacity for the purpose of estimating the queue service time. This requirement is met in the polygons shown because the queue size equals 0.0 vehicles at some point during the cycle.

Step 3. Define Arrival–Departure Polygon for Fully Stopped Vehicles

During this step, the polygon defined in the previous step is enhanced to include the polygon shape for the fully stopped vehicles. The fully stopped vehicle polygon is defined by dashed lines in Exhibit 31-25 through Exhibit 31-31.

Two rules guide the development of this polygon feature. First, the dashed line that corresponds to arrivals at the stopped queue *lags* behind the solid arrival line by $d_a/2$ s. Second, the dashed line that corresponds to initiation of the departure process *leads* the solid departure line by $d_a/2$ s.

Step 4. Compute Service Time for Fully Stopped Vehicles

The service time t_f is computed for each polygon constructed in the previous step. When the polygon in Exhibit 31-25 applies, then either Equation 31-137 or Equation 31-138 can be used to compute this time.

If $d_a \leq (1 - P) g X$, then

Equation 31-137

$$t_f = \frac{q C (1 - P - P d_a/g)}{s [1 - \min(1, X) P]}$$

otherwise

Equation 31-138

$$t_f = \frac{q C (1 - P)(r - d_a)}{s [r - \min(1, X) (1 - P)g]}$$

where X is the volume-to-capacity ratio.

The saturation flow rate s used in Equation 31-137 and Equation 31-138 represents the adjusted saturation flow rate that is computed by the procedure described in Section 3 of Chapter 19, Signalized Intersections.

Step 5. Compute the Number of Fully Stopped Vehicles

The number of fully stopped vehicles N_f is computed for each polygon constructed in Step 3. When the polygon in Exhibit 31-25 applies, then Equation 31-139 or Equation 31-140 can be used to compute the number of stops.

If $d_a \leq (1 - P) g X$, then

Equation 31-139

$$N_f = q_r r + q_g (t_f - d_a)$$

otherwise

Equation 31-140

$$N_f = q_r (r - d_a + t_f)$$

Step 6. Compute the First-Term Back-of-Queue Size

The first-term back-of-queue estimate Q_1 (in vehicles per lane) is computed by using the number of fully stopped vehicles from the previous step. It is computed with Equation 31-141, where N_f is the number of fully stopped vehicles.

$$Q_1 = N_f$$

Equation 31-141

For some of the more complex ADPs that include left-turn movements operating with the permitted mode, the queue may dissipate at two or more points during the cycle. If this occurs, then N_{fi} is computed for each of the i periods between queue dissipation points. The first-term back-of-queue estimate is then equal to the largest of the N_{fi} values computed in this manner.

Step 7. Compute the Second-Term Back-of-Queue Size

Equation 31-142 is used to compute the second-term back-of-queue estimate Q_2 for lane groups served by an actuated phase.

$$Q_2 = \frac{c_A}{3,600 N} d_2$$

Equation 31-142

where

Q_2 = second-term back-of-queue size (veh/ln),

c_A = average capacity (veh/h),

d_2 = incremental delay (s/veh), and

N = number of lanes in lane group (ln).

If there is no initial queue, then the average capacity c_A is equal to the lane group capacity c . The procedure for computing this capacity is described in Section 3 of Chapter 19. If there is an initial queue, then the average capacity is computed with the procedure described in Section 4 of Chapter 19.

Step 8. Compute the Third-Term Back-of-Queue Size

The third-term back-of-queue estimate Q_3 is calculated with Equation 31-143 through Equation 31-148.

$$Q_3 = \frac{1}{N T} \left(t_A \frac{Q_b + Q_e - Q_{eo}}{2} \right)$$

Equation 31-143

with

$$Q_e = Q_b + t_A(v - c_A)$$

Equation 31-144

If $v \geq c_A$, then

$$Q_{eo} = T(v - c_A)$$

Equation 31-145

$$t_A = T$$

Equation 31-146

If $v < c_A$, then

$$Q_{eo} = 0.0 \text{ veh}$$

Equation 31-147

$$t_A = Q_b / (c_A - v) \leq T$$

Equation 31-148

where

Q_3 = third-term back-of-queue size (veh/ln),

t_A = adjusted duration of unmet demand in the analysis period (h),

T = analysis period duration (h),

Q_b = initial queue at the start of the analysis period (veh),

Q_e = queue at the end of the analysis period (veh), and

Q_{eo} = queue at the end of the analysis period when $v \geq c_A$ and $Q_b = 0.0$ (veh).

Step 9. Compute the Back-of-Queue Size

The average back-of-queue estimate Q for a lane group (in vehicles per lane) is computed with Equation 31-149 (all other variables are as previously defined).

Equation 31-149

$$Q = Q_1 + Q_2 + Q_3$$

If desired, a percentile back-of-queue estimate $Q_{\%}$ can be computed with Equation 31-150, and Equation 31-151 through Equation 31-153 can be used to compute the percentile back-of-queue factor $f_{B\%}$.

Equation 31-150

$$Q_{\%} = (Q_1 + Q_2)f_{B\%} + Q_3$$

with

If $v \geq c_A$, then

Equation 31-151

$$f_{B\%} = \min \left(1.8, 1.0 + z \sqrt{\frac{I}{Q_1 + Q_2}} + 0.60 z^{0.24} \left(\frac{g}{C}\right)^{0.33} (1.0 - e^{2-2X_A}) \right)$$

Equation 31-152

$$X_A = v/c_A$$

If $v < c_A$, then

Equation 31-153

$$f_{B\%} = \min \left(1.8, 1.0 + z \sqrt{\frac{I}{Q_1 + Q_2}} \right)$$

where

$Q_{\%}$ = percentile back-of-queue size (veh/ln);

$f_{B\%}$ = percentile back-of-queue factor;

z = percentile parameter = 1.04 for 85th percentile queue, 1.28 for 90th percentile queue, and 1.64 for 95th percentile queue;

I = upstream filtering adjustment factor; and

X_A = average volume-to-capacity ratio.

Step 10. Compute Queue Storage Ratio

If the lane group is served by a bay or lane of limited storage length, then the queue storage ratio can be computed by using Equation 31-154 with Equation 31-155.

$$R_Q = \frac{L_h Q}{L_a}$$

Equation 31-154

with

$$L_h = L_{pc}(1 - 0.01 P_{HV}) + 0.01 L_{HV}P_{HV}$$

Equation 31-155

where

R_Q = queue storage ratio,

L_a = available queue storage distance (ft/ln),

L_h = average vehicle spacing in stationary queue (ft/veh),

L_{pc} = stored passenger car lane length = 25 (ft),

L_{HV} = stored heavy-vehicle lane length = 45 (ft), and

P_{HV} = percentage heavy vehicles in the corresponding movement group (%).

Average vehicle spacing is the average length between the front bumpers of two successive vehicles in a stationary queue. The available queue storage distance is equal to the turn bay (or lane) length.

The queue storage ratio is useful for quantifying the potential blockage of the available queue storage distance. If the queue storage ratio is less than 1.0, then blockage will not occur during the analysis period. Blockage will occur if the queue storage ratio is equal to or greater than 1.0.

If desired, a percentile queue storage ratio can be computed with Equation 31-156.

$$R_{Q\%} = \frac{L_h Q\%}{L_a}$$

Equation 31-156

where $R_{Q\%}$ is the percentile queue storage ratio.

5. PLANNING-LEVEL ANALYSIS APPLICATION

The planning-level analysis application described in this section is intended to provide the user a means for conducting a simplified and approximate analysis of signalized intersection operations for motorized vehicles. Chapter 19, Signalized Intersections, provides a more detailed methodology. The objective of the planning-level analysis application is to assess whether an intersection's geometric conditions are sufficient to handle the projected demand volume. Within this framework, many of the data required for a full operational analysis are not needed. This method has several potential uses and applications:

- Conducting sketch-level analyses to quickly assess whether an intersection's lane geometry is sufficient to accommodate a given set of turn-movement demand volumes;
- Evaluating intersection geometry and lane widening alternatives;
- Estimating signal phasing and timing;
- Comparing analysis results against traffic operational performance results produced by other methods; and
- Educating students, transportation professionals, and nontransportation professionals about the fundamentals of traffic signal operational performance.

OVERVIEW OF THE APPLICATION

This subsection provides an overview of the two parts of the planning-level analysis application. Part I provides an estimate of intersection capacity sufficiency. Part II extends the analysis from Part I to provide an estimate of delay and level of service (LOS).

The planning-level analysis application is designed to evaluate the performance of designated groups of lanes, an intersection approach, and the entire intersection. A group of lanes designated for separate analysis is referred to as a *lane group*. Lane groups form the basis for intersection analysis in the planning-level analysis application and in the motorized vehicle methodology described in Chapter 19. However, the criteria for defining a lane group are different between the two methodologies.

For the planning-level analysis application, all traffic movements for a given approach (i.e., left, through, and right) must be assigned to at least one lane group. A lane group can consist of one or more lanes. There are two guidelines to follow for assigning traffic movements to lane groups:

1. When a traffic movement uses only an exclusive lane (or lanes), it is analyzed as an exclusive lane group.
2. When two or more traffic movements share a lane, all lanes that convey those traffic movements are analyzed as a mixed lane group.

When a right-turn movement is shared with a through movement, it is considered to be a part of the through movement lane group. When a right-turn movement is shared with a left-turn movement (such as at a T-intersection), it is

considered to be a part of the left-turn movement lane group. The concept of lane group is discussed in more detail in the Methodology subsection.

Part I: Intersection Sufficiency Assessment

Part I provides an estimate of the intersection's volume-to-capacity ratio, which can be used to assess whether the intersection is likely to operate under, near, or over capacity during the analysis period. This assessment is predicated on the critical movement analysis technique developed originally as part of *Transportation Research Circular 212 (6)*.

Part I generally requires only two inputs: turn movement volume and lane geometry. Other input data are allowed, but they can also be set to default values if they are not explicitly known. Part I can be applied by using manual calculations; it does not require software to implement.

Part I consists of the following steps:

1. Determine left-turn operation.
2. Convert movement volumes to through passenger-car equivalents.
3. Assign flow rates to lane groups.
4. Determine critical lane groups.
5. Determine intersection sufficiency.

Part II: Delay and Level of Service Assessment

Part II extends the results from Part I to produce estimates of volume-to-capacity ratio, delay, and LOS. For practical purposes, Part II requires a spreadsheet or other software to compute estimates of delay and LOS. A Part II analysis requires the initial completion of Steps 1 to 5 of Part I. It then continues with the following steps:

6. Calculate capacity.
7. Determine delay and LOS.

Limitations

The planning-level analysis application has the following limitations:

- It only considers the performance of motorized vehicles;
- It is based on pretimed operation and thus does not account for the effects of actuated control;
- It does not analyze all potential combinations of left-turn operation for opposing approaches (e.g., protected left-turn operation opposed by permitted left-turn operation is not addressed by the application);
- It does not explicitly consider the effects of poorly timed signals;
- It does not account for upstream or downstream impedances and effects of short lanes; and
- It does not consider the effects of grade, lane width, bus activity, area type, pedestrian-vehicle conflicts, or pedestrian-bicycle conflicts;

however, an “equivalency factor for other conditions” is provided to allow the analyst to account for these (or other) nonideal conditions.

REQUIRED DATA AND SOURCES

Exhibit 31-32 describes the input data requirements for conducting an analysis using the planning-level analysis application.

Exhibit 31-32
Required Input Data for the
Planning-Level Analysis
Application

Data Item	Comments
<i>Part I</i>	
Number of lanes and lane use	Required. Exclusive or shared lane use.
Turn movement volumes	Required
Intersection peak hour factor	Use default value of 0.92 if not known.
Percentage heavy vehicles	Use default value of 3% if not known.
On-street parking presence	No (default)
Level of pedestrian activity	None (default) Low – 50 p/h Medium – 200 p/h High – 400 p/h Extreme – 800 p/h
Left-turn operation and phase sequence	Protected operation—with left-turn phase Permitted operation—no left-turn phase Protected operation—split phasing Protected-permitted operation—with left-turn phase (Can be estimated—use guidance provided in the application)
Base saturation flow rate	(Can be estimated—use guidance provided in the application)
Cycle length	(Can be estimated—use guidance provided in the application)
Effective green time	Required to evaluate protected-permitted operation, if present (Can be estimated—use guidance provided in the application)
<i>Part II</i>	
Effective green time	(Can be estimated—use guidance provided in the application)
Progression quality	Good progression Random arrivals (default) Poor progression

The analyst is required to specify values for two data items: (a) the volume for each movement and (b) the number of lanes (and the turn designation for each lane) on each approach. The effective green time is also required if protected-permitted left-turn operation is to be evaluated. Default values can be assumed for the other input data, or the user can specify these values if they are known.

METHODOLOGY

Part I: Intersection Sufficiency Assessment

The first part of the application consists of five steps. These steps are completed in sequence to evaluate the capacity sufficiency of the intersection.

Step 1: Determine Left-Turn Operation

For approaches with left-turn movements, the left-turn operational mode and phase sequence must be defined. The following mode and sequence combinations are addressed in the planning-level analysis application:

- **Protected operation – with left-turn phase.** This combination enables the subject left-turn movement to proceed concurrently with either the adjacent through movement or the opposing left-turn movement.

- **Permitted operation—no left-turn phase.** This combination enables the subject left-turn movement to proceed through the intersection during the same phase indication as the opposing through movement. It generally results in higher capacity for the intersection than other combinations. However, it also produces the highest potential safety conflicts.
- **Protected operation—split phasing.** With split phasing, the through and left-turn movements on the subject approach are served in a protected manner during a common phase. This combination is generally the least efficient type of operation and is oftentimes used when geometric properties of the intersection preclude movements on opposing approaches from proceeding at the same time, or when traffic volumes on opposite approaches are unbalanced.
- **Protected-permitted operation—with left-turn phase.** This combination serves left turns in a protected manner during a left-turn phase and in a permitted manner during a through phase. If this combination is to be evaluated, the analyst should refer to the supplemental procedure in the Protected-Permitted Left-Turn Operations section.

If the operational mode is not known, the following general rules can be applied to determine if protected operation is appropriate for planning-level analysis purposes. Protected operation should be assumed if any of the following conditions are met:

1. The left-turn volume is greater than or equal to 240 veh/h.
2. The product of the left-turn volume and the opposing through volume exceeds a given threshold (50,000 if there is one opposing through lane, 90,000 if there are two opposing through lanes, and 110,000 if there are three or more opposing through lanes).
3. There is more than one left-turn lane on the approach.

Several other considerations for choosing a left-turn operation are not considered to be an explicit part of a planning method. The *Traffic Engineering Handbook* (7) provides additional criteria that include the speed of vehicles on the opposing approach, restrictive sight distances, and accident rates, among others. Therefore, protected left-turn operation may be appropriate even when the above conditions are not satisfied.

In some cases, an intersection may have protected left-turn operation on one approach and permitted left-turn operation on the opposite approach. When this situation occurs, it is necessary to assume both approaches have protected operation to use the planning-level analysis application.

Step 2: Convert Movement Volumes to Through Passenger-Car Equivalents

The objective of this step is to convert all movement volumes into through passenger-car equivalents. The conversion considers one or more of the following factors:

- Effect of heavy vehicles,
- Variation in flow during the hour,

- Impact of opposing through vehicles on permitted left-turn vehicles,
- Impact of pedestrians on right-turn vehicles,
- Impact of parking maneuvers, and
- Lane utilization.

Equation 31-157 provides the volume adjustment equation. Each of the factors in this equation is described in the subsequent paragraphs.

Equation 31-157

$$v_{adj} = V E_{HV} E_{PHF} E_{LT} E_{RT} E_p E_{LU} E_{other}$$

where

v_{adj} = equivalent through movement flow rate expressed in through passenger cars per hour (tpc/h),

V = movement volume (veh/h),

E_{HV} = equivalency factor for heavy vehicles,

E_{PHF} = equivalency factor for peaking characteristics,

E_{RT} = equivalency factor for right turns,

E_{LT} = equivalency factor for left turns,

E_p = equivalency factor for parking activity,

E_{LU} = equivalency factor for lane utilization, and

E_{other} = equivalency factor for other conditions.

Adjustment for Heavy Vehicles

The equivalency factor to convert the mixed traffic stream into passenger car equivalents is computed with Equation 31-158.

Equation 31-158

$$E_{HV} = 1 + 0.01 P_{HV} (E_T - 1)$$

where

P_{HV} = percentage of heavy vehicles in the corresponding lane group (%), and

E_T = equivalent number of through cars for each heavy vehicle = 2.0.

The recommended passenger car equivalent E_T in this method is 2.0. If the user has more detailed or localized information about the value of E_T , then this value may be used in Equation 31-158.

Adjustment for Variation in Flow During the Hour

The movement volume is adjusted by the peak hour factor to reflect the peak 15-min flow rate, similar to the procedure used in the operational method. Equation 31-159 is used to compute the peak hour adjustment factor.

Equation 31-159

$$E_{PHF} = \frac{1}{PHF}$$

where PHF is the peak hour factor (varies between 0.25 and 1.00).

Adjustment for Impedances Experienced by Turning Vehicles

The equivalency factors used to account for impedances experienced by left- and right-turn movements are shown in Exhibit 31-33 and Exhibit 31-34.

Left-Turn Operation	Total Opposing Volume V_o (veh/h) ^a	Equivalency Factor for Left Turns E_{LT}
Protected—with left-turn phase	Any	1.05
Protected—split phasing		
Permitted—no left-turn phase	<200	1.1
	200–599	2.0
	600–799	3.0
	800–999	4.0
	≥1,000	5.0
Protected-permitted—with left-turn phase	Refer to guidance in the Protected-Permitted Left-Turn Operations section	

Note: ^a Includes the sum of through and right-turn volumes on the opposing approach, regardless of whether the right-turn volume is served in an exclusive right-turn lane.

Level of Pedestrian Activity	Pedestrian Volume (p/h)	Equivalency Factor for Right Turns E_{RT}
None or low	0–199	1.2
Moderate	200–399	1.3
High	400–799	1.5
Extreme	≥800	2.1

In Exhibit 31-33, the equivalency factor that is applicable to permitted left-turn movements is based on the opposing volume. This volume is defined as the sum of opposing through and right-turn movements, regardless of whether the right-turn volume is served in an exclusive right-turn lane. The equivalency factor for right turns is a function of the pedestrian activity in the crosswalk that conflicts with the subject right-turn movement.

Adjustment for Parking Activity

The equivalency factor for on-street parking activity is shown in Exhibit 31-35. This factor is applicable to through and right-turn vehicles. It is also applicable to left-turn vehicles on a one-way street when parking is allowed on the left side.

On-Street Parking Presence	No. of Lanes in Lane Group	Equivalency Factor for Parking Activity E_p
No	All	1.00
Yes	1	1.20
	2	1.10
	3	1.05

Adjustment for Lane Utilization

The planning-level analysis application analyzes the performance of the heaviest-traveled lane. For lane groups with two or more lanes, the volume is adjusted to reflect the heaviest-traveled lane. The appropriate equivalency factor to account for lane utilization is selected from Exhibit 31-36.

Exhibit 31-33
Planning-Level Analysis:
Equivalency Factor for Left Turns

Exhibit 31-34
Planning-Level Analysis:
Equivalency Factor for Right Turns

Exhibit 31-35
Planning-Level Analysis:
Equivalency Factor for Parking Activity

Exhibit 31-36
 Planning-Level Analysis:
 Equivalency Factor for Lane
 Utilization

Lane Group Movement	No. of Lanes in Lane Group	Equivalency Factor for Lane Utilization E_{LU}
Through or shared	1	1.00
	2	1.05
	≥ 3	1.10
Exclusive left turn	1	1.00
	≥ 2	1.03
Exclusive right turn	1	1.00
	≥ 2	1.13

Adjustment for "Other" Conditions

An adjustment factor for "other" is provided in Equation 31-157. This factor is a placeholder to allow the user to further adjust the movement volume for conditions that are not captured by any other adjustment factor. The analyst may apply any combination of the saturation flow rate adjustment factors presented in Section 3 of Chapter 19 to reflect other nonideal conditions. In this situation, E_{other} is computed as the product of the inverted factors (i.e., $E_{other} = 1/f_i \times 1/f_j \times \dots \times 1/f_w$ where $f_i, f_j,$ and f_n represent the factors in Chapter 19 that are applicable to the subject movement).

Step 3: Assign Flow Rates to Lane Groups

Initially, lane groups should be checked to determine if a de facto turn lane exists. A de facto turn lane occurs on approaches with multilane lane groups where (a) either a left- or right-turn movement is shared with a through movement and (b) the turning flow rates are sufficiently high, or the impedance to the turning traffic is sufficiently great, to reasonably expect that the through vehicles use only the adjacent exclusive through lane(s) and avoid the shared lane.

The presence of a de facto turn lane can be determined by comparing the total flow rate of turning traffic (left or right) with the lane-equivalent adjusted flow rate in the shared lane as calculated in Step 2. If the flow rate of turning traffic is greater than the lane-equivalent adjusted flow rate, a de facto turn lane should be assumed. De facto turn lanes should be analyzed as exclusive turn lanes, and thus all through movements should be assigned to the through-only lane(s).

In cases in which there are multiple turn lanes and one lane is shared with a through movement, these lanes should be treated as a single lane group that is designated as the through lane group. For approaches at a T-intersection where there are only left- and right-turn movements and multiple lanes, and one of the lanes is shared, the user has the option of coding all lanes as either the right-turn lane group or the left-turn lane group.

Once lane groups have been defined, the lane group flow rate is divided by the number of lanes associated with the lane group to obtain the lane flow rate. Equation 31-160 is used for this purpose.

$$v_i = \frac{v_{adj,i}}{N_i}$$

where

v_i = lane flow rate for lane group i expressed in through passenger cars per hour per lane (tpc/h/ln);

Equation 31-160

$v_{adj,i}$ = equivalent through movement flow rate for lane group i (tpc/h); and

N_i = number of lanes associated with lane group i , accounting for de facto lanes (ln).

Step 4: Determine Critical Lane Groups

The critical lane groups are identified and the sum of critical-lane flow rates is determined in this step. Critical lane groups represent the unique combination of conflicting lane groups that have the highest total flow rate. These critical lane groups dictate the amount of green time required during each phase. They also dictate the total cycle length required for the intersection. The critical lane groups for the north–south and east–west approaches are assessed independently.

This step consists of three tasks. During the first task, the right-turn flow rate is adjusted to account for right-turn capacity during the complementary left-turn phase. During the second task, the critical lane groups are identified. During the third task, the critical-lane group flow rates are added to determine the sum of critical-lane flow rates.

Step 4a. Adjust Right-Turn Flow Rate

There may be situations in which an exclusive right-turn lane could have a higher flow rate than the adjacent through lane(s). In this situation, the right turns that could occur simultaneously with a protected left-turn movement from the cross street should be deducted from the right-turn flow rate. For example, if the exclusive northbound right-turn flow rate is 300 tpc/h/ln and the protected westbound left-turn flow rate is 125 tpc/h/ln, 125 northbound right-turn vehicles should be assumed to depart the intersection during the westbound left-turn phase. Thus, 125 should be deducted from the total northbound right-turn flow rate, resulting in an adjusted northbound right-turn flow rate of 175 tpc/h/ln. This adjustment is only necessary when the right-turn lane group is critical. If that is the case, the rules described in Step 4b should replace the through lane group flow rate with the right-turn lane group flow rate.

Step 4b. Identify Critical Lane Groups

The lane groups that are determined to be critical are identified in this task. The rules for making this determination are dependent on the left-turn operational mode and phase sequence. Each of the combinations addressed by the planning-level analysis application is discussed in the following paragraphs.

Protected operation—with left-turn phase. When opposing approaches use protected left-turn operation, there are two possible lane group combinations that could determine the critical-lane flow rate. Each combination comprises a left-turn lane group and its opposing through (or right-turn) lane group. The flow rate for each lane group pair is added. The maximum of these two sums defines the critical-lane flow rate. For the east–west approaches, the critical-lane flow rate is computed with Equation 31-161.

Equation 31-161

$$V_{c,prot,1} = \max \begin{bmatrix} v_{EBlt} + v_{WBth} \\ v_{WBlt} + v_{EBth} \end{bmatrix}$$

where

$V_{c,prot,1}$ = critical-lane flow rate for protected left-turn operation on the east–west approaches (tpc/h/ln), and

v_i = lane flow rate for lane group i ($i = EBlt$: eastbound left turn, $WBlt$: westbound left turn, $EBth$: eastbound through, $WBth$: westbound through) (tpc/h/ln).

The two lane groups that add to produce the largest critical-lane flow rate in Equation 31-161 represent the critical lane groups for the east–west street.

Similarly, for north–south approaches with protected left-turn operation, the critical-lane flow rate is computed with Equation 31-162.

Equation 31-162

$$V_{c,prot,2} = \max \begin{bmatrix} v_{NBlt} + v_{SBth} \\ v_{SBlt} + v_{NBth} \end{bmatrix}$$

where

$V_{c,prot,2}$ = critical-lane flow rate for protected left-turn operation on the north–south approaches (tpc/h/ln), and

v_i = lane flow rate for lane group i ($i = NBlt$: northbound left turn, $SBlt$: southbound left turn, $NBth$: northbound through, $SBth$: southbound through) (tpc/h/ln).

The two lane groups that add to produce the largest critical-lane flow rate in Equation 31-162 represent the critical lane groups for the north–south street.

Permitted operation—no left-turn phase. When opposing approaches use permitted operation, the critical-lane flow rate will be the highest lane flow rate of all lane groups associated with the pair of approaches. For the east–west approaches, the critical-lane flow rate is computed with Equation 31-163.

Equation 31-163

$$V_{c,perm,1} = \max (v_{EBlt}, v_{EBth}, v_{EBrt}, v_{WBlt}, v_{WBth}, v_{WBrt})$$

where

$V_{c,perm,1}$ = critical-lane flow rate for permitted left-turn operation on the east–west approaches (tpc/h/ln), and

v_i = lane flow rate for lane group i ($i = EBlt$: eastbound left turn, $WBlt$: westbound left turn, $EBth$: eastbound through, $WBth$: westbound through, $EBrt$: eastbound right turn, $WBrt$: westbound right turn) (tpc/h/ln).

The lane group that produces the largest critical-lane flow rate in Equation 31-163 represents the critical lane group for the east–west street.

Similarly, for north–south approaches with permitted left-turn operation, the critical-lane flow rate is computed with Equation 31-164.

Equation 31-164

$$V_{c,perm,2} = \max (v_{SBlt}, v_{SBth}, v_{SBrt}, v_{NBlt}, v_{NBth}, v_{NBrt})$$

where

$V_{c,perm,2}$ = critical-lane flow rate for permitted left-turn operation on the north-south approaches (tpc/h/ln), and

v_i = lane flow rate for lane group i ($i = SBlt$: southbound left turn, $NBlT$: northbound left turn, $SBth$: southbound through, $NBth$: northbound through, $SBrT$: southbound right turn, $NBrT$: northbound right turn) (tpc/h/ln).

The lane group that produces the largest critical-lane flow rate in Equation 31-164 represents the critical lane group for the north-south street.

Protected operation—split phasing. When opposing approaches use split phasing (i.e., when only one approach is served during a phase), the critical-lane flow rate for a given approach will be the highest lane flow rate of all lane groups for that approach. The critical-lane flow rate for the two opposing approaches will be the sum of the highest lane flow rate for each approach. For the east-west approaches, the critical-lane flow rate is computed with Equation 31-165.

$$V_{c,split,1} = \max(v_{EBlt}, v_{EBth}, v_{EBrt}) + \max(v_{WBlt}, v_{WBth}, v_{WBrt})$$

Equation 31-165

where $V_{c,split,1}$ is the critical-lane flow rate for split phasing on the east-west approaches (tpc/h/ln).

The two lane groups that add to produce the largest critical-lane flow rate in Equation 31-165 represent the critical lane groups for the east-west street.

Similarly, for the north-south approaches with split phasing, the critical-lane flow rate is computed with Equation 31-166.

$$V_{c,split,2} = \max(v_{SBlt}, v_{SBth}, v_{SBrT}) + \max(v_{NBlT}, v_{NBth}, v_{NBrT})$$

Equation 31-166

where $V_{c,split,2}$ is the critical-lane flow rate for split phasing on the north-south approaches (tpc/h/ln).

The two lane groups that add to produce the largest critical-lane flow rate in Equation 31-166 represent the critical lane groups for the north-south street.

Protected-permitted operation—with left-turn phase. If protected-permitted operation is to be evaluated, the analyst should refer to the supplemental procedure in the Protected-Permitted Left-Turn Operations subsection.

Step 4c. Calculate the Sum of Critical-Lane Flow Rates

Once the critical lane groups have been identified, the sum of critical-lane flow rates for the intersection can be computed by adding the lane flow rate associated with each critical lane group. Alternatively, the sum of critical-lane flow rates can be computed by adding the critical-lane group flow rate for each intersecting street, as calculated in the previous task. The following four cases illustrate this technique for some example combinations of left-turn operation and phase sequence using Equation 31-167 through Equation 31-170.

Case 1: East-west and north-south approaches use protected operation—with left-turn phase.

$$V_c = V_{c,prot,1} + V_{c,prot,2}$$

Equation 31-167

where V_c is the sum of the critical-lane flow rates (tpc/h/ln).

Case 2: East–west and north–south approaches use permitted operation—no left-turn phase.

Equation 31-168

$$V_c = V_{c,perm,1} + V_{c,perm,2}$$

Case 3: East–west approaches use protected operation—with left-turn phase and north–south approaches use permitted operation—no left-turn phase.

Equation 31-169

$$V_c = V_{c,prot,1} + V_{c,perm,2}$$

Case 4: East–west approaches use protected operation—with left-turn phase and north–south approaches use protected operation—split phasing.

Equation 31-170

$$V_c = V_{c,prot,1} + V_{c,split,2}$$

Step 4d. Identify Critical Phases

The critical phases identified in this task are used in Part II. If Part II is not part of the analysis, then this task can be skipped.

For this task, one critical phase is associated with each critical lane group, as identified in Step 4b. The flow rate that corresponds to a critical lane group (and critical phase i) is called the critical-lane flow rate $v_{c,i}$. By definition, the sum of these critical-lane flow rates equals the sum of critical-lane flow rates V_c .

For example, consider an intersection for which Equation 31-167 is determined to be applicable (i.e., the intersection has protected operation—with left-turn phase on both approaches). If the eastbound left-turn and westbound through phases are found to yield the critical-lane flow rate $V_{c,prot,1}$, then the eastbound left-turn phase and the westbound through phase are identified as critical phases. The critical-lane flow rates for the east–west approaches are $v_{c,EBlt}$ ($= v_{EBlt}$) and $v_{c,WBth}$ ($= v_{WBth}$).

Step 5: Determine Intersection Sufficiency

This step consists of four tasks. The first task is to determine the cycle length, and the second is to calculate intersection capacity. The third task is to compute the intersection volume-to-capacity ratio. The fourth task is to determine whether the intersection is operating under, near, or over its capacity.

If local data describing cycle length and base saturation flow rate are not available, then a default intersection capacity c_i of 1,650 tpc/h/ln can be used. This default value reflects a base saturation flow rate of 1,900 pc/h/ln, a lost time of 4.0 s per phase, and a cycle length equal to 30 s per critical phase. If the default intersection capacity is used, then the analyst can proceed to Step 5c.

Step 5a. Calculate Cycle Length

If cycle length is known, then the analyst can proceed to Step 5b.

For purposes of conducting a planning-level analysis, the analyst can assume a cycle length equal to 30 s for each critical phase. For example, an intersection with a protected left-turn phase for each of the eastbound and westbound approaches and permitted left-turn operation for the northbound and southbound approaches could be assumed to have a 90-s cycle length. The selection of a cycle length in practice should be based on consideration of

multiple factors including (a) local agency policies and practices and (b) needs of nonmotorized users.

Step 5b. Calculate Intersection Capacity

Intersection capacity is calculated with Equation 31-171.

$$c_I = s_o \frac{C - (n_{cp} l_t)}{C}$$

Equation 31-171

where

c_I = intersection capacity (tpc/h/ln),

s_o = base saturation flow rate (pc/h/ln),

C = cycle length (s),

n_{cp} = number of critical phases, and

l_t = phase lost time (s).

A default phase lost time of 4.0 s for each critical phase is recommended. A default value for base saturation flow rate can be obtained from Exhibit 19-11.

Step 5c. Calculate the Intersection Volume-to-Capacity Ratio

The critical intersection volume-to-capacity ratio is calculated with Equation 31-172.

$$X_c = \frac{V_c}{c_I}$$

Equation 31-172

where

X_c = critical intersection volume-to-capacity ratio,

V_c = sum of critical-lane flow rates (tpc/h/ln), and

c_I = intersection capacity (tpc/h/ln).

Step 5d. Assess Intersection Sufficiency

The objective of this task is to assess the sufficiency of the intersection in terms of its ability to accommodate a given demand level. Exhibit 31-37 provides guidance for determining whether an intersection is operating under, near, or over its available capacity.

The analyst may stop at this point or may continue with Part II to determine delay and LOS.

Exhibit 31-37
 Planning-Level Analysis:
 Intersection Volume-to-
 Capacity Ratio Assessment
 Levels

Critical Intersection Volume-to-Capacity Ratio	Description	Capacity Assessment
<0.85	All demand is able to be accommodated; delays are low to moderate.	Under
0.85–0.98	Demand for critical lane groups is near capacity and some lane groups require more than one cycle to clear the intersection; all demand is able to be processed within the analysis period; delays are moderate to high.	Near
>0.98	Demand for critical lane groups is just able to be accommodated within a cycle but often requires multiple cycles to clear the intersection; delays are high and queues are long.	Over

Part II: Delay and Level of Service

Part II builds on the results of Part I by allowing the user to calculate capacity, delay, and LOS.

Step 6: Calculate Capacity

This step consists of two tasks. For the first task, the analyst calculates the effective green time for each critical phase. For the second task, the analyst calculates the volume-to-capacity ratio for each lane group.

Step 6a. Calculate Effective Green Times

If the effective green time for each critical phase is known, then the analyst can proceed to Step 6b.

The total effective green time available for all critical phases is equal to the cycle length minus the total lost time per cycle. This calculation is shown in Equation 31-173.

Equation 31-173

$$g_{tot} = C - (n_{cp}l_t)$$

where

g_{tot} = total effective green time in the cycle (s),

C = cycle length (s),

n_{cp} = number of critical phases, and

l_t = phase lost time (s).

A default phase lost time of 4.0 s for each critical phase is recommended.

The total effective green time is allocated to each critical phase in proportion to the lane flow rate for each critical phase. Equation 31-174 is used to compute the effective green time for a given critical lane group.

Equation 31-174

$$g_{c,i} = g_{tot} \left(\frac{v_{c,i}}{V_c} \right)$$

where

$g_{c,i}$ = effective green time for critical lane group i (s),

g_{tot} = total effective green time in the cycle (s),

$v_{c,i}$ = lane flow rate for critical lane group i (tpc/h/ln), and
 V_c = sum of the critical-lane flow rates (tpc/h/ln).

The effective green time for a noncritical lane group is set equal to the effective green time for its counterpart critical lane group that occurs concurrently during the same phase.

Finally, the effective green time g_i for each phase i is set equal to the effective green time that is computed for the corresponding lane group. The effective green time computed in this manner should be reviewed against policy requirements and other considerations (such as the minimum green time based on driver expectancy and the time required for pedestrians to cross the approach).

Step 6b. Calculate Capacity and Volume-to-Capacity Ratios

The lane group capacity and volume-to-capacity ratio can be computed with Equation 31-175 and Equation 31-176, respectively.

$$c_i = s_o N_i \frac{g_i}{C}$$

$$X_i = \frac{N_i v_i}{c_i}$$

Equation 31-175

Equation 31-176

where

- c_i = capacity of lane group i (tpc/h);
- g_i = effective green time for lane group i (s);
- N_i = number of lanes associated with lane group i , accounting for de facto lanes (ln);
- X_i = volume-to-capacity ratio for lane group i ;
- v_i = lane flow rate for lane group i (tpc/h/ln); and
- C = cycle length (s).

The capacity for each lane group is based on the base saturation flow rate s_o . A default value for base saturation flow rate can be obtained from Exhibit 19-11. This rate is not adjusted for parking activity, heavy vehicles, and so forth because these adjustments are applied in Step 2 to the lane group flow rate.

Equation 31-177 and Equation 31-178 can be used to compute the intersection capacity and intersection volume-to-capacity ratio, respectively.

$$c_{sum} = s_o \frac{\sum_{i=1}^{n_{cp}} g_{c,i}}{C}$$

$$X_c = \frac{V_c}{c_{sum}}$$

Equation 31-177

Equation 31-178

where c_{sum} is the intersection capacity (tpc/h/ln).

Step 7: Determine Delay and Level of Service

The control delay for each lane group is calculated by using Equation 31-179 with Equation 31-180 and Equation 31-181.

Equation 31-179

$$d_i = d_{1,i} + d_{2,i}$$

with

Equation 31-180

$$d_{1,i} = PF_i \frac{0.5 C (1 - g_i/C)^2}{1 - [\min(1, X_i) g_i/C]}$$

Equation 31-181

$$d_{2,i} = 225 \left[(X_i - 1) + \sqrt{(X_i - 1)^2 + \frac{16 X_i}{c_i}} \right]$$

where

d_i = control delay for lane group i (s/veh),

$d_{1,i}$ = uniform delay for lane group i (s/veh),

$d_{2,i}$ = incremental delay for lane group i (s/veh),

PF_i = progression adjustment factor for lane group i , and

all other variables are as previously defined.

The progression adjustment factor describes the arrival distribution for the subject lane group, which may be influenced by an upstream traffic signal. Recommended progression adjustment factors are shown in Exhibit 31-38.

Exhibit 31-38

Planning-Level Analysis:
Progression Adjustment
Factor

Quality of Progression	Conditions That Describe Arrivals Associated with the Subject Lane Group	Progression Factor PF
Good progression	(a) Vehicles arrive in platoons during the green interval, OR (b) most vehicles arrive during the green interval.	0.70
Random arrivals (default)	(a) The phase serving the subject lane group is not coordinated with the upstream traffic signal, OR (b) the intersection is sufficiently distant from other signalized intersections as to be considered isolated.	1.00
Poor progression	(a) Vehicles arrive in platoons during the red interval, OR (b) most vehicles arrive during the red indication.	1.25

Lane group delay may be aggregated for each approach and for the intersection as a whole. The aggregation process is the same as that in the motorized vehicle methodology in Chapter 19 using Equation 19-28 and Equation 19-29.

Delay values may be compared with the criteria in Exhibit 19-8 to determine the LOS for a lane group, approach, or the intersection as a whole.

Protected-Permitted Left-Turn Operations

The procedure described in this subsection applies to the analysis of protected-permitted left-turn operation. The effective green time is a required input data item. If it is known or can be estimated, then the supplemental guidance in this subsection can be used with the planning-level analysis application.

Step 2: Convert Movement Volumes to Through Passenger-Car Equivalents

The guidance provided in this subsection supplements that provided in Step 2 of the planning-level analysis application. The objective is to compute an

equivalency factor for protected-permitted left-turn operation that reflects the left-turn vehicle's overall effect on operations.

A single left-turn equivalency factor is computed for both the protected and the permitted time periods. Exhibit 31-33 is used to identify the equivalency factor for protected left-turn operation during the left-turn phase. It is also used to identify the equivalency factor for permitted left-turn operation during the through phase. A single factor is calculated that weighs these two equivalency factors in proportion to the effective green times of each time period. Equation 31-182 is used to compute the single equivalency factor for left turns.

$$E_{LT} = \frac{E_{LT,pt} g_{lt,pt} + E_{LT,pm} g_{lt,pm}}{g_{lt,pt} + g_{lt,pm}}$$

Equation 31-182

where

E_{LT} = equivalency factor for left turns,

$E_{LT,pt}$ = equivalency factor for protected left-turn operation,

$E_{LT,pm}$ = equivalency factor for permitted left-turn operation,

$g_{lt,pt}$ = effective green time for the protected left-turn phase (s), and

$g_{lt,pm}$ = effective green time for permitted left-turn operation during the through phase (s).

The equivalency factor computed with Equation 31-182 is used in Equation 31-157 to compute the equivalent through movement flow rate for the left-turn lane group. The effective green time for the first time period of the protected-permitted operation includes the yellow interval that occurs between the two periods.

Step 4: Determine Critical Lane Groups

The guidance provided in this subsection supplements that provided in Step 4 of the planning-level analysis application. The objective is to compute the left-turn lane flow rate during the protected left-turn phase and then use this value to identify the critical lane groups.

The equivalent through-car flow rate in the left lane during the protected left-turn phase is estimated by distributing the lane flow rate for the left-turn lane group proportionally among the protected and permitted periods. The flow rate for the protected left-turn period is computed with Equation 31-183.

$$v_{lt,pt} = v_{lt} \frac{g_{lt,pt}}{g_{lt,pt} + g_{lt,pm}}$$

Equation 31-183

where

$v_{lt,pt}$ = lane flow rate for the left-turn lane group during the protected left-turn phase (tpc/h/ln), and

v_{lt} = lane flow rate for the left-turn lane group (tpc/h/ln).

In the process of identifying the critical lane groups (and related flow rate), only the lane flow rate during the protected left-turn phase $v_{lt,pl}$ is used for the left-turn lane group. The critical-lane flow rate is then determined by using the rules described for protected operation—with left-turn phase in Step 4b above.

The remainder of the planning-level analysis application does not change. In Step 7, the lane flow rate for the left-turn lane group v_{lt} is used to determine the delay and LOS.

WORKSHEETS

This subsection includes a series of worksheets that can be used to document an application of the planning-level analysis application. These worksheets are as follows:

- Input Worksheet (Exhibit 31-39),
- Left-Turn Treatment Worksheet (Exhibit 31-40),
- Intersection Sufficiency Worksheet (Exhibit 31-41), and
- Delay and LOS Worksheet (Exhibit 31-42).

Exhibit 31-39
Planning-Level Analysis: Input Worksheet

PLANNING-LEVEL ANALYSIS: INPUT WORKSHEET												
General Information						Site Information						
Analyst						Intersection						
Agency or Company						Jurisdiction						
Date Performed						Analysis Year						
Analysis Time Period												
Intersection Geometry												
Volume and Signal Input												
	EB			WB			NB			SB		
	LT	TH	RT	LT	TH	RT	LT	TH	RT	LT	TH	RT
Required Data												
Volume (veh/h)												
Number of lanes												
Lane use (exclusive or shared)												
Optional Data¹												
Heavy vehicles (%)												
On-street parking presence (no, yes)												
Pedestrian activity (none, low, med., high, extreme)												
Left-turn operation and phase sequence ²												
Effective green time (s) ^{3,4}												
Progression quality (good, random, poor) ⁴												
Peak hour factor		Cycle length (s)		Base saturation flow rate (pc/h/ln)								
Notes												
<ol style="list-style-type: none"> 1. Optional input data (guidance is provided for estimating these data if they are not known). 2. Combinations addressed: (a) protected operation—with left-turn phase, (b) permitted operation—no left-turn phase, (c) protected operation—split phasing, (d) protected-permitted operation—with left-turn phase 3. Data required for Part I analysis if "protected-permitted operation—with left-turn phase" is present. 4. Data required for Part II analysis. 												

Exhibit 31-40
 Planning-Level Analysis: Left-Turn Treatment Worksheet

PLANNING-LEVEL ANALYSIS: LEFT-TURN TREATMENT WORKSHEET														
General Information														
Description _____														
Check # 1. Left-Turn Lane Check														
Approach	EB	WB	NB	SB										
Number of left-turn lanes														
Protected left turn (Y or N)?														
If the number of left-turn lanes on any approach exceeds 1, then it is recommended that the left turns on that the approach be protected. Those approaches with protected left turns need not be evaluated in subsequent checks.														
Check # 2. Minimum Volume Check														
Approach	EB	WB	NB	SB										
Left-turn volume														
Protected left turn (Y or N)?														
If left-turn volume on any approach exceeds 240 veh/h, then it is recommended that the left turns on that the approach be protected. Those approaches with protected left turns need not be evaluated in subsequent checks.														
Check # 3. Minimum Cross-Product Check														
Approach	EB	WB	NB	SB										
Left-turn volume, V_L (veh/h)														
Opposing mainline volume, V_o (veh/h)														
Cross product ($V_L * V_o$)														
Opposing through lanes														
Protected left turn (Y or N)?														
<table border="0" style="width: 100%; text-align: center;"> <tr> <td colspan="2">Minimum Cross-Product Values for Recommending Left-Turn Protection</td> </tr> <tr> <td><u>Number of Through Lanes</u></td> <td><u>Minimum Cross Product</u></td> </tr> <tr> <td>1</td> <td>50,000</td> </tr> <tr> <td>2</td> <td>90,000</td> </tr> <tr> <td>3</td> <td>110,000</td> </tr> </table>					Minimum Cross-Product Values for Recommending Left-Turn Protection		<u>Number of Through Lanes</u>	<u>Minimum Cross Product</u>	1	50,000	2	90,000	3	110,000
Minimum Cross-Product Values for Recommending Left-Turn Protection														
<u>Number of Through Lanes</u>	<u>Minimum Cross Product</u>													
1	50,000													
2	90,000													
3	110,000													
If the cross product on any approach exceeds the above values, then it is recommended that the left turns on that approach be protected. Those approaches with protected left turns need not be evaluated in subsequent checks.														
Notes														
1. If any approach is recommended for left-turn protection but the analyst evaluates it as having permitted operation, then the planning-level analysis method may give overly optimistic results. The analyst should instead use the automobile methodology described in Chapter 19, Signalized Intersections. 2. All volumes used in this worksheet are unadjusted hourly volumes.														

PLANNING-LEVEL ANALYSIS: INTERSECTION SUFFICIENCY WORKSHEET						
General Information						
Description:						
East-West Approaches						
	Eastbound			Westbound		
	Left	Through	Right	Left	Through	Right
Movement volume, V (veh/h)						
Equivalency factor for heavy vehicles, E_{HV}						
Equivalency factor for peaking char., E_{PHF}						
Equivalency factor for right turns, E_{RT}						
Equivalency factor for left turns, E_{LT}^{-1}						
Equivalency factor for parking activity, E_p						
Equivalency factor for lane utilization, E_{LU}						
Equivalency factor for other conditions, E_{other}						
Equivalent through mvmt. flow rate (tpc/h) v_{adj} $= V E_{HV} E_{PHF} E_{LT} E_{RT} E_p E_{LU} E_{other}$						
Number of lanes, N						
Lane flow rate, v (tpc/h/ln) $v = v_{adj} / N$						
Critical lane flow rate, V_c (tpc/h/ln)						
Critical lane group (indicate with "X")						
Critical lane group flow rate, v_c (tpc/h/ln)						
Supplemental Calculations for Protected-Permitted Operation						
Equivalency factor for prot. left turn, $E_{LT,pt}$						
Equivalency factor for perm. left turn, $E_{LT,pm}$						
Effective green for prot. left turn, $g_{lt,pt}$ (s)						
Effective green for perm. left turn, $g_{lt,pm}$ (s)						
Equivalency factor for left turns, E_{LT} $E_{LT} = (E_{LT,pt} g_{lt,pt} + E_{LT,pm} g_{lt,pm}) / (g_{lt,pt} + g_{lt,pm})$						
North-South Approaches						
	Northbound			Southbound		
	Left	Through	Right	Left	Through	Right
Movement volume, V (veh/h)						
Equivalency factor for heavy vehicles, E_{HV}						
Equivalency factor for peaking char., E_{PHF}						
Equivalency factor for right turns, E_{RT}						
Equivalency factor for left turns, E_{LT}^{-1}						
Equivalency factor for parking activity, E_p						
Equivalency factor for lane utilization, E_{LU}						
Equivalency factor for other conditions, E_{other}						
Equivalent through mvmt. flow rate (tpc/h) v_{adj} $= V E_{HV} E_{PHF} E_{LT} E_{RT} E_p E_{LU} E_{other}$						
Number of lanes, N						
Lane flow rate, v (tpc/h/ln) $v = v_{adj} / N$						
Critical lane flow rate, V_c (tpc/h/ln)						
Critical lane group (indicate with "X")						
Critical lane group flow rate, v_c (tpc/h/ln)						
Supplemental Calculations for Protected-Permitted Operation						
Equivalency factor for prot. left turn, $E_{LT,pt}$						
Equivalency factor for perm. left turn, $E_{LT,pm}$						
Effective green for prot. left turn, $g_{lt,pt}$ (s)						
Effective green for perm. left turn, $g_{lt,pm}$ (s)						
Equivalency factor for left turns, E_{LT} $E_{LT} = (E_{LT,pt} g_{lt,pt} + E_{LT,pm} g_{lt,pm}) / (g_{lt,pt} + g_{lt,pm})$						
Intersection Sufficiency Assessment						
Number of critical phases, n_{cp}		Intersection capacity, c_I (tpc/h/ln) $c_I = s_o [C - (n_{cp} 4.0)] / C$				
Sum of critical lane flow rates, V_c (tpc/h/ln)		Critical intersection vol.-to-capacity ratio, X_c $X_c = V_c / c_I$				
Intersection status (relationship to capacity)		Under ___ Near ___ Over ___				
Note						
1. If the approach has protected-permitted operation, use the supplemental calculations section to compute E_{LT} .						

Exhibit 31-41
Planning Level Analysis:
Intersection Sufficiency
Worksheet

Exhibit 31-42
 Planning-Level Analysis: Delay
 and LOS Worksheet

PLANNING-LEVEL ANALYSIS: DELAY AND LOS WORKSHEET								
General Information								
Description _____								
Green Time Calculation								
Total effective green time, g_{tot} (s) $g_{tot} = C - (n_{cp} \cdot 4.0)$								
East-West Approaches								
	Eastbound			Westbound				
	Left	Through	Right	Left	Through	Right		
Critical lane group flow rate, v_c (tpc/h/ln) ¹								
Effective green time for critical lane group, g_c (s) $g_c = g_{tot} \cdot v_c / V_c$								
	Phase No. 1		Phase No. 2		Phase No. 3			
Effective green time, g (s)								
North-South Approaches								
	Northbound			Southbound				
	Left	Through	Right	Left	Through	Right		
Critical lane group flow rate, v_c (tpc/h/ln) ¹								
Effective green time for critical lane group, g_c (s) $g_c = g_{tot} \cdot v_c / V_c$								
	Phase No. 1		Phase No. 2		Phase No. 3			
Effective green time, g (s)								
Control Delay and LOS								
	EB		WB		NB		SB	
Lane group								
Effective green time, g (s)								
Green-to-cycle-length ratio, g/C								
Number of lanes, N^1								
Lane group capacity, c (veh/h) $c = 1900 N g/C$								
Lane flow rate, v (tpc/h/ln) ¹								
Volume-to-capacity ratio, X $X = (N v)/c$								
Progression adjustment factor, PF								
Uniform delay, d_1 (s/veh)								
Incremental delay, d_2 (s/veh)								
Control delay, $d = d_1 + d_2$ (s/veh)								
Approach delay, d_A (s/veh) $d_A = \Sigma(d N v) / \Sigma(N v)$								
Approach flow rate, V_A (veh/h)								
Intersection delay, d_I (s/veh) $d_I = \Sigma(d_A V_A) / \Sigma V_A$			Intersection LOS (Exhibit 19-8)					
Intersection capacity, c_{sum} (tpc/h/ln) $c_{sum} = 1900 (\Sigma g_c) / C$			Critical intersection vol.-to-capacity ratio, X_c $X_c = V_c / c_{sum}$					
Notes								
1. Value obtained from the Intersection Sufficiency Worksheet.								

6. FIELD MEASUREMENT TECHNIQUES

This section describes two techniques for estimating key traffic characteristics by using field data. The first subsection describes a technique for estimating control delay. The second subsection describes a technique for estimating saturation flow rate.

FIELD MEASUREMENT OF INTERSECTION CONTROL DELAY

Delay can be measured at existing intersections as an alternative to estimating delay by using the motorized vehicle methodology in Chapter 19, Signalized Intersections. Various techniques can be used for measuring delay, including a test-car survey, vehicle path tracing, input–output analysis, and queue counting. The first three techniques tend to require more time to implement than the last technique, but they provide more accurate delay estimates. They are often limited to sampling when implemented manually. They may be more appropriate when oversaturated conditions are present. The first two techniques can be used to estimate delay on either a movement basis or a lane group basis. The last two techniques are more amenable to delay measurement on a lane group basis.

The queue-count technique is recommended for control delay measurement. It is based on direct observation of vehicle-in-queue counts for a subject lane group. It normally requires two field personnel for each lane group surveyed. Also needed are (a) a multifunction digital watch that includes a countdown-repeat timer, with the countdown interval in seconds; and (b) a volume-count board with at least two tally counters. Alternatively, a laptop computer can be programmed to emit audio count markers at user-selected intervals, take volume counts, and execute real-time delay computations.

The queue-count technique is applicable to all undersaturated lane groups. Significant queue buildup can make the technique impractical for oversaturated lane groups or lane groups with limited storage length. If queues are lengthy, then the technique should be modified by subdividing the lane group into manageable segments (or zones) and assigning an observer to each zone. Each observer then counts queued vehicles in his or her assigned zone.

If queues are lengthy or the volume-to-capacity ratio is near 1.0, then care must be taken to continue the vehicle-in-queue count past the end of the arrival count period, as detailed in subsequent paragraphs. This extended counting period is required for consistency with the analytic delay equation used in the chapter text.

The queue-count technique does not directly measure delay during deceleration and during a portion of acceleration. These delay elements are very difficult to measure without sophisticated tracking equipment. Nevertheless, this technique has been shown to yield a reasonable estimate of control delay by application of appropriate adjustment factors (8, 9). One adjustment factor accounts for sampling errors that may occur. Another factor accounts for

unmeasured acceleration–deceleration delay. This adjustment factor is a function of the number of vehicles in queue each cycle and the approach speed.

Approach Speed

Exhibit 31-43 shows a worksheet that can be used for recording observations and computing control delay for the subject lane group. Before starting the survey, observers need to estimate the average approach speed during the study period. Approach speed is the speed at which vehicles would pass unimpeded through the intersection if the signal were green for an extended period and volume was light. This speed may be obtained by driving through the intersection a few times when the signal is green and there is no queue. The approach speed is recorded at an upstream location that is least affected by the operation of the subject signalized intersection as well as the operation of any other signalized intersection.

Survey Period

The duration of the survey period must be clearly defined in advance so the last arriving vehicle or vehicles that stop in the period can be identified and counted until they exit the intersection. It is logical to define the survey period on the basis of the same considerations used to define an evaluation analysis period (as described in Section 3 of Chapter 19). A typical survey period is 15 min.

Count Interval

The survey technique is based on recording a vehicle-in-queue count at specific points in time. A count interval in the range of 10 to 20 s has been found to provide a good balance between delay estimate precision and observer capability. The actual count interval selected from this range is based on consideration of survey period duration and the type of control used at the intersection.

The count interval *should* be an integral divisor of the survey period duration. This characteristic ensures that a complete count of events is taken for the full survey period. It also allows easier coordination of observer tasks during the field study. For example, if the study period is 15 min, the count interval can be 10, 12, 15, 18, or 20 s.

If the intersection has pretimed or coordinated-actuated control, the count interval *should not* be an integral divisor of the cycle length. This characteristic eliminates potential survey bias due to queue buildup in a cyclical pattern. For example, if the cycle length is 120 s, the count interval can be 11, 13, 14, 16, 17, 18, or 19 s.

If the intersection has actuated control, the count interval may be chosen as the most convenient value for conducting the field survey with consideration of survey period duration.

stopped vehicle and is itself about to stop. This definition is used because of the difficulty of keeping track of the moment when a vehicle comes to a stop.

2. At the start of each count interval, Observer 1 records the number of vehicles in queue in all lanes of the subject lane group. The countdown-repeat timer on a digital watch can be used to signal the count time. This count includes vehicles that arrive when the signal is actually green but stop because queued vehicles ahead have not yet started moving. All vehicles that join a queue are included in the vehicle-in-queue count until they “exit” the intersection. A through vehicle exits the intersection when its rear axle crosses the stop line. A turning vehicle exits the intersection the instant it clears the opposing through traffic (or pedestrians to which it must yield) and begins accelerating back to the approach speed. The vehicle-in-queue count often includes some vehicles that have regained speed but have not yet exited the intersection.
3. Observer 1 records the vehicle-in-queue count in the appropriate count-interval box on the worksheet. Ten boxes are provided for each “count cycle” (note that a count cycle is not the same as a signal cycle). Any number of boxes can be used to define the count cycle; however, as many as possible should be used to ensure best use of worksheet space. The clock time at the start of the count cycle is recorded in the first (far-left) column. The count cycle number is recorded in the second column of the sheet.
4. At the end of the survey period, Observer 1 continues taking vehicle-in-queue counts for all vehicles that arrived during the survey period until all of them have exited the intersection. This step requires the observer to make a mental note of the last stopping vehicle that arrived during the survey period in each lane of the lane group and continue the vehicle-in-queue counts until the last stopping vehicle or vehicles, plus all vehicles in front of the last stopping vehicle(s), exit the intersection. Stopping vehicles that arrive after the end of the survey period are not included in the final vehicle-in-queue counts.

Observer 2 Tasks

5. Observer 2 maintains three counts during the survey period. The first is a count of the vehicles that arrive during the survey period. The second is a count of the vehicles that arrive during the survey period and that stop one or more times. A vehicle stopping multiple times is counted only once as a stopping vehicle. The third count is the count of signal cycles, as measured by the number of times the red indication is presented for the subject lane group. For lane groups with a turn movement and protected or protected-permitted operation, the protected red indication is used for this purpose. If the survey period does not start or end at the same time as the presentation of a red indication, then the number of count intervals that occur in the interim can be used to estimate the fraction of the cycle that occurred at the start or end of the survey period.
6. Observer 2 enters all counts in the appropriate boxes on the worksheet.

Data Reduction Tasks

7. Sum each column of vehicle-in-queue counts, then sum the column totals for the entire survey period.
8. A vehicle recorded as part of a vehicle-in-queue count is assumed to be in queue, on average, for the time interval between counts. On this basis, the average time in queue per vehicle arriving during the survey period is estimated with Equation 31-184.

$$d_{vq} = 0.9 \left(I_s \frac{\sum V_{iq}}{V_{tot}} \right)$$

Equation 31-184

where

d_{vq} = time in queue per vehicle (s/veh),

I_s = interval between vehicle-in-queue counts (s),

$\sum V_{iq}$ = sum of vehicle-in-queue counts (veh), and

V_{tot} = total number of vehicles arriving during the survey period (veh).

The 0.9 adjustment factor in Equation 31-184 accounts for the errors that may occur when the queue-count technique is used to estimate delay. Research has shown the adjustment factor value is fairly constant for a variety of conditions (8).

9. Compute the fraction of vehicles stopping and the average number of vehicles stopping per lane in each signal cycle, as indicated on the worksheet.
10. Use Exhibit 31-44 to look up the correction factor appropriate to the lane group approach speed and the average number of vehicles stopping per lane in each cycle. This factor adjusts for deceleration and acceleration delay, which cannot be measured directly with manual techniques (9).

Approach Speed (mi/h)	Acceleration–Deceleration Correction Factor CF (s/veh) As a Function of the Average Number of Vehicles Stopping		
	≤ 7 veh/ln/cycle	8–19 veh/ln/cycle	20–30 veh/ln/cycle ^a
≤ 37	+5	+2	-1
>37–45	+7	+4	+2
>45	+9	+7	+5

Exhibit 31-44
Acceleration–Deceleration Correction Factor

Note: ^a Vehicle-in-queue counts in excess of about 30 veh/ln/cycle are typically unreliable.

11. Multiply the correction factor by the fraction of vehicles stopping. Add this product to the time-in-queue value from Task 2 to obtain the estimate of control delay for the subject lane group.

Example Application

Exhibit 31-45 presents sample data for a lane group during a 15-min survey period. The intersection has a 115-s cycle. A 15-s count interval is selected because 15 is not an integral divisor of the cycle length, but it is an integral divisor of the survey period.

Concepts

The saturation flow rate represents the maximum rate of flow in a traffic lane, as measured at the stop line during the green indication. It is usually achieved after 10 to 14 s of green, which corresponds to the front axle of the fourth to sixth queued passenger car crossing the stop line.

The base saturation flow rate represents the saturation flow rate for a traffic lane that is 12 ft wide and has no heavy vehicles, a flat grade, no parking, no buses that stop at the intersection, even lane utilization, and no turning vehicles. It is usually stable over a period of time in a given area and normally exhibits a relatively narrow distribution among intersections in that area.

The prevailing saturation flow rate is the rate measured in the field for a specific lane group at a specific intersection. It may vary significantly among intersections with similar lane groups because of differences in lane width, traffic composition (i.e., percentage of heavy vehicles), grade, parking, bus stops, lane use, and turning vehicle operation. If the intersections are located in different areas, then the prevailing saturation flow rate may also vary because of areawide differences in the base saturation flow rate.

The adjusted saturation flow rate is the rate computed by the procedure described in Chapter 19. It represents an estimate of the prevailing saturation flow rate. It can vary among intersections for the same reasons as stated above for the prevailing saturation flow rate. Any potential bias in the estimate is minimized by local calibration of the base saturation flow rate.

The prevailing saturation flow rate and the adjusted saturation flow rate are both expressed in units of vehicles. As a result, their value reflects the traffic composition in the subject traffic lane. In contrast, the base saturation flow rate is expressed in units of passenger cars and does not reflect traffic composition.

Measurement Technique

This subsection describes the technique for measuring the prevailing saturation flow rate for a given traffic lane. In general, vehicles are recorded when their front axles cross the stop line. The measurement period starts at the beginning of the green interval or when the front axle of the first vehicle in the queue passes the stop line. Saturation flow rate is calculated only from the data recorded after the fourth vehicle in the queue passes the stop line.

The vehicle's front axle, the stop line, and the time the fourth queued vehicle crosses the stop line represent three key reference points for saturation flow measurement. These three reference points must be maintained to ensure consistency with the procedure described in Chapter 19 and to facilitate comparability of results with other studies. The use of other reference points on the vehicle, on the road, or in time may yield different saturation flow rates.

If the stop line is not visible or if vehicles consistently stop beyond the stop line, then an alternative reference line must be established. This reference line should be established just beyond the typical stopping position of the first queued vehicle. Vehicles should consistently stop behind this line. Observation of several cycles before the start of the study should be sufficient to identify this substitute reference line.

The following paragraphs describe the tasks associated with a single-lane saturation flow survey. A two-person field crew is recommended. However, one person with a tape recorder, push-button event recorder, or a notebook computer with appropriate software will suffice. The field notes and tasks identified in the following paragraphs must be adjusted according to the type of equipment used. A sample field worksheet for recording observations is included as Exhibit 31-47.

Exhibit 31-47
Saturation Flow Rate Field Study Worksheet

FIELD SATURATION FLOW RATE STUDY WORKSHEET																		
General Information									Site Information									
Analyst _____ Agency or Company _____ Date Performed _____ Analysis Time Period _____									Intersection _____ Area Type <input type="checkbox"/> CBD <input type="checkbox"/> Other Jurisdiction _____ Analysis Year _____									
Lane Movement Input																		
Input Field Measurement																		
Veh. in queue	Cycle 1			Cycle 2			Cycle 3			Cycle 4			Cycle 5			Cycle 6		
	Time	HV	T	Time	HV	T	Time	HV	T	Time	HV	T	Time	HV	T	Time	HV	T
1																		
2																		
3																		
4																		
5																		
6																		
7																		
8																		
9																		
10																		
11																		
12																		
13																		
14																		
15																		
16																		
17																		
18																		
19																		
20																		
End of saturation	██████████			██████████			██████████			██████████			██████████			██████████		
End of green	██████████			██████████			██████████			██████████			██████████			██████████		
No. veh. > 20																		
No. veh. on yellow																		
Glossary and Notes																		
HV = Heavy vehicles (vehicles with more than 4 tires on pavement) T = Turning vehicles (L = Left, R = Right) Pedestrians and buses that block vehicles should be noted with the time that they block traffic, for example, P12 = Pedestrians blocked traffic for 12 s B15 = Bus blocked for 15 s																		

General Tasks

Measure and record the area type as well as the width and grade of the lane being studied. Enter these data in the lane movement input section of the field worksheet.

Select an observation point where the roadway reference line (e.g., stop line) for the surveyed lane and the corresponding signal heads are clearly visible. When a vehicle crosses this line unimpeded, it has entered the intersection conflict space for the purpose of saturation flow measurement. Left- or right-turning vehicles yielding to opposing through traffic or yielding to pedestrians are not recorded until they proceed through the opposing traffic or pedestrians.

Recorder Tasks

During the measurement period, note the last vehicle in the stopped queue when the signal turns green. Describe the last vehicle to the timer. Note on the worksheet which vehicles are heavy vehicles and which vehicles turn left or right. Record the time called out by the timer.

Timer Tasks

Start the stopwatch at the beginning of the green indication and notify the recorder. Count aloud each vehicle in the queue as its front axle crosses the stop line and note the time of crossing. Call out the time of the fourth, 10th, and last vehicle in the stopped queue as its front axle crosses the stop line.

If queued vehicles are still entering the intersection at the end of the green interval, call out “saturation through the end of green—last vehicle was number XX.” Note any unusual events that may have influenced the saturation flow rate, such as buses, stalled vehicles, and unloading trucks.

The period of saturation flow begins when the front axle of the fourth vehicle in the queue crosses the roadway reference line (e.g., stop line) and ends when the front axle of the last queued vehicle crosses this line. The last queued vehicle may be a vehicle that joined the queue during the green indication.

Data Reduction

Measurements are taken cycle by cycle. To reduce the data for each cycle, the time recorded for the fourth vehicle is subtracted from the time recorded for the last vehicle in the queue. This value represents the sum of the headways for the fifth through n th vehicle, where n is the number of the last vehicle surveyed (which may not be the last vehicle in the queue). This sum is divided by the number of headways after the fourth vehicle [i.e., divided by $(n - 4)$] to obtain the average headway per vehicle under saturation flow. The saturation flow rate is 3,600 divided by this average headway.

For example, if the time for the fourth vehicle was observed as 10.2 s and the time for the 14th and last vehicle surveyed was 36.5 s, the average saturation headway per vehicle is as follows:

$$\frac{(36.5 - 10.2)}{(14 - 4)} = \frac{26.3}{10} = 2.63 \text{ s/veh}$$

The prevailing saturation flow rate in that cycle is as follows:

$$\frac{3,600}{2.63} = 1,369 \text{ veh/h/ln}$$

To obtain a statistically significant value, a minimum of 15 signal cycles (each with more than eight vehicles in the initial queue) is typically required. The average of the saturation headway per vehicle values from the individual cycles is divided into 3,600 to obtain the prevailing saturation flow rate for the surveyed lane. The percentage of heavy vehicles and turning vehicles in the sample should be determined and noted for reference.

Calibration Technique

This subsection describes a technique for quantifying the base saturation flow rate at a local level. It consists of three tasks. The first task entails measuring the prevailing saturation flow rate at representative locations in the local area. The second task requires the calculation of an adjusted saturation flow rate for the same locations where a prevailing saturation flow rate was measured. The third task combines the information to compute the local base saturation flow rate.

This technique will require some resource investment by the agency. However, it should need to be completed only once every few years. In fact, it should be repeated only when there is evidence of a change in local driver behavior. The benefit of this calibration activity will be realized by the agency in terms of more accurate estimates of motorized vehicle performance, which should translate into more effective decisions related to infrastructure investment and system management.

Task 1. Measure Prevailing Saturation Flow Rate

This task requires measuring the prevailing saturation flow rate of one or more lane groups at each of several representative intersections in the local area. The minimum number of lane groups needed in the data set is difficult to judge for all situations; however, it should reflect a statistically valid sample. The data set should also provide a reasonable geographic and physical representation of the population of signalized intersections in the local area.

The lane groups for which the prevailing saturation flow rate is measured should include a representative mix of left-turn, through, and right-turn lane groups. It should not include left-turn lane groups that operate in the permitted or the protected-permitted mode or right-turn lane groups that have protected-permitted operation. These lane groups are excluded because of the complex nature of permitted and protected-permitted operation. The saturation flow rate for these lane groups tends to have a large amount of random variation that makes it more difficult to quantify the local base saturation flow rate with an acceptable level of precision.

Once the set of lane groups is identified, the technique described in the previous subsection is used to measure the prevailing saturation flow rate at each location.

Task 2. Compute Adjusted Saturation Flow Rate

For this task, the saturation flow rate calculation procedure in Chapter 19 is used to compute the adjusted saturation flow rate for each lane group in the data set. If a lane group is at an intersection with actuated control for one or more phases, the motorized vehicle methodology (as opposed to just the saturation flow rate procedure) will be needed to compute the adjusted saturation flow rate accurately. Regardless, the base saturation flow rate used with the procedure (or methodology) for this task must be 1,900 pc/h/ln.

Task 3. Compute Local Base Saturation Flow Rate

The local base saturation flow rate is computed with Equation 31-185.

Equation 31-185

$$s_{o,local} = 1,900 \frac{\sum_{i=1}^m s_{prevailing,i}}{\sum_{i=1}^m s_i}$$

where

$s_{o,local}$ = local base saturation flow rate (pc/h/ln),

$s_{prevailing,i}$ = prevailing saturation flow rate for lane group i (veh/h/ln),

s_i = (adjusted) saturation flow rate for lane group i (veh/h/ln), and

m = number of lane groups.

Once the local base saturation flow rate $s_{o,local}$ is quantified by this technique, it is substituted thereafter for s_o in any equation in an HCM chapter that refers to this variable.

7. COMPUTATIONAL ENGINE DOCUMENTATION

This section uses a series of flowcharts and linkage lists to document the logic flow for the computational engine.

FLOWCHARTS

The methodology flowchart is shown in Exhibit 31-48. The methodology is shown to consist of four main modules:

- Setup module,
- Signalized intersection module,
- Initial queue delay module, and
- Performance measures module.

This subsection provides a separate flowchart for each of these modules.

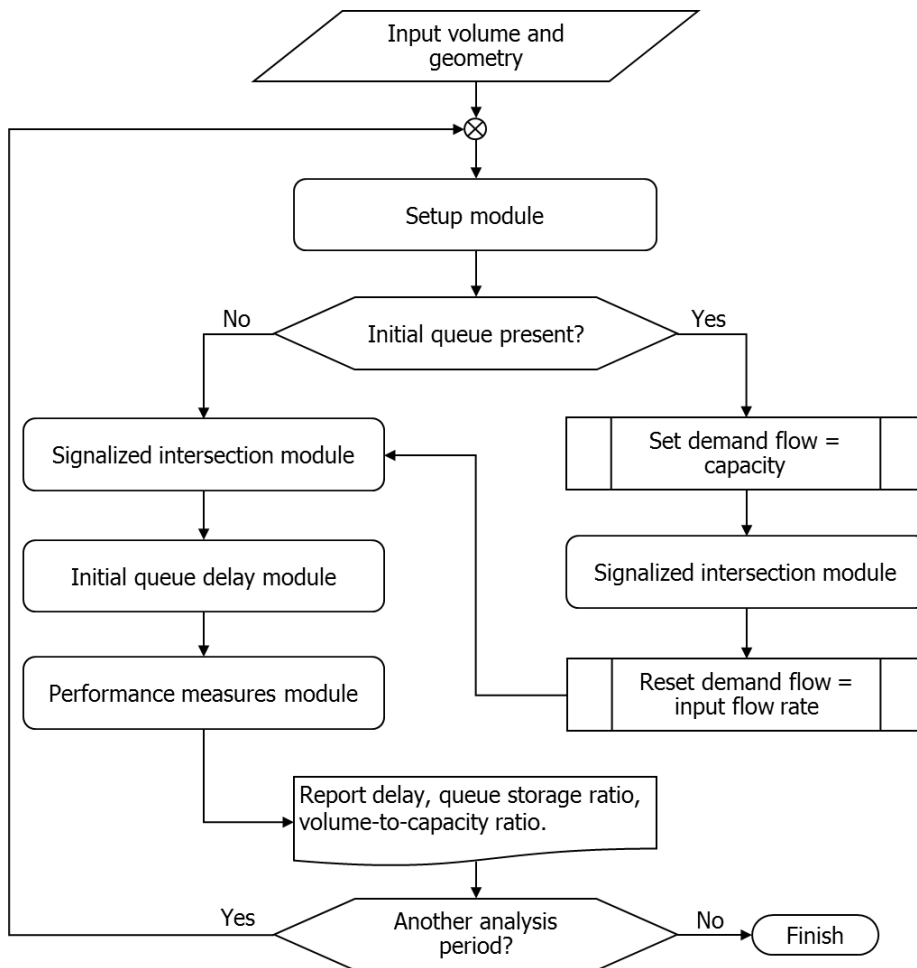
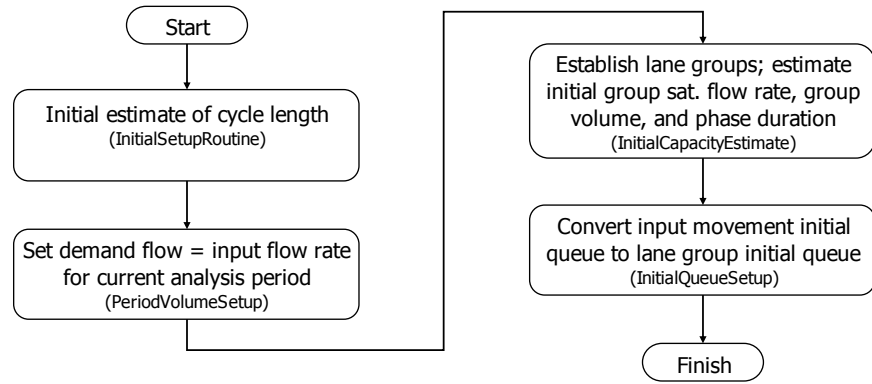


Exhibit 31-48
Methodology Flowchart

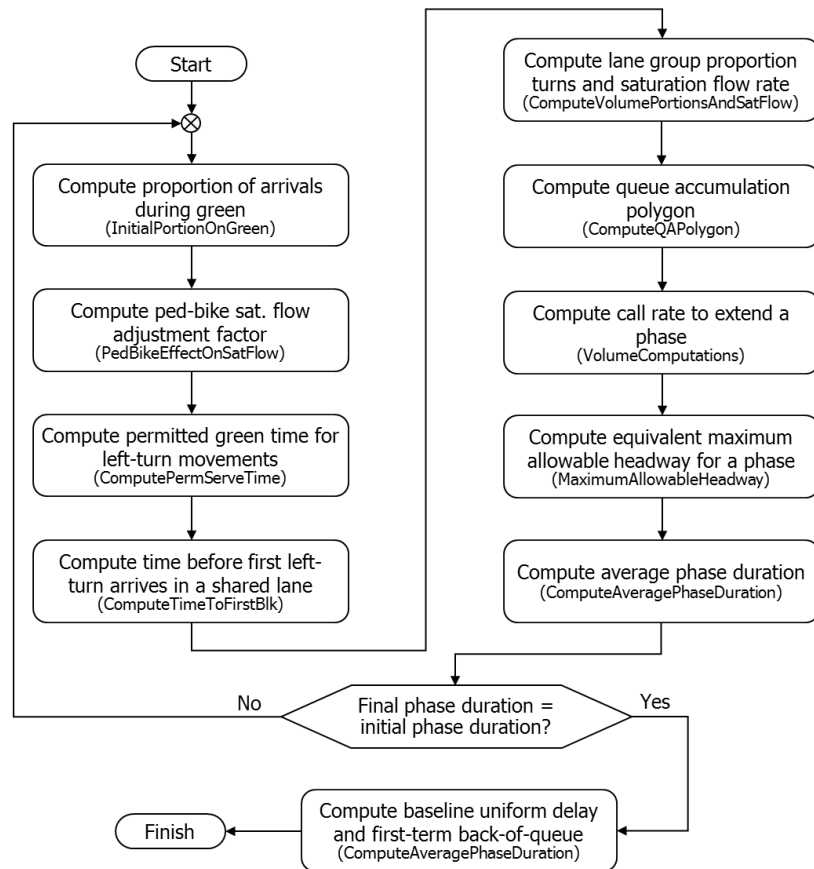
The setup module is shown in Exhibit 31-49. It consists of four main routines, as shown in the large rectangles of the exhibit. The main function of each routine, as well as the name given to it in the computational engine, is shown in the exhibit. These routines are described further in the next subsection.

Exhibit 31-49
Setup Module



The signalized intersection module is shown in Exhibit 31-50. It consists of nine main routines followed by a tenth and final computation routine performed after the final phase duration equals the initial phase duration. The main function of each routine, as well as the name given to it in the computational engine, is shown in the exhibit. These routines are described further in the next subsection.

Exhibit 31-50
Signalized Intersection Module



The initial queue delay module is shown in Exhibit 31-51. It consists of four main routines. The main function of each routine is shown in the exhibit.

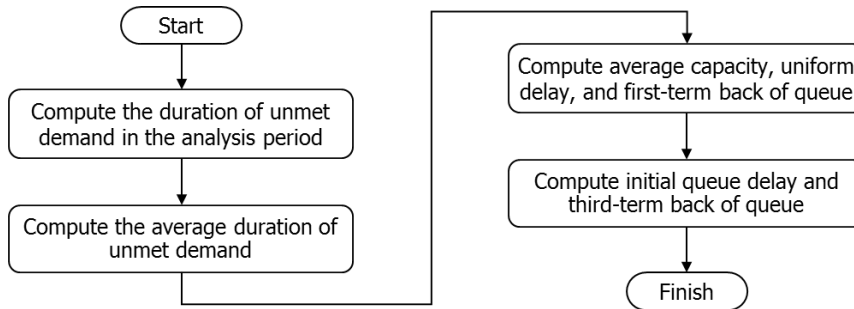


Exhibit 31-51
Initial Queue Delay Module

The performance measures module is shown in Exhibit 31-52. It consists of four main routines. The main function of each routine is shown in the exhibit. Two of the routines are complicated enough to justify their development as separate entities in the computational engine. The name given to each of these two routines is also shown in the exhibit, and they are described further in the next subsection.

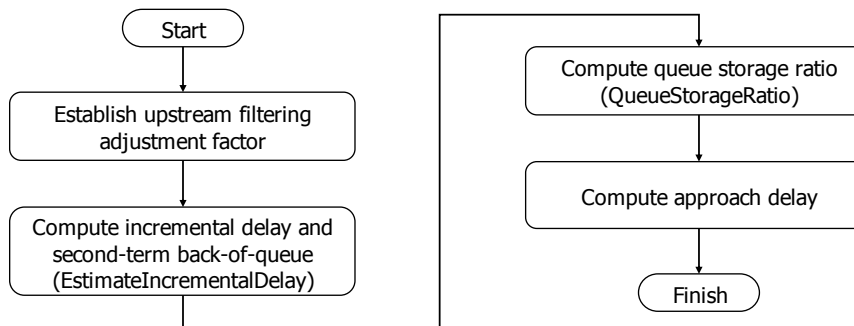


Exhibit 31-52
Performance Measures Module

LINKAGE LISTS

This subsection uses linkage lists to describe the main routines that compose the computational engine. Each list is provided in a table (an exhibit) that identifies the routine and the various subroutines to which it refers. Conditions for which the subroutines are used are also provided.

The lists are organized by module, as described in the previous subsection. Four tables are provided to address the following three modules:

- Setup module (one table),
- Signalized intersection module (two tables), and
- Performance measures module (one table).

The initial queue delay module does not have a linkage list because it does not call any specific routines.

The linkage list for the setup module is provided in Exhibit 31-53. The main routines are listed in the far-left column of the exhibit and are identified in Exhibit 31-49.

Exhibit 31-53
Setup Module Routines

Routine	Subroutine	Conditions for Use
InitialSetupRoutine	Compute change period ($Y + R_c$).	None
	Compute initial estimate of cycle length C .	None
PeriodVolumeSetup	a. Compute period volume before initial queue analysis, and b. Restore period volume if initial queue analysis conducted.	Used for multiple-period analysis
	a. Save input volume as it will be overwritten if initial queue is present, and b. Restore input volume if initial queue analysis conducted.	Used for single-period analysis
InitialCapacityEstimate	getPermissiveLeftServiceTime (computes g_u , the duration of the permitted period that is not blocked by an opposing queue)	Used if subject phase serves a left-turn movement with a. permitted mode or b. protected-permitted mode
	getPermissiveLeftEffGreen (computes g_p , the duration of the permitted green for permitted left-turn movements)	Used if subject phase serves a left-turn movement with a. permitted mode or b. protected-permitted mode
	Define lane groups for each approach.	None
	Establish initial estimate of lane group volume, saturation flow rate, and number of lanes capacity.	None
	Establish initial estimate of proportion of turns in a shared-lane lane group.	Used for shared-lane lane groups
	PermittedSatFlow (computes permitted left-turn saturation flow rate s_p)	Used if lane group serves a left-turn movement with protected-permitted mode
	getParkBusSatFlowAdj (computes combined parking and bus blockage saturation flow adjustment factors)	Used if lane group is adjacent to on-street parking or a local bus stop
InitialQueueSetup	Distribute input movement initial queue to corresponding lane groups.	Used for first analysis period
	Assign residual queue from last period to initial queue of current period, and distribute initial queue among affected lane groups.	Used for second and subsequent analysis periods

The linkage list for the signalized intersection module is provided in Exhibit 31-54. The main routines are listed in the far-left column of the exhibit and are identified in Exhibit 31-50. The ComputeQAPolygon routine is complex enough to justify the presentation of its subroutines in a separate linkage list. This supplemental list is provided in Exhibit 31-55.

Routine	Subroutine	Conditions for Use
InitialPortionOnGreen	Compute portion arriving during green P .	None
PedBikeEffectOnSatFlow	PedBikeEffectOnLefts	Used if subject phase serves a left-turn movement with a. permitted mode or b. protected-permitted mode
	PedBikeEffectOnRights	Used if subject phase serves a right-turn movement
	PedBikeEffectOnLeftsUnopposed	Used if subject phase serves a left-turn movement with split phasing
ComputePermServeTime	getPermissiveLeftServiceTime (computes g_u , the duration of the permitted period that is not blocked by an opposing queue)	Used if subject phase serves a left-turn movement with a. permitted mode or b. protected-permitted mode
	getPermissiveLeftEffGreen (computes g_p , the duration of the permitted green for permitted left-turn movements)	Used if subject phase serves a left-turn movement with a. permitted mode or b. protected-permitted mode
ComputeTimeToFirstBlk	getTimetoFirstBlk (computes g_r , the time before the first left-turning vehicle arrives and blocks the shared lane)	Used if subject phase serves a left-turn movement in a shared lane with a. permitted mode or b. protected-permitted mode
ComputeVolumePortions-AndSatFlow	PermittedSatFlow (computes permitted left-turn saturation flow rate s_p)	Used if lane group serves a left-turn movement with protected-permitted mode
	PortionTurnsInSharedTRLane (computes proportion of right-turning vehicles in shared lane P_R)	Used if approach has exclusive left-turn lane and subject lane group is a shared lane serving through and right-turning vehicles
	SatFlowforPermExclLefts	Used if lane group serves a left-turn movement with a permitted mode in an exclusive lane
	PortionTurnsInSharedLTRLane (computes proportion of right-turning vehicles in shared lane P_R and proportion of left-turning vehicles in shared lane P_L)	Used if approach has a shared lane serving left-turn and through vehicles
ComputeQAPolygon	QAP_ProtPermExclLane	Used if lane group serves a left-turn movement in an exclusive lane with the protected-permitted mode
	QAP_ProtMvmtExclLane	Used if lane group's movement has an exclusive lane and is served with protected mode
	QAP_ProtSharedLane	Used if lane group has a. a shared lane with through and right-turning movements b. a shared lane with through and left-turning movements served with split phasing
	QAP_PermLeftExclLane	Used if lane group serves a left-turn movement in an exclusive lane with the permitted mode
	QAP_PermSharedLane	Used if lane group serves a left-turn movement in a shared lane with the permitted mode

Exhibit 31-54
Signalized Intersection
Module: Main Routines

Exhibit 31-54 (continued)
 Signalized Intersection
 Module: Main Routines

Routine	Subroutine	Conditions for Use
VolumeComputations	Determine call rate to extend green λ .	None
	Determine call rate to activate a phase q_v, q_p	None
MaximumAllowable-Headway	Compute maximum allowable headway for each lane group MAH .	Calculations vary depending on lane group movements, lane assignment, phase sequence, and left-turn operational mode.
	Compute equivalent maximum allowable headway for each phase and timer MAH^* .	None
ComputeAverage-PhaseDuration	Compute probability of green extension p .	Computed for all phases except for the timer that serves the protected left-turn movement in a shared lane
	Compute maximum queue service time for all lane groups served during the phase.	None
	Compute probability of phase termination by extension to maximum limit (i.e., max-out).	None
	Compute green extension time g_e .	None
	Compute probability of a phase call p_c .	None
	Compute unbalanced green duration G_u .	None
	Compute average phase duration D_p .	None

Routine	Subroutine	Conditions for Use
QAP_ProtPermExclLane	ADP_ProtPermExcl (compute baseline first-term back-of-queue estimate $Q_{1,b}$)	Used for lane groups with left-turn movements in exclusive lane and served by protected-permitted mode
	getUniformDelay (compute baseline uniform delay $d_{1,b}$)	None
	Compute queue service time g_s .	None
	Compute lane group available capacity.	None
	Compute movement capacity.	None
QAP_ProtMvmtExclLane	ADP_ProtMvmt (compute baseline first-term back-of-queue estimate $Q_{1,b}$)	Used for lane groups with one service period
	getUniformDelay (compute baseline uniform delay $d_{1,b}$)	None
	Compute queue service time g_s .	None
	Compute lane group available capacity.	None
	Compute movement capacity.	None
QAP_ProtSharedLane	ADP_ProtMvmt (compute baseline first-term back-of-queue estimate $Q_{1,b}$)	Used for lane groups with one service period
	getUniformDelay (compute baseline uniform delay $d_{1,b}$)	None
	Compute queue service time g_s .	None
	Compute lane group available capacity.	None
	Compute movement capacity.	None
QAP_PermLeftExclLane	ADP_PermLeftExclLane (compute baseline first-term back-of-queue estimate $Q_{1,b}$)	Used for lane groups with left-turn movements in exclusive lane and served by permitted mode
	getUniformDelay (compute baseline uniform delay $d_{1,b}$)	None
	Compute queue service time g_s .	None
	Compute lane group available capacity.	None
	Compute movement capacity.	None
QAP_PermSharedLane	ADP_PermSharedMvmt (compute baseline first-term back-of-queue estimate $Q_{1,b}$)	Used for shared-lane lane groups with a permitted left-turn movement
	ADP_ProtMvmt (compute baseline first-term back-of-queue estimate $Q_{1,b}$)	Used for lane groups with one service period
	ADP_ProtPermShared (compute baseline first-term back-of-queue estimate $Q_{1,b}$)	Used for lane groups with left-turn movements in shared-lane lane group and served by protected-permitted mode
	getUniformDelay (compute baseline uniform delay $d_{1,b}$)	None
	Compute queue service time g_s .	None
	Compute lane group available capacity.	None
	Compute movement capacity.	None

Exhibit 31-55
Signalized Intersection
Module: ComputeQAPolygon
Routines

The linkage list for the performance measures module is provided in Exhibit 31-56. The main routines are listed in the far-left column and are identified in Exhibit 31-52.

Exhibit 31-56
Performance Measures
Module Routines

Routine	Subroutine	Conditions for Use
EstimateIncrementalDelay	Compute incremental delay d_2 and second-term back-of-queue estimate Q_2 .	None
QueueStorageRatio	Compute queue storage ratio L_Q .	None

8. USE OF ALTERNATIVE TOOLS

This section illustrates the use of alternative evaluation tools to evaluate the operation of a signalized intersection. The intersection described in Example Problem 1 of Section 9 is used for this purpose. There are no limitations in this example that would suggest the need for alternative tools. However, it is possible to introduce situations, such as short left-turn bays, for which an alternative tool might provide a more realistic assessment of intersection operation.

The basic layout of the example intersection is shown in the second exhibit of Example Problem 1 of Section 9. The left-turn movements on the north-south street operate under protected-permitted control and lead the opposing through movements (i.e., a lead-lead phase sequence). The left-turn movements on the east-west street operate as permitted. To simplify the discussion, the pedestrian and parking activity is removed. A pretimed signal operation is used.

EFFECT OF STORAGE BAY OVERFLOW

The effect of left-turn storage bay overflow is described in this subsection as a means of illustrating the use of alternative tools. The motorized vehicle methodology in Chapter 19 can be used to compute a queue storage ratio that compares the back-of-queue estimate with the available storage length. This ratio is used to identify bays that have inadequate storage. Overflow from a storage bay can be expected to reduce approach capacity and increase the approach delay. However, these effects of bay overflow are not addressed by the motorized vehicle methodology.

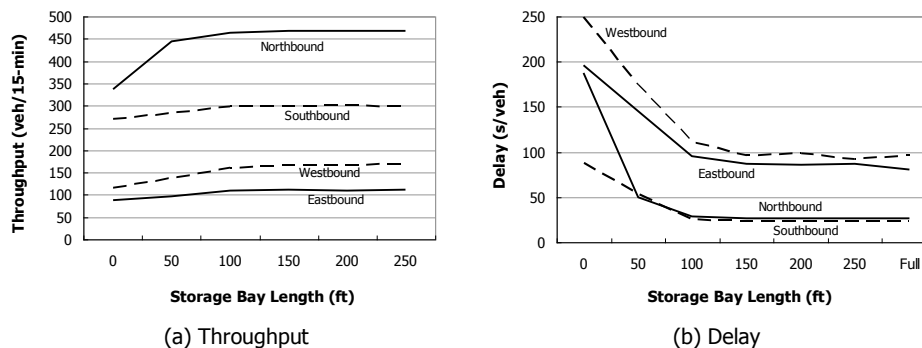
Effect of Overflow on Approach Throughput and Delay

A simulation software product was selected as the alternative tool for this analysis. The intersection was simulated for a range of storage bay lengths from 0 to 250 ft. All other input data remained the same. The results presented here represent the average of 30 simulation runs for each case.

The effect of bay overflow was assessed by examining the relationship between bay length, approach throughput, and approach delay. Exhibit 31-57 shows this effect. The throughput on each approach is equal to the demand volume when storage is adequate but drops off when the bay length is decreased.

A delay comparison is also presented in Exhibit 31-57. The delay on each approach increases as bay length is reduced. The highest delay is associated with a zero-length bay, which is effectively a shared lane. The zero-length case is included here to establish a boundary condition. The delay value becomes excessive when overflow occurs. This situation often degrades into oversaturation, and a proper assessment of delay would require a multiple-period analysis to account for the buildup of long-term queues.

Exhibit 31-57
Effect of Storage Bay Length on Throughput and Delay



For case-specific applications, parameters that could influence the evaluation of bay overflow include the following:

- Number of lanes for each movement,
- Demand volumes for each movement,
- Impedance of left-turning vehicles by oncoming traffic during permitted periods,
- Signal-timing plan (cycle length and phase times),
- Factors that affect the number of left-turn sneakers for left-turn movements that have permitted operation, and
- Other factors that influence the saturation flow rates.

The example intersection described here had two through lanes in all directions. If only one through lane had existed, the blockage effect would have been much more severe.

Effect of Overflow on Through Movement Capacity

This subsection illustrates how an alternative tool can be used to model congestion due to storage bay overflow. An example was set up involving constant blockage of a through lane by left-turning vehicles. This condition arises only under very severe oversaturation.

The following variables are used for this examination:

- Cycle length is 90 s,
- Effective green time is 41 s, and
- Saturation flow rate is 1,800 veh/h/ln.

The approach has two through lanes. Traffic volumes were sufficient to overload both lanes, so that the number of trips processed by the simulation model was determined to be an indication of through movement capacity. With no storage bay overflow effect, this capacity is computed as 1,640 veh/h ($= 3,600 \times 41/90$). So, in a 15-min period, 410 trips were processed on average when there was no overflow.

Exhibit 31-58 shows the effect of the storage bay length on the through movement capacity. The percentage of the full capacity is plotted as a function of the storage bay length over the range of 0 to 600 ft. As expected, a zero-length bay reduces the capacity to 50% of its full value because one lane would be

constantly blocked. At the other extreme, the “no blockage” condition, achieved by setting the left-turn volume to zero, indicates the full capacity was available. The loss of capacity is more or less linear for storage lengths up to 600 ft, at which point about 90% of the full capacity is achieved.

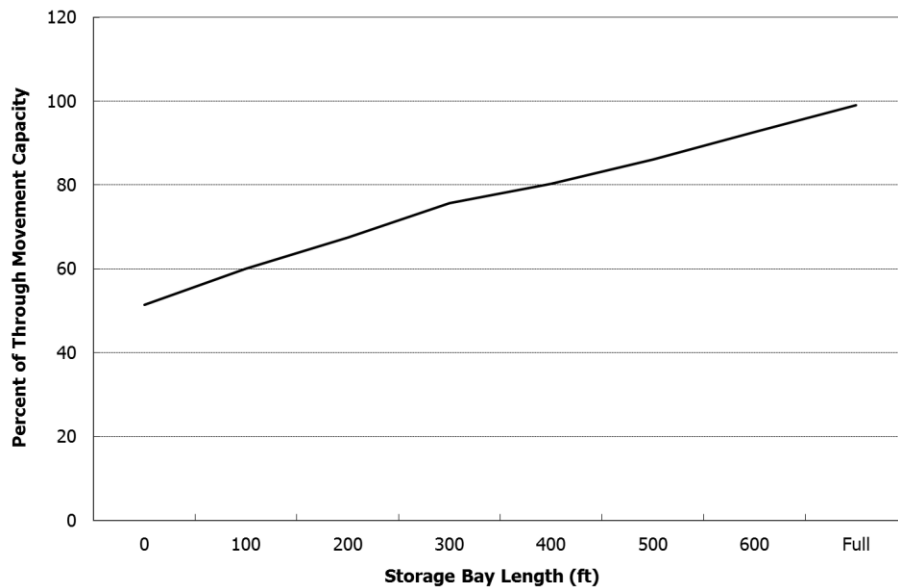


Exhibit 31-58
Effect of Storage Bay Length on Capacity

Bay overflow is a very difficult phenomenon to deal with analytically, and a substantial variation in its treatment is expected among alternative tools. The main issue for modeling is the behavior of left-turning drivers denied access to the left-turn bay because of the overflow. The animated graphics display produced by some tools can often be used to examine this behavior and assess the tool’s validity. Typically, some model parameters can be adjusted so that the resulting behavior is more realistic.

EFFECT OF RIGHT-TURN-ON-RED OPERATION

The treatment of right-turn-on-red (RTOR) operation in the motorized vehicle methodology is limited to the removal of RTOR vehicles from the right-turn demand volume. If the right-turn movement is served by an exclusive lane, the methodology suggests RTOR volume can be estimated as equal to the left-turn demand of the complementary cross street left-turn movement, whenever this movement is provided a left-turn phase. Given the simplicity of this treatment, it may be preferable to use an alternative tool to evaluate RTOR operation under the following conditions:

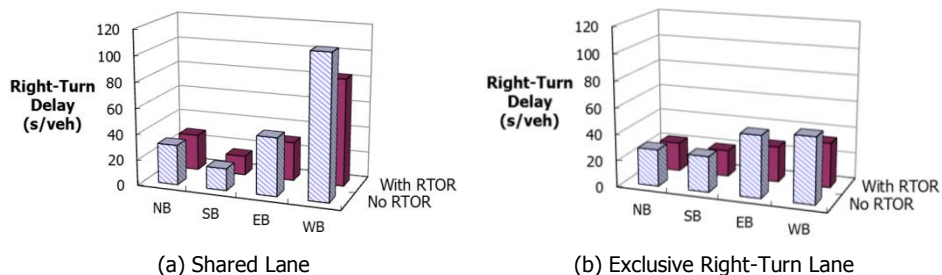
- RTOR operation occurs at the intersection,
- Right turns are a critical element of the operation,
- An acceptable LOS depends on RTOR movements, or
- Detailed phasing alternatives involving RTOR are being considered.

The remainder of this subsection examines the RTOR treatment offered in the motorized vehicle methodology. The objective of this discussion is to illustrate when alternative tools should be considered.

Effect of Right-Turn Lane Allocation

This subsection examines the effect of the lane allocation for the right-turn movement. The lane-allocation scenarios considered include (a) provision of a shared lane for the right-turn movement and (b) provision of an exclusive right-turn lane. Exhibit 31-59 shows the results of the analysis. The intersection was simulated with (and without) the RTOR volume.

Exhibit 31-59
Effect of Right-Turn-on-Red and Lane Allocation on Delay



The trends in Exhibit 31-59 indicate there are only minimal differences in delay when RTOR is allowed relative to when it is not allowed. The northbound and southbound approaches had no shadowing opportunities because the eastbound and westbound movements did not have a protected left-turn phase. As a result, the effect of lane allocation and RTOR operation was negligible for the northbound and southbound right-turn movements.

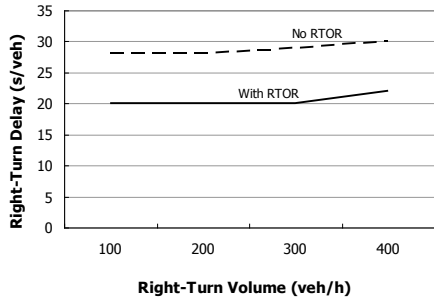
In contrast, the eastbound and westbound right-turn movements were shadowed by the protected left-turn phases for the northbound and southbound approaches. As a result, the effect of lane allocation was more notable for the eastbound and the westbound right-turn movements.

Effect of Right-Turn Demand Volume

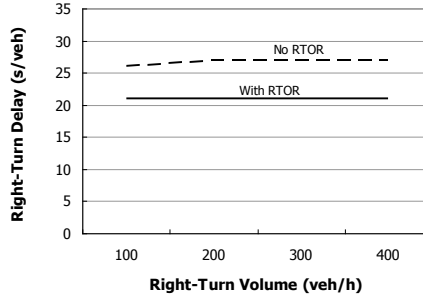
This subsection examines the effect of right-turn demand volume on right-turn delay, with and without RTOR allowed. The right-turn volumes varied from 100 to 400 veh/h on all approaches. Exclusive right-turn storage bays were provided on each approach.

The results are shown in Exhibit 31-60. They indicate delay to the northbound and southbound right-turn movements was fairly insensitive to right-turn volume, with or without RTOR allowed. The available green time on these approaches provided adequate capacity for the right turns. RTOR operation provided about a 25% delay reduction.

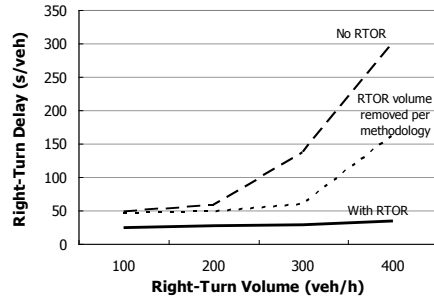
The delay to the eastbound and westbound right-turn movements increased rapidly with right-turn volume when RTOR was not allowed. At 300 veh/h and no RTOR, the right-turn delay becomes excessive in both directions. With RTOR, delay is less sensitive to right-turn volume. This trend indicates the additional capacity provided by RTOR is beneficial for higher right-turn volume levels.



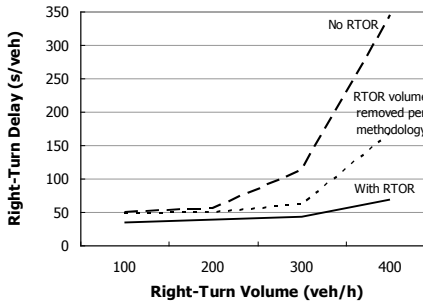
(a) Northbound



(b) Southbound



(c) Eastbound



(d) Westbound

Exhibit 31-60
Effect of Right-Turn-on-Red and Right-Turn Volume on Delay

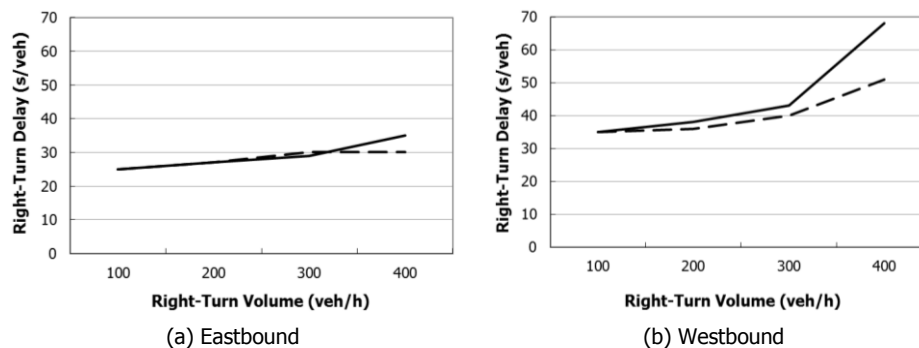
The treatment of RTOR suggested in the motorized vehicle methodology (i.e., removal of the RTOR vehicles from the right-turn volume) was also examined. The simulation analysis was repeated with the right-turn volumes reduced in this manner to explore the validity of this treatment.

The results of this analysis are shown in Exhibit 31-60 for the eastbound and westbound approaches. The trends shown suggest the treatment yields a result that is closer to the “with RTOR” case, as intended. However, use of the treatment in this case could still lead to erroneous conclusions about right-turn delay at intersections with high right-turn volumes.

Effect of a Protected Right-Turn Phase

This subsection compares the effect of adding a protected right-turn phase without RTOR allowed relative to just allowing RTOR. The example intersection was modified to include an exclusive right-turn storage bay and a protected right-turn phase for both the eastbound and westbound approaches. Each phase was timed concurrently with the complementary northbound or southbound left-turn phase, as appropriate. The results are shown in Exhibit 31-61. The trends in the exhibit indicate the protected phase does not improve over RTOR operation at low volume levels. However, it does provide some delay reduction at the high end of the volume scale.

Exhibit 31-61
Effect of Right-Turn-on-Red and Right-Turn Protection on Delay



This examination indicates RTOR operation can have some effect on right-turn delay. The effect is most notable when there are no shadowing opportunities in the phase sequence for right-turn service or the right-turn volume is high. The use of an alternative tool to evaluate RTOR operation may provide a more realistic estimate of delay than simply removing RTOR vehicles from the right-turn demand volume, as suggested in Chapter 19.

EFFECT OF SHORT THROUGH LANES

One identified limitation of the motorized vehicle methodology is its inability to evaluate short through lanes that are added or dropped at the intersection. This subsection describes the results from an evaluation of this geometry for the purpose of illustrating the effect of short through lanes.

Several alternative tools can address the effect of short through lanes. Each tool will have its own unique method of representing lane drop or add geometry and models of driver behavior. Some degree of approximation is involved with all evaluation tools.

The question under consideration is, “How much additional through traffic could the northbound approach accommodate if a lane were added both 150 ft upstream and 150 ft downstream of the intersection?” The capacity of the original two northbound lanes was computed as 1,778 veh/h (i.e., 889 veh/h/ln) by using the motorized vehicle methodology. The simulation tool’s start-up lost time and saturation headway parameters were then adjusted so the simulation tool produced the same capacity. It was found in this case that a 2.3-s headway and 3.9-s start-up lost time produced the desired capacity.

Finally, the additional through lane was added to the simulated intersection, and the process of determining capacity was repeated. On the basis of an average of 30 runs, the capacity of the additional lane was computed as 310 veh/h. Theoretically, the addition of a full lane would increase the capacity by another 889 veh/h, for a total of 2,667 veh/h.

The alternative tool indicates the additional lane contributes only 0.35 equivalent lane (= 310/889). This result cannot be stated as a general conclusion that applies to all cases because other parameters (such as the signal-timing plan and the proportion of right turns in the lane group) will influence the results. More important, the results are likely to vary among alternative tools given the likely differences in their driver behavior models.

EFFECT OF CLOSELY SPACED INTERSECTIONS

The effect of closely spaced intersections is examined in this subsection. The motorized vehicle methodology does not account for the effect of queue cyclic spillback from a downstream signal or demand starvation from an upstream signal. It is generally accepted that simulation of these effects is desirable when two closely spaced signalized intersections interact with each other in this manner.

Consider two intersections separated by 200 ft along the north–south roadway. They operate with the same cycle length and the same northbound and southbound green time. To keep the problem simple, only through movements are allowed at these intersections. The northbound approach is used in this discussion to illustrate the effect of the adjacent intersection. The layout of this system and the resulting lane blockage are illustrated in Exhibit 31-62.

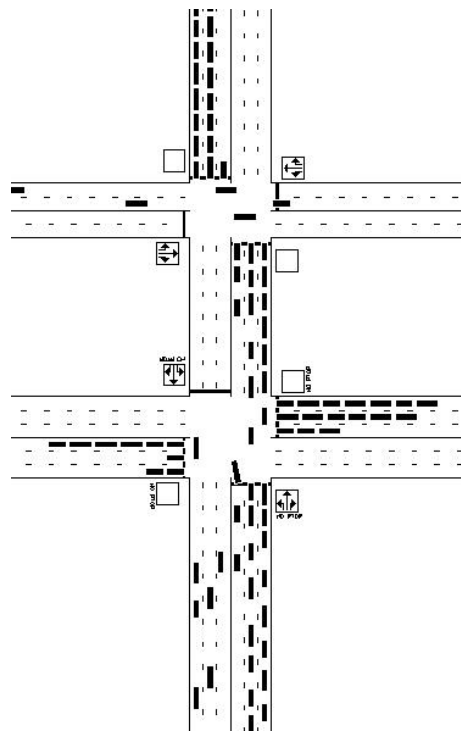


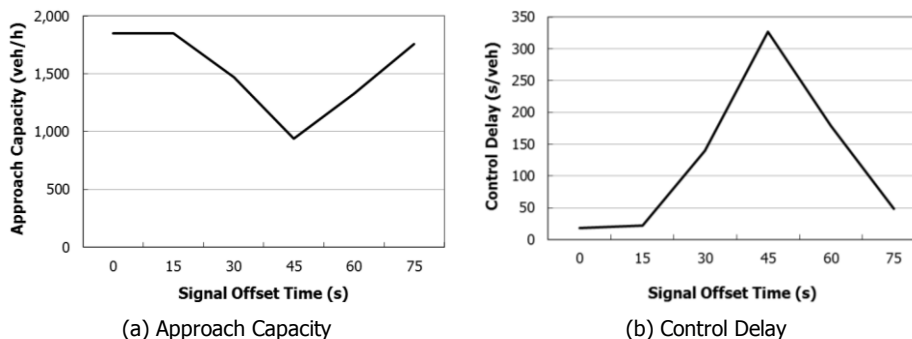
Exhibit 31-62
Closely Spaced Intersections

Exhibit 31-62 illustrates both cyclic spillback and demand starvation at one point in the cycle. For the northbound direction, traffic queues have spilled back from the downstream intersection to block the upstream intersection. For the southbound direction, the traffic at the upstream intersection is prevented from reaching the downstream intersection by the red signal at the upstream intersection. Valuable green time is being wasted in both travel directions at the southern intersection.

Exhibit 31-63 illustrates the relationship between signal offset and the performance of the northbound travel direction. In terms of capacity, the exhibit shows that under the best-case condition (i.e., zero offset), the capacity is maintained at a value slightly above the demand volume. Under the worst-case

Exhibit 31-63
Effect of Closely Spaced
Intersections on Capacity and
Delay

condition, the capacity is reduced to slightly below 1,000 veh/h. The demand volume-to-capacity ratio under this condition is about 1.7.



The effect of signal offset time on the delay to northbound traffic approaching the first intersection is also shown in Exhibit 31-63. As expected, the delay is minimal under favorable offsets, but it increases rapidly as the offset becomes less favorable. Delay is at its maximum value with a 45-s offset time. The large value of delay suggests that approach is severely oversaturated.

The delay reported by most simulation tools represents the delay incurred by vehicles when they *depart* the system during the analysis period, as opposed to the delay incurred by vehicles that *arrive* during the analysis period. The latter measure represents the delay reported by the motorized vehicle methodology.

For oversaturated conditions, the delay reported by a simulation tool may be biased when the street system is not adequately represented. This bias occurs when the street system represented to the tool does not physically extend beyond the limits of the longest queue that occurs during the analysis period.

The issues highlighted in the preceding paragraphs must be considered when an alternative tool is used. Specifically, a multiple-period analysis must be conducted that temporally spans the period of oversaturation. Also, the spatial boundaries of the street system must be large enough to encompass all queues during the saturated time periods. A more detailed discussion of multiple-period analyses is presented in Chapter 7, Interpreting HCM and Alternative Tool Results.

9. EXAMPLE PROBLEMS

This section describes the application of each of the motorized vehicle, pedestrian, and bicycle methodologies through the use of example problems. Exhibit 31-64 provides an overview of these problems. The examples focus on the operational analysis level. The planning and preliminary engineering analysis level is identical to the operational analysis level in terms of the calculations, except that default values are used when field-measured values are not available.

Problem Number	Description	Analysis Level
1	Motorized vehicle LOS	Operational
2	Pedestrian LOS	Operational
3	Bicycle LOS	Operational

Exhibit 31-64
Example Problems

EXAMPLE PROBLEM 1: MOTORIZED VEHICLE LOS

The Intersection

The intersection of 5th Avenue and 12th Street is an intersection of two urban arterial streets. The intersection plan view is shown in Exhibit 31-65.

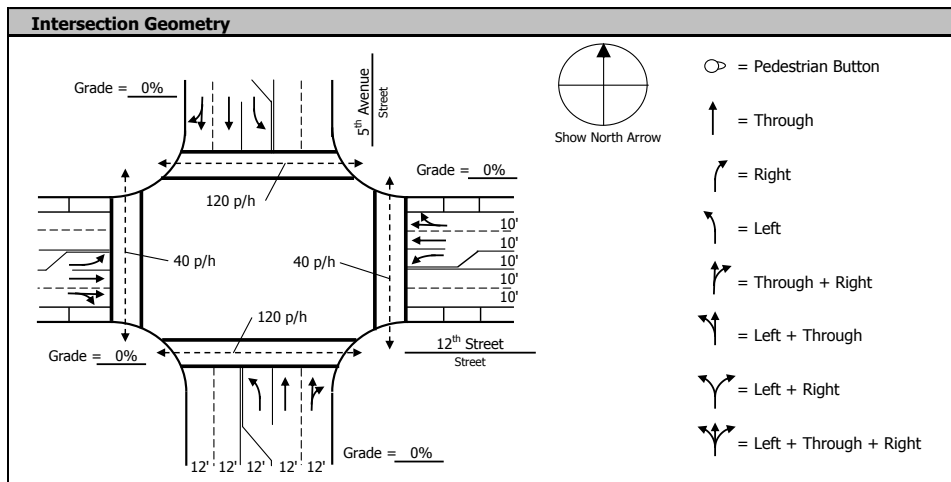


Exhibit 31-65
Example Problem 1:
Intersection Plan View

The Question

What is the motorist delay and LOS during the analysis period for each lane group and the intersection as a whole?

The Facts

The intersection's traffic, geometric, and signalization conditions are listed in Exhibit 31-66, Exhibit 31-67, and Exhibit 31-68, respectively. Exhibit 31-69 presents additional data. The volume data provided represent the demand flow rate during the 0.25-h analysis period, so a peak hour factor is not applicable to this evaluation.

Exhibit 31-66
Example Problem 1: Traffic Characteristics Data

Input Data Element	Eastbound			Westbound			Northbound			Southbound		
	L	T	R	L	T	R	L	T	R	L	T	R
Demand flow rate (veh/h)	71	318	106	118	600	24	133	1644	111	194	933	111
RTOR flow rate (veh/h)			0			0			22			33
Percentage heavy vehicles (%)	5	5		5	5		2	2		2	2	
Platoon ratio	1.00	1.00		1.00	1.00		1.00	1.00		1.00	1.00	
Upstream filtering adjustment factor	1.00	1.00		1.00	1.00		1.00	1.00		1.00	1.00	
Initial queue (veh)	0	0		0	0		0	0		0	0	
Base saturation flow rate (pc/h/ln)	1,900	1,900		1,900	1,900		1,900	1,900		1,900	1,900	
Pedestrian flow rate (p/h)		120			120			40			40	
Bicycle flow rate (bicycles/h)		0			0			0			0	
On-street parking maneuver rate (maneuvers/h)		5			5							
Local bus stopping rate (buses/h)		0			0			0			0	

Note: L = left turn; T = through; R = right turn.

Exhibit 31-67
Example Problem 1: Geometric Design Data

Input Data Element	Eastbound			Westbound			Northbound			Southbound		
	L	T	R	L	T	R	L	T	R	L	T	R
Number of lanes (ln)	1	2	0	1	2	0	1	2	0	1	2	0
Average lane width (ft)	10.0	10.0		10.0	10.0		12.0	12.0		12.0	12.0	
Number of receiving lanes (ln)		2			2			2			2	
Turn bay length (ft)	200			200			200			200		
Presence of on-street parking	No		Yes	No		Yes	No		No	No		No
Approach grade (%)		0			0			0			0	

Note: L = left turn; T = through; R = right turn.

Exhibit 31-68
Example Problem 1: Signal Control Data

Input Data Element	Eastbound	Westbound	Northbound	Southbound
Type of signal control	Actuated	Actuated	Actuated	Actuated
Phase sequence	No left-turn phase	No left-turn phase	Leading left	Lagging left
Phase number	2	6	3	7
Movement	L+T+R	L+T+R	L T+R	L T+R
Left-turn operational mode	Perm.	Perm.	Prot.-Perm.	Prot.-Perm.
Dallas left-turn phasing option			No	No
Passage time (s)	2.0	2.0	2.0	2.0
Maximum green (s)	30	30	25	50
Minimum green (s)	5	5	5	5
Yellow change (s)	4.0	4.0	4.0	4.0
Red clearance (s)	0	0	0	0
Walk (s)	5	5	5	5
Pedestrian clear (s)	14	14	16	16
Phase recall	No	No	No	No
Dual entry	Yes	Yes	No	Yes
Simultaneous gap-out		Yes		Yes

Note: L = left turn; T = through; R = right turn; Prot. = protected; Perm. = permitted.

Input Data Element	Eastbound			Westbound			Northbound			Southbound		
	L	T	R	L	T	R	L	T	R	L	T	R
Analysis period duration (h)	0.25			0.25			0.25			0.25		
Speed limit (mi/h)	35			35			35			35		
Stop-line detector length (ft)	40	40		40	40		40	40		40	40	
Detection mode	Pres.	Presence		Pres.	Presence		Pres.	Presence		Pres.	Presence	
Area type	Central business district											

Exhibit 31-69
Example Problem 1: Other Data

Note: L = left turn; T = through; R = right turn; Pres. = presence.

The intersection is located in a central business district-type environment. Adjacent signals are somewhat distant so the intersection is operated by using fully actuated control. Vehicle arrivals to each approach are characterized as “random” and are described by using a platoon ratio of 1.0.

The left-turn movements on the north-south street operate under protected-permitted control and lead the opposing through movements (i.e., a lead-lead phase sequence). The left-turn movements on the east-west street operate as permitted.

All intersection approaches have a 200-ft left-turn bay, an exclusive through lane, and a shared through and right-turn lane. The average width of the traffic lanes on the east-west street is 10 ft. The average width of the traffic lanes on the north-south street is 12 ft.

Crosswalks are provided on each intersection leg. A two-way flow rate of 120 p/h is estimated to use each of the east-west crosswalks and a two-way flow rate of 40 p/h is estimated to use each of the north-south crosswalks.

On-street parking is present on the east-west street. It is estimated that parking maneuvers on each intersection approach occur at a rate of 5 maneuvers/h during the analysis period.

The speed limit is 35 mi/h on each intersection approach. The analysis period is 0.25 h. There is no initial queue for any movement.

As noted in the next section, none of the intersection movements have two or more exclusive lanes. For this reason, the saturation flow rate adjustment factor for lane utilization is not applicable. Any unequal lane use that may occur due to the shared through and right-turn lane groups will be accounted for in the lane group flow rate calculation, as described in the Lane Group Flow Rate on Multiple-Lane Approaches subsection of Section 2.

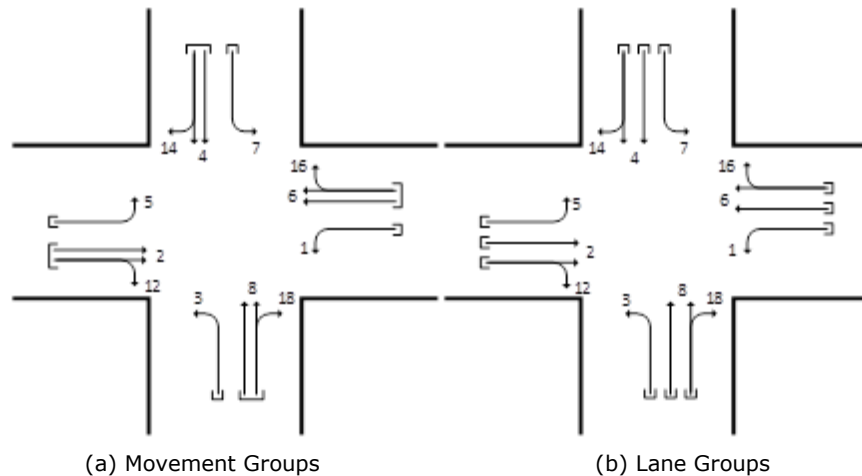
Outline of Solution

The solution follows the steps listed in Exhibit 19-18 of Chapter 19.

Step 1: Determine Movement Groups and Lane Groups

The left-turn lanes are designated as separate movement groups according to the rules described in Chapter 19. The through and shared right-turn and through lanes are combined into one movement group on each approach. The movement group designations are shown in Exhibit 31-70a with brackets showing how the individual movements are combined into movement groups.

Exhibit 31-70
Example Problem 1:
Movement Groups and Lane Groups



Each lane is analyzed as a separate lane group according to the rules in Chapter 19. The lane group designations are shown in Exhibit 31-70b with brackets showing how the individual lanes are combined into lane groups.

Step 2: Determine Movement Group Flow Rate

Exhibit 31-71 shows the movement group flow rates, which are based on the movement groups identified in Exhibit 31-70a. The RTOR flow rate is subtracted from the right-turn volume for the northbound and southbound through-and-right-turn movement groups.

Exhibit 31-71
Example Problem 1:
Movement Group Flow Rates

Data Element	Eastbound		Westbound		Northbound		Southbound	
Movement group	L	T+R	L	T+R	L	T+R	L	T+R
Number of lanes (ln)	1	2	1	2	1	2	1	2
Movement group flow rate (veh/h)	71	318 + 106 = 424	118	600 + 24 = 624	133	1,644 + 111 - 22 = 1,733	194	933 + 111 - 33 = 1,011

Note: L = left turn; T+R = combined through and right turn.

Step 3: Determine Lane Group Flow Rate

There is one shared lane and two or more lanes on each intersection approach. For this configuration, the lane group flow rates for the through-and-right-turn movement groups are computed by the procedures in the Lane Group Flow Rate on Multiple-Lane Approaches subsection of Section 2. The results of these calculations are given in Exhibit 31-72. The left-turn lane group volumes remain unchanged from Exhibit 31-71 because the movement groups and the lane groups are the same for the left-turn lanes. The volumes shown for the through lane group and the shared lane group represent the flow rates obtained from the Section 2 procedure.

Exhibit 31-72
Example Problem 1: Lane
Group Flow Rates

Data Element	Eastbound			Westbound			Northbound			Southbound		
Lane group	L	T	T+R	L	T	T+R	L	T	T+R	L	T	T+R
Number of lanes (ln)	1	1	1	1	1	1	1	1	1	1	1	1
Flow rate (veh/h)	71	239	185	118	337	287	133	870	863	194	513	497

Note: L = left turn; T = through; T+R = combined through and right turn.

Step 4: Determine Adjusted Saturation Flow Rate

The base saturation flow rate is 1,900 veh/h/ln for each lane group. Adjustments made for each of the lane groups are summarized in the following paragraphs.

The left-turn lane groups for the eastbound and westbound approaches operate with the permitted mode. The saturation flow rate of a permitted left-turn movement s_p is determined with Equation 31-100. For example, the saturation flow rate for the eastbound left-turn lane group is computed with the following equation.

$$s_p = \frac{v_o e^{-v_o t_{cg}/3,600}}{1 - e^{-v_o t_{fh}/3,600}} = \frac{624 e^{-624(4.5)/3,600}}{1 - e^{-624(2.5)/3,600}} = 813 \text{ veh/h/ln}$$

The adjustment factor for the existence of parking and parking activity f_p is applied to the shared-lane lane groups for the eastbound and westbound approaches. This factor is computed with Equation 19-11.

The adjustment factor for area type f_a is applied to all lane groups. Guidance for determining this factor's value is provided in Section 3 of Chapter 19 (in the subsection titled Adjustment for Area Type).

The adjustment factor for heavy vehicles and grade f_{HVg} is computed with Equation 19-10. This factor is applicable to all lane groups.

The adjustment factors and the adjusted saturation flow rate for each movement are shown in Exhibit 31-73.

Data Element	Eastbound			Westbound			Northbound			Southbound		
	L	T	T+R	L	T	T+R	L	T	T+R	L	T	T+R
Lane group	L	T	T+R	L	T	T+R	L	T	T+R	L	T	T+R
Phase number	2	2	2	6	6	6	3	8	8	7	4	4
Base saturation flow rate s_o (pc/h/ln)		1,900	1,900		1,900	1,900	1,900	1,900	1,900	1,900	1,900	1,900
Permitted left turn saturation flow rate s_p (veh/h/ln)	813			978								
Adjustment factor for left-turn vehicle presence, f_{LT}							0.95			0.95		
Adjustment factor for heavy vehicles and grade, f_{HVg}	0.96	0.96	0.96	0.96	0.96	0.96	0.98	0.98	0.98	0.98	0.98	0.98
Adjustment factor for existence of parking lane and parking activity, f_p			0.88			0.88						
Adjustment factor for area type, f_a	0.90	0.90	0.90	0.90	0.90	0.90	0.90	0.90	0.90	0.90	0.90	0.90
Pedestrian adjustment factor for left-turn groups, f_{Lpb}	1.00			0.98			1.00			1.00		
Pedestrian-bicycle adjustment factor for right-turn groups, f_{Rpb}			0.88			0.88			0.98			0.98
Adjusted saturation flow rate (veh/h/ln)	702	1,643	1,201	825	1,643	1,398	1,603	1,683	1,648	1,603	1,683	1,630

Exhibit 31-73
Example Problem 1: Adjusted Saturation Flow Rate

Notes: L = left turn; T = through; T+R = combined through and right turn.
Calculated values are based on maintaining six or more significant digits for all computed values through all calculations. These values are shown with fewer digits for presentation purposes only.

Equation 19-8 shows all the adjustment factors that might be applied in the calculation of saturation flow rate. However, when this equation is applied to a given lane group, some of the factors are not applicable (or have a value of 1.0) and can be removed from the equation. The reduced form of the saturation flow rate equation is described in the following paragraphs for several of the lane groups at the subject intersection.

For the eastbound and westbound left-turn lane groups, the adjusted saturation flow rate is calculated with the following equation.

$$s = s_p f_{HVg} f_a f_{Lpb}$$

The northbound and southbound left-turn lane groups operate in the protected-permitted mode. The adjusted saturation flow rate for the protected left-turn phase is calculated with the following equation.

$$s = s_o f_{LT} f_{HVg} f_a$$

The adjusted saturation flow rate for the permitted left-turn period is calculated with the same equation as for the eastbound and westbound left-turn lane groups.

For the through lane groups on each approach, the adjusted saturation flow rate is computed with the following equation.

$$s = s_o f_{HVg} f_a$$

For the shared-lane lane groups, the adjusted saturation flow rate is computed by using Equation 31-105. This equation is reproduced below for the eastbound shared right-turn and through lane group.

$$s_{sr} = \frac{s_{th}}{1 + P_R \left(\frac{E_R}{f_{Rpb}} - 1 \right)} = \frac{1,438}{1 + \left(\frac{106}{186} \right) \left(\frac{1.18}{0.88} - 1 \right)} = 1,201 \text{ veh/h/ln}$$

with

$$s_{th} = s_o f_{HVg} f_p f_a = 1,900 \times 0.96 \times 0.88 \times 0.90 = 1,438 \text{ veh/h/ln}$$

The calculated adjustment factors and saturation flow rates in the previous equations are based on maintaining six or more significant digits for all computed values through all calculations. These values are shown with fewer digits for presentation purposes only.

Step 5: Determine Proportion Arriving During Green

The proportion arriving during green *P* is computed using Equation 19-15. The results are shown in Exhibit 31-74. The effective green time *g* and cycle length *C* are determined by using the results from the final iteration of Step 6.

Exhibit 31-74
Example Problem 1:
Proportion Arriving During
Green

Data Element	Eastbound			Westbound			Northbound			Southbound		
Lane group	L	T	T+R	L	T	T+R	L	T	T+R	L	T	T+R
Phase number	2	2	2	6	6	6	3	8	8	7	4	4
Effective green time <i>g</i> (s)	30.0	30.0	30.0	30.0	30.0	30.0	6.2	50.0	50.0	9.8	53.6	53.6
Proportion arriving on green, <i>P</i>	0.29	0.29	0.29	0.29	0.29	0.29	0.06	0.49	0.49	0.10	0.53	0.53

Note: L = left turn; T = through; T+R = combined through and right turn.
Calculated values are based on maintaining six or more significant digits for all computed values through all calculations. These values are shown with fewer digits for presentation purposes only.

Step 6: Determine Signal Phase Duration

The duration of each signal phase is determined by using the procedure described in Section 2 (in the subsection titled Actuated Phase Duration). The results of this iterative process are shown in Exhibit 31-75. The resulting cycle length is 101.8 s.

Data Element	Eastbound	Westbound	Northbound		Southbound	
Phase number	2	6	3	8	7	4
Assigned movements	L+T+R	L+T+R	L	T+R	L	T+R
Phase duration D_p (s)	34.0	34.0	10.2	54.0	13.8	57.6
Maximum allowable headway MAH (s)	3.4	3.4	3.1	3.1	3.1	3.1
Maximum queue clearance time g_c (s)	28.7	27.2	4.1	50.0	7.6	21.2
Green extension time g_e (s)	0.0	0.4	0.2	0.0	0.3	7.8
Probability that subject phase is called, p_c	1.00	1.00	0.98	1.00	1.00	1.00
Probability of max-out, p_x	1.00	1.00	0.0	1.00	0.0	0.18
Duration of permitted left-turn green not blocked by an opposing queue, g_u (s)	11.4	17.0	32.5		0.0	

Exhibit 31-75
Example Problem 1: Signal Phase Duration

Notes: L = left turn; T = through; T+R = combined through and right turn; L+T+R = combined left, through, and right turn.
Calculated values are based on maintaining six or more significant digits for all computed values through all calculations. These values are shown with fewer digits for presentation purposes only.

Step 7: Determine Capacity and Volume-to-Capacity Ratio

The capacity of each through lane group and each shared-lane lane group is computed with Equation 19-16. The capacity for the permitted left-turn lane groups is computed with Equation 31-119. The latter equation is reproduced below for the eastbound left-turn lane group.

$$c_{l,e} = \frac{g_u s_l + 3,600 n_s f_{ms} f_{sp}}{C} N_l$$

$$c_{l,e} = \frac{(11.4 \times 702) + (3,600 \times 2 \times 1.0 \times 1.0)}{101.8} \times 1 = 149 \text{ veh/h}$$

The capacity for the protected-permitted left-turn lane groups on the northbound and southbound approaches is computed with Equation 31-124. The results from the capacity and the volume-to-capacity ratio calculations are shown in Exhibit 31-76.

Data Element	Eastbound			Westbound			Northbound			Southbound		
Lane group	L	T	T+R	L	T	T+R	L	T	T+R	L	T	T+R
Phase number	2	2	2	6	6	6	3	8	8	7	4	4
Number of lanes N (ln)	1	1	1	1	1	1	1	1	1	1	1	1
Flow rate v (veh/h)	71	239	185	118	337	287	133	870	863	194	513	497
Adjusted saturation flow rate s (veh/h/ln)	702	1,643	1,201	825	1,643	1,398	1,603	1,683	1,648	1,603	1,683	1,630
Effective green time g (s)	30.0	30.0	30.0	30.0	30.0	30.0	6.2	50.0	50.0	9.8	53.6	53.6
Capacity c (veh/h)	149	484	354	208	484	412	328	827	809	225	887	859
Volume-to-capacity ratio X	0.47	0.49	0.52	0.57	0.70	0.70	0.41	1.05	1.07	0.86	0.58	0.58

Exhibit 31-76
Example Problem 1: Capacity and Volume-to-Capacity Ratio

Note: L = left turn; T = through; T+R = combined through and right turn.
Calculated values are based on maintaining six or more significant digits for all computed values through all calculations. These values are shown with fewer digits for presentation purposes only.

Step 8: Determine Delay

The control delay for each movement and approach, and for the intersection as a whole, is calculated with Equation 19-18. The results of the delay calculations are shown in Exhibit 31-77.

Exhibit 31-77
Example Problem 1: Control Delay

Data Element	Eastbound			Westbound			Northbound			Southbound		
	L	T	T+R	L	T	T+R	L	T	T+R	L	T	T+R
Lane group	L	T	T+R	L	T	T+R	L	T	T+R	L	T	T+R
Phase number	2	2	2	6	6	6	3	8	8	7	4	4
Uniform delay d_1 (s/veh)	44.6	29.6	29.9	41.3	31.9	31.9	13.2	25.9	25.9	28.9	16.4	16.4
Incremental delay d_2 (s/veh)	0.9	0.3	0.7	2.3	3.6	4.3	0.3	46.0	50.8	3.8	0.6	0.7
Initial queue delay d_3 (s/veh)	0.0	0.0	0.0	0.0	0.0	0.0	0.0	0.0	0.0	0.0	0.0	0.0
Control delay d (s/veh)	45.5	29.9	30.6	43.5	35.5	36.2	13.5	72.0	76.7	32.6	17.0	17.1
Level of service	D	C	C	D	D	D	B	F	F	C	B	B
Approach delay d_A (s/veh)		32.4			37.0			70.0			19.6	
Approach LOS		C			D			E			B	
Intersection delay d_i (s/veh)							45.9					
Intersection LOS							D					

Note: L = left turn; T = through; T+R = combined through and right turn.
Calculated values are based on maintaining six or more significant digits for all computed values through all calculations. These values are shown with fewer digits for presentation purposes only.

Step 9: Determine LOS

LOS is based on the control delay. LOS values for each approach and for the entire intersection are shown in Exhibit 31-77. The determination of LOS is based on the LOS thresholds in Exhibit 19-8.

Step 10: Determine Queue Storage Ratio

The procedure for calculating the percentile back-of-queue size and queue storage ratio is described in Section 4. This procedure was used to compute the 50th percentile values for both variables. The results are shown in Exhibit 31-78.

Exhibit 31-78
Example Problem 1: Back of Queue and Queue Storage Ratio

Data Element	Eastbound			Westbound			Northbound			Southbound		
	L	T	T+R	L	T	T+R	L	T	T+R	L	T	T+R
Lane group	L	T	T+R	L	T	T+R	L	T	T+R	L	T	T+R
Phase number	2	2	2	6	6	6	3	8	8	7	4	4
50th percentile back of queue Q_{50} (veh/ln)	1.8	4.8	3.8	3.0	7.6	6.6	1.4	28.9	29.4	4.9	7.7	7.5
50th percentile queue storage ratio $R_{Q_{50}}$	0.23	0.12	0.10	0.38	0.20	0.17	0.18	0.74	0.75	0.62	0.20	0.19

Note: L = left turn; T = through; T+R = combined through and right turn.

Queue Accumulation Polygon

The QAP is a useful way of illustrating the signal timing and performance of a signalized intersection. The evolution of the queue length during the cycle is shown in the QAP. In addition, the area of the QAP is the total uniform delay experienced by all vehicles during the cycle. The variables needed to construct the QAP for the northbound through lane group are provided in the following list. The QAP for this movement is shown in Exhibit 31-79.

- Flow rate: 870 veh/h,
- Adjusted saturation flow rate: 1,683 veh/h/ln,
- Cycle length: 101.8 s,
- Effective green time: 50.0 s,

- Effective red time: 51.8 s,
- Maximum queue clearance time: 50.0 s,
- Green extension time: 0.0 s, and
- Queue length at end of effective red: 13.4 veh/ln.

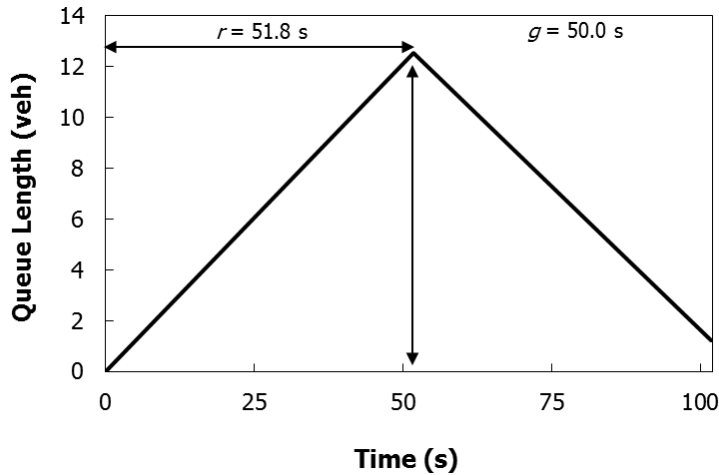


Exhibit 31-79
Example Problem 1: Queue Accumulation Polygon

EXAMPLE PROBLEM 2: PEDESTRIAN LOS

The Intersection

The pedestrian crossing of interest crosses the north leg at a signalized intersection. The north-south street is the minor street and the east-west street is the major street. The intersection serves all north-south traffic concurrently (i.e., no left-turn phases) and all east-west traffic concurrently. The signal has an 80-s cycle length. The crosswalk and intersection corners that are the subject of this example problem are shown in Exhibit 31-80.

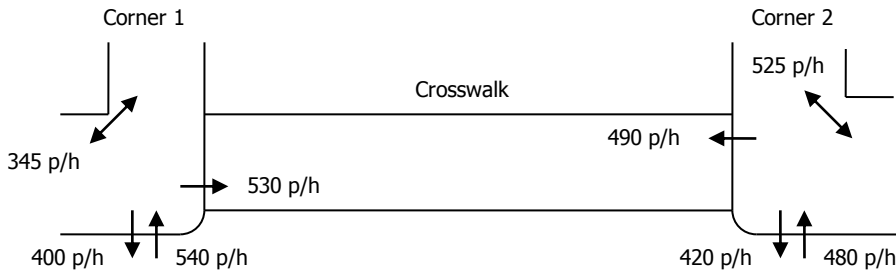


Exhibit 31-80
Example Problem 2: Pedestrian Flow Rates

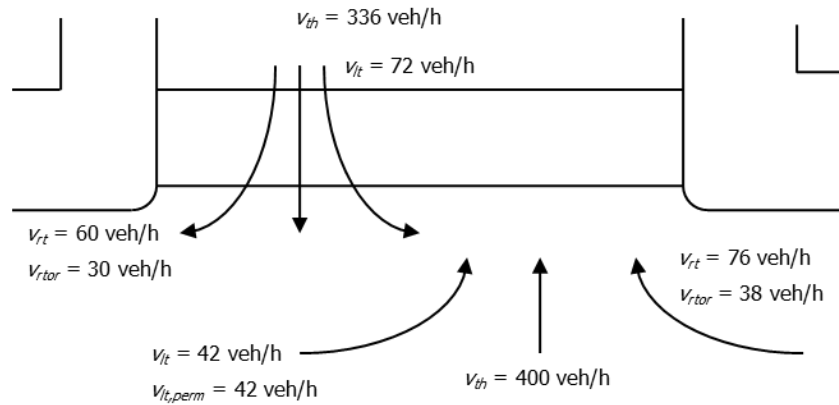
The Question

What is the pedestrian LOS for the crossing?

The Facts

Pedestrian flow rates are shown in Exhibit 31-80. Vehicular flow rates are shown in Exhibit 31-81.

Exhibit 31-81
 Example Problem 2: Vehicular
 Demand Flow Rates



In addition, the following facts are known about the crosswalk and the intersection corners:

- Major street: Phase duration, $D_{p,mj} = 48$ s
 Yellow change interval, $Y_{mj} = 4$ s
 Red clearance interval, $R_{mj} = 1$ s
 Walk setting, $Walk_{mj} = 7$ s
 Pedestrian clear setting, $PC_{mj} = 8$ s
 Four traffic lanes (no turn bays)
- Minor street: Phase duration, $D_{p,mi} = 32$ s
 Yellow change interval, $Y_{mi} = 4$ s
 Red clearance interval, $R_{mi} = 1$ s
 Walk setting, $Walk_{mi} = 7$ s
 Pedestrian clear setting, $PC_{mi} = 13$ s
 Two traffic lanes (no turn bays)
 85th percentile speed at a midsegment location, $S_{85,mi} = 35$ mi/h
- Corner 1: Total walkway width, $W_a = W_b = 16$ ft
 Corner radius, $R = 15$ ft
- Corner 2: Total walkway width, $W_a = W_b = 18$ ft
 Corner radius, $R = 15$ ft
- Other data: Effective crosswalk width, $W_c = 16$ ft
 Crosswalk length, $L_c = 28$ ft
 Walking speed, $S_p = 4$ ft/s
 No right-turn channelizing islands are provided on any corner.
 Pedestrian signal indications are provided for each crosswalk.
 Rest-in-walk mode is not used for any phase.

Comments

On the basis of the variable notation in Exhibit 19-29, the subject crosswalk is Crosswalk C because it crosses the minor street. The outbound pedestrian flow rate v_{co} at Corner 1 equals inbound flow rate v_{ci} at Corner 2, and the inbound flow rate v_{ci} at Corner 1 equals the outbound flow rate v_{co} at Corner 2.

Outline of Solution

First, the circulation area is calculated for both corners. Next, the circulation area is calculated for the crosswalk. The street corner and crosswalk circulation areas are then compared with the qualitative descriptions of pedestrian space listed in Exhibit 19-28.

Pedestrian delay and the pedestrian LOS score are then calculated for the crossing. Finally, LOS for the crossing is determined on the basis of the computed score and the threshold values in Exhibit 19-9.

Computational Steps

The solution follows the steps listed in Exhibit 19-33 of Chapter 19.

Step 1: Determine Street Corner Circulation Area

A. Compute Available Time-Space

For Corner 1, the available time-space is computed with Equation 19-51.

$$\begin{aligned} TS_{\text{corner}} &= C(W_a W_b - 0.215 R^2) \\ TS_{\text{corner}} &= 80[16 \times 16 - 0.215(15)^2] \\ TS_{\text{corner}} &= 16,610 \text{ ft}^2\text{-s} \end{aligned}$$

B. Compute Holding-Area Waiting Time

Because pedestrian signal indications are provided and rest-in-walk is not enabled, the effective walk time for the phase serving the major street is computed with Equation 19-54.

$$\begin{aligned} g_{\text{Walk},mj} &= \text{Walk}_{mj} + 4.0 \\ g_{\text{Walk},mj} &= 7.0 + 4.0 = 11 \text{ s} \end{aligned}$$

The number of pedestrians arriving at the corner during each cycle to cross the minor street is computed with Equation 19-53.

$$\begin{aligned} N_{co} &= \frac{v_{co}}{3,600} C \\ N_{co} &= \frac{530}{3,600} (80) = 11.8 \text{ p} \end{aligned}$$

The total time spent by pedestrians waiting to cross the minor street during one cycle is then calculated with Equation 19-52.

$$\begin{aligned} Q_{tco} &= \frac{N_{co} (C - g_{\text{Walk},mj})^2}{2 C} \\ Q_{tco} &= \frac{(11.8)(80 - 11)^2}{2(80)} = 350.5 \text{ p-s} \end{aligned}$$

By the same procedure, the total time spent by pedestrians waiting to cross the major street during one cycle (Q_{tdo}) is found to be 264.5 p-s.

C. Compute Circulation Time–Space

The circulation time–space is found by using Equation 19-57.

$$TS_c = TS_{\text{corner}} - [5.0(Q_{tdo} + Q_{tco})]$$

$$TS_c = 16,610 - [5.0(350.5 + 264.5)] = 13,535 \text{ ft}^2\text{-s}$$

D. Compute Pedestrian Corner Circulation Area

The total number of circulating pedestrians is computed with Equation 19-59.

$$N_{tot} = \frac{v_{ci} + v_{co} + v_{di} + v_{do} + v_{a,b}}{3,600} C$$

$$N_{tot} = \frac{490 + 530 + 540 + 400 + 345}{3,600} (80) = 51.2 \text{ p}$$

Finally, the corner circulation area per pedestrian is calculated with Equation 19-58.

$$M_{\text{corner}} = \frac{TS_c}{4.0 N_{tot}}$$

$$M_{\text{corner}} = \frac{13,535}{4.0(51.2)} = 66.1 \text{ ft}^2/\text{p}$$

By following the same procedure, the corner circulation area per pedestrian for Corner 2 is found to be 87.6 ft²/p. According to the qualitative descriptions provided in Exhibit 19-28, pedestrians at both corners will have the ability to move in the desired path without needing to alter their movements to avoid conflicts.

Step 2: Determine Crosswalk Circulation Area

The analysis conducted in this step describes the circulation area for pedestrians in the subject crosswalk.

A. Establish Walking Speed

As given in the subsection titled The Facts, the average walking speed is determined to be 4.0 ft/s.

B. Compute Available Time–Space

Rest-in-walk is not enabled, so the pedestrian service time g_{ped} is estimated to equal the sum of the walk and pedestrian clear settings. The time–space available in the crosswalk is found with Equation 19-60.

$$TS_{cw} = L_c W_c g_{\text{Walk},mj}$$

$$TS_{cw} = (28)(16)(11) = 4,928 \text{ ft}^2\text{-s}$$

C. Compute Effective Available Time–Space

The number of turning vehicles during the walk and pedestrian clear intervals is calculated with Equation 19-63.

$$N_{tv} = \frac{v_{lt,perm} + v_{rt} - v_{rtor}}{3,600} C$$

$$N_{tv} = \frac{42 + 76 - 38}{3,600} (80) = 1.8 \text{ veh}$$

The time-space occupied by turning vehicles can then be computed with Equation 19-62.

$$TS_{tv} = 40 N_{tv} W_c$$

$$TS_{tv} = 40(1.8)(16) = 1,138 \text{ ft}^2\text{-s}$$

The effective available crosswalk time-space TS_{cw}^* is found by subtracting the total available crosswalk time-space TS_{cw} from the time-space occupied by turning vehicles, as shown by Equation 19-61.

$$TS_{cw}^* = TS_{cw} - TS_{tv}$$

$$TS_{cw}^* = 4,928 - 1,138 = 3,970 \text{ ft}^2\text{-s}$$

D. Compute Pedestrian Service Time

The number of pedestrians exiting the curb when the WALK indication is presented is computed by using Equation 19-66.

$$N_{ped,co} = N_{co} \frac{C - g_{Walk,mj}}{C}$$

$$N_{ped,co} = (11.8) \frac{80 - 11}{80} = 10.2 \text{ p}$$

Because the crosswalk width is greater than 10 ft, the pedestrian service time is computed by using Equation 19-64.

$$t_{ps,co} = 3.2 + \frac{L_c}{S_p} + 2.7 \frac{N_{ped,co}}{W_c}$$

$$t_{ps,co} = 3.2 + \frac{28}{4.0} + (2.7) \frac{10.2}{16} = 11.9 \text{ s}$$

The other travel direction in the crosswalk is analyzed next. The number of pedestrians arriving at Corner 1 each cycle by crossing the minor street is computed by using Equation 19-68.

$$N_{ci} = \frac{v_{ci}}{3,600} C$$

$$N_{ci} = \frac{490}{3,600} (80) = 10.9 \text{ p}$$

The sequence of calculations is repeated for this second travel direction in the subject crosswalk to indicate that $N_{ped,ci}$ is equal to 9.4 p and $t_{ps,ci}$ is 11.8.

E. Compute Crosswalk Occupancy Time

The crosswalk occupancy time for the crosswalk is computed by using Equation 19-67.

$$T_{occ} = t_{ps,co} N_{co} + t_{ps,ci} N_{ci}$$

$$T_{occ} = 11.9(11.8) + 11.8(10.9) = 268.6 \text{ p-s}$$

F. Compute Pedestrian Crosswalk Circulation Area

Finally, the crosswalk circulation area per pedestrian for the crosswalk is computed by using Equation 19-69.

$$M_{cw} = \frac{TS_{cw}^*}{T_{occ}}$$

$$M_{cw} = \frac{3,790}{268.6} = 14.1 \text{ ft}^2/\text{p}$$

The crosswalk circulation area is found to be 14.1 ft²/p. According to the qualitative descriptions provided in Exhibit 19-28, pedestrians will find their walking speed is restricted, with very limited ability to pass slower pedestrians. Improvements to the crosswalk should be considered and may include a wider crosswalk or a longer walk interval.

Step 3: Determine Pedestrian Delay

The pedestrian delay is calculated by using Equation 19-70.

$$d_p = \frac{(C - g_{Walk,mj})^2}{2C}$$

$$d_p = \frac{(80 - 11)^2}{2(80)} = 29.8 \text{ s/p}$$

Step 4: Determine Pedestrian LOS Score for Intersection

The number of vehicles traveling on the minor street during a 15-min period is computed by using Equation 19-76.

$$n_{15,mi} = \frac{0.25}{N_c} \sum v_i$$

$$n_{15,mi} = \frac{0.25}{2} (72 + 336 + 60 + 42 + 400 + 76) = 123.3 \text{ veh/ln}$$

The cross-section adjustment factor is calculated by using Equation 19-72.

$$F_w = 0.681(N_c)^{0.514}$$

$$F_w = 0.681(2)^{0.514} = 0.972$$

The motorized vehicle adjustment factor is computed with Equation 19-73.

$$F_v = 0.00569 \left(\frac{v_{rtor} + v_{lt,perm}}{4} \right) - N_{rtci,c} (0.0027n_{15,mi} - 0.1946)$$

$$F_v = 0.00569 \left(\frac{30 + 42}{4} \right) - (0)(0.0027(123.3) - 0.1946) = 0.102$$

The motorized vehicle speed adjustment factor is then computed with Equation 19-74.

$$F_s = 0.00013 n_{15,mi} S_{85,mi}$$

$$F_s = 0.00013(123.3)(35) = 0.561$$

The pedestrian delay adjustment factor is calculated with Equation 19-75.

$$F_{delay} = 0.0401 \ln(d_{p,c})$$

$$F_{delay} = 0.0401 \ln(29.8) = 0.136$$

The pedestrian LOS score for the intersection $I_{p,int}$ is then computed with Equation 19-71.

$$I_{p,int} = 0.5997 + F_w + F_v + F_s + F_{delay}$$

$$I_{p,int} = 0.5997 + 0.972 + 0.102 + 0.561 + 0.136 = 2.37$$

Step 5: Determine LOS

According to Exhibit 19-9, the crosswalk operates at LOS B.

Discussion

The crosswalk was found to operate at LOS B in Step 5. It was determined in Step 1 that the pedestrians at both corners have adequate space to allow freedom of movement. However, crosswalk circulation area was found to be restricted in Step 2 and improvements are probably justified. Moreover, the pedestrian delay computed in Step 3 was found to be slightly less than 30 s/p. With this much delay, some pedestrians may not comply with the signal indication.

EXAMPLE PROBLEM 3: BICYCLE LOS

The Intersection

A 5-ft-wide bicycle lane is provided at a signalized intersection.

The Question

What is the LOS of this bicycle lane?

The Facts

- Saturation flow rate for bicycles = 2,000 bicycles/h
- Effective green time = 48 s
- Cycle length = 120 s
- Bicycle flow rate = 120 bicycles/h
- No on-street parking

The vehicular flow rates and street cross-section element widths are as shown in Exhibit 31-82.

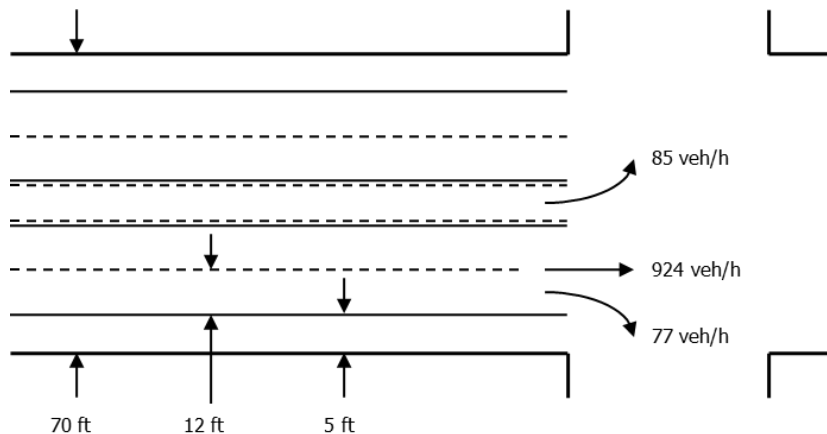


Exhibit 31-82
Example Problem 3: Vehicular Demand Flow Rates and Cross-Section Element Widths

Outline of Solution

Bicycle delay and the bicycle LOS score are computed. LOS is then determined on the basis of the computed score and the threshold values in Exhibit 19-9.

Computational Steps

The solution follows the steps listed in Exhibit 19-35 of Chapter 19.

Step 1: Determine Bicycle Delay

A. Compute Bicycle Lane Capacity

The capacity of the bicycle lane is calculated with Equation 19-77.

$$c_b = s_b \frac{g_b}{C}$$

$$c_b = (2,000) \frac{48}{120} = 800 \text{ bicycles/h}$$

B. Compute Bicycle Delay

Bicycle delay is computed with Equation 19-78.

$$d_b = \frac{0.5 C (1 - g_b/C)^2}{1 - \min\left(\frac{v_{bic}}{c_b}, 1.0\right) \frac{g_b}{C}}$$

$$d_b = \frac{0.5(120)(1 - 48/120)^2}{1 - \min\left(\frac{120}{800}, 1.0\right) \times \frac{48}{120}} = 23.0 \text{ s/bicycle}$$

Step 2: Determine Bicycle LOS Score for Intersection

As shown in Exhibit 31-82, the total width of the outside through lane, bicycle lane, and paved shoulder W_t is 17 ft (= 12 + 5 + 0 + 0). There is no on-street parking. The cross-section adjustment factor can then be calculated with Equation 19-80.

$$F_w = 0.0153 W_{cd} - 0.2144 W_t$$

$$F_w = 0.0153(70) - 0.2144(17) = -2.57$$

The motor-vehicle volume adjustment factor must be calculated by using Equation 19-81.

$$F_v = 0.0066 \frac{v_{lt} + v_{th} + v_{rt}}{4 N_{th}}$$

$$F_v = 0.0066 \frac{85 + 924 + 77}{4(2)} = 0.90$$

The bicycle LOS score can then be computed with Equation 19-79.

$$I_{b,int} = 4.1324 + F_w + F_v$$

$$I_{b,int} = 4.1324 - 2.57 + 0.90 = 2.45$$

Step 3: Determine LOS

According to Exhibit 19-9, the bicycle lane will operate at LOS B through the signalized intersection.

Discussion

The bicycle lane was found to operate at LOS B. The bicycle delay was found to be 23.0 s/bicycle, which is low enough that most bicyclists are not likely to be impatient. However, if the signal timing at the intersection were to be changed, the bicycle delay would need to be computed again to verify that it does not rise above 30 s/bicycle.

Many of these references are available in the Technical Reference Library in Volume 4.

10. REFERENCES

1. Zegeer, C., K. Opiela, and M. Cynecki. *Pedestrian Signalization Alternatives*. Report FHWA/RD-83/102. Federal Highway Administration, Washington, D.C., 1983.
2. Lieberman, E. B. Determining the Lateral Deployment of Traffic on an Approach to an Intersection. In *Transportation Research Record 772*, Transportation Research Board, National Research Council, Washington, D.C., 1980, pp. 1–5.
3. Bonneson, J. Lane Volume and Saturation Flow Rate for a Multilane Intersection Approach. *Journal of Transportation Engineering*, Vol. 124, No. 3, 1998, pp. 240–246.
4. Bonneson, J. A., and P. T. McCoy. *NCHRP Report 395: Capacity and Operational Effects of Midblock Left-Turn Lanes*. Transportation Research Board, National Research Council, Washington, D.C., 1997.
5. Teply, S. Accuracy of Delay Surveys at Signalized Intersections. In *Transportation Research Record 1225*, Transportation Research Board, National Research Council, Washington, D.C., 1989, pp. 24–32.
6. *Transportation Research Circular 212: Interim Materials on Highway Capacity*. Transportation Research Board, National Research Council, Washington, D.C., 1980.
7. Pline, J. L. (ed.). *Traffic Engineering Handbook*, 5th ed. ITE, Washington, D.C., 1999.
8. Reilly, W. R., and C. C. Gardner. Technique for Measuring Delay at Intersections. In *Transportation Research Record 644*, Transportation Research Board, National Research Council, Washington, D.C., 1977, pp. 1–7.
9. Powell, J. L. Field Measurement of Signalized Intersection Delay for 1997 Update of the *Highway Capacity Manual*. In *Transportation Research Record 1646*, Transportation Research Board, National Research Council, Washington, D.C., 1998, pp. 79–86.



HIGHWAY CAPACITY MANUAL

6TH EDITION | A GUIDE FOR MULTIMODAL MOBILITY ANALYSIS

VOLUME 4: APPLICATIONS GUIDE

The National Academies of
SCIENCES • ENGINEERING • MEDICINE

TRANSPORTATION RESEARCH BOARD
WASHINGTON, D.C. | WWW.TRB.ORG

TRANSPORTATION RESEARCH BOARD 2016 EXECUTIVE COMMITTEE *

Chair: James M. Crites, Executive Vice President of Operations,
Dallas–Fort Worth International Airport, Texas

Vice Chair: Paul Trombino III, Director, Iowa Department of
Transportation, Ames

Executive Director: Neil J. Pedersen, Transportation Research Board

Victoria A. Arroyo, Executive Director, Georgetown Climate Center;
Assistant Dean, Centers and Institutes; and Professor and Director,
Environmental Law Program, Georgetown University Law Center,
Washington, D.C.

Scott E. Bennett, Director, Arkansas State Highway and Transportation
Department, Little Rock

Jennifer Cohan, Secretary, Delaware Department of Transportation, Dover

Malcolm Dougherty, Director, California Department of
Transportation, Sacramento

A. Stewart Fotheringham, Professor, School of Geographical Sciences
and Urban Planning, Arizona State University, Tempe

John S. Halikowski, Director, Arizona Department of Transportation,
Phoenix

Susan Hanson, Distinguished University Professor Emerita, Graduate
School of Geography, Clark University, Worcester, Massachusetts

Steve Heminger, Executive Director, Metropolitan Transportation
Commission, Oakland, California

Chris T. Hendrickson, Hamerschlag Professor of Engineering, Carnegie
Mellon University, Pittsburgh, Pennsylvania

Jeffrey D. Holt, Managing Director, Power, Energy, and Infrastructure
Group, BMO Capital Markets Corporation, New York

S. Jack Hu, Vice President for Research and J. Reid and Polly Anderson
Professor of Manufacturing, University of Michigan, Ann Arbor

Roger B. Huff, President, HGLC, LLC, Farmington Hills, Michigan

Geraldine Knatz, Professor, Sol Price School of Public Policy, Viterbi
School of Engineering, University of Southern California, Los Angeles

Ysela Llort, Consultant, Miami, Florida

Melinda McGrath, Executive Director, Mississippi Department of
Transportation, Jackson

James P. Redeker, Commissioner, Connecticut Department of
Transportation, Newington

Mark L. Rosenberg, Executive Director, The Task Force for Global
Health, Inc., Decatur, Georgia

Kumares C. Sinha, Olson Distinguished Professor of Civil Engineering,
Purdue University, West Lafayette, Indiana

Daniel Sperling, Professor of Civil Engineering and Environmental
Science and Policy; Director, Institute of Transportation Studies,
University of California, Davis

Kirk T. Steudle, Director, Michigan Department of Transportation,
Lansing (Past Chair, 2014)

Gary C. Thomas, President and Executive Director, Dallas Area Rapid
Transit, Dallas, Texas

Pat Thomas, Senior Vice President of State Government Affairs, United
Parcel Service, Washington, D.C.

Katherine F. Turnbull, Executive Associate Director and Research
Scientist, Texas A&M Transportation Institute, College Station

Dean Wise, Vice President of Network Strategy, Burlington Northern
Santa Fe Railway, Fort Worth, Texas

Thomas P. Bostick (Lieutenant General, U.S. Army), Chief of Engineers
and Commanding General, U.S. Army Corps of Engineers, Washington,
D.C. (ex officio)

James C. Card (Vice Admiral, U.S. Coast Guard, retired), Maritime
Consultant, The Woodlands, Texas, and Chair, TRB Marine Board
(ex officio)

T. F. Scott Darling III, Acting Administrator and Chief Counsel, Federal
Motor Carrier Safety Administration, U.S. Department of Transportation
(ex officio)

Marie Therese Dominguez, Administrator, Pipeline and Hazardous
Materials Safety Administration, U.S. Department of Transportation
(ex officio)

Sarah Feinberg, Administrator, Federal Railroad Administration,
U.S. Department of Transportation (ex officio)

Carolyn Flowers, Acting Administrator, Federal Transit Administration,
U.S. Department of Transportation (ex officio)

LeRoy Gishi, Chief, Division of Transportation, Bureau of Indian
Affairs, U.S. Department of the Interior, Washington, D.C. (ex officio)

John T. Gray II, Senior Vice President, Policy and Economics,
Association of American Railroads, Washington, D.C. (ex officio)

Michael P. Huerta, Administrator, Federal Aviation Administration,
U.S. Department of Transportation (ex officio)

Paul N. Jaenichen, Sr., Administrator, Maritime Administration,
U.S. Department of Transportation (ex officio)

Bevan B. Kirley, Research Associate, University of North Carolina
Highway Safety Research Center, Chapel Hill, and Chair, TRB Young
Members Council (ex officio)

Gregory G. Nadeau, Administrator, Federal Highway Administration,
U.S. Department of Transportation (ex officio)

Wayne Nastri, Acting Executive Officer, South Coast Air Quality
Management District, Diamond Bar, California (ex officio)

Mark R. Rosekind, Administrator, National Highway Traffic Safety
Administration, U.S. Department of Transportation (ex officio)

Craig A. Rutland, U.S. Air Force Pavement Engineer, U.S. Air Force
Civil Engineer Center, Tyndall Air Force Base, Florida (ex officio)

Reuben Sarkar, Deputy Assistant Secretary for Transportation,
U.S. Department of Energy (ex officio)

Richard A. White, Acting President and CEO, American Public
Transportation Association, Washington, D.C. (ex officio)

Gregory D. Winfree, Assistant Secretary for Research and Technology,
Office of the Secretary, U.S. Department of Transportation (ex officio)

Frederick G. (Bud) Wright, Executive Director, American Association
of State Highway and Transportation Officials, Washington, D.C.
(ex officio)

Paul F. Zukunft (Admiral, U.S. Coast Guard), Commandant, U.S. Coast
Guard, U.S. Department of Homeland Security (ex officio)

Transportation Research Board publications are available by ordering
individual publications directly from the TRB Business Office, through
the Internet at www.TRB.org, or by annual subscription through
organizational or individual affiliation with TRB. Affiliates and library
subscribers are eligible for substantial discounts. For further information,
contact the Transportation Research Board Business Office, 500 Fifth
Street, NW, Washington, DC 20001 (telephone 202-334-3213;
fax 202-334-2519; or e-mail TRBsales@nas.edu).

Copyright 2016 by the National Academy of Sciences.

All rights reserved.

Printed in the United States of America.

ISBN 978-0-309-36997-8 [Slipcased set of three volumes]

ISBN 978-0-309-36998-5 [Volume 1]

ISBN 978-0-309-36999-2 [Volume 2]

ISBN 978-0-309-37000-4 [Volume 3]

ISBN 978-0-309-37001-1 [Volume 4, online only]

The National Academies of
SCIENCES • ENGINEERING • MEDICINE

The **National Academy of Sciences** was established in 1863 by an Act of Congress, signed by President Lincoln, as a private, nongovernmental institution to advise the nation on issues related to science and technology. Members are elected by their peers for outstanding contributions to research. Dr. Ralph J. Cicerone is president.

The **National Academy of Engineering** was established in 1964 under the charter of the National Academy of Sciences to bring the practices of engineering to advising the nation. Members are elected by their peers for extraordinary contributions to engineering. Dr. C. D. Mote, Jr., is president.

The **National Academy of Medicine** (formerly the Institute of Medicine) was established in 1970 under the charter of the National Academy of Sciences to advise the nation on medical and health issues. Members are elected by their peers for distinguished contributions to medicine and health. Dr. Victor J. Dzau is president.

The three Academies work together as the National Academies of Sciences, Engineering, and Medicine to provide independent, objective analysis and advice to the nation and conduct other activities to solve complex problems and inform public policy decisions. The Academies also encourage education and research, recognize outstanding contributions to knowledge, and increase public understanding in matters of science, engineering, and medicine.

Learn more about the National Academies of Sciences, Engineering, and Medicine at **www.national-academies.org**.

The **Transportation Research Board** is one of seven major programs of the National Academies of Sciences, Engineering, and Medicine. The mission of the Transportation Research Board is to increase the benefits that transportation contributes to society by providing leadership in transportation innovation and progress through research and information exchange, conducted within a setting that is objective, interdisciplinary, and multimodal. The Board's varied committees, task forces, and panels annually engage about 7,000 engineers, scientists, and other transportation researchers and practitioners from the public and private sectors and academia, all of whom contribute their expertise in the public interest. The program is supported by state transportation departments, federal agencies including the component administrations of the U.S. Department of Transportation, and other organizations and individuals interested in the development of transportation.

Learn more about the Transportation Research Board at **www.TRB.org**.

CHAPTER 32
STOP-CONTROLLED INTERSECTIONS: SUPPLEMENTAL

CONTENTS

1. INTRODUCTION 32-1

2. TWSC POTENTIAL CAPACITY 32-2

3. TWSC EXAMPLE PROBLEMS 32-4

 TWSC Example Problem 1: TWSC at an Intersection with Three Legs 32-4

 TWSC Example Problem 2: Pedestrian Crossing at a TWSC
 Intersection..... 32-10

 TWSC Example Problem 3: Flared Approaches and Median Storage 32-13

 TWSC Example Problem 4: TWSC Intersection Within A Signalized
 Urban Street Segment..... 32-28

 TWSC Example Problem 5: Six-Lane Street with U-Turns and
 Pedestrians..... 32-38

**4. AWSC SUPPLEMENTAL ANALYSIS FOR THREE-LANE
 APPROACHES 32-47**

5. AWSC EXAMPLE PROBLEMS..... 32-56

 AWSC Example Problem 1: Single-Lane, Three-Leg Intersection 32-56

 AWSC Example Problem 2: Multilane, Four-Leg Intersection..... 32-61

LIST OF EXHIBITS

Exhibit 32-1 Potential Capacity $c_{p,x}$ for Two-Lane Major Streets 32-2

Exhibit 32-2 Potential Capacity $c_{p,x}$ for Four-Lane Major Streets..... 32-3

Exhibit 32-3 Potential Capacity $c_{p,x}$ for Six-Lane Major Streets..... 32-3

Exhibit 32-4 TWSC Example Problems 32-4

Exhibit 32-5 TWSC Example Problem 1: 15-min Volumes and Lane Configurations..... 32-4

Exhibit 32-6 TWSC Example Problem 1: Movement Numbers and Calculation of Peak 15-min Flow Rates 32-5

Exhibit 32-7 TWSC Example Problem 3: 15-min Volumes and Lane Configurations..... 32-13

Exhibit 32-8 TWSC Example Problem 3: Movement Numbers and Calculation of Peak 15-min Flow Rates 32-14

Exhibit 32-9 TWSC Example Problem 4: TWSC Intersection Within a Signalized Urban Street Segment 32-29

Exhibit 32-10 TWSC Example Problem 4: 15-min Flow Rates and Lane Configurations..... 32-29

Exhibit 32-11 TWSC Example Problem 4: Movement-Based Access Point Output (from Chapter 30, Example Problem 1) 32-29

Exhibit 32-12 TWSC Example Problem 4: Movement Numbers and Calculation of Peak 15-min Flow Rates 32-30

Exhibit 32-13 TWSC Example Problem 5: Volumes and Lane Configurations..... 32-39

Exhibit 32-14 TWSC Example Problem 5: Movement Numbers and Calculation of Peak 15-min Flow Rates 32-39

Exhibit 32-15 Probability of Degree-of-Conflict Case: Multilane AWSC Intersections (Three-Lane Approaches, by Lane) 32-47

Exhibit 32-16 AWSC Example Problems 32-56

Exhibit 32-17 AWSC Example Problem 1: Volumes and Lane Configurations..... 32-56

Exhibit 32-18 AWSC Example Problem 1: Applicable Degree-of-Conflict Cases 32-58

Exhibit 32-19 AWSC Example Problem 1: Eastbound Saturation Headways 32-59

Exhibit 32-20 AWSC Example Problem 1: Convergence Check..... 32-60

Exhibit 32-21 AWSC Example Problem 2: 15-min Volumes and Lane Configurations..... 32-62

Exhibit 32-22 AWSC Example Problem 2: 15-min Volumes Converted to Hourly Flow Rates 32-62

Exhibit 32-23 AWSC Example Problem 2: Convergence Check..... 32-66

1. INTRODUCTION

Chapter 32 is the supplemental chapter for Chapter 20, Two-Way STOP-Controlled Intersections, and Chapter 21, All-Way STOP-Controlled Intersections, which are found in Volume 3 of the *Highway Capacity Manual*. This chapter provides supplemental material on (a) determining the potential capacity of two-way STOP-controlled (TWSC) intersections and (b) identifying the 512 combinations of degree-of-conflict cases for all-way STOP-controlled (AWSC) intersections with three-lane approaches. The chapter also provides example problems demonstrating the application of the TWSC and AWSC methodologies.

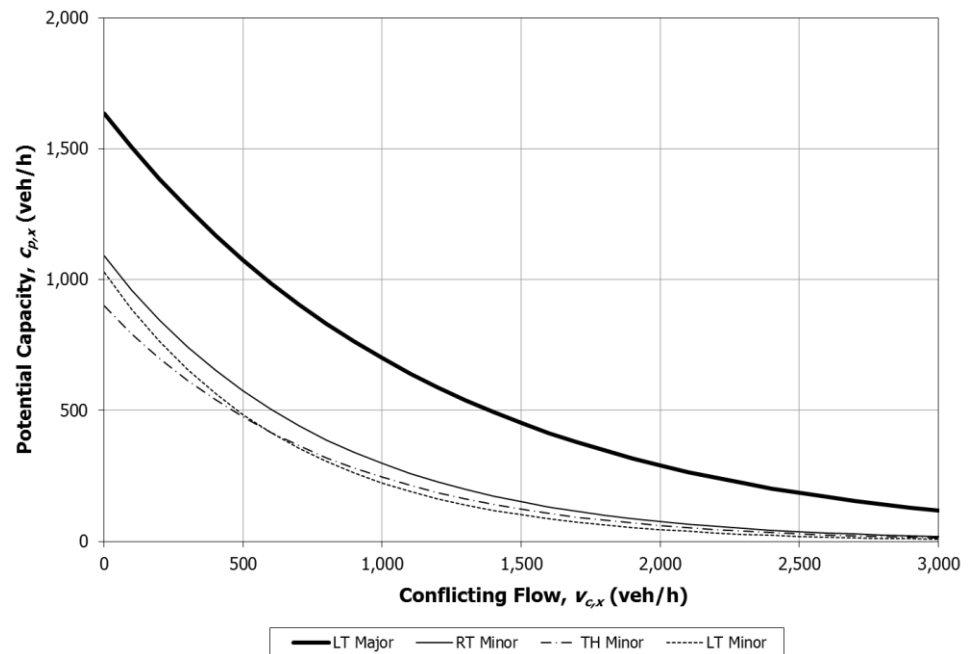
VOLUME 4: APPLICATIONS GUIDE

- 25. Freeway Facilities: Supplemental
- 26. Freeway and Highway Segments: Supplemental
- 27. Freeway Weaving: Supplemental
- 28. Freeway Merges and Diverges: Supplemental
- 29. Urban Street Facilities: Supplemental
- 30. Urban Street Segments: Supplemental
- 31. Signalized Intersections: Supplemental
- 32. STOP-Controlled Intersections: Supplemental**
- 33. Roundabouts: Supplemental
- 34. Interchange Ramp Terminals: Supplemental
- 35. Pedestrians and Bicycles: Supplemental
- 36. Concepts: Supplemental
- 37. ATDM: Supplemental

2. TWSC POTENTIAL CAPACITY

The gap acceptance model to estimate potential capacity (presented in Chapter 20, Equation 20-32) can be plotted for each of the non-Rank 1 movements by using values of critical headway and follow-up headway from Chapter 20 (Exhibit 20-12 and Exhibit 20-13, respectively). These graphs are presented in Exhibit 32-1, Exhibit 32-2, and Exhibit 32-3 for a major street with two lanes, four lanes, and six lanes, respectively. The potential capacity is expressed as vehicles per hour. The exhibits indicate the potential capacity is a function of the conflicting flow rate $v_{c,x}$ expressed as an hourly rate, as well as the type of minor-street movement.

Exhibit 32-1
Potential Capacity $c_{p,x}$ for
Two-Lane Major Streets



Note: LT = left turn, RT = right turn, and TH = through.

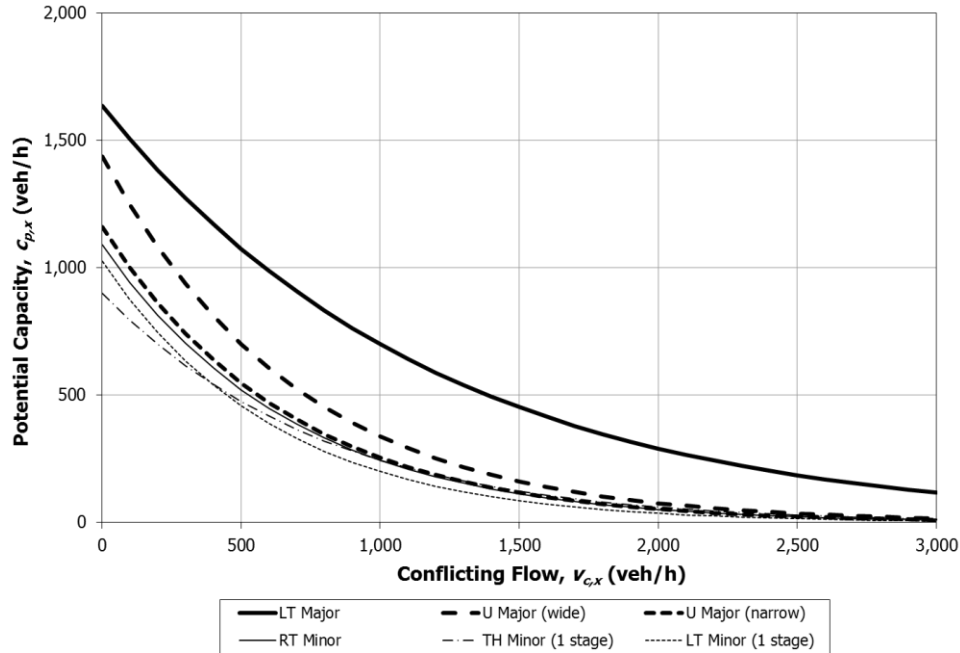


Exhibit 32-2
Potential Capacity $c_{p,x}$ for
Four-Lane Major Streets

Note: LT = left turn, U = U-turn, RT = right turn, and TH = through.

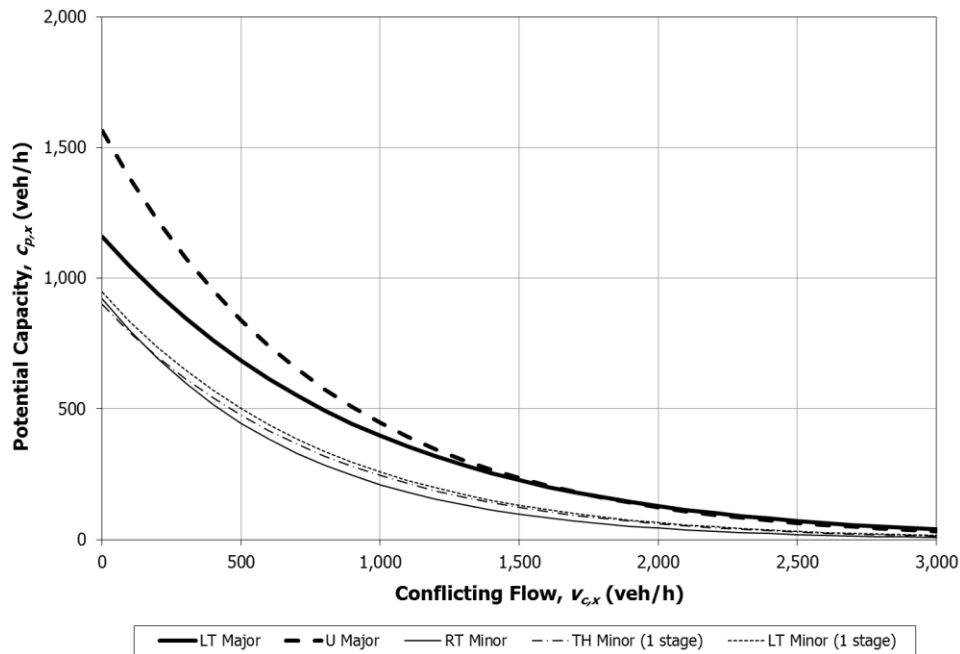


Exhibit 32-3
Potential Capacity $c_{p,x}$ for
Six-Lane Major Streets

Note: LT = left turn, U = U-turn, RT = right turn, and TH = through.

3. TWSC EXAMPLE PROBLEMS

This section provides example problems for use of the TWSC methodology. Exhibit 32-4 provides an overview of these problems. The examples focus on the operational analysis level. The planning and preliminary engineering analysis level is identical to the operations analysis level in terms of the calculations, except that default values are used when available.

Exhibit 32-4
TWSC Example Problems

Problem Number	Description	Analysis Level
1	TWSC at an intersection with three legs	Operational
2	Pedestrian crossing at a TWSC intersection	Operational
3	TWSC intersection with flared approaches and median storage	Operational
4	TWSC intersection within a signalized urban street segment	Operational
5	TWSC intersection on a six-lane street with U-turns and pedestrians	Operational

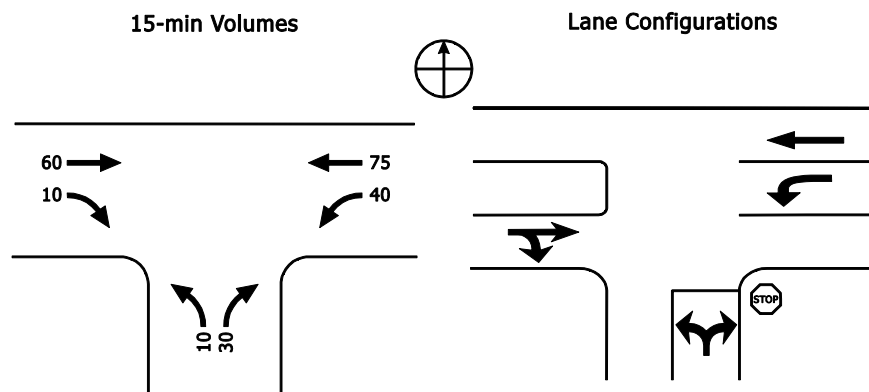
TWSC EXAMPLE PROBLEM 1: TWSC AT AN INTERSECTION WITH THREE LEGS

The Facts

The following data are available to describe the traffic and geometric characteristics of this location:

- T-intersection,
- Major street with one lane in each direction,
- Minor street with one lane in each direction and STOP-controlled on the minor-street approach,
- Level grade on all approaches,
- Percentage heavy vehicles on all approaches = 10%,
- No other unique geometric considerations or upstream signal considerations,
- No pedestrians,
- Length of analysis period = 0.25 h, and
- Volumes during the peak 15-min period and lane configurations as shown in Exhibit 32-5.

Exhibit 32-5
TWSC Example Problem 1:
15-min Volumes and Lane
Configurations



Comments

All input parameters are known, so no default values are needed or used.

Steps 1 and 2: Convert Movement Demand Volumes to Flow Rates and Label Movement Priorities

Because peak 15-min volumes have been provided, each volume is multiplied by four to determine a peak 15-min flow rate (in vehicle per hour) for each movement. These values, along with the associated movement numbers, are shown in Exhibit 32-6.

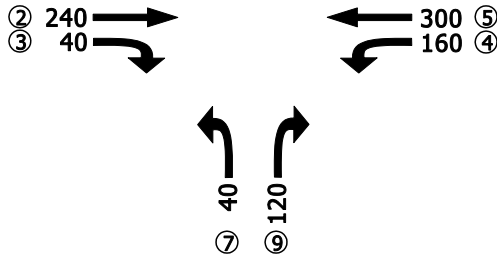


Exhibit 32-6
TWSC Example Problem 1:
Movement Numbers and
Calculation of Peak 15-min
Flow Rates

Step 3: Compute Conflicting Flow Rates

The conflicting flow rates for each minor movement at the intersection are computed according to Equation 20-3, Equation 20-4, Equation 20-18, and Equation 20-24. The conflicting flow for the major-street left-turn $v_{c,4}$ is

$$v_{c,4} = v_2 + v_3 + v_{15}$$

$$v_{c,4} = 240 + 40 + 0 = 280 \text{ veh/h}$$

The conflicting flow for the minor-street right-turn movement $v_{c,9}$ is

$$v_{c,9} = v_2 + 0.5v_3 + v_{14} + v_{15}$$

$$v_{c,9} = 240 + 0.5(40) + 0 + 0 = 260 \text{ veh/h}$$

Finally, the conflicting flow for the minor-street left-turn movement $v_{c,7}$ is computed. Because two-stage gap acceptance is not present at this intersection, the conflicting flow rates shown in Stage I (Equation 20-18) and Stage II (Equation 20-24) are added together and considered as one conflicting flow rate. The conflicting flow for $v_{c,7}$ is computed as follows:

$$v_{c,7} = 2v_1 + v_2 + 0.5v_3 + v_{15} + 2v_4 + v_5 + 0.5v_6 + 0.5v_{12} + 0.5v_{11} + v_{13}$$

$$v_{c,7} = 2(0) + 240 + 0.5(40) + 0 + 2(160) + 300 + 0.5(0) + 0.5(0) + 0.5(0) + 0 = 880 \text{ veh/h}$$

Step 4: Determine Critical Headways and Follow-Up Headways

The critical headway for each minor movement is computed beginning with the base critical headway given in Exhibit 20-12. The base critical headway for each movement is then adjusted according to Equation 20-30. The critical headway for the major-street left-turn movement $t_{c,4}$ is computed as follows:

$$t_{c,4} = t_{c,\text{base}} + t_{c,HV}P_{HV} + t_{c,G}G - t_{3,LT}$$

$$t_{c,4} = 4.1 + 1.0(0.1) + 0(0) - 0 = 4.2 \text{ s}$$

Similarly, the critical headway for the minor-street right-turn movement $t_{c,9}$ is

$$t_{c,9} = 6.2 + 1.0(0.1) + 0.1(0) - 0 = 6.3 \text{ s}$$

Finally, the critical headway for the minor-street left-turn movement $t_{c,7}$ is

$$t_{c,7} = 7.1 + 1.0(0.1) + 0.2(0) - 0.7 = 6.5 \text{ s}$$

The follow-up headway for each minor movement is computed beginning with the base follow-up headway given in Exhibit 20-13. The base follow-up headway for each movement is then adjusted according to Equation 20-31. The follow-up headway for the major-street left-turn movement $t_{f,4}$ is computed as follows:

$$t_{f,4} = t_{f,base} + t_{f,HV}P_{HV}$$

$$t_{f,4} = 2.2 + 0.9(0.1) = 2.29 \text{ s}$$

Similarly, the follow-up headway for the minor-street right-turn movement $t_{f,9}$ is

$$t_{f,9} = 3.3 + 0.9(0.1) = 3.39 \text{ s}$$

Finally, the follow-up headway for the minor-street left-turn movement $t_{f,7}$ is

$$t_{f,7} = 3.5 + 0.9(0.1) = 3.59 \text{ s}$$

Step 5: Compute Potential Capacities

The computation of a potential capacity for each movement provides the analyst with a definition of capacity under the assumed base conditions. The potential capacity will be adjusted in later steps to estimate the movement capacity for each movement. The potential capacity for each movement is a function of the conflicting flow rate, critical headway, and follow-up headway computed in the previous steps. The potential capacity for the major-street left-turn movement $c_{p,4}$ is computed as follows from Equation 20-32:

$$c_{p,4} = v_{c,4} \frac{e^{-v_{c,4}t_{c,4}/3,600}}{1 - e^{-v_{c,4}t_{f,4}/3,600}}$$

$$c_{p,4} = 280 \frac{e^{-(280)(4.2)/3,600}}{1 - e^{-(280)(2.29)/3,600}} = 1,238 \text{ veh/h}$$

Similarly, the potential capacity for the minor-street right-turn movement $c_{p,9}$ is computed as follows:

$$c_{p,9} = 260 \frac{e^{-(260)(6.3)/3,600}}{1 - e^{-(260)(3.39)/3,600}} = 760 \text{ veh/h}$$

Finally, the potential capacity for the minor-street left-turn movement $c_{p,7}$ is

$$c_{p,7} = 880 \frac{e^{-(880)(6.5)/3,600}}{1 - e^{-(880)(3.59)/3,600}} = 308 \text{ veh/h}$$

There are no upstream signals, so the adjustments for upstream signals are ignored.

Step 6: Compute Rank 1 Movement Capacities

There are no pedestrians at the intersection; therefore, all pedestrian impedance factors are equal to 1.0, and this step can be ignored.

Step 7: Compute Rank 2 Movement Capacities

The movement capacity for the major-street left-turn movement (Rank 2) $c_{m,4}$ is computed as follows from Equation 20-36:

$$c_{m,4} = c_{p,4} = 1,238 \text{ veh/h}$$

Similarly, the movement capacity for the minor-street right-turn movement (Rank 2) $c_{m,9}$ is computed with Equation 20-37:

$$c_{m,9} = c_{p,9} = 760 \text{ veh/h}$$

Step 8: Compute Rank 3 Movement Capacities

The computation of vehicle impedance effects accounts for the reduction in potential capacity due to the impacts of the congestion of a high-priority movement on lower-priority movements.

Major-street movements of Rank 1 and Rank 2 are assumed to be unimpeded by other vehicular movements. Minor-street movements of Rank 3 can be impeded by major-street left-turn movements due to a major-street left-turning vehicle waiting for an acceptable gap at the same time as vehicles of Rank 3. The magnitude of this impedance depends on the probability that major-street left-turning vehicles will be waiting for an acceptable gap at the same time as vehicles of Rank 3. In this example, only the minor-street left-turn movement is defined as a Rank 3 movement. Therefore, the probability of the major-street left-turn movement operating in a queue-free state ($p_{0,4}$) is computed from Equation 20-42:

$$p_{0,4} = 1 - \frac{v_4}{c_{m,4}} = 1 - \frac{160}{1,238} = 0.871$$

The movement capacity for the minor-street left-turn movement (Rank 3) $c_{m,7}$ is found by first computing a capacity adjustment factor that accounts for the impeding effects of higher-ranked movements. The capacity adjustment factor for the minor-street left-turn movement f_7 is computed with Equation 20-46:

$$f_7 = \prod_j p_{0,j} = 0.871$$

The movement capacity for the minor-street left-turn movement (Rank 3) $c_{m,7}$ is computed with Equation 20-47:

$$c_{m,7} = c_{p,7} \times f_7 = 308(0.871) = 268 \text{ veh/h}$$

Step 9: Compute Rank 4 Movement Capacities

There are no Rank 4 movements in this example problem, so this step does not apply.

Step 10: Compute Capacity Adjustment Factors

In this example, the minor-street approach is a single lane shared by right-turn and left-turn movements; therefore, the capacity of these two movements must be adjusted to compute an approach capacity based on shared-lane effects.

The shared-lane capacity for the northbound minor-street approach $c_{SH,NB}$ is computed from Equation 20-59:

$$c_{SH,NB} = \frac{\sum_y v_y}{\sum_y \frac{v_y}{c_{m,y}}} = \frac{v_7 + v_9}{\frac{v_7}{c_{m,7}} + \frac{v_9}{c_{m,9}}} = \frac{40 + 120}{\frac{40}{268} + \frac{120}{760}} = 521 \text{ veh/h}$$

No other adjustments apply.

Step 11: Compute Control Delay

The control delay computation for any movement includes initial deceleration delay, queue move-up time, stopped delay, and final acceleration delay.

Step 11a: Compute Control Delay to Rank 2 Through Rank 4 Movements

The control delay for the major-street left-turn movement (Rank 2) d_4 is computed with Equation 20-64:

$$d = \frac{3,600}{c_{m,x}} + 900T \left[\frac{v_x}{c_{m,x}} - 1 + \sqrt{\left(\frac{v_x}{c_{m,x}} - 1\right)^2 + \frac{\left(\frac{3,600}{c_{m,x}}\right)\left(\frac{v_x}{c_{m,x}}\right)}{450T}} \right] + 5$$

$$d_4 = \frac{3,600}{1,238} + 900(0.25) \left[\frac{160}{1,238} - 1 + \sqrt{\left(\frac{160}{1,238} - 1\right)^2 + \frac{\left(\frac{3,600}{1,238}\right)\left(\frac{160}{1,238}\right)}{450(0.25)}} \right] + 5$$

$$d_4 = 8.3 \text{ s}$$

On the basis of Exhibit 20-2, the westbound left-turn movement is assigned level of service (LOS) A.

The control delay for the minor-street right-turn and left-turn movements is computed by using the same formula; however, one significant difference from the major-street left-turn computation of control delay is that these movements share the same lane. Therefore, the control delay is computed for the approach as a whole, and the shared-lane volume and shared-lane capacity must be used as follows:

$$d_{SH,NB} = \frac{3,600}{521} + 900(0.25) \left[\frac{160}{521} - 1 + \sqrt{\left(\frac{160}{521} - 1\right)^2 + \frac{\left(\frac{3,600}{521}\right)\left(\frac{160}{521}\right)}{450(0.25)}} \right] + 5$$

$$d_{SH,NB} = 14.9 \text{ s}$$

On the basis of Exhibit 20-2, the northbound approach is assigned LOS B.

Step 11b: Compute Control Delay to Rank 1 Movements

This step is not applicable as the westbound major-street through movement v_5 and westbound major-street left-turn movement v_4 have exclusive lanes at this intersection. It is assumed the eastbound through movement v_2 and eastbound major-street right-turn movement v_3 do not incur any delay at this intersection.

Step 12: Compute Approach and Intersection Control Delay

The control delays to all vehicles on the eastbound approach are assumed to be negligible as described in Step 11b. The control delay for the westbound approach $d_{A,WB}$ is computed with Equation 20-66:

$$d_A = \frac{d_r v_r + d_t v_t + d_l v_l}{v_r + v_t + v_l}$$

$$d_{A,WB} = \frac{0(0) + 0(300) + 8.3(160)}{0 + 300 + 160} = 2.9 \text{ s}$$

It is assumed the westbound through movement incurs no control delay at this intersection. The control delay for the northbound approach was computed in Step 11a as $d_{SH,NB}$.

The intersection control delay d_I is computed from Equation 20-67:

$$d_I = \frac{d_{A,EB} v_{A,EB} + d_{A,WB} v_{A,WB} + d_{A,NB} v_{A,NB}}{v_{A,EB} + v_{A,WB} + v_{A,NB}}$$

$$d_I = \frac{0(280) + 2.9(460) + 14.9(160)}{280 + 460 + 160} = 4.1 \text{ s}$$

As noted in Chapter 20, neither major-street approach LOS nor intersection LOS is defined.

Step 13: Compute 95th Percentile Queue Lengths

The 95th percentile queue length for the major-street westbound left-turn movement $Q_{95,4}$ is computed from Equation 20-68:

$$Q_{95,4} \approx 900T \left[\frac{v_4}{c_{m,4}} - 1 + \sqrt{\left(\frac{v_4}{c_{m,4}} - 1 \right)^2 + \frac{\left(\frac{3,600}{c_{m,4}} \right) \left(\frac{v_x}{c_{m,4}} \right)}{150T}} \right] \left(\frac{c_{m,4}}{3,600} \right)$$

$$Q_{95,4} \approx 900(0.25) \left[\frac{160}{1,238} - 1 + \sqrt{\left(\frac{160}{1,238} - 1 \right)^2 + \frac{\left(\frac{3,600}{1,238} \right) \left(\frac{160}{1,238} \right)}{150(0.25)}} \right] \left(\frac{1,238}{3,600} \right)$$

$$Q_{95,4} = 0.4 \text{ veh}$$

The result of 0.4 vehicles for the 95th percentile queue indicates a queue of more than one vehicle will occur very infrequently for the major-street left-turn movement.

The 95th percentile queue length for the northbound approach is computed by using the same formula. Similar to the control delay computation, the shared-lane volume and shared-lane capacity must be used as shown:

$$Q_{95,NB} \approx 900(0.25) \left[\frac{160}{521} - 1 + \sqrt{\left(\frac{160}{521} - 1 \right)^2 + \frac{\left(\frac{3,600}{521} \right) \left(\frac{160}{521} \right)}{150(0.25)}} \right] \left(\frac{521}{3,600} \right)$$

$$Q_{95,NB} = 1.3 \text{ veh}$$

The result suggests that a queue of more than one vehicle will occur only occasionally for the northbound approach.

Discussion

Overall, the results indicate this three-leg TWSC intersection will operate well with brief delays and little queuing for all minor movements.

TWSC EXAMPLE PROBLEM 2: PEDESTRIAN CROSSING AT A TWSC INTERSECTION

Calculate the pedestrian LOS of a pedestrian crossing of a major street at a TWSC intersection under the following circumstances:

- Scenario A: unmarked crosswalk, no median refuge island;
- Scenario B: unmarked crosswalk, median refuge island; and
- Scenario C: marked crosswalk with high-visibility treatments, median refuge island.

The Facts

The following data are available to describe the traffic and geometric characteristics of this location:

- Four-lane major street;
- 1,700 peak hour vehicles, bidirectional;
- Crosswalk length without median = 46 ft;
- Crosswalk length with median = 40 ft;
- Observed pedestrian walking speed = 4 ft/s;
- Pedestrian start-up time = 3 s; and
- No pedestrian platooning.

Comments

In addition to the input data listed above, information is required on motor vehicle yield rates under the various scenarios. On the basis of an engineering study of similar intersections in the vicinity, it is determined motor vehicle yield rates are 0% with unmarked crosswalks and 50% with high-visibility marked crosswalks.

Step 1: Identify Two-Stage Crossings

Scenario A does not have two-stage pedestrian crossings, as no median refuge is available. Analysis for Scenarios B and C should assume two-stage crossings. Thus, analysis for Scenarios B and C will combine two equidistant pedestrian crossings of 20 ft each to determine the total delay.

Step 2: Determine Critical Headway

Because there is no pedestrian platooning, the critical headway t_c is determined with Equation 20-77:

Scenario A: $t_c = (46 \text{ ft})/(4 \text{ ft/s}) + 3 \text{ s} = 14.5 \text{ s}$

Scenario B: $t_c = (20 \text{ ft})/(4 \text{ ft/s}) + 3 \text{ s} = 8 \text{ s}$

Scenario C: $t_c = (20 \text{ ft})/(4 \text{ ft/s}) + 3 \text{ s} = 8 \text{ s}$

Step 3: Estimate Probability of a Delayed Crossing

Equation 20-81 and Equation 20-82 are used to calculate P_b , the probability of a blocked lane, and P_d , the probability of a delayed crossing, respectively. In the case of Scenario A, the crossing consists of four lanes. Scenarios B and C have only two lanes, given the two-stage crossing opportunity.

For the single-stage crossing, v is $(1,700 \text{ veh/h})/(3,600 \text{ s/h}) = 0.47 \text{ veh/s}$.

For the two-stage crossing, without any information on directional flows, one-half the volume is used, and v is therefore $(850 \text{ veh/h})/(3,600 \text{ s/h}) = 0.24 \text{ veh/s}$.

Scenario A:

$$P_b = 1 - e^{-\frac{t_c G v}{N_L}}$$

$$P_d = 1 - (1 - P_b)^{N_L}$$

$$P_b = 1 - e^{-\frac{14.5(0.47)}{4}} = 0.82$$

$$P_d = 1 - (1 - 0.18)^4 = 0.999$$

Scenario B:

$$P_b = 1 - e^{-\frac{8(0.24)}{2}} = 0.61$$

$$P_d = 1 - (1 - 0.39)^2 = 0.85$$

Scenario C:

$$P_b = 1 - e^{-\frac{8(0.24)}{2}} = 0.61$$

$$P_d = 1 - (1 - 0.39)^2 = 0.85$$

Step 4: Calculate Average Delay to Wait for Adequate Gap

Average gap delay d_g and average gap delay when delay is nonzero d_{gd} are calculated by Equation 20-83 and Equation 20-84, respectively.

Scenario A:

$$d_g = \frac{1}{v} (e^{vt_{c,G}} - vt_{c,G} - 1)$$

$$d_g = \frac{1}{0.47} (e^{0.47(14.5)} - 0.47(14.5) - 1) = 1,977 \text{ s}$$

$$d_{gd} = \frac{d_g}{P_d} = \frac{1,977}{0.999} = 1,979 \text{ s}$$

Scenario B:

$$d_g = \frac{1}{0.24} (e^{0.24(8)} - 0.24(8) - 1) = 15.8 \text{ s}$$

$$d_{gd} = \frac{15.8}{0.85} = 18.6 \text{ s}$$

Scenario C:

$$d_g = \frac{1}{0.24} (e^{0.24(8)} - 0.24(8) - 1) = 15.8 \text{ s}$$

$$d_{gd} = \frac{15.8}{0.85} = 18.6 \text{ s}$$

Step 5: Estimate Delay Reduction Due to Yielding Vehicles

Under Scenarios A and B, the motorist yield rates are approximately 0%. Therefore, there is no reduction in delay due to yielding vehicles, and average delay is the same as that shown in Step 4. Under Scenario C, motorist yield rates are 50%. The two-stage crossing requires the use of Equation 20-88 to determine $P(Y_i)$:

$$P(Y_i) = \left[P_d - \sum_{j=0}^{i-1} P(Y_j) \right] \left[\frac{(2P_b[1 - P_b]M_y) + (P_b^2 M_y^2)}{P_d} \right]$$

$$P(Y_1) = [0.85 - 0] \left[\frac{(2[0.61][1 - 0.61][0.5]) + (0.61^2 0.50^2)}{0.85} \right] = 0.33$$

$$P(Y_2) = [0.85 - 0.33] \left[\frac{(2[0.61][1 - 0.61][0.5]) + (0.61^2 0.50^2)}{0.85} \right] = 0.20$$

The results of Equation 20-88 are substituted into Equation 20-85 to determine average pedestrian delay.

$$d_p = \sum_{i=1}^n h(i - 0.5)P(Y_i) + \left(P_d - \sum_{i=1}^n P(Y_i) \right) d_{gd}$$

$$h = \frac{N_L}{v} = \frac{2}{(0.24)} = 8.3 \text{ s}$$

$$n = \text{int} \left(\frac{d_{gd}}{h} \right) = \text{int} \left(\frac{18.6}{8.3} \right) = 2$$

$$d_p = (8.3)(1 - 0.5)(0.33) + (8.3)(2 - 0.5)(0.20) + (0.85 - 0.53)(18.6) = 9.8 \text{ s}$$

Step 6: Calculate LOS

Average pedestrian delays and the corresponding pedestrian LOS under each of the three scenarios are determined from Exhibit 20-3 as follows:

Scenario A = 1,979 s = LOS F

Scenario B = 2 × 15.8 s = 31.6 s = LOS E

Scenario C = 2 × 9.8 s = 19.6 s = LOS C

TWSC EXAMPLE PROBLEM 3: FLARED APPROACHES AND MEDIAN STORAGE

The Facts

The following data are available to describe the traffic and geometric characteristics of this location:

- Major street with two lanes in each direction, minor street with one lane on each approach that flares with storage for one vehicle in the flare area, and median storage for two vehicles at one time available for minor-street through and left-turn movements;
- Level grade on all approaches;
- Percentage heavy vehicles on all approaches = 10%;
- Peak hour factor on all approaches = 0.92;
- Length of analysis period = 0.25 h; and
- Volumes and lane configurations as shown in Exhibit 32-7.

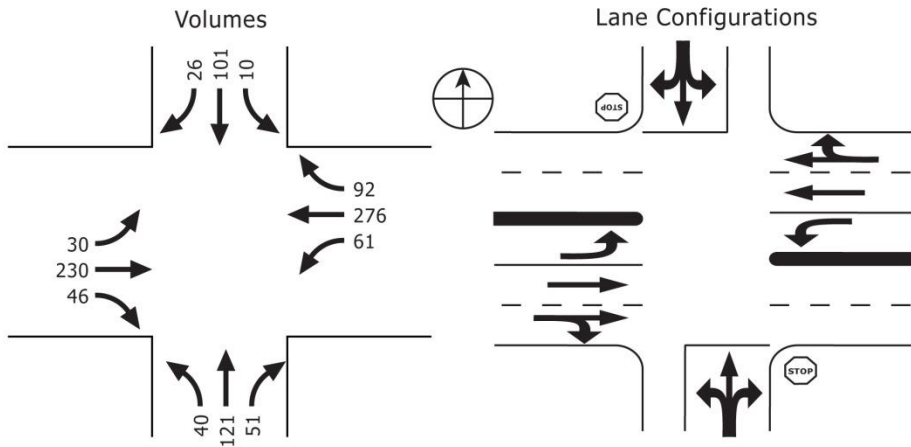


Exhibit 32-7
TWSC Example Problem 3:
15-min Volumes and Lane
Configurations

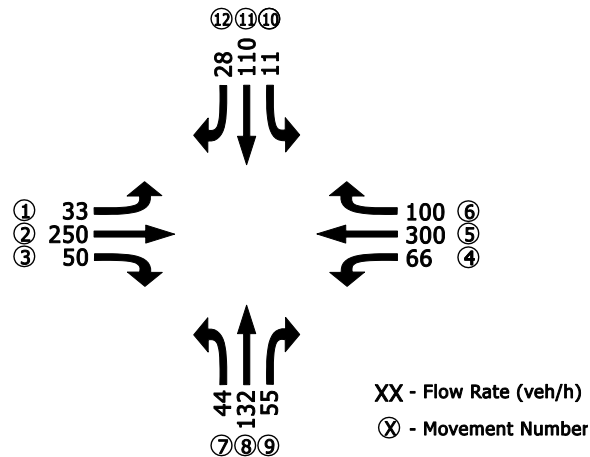
Comments

All relevant input parameters are known, so no default values are needed or used.

Steps 1 and 2: Convert Movement Demand Volumes to Flow Rates and Label Movement Priorities

Because hourly volumes and a peak hour factor have been provided, each hourly volume is divided by the peak hour factor to determine a peak 15-min flow rate (in vehicles per hour) for each movement. These values are shown in Exhibit 32-8.

Exhibit 32-8
 TWSC Example Problem 3:
 Movement Numbers and
 Calculation of Peak 15-min
 Flow Rates



Step 3: Compute Conflicting Flow Rates

The conflicting flow rates for each minor movement at the intersection are computed according to the equations in Chapter 20. The conflicting flow for the eastbound major-street left-turn movement $v_{c,1}$ is computed according to Equation 20-2 as follows:

$$v_{c,1} = v_5 + v_6 + v_{16} = 300 + 100 + 0 = 400 \text{ veh/h}$$

Similarly, the conflicting flow for the westbound major-street left-turn movement $v_{c,4}$ is computed according to Equation 20-3 as follows:

$$v_{c,4} = v_2 + v_3 + v_{15} = 250 + 50 + 0 = 300 \text{ veh/h}$$

The conflicting flows for the northbound minor-street right-turn movement $v_{c,9}$ and southbound minor-street right-turn movement $v_{c,12}$ are computed with Equation 20-6 and Equation 20-7, respectively, as follows (with no U-turns and pedestrians, the last three terms can be assigned zero):

$$v_{c,9} = 0.5v_2 + 0.5v_3 + v_{4U} + v_{14} + v_{15}$$

$$v_{c,9} = 0.5(250) + 0.5(50) + 0 + 0 + 0 = 150 \text{ veh/h}$$

$$v_{c,12} = 0.5v_5 + 0.5v_6 + v_{1U} + v_{13} + v_{16}$$

$$v_{c,12} = 0.5(300) + 0.5(100) + 0 + 0 + 0 = 200 \text{ veh/h}$$

Next, the conflicting flow for the northbound minor-street through movement $v_{c,8}$ is computed. Because two-stage gap acceptance is available for this movement, the conflicting flow rates shown in Stage I and Stage II must be computed separately. The conflicting flow for Stage I $v_{c,I,8}$ is computed from Equation 20-14:

$$v_{c,I,8} = 2(v_1 + v_{1U}) + v_2 + 0.5v_3 + v_{15}$$

$$v_{c,I,8} = 2(33 + 0) + 250 + 0.5(50) + 0 = 341 \text{ veh/h}$$

The conflicting flow for Stage II $v_{c,II,8}$ is computed from Equation 20-16:

$$v_{c,II,8} = 2(v_4 + v_{4U}) + v_5 + v_6 + v_{16}$$

$$v_{c,II,8} = 2(66 + 0) + 300 + 100 + 0 = 532 \text{ veh/h}$$

The total conflicting flow for the northbound through movement $v_{c,8}$ is computed as follows:

$$v_{c,8} = v_{c,I,8} + v_{c,II,8} = 341 + 532 = 873 \text{ veh/h}$$

Similarly, the conflicting flow for the southbound minor-street through movement $v_{c,11}$ is computed in two stages as follows:

$$v_{c,I,11} = 2(66 + 0) + 300 + 0.5(100) + 0 = 482 \text{ veh/h}$$

$$v_{c,II,11} = 2(33 + 0) + 250 + 50 + 0 = 366 \text{ veh/h}$$

$$v_{c,11} = v_{c,I,11} + v_{c,II,11} = 482 + 366 = 848 \text{ veh/h}$$

Next, the conflicting flow for the northbound minor-street left-turn movement $v_{c,7}$ is computed. Because two-stage gap acceptance is available for this movement, the conflicting flow rates shown in Stage I and Stage II must be computed separately. The conflicting flow for Stage I $v_{c,I,7}$ is computed with Equation 20-20 as follows:

$$v_{c,I,7} = 2(v_1 + v_{1U}) + v_2 + 0.5v_3 + v_{15}$$

$$v_{c,I,7} = 2(33 + 0) + 250 + 0.5(50) + 0 = 341 \text{ veh/h}$$

The conflicting flow for Stage II $v_{c,II,7}$ is computed with Equation 20-26 as follows:

$$v_{c,II,7} = 2(v_4 + v_{4U}) + 0.5v_5 + 0.5v_{11} + v_{13}$$

$$v_{c,II,7} = 2(66 + 0) + 0.5(300) + 0.5(110) + 0 = 337 \text{ veh/h}$$

The total conflicting flow for the northbound left-turn movement $v_{c,7}$ is computed as follows:

$$v_{c,7} = v_{c,I,7} + v_{c,II,7} = 341 + 337 = 678 \text{ veh/h}$$

Similarly, the conflicting flow for the southbound minor-street left-turn movement $v_{c,10}$ is computed in two stages as follows:

$$v_{c,I,10} = 2(66 + 0) + 300 + 0.5(100) + 0 = 482 \text{ veh/h}$$

$$v_{c,II,10} = 2(33 + 0) + 0.5(250) + 0.5(132) + 0 = 257 \text{ veh/h}$$

$$v_{c,10} = v_{c,I,10} + v_{c,II,10} = 482 + 257 = 739 \text{ veh/h}$$

Step 4: Determine Critical Headways and Follow-Up Headways

The critical headway for each minor movement is computed beginning with the base critical headway given in Exhibit 20-12. The base critical headway for each movement is then adjusted according to Equation 20-30. The critical headways for the eastbound and westbound major-street left turns $t_{c,1}$ and $t_{c,4}$ (in this case, $t_{c,1} = t_{c,4}$) are computed as follows:

$$t_{c,1} = t_{c,4} = t_{c,\text{base}} + t_{c,HV}P_{HV} + t_{c,G}G - t_{3,LT}$$

$$t_{c,1} = t_{c,4} = 4.1 + 2.0(0.1) + 0(0) - 0 = 4.3 \text{ s}$$

Next, the critical headways for the northbound and southbound minor-street right-turn movements $t_{c,9}$ and $t_{c,12}$ (in this case, $t_{c,9} = t_{c,12}$) are computed as follows:

$$t_{c,9} = t_{c,12} = 6.9 + 2.0(0.1) + 0.1(0) - 0 = 7.1 \text{ s}$$

Next, the critical headways for the northbound and southbound minor-street through movements $t_{c,8}$ and $t_{c,11}$ (in this case, $t_{c,8} = t_{c,11}$) are computed. Because

two-stage gap acceptance is available for these movements, the critical headways for Stage I and Stage II must be computed, along with the critical headways for these movements assuming single-stage gap acceptance. The critical headways for Stage I and Stage II, $t_{c,I,8}$, $t_{c,I,11}$ and $t_{c,II,8}$, $t_{c,II,11}$, respectively (in this case, $t_{c,I,8} = t_{c,II,8} = t_{c,I,11} = t_{c,II,11}$), are computed as follows:

$$t_{c,I,8} = t_{c,II,8} = t_{c,I,11} = t_{c,II,11} = 5.5 + 2.0(0.1) + 0.2(0) - 0 = 5.7 \text{ s}$$

The critical headways for $t_{c,8}$ and $t_{c,11}$ (in this case, $t_{c,8} = t_{c,11}$), assuming single-stage gap acceptance, are computed as follows:

$$t_{c,8} = t_{c,11} = 6.5 + 2.0(0.1) + 0.2(0) - 0 = 6.7 \text{ s}$$

Finally, the critical headways for the northbound and southbound minor-street left-turn movements $t_{c,7}$ and $t_{c,10}$ (in this case, $t_{c,7} = t_{c,10}$) are computed. Because two-stage gap acceptance is available for these movements, the critical headways for Stage I and Stage II must be computed, along with the critical headways for these movements assuming single-stage gap acceptance. The critical headways for Stage I and Stage II, $t_{c,I,7}$, $t_{c,I,10}$ and $t_{c,II,7}$, $t_{c,II,10}$, respectively (in this case, $t_{c,I,7} = t_{c,II,7} = t_{c,I,10} = t_{c,II,10}$), are computed as follows:

$$t_{c,I,7} = t_{c,II,7} = t_{c,I,10} = t_{c,II,10} = 6.5 + 2.0(0.1) + 0.2(0) - 0 = 6.7 \text{ s}$$

The critical headways for $t_{c,7}$ and $t_{c,10}$ (in this case, $t_{c,7} = t_{c,10}$), assuming single-stage gap acceptance, are computed as follows:

$$t_{c,7} = t_{c,10} = 7.5 + 2.0(0.1) + 0.2(0) - 0 = 7.7 \text{ s}$$

The follow-up headway for each minor movement is computed beginning with the base follow-up headway given in Exhibit 20-13. The base follow-up headway for each movement is then adjusted according to Equation 20-31. The follow-up headways for the northbound and southbound major-street left-turn movements $t_{f,1}$ and $t_{f,4}$ (in this case, $t_{f,1} = t_{f,4}$) are computed as follows:

$$t_{f,1} = t_{f,4} = t_{f,base} + t_{f,HV}P_{HV}$$

$$t_{f,1} = t_{f,4} = 2.2 + 1.0(0.1) = 2.3 \text{ s}$$

Next, the follow-up headways for the northbound and southbound minor-street right-turn movements $t_{f,9}$ and $t_{f,12}$ (in this case, $t_{f,9} = t_{f,12}$) are computed as follows:

$$t_{f,9} = t_{f,12} = 3.3 + 1.0(0.1) = 3.4 \text{ s}$$

Next, the follow-up headways for the northbound and southbound minor-street through movements $t_{f,8}$ and $t_{f,11}$ (in this case, $t_{f,8} = t_{f,11}$) are computed as follows:

$$t_{f,8} = t_{f,11} = 4.0 + 1.0(0.1) = 4.1 \text{ s}$$

Finally, the follow-up headways for the northbound and southbound minor-street left-turn movements $t_{f,7}$ and $t_{f,10}$ (in this case, $t_{f,7} = t_{f,10}$) are computed as follows:

$$t_{f,7} = t_{f,10} = 3.5 + 1.0(0.1) = 3.6 \text{ s}$$

Follow-up headways for the minor-street through and left-turn movements are computed for the movement as a whole. Follow-up headways are not broken up by stage because they apply only to vehicles as they exit the approach and enter the intersection.

Step 5: Compute Potential Capacities

Because no upstream signals are present, the procedure in Step 5a is followed.

The computation of a potential capacity for each movement provides the analyst with a definition of capacity under the assumed base conditions. The potential capacity will be adjusted in later steps to estimate the movement capacity for each movement. The potential capacity for each movement is a function of the conflicting flow rate, critical headway, and follow-up headway computed in the previous steps. The potential capacity for the northbound major-street left-turn movement $c_{p,1}$ is computed from Equation 20-32:

$$c_{p,1} = v_{c,1} \frac{e^{-v_{c,1}t_{c,1}/3,600}}{1 - e^{-v_{c,1}t_{f,1}/3,600}}$$

$$c_{p,1} = 400 \frac{e^{-(400)(4.3)/3,600}}{1 - e^{-(400)(2.3)/3,600}} = 1,100 \text{ veh/h}$$

Similarly, the potential capacities for Movements 4, 9, and 12 ($c_{p,4}$, $c_{p,9}$, and $c_{p,12}$, respectively) are computed as follows:

$$c_{p,4} = 300 \frac{e^{-(300)(4.3)/3,600}}{1 - e^{-(300)(2.3)/3,600}} = 1,202 \text{ veh/h}$$

$$c_{p,9} = 150 \frac{e^{-(150)(7.1)/3,600}}{1 - e^{-(150)(3.4)/3,600}} = 845 \text{ veh/h}$$

$$c_{p,12} = 200 \frac{e^{-(200)(7.1)/3,600}}{1 - e^{-(200)(3.4)/3,600}} = 783 \text{ veh/h}$$

Because the two-stage gap-acceptance adjustment procedure will be implemented for estimating the capacity of the minor-street movements, three potential capacity values must be computed for each of Movements 7, 8, 10, and 11. First, the potential capacity must be computed for Stage I, $c_{p,I,8}$, $c_{p,I,11}$, $c_{p,I,7}$, and $c_{p,I,10}$, for each movement as follows:

$$c_{p,I,8} = 341 \frac{e^{-(341)(5.7)/3,600}}{1 - e^{-(341)(4.1)/3,600}} = 618 \text{ veh/h}$$

$$c_{p,I,11} = 482 \frac{e^{-(482)(5.7)/3,600}}{1 - e^{-(482)(4.1)/3,600}} = 532 \text{ veh/h}$$

$$c_{p,I,7} = 341 \frac{e^{-(341)(6.7)/3,600}}{1 - e^{-(341)(3.6)/3,600}} = 626 \text{ veh/h}$$

$$c_{p,I,10} = 482 \frac{e^{-(482)(6.7)/3,600}}{1 - e^{-(482)(3.6)/3,600}} = 514 \text{ veh/h}$$

Next, the potential capacity must be computed for Stage II for each movement, $c_{p,II,8}$, $c_{p,II,11}$, $c_{p,II,7}$, and $c_{p,II,10}$, as follows:

$$c_{p,II,8} = 532 \frac{e^{-(532)(5.7)/3,600}}{1 - e^{-(532)(4.1)/3,600}} = 504 \text{ veh/h}$$

$$c_{p,II,11} = 366 \frac{e^{-(366)(5.7)/3,600}}{1 - e^{-(366)(4.1)/3,600}} = 601 \text{ veh/h}$$

$$c_{p,11,7} = 337 \frac{e^{-(337)(6.7)/3,600}}{1 - e^{-(337)(3.6)/3,600}} = 629 \text{ veh/h}$$

$$c_{p,1,10} = 257 \frac{e^{-(257)(6.7)/3,600}}{1 - e^{-(257)(3.6)/3,600}} = 703 \text{ veh/h}$$

Finally, the potential capacity must be computed assuming single-stage gap acceptance for each movement, $c_{p,8}$, $c_{p,11}$, $c_{p,7}$, and $c_{p,10}$, as follows:

$$c_{p,8} = 873 \frac{e^{-(873)(6.7)/3,600}}{1 - e^{-(873)(4.1)/3,600}} = 273 \text{ veh/h}$$

$$c_{p,11} = 848 \frac{e^{-(848)(6.7)/3,600}}{1 - e^{-(848)(4.1)/3,600}} = 283 \text{ veh/h}$$

$$c_{p,7} = 678 \frac{e^{-(678)(7.7)/3,600}}{1 - e^{-(678)(3.6)/3,600}} = 323 \text{ veh/h}$$

$$c_{p,10} = 739 \frac{e^{-(739)(7.7)/3,600}}{1 - e^{-(739)(3.6)/3,600}} = 291 \text{ veh/h}$$

Steps 6–9: Compute Movement Capacities

Because no pedestrians are present, the procedures given in Chapter 20 are followed.

Step 6: Compute Rank 1 Movement Capacities

There is no computation for this step.

Step 7: Compute Rank 2 Movement Capacities

Step 7a: Movement Capacity for Major-Street Left-Turn Movements

The movement capacity of each Rank 2 major-street left-turn movement is equal to its potential capacity:

$$c_{m,1} = c_{p,1} = 1,100 \text{ veh/h}$$

$$c_{m,4} = c_{p,4} = 1,202 \text{ veh/h}$$

Step 7b: Movement Capacity for Minor-Street Right-Turn Movements

The movement capacity of each minor-street right-turn movement is equal to its potential capacity:

$$c_{m,9} = c_{p,9} = 845 \text{ veh/h}$$

$$c_{m,12} = c_{p,12} = 783 \text{ veh/h}$$

Step 7c: Movement Capacity for Major-Street U-Turn Movements

No U-turns are present, so this step is skipped.

Step 7d: Effect of Major-Street Shared Through and Left-Turn Lane

Separate major-street left-turn lanes are provided, so this step is skipped.

Step 8: Compute Rank 3 Movement Capacities

The movement capacity of each Rank 3 movement is equal to its potential capacity, factored by any impedance due to conflicting pedestrian or vehicular movements.

Step 8a: Rank 3 Capacity for One-Stage Movements

As there are no pedestrians assumed at this intersection, the Rank 3 movements will be impeded only by other vehicular movements. Specifically, the Rank 3 movements will be impeded by major-street left-turning traffic, and as a first step in determining the impact of this impedance, the probability that these movements will operate in a queue-free state must be computed according to Equation 20-42:

$$p_{0,1} = 1 - \frac{v_1}{c_{m,1}} = 1 - \frac{33}{1,100} = 0.970$$

$$p_{0,4} = 1 - \frac{66}{1,202} = 0.945$$

Next, by using the probabilities computed above, capacity adjustment factors f_8 and f_{11} can be computed according to Equation 20-46:

$$f_8 = f_{11} = p_{0,1} \times p_{0,4} = (0.970)(0.945) = 0.917$$

Finally, under the single-stage gap-acceptance assumption, the movement capacities $c_{m,8}$ and $c_{m,11}$ can be computed according to Equation 20-47:

$$c_{m,8} = c_{p,8} \times f_8 = (273)(0.917) = 250 \text{ veh/h}$$

$$c_{m,11} = c_{p,11} \times f_{11} = (283)(0.917) = 260 \text{ veh/h}$$

Because Movements 8 and 11 will operate under two-stage gap acceptance, the capacity adjustment procedure for estimating the capacity of Stage I and Stage II of these movements must be completed.

To begin the process of estimating Stage I and Stage II movement capacities, the probabilities of queue-free states on conflicting Rank 2 movements calculated above are entered into Equation 20-46 as before, but this time capacity adjustment factors are estimated for each individual stage as follows:

$$f_{I,8} = p_{0,1} = 0.970$$

$$f_{I,11} = p_{0,4} = 0.945$$

$$f_{II,8} = p_{0,4} = 0.945$$

$$f_{II,11} = p_{0,1} = 0.970$$

The Stage I movement capacities are then computed as follows:

$$c_{m,I,8} = c_{p,I,8} \times f_{I,8} = (618)(0.970) = 599 \text{ veh/h}$$

$$c_{m,I,11} = c_{p,I,11} \times f_{I,11} = (532)(0.945) = 503 \text{ veh/h}$$

The Stage II movement capacities are then computed as follows:

$$c_{m,II,8} = c_{p,II,8} \times f_{II,8} = (504)(0.945) = 476 \text{ veh/h}$$

$$c_{m,II,11} = c_{p,II,11} \times f_{II,11} = (601)(0.970) = 583 \text{ veh/h}$$

Step 8b: Rank 3 Capacity for Two-Stage Movements

The two-stage gap-acceptance procedure will result in a total capacity estimate for Movements 8 and 11. To begin the procedure, an adjustment factor a must be computed for each movement by using Equation 20-48, under the assumption there is storage for two vehicles in the median refuge area; thus, $n_m = 2$.

$$a_8 = a_{11} = 1 - 0.32e^{-1.3\sqrt{n_m}} = 1 - 0.32e^{-1.3\sqrt{2}} = 0.949$$

Next, an intermediate variable, y , must be computed for each movement by using Equation 20-49:

$$y_8 = \frac{c_{m,I,8} - c_{m,8}}{c_{m,II,8} - v_1 - c_{m,8}} = \frac{599 - 250}{476 - 33 - 250} = 1.808$$

$$y_{11} = \frac{c_{m,I,11} - c_{m,11}}{c_{m,II,11} - v_4 - c_{m,11}} = \frac{503 - 260}{583 - 66 - 260} = 0.946$$

Finally, the total capacity for each movement $c_{T,8}$ and $c_{T,11}$ is computed according to Equation 20-50, because $y \neq 1$:

$$c_{m,T,8} = \frac{a_8}{y_8^{n_m+1} - 1} [y_8(y_8^{n_m} - 1)(c_{m,II,8} - v_1) + (y_8 - 1)c_{m,8}]$$

$$c_{m,T,8} = \frac{0.949}{1.808^{2+1} - 1} [(1.808)(1.808^2 - 1)(476 - 33) + (1.808 - 1)(250)]$$

$$c_{m,T,8} = 390 \text{ veh/h}$$

$$c_{m,T,11} = \frac{a_{11}}{y_{11}^{n_m+1} - 1} [y_{11}(y_{11}^{n_m} - 1)(c_{m,II,11} - v_4) + (y_{11} - 1)c_{m,11}]$$

$$c_{m,T,11} = \frac{0.949}{0.946^{2+1} - 1} [(0.946)(0.946^2 - 1)(583 - 66) + (0.946 - 1)(260)]$$

$$c_{m,T,11} = 405 \text{ veh/h}$$

Step 9: Compute Rank 4 Movement Capacities
Step 9a: Rank 4 Capacity for One-Stage Movements

The vehicle impedance effects for Rank 4 movements are first estimated by assuming single-stage gap acceptance. Rank 4 movements are impeded by all the same movements impeding Rank 2 and Rank 3 movements with the addition of impedances due to the minor-street crossing movements and minor-street right-turn movements. The probability that these movements will operate in a queue-free state must be incorporated into the procedure.

The probabilities that the minor-street right-turn movements will operate in a queue-free state ($p_{0,9}$ and $p_{0,12}$) are computed as follows:

$$p_{0,9} = 1 - \frac{v_9}{c_{m,9}} = 1 - \frac{55}{845} = 0.935$$

$$p_{0,12} = 1 - \frac{28}{783} = 0.964$$

To compute p' , the probability that both the major-street left-turn movements and the minor-street crossing movements will operate in a queue-free state simultaneously, the analyst must first compute $p_{0,k}$ which is done in the same

manner as the computation of $p_{0,j}$, except k represents Rank 3 movements. The values for $p_{0,k}$ are computed as follows:

$$p_{0,8} = 1 - \frac{v_8}{c_{m,T,8}} = 1 - \frac{132}{390} = 0.662$$

$$p_{0,11} = 1 - \frac{110}{405} = 0.728$$

Next, the analyst must compute p'' , which, under the single-stage gap-acceptance assumption, is simply the product of f_j and $p_{0,k}$. The value for $f_8 = f_{11} = 0.917$ is as computed above. The value for $p_{0,11}$ is computed by using the total capacity for Movement 11 calculated in the previous step:

$$p''_7 = p_{0,11} \times f_{11} = (0.728)(0.917) = 0.668$$

$$p''_{10} = p_{0,8} \times f_8 = (0.662)(0.917) = 0.607$$

With the values for p'' , the probability of a simultaneous queue-free state for each movement can be computed by using Equation 20-52 as follows:

$$p'_7 = 0.65p''_7 - \frac{p''_7}{p''_7 + 3} + 0.6\sqrt{p''_7}$$

$$p'_7 = 0.65(0.668) - \frac{0.668}{0.668 + 3} + 0.6\sqrt{0.668} = 0.742$$

$$p'_{10} = 0.65(0.607) - \frac{0.607}{0.607 + 3} + 0.6\sqrt{0.607} = 0.694$$

Next, with the probabilities computed above, capacity adjustment factors f_7 and f_{10} can be computed according to Equation 20-53:

$$f_7 = p'_7 \times p_{0,12} = (0.742)(0.964) = 0.715$$

$$f_{10} = p'_{10} \times p_{0,9} = (0.694)(0.935) = 0.649$$

Finally, under the single-stage gap-acceptance assumption, the movement capacities $c_{m,7}$ and $c_{m,10}$ can be computed according to Equation 20-54:

$$c_{m,7} = c_{p,7} \times f_7 = (323)(0.715) = 231 \text{ veh/h}$$

$$c_{m,10} = c_{p,10} \times f_{10} = (291)(0.649) = 189 \text{ veh/h}$$

Step 9b: Rank 4 Capacity for Two-Stage Movements

Similar to the minor-street crossing movements at this intersection, Movements 7 and 10 will also operate under two-stage gap acceptance. Therefore, the capacity adjustment procedure for estimating the capacity of Stage I and Stage II of these movements must be completed.

Under the assumption of two-stage gap acceptance with a median refuge area, the minor-street left-turn movements operate as Rank 3 movements in each individual stage of completing the left-turn maneuver. To begin the process of estimating two-stage movement capacities, the probabilities of queue-free states on conflicting Rank 2 movements for Stage I of the minor-street left-turn movement are entered into Equation 20-46, and capacity adjustment factors for Stage I are computed as follows:

$$f_{1,7} = p_{0,1} = 0.970$$

$$f_{1,10} = p_{0,4} = 0.945$$

The Stage I movement capacities can then be computed as follows:

$$c_{m,I,7} = c_{p,I,7} \times f_{I,7} = (626)(0.970) = 607 \text{ veh/h}$$

$$c_{m,I,10} = c_{p,I,10} \times f_{I,10} = (514)(0.945) = 486 \text{ veh/h}$$

Next, the probabilities of queue-free states on conflicting Rank 2 movements for Stage II of the minor-street left-turn movement are entered into Equation 20-46. However, before estimating these probabilities, the probability of a queue-free state for the first stage of the minor-street crossing movement must be estimated as it impedes Stage II of the minor-street left-turn movement. These probabilities are estimated with Equation 20-42:

$$p_{0,I,8} = 1 - \frac{v_8}{c_{m,I,8}} = 1 - \frac{132}{599} = 0.780$$

$$p_{0,I,11} = 1 - \frac{110}{503} = 0.781$$

The capacity adjustment factors for Stage II are then computed as follows:

$$f_{II,7} = p_{0,4} \times p_{0,12} \times p_{0,I,11} = (0.945)(0.964)(0.781) = 0.711$$

$$f_{II,10} = p_{0,1} \times p_{0,9} \times p_{0,I,8} = (0.970)(0.935)(0.780) = 0.707$$

Finally, the movement capacities for Stage II are computed as follows:

$$c_{m,II,7} = c_{p,II,7} \times f_{II,7} = (629)(0.711) = 447 \text{ veh/h}$$

$$c_{m,II,10} = (703)(0.707) = 497 \text{ veh/h}$$

The final result of the two-stage gap-acceptance procedure will be a total capacity estimate for Movements 7 and 10. To begin the procedure, an adjustment factor a must be computed for each movement by using Equation 20-55, under the assumption there is storage for two vehicles in the median refuge area; thus, $n_m = 2$.

$$a_7 = a_{10} = 1 - 0.32e^{-1.3\sqrt{n_m}} = 1 - 0.32e^{-1.3\sqrt{2}} = 0.949$$

Next, an intermediate variable y must be computed for each movement by using Equation 20-56:

$$y_7 = \frac{c_{m,I,7} - c_{m,7}}{c_{m,II,7} - v_1 - c_{m,7}} = \frac{607 - 231}{447 - 33 - 231} = 2.055$$

$$y_{10} = \frac{c_{m,I,10} - c_{m,10}}{c_{m,II,10} - v_4 - c_{m,10}} = \frac{486 - 189}{497 - 66 - 189} = 1.227$$

Finally, the total capacity for each movement, $c_{T,7}$ and $c_{T,10}$, is computed according to Equation 20-57, as $y \neq 1$:

$$c_{T,7} = \frac{a_7}{y_7^{n_m+1} - 1} [y_7(y_7^{n_m} - 1)(c_{m,II,7} - v_1) + (y_7 - 1)c_{m,7}]$$

$$c_{T,7} = \frac{0.949}{2.055^{2+1} - 1} [(2.055)(2.055^2 - 1)(447 - 33) + (2.055 - 1)(231)]$$

$$c_{T,7} = 369 \text{ veh/h}$$

$$c_{T,10} = \frac{a_{10}}{y_{10}^{n_m+1} - 1} [y_{10}(y_{10}^{n_m} - 1)(c_{m,II,10} - v_4) + (y_{10} - 1)c_{m,10}]$$

$$c_{T,10} = \frac{0.949}{1.227^{2+1} - 1} [(1.227)(1.227^2 - 1)(497 - 66) + (1.227 - 1)(189)]$$

$$c_{T,10} = 347 \text{ veh/h}$$

Step 10: Compute Final Capacity Adjustments

In this example problem, several final capacity adjustments must be made to account for the effect of the shared lanes and the flared lanes on the minor-street approaches. Initially, the shared-lane capacities for each of the minor-street approaches must be computed on the assumption of no flared lanes; after these computations are completed, the effects of the flare can be incorporated to compute an actual capacity for each minor-street approach.

Step 10a: Shared-Lane Capacity of Minor-Street Approaches

In this example, both minor-street approaches have single-lane entries, meaning that all movements on the minor street share one lane. The shared-lane capacities for the minor-street approaches are computed according to Equation 20-59:

$$c_{SH,NB} = \frac{\sum_y v_y}{\sum_y \frac{v_y}{c_{m,y}}} = \frac{v_7 + v_8 + v_9}{\frac{v_7}{c_{m,7}} + \frac{v_8}{c_{m,8}} + \frac{v_9}{c_{m,9}}} = \frac{44 + 132 + 55}{\frac{44}{369} + \frac{132}{390} + \frac{55}{845}} = 442 \text{ veh/h}$$

$$c_{SH,SB} = \frac{\sum_y v_y}{\sum_y \frac{v_y}{c_{m,y}}} = \frac{11 + 110 + 28}{\frac{11}{347} + \frac{110}{405} + \frac{28}{783}} = 439 \text{ veh/h}$$

Step 10b: Flared Minor-Street Lane Effects

In this example, the capacity of each minor-street approach will be greater than the shared capacities computed in the previous step due to the shared-lane condition on each approach. On each approach, it is assumed one vehicle at a time can queue in the flared area; therefore, $n = 1$.

First, the analyst must estimate the average queue length for each movement sharing the lane on each approach. Required input data for this estimation include the flow rates and control delays for each movement. Although the flow rates are known input data, the control delays have not yet been computed. Therefore, the control delay for each movement, assuming a 15-min analysis period and separate lanes for each movement, is computed with Equation 20-64:

$$d_7 = \frac{3,600}{c_7} + 900T \left[\frac{v_7}{c_{m,7}} - 1 + \sqrt{\left(\frac{v_7}{c_{m,7}} - 1\right)^2 + \frac{\left(\frac{3,600}{c_{m,7}}\right)\left(\frac{v_7}{c_{m,7}}\right)}{450T}} \right] + 5$$

$$d_7 = \frac{3,600}{369} + 900(0.25) \left[\frac{44}{369} - 1 + \sqrt{\left(\frac{44}{369} - 1\right)^2 + \frac{\left(\frac{3,600}{369}\right)\left(\frac{44}{369}\right)}{450(0.25)}} \right] + 5$$

$$d_7 = 16.07 \text{ s}$$

$$d_8 = \frac{3,600}{390} + 900(0.25) \left[\frac{132}{390} - 1 + \sqrt{\left(\frac{132}{390} - 1\right)^2 + \frac{\left(\frac{3,600}{390}\right)\left(\frac{132}{390}\right)}{450(0.25)}} \right] + 5$$

$$d_8 = 18.88 \text{ s}$$

$$d_9 = \frac{3,600}{845} + 900(0.25) \left[\frac{55}{845} - 1 + \sqrt{\left(\frac{55}{845} - 1\right)^2 + \frac{\left(\frac{3,600}{845}\right)\left(\frac{55}{845}\right)}{450(0.25)}} \right] + 5$$

$$d_9 = 9.57 \text{ s}$$

$$d_{10} = \frac{3,600}{347} + 900(0.25) \left[\frac{11}{347} - 1 + \sqrt{\left(\frac{11}{347} - 1\right)^2 + \frac{\left(\frac{3,600}{347}\right)\left(\frac{11}{347}\right)}{450(0.25)}} \right] + 5$$

$$d_{10} = 15.71 \text{ s}$$

$$d_{11} = \frac{3,600}{405} + 900(0.25) \left[\frac{110}{405} - 1 + \sqrt{\left(\frac{110}{405} - 1\right)^2 + \frac{\left(\frac{3,600}{405}\right)\left(\frac{110}{405}\right)}{450(0.25)}} \right] + 5$$

$$d_{11} = 17.17 \text{ s}$$

$$d_{12} = \frac{3,600}{783} + 900(0.25) \left[\frac{28}{783} - 1 + \sqrt{\left(\frac{28}{783} - 1\right)^2 + \frac{\left(\frac{3,600}{783}\right)\left(\frac{28}{783}\right)}{450(0.25)}} \right] + 5$$

$$d_{12} = 9.77 \text{ s}$$

In this example, all movements on the minor-street approach share one lane; therefore, the average queue lengths for each minor-street movement are computed as follows from Equation 20-60:

$$Q_{sep,7} = \frac{d_{sep,7} v_{sep,7}}{3,600} = \frac{(16.07)(44)}{3,600} = 0.20 \text{ veh}$$

$$Q_{sep,8} = \frac{(18.88)(132)}{3,600} = 0.69 \text{ veh}$$

$$Q_{sep,9} = \frac{(9.57)(55)}{3,600} = 0.15 \text{ veh}$$

$$Q_{sep,10} = \frac{(15.71)(11)}{3,600} = 0.05 \text{ veh}$$

$$Q_{sep,11} = \frac{(17.17)(110)}{3,600} = 0.53 \text{ veh}$$

$$Q_{sep,12} = \frac{(9.77)(28)}{3,600} = 0.08 \text{ veh}$$

Next, the required length of the storage area so that each approach would operate effectively as separate lanes is computed with Equation 20-61:

$$n_{Max} = \max_i [\text{round}(Q_{sep,i} + 1)]$$

$$n_{Max,NB} = \max_{NB} [\text{round}(Q_{sep,7} + 1), \text{round}(Q_{sep,8} + 1), \text{round}(Q_{sep,9} + 1)]$$

$$n_{Max,NB} = \max_{NB} [\text{round}(0.20 + 1), \text{round}(0.69 + 1), \text{round}(0.15 + 1)] = 2$$

$$n_{Max,SB} = \max_{SB} [\text{round}(0.05 + 1), \text{round}(0.53 + 1), \text{round}(0.08 + 1)] = 2$$

The next step involves estimating separate lane capacities, with consideration of the limitation of the amount of right-turn traffic that could actually move into a separate right-turn lane given a queue before the location of the flare. To compute separate lane capacities, the shared-lane capacities of the through plus left-turn movement on each approach must first be estimated according to Equation 20-59:

$$c_{L+TH,NB} = \frac{\sum_y v_y}{\sum_y \frac{v_y}{c_{m,y}}} = \frac{v_7 + v_8}{\frac{v_7}{c_{m,7}} + \frac{v_8}{c_{m,8}}} = \frac{44 + 132}{\frac{44}{369} + \frac{132}{390}} = 385 \text{ veh/h}$$

$$c_{L+TH,SB} = \frac{\sum_y v_y}{\sum_y \frac{v_y}{c_{m,y}}} = \frac{v_{10} + v_{11}}{\frac{v_{10}}{c_{m,10}} + \frac{v_{11}}{c_{m,11}}} = \frac{11 + 110}{\frac{11}{347} + \frac{110}{405}} = 399 \text{ veh/h}$$

Then, the capacity of the separate lane condition c_{sep} for each approach can be computed according to Equation 20-62:

$$c_{sep} = \min \left[c_R \left(1 + \frac{v_{L+TH}}{v_R} \right), c_{L+TH} \left(1 + \frac{v_R}{v_{L+TH}} \right) \right]$$

$$c_{sep,NB} = \min \left[c_{m,9} \left(1 + \frac{v_{L+TH,NB}}{v_9} \right), c_{L+TH,NB} \left(1 + \frac{v_9}{v_{L+TH,NB}} \right) \right]$$

$$c_{sep,NB} = \min \left[(845) \left(1 + \frac{44 + 132}{55} \right), (385) \left(1 + \frac{55}{44 + 132} \right) \right] = 505 \text{ veh/h}$$

$$c_{sep,SB} = \min \left[c_{m,12} \left(1 + \frac{v_{L+TH,SB}}{v_{12}} \right), c_{L+TH,SB} \left(1 + \frac{v_{12}}{v_{L+TH,SB}} \right) \right]$$

$$c_{sep,SB} = \min \left[(783) \left(1 + \frac{11 + 110}{28} \right), (399) \left(1 + \frac{28}{11 + 110} \right) \right] = 491 \text{ veh/h}$$

Finally, the capacities of the flared minor-street lanes are computed according to Equation 20-63:

$$c_R = \begin{cases} (c_{sep} - c_{SH}) \frac{n_R}{n_{Max}} + c_{SH} & \text{if } n_R \leq n_{Max} \\ c_{sep} & \text{if } n_R > n_{Max} \end{cases}$$

Because $n_R = 1$ and $n_{Max} = 2$, the first condition is evaluated:

$$c_{R,NB} = (505 - 442) \left(\frac{1}{2} \right) + 442 = 474 \text{ veh/h}$$

Similarly,

$$c_{R,SB} = (491 - 439) \left(\frac{1}{2} \right) + 439 = 465 \text{ veh/h}$$

Step 11: Compute Control Delay

The control delay computation for any movement includes initial deceleration delay, queue move-up time, stopped delay, and final acceleration delay.

Step 11a: Compute Control Delay to Rank 2 Through Rank 4 Movements

The control delays for the major-street left-turn movements (Rank 2) d_1 and d_4 and the minor-street approaches d_{NB} and d_{SB} are computed with Equation 20-64:

$$d_1 = \frac{3,600}{1,100} + 900(0.25) \left[\frac{33}{1,100} - 1 + \sqrt{\left(\frac{33}{1,100} - 1\right)^2 + \frac{\left(\frac{3,600}{1,100}\right)\left(\frac{33}{1,100}\right)}{450(0.25)}} \right] + 5$$

$$d_1 = 8.4 \text{ s}$$

$$d_4 = \frac{3,600}{1,202} + 900(0.25) \left[\frac{66}{1,202} - 1 + \sqrt{\left(\frac{66}{1,202} - 1\right)^2 + \frac{\left(\frac{3,600}{1,202}\right)\left(\frac{66}{1,202}\right)}{450(0.25)}} \right] + 5$$

$$d_4 = 8.2 \text{ s}$$

$$d_{NB} = \frac{3,600}{474} + 900(0.25) \left[\frac{231}{474} - 1 + \sqrt{\left(\frac{231}{474} - 1\right)^2 + \frac{\left(\frac{3,600}{474}\right)\left(\frac{231}{474}\right)}{450(0.25)}} \right] + 5$$

$$d_{NB} = 19.6 \text{ s}$$

$$d_{SB} = \frac{3,600}{465} + 900(0.25) \left[\frac{149}{465} - 1 + \sqrt{\left(\frac{149}{465} - 1\right)^2 + \frac{\left(\frac{3,600}{465}\right)\left(\frac{149}{465}\right)}{450(0.25)}} \right] + 5$$

$$d_{SB} = 16.3 \text{ s}$$

According to Exhibit 20-2, LOS for the major-street left-turn movements and the minor-street approaches are as follows:

- Eastbound major-street left turn (Movement 1): LOS A,
- Westbound major-street left turn (Movement 4): LOS A,
- Northbound minor-street approach: LOS C, and
- Southbound minor-street approach: LOS C.

Step 11b: Compute Control Delay to Rank 1 Movements

This step is not applicable as the major-street through movements v_2 and v_5 and westbound major-street left-turn movements v_1 and v_4 have exclusive lanes at this intersection.

Step 12: Compute Approach and Intersection Control Delay

The control delay for the eastbound approach $d_{A,EB}$ is computed with Equation 20-66:

$$d_A = \frac{d_r v_r + d_t v_t + d_l v_l}{v_r + v_t + v_l}$$

$$d_{A,EB} = \frac{0(50) + 0(250) + 8.2(33)}{50 + 250 + 33} = 0.8 \text{ s}$$

The control delay for the westbound approach $d_{A,WB}$ is computed according to the same equation as for the eastbound approach:

$$d_{A,WB} = \frac{0(100) + 0(300) + 8.4(66)}{100 + 300 + 66} = 1.2 \text{ s}$$

The intersection delay d_I is computed from Equation 20-67:

$$d_I = \frac{d_{A,EB} v_{A,EB} + d_{A,WB} v_{A,WB} + d_{A,NB} v_{A,NB} + d_{A,SB} v_{A,SB}}{v_{A,EB} + v_{A,WB} + v_{A,NB} + v_{A,SB}}$$

$$d_I = \frac{0.8(333) + 1.2(466) + 19.6(231) + 16.3(149)}{333 + 466 + 231 + 149} = 6.6 \text{ s}$$

LOS is not defined for the intersection as a whole or for the major-street approaches.

Step 13: Compute 95th Percentile Queue Lengths

The 95th percentile queue length for the major-street eastbound left-turn movement $Q_{95,1}$ is computed from Equation 20-68:

$$Q_{95,1} \approx 900T \left[\frac{v_1}{c_{m,1}} - 1 + \sqrt{\left(\frac{v_1}{c_{m,1}} - 1\right)^2 + \frac{\left(\frac{3,600}{c_{m,1}}\right)\left(\frac{v_x}{c_{m,1}}\right)}{150T}} \right] \left(\frac{c_{m,1}}{3,600}\right)$$

$$Q_{95,1} \approx 900(0.25) \left[\frac{33}{1,100} - 1 + \sqrt{\left(\frac{33}{1,100} - 1\right)^2 + \frac{\left(\frac{3,600}{1,100}\right)\left(\frac{33}{1,100}\right)}{150(0.25)}} \right] \left(\frac{1,100}{3,600}\right)$$

$$Q_{95,1} \approx 0.1 \text{ veh}$$

The result of 0.1 vehicles for the 95th percentile queue indicates a queue of more than one vehicle will occur very infrequently for the eastbound major-street left-turn movement.

The 95th percentile queue length for the major-street westbound left-turn movement $Q_{95,4}$ is computed as follows:

$$Q_{95,4} \approx 900(0.25) \left[\frac{66}{1,202} - 1 + \sqrt{\left(\frac{66}{1,202} - 1\right)^2 + \frac{\left(\frac{3,600}{1,202}\right)\left(\frac{66}{1,202}\right)}{150(0.25)}} \right] \left(\frac{1,202}{3,600}\right)$$

$$Q_{95,4} \approx 0.2 \text{ veh}$$

The result of 0.2 vehicles for the 95th percentile queue indicates a queue of more than one vehicle will occur very infrequently for the westbound major-street left-turn movement.

The 95th percentile queue length for the northbound approach is computed by using the same formula, but similar to the control delay computation, the shared-lane volume and shared-lane capacity must be used.

$$Q_{95,NB} \approx 900(0.25) \left[\frac{231}{474} - 1 + \sqrt{\left(\frac{231}{474} - 1\right)^2 + \frac{\left(\frac{3,600}{474}\right)\left(\frac{231}{474}\right)}{150(0.25)}} \right] \left(\frac{474}{3,600}\right)$$

$$Q_{95,NB} \approx 2.6 \text{ veh}$$

The result of 2.6 vehicles for the 95th percentile queue indicates a queue of more than two vehicles will occur occasionally for the northbound approach.

The 95th percentile queue length for the southbound approach is computed by using the same formula, but similar to the control delay computation, the shared-lane volume and shared-lane capacity must be used.

$$Q_{95,SB} \approx 900(0.25) \left[\frac{149}{465} - 1 + \sqrt{\left(\frac{149}{465} - 1\right)^2 + \frac{\left(\frac{3,600}{465}\right)\left(\frac{149}{465}\right)}{150(0.25)}} \right] \left(\frac{465}{3,600}\right)$$

$$Q_{95,SB} \approx 1.4 \text{ veh}$$

The result of 1.4 vehicles for the 95th percentile queue indicates a queue of more than one vehicle will occur occasionally for the southbound approach.

Discussion

Overall, the results indicate the four-leg TWSC intersection with two-stage gap acceptance and flared minor-street approaches will operate satisfactorily with low delays for major-street movements and average delays for the minor-street approaches.

TWSC EXAMPLE PROBLEM 4: TWSC INTERSECTION WITHIN A SIGNALIZED URBAN STREET SEGMENT

The Facts

This problem analyzes the performance of the TWSC intersection at Access Point 1 (AP1) from Example Problem 1 in Chapter 30, Urban Street Segments: Supplemental, which looks at the motor vehicle performance of the urban street segment bounded by two signalized intersections, as shown in Exhibit 32-9. The street has a four-lane cross section with two lanes in each direction.

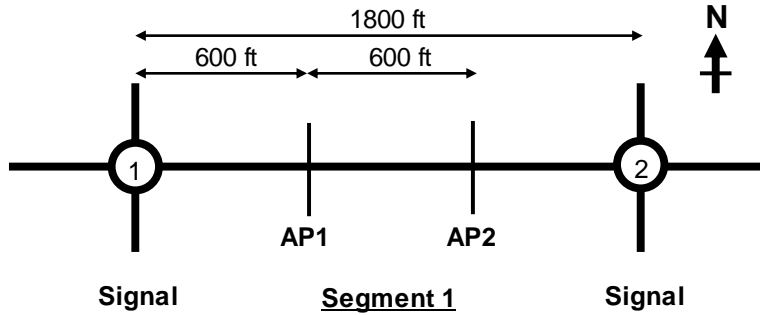


Exhibit 32-9
TWSC Example Problem 4:
TWSC Intersection Within a
Signalized Urban Street
Segment

From Example Problem 1 in Chapter 30, the following data are relevant:

- Major street with two lanes in each direction,
- Minor street with separate left-turn and right-turn lanes in each direction (through movements considered negligible) and STOP control on minor-street approach,
- Level grade on all approaches,
- Percentage heavy vehicles on all approaches = 1%,
- Length of analysis period = 0.25 h, and
- Flow rates and lane configurations as shown in Exhibit 32-10.

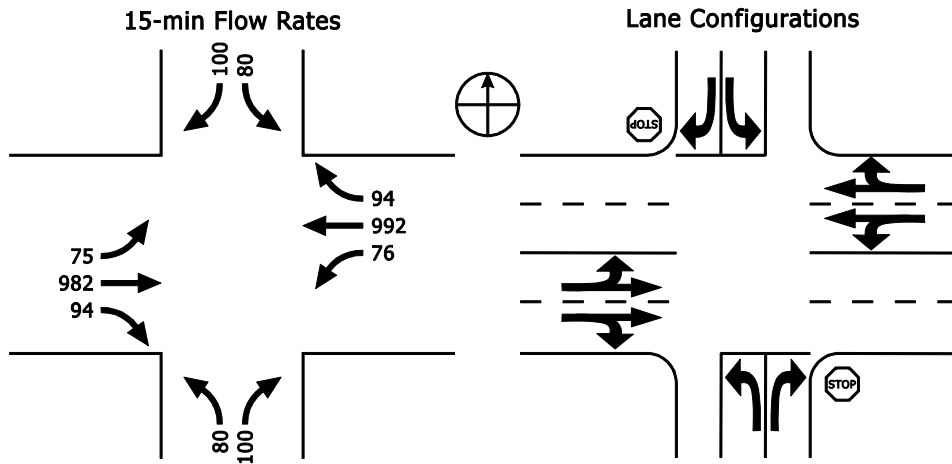


Exhibit 32-10
TWSC Example Problem 4:
15-min Flow Rates and Lane
Configurations

The proportion time blocked and delay to through vehicles from the methodology of Chapter 18, Urban Street Segments, are as shown in Exhibit 32-11.

Access Point Data	EB	EB	EB	WB	WB	WB	NB	NB	NB	SB	SB	SB
Segment 1	L	T	R	L	T	R	L	T	R	L	T	R
Access Point Intersection No. 1	1	2	3	4	5	6	7	8	9	10	11	12
1: Volume, veh/h	74.80	981.71	93.50	75.56	991.70	94.45	80.00	0.00	100.00	80.00	0.00	100.00
1: Lanes	0	2	0	0	2	0	1	0	1	1	0	1
1: Proportion time blocked	0.170			0.170			0.260	0.260	0.170	0.260	0.260	0.170
1: Delay to through vehicles, s/veh		0.163			0.164							
1: Prob. inside lane blocked by left		0.101			0.101							
1: Dist. from West/South signal, ft		600										
Access Point Intersection No. 2												
2: Volume, veh/h	75.56	991.70	94.45	74.80	981.71	93.50	80.00	0.00	100.00	80.00	0.00	100.00
2: Lanes	0	2	0	0	2	0	1	0	1	1	0	1
2: Proportion time blocked	0.170			0.170			0.260	0.260	0.170	0.260	0.260	0.170
2: Delay to through vehicles, s/veh		0.164			0.163							
2: Prob. inside lane blocked by left		0.101			0.101							
2: Dist. from West/South signal, ft		1200										

Exhibit 32-11
TWSC Example Problem 4:
Movement-Based Access Point
Output (from Chapter 30,
Example Problem 1)

Comments

Default values are needed for the saturation flow rates of the major-street through and right-turn movements for the analysis of shared or short major-street left-turn lanes:

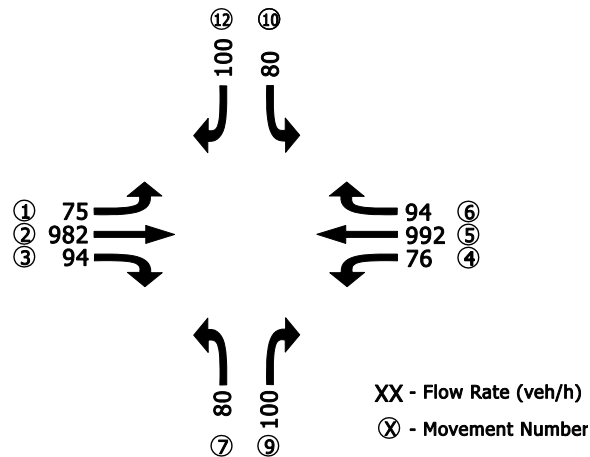
- Major-street through movement, $s_{i1} = 1,800$ veh/h; and
- Major-street right-turn movement, $s_{i2} = 1,500$ veh/h.

All other input parameters are known.

Steps 1 and 2: Convert Movement Demand Volumes to Flow Rates and Label Movement Priorities

Flow rates for each turning movement have been provided from the methodology of Chapter 17, Urban Street Reliability and ATDM. They are assigned movement numbers as shown in Exhibit 32-12.

Exhibit 32-12
 TWSC Example Problem 4:
 Movement Numbers and
 Calculation of Peak 15-min
 Flow Rates



Step 3: Compute Conflicting Flow Rates

Major-Street Left-Turn Movements (Rank 2, Movements 1 and 4)

The conflicting flows for the major-street left-turn movements are computed from Equation 20-2 and Equation 20-3 as follows:

$$v_{c,1} = v_5 + v_6 + v_{16} = 992 + 94 + 0 = 1,086 \text{ veh/h}$$

$$v_{c,4} = v_2 + v_3 + v_{15} = 982 + 94 + 0 = 1,076 \text{ veh/h}$$

Minor-Street Right-Turn Movements (Rank 2, Movements 9 and 12)

The conflicting flows for minor-street right-turn movements are computed from Equation 20-6 and Equation 20-7 as follows:

$$v_{c,9} = 0.5v_2 + 0.5v_3 + v_{4U} + v_{14} + v_{15}$$

$$v_{c,9} = 0.5(982) + 0.5(94) + 0 + 0 + 0 = 538 \text{ veh/h}$$

$$v_{c,12} = 0.5v_5 + 0.5v_6 + v_{1U} + v_{13} + v_{16}$$

$$v_{c,12} = 0.5(992) + 0.5(94) + 0 + 0 + 0 = 543 \text{ veh/h}$$

Major-Street U-Turn Movements (Rank 2, Movements 1U and 4U)

U-turns are assumed to be negligible.

Minor-Street Pedestrian Movements (Rank 2, Movements 13 and 14)

Minor-street pedestrian movements are assumed to be negligible.

Minor-Street Through Movements (Rank 3, Movements 8 and 11)

Because there are no minor-street through movements, this step can be skipped.

Minor-Street Left-Turn Movements (Rank 4, Movements 7 and 10)

Because the major street has four lanes without left-turn lanes or other possible median storage, the minor-street left-turn movement is assumed to be conducted in one stage. As a result, the conflicting flows for Stages I and II can be combined.

$$v_{c,7} = 2(v_1 + v_{1U}) + v_2 + 0.5v_3 + v_{15} + 2(v_4 + v_{4U}) + 0.5v_5 + 0.5v_{11} + v_{13}$$

$$v_{c,7} = 2(75 + 0) + 982 + 0.5(94) + 0 + 2(76 + 0) + 0.5(992) + 0.5(0) + 0$$

$$v_{c,7} = 1,827 \text{ veh/h}$$

$$v_{c,10} = 2(v_4 + v_{4U}) + v_5 + 0.5v_6 + v_{16} + 2(v_1 + v_{1U}) + 0.5v_2 + 0.5v_8 + v_{14}$$

$$v_{c,10} = 2(76 + 0) + 992 + 0.5(94) + 0 + 2(75 + 0) + 0.5(982) + 0.5(0) + 0$$

$$v_{c,10} = 1,832 \text{ veh/h}$$

Step 4: Determine Critical Headways and Follow-Up Headways

Critical headways for each movement are computed from Equation 20-30:

$$t_{c,x} = t_{c,\text{base}} + t_{c,HV}P_{HV} + t_{c,G}G - t_{3,LT}$$

$$t_{c,1} = t_{c,4} = 4.1 + (2.0)(0.01) + 0 - 0 = 4.12 \text{ s}$$

$$t_{c,9} = t_{c,12} = 6.9 + (2.0)(0.01) + 0.1(0) - 0 = 6.92 \text{ s}$$

$$t_{c,7} = t_{c,10} = 7.5 + (2.0)(0.01) + 0.2(0) - 0 = 7.52 \text{ s}$$

Follow-up headways for each movement are computed from Equation 20-31:

$$t_{f,x} = t_{f,\text{base}} + t_{f,HV}P_{HV}$$

$$t_{f,1} = t_{f,4} = 2.2 + (1.0)(0.01) = 2.21 \text{ s}$$

$$t_{f,9} = t_{f,12} = 3.3 + (1.0)(0.01) = 3.31 \text{ s}$$

$$t_{f,7} = t_{f,10} = 3.5 + (1.0)(0.01) = 3.51 \text{ s}$$

Step 5: Compute Potential Capacities

Because upstream signals are present, Step 5b is used. The proportion time blocked for each movement x is given as $p_{b,x}$ and has been computed by the Chapter 18 procedure.

The flow for the unblocked period (no platoons) is determined by first computing the conflicting flow for each movement during the unblocked period (Equation 20-33). The minimum platooned flow rate $v_{c,\text{min}}$ over two lanes is assumed to be equal to $1,000N = 1,000(2) = 2,000$. The flow rate assumed to occur during the blocked period is calculated as follows:

$$v_{c,u,x} = \begin{cases} \frac{v_{c,x} - 1.5v_{c,min}p_{b,x}}{1 - p_{b,x}} & \text{if } v_{c,x} > 1.5v_{c,min}p_{b,x} \\ 0 & \text{otherwise} \end{cases}$$

$$1.5v_{c,min}p_{b,1} = 1.5(2,000)(0.170) = 510 \text{ veh/h}$$

The value for $v_{c,1} = 1,086$ exceeds this value, which indicates some of the conflicting flow occurs in the unblocked period. Therefore, $v_{c,u,1}$ is calculated as follows:

$$v_{c,u,1} = \frac{v_{c,1} - 1.5v_{c,min}p_{b,1}}{1 - p_{b,1}} = \frac{1,086 - 1.5(2,000)(0.170)}{1 - 0.170} = 694 \text{ veh/h}$$

Similar calculations are made for the other movements:

$$v_{c,u,4} = \frac{1,076 - 1.5(2,000)(0.170)}{1 - 0.170} = 682 \text{ veh/h}$$

$$v_{c,u,9} = \frac{538 - 1.5(2,000)(0.170)}{1 - 0.170} = 34 \text{ veh/h}$$

$$v_{c,u,12} = \frac{543 - 1.5(2,000)(0.170)}{1 - 0.170} = 40 \text{ veh/h}$$

$$v_{c,u,7} = \frac{1,827 - 1.5(2,000)(0.260)}{1 - 0.260} = 1,415 \text{ veh/h}$$

$$v_{c,u,10} = \frac{1,832 - 1.5(2,000)(0.260)}{1 - 0.260} = 1,422 \text{ veh/h}$$

The potential capacity for each movement is then calculated with Equation 20-34 and Equation 20-35 (combined) as follows:

$$c_{p,1} = (1 - p_{b,1})(v_{c,u,1}) \frac{e^{-v_{c,u,1}t_{c,1}/3,600}}{1 - e^{-v_{c,u,1}t_{f,1}/3,600}}$$

$$c_{p,1} = (1 - 0.170)(694) \frac{e^{-(694)(4.12)/3,600}}{1 - e^{-(694)(2.21)/3,600}} = 750 \text{ veh/h}$$

$$c_{p,4} = (1 - 0.170)(682) \frac{e^{-(682)(4.12)/3,600}}{1 - e^{-(682)(2.21)/3,600}} = 758 \text{ veh/h}$$

$$c_{p,9} = (1 - 0.170)(34) \frac{e^{-(34)(6.92)/3,600}}{1 - e^{-(34)(3.31)/3,600}} = 859 \text{ veh/h}$$

$$c_{p,12} = (1 - 0.170)(40) \frac{e^{-(40)(6.92)/3,600}}{1 - e^{-(40)(3.31)/3,600}} = 851 \text{ veh/h}$$

$$c_{p,7} = (1 - 0.260)(1,415) \frac{e^{-(1,415)(7.52)/3,600}}{1 - e^{-(1,415)(3.51)/3,600}} = 73 \text{ veh/h}$$

$$c_{p,10} = (1 - 0.260)(1,422) \frac{e^{-(1,422)(7.52)/3,600}}{1 - e^{-(1,422)(3.51)/3,600}} = 72 \text{ veh/h}$$

Steps 6–9: Compute Movement Capacities

Because no pedestrians are present, the procedures given in Chapter 20 are followed.

Step 6: Compute Rank 1 Movement Capacities

There is no computation for this step. The adjustment for the delay to through movements caused by left-turn movements in the shared left-through lane is accounted for by using adjustments provided later in this procedure.

Step 7: Compute Rank 2 Movement Capacities

Step 7a: Movement Capacity for Major-Street Left-Turn Movements

The movement capacity of each Rank 2 major-street left-turn movement is equal to its potential capacity as follows:

$$c_{m,1} = c_{p,1} = 750 \text{ veh/h}$$

$$c_{m,4} = c_{p,4} = 758 \text{ veh/h}$$

Step 7b: Movement Capacity for Minor-Street Right-Turn Movements

The movement capacity of each minor-street right-turn movement is equal to its potential capacity:

$$c_{m,9} = c_{p,9} = 859 \text{ veh/h}$$

$$c_{m,12} = c_{p,12} = 851 \text{ veh/h}$$

Step 7c: Movement Capacity for Major-Street U-Turn Movements

No U-turns are present, so this step is skipped.

Step 7d: Effect of Major-Street Shared Through and Left-Turn Lane

The probability that the major-street left-turning traffic will operate in a queue-free state, assuming the left-turn movement occupies its own lane, is calculated with Equation 20-42 as follows:

$$p_{0,1} = 1 - \frac{v_1}{c_{m,1}} = 1 - \frac{75}{750} = 0.900$$

$$p_{0,4} = 1 - \frac{v_4}{c_{m,4}} = 1 - \frac{76}{758} = 0.900$$

However, for this problem the major-street left-turn movement shares a lane with the through movement. First, the combined degree of saturation for the major-street through and right-turn movements is calculated as follows (using default values for s):

$$x_{2+3} = \frac{v_2}{s_2} + \frac{v_3}{s_3} = \frac{982}{1,800} + \frac{94}{1,500} = 0.608$$

$$x_{5+6} = \frac{v_5}{s_5} + \frac{v_6}{s_6} = \frac{992}{1,800} + \frac{94}{1,500} = 0.614$$

Next, the probability that there will be no queue in the major-street shared lane $p_{0,j}^*$ is calculated according to the special case ($n_L = 0$) given in Equation 20-45:

$$p_{0,1}^* = 1 - \frac{1 - p_{0,1}}{1 - x_{2+3}} = 1 - \frac{1 - 0.900}{1 - 0.608} = 0.745$$

$$p_{0,4}^* = 1 - \frac{1 - p_{0,4}}{1 - x_{5+6}} = 1 - \frac{1 - 0.900}{1 - 0.614} = 0.741$$

These values of $p_{0,1}^*$ and $p_{0,4}^*$ are used in lieu of $p_{0,1}$ and $p_{0,4}$ for the remaining calculations.

Step 8: Compute Rank 3 Movement Capacities

Step 8a: Rank 3 Capacity for One-Stage Movements

Because there are no minor-street through movements, it is not necessary to compute the movement capacities for those movements. However, capacity adjustment factors f_8 and f_{11} are needed for subsequent steps and can be computed as follows:

$$f_8 = f_{11} = p_{0,1}^* p_{0,4}^* = (0.745)(0.741) = 0.552$$

Step 8b: Rank 3 Capacity for Two-Stage Movements

No two-stage movements are present, so this step is skipped.

Step 9: Compute Rank 4 Movement Capacities

Step 9a: Rank 4 Capacity for One-Stage Movements

The probabilities that the minor-street right-turn movements will operate in the queue-free state $p_{0,9}$ and $p_{0,12}$ are computed as follows:

$$p_{0,9} = 1 - \frac{v_9}{c_{m,9}} = 1 - \frac{100}{859} = 0.884$$

$$p_{0,12} = 1 - \frac{v_{12}}{c_{m,12}} = 1 - \frac{100}{851} = 0.882$$

To compute p' , the probability that both the major-street left-turn movements and the minor-street crossing movements will operate in a queue-free state simultaneously, the analyst must first compute $p_{0,k}$ which is done in the same manner as the computation of $p_{0,j}$, except k represents Rank 3 movements. The values for $p_{0,k}$ are computed as follows:

$$p_{0,8} = 1 - \frac{v_8}{c_{m,8}} = 1 - 0 = 1$$

$$p_{0,11} = 1 - \frac{v_{11}}{c_{m,11}} = 1 - 0 = 1$$

Next, the analyst must compute p'' , which, under the single-stage gap-acceptance assumption, is simply the product of f_j and $p_{0,k}$. The value for $f_8 = f_{11} = 0.552$ is as computed above. The value for $p_{0,11}$ is computed by using the total capacity for Movement 11 calculated in the previous step:

$$p_7'' = p_{0,11} \times f_{11} = (1)(0.552) = 0.552$$

$$p_{10}'' = p_{0,8} \times f_8 = (1)(0.552) = 0.552$$

By using the values for p'' , the probability of a simultaneous queue-free state for each movement can be computed with Equation 20-52 as follows:

$$p'_7 = 0.65p''_7 - \frac{p''_7}{p''_7 + 3} + 0.6\sqrt{p''_7}$$

$$p'_7 = 0.65(0.552) - \frac{(0.552)}{0.552 + 3} + 0.6\sqrt{0.552} = 0.649$$

$$p'_{10} = 0.65(0.552) - \frac{(0.552)}{0.552 + 3} + 0.6\sqrt{0.552} = 0.649$$

Next, by using the probabilities computed above, capacity adjustment factors f_7 and f_{10} can be computed as follows:

$$f_7 = p'_7 \times p_{0,12} = (0.649)(0.882) = 0.572$$

$$f_{10} = p'_{10} \times p_{0,9} = (0.649)(0.884) = 0.574$$

Finally, the movement capacities $c_{m,7}$ and $c_{m,10}$ can be computed as follows:

$$c_{m,7} = c_{p,7} \times f_7 = (73)(0.572) = 42 \text{ veh/h}$$

$$c_{m,10} = c_{p,10} \times f_{10} = (72)(0.574) = 41 \text{ veh/h}$$

Step 9b: Rank 4 Capacity for Two-Stage Movements

No two-stage movements are present, so this step is skipped.

Step 10: Final Capacity Adjustments

Step 10a: Shared-Lane Capacity of Minor-Street Approaches

No shared lanes are present on the side street, so this step is skipped.

Step 10b: Flared Minor-Street Lane Effects

No flared lanes are present, so this step is skipped.

Step 11: Compute Movement Control Delay

Step 11a: Compute Control Delay to Rank 2 Through Rank 4 Movements

The delay for each minor-street movement is calculated from Equation 20-64:

$$d_1 = \frac{3,600}{750} + 900(0.25) \left[\frac{75}{750} - 1 + \sqrt{\left(\frac{75}{750} - 1\right)^2 + \frac{\left(\frac{3,600}{750}\right)\left(\frac{75}{750}\right)}{450(0.25)}} \right] + 5$$

$$d_1 = 10.3 \text{ s}$$

$$d_4 = \frac{3,600}{758} + 900(0.25) \left[\frac{76}{758} - 1 + \sqrt{\left(\frac{76}{758} - 1\right)^2 + \frac{\left(\frac{3,600}{758}\right)\left(\frac{76}{758}\right)}{450(0.25)}} \right] + 5$$

$$d_4 = 10.3 \text{ s}$$

$$d_9 = \frac{3,600}{859} + 900(0.25) \left[\frac{100}{859} - 1 + \sqrt{\left(\frac{100}{859} - 1\right)^2 + \frac{\left(\frac{3,600}{859}\right)\left(\frac{100}{859}\right)}{450(0.25)}} \right] + 5$$

$$d_9 = 9.7 \text{ s}$$

$$d_{12} = \frac{3,600}{851} + 900(0.25) \left[\frac{100}{851} - 1 + \sqrt{\left(\frac{100}{851} - 1\right)^2 + \frac{\left(\frac{3,600}{851}\right)\left(\frac{100}{851}\right)}{450(0.25)}} \right] + 5$$

$$d_{12} = 9.8 \text{ s}$$

$$d_7 = \frac{3,600}{42} + 900(0.25) \left[\frac{80}{42} - 1 + \sqrt{\left(\frac{80}{42} - 1\right)^2 + \frac{\left(\frac{3,600}{42}\right)\left(\frac{80}{42}\right)}{450(0.25)}} \right] + 5$$

$$d_7 = 633 \text{ s}$$

$$d_{10} = \frac{3,600}{41} + 900(0.25) \left[\frac{80}{41} - 1 + \sqrt{\left(\frac{80}{41} - 1\right)^2 + \frac{\left(\frac{3,600}{41}\right)\left(\frac{80}{41}\right)}{450(0.25)}} \right] + 5$$

$$d_{10} = 657 \text{ s}$$

According to Exhibit 20-2, the LOS for the major-street left-turn movements and the minor-street approaches are as follows:

- Eastbound major-street left turn (Movement 1): LOS B,
- Westbound major-street left turn (Movement 4): LOS B,
- Northbound minor-street right turn (Movement 9): LOS A,
- Southbound minor-street right turn (Movement 12): LOS A,
- Northbound minor-street left turn (Movement 7): LOS F, and
- Southbound minor-street left turn (Movement 10): LOS F.

Step 11b: Compute Control Delay to Rank 1 Movements

The presence of a shared left-through lane on the major street creates delay for Rank 1 movements (major-street through movements). Assuming that major-street through vehicles distribute equally across both lanes, then $v_{i,1} = v_2/N = 982/2 = 491$. The number of major-street turning vehicles in the shared lane is equal to the major-street left-turn flow rate; therefore, $v_{i,2} = 75$.

The average delay to Rank 1 vehicles is computed with Equation 20-65 as follows:

$$d_{Rank1} = \begin{cases} \frac{(1 - p_{0,j}^*) d_{M,LT} \left(\frac{v_{i,1}}{N}\right)}{v_{i,1} + v_{i,2}} & N > 1 \\ (1 - p_{0,j}^*) d_{M,LT} & N = 1 \end{cases}$$

$$d_2 = \frac{(1 - p_{0,1}^*) d_1 \left(\frac{v_{i,1}}{N}\right)}{v_{i,1} + v_{i,2}} = \frac{(1 - 0.745)(10.3) \left(\frac{491}{2}\right)}{491 + 75} = 1.1 \text{ s}$$

Similarly, for the opposite direction, $v_{i,1} = v_5/N = 992/2 = 496$. The number of major-street turning vehicles in the shared lane is equal to the major-street left-turn flow rate; therefore, $v_{i,2} = 76$.

$$d_5 = \frac{(1 - p_{0,4}^*) d_4 \left(\frac{v_{i,1}}{N}\right)}{v_{i,1} + v_{i,2}} = \frac{(1 - 0.741)(10.3) \left(\frac{496}{2}\right)}{496 + 76} = 1.2 \text{ s}$$

The procedures in Chapter 18 provide a better estimate of delay to major-street through vehicles: $d_2 = 0.2$ and $d_5 = 0.2$. These values account for the likelihood of major-street through vehicles shifting out of the shared left-through lane to avoid being delayed by major-street left-turning vehicles. These values are used in the calculations in Step 12.

Step 12: Compute Approach and Intersection Control Delay

The control delay for each approach is computed as follows:

$$d_A = \frac{d_r v_r + d_t v_t + d_l v_l}{v_r + v_t + v_l}$$

$$d_{A,EB} = \frac{0(94) + 1.1(982) + 10.3(75)}{94 + 982 + 75} = 1.6 \text{ s}$$

$$d_{A,WB} = \frac{0(94) + 1.2(992) + 10.3(76)}{94 + 992 + 76} = 1.7 \text{ s}$$

$$d_{A,NB} = \frac{9.7(100) + 0 + 633(80)}{100 + 0 + 80} = 287 \text{ s}$$

$$d_{A,SB} = \frac{9.8(100) + 0 + 657(80)}{100 + 0 + 80} = 297 \text{ s}$$

The intersection delay d_I is computed as follows:

$$d_I = \frac{d_{A,EB} v_{A,EB} + d_{A,WB} v_{A,WB} + d_{A,NB} v_{A,NB} + d_{A,SB} v_{A,SB}}{v_{A,EB} + v_{A,WB} + v_{A,NB} + v_{A,SB}}$$

$$d_I = \frac{1.6(1,151) + 1.7(1,162) + 287(180) + 297(180)}{1,151 + 1,162 + 180 + 180} = 40.8 \text{ s}$$

LOS is not defined for the intersection as a whole or for the major-street approaches. This fact is particularly important for this problem, as the assignment of LOS to the intersection as a whole would mask the severe LOS F condition on the minor-street left-turn movement.

Step 13: Compute 95th Percentile Queue Lengths

The 95th percentile queue length for each movement is computed by using Equation 20-68:

$$Q_{95,1} \approx 900T \left[\frac{v_1}{c_{m,1}} - 1 + \sqrt{\left(\frac{v_1}{c_{m,1}} - 1\right)^2 + \frac{\left(\frac{3,600}{c_{m,1}}\right) \left(\frac{v_1}{c_{m,1}}\right)}{150T}} \right] \left(\frac{c_{m,1}}{3,600}\right)$$

$$Q_{95,1} \approx 900(0.25) \left[\frac{75}{750} - 1 + \sqrt{\left(\frac{75}{750} - 1\right)^2 + \frac{\left(\frac{3,600}{750}\right) \left(\frac{75}{750}\right)}{150(0.25)}} \right] \left(\frac{750}{3,600}\right)$$

$$Q_{95,1} \approx 0.3 \text{ veh}$$

$$Q_{95,4} \approx 900(0.25) \left[\frac{76}{758} - 1 + \sqrt{\left(\frac{76}{758} - 1\right)^2 + \frac{\left(\frac{3,600}{758}\right)\left(\frac{76}{758}\right)}{150(0.25)}} \right] \left(\frac{758}{3,600}\right)$$

$$Q_{95,4} \approx 0.3 \text{ veh}$$

$$Q_{95,9} \approx 900(0.25) \left[\frac{100}{859} - 1 + \sqrt{\left(\frac{100}{859} - 1\right)^2 + \frac{\left(\frac{3,600}{859}\right)\left(\frac{100}{859}\right)}{150(0.25)}} \right] \left(\frac{859}{3,600}\right)$$

$$Q_{95,9} \approx 0.4 \text{ veh}$$

$$Q_{95,12} \approx 900(0.25) \left[\frac{100}{851} - 1 + \sqrt{\left(\frac{100}{851} - 1\right)^2 + \frac{\left(\frac{3,600}{851}\right)\left(\frac{100}{851}\right)}{150(0.25)}} \right] \left(\frac{851}{3,600}\right)$$

$$Q_{95,12} \approx 0.4 \text{ veh}$$

$$Q_{95,7} \approx 900(0.25) \left[\frac{80}{42} - 1 + \sqrt{\left(\frac{80}{42} - 1\right)^2 + \frac{\left(\frac{3,600}{42}\right)\left(\frac{80}{42}\right)}{150(0.25)}} \right] \left(\frac{42}{3,600}\right)$$

$$Q_{95,7} \approx 8.3 \text{ veh}$$

$$Q_{95,10} \approx 900(0.25) \left[\frac{80}{41} - 1 + \sqrt{\left(\frac{80}{41} - 1\right)^2 + \frac{\left(\frac{3,600}{41}\right)\left(\frac{80}{41}\right)}{150(0.25)}} \right] \left(\frac{41}{3,600}\right)$$

$$Q_{95,10} \approx 8.4 \text{ veh}$$

The results indicate that queues of more than one vehicle will rarely occur for the major-street left-turn and minor-street right-turn movements. Longer queues are expected for the minor-street left-turn movements, and these queues are likely to be unstable under the significantly oversaturated conditions.

Discussion

The results indicate that Access Point 1 will operate over capacity (LOS F) for the minor-street left-turn movements. All other movements are expected to operate at LOS B or better, with low average delays and short queue lengths.

TWSC EXAMPLE PROBLEM 5: SIX-LANE STREET WITH U-TURNS AND PEDESTRIANS

The Facts

The following data are available to describe the traffic and geometric characteristics of this location:

- T-intersection,
- Major street with three lanes in each direction,

- Minor street with separate left-turn and right-turn lanes and STOP control on the minor-street approach (minor-street left turns operate in two stages with room for storage of one vehicle),
- Level grade on all approaches,
- Percentage heavy vehicles on all approaches = 0%,
- Lane width = 12 ft,
- No other unique geometric considerations or upstream signal considerations,
- 20 p/h crossing both the west and south legs [each pedestrian is assumed to cross in his or her own group (i.e., independently)],
- Peak hour factor = 1.00,
- Length of analysis period = 0.25 h, and
- Hourly volumes and lane configurations as shown in Exhibit 32-13.

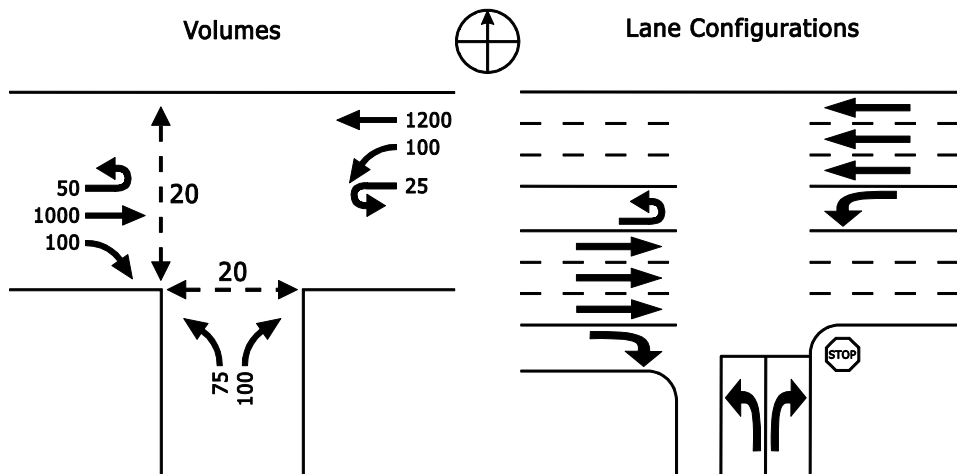


Exhibit 32-13
TWSC Example Problem 5:
Volumes and Lane
Configurations

Comments

The assumed walking speed of pedestrians is 3.5 ft/s.

Steps 1 and 2: Convert Movement Demand Volumes to Flow Rates and Label Movement Priorities

Flow rates for each turning movement are the same as the peak hour volumes because the peak hour factor equals 1.0. These movements are assigned numbers as shown in Exhibit 32-14.

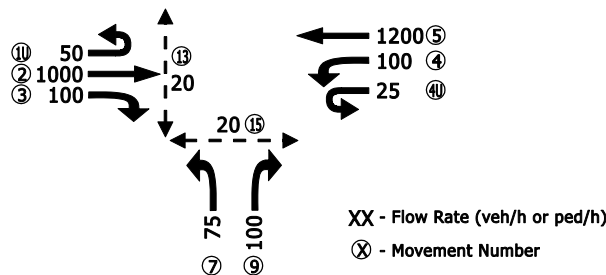


Exhibit 32-14
TWSC Example Problem 5:
Movement Numbers and
Calculation of Peak 15-min
Flow Rates

Step 3: Compute Conflicting Flow Rates

Major-Street Left-Turn Movement (Rank 2, Movement 4)

The conflicting flow rate for the major-street left-turn movement is computed as follows:

$$v_{c,4} = v_2 + v_3 + v_{15} = 1,000 + 100 + 20 = 1,120 \text{ veh/h}$$

Minor-Street Right-Turn Movement (Rank 2, Movement 9)

The conflicting flow rate for the minor-street right-turn movement is computed as follows (dropping the v_3 term due to a separate major-street right-turn lane):

$$\begin{aligned} v_{c,9} &= 0.5v_2 + 0.5v_3 + v_{4U} + v_{14} + v_{15} \\ v_{c,9} &= 0.5(1,000) + 0.5(0) + 0 + 0 + 20 = 520 \text{ veh/h} \end{aligned}$$

Major-Street U-Turn Movements (Rank 2, Movements 1U and 4U)

The conflicting flow rates for the major-street U-turns are computed as follows (again dropping the v_3 term):

$$\begin{aligned} v_{c,1U} &= 0.73v_5 + 0.73v_6 = 0.73(1,200) + 0 = 876 \text{ veh/h} \\ v_{c,4U} &= 0.73v_2 + 0.73v_3 = 0.73(1,000) + 0 = 730 \text{ veh/h} \end{aligned}$$

Minor-Street Left-Turn Movements (Rank 3, Movement 7)

The conflicting flow rate for Stage I of the minor-street left-turn movement is computed as follows (the v_3 term in these equations is assumed to be zero because of the right-turn lane on the major street):

$$\begin{aligned} v_{c,I,7} &= 2(v_1 + v_{1U}) + v_2 + 0.5v_3 + v_{15} \\ v_{c,I,7} &= 2(0 + 50) + 1,000 + 0 + 20 = 1,120 \text{ veh/h} \end{aligned}$$

The conflicting flow rate for Stage II of the minor-street left-turn movement is computed as follows:

$$\begin{aligned} v_{c,II,7} &= 2(v_4 + v_{4U}) + 0.4v_5 + 0.5v_{11} + v_{13} \\ v_{c,II,7} &= 2(100 + 25) + 0.4(1,200) + 0 + 20 = 750 \text{ veh/h} \\ v_{c,7} &= v_{c,I,7} + v_{c,II,7} = 1,120 + 750 = 1,870 \text{ veh/h} \end{aligned}$$

Step 4: Determine Critical Headways and Follow-Up Headways

Critical headways for each minor movement are computed as follows:

$$\begin{aligned} t_{c,x} &= t_{c,\text{base}} + t_{c,HV}P_{HV} + t_{c,G}G - t_{3,LT} \\ t_{c,1U} &= 5.6 + 0 + 0 - 0 = 5.6 \text{ s} \\ t_{c,4} &= 5.3 + 0 + 0 - 0 = 5.3 \text{ s} \\ t_{c,4U} &= 5.6 + 0 + 0 - 0 = 5.6 \text{ s} \\ t_{c,9} &= 7.1 + 0 + 0 - 0 = 7.1 \text{ s} \\ t_{c,7} &= 6.4 + 0 + 0 - 0.7 = 5.7 \text{ s} \\ t_{c,I,7} &= 7.3 + 0 + 0 - 0.7 = 6.6 \text{ s} \\ t_{c,II,7} &= 6.7 + 0 + 0 - 0.7 = 6.0 \text{ s} \end{aligned}$$

Follow-up headways for each minor movement are computed as follows:

$$t_{f,x} = t_{f,\text{base}} + t_{f,HV} P_{HV}$$

$$t_{f,1U} = 2.3 + 0 = 2.3 \text{ s}$$

$$t_{f,A} = 3.1 + 0 = 3.1 \text{ s}$$

$$t_{f,4U} = 2.3 + 0 = 2.3 \text{ s}$$

$$t_{f,9} = 3.9 + 0 = 3.9 \text{ s}$$

$$t_{f,7} = 3.8 + 0 = 3.8 \text{ s}$$

Step 5: Compute Potential Capacities

Because no upstream signals are present, Step 5a is used. The potential capacity $c_{p,x}$ for each movement is computed as follows:

$$c_{p,x} = v_{c,x} \frac{e^{-v_{c,x} t_{c,x}/3,600}}{1 - e^{-v_{c,x} t_{f,x}/3,600}}$$

$$c_{p,1U} = v_{c,1U} \frac{e^{-v_{c,1U} t_{c,1U}/3,600}}{1 - e^{-v_{c,1U} t_{f,1U}/3,600}} = 876 \frac{e^{-(876)(5,6)/3,600}}{1 - e^{-(876)(2,3)/3,600}} = 523 \text{ veh/h}$$

$$c_{p,4} = 1,120 \frac{e^{-(1,120)(5,3)/3,600}}{1 - e^{-(1,120)(3,1)/3,600}} = 348 \text{ veh/h}$$

$$c_{p,4U} = 730 \frac{e^{-(730)(5,6)/3,600}}{1 - e^{-(730)(2,3)/3,600}} = 629 \text{ veh/h}$$

$$c_{p,9} = 520 \frac{e^{-(520)(7,1)/3,600}}{1 - e^{-(520)(3,9)/3,600}} = 433 \text{ veh/h}$$

$$c_{p,7} = 1,870 \frac{e^{-(1,870)(5,7)/3,600}}{1 - e^{-(1,870)(3,8)/3,600}} = 112 \text{ veh/h}$$

$$c_{p,l,7} = 1,120 \frac{e^{-(1,120)(6,6)/3,600}}{1 - e^{-(1,120)(3,8)/3,600}} = 207 \text{ veh/h}$$

$$c_{p,II,7} = 750 \frac{e^{-(750)(6,0)/3,600}}{1 - e^{-(750)(3,8)/3,600}} = 393 \text{ veh/h}$$

Steps 6–9: Compute Movement Capacities

Because of the presence of pedestrians, the computation steps provided earlier in this chapter should be used.

Step 6: Compute Rank 1 Movement Capacities

The methodology assumes Rank 1 vehicles are unimpeded by pedestrians.

Step 7: Compute Rank 2 Movement Capacities

Step 7a: Pedestrian Impedance

The factor accounting for pedestrian blockage is computed by Equation 20-69 as follows:

$$f_{pb} = \frac{v_x \times \frac{w}{S_p}}{3,600}$$

$$f_{pb,13} = \frac{v_{13} \times \frac{w}{S_p}}{3,600} = \frac{20 \times \frac{12}{3.5}}{3,600} = 0.019$$

$$f_{pb,15} = \frac{20 \times \frac{12}{3.5}}{3,600} = 0.019$$

The pedestrian impedance factor for each pedestrian movement x , $p_{p,x}$ is computed by Equation 20-70 as follows:

$$p_{p,13} = 1 - f_{pb,13} = 1 - 0.019 = 0.981$$

$$p_{p,15} = 1 - f_{pb,15} = 1 - 0.019 = 0.981$$

Step 7b: Movement Capacity for Major-Street Left-Turn Movements

On the basis of Exhibit 20-18, vehicular Movement 4 is impeded by pedestrian Movement 15. Therefore, the movement capacity for Rank 2 major-street left-turn movements is computed as follows:

$$c_{m,4} = c_{p,4} \times p_{p,15} = (348)(0.981) = 341 \text{ veh/h}$$

Step 7c: Movement Capacity for Minor-Street Right-Turn Movements

The northbound minor-street right-turn movement (Movement 9) is impeded by one conflicting pedestrian movement: Movement 15.

$$f_9 = p_{p,15} = 0.981$$

The movement capacity is then computed as follows:

$$c_{m,9} = c_{p,9} \times f_9 = (433)(0.981) = 425 \text{ veh/h}$$

Step 7d: Movement Capacity for Major-Street U-Turn Movements

The eastbound U-turn is unimpeded by queues from any other movement. Therefore, $f_{1U} = 1$, and the movement capacity is computed as follows:

$$c_{m,1U} = c_{p,1U} \times f_{1U} = (523)(0.981) = 523 \text{ veh/h}$$

For the westbound U-turn, the movement capacity is found by first computing a capacity adjustment factor that accounts for the impeding effects of minor-street right turns as follows:

$$f_{4U} = p_{0,9} = 1 - \frac{v_9}{c_{m,9}} = 1 - \frac{100}{425} = 0.765$$

The movement capacity is therefore computed as follows:

$$c_{m,4U} = c_{p,4U} \times f_{4U} = (629)(0.765) = 481 \text{ veh/h}$$

Because the westbound left-turn and U-turn movements are conducted from the same lane, their shared-lane capacity is computed as follows:

$$c_{m,4+4U} = \frac{v_4 + v_{4U}}{\frac{v_4}{c_{m,4}} + \frac{v_{4U}}{c_{m,4U}}} = \frac{100 + 25}{\frac{100}{341} + \frac{25}{481}} = 362 \text{ veh/h}$$

Step 7e: Effect of Major-Street Shared Through and Left-Turn Lane

This step is skipped.

Step 8: Compute Rank 3 Movement Capacities

There are no minor-street through movements, so the minor-street left-turn movement is treated as a Rank 3 movement.

Step 8a: Pedestrian Impedance

The northbound minor-street left turn (Movement 7) must yield to pedestrian Movements 13 and 15. Therefore, the impedance factor for pedestrians is as follows:

$$p_{p,7} = p_{p,15} \times p_{p,13} = (0.981)(0.981) = 0.962$$

Step 8b: Rank 3 Capacity for One-Stage Movements

The movement capacity $c_{m,k}$ for all Rank 3 movements is found by first computing a capacity adjustment factor that accounts for the impeding effects of higher-ranked movements, assuming the movement operates in one stage. This value is computed as follows:

$$f_7 = p_{0,1U} \times p_{0,4+4U} \times p_{p,7} = \left(1 - \frac{v_{1U}}{c_{m,1U}}\right) \left(1 - \frac{v_{4+4U}}{c_{m,4+4U}}\right) (p_{p,7})$$

$$f_7 = \left(1 - \frac{50}{523}\right) \left(1 - \frac{100 + 25}{362}\right) (0.962) = 0.570$$

$$c_{m,7} = c_{p,7} \times f_7 = (112)(0.570) = 64 \text{ veh/h}$$

Step 8c: Rank 3 Capacity for Two-Stage Movements

Because the minor-street left-turn movement operates in two stages, the procedure for computing the total movement capacity for the subject movement considering the two-stage gap-acceptance process is followed.

First, the movement capacities for each stage of the left-turn movement are computed on the basis of the impeding movements for each stage. For Stage I, the left-turn movement is impeded by the major-street left and U-turns and by pedestrian Movement 15. Therefore,

$$f_{1,7} = p_{0,1U} \times p_{0,4+4U} \times p_{p,15} = \left(1 - \frac{v_{1U}}{c_{m,1U}}\right) \left(1 - \frac{v_{4+4U}}{c_{m,4+4U}}\right) (p_{p,15})$$

$$f_{1,7} = \left(1 - \frac{50}{523}\right) \left(1 - \frac{100 + 25}{362}\right) (0.981) = 0.581$$

$$c_{m,1,7} = c_{p,1,7} \times f_{1,7} = (207)(0.581) = 120 \text{ veh/h}$$

For Stage II, the left-turn movement is impeded only by pedestrian Movement 13. Therefore,

$$f_{II,7} = p_{p,13} = 0.981$$

$$c_{m,II,7} = c_{p,II,7} \times f_{II,7} = (393)(0.981) = 386 \text{ veh/h}$$

Next, an adjustment factor a and an intermediate variable y are computed for Movement 7 as follows:

$$a_7 = 1 - 0.32e^{-1.3\sqrt{n_m}} = 1 - 0.32e^{-1.3\sqrt{1}} = 0.913$$

$$y_7 = \frac{c_{m,I,7} - c_{m,7}}{c_{m,II,7} - v_{4+4U} - c_{m,7}} = \frac{120 - 64}{386 - 125 - 64} = 0.284$$

Therefore, the total capacity c_T is computed as follows:

$$c_{m,T,7} = \frac{a_7}{y_7^{n_m+1} - 1} [y_7(y_7^{n_m} - 1)(c_{m,II,7} - v_{4+4U}) + (y_7 - 1)c_{m,7}]$$

$$c_{m,T,7} = \frac{0.913}{0.284^{1+1} - 1} [(0.284)(0.284^1 - 1)(386 - 125) + (0.284 - 1)(64)]$$

$$c_{m,T,7} = 98 \text{ veh/h}$$

Step 9: Compute Rank 4 Movement Capacities

Because there are no Rank 4 movements, this step is skipped.

Step 10: Final Capacity Adjustments

There are no shared or flared lanes on the minor street, so this step is skipped.

Step 11: Compute Movement Control Delay

Step 11a: Compute Control Delay to Rank 2 Through Rank 4 Movements

The control delay for each minor movement is computed as follows:

$$d_{1U} = \frac{3,600}{523} + 900(0.25) \left[\frac{50}{523} - 1 + \sqrt{\left(\frac{50}{523} - 1\right)^2 + \frac{\left(\frac{3,600}{523}\right)\left(\frac{50}{523}\right)}{450(0.25)}} \right] + 5$$

$$d_1 = 12.6 \text{ s}$$

This movement would be assigned LOS B.

$$d_{4+4U} = \frac{3,600}{362} + 900(0.25) \left[\frac{125}{362} - 1 + \sqrt{\left(\frac{125}{362} - 1\right)^2 + \frac{\left(\frac{3,600}{362}\right)\left(\frac{125}{362}\right)}{450(0.25)}} \right] + 5$$

$$d_{4+4U} = 20.1 \text{ s}$$

This movement would be assigned LOS C.

$$d_9 = \frac{3,600}{425} + 900(0.25) \left[\frac{100}{425} - 1 + \sqrt{\left(\frac{100}{425} - 1\right)^2 + \frac{\left(\frac{3,600}{425}\right)\left(\frac{100}{425}\right)}{450(0.25)}} \right] + 5$$

$$d_9 = 16.1 \text{ s}$$

This movement would be assigned LOS C.

$$d_7 = \frac{3,600}{98} + 900(0.25) \left[\frac{75}{98} - 1 + \sqrt{\left(\frac{75}{98} - 1\right)^2 + \frac{\left(\frac{3,600}{98}\right)\left(\frac{75}{98}\right)}{450(0.25)}} \right] + 5$$

$$d_1 = 113 \text{ s}$$

This movement would be assigned LOS F.

Step 11b: Compute Control Delay to Rank 1 Movements

No shared lanes are present on the major street, so this step is skipped.

Step 12: Compute Approach and Intersection Control Delay

The control delay for each approach is computed as follows:

$$d_{A,EB} = \frac{0(100) + 0(1,000) + 12.6(50)}{100 + 1,000 + 50} = 0.5 \text{ s}$$

$$d_{A,WB} = \frac{0(1,200) + 20.1(125)}{1,200 + 125} = 1.9 \text{ s}$$

$$d_{A,NB} = \frac{16.1(100) + 113(75)}{100 + 75} = 57.6 \text{ s}$$

The northbound approach is assigned LOS F. No LOS is assigned to the major-street approaches.

The intersection delay d_I is computed as follows:

$$d_I = \frac{d_{A,EB}v_{A,EB} + d_{A,WB}v_{A,WB} + d_{A,NB}v_{A,NB}}{v_{A,EB} + v_{A,WB} + v_{A,NB}}$$

$$d_I = \frac{0.5(1,150) + 1.9(1,325) + 57.6(175)}{1,150 + 1,325 + 175} = 5.0 \text{ s}$$

LOS is not defined for the intersection as a whole.

Step 13: Compute 95th Percentile Queue Lengths

The 95th percentile queue length for each movement is computed from Equation 20-68:

$$Q_{95,1U} \approx 900(0.25) \left[\frac{50}{523} - 1 + \sqrt{\left(\frac{50}{523} - 1\right)^2 + \frac{\left(\frac{3,600}{523}\right)\left(\frac{50}{523}\right)}{150(0.25)}} \right] \left(\frac{523}{3,600}\right)$$

$$Q_{95,1} \approx 0.3 \text{ veh}$$

$$Q_{95,4+4U} \approx 900(0.25) \left[\frac{125}{362} - 1 + \sqrt{\left(\frac{125}{362} - 1\right)^2 + \frac{\left(\frac{3,600}{362}\right)\left(\frac{125}{362}\right)}{150(0.25)}} \right] \left(\frac{362}{3,600}\right)$$

$$Q_{95,4+4U} \approx 1.5 \text{ veh}$$

$$Q_{95,9} \approx 900(0.25) \left[\frac{100}{425} - 1 + \sqrt{\left(\frac{100}{425} - 1\right)^2 + \frac{\left(\frac{3,600}{425}\right)\left(\frac{100}{425}\right)}{150(0.25)}} \right] \left(\frac{425}{3,600}\right)$$

$$Q_{95,9} \approx 0.9 \text{ veh}$$

$$Q_{95,7} \approx 900(0.25) \left[\frac{75}{98} - 1 + \sqrt{\left(\frac{75}{98} - 1\right)^2 + \frac{\left(\frac{3,600}{98}\right)\left(\frac{75}{98}\right)}{150(0.25)}} \right] \left(\frac{98}{3,600}\right)$$

$$Q_{95,7} \approx 4.1 \text{ veh}$$

Discussion

Overall, the results indicate that although most minor movements are operating at low to moderate delays and at LOS C or better, the minor-street left turn experiences high delays and operates at LOS F.

4. AWSC SUPPLEMENTAL ANALYSIS FOR THREE-LANE APPROACHES

Exhibit 32-15 provides the 512 possible combinations of probability of degree-of-conflict cases when alternative lane occupancies are considered for three-lane approaches. A 1 indicates a vehicle is in the lane; a 0 indicates a vehicle is not in the lane.

<i>i</i>	DOC Case	No. of Vehicles	Opposing Approach			Conflicting Left Approach			Conflicting Right Approach			
			L1	L2	L3	L1	L2	L3	L1	L2	L3	
1	1	0	0	0	0	0	0	0	0	0	0	
2	2	1	1	0	0	0	0	0	0	0	0	
3			0	1	0	0	0	0	0	0	0	
4			0	0	1	0	0	0	0	0	0	
5		2	1	1	0	0	0	0	0	0	0	
6			0	1	1	0	0	0	0	0	0	
7			1	0	1	0	0	0	0	0	0	
8		3	3	1	1	1	0	0	0	0	0	
9	3	1	0	0	0	1	0	0	0	0	0	
10			0	0	0	0	1	0	0	0	0	
11			0	0	0	0	0	1	0	0	0	
12			0	0	0	0	0	0	0	1	0	
13			0	0	0	0	0	0	0	0	1	0
14			0	0	0	0	0	0	0	0	0	1
15			2	0	0	0	1	1	0	0	0	0
16		0		0	0	0	1	1	1	0	0	0
17		0		0	0	1	0	1	0	0	0	0
18		0		0	0	0	0	0	0	1	1	0
19		0		0	0	0	0	0	0	0	1	1
20		0		0	0	0	0	0	0	1	0	1
21		3		3	0	0	0	1	1	1	0	0
22			0		0	0	0	0	0	1	1	1
23	4	2	1	0	0	1	0	0	0	0	0	
24			1	0	0	0	1	0	0	0	0	0
25			1	0	0	0	0	0	1	0	0	0
26			0	1	0	0	1	0	0	0	0	0
27			0	1	0	0	0	1	0	0	0	0
28			0	1	0	0	0	0	1	0	0	0
29			0	0	1	1	0	0	0	0	0	0
30			0	0	1	0	1	0	0	0	0	0
31			0	0	1	0	0	1	0	0	0	0
32			1	0	0	0	0	0	0	1	0	0
33			1	0	0	0	0	0	0	0	1	0
34			1	0	0	0	0	0	0	0	0	1
35			0	1	0	0	0	0	0	1	0	0
36			0	1	0	0	0	0	0	0	1	0
37		0	1	0	0	0	0	0	0	0	1	
38		0	0	1	0	0	0	0	1	0	0	
39		0	0	1	0	0	0	0	0	1	0	
40		0	0	1	0	0	0	0	0	0	1	
41		0	0	0	1	0	0	0	1	0	0	
42		0	0	0	1	0	0	0	0	1	0	
43		0	0	0	0	1	0	0	0	0	1	
44		0	0	0	0	0	1	0	1	0	0	
45		0	0	0	0	0	1	0	0	1	0	
46		0	0	0	0	0	1	0	0	0	1	
47		0	0	0	0	0	0	1	1	0	0	
48		0	0	0	0	0	0	1	0	1	0	
49		0	0	0	0	0	0	1	0	0	1	

Exhibit 32-15
Probability of Degree-of-Conflict Case: Multilane AWSC Intersections (Three-Lane Approaches, by Lane) (Cases 1–49)

Exhibit 32-15 (cont'd.)
 Probability of Degree-of-Conflict Case: Multilane AWSC Intersections (Three-Lane Approaches, by Lane) (Cases 50–112)

<i>i</i>	DOC Case	No. of Vehicles	Opposing Approach			Conflicting Left Approach			Conflicting Right Approach					
			L1	L2	L3	L1	L2	L3	L1	L2	L3			
50	4 (cont'd.)	3	1	1	0	1	0	0	0	0	0			
51			1	1	0	0	1	0	0	0	0	0		
52			1	1	0	0	0	1	0	0	0	0		
53			0	1	1	1	0	0	0	0	0	0		
54			0	1	1	0	1	0	0	0	0	0		
55			0	1	1	0	0	1	0	0	0	0		
56			1	0	1	1	0	0	0	0	0	0		
57			1	0	1	0	1	0	0	0	0	0		
58			1	0	1	0	0	1	0	0	0	0		
59			1	1	0	0	0	0	0	1	0	0		
60			1	1	0	0	0	0	0	0	1	0		
61			1	1	0	0	0	0	0	0	0	1		
62			0	1	1	0	0	0	0	1	0	0		
63			0	1	1	0	0	0	0	0	1	0		
64			0	1	1	0	0	0	0	0	0	1		
65			1	0	1	0	0	0	0	1	0	0		
66			1	0	1	0	0	0	0	0	1	0		
67			1	0	1	0	0	0	0	0	0	1		
68			1	0	0	1	1	1	0	0	0	0		
69			1	0	0	0	0	1	1	0	0	0		
70			1	0	0	1	0	1	1	0	0	0		
71			0	1	0	0	1	1	0	0	0	0		
72			0	1	0	0	0	1	1	0	0	0		
73			0	1	0	1	1	0	1	0	0	0		
74			0	0	1	1	1	1	0	0	0	0		
75			0	0	1	0	1	1	1	0	0	0		
76			0	0	1	1	0	1	1	0	0	0		
77			0	0	0	1	1	1	0	1	0	0		
78			0	0	0	1	1	1	0	0	1	0		
79			0	0	0	1	1	1	0	0	0	1		
80			0	0	0	0	0	1	1	1	0	0		
81			0	0	0	0	0	1	1	0	1	0		
82			0	0	0	0	0	1	1	0	0	1		
83			0	0	0	1	0	1	1	1	0	0		
84			0	0	0	1	0	1	1	0	1	0		
85			0	0	0	1	0	1	1	0	0	1		
86			1	0	0	0	0	0	0	1	1	0		
87			1	0	0	0	0	0	0	0	1	1		
88			1	0	0	0	0	0	0	1	0	1		
89			0	1	0	0	0	0	0	1	1	0		
90			0	1	0	0	0	0	0	0	1	1		
91			0	1	0	0	0	0	0	1	0	1		
92			0	0	1	0	0	0	0	1	1	0		
93			0	0	1	0	0	0	0	0	1	1		
94			0	0	1	0	0	0	0	1	0	1		
95			0	0	0	1	0	0	0	1	1	0		
96			0	0	0	1	0	0	0	0	1	1		
97			0	0	0	1	0	0	0	1	0	1		
98			0	0	0	0	0	1	0	1	1	0		
99			0	0	0	0	0	1	0	0	1	1		
100			0	0	0	0	0	1	0	1	0	1		
101			0	0	0	0	0	0	1	1	1	0		
102			0	0	0	0	0	0	1	0	1	1		
103			0	0	0	0	0	0	1	1	0	1		
104			4	4	1	1	0	1	1	0	0	0	0	
105					1	1	0	0	1	1	0	0	0	0
106					1	1	0	1	0	1	0	0	0	0
107					0	1	1	1	1	0	0	0	0	0
108					0	1	1	0	1	1	0	0	0	0
109					0	1	1	1	1	0	1	0	0	0
110					1	0	1	1	1	0	0	0	0	0
111					1	0	1	0	1	1	0	0	0	0
112					1	0	1	1	0	1	0	0	0	0

i	DOC Case	No. of Vehicles	Opposing Approach			Conflicting Left Approach			Conflicting Right Approach				
			L1	L2	L3	L1	L2	L3	L1	L2	L3		
113	4 (cont'd.)	4 (cont'd.)	1	1	0	0	0	0	1	1	0		
114			1	1	0	0	0	0	0	1	1		
115			1	1	0	0	0	0	1	0	1		
116			0	1	1	0	0	0	1	1	0		
117			0	1	1	0	0	0	0	1	1		
118			0	1	1	0	0	0	1	0	1		
119			1	0	1	0	0	0	1	1	0		
120			1	0	1	0	0	0	0	1	1		
121			1	0	1	0	0	0	1	0	1		
122			0	0	0	1	1	0	1	1	0		
123			0	0	0	1	1	0	0	1	1		
124			0	0	0	1	1	0	1	0	1		
125			0	0	0	0	1	1	1	1	0		
126			0	0	0	0	1	1	1	0	1		
127			0	0	0	0	1	1	1	1	0		
128			0	0	0	1	0	1	1	1	0		
129			0	0	0	1	0	1	0	1	1		
130			0	0	0	1	0	1	1	0	1		
131			1	1	1	1	0	0	0	0	0		
132			1	1	1	0	1	0	0	0	0		
133			1	1	1	0	0	1	0	0	0		
134			1	1	1	0	0	0	1	0	0		
135			1	1	1	0	0	0	0	1	0		
136			1	1	1	0	0	0	0	0	1		
137			1	0	0	1	1	1	0	0	0		
138			0	1	0	1	1	1	0	0	0		
139			0	0	1	1	1	1	0	0	0		
140			0	0	0	1	1	1	1	0	0		
141			0	0	0	1	1	1	0	1	0		
142			0	0	0	1	1	1	0	0	1		
143			1	0	0	0	0	0	1	1	1		
144			0	1	0	0	0	0	1	1	1		
145			0	0	1	0	0	0	1	1	1		
146			0	0	0	1	0	0	1	1	1		
147			0	0	0	0	1	0	1	1	1		
148			0	0	0	0	0	1	1	1	1		
149			5	5	1	1	1	1	1	0	0	0	0
150					1	1	1	0	1	1	0	0	0
151					1	1	1	1	0	1	0	0	0
152					1	1	1	0	0	0	1	1	0
153					1	1	1	0	0	0	0	1	1
154					1	1	1	0	0	0	1	0	1
155					1	1	0	1	1	1	0	0	0
156					0	1	1	1	1	1	0	0	0
157					1	0	1	1	1	1	0	0	0
158					0	0	0	1	1	1	1	1	0
159					0	0	0	1	1	1	0	1	1
160					0	0	0	1	1	1	1	0	1
161	1	1			0	0	0	0	1	1	1		
162	0	1			1	0	0	0	1	1	1		
163	1	0			1	0	0	0	1	1	1		
164	0	0			0	1	1	0	1	1	1		
165	0	0			0	0	1	1	1	1	1		
166	0	0			0	1	0	1	1	1	1		
167	6	6	1	1	1	1	1	1	0	0	0		
168			1	1	1	0	0	0	1	1	1		
169			0	0	0	1	1	1	1	1	1		
170	5	3	1	0	0	1	0	0	1	0	0		
171			1	0	0	1	0	0	0	1	0		
172			1	0	0	1	0	0	0	0	1		
173			1	0	0	0	1	0	1	0	0		
174			1	0	0	0	1	0	0	1	0		
175			1	0	0	0	1	0	0	0	1		

Exhibit 32-15 (cont'd.)
 Probability of Degree-of-Conflict Case: Multilane AWSC Intersections (Three-Lane Approaches, by Lane) (Cases 113-175)

Exhibit 32-15 (cont'd.)
 Probability of Degree-of-Conflict Case: Multilane AWSC Intersections (Three-Lane Approaches, by Lane) (Cases 176–238)

<i>i</i>	DOC Case	No. of Vehicles	Opposing Approach			Conflicting Left Approach			Conflicting Right Approach		
			L1	L2	L3	L1	L2	L3	L1	L2	L3
176	5 (cont'd.)	3 (cont'd.)	1	0	0	0	0	1	1	0	0
177			1	0	0	0	0	1	0	1	0
178			1	0	0	0	0	1	0	0	1
179			0	1	0	1	0	0	1	0	0
180			0	1	0	1	0	0	0	1	0
181			0	1	0	1	0	0	0	0	1
182			0	1	0	0	1	0	1	0	0
183			0	1	0	0	1	0	0	1	0
184			0	1	0	0	1	0	0	0	1
185			0	1	0	0	0	1	1	0	0
186			0	1	0	0	0	1	0	1	0
187			0	1	0	0	0	1	0	0	1
188			0	0	1	1	0	0	1	0	0
189			0	0	1	1	0	0	0	1	0
190			0	0	1	1	0	0	0	0	1
191			0	0	1	0	1	0	1	0	0
192			0	0	1	0	1	0	0	1	0
193			0	0	1	0	1	0	0	0	1
194			0	0	1	0	0	1	1	0	0
195	0	0	1	0	0	1	0	1	0		
196	0	0	1	0	0	1	0	0	1		
197	4	4	1	1	0	1	0	0	1	0	0
198			1	1	0	1	0	0	0	1	0
199			1	1	0	1	0	0	0	0	1
200			1	1	0	0	1	0	1	0	0
201			1	1	0	0	1	0	0	1	0
202			1	1	0	0	1	0	0	0	1
203			1	1	0	0	0	1	1	0	0
204			1	1	0	0	0	1	0	1	0
205			1	1	0	0	0	1	0	0	1
206			0	1	1	1	0	0	1	0	0
207			0	1	1	1	1	0	0	0	1
208			0	1	1	1	1	0	0	0	1
209			0	1	1	0	1	0	1	0	0
210			0	1	1	0	1	0	0	1	0
211			0	1	1	0	1	0	0	0	1
212			0	1	1	0	0	1	1	0	0
213			0	1	1	0	0	1	0	1	0
214			0	1	1	0	0	1	0	0	1
215			1	0	1	1	0	0	1	0	0
216			1	0	1	1	0	0	0	1	0
217			1	0	1	1	0	0	0	0	1
218			1	0	1	0	1	0	1	0	0
219			1	0	1	0	1	0	0	1	0
220			1	0	1	0	1	0	0	0	1
221			1	0	1	0	0	1	1	0	0
222			1	0	1	0	0	1	0	1	0
223			1	0	1	0	0	1	0	0	1
224			1	0	0	1	1	0	1	0	0
225			1	0	0	1	1	0	0	1	0
226			1	0	0	1	1	0	0	0	1
227			1	0	0	0	1	1	1	0	0
228			1	0	0	0	1	1	0	1	0
229			1	0	0	0	1	1	0	0	1
230			1	0	0	1	0	1	1	0	0
231			1	0	0	1	0	1	0	1	0
232			1	0	0	1	0	1	0	0	1
233			0	1	0	1	1	0	1	0	0
234			0	1	0	1	1	0	0	1	0
235			0	1	0	1	1	0	0	0	1
236			0	1	0	0	1	1	1	0	0
237			0	1	0	0	1	1	0	1	0
238			0	1	0	0	1	1	0	0	1

<i>i</i>	DOC Case	No. of Vehicles	Opposing Approach			Conflicting Left Approach			Conflicting Right Approach		
			L1	L2	L3	L1	L2	L3	L1	L2	L3
239	5	4	0	1	0	1	0	1	1	0	0
240	(cont'd.)	(cont'd.)	0	1	0	1	0	1	0	1	0
241			0	1	0	1	0	1	0	0	1
242			0	0	1	1	1	0	1	0	0
243			0	0	1	1	1	0	0	1	0
244			0	0	1	1	1	0	0	0	1
245			0	0	1	0	1	1	1	0	0
246			0	0	1	0	1	1	0	1	0
247			0	0	1	0	1	1	0	0	1
248			0	0	1	1	0	1	1	0	0
249			0	0	1	1	0	1	0	1	0
250			0	0	1	1	0	1	0	0	1
251			1	0	0	1	0	0	1	1	0
252			1	0	0	1	0	0	0	1	1
253			1	0	0	1	0	0	1	0	1
254			1	0	0	0	1	0	1	1	0
255			1	0	0	0	1	0	0	1	1
256			1	0	0	0	1	0	1	0	1
257			1	0	0	0	0	1	1	1	0
258			1	0	0	0	0	1	0	1	1
259			1	0	0	0	0	1	1	0	1
260			0	1	0	1	0	0	1	1	0
261			0	1	0	1	0	0	0	1	1
262			0	1	0	1	0	0	1	0	1
263			0	1	0	0	1	0	1	1	0
264			0	1	0	0	1	0	0	1	1
265			0	1	0	0	1	0	1	0	1
266			0	1	0	0	0	1	1	1	0
267			0	1	0	0	0	1	0	1	1
268			0	1	0	0	0	1	1	0	1
269			0	0	1	1	0	0	1	1	0
270			0	0	1	1	0	0	0	1	1
271			0	0	1	1	0	0	1	0	1
272			0	0	1	0	1	0	1	1	0
273			0	0	1	0	1	0	0	1	1
274			0	0	1	0	1	0	1	0	1
275			0	0	1	0	0	1	1	1	0
276			0	0	1	0	0	1	0	1	1
277			0	0	1	0	0	1	1	0	1
278		5	1	1	0	1	1	0	1	0	0
279			1	1	0	1	1	0	0	1	0
280			1	1	0	1	1	0	0	0	1
281			1	1	0	0	1	1	1	0	0
282			1	1	0	0	1	1	0	1	0
283			1	1	0	0	1	1	0	0	1
284			1	1	0	1	0	1	1	0	0
285			1	1	0	1	0	1	0	1	0
286			1	1	0	1	0	1	0	0	1
287			0	1	1	1	1	0	1	0	0
288			0	1	1	1	1	0	0	1	0
289			0	1	1	1	1	0	0	0	1
290			0	1	1	0	1	1	1	0	0
291			0	1	1	0	1	1	0	1	0
292			0	1	1	0	1	1	0	0	1
293			0	1	1	1	0	1	1	0	0
294			0	1	1	1	0	1	0	1	0
295			0	1	1	1	0	1	0	0	1
296			1	0	1	1	1	0	1	0	0
297			1	0	1	1	1	0	0	1	0
298			1	0	1	1	1	0	0	0	1
299			1	0	1	0	1	1	1	0	0
300			1	0	1	0	1	1	0	1	0
301			1	0	1	0	1	1	0	0	1

Exhibit 32-15 (cont'd.)
 Probability of Degree-of-Conflict Case: Multilane AWSC Intersections (Three-Lane Approaches, by Lane) (Cases 239–301)

Exhibit 32-15 (cont'd.)
 Probability of Degree-of-Conflict Case: Multilane AWSC Intersections (Three-Lane Approaches, by Lane) (Cases 302–364)

<i>i</i>	DOC Case	No. of Vehicles	Opposing Approach			Conflicting Left Approach			Conflicting Right Approach		
			L1	L2	L3	L1	L2	L3	L1	L2	L3
302	5	5	1	0	1	1	0	1	1	0	0
303	(cont'd.)	(cont'd.)	1	0	1	1	0	1	0	1	0
304			1	0	1	1	0	1	0	0	1
305			1	1	0	1	0	0	1	1	0
306			1	1	0	0	1	0	1	1	0
307			1	1	0	0	0	1	1	1	0
308			1	1	0	1	0	0	0	1	1
309			1	1	0	0	1	0	0	1	1
310			1	1	0	0	0	1	0	1	1
311			1	1	0	1	0	0	1	0	1
312			1	1	0	0	1	0	1	0	1
313			1	1	0	0	0	1	1	0	1
314			0	1	1	1	0	0	1	1	0
315			0	1	1	0	1	0	1	1	0
316			0	1	1	0	0	1	1	1	0
317			0	1	1	1	0	0	0	1	1
318			0	1	1	0	1	0	0	1	1
319			0	1	1	0	0	1	0	1	1
320			0	1	1	1	0	0	1	0	1
321			0	1	1	0	1	0	1	0	1
322			0	1	1	0	0	1	1	0	1
323			1	0	1	1	0	0	1	1	0
324			1	0	1	0	1	0	1	1	0
325			1	0	1	0	0	1	1	1	0
326			1	0	1	1	0	0	0	1	1
327			1	0	1	0	1	0	0	1	1
328			1	0	1	0	0	1	0	1	1
329			1	0	1	1	0	0	1	0	1
330			1	0	1	0	1	0	1	0	1
331			1	0	1	0	0	1	1	0	1
332			1	0	0	1	1	0	1	1	0
333			1	0	0	1	1	0	0	1	1
334			1	0	0	1	1	0	1	0	1
335			1	0	0	0	1	1	1	1	0
336			1	0	0	0	1	1	0	1	1
337			1	0	0	0	1	1	1	0	1
338			1	0	0	1	0	1	1	1	0
339			1	0	0	1	0	1	0	1	1
340			1	0	0	1	0	1	1	0	1
341			0	1	0	1	1	0	1	1	0
342			0	1	0	1	1	0	0	1	1
343			0	1	0	1	1	0	1	0	1
344			0	1	0	0	1	1	1	1	0
345			0	1	0	0	1	1	0	1	1
346			0	1	0	0	1	1	1	0	1
347			0	1	0	1	0	1	1	1	0
348			0	1	0	1	0	1	0	1	1
349			0	1	0	1	0	1	1	0	1
350			0	0	1	1	1	0	1	1	0
351			0	0	1	1	1	0	0	1	1
352			0	0	1	1	1	0	1	0	1
353			0	0	1	0	1	1	1	1	0
354			0	0	1	0	1	1	0	1	1
355			0	0	1	0	1	1	1	0	1
356			0	0	1	1	0	1	1	1	0
357			0	0	1	1	0	1	0	1	1
358			0	0	1	1	0	1	1	0	1
359			1	1	1	1	0	0	1	0	0
360			1	1	1	1	0	0	0	1	0
361			1	1	1	1	0	0	0	0	1
362			1	1	1	0	1	0	1	0	0
363			1	1	1	0	1	0	0	1	0
364			1	1	1	0	1	0	0	0	1

i	DOC Case	No. of Vehicles	Opposing Approach			Conflicting Left Approach			Conflicting Right Approach				
			L1	L2	L3	L1	L2	L3	L1	L2	L3		
365	5 (cont'd.)	5 (cont'd.)	1	1	1	0	0	1	1	0	0		
366			1	1	1	0	0	1	0	1	0		
367			1	1	1	0	0	1	0	0	1		
368			1	0	0	1	1	1	1	0	0		
369			1	0	0	1	1	1	1	0	1		
370			1	0	0	1	1	1	1	0	0		
371			0	1	0	1	1	1	1	1	0		
372			0	1	0	1	1	1	1	0	1		
373			0	1	0	1	1	1	1	0	0		
374			0	0	1	1	1	1	1	1	0		
375			0	0	1	1	1	1	1	0	1		
376			0	0	1	1	1	1	1	0	0		
377			1	0	0	1	0	0	0	1	1		
378			1	0	0	0	0	1	0	1	1		
379			1	0	0	0	0	0	1	1	1		
380			0	1	0	1	0	0	0	1	1		
381			0	1	0	0	0	1	0	1	1		
382			0	1	0	0	0	0	1	1	1		
383			0	0	1	1	0	0	0	1	1		
384			0	0	1	0	1	0	0	1	1		
385			0	0	1	0	0	0	1	1	1		
386			6	6	1	1	0	1	1	0	1	1	0
387					1	1	0	1	1	0	0	1	1
388					1	1	0	1	1	0	1	0	1
389					1	1	0	0	1	1	1	1	0
390					1	1	0	0	1	1	0	1	1
391					1	1	0	0	1	1	1	0	1
392					1	1	0	1	0	1	1	1	0
393					1	1	0	1	0	1	0	1	1
394					1	1	0	1	0	1	1	0	1
395					0	1	1	1	1	0	1	1	0
396					0	1	1	1	1	0	0	1	1
397					0	1	1	1	1	0	1	0	1
398					0	1	1	0	1	1	1	1	0
399					0	1	1	0	1	1	0	1	1
400	0	1			1	0	1	1	1	0	1		
401	0	1			1	1	0	1	1	1	0		
402	0	1			1	1	0	1	0	1	1		
403	0	1			1	1	0	1	1	0	1		
404	1	0			1	1	1	0	1	1	0		
405	1	0			1	1	1	0	0	1	1		
406	1	0			1	1	1	0	1	0	1		
407	1	0			1	0	1	1	1	1	0		
408	1	0			1	0	1	1	0	1	1		
409	1	0			1	0	1	1	1	0	1		
410	1	0			1	1	0	1	1	1	0		
411	1	0			1	1	0	1	0	1	1		
412	1	0			1	1	0	1	1	0	1		
413	1	1			1	1	1	0	1	0	0		
414	1	1			1	1	1	0	0	1	0		
415	1	1			1	1	1	0	0	0	1		
416	1	1			1	0	1	1	1	0	0		
417	1	1			1	0	1	1	0	1	0		
418	1	1			1	0	1	1	0	0	1		
419	1	1			1	1	0	1	1	0	0		
420	1	1			1	1	0	1	0	1	0		
421	1	1			1	1	0	1	0	0	1		
422	1	1			1	1	0	0	1	1	0		
423	1	1			1	1	0	0	0	1	1		
424	1	1			1	1	0	0	1	0	1		
425	1	1			1	0	1	0	1	1	0		
426	1	1			1	0	1	0	0	1	1		
427	1	1			1	0	1	0	1	0	1		

Exhibit 32-15 (cont'd.)
Probability of Degree-of-Conflict Case: Multilane AWSC Intersections (Three-Lane Approaches, by Lane) (Cases 365–427)

Exhibit 32-15 (cont'd.)
 Probability of Degree-of-Conflict Case: Multilane AWSC Intersections (Three-Lane Approaches, by Lane) (Cases 428–490)

<i>i</i>	DOC Case	No. of Vehicles	Opposing Approach			Conflicting Left Approach			Conflicting Right Approach				
			L1	L2	L3	L1	L2	L3	L1	L2	L3		
428	5 (cont'd.)	6 (cont'd.)	1	1	1	0	0	1	1	1	0		
429			1	1	1	0	0	1	0	1	1		
430			1	1	1	0	0	1	1	0	1		
431			1	1	0	1	1	1	1	0	0		
432			1	1	0	1	1	1	0	1	0		
433			1	1	0	1	1	1	0	0	1		
434			0	1	1	1	1	1	1	0	0		
435			0	1	1	1	1	1	1	0	0		
436			0	1	1	1	1	1	1	0	0		
437			1	0	1	1	1	1	1	1	0	0	
438			1	0	1	1	1	1	1	0	1	0	
439			1	0	1	1	1	1	1	0	0	1	
440			1	0	0	1	1	1	1	1	1	0	
441			1	0	0	1	1	1	1	0	1	1	
442			1	0	0	1	1	1	1	1	0	1	
443			0	1	0	1	1	1	1	1	1	0	
444			0	1	0	1	1	1	1	0	1	1	
445			0	1	0	1	1	1	1	1	0	1	
446			0	0	1	1	1	1	1	1	1	0	
447			0	0	1	1	1	1	1	0	1	1	
448			0	0	1	1	1	1	1	1	0	1	
449			1	1	0	1	0	0	1	1	1	1	
450			1	1	0	0	1	0	1	1	1	1	
451			1	1	0	0	0	0	1	1	1	1	
452			0	1	1	1	1	0	0	1	1	1	
453			0	1	1	1	0	1	0	1	1	1	
454			0	1	1	1	0	0	1	1	1	1	
455			1	0	1	1	1	0	0	1	1	1	
456			1	0	1	1	0	1	0	1	1	1	
457			1	0	1	1	0	0	1	1	1	1	
458			1	0	0	1	1	1	0	1	1	1	
459			1	0	0	0	0	1	1	1	1	1	
460			1	0	0	1	1	0	1	1	1	1	
461			0	1	0	1	1	1	0	1	1	1	
462			0	1	0	0	0	1	1	1	1	1	
463			0	1	0	1	1	0	1	1	1	1	
464			0	0	1	1	1	1	0	1	1	1	
465			0	0	1	1	0	1	1	1	1	1	
466			0	0	1	1	1	0	1	1	1	1	
467			7	7	1	1	1	1	1	0	1	1	0
468					1	1	1	1	1	0	0	1	1
469					1	1	1	1	1	0	1	0	1
470					1	1	1	0	1	1	1	1	0
471					1	1	1	0	1	1	0	1	1
472					1	1	1	0	1	1	1	0	1
473					1	1	1	1	0	1	1	1	0
474	1	1			1	1	0	1	0	1	1		
475	1	1			1	1	0	1	1	0	1		
476	1	1			0	1	1	1	1	1	0		
477	1	1			0	1	1	1	1	0	1		
478	1	1			0	1	1	1	1	0	1		
479	0	1			1	1	1	1	1	1	0		
480	0	1			1	1	1	1	1	0	1		
481	0	1			1	1	1	1	1	1	0		
482	1	0			1	1	1	1	1	1	0		
483	1	0			1	1	1	1	1	0	1		
484	1	0			1	1	1	1	1	1	0		
485	1	1			0	1	1	0	1	1	1		
486	1	1			0	0	1	1	1	1	1		
487	1	1			0	1	0	1	1	1	1		
488	0	1			1	1	1	0	1	1	1		
489	0	1			1	1	0	1	1	1	1		
490	0	1			1	1	1	0	1	1	1		

<i>i</i>	DOC Case	No. of Vehicles	Opposing Approach			Conflicting Left Approach			Conflicting Right Approach				
			L1	L2	L3	L1	L2	L3	L1	L2	L3		
491	5 (cont'd.)	7 (cont'd.)	1	0	1	1	1	0	1	1	1		
492			1	0	1	0	1	1	1	1	1	1	
493			1	0	1	1	0	1	1	1	1	1	
494			1	1	1	1	1	1	1	1	0	0	
495			1	1	1	1	1	1	1	0	1	0	
496			1	1	1	1	1	1	1	0	0	1	
497			1	1	1	1	1	0	0	1	1	1	
498			1	1	1	1	0	1	0	1	1	1	
499			1	1	1	1	0	0	1	1	1	1	
500			1	0	0	1	1	1	1	1	1	1	
501			0	1	0	1	1	1	1	1	1	1	
502			0	0	1	1	1	1	1	1	1	1	
503			8		1	1	1	1	1	1	1	1	0
504					1	1	1	1	1	1	1	0	1
505	1	1			1	1	1	1	1	1	0	1	
506	1	1			1	1	1	1	0	1	1	1	
507	1	1			1	0	1	1	1	1	1	1	
508	1	1			1	1	0	1	1	1	1	1	
509	1	1			0	1	1	1	1	1	1	1	
510	0	1			1	1	1	1	1	1	1	1	
511	1	0			1	1	1	1	1	1	1	1	
512	9		1	1	1	1	1	1	1	1			

Exhibit 32-15 (cont'd.)
Probability of Degree-of-Conflict Case: Multilane AWSC Intersections (Three-Lane Approaches, by Lane) (Cases 491–512)

Note: DOC = degree-of-conflict; No. of vehicles = total number of vehicles on the opposing and conflicting approaches; L1, L2, and L3 = Lane 1, 2, and 3, respectively.

5. AWSC EXAMPLE PROBLEMS

This part of the chapter provides example problems for use of the AWSC methodology. Exhibit 32-16 provides an overview of these problems. The examples focus on the operational analysis level. The planning and preliminary engineering analysis level is identical to the operations analysis level in terms of the calculations, except default values are used when available.

Exhibit 32-16
AWSC Example Problems

Problem Number	Description	Analysis Level
1	Single-lane, three-leg AWSC intersection	Operational
2	Multilane, four-leg AWSC intersection	Operational

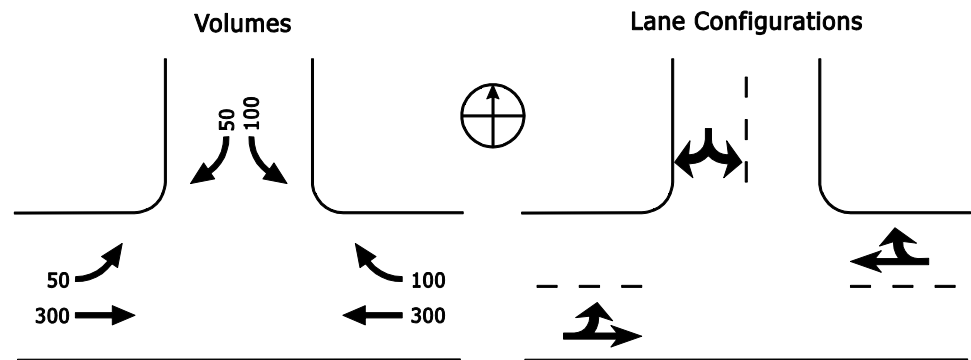
AWSC EXAMPLE PROBLEM 1: SINGLE-LANE, THREE-LEG INTERSECTION

The Facts

The following describes this location's traffic and geometric characteristics:

- Three legs (T-intersection),
- One-lane entries on each leg,
- Percentage heavy vehicles on all approaches = 2%,
- Peak hour factor = 0.95, and
- Volumes and lane configurations are as shown in Exhibit 32-17.

Exhibit 32-17
AWSC Example Problem 1:
Volumes and Lane Configurations



Length of study period = 0.25 h

Comments

All input parameters are known, so no default values are needed or used. The use of a spreadsheet or software is recommended because of the repetitive computations required. Slight differences in reported values may result from rounding differences between manual and software computations. Because showing all the individual computations is not practical, this example problem shows how one or more computations are made. All computational results can be found in the spreadsheet output located in the Volume 4 Technical Reference Library section for Chapter 32.

The use of a spreadsheet or software for AWSC intersection analysis is recommended because of the repetitive and iterative computations required.

Step 1: Convert Movement Demand Volumes to Flow Rates

Peak 15-min flow rates for each turning movement at the intersection are equal to the hourly volumes divided by the peak hour factor (Equation 21-12). For example, the peak 15-min flow rate for the eastbound through movement is as follows:

$$v_{EBTH} = \frac{V_{EBTH}}{PHF} = \frac{300}{0.95} = 316 \text{ veh/h}$$

Step 2: Determine Lane Flow Rates

This step does not apply because the intersection has one-lane approaches on all legs.

Step 3: Determine Geometry Group for Each Approach

Exhibit 21-11 shows each approach should be assigned to Geometry Group 1.

Step 4: Determine Saturation Headway Adjustments

Exhibit 21-12 shows the headway adjustments for left turns, right turns, and heavy vehicles are 0.2, -0.6, and 1.7, respectively. These values apply to all approaches because all are assigned to Geometry Group 1. The saturation headway adjustment for the eastbound approach is calculated from Equation 21-13 as follows:

$$h_{adj} = h_{LT,adj}P_{LT} + h_{RT,adj}P_{RT} + h_{HV,adj}P_{HV}$$

$$h_{adj,EB} = 0.2 \frac{53}{53 + 316} - 0.6(0) + 1.7(0.02) = 0.063$$

Similarly, the saturation headway adjustments for the westbound and northbound approaches are as follows:

$$h_{adj,WB} = 0.2(0) - 0.6 \left(\frac{105}{105 + 316} \right) + 1.7(0.02) = -0.116$$

$$h_{adj,NB} = 0.2 \frac{105}{105 + 53} - 0.6 \left(\frac{53}{105 + 53} \right) + 1.7(0.02) = -0.034$$

Steps 5–11: Determine Departure Headways

These steps are iterative. The following narrative highlights some of the key calculations using the eastbound approach for Iteration 1.

Step 6: Calculate Initial Degree of Utilization

By using the lane flow rates from Step 2 and the assumed initial departure headway from Step 5, the initial degree of utilization x is computed as follows from Equation 21-14:

$$x_{EB} = \frac{vh_d}{3,600} = \frac{(368)(3.2)}{3,600} = 0.327$$

$$x_{WB} = \frac{(421)(3.2)}{3,600} = 0.374$$

$$x_{NB} = \frac{(158)(3.2)}{3,600} = 0.140$$

Step 7: Compute Probability States

The probability state of each combination i is determined with Equation 21-15.

$$P(i) = \prod_j P(a_j) = P(a_O) \times P(a_{CL}) \times P(a_{CR})$$

For an intersection with single-lane approaches, only eight cases from Exhibit 21-14 apply, as shown in Exhibit 32-18:

Exhibit 32-18
 AWSC Example Problem 1:
 Applicable Degree-of-Conflict
 Cases

i	DOC Case	No. of Vehicles	Opposing Approach	Conflicting Left Approach	Conflicting Right Approach
1	1	0	0	0	0
2	2	1	1	0	0
5	3	1	0	1	0
7	3	1	0	0	1
13	4	2	0	1	1
16	4	2	1	1	0
21	4	2	1	0	1
45	5	3	1	1	1

For example, the probability state for the eastbound leg under the condition of no opposing vehicles on the other approaches (degree-of-conflict Case 1, $i = 1$) is as follows:

$$P(a_O) = 1 - x_O = 1 - 0.374 = 0.626 \quad (\text{no opposing vehicle present})$$

$$P(a_{CL}) = 1 - x_{CL} = 1 - 0.140 = 0.860 \quad (\text{no conflicting vehicle from left})$$

$$P(a_{CR}) = 1 \quad (\text{no approach conflicting from right})$$

Therefore,

$$P(1) = P(a_O) \times P(a_{CL}) \times P(a_{CR}) = (0.626)(0.860)(1) = 0.538$$

Similarly,

$$P(2) = (0.374)(0.860)(1) = 0.322$$

$$P(5) = (0.626)(0.140)(1) = 0.088$$

$$P(7) = (0.626)(0.860)(0) = 0$$

$$P(13) = (0.626)(0.140)(0) = 0$$

$$P(16) = (0.374)(0.140)(1) = 0.052$$

$$P(21) = (0.374)(0.860)(0) = 0$$

$$P(45) = (0.374)(0.140)(0) = 0$$

Step 8: Compute Probability Adjustment Factors

The probability adjustment is computed as follows, using Equation 21-16 through Equation 21-20:

$$P(C_1) = P(1) = 0.538$$

$$P(C_2) = P(2) = 0.322$$

$$P(C_3) = P(5) + P(7) = 0.088 + 0 = 0.088$$

$$P(C_4) = P(13) + P(16) + P(21) = 0 + 0.052 + 0 = 0.052$$

$$P(C_5) = P(45) = 0$$

The probability adjustment factors for the nonzero cases are calculated from Equation 21-21 through Equation 21-25:

$$AdjP(1) = 0.01[0.322 + 2(0.088) + 3(0.052) + 0]/1 = 0.0065$$

$$AdjP(2) = 0.01[0.088 + 2(0.052) + 0 - 0.322]/3 = -0.0004$$

$$AdjP(5) = 0.01[0.052 + 2(0) - 3(0.088)]/6 = -0.0004$$

$$AdjP(16) = 0.01[0 - 6(0.052)]/27 = -0.0001$$

Therefore, the adjusted probability for Combination 1, for example, is as follows from Equation 21-16:

$$P'(1) = P(1) + AdjP(1) = 0.538 + 0.0065 = 0.5445$$

Step 9: Compute Saturation Headways

The base saturation headways for each combination can be determined with Exhibit 21-15. They are adjusted by using the adjustment factors calculated in Step 4 and added to the base saturation headways to determine saturation headways as shown in Exhibit 32-19 (eastbound illustrated):

<i>i</i>	<i>h_{base}</i>	<i>h_{adj}</i>	<i>h_{si}</i>
1	3.9	0.063	3.963
2	4.7	0.063	4.763
5	5.8	0.063	5.863
7	7.0	0.063	7.063

Exhibit 32-19
AWSC Example Problem 1:
Eastbound Saturation
Headways

Step 10: Compute Departure Headways

The departure headway of the lane is the sum of the products of the adjusted probabilities and the saturation headways as follows (eastbound illustrated):

$$h_d = \sum_{i=1}^{64} P'(i)h_{si}$$

$$h_{d,EB} = (0.5445)(3.963) + (0.3213)(4.763) + (0.0875)(5.863) + (0.0524)(7.063)$$

$$h_{d,EB} = 4.57 \text{ s}$$

Step 11: Check for Convergence

The calculated values of *h_d* are checked against the initial values assumed for *h_d*. After one iteration, each calculated headway differs from the initial value by more than 0.1 s. Therefore, the new calculated headway values are used as initial values in a second iteration. For this problem, four iterations are required for convergence, as shown in Exhibit 32-20.

Exhibit 32-20

 AWSC Example Problem 1:
 Convergence Check

	EB L1	EB L2	WB L1	WB L2	NB L1	NB L2	SB L1	SB L2
Total Lane Flow Rate	368		421				158	
hd, initial value, iteration 1	3.2		3.2				3.2	
x, initial, iteration 1	0.327		0.374				0.140	
hd, computed value, iteration 1	4.57		4.35				5.14	
Convergence?	N		N				N	
hd, initial value, iteration 2	4.57		4.35				5.14	
x, initial, iteration 2	0.468		0.509				0.225	
hd, computed value, iteration 2	4.88		4.66				5.59	
Convergence?	N		N				N	
hd, initial value, iteration 3	4.88		4.66				5.59	
x, initial, iteration 3	0.499		0.545				0.245	
hd, computed value, iteration 3	4.95		4.73				5.70	
Convergence?	Y		Y				N	
hd, initial value, iteration 4	4.88		4.66				5.70	
x, initial, iteration 4	0.499		0.545				0.250	
hd, computed value, iteration 4	4.97		4.74				5.70	
Convergence?	Y		Y				Y	

Step 12: Compute Capacities

The capacity of each lane in a subject approach is computed by increasing the given flow rate on the subject lane (assuming the flows on the opposing and conflicting approaches are constant) until the degree of utilization for the subject lane reaches 1. This level of calculation requires running an iterative procedure many times, which is practical for a spreadsheet or software implementation.

Here, the eastbound lane capacity is approximately 720 veh/h, which is lower than the value that could be estimated by dividing the lane volume by the degree of utilization ($368/0.492 = 748$ veh/h). The difference is due to the interaction effects among the approaches: increases in eastbound traffic volume increase the departure headways of the lanes on the other approaches, which in turn increases the departure headways of the lane(s) on the subject approach.

Step 13: Compute Service Times

The service time required to calculate control delay is computed on the basis of the final calculated departure headway and the move-up time by using Equation 21-29. For the eastbound lane (using a value for m of 2.0 for Geometry Group 1), the calculation is as follows:

$$t_{s,EB} = h_{d,EB} - m = 4.97 - 2.0 = 2.97 \text{ s}$$

Step 14: Compute Control Delay and Determine LOS for Each Lane

The control delay for each lane is computed with Equation 21-30 as follows (eastbound illustrated):

$$d_{EB} = t_{s,EB} + 900T \left[(x_{EB} - 1) + \sqrt{(x_{EB} - 1)^2 + \frac{h_{d,EB}x_{EB}}{450T}} \right] + 5$$

$$d_{EB} = 2.97 + 900(0.25) \left[(0.508 - 1) + \sqrt{(0.508 - 1)^2 + \frac{4.97(0.508)}{450(0.25)}} \right] + 5$$

$$d_{EB} = 13.0 \text{ s}$$

By using Exhibit 21-8, the eastbound lane (and thus approach) is assigned LOS B. A similar calculation for the westbound and southbound lanes (and thus approaches) yields 13.5 and 10.6 s, respectively.

Step 15: Compute Control Delay and Determine LOS for the Intersection

The control delays for the approaches can be combined into an intersection control delay by using a weighted average as follows:

$$d_{\text{intersection}} = \frac{\sum d_a v_a}{\sum v_a}$$

$$d_{\text{intersection}} = \frac{(13.0)(368) + (13.5)(421) + (10.6)(158)}{368 + 421 + 158} = 12.8 \text{ s}$$

This value of delay is assigned LOS B.

Step 16: Compute Queue Lengths

The 95th percentile queue for each lane is computed with Equation 21-33 as follows (eastbound approach illustrated):

$$Q_{95,EB} \approx \frac{900T}{h_{d,EB}} \left[(x_{EB} - 1) + \sqrt{(x_{EB} - 1)^2 + \frac{h_{d,EB} x_{EB}}{150T}} \right]$$

$$Q_{95,EB} \approx \frac{900(0.25)}{4.97} \left[(0.508 - 1) + \sqrt{(0.508 - 1)^2 + \frac{4.97(0.508)}{150(0.25)}} \right] = 2.9 \text{ veh}$$

This queue length would be reported as three vehicles.

Discussion

The results indicate the intersection operates well with brief delays.

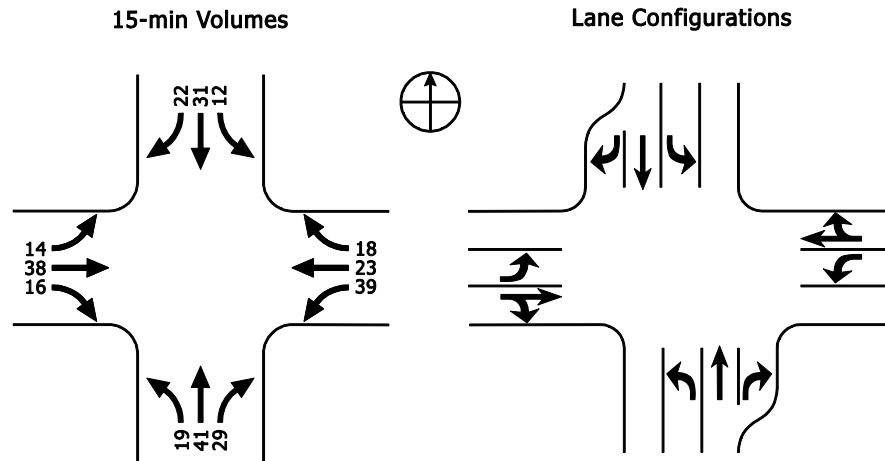
AWSC EXAMPLE PROBLEM 2: MULTILANE, FOUR-LEG INTERSECTION

The Facts

The following data are available to describe the traffic and geometric characteristics of this location:

- Four legs;
- Two-lane approaches on the east and west legs;
- Three-lane approaches on the north and south legs;
- Percentage heavy vehicles on all approaches = 2%;
- Demand volumes are provided in 15-min intervals (therefore, a peak hour factor is not required), and the analysis period length is 0.25 h; and
- Volumes and lane configurations are as shown in Exhibit 32-21.

Exhibit 32-21
 AWSC Example Problem 2:
 15-min Volumes and Lane
 Configurations



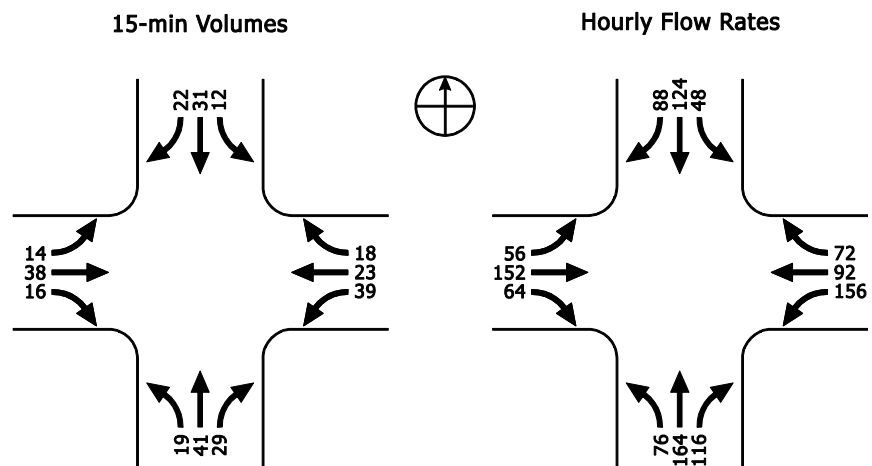
Comments

All input parameters are known, so no default values are needed or used. The use of a spreadsheet or software is required because of the several thousand repetitive computations needed. Slight differences in reported values may result from rounding differences between manual and software computations. Because showing all the individual computations is not practical, this example problem shows how one or more computations are made. All computational results can be found in the spreadsheet output located in the Volume 4 Technical Reference Library section for Chapter 32.

Step 1: Convert Movement Demand Volumes to Flow Rates

To convert the peak 15-min demand volumes to hourly flow rates, the individual movement volumes are simply multiplied by four, as shown in Exhibit 32-22:

Exhibit 32-22
 AWSC Example Problem 2:
 15-min Volumes Converted to
 Hourly Flow Rates



Step 2: Determine Lane Flow Rates

This step simply involves assigning the turning movement volume to each of the approach lanes. The left-turn volume is assigned to the separate left-turn lane on each approach. For the east and west approaches, the through and right-turn volumes are assigned to the shared through and right lanes. For the north and

south approaches, the through volumes are assigned to the through lanes and the right-turn volumes are assigned to the right-turn lanes.

Step 3: Determine Geometry Group for Each Approach

Exhibit 21-11 shows each approach should be assigned to Geometry Group 6.

Step 4: Determine Saturation Headway Adjustments

Exhibit 21-12 shows the headway adjustments for left turns, right turns, and heavy vehicles are 0.5, -0.7, and 1.7, respectively. These values apply to all approaches as all are assigned Geometry Group 6. The saturation headway adjustment for the eastbound approach is as follows for Lane 1 (the left-turn lane):

$$h_{adj} = h_{LT,adj}P_{LT} + h_{RT,adj}P_{RT} + h_{HV,adj}P_{HV}$$

$$h_{adj,EB,1} = 0.5(1.0) - 0.7(0) + 1.7(0.02) = 0.534$$

Similarly, the saturation headway adjustment for Lane 2 of the eastbound approach is as follows:

$$h_{adj,EB,2} = 0.5(0) - 0.7\left(\frac{64}{64 + 152}\right) + 1.7(0.02) = -0.173$$

The saturation headway adjustment for all the remaining lanes by approach is similarly calculated. The full computational results can be seen in the "HdwyAdj" spreadsheet tab.

Steps 5–11: Determine Departure Headways

These steps are iterative and, for this example, involve several thousand calculations. The following narrative highlights some of the key calculations using the eastbound approach for Iteration 1, but it does not attempt to reproduce all calculations for all iterations. The full computational results for each of the iterative computations can be seen in the "DepHdwyIterX" spreadsheet tab, where "X" is the iteration.

Step 6: Calculate Initial Degree of Utilization

The remainder of this example illustrates the calculations needed to evaluate Lane 1 on the eastbound approach (eastbound left turn). Step 6 requires calculating the initial degree of utilization for all the opposing and conflicting lanes. They are computed as follows:

$$x_{WB,1} = \frac{vh_d}{3,600} = \frac{(156)(3.2)}{3,600} = 0.1387$$

$$x_{WB,2} = \frac{vh_d}{3,600} = \frac{(164)(3.2)}{3,600} = 0.1458$$

$$x_{NB,1} = \frac{vh_d}{3,600} = \frac{(76)(3.2)}{3,600} = 0.0676$$

$$x_{NB,2} = \frac{vh_d}{3,600} = \frac{(164)(3.2)}{3,600} = 0.1458$$

$$x_{NB,3} = \frac{vh_d}{3,600} = \frac{(116)(3.2)}{3,600} = 0.1031$$

$$x_{SB,1} = \frac{vh_d}{3,600} = \frac{(48)(3.2)}{3,600} = 0.0427$$

$$x_{SB,2} = \frac{vh_d}{3,600} = \frac{(124)(3.2)}{3,600} = 0.1102$$

$$x_{SB,3} = \frac{vh_d}{3,600} = \frac{(88)(3.2)}{3,600} = 0.0782$$

Step 7: Compute Probability States

Because three-lane approaches are involved, the modified methodology presented in Section 4 of Chapter 21 is used.

The probability state of each combination *i* is determined with Equation 21-34:

$$P(i) = \prod_j P(a_j) = P(a_O) \times P(a_{CL}) \times P(a_{CR})$$

For example, the probability state for the eastbound leg under the condition of no opposing vehicles on the other approaches (Degree-of-Conflict Case 1, *i* = 1) is as follows (using Exhibit 21-16):

$$P(a_{O1}) = 1 - x_{O1} = 1 - 0.1387 = 0.8613 \quad (\text{opposing westbound Lane 1})$$

$$P(a_{O2}) = 1 - x_{O2} = 1 - 0.1458 = 0.8542 \quad (\text{opposing westbound Lane 2})$$

$$P(a_{CL1}) = 1 - x_{CL1} = 1 - 0.0427 = 0.9573 \quad (\text{conflicting from left Lane 1})$$

$$P(a_{CL2}) = 1 - x_{CL2} = 1 - 0.1102 = 0.8898 \quad (\text{conflicting from left Lane 2})$$

$$P(a_{CL3}) = 1 - x_{CL3} = 1 - 0.0782 = 0.9218 \quad (\text{conflicting from left Lane 3})$$

$$P(a_{CR1}) = 1 - x_{CR1} = 1 - 0.0676 = 0.9324 \quad (\text{conflicting from right Lane 1})$$

$$P(a_{CR2}) = 1 - x_{CR2} = 1 - 0.1458 = 0.8542 \quad (\text{conflicting from right Lane 2})$$

$$P(a_{CR3}) = 1 - x_{CR3} = 1 - 0.1031 = 0.8969 \quad (\text{conflicting from right Lane 3})$$

Therefore,

$$P(1) = P(a_{O1}) \times P(a_{O2}) \times P(a_{CL1}) \times P(a_{CL2}) \times P(a_{CL3}) \times P(a_{CR1}) \times P(a_{CR2}) \times P(a_{CR3})$$

$$P(1) = (0.8613)(0.8542)(0.9573)(0.8898)(0.9218)(0.9324)(0.8542)(0.8969)$$

$$P(1) = 0.4127$$

To complete the calculations for Step 7, the computations are completed for the remaining 511 possible combinations. The full computational results for the eastbound leg (Lane 1) can be seen in the “DepHdwyIter1” spreadsheet tab, Rows 3118–3629 (Columns C–K).

Step 8: Compute Probability Adjustment Factors

The probability adjustment is computed with Equation 21-35 through Equation 21-39 to account for the serial correlation in the previous probability computation. First, the probability of each degree-of-conflict case must be determined. For the example of eastbound Lane 1, these computations are made by summing Rows 3118–3629 in the spreadsheet for each of the five cases (Columns R–V). The resulting computations are shown in Row 3630 (Columns R–V), where

$$P(C_1) = P(1) = 0.4127$$

$$P(C_2) = \sum_{i=2}^8 P(i) = 0.1482$$

$$P(C_3) = \sum_{i=9}^{22} P(i) = 0.2779$$

$$P(C_4) = \sum_{i=23}^{169} P(i) = 0.1450$$

$$P(C_5) = \sum_{i=170}^{512} P(i) = 0.0162$$

The probability adjustment factors are then computed with Equation 21-40 through Equation 21-44, where α equals 0.01 (or 0.00 if correlation among saturation headways is not taken into account).

For example, by using Equation 21-35, $AdjP(1)$ is calculated as follows:

$$AdjP(1) = 0.01[0.1482 + 2(0.2779) + 3(0.1450) + 4(0.0162)]/1 = 0.01204$$

The results of the remaining computations for eastbound Lane 1 are located in Row 3632 of the spreadsheet (Columns S–V).

Step 9: Compute Saturation Headways

The base saturation headways for each of the 512 combinations can be determined with Exhibit 21-15. They are adjusted by using the adjustment factors calculated in Step 4 and added to the base saturation headways to determine saturation headways.

For the example of eastbound Lane 1, these computations are shown in Rows 3118–3629 of the spreadsheet (Columns M–O).

Step 10: Compute Departure Headways

The departure headway of the lane is the sum of the products of the adjusted probabilities and the saturation headways. For the example of eastbound Lane 1, these computations are made by summing the product of Columns O and Y for Rows 3118–3629 in the example spreadsheet.

Step 11: Check for Convergence

The calculated values of h_d are checked against the assumed initial values for h_d . After one iteration, each calculated headway differs from the initial value by more than 0.1 s. Therefore, the new calculated headway values are used as initial values in a second iteration. For this problem, five iterations were required for convergence, as shown in Exhibit 32-23.

Exhibit 32-23
AWSC Example Problem 2:
Convergence Check

	EB L1	EB L2	EB L3	WB L1	WB L2	WB L3	NB L1	NB L2	NB L3	SB L1	SB L2	SB L3
Total lane flow rate	56	216		156	164		76	164	116	48	124	88
hd, initial value, Iteration 1	3.2	3.2		3.2	3.2		3.2	3.2	3.2	3.2	3.2	3.2
x, initial, Iteration 1	0.0498	0.192		0.1387	0.1458		0.0676	0.1458	0.1031	0.0427	0.1102	0.0782
hd, computed value, Iteration 1	6.463	5.755		6.405	5.597		6.440	5.935	5.228	6.560	6.055	5.347
Convergence?	N	N		N	N		N	N	N	N	N	N
hd, initial value, Iteration 2	6.463	5.755		6.405	5.597		6.440	5.935	5.228	6.560	6.055	5.347
x, initial, Iteration 2	0.1005	0.3453		0.2776	0.255		0.136	0.2704	0.1685	0.0875	0.2086	0.1307
hd, computed value, Iteration 2	7.550	6.838		7.440	6.629		7.537	7.027	6.313	7.740	7.230	6.515
Convergence?	N	N		N	N		N	N	N	N	N	N
hd, initial value, Iteration 3	7.550	6.838		7.440	6.629		7.537	7.027	6.313	7.740	7.230	6.515
x, initial, Iteration 3	0.1174	0.4103		0.3224	0.302		0.1591	0.3201	0.2034	0.1032	0.249	0.1593
hd, computed value, Iteration 3	7.970	7.257		7.854	7.041		7.954	7.442	6.725	8.187	7.675	6.957
Convergence?	N	N		N	N		N	N	N	N	N	N
hd, initial value, Iteration 4	7.970	7.257		7.854	7.041		7.954	7.442	6.725	8.187	7.675	6.957
x, initial, Iteration 4	0.124	0.4354		0.3404	0.3208		0.1679	0.339	0.2167	0.1092	0.2643	0.17
hd, computed value, Iteration 4	8.130	7.416		8.010	7.196		8.114	7.601	6.884	8.359	7.845	7.126
Convergence?	N	N		N	N		N	N	N	N	N	N
hd, initial value, Iteration 5	8.130	7.416		8.010	7.196		8.114	7.601	6.884	8.359	7.845	7.126
x, initial, Iteration 5	0.1265	0.445		0.3471	0.3278		0.1713	0.3463	0.2218	0.1115	0.2702	0.1742
hd, computed value, Iteration 5	8.191	7.476		8.069	7.255		8.174	7.661	6.943	8.424	7.910	7.190
Convergence?	Y	Y		Y	Y		Y	Y	Y	Y	Y	Y

Step 12: Compute Capacity

As noted in the procedure, the capacity of each lane in a subject approach is computed by increasing the given flow rate on the subject lane (assuming the flows on the opposing and conflicting approaches are constant) until the degree of utilization for the subject lane reaches 1. This level of calculation requires running an iterative procedure many times, which is practical only for a spreadsheet or software implementation.

For this example, the capacity of eastbound Lane 1 can be found to be approximately 420 veh/h. This value is lower than the value that could be estimated by dividing the lane volume by the degree of utilization (56/0.1265 = 443 veh/h). The difference is due to the interaction effects among the approaches: increases in eastbound traffic volume increase the departure headways of the lanes on the other approaches, which increases the departure headways of the lanes on the subject approach.

Step 13: Compute Service Times

The service time required to calculate control delay is computed on the basis of the final calculated departure headway and the move-up time by using Equation 21-29. For the eastbound Lane 1 (using a value for *m* of 2.3 for Geometry Group 6), the calculation is as follows:

$$t_{s,EB,1} = h_{d,EB,1} - m = 8.19 - 2.3 = 5.89 \text{ s}$$

Step 14: Compute Control Delay and Determine LOS for Each Lane

The control delay for each lane is computed with Equation 21-30 as follows (eastbound Lane 1 illustrated):

$$d_{EB,1} = t_{s,EB,1} + 900T \left[(x_{EB,1} - 1) + \sqrt{(x_{EB,1} - 1)^2 + \frac{h_{d,EB,1}x_{EB,1}}{450T}} \right] + 5$$

$$d_{EB,1} = 5.89 + 900(0.25) \left[(0.1274 - 1) + \sqrt{(0.1274 - 1)^2 + \frac{8.19(0.1274)}{450(0.25)}} \right] + 5$$

$$d_{EB,1} = 12.1 \text{ s}$$

On the basis of Exhibit 20-2, eastbound Lane 1 is assigned LOS B.

Step 15: Compute Control Delay and Determine LOS for Each Approach and the Intersection

The control delay for each approach is calculated using Equation 21-31 as follows (eastbound approach illustrated):

$$d_{EB} = \frac{(12.1)(272) + (16.1)(216)}{56 + 216} = 15.3 \text{ s}$$

This value of delay is assigned LOS C.

Similarly, the control delay for the intersection is calculated as follows:

$$d_{\text{intersection}} = \frac{(15.3)(272) + (14.3)(320) + (13.1)(356) + (12.6)(260)}{272 + 320 + 356 + 260} = 14.0 \text{ s}$$

This value of delay is assigned LOS B.

Step 16: Compute Queue Lengths

The 95th percentile queue for each lane is computed with Equation 21-33 as follows for eastbound Lane 1:

$$Q_{95,EB1} \approx \frac{900(0.25)}{8.19} \left[(0.1274 - 1) + \sqrt{(0.1274 - 1)^2 + \frac{8.19(0.1274)}{150(0.25)}} \right]$$

$$Q_{95,EB1} \approx 0.4 \text{ veh}$$

This queue length commonly would be rounded up to one vehicle.

Discussion

The overall results can be found in the “DelayLOS” spreadsheet tab. As indicated in the output, all movements at the intersection are operating well with small delays. The worst-performing movement is eastbound Lane 2, which is operating with a volume-to-capacity ratio of 0.45 and a control delay of 16.1 s/veh, which results in LOS C. The intersection as a whole operates at LOS B, so the reporting of individual movements is important to avoid masking results caused by aggregating delays.



HIGHWAY CAPACITY MANUAL

6TH EDITION | A GUIDE FOR MULTIMODAL MOBILITY ANALYSIS

VOLUME 4: APPLICATIONS GUIDE

The National Academies of
SCIENCES • ENGINEERING • MEDICINE

TRANSPORTATION RESEARCH BOARD
WASHINGTON, D.C. | WWW.TRB.ORG

TRANSPORTATION RESEARCH BOARD 2016 EXECUTIVE COMMITTEE *

Chair: James M. Crites, Executive Vice President of Operations,
Dallas–Fort Worth International Airport, Texas

Vice Chair: Paul Trombino III, Director, Iowa Department of
Transportation, Ames

Executive Director: Neil J. Pedersen, Transportation Research Board

Victoria A. Arroyo, Executive Director, Georgetown Climate Center;
Assistant Dean, Centers and Institutes; and Professor and Director,
Environmental Law Program, Georgetown University Law Center,
Washington, D.C.

Scott E. Bennett, Director, Arkansas State Highway and Transportation
Department, Little Rock

Jennifer Cohan, Secretary, Delaware Department of Transportation, Dover

Malcolm Dougherty, Director, California Department of
Transportation, Sacramento

A. Stewart Fotheringham, Professor, School of Geographical Sciences
and Urban Planning, Arizona State University, Tempe

John S. Halikowski, Director, Arizona Department of Transportation,
Phoenix

Susan Hanson, Distinguished University Professor Emerita, Graduate
School of Geography, Clark University, Worcester, Massachusetts

Steve Heminger, Executive Director, Metropolitan Transportation
Commission, Oakland, California

Chris T. Hendrickson, Hamerschlag Professor of Engineering, Carnegie
Mellon University, Pittsburgh, Pennsylvania

Jeffrey D. Holt, Managing Director, Power, Energy, and Infrastructure
Group, BMO Capital Markets Corporation, New York

S. Jack Hu, Vice President for Research and J. Reid and Polly Anderson
Professor of Manufacturing, University of Michigan, Ann Arbor

Roger B. Huff, President, HGLC, LLC, Farmington Hills, Michigan

Geraldine Knatz, Professor, Sol Price School of Public Policy, Viterbi
School of Engineering, University of Southern California, Los Angeles

Ysela Llort, Consultant, Miami, Florida

Melinda McGrath, Executive Director, Mississippi Department of
Transportation, Jackson

James P. Redeker, Commissioner, Connecticut Department of
Transportation, Newington

Mark L. Rosenberg, Executive Director, The Task Force for Global
Health, Inc., Decatur, Georgia

Kumares C. Sinha, Olson Distinguished Professor of Civil Engineering,
Purdue University, West Lafayette, Indiana

Daniel Sperling, Professor of Civil Engineering and Environmental
Science and Policy; Director, Institute of Transportation Studies,
University of California, Davis

Kirk T. Steudle, Director, Michigan Department of Transportation,
Lansing (Past Chair, 2014)

Gary C. Thomas, President and Executive Director, Dallas Area Rapid
Transit, Dallas, Texas

Pat Thomas, Senior Vice President of State Government Affairs, United
Parcel Service, Washington, D.C.

Katherine F. Turnbull, Executive Associate Director and Research
Scientist, Texas A&M Transportation Institute, College Station

Dean Wise, Vice President of Network Strategy, Burlington Northern
Santa Fe Railway, Fort Worth, Texas

Thomas P. Bostick (Lieutenant General, U.S. Army), Chief of Engineers
and Commanding General, U.S. Army Corps of Engineers, Washington,
D.C. (ex officio)

James C. Card (Vice Admiral, U.S. Coast Guard, retired), Maritime
Consultant, The Woodlands, Texas, and Chair, TRB Marine Board
(ex officio)

T. F. Scott Darling III, Acting Administrator and Chief Counsel, Federal
Motor Carrier Safety Administration, U.S. Department of Transportation
(ex officio)

Marie Therese Dominguez, Administrator, Pipeline and Hazardous
Materials Safety Administration, U.S. Department of Transportation
(ex officio)

Sarah Feinberg, Administrator, Federal Railroad Administration,
U.S. Department of Transportation (ex officio)

Carolyn Flowers, Acting Administrator, Federal Transit Administration,
U.S. Department of Transportation (ex officio)

LeRoy Gishi, Chief, Division of Transportation, Bureau of Indian
Affairs, U.S. Department of the Interior, Washington, D.C. (ex officio)

John T. Gray II, Senior Vice President, Policy and Economics,
Association of American Railroads, Washington, D.C. (ex officio)

Michael P. Huerta, Administrator, Federal Aviation Administration,
U.S. Department of Transportation (ex officio)

Paul N. Jaenichen, Sr., Administrator, Maritime Administration,
U.S. Department of Transportation (ex officio)

Bevan B. Kirley, Research Associate, University of North Carolina
Highway Safety Research Center, Chapel Hill, and Chair, TRB Young
Members Council (ex officio)

Gregory G. Nadeau, Administrator, Federal Highway Administration,
U.S. Department of Transportation (ex officio)

Wayne Nastri, Acting Executive Officer, South Coast Air Quality
Management District, Diamond Bar, California (ex officio)

Mark R. Rosekind, Administrator, National Highway Traffic Safety
Administration, U.S. Department of Transportation (ex officio)

Craig A. Rutland, U.S. Air Force Pavement Engineer, U.S. Air Force
Civil Engineer Center, Tyndall Air Force Base, Florida (ex officio)

Reuben Sarkar, Deputy Assistant Secretary for Transportation,
U.S. Department of Energy (ex officio)

Richard A. White, Acting President and CEO, American Public
Transportation Association, Washington, D.C. (ex officio)

Gregory D. Winfree, Assistant Secretary for Research and Technology,
Office of the Secretary, U.S. Department of Transportation (ex officio)

Frederick G. (Bud) Wright, Executive Director, American Association
of State Highway and Transportation Officials, Washington, D.C.
(ex officio)

Paul F. Zukunft (Admiral, U.S. Coast Guard), Commandant, U.S. Coast
Guard, U.S. Department of Homeland Security (ex officio)

Transportation Research Board publications are available by ordering
individual publications directly from the TRB Business Office, through
the Internet at www.TRB.org, or by annual subscription through
organizational or individual affiliation with TRB. Affiliates and library
subscribers are eligible for substantial discounts. For further information,
contact the Transportation Research Board Business Office, 500 Fifth
Street, NW, Washington, DC 20001 (telephone 202-334-3213;
fax 202-334-2519; or e-mail TRBsales@nas.edu).

Copyright 2016 by the National Academy of Sciences.

All rights reserved.

Printed in the United States of America.

ISBN 978-0-309-36997-8 [Slipcased set of three volumes]

ISBN 978-0-309-36998-5 [Volume 1]

ISBN 978-0-309-36999-2 [Volume 2]

ISBN 978-0-309-37000-4 [Volume 3]

ISBN 978-0-309-37001-1 [Volume 4, online only]

The National Academies of
SCIENCES • ENGINEERING • MEDICINE

The **National Academy of Sciences** was established in 1863 by an Act of Congress, signed by President Lincoln, as a private, nongovernmental institution to advise the nation on issues related to science and technology. Members are elected by their peers for outstanding contributions to research. Dr. Ralph J. Cicerone is president.

The **National Academy of Engineering** was established in 1964 under the charter of the National Academy of Sciences to bring the practices of engineering to advising the nation. Members are elected by their peers for extraordinary contributions to engineering. Dr. C. D. Mote, Jr., is president.

The **National Academy of Medicine** (formerly the Institute of Medicine) was established in 1970 under the charter of the National Academy of Sciences to advise the nation on medical and health issues. Members are elected by their peers for distinguished contributions to medicine and health. Dr. Victor J. Dzau is president.

The three Academies work together as the National Academies of Sciences, Engineering, and Medicine to provide independent, objective analysis and advice to the nation and conduct other activities to solve complex problems and inform public policy decisions. The Academies also encourage education and research, recognize outstanding contributions to knowledge, and increase public understanding in matters of science, engineering, and medicine.

Learn more about the National Academies of Sciences, Engineering, and Medicine at **www.national-academies.org**.

The **Transportation Research Board** is one of seven major programs of the National Academies of Sciences, Engineering, and Medicine. The mission of the Transportation Research Board is to increase the benefits that transportation contributes to society by providing leadership in transportation innovation and progress through research and information exchange, conducted within a setting that is objective, interdisciplinary, and multimodal. The Board's varied committees, task forces, and panels annually engage about 7,000 engineers, scientists, and other transportation researchers and practitioners from the public and private sectors and academia, all of whom contribute their expertise in the public interest. The program is supported by state transportation departments, federal agencies including the component administrations of the U.S. Department of Transportation, and other organizations and individuals interested in the development of transportation.

Learn more about the Transportation Research Board at **www.TRB.org**.

CHAPTER 33
ROUNDBABOUTS: SUPPLEMENTAL

CONTENTS

1. INTRODUCTION 33-1

2. SUPPLEMENTAL GUIDANCE..... 33-2

 Variability and Uncertainty 33-2

 Lane-Use Assignment..... 33-4

 Capacity Model Calibration 33-6

3. EXAMPLE PROBLEMS 33-8

 Example Problem 1: Single-Lane Roundabout with Bypass Lanes 33-8

 Example Problem 2: Multilane Roundabout..... 33-13

4. REFERENCES..... 33-19

LIST OF EXHIBITS

Exhibit 33-1 Observed Combinations of Entry Flow and Conflicting Flow
During 1-min Periods of Continuous Queuing: One-Lane Entry
Opposed by One Circulating Lane..... 33-2

Exhibit 33-2 Observed Combinations of Entry Flow and Conflicting Flow
During 1-min Periods of Continuous Queuing: Both Lanes of Two-
Lane Entry Opposed by One Circulating Lane 33-3

Exhibit 33-3 Observed Combinations of Entry Flow and Conflicting Flow
During 1-min Periods of Continuous Queuing: Left Lane of Two-
Lane Entry Opposed by Two Circulating Lanes 33-3

Exhibit 33-4 Observed Combinations of Entry Flow and Conflicting Flow
During 1-min Periods of Continuous Queuing: Right Lane of Two-
Lane Entry Opposed by Two Circulating Lanes 33-4

Exhibit 33-5 Roundabout Example Problems 33-8

Exhibit 33-6 Example Problem 1: Demand Volumes and Lane
Configurations..... 33-8

Exhibit 33-7 Example Problem 1: Adjusted Flow Rates 33-9

Exhibit 33-8 Example Problem 1: LOS by Lane 33-12

Exhibit 33-9 Example Problem 2: Demand Volumes and Lane
Configurations..... 33-13

Exhibit 33-10 Example Problem 2: Adjusted Flow Rates 33-14

Exhibit 33-11 Example Problem 2: LOS by Lane 33-17

1. INTRODUCTION

Chapter 33 is the supplemental chapter for Chapter 22, Roundabouts, which is found in Volume 3 of the *Highway Capacity Manual* (HCM). This chapter presents detailed information about the following aspects of the Chapter 22 motorized vehicle methodology:

- Information about the large variability in U.S. driver behavior at roundabouts,
- Guidance on making an appropriate selection of a lane utilization factor, and
- Guidance on calibrating the capacity model to reflect local conditions.

This chapter also provides two example problems that demonstrate the application of the Chapter 22 methodology to single-lane and multilane roundabouts.

VOLUME 4: APPLICATIONS
GUIDE

- 25. Freeway Facilities:
Supplemental
- 26. Freeway and Highway
Segments: Supplemental
- 27. Freeway Weaving:
Supplemental
- 28. Freeway Merges and
Diverges: Supplemental
- 29. Urban Street Facilities:
Supplemental
- 30. Urban Street Segments:
Supplemental
- 31. Signalized Intersections:
Supplemental
- 32. STOP-Controlled
Intersections:
Supplemental
- 33. Roundabouts:
Supplemental**
- 34. Interchange Ramp
Terminals: Supplemental
- 35. Pedestrians and Bicycles:
Supplemental
- 36. Concepts: Supplemental
- 37. ATDM: Supplemental

2. SUPPLEMENTAL GUIDANCE

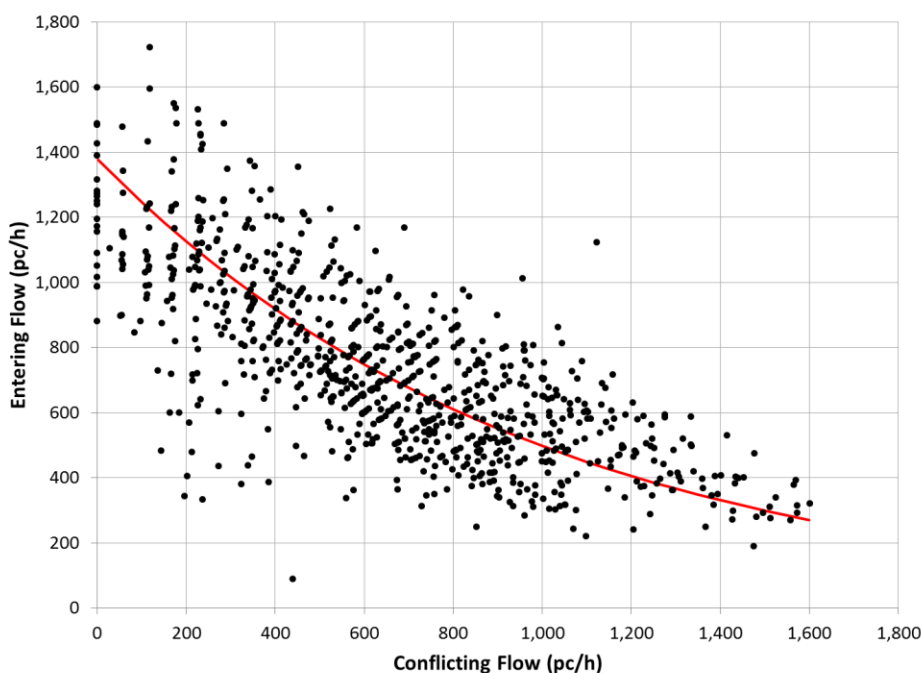
This section presents supplemental guidance on the methodology provided in Chapter 22, Roundabouts.

VARIABILITY AND UNCERTAINTY

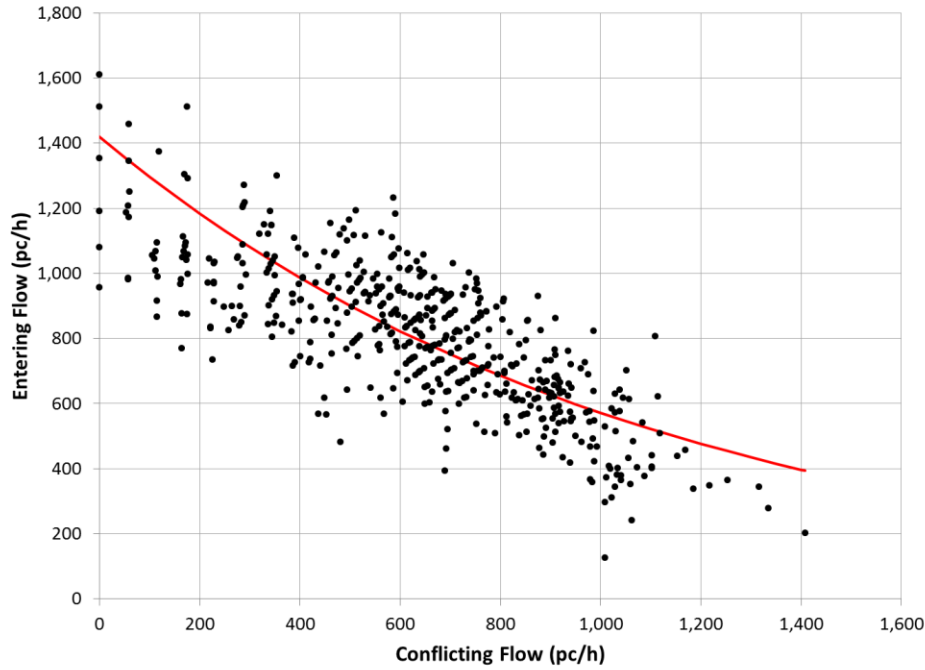
The analyst should be aware of the large observed variation in driver behavior at roundabouts. Exhibit 33-1 through Exhibit 33-4 show observed combinations of entry flow and conflicting flow at different roundabout configurations, along with the capacity models for the respective configuration as presented in Chapter 22. The bulk of this variation is attributable to variations in driver behavior, truck percentage, and exiting vehicles. As there is no external control device regulating flow interactions at roundabouts, driver interactions govern the operation, and they are highly variable by nature.

This variability should be considered by the analyst when evaluating a roundabout approach.

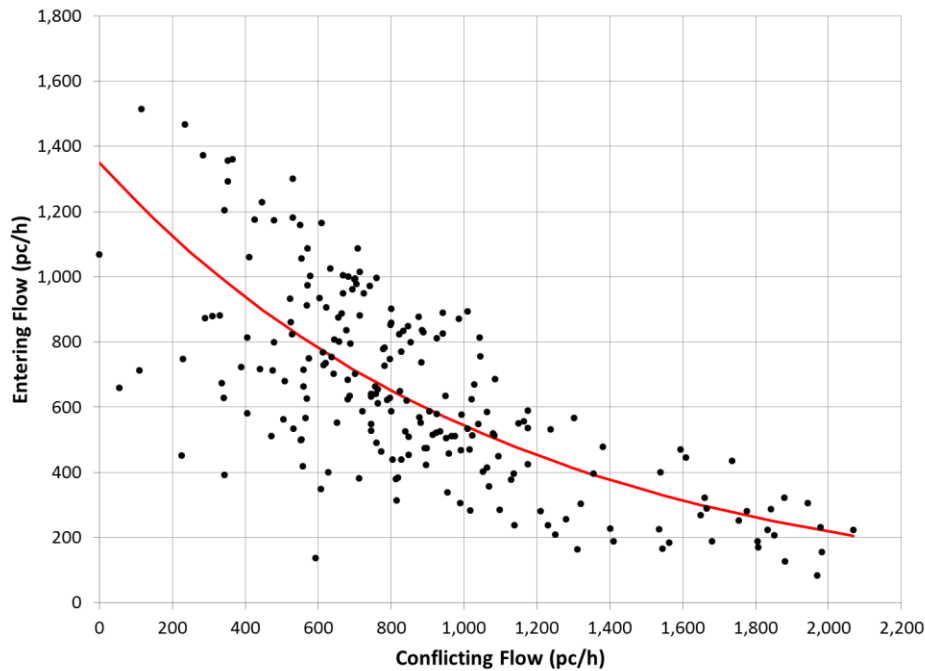
Exhibit 33-1
Observed Combinations of Entry Flow and Conflicting Flow During 1-min Periods of Continuous Queuing: One-Lane Entry Opposed by One Circulating Lane



Source: Rodederdt et al. (1).



Source: Rodederdts et al. (1).



Source: Rodederdts et al. (1).

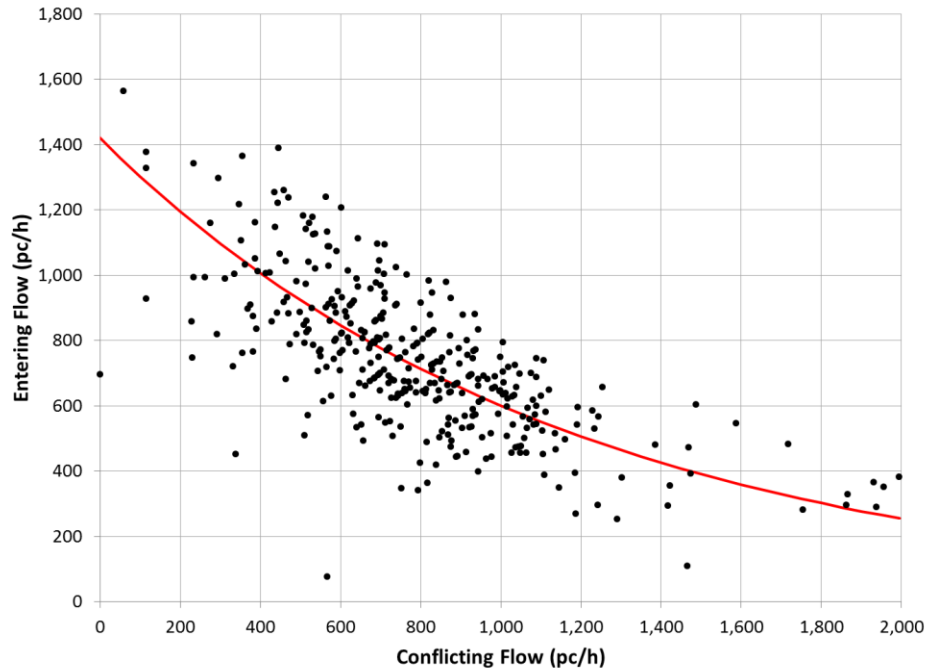
Exhibit 33-2

Observed Combinations of Entry Flow and Conflicting Flow During 1-min Periods of Continuous Queuing: Both Lanes of Two-Lane Entry Opposed by One Circulating Lane

Exhibit 33-3

Observed Combinations of Entry Flow and Conflicting Flow During 1-min Periods of Continuous Queuing: Left Lane of Two-Lane Entry Opposed by Two Circulating Lanes

Exhibit 33-4
 Observed Combinations of Entry Flow and Conflicting Flow During 1-min Periods of Continuous Queuing: Right Lane of Two-Lane Entry Opposed by Two Circulating Lanes



Source: Rodegerdts et al. (1).

LANE-USE ASSIGNMENT

Lane-use assignment is best determined by measuring lane use in the field under the conditions being analyzed. In the absence of this information, default values or estimates can be used. This section provides background on the process by which an analyst can make an appropriate selection of a lane utilization factor.

In general, several factors contribute to the assignment of traffic flow to each lane:

1. The assignment of turning movements to each lane (either as exclusive lanes or as shared lanes) directly influences the assignment of traffic volumes to each lane. Lane assignment is generally accomplished through the use of signs and pavement markings that designate the lane use for each lane. Multilane entries with no lane-use signing or pavement markings may be assumed to operate with a shared left-through lane in the left lane and a shared through-right lane in the right lane, although field observations should be made to confirm the lane-use pattern of an existing roundabout.
2. Dominant turning movements may create de facto lane assignments for which there is no advantage for drivers in using both lanes assigned to a given turning movement. For example, at an entry with left-through and through-right lanes and a dominant left-turn movement, there may be no advantage for through drivers in using the left lane. In addition, a lack of lane balance through the roundabout (e.g., two entry lanes but only one downstream circulating lane or one downstream exit lane) can create de facto lane-use assignments for a particular entry.

Turning movement patterns greatly influence lane assignments.

Dominant turning movements may create de facto lanes. A de facto lane is one designated for multiple movements but that may operate as an exclusive lane because of a dominant movement demand. A common example is a left-through lane with a left-turn flow rate that greatly exceeds the through flow rate.

3. Destinations downstream of a roundabout may influence the lane choice at the roundabout entry. A downstream destination such as a freeway on-ramp may increase use of the right entry lane, for example, even though both lanes could be used.
4. The alignment of the lane relative to the circulatory roadway seems to influence the use of entry lanes where drivers can choose between lanes. Some roundabouts have been designed with rather perpendicular entries that have a natural alignment of the right entry lane into the left lane of the circulatory roadway. Under this design, the left entry lane is naturally aimed at the central island and is thus less comfortable and less desirable for drivers. This phenomenon of poor path alignment, documented elsewhere (2), may result in poor use of the left entry lane. Similarly, poorly aligned multilane exits, where vehicles exiting in the inside lane cross the path of vehicles exiting in the outside lane, may influence lane use on upstream entries. In either case, the effect is most readily measured in the field at existing roundabouts, and it should be avoided in the design of new roundabouts.
5. Drivers may be uncertain about lane use when they use the roundabout, particularly at roundabouts without designated lane assignments approaching or circulating through the roundabout. This uncertainty may contribute to the generally incorrect use of the right entry lane for left turns, for example, because of a perceived or real difficulty in exiting from the inside lane of the circulatory roadway. Proper signing and striping of lane use on the approach and through the roundabout may reduce this uncertainty, although it is likely to be present to some extent at multilane roundabouts.

The first three factors described above are common to all intersections and are accounted for in the assignment of turning-movement patterns to individual lanes; the remaining two factors are unique to roundabouts. The fourth factor should be addressed through proper alignment of the entry relative to the circulatory roadway and thus may not need to be considered in the analysis of new facilities. However, existing roundabouts may exhibit poor path alignment, resulting in poor lane utilization. It may be possible to reduce the fifth factor through proper design, particularly through lane-use arrows and striping. These factors collectively make accurate estimation of lane utilization difficult, but it can be measured at existing roundabouts.

For entries with two through lanes, limited field data suggest drivers generally have a bias for the right lane. For entries with two left-turn lanes (e.g., left-turn-only and shared left-through-right lanes), limited field data suggest drivers have a bias for the left lane. Although no field observations have been documented for entries with two right-turn lanes, experience at other types of intersections with two right-turn lanes suggests drivers have a bias for the right lane.

Downstream destinations may influence lane assignment.

Poor geometric alignment of the entry may cause drivers to avoid the left lane.

Unfamiliar drivers may incorrectly select lanes for their intended movements.

Multilane roundabouts generally exhibit a bias to the right lane except where a double left-turn movement is present.

CAPACITY MODEL CALIBRATION

As discussed in Chapter 22, Roundabouts, the capacity model can be calibrated by using one of two methods: using two parameters, the critical headway t_c and the follow-up headway t_f , or using only the follow-up headway t_f .

An example of calibration using two parameters was performed for roundabouts in California (3). Field-measured values for critical headway and follow-up headway were determined as follows:

- Critical headway:
 - Single-lane roundabouts: 4.8 s;
 - Multilane roundabouts, left lane: 4.7 s; and
 - Multilane roundabouts, right lane: 4.4 s.
- Follow-up headway:
 - Single-lane roundabouts: 2.5 s;
 - Multilane roundabouts, left lane: 2.2 s; and
 - Multilane roundabouts, right lane: 2.2 s.

By using these values and the expressions in Equation 22-21 through Equation 22-23, the capacity equation for single-lane roundabouts can be expressed as follows:

$$A = \frac{3,600}{t_f} = \frac{3,600}{2.5} = 1,440$$

$$B = \frac{t_c - (t_f/2)}{3,600} = \frac{4.8 - (2.5/2)}{3,600} = 1.0 \times 10^{-3}$$

$$c_{pce} = Ae^{(-Bv_c)} = 1,440e^{(-1.0 \times 10^{-3}v_c)}$$

Therefore, the model resulting from the use of California-specific data for critical headway and follow-up time has a higher intercept, and thus higher capacity, over its entire range than does the model based on the national study. These equations replace the equations in Step 5 of the Chapter 22 methodology.

An example of calibration using only follow-up headway can be demonstrated using data collected as part of a national study for the US-9/Warren Street/Hudson Avenue/Glen Street intersection in Glen Falls, New York (1). Field-measured values for follow-up headway for the five-legged roundabout were determined as follows (rounded to the nearest 0.1 s):

- East leg: 2.9 s,
- Northwest leg: 2.8 s,
- South leg: 2.9 s,
- West leg: 2.7 s, and
- North leg: 2.8 s.

The mean value using unrounded values for follow-up time for the intersection is 2.85 s. The intercept can therefore be calculated as follows:

$$A = \frac{3,600}{t_f} = \frac{3,600}{2.85} = 1,260$$

With this value for the intercept, the resulting capacity model is

$$c_{pce} = Ae^{(-Bv_c)} = 1,260e^{(-1.02 \times 10^{-3} v_c)}$$

The resulting model has a lower intercept than the national model. Based on the observations of each approach of this intersection under queued conditions from the national study, this site-specific model has a better goodness of fit than the national model (an improvement in the root mean squared error from 164 to 126 pc/h). Variation in driver behavior between individual drivers or from minute to minute makes eliminating prediction error impossible, but calibration can improve the accuracy of the prediction.

3. EXAMPLE PROBLEMS

This section illustrates the application of the roundabout methodology through the two example problems listed in Exhibit 33-5.

Exhibit 33-5
Roundabout Example Problems

Example Problem	Description	Application
1	Single-lane roundabout with bypass lanes	Operational analysis
2	Multilane roundabout	Operational analysis

EXAMPLE PROBLEM 1: SINGLE-LANE ROUNDABOUT WITH BYPASS LANES

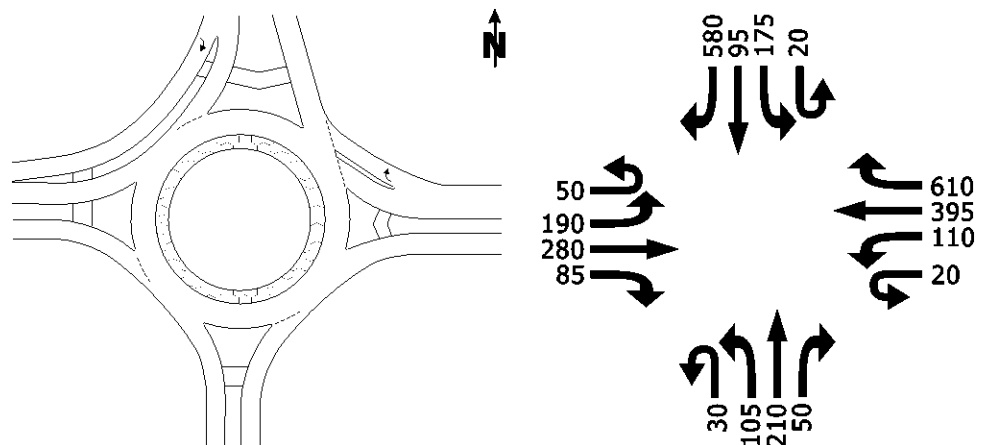
The Facts

The following data are available to describe the traffic and geometric characteristics of this location:

- Four legs,
- One-lane entries on each leg,
- A westbound right-turn bypass lane that yields to exiting vehicles,
- A southbound right-turn bypass lane that forms its own lane adjacent to exiting vehicles,
- Percentage heavy vehicles for all movements = 2%,
- Peak hour factor = 0.94,
- Demand volumes and lane configurations as shown in Exhibit 33-6, and
- 50 p/h across the south leg and negligible pedestrian activity across the other three legs.

This is an example of an operational analysis. It uses traffic data and geometric characteristics to determine capacities, control delay, and LOS.

Exhibit 33-6
Example Problem 1: Demand Volumes and Lane Configurations



Comments

All input parameters are known, so no default values are needed or used.

Step 1: Convert Movement Demand Volumes to Flow Rates

Each turning-movement volume given in the problem is converted to a demand flow rate by dividing by the peak hour factor. As an example, the northbound left-turn volume is converted to a flow rate as follows by using Equation 22-8:

$$v_{NBL} = \frac{V_{NBL}}{PHF} = \frac{105}{0.94} = 112 \text{ pc/h}$$

Step 2: Adjust Flow Rates for Heavy Vehicles

The flow rate for each movement may be adjusted to account for vehicle stream characteristics by using Equations 22-9 and 22-10 as follows (northbound left turn illustrated):

$$f_{HV} = \frac{1}{1 + P_T(E_T - 1)} = \frac{1}{1 + 0.02(2 - 1)} = 0.980$$

$$v_{NBL,pce} = \frac{v_{NBL}}{f_{HV}} = \frac{112}{0.980} = 114 \text{ pc/h}$$

The resulting adjusted flow rates for all movements, accounting for Steps 1 and 2, are therefore computed as shown in Exhibit 33-7:

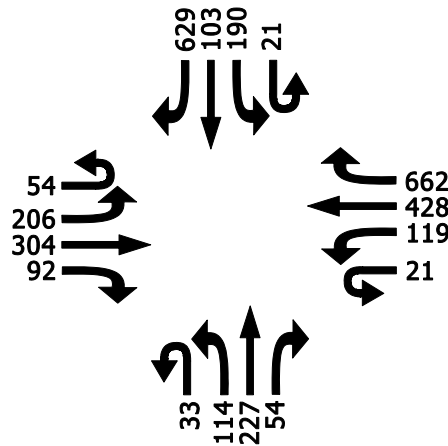


Exhibit 33-7
Example Problem 1:
Adjusted Flow Rates

Step 3: Determine Circulating and Exiting Flow Rates

The circulating and exiting flows are calculated for each leg. For the south leg (northbound entry), the circulating flow is calculated by using the process illustrated by Equation 22-11 as follows:

$$v_{c,NB,pce} = v_{WBU,pce} + v_{SBL,pce} + v_{SBU,pce} + v_{EBT,pce} + v_{EBL,pce} + v_{EBU,pce}$$

$$v_{c,NB,pce} = 21 + 190 + 21 + 304 + 206 + 54 = 796 \text{ pc/h}$$

Similarly, $v_{c,SB,pce} = 769 \text{ pc/h}$; $v_{c,EB,pce} = 487 \text{ pc/h}$; and $v_{c,WB,pce} = 655 \text{ pc/h}$.

For this problem, one exit flow rate is needed: the northbound exit flow rate, which serves as the conflicting flow for the westbound bypass lane. Because all westbound right turns are assumed to use the bypass lane, they are excluded from the conflicting exit flow by using the process illustrated by Equation 22-12 as follows:

$$v_{ex,NB,pce} = v_{SBU,pce} + v_{EBL,pce} + v_{NBT,pce} + v_{WBR,pce} - v_{WBR,bypass,pce}$$

$$v_{ex,NB,pce} = 21 + 206 + 227 + 662 - 662 = 454 \text{ pc/h}$$

Step 4: Determine Entry Flow Rates by Lane

The entry flow rate is calculated by summing the movement flow rates that enter the roundabout (without using a bypass lane). Because this is a single-lane roundabout, no lane-use calculations are needed.

The entry flow rates are calculated as follows, assuming all right-turn volumes on the westbound and southbound approaches use the bypass lane provided and not the entry:

$$v_{e,NB,pce} = v_{NBU,pce} + v_{NBL,pce} + v_{NBT,pce} + v_{NBR,e,pce}$$

$$v_{e,NB,pce} = 33 + 114 + 227 + 54 = 428 \text{ pc/h}$$

$$v_{e,SB,pce} = v_{SBU,pce} + v_{SBL,pce} + v_{SBT,pce} + v_{SBR,e,pce}$$

$$v_{e,SB,pce} = 21 + 190 + 103 + 0 = 314 \text{ pc/h}$$

$$v_{e,EB,pce} = v_{EBU,pce} + v_{EBL,pce} + v_{EBT,pce} + v_{EBR,e,pce}$$

$$v_{e,EB,pce} = 54 + 206 + 304 + 92 = 656 \text{ pc/h}$$

$$v_{e,WB,pce} = v_{WBU,pce} + v_{WBL,pce} + v_{WBT,pce} + v_{WBR,e,pce}$$

$$v_{e,WB,pce} = 21 + 119 + 428 + 0 = 568 \text{ pc/h}$$

Step 5: Determine the Capacity of Each Entry Lane and Bypass Lane as Appropriate in Passenger Car Equivalents

By using the single-lane capacity equation (Equation 22-1), the capacity for each entry lane is given as follows:

$$C_{pce,NB} = 1,380e^{(-1.02 \times 10^{-3})v_{c,pce,NB}} = 1,380e^{(-1.02 \times 10^{-3})(796)} = 613 \text{ pc/h}$$

$$C_{pce,SB} = 1,380e^{(-1.02 \times 10^{-3})v_{c,pce,SB}} = 1,380e^{(-1.02 \times 10^{-3})(769)} = 630 \text{ pc/h}$$

$$C_{pce,EB} = 1,380e^{(-1.02 \times 10^{-3})v_{c,pce,EB}} = 1,380e^{(-1.02 \times 10^{-3})(487)} = 840 \text{ pc/h}$$

$$C_{pce,WB} = 1,380e^{(-1.02 \times 10^{-3})v_{c,pce,WB}} = 1,380e^{(-1.02 \times 10^{-3})(655)} = 708 \text{ pc/h}$$

By using the equation for a bypass lane opposed by a single exit lane (Equation 22-6), the capacity for the westbound bypass lane is given as follows:

$$C_{bypass,pce,WB} = 1,380e^{(-1.02 \times 10^{-3})v_{ex,pce,NB}} = 1,380e^{(-1.02 \times 10^{-3})(454)} = 868 \text{ pc/h}$$

Step 6: Determine Pedestrian Impedance to Vehicles

The south leg (northbound entry) has a conflicting pedestrian flow rate, n_{ped} , of 50 p/h. The pedestrian impedance factor is calculated by using Exhibit 22-18 as follows:

$$f_{ped} = 1 - 0.000137n_{ped} = 1 - 0.000137(50) = 0.993$$

Because the other legs and bypass lanes have negligible pedestrian activity ($n_{ped} = 0$), they have $f_{ped} = 1$.

Step 7: Convert Lane Flow Rates and Capacities into Vehicles per Hour

The capacity for a given lane is converted back to vehicles by first determining the heavy-vehicle adjustment factor for the lane and then multiplying it by the capacity in passenger car equivalents (Equation 22-14). For this example, because all turning movements on each entry have the same f_{HV} , each entry will also have the same f_{HV} , 0.980. The capacities for each of the entries are also adjusted by the pedestrian impedance factor.

$$c_{NB} = c_{pce,NB} f_{HV,e,NB} f_{ped} = (613)(0.980)(0.993) = 597 \text{ veh/h}$$

$$c_{SB} = c_{pce,SB} f_{HV,e,SB} f_{ped} = (630)(0.980)(1) = 618 \text{ veh/h}$$

$$c_{EB} = c_{pce,EB} f_{HV,e,EB} f_{ped} = (840)(0.980)(1) = 824 \text{ veh/h}$$

$$c_{WB} = c_{pce,WB} f_{HV,e,WB} f_{ped} = (708)(0.980)(1) = 694 \text{ veh/h}$$

$$c_{bypass,WB} = c_{bypass,pce,WB} f_{HV,e,WB} f_{ped} = (868)(0.980)(1) = 851 \text{ veh/h}$$

Calculations for the entry flow rates are as follows (Equation 22-13):

$$v_{NB} = v_{pce,NB} f_{HV,e,NB} = (428)(0.980) = 420 \text{ veh/h}$$

$$v_{SB} = v_{pce,SB} f_{HV,e,SB} = (314)(0.980) = 308 \text{ veh/h}$$

$$v_{EB} = v_{pce,EB} f_{HV,e,EB} = (656)(0.980) = 643 \text{ veh/h}$$

$$v_{WB} = v_{pce,WB} f_{HV,e,WB} = (568)(0.980) = 557 \text{ veh/h}$$

$$v_{bypass,WB} = v_{bypass,pce,WB} f_{HV,e,WB} = (662)(0.980) = 649 \text{ veh/h}$$

Step 8: Compute the Volume-to-Capacity Ratio for Each Lane

The volume-to-capacity ratios for each entry lane are calculated from Equation 22-16 as follows:

$$x_{NB} = \frac{420}{597} = 0.70$$

$$x_{SB} = \frac{308}{618} = 0.50$$

$$x_{EB} = \frac{643}{824} = 0.78$$

$$x_{WB} = \frac{557}{694} = 0.80$$

$$x_{bypass,WB} = \frac{649}{851} = 0.76$$

Step 9: Compute the Average Control Delay for Each Lane

The control delay for the northbound entry lane is computed from Equation 22-17 as follows:

$$d_{NB} = \frac{3,600}{597} + 900(0.25) \left[0.70 - 1 + \sqrt{(0.70 - 1)^2 + \frac{\left(\frac{3,600}{597}\right) 0.70}{450(0.25)}} \right] + 5(\min[0.70, 1])$$

$$d_{NB} = 22.6 \text{ s/veh}$$

Similarly, $d_{SB} = 14.0$ s; $d_{bypass,SB} = 0$ s (assumed); $d_{EB} = 22.0$ s; $d_{WB} = 26.8$ s; and $d_{bypass,WB} = 20.2$ s.

Step 10: Determine LOS for Each Lane on Each Approach

From Exhibit 22-8, the level of service (LOS) for each lane is determined as shown in Exhibit 33-8:

Exhibit 33-8
Example Problem 1:
LOS by Lane

Lane	Control Delay (s/veh)	LOS
Northbound entry	22.6	C
Southbound entry	14.0	B
Southbound bypass lane	0 (assumed)	A
Eastbound entry	22.0	C
Westbound entry	26.8	D
Westbound bypass lane	20.2	C

Step 11: Compute the Average Control Delay and Determine LOS for Each Approach and the Roundabout as a Whole

The control delays for the northbound and eastbound approaches are equal to the control delay for the entry lanes, as both of these approaches have only one lane. On the basis of Exhibit 22-8, these approaches are both assigned LOS C.

The control delay calculations for the westbound and southbound approaches include the effects of their bypass lanes as follows (Equation 22-18):

$$d_{WB} = \frac{(26.8)(557) + (20.2)(649)}{557 + 649} = 23.3 \text{ s/veh}$$

$$d_{SB} = \frac{(14.0)(308) + (0.0)(617)}{308 + 617} = 4.7 \text{ s/veh}$$

On the basis of Exhibit 22-8, these approaches are respectively assigned LOS C and LOS A.

Similarly, intersection control delay is computed as follows (Equation 22-19):

$$d_{\text{intersection}} = \frac{(22.6)(420) + (4.7)(925) + (22.0)(643) + (23.3)(1,206)}{420 + 925 + 643 + 1,206}$$

$$d_{\text{intersection}} = 17.5 \text{ s/veh}$$

On the basis of Exhibit 22-8, the intersection is assigned LOS C.

Step 12: Compute 95th Percentile Queues for Each Lane

The 95th percentile queue is computed for each lane. An example calculation for the northbound entry is given as follows (Equation 22-20):

$$Q_{95,NB} = 900(0.25) \left[0.70 - 1 + \sqrt{(1 - 0.70)^2 + \frac{\left(\frac{3,600}{597}\right) 0.70}{150(0.25)}} \right] \left(\frac{597}{3,600}\right)$$

$$Q_{95,NB} = 5.7 \text{ veh}$$

For design purposes, this value is typically rounded up to the nearest vehicle, which for this case would be six vehicles.

Similarly, $Q_{95,SB} = 2.8$ veh; $Q_{95,EB} = 7.9$ veh; $Q_{95,WB} = 8.2$ veh; and $Q_{95,bypass,WB} = 7.4$ veh.

Discussion

The results indicate the overall roundabout is operating at LOS C. However, one lane (the westbound entry) is operating at LOS D. If, for example, the performance standard for this intersection was LOS C, this entry would not meet the standard, even though the overall intersection meets the standard. For these reasons, the analyst should consider reporting volume-to-capacity ratios, control delay, and queue lengths for each lane, in addition to the aggregated measures, for a more complete picture of operational performance.

The analyst should be careful not to mask key operational performance issues by reporting overall intersection performance without also reporting the performance of each lane, or at least the worst-performing lane.

EXAMPLE PROBLEM 2: MULTILANE ROUNDABOUT

The Facts

The following data are available to describe the traffic and geometric characteristics of this location:

- Percentage heavy vehicles for eastbound and westbound movements = 5%,
- Percentage heavy vehicles for northbound and southbound movements = 2%,
- Peak hour factor = 0.95,
- Negligible pedestrian activity, and
- Volumes and lane configurations as shown in Exhibit 33-9.

Example Problem 2 is also an example of an operational analysis, despite the fact that lane utilization data are unknown and must be assumed.

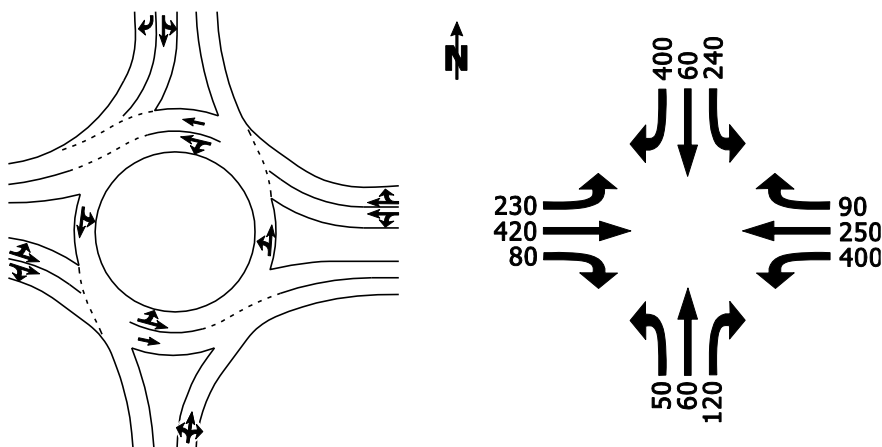


Exhibit 33-9
Example Problem 2: Demand Volumes and Lane Configurations

Comments

Lane use is not specified for the eastbound and westbound approaches; therefore, the percentage flow in the right lane is assumed to be 53%, as specified in Exhibit 22-9.

Step 1: Convert Movement Demand Volumes to Flow Rates

Each turning-movement demand volume given in the problem is converted to a demand flow rate by dividing by the peak hour factor. As an example, the eastbound-left demand volume is converted to a demand flow rate by using Equation 22-8 as follows:

$$v_{EBL} = \frac{V_{EBL}}{PHF} = \frac{230}{0.95} = 242 \text{ veh/h}$$

Step 2: Adjust Flow Rates for Heavy Vehicles

The heavy-vehicle adjustment factor for the eastbound and westbound movements is calculated by using Equation 22-10 as follows:

$$f_{HV} = \frac{1}{1 + P_T(E_T - 1)} = \frac{1}{1 + 0.05(2 - 1)} = 0.952$$

Similarly, the heavy-vehicle adjustment factor for the northbound and southbound movements is calculated as follows:

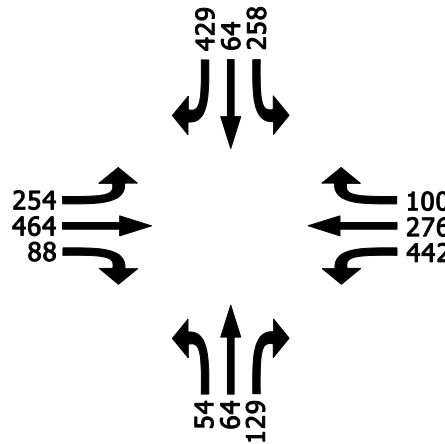
$$f_{HV} = \frac{1}{1 + P_T(E_T - 1)} = \frac{1}{1 + 0.02(2 - 1)} = 0.980$$

This factor is applied to each movement by using Equation 22-9 as follows (eastbound left turn illustrated):

$$v_{EBL,pce} = \frac{v_{EBL}}{f_{HV}} = \frac{242}{0.952} = 254 \text{ pc/h}$$

The resulting adjusted flow rates for all movements, accounting for Steps 1 and 2, are therefore as shown in Exhibit 33-10:

Exhibit 33-10
Example Problem 2:
Adjusted Flow Rates



Step 3: Determine Circulating and Exiting Flow Rates

For this problem, only circulating flows need to be calculated for each leg. For the west leg (eastbound entry), the circulating flow is calculated by using the process illustrated by Equation 22-11 as follows:

$$v_{c,EB,pce} = v_{NBU,pce} + v_{WBL,pce} + v_{WBU,pce} + v_{SBT,pce} + v_{SBL,pce} + v_{SBU,pce}$$

$$v_{c,EB,pce} = 0 + 442 + 0 + 64 + 258 + 0 = 764 \text{ pc/h}$$

Similarly, $v_{c,WB,pce} = 372 \text{ pc/h}$; $v_{c,NB,pce} = 976 \text{ pc/h}$; and $v_{c,SB,pce} = 772 \text{ pc/h}$.

Step 4: Determine Entry Flow Rates by Lane

The entry flow rate is calculated by summing up the movement flow rates that enter the roundabout. This problem presents four unique cases.

- *Northbound:* The northbound entry has only one lane. Therefore, the entry flow is simply the sum of the movements, or $54 + 64 + 129 = 247 \text{ pc/h}$.

- *Southbound*: The southbound entry has two lanes: a shared through–left lane and a right-turn-only lane. Therefore, the flow rate in the right lane is simply the right-turn movement flow, or 429 pc/h, and the flow rate in the left lane is the sum of the left-turn and through movements, or $258 + 64 = 322$ pc/h.
- *Eastbound*: The eastbound entry has shared left–through and through–right lanes. A check is needed to determine whether any de facto lanes are in effect. These checks are as follows:
 - *Left lane*: The left-turn flow rate, 254 pc/h, is less than the sum of the through and right-turn flow rates, $464 + 88 = 552$ pc/h. Therefore, some of the through volume is assumed to use the left lane, and no de facto left-turn lane condition is present.
 - *Right lane*: The right-turn flow rate, 88 pc/h, is less than the sum of the left-turn and through flow rates, $254 + 464 = 718$ pc/h. Therefore, some of the through volume is assumed to use the right lane, and no de facto right-turn lane condition is present.

The total entry flow ($254 + 464 + 88 = 806$ pc/h) is therefore distributed over the two lanes, with flow biased to the right lane by using the assumed lane-use factor identified previously:

- *Right lane*: $(806)(0.53) = 427$ pc/h, and
- *Left lane*: $806 - 427 = 379$ pc/h.
- *Westbound*: The westbound entry also has shared left–through and through–right lanes, and so a similar check is needed for de facto lanes. The left-turn flow rate, 442 pc/h, is greater than the sum of the through and right-turn flow rates, $276 + 100 = 376$ pc/h. Therefore, the left lane is assumed to operate as a de facto left-turn lane. Therefore, the left-lane flow rate is equal to the left-turn flow rate, or 442 pc/h, and the right-lane flow rate is equal to the sum of the through- and right-turn-movement flow rates, or 376 pc/h.

Step 5: Determine the Capacity of Each Entry Lane and Bypass Lane as Appropriate in Passenger Car Equivalents

The capacity calculations for each approach are calculated as follows:

- *Northbound*: The northbound entry is a single-lane entry opposed by two circulating lanes. Therefore, Equation 22-3 is used as follows:

$$c_{pce,NB} = 1,420e^{(-0.85 \times 10^{-3})(976)} = 619 \text{ pc/h}$$

- *Southbound*: The southbound entry is a two-lane entry opposed by two circulating lanes. Therefore, Equation 22-4 is used for the right lane, and Equation 22-5 is used for the left lane:

$$c_{pce,SB,R} = 1,420e^{(-0.85 \times 10^{-3})(772)} = 737 \text{ pc/h}$$

$$c_{pce,SB,L} = 1,350e^{(-0.92 \times 10^{-3})(772)} = 664 \text{ pc/h}$$

- *Eastbound*: The eastbound entry is a two-lane entry opposed by one circulating lane. Therefore, the capacity for each lane is calculated by using Equation 22-2 as follows:

$$c_{pce,EB,R} = c_{pce,EB,L} = 1,420e^{(-0.91 \times 10^{-3})(764)} = 709 \text{ pc/h}$$

- *Westbound*: The westbound entry is also a two-lane entry opposed by one circulating lane, so its capacity calculation is similar to that for the eastbound entry:

$$c_{pce,WB} = 1,420e^{(-0.91 \times 10^{-3})(372)} = 1,012 \text{ pc/h}$$

There are no bypass lanes in this example problem.

Step 6: Determine Pedestrian Impedance to Vehicles

For this problem pedestrians have been assumed to be negligible, so no impedance calculations are performed.

Step 7: Convert Lane Flow Rates and Capacities into Vehicles per Hour

The capacity for a given lane is converted back to vehicles by first determining the heavy-vehicle adjustment factor for the lane and then multiplying it by the capacity in passenger car equivalents (Equation 22-14). For this example, because all turning movements on the eastbound and westbound entries have the same f_{HV} , each of the lanes on the eastbound and westbound entries can be assumed to have the same f_{HV} , 0.952.

$$c_{EB,R} = c_{pce,EB,R} f_{HV,e,EB} = (709)(0.952) = 675 \text{ veh/h}$$

Similarly, $c_{EB,L} = 675 \text{ veh/h}$; $c_{WB,L} = 964 \text{ veh/h}$; and $c_{WB,R} = 964 \text{ veh/h}$.

Because all turning movements on the northbound and southbound entries have the same f_{HV} , each of the lanes on those entries can be assumed to have the same f_{HV} , 0.980.

$$c_{NB} = c_{pce,NB} f_{HV,e,NB} = (619)(0.980) = 607 \text{ veh/h}$$

Similarly, $c_{SB,L} = 651 \text{ veh/h}$, and $c_{SB,R} = 723 \text{ veh/h}$.

Calculations for the entry flow rates are as follows (Equation 22-13):

$$v_{EB,R} = v_{pce,EB,R} f_{HV,e,EB} = (427)(0.952) = 407 \text{ veh/h}$$

$$v_{NB} = v_{pce,NB} f_{HV,e,NB} = (247)(0.980) = 242 \text{ veh/h}$$

Similarly, $v_{EB,L} = 361 \text{ veh/h}$; $v_{WB,L} = 421 \text{ veh/h}$; $v_{WB,R} = 358 \text{ veh/h}$; $v_{SB,L} = 316 \text{ veh/h}$; and $v_{SB,R} = 421 \text{ veh/h}$.

Step 8: Compute the Volume-to-Capacity Ratio for Each Lane

The volume-to-capacity ratio for each lane is calculated from Equation 22-16 as follows:

$$x_{NB} = \frac{242}{607} = 0.40$$

$$x_{SB,L} = \frac{316}{651} = 0.48$$

$$x_{SB,R} = \frac{421}{723} = 0.58$$

$$x_{EB,L} = \frac{361}{675} = 0.53$$

$$x_{EB,R} = \frac{407}{675} = 0.60$$

$$x_{WB,L} = \frac{421}{964} = 0.44$$

$$x_{WB,R} = \frac{358}{964} = 0.37$$

Step 9: Compute the Average Control Delay for Each Lane

The control delay for the northbound entry lane is computed from Equation 22-17 as follows:

$$d_{NB} = \frac{3,600}{607} + 900(0.25) \left[\frac{242}{607} - 1 + \sqrt{\left(\frac{242}{607} - 1\right)^2 + \frac{(3,600) 242}{450(0.25) 607}} \right] + 5 \left(\min \left[\frac{242}{607}, 1 \right] \right)$$

$$d_{NB} = 11.8 \text{ s/veh}$$

Similarly, $d_{SB,L} = 13.0$ s/veh; $d_{SB,R} = 14.6$ s/veh; $d_{EB,L} = 14.0$ s/veh; $d_{EB,R} = 16.1$ s/veh; $d_{WB,L} = 8.8$ s/veh; and $d_{WB,R} = 7.8$ s/veh.

Step 10: Determine LOS for Each Lane on Each Approach

On the basis of Exhibit 22-8, the LOS for each lane is determined as shown in Exhibit 33-11:

Critical Lane	Control Delay (s/veh)	LOS
Northbound entry	11.8	B
Southbound left lane	13.0	B
Southbound right lane	14.6	B
Eastbound left lane	14.0	B
Eastbound right lane	16.1	C
Westbound left lane	8.8	A
Westbound right lane	7.8	A

Exhibit 33-11
Example Problem 2:
LOS by Lane

Step 11: Compute the Average Control Delay and Determine LOS for Each Approach and the Roundabout as a Whole

The control delay for the northbound approaches is equal to the control delay for the entry lane, 11.8 s, as the approach has only one lane. The control delays for the other approaches are as follows (Equation 22-18):

$$d_{SB} = \frac{(13.0)(316) + (14.6)(421)}{316 + 421} = 13.9 \text{ s/veh}$$

$$d_{EB} = \frac{(14.0)(361) + (16.1)(407)}{361 + 407} = 15.1 \text{ s/veh}$$

$$d_{WB} = \frac{(8.8)(421) + (7.8)(358)}{421 + 358} = 8.3 \text{ s/veh}$$

On the basis of Exhibit 22-8, these approaches are respectively assigned LOS B, LOS B, LOS C, and LOS A.

Similarly, control delay for the intersection is computed as follows (Equation 22-19):

$$d_{\text{intersection}} = \frac{(11.8)(242) + (13.9)(736) + (15.1)(768) + (8.3)(779)}{242 + 736 + 768 + 779}$$

$$d_{\text{intersection}} = 12.3 \text{ s/veh}$$

On the basis of Exhibit 22-8, the intersection is assigned LOS B.

Step 12: Compute 95th Percentile Queues for Each Lane

The 95th percentile queue is computed for each lane. An example calculation for the northbound entry is given as follows (Equation 22-20):

$$Q_{95,NB} = 900(0.25) \left[\frac{242}{607} - 1 + \sqrt{\left(1 - \frac{242}{607}\right)^2 + \frac{\left(\frac{3,600}{607}\right)\left(\frac{242}{607}\right)}{150(0.25)}} \right] \left(\frac{607}{3,600}\right)$$

$$Q_{95,NB} = 1.9 \text{ veh}$$

For design purposes, this value is typically rounded up to the nearest vehicle, in this case two vehicles.

Discussion

The results indicate the intersection as a whole operates at LOS B on the basis of control delay during the peak 15 min of the analysis hour. However, the eastbound approach operates at LOS C, as does the right lane of the eastbound approach. The analyst should consider reporting both the overall performance and those of the individual lanes to provide a more complete picture of operational performance.

4. REFERENCES

1. Rodegerdts, L. A., A. Malinge, P. S. Marnell, S. G. Beaird, M. J. Kittelson, and Y. S. Mereszczak. *Assessment of Roundabout Capacity Models for the Highway Capacity Manual: Volume 2 of Accelerating Roundabout Implementation in the United States*. Report FHWA-SA-15-070. Federal Highway Administration, Washington, D.C., Sept. 2015.
2. Rodegerdts, L., J. Bansen, C. Tiesler, J. Knudsen, E. Myers, M. Johnson, M. Moule, B. Persaud, C. Lyon, S. Hallmark, H. Isebrands, R. B. Crown, B. Guichet, and A. O'Brien. *NCHRP Report 672: Roundabouts: An Informational Guide*, 2nd ed. Transportation Research Board of the National Academies, Washington, D.C., 2010.
3. Tian, Z. Z., F. Xu, L. A. Rodegerdts, W. E. Scarbrough, B. L. Ray, W. E. Bishop, T. C. Ferrara, and S. Mam. *Roundabout Geometric Design Guidance*. Report No. F/CA/RI-2006/13. Division of Research and Innovation, California Department of Transportation, Sacramento, Calif., June 2007.

Many of these references can be found in the Technical Reference Library in Volume 4.



HIGHWAY CAPACITY MANUAL

6TH EDITION | A GUIDE FOR MULTIMODAL MOBILITY ANALYSIS

VOLUME 4: APPLICATIONS GUIDE

The National Academies of
SCIENCES • ENGINEERING • MEDICINE

TRANSPORTATION RESEARCH BOARD
WASHINGTON, D.C. | WWW.TRB.ORG

TRANSPORTATION RESEARCH BOARD 2016 EXECUTIVE COMMITTEE *

Chair: James M. Crites, Executive Vice President of Operations,
Dallas–Fort Worth International Airport, Texas

Vice Chair: Paul Trombino III, Director, Iowa Department of
Transportation, Ames

Executive Director: Neil J. Pedersen, Transportation Research Board

Victoria A. Arroyo, Executive Director, Georgetown Climate Center;
Assistant Dean, Centers and Institutes; and Professor and Director,
Environmental Law Program, Georgetown University Law Center,
Washington, D.C.

Scott E. Bennett, Director, Arkansas State Highway and Transportation
Department, Little Rock

Jennifer Cohan, Secretary, Delaware Department of Transportation, Dover

Malcolm Dougherty, Director, California Department of
Transportation, Sacramento

A. Stewart Fotheringham, Professor, School of Geographical Sciences
and Urban Planning, Arizona State University, Tempe

John S. Halikowski, Director, Arizona Department of Transportation,
Phoenix

Susan Hanson, Distinguished University Professor Emerita, Graduate
School of Geography, Clark University, Worcester, Massachusetts

Steve Heminger, Executive Director, Metropolitan Transportation
Commission, Oakland, California

Chris T. Hendrickson, Hamerschlag Professor of Engineering, Carnegie
Mellon University, Pittsburgh, Pennsylvania

Jeffrey D. Holt, Managing Director, Power, Energy, and Infrastructure
Group, BMO Capital Markets Corporation, New York

S. Jack Hu, Vice President for Research and J. Reid and Polly Anderson
Professor of Manufacturing, University of Michigan, Ann Arbor

Roger B. Huff, President, HGLC, LLC, Farmington Hills, Michigan

Geraldine Knatz, Professor, Sol Price School of Public Policy, Viterbi
School of Engineering, University of Southern California, Los Angeles

Ysela Llort, Consultant, Miami, Florida

Melinda McGrath, Executive Director, Mississippi Department of
Transportation, Jackson

James P. Redeker, Commissioner, Connecticut Department of
Transportation, Newington

Mark L. Rosenberg, Executive Director, The Task Force for Global
Health, Inc., Decatur, Georgia

Kumares C. Sinha, Olson Distinguished Professor of Civil Engineering,
Purdue University, West Lafayette, Indiana

Daniel Sperling, Professor of Civil Engineering and Environmental
Science and Policy; Director, Institute of Transportation Studies,
University of California, Davis

Kirk T. Steudle, Director, Michigan Department of Transportation,
Lansing (Past Chair, 2014)

Gary C. Thomas, President and Executive Director, Dallas Area Rapid
Transit, Dallas, Texas

Pat Thomas, Senior Vice President of State Government Affairs, United
Parcel Service, Washington, D.C.

Katherine F. Turnbull, Executive Associate Director and Research
Scientist, Texas A&M Transportation Institute, College Station

Dean Wise, Vice President of Network Strategy, Burlington Northern
Santa Fe Railway, Fort Worth, Texas

Thomas P. Bostick (Lieutenant General, U.S. Army), Chief of Engineers
and Commanding General, U.S. Army Corps of Engineers, Washington,
D.C. (ex officio)

James C. Card (Vice Admiral, U.S. Coast Guard, retired), Maritime
Consultant, The Woodlands, Texas, and Chair, TRB Marine Board
(ex officio)

T. F. Scott Darling III, Acting Administrator and Chief Counsel, Federal
Motor Carrier Safety Administration, U.S. Department of Transportation
(ex officio)

Marie Therese Dominguez, Administrator, Pipeline and Hazardous
Materials Safety Administration, U.S. Department of Transportation
(ex officio)

Sarah Feinberg, Administrator, Federal Railroad Administration,
U.S. Department of Transportation (ex officio)

Carolyn Flowers, Acting Administrator, Federal Transit Administration,
U.S. Department of Transportation (ex officio)

LeRoy Gishi, Chief, Division of Transportation, Bureau of Indian
Affairs, U.S. Department of the Interior, Washington, D.C. (ex officio)

John T. Gray II, Senior Vice President, Policy and Economics,
Association of American Railroads, Washington, D.C. (ex officio)

Michael P. Huerta, Administrator, Federal Aviation Administration,
U.S. Department of Transportation (ex officio)

Paul N. Jaenichen, Sr., Administrator, Maritime Administration,
U.S. Department of Transportation (ex officio)

Bevan B. Kirley, Research Associate, University of North Carolina
Highway Safety Research Center, Chapel Hill, and Chair, TRB Young
Members Council (ex officio)

Gregory G. Nadeau, Administrator, Federal Highway Administration,
U.S. Department of Transportation (ex officio)

Wayne Nastri, Acting Executive Officer, South Coast Air Quality
Management District, Diamond Bar, California (ex officio)

Mark R. Rosekind, Administrator, National Highway Traffic Safety
Administration, U.S. Department of Transportation (ex officio)

Craig A. Rutland, U.S. Air Force Pavement Engineer, U.S. Air Force
Civil Engineer Center, Tyndall Air Force Base, Florida (ex officio)

Reuben Sarkar, Deputy Assistant Secretary for Transportation,
U.S. Department of Energy (ex officio)

Richard A. White, Acting President and CEO, American Public
Transportation Association, Washington, D.C. (ex officio)

Gregory D. Winfree, Assistant Secretary for Research and Technology,
Office of the Secretary, U.S. Department of Transportation (ex officio)

Frederick G. (Bud) Wright, Executive Director, American Association
of State Highway and Transportation Officials, Washington, D.C.
(ex officio)

Paul F. Zukunft (Admiral, U.S. Coast Guard), Commandant, U.S. Coast
Guard, U.S. Department of Homeland Security (ex officio)

Transportation Research Board publications are available by ordering
individual publications directly from the TRB Business Office, through
the Internet at www.TRB.org, or by annual subscription through
organizational or individual affiliation with TRB. Affiliates and library
subscribers are eligible for substantial discounts. For further information,
contact the Transportation Research Board Business Office, 500 Fifth
Street, NW, Washington, DC 20001 (telephone 202-334-3213;
fax 202-334-2519; or e-mail TRBsales@nas.edu).

Copyright 2016 by the National Academy of Sciences.

All rights reserved.

Printed in the United States of America.

ISBN 978-0-309-36997-8 [Slipcased set of three volumes]

ISBN 978-0-309-36998-5 [Volume 1]

ISBN 978-0-309-36999-2 [Volume 2]

ISBN 978-0-309-37000-4 [Volume 3]

ISBN 978-0-309-37001-1 [Volume 4, online only]

The National Academies of
SCIENCES • ENGINEERING • MEDICINE

The **National Academy of Sciences** was established in 1863 by an Act of Congress, signed by President Lincoln, as a private, nongovernmental institution to advise the nation on issues related to science and technology. Members are elected by their peers for outstanding contributions to research. Dr. Ralph J. Cicerone is president.

The **National Academy of Engineering** was established in 1964 under the charter of the National Academy of Sciences to bring the practices of engineering to advising the nation. Members are elected by their peers for extraordinary contributions to engineering. Dr. C. D. Mote, Jr., is president.

The **National Academy of Medicine** (formerly the Institute of Medicine) was established in 1970 under the charter of the National Academy of Sciences to advise the nation on medical and health issues. Members are elected by their peers for distinguished contributions to medicine and health. Dr. Victor J. Dzau is president.

The three Academies work together as the National Academies of Sciences, Engineering, and Medicine to provide independent, objective analysis and advice to the nation and conduct other activities to solve complex problems and inform public policy decisions. The Academies also encourage education and research, recognize outstanding contributions to knowledge, and increase public understanding in matters of science, engineering, and medicine.

Learn more about the National Academies of Sciences, Engineering, and Medicine at **www.national-academies.org**.

The **Transportation Research Board** is one of seven major programs of the National Academies of Sciences, Engineering, and Medicine. The mission of the Transportation Research Board is to increase the benefits that transportation contributes to society by providing leadership in transportation innovation and progress through research and information exchange, conducted within a setting that is objective, interdisciplinary, and multimodal. The Board's varied committees, task forces, and panels annually engage about 7,000 engineers, scientists, and other transportation researchers and practitioners from the public and private sectors and academia, all of whom contribute their expertise in the public interest. The program is supported by state transportation departments, federal agencies including the component administrations of the U.S. Department of Transportation, and other organizations and individuals interested in the development of transportation.

Learn more about the Transportation Research Board at **www.TRB.org**.

**CHAPTER 34
INTERCHANGE RAMP TERMINALS: SUPPLEMENTAL**

CONTENTS

1. INTRODUCTION 34-1

2. EXAMPLE PROBLEMS 34-2

 Introduction 34-2

 Intersection Traffic Movements 34-2

 Example Problem 1: Diamond Interchange 34-3

 Example Problem 2: Parclo A-2Q Interchange 34-9

 Example Problem 3: Diamond Interchange with Queue Spillback 34-16

 Example Problem 4: Diamond Interchange with Demand Starvation 34-23

 Example Problem 5: Diverging Diamond Interchange with Signal Control 34-30

 Example Problem 6: Diverging Diamond Interchange with Yield Control 34-34

 Example Problem 7: Single-Point Urban Interchange 34-37

 Example Problem 8: Diamond Interchange with Adjacent Intersection 34-43

 Example Problem 9: Diamond Interchange with Roundabouts 34-51

 Example Problem 10: Operational Analysis for Type Selection 34-53

 Example Problem 11: Alternative Analysis Tool 34-58

 Example Problem 12: Four-Legged Restricted Crossing U-Turn Intersection with Merges 34-64

 Example Problem 13: Three-Legged Restricted Crossing U-Turn Intersection with Stop Signs 34-67

 Example Problem 14: Four-Legged Restricted Crossing U-Turn Intersection with Signals 34-71

 Example Problem 15: Four-Legged Median U-Turn Intersection with Stop Signs 34-75

 Example Problem 16: Partial Displaced Left-Turn Intersection 34-79

 Example Problem 17: Full Displaced Left-Turn Intersection 34-84

3. OPERATIONAL ANALYSIS FOR INTERCHANGE TYPE SELECTION 34-91

 Introduction 34-91

 Inputs and Applications 34-92

 Saturation Flow Rates 34-92

 Computational Steps 34-93

4. O-D AND TURNING MOVEMENTS 34-100
 O-D and Turning Movements for Interchanges with Roundabouts..... 34-100
 O-D and Turning Movements for Conventional Interchanges..... 34-102

5. REFERENCES..... 34-108

LIST OF EXHIBITS

Exhibit 34-1 Example Problem Descriptions 34-2

Exhibit 34-2 Intersection Traffic Movements and Numbering Scheme 34-2

Exhibit 34-3 Example Problem 1: Interchange Volumes and
Channelization..... 34-3

Exhibit 34-4 Example Problem 1: Signalization Information..... 34-3

Exhibit 34-5 Example Problem 1: Adjusted O-D Table..... 34-4

Exhibit 34-6 Example Problem 1: Lane Utilization Adjustment
Calculations..... 34-4

Exhibit 34-7 Example Problem 1: Saturation Flow Rate Calculation for
Eastbound and Westbound Approaches..... 34-5

Exhibit 34-8 Example Problem 1: Saturation Flow Rate Calculation for
Northbound and Southbound Approaches 34-5

Exhibit 34-9 Example Problem 1: Common Green Calculations..... 34-6

Exhibit 34-10 Example Problem 1: Lost Time due to Downstream Queues..... 34-6

Exhibit 34-11 Example Problem 1: Lost Time due to Demand Starvation..... 34-7

Exhibit 34-12 Example Problem 1: Queue Storage Ratio for Eastbound
and Westbound Movements..... 34-7

Exhibit 34-13 Example Problem 1: Queue Storage Ratio for Northbound
and Southbound Movements..... 34-8

Exhibit 34-14 Example Problem 1: Control Delay for Eastbound and
Westbound Movements 34-8

Exhibit 34-15 Example Problem 1: Control Delay for Northbound and
Southbound Movements..... 34-9

Exhibit 34-16 Example Problem 1: O-D Movement LOS..... 34-9

Exhibit 34-17 Example Problem 2: Intersection Plan View 34-10

Exhibit 34-18 Example Problem 2: Signalization Information 34-10

Exhibit 34-19 Example Problem 2: Adjusted O-D Table..... 34-11

Exhibit 34-20 Example Problem 2: Lane Utilization Adjustment
Calculations..... 34-11

Exhibit 34-21 Example Problem 2: Saturation Flow Rate Calculation for
Northbound and Southbound Approaches 34-11

Exhibit 34-22 Example Problem 2: Saturation Flow Rate Calculation for
Eastbound and Westbound Approaches..... 34-12

Exhibit 34-23 Example Problem 2: Common Green Calculations..... 34-12

Exhibit 34-24 Example Problem 2: Lost Time due to Downstream Queues..... 34-13

Exhibit 34-25 Example Problem 2: Queue Storage Ratio for Eastbound
and Westbound Movements 34-13

Exhibit 34-26 Example Problem 2: Queue Storage Ratio for Northbound and Southbound Movements..... 34-14

Exhibit 34-27 Example Problem 2: Control Delay for Eastbound and Westbound Movements 34-14

Exhibit 34-28 Example Problem 2: Control Delay for Northbound and Southbound Movements..... 34-15

Exhibit 34-29 Example Problem 2: O-D Movement LOS..... 34-15

Exhibit 34-30 Example Problem 3: Intersection Plan View 34-16

Exhibit 34-31 Example Problem 3: Signalization Information..... 34-16

Exhibit 34-32 Example Problem 3: Adjusted O-D Table 34-17

Exhibit 34-33 Example Problem 3: Lane Utilization Adjustment Calculations 34-17

Exhibit 34-34 Example Problem 3: Saturation Flow Rate Calculation for Eastbound and Westbound Approaches..... 34-18

Exhibit 34-35 Example Problem 3: Saturation Flow Rate Calculation for Northbound and Southbound Approaches 34-18

Exhibit 34-36 Example Problem 3: Common Green Calculations..... 34-19

Exhibit 34-37 Example Problem 3: Lost Time due to Downstream Queues..... 34-19

Exhibit 34-38 Example Problem 3: Lost Time due to Demand Starvation Calculations 34-20

Exhibit 34-39 Example Problem 3: Queue Storage Ratio for Eastbound and Westbound Movements 34-20

Exhibit 34-40 Example Problem 3: Queue Storage Ratio for Northbound and Southbound Movements..... 34-21

Exhibit 34-41 Example Problem 3: Control Delay for Eastbound and Westbound Movements 34-21

Exhibit 34-42 Example Problem 3: Control Delay for Northbound and Southbound Movements..... 34-22

Exhibit 34-43 Example Problem 3: O-D Movement LOS..... 34-22

Exhibit 34-44 Example Problem 4: Intersection Plan View 34-23

Exhibit 34-45 Example Problem 4: Signalization Information..... 34-23

Exhibit 34-46 Example Problem 4: Adjusted O-D Table 34-24

Exhibit 34-47 Example Problem 4: Lane Utilization Adjustment Calculations 34-24

Exhibit 34-48 Example Problem 4: Saturation Flow Rate Calculation for Eastbound and Westbound Approaches..... 34-25

Exhibit 34-49 Example Problem 4: Saturation Flow Rate Calculation for Northbound and Southbound Approaches 34-25

Exhibit 34-50 Example Problem 4: Common Green Calculations..... 34-26

Exhibit 34-51 Example Problem 4: Lost Time due to Downstream Queues..... 34-26

Exhibit 34-52 Example Problem 4: Lost Time due to Demand Starvation Calculations.....	34-27
Exhibit 34-53 Example Problem 4: Queue Storage Ratio for Eastbound and Westbound Movements	34-27
Exhibit 34-54 Example Problem 4: Queue Storage Ratio for Northbound and Southbound Movements.....	34-28
Exhibit 34-55 Example Problem 4: Control Delay for Eastbound and Westbound Movements	34-28
Exhibit 34-56 Example Problem 4: Control Delay for Northbound and Southbound Movements.....	34-29
Exhibit 34-57 Example Problem 4: O-D Movement LOS.....	34-29
Exhibit 34-58 Example Problem 5: DDI Geometry, Lane, and Volume Inputs	34-30
Exhibit 34-59 Example Problem 5: Signal Timing and Volume Inputs.....	34-31
Exhibit 34-60 Example Problem 5: Adjusted O-D Table.....	34-31
Exhibit 34-61 Example Problem 5: Lane Utilization Adjustment Calculations.....	34-32
Exhibit 34-62 Example Problem 5: Saturation Flow Rate Calculation for All Approaches.....	34-32
Exhibit 34-63 Example Problem 5: Lost Time and Effective Green Calculations.....	34-33
Exhibit 34-64 Example Problem 5: Performance Results.....	34-33
Exhibit 34-65 Example Problem 5: ETT and LOS Results.....	34-34
Exhibit 34-66 Example Problem 6: Geometry, Lane, and Volume Inputs	34-34
Exhibit 34-67 Example Problem 6: Capacity of Blocked Regime	34-35
Exhibit 34-68 Example Problem 6: Capacity of Gap Acceptance Regime	34-36
Exhibit 34-69 Example Problem 6: Capacity of No-Opposing-Flow Regime	34-36
Exhibit 34-70 Example Problem 6: Performance Results.....	34-36
Exhibit 34-71 Example Problem 6: ETT and LOS Results.....	34-37
Exhibit 34-72 Example Problem 7: Intersection Plan View	34-37
Exhibit 34-73 Example Problem 7: Signalization Information.....	34-37
Exhibit 34-74 Example Problem 7: Adjusted O-D Table.....	34-38
Exhibit 34-75 Example Problem 7: Saturation Flow Rate Calculation for Eastbound and Westbound Approaches.....	34-39
Exhibit 34-76 Example Problem 7: Saturation Flow Rate Calculation for Northbound and Southbound Approaches	34-39
Exhibit 34-77 Example Problem 7: Uniform Delay Calculations for Left Turns Featuring Both Permissive and Protected Phasing.....	34-40

Exhibit 34-78 Example Problem 7: Queue Storage Ratio for Eastbound and Westbound Movements 34-41

Exhibit 34-79 Example Problem 7: Queue Storage Ratio for Northbound and Southbound Movements..... 34-41

Exhibit 34-80 Example Problem 7: Control Delay for Eastbound and Westbound Movements 34-42

Exhibit 34-81 Example Problem 7: Control Delay for Northbound and Southbound Movements..... 34-42

Exhibit 34-82 Example Problem 7: O-D Movement LOS..... 34-42

Exhibit 34-83 Example Problem 8: Intersection Plan View 34-43

Exhibit 34-84 Example Problem 8: Signalization Information..... 34-43

Exhibit 34-85 Example Problem 8: Lane Utilization Adjustment Calculations 34-44

Exhibit 34-86 Example Problem 8: Saturation Flow Rate Calculation for Interchange Eastbound and Westbound Approaches..... 34-44

Exhibit 34-87 Example Problem 8: Saturation Flow Rate Calculation for Interchange Northbound and Southbound Approaches..... 34-45

Exhibit 34-88 Example Problem 8: Saturation Flow Rate Calculation for Adjacent Intersection..... 34-45

Exhibit 34-89 Example Problem 8: Common Green Calculations..... 34-46

Exhibit 34-90 Example Problem 8: Lost Time due to Downstream Queues..... 34-47

Exhibit 34-91 Example Problem 8: Queue Storage Ratio for Interchange Eastbound and Westbound Movements 34-48

Exhibit 34-92 Example Problem 8: Queue Storage Ratio for Interchange Northbound and Southbound Movements 34-48

Exhibit 34-93 Example Problem 8: Queue Storage Ratio for Adjacent Intersection Movements..... 34-49

Exhibit 34-94 Example Problem 8: Control Delay for Interchange Eastbound and Westbound Movements 34-49

Exhibit 34-95 Example Problem 8: Control Delay for Interchange Northbound and Southbound Movements 34-50

Exhibit 34-96 Example Problem 8: Control Delay for Adjacent Intersection Movements..... 34-50

Exhibit 34-97 Example Problem 8: Interchange O-D Movement LOS 34-51

Exhibit 34-98 Example Problem 8: Adjacent Intersection Movement LOS 34-51

Exhibit 34-99 Example Problem 9: Intersection Plan View 34-51

Exhibit 34-100 Example Problem 9: Adjusted O-D Table 34-52

Exhibit 34-101 Example Problem 9: Approach Capacity and Delay Calculations 34-52

Exhibit 34-102 Example Problem 9: Control Delay and LOS for Each O-D Movement	34-53
Exhibit 34-103 Example Problem 10: O-D Demand Information for the Interchange.....	34-54
Exhibit 34-104 Example Problem 10: NEMA Flows (veh/h) for the Interchange.....	34-54
Exhibit 34-105 Example Problem 10: NEMA Flows for the Interchange Without Channelized Right Turns	34-55
Exhibit 34-106 Example Problem 10: SPUI Critical Flow Ratio Calculations.....	34-55
Exhibit 34-107 Example Problem 10: TUDI Critical Flow Ratio Calculations.....	34-55
Exhibit 34-108 Example Problem 10: CUDI Critical Flow Ratio Calculations.....	34-55
Exhibit 34-109 Example Problem 10: CDI Critical Flow Ratio Calculations.....	34-56
Exhibit 34-110 Example Problem 10: Parclo A-4Q Critical Flow Ratio Calculations.....	34-56
Exhibit 34-111 Example Problem 10: Parclo A-2Q Critical Flow Ratio Calculations.....	34-57
Exhibit 34-112 Example Problem 10: Parclo B-4Q Critical Flow Ratio Calculations.....	34-57
Exhibit 34-113 Example Problem 10: Parclo B-2Q Critical Flow Ratio Calculations.....	34-57
Exhibit 34-114 Example Problem 10: Interchange Delay for the Eight Interchange Types.....	34-58
Exhibit 34-115 Example Problem 11: Interchange Configuration and Demand Volumes	34-59
Exhibit 34-116 Example Problem 11: Signal Timing Plan	34-59
Exhibit 34-117 Example Problem 11: Physical Configurations Examined	34-60
Exhibit 34-118 Example Problem 11: Congested Approaches to Diamond Interchange.....	34-60
Exhibit 34-119 Example Problem 11: Discharge from the Diamond Interchange Under the Full Range of Arterial Demand	34-61
Exhibit 34-120 Example Problem 11: Discharge from the Southbound Exit Ramp Under the Full Range of Ramp Demand	34-62
Exhibit 34-121 Example Problem 11: Congested Approaches to the TWSC Intersection.....	34-62
Exhibit 34-122 Example Problem 11: Effect of Arterial Demand on Minor-Street Discharge at the TWSC Intersection.....	34-63
Exhibit 34-123 Example Problem 12: Turning Movement Demands	34-64

Exhibit 34-124 Example Problem 12: Demands Converted to the RCUT
 Geometry..... 34-64

Exhibit 34-125 Example Problem 12: Flow Rates in the RCUT Geometry..... 34-65

Exhibit 34-126 Example Problem 13: Turning Movement Demands 34-67

Exhibit 34-127 Example Problem 13: Demands Converted to the RCUT
 Geometry..... 34-68

Exhibit 34-128 Example Problem 13: Flow Rates in the RCUT Geometry..... 34-68

Exhibit 34-129 Example Problem 14: Turning Movement Demands 34-71

Exhibit 34-130 Example Problem 14: Demands Converted to the RCUT
 Geometry..... 34-72

Exhibit 34-131 Example Problem 14: Flow Rates in the RCUT Geometry..... 34-72

Exhibit 34-132 Example Problem 14: Control Delay for Each Junction..... 34-73

Exhibit 34-133 Example Problem 14: ETT and LOS Results 34-74

Exhibit 34-134 Example Problem 15: Turning Movement Demands and
 Average Interval Durations..... 34-75

Exhibit 34-135 Example Problem 15: Demands Converted to the MUT
 Geometry..... 34-76

Exhibit 34-136 Example Problem 15: Flow Rates in the MUT Geometry 34-76

Exhibit 34-137 Example Problem 15: Control Delay for Each Junction..... 34-77

Exhibit 34-138 Example Problem 15: ETT and LOS Results 34-78

Exhibit 34-139 Example Problem 16: Intersection Volumes and
 Channelization 34-79

Exhibit 34-140 Example Problem 16: Intersection Signalization 34-79

Exhibit 34-141 Example Problem 16: Flow Rates at the Supplemental and
 Main Intersections..... 34-80

Exhibit 34-142 Example Problem 16: Lane Geometries at the
 Supplemental and Main Intersections 34-80

Exhibit 34-143 Example Problem 16: Signalization at the DLT
 Intersections..... 34-81

Exhibit 34-144 Example Problem 16: Maximum Phase Times at the Main
 Intersection..... 34-82

Exhibit 34-145 Example Problem 16: Weighted Average Control Delays 34-83

Exhibit 34-146 Example Problem 17: Flow Rates at the Supplemental and
 Main Intersections..... 34-85

Exhibit 34-147 Example Problem 17: Lane Geometries at the
 Supplemental and Main Intersections 34-85

Exhibit 34-148 Example Problem 17: East–West Signalization at the DLT
 Intersections..... 34-86

Exhibit 34-149 Example Problem 17: North–South Signalization at the
 DLT Intersections 34-88

Exhibit 34-150 Example Problem 17: Weighted Average Control Delays 34-89

Exhibit 34-151 Default Values of Saturation Flow Rate for Use with the
Operational Analysis for Interchange Type Selection 34-93

Exhibit 34-152 Mapping of Interchange Origins and Destinations into
Phase Movements for Operational Interchange Type Selection
Analysis 34-94

Exhibit 34-153 Phase Movements in a SPUI 34-94

Exhibit 34-154 Phase Movements in a Tight Urban or Compressed Urban
Diamond Interchange 34-95

Exhibit 34-155 Default Values for y_i 34-95

Exhibit 34-156 Phase Movements in a CDI 34-96

Exhibit 34-157 Phase Movements in Parclo A-2Q and A-4Q Interchanges 34-97

Exhibit 34-158 Phase Movements in Parclo B-2Q and B-4Q Interchanges 34-97

Exhibit 34-159 Estimation of Interchange Delay d_i for Eight Basic
Interchange Types 34-99

Exhibit 34-160 Illustration and Notation of O-D Demands at an
Interchange with Roundabouts 34-100

Exhibit 34-161 Notation of O-D Demands at Interchanges with
Roundabouts 34-101

Exhibit 34-162 O-D Flows for Each Interchange Configuration 34-102

Exhibit 34-163 Worksheet for Obtaining O-D Movements from Turning
Movements for Parclo A-2Q Interchanges 34-103

Exhibit 34-164 Worksheet for Obtaining O-D Movements from Turning
Movements for Parclo A-4Q Interchanges 34-103

Exhibit 34-165 Worksheet for Obtaining O-D Movements from Turning
Movements for Parclo AB-2Q Interchanges 34-103

Exhibit 34-166 Worksheet for Obtaining O-D Movements from Turning
Movements for Parclo AB-4Q Interchanges 34-104

Exhibit 34-167 Worksheet for Obtaining O-D Movements from Turning
Movements for Parclo B-2Q Interchanges 34-104

Exhibit 34-168 Worksheet for Obtaining O-D Movements from Turning
Movements for Parclo B-4Q Interchanges 34-104

Exhibit 34-169 Worksheet for Obtaining O-D Movements from Turning
Movements for Diamond Interchanges 34-105

Exhibit 34-170 Worksheet for Obtaining O-D Movements from Turning
Movements for SPUIs 34-105

Exhibit 34-171 Worksheet for Obtaining Turning Movements from O-D
Movements for Parclo A-2Q and Parclo A-4Q Interchanges 34-105

Exhibit 34-172 Worksheet for Obtaining Turning Movements from O-D
Movements for Parclo AB-2Q Interchanges 34-106

Exhibit 34-173 Worksheet for Obtaining Turning Movements from O-D
Movements for Parclo AB-4Q Interchanges 34-106

Exhibit 34-174 Worksheet for Obtaining Turning Movements from O-D
Movements for Parclo B-2Q Interchanges..... 34-106

Exhibit 34-175 Worksheet for Obtaining Turning Movements from O-D
Movements for Parclo B-4Q Interchanges..... 34-107

Exhibit 34-176 Worksheet for Obtaining Turning Movements from O-D
Movements for Diamond Interchanges..... 34-107

Exhibit 34-177 Worksheet for Obtaining Turning Movements from O-D
Movements for SPUIs..... 34-107

1. INTRODUCTION

Chapter 34 is the supplemental chapter for Chapter 23, Ramp Terminals and Alternative Intersections, which is found in Volume 3 of the *Highway Capacity Manual* (HCM). This chapter provides 17 example problems demonstrating the application of the Chapter 23 methodologies for evaluating the performance of distributed intersections, including restricted crossing U-turn (RCUT), median U-turn (MUT), and displaced left-turn (DLT) intersections. It also presents a procedure for interchange type selection, which can be used to evaluate the operational performance of various interchange types. Finally, this chapter provides worksheets for converting origin–destination (O-D) flows to turn movement flows, and vice versa, for various interchange types.

Methodologies for the analysis of interchanges involving freeways and surface streets (i.e., service interchanges) were developed primarily on the basis of research conducted through the National Cooperative Highway Research Program (1–3) and elsewhere (4). Development of HCM analysis procedures for alternative intersection and interchange designs was conducted through the Federal Highway Administration (5).

VOLUME 4: APPLICATIONS GUIDE

- 25. Freeway Facilities: Supplemental
- 26. Freeway and Highway Segments: Supplemental
- 27. Freeway Weaving: Supplemental
- 28. Freeway Merges and Diverges: Supplemental
- 29. Urban Street Facilities: Supplemental
- 30. Urban Street Segments: Supplemental
- 31. Signalized Intersections: Supplemental
- 32. STOP-Controlled Intersections: Supplemental
- 33. Roundabouts: Supplemental
- 34. Interchange Ramp Terminals: Supplemental**
- 35. Pedestrians and Bicycles: Supplemental
- 36. Concepts: Supplemental
- 37. ATDM: Supplemental

2. EXAMPLE PROBLEMS

INTRODUCTION

This section describes the application of each of the final design, operational analysis for interchange type selection, and roundabouts analysis methods through the use of example problems. Exhibit 34-1 describes each of the example problems included in this chapter and indicates the methodology applied.

Exhibit 34-1
Example Problem Descriptions

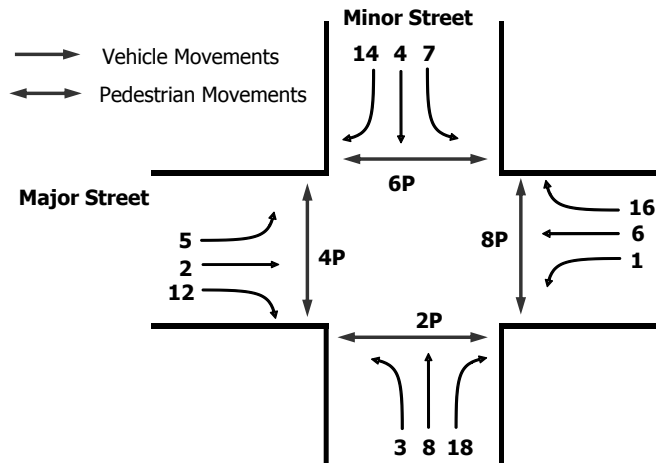
Example Problem	Description	Application
1	Diamond interchange	Operational
2	Parclo A-2Q interchange	Operational
3	Diamond interchange with four-phase signalization and queue spillback	Operational
4	Diamond interchange with demand starvation	Operational
5	Diverging diamond interchange with signalized control	Operational
6	Diverging diamond interchange with YIELD-controlled turns	Operational
7	Single-point urban interchange	Operational
8	Diamond interchange with closely spaced intersections	Operational
9	Diamond interchange with roundabouts	Operational
10	Compare eight types of signalized interchanges	Interchange type selection
11	Diamond interchange analysis using simulation	Alternative tools
12	Four-legged RCUT with merges	Operational
13	Three-legged RCUT with STOP signs	Operational
14	Four-legged RCUT with signals	Operational
15	Four-legged MUT with STOP signs	Operational
16	Partial DLT intersection	Operational
17	Full DLT intersection	Operational

Note: Parclo = partial cloverleaf, RCUT = restricted crossing U-turn, MUT = median U-turn, DLT = displaced left turn.

INTERSECTION TRAFFIC MOVEMENTS

Exhibit 34-2 illustrates typical vehicle and pedestrian traffic movements for the intersections in this chapter. Three vehicular traffic movements and one pedestrian traffic movement are shown for each intersection approach. Each movement is assigned a unique number or a number and letter combination. The letter P denotes a pedestrian movement. The number assigned to each left-turn and through movement is the same as the number assigned to each phase by National Electrical Manufacturers Association (NEMA) specification.

Exhibit 34-2
Intersection Traffic Movements and Numbering Scheme



Intersection traffic movements are assigned the right-of-way by the signal controller. Each movement is assigned to one or more signal phases. A phase is defined as the green, yellow change, and red clearance intervals in a cycle that are assigned to a specified traffic movement (or movements) (6). The assignment of movements to phases varies in practice with the desired phase sequence and the movements present at the intersection.

EXAMPLE PROBLEM 1: DIAMOND INTERCHANGE

The Interchange

The interchange of I-99 (northbound/southbound, NB/SB) and University Drive (eastbound/westbound, EB/WB) is a diamond interchange. Exhibit 34-3 provides the interchange volumes and channelization, and Exhibit 34-4 provides the signalization information. The offset is referenced to the beginning of green on the EB direction of the arterial.

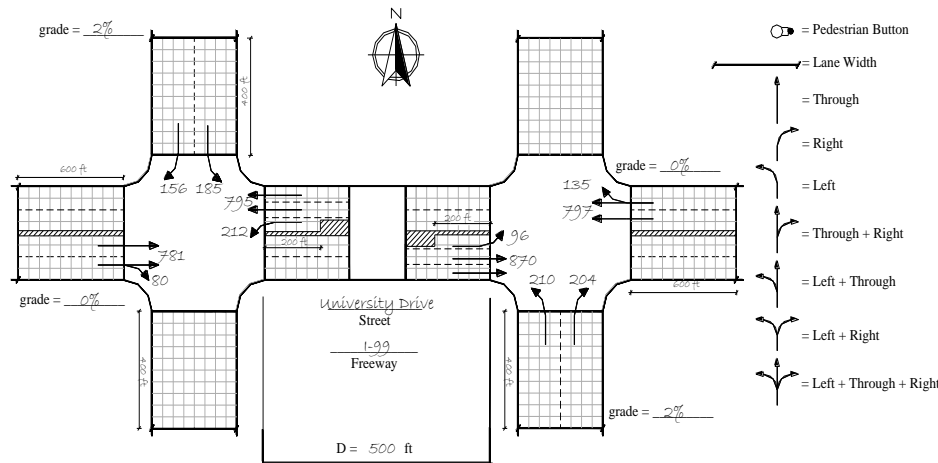


Exhibit 34-3
Example Problem 1:
Interchange Volumes and
Channelization

Phase	Intersection I			Intersection II		
	1	2	3	1	2	3
NEMA	Φ (2+6)	Φ (1+6)	Φ (4+7)	Φ (2+6)	Φ (3+8)	Φ (2+5)
Green time (s)	63	43	39	63	53	29
Yellow + all red (s)	5	5	5	5	5	5
Offset (s)		19			9	

Exhibit 34-4
Example Problem 1:
Signalization Information

The Question

What are the control delay, queue storage ratio, and level of service (LOS) for this interchange?

The Facts

There are no closely spaced intersections to this interchange, and it operates as a pretimed signal with no right turns on red allowed. Travel path radii are 50 ft for all right-turning movements and 75 ft for all left-turning movements. Arrival Type 4 is assumed for all arterial movements and Arrival Type 3 for all other movements. Extra distance traveled along each freeway ramp is 100 ft.

Heavy vehicles account for 6.1% of both the external and the internal through movements, and the peak hour factor (PHF) for the interchange is estimated to be 0.90. Start-up lost time and extension of effective green are both 2 s for all approaches. During the analysis period, there is no parking, and no buses, bicycles, or pedestrians utilize the interchange. The grade is 2% on the NB and SB approaches.

Solution

Calculation of Origin–Destination Movements

O-D movements through this diamond interchange are calculated on the basis of the worksheet provided in Exhibit 34-169 in Section 4. Since all movements utilize the signal, O-Ds can be calculated directly from the turning movements at the two intersections. The results of these calculations and the PHF-adjusted values are presented in Exhibit 34-5.

Exhibit 34-5
Example Problem 1: Adjusted O-D Table

O-D Movement	Demand (veh/h)	PHF-Adjusted Demand (veh/h)
A	210	233
B	204	227
C	156	173
D	185	206
E	96	107
F	80	89
G	135	150
H	212	236
I	685	761
J	585	650
K	0	0
L	0	0
M	0	0
N	0	0

Lane Utilization and Saturation Flow Rate Calculations

Both external approaches to this interchange consist of a two-lane shared right and through lane group. Lane utilization factors for the external through approaches are presented in Exhibit 34-6.

Exhibit 34-6
Example Problem 1: Lane Utilization Adjustment Calculations

Approach	V_1	V_2	Maximum Lane Utilization	Lane Utilization Factor
Eastbound external	0.5056	0.4944	0.5056	0.9890
Westbound external	0.5181	0.4819	0.5181	0.9651

Saturation flow rates are calculated on the basis of reductions in the base saturation flow rate of 1,900 pc/hg/ln by using Equation 23-14. The lane utilization of the approaches external to the interchange is obtained as shown above in Exhibit 34-6. Traffic pressure is calculated by using Equation 23-15. The left- and right-turn adjustment factors are estimated by using Equations 23-20 through 23-23. These equations use an adjustment factor for travel path radius calculated by Equation 23-19. The remaining adjustment factors are calculated as indicated in Chapter 19, Signalized Intersections. The estimated saturation flow rates for all approaches are shown in Exhibit 34-7 and Exhibit 34-8.

Value	Eastbound			Westbound		
	EXT-TH&R	INT-TH	INT-L	EXT-TH&R	INT-TH	INT-L
Base saturation flow (s_0 , pc/hg/ln)	1,900	1,900	1,900	1,900	1,900	1,900
Number of lanes (N)	2	2	1	2	2	1
Lane width adjustment (f_w)	1.000	1.000	1.000	1.000	1.000	1.000
Heavy vehicle and grade adjustment (f_{HVG})	0.952	0.952	1.000	0.952	0.952	1.000
Parking adjustment (f_p)	1.000	1.000	1.000	1.000	1.000	1.000
Bus blockage adjustment (f_{bb})	1.000	1.000	1.000	1.000	1.000	1.000
Area type adjustment (f_a)	1.000	1.000	1.000	1.000	1.000	1.000
Lane utilization adjustment (f_{LU})	0.989	0.952	1.000	0.965	0.952	1.000
Left-turn adjustment (f_{LT})	1.000	1.000	0.930	1.000	1.000	0.930
Right-turn adjustment (f_{RT})	0.999	1.000	1.000	0.998	1.000	1.000
Left-turn pedestrian-bicycle adjustment (f_{LPB})	1.000	1.000	1.000	1.000	1.000	1.000
Right-turn pedestrian-bicycle adjustment (f_{RPB})	1.000	1.000	1.000	1.000	1.000	1.000
Turn radius adjustment for lane group (f_R)	0.991	1.000	0.930	0.985	1.000	0.930
Traffic pressure adjustment for lane group (f_v)	1.034	1.036	0.963	1.044	1.026	1.000
Adjusted saturation flow (s , veh/hg/ln)	3,700	3,568	1,703	3,637	3,535	1,767

Notes: EXT = external, INT = internal, TH = through, R = right, L = left.

Value	Northbound		Southbound	
	Left	Right	Left	Right
Base saturation flow (s_0 , pc/hg/ln)	1,900	1,900	1,900	1,900
Number of lanes (N)	1	1	1	1
Lane width adjustment (f_w)	1.000	1.000	1.000	1.000
Heavy vehicle and grade adjustment (f_{HVG})	0.990	0.990	0.990	0.990
Parking adjustment (f_p)	1.000	1.000	1.000	1.000
Bus blockage adjustment (f_{bb})	1.000	1.000	1.000	1.000
Area type adjustment (f_a)	1.000	1.000	1.000	1.000
Lane utilization adjustment (f_{LU})	1.000	1.000	1.000	1.000
Left-turn adjustment (f_{LT})	0.930	1.000	0.930	1.000
Right-turn adjustment (f_{RT})	1.000	0.899	1.000	0.899
Left-turn pedestrian-bicycle adjustment (f_{LPB})	1.000	1.000	1.000	1.000
Right-turn pedestrian-bicycle adjustment (f_{RPB})	1.000	1.000	1.000	1.000
Turn radius adjustment for lane group (f_R)	0.930	0.899	0.930	0.899
Traffic pressure adjustment for lane group (f_v)	1.000	0.979	0.991	0.968
Adjusted saturation flow (s , veh/hg/ln)	1,749	1,656	1,734	1,638

Common Green and Lost Time due to Downstream Queue and Demand Starvation Calculations

Exhibit 34-9 first provides the beginning and end times of the green for each phase at the two intersections on the assumption that Phase 1 of the first intersection begins at time zero. On the basis of the information provided in Exhibit 34-9, the relative offset between the two intersections is $\text{Offset 2} - \text{Offset 1} + n \times \text{cycle length} = 9 - 19 + 160 = 150$ s. Next, the exhibit provides the beginning and end of green for the six pairs of movements between the two intersections and the respective common green time for each pair of movements. For example, the EB external through movement has the green between 0 and 63 s, while the EB internal through movement has the green twice during the cycle, between 150 and 53 s and between 116 and 150 s. The common green time when both movements have the green is between 0 and 53 s, for a duration of 53 s.

Exhibit 34-7

Example Problem 1:
Saturation Flow Rate
Calculation for Eastbound and
Westbound Approaches

Exhibit 34-8

Example Problem 1:
Saturation Flow Rate
Calculation for Northbound
and Southbound Approaches

Exhibit 34-9

Example Problem 1: Common Green Calculations

Phase	Intersection I		Intersection II		Common Green Time
	Green Begin	Green End	Green Begin	Green End	
Phase 1	0	63	150	53	
Phase 2	68	111	58	111	
Phase 3	116	155	116	145	
Movement	First Green Time Within Cycle		Second Green Time Within Cycle		Common Green Time
	Begin	End	Begin	End	
EB EXT THRU	0	63			53
EB INT THRU	150	53	116	150	
WB EXT THRU	150	53			53
WB INT THRU	0	111			
SB RAMP	116	155			34
EB INT THRU	150	53	116	150	
NB RAMP	58	111			53
WB INT THRU	0	111			
WB INT LEFT	68	111			0
EB INT THRU	150	53			
EB INT LEFT	116	145			0
WB INT THRU	0	111			

Notes: EXT = external, INT = internal, THRU = through, EB = eastbound, WB = westbound, SB = southbound, NB = northbound.

The next step involves the calculation of lost time due to downstream queues. First, the queues at the beginning of the upstream arterial phase and at the beginning of the upstream ramp phase must be calculated by using Equation 23-33 and Equation 23-34, respectively. Exhibit 34-10 presents the calculation of these downstream queues followed by the calculation of the respective lost time due to those queues.

Exhibit 34-10

Example Problem 1: Lost Time due to Downstream Queues

Value	Movement			
	EB EXT-TH	SB-L	WB EXT-TH	NB-L
<i>Downstream Queue Calculations</i>				
V_R or V_A (veh/h)	206	868	233	886
N_R or N_A	1	2	1	2
G_R or G_A (s)	39	63	53	63
G_D (s)	97	97	111	111
C (s)	160	160	160	160
CG_{UD} or CG_{RD} (s)	53	34	53	53
Queue length (Q_A or Q_R) (ft)	0.0	4.1	0.0	0.0
<i>Lost Time Calculations</i>				
G_R or G_A (s)	63	39	63	53
C (s)	160	160	160	160
D_{QA} or D_{QR} (ft)	500	496	500	500
CG_{UD} or CG_{RD} (s)	53	34	53	53
Additional lost time, L_{D-A} or L_{D-R} (s)	0.0	0.0	0.0	0.0
Total lost time, t'_l (s)	5.0	5.0	5.0	5.0
Effective green time, g' (s)	63.0	39.0	63.0	53.0

Notes: EXT = external, TH = through, L = left, EB = eastbound, WB = westbound, NB = northbound, SB = southbound.

The lost time due to demand starvation is calculated by using Equation 23-38. The respective calculations are presented in Exhibit 34-11. As shown, in this case there is no lost time due to demand starvation ($L_{DS} = 0$).

Value	Movement	
	EB-INT-TH	WB-INT-TH
V_{Ramp-L} (veh/h)	206	233
$V_{Arterial}$ (veh/h)	868	886
C (s)	160	160
N_{Ramp-L}	1	1
$N_{Arterial}$	2	2
CG_{RD} (s)	34	53
CG_{UD} (s)	53	53
H_I	2.02	2.04
$Q_{Initial}$ (ft)	0	0
CG_{DS} (s)	0	0
L_{DS} (s)	0	0
t'_L (s)	5	5
Effective green time, g'' (s)	97	111

Notes: EB-INT-TH = eastbound internal through, WB-INT-TH = westbound internal through.

Exhibit 34-11

Example Problem 1: Lost Time due to Demand Starvation

Queue Storage and Control Delay

The queue storage ratio is estimated as the ratio of the average maximum queue to the available queue storage by using Equation 31-154. Exhibit 34-12 and Exhibit 34-13 present the calculations of the queue storage ratio for all movements in Example 1. Those exhibits also show the volume-to-capacity (v/c) ratio for each movement. Control delay for each movement is calculated according to Equation 19-18. Exhibit 34-14 and Exhibit 34-15 provide the control delay for each movement of the interchange.

Value	Eastbound Movements			Westbound Movements		
	EXT-TH&R	INT-L	INT-TH	EXT-TH&R	INT-L	INT-TH
Q_{bl} (ft)	0.0	0.0	0.0	0.0	0.0	0.0
v (veh/h/ln group)	957	107	967	1,036	236	883
s (veh/h/ln)	1,850	1,703	1,784	1,819	1,768	1,768
g (s)	63	29	97	63	43	111
g/C	0.39	0.18	0.61	0.39	0.27	0.69
I	1.00	0.71	0.71	1.00	0.62	0.62
c (veh/h/ln group)	1,459	309	2,163	1,437	475	2,452
$X = v/c$	0.66	0.35	0.45	0.72	0.50	0.36
r_a (ft/s ²)	3.5	3.5	3.5	3.5	3.5	3.5
r_d (ft/s ²)	4.0	4.0	4.0	4.0	4.0	4.0
S_s (mi/h)	5	5	5	5	5	5
S_{pl} (mi/h)	40	40	40	40	40	40
S_s (mi/h)	39.96	39.96	39.96	39.96	39.96	39.96
d_b (s)	12.04	12.04	12.04	12.04	12.04	12.04
Rp	1.000	1.333	1.333	1.000	1.333	1.333
P	0.39	0.24	0.81	0.39	0.36	0.92
r (s)	97	131	63	97	117	49
t_r (s)	0.01	0.00	0.00	0.01	0.00	0.00
q (veh/s)	0.27	0.03	0.27	0.27	0.07	0.25
q_g (veh/s)	0.27	0.04	0.36	0.28	0.13	0.25
q_r (veh/s)	0.27	0.03	0.13	0.72	0.50	0.36
Q_1 (veh)	15.2	3.5	3.8	13.9	6.9	1.2
Q_2 (veh)	0.9	0.2	0.1	1.2	0.3	0.1
T	0.25	0.25	0.25	0.25	0.25	0.25
Q_{eo} (veh)	0.00	0.00	0.00	0.00	0.00	0.00
t_a	0	0	0	0	0	0
Q_e (veh)	0.00	0.00	0.00	0.00	0.00	0.00
Q_b (veh)	0.00	0.00	0.00	0.00	0.00	0.00
Q_3 (veh)	0.0	0.0	0.0	0.0	0.0	0.0
Q (veh)	16.2	3.7	4.0	15.2	7.2	1.3
L_n (ft)	25.01	25.00	25.01	25	25	25
L_a (ft)	600	200	500	600	200	500
R_Q	0.67	0.46	0.20	0.63	0.90	0.06

Notes: EXT = external, INT = internal, TH = through, R = right, L = left.

Exhibit 34-12

Example Problem 1: Queue Storage Ratio for Eastbound and Westbound Movements

Exhibit 34-13

Example Problem 1: Queue Storage Ratio for Northbound and Southbound Movements

Value	Northbound Movements		Southbound Movements	
	Left	Right	Left	Right
Q_{bl} (ft)	0.0	0.0	0.0	0.0
v (veh/h/ln group)	233	227	206	173
s (veh/h/ln)	1,749	1,656	1,734	1,638
g (s)	53	53	39	39
g/C	0.33	0.33	0.24	0.24
I	1.00	1.00	1.00	1.00
c (veh/h/ln group)	580	549	423	399
$X = v/c$	0.40	0.41	0.49	0.43
r_a (ft/s ²)	3.5	3.5	3.5	3.5
r_d (ft/s ²)	4.0	4.0	4.0	4.0
S_s (mi/h)	5	5	5	5
S_{pl} (mi/h)	40	40	40	40
S_a (mi/h)	39.96	39.96	39.96	39.96
d_b (s)	12.04	12.04	12.04	12.04
Rp	1.000	1.000	1.000	1.000
P	0.33	0.33	0.24	0.24
r (s)	107.00	107.00	121.00	121.00
t_r (s)	0.00	0.00	0.00	0.00
q (veh/s)	0.06	0.06	0.06	0.05
q_d (veh/s)	0.06	0.06	0.06	0.05
q_r (veh/s)	0.06	0.06	0.06	0.05
Q_1 (veh)	7.1	6.9	7.1	5.9
Q_2 (veh)	0.3	0.3	0.5	0.4
T	0.25	0.25	0.25	0.25
Q_{eo} (veh)	0.00	0.00	0.00	0.00
t_a	0	0	0	0
Q_e (veh)	0.00	0.00	0.00	0.00
Q_b (veh)	0.00	0.00	0.00	0.00
Q_3 (veh)	0.0	0.0	0.0	0.0
Q (veh)	7.4	7.3	7.5	6.2
L_f (ft)	25	25	25	25
L_s (ft)	400	400	400	400
R_Q	0.46	0.45	0.47	0.39

Exhibit 34-14

Example Problem 1: Control Delay for Eastbound and Westbound Movements

Value	Eastbound Movements			Westbound Movements		
	EXT-TH&R	INT-L	INT-TH	EXT-TH&R	INT-L	INT-TH
g (s)	-	29	97	-	43	111
g' (s)	63	-	-	63	-	-
g/C or g'/C	0.39	0.18	0.61	0.39	0.27	0.69
c (veh/h)	1,459	309	2,163	1,437	475	2,452
$X = v/c$	0.66	0.35	0.45	0.72	0.50	0.36
d_1 (s/veh)	39.6	52.8	7.3	31.3	42.9	2.0
k	0.5	0.5	0.5	0.5	0.5	0.5
d_2 (s/veh)	4.6	2.2	0.5	6.2	2.3	0.3
d_3 (s/veh)	0.0	0.0	0.0	0.0	0.0	0.0
PF	1.000	1.000	0.560	1.000	1.000	0.283
K_{min}	0.04	0.04	0.04	0.04	0.04	0.04
u	0	0	0	0	0	0
t	0	0	0	0	0	0
d (s/veh)	44.1	55.0	7.8	37.5	45.2	2.3

Notes: EXT = external, INT = internal, TH = through, R = right, L = left.

Value	Northbound Movements		Southbound Movements	
	Left	Right	Left	Right
g (s)	-	53	-	39
g' (s)	53	-	39	-
g/C or g'/C	0.33	0.33	0.24	0.24
c (veh/h)	580	549	423	399
$X = v/c$	0.42	0.41	0.49	0.43
d_1 (s/veh)	41.3	41.5	51.9	51.2
k	0.5	0.5	0.5	0.5
d_2 (s/veh)	2.1	2.1	4.0	3.4
d_3 (s/veh)	0.0	0.0	0.0	0.0
PF	1.000	1.000	1.000	1.000
k_{min}	0.04	0.04	0.04	0.04
u	0	0	0	0
t	0	0	0	0
d (s/veh)	43.4	43.4	55.9	54.6

Exhibit 34-15

Example Problem 1: Control Delay for Northbound and Southbound Movements

Results

Delay for each O-D is estimated as the sum of the movement delays for each movement utilized by the O-D, as indicated in Equation 23-2. Next, the v/c and queue storage ratios are checked. If either of these parameters exceeds 1, the LOS for all O-Ds that utilize that movement is F. Exhibit 34-16 summarizes the results for all O-D movements at this interchange. As shown, all the movements have v/c and queue storage ratios less than 1; for these O-D movements, the LOS is determined by using Exhibit 23-10. After extra distances are measured according to the Exhibit 23-8 discussion, EDTT can be obtained from Equation 23-50 [i.e., $EDTT = 100 / (1.47 \times 35) + 0 = 1.9$ s/veh]. Intersection-wide performance measures are not calculated for interchange ramp terminals.

O-D Movement	Control Delay (s/veh)	EDTT (s/veh)	ETT (s/veh)	$v/c > 1?$	$R_q > 1?$	LOS
A	45.6	1.9	47.5	No	No	C
B	43.7	-1.9	41.8	No	No	C
C	54.6	-1.9	52.7	No	No	C
D	63.6	1.9	65.5	No	No	D
E	99.2	1.9	101.1	No	No	E
F	44.2	-1.9	42.3	No	No	C
G	37.5	-1.9	35.6	No	No	C
H	82.7	1.9	84.6	No	No	D
I	52.0	0.0	52.0	No	No	C
J	39.8	0.0	39.8	No	No	C

Exhibit 34-16

Example Problem 1: O-D Movement LOS

EXAMPLE PROBLEM 2: PARCLO A-2Q INTERCHANGE
The Interchange

The interchange of I-75 (NB/SB) and Newberry Avenue (EB/WB) is a Parclo A-2Q interchange. Exhibit 34-17 provides the interchange volumes and channelization, while Exhibit 34-18 provides the signalization information. The offset is referenced to the beginning of green on the EB direction of the arterial.

Exhibit 34-17
Example Problem 2:
Intersection Plan View

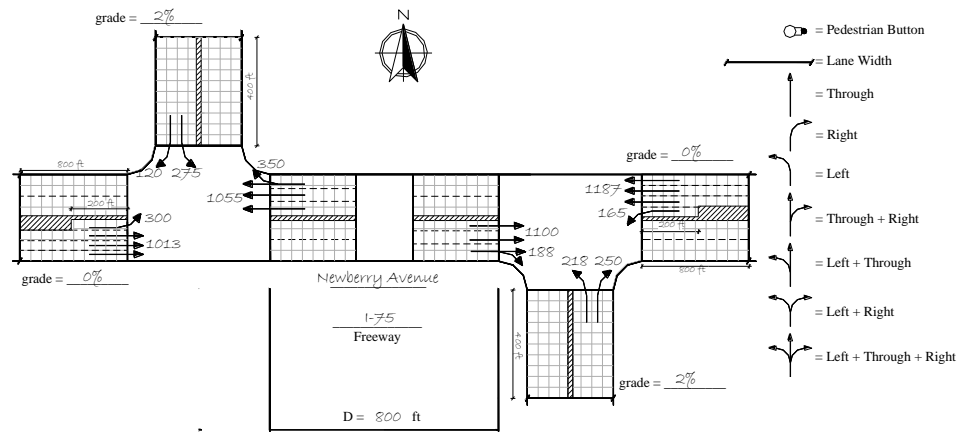


Exhibit 34-18
Example Problem 2:
Signalization Information

Phase	Intersection I			Intersection II		
	1	2	3	1	2	3
NEMA	Φ (2+5)	Φ (2+6)	Φ (4+7)	Φ (1+6)	Φ (3+8)	Φ (2+6)
Green time (s)	25	60	40	25	35	65
Yellow + all red (s)	5	5	5	5	5	5
Offset (s)		0			0	

The Question

What are the control delay, queue storage ratio, and LOS for this interchange?

The Facts

There are no closely spaced intersections to this interchange, and it operates as a pretimed signal with no right turns on red allowed. The eastbound and westbound left-turn radii are 80 ft, while all remaining turning movements have radii of 50 ft. The arrival type is assumed to be 4 for all arterial movements and 3 for all other movements. Extra distance traveled along each freeway loop ramp is 1,600 ft. The grade is 2% on the NB and SB approaches.

There are 11.7% heavy vehicles on both the external and the internal through movements, and the PHF for the interchange is estimated to be 0.95. Start-up lost time is 3 s for all approaches, while the extension of effective green is 2 s for all approaches. During the analysis period, there is no parking, and no buses, bicycles, or pedestrians utilize the interchange.

Solution

Calculation of Origin–Destination Movements

O-Ds through this parclo interchange are calculated on the basis of the worksheet provided in Exhibit 34-163 in Section 4. Since all movements utilize the signal, O-Ds can be calculated directly from the turning movements at the two intersections. The results of these calculations and the PHF-adjusted values are presented in Exhibit 34-19.

O-D Movement	Demand (veh/h)	PHF-Adjusted Demand (veh/h)
A	218	229
B	250	263
C	120	126
D	275	289
E	188	198
F	300	316
G	165	174
H	350	368
I	825	868
J	837	881
K	0	0
L	0	0
M	0	0
N	0	0

Exhibit 34-19
Example Problem 2: Adjusted O-D Table

Lane Utilization and Saturation Flow Rate Calculations

The external approaches to this interchange consist of a three-lane through lane group. Use of the three-lane model from Exhibit 23-24 results in the predicted lane utilization percentages for the external through approaches that are presented in Exhibit 34-20.

Approach	V_1	V_2	V_3	Maximum Lane Utilization	Lane Utilization Factor
Eastbound external	0.2660	0.2791	0.4549	0.4549	0.7328
Westbound external	0.2263	0.2472	0.5265	0.5265	0.6332

Exhibit 34-20
Example Problem 2: Lane Utilization Adjustment Calculations

Saturation flow rates are calculated on the basis of reductions in the base saturation flow rate of 1,900 pc/hg/ln by using Equation 23-14. The lane utilization of the approaches external to the interchange is obtained as shown above in Exhibit 34-20. Traffic pressure is calculated by using Equation 23-15. The left- and right-turn adjustment factors are estimated by using Equations 23-20 through 23-23. These equations use an adjustment factor for travel path radius calculated by Equation 23-19. The remaining adjustment factors are calculated according to Chapter 19, Signalized Intersections. The results of these calculations for all approaches are presented in Exhibit 34-21 and Exhibit 34-22.

Value	Northbound		Southbound	
	Left	Right	Left	Right
Base saturation flow (s_0 , pc/hg/ln)	1,900	1,900	1,900	1,900
Number of lanes (N)	1	1	1	1
Lane width adjustment (f_w)	1.000	1.000	1.000	1.000
Heavy vehicle and grade adjustment (f_{HVg})	0.990	0.990	0.990	0.990
Parking adjustment (f_p)	1.000	1.000	1.000	1.000
Bus blockage adjustment (f_{bb})	1.000	1.000	1.000	1.000
Area type adjustment (f_a)	1.000	1.000	1.000	1.000
Lane utilization adjustment (f_{LU})	1.000	1.000	1.000	1.000
Left-turn adjustment (f_{LT})	0.899	1.000	0.899	1.000
Right-turn adjustment (f_{RT})	1.000	0.899	1.000	0.899
Left-turn pedestrian-bicycle adjustment (f_{LPB})	1.000	1.000	1.000	1.000
Right-turn pedestrian-bicycle adjustment (f_{RPB})	1.000	1.000	1.000	1.000
Turn radius adjustment for lane group (f_R)	0.899	0.899	0.899	0.899
Traffic pressure adjustment for lane group (f_v)	0.990	0.980	1.006	0.956
Adjusted saturation flow (s , veh/hg/ln)	1,674	1,658	1,701	1,617

Exhibit 34-21
Example Problem 2: Saturation Flow Rate Calculation for Northbound and Southbound Approaches

Exhibit 34-22

Example Problem 2:
Saturation Flow Rate
Calculation for Eastbound and
Westbound Approaches

Value	Eastbound			Westbound		
	EXT-TH	EXT-L	INT-TH&R	EXT-TH	EXT-L	INT-TH&R
Base saturation flow (s_0 , pc/hg/ln)	1,900	1,900	1,900	1,900	1,900	1,900
Number of lanes (N)	3	1	3	3	1	3
Lane width adjustment (f_w)	1.000	1.000	1.000	1.000	1.000	1.000
Heavy vehicle and grade adjustment (f_{HVg})	0.909	1.000	0.909	0.909	1.000	0.909
Parking adjustment (f_p)	1.000	1.000	1.000	1.000	1.000	1.000
Bus blockage adjustment (f_{bb})	1.000	1.000	1.000	1.000	1.000	1.000
Area type adjustment (f_a)	1.000	1.000	1.000	1.000	1.000	1.000
Lane utilization adjustment (f_{LU})	0.733	1.000	1.000	0.633	1.000	1.000
Left-turn adjustment (f_{LT})	1.000	0.934	1.000	1.000	0.934	1.000
Right-turn adjustment (f_{RT})	1.000	1.000	0.998	1.000	1.000	0.994
Left-turn pedestrian-bicycle adjustment (f_{Lpb})	1.000	1.000	1.000	1.000	1.000	1.000
Right-turn pedestrian-bicycle adjustment (f_{Rpb})	1.000	1.000	1.000	1.000	1.000	1.000
Turn radius adjustment for lane group (f_R)	1.000	0.934	0.985	1.000	0.934	0.975
Traffic pressure adjustment for lane group (f_v)	0.997	1.013	1.016	1.009	0.976	1.024
Adjusted saturation flow (s , veh/hg/ln)	3,786	1,798	5,253	3,310	1,733	5,271

Notes: EXT = external, INT = internal, TH = through, R = right, L = left.

Common Green and Lost Time due to Downstream Queue and Demand Starvation Calculations

Exhibit 34-23 provides the beginning and end times of the green for each phase followed by the beginning and end of green for the four pairs of movements at the two intersections. Phase 1 of the first intersection is assumed to begin at time zero (in this case the offset for both intersections is zero, and therefore the beginning of Phase 1 for the second intersection is also zero).

Exhibit 34-23

Example Problem 2: Common
Green Calculations

Phase	Intersection I		Intersection II		Common Green Time
	Green Begin	Green End	Green Begin	Green End	
Phase 1	0	25	0	25	
Phase 2	30	90	30	65	
Phase 3	95	135	70	135	
Movement	First Green Time Within Cycle		Second Green Time Within Cycle		Common Green Time
	Begin	End	Begin	End	
EB EXT THRU	0	90			20
EB INT THRU	70	135			
WB EXT THRU	0	25	70	135	20
WB INT THRU	30	90			
SB RAMP	95	135			40
EB INT THRU	70	135			
NB RAMP	30	65			35
WB INT THRU	30	90			

Notes: EXT = external, INT = internal, EB = eastbound, WB = westbound, NB = northbound, SB = southbound, THRU = through.

The next step involves the calculation of lost time due to downstream queues. First, the queues at the beginning of the upstream arterial phase and at the beginning of the upstream ramp phase must be calculated by using Equation 23-33 and Equation 23-34, respectively. Exhibit 34-24 presents the calculation of these downstream queues followed by the calculation of the respective lost time due to those queues.

Value	Movement			
	EB EXT-TH	SB-L	WB EXT-TH	NB-L
<i>Downstream Queue Calculations</i>				
V_R or V_A (veh/h)	289	1,066	229	1,249
N_R or N_A	1	3	1	3
G_R or G_A (s)	40	90	35	95
G_D (s)	65	65	60	60
C (s)	140	140	140	140
CG_{UD} or CG_{RD} (s)	20	40	20	35
Queue length (Q_A or Q_R) (ft)	0.9	48.6	0.0	89.4
<i>Lost Time Calculations</i>				
G_R or G_A (s)	90	40	95	35
C (s)	140	140	140	140
D_{QA} or D_{QR} (ft)	799	751	800	711
CG_{UD} or CG_{RD} (s)	20	40	20	35
Additional lost time, L_{D-A} or L_{D-R} (s)	0	0	0	0
Total lost time, t'_l (s)	6	6	6	6
Effective green time, g' (s)	89	39	94	34

Notes: EXT = external, TH = through, L = left, EB = eastbound, WB = westbound, NB = northbound, SB = southbound.

Queue Storage and Control Delay

The queue storage ratio is estimated as the ratio of the average maximum queue to the available queue storage by using Equation 31-154. Exhibit 34-25 and Exhibit 34-26 present the calculation of the queue storage ratio for all movements in Example Problem 2. The exhibit also shows the v/c ratio for each movement. Control delay for each movement is calculated according to Equation 19-18. Exhibit 34-27 and Exhibit 34-28 provide the control delay for each movement of this interchange.

Value	Eastbound Movements			Westbound Movements		
	EXT-TH	EXT-L	INT-TH&R	EXT-TH	EXT-L	INT-TH&R
Q_{bl} (ft)	0.0	0.0	0.0	0.0	0.0	0.0
v (veh/h/ln group)	1,066	316	1,282	1,249	174	1,479
s (veh/h/ln)	1,262	1,798	1,751	1,103	1,733	1,757
g (s)	89	24	64	94	24	59
g/C	0.64	0.17	0.46	0.67	0.17	0.42
I	1.00	1.00	0.90	1.00	1.00	0.81
c (veh/h/ln group)	2,407	308	2,401	2,222	297	2,221
$X = v/c$	0.44	1.02	0.54	0.56	0.58	0.67
r_a (ft/s ²)	3.5	3.5	3.5	3.5	3.5	3.5
r_d (ft/s ²)	4.0	4.0	4.0	4.0	4.0	4.0
S_s (mi/h)	5	5	5	5	5	5
S_{pl} (mi/h)	40	40	40	40	40	40
S_s (mi/h)	39.96	39.96	39.96	39.96	39.96	39.96
d_b (s)	12.04	12.04	12.04	12.04	12.04	12.04
Rp	1.000	1.000	1.333	1.000	1.000	1.333
P	0.636	0.171	0.609	0.671	0.171	0.562
r (s)	51	116	76	46	116	81
t_r (s)	0.00	0.01	0.00	0.01	0.00	0.01
q (veh/s)	0.30	0.09	0.38	0.35	0.05	0.41
q_b (veh/s)	0.30	0.09	0.50	0.35	0.05	0.55
q_r (veh/s)	0.30	0.09	0.27	0.35	0.05	0.31
Q_1 (veh)	5.4	10.7	6.9	6.3	5.6	10.4
Q_2 (veh)	0.1	4.9	0.3	0.2	0.7	0.5
T	0.25	0.25	0.25	0.25	0.25	0.25
Q_{ev} (veh)	0.00	0.00	0.00	0.00	0.00	0.00
t_A	0	0	0	0	0	0
Q_e (veh)	0.00	0.00	0.00	0.00	0.00	0.00
Q_b (veh)	0.00	0.00	0.00	0.00	0.00	0.00
Q_s (veh)	0.0	0.0	0.0	0.0	0.0	0.0
Q (veh)	5.5	15.7	7.2	6.5	6.3	10.9
L_h (ft)	25.02	25.00	25.02	25.02	25.00	25.02
L_s (ft)	800	200	800	800	200	800
R_Q	0.17	1.96	0.23	0.20	0.78	0.34

Notes: EXT = external, INT = internal, TH = through, R = right, L = left.

Exhibit 34-24
Example Problem 2: Lost Time due to Downstream Queues

Exhibit 34-25
Example Problem 2: Queue Storage Ratio for Eastbound and Westbound Movements

Exhibit 34-26

Example Problem 2: Queue Storage Ratio for Northbound and Southbound Movements

Value	Northbound Movements		Southbound Movements	
	Left	Right	Left	Right
Q_{bl} (ft)	0.0	0.0	0.0	0.0
v (veh/h/ln group)	229	263	289	126
s (veh/h/ln)	1,674	1,658	1,701	1,617
g (s)	34	34	39	39
g/C	0.24	0.24	0.28	0.28
I	1.00	1.00	1.00	1.00
c (veh/h/ln group)	407	403	474	450
$X = v/c$	0.56	0.65	0.61	0.28
r_a (ft/s ²)	3.5	3.5	3.5	3.5
r_l (ft/s ²)	4.0	4.0	4.0	4.0
S_s (mi/h)	5	5	5	5
S_{pl} (mi/h)	40	40	40	40
S_b (mi/h)	39.96	39.96	39.96	39.96
d_a (s)	12.04	12.04	12.04	12.04
Rp	1.000	1.000	1.000	1.000
P	0.243	0.243	0.279	0.279
r (s)	106	106	101	101
t_r (s)	0.00	0.00	0.01	0.00
q (veh/s)	0.06	0.07	0.08	0.04
q_g (veh/s)	0.06	0.07	0.08	0.04
q_r (veh/s)	0.06	0.07	0.08	0.04
Q_1 (veh)	7.8	9.2	9.8	3.4
Q_2 (veh)	0.6	0.9	0.8	0.2
T	0.25	0.25	0.25	0.25
Q_{eo} (veh)	0.00	0.00	0.00	0.00
t_a	0	0	0	0
Q_e (veh)	0.00	0.00	0.00	0.00
Q_b (veh)	0.00	0.00	0.00	0.00
Q_s (veh)	0.0	0.0	0.0	0.0
Q (veh)	8.5	10.1	10.5	3.6
L_h (ft)	25	25	25	25
L_a (ft)	400	400	400	400
R_Q	0.53	0.63	0.66	0.22

Exhibit 34-27

Example Problem 2: Control Delay for Eastbound and Westbound Movements

Value	Eastbound Movements			Westbound Movements		
	EXT-TH	EXT-L	INT-TH&R	EXT-TH	EXT-L	INT-TH&R
g (s)	-	24	64	-	24	59
g' (s)	89	-	-	94	-	-
g/C or g'/C	0.64	0.17	0.46	0.67	0.17	0.42
c (veh/h)	2,407	308	2,401	2,222	297	2,221
$X = v/c$	0.44	1.02	0.56	0.56	0.58	0.67
d_1 (s/veh)	12.9	58.0	18.8	12.1	53.4	24.1
k	0.5	0.5	0.5	0.5	0.5	0.5
d_2 (s/veh)	0.6	57.7	1.5	1.0	8.2	2.6
d_3 (s/veh)	0.0	0.0	0.0	0.0	0.0	0.0
PF	1.000	1.000	0.827	1.000	1.000	0.871
K_{min}	0.04	0.04	0.04	0.04	0.04	0.04
u	0	0	0	0	0	0
t	0	0	0	0	0	0
d (s/veh)	13.5	115.7	20.3	13.2	61.6	26.8

Notes: EXT = external, INT = internal, TH = through, R = right, L = left.

Value	Northbound Movements		Southbound Movements	
	Left	Right	Left	Right
g (s)	-	34	39	-
g' (s)	34	-	-	39
g/C or g'/C	0.24	0.24	0.28	0.28
c (veh/h)	407	403	474	450
$X = v/c$	0.56	0.65	0.61	0.28
d_1 (s/veh)	46.5	47.7	43.9	39.5
k	0.5	0.5	0.5	0.5
d_2 (s/veh)	5.6	8.0	5.8	1.6
d_3 (s/veh)	0.0	0.0	0.0	0.0
PF	1.000	1.000	1.000	1.000
k_{min}	0.04	0.04	0.04	0.04
u	0	0	0	0
t	0	0	0	0
d (s/veh)	52.1	55.7	49.7	41.1

Exhibit 34-28

Example Problem 2: Control Delay for Northbound and Southbound Movements

Results

Delay for each O-D is estimated as the sum of the movement delays for each movement utilized by the O-D, as indicated in Equation 23-2. Next, the v/c and queue storage ratios are checked. If either of these parameters exceeds 1, the LOS for all O-Ds that utilize that movement is F. Exhibit 34-29 presents the resulting delay, v/c ratio, and R_Q for each O-D movement. As shown, O-D Movement F (which consists of the EB external left movement) has v/c and R_Q ratios greater than 1, resulting in LOS F. For the remaining movements, the LOS is determined by using Exhibit 23-10. After extra distances are measured according to the Exhibit 23-9 discussion, EDTT can be obtained from Equation 23-50 [i.e., $EDTT = 1,200 / (1.47 \times 25) + 5 = 37.7$ s/veh]. Intersectionwide performance measures are not calculated for interchange ramp terminals.

O-D Movement	Control Delay (s/veh)	EDTT (s/veh)	ETT (s/veh)	$v/c > 1?$	$R_Q > 1?$	LOS
A	78.9	20.6	99.5	No	No	E
B	55.7	-15.6	40.1	No	No	C
C	41.1	-15.6	25.5	No	No	B
D	70.0	20.6	90.6	No	No	E
E	33.8	37.7	71.5	No	No	D
F	115.7	20.6	136.3	Yes	Yes	F
G	61.6	20.6	82.2	No	No	D
H	40.0	37.7	77.7	No	No	D
I	33.8	0.0	33.8	No	No	C
J	40.0	0.0	40.0	No	No	C

Exhibit 34-29

Example Problem 2: O-D Movement LOS

EXAMPLE PROBLEM 3: DIAMOND INTERCHANGE WITH QUEUE SPILLBACK

The Interchange

The interchange of I-95 (NB/SB) and 22nd Avenue (EB/WB) is a diamond interchange. The traffic, geometric, and signalization conditions for this study site are provided in Exhibit 34-30 and Exhibit 34-31. The offset is referenced to the beginning of green on the EB direction of the arterial.

Exhibit 34-30
Example Problem 3:
Intersection Plan View

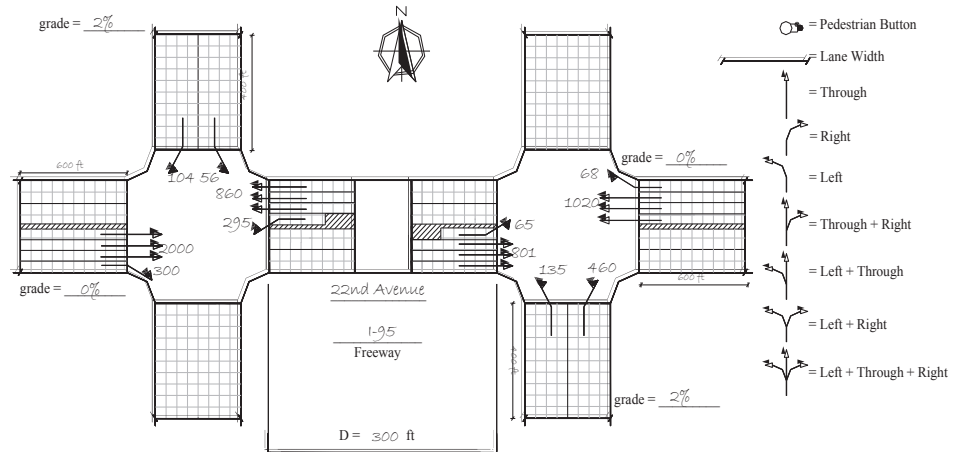


Exhibit 34-31
Example Problem 3:
Signalization Information

Phase	Intersection I			Intersection II		
	1	2	3	1	2	3
NEMA	Φ (4+7)	Φ (2+6)	Φ (1+6)	Φ (2+5)	Φ (2+6)	Φ (3+8)
Green time (s)	27	59	19	27	39	39
Yellow + all red (s)	5	5	5	5	5	5
Offset (s)		0			0	

The Question

What are the control delay, queue storage ratio, and LOS for this interchange?

The Facts

There are no closely spaced intersections to this interchange, and it operates as a pretimed signal with no right turns on red allowed. Travel path radii are 50 ft for all turning movements except the eastbound and westbound left movements, which have radii of 75 ft. Extra distance traveled along each freeway ramp is 60 ft. The grade is 2% on the NB and SB approaches.

There are 6.1% heavy vehicles on both the external and the internal through movements, and the PHF for the interchange is 0.97. Start-up lost time and extension of effective green are both 2 s for all approaches. During the analysis period, there is no parking, and no buses, bicycles, or pedestrians utilize the interchange.

Solution

Calculation of Origin–Destination Movements

O-Ds through this diamond interchange are calculated on the basis of the worksheet provided in Exhibit 34-169 in Section 4. Since all movements utilize

the signal, O-Ds can be calculated directly from the turning movements at the two intersections. The results of these calculations and the PHF-adjusted values are presented in Exhibit 34-32.

O-D Movement	Demand (veh/h)	PHF-Adjusted Demand (veh/h)
A	135	139
B	460	474
C	104	107
D	56	58
E	1,255	1,294
F	300	309
G	68	70
H	295	304
I	745	768
J	725	747
K	0	0
L	0	0
M	0	0
N	0	0

Exhibit 34-32
Example Problem 3: Adjusted O-D Table

Lane Utilization and Saturation Flow Rate Calculations

This interchange consists of external approaches with three through lanes and an exclusive right-turn lane. The lane utilization for Lane 1 is predicted by using the three-lane model of Exhibit 23-24. Since there is an exclusive right-turn lane for both external approaches, according to the first note of Exhibit 23-24 the lane utilization for Lane 3 should be estimated by assuming that the right-turning O-D (v_r, v_c) is zero. Exhibit 34-33 presents the calculation results and the lane utilization factor for each approach.

Approach	V_1	V_2	V_3	Maximum Lane Utilization	Lane Utilization Factor
3-lane EB	0.5551	0.2224	0.2224	0.5551	0.6005
3-lane WB	0.4441	0.2779	0.2779	0.4441	0.7506

Notes: EB = eastbound, WB = westbound.

Exhibit 34-33
Example Problem 3: Lane Utilization Adjustment Calculations

Saturation flow rates are calculated on the basis of reductions in the base saturation flow rate of 1,900 pc/hg/ln by using Equation 23-14. The lane utilization of the approaches external to the interchange is obtained as shown above in Exhibit 34-6. Traffic pressure is calculated by using Equation 23-15. The left- and right-turn adjustment factors are estimated by using Equations 23-20 through 23-23. These equations use an adjustment factor for travel path radius calculated by Equation 23-19. The remaining adjustment factors are calculated as indicated in Chapter 19, Signalized Intersections. The results of these calculations for all approaches are presented in Exhibit 34-34 and Exhibit 34-35.

Exhibit 34-34

Example Problem 3:
Saturation Flow Rate
Calculation for Eastbound and
Westbound Approaches

Value	Eastbound				Westbound			
	EXT-TH	EXT-R	INT-TH	INT-L	EXT-TH	EXT-R	INT-TH	INT-L
Base saturation flow (s_0 , pc/hg/ln)	1,900	1,900	1,900	1,900	1,900	1,900	1,900	1,900
Number of lanes (N)	3	1	3	1	3	1	3	1
Lane width adjustment (f_w)	1.000	1.000	1.000	1.000	1.000	1.000	1.000	1.000
Heavy vehicle and grade adjustment (f_{HVg})	0.952	1.000	0.952	1.000	0.952	1.000	0.952	1.000
Parking adjustment (f_p)	1.000	1.000	1.000	1.000	1.000	1.000	1.000	1.000
Bus blockage adjustment (f_{bb})	1.000	1.000	1.000	1.000	1.000	1.000	1.000	1.000
Area type adjustment (f_a)	1.000	1.000	1.000	1.000	1.000	1.000	1.000	1.000
Lane utilization adjustment (f_{LU})	0.600	1.000	0.908	1.000	0.751	1.000	0.908	1.000
Left-turn adjustment (f_{LT})	1.000	1.000	1.000	0.930	1.000	1.000	1.000	0.930
Right-turn adjustment (f_{RT})	1.000	0.899	1.000	1.000	1.000	0.899	1.000	1.000
Left-turn pedestrian-bicycle adjustment (f_{LPB})	1.000	1.000	1.000	1.000	1.000	1.000	1.000	1.000
Right-turn pedestrian-bicycle adjustment (f_{RPB})	1.000	1.000	1.000	1.000	1.000	1.000	1.000	1.000
Turn radius adjustment for lane group (f_R)	1.000	0.899	1.000	0.930	1.000	0.899	1.000	0.930
Traffic pressure adjustment for lane group (f_v)	1.043	0.980	0.975	0.948	0.987	0.945	0.978	0.998
Adjusted saturation flow (s , veh/hg/ln)	3,400	1,675	4,807	1,676	4,021	1,614	4,822	1,764

Notes: EXT = external, INT = internal, TH = through, R = right, L = left.

Exhibit 34-35

Example Problem 3:
Saturation Flow Rate
Calculation for Northbound
and Southbound Approaches

Value	Northbound		Southbound	
	Left	Right	Left	Right
Base saturation flow (s_0 , pc/hg/ln)	1,900	1,900	1,900	1,900
Number of lanes (N)	1	1	1	1
Lane width adjustment (f_w)	1.000	1.000	1.000	1.000
Heavy vehicle adjustment (f_{HV})	1.000	1.000	1.000	1.000
Grade adjustment (f_g)	0.990	0.990	0.990	0.990
Parking adjustment (f_p)	1.000	1.000	1.000	1.000
Bus blockage adjustment (f_{bb})	1.000	1.000	1.000	1.000
Area type adjustment (f_a)	1.000	1.000	1.000	1.000
Lane utilization adjustment (f_{LU})	1.000	1.000	1.000	1.000
Left-turn adjustment (f_{LT})	0.899	1.000	0.899	1.000
Right-turn adjustment (f_{RT})	1.000	0.899	1.000	0.899
Left-turn pedestrian-bicycle adjustment (f_{LPB})	1.000	1.000	1.000	1.000
Right-turn pedestrian-bicycle adjustment (f_{RPB})	1.000	1.000	1.000	1.000
Turn radius adjustment for lane group (f_R)	0.899	0.899	0.899	0.899
Traffic pressure adjustment for lane group (f_v)	0.963	1.007	0.946	0.950
Adjusted saturation flow (s , veh/hg/ln)	1,628	1,703	1,600	1,606

Common Green and Lost Time due to Downstream Queue and Demand Starvation Calculations

Exhibit 34-36 first provides the beginning and ending of the green time for each phase at the two intersections, on the assumption that Phase 1 of the first intersection begins at time zero. In this case, the offset for both intersections is zero; therefore, the beginning of Phase 1 for the second intersection is also zero.

Phase	Intersection I		Intersection II		
	Green Begin	Green End	Green Begin	Green End	
Phase 1	0	27	0	27	
Phase 2	32	91	32	71	
Phase 3	96	115	76	115	
Movement	First Green Time Within Cycle		Second Green Time Within Cycle		Common Green Time
	Begin	End	Begin	End	
EB EXT THRU	32.0	91.0			39
EB INT THRU	0.0	71.0			
WB EXT THRU	32.0	71.0			39
WB INT THRU	32.0	115.0			
SB RAMP	0.0	27.0			27
EB INT THRU	0.0	71.0			
NB RAMP	76.0	115.0			39
WB INT THRU	32.0	115.0			
WB INT LEFT	96.0	115.0			0
EB INT THRU	0.0	71.0			
EB INT LEFT	0.0	27.0			0
WB INT THRU	32.0	115.0			

Notes: EXT = external, INT = internal, EB = eastbound, WB = westbound, NB = northbound, SB = southbound, THRU = through.

The next step involves the calculation of lost time due to downstream queues. First, the queues at the beginning of the upstream arterial phase and at the beginning of the upstream ramp phase must be calculated by using Equation 23-33 and Equation 23-34, respectively. Exhibit 34-37 presents the calculation of these downstream queues followed by the calculation of the respective lost time due to those queues. As shown, the SB-L movement has additional lost time of 5.5 s due to the downstream queue.

The lost time due to demand starvation is calculated by using Equation 23-38. The respective calculations are presented in Exhibit 34-38. As shown, in this case there is no lost time due to demand starvation.

Value	Movement			
	EB EXT-TH	SB-L	WB EXT-TH	NB-L
<i>Downstream Queue Calculations</i>				
V_R or V_A (veh/h)	58	2,062	139	1,052
N_R or N_A	1	3	1	3
G_R or G_A (s)	27	59	39	39
G_D (s)	71	71	83	83
C (s)	120	120	120	120
CG_{LD} or CG_{RD} (s)	39.0	27.0	39.0	39.0
Queue length (Q_A or Q_R) (ft)	0.0	108.60	0.0	0.0
<i>Lost Time Calculations</i>				
G_R or G_A (s)	59	27	39	39
C (s)	120	120	120	120
D_{QA} or D_{QR} (ft)	300	191	300	300
CG_{LD} or CG_{RD} (s)	39.0	27	39	39
Additional lost time, L_{D-A} or L_{D-R} (s)	0.0	5.5	0.0	0.0
Total lost time, t'_L (s)	5.0	10.5	5.0	5.0
Effective green time, g' (s)	59.0	21.5	39.0	39.0

Notes: EXT = external, TH = through, L = left, EB = eastbound, WB = westbound, NB = northbound, SB = southbound.

Exhibit 34-36
Example Problem 3: Common Green Calculations

Exhibit 34-37
Example Problem 3: Lost Time due to Downstream Queues

Exhibit 34-38

Example Problem 3: Lost Time due to Demand Starvation Calculations

Value	Movement	
	EB-INT-TH	WB-INT-TH
V_{Ramp-L} (veh/h)	58	139
$V_{Arterial}$ (veh/h)	2,062	1,052
C (s)	120	120
N_{Ramp-L}	1	1
$N_{Arterial}$	3	3
CG_{RD} (s)	27	39
CG_{UD} (s)	39	39
H_I	2.25	2.24
$Q_{initial}$ (ft)	0	0
CG_{DS} (s)	0	0
L_{DS} (s)	0	0
t''_L (s)	5	5
Effective green time, g'' (s)	71	83

Notes: EB-INT-TH = eastbound internal through, WB-INT-TH = westbound internal through.

Queue Storage and Control Delay

The queue storage ratio is estimated as the ratio of the average maximum queue to the available queue storage by using Equation 31-154. Exhibit 34-39 and Exhibit 34-40 present the calculations of the queue storage ratio for all movements. Those exhibits also provide the v/c ratio for each movement. Control delay for each movement is calculated according to Equation 19-18. Exhibit 34-41 and Exhibit 34-42 provide the control delay for each movement of the interchange.

Exhibit 34-39

Example Problem 3: Queue Storage Ratio for Eastbound and Westbound Movements

Value	Eastbound Movements				Westbound Movements			
	EXT-TH	EXT-R	INT-L	INT-TH	EXT-TH	EXT-R	INT-L	INT-TH
Q_{bl} (ft)	0.0	0.0	0.0	0.0	0.0	0.0	0.0	0.0
v (veh/h/ln group)	2,062	309	67	826	1,052	70	304	887
s (veh/h/ln)	1,133	1,675	1,676	1,602	1,340	1,614	1,764	1,607
g (s)	59.0	59.0	27.0	71.0	39.0	39.0	19.0	83.0
g/C	0.49	0.49	0.23	0.59	0.33	0.33	0.16	0.69
I	1.00	1.00	0.09	0.09	1.00	1.00	0.49	0.49
c (veh/h/ln group)	1,672	824	377	2,844	1,307	524	279	3,336
$X = v/c$	1.23	0.38	0.18	0.29	0.80	0.13	1.09	0.27
r_a (ft/s ²)	3.5	3.5	3.5	3.5	3.5	3.5	3.5	3.5
r_d (ft/s ²)	4	4	4	4	4	4	4	4
S_s (mi/h)	5	5	5	5	5	5	5	5
S_{pl} (mi/h)	40	40	40	40	40	40	40	40
S_a (mi/h)	39.96	39.96	39.96	39.96	39.96	39.96	39.96	39.96
d_s (s)	12.04	12.04	12.04	12.04	12.04	12.04	12.04	12.04
RP	1	1	1	1.333	1	1	1	1.333
P	0.49	0.49	0.23	0.79	0.33	0.33	0.16	0.92
r (s)	61.00	61.00	93.00	49.00	81.00	81.00	101.00	37.00
t_r (s)	0.02	0.00	0.00	0.00	0.01	0.00	0.01	0.00
q (veh/s)	0.57	0.09	0.02	0.23	0.29	0.02	0.08	0.25
q_B (veh/s)	0.57	0.09	0.02	0.31	0.29	0.02	0.08	0.33
q_T (veh/s)	0.57	0.09	0.02	0.12	0.29	0.02	0.08	0.06
Q_1 (veh)	14.9	5.2	1.6	1.6	9.1	1.4	8.2	0.5
Q_2 (veh)	17.1	0.3	0.0	0.0	0.6	0.1	5.0	0.1
T	0.25	0.25	0.25	0.25	0.25	0.25	0.25	0.25
Q_{ev} (veh)	97.50	0.00	0.00	0.00	0.00	0.00	6.22	0.00
t_a	0.25	0	0	0	0	0	0.25	0
Q_e (veh)	97.50	0.00	0.00	0.00	0.00	0.00	6.22	0.00
Q_b (veh)	0	0	0	0	0	0	0	0
Q_s (veh)	0.0	0.0	0.0	0.0	0.0	0.0	0.0	0.0
Q (veh)	32.0	5.5	1.6	1.6	9.7	1.5	13.2	0.6
L_h (ft)	25	25	25	25	25	25	25	25
L_s (ft)	600	600	200	300	600	600	200	300
R_Q	1.33	0.23	0.20	0.13	0.41	0.06	1.65	0.12

Notes: EXT = external, INT = internal, TH = through, R = right, L = left.

Value	Northbound Movements		Southbound Movements	
	Left	Right	Left	Right
Q_{bl} (ft)	0.0	0.0	0.0	0.0
v (veh/h/ln group)	139	474	58	107
s (veh/h/ln)	1,628	1,703	1,600	1,607
g (s)	39.0	39.0	22.0	27.0
g/C	0.33	0.33	0.18	0.23
I	1.00	1.00	1.00	1.00
c (veh/h/ln group)	529	553	287	362
$X = v/c$	0.26	0.86	0.20	0.30
r_a (ft/s ²)	3.5	3.5	3.5	3.5
r_d (ft/s ²)	4	4	4	4
S_s (mi/h)	5	5	5	5
S_{pl} (mi/h)	40	40	40	40
S_b (mi/h)	39.96	39.96	39.96	39.96
d_a (s)	12.04	12.04	12.04	12.04
Rp	1	1	1	1
P	0.33	0.33	0.18	0.23
r (s)	81.00	81.00	98.50	93.00
t_r (s)	0.00	0.01	0.00	0.00
q (veh/s)	0.04	0.13	0.02	0.03
q_g (veh/s)	0.04	0.13	0.02	0.03
q_r (veh/s)	0.04	0.13	0.02	0.03
Q_1 (veh)	2.9	12.6	1.4	2.6
Q_2 (veh)	0.2	2.4	0.1	0.2
T	0.25	0.25	0.25	0.25
Q_{eo} (veh)	0.0	0.0	0.0	0.0
t_a	0.0	0.0	0.0	0.0
Q_e (veh)	0.0	0.0	0.0	0.0
Q_b (veh)	0.0	0.0	0.0	0.0
Q_s (veh)	0.0	0.0	0.0	0.0
Q (veh)	3.1	15.0	1.6	2.8
L_h (ft)	25	25	25	25
L_a (ft)	400	400	400	400
R_Q	0.19	0.94	0.10	0.17

Exhibit 34-40

Example Problem 3: Queue Storage Ratio for Northbound and Southbound Movements

Value	Eastbound Movements				Westbound Movements			
	EXT-TH	EXT-R	INT-L	INT-TH	EXT-TH	EXT-R	INT-L	INT-TH
g (s)	-	59	27	71	-	39	19	83
g' (s)	59	-	-	-	39	-	-	-
g/C or g'/C	0.49	0.49	0.23	0.59	0.33	0.33	0.16	0.69
c (veh/h)	1,672	824	377	2,844	1,307	524	279	3,336
$X = v/c$	1.23	0.38	0.18	0.29	0.80	0.13	1.09	0.27
d_1 (s/veh)	30.5	19.0	37.5	5.8	37.0	28.6	50.5	1.5
k	0.5	0.5	0.5	0.5	0.5	0.5	0.5	0.5
d_2 (s/veh)	110.5	1.3	0.1	0.0	5.4	0.5	64.1	0.1
d_3 (s/veh)	0	0	0	0	0	0	0	0
PF	1.000	1.000	1.000	0.595	1.000	1.000	1.000	0.291
K_{min}	0.04	0.04	0.04	0.04	0.04	0.04	0.04	0.04
u	0	0	0	0	0	0	0	0
t	0	0	0	0	0	0	0	0
d (s/veh)	141.0	20.3	37.6	5.8	42.4	29.1	114.6	1.6

Notes: EXT = external, INT = internal, TH = through, R = right, L = left.

Exhibit 34-41

Example Problem 3: Control Delay for Eastbound and Westbound Movements

Exhibit 34-42

Example Problem 3: Control Delay for Northbound and Southbound Movements

Value	Northbound Movements		Southbound Movements	
	Left	Right	Left	Right
g (s)	-	39	-	27
g' (s)	39	-	21.5	-
g/C or g'/C	0.33	0.33	0.18	0.23
c (veh/h)	529	553	287	361
$X = v/c$	0.26	0.86	0.20	0.30
d_1 (s/veh)	29.9	37.9	41.9	38.6
k	0.5	0.5	0.5	0.5
d_2 (s/veh)	1.2	15.7	1.6	2.1
d_3 (s/veh)	0.0	0.0	0.0	0.0
PF	1.000	1.000	1.000	1.000
k_{min}	0.04	0.04	0.04	0.04
u	0	0	0	0
t	0	0	0	0
d (s/veh)	31.1	53.6	43.5	40.7

Results

Delay for each O-D is estimated as the sum of the movement delays for each movement utilized by the O-D, as indicated in Equation 23-2. Next, the v/c ratio and queue storage ratio are checked. If either of these parameters exceeds 1, the LOS for all O-Ds that utilize that movement is F. Exhibit 34-43 presents a summary of the results for all O-D movements at this interchange. As shown, v/c and R_Q for parts of O-Ds E, H, I, and M exceed 1; therefore, these O-Ds operate in LOS F. O-D E and O-D I include the EB external through movement, while O-D H and O-D M include the WB internal left. These movements have v/c ratios exceeding 1. The remaining movements have v/c and queue storage ratios less than 1; the LOS for these O-D movements is determined by using Exhibit 23-10. After extra distances are measured according to the Exhibit 23-8 discussion, EDTT can be obtained from Equation 23-50 [i.e., $EDTT = 60 / (1.47 \times 35) + 0 = 1.2$ s/veh]. Intersectionwide performance measures are not calculated for interchange ramp terminals.

Exhibit 34-43

Example Problem 3: O-D Movement LOS

O-D Movement	Control Delay (s/veh)	EDTT (s/veh)	ETT (s/veh)	$v/c > 1?$	$R_Q > 1?$	LOS
A	32.7	1.2	33.9	No	No	C
B	53.6	-1.2	52.4	No	No	C
C	40.7	-1.2	39.5	No	No	C
D	49.3	1.2	50.5	No	No	C
E	178.6	1.2	179.8	Yes	Yes	F
F	20.3	-1.2	19.1	No	No	B
G	29.1	-1.2	27.9	No	No	B
H	157.0	1.2	158.2	Yes	Yes	F
I	146.8	0.0	146.8	Yes	Yes	F
J	44.0	0.0	44.0	No	No	C

EXAMPLE PROBLEM 4: DIAMOND INTERCHANGE WITH DEMAND STARVATION

The Interchange

The interchange of I-75 (NB/SB) and Archer Road (EB/WB) is a diamond interchange. The traffic, geometric, and signalization conditions for this interchange are provided in Exhibit 34-44 and Exhibit 34-45. The offset is referenced to the beginning of green on the EB direction of the arterial.

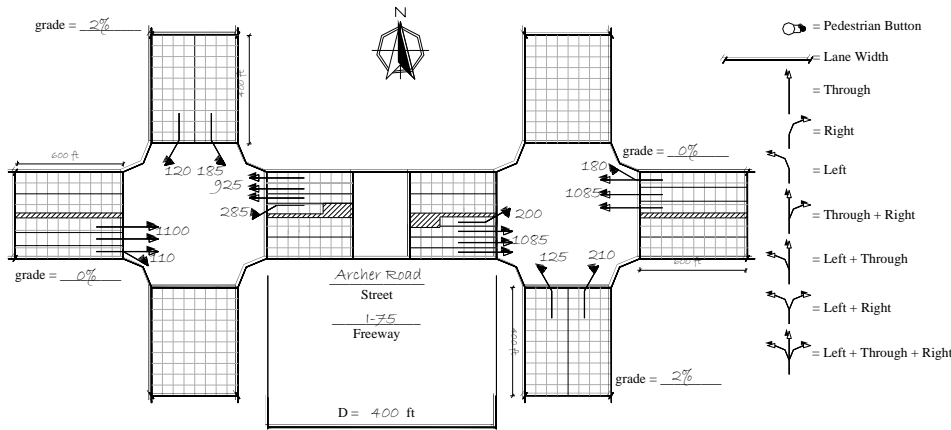


Exhibit 34-44
Example Problem 4:
Intersection Plan View

Phase	Intersection I			Intersection II		
	1	2	3	1	2	3
NEMA	$\Phi (1+6)$	$\Phi (2+6)$	$\Phi (4+7)$	$\Phi (2+6)$	$\Phi (2+5)$	$\Phi (3+8)$
Green time (s)	30	25	30	30	25	30
Yellow + all red (s)	5	5	5	5	5	5
Offset (s)		0			0	

Exhibit 34-45
Example Problem 4:
Signalization Information

The Question

What are the control delay, queue storage ratio, and LOS for this interchange?

The Facts

There are no closely spaced intersections to this interchange, and it operates as a pretimed signal with no right turns on red allowed. Travel path radii are 50 ft for all turning movements except the eastbound and westbound left, which are 75 ft. Extra distance traveled along each freeway ramp is 100 ft.

There are 6.1% heavy vehicles on both external and internal through movements, and the PHF for the interchange is estimated to be 0.97. Start-up lost time and extension of effective green are both 2 s for all approaches. During the analysis interval, there is no parking, and no buses, bicycles, or pedestrians utilize the interchange. The grade is 2% on the NB and SB approaches.

Solution

Calculation of Origin–Destination Movements

O-Ds through this diamond interchange are calculated by using the worksheet given in Exhibit 34-169 in Section 4. Since all movements utilize the signal, O-Ds can be calculated directly from the turning movements at the two intersections. The results of these O-D calculations and the PHF-adjusted values are presented in Exhibit 34-46.

Exhibit 34-46
Example Problem 4: Adjusted O-D Table

O-D Movement	Demand (veh/h)	PHF-Adjusted Demand (veh/h)
A	125	129
B	210	216
C	120	124
D	185	191
E	200	206
F	110	113
G	180	186
H	285	294
I	900	928
J	800	825
K	0	0
L	0	0
M	0	0
N	0	0

Lane Utilization and Saturation Flow Rate Calculations

This interchange consists of a three-lane shared right and through lane group for the external approaches. Use of the three-lane model from Exhibit 23-24 results in the predicted lane utilization percentages for the external through approaches that are presented in Exhibit 34-47.

Exhibit 34-47
Example Problem 4: Lane Utilization Adjustment Calculations

Approach	V_1	V_2	V_3	Maximum Lane Utilization	Lane Utilization Factor
3-lane EB	0.3879	0.2773	0.3348	0.3879	0.8593
3-lane WB	0.4032	0.2502	0.3465	0.4032	0.8266

Notes: EB = eastbound, WB = westbound.

Saturation flow rates are calculated on the basis of reductions in the base saturation flow rate of 1,900 pc/hg/ln by using Equation 23-14. The lane utilization of the approaches external to the interchange is obtained as shown above in Exhibit 34-6. Traffic pressure is calculated by using Equation 23-15. The left- and right-turn adjustment factors are estimated by using Equations 23-20 through 23-23. These equations use an adjustment factor for travel path radius calculated by Equation 23-19. The remaining adjustment factors are calculated as indicated in Chapter 19, Signalized Intersections. The results of the saturation flow rate calculations for all approaches are presented in Exhibit 34-48 and Exhibit 34-49.

Value	Eastbound			Westbound		
	EXT-TH&R	INT-TH	INT-L	EXT-TH&R	INT-TH	INT-L
Base saturation flow (s_0 , pc/hg/ln)	1,900	1,900	1,900	1,900	1,900	1,900
Number of lanes (N)	3	3	1	3	3	1
Lane width adjustment (f_w)	1.000	1.000	1.000	1.000	1.000	1.000
Heavy vehicle and grade adjustment (f_{HVg})	0.952	0.952	1.000	0.952	0.952	1.000
Parking adjustment (f_p)	1.000	1.000	1.000	1.000	1.000	1.000
Bus blockage adjustment (f_{bb})	1.000	1.000	1.000	1.000	1.000	1.000
Area type adjustment (f_a)	1.000	1.000	1.000	1.000	1.000	1.000
Lane utilization adjustment (f_{LU})	0.859	0.908	1.000	0.827	0.908	1.000
Left-turn adjustment (f_{LT})	1.000	1.000	0.930	1.000	1.000	0.930
Right-turn adjustment (f_{RT})	0.999	1.000	1.000	0.998	1.000	1.000
Left-turn pedestrian-bicycle adjustment (f_{LPb})	1.000	1.000	1.000	1.000	1.000	1.000
Right-turn pedestrian-bicycle adjustment (f_{RPb})	1.000	1.000	1.000	1.000	1.000	1.000
Turn radius adjustment for lane group (f_R)	0.991	1.000	0.930	0.986	1.000	0.930
Traffic pressure adjustment for lane group (f_i)	0.986	0.981	0.969	0.989	0.974	0.985
Adjusted saturation flow (s , veh/hg/ln)	4,597	4,834	1,714	4,428	4,799	1,741

Notes: EXT = external, INT = internal, TH = through, R = right, L = left.

Exhibit 34-48

Example Problem 4:
Saturation Flow Rate
Calculation for Eastbound and
Westbound Approaches

Value	Northbound		Southbound	
	Left	Right	Left	Right
Base saturation flow (s_0 , pc/hg/ln)	1,900	1,900	1,900	1,900
Number of lanes (N)	1	1	1	1
Lane width adjustment (f_w)	1.000	1.000	1.000	1.000
Heavy vehicle and grade adjustment (f_{HVg})	0.990	0.990	0.990	0.990
Parking adjustment (f_p)	1.000	1.000	1.000	1.000
Bus blockage adjustment (f_{bb})	1.000	1.000	1.000	1.000
Area type adjustment (f_a)	1.000	1.000	1.000	1.000
Lane utilization adjustment (f_{LU})	1.000	1.000	1.000	1.000
Left-turn adjustment (f_{LT})	0.899	1.000	0.899	1.000
Right-turn adjustment (f_{RT})	1.000	0.899	1.000	0.899
Left-turn pedestrian-bicycle adjustment (f_{LPb})	1.000	1.000	1.000	1.000
Right-turn pedestrian-bicycle adjustment (f_{RPb})	1.000	1.000	1.000	1.000
Turn radius adjustment for lane group (f_R)	0.899	0.899	0.899	0.899
Traffic pressure adjustment for lane group (f_i)	0.956	0.961	0.967	0.949
Adjusted saturation flow (s , veh/hg/ln)	1,617	1,625	1,635	1,605

Exhibit 34-49

Example Problem 4:
Saturation Flow Rate
Calculation for Northbound
and Southbound Approaches

Common Green and Lost Time due to Downstream Queue and Demand Starvation Calculations

Exhibit 34-50 presents the beginning and end times of the green for each phase at the two intersections. Phase 1 of the first intersection is assumed to begin at time zero. In this case the offset for both intersections is zero; therefore the beginning of Phase 1 for the second intersection is also zero.

Exhibit 34-50

Example Problem 4: Common Green Calculations

Phase	Intersection I		Intersection II		
	Green Begin	Green End	Green Begin	Green End	
Phase 1	0	30	0	30	
Phase 2	35	60	35	60	
Phase 3	65	95	65	95	
Movement	First Green Time Within Cycle		Second Green Time Within Cycle		Common Green Time
	Begin	End	Begin	End	
EB EXT THRU	35	60			25
EB INT THRU	0	60			
WB EXT THRU	0	30			30
WB INT THRU	0	60			
SB RAMP	65	95			0
EB INT THRU	35	60			
NB RAMP	65	95			0
WB INT THRU	0	60			
WB INT LEFT	0	30			30
EB INT THRU	0	60			
EB INT LEFT	35	60			25
WB INT THRU	0	60			

Notes: EXT = external, INT = internal, EB = eastbound, WB = westbound, NB = northbound, SB = southbound, THRU = through.

The next step involves the calculation of lost time due to downstream queues. First, the queues at the beginning of the upstream arterial phase and at the beginning of the upstream ramp phase must be calculated by using Equation 23-33 and Equation 23-34, respectively. Exhibit 34-51 presents the calculation of these downstream queues followed by the calculation of the respective lost time due to those queues. As shown, there is no additional lost time due to downstream queues.

Exhibit 34-51

Example Problem 4: Lost Time due to Downstream Queues

Value	Movement			
	EB EXT-TH	SB-L	WB EXT-TH	NB-L
<i>Downstream Queue Calculations</i>				
V_R or V_A (veh/h)	191	1,134	129	1,119
N_R or N_A	1	3	1	3
G_R or G_A (s)	30	25	30	30
G_D (s)	60	60	60	60
C (s)	100	100	100	100
CG_{UD} or CG_{RD} (s)	25	0	30	0
Queue length (Q_A or Q_R) (ft)	0.0	31.5	0.0	40
<i>Lost Time Calculations</i>				
G_R or G_A (s)	25	30	30	30
C (s)	100	100	100	100
D_{QA} or D_{QR} (ft)	400	369	400	360
CG_{UD} or CG_{RD} (s)	25	0	30	0
Additional lost time, L_{D-A} or L_{D-R} (s)	0	0	0	0
Total lost time, t'_L (s)	5	5	5	5
Effective green time, g' (s)	25	30	30	30

Notes: EXT = external, EB = eastbound, WB = westbound, NB = northbound, SB = southbound, TH = through, L = left.

The lost time due to demand starvation is calculated by using Equation 23-38. The respective calculations are presented in Exhibit 34-52. As shown, both internal through movements experience lost time due to demand starvation.

Value	Movement	
	EB-INT-TH	WB-INT-TH
V_{Ramp-L} (veh/h)	191	129
$V_{Arterial}$ (veh/h)	1,134	1,119
C (s)	100	100
N_{Ramp-L}	1	1
$N_{Arterial}$	3	3
CG_{RD} (s)	5	5
CG_{UD} (s)	25	30
H_I	2.23	2.25
$Q_{initial}$ (ft)	6.8	2.8
CG_{DS} (s)	30	25
L_{DS} (s)	14.7	18.6
t'_L (s)	19.7	23.6
Effective green time, g'' (s)	45.3	41.4

Notes: EB-INT-TH = eastbound internal through, WB-INT-TH = westbound internal through.

Queue Storage and Control Delay

The queue storage ratio is estimated as the ratio of the average maximum queue to the available queue storage by using Equation 31-154. Exhibit 34-53 and Exhibit 34-54 present the calculations of the queue storage ratio for all movements. These exhibits also provide the v/c ratios for all movements. Control delay for each movement is calculated according to Equation 19-18. Exhibit 34-55 and Exhibit 34-56 provide the control delay for each movement of the interchange.

Value	Eastbound Movements			Westbound Movements		
	EXT-TH&R	INT-L	INT-TH	EXT-TH&R	INT-L	INT-TH
Q_{bl} (ft)	0.0	0.0	0.0	0.0	0.0	0.0
v (veh/h/ln group)	1,247	206	1,119	1,304	294	954
s (veh/h/ln)	1,532	1,714	1,611	1,476	1,741	1,600
g (s)	25	25	45	30	30	41
g/C	0.25	0.25	0.45	0.30	0.30	0.41
I	1.00	0.09	0.09	1.00	0.13	0.13
c (veh/h/ln group)	1,198	428	2,190	1,383	522	1,987
$X = v/c$	1.04	0.48	0.51	0.94	0.56	0.48
r_a (ft/s ²)	3.5	3.5	3.5	3.5	3.5	3.5
r_d (ft/s ²)	4	4	4	4	4	4
S_s (mi/h)	5	5	5	5	5	5
S_{pl} (mi/h)	40	40	40	40	40	40
S_a (mi/h)	39.96	39.96	39.96	39.96	39.96	39.96
d_s (s)	12.04	12.04	12.04	12.04	12.04	12.04
R_D	1.000	1.000	1.333	1.000	1.000	1.333
P	0.25	0.25	0.60	0.30	0.30	0.55
r (s)	75.00	75.00	54.71	70.00	70.00	58.64
t_r (s)	0.01	0.00	0.00	0.01	0.00	0.00
q (veh/s)	0.35	0.06	0.31	0.36	0.08	0.26
q_B (veh/s)	0.35	0.06	0.41	0.36	0.08	0.35
q_r (veh/s)	0.35	0.06	0.23	0.36	0.08	0.20
Q_1 (veh)	9.2	4.1	3.8	9.8	5.7	3.7
Q_2 (veh)	5.5	0.0	0.0	3.0	0.1	0.0
T	0.25	0.25	0.25	0.25	0.25	0.25
Q_{ev} (veh)	24.54	0.00	0.00	0.00	0.00	0.00
t_a	0.25	0	0	0	0	0
Q_e (veh)	24.54	0.00	0.00	0.00	0.00	0.00
Q_b (veh)	0	0	0	0	0	0
Q_s (veh)	0.0	0.0	0.0	0.0	0.0	0.0
Q (veh)	14.7	4.1	3.9	12.8	5.8	3.7
L_h (ft)	25	25	25	25	25	25
L_s (ft)	600	200	400	600	200	400
R_Q	0.61	0.52	0.24	0.53	0.72	0.23

Notes: EXT = external, INT = internal, TH = through, R = right, L = left.

Exhibit 34-52

Example Problem 4: Lost Time due to Demand Starvation Calculations

Exhibit 34-53

Example Problem 4: Queue Storage Ratio for Eastbound and Westbound Movements

Exhibit 34-54

Example Problem 4: Queue Storage Ratio for Northbound and Southbound Movements

Value	Northbound Movements		Southbound Movements	
	Left	Right	Left	Right
Q_{bl} (ft)	0.0	0.0	0.0	0.0
v (veh/h/ln group)	129	216	191	124
s (veh/h/ln)	1,617	1,625	1,635	1,606
g (s)	30	30	30	30
g/C	0.30	0.30	0.30	0.30
I	1.00	1.00	1.00	1.00
c (veh/h/ln group)	485	487	491	482
$X = v/c$	0.27	0.44	0.39	0.26
r_a (ft/s ²)	3.5	3.5	3.5	3.5
r_d (ft/s ²)	4	4	4	4
S_s (mi/h)	5	5	5	5
S_{pl} (mi/h)	40	40	40	40
S_s (mi/h)	39.96	39.96	39.96	39.96
d_b (s)	12.04	12.04	12.04	12.04
Rp	1.00	1.00	1.00	1.00
P	0.30	0.30	0.30	0.30
r (s)	70.00	70.00	70.00	70.00
t_r (s)	0.00	0.00	0.00	0.00
q (veh/s)	0.04	0.06	0.05	0.03
q_g (veh/s)	0.04	0.06	0.05	0.03
q_r (veh/s)	0.04	0.06	0.05	0.03
Q_1 (veh)	2.3	4.0	3.5	2.2
Q_2 (veh)	0.2	0.4	0.3	0.2
T	0.25	0.25	0.25	0.25
Q_{e0} (veh)	0.00	0.00	0.00	0.00
t_a	0	0	0	0
Q_e (veh)	0.00	0.00	0.00	0.00
Q_b (veh)	0	0	0	0
Q_s (veh)	0.0	0.0	0.0	0.0
Q (veh)	2.4	4.4	3.8	2.3
L_h (ft)	25	25	25	25
L_s (ft)	400	400	400	400
R_Q	0.15	0.28	0.24	0.15

Exhibit 34-55

Example Problem 4: Control Delay for Eastbound and Westbound Movements

Value	Eastbound Movements			Westbound Movements		
	EXT-TH&R	INT-L	INT-TH	EXT-TH&R	INT-L	INT-TH
g (s)	-	25	45	-	30	41
g' (s)	25	-	-	30	-	-
g/C or g'/C	0.25	0.25	0.45	0.30	0.30	0.41
c (veh/h)	1,198	428	2,190	1,385	522	1,985
$X = v/c$	1.04	0.48	0.51	0.94	0.56	0.48
d_1 (s/veh)	37.4	32.0	13.5	34.2	29.5	15.8
k	0.5	0.5	0.5	0.5	0.5	0.5
d_2 (s/veh)	50.3	0.3	0.1	23.7	0.6	0.1
d_3 (s/veh)	0.0	0.0	0.0	0.0	0.0	0.0
PF	1.000	1.000	0.863	1.000	1.000	0.902
K_{min}	0.04	0.04	0.04	0.04	0.04	0.04
u	0	0	0	0	0	0
t	0	0	0	0	0	0
d (s/veh)	87.6	32.3	13.5	57.9	30.1	16.0

Notes: EXT = external, INT = internal, TH = through, R = right, L = left.

Value	Northbound Movements		Southbound Movements	
	Left	Right	Left	Right
g (s)	-	30	-	30
g' (s)	30	-	30	-
g/C or g'/C	0.30	0.30	0.30	0.30
c (veh/h)	485	487	490	482
$X = v/c$	0.27	0.44	0.39	0.26
d_1 (s/veh)	26.6	28.3	27.7	26.5
k	0.5	0.5	0.5	0.5
d_2 (s/veh)	1.3	2.9	2.3	1.3
d_3 (s/veh)	0.0	0.0	0.0	0.0
PF	1.000	1.000	1.000	1.000
k_{min}	0.04	0.04	0.04	0.04
u	0	0	0	0
t	0	0	0	0
d (s/veh)	28.0	31.2	30.1	27.8

Exhibit 34-56

Example Problem 4: Control Delay for Northbound and Southbound Movements

Results

Delay for each O-D is estimated as the sum of the movement delays for each movement utilized by the O-D, as indicated in Equation 23-2. Next, the v/c and queue storage ratios are checked. If either of these parameters exceeds 1, the LOS for all O-Ds that utilize that movement is F. Exhibit 34-57 summarizes the results for all O-D movements at this interchange. As shown, the v/c ratio exceeds 1 for O-D Movements E, F, and I, all of which include the EB external through and right movements. Therefore, these O-D movements operate in LOS F. The remaining movements have v/c and queue storage ratios less than 1; the LOS is determined by using Exhibit 23-10 for these movements. After extra distances are measured according to the Exhibit 23-8 discussion, EDTT can be obtained from Equation 23-50 [i.e., $EDTT = 80 / (1.47 \times 35) + 0 = 1.6$ s/veh]. Intersectionwide performance measures are not calculated for interchange ramp terminals.

O-D Movement	Control Delay (s/veh)	EDTT (s/veh)	ETT (s/veh)	$v/c > 1?$	$R_0 > 1?$	LOS
A	43.9	1.6	45.5	No	No	C
B	31.2	-1.6	29.6	No	No	B
C	27.8	-1.6	26.2	No	No	B
D	43.6	1.6	45.2	No	No	C
E	119.9	1.6	121.5	Yes	No	F
F	87.6	-1.6	86.0	Yes	No	F
G	57.9	-1.6	56.3	No	No	D
H	88.0	1.6	89.6	No	No	E
I	101.1	0.0	101.1	Yes	No	F
J	73.9	0.0	73.9	No	No	D

Exhibit 34-57

Example Problem 4: O-D Movement LOS

EXAMPLE PROBLEM 5: DIVERGING DIAMOND INTERCHANGE WITH SIGNAL CONTROL

The Interchange

The interchange of Main Street at Interstate I-40 is a diverging diamond interchange (DDI) with signalized right turns and left turns controlling movements from the freeway onto the Main Street arterial. The turning movements onto the freeway from Main Street are not signalized. The traffic, geometric, and signalization conditions of the interchange are provided in Exhibit 34-58 and Exhibit 34-59.

Exhibit 34-58
Example Problem 5: DDI
Geometry, Lane, and Volume Inputs

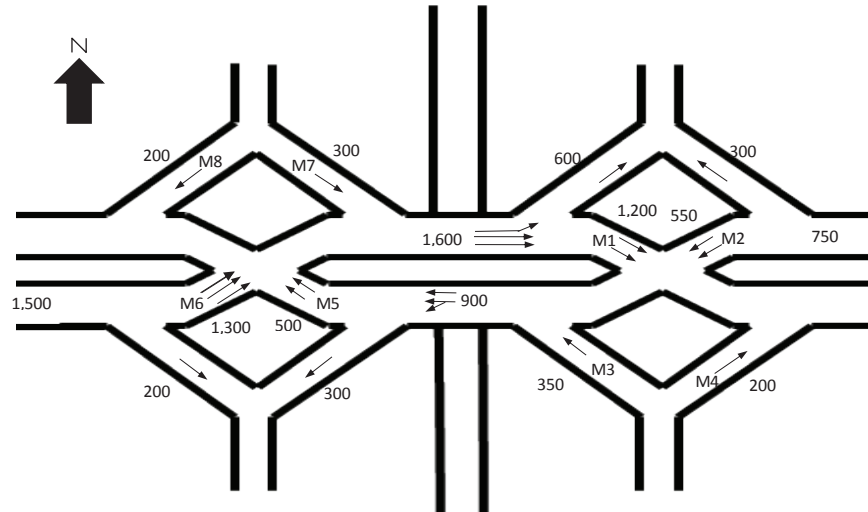


Exhibit 34-58 shows movement numbers M1 through M8, their associated volume levels (in vehicles per hour), and the number of lanes for each movement approach. Note that the eastbound movement has an exclusive left-turn lane onto the freeway between crossovers, which is carried through the external crossover at Movement M6. For the westbound movement, the left turn onto the freeway is made from a shared lane, which is expected to affect the lane utilization of Movement M2.

The Question

What are the control delays, experienced travel time, and LOS for this interchange?

The Facts

There are no closely spaced intersections to this interchange, and it operates as a pretimed signal with no right turns on red allowed. Travel path radii are 75 ft for right-turn movements and 150 ft for left turns.

There are 6.1% heavy vehicles for all movements, and the PHF for the interchange is 0.95. Start-up lost time and extension of effective green are both 2 s for all approaches. During the analysis period, there is no parking, and no buses, bicycles, or pedestrians utilize the interchange.

Exhibit 34-59 provides basic signal timing information for the DDI. The cycle length is set at 70 s for this pretimed signal. The arterial street free-flow speed is 35 mi/h.

Movement	West Crossover				East Crossover			
	M5	M6	M7	M8	M1	M2	M3	M4
Green time (s)	25	35	25	35	35	25	35	25
Yellow time (s)	4	4	4	4	4	4	4	4
All-red time (s)	1	1	1	1	1	1	1	1
Phase split (s)	30	40	30	40	40	30	40	30
Turn radius (ft)			150	75			150	75
Width of clear zone (ft)			200	100			200	100
Shortest distance, stop bar to conflict point (ft)			20	60			20	60
Volume (veh/h)	500	1,300	300	200	1,000	450	350	200

Exhibit 34-59
Example Problem 5: Signal Timing and Volume Inputs

The DDI is timed with two critical phases to allow the northbound and southbound through movements to be processed through the interchange sequentially. The signalized right-turn movements from the freeway move concurrently with the inbound through movement into the interchange at each crossover, and the left turns move concurrently with the outbound through movements. Overlap phasing is used to reduce the lost time for the through movement while providing adequate clearance times for the turning traffic. In the methodology, this results in additional lost time applied to the ramp movements (Step 4 of DDI methodology in Chapter 23).

Solution

Calculation of Origin–Destination Movements

O-D movements through this diamond interchange are calculated by using the worksheet in Exhibit 34-169 in Section 4. Because all movements utilize the signal, O-Ds can be calculated directly from the turning movements at the two intersections. The results of these calculations and the PHF-adjusted values are presented in Exhibit 34-60.

O-D Movement	Demand (veh/h)	PHF-Adjusted Demand (veh/h)
A	350	368
B	200	211
C	200	211
D	300	316
E	600	632
F	200	211
G	300	316
H	300	316
I	700	737
J	150	158
K	0	0
L	0	0
M	0	0
N	0	0

Exhibit 34-60
Example Problem 5: Adjusted O-D Table

Lane Utilization and Saturation Flow Rate Calculations

Lane utilization for DDIs is calculated by using Exhibit 23-26 for the two external approaches to the DDI. The eastbound movement has an exclusive left-turn lane onto the freeway between crossovers, which is carried through the external crossover at Movement M6. For the westbound movement, the left turn onto the freeway is made from a shared lane, which is expected to affect lane utilization at Movement M2. The calculated maximum lane utilization and associated lane utilization factors are shown in Exhibit 34-61.

Exhibit 34-61
Example Problem 5: Lane Utilization Adjustment Calculations

Approach	Lane Configuration	Left-Turn Demand Ratio	Maximum Lane Utilization	Lane Utilization Factor
Eastbound external	3-lane exclusive	0.46	0.45	0.74
Westbound external	2-lane shared	0.67	0.77	0.65

Saturation flow rates are calculated on the basis of reductions in the base saturation flow rate of 1,900 pc/hg/ln by using Equation 23-14. The lane utilization of the approaches external to the interchange is obtained as shown above. Traffic pressure is calculated by using Equation 23-15. The left- and right-turn adjustment factors are estimated by using Equation 23-20 through Equation 23-23. These equations use an adjustment factor for travel path radius calculated by Equation 23-19. The DDI adjustment factor is applied to the internal and external through movements at both crossovers. The remaining adjustment factors are calculated as indicated in Chapter 19, Signalized Intersections. The estimated saturation flow rates for all approaches are shown in Exhibit 34-62.

Exhibit 34-62
Example Problem 5: Saturation Flow Rate Calculation for All Approaches

Value	West Crossover				East Crossover			
	M5	M6	M7	M8	M1	M2	M3	M4
Base saturation flow (s_0 , pc/hg/ln)	1,900	1,900	1,900	1,900	1,900	1,900	1,900	1,900
Number of lanes (N)	2	3	1	1	2	2	1	1
Lane width adjustment (f_w)	1.000	1.000	1.000	1.000	1.000	1.000	1.000	1.000
Heavy vehicle and grade adjustment (f_{HVg})	0.952	0.952	0.952	0.952	0.952	0.952	0.952	0.952
Parking adjustment (f_p)	1.000	1.000	1.000	1.000	1.000	1.000	1.000	1.000
Bus blockage adjustment (f_{bb})	1.000	1.000	1.000	1.000	1.000	1.000	1.000	1.000
Area type adjustment (f_a)	1.000	1.000	1.000	1.000	1.000	1.000	1.000	1.000
Lane utilization adjustment (f_{LU})	1.000	0.740	1.000	1.000	1.000	0.649	1.000	1.000
Left-turn adjustment (f_{LT})	1.000	1.000	0.964	1.000	1.000	1.000	0.964	1.000
Right-turn adjustment (f_{RT})	1.000	1.000	1.000	0.930	1.000	1.000	1.000	0.930
Left-turn pedestrian-bicycle adjustment (f_{LPB})	1.000	1.000	1.000	1.000	1.000	1.000	1.000	1.000
Right-turn pedestrian-bicycle adjustment (f_{RPB})	1.000	1.000	1.000	1.000	1.000	1.000	1.000	1.000
Turn radius adjustment for lane group (f_r)	1.000	1.000	1.000	1.000	1.000	1.000	1.000	1.000
Traffic pressure adjustment for lane group (f_t)	0.956	0.972	0.960	0.951	0.978	0.954	0.964	0.951
DDI adjustment factor (f_{DDI})	0.913	0.913	1.000	1.000	0.913	0.913	1.000	1.000
Adjusted saturation flow per lane (s , veh/hg/ln)	1,578	1,188	1,674	1,601	1,615	1,022	1,682	1,601
Adjusted approach saturation flow (s , veh/hg)	3,156	3,563	1,674	1,601	3,229	2,045	1,682	1,601

Effective Green and Lost Time Calculations

Next, effective green time adjustments for the DDI movements are calculated according to Step 4 of the DDI methodology, as shown in Exhibit 34-63. The lost time adjustment due to internal queues was illustrated in previous examples and is assumed to be 4 s/veh for this example. Lost time due to demand starvation does not apply to DDIs and is set at zero. Lost time due to overlap phasing for the DDI ramp movements is calculated from Equation 23-37.

Value	West Crossover				East Crossover			
	M5	M6	M7	M8	M1	M2	M3	M4
Lost time due to internal queues (s)	0	4	4	0	0	4	4	0
Lost time due to demand starvation (s)	0	0	0	0	0	0	0	0
Lost time on DDI ramps from overlap phasing (s)	0	0	6.5	4.9	0	0	6.5	4.9
Start-up lost time (s)	2	2	2	2	2	2	2	2
Extension of effective green (s)	2	2	2	2	2	2	2	2
Adjusted lost time, external (s)		8	15	9		9	15	9
Adjusted lost time, internal (s)	4				4			
Effective green time (s)	25	31	14	30	35	20	24	20

Exhibit 34-63
Example Problem 5:
Lost Time and Effective
Green Calculations

Results

With the effective green time and saturation flow adjustments complete, the volume-to-capacity ratios for each lane group are calculated from Equation 23-48. Because this is an isolated DDI, no adjustments due to closely spaced intersections apply. Because all turning movements from the freeway are signalized, Step 6 for estimating performance of YIELD-controlled turns also does not apply. The results are shown in Exhibit 34-64.

Control delay and its various components (uniform delay, incremental delay, and initial queue delay) are calculated by using the procedures in Chapter 19, and the results are shown in Exhibit 34-64.

Value	West Crossover				East Crossover			
	M5	M6	M7	M8	M1	M2	M3	M4
Demand flow rate, lane group (veh/h)	500	1,300	300	200	1,000	450	350	200
Saturation flow rate, lane group (veh/h)	3,156	3,563	1,674	1,601	3,229	2,045	1,682	1,601
Effective green time (s)	25	31	14	30	35	20	24	20
Cycle length (s)	70	70	70	70	70	70	70	70
g/C ratio	0.36	0.44	0.21	0.43	0.50	0.29	0.35	0.29
v/c ratio for lane group	0.44	0.82	0.87	0.29	0.62	0.77	0.60	0.44
Uniform delay (s/veh)	16.0	17.6	26.8	13.2	21.7	25.4	19.1	22.3
Incremental delay (s/veh)	1.2	5.2	25.7	0.1	0.2	23	1.9	0.6
Initial queue delay (s/veh)	0	0	0	0	0	0	0	0
Control delay (s/veh)	17.2	22.8	52.5	13.3	21.9	48.4	21.0	22.9

Exhibit 34-64
Example Problem 5:
Performance Results

From these results, the performance measures are aggregated for each O-D movement. The naming convention for converting turning movements to O-Ds is followed. Furthermore, for each O-D movement, the EDTT is calculated with Equation 23-50. The LOS for each lane group can then be determined from Exhibit 23-10. The results of all steps are shown in Exhibit 34-65.

In the exhibit, the extra distance traveled is 100 ft for the left turn from the freeway (Movements A and D), reflecting some out-of-direction travel distance at the interchange. Similarly, 40 ft of added travel distance is applied to the arterial through movements (I and J) to account for the two crossover shifts. For an

actual site, these distances should be measured from design drawings or aerial images. The EDTT is then calculated on the assumption of a travel speed of 35 mi/h for that added distance. Note that the methodology does not consider delays for the free-flow right-turn bypass movements onto the freeway, which are therefore assumed to be zero. Intersectionwide performance measures are not calculated for interchange ramp terminals.

Exhibit 34-65
Example Problem 5: ETT and LOS Results

O-D	PHF-Adjusted Demand (veh/h)	Movement	Control Delay Components	Total Control Delay (s/veh)	Extra Distance (ft)	EDTT (s/veh)	ETT (s/veh)	LOS
A	368	NB L	M3 + M5	38.2	100	1.9	40.1	C
B	211	NB R	M4	22.9	-100	-1.9	21.0	B
C	211	SB R	M8	13.3	-100	-1.9	11.4	A
D	316	SB L	M7 + M1	74.4	100	1.9	76.3	D
E	632	EB L	M6	22.8	100	1.9	24.7	B
F	211	EB R	N/A	0.0	0	0.0	0.0	A
G	316	WB R	N/A	0.0	0	0.0	0.0	A
H	316	WB L	M2	48.4	100	1.9	50.3	C
I	737	EB T	M6 + M1	44.7	40	0.8	45.5	C
J	158	WB T	M2 + M5	65.6	40	0.8	66.4	D

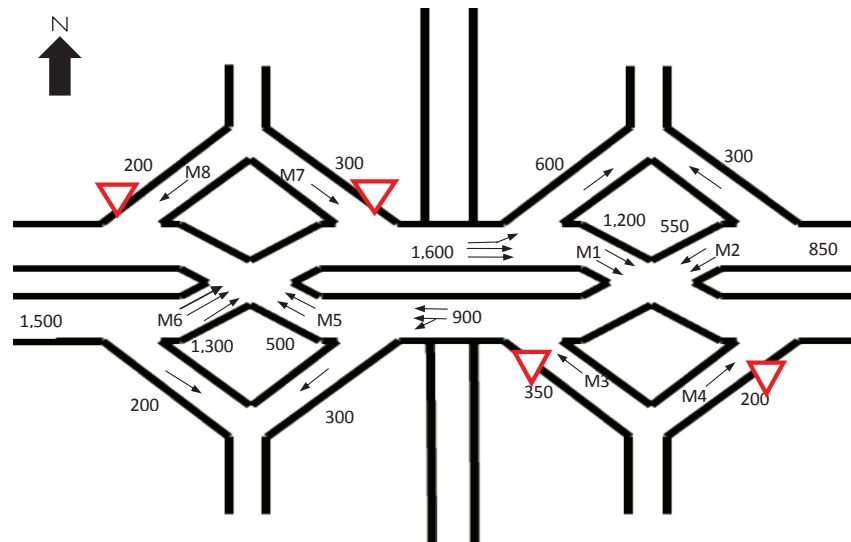
Note: NB = northbound, SB = southbound, EB = eastbound, WB = westbound, L = left, R = right, T = through, N/A = not applicable.

EXAMPLE PROBLEM 6: DIVERGING DIAMOND INTERCHANGE WITH YIELD CONTROL

The Interchange

In this example, the same DDI is used that was introduced in Example Problem 5. The only difference is that the left turns (M3 and M7) and right turns (M4 and M8) from the freeway off-ramps are now YIELD-controlled movements. The estimation of control delays for Movements M1, M2, M5, and M6 is unchanged from the previous example. The geometry is shown in Exhibit 34-66.

Exhibit 34-66
Example Problem 6:
Geometry, Lane, and Volume Inputs



The Question

What are the control delays, experienced travel time, and LOS for the turning movements off the freeway for this interchange if they are controlled by YIELD signs?

The Facts

The basic assumptions for this freeway are the same as for Example Problem 5. Similarly, Steps 1 through 5 are unchanged for the signalized movements.

Solution

Capacity of YIELD-Controlled Movement

Step 6 of the interchange methodology evaluates the capacity of the YIELD-controlled movement in three regimes: (a) Regime 1—blocked by conflicting platoon when the conflicting signal has just turned green, with zero capacity for turning movement; (b) Regime 2—gap acceptance in conflicting traffic after the initial platoon has cleared, with gap acceptance controlled by the critical gap, follow-up time, and conflicting flow rate; and (c) Regime 3—no conflicting flow when the conflicting signal is red, with full capacity, controlled by the follow-up time of the YIELD-controlled approach.

For each regime, the methodology computes the proportion of time the regime is active, as well as the capacity that applies over that period of time. The evaluation is performed for the two right-turn movements (M4 and M8) and the two left-turn movements (M3 and M7).

In Regime 1, the capacity is equal to zero, since no YIELD-controlled movements can enter the interchange while the opposing queue clears. The duration of the blocked period is estimated from Equation 23-51. For an isolated interchange, Equation 23-52 and Equation 23-54 are used to estimate the time to clear the opposing queue and the time for the last queued vehicle to clear the conflict point, respectively. The calculation results are shown in Exhibit 34-67.

Value	M7	M8	M3	M4
Green time for opposing movement (s)	31	25	20	35
Red time for opposing movement (s)	39	45	50	35
Volume of opposing movement per lane (veh/h/ln)	433	250	225	500
Saturation flow rate for opposing movement (veh/h)	1,188	1,578	1,022	1,615
Time to clear queue, t_{CQ} (s)	22.4	8.5	14.1	15.7
Distance to clear, x_{clear} (ft)	200.0	100.0	200.0	100.0
Speed of opposing movement (mi/h)	25.0	25.0	25.0	25.0
Time to clear last vehicle, t_{clear} (s)	5.5	2.7	5.5	2.7
Proportion of time blocked, p_b	0.40	0.16	0.28	0.26
Capacity of blocked period, c_b (veh/h)	0	0	0	0

Exhibit 34-67
Example Problem 6: Capacity of Blocked Regime

In Regime 2, the capacity of the YIELD-controlled movement when gaps are accepted in opposing traffic is estimated by using Equation 23-42. The proportion of time for that gap acceptance regime is estimated from Equation 23-43. The computation results are shown in Exhibit 34-68. Note that in the exhibit, the p_{GA} time calculated for M3 was originally negative and therefore was set to zero.

Exhibit 34-68

Example Problem 6: Capacity of Gap Acceptance Regime

Value	M7	M8	M3	M4
Critical gap, t_c (s)	3.9	1.8	3.9	1.8
Follow-up time, t_f (s)	2.6	2.4	2.6	2.4
Conflicting flow rate, q_c (veh/h)	1,300	500	450	1,200
Capacity of gap acceptance regime, C_{GA} (veh/h)	541	1,380	1,000	1,228
Proportion of time of gap acceptance, P_{GA}	0.04	0.20	0.00 ^a	0.24

Note: ^a Set to zero to avoid negative numbers.

In Regime 3, conflicting flow is stopped at the crossover signal, and the capacity is estimated from Equation 23-44. The proportion of time for this regime is estimated from Equation 23-45. The results are shown in Exhibit 34-69.

Exhibit 34-69

Example Problem 6: Capacity of No-Opposing-Flow Regime

Value	M7	M8	M3	M4
Capacity of no-opposing-flow regime, C_{NOF} (veh/h)	1,385	1,500	1,385	1,500
Proportion of time with no opposing flow, P_{NOF}	0.56	0.64	0.71	0.50

Results

The combined capacity of the YIELD-controlled movement is estimated from Equation 23-46 or Equation 23-47. With that capacity and the movement demand, a volume-to-capacity ratio can be estimated. The control delay for the movement is then estimated by using the control delay procedure for roundabouts given in Equation 22-17. The computations of other terms contributing to the experienced travel time service measure are consistent with Example Problem 5. The results are shown in Exhibit 34-70.

Exhibit 34-70

Example Problem 6: Performance Results

Value	M7	M8	M3	M4
Demand flow rate for lane group (veh/h)	300	200	350	200
v/c ratio for lane group (decimal)	0.38	0.16	0.35	0.19
Control delay (s/veh)	34.7	13.4	31.0	16.3

The results suggest that under these assumptions, YIELD-controlled left-turn Movements M7 and M4 perform better than the signalized alternatives evaluated in Example Problem 5, while unsignalized right-turn Movements M8 and M3 show slightly higher delay than with the signal.

From these results, the performance measures are aggregated for each O-D movement. The naming convention for converting turning movements to O-Ds is followed. Furthermore, for each O-D movement, the EDTT is calculated with Equation 23-50. From the O-D ETT, the LOS for each lane group is estimated from Exhibit 23-10. The results of all steps are shown in Exhibit 34-71.

In the exhibit, the extra distance traveled is 100 ft for the left turn from the freeway (Movements A and D), reflecting some out-of-direction travel distance at the interchange. For right turns from the freeway (Movements B and C), an equivalent negative extra travel distance is applied. Similarly, 40 ft of added travel distance is applied to the arterial through movements (I and J) to account for the two crossover shifts. For an actual site, these distances should be measured from design drawings or aerial images. The EDTT is then calculated on the assumption of a travel speed of 35 mi/h for that added distance. Note that the methodology does not consider delays for the free-flow right-turn bypass movements onto the freeway, which are therefore assumed to be zero.

Intersectionwide performance measures are not calculated for interchange ramp terminals.

O-D	PHF-Adjusted Demand (veh/h)	Movement	Control Delay Components	Total Control Delay (s/veh)	Extra Distance (ft)	EDTT (s/veh)	ETT (s/veh)	LOS
A	368	NB L	M3 + M5	48.2	100	1.9	50.2	D
B	211	NB R	M4	16.3	-100	-1.9	14.3	A
C	211	SB R	M8	13.4	-100	-1.9	11.5	A
D	316	SB L	M7 + M1	56.6	100	1.9	58.5	D
E	632	EB L	M6	22.8	100	1.9	24.7	B
F	211	EB R	N/A	0.0	0	0.0	0.0	A
G	316	WB R	N/A	0.0	0	0.0	0.0	A
H	316	WB L	M2	48.4	100	1.9	50.3	C
I	737	EB T	M6 + M1	44.7	40	0.8	45.5	C
J	158	WB T	M2 + M5	65.6	40	0.8	66.4	D

Note: NB = northbound, SB = southbound, EB = eastbound, WB = westbound, L = left, R = right, T = through, N/A = not applicable.

Exhibit 34-71
Example Problem 6: ETT and LOS Results

EXAMPLE PROBLEM 7: SINGLE-POINT URBAN INTERCHANGE

The Interchange

The interchange of I-95 (NB/SB) and University Drive (EB/WB) is a single-point urban interchange (SPUI). The traffic, geometric, and signalization conditions of the interchange are provided in Exhibit 34-72 and Exhibit 34-73.

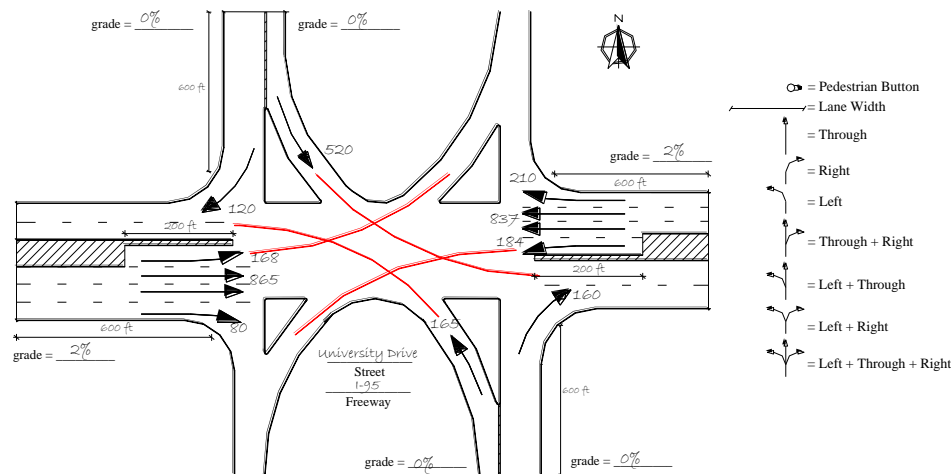


Exhibit 34-72
Example Problem 7:
Intersection Plan View

Phase	SPUI Interchange		
	1	2	3
NEMA	$\Phi (1+5+4R+8R)$	$\Phi (2+6)$	$\Phi (3+8+2R+6R)$
Green time (s)	16	32	38
Yellow + all red (s)	8	8	8

Exhibit 34-73
Example Problem 7:
Signalization Information

The Question

What are the control delay, queue storage ratio, and LOS for this interchange?

The Facts

There are no closely spaced intersections to this interchange, and it operates as a pretimed signal with no right turns on red allowed. Travel path radii are 87

ft and 50 ft for all left-turn and right-turn movements, respectively. Lane widths are 10.3 ft for all lanes. There is no extra distance traveled along the freeway ramps. The grade is 2% on the eastbound and westbound approaches.

There are 3.4% heavy vehicles on all eastbound and westbound movements. There are 5% heavy vehicles on all northbound and southbound movements. The PHF for the interchange is 0.95. Start-up lost time and extension of effective green are both 2 s for all approaches. During the analysis period, there is no parking, and no buses, bicycles, or pedestrians utilize the interchange.

Solution

Calculation of Origin–Destination Movements

O-Ds through this SPUI are calculated on the basis of the worksheet provided in Exhibit 34-170. O-Ds can be calculated directly from the turning movements at a SPUI because it has only one intersection. The O-Ds and the corresponding PHF-adjusted values are presented in Exhibit 34-74.

Exhibit 34-74
Example Problem 7: Adjusted
O-D Table

O-D Movement	Demand (veh/h)	PHF-Adjusted Demand (veh/h)
A	165	174
B	160	168
C	120	126
D	520	547
E	168	177
F	80	84
G	210	221
H	184	194
I	865	911
J	837	881
K	0	0
L	0	0
M	0	0
N	0	0

Saturation Flow Rate Calculations

Saturation flow rates are calculated on the basis of reductions in the base saturation flow rate of 1,900 pc/hg/ln by using Equation 23-14. Traffic pressure is calculated by using Equation 23-15. The left- and right-turn adjustment factors are estimated by using Equation 23-20 through Equation 23-23. These equations use an adjustment factor for travel path radius calculated by Equation 23-19. The remaining adjustment factors are calculated as indicated in Chapter 19, Signalized Intersections. The results of the saturation flow rate calculations for all approaches are presented in Exhibit 34-75 and Exhibit 34-76.

Value	Eastbound				Westbound			
	Left Prot.	Left Perm.	Through	Right	Left Prot.	Left Perm.	Through	Right
Base saturation flow (s_0 , pc/hg/ln)	1,900	1,900	1,900	1,900	1,900	1,900	1,900	1,900
Number of lanes (N)	1	1	2	1	1	1	2	1
Lane width adjustment (f_w)	0.967	0.967	0.967	0.967	0.967	0.967	0.967	0.967
Heavy vehicle and grade adjustment (f_{HVg})	0.961	0.961	0.961	0.961	0.961	0.961	0.961	0.961
Parking adjustment (f_p)	1.000	1.000	1.000	1.000	1.000	1.000	1.000	1.000
Bus blockage adjustment (f_{bb})	1.000	1.000	1.000	1.000	1.000	1.000	1.000	1.000
Area type adjustment (f_a)	1.000	1.000	1.000	1.000	1.000	1.000	1.000	1.000
Lane utilization adjustment (f_{LU})	1.000	1.000	0.952	1.000	1.000	1.000	0.952	1.000
Left-turn adjustment (f_{LT})	0.930	0.136	1.000	1.000	0.930	0.125	1.000	1.000
Right-turn adjustment (f_{RT})	1.000	1.000	1.000	0.994	1.000	1.000	1.000	0.983
Left-turn pedestrian-bicycle adjustment (f_{LPB})	1.000	1.000	1.000	1.000	1.000	1.000	1.000	1.000
Right-turn pedestrian-bicycle adjustment (f_{RPB})	1.000	1.000	1.000	1.000	1.000	1.000	1.000	1.000
Turn radius adjustment for lane group (f_R)	0.930	0.930	1.000	0.899	0.930	0.930	1.000	0.899
Traffic pressure adjustment for lane group (f_v)	0.950	0.951	0.998	0.946	0.950	0.954	0.995	0.964
Adjusted saturation flow (s , veh/hg/ln)	1,560	228	3,353	1,659	1,561	211	3,346	1,673

Note: Prot. = protected, Perm. = permitted.

Value	Northbound			Southbound		
	Left	Through	Right	Left	Through	Right
Base saturation flow (s_0 , pc/hg/ln)	1,900	1,900	1,900	1,900	1,900	1,900
Number of lanes (N)	1	1	1	1	1	1
Lane width adjustment (f_w)	0.967	0.967	0.967	0.967	0.967	0.967
Heavy vehicle and grade adjustment (f_{HVg})	1.000	1.000	1.000	1.000	1.000	1.000
Parking adjustment (f_p)	1.000	1.000	1.000	1.000	1.000	1.000
Bus blockage adjustment (f_{bb})	1.000	1.000	1.000	1.000	1.000	1.000
Area type adjustment (f_a)	1.000	1.000	1.000	1.000	1.000	1.000
Lane utilization adjustment (f_{LU})	1.000	1.000	1.000	1.000	1.000	1.000
Left-turn adjustment (f_{LT})	0.899	1.000	1.000	0.899	1.000	1.000
Right-turn adjustment (f_{RT})	1.000	1.000	0.899	1.000	1.000	0.899
Left-turn pedestrian-bicycle adjustment (f_{LPB})	1.000	1.000	1.000	1.000	1.000	1.000
Right-turn pedestrian-bicycle adjustment (f_{RPB})	1.000	1.000	1.000	1.000	1.000	1.000
Turn radius adjustment for lane group (f_R)	0.899	1.000	0.899	0.899	1.000	0.899
Traffic pressure adjustment for lane group (f_v)	0.967	0.935	0.957	1.044	0.935	0.951
Adjusted saturation flow (s , veh/hg/ln)	1,597	1,717	1,580	1,724	1,717	1,571

Exhibit 34-75

Example Problem 7:
Saturation Flow Rate
Calculation for Eastbound and
Westbound Approaches

Exhibit 34-76

Example Problem 7:
Saturation Flow Rate
Calculation for Northbound
and Southbound Approaches

Supplemental Uniform Delay Worksheet for Left Turns from Exclusive Lanes with Protected and Permitted Phases

Uniform delay for the eastbound and westbound left-turn movements must be calculated with a supplemental worksheet since both of these exclusive left-turn lanes have both protected and permitted movements. The intermediate calculations and uniform delay for the eastbound and westbound left turns are completed according to the methodology of Chapter 19, Signalized Intersections, and are shown in Exhibit 34-77.

Exhibit 34-77

Example Problem 7: Uniform Delay Calculations for Left Turns Featuring Both Permissive and Protected Phasing

Value	Eastbound Left	Westbound Left
C (s)	110	110
Leading left?	Yes	Yes
g (s)	16	16
g_{σ} (s)	17	20
g_u (s)	13.01	11.78
r (s)	62.00	62.00
$X = v/c$	0.60	0.67
q_{σ} (veh/s)	0.05	0.05
s_p (veh/s)	0.43	0.43
s_s (veh/s)	0.16	0.16
X_{perm}	0.78	0.92
X_{prot}	0.55	0.60
Case	1	1
Q_A (ft)	3.0	3.3
Q_u (ft)	0.9	1.1
Q_r (ft)	0.0	0.0
d_1 (s/veh)	22.1	22.7

Queue Storage and Control Delay

The queue storage ratio is estimated as the ratio of the average maximum queue to the available queue storage by using Equation 31-154. Exhibit 34-78 and Exhibit 34-79 present the calculations of the queue storage ratio for all movements. These exhibits also show the v/c ratio for each movement. Control delay for each movement is calculated according to Equation 19-18. Exhibit 34-80 and Exhibit 34-81 provide the control delay for each movement of the interchange. The eastbound left turns for the permissive and protected phases are treated in combination in these calculations.

Value	Eastbound Movements			Westbound Movements		
	Left	Through	Right	Left	Through	Right
Q_{bl} (ft)	0.0	0.0	0.0	0.0	0.0	0.0
v (veh/h/ln group)	177	911	84	194	881	221
s (veh/h/ln)	672	1,676	1,659	661	1,673	1,673
g (s)	48.0	32.0	38.0	48.0	32.0	38.0
g/C	0.44	0.29	0.35	0.44	0.29	0.35
I	1.0	1.0	1.0	1.0	1.0	1.0
c (veh/h/ln group)	293	975	573	288	973	578
$X = v/c$	0.60	0.93	0.15	0.67	0.91	0.38
r_a (ft/s ²)	3.5	3.5	3.5	3.5	3.5	3.5
r_d (ft/s ²)	4	4	4	4	4	4
S_s (mi/h)	5	5	5	5	5	5
S_{pl} (mi/h)	40	40	40	40	40	40
S_a (mi/h)	39.96	39.96	39.96	39.96	39.96	39.96
d_b (s)	12.04	12.04	12.04	12.04	12.04	12.04
RP	1	1	1	1	1	1
P	0.44	0.29	0.35	0.44	0.29	0.35
r (s)	62.0	78.0	72.0	62.0	78.0	72.0
t_r (s)	0.00	0.01	0.00	0.01	0.01	0.00
q (veh/s)	0.05	0.25	0.02	0.05	0.24	0.06
q_g (veh/s)	0.05	0.25	0.02	0.05	0.24	0.06
q_r (veh/s)	0.05	0.25	0.02	0.05	0.24	0.06
Q_1 (veh)	4.1	14.2	1.8	4.7	13.6	5.1
Q_2 (veh)	0.7	2.3	0.1	0.9	1.9	0.3
T	0.25	0.25	0.25	0.25	0.25	0.25
Q_{eo} (veh)	0.00	0.00	0.00	0.00	0.00	0.00
t_a	0	0	0	0	0	0
Q_e (veh)	0.00	0.00	0.00	0.00	0.00	0.00
Q_b (veh)	0	0	0	0	0	0
Q_s (veh)	0	0	0	0	0	0
Q (veh)	4.9	16.5	1.9	5.7	15.4	5.4
L_h (ft)	25,006	25,006	25,006	25,006	25,006	25,006
L_s (ft)	200	600	600	200	600	600
R_Q	0.61	0.69	0.08	0.71	0.64	0.23

Exhibit 34-78

Example Problem 7: Queue Storage Ratio for Eastbound and Westbound Movements

Value	Northbound Movements			Southbound Movements		
	Left	Through	Right	Left	Through	Right
Q_{bl} (ft)	0.0	0.0	0.0	0.0	0.0	0.0
v (veh/h/ln group)	174	0	168	547	0	126
s (veh/h/ln)	1,597	1,717	1,580	1,724	1,717	1,571
g (s)	38.0	38.0	16.0	38.0	38.0	16.0
g/C	0.35	0.35	0.15	0.35	0.35	0.15
I	1.0	1.0	1.0	1.0	1.0	1.0
c (veh/h/ln group)	552	593	230	596	593	228
$X = v/c$	0.31	0.00	0.73	0.92	0.00	0.55
r_a (ft/s ²)	3.5	3.5	3.5	3.5	3.5	3.5
r_d (ft/s ²)	4	4	4	4	4	4
S_s (mi/h)	5	5	5	5	5	5
S_{pl} (mi/h)	40	40	40	40	40	40
S_a (mi/h)	39.96	39.96	39.96	39.96	39.96	39.96
d_b (s)	12.04	12.04	12.04	12.04	12.04	12.04
RP	1	1	1	1	1	1
P	0.35	0.35	0.15	0.35	0.35	0.15
r (s)	72.0	72.0	94.0	72.0	72.0	94.0
t_r (s)	0.00	0.00	0.00	0.01	0.00	0.00
q (veh/s)	0.05	0.00	0.05	0.15	0.00	0.04
q_g (veh/s)	0.05	0.00	0.05	0.15	0.00	0.04
q_r (veh/s)	0.05	0.00	0.05	0.15	0.00	0.04
Q_1 (veh)	3.9	0.0	4.9	16.0	0.0	3.6
Q_2 (veh)	0.2	0.0	1.2	3.6	0.0	0.6
T	0.25	0.25	0.25	0.25	0.25	0.25
Q_{eo} (veh)	0.00	0.00	0.00	0.00	0.00	0.00
t_a	0	0	0	0	0	0
Q_e (veh)	0.00	0.00	0.00	0.00	0.00	0.00
Q_b (veh)	0	0	0	0	0	0
Q_s (veh)	0	0	0	0	0	0
Q (veh)	4.1	0.0	6.1	19.6	0.0	4.2
L_h (ft)	25	25	25	25	25	25
L_s (ft)	600	600	600	600	600	600
R_Q	0.17	0.00	0.25	0.82	0.00	0.17

Exhibit 34-79

Example Problem 7: Queue Storage Ratio for Northbound and Southbound Movements

Exhibit 34-80

Example Problem 7: Control Delay for Eastbound and Westbound Movements

Value	Eastbound Movements			Westbound Movements		
	Left	Through	Right	Left	Through	Right
g (s)	-	32	38	-	32	38
g' (s)	48	-	-	48	-	-
g/C or g'/C	0.44	0.29	0.35	0.44	0.29	0.35
c (veh/h)	293	975	573	288	973	578
$X = v/c$	0.60	0.93	0.15	0.67	0.91	0.38
d_1 (s/veh)	22.1	38.0	24.8	22.8	37.5	27.2
k	0.5	0.5	0.5	0.5	0.5	0.5
d_2 (s/veh)	8.9	16.6	0.5	11.8	13.4	1.9
d_3 (s/veh)	0.0	0.0	0.0	0.0	0.0	0.0
PF	1.000	1.000	1.000	1.000	1.000	1.000
k_{min}	0.04	0.04	0.04	0.04	0.04	0.04
u	0	0	0	0	0	0
t	0	0	0	0	0	0
d (s/veh)	31.0	54.6	25.4	34.6	51.0	29.1

Exhibit 34-81

Example Problem 7: Control Delay for Northbound and Southbound Movements

Value	Northbound Movements			Southbound Movements		
	Left	Through	Right	Left	Through	Right
g (s)	-	38	16	-	38	16
g' (s)	38	-	-	38	-	-
g/C or g'/C	0.35	0.35	0.15	0.35	0.35	0.15
c (veh/h)	552	593	230	596	593	228
$X = v/c$	0.31	0.00	0.73	0.92	0.00	0.55
d_1 (s/veh)	26.4	23.6	45.0	34.5	23.6	43.7
k	0.5	0.5	0.5	0.5	0.5	0.5
d_2 (s/veh)	1.5	0.0	18.6	21.5	0.0	9.3
d_3 (s/veh)	0.0	0.0	0.0	0.0	0.0	0.0
PF	1.000	1.000	1.000	1.000	1.000	1.000
k_{min}	0.04	0.04	0.04	0.04	0.04	0.04
u	0	0	0	0	0	0
t	0	0	0	0	0	0
d (s/veh)	27.9	23.6	63.6	56.0	23.6	53.0

Results

Delay for each O-D is estimated as the movement delay for the corresponding movement, as shown in Exhibit 34-82. Next, the v/c and queue storage ratios are checked. If either of these parameters exceeds 1, the LOS for the respective O-D is F. As shown, no movements have a v/c ratio or R_Q exceeding 1, and therefore the LOS result is based on the second column of Exhibit 23-10. Intersectionwide performance measures are not calculated for interchange ramp terminals.

Exhibit 34-82

Example Problem 7: O-D Movement LOS

O-D Movement	ETT (s/veh)	$v/c > 1?$	$R_Q > 1?$	LOS
A	27.9	No	No	B
B	63.6	No	No	D
C	53.0	No	No	C
D	56.0	No	No	D
E	31.0	No	No	C
F	25.4	No	No	B
G	29.1	No	No	B
H	34.6	No	No	C
I	54.6	No	No	C
J	51.0	No	No	C

EXAMPLE PROBLEM 8: DIAMOND INTERCHANGE WITH ADJACENT INTERSECTION

The Interchange

At the diamond interchange described in Example Problem 1 (I-99 and University Drive), an adjacent intersection was built 300 ft to the west of the interchange (Spring Street, NB/SB, and University Drive, EB/WB). The traffic, geometric, and signalization conditions are shown in Exhibit 34-83 and Exhibit 34-84. The offset is referenced to the beginning of the green for the respective EB arterial approach.

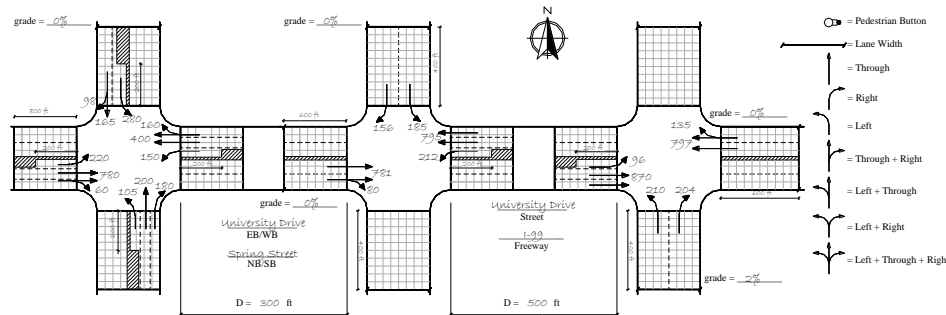


Exhibit 34-83
Example Problem 8:
Intersection Plan View

Phase	Intersection I			Intersection II		
	1	2	3	1	2	3
NEMA	Φ (2+6)	Φ (1+6)	Φ (4+7)	Φ (2+6)	Φ (3+8)	Φ (2+5)
Green time (s)	63	43	39	63	53	29
Yellow + all red (s)	5	5	5	5	5	5
Offset (s)		19			9	

Phase	Adjacent Intersection			
	1	2	3	4
NEMA	Φ (1+5)	Φ (2+6)	Φ (4+7)	Φ (3+8)
Green time (s)	33	59	24	24
Yellow + all red (s)	5	5	5	5
Offset (s)			19	

Exhibit 34-84
Example Problem 8:
Signalization Information

The Question

What are the control delay, queue storage ratio, and LOS for this interchange and the adjacent intersection?

The Facts

The closely spaced intersection operates as a pretimed signal with no right turns on red allowed. Travel path radii at the interchange are 50 ft for all right-turning movements and 75 ft for all left-turning movements. Extra distance traveled along each freeway ramp is 100 ft.

There are 6.1% heavy vehicles on eastbound and westbound through movements of the interchange and all movements of the adjacent intersection. The PHF for the interchange-intersection system is 0.97. Start-up lost time and extension of effective green are both 2 s for all approaches. During the analysis period, there is no parking, and no buses, bicycles, or pedestrians utilize the interchange. The grade is 2% on the northbound approach.

Solution

Calculation of Origin–Destination Movements

The O-Ds for the interchange are obtained as explained in Example Problem 1 and were presented in Exhibit 34-5.

Lane Utilization and Saturation Flow Rate Calculations

The adjacent intersection has a two-lane shared right and through lane group for both the inbound (arriving at the interchange) and the outbound (leaving the interchange) approaches. The lane utilization factors for the inbound and outbound approaches of the closely spaced intersection are estimated by obtaining the respective lane utilization values (through or shared) from Exhibit 19-15 and subtracting 0.05. The resulting lane utilization factors are shown in Exhibit 34-85.

Exhibit 34-85
Example Problem 8: Lane Utilization Adjustment Calculations

Lane Group	Lane Utilization Factor
2-lane group eastbound (inbound)	0.902
2-lane group westbound (outbound)	0.902

Saturation flow rates are calculated on the basis of reductions in the base saturation flow rate of 1,900 pc/h/ln by using Equation 23-14. The saturation flows for each lane group of the adjacent intersection are estimated according to Chapter 19, Signalized Intersections. The results of the saturation flow rate calculations for all movements of the adjacent intersection and the interchange are presented in Exhibit 34-86 through Exhibit 34-88. Note that turn radius and traffic pressure adjustments are not considered in the adjacent intersection.

Exhibit 34-86
Example Problem 8: Saturation Flow Rate Calculation for Interchange Eastbound and Westbound Approaches

Value	Eastbound			Westbound		
	EXT-TH&R	INT-TH	INT-L	EXT-TH&R	INT-TH	INT-L
Base saturation flow (s_0 , pc/hg/ln)	1,900	1,900	1,900	1,900	1,900	1,900
Number of lanes (N)	2	2	1	2	2	1
Lane width adjustment (f_w)	1.000	1.000	1.000	1.000	1.000	1.000
Heavy vehicle and grade adjustment (f_{HVg})	0.952	0.952	1.000	0.952	0.952	1.000
Parking adjustment (f_p)	1.000	1.000	1.000	1.000	1.000	1.000
Bus blockage adjustment (f_{bb})	1.000	1.000	1.000	1.000	1.000	1.000
Area type adjustment (f_a)	1.000	1.000	1.000	1.000	1.000	1.000
Lane utilization adjustment (f_{LU})	0.989	0.952	1.000	0.965	0.952	1.000
Left-turn adjustment (f_{LT})	1.000	1.000	0.930	1.000	1.000	0.930
Right-turn adjustment (f_{RT})	0.999	1.000	1.000	0.998	1.000	1.000
Left-turn pedestrian–bicycle adjustment (f_{LPB})	1.000	1.000	1.000	1.000	1.000	1.000
Right-turn pedestrian–bicycle adjustment (f_{RPB})	1.000	1.000	1.000	1.000	1.000	1.000
Turn radius adjustment for lane group (f_R)	0.991	1.000	0.930	0.985	1.000	0.930
Traffic pressure adjustment for lane group (f_T)	1.027	1.028	0.961	1.044	1.019	0.995
Adjusted saturation flow (s , veh/hg/ln)	3,670	3,540	1,698	3,637	3,510	1,759

Notes: EXT = external, INT = internal, TH = through, R = right, L = left.

Value	Northbound		Southbound	
	Left	Right	Left	Right
Base saturation flow (s_0 , pc/hg/ln)	1,900	1,900	1,900	1,900
Number of lanes (N)	1	1	1	1
Lane width adjustment (f_w)	1.000	1.000	1.000	1.000
Heavy vehicle and grade adjustment (f_{HVg})	0.990	0.990	0.990	0.990
Parking adjustment (f_p)	1.000	1.000	1.000	1.000
Bus blockage adjustment (f_{bb})	1.000	1.000	1.000	1.000
Area type adjustment (f_a)	1.000	1.000	1.000	1.000
Lane utilization adjustment (f_{LU})	1.000	1.000	1.000	1.000
Left-turn adjustment (f_{LT})	0.899	1.000	0.899	1.000
Right-turn adjustment (f_{RT})	1.000	0.899	1.000	0.899
Left-turn pedestrian-bicycle adjustment (f_{LPb})	1.000	1.000	1.000	1.000
Right-turn pedestrian-bicycle adjustment (f_{RPb})	1.000	1.000	1.000	1.000
Turn radius adjustment for lane group (f_R)	0.899	0.899	0.899	0.899
Traffic pressure adjustment for lane group (f_i)	0.995	0.971	0.987	0.966
Adjusted saturation flow (s , veh/hg/ln)	1,682	1,650	1,669	1,633

Exhibit 34-87

Example Problem 8:
Saturation Flow Rate
Calculation for Interchange
Northbound and Southbound
Approaches

Value	Eastbound		Westbound		Northbound			Southbound	
	TH&R	L	TH&R	L	TH	R	L	TH&R	L
Base saturation flow (s_0 , pc/hg/ln)	1,900	1,900	1,900	1,900	1,900	1,900	1,900	1,900	1,900
Number of lanes (N)	2	1	2	1	1	1	1	2	1
Lane width adjustment (f_w)	1.000	1.000	1.000	1.000	1.000	1.000	1.000	1.000	1.000
Heavy vehicle and grade adjustment (f_{HVg})	0.952	0.952	0.952	0.952	0.952	0.952	0.952	0.952	0.952
Parking adjustment (f_p)	1.000	1.000	1.000	1.000	1.000	1.000	1.000	1.000	1.000
Bus blockage adjustment (f_{bb})	1.000	1.000	1.000	1.000	1.000	1.000	1.000	1.000	1.000
Area type adjustment (f_a)	1.000	1.000	1.000	1.000	1.000	1.000	1.000	1.000	1.000
Lane utilization adjustment (f_{LU})	0.902	1.000	0.902	1.000	1.000	1.000	1.000	1.000	1.000
Left-turn adjustment (f_{LT})	1.000	0.930	1.000	0.930	1.000	1.000	0.899	1.000	0.899
Right-turn adjustment (f_{RT})	1.000	1.000	1.000	1.000	1.000	0.899	1.000	1.000	1.000
Left-turn pedestrian-bicycle adjustment (f_{LPb})	1.000	1.000	1.000	1.000	1.000	1.000	1.000	1.000	1.000
Right-turn pedestrian-bicycle adjustment (f_{RPb})	1.000	1.000	1.000	1.000	1.000	1.000	1.000	1.000	1.000
Adjusted saturation flow (s , veh/hg/ln)	3,359	1,680	3,251	1,645	1,765	1,580	1,568	3,434	1,654

Exhibit 34-88

Example Problem 8:
Saturation Flow Rate
Calculation for Adjacent
Intersection

Notes: TH = through, R = right, L = left.

Common Green and Lost Time due to Downstream Queue Calculations

Common green is calculated between certain movements that can contribute to excessive downstream queues or demand starvation, depending on the signal phasing sequence. The adjacent intersection is offset by 10 s from Intersection 2 and by 0 s from Intersection 1. Exhibit 34-89 presents the beginning and end of each phase at the three intersections and the calculations of common green between the relevant movements at the three intersections.

Exhibit 34-89

Example Problem 8: Common Green Calculations

Phase	Intersection I		Intersection II		
	Green Begin	Green End	Green Begin	Green End	
Phase 1	0	63	150	53	
Phase 2	68	111	58	111	
Phase 3	116	155	116	145	
Adjacent Intersection					
Phase	Phase Begin	Phase End			
Phase 1	0	33			
Phase 2	38	62			
Phase 3	67	96			
Phase 4	96	155			
Movement	First Green Time Within Cycle		Second Green Time Within Cycle		Common Green Time
	Begin	End	Begin	End	
EB EXT THRU	0	63			53
EB INT THRU	150	53	116	150	
WB EXT THRU	150	53			53
WB INT THRU	0	111			
SB RAMP	116	155			
EB INT THRU	150	53	116	150	34
NB RAMP	58	111			
WB INT THRU	0	111			53
WB INT LEFT	68	111			
EB INT THRU	150	53			0
EB INT LEFT	116	145			
WB INT THRU	0	111			0
EB EXT THRU	0	63			
ADJ EB THRU	38	97			25
EB EXT THRU	0	63			
ADJ SB LEFT	102	126			0
EB EXT THRU	0	63			
ADJ NB RIGHT	131	155			0
ADJ WB THRU	38	97			
WB INT THRU	0	111			59
ADJ WB THRU	38	97			
SB RAMP	116	155			0

Notes: ADJ = adjacent, EXT = external, INT = internal, THRU = through, EB = eastbound, WB = westbound, NB = northbound, SB = southbound.

The next step is the calculation of lost time due to downstream queues. At an adjacent intersection, additional lost time due to interchange operations may occur at the intersection’s eastbound, southbound left-turn, and northbound right-turn approaches. Furthermore, the interchange westbound internal link and southbound ramp may experience additional lost time due to operations at the adjacent closely spaced intersection.

To estimate whether these approaches experience additional lost time, the procedure determines the queue at the beginning of the intersection’s eastbound through arterial phase, southbound left-turn phase, and northbound right-turn phase. They are calculated by using Equation 23-24 and Equation 23-25. The resulting queues are subtracted from the downstream link length (link between the closely spaced intersection and the interchange) to determine the storage at the beginning of each phase. Exhibit 34-90 presents the calculation of lost time due to downstream queues. The results indicate that the southbound left-turn and northbound right-turn movements of the adjacent intersection experience additional lost time of 2.10 and 3.07 s, respectively.

Exhibit 34-90
Example Problem 8: Lost Time due to Downstream Queues

Movement	Interchange				
	EB EXT-TH	SB-L	WB EXT-TH	NB-L	
V_R or V_A (veh/h)	191	805	216	822	
N_R or N_A	1	2	1	2	
G_R or G_A (s)	39	63	53	63	
G_D (s)	97	97	111	111	
C (s)	160	160	160	160	
CG_{UD} or CG_{RD} (s)	53	34	53	53	
Queue length (Q_A or Q_R) (ft)	0.0	0.0	0.0	0.0	
Lost Time due to Downstream Queue					
Effective Green Adjustment	Interchange				
	EB EXT-TH	SB-L	WB EXT-TH	NB-L	
G_R or G_A (s)	63	39	63	53	
C (s)	160	160	160	160	
D_{QA} or D_{QR} (ft)	500	500	500	500	
CG_{UD} or CG_{RD} (s)	53	34	53	53	
Additional lost time, L_{D-A} or L_{D-R} (s)	0.0	0.0	0.0	0.0	
Total lost time, t'_L (s)	5.0	5.0	5.0	5.0	
Effective green time, g' (s)	63	39	63	53	
Movement	Adjacent Intersection			Interchange	
	EB-TH	SB-L	NB-R	WB INT-TH	SB-R
V_R or V_A (veh/h)	474	804	804	156	795
N_R or N_A	1	2	2	1	2
G_R or G_A (s)	48	59	59	39	111
G_D (s)	63	63	63	59	59
C (s)	160	160	160	160	160
CG_{UD} or CG_{RD} (s)	25.0	0.0	0.0	15	39
Queue length (Q_A or Q_R) (ft)	56.9	102.6	102.6	0.0	91.1
Lost Time due to Downstream Queue					
Effective Green Adjustment	Adjacent Intersection			Interchange	
	EB-TH	SB-L	NB-R	WB INT-TH	SB-R
G_R or G_A (s)	59	24	24	119	39
C (s)	160	160	160	160	160
D_{QA} or D_{QR} (ft)	243	197	197	300	209
CG_{UD} or CG_{RD} (s)	25.0	29	0	15	39
Additional lost time, L_{D-A} or L_{D-R} (s)	0.00	2.10	3.07	0.0	0.0
Total lost time, t'_L (s)	5.00	7.10	8.07	5.0	5.0
Effective green time, g' (s)	59.0	21.9	20.9	119	39

Notes: EXT = external, INT = internal, TH = through, L = left, R = right, EB = eastbound, WB = westbound, NB = northbound, SB = southbound.

Queue Storage and Control Delay

The queue storage ratio is estimated as the average maximum queue divided by the available queue storage by using Equation 31-154. Exhibit 34-91 and Exhibit 34-92 present the calculations of the queue storage ratio for all approaches of the interchange, while Exhibit 34-93 gives the results of all approaches of the adjacent intersection. The v/c ratio for the respective movements is also provided in these exhibits.

Control delay for each movement is calculated according to Equation 19-18. Exhibit 34-94 through Exhibit 34-96 summarize the control delay estimates for all approaches of the interchange and adjacent signalized intersection.

Exhibit 34-91

Example Problem 8: Queue Storage Ratio for Interchange Eastbound and Westbound Movements

Value	Eastbound Movements			Westbound Movements		
	EXT-TH&R	INT-L	INT-TH	EXT-TH&R	INT-L	INT-TH
Q_{bl} (ft)	0.0	0.0	0.0	0.0	0.0	0.0
v (veh/h/ln group)	888	99	897	961	219	820
s (veh/h/ln)	1,835	1,699	1,770	1,819	1,759	1,755
g (s)	63	29	97	63	43	111
g/C	0.39	0.18	0.61	0.39	0.27	0.69
I	1.00	0.75	0.75	1.00	0.68	0.68
c (veh/h/ln group)	1,448	308	2,146	1,448	473	2,435
$X = v/c$	0.61	0.32	0.42	0.66	0.46	0.34
r_a (ft/s ²)	3.5	3.5	3.5	3.5	3.5	3.5
r_d (ft/s ²)	4	4	4	4	4	4
S_s (mi/h)	5	5	5	5	5	5
S_{pl} (mi/h)	40	40	40	40	40	40
S_s (mi/h)	39.96	39.96	39.96	39.96	39.96	39.96
d_a (s)	12.04	12.04	12.04	12.04	12.04	12.04
Rp	1.000	1.000	1.333	1.000	1.000	1.333
P	0.39	0.18	0.81	0.39	0.27	0.92
r (s)	97.00	131.00	63.00	97.00	117.00	49.00
t_r (s)	0.01	0.00	0.00	0.01	0.00	0.00
q (veh/s)	0.25	0.03	0.25	0.27	0.06	0.23
q_b (veh/s)	0.25	0.03	0.33	0.27	0.06	0.30
q_r (veh/s)	0.25	0.03	0.12	0.27	0.06	0.06
Q_1 (veh)	13.8	3.5	8.5	13.0	7.3	1.1
Q_2 (veh)	0.8	0.2	0.1	1.1	0.3	0.1
T	0.25	0.25	0.25	0.25	0.25	0.25
Q_{eo} (veh)	0.00	0.00	0.00	0.00	0.00	0.00
t_a	0	0	0	0	0	0
Q_e (veh)	0.00	0.00	0.00	0.00	0.00	0.00
Q_b (veh)	0	0	0	0	0	0
Q_s (veh)	0.0	0.0	0.0	0.0	0.0	0.0
Q (veh)	14.6	3.7	8.6	14.1	7.6	1.2
L_h (ft)	25	25	25	25	25	25
L_s (ft)	600	200	500	600	200	500
RQ	0.61	0.46	0.43	0.59	0.95	0.06

Notes: EXT = external, INT = internal, TH = through, L = left, R = right.

Exhibit 34-92

Example Problem 8: Queue Storage Ratio for Interchange Northbound and Southbound Movements

Value	Northbound Movements		Southbound Movements	
	Left	Right	Left	Right
Q_{bl} (ft)	0.0	0.0	0.0	0.0
v (veh/h/ln group)	216	210	191	161
s (veh/h/ln)	1,682	1,651	1,669	1,634
g (s)	53	53	39	39
g/C	0.33	0.33	0.24	0.24
I	1.00	1.00	1.00	1.00
c (veh/h/ln group)	557	547	407	398
$X = v/c$	0.39	0.38	0.47	0.40
r_a (ft/s ²)	3.5	3.5	3.5	3.5
r_d (ft/s ²)	4	4	4	4
S_s (mi/h)	5	5	5	5
S_{pl} (mi/h)	40	40	40	40
S_s (mi/h)	39.96	39.96	39.96	39.96
d_a (s)	12.04	12.04	12.04	12.04
Rp	1.000	1.000	1.000	1.000
P	0.33	0.33	0.24	0.24
r (s)	107.00	107.00	121.00	121.00
t_r (s)	0.00	0.00	0.00	0.00
q (veh/s)	0.06	0.06	0.05	0.04
q_b (veh/s)	0.06	0.06	0.05	0.04
q_r (veh/s)	0.06	0.06	0.05	0.04
Q_1 (veh)	6.6	6.4	6.5	5.4
Q_2 (veh)	0.3	0.3	0.4	0.3
T	0.25	0.25	0.25	0.25
Q_{eo} (veh)	0.00	0.00	0.00	0.00
t_a	0	0	0	0
Q_e (veh)	0.00	0.00	0.00	0.00
Q_b (veh)	0	0	0	0
Q_s (veh)	0.0	0.0	0.0	0.0
Q (veh)	6.9	6.7	7.0	5.7
L_h (ft)	25	25	25	25
L_s (ft)	400	400	400	400
RQ	0.43	0.42	0.43	0.36

Value	Eastbound		Westbound		Northbound			Southbound	
	Through & Right	Left	Through & Right	Left	Through	Right	Left	Through & Right	Left
Q_{bl} (ft)	0.0	0.0	0.0	0.0	0.0	0.0	0.0	0.0	0.0
v (veh/h/ln group)	866	227	577	309	206	186	108	542	289
s (veh/h/ln)	1,679	1,680	1,650	1,722	1,765	1,580	1,568	1,717	1,654
g (s)	59.0	33	59	33	24.0	20.9	24.0	24	21.9
g/C	0.37	0.21	0.37	0.21	0.15	0.13	0.15	0.15	0.14
I	1.00	1.00	1.00	1.00	1.00	1.00	1.00	1.00	1.00
c (veh/h/ln group)	1,288	346	1,218	355	265	237	235	515	248
$X = v/c$	0.67	0.65	0.47	0.46	0.78	0.90	0.46	1.05	1.28
r_a (ft/s ²)	3.5	3.5	3.5	3.5	3.5	3.5	3.5	3.5	3.5
r_d (ft/s ²)	4	4	4	4	4	4	4	4	4
S_s (mi/h)	5	5	5	5	5	5	5	5	5
S_{pl} (mi/h)	40	40	40	40	40	40	40	40	40
S_{pl} (mi/h)	39.96	39.96	39.96	39.96	39.96	39.96	39.96	39.96	39.96
d_b (s)	12.04	12.04	12.04	12.04	12.04	12.04	12.04	12.04	12.04
Rp	1.000	1.000	1.000	1.000	1.000	1.000	1.000	1.000	1.000
P	0.37	0.21	0.37	0.21	0.15	0.13	0.15	0.15	0.14
r (s)	101.00	127.00	101.00	127.00	136.00	139.07	136.00	136.00	138.10
t_r (s)	0.01	0.00	0.01	0.00	0.00	0.00	0.00	0.01	0.01
q (veh/s)	0.24	0.06	0.16	0.04	0.06	0.05	0.03	0.08	0.08
q_p (veh/s)	0.24	0.06	0.16	0.04	0.06	0.05	0.03	0.08	0.08
q_r (veh/s)	0.24	0.06	0.16	0.04	0.06	0.05	0.03	0.08	0.08
Q_1 (veh)	14.3	8.4	8.7	5.5	8.0	7.4	4.0	10.4	9.2
Q_2 (veh)	1.1	0.9	0.5	0.4	1.5	2.3	0.4	5.0	9.7
T	0.25	0.25	0.25	0.25	0.25	0.25	0.25	0.25	0.25
Q_{eo} (veh)	0.00	0.00	0.00	0.00	0.00	0.00	0.00	3.39	15.6
t_a	0	0	0	0	0	0	0	0.25	0.25
Q_e (veh)	0.00	0.00	0.00	0.00	0.00	0.00	0.00	3.39	15.6
Q_b (veh)	0	0	0	0	0	0	0	0	0
Q_3 (veh)	0.0	0.0	0.0	0.0	0.0	0.0	0.0	0.0	0.0
Q (veh)	15.4	9.3	9.1	5.9	9.5	9.8	4.4	15.5	18.8
L_h (ft)	25	25	25	25	25	25	25	25	25
L_e (ft)	800	200	300	200	800	800	200	800	200
R_Q	0.48	1.16	0.76	0.73	0.30	0.30	0.55	0.48	2.36

Exhibit 34-93

Example Problem 8: Queue Storage Ratio for Adjacent Intersection Movements

Value	Eastbound Movements			Westbound Movements		
	EXT-TH&R	INT-L	INT-TH	EXT-TH&R	INT-L	INT-TH
g (s)	-	29	97	-	43	111
g' (s)	63	-	-	63	-	-
g/C or g'/C	0.39	0.18	0.61	0.39	0.27	0.69
c (veh/h)	1,448	308	2,146	1,448	473	2,435
$X = v/c$	0.61	0.32	0.42	0.68	0.46	0.34
d_1 (s/veh)	38.8	56.9	16.6	30.6	48.8	2.0
k	0.5	0.5	0.5	0.5	0.5	0.5
d_2 (s/veh)	3.9	2.1	0.5	5.4	2.2	0.3
d_3 (s/veh)	0.0	0.0	0.0	0.0	0.0	0.0
PF	1.000	1.000	0.560	1.000	1.000	0.283
k_{min}	0.04	0.04	0.04	0.04	0.04	0.04
u	0	0	0	0	0	0
t	0	0	0	0	0	0
d (s/veh)	42.6	59.0	17.1	36.0	51.0	2.2

Notes: EXT = external, INT = internal, TH = through, L = left, R = right.

Exhibit 34-94

Example Problem 8: Control Delay for Interchange Eastbound and Westbound Movements

Exhibit 34-95

Example Problem 8: Control Delay for Interchange Northbound and Southbound Movements

Value	Northbound Movements		Southbound Movements	
	Left	Right	Left	Right
g (s)	-	53	-	39
g' (s)	53	-	39	-
g/C or g'/C	0.33	0.33	0.24	0.24
c (veh/h)	557	547	407	398
$X = v/c$	0.39	0.38	0.47	0.40
d_1 (s/veh)	41.1	41.0	51.7	50.7
k	0.5	0.5	0.5	0.5
d_2 (s/veh)	2.0	2.0	3.8	3.0
d_3 (s/veh)	0.0	0.0	0.0	0.0
PF	1	1	1	1
k_{min}	0.04	0.04	0.04	0.04
u	0	0	0	0
t	0	0	0	0
d (s/veh)	43.1	43.0	55.5	53.8

Exhibit 34-96

Example Problem 8: Control Delay for Adjacent Intersection Movements

Value	Eastbound		Westbound		Northbound			Southbound	
	Through & Right	Left	Through & Right	Left	Through	Right	Left	Through & Right	Left
g (s)	-	33.0	59.0	33.0	24.0	-	24.0	24.0	-
g' (s)	59.0	-	-	-	-	20.9	-	-	21.9
g/C or g'/C	0.37	0.21	0.37	0.21	0.15	0.13	0.15	0.15	0.14
c (veh/h)	1,288	346	1,218	355	265	237	235	258	248
$X = v/c$	0.67	0.65	0.47	0.87	0.78	0.78	0.46	1.05	1.28
d_1 (s/veh)	42.5	58.3	38.7	55.6	65.4	68.5	62.1	68.0	69.0
k	0.5	0.5	0.5	0.5	0.5	0.5	0.5	0.5	0.5
d_2 (s/veh)	6.0	9.3	2.7	4.4	20.0	40.7	6.4	70.6	153.6
d_3 (s/veh)	0	0	0	0	0	0	0	0	0
PF	1.000	1.000	1.000	1.000	1.000	1.000	1.000	1.000	1.000
k_{min}	0.04	0.04	0.04	0.04	0.04	0.04	0.04	0.04	0.04
u	0	0	0	0	0	0	0	0	0
t	0	0	0	0	0	0	0	0	0
d (s/veh)	48.5	67.6	41.4	60.0	85.4	109.1	68.4	138.6	226.6

Results

Delay for each O-D is estimated as the sum of the movement delays for each movement utilized by the O-D, as indicated in Equation 23-2. The v/c and queue storage ratios are checked next. If either of these parameters exceeds 1, the LOS for all O-Ds that utilize that movement is F. The final delay calculations and resulting LOS for each O-D and each lane group are presented in Exhibit 34-97 and Exhibit 34-98. As shown, the v/c ratio and R_Q for all O-Ds are all below 1, and therefore the LOS for all O-Ds is determined by using the second column of Exhibit 23-10. The LOS for each lane group at the adjacent intersection is assigned on the basis of Chapter 19, Signalized Intersections. After extra distances are measured according to the Exhibit 23-8 discussion, EDTT can be obtained from Equation 23-50 [i.e., $EDTT = 100 / (1.47 \times 35) + 0 = 1.9$ s]. Intersectionwide performance measures are not calculated for interchange ramp terminals.

O-D Movement	Control Delay (s/veh)	EDTT (s/veh)	ETT (s/veh)	v/c > 1?	R ₀ > 1?	LOS
A	45.3	1.9	47.2	No	No	C
B	43.0	-1.9	41.1	No	No	C
C	53.8	-1.9	51.9	No	No	C
D	72.6	1.9	74.5	No	No	D
E	98.1	1.9	100.0	No	No	E
F	39.1	-1.9	37.2	No	No	C
G	36.0	-1.9	34.1	No	No	C
H	87.0	1.9	88.9	No	No	E
I	56.2	0.0	56.2	No	No	D
J	38.2	0.0	38.2	No	No	C

Exhibit 34-97
Example Problem 8:
Interchange O-D Movement
LOS

Approach	Lane Group	Control Delay (s)	LOS
EB	Through and right	48.5	C
	Left	67.6	D
WB	Through and right	41.4	C
	Left	60.0	D
NB	Through	85.4	E
	Right	109.1	E
	Left	68.4	D
SB	Through and right	138.6	F
	Left	226.6	F

Notes: EB = eastbound, WB = westbound, NB = northbound, SB = southbound.

Exhibit 34-98
Example Problem 8: Adjacent
Intersection Movement LOS

EXAMPLE PROBLEM 9: DIAMOND INTERCHANGE WITH ROUNDABOUTS

The Interchange

The interchange of I-99 (NB/SB) and University Drive (EB/WB) is a diamond interchange featuring roundabouts. The traffic conditions of the interchange are provided in Exhibit 34-99.

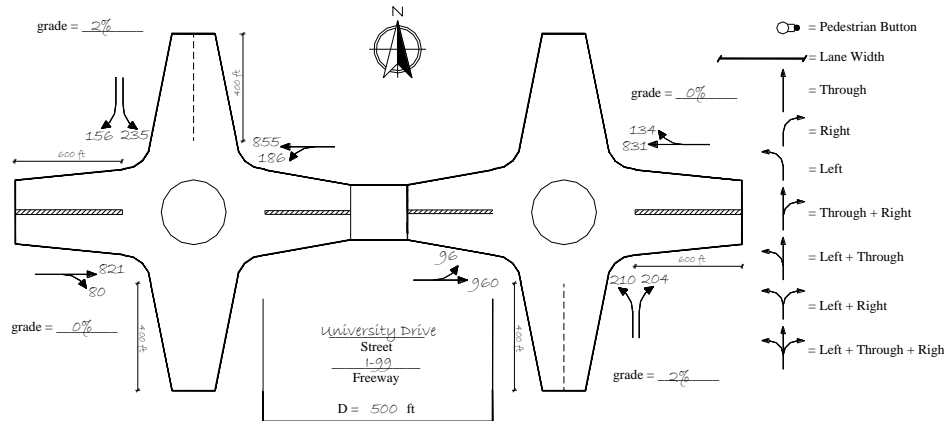


Exhibit 34-99
Example Problem 9:
Intersection Plan View

The Question

What are the control delay and LOS for this interchange?

The Facts

There are no closely spaced intersections to this interchange. This interchange has 3% heavy vehicles and a PHF of 0.97. During the analysis period, there is no parking, and no buses, bicycles, or pedestrians utilize the interchange.

Extra distance traveled along each freeway ramp is 100 ft. The grade is 2% on the NB and SB approaches.

Solution

Calculation of Origin–Destination Movements

O-Ds through this diamond interchange are calculated by using the worksheet provided in Exhibit 34-169 in Section 4. The results of the O-D calculations and the resulting PHF-adjusted values are presented in Exhibit 34-100.

Exhibit 34-100
Example Problem 9: Adjusted
O-D Table

O-D Movement	Demand (veh/h)	PHF-Adjusted Demand (veh/h)	Heavy Vehicle–Adjusted Demand (pc/h)
A	179	185	191
B	169	174	179
C	122	126	130
D	228	235	242
E	93	96	99
F	78	80	82
G	94	97	100
H	119	123	127
I	509	525	541
J	529	545	561
K	0	0	0
L	0	0	0
M	0	0	0
N	0	0	0

Calculation of Approach Capacity and Control Delay

To estimate the delay of each approach to the roundabout, the procedures outlined in Section 4 are used to estimate the entering and conflicting flow rates and the resulting capacity of each approach. Exhibit 34-160 and Exhibit 34-161 are used to determine the entering and conflicting flow rates for each approach of the interchange. For example, the northbound ramp movement (Number 13 in Exhibit 34-160) consists of O-D Movements A, B, K, and M at a diamond interchange (Exhibit 34-161). The conflicting flow (Number 12) consists of O-D Movements D, E, I, and N. Exhibit 34-101 shows the entering and conflicting flow for each approach, along with the corresponding capacity and delay.

Exhibit 34-101
Example Problem 9: Approach
Capacity and Delay
Calculations

Approach	Entering Flow (pc/h)	Conflicting Flow (pc/h)	Capacity (pc/h)	Control Delay (s/veh)
EB EXT	722	369	782	34.5
EB INT	882	0	1,130	13.4
WB EXT	788	289	846	33.8
WB INT	879	0	1,130	13.3
NB RAMP	370	882	468	30.9
SB RAMP	372	879	469	31.1

Notes: EXT = external, INT = internal, EB = eastbound, WB = westbound, NB = northbound, SB = southbound.

O-D Movement Control Delay and LOS

Delay for each O-D is estimated as the sum of approach delays for each approach utilized by the O-D. For example, O-D Movement A will utilize the northbound ramp approach and westbound internal through approach. Control delays for these approaches are then summed to estimate control delay for O-D Movement A. LOS for each O-D is assigned on the basis of Exhibit 23-14. The

resulting control delay and LOS for all movements are shown in Exhibit 34-102. After extra distances are measured according to the Exhibit 23-8 discussion, EDTT can be obtained from Equation 23-50 [i.e., $EDTT = 100 / (1.47 \times 35) + 0 = 1.9$ s]. Intersectionwide performance measures are not calculated for interchange ramp terminals.

O-D	Control Delay (s/veh)	EDTT (s/veh)	ETT (s/veh)	LOS
A	44.2	1.9	46.1	D
B	30.9	-1.9	29.0	C
C	31.1	-1.9	29.2	C
D	44.5	1.9	46.4	D
E	47.9	1.9	49.8	D
F	34.5	-1.9	32.6	C
G	33.8	-1.9	31.9	C
H	47.1	1.9	49.0	D
I	47.9	0.0	47.9	D
J	47.1	0.0	47.1	D

Exhibit 34-102

Example Problem 9: Control Delay and LOS for Each O-D Movement

EXAMPLE PROBLEM 10: OPERATIONAL ANALYSIS FOR TYPE SELECTION

The Interchange

An interchange is to be built at the junction of I-83 (NB/SB) and Archer Road (EB/WB) in an urban area. The interchange type selection methodology described in Section 3 is used.

The Question

Which interchange type is likely to operate better under the given demands?

The Facts

This interchange will have two-lane approaches with single left-turn lanes on the arterial approaches. Freeway ramps will consist of two-lane approaches with channelized right turns in addition to the main ramp lanes. Default saturation flow rates for use in the type selection analysis are given in Exhibit 34-151. The O-D movements of traffic through this interchange are shown in Exhibit 34-103.

Exhibit 34-103

Example Problem 10: O-D Demand Information for the Interchange

O-D Movement	Volume (veh/h)
A	400
B	350
C	400
D	550
E	150
F	200
G	225
H	185
I	600
J	800
K	2,500
L	3,200
M	0
N	10

Outline of Solution

Mapping O-D Flows into Interchange Movements

The primary objective of this example is to compare up to eight interchange types against a given set of design volumes. The first step is to convert these O-D flows into movement flows through the signalized interchange. The interchange type methodology uses the standard NEMA numbering sequence for interchange phasing, and Exhibit 34-152 in Section 3 demonstrates which O-Ds make up each NEMA phase at the eight interchange types. Exhibit 34-104 shows the corresponding volumes for this example on the basis of the O-Ds from Exhibit 34-103. Since this interchange has channelized right turns, Exhibit 34-105 shows only the NEMA phasing volumes utilizing the signals.

Exhibit 34-104

Example Problem 10: NEMA Flows (veh/h) for the Interchange

Interchange Type	NEMA Phase Movement Number							
	1	2	3	4	5	6	7	8
SPUI	185	800	400	400	150	1,025	560	350
TUDI /CUDI	185	950	--	960	160	1,210	--	750
CDI (I)	185	950	--	960	--	1,200	--	--
CDI (II)	--	1,150	--	--	160	1,210	--	750
Parclo A-4Q (I)	--	750	--	960	--	1,385	--	--
Parclo A-4Q (II)	--	1,310	--	--	--	985	--	750
Parclo A-2Q (I)	--	750	--	960	200	1,385	--	--
Parclo A-2Q (II)	225	1,310	--	--	--	985	--	750
Parclo B-4Q (I)	185	950	--	--	--	1,200	--	--
Parclo B-4Q (II)	--	1,150	--	--	160	1,210	--	--
Parclo B-2Q (I)	185	950	--	--	--	1,200	--	400
Parclo B-2Q (II)	--	1,150	--	350	160	1,210	--	--

Notes: SPUI = single-point urban interchange, TUDI = tight urban diamond interchange, CUDI = compressed urban diamond interchange, CDI = conventional diamond interchange, Parclo = partial cloverleaf. (I) and (II) indicate the intersections within the interchange type. -- indicates that the movement does not exist in this interchange type.

Interchange Type	NEMA Phase Movement Number							
	1	2	3	4	5	6	7	8
SPUI	185	600	400	0	150	1,025	560	350
TUDI /CUDI	185	750	--	560	160	1,210	--	750
CDI (I)	185	750	--	560	--	1,200	--	--
CDI (II)	--	1,150	--	--	160	1,210	--	750
Parclo A-4Q (I)	--	750	--	560	--	1,385	--	--
Parclo A-4Q (II)	--	1,150	--	--	--	985	--	750
Parclo A-2Q (I)	--	750	--	560	200	1,385	--	--
Parclo A-2Q (II)	225	1,150	--	--	--	985	--	750
Parclo B-4Q (I)	185	750	--	--	--	1,200	--	--
Parclo B-4Q (II)	--	1,150	--	--	160	1,210	--	--
Parclo B-2Q (I)	185	750	--	--	--	1,200	--	400
Parclo B-2Q (II)	--	1,150	--	350	160	1,210	--	--

Notes: (I) and (II) indicate the intersections within the interchange type.
 -- indicates that the movement does not exist in this interchange type.

Computation of Critical Flow Ratios

Comparison between the eight intersection types begins with computation of the critical flow ratio at each interchange type. The first intersection type to be calculated is the SPUI by using Equation 34-1. On the basis of the default saturation flow rate for a SPUI and the values for the NEMA phases, Exhibit 34-106 shows the output from these calculations for a SPUI. The TUDI critical flow ratios are calculated by using Equation 34-4. Exhibit 34-107 shows these calculations for a 300-ft distance between the two TUDI intersections.

Value	Signalized Right Turns	Channelized Right Turns
Critical flow ratio for the arterial movements, A	0.368	0.306
Critical flow ratio for the ramp movements, R	0.350	0.156
Sum of critical flow ratios, Y_c	0.718	0.462

Exhibit 34-105

Example Problem 10: NEMA Flows for the Interchange Without Channelized Right Turns

Value	Signalized Right Turns	Channelized Right Turns
Effective flow ratio for concurrent phase when dictated by travel time, γ_t	0.070	0.070
Effective flow ratio for concurrent Phase 3, γ_3	0.070	0.070
Effective flow ratio for concurrent Phase 7, γ_7	0.070	0.070
Critical flow ratio for the arterial movements, A	0.461	0.294
Critical flow ratio for the ramp movements, R	0.474	0.315
Sum of critical flow ratios, Y_c	0.935	0.609

Exhibit 34-106

Example Problem 10: SPUI Critical Flow Ratio Calculations

Exhibit 34-107

Example Problem 10: TUDI Critical Flow Ratio Calculations

Value	Signalized Right Turns	Channelized Right Turns
Flow ratio for Phase 2 with consideration of pre-positioning, γ_2	0.264	0.208
Flow ratio for Phase 6 with consideration of pre-positioning, γ_6	0.208	0.208
Critical flow ratio for the arterial movements, A	0.373	0.332
Critical flow ratio for the ramp movements, R	0.267	0.156
Sum of critical flow ratios, Y_c	0.640	0.488

Exhibit 34-108

Example Problem 10: CUDI Critical Flow Ratio Calculations

Exhibit 34-109

Example Problem 10: CDI
Critical Flow Ratio Calculations

Value	Signalized Right Turns	Channelized Right Turns
Critical flow ratio for the arterial movements at Intersection I, A_I	0.373	0.333
Critical flow ratio for the ramp movements at Intersection I, R_I	0.282	0.165
Sum of critical flow ratios at Intersection I, $Y_{c,I}$	0.655	0.498
Critical flow ratio for the arterial movements at Intersection II, A_{II}	0.430	0.368
Critical flow ratio for the ramp movements at Intersection II, R_{II}	0.221	0.118
Sum of critical flow ratios at Intersection II, $Y_{c,II}$	0.651	0.486
Maximum sum of critical flow ratios, Y_c	0.655	0.498

The CUDI critical flow ratios are calculated by using Equation 34-9. Exhibit 34-108 shows these calculations for a CUDI with the given O-D flows.

The CDI, Parclo A-4Q, Parclo A-2Q, Parclo B-4Q, and Parclo B-2Q all use separate controllers. For these interchanges the critical flow ratios are calculated for each intersection, and then the maximum is taken for the overall interchange critical flow ratio. These numbers are all calculated by using Equation 34-14 and the default saturation flows. Exhibit 34-109 through Exhibit 34-113 show the calculations for these interchanges utilizing two controllers.

Exhibit 34-110

Example Problem 10: Parclo
A-4Q Critical Flow Ratio
Calculations

Value	Signalized Right Turns	Channelized Right Turns
Critical flow ratio for the arterial movements at Intersection I, A_I	0.385	0.333
Critical flow ratio for the ramp movements at Intersection I, R_I	0.282	0.282
Sum of critical flow ratios at Intersection I, $Y_{c,I}$	0.667	0.615
Critical flow ratio for the arterial movements at Intersection II, A_{II}	0.364	0.333
Critical flow ratio for the ramp movements at Intersection II, R_{II}	0.208	0.111
Sum of critical flow ratios at Intersection II, $Y_{c,II}$	0.572	0.444
Maximum sum of critical flow ratios, Y_c	0.667	0.615

Value	Signalized Right Turns	Channelized Right Turns
Critical flow ratio for the arterial movements at Intersection I, A_I	0.502	0.451
Critical flow ratio for the ramp movements at Intersection I, R_I	0.282	0.165
Sum of critical flow ratios at Intersection I, $Y_{c,I}$	0.784	0.616
Critical flow ratio for the arterial movements at Intersection II, A_{II}	0.430	0.452
Critical flow ratio for the ramp movements at Intersection II, R_{II}	0.221	0.111
Sum of critical flow ratios at Intersection II, $Y_{c,II}$	0.651	0.563
Maximum sum of critical flow ratios, Y_c	0.784	0.616

Exhibit 34-111

Example Problem 10: Parclo A-2Q Critical Flow Ratio Calculations

Value	Signalized Right Turns	Channelized Right Turns
Critical flow ratio for the arterial movements at Intersection I, A_I	0.373	0.333
Critical flow ratio for the ramp movements at Intersection I, R_I	0.000	0.000
Sum of critical flow ratios at Intersection I, $Y_{c,I}$	0.373	0.333
Critical flow ratio for the arterial movements at Intersection II, A_{II}	0.430	0.368
Critical flow ratio for the ramp movements at Intersection II, R_{II}	0.000	0.000
Sum of critical flow ratios at Intersection II, $Y_{c,II}$	0.430	0.368
Maximum sum of critical flow ratios, Y_c	0.430	0.368

Exhibit 34-112

Example Problem 10: Parclo B-4Q Critical Flow Ratio Calculations

Value	Signalized Right Turns	Channelized Right Turns
Critical flow ratio for the arterial movements at Intersection I, A_I	0.373	0.333
Critical flow ratio for the ramp movements at Intersection I, R_I	0.111	0.111
Sum of critical flow ratios at Intersection I, $Y_{c,I}$	0.484	0.444
Critical flow ratio for the arterial movements at Intersection II, A_{II}	0.430	0.368
Critical flow ratio for the ramp movements at Intersection II, R_{II}	0.103	0.103
Sum of critical flow ratios at Intersection II, $Y_{c,II}$	0.533	0.471
Maximum sum of critical flow ratios, Y_c	0.533	0.471

Exhibit 34-113

Example Problem 10: Parclo B-2Q Critical Flow Ratio Calculations

Estimation of Interchange Delay

Estimation of interchange delay is the final step when interchange types are compared. On the basis of the critical flow ratios calculated previously, Exhibit 34-159 in Section 3 can be used to calculate the delay at the eight interchange types. Exhibit 34-114 shows the solutions to these calculations.

Exhibit 34-114
 Example Problem 10:
 Interchange Delay for the
 Eight Interchange Types

Intersection Type	Interchange Delay d_I (s/veh)	
	Right Turns Signalized	Right Turns Free or YIELD-Controlled
SPUI	62.9	22.0
TUDI	217.7	33.3
CUDI	35.9	27.4
CDI	26.6	21.7
Parclo A-4Q	26.2	21.6
Parclo A-2Q	47.4	29.0
Parclo B-4Q	11.9	11.3
Parclo B-2Q	30.7	29.0

Results

As demonstrated by Exhibit 34-114, a Parclo B-4Q would be the best interchange type to select in terms of operational performance for the given O-D flows at this interchange. For the final interchange type selection, however, additional criteria should be considered, including those related to economic, environmental, and land use concerns.

EXAMPLE PROBLEM 11: ALTERNATIVE ANALYSIS TOOL

This example presents a simulation analysis of the diamond interchange configuration originally described in Example Problem 1. A few changes have been made to introduce elements that are beyond the stated limitations of the interchange ramp terminal procedures. The use of a typical simulation tool to address the limitations is described in this section. The need to determine performance measures from analysis of vehicle trajectories was emphasized in Chapter 7, Interpreting HCM and Alternative Tool Results. Specific procedures for defining measures in terms of vehicle trajectories were proposed to guide the development of alternative tools. Pending further development, the example presented in this chapter applied existing versions of alternative tools and thus does not reflect the trajectory-based measures described in Chapter 7.

Operational Characteristics

A two-way STOP-controlled (TWSC) intersection was introduced 600 ft west of the first signalized intersection of the interchange. Ramp metering signals were installed on both of the freeway entrance ramps. Right-turn storage bays were introduced on all approaches to the interchange that accommodated right turns. The demand volumes were modified to introduce conditions that varied from undersaturated to heavily oversaturated. The signal timing plan was modified to accommodate the distribution of volumes. Exhibit 34-115 shows the interchange configuration and demand volumes. The demand volumes are referenced to the total directional arterial demand d , which varies from 600 to 1,800 veh/h. The turning movement volumes entering and leaving the arterial have been balanced for continuity of traffic flow. The turning movements entering and leaving the freeway were set at 25% of the total approach volumes and were adjusted proportionally to match the arterial demand volumes. The cross-street entry demand from the TWSC intersection was held constant at 100 veh/h in each direction, with 50% assigned to the left and right turns. No through vehicles were assigned from the cross street at this intersection.

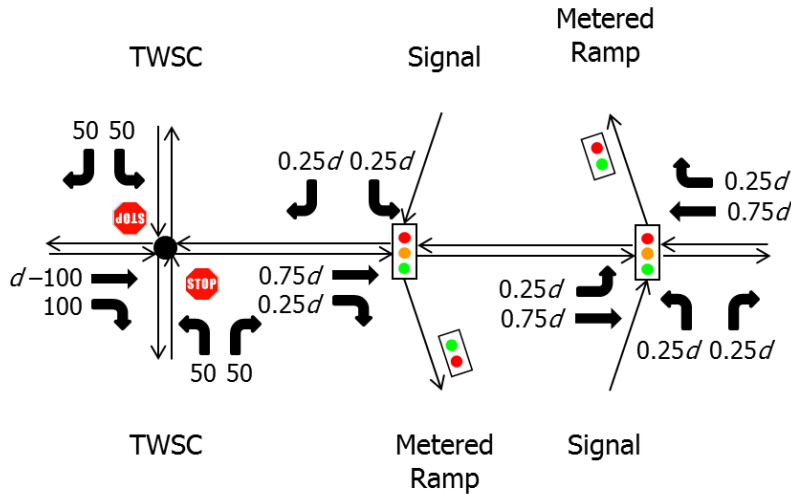


Exhibit 34-115
Example Problem 11:
Interchange Configuration and
Demand Volumes

Note: TWSC = two-way STOP control.

Exhibit 34-116 shows the signal timing plan for both intersections of the diamond interchange. A simple three-phase operation at each intersection is depicted in this table. No attempt has been made to optimize the phasing or timing since the main purpose of this example is to demonstrate self-aggravating phenomena that are not recognized by the Chapter 23 procedures. The ramp metering signals installed on each of the entrance ramps were set to release a single vehicle at 10-s intervals, giving a capacity of 360 veh/h for each ramp.

Movement	Green (s)	Yellow (s)	All Red (s)
Entry through/left	20	4	1
Entry and exit through/right	45	4	1
Ramp	20	4	1
Cycle length (s)	100		

Exhibit 34-116
Example Problem 11: Signal
Timing Plan

Summary of Simulation Runs

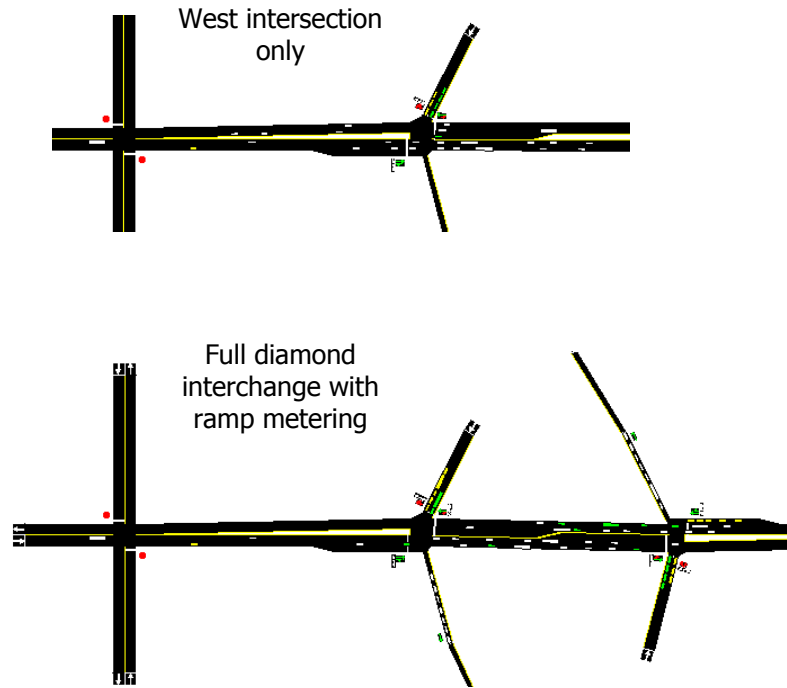
Operation of this interchange was simulated by using demand volumes d ranging from 600 veh/h (very undersaturated) to 1,800 veh/h (very oversaturated). The volume increment was 200 veh/h. Thirty simulations were run for each condition to capture stochastic variations inherent to simulation.

Two configurations were examined for each of the demand levels:

1. A single intersection at the west end of the diamond interchange and
2. The full diamond interchange with ramp metering.

Both of these configurations are illustrated in Exhibit 34-117. The west intersection was examined separately to show the difference between a signalized intersection operating independently and one operating as part of a diamond interchange with mutual interactions between intersections at each end.

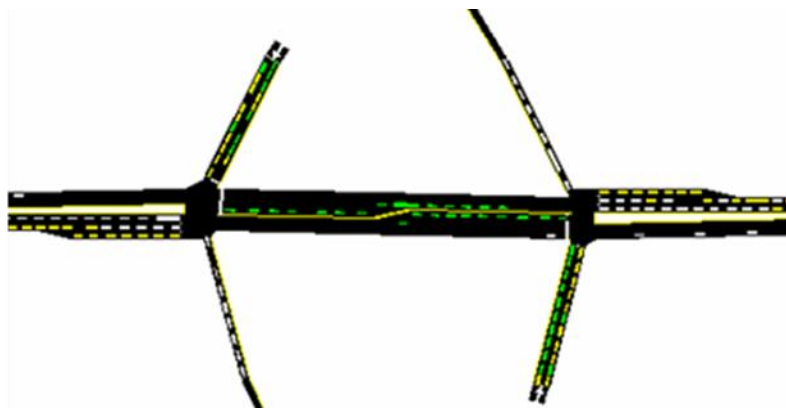
Exhibit 34-117
Example Problem 11: Physical
Configurations Examined



Diamond Interchange Operation

Exhibit 34-118 illustrates the self-aggravating effects from interactions among the two signals that make up the interchange and the ramp metering. Backup and congestion are observed at high demands on all approaches. The left-turn bays on the internal interchange segments spill over to block through traffic. Backup from the ramp metering signals causes additional impediment to traffic trying to leave the interchange.

Exhibit 34-118
Example Problem 11:
Congested Approaches to
Diamond Interchange



Excessive delays will be associated with the oversaturated operation. However, for purposes of this example, the reduction in capacity is of more interest because capacity reductions due to self-aggravating phenomena are not fully recognized by the Chapter 23 methodology. Proper assessment of delay with heavy oversaturation would require a more complex procedure involving multiperiod analysis with possible consideration of route diversion due to the excessive congestion. Therefore, this example will be limited to examining the

capacity reduction that results from interaction between the elements within this system. The extent of the capacity reduction will be estimated by the relationship between demand (input) and discharge (output) on the various segments.

Exhibit 34-119 shows the westbound arterial discharge from the diamond interchange (through plus left turns) as a function of arterial demand d . Note that the discharge tracks the demand at low volumes, which indicates that all arrivals were accommodated. As the demand increases, the discharge levels off at a point that indicates the capacity of the approach. When the approach is a part of an isolated intersection, the capacity nears 1,600 veh/h. A much lower capacity (about 850 veh/h) is attainable in the case of the diamond interchange with ramp metering. A number of self-aggravating phenomena reduce the capacity. Some westbound vehicles are unable to enter the east intersection because of backup from internal westbound left-turn bay spillover. Other westbound vehicles are unable to exit the interchange because of backup from the ramp metering signal and because of blockage of the intersection by left-turning exit ramp vehicles. The net result is a substantial reduction in capacity that would not be evident from application of the Chapter 23 methodology.

Exhibit 34-120 shows the effect of the demand volume on the southbound exit ramp discharge at the west signal of the diamond interchange. With an isolated signal, the discharge levels off at the approach capacity. As shown, the capacity is reduced slightly when the signal is part of a diamond interchange. The reduction was not as apparent as it was for the arterial movements because the blockage effects are not as significant. Some left turns were unable to enter the intersection because of backup from the east signal. The right turns from the ramp were not subject to any blockage effects.

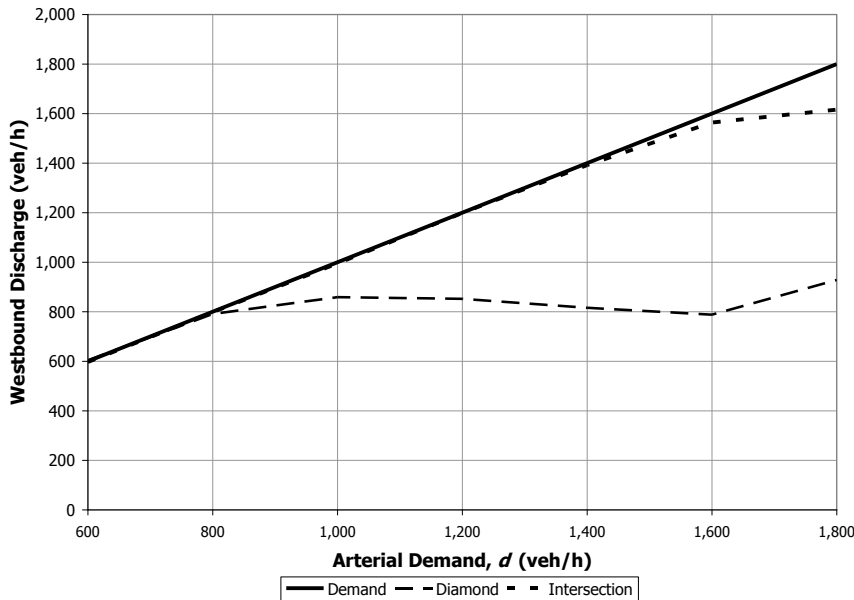
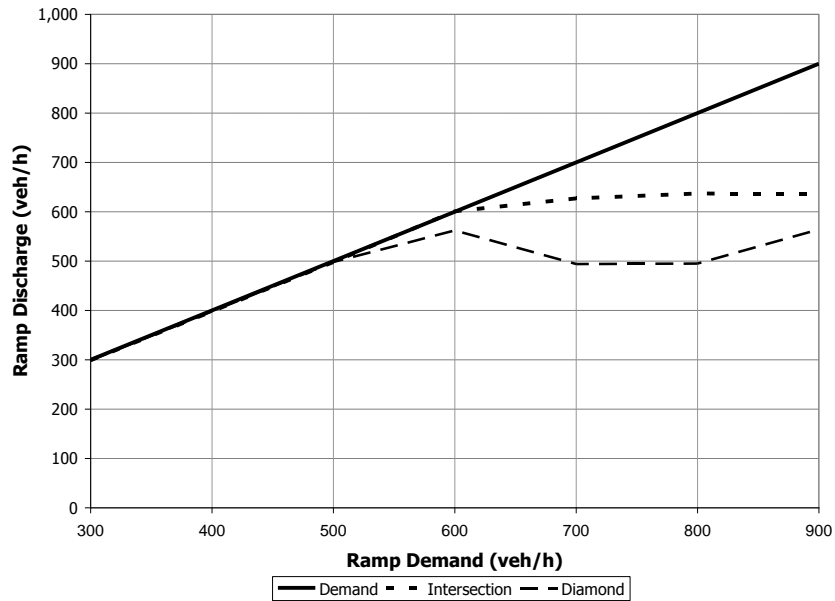


Exhibit 34-119
 Example Problem 11:
 Discharge from the Diamond
 Interchange Under the Full
 Range of Arterial Demand

Exhibit 34-120
 Example Problem 11:
 Discharge from the
 Southbound Exit Ramp Under
 the Full Range of Ramp
 Demand



TWSC Intersection Operation

The TWSC analysis procedures prescribed in Chapter 20 recognize the effects of adjacent signalized intersections to some extent, but they do not address cases in which an approach is blocked throughout part of a cycle by stationary queues that prevent vehicles from entering on the minor street. This situation is depicted in Exhibit 34-121, in which a stationary queue of eastbound vehicles backed up from the west intersection of the diamond interchange has blocked the entry to the intersection for three of the four minor-street movements.

Exhibit 34-121
 Example Problem 11:
 Congested Approaches to the
 TWSC Intersection

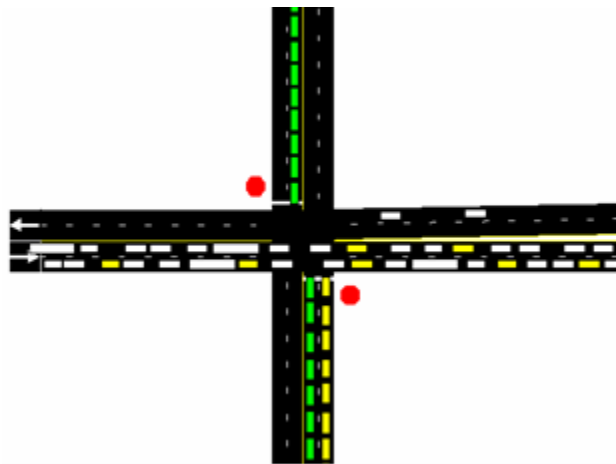
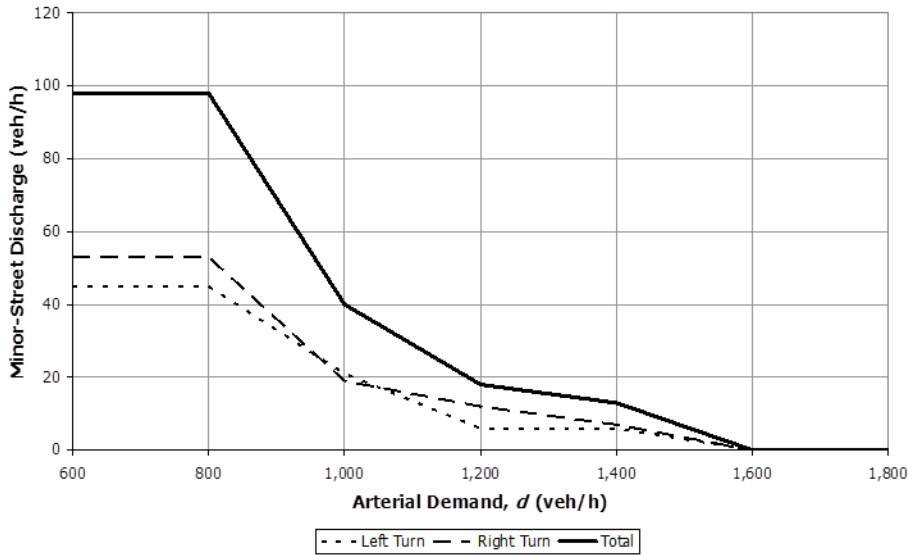
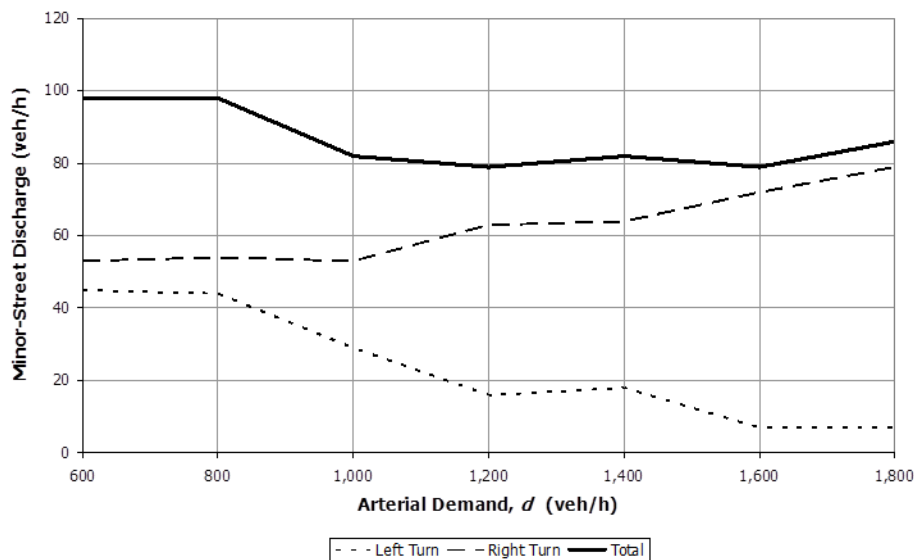


Exhibit 34-122 shows the minor-street entry as a function of the arterial demand. Unlike the other movements in this example, the minor-street demand was kept constant throughout the entire range of arterial demand. According to a well-established principle of TWSC analysis, the entry capacity for minor-street movements diminishes with increasing major-street volumes. That phenomenon is depicted clearly for northbound traffic in Exhibit 34-121. It is evident here that capacity begins to drop below demand at about 800 veh/h in each arterial direction. The southbound situation, on the other hand, presents some surprising

results. The southbound left turn is impeded by a queue of westbound vehicles backed up from the interchange, as expected. The southbound right turn, assisted by gaps created by the interchange signal, experiences an increase in capacity, producing entry volumes that exceed the original demand. Animated graphics indicate that some of the southbound left-turn vehicles were unable to maneuver into the proper lane. The driver behavior model of the simulation tool reassigned these vehicles to right turns because of excessive waiting times. This effect provides a clear example of the difference between simulation modeling and the analytical approach presented throughout the HCM.



(a) Northbound



(b) Southbound

Exhibit 34-122

Example Problem 11: Effect of Arterial Demand on Minor-Street Discharge at the TWSC Intersection

EXAMPLE PROBLEM 12: FOUR-LEGGED RESTRICTED CROSSING U-TURN INTERSECTION WITH MERGES

The Intersection

An RCUT with merges in a rural area has four approaches.

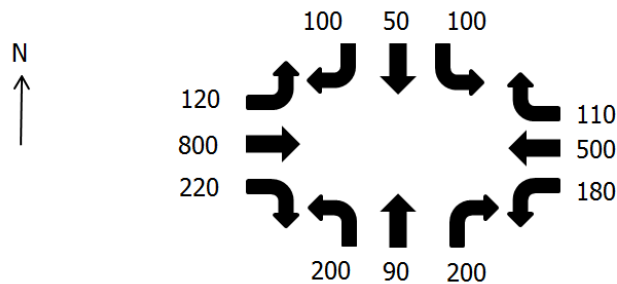
The Question

What is the LOS for each of the 12 movements at the intersection?

The Facts

The geometry is as pictured in Exhibit 23-42, with the main street running east-west. The distance from the main intersection to each U-turn crossover is 2,000 ft. The storage bay length for each left-turn crossover is 300 ft. The PHF is 0.92. Free-flow speed on the major street is 60 mi/h. The truck percentages are zero, and there are no significant grades on any approach. Exhibit 34-123 shows the vehicular demands (veh/h).

Exhibit 34-123
Example Problem 12: Turning Movement Demands



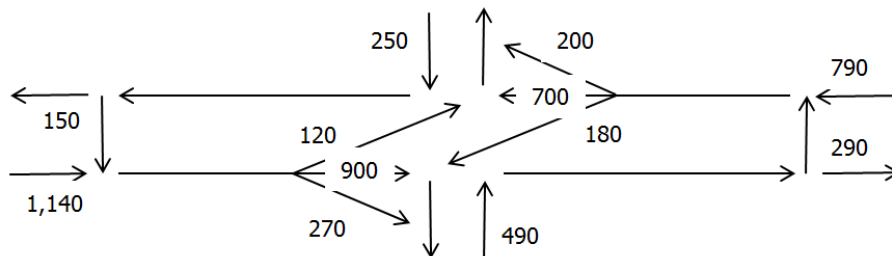
Solution

The solution follows the 10-step procedure outlined in Chapter 23. Once the v/c ratio, 95% queue-to-storage ratio, and experienced travel time have been determined for a movement, its LOS will be found by using Exhibit 23-13.

Determination of O-D Demands and Movement Demands

Exhibit 34-124 shows the demands (veh/h) redistributed to the different junctions of the RCUT.

Exhibit 34-124
Example Problem 12: Demands Converted to the RCUT Geometry



Determination of Lane Groups

RCUTs with merges do not have signals, so there is no need to determine lane or movement groups at each approach. Exhibit 34-125 shows the redistributed demands converted to flow rates (veh/h) by using the PHF and Equation 23-55.

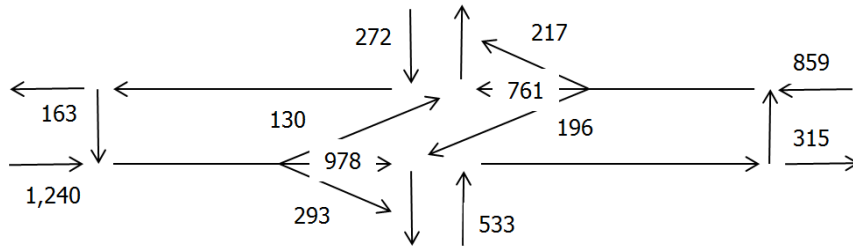


Exhibit 34-125
Example Problem 12: Flow Rates in the RCUT Geometry

Determination of Lane Utilization

This step is not needed for an RCUT with merges.

Calculation of Signal Progression Adjustments

This step is not needed for an RCUT with merges.

Calculation of Additional Control-Based Adjustments

For an RCUT with merges, the analyst may use judgment to determine whether significant weaving delay exists. When significant weaving delay exists, the analyst must develop an estimate of this delay from field measurements or an alternative tool and add it to the EDTT estimate calculated later.

Calculation of Junction-Specific Performance Measures

At an RCUT with merges that passes the weaving area tests in Step 5, control delay is only experienced by the major-street left turns. Use of the methods of Chapter 20 with the inputs listed above, and with default values for all other factors provided, produces the following results:

- For the eastbound left turn (at the north main intersection), $v/c = 0.18$, 95% queue length = 0.66 veh or 16.5 ft at 25 ft/veh, and control delay = 11.2 s/veh; and
- For the westbound left turn (at the south main intersection), $v/c = 0.35$, 95% queue length = 1.58 veh or 39.5 ft at 25 ft/veh, and control delay = 15.0 s/veh.

Calculation of Extra Distance Travel Time

The bottom portion of Exhibit 23-48 shows that at a four-legged RCUT with merges, extra travel distance is experienced by the left turns from the minor street and by the through movements on the minor street. Both minor left turns will experience the same extra distance travel time (EDTT) since the distances from the main intersection to both U-turn crossovers are the same. Use of Equation 23-56 results in the following EDTT:

$$EDTT = \frac{D_t + D_f}{1.47 \times FFS} + a$$

$$EDTT = \frac{2,000 + 2,000}{1.47 \times 60} + 10 = 55.4 \text{ s/veh}$$

Both minor-street through movements will experience the same EDTT, since the distances from the main intersection to both U-turn crossovers are the same. Use of Equation 23-56 results in the following EDTT:

$$EDTT = \frac{2,000 + 2,000}{1.47 \times 60} + 15 = 60.4 \text{ s/veh}$$

Calculation of Additional Weaving Delay

In this example problem, it is assumed that no significant weaving delay exists, in the analyst’s judgment. Therefore, there are no adjustments to make in this step.

Calculation of Experienced Travel Time

Experienced travel time (ETT) is computed with Equation 23-58:

$$ETT = \sum d_i + \sum EDTT$$

The bottom portion of Exhibit 23-48 gives the following:

- For the EB left from the major street, ETT = 11.2 + 0 = 11.2 s/veh.
- For the WB left from the major street, ETT = 15.0 + 0 = 15.0 s/veh.
- For the major-street through movements, ETT = 0 + 0 = 0 s/veh.
- For the major-street right-turn movements, ETT = 0 + 0 = 0 s/veh.
- For the left turns from the minor street, ETT = (0 + 0) + 55.4 = 55.4 s/veh.
- For the through movements from the minor street, ETT = (0 + 0) + 60.4 = 60.4 s/veh.
- For the right turns from the minor street, ETT = 0 + 0 = 0 s/veh.

Determination of Level of Service

The LOS for each movement is obtained with Exhibit 23-13 (it has been established that the *v/c* ratio was less than 1.0 at all junctions and that the queue-to-storage ratios were well below 1.0 for the 300-ft bay lengths provided):

- For the eastbound left from the major street, LOS = B.
- For the westbound left from the major street, LOS = B.
- For the major-street through movements, LOS = A.
- For the major-street right-turn movements, LOS = A.
- For the minor-street left turns, LOS = E.
- For the minor-street through movements, LOS = E.
- For minor-street right turns, LOS = A.

Discussion

The minor-street left-turn and through movements experience LOS E because of the distances from the main intersection to the U-turn crossovers and the major-street free-flow speed. Chapter 23 explores the sensitivity of EDTT and LOS to these factors. It shows that, over typical ranges, there is some change in EDTT and LOS as a result of these factors but that achievement of a LOS better than D or E for minor-street left-turn and through movements with this design will be difficult.

**EXAMPLE PROBLEM 13: THREE-LEGGED RESTRICTED CROSSING
U-TURN INTERSECTION WITH STOP SIGNS**

The Intersection

An RCUT with STOP signs in a rural area has three approaches.

The Question

What is the LOS for each of the six movements at the intersection?

The Facts

The main street runs north–south. The distance from the main intersections to the U-turn crossover is 700 ft. The storage bay lengths for the left-turn and U-turn crossovers are 400 ft. The PHF is 0.90. The free-flow speed on the major street is 60 mi/h. The truck percentage is 5.9% on the EB approach and 6.1% on all other approaches. The grade on the EB approach is 2%, there are no pedestrians, and there are no nearby traffic signals. Exhibit 34-126 shows the vehicular demands (veh/h).

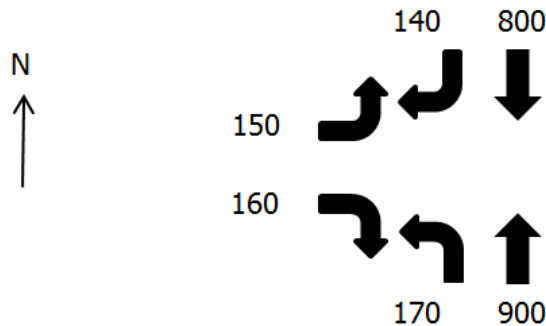


Exhibit 34-126
Example Problem 13: Turning
Movement Demands

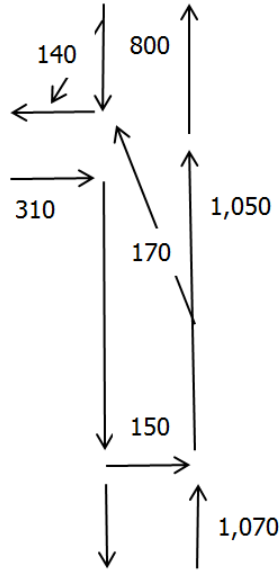
Solution

The solution follows the 10-step procedure outlined in Chapter 23. Once the v/c ratio, queue-to-storage ratio, and experienced travel time have been determined for a movement, its LOS will be found with Exhibit 23-13.

Determination of O-D Demands and Movement Demands

Exhibit 34-127 shows the demands (veh/h) redistributed to the various junctions of the RCUT.

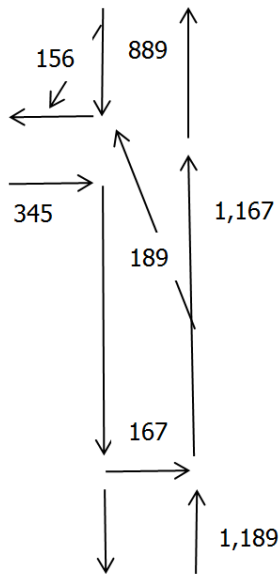
Exhibit 34-127
 Example Problem 13:
 Demands Converted to the
 RCUT Geometry



Determination of Lane Groups

RCUTs with STOP signs do not have traffic signals, so there is no need to determine lane or movement groups at each approach. Exhibit 34-128 shows the redistributed demands converted to flow rates (veh/h) on the basis of the PHF and Equation 23-55.

Exhibit 34-128
 Example Problem 13: Flow
 Rates in the RCUT Geometry



Determination of Lane Utilization

This step is not needed for an RCUT with STOP signs.

Calculation of Signal Progression Adjustments

This step is not needed for an RCUT with STOP signs.

Calculation of Additional Control-Based Adjustments

For this RCUT with STOP signs, no field data on the base critical headway and base follow-up time are available, so the solution will use the default values suggested in Chapter 23.

Calculation of Junction-Specific Performance Measures

The bottom of Exhibit 23-49 shows that, for a three-legged RCUT with STOP signs, control delay is experienced by the major-street left-turn and minor-street left-turn and right-turn vehicles at the main junction and by the minor-street left-turn vehicles at the U-turn crossover. The methods of Chapter 20, with the inputs listed above and default values for all other factors, provide the following results:

- For the eastbound minor-street left-turn and through vehicles at the main junction, $v/c = 0.59$, 95% queue length = 3.8 veh or 95 ft at 25 ft/veh, and control delay = 19.4 s/veh.
- For the northbound major-street left turn at the main junction, $v/c = 0.29$, 95% queue length = 1.2 veh or 30 ft at 25 ft/veh, and control delay = 12.9 s/veh.
- For the eastbound minor-street left turn at the U-turn crossover, $v/c = 0.19$, 95% queue length = 0.69 veh or 17 ft at 25 ft/veh, and control delay = 10.0 s/veh.

Calculation of Extra Distance Travel Time

The bottom portion of Exhibit 23-49 shows that at a three-legged RCUT with STOP signs, extra travel distance is experienced by the left turns from the minor street. Use of Equation 23-57 gives the extra distance travel time (EDTT):

$$EDTT = \frac{D_t + D_f}{1.47 \times FFS}$$

$$EDTT = \frac{700 + 700}{1.47 \times 60} = 15.9 \text{ s/veh}$$

Calculation of Additional Weaving Delay

For an RCUT with STOP signs there are no adjustments to make in this step.

Calculation of Experienced Travel Time

Experienced travel time (ETT) is computed with Equation 23-58:

$$ETT = \sum d_i + \sum EDTT$$

Use of the bottom portion of Exhibit 23-49 gives the following:

- For the northbound left from the major street, $ETT = 12.9 + 0 = 12.9$ s/veh.
- For the major-street through movements, $ETT = 0 + 0 = 0$ s/veh.
- For the major-street right-turn movement, $ETT = 0 + 0 = 0$ s/veh.
- For the left turn from the minor street, $ETT = (19.4 + 10.0) + 15.9 = 45.3$ s/veh.
- For the right turn from the minor street, $ETT = 19.4 + 0 = 19.4$ s/veh.

Determination of Level of Service

LOS for each movement is obtained with Exhibit 23-13 (it has been established that the v/c ratio was less than 1.0 at all junctions and that the queue-to-storage ratios were well below 1.0 for the 400-ft bay lengths provided):

- For the eastbound left from the major street, LOS = B.
- For the major-street through movements, LOS = A.
- For the major-street right-turn movement, LOS = A.
- For the left turn from the minor street, LOS = D.
- For the right turn from the minor street, LOS = B.

Discussion

Interesting factors to examine in this problem are the base critical headway and base follow-up time at the U-turn crossover and the minor-street left-turn demand. Recalculation of the example by using the default values for base critical headway and base follow-up time for minor-street left turns (7.1 s and 3.5 s, respectively) results in control delay at the U-turn crossover rising from 10.0 to 18.6 s/veh. In turn, this changes the EDTT value for the minor-street left-turn movement to 52.7 s/veh, which is still LOS D. It is apparent that the base critical headway and base follow-up time values used in the U-turn crossover analysis could affect LOS by one level.

In general, the RCUT design requires extra travel time for the minor-street left-turn and through movements while minimizing delays for the major-street movements. Chapter 23 shows, for the conditions in this example, how far the minor street can be pushed before it reaches LOS F. In this case, a demand of more than 250 veh/h minor-street left turns in conjunction with 250 veh/h minor-street right turns results in LOS F. If these are peak-period flows and typical K - and D -factors apply, these demand levels translate to annual average daily traffic values of 8,000 to 10,000 veh/day. Of course, better levels of service can be achieved on the minor-street approach with an additional lane. Chapter 23 also illustrates that minor-street left-turn LOS at an RCUT with STOP signs will rarely achieve better than LOS D. It is apparent that the LOS constraint at an RCUT will typically be the minor-street approach, which serves more movements than the major-street left-turn crossover or the U-turn crossover.

EXAMPLE PROBLEM 14: FOUR-LEGGED RESTRICTED CROSSING U-TURN INTERSECTION WITH SIGNALS

The Intersection

An RCUT with signals in a suburban area has four approaches.

The Question

What is the LOS for each of the 12 movements at the intersection and for the facility as a whole?

The Facts

The main street runs north–south. The distance from the main intersections to the U-turn crossovers is 800 ft. The storage bay lengths for the left-turn and U-turn crossovers are 400 ft. The median is 40 ft wide. All crossovers have a single lane. The major street has two through lanes and exclusive right-turn lanes at the main junction in each direction. The minor street has two lanes on each of the approaches to the main junctions. The PHF is 0.93. Free-flow speed on the major street is 50 mi/h. The truck percentages are 3.7%. Grades are flat on all approaches. There are no pedestrians, and there are no significant volumes turning on a red signal. Exhibit 34-129 shows the vehicular demands (veh/h).

The signals are pretimed as part of a longer RCUT corridor. The arrival type is 6 on the major street at the U-turn crossover signals in both directions and 3 for the minor street. At both southbound signals, the cycle length is 90 s, with 60 s of major-street green, 20 s of minor-street or crossover green, 4 s of yellow, and 1 s of all-red. At both northbound signals, the cycle length is 60 s, with 25 s of major-street green, 25 s of minor-street or crossover green, 4 s of yellow, and 1 s of all-red.

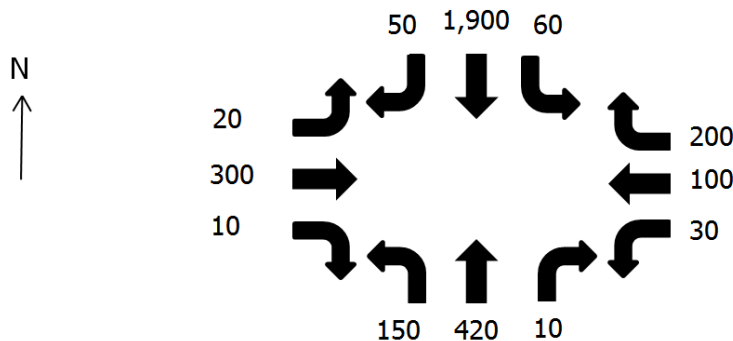


Exhibit 34-129
Example Problem 14: Turning Movement Demands

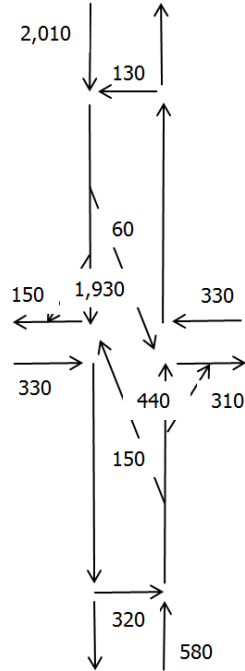
Solution

The solution follows the 10-step procedure outlined in Chapter 23. Once the v/c ratio, queue-to-storage ratio, and experienced travel time have been determined for a movement, its LOS will be found with Exhibit 23-13.

Determination of O-D Demands and Movement Demands

Exhibit 34-130 shows the demands (veh/h) redistributed to the various junctions of the RCUT.

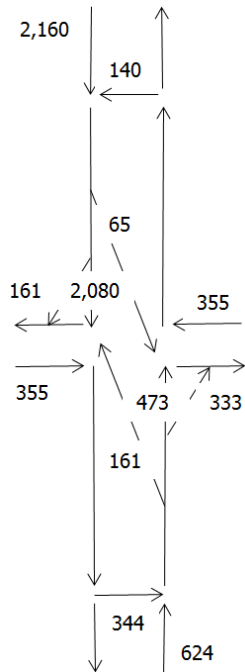
Exhibit 34-130
 Example Problem 14:
 Demands Converted to the
 RCUT Geometry



Determination of Lane Groups

Lane and movement groups at each approach are determined with the methods of Chapter 19. Exhibit 34-131 shows the redistributed demands converted to flow rates (veh/h) obtained by using the PHF and Equation 23-55.

Exhibit 34-131
 Example Problem 14: Flow
 Rates in the RCUT Geometry



Determination of Lane Utilization

With no field data on hand, the default lane distribution is applied to all approaches to signals.

Calculation of Signal Progression Adjustments

The top portion of Exhibit 23-51 is used to find arrival types for each approach to each signal after the first signal encountered.

Calculation of Additional Control-Based Adjustments

For this RCUT with signals, no field data are available on the saturation flow rate for traffic in the U-turn crossover, so the solution will use the default value of 0.85 suggested in Exhibit 23-52 for a 40-ft median width.

Calculation of Junction-Specific Performance Measures

The top portion of Exhibit 23-48 shows that, for a four-legged RCUT with signals, one to three increments of control delay are experienced by each movement. The methods of Chapter 19 are applied to calculate these delays, on the basis of the inputs listed above and defaults for all other values. The results are shown in Exhibit 34-132.

Junction	Movement	v/c	95% Queue Length (veh)	Control Delay (s/veh)
North crossover	SB through	0.92	4.4	7.6
	WB crossover	0.40	5.0	33.3
West main intersection	SB through	0.89	3.2	5.4
	SB right turn	0.16	0.2	0.3
	EB right turn	0.58	6.4	35.1
	NB left turn	0.41	5.7	33.2
South crossover	NB through	0.43	1.4	4.1
	EB crossover	0.53	5.9	16.1
East main intersection	NB through	0.32	1.7	6.4
	NB right turn	0.51	3.1	9.1
	WB right turn	0.31	2.4	12.4
	SB left turn	0.09	0.8	10.8

Notes: EB = eastbound, WB = westbound, NB = northbound, SB = southbound.

Exhibit 34-132
Example Problem 14: Control Delay for Each Junction

Calculation of Extra Distance Travel Time

The top portion of Exhibit 23-48 shows that at a four-legged RCUT with signals, extra travel distance is experienced by the left turns and through movements from the minor street. Use of Equation 23-57 gives the following extra distance travel time (EDTT):

$$EDTT = \frac{D_t + D_f}{1.47 \times S_f}$$

$$EDTT = \frac{800 + 800}{1.47 \times 50} = 21.8 \text{ s/veh}$$

Calculation of Additional Weaving Delay

For an RCUT with signals, there are no adjustments to make in this step.

Calculation of Experienced Travel Time

Experienced travel time (ETT) is computed with Equation 23-58:

$$ETT = \sum d_i + \sum EDTT$$

Use of the top portion of Exhibit 23-48 gives the results in Exhibit 34-133.

Exhibit 34-133

Example Problem 14: ETT and LOS Results

Movement	Control Delay (s/veh) by Traffic Control Device			EDTT (s/veh)	ETT (s/veh)	LOS
	First	Second	Third			
NB left	4.1	33.2	None	0	37.3	D
SB left	7.6	10.8	None	0	18.4	B
NB through	4.1	6.4	None	0	10.5	B
SB through	7.6	5.4	None	0	13.0	B
NB right	4.1	9.1	None	0	13.2	B
SB right	7.6	0.3	None	0	7.9	A
EB left	35.1	16.1	6.4	21.8	79.4	E
WB left	12.4	33.3	5.4	21.8	72.9	E
EB through	35.1	16.1	9.1	21.8	82.1	F
WB through	12.4	33.3	0.3	21.8	67.8	E
EB right	35.1	None	None	0	35.1	D
WB right	12.4	None	None	0	12.4	B

Notes: EB = eastbound, WB = westbound, NB = northbound, SB = southbound.

Determination of Level of Service

Levels of service for each movement are shown above in Exhibit 34-133. The results were obtained with Exhibit 23-13, after establishing that the v/c ratio was less than 1.0 at all junctions and that the queue-to-storage ratios were well below 1.0 for the 400-ft bay lengths provided.

The ETT for the entire intersection is obtained from Equation 23-60:

$$ETT_I = \frac{\sum(ETT_j \times v_j)}{\sum v_j}$$

ETT_I is $79,900 / 3,500 = 22.8$ s/veh, which corresponds to LOS C.

Discussion

One of the concerns at an RCUT is the possibility of uneven lane distribution on a multilane minor-street approach or a multilane U-turn crossover. The results above were produced by assuming a relatively even lane distribution on the two-lane minor-street approaches. On the westbound minor-street approach, there was a demand of 200 veh/h to turn right and 130 veh/h to turn left or make a through movement. Placing all of the right-turn vehicles in the right lane and all of the other vehicles in the left lane would add just 0.3 s/veh of control delay to those movements, which indicates that for situations like the one in this example, lane distribution may not matter too much.

The effect of the saturation flow adjustment factor for U-turns can also be examined. The default suggested in Exhibit 23-52 for this case, with a 40-ft-wide median, is 0.85. If field data showed that the factor should be 0.8, control delay for each movement using a crossover would increase by 0.7 to 0.9 s/veh from the results in Exhibit 34-133. On the other hand, if field data showed that the factor should be 0.9, the control delay for each movement using a crossover would decrease by 0.6 to 0.7 s/veh, compared with the results in Exhibit 34-133. Overall, the U-turn saturation flow adjustment factor only makes a small difference in this problem.

EXAMPLE PROBLEM 15: FOUR-LEGGED MEDIAN U-TURN INTERSECTION WITH STOP SIGNS

The Intersection

An MUT with STOP signs at the U-turn crossovers in a suburban area has four approaches.

The Question

What is the LOS for each of the 12 movements at the intersection?

The Facts

The main street runs north–south. The distance from the main intersections to the U-turn crossovers is 600 ft. The storage bay lengths for the left-turn and U-turn crossovers are 500 ft. Both U-turn crossovers have a single lane. The major street has two through lanes at the main junction, with shared right-turn lanes. The minor street has one through lane and one exclusive right-turn lane on each approach to the main junction. The PHF is 0.95. Free-flow speed on the major street is 40 mi/h. The truck percentages are 2.6%. Grades are flat on all approaches. There are 100 pedestrians per hour on each crosswalk at the main junction, and there are no turns on red at the signal due to the pedestrians. Exhibit 34-134 shows the vehicular demands (veh/h). The signal is actuated and not coordinated. The yellow time is 4 s and the all-red is 1 s. Maximum green times are 30 s for east–west phases and 50 s for north–south phases.

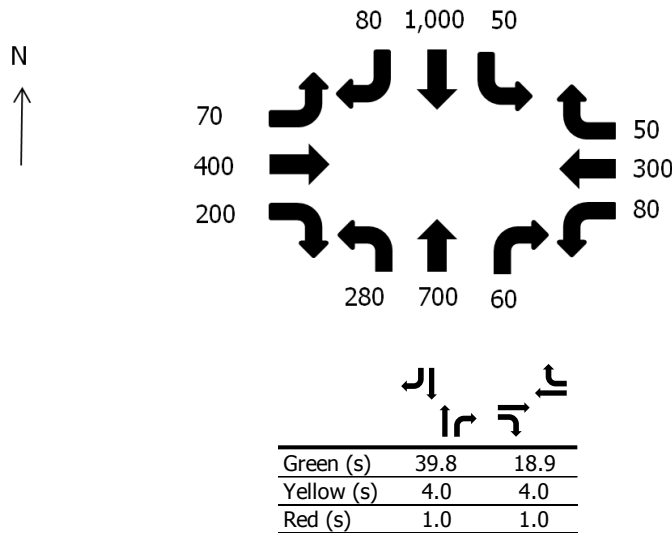


Exhibit 34-134

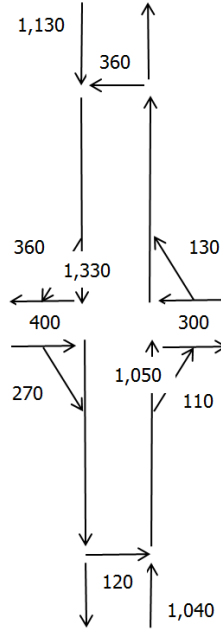
Example Problem 15: Turning Movement Demands and Average Interval Durations

Solution

Determination of O-D Demands and Movement Demands

Exhibit 34-135 shows the demands (veh/h) redistributed to the various junctions of the MUT.

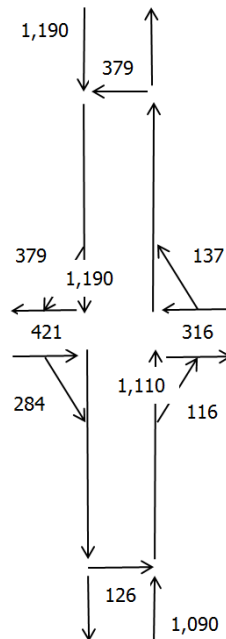
Exhibit 34-135
 Example Problem 15:
 Demands Converted to the
 MUT Geometry



Determination of Lane Groups

Lane and movement groups at each approach are determined with the methods of Chapter 19. Exhibit 34-136 shows the redistributed demands converted to flow rates (veh/h) obtained by using the PHF and Equation 23-55.

Exhibit 34-136
 Example Problem 15: Flow
 Rates in the MUT Geometry



Determination of Lane Utilization

With no field data on hand, the default lane distribution is applied to the major-street approaches to the signal.

Calculation of Signal Progression Adjustments

Because the signal is not coordinated, arrival types of 3 will be used on all approaches to the signal.

Calculation of Additional Control-Based Adjustments

For this MUT with STOP signs at the U-turn crossovers, no field data on the base critical headway and no base follow-up time are available, so the solution uses the default values suggested in Chapter 23.

Calculation of Junction-Specific Performance Measures

The middle portion of Exhibit 23-50 shows that, for a four-legged MUT with STOP signs at the U-turn crossovers, one to three increments of control delay are experienced by each movement. The methods of Chapters 19 and 20 are applied, by using the inputs listed above and defaults for all other values. The results are shown in Exhibit 34-137.

Junction	Movement	v/c	95% Queue Length (veh)	Control Delay (s/veh)
North crossover	WB crossover	0.78	7.1	34.6
Main intersection	EB through	0.82	10.2	25.1
	EB right turn	0.74	7.1	23.7
	WB through	0.62	7.5	22.2
	WB right turn	0.35	3.0	20.2
	NB through	0.58	8.3	9.3
	NB right turn	0.58	8.0	9.4
	SB through	0.76	12.2	12.3
	SB right turn	0.80	12.0	13.7
South crossover	EB crossover	0.24	0.9	14.0

Notes: EB = eastbound, WB = westbound, NB = northbound, SB = southbound.

Calculation of Extra Distance Travel Time

The middle portion of Exhibit 23-50 shows that at a four-legged MUT with STOP signs at the U-turn crossovers, extra travel distance is experienced by the left turns from the major and minor streets. Use of Equation 23-57 gives the extra distance travel time (EDTT) as follows:

$$EDTT = \frac{D_t + D_f}{1.47 \times S_f}$$

$$EDTT = \frac{800 + 800}{1.47 \times 50} = 21.8 \text{ s/veh}$$

Calculation of Additional Weaving Delay

For an MUT, there are no adjustments to make in this step.

Exhibit 34-137
Example Problem 15: Control Delay for Each Junction

Calculation of Experienced Travel Time

Experienced travel time (ETT) is computed with Equation 23-58:

$$ETT = \sum d_i + \sum EDTT$$

Use of the middle portion of Exhibit 23-50 gives the results in Exhibit 34-138.

Exhibit 34-138
Example Problem 15: ETT and
LOS Results

Movement	Control Delay (s/veh) by Traffic Control Device			EDTT (s/veh)	ETT (s/veh)	LOS
	First	Second	Third			
NB left	9.3	34.6	13.7	20.4	78.0	E
SB left	12.3	14.0	9.4	20.4	56.1	E
NB through	9.3	None	None	0	9.3	A
SB through	12.3	None	None	0	12.3	B
NB right	9.4	None	None	0	9.4	A
SB right	13.7	None	None	0	13.7	B
EB left	23.7	14.0	9.3	20.4	67.4	E
WB left	20.2	34.6	12.3	20.4	87.5	F
EB through	25.1	None	None	0	25.1	C
WB through	22.2	None	None	0	22.2	C
EB right	23.7	None	None	0	23.7	C
WB right	20.2	None	None	0	20.2	C

Notes: EB = eastbound, WB = westbound, NB = northbound, SB = southbound.

Determination of Level of Service

LOS for each movement is shown above in Exhibit 34-138. The results were obtained by using Exhibit 23-13, having established that the *v/c* ratio was less than 1.0 at all junctions and that the queue-to-storage ratios were well below 1.0 for the 500-ft bay lengths provided.

Discussion

MUT and RCUT intersections are particularly aided by right turns and U-turns on red because the demands for those movements are relatively higher than at conventional intersections. If right turns on red were allowed from the minor-street approaches in this case, where there are exclusive right-turn lanes, the Chapter 23 example results in Part C show the effects on ETT. If 40% of the right-turning volume (which includes the traffic that will eventually turn left) is able to turn on red, with an estimated zero control delay, ETT will be reduced by more than 11 s/veh for some of the minor-street movements, which will change LOS by one level in some cases.

EXAMPLE PROBLEM 16: PARTIAL DISPLACED LEFT-TURN INTERSECTION

The Intersection

The intersection of Speedway Boulevard (east–west) and Campbell Avenue (north–south) has multiple failing movements and heavy left-turn demands. Many of the nonfailing movements are close to failing, and future traffic growth is a concern. Exhibit 34-139 provides the intersection volumes and channelization, and Exhibit 34-140 provides the signalization information. Volumes (hourly flow rates) listed in Exhibit 34-139 are only valid during the peak 15-min period.

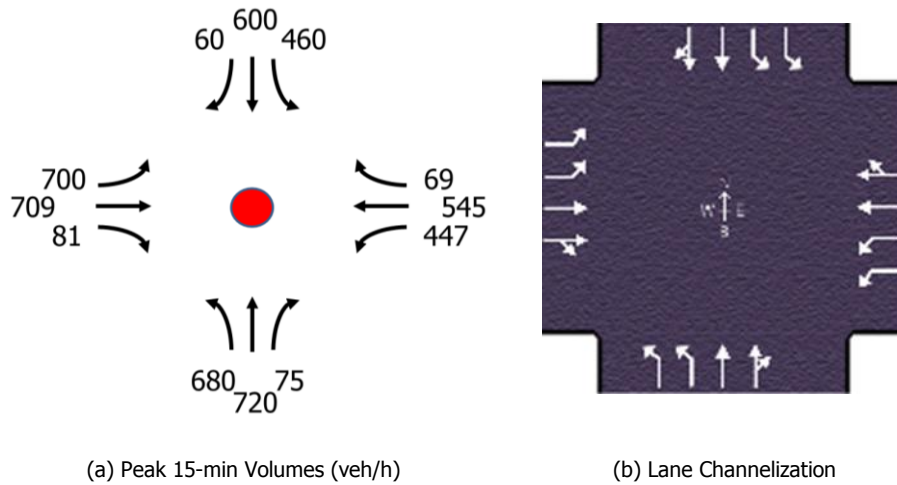


Exhibit 34-139
Example Problem 16:
Intersection Volumes and
Channelization

Green (s)	20.9	5.9	23.0	21.6	4.4	26.0
Yellow (s)	4.0	4.0	4.0	4.0	4.0	4.0
Red (s)	1.0	1.0	1.0	1.0	1.0	1.0

Exhibit 34-140
Example Problem 16:
Intersection Signalization

The Question

Will displacing the left turns on the major street significantly improve performance of this intersection?

The Facts

No other signalized intersections exist within 1 mi. The intersection is controlled by a fully actuated signal, with no right turns on red allowed. There are no heavy vehicles, and the PHF is estimated to be 0.92. The start-up lost time and the extension of effective green are both 2 s for all approaches. During the analysis period, there is no parking, and no buses, bicycles, or pedestrians utilize the intersection.

Solution

The analyst wishes to evaluate potential improvements when the east-west left turns are displaced 350 ft upstream of the main intersection. These upstream locations are now classified as the supplemental intersections. In the HCM context, a DLT intersection analysis can be considered an extension of the urban streets procedure. Thus, definitions of volume, geometric, and signalization data for an urban street having three intersections are necessary at this stage.

Determination of Movement Demands

Exhibit 34-141 illustrates the demand volumes at each intersection in the partial DLT configuration. The displaced eastbound and westbound left-turn volumes are assumed to be zero at the main intersection, according to Step 1 of the DLT computational procedure. At the western supplemental intersection, eastbound through (709 veh/h) and right-turn (81 veh/h) demands at the main intersection are combined into a single through (790 veh/h) demand. Similarly, three feeding demands (northbound left, westbound through, and southbound right) at the main intersection are combined into a westbound through (1,285 veh/h) demand. Similar flow aggregations are made at the eastern supplemental intersection. Exhibit 34-142 illustrates lane geometries in the DLT configuration.

Exhibit 34-141
Example Problem 16: Flow Rates at the Supplemental and Main Intersections

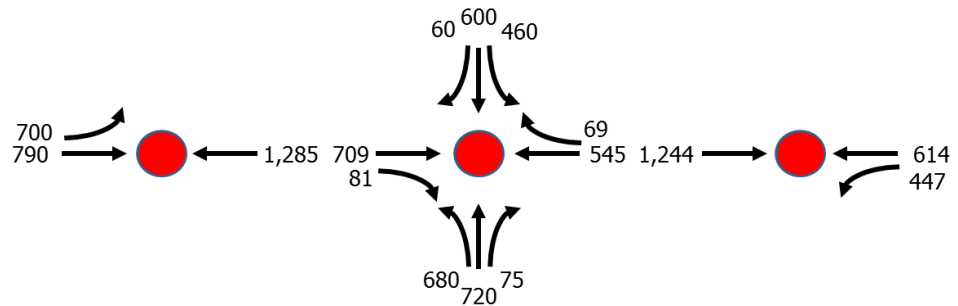
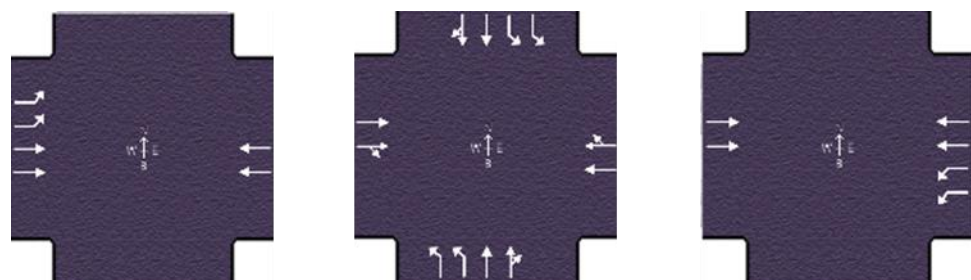


Exhibit 34-142
Example Problem 16: Lane Geometries at the Supplemental and Main Intersections



Determination of Lane Groups, Lane Utilization, and Signal Progression Adjustments

Steps 2 through 4 of the DLT procedure involve lane group determination, lane utilization, and arrival type adjustments, respectively. Lane group determination and lane utilization are performed by the Chapter 19, Signalized Intersections, procedures. Arrival type adjustments are handled by the flow profile analysis from Chapter 18, Urban Street Segments.

Calculation of Additional Control-Based Adjustments

In Step 5 of the DLT procedure, a right-turn saturation flow rate adjustment factor is applied to the left-turn movements at the supplemental intersections. In addition, signalization offsets must be set such that displaced left-turn vehicles always arrive during the guaranteed green window at the main intersection. The signalization information provided in Exhibit 34-140 should no longer be used in a potential DLT configuration, because the major-street left-turn phases will no longer exist at the main intersection. To ensure proper coordination, the supplemental intersections must have the same cycle length as the main intersection, and major-street through phases must now be treated as non-actuated phases. Exhibit 34-143 provides the new timing plans at each intersection. The new timing plans were generated by an alternative tool for signal optimization.

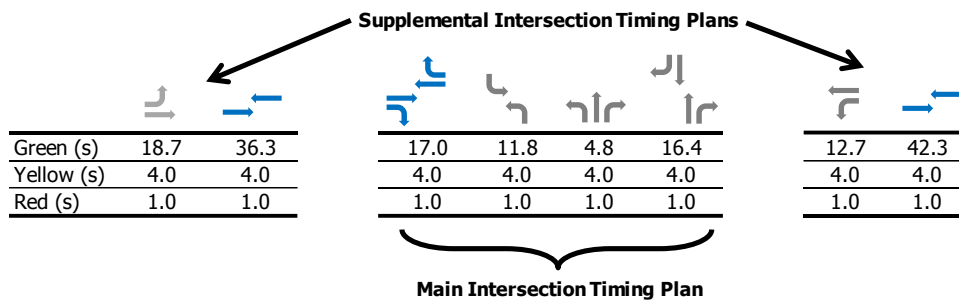


Exhibit 34-143
Example Problem 16:
Signalization at the DLT
Intersections

After the overall new timing plans are determined, the signalization offsets can be recalculated according to Step 5. The following steps represent the offset computation process for DLT intersections in Chapter 23:

1. Determine the travel distance for (i.e., segment length of) the displaced left-turn roadway TD_{DLT} , in feet. The displaced left-turn roadway is the roadway used by displaced left-turning vehicles as they travel from the upstream crossover at the supplemental intersection to the stop bar at the main intersection. In this case, the distance is 350 ft.
2. Compute the left-turn travel time TT_{DLT} with Equation 23-61:

$$TT_{DLT} = \frac{TD_{DLT}}{S_{f,DLT} \times 1.47}$$

$$TT_{DLT} = \frac{350}{35 \times 1.47} = 6.8 \text{ s}$$


3. For the upstream supplemental intersection, obtain the duration between the reference point and the start of the displaced left-turn phase LAG_{DLT} in seconds. For the downstream main intersection, obtain the duration between the reference point and the start of the major-street through phase LAG_{TH} in seconds. These durations should be based on input phase splits instead of output phase durations.

In this example, the reference point at all intersections is assumed to be the end of the major-street through phase. From Exhibit 34-143, the supplemental intersection's displaced left-turn phases always begin

Exhibit 34-144
 Example Problem 16:
 Maximum Phase Times at the
 Main Intersection

exactly when the major-street through phases end, so that LAG_{DLT} is equal to zero.

Exhibit 34-143 indicates that at the main intersection, after the major-street through phase ends, the signal must cycle through all minor-street phases before reaching a point where the major-street through phase begins. However, Exhibit 34-143 illustrates average phase durations. To determine the window of green time that is guaranteed to occur on the major street, it is necessary to observe what the timing plan would be if actuated phases were driven to their maximum durations. Exhibit 34-144 illustrates this timing plan.



Green (s)	8.0	21.0	1.0	15.0
Yellow (s)	4.0	4.0	4.0	4.0
Red (s)	1.0	1.0	1.0	1.0

Thus LAG_{TH} is equal to $21 + 4 + 1 + 1 + 4 + 1 + 15 + 4 + 1 = 52$ s. This means that the major-street through phase begins 52 s after the reference point.

- Obtain the offsets at the upstream supplemental intersection O_{SUPP} and the downstream main intersection O_{MAIN} , both in seconds.

In this example, the initial offsets at all intersections are assumed equal to 0 s. When an existing DLT intersection having nonzero offsets is evaluated, the existing offsets would be assigned here.

- Compute the system start time of the displaced left-turn phase ST_{DLT} , in seconds, for the upstream crossover at the supplemental intersection, by using Equation 23-62:

$$ST_{DLT} = LAG_{DLT} + O_{SUPP}$$

$$ST_{DLT} = 0 + 0 = 0 \text{ s}$$

- Compute the system start time of the major-street through phase ST_{TH} at the main intersection by using Equation 23-63:

$$ST_{TH} = LAG_{TH} + O_{MAIN}$$

$$ST_{TH} = 52 + 0 = 52 \text{ s}$$

- Change O_{SUPP} so that ST_{TH} is equal to $ST_{DLT} + TT_{DLT}$ by using Equation 23-64:

$$O_{SUPP} = O_{SUPP} - ST_{DLT} + ST_{TH} - TT_{DLT}$$

$$O_{SUPP} = 0 - 0 + 52 - 7 = 45 \text{ s}$$

- If the offset value is greater than the background cycle length value, decrement the offset value by the cycle length C to obtain an equivalent offset within the valid range.

In this example, the new offset value of 45 s is not greater than the cycle length value of 65 s.

9. If any offset value is lower than zero, increment the offset value by the cycle length to obtain an equivalent offset within the valid range.

In this example, the new offset value of 45 s is not lower than zero. Thus, when the offset is set to 45 s at the supplemental intersections, displaced left-turn vehicles are expected to pass through the main intersection without stopping.

Calculation of Junction-Specific Performance Measures

After the offset calculation in Step 5, Step 6 of the alternative intersection procedure estimates the *v/c* ratio and control delay at each intersection. Steps 7 through 9 are not applicable to DLT intersections, and Step 10 is the LOS determination.

For the conventional intersection design from Exhibit 34-139, intersection-wide control delay is calculated as 64.1 s/veh by using Chapter 19 methods. For the DLT intersection design from Exhibit 34-141, after Steps 1 through 5 of the alternative intersection procedure are used to adjust the input data, *v/c* and control delay for each isolated turn movement can be calculated by using methods from Chapters 18 and 19. However at the overall DLT facility, turn movement-specific control delays are encountered sequentially at each intersection, as shown in Exhibit 34-145.

Move- ment	Flows				Delays			Products		
	Orig.	Int 1	Int 2	Int 3	Int 1	Int 2	Int 3	Int 1	Int 2	Int 3
EB L	761	761			22.5			17,123	0	0
EB TH	437	859	437	1,352	0.4	41.9	2.5	344	18,310	3,380
EB R	422		422			42.5		0	17,935	0
WB L	486			486			25.7	0	0	12,490
WB TH	340	1,397	340	667	4.0	29.3	0.4	5,588	9,962	267
WB R	328		328			29.7		0	9,742	0
NB L	739		739			23.7		0	17,514	0
NB TH	439		439			19.8		0	8,692	0
NB R	425		425			19.8		0	8,415	0
SB L	500		500			26.2		0	13,100	0
SB TH	364		364			23.4		0	8,518	0
SB R	353		353			23.5		0	8,296	0
Total	5,594							159,675		
Avg.								28.5		

Notes: EB = eastbound, WB = westbound, NB = northbound, SB = southbound, TH = through, L = left, R = right, Orig. = original (non-DLT) intersection, Int = intersection, Avg. = average.

Determination of Level of Service

Comparison of the conventional intersection delay of 64.1 s/veh with the alternative intersection delay of 28.5 s/veh indicates that the alternative design is expected to offer a 55% average delay reduction while processing the same number (5,594) of vehicle trips. For DLT intersections, experienced travel time (ETT) can be assumed as equal to control delay. According to the LOS thresholds given in Chapter 19, Signalized Intersections, the overall DLT intersection would operate at LOS C, in contrast to the conventional intersection operating at LOS E. This raises the question of what might happen if left turns could be displaced on all four intersection approaches. This is the subject of Example Problem 17.

Exhibit 34-145
Example Problem 16:
Weighted Average Control
Delays

Validity Checks

Chapter 23 cites a number of conditions that would invalidate the DLT analysis method. If any of these conditions are met, the analysis results are unreliable, and alternative tool analysis is recommended:

- Displaced left-turn vehicles are significantly delayed at the main intersection,
- Displaced left-turn approach's through and left-turning movements are not served by exactly the same signal phasing and timing,
- Green times at the main intersection are not long enough to serve displaced left-turning vehicle demands fully, or
- Side street green durations do not exceed the sum of (a) main street travel time between supplemental and main intersections and (b) displaced left-turn queue clearance time.

EXAMPLE PROBLEM 17: FULL DISPLACED LEFT-TURN INTERSECTION

The Intersection

The conventional intersection conditions in Example Problem 17 are identical to those given in Example Problem 16, before DLT conversion.

The Question

Will displacement of left-turn movements on all four approaches significantly improve performance of this intersection?

The Facts

The facts of the example problem are the same as in Example Problem 16.

Solution

The analyst wishes to evaluate potential improvements when left turns on all four approaches are displaced 350 ft upstream of the main intersection. In this case, two partial DLT analyses must be performed: one for the major street and one for the minor street.

Determination of Movement Demands (East–West Partial DLT Analysis)

Exhibit 34-146 illustrates the major-street flow rates. Displaced left-turn volumes are again assumed to be zero at the main intersection, according to Step 1 of the DLT computational procedure. Unlike partial DLT intersections, pseudo right-turn modeling adjustments are needed at full DLT intersections. Minor-street left-turn lanes have been converted to pseudo right-turn lanes on the opposite side of the intersection. Similarly, minor-street left-turn volumes have been combined with right-turn volumes on the opposite side of the intersection. Exhibit 34-147 further illustrates the lane geometries at all three intersections in the DLT configuration.

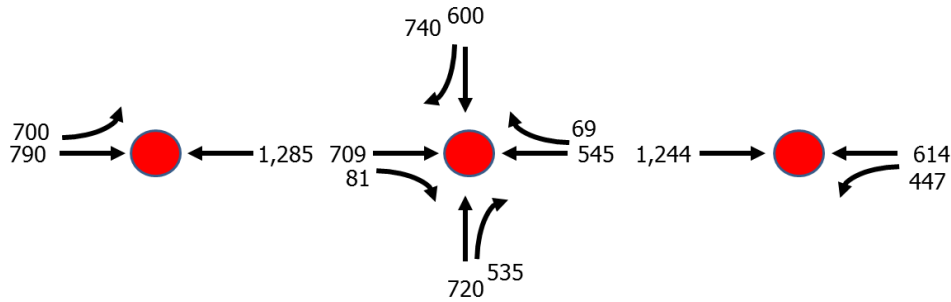


Exhibit 34-146
Example Problem 17: Flow Rates at the Supplemental and Main Intersections

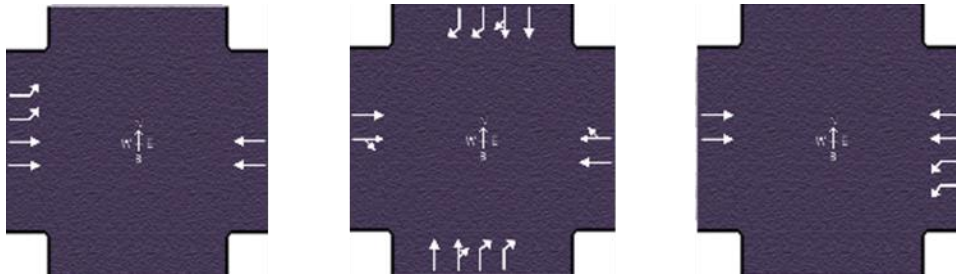


Exhibit 34-147
Example Problem 17: Lane Geometries at the Supplemental and Main Intersections

Determination of Lane Groups, Lane Utilization, and Signal Progression Adjustments (East–West Partial DLT Analysis)

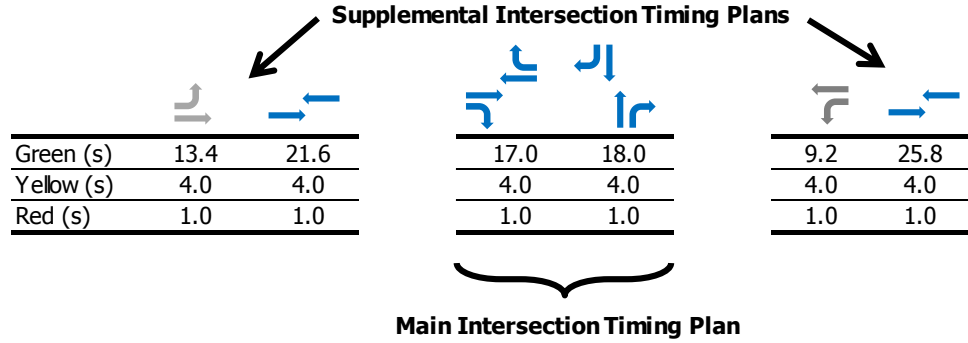
Steps 2 through 4 of the DLT procedure involve lane group determination, lane utilization, and arrival type adjustments, respectively. Lane group determination and lane utilization are performed by the Chapter 19, Signalized Intersections, procedures. Arrival type adjustments should be handled by the flow profile analysis from Chapter 18, Urban Street Segments.

Determination of Additional Control-Based Adjustments (East–West Partial DLT Analysis)

In Step 5 of the DLT procedure, a right-turn saturation flow rate adjustment factor is applied to the left-turn movements at the supplemental intersections. A left-turn saturation flow rate adjustment factor is applied to both pseudo right-turn movements at the main intersection. A start-up lost time of 0 s is assumed for both pseudo right-turn movements at the main intersection.

Signalization offsets must then be set to allow displaced left-turn vehicles to arrive during the guaranteed green window at the main intersection. The signalization information provided in Exhibit 34-140 should no longer be used in a potential DLT configuration, because the major-street left-turn phases will no longer exist at the main intersection. To ensure proper coordination, the supplemental intersections must have the same cycle length as the main intersection. Because of the full DLT configuration, all phases at the main intersection are nonactuated phases. Exhibit 34-148 illustrates new timing plans (in units of seconds) at each intersection. The new timing plans were generated by an alternative tool for signal optimization.

Exhibit 34-148
 Example Problem 17: East–
 West Signalization at the DLT
 Intersections



After the overall new timing plans are determined, signalization offsets can be recalculated according to Step 5. The following steps represent the offset computation process for DLT intersections in Chapter 23:

1. Determine the travel distance for (i.e., segment length of) the displaced left-turn roadway TD_{DLT} , in feet. The displaced left-turn roadway is the roadway used by displaced left-turning vehicles as they travel from the upstream crossover at the supplemental intersection to the stop bar at the main intersection. In this case, the distance is 350 ft.
2. Compute the left-turn travel time TT_{DLT} by using Equation 23-61:

$$TT_{DLT} = \frac{TD_{DLT}}{FFS_{DLT} \times 1.47}$$

$$TT_{DLT} = \frac{350}{35 \times 1.47} = 6.8 \text{ s}$$

3. For the upstream supplemental intersection, obtain the duration between the reference point and the start of the displaced left-turn phase LAG_{DLT} , in seconds. For the downstream main intersection, obtain the duration between the reference point and the start of the major-street through phase LAG_{TH} , in seconds. These durations should be based on input phase splits instead of output phase durations.

In this example, the reference point at all intersections is assumed to be the end of the major-street through phase. From Exhibit 34-148, the supplemental intersection’s displaced left-turn phases always begin exactly when the major-street through phases end, so that LAG_{DLT} is equal to zero.

From Exhibit 34-148 at the main intersection, after the major-street through phase ends, the signal must cycle through the minor-street phase before reaching a point where the major-street through phase begins. For partial DLTs, it is necessary to observe what the timing plan would be if actuated phases were driven to their maximum durations, but for full DLTs, no phases are allowed to be actuated at the main intersection. Thus LAG_{TH} is equal to $18 + 4 + 1 = 23$ s. This means that the major-street through phase begins 23 s after the reference point.

- Obtain the offsets at the upstream supplemental intersection O_{SUPP} and the downstream main intersection O_{MAIN} , both in seconds.

For this example, the initial offsets at all intersections are assumed equal to 0 s. When an existing DLT intersection having nonzero offsets is evaluated, the existing offsets would be assigned here.

- Compute the system start time of the displaced left-turn phase ST_{DLT} , in seconds, for the upstream crossover at the supplemental intersection by using Equation 23-62:

$$ST_{DLT} = LAG_{DLT} + O_{SUPP}$$

$$ST_{DLT} = 0 + 0 = 0 \text{ s}$$

- Compute the system start time of the major-street through phase ST_{TH} at the main intersection by using Equation 23-63:

$$ST_{TH} = LAG_{TH} + O_{MAIN}$$

$$ST_{TH} = 23 + 0 = 23 \text{ s}$$

- Change O_{SUPP} so that ST_{TH} is equal to $ST_{DLT} + TT_{DLT}$ by using Equation 23-64:

$$O_{SUPP} = O_{SUPP} - ST_{DLT} + ST_{TH} - TT_{DLT}$$

$$O_{SUPP} = 0 - 0 + 23 - 7 = 16 \text{ s}$$

- If the offset value is greater than the background cycle length value, decrement the offset value by the cycle length C to obtain an equivalent offset within the valid range.

In this example, the new offset value of 16 s is not greater than the cycle length value of 45 s.

- If any offset value is lower than zero, increment the offset value by the cycle length to obtain an equivalent offset within the valid range.

In this example, the new offset value of 16 is not lower than zero. Thus, with offset values of 16 s at the east–west supplemental intersections, displaced left-turn vehicles are expected to pass through the main intersection without stopping. This completes the input data adjustments for a partial DLT analysis in the east–west direction.

North–South Partial DLT Analysis

Input data adjustments must now be performed for a second partial DLT analysis in the north–south direction. The cycle length of 45 s from the east–west partial DLT analysis must now be applied to the north–south partial DLT analysis. The main intersection timing plan from Exhibit 34-148 must not be changed in the north–south partial DLT analysis.

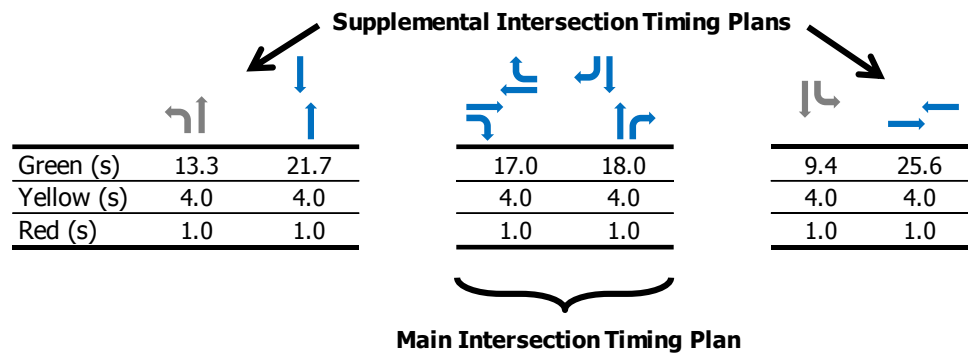
Step 1 of the north–south partial DLT analysis is similar to what was illustrated in Exhibit 34-146 and Exhibit 34-147. Steps 2 through 4 are again handled by the Chapter 19, Signalized Intersections, and Chapter 18, Urban Street Segments, procedures. In Step 5, a right-turn saturation flow rate adjustment factor is again applied to the supplemental intersection left-turn movements. A left-turn saturation flow rate adjustment factor is applied to both

pseudo right-turn movements at the main intersection. A start-up lost time of 0 s is assumed for both pseudo right-turn movements at the main intersection.

Signalization offsets must now be set to allow displaced left-turn vehicles to arrive during the guaranteed green window at the main intersection. Before the offsets are calculated, green splits must be optimized in the north–south direction, while constrained to the cycle length of 45 s. Exhibit 34-149 illustrates new timing plans (in units of seconds) at each intersection. The new timing plans were generated by an alternative tool for signal optimization.

After the overall new timing plans are determined, signalization offsets can be recalculated according to Step 5. The north–south and east–west offset calculations are mostly identical. However, LAG_{TH} is now equal to $17 + 4 + 1 = 22$ s, ultimately leading to 15-s offsets at the north–south supplemental intersections. With offset values of 15 s at the north–south supplemental intersections, displaced left-turn vehicles are expected to pass through the main intersection without stopping.

Exhibit 34-149
Example Problem 17: North–South Signalization at the DLT Intersections



Calculation of Junction-Specific Performance Measures

After the offset calculation in Step 5, Step 6 of the alternative intersection procedure estimates the v/c ratio and control delay at each intersection. Steps 7 through 9 are not applicable to DLT intersections, and Step 10 is the LOS determination.

For the conventional intersection design from Exhibit 34-139, intersectionwide control delay is calculated as 64.1 s/veh by using Chapter 19’s methods.

For the DLT intersection design, after Steps 1 through 5 of the alternative intersection procedure are used to adjust the input data, v/c ratio and control delay for each isolated turn movement can be calculated with methods from Chapter 19, Signalized Intersections, and Chapter 18, Urban Street Segments. However, for the overall DLT facility, turn movement–specific control delays are encountered sequentially at each intersection, as shown in Exhibit 34-150. To avoid double counting, minor-street performance measures are not tabulated in either of the two partial DLT analyses.

The full DLT delay computed here (29.0 s/veh) is similar to the partial DLT delay (28.5 s/veh) from Example Problem 16. For DLT intersections, experienced travel time can be assumed equal to control delay. According to Chapter 19’s LOS thresholds, the overall DLT intersection would operate at LOS C, in contrast to the conventional intersection operating at LOS E.

Since the major-street and minor-street demands were all relatively heavy in Example Problems 16 and 17, the failure of the full DLT configuration to outperform the partial DLT configuration was surprising. However, when the same exercise was performed with 800-ft spacings between supplemental and main intersections, the full DLT (25.3 s/veh) outperformed the partial DLT (28.4 s/veh) by more than 10%. This shows that the DLT results are sensitive to intersection spacings and that intersection spacings should be taken into consideration in designing a new DLT facility.

Move- ment	Flows					Delays					
	Orig.	Int 1	Int 2	Int 3	Int 4	Int 5	Int 1	Int 2	Int 3	Int 4	Int 5
EB L	761	761					15.8				
EB TH	437	859	437	1,352			0.6	14.5	10.4		
EB R	422		422					14.6			
WB L	486			486					17.5		
WB TH	340	1,397	340	667			17.9	12.8	0.5		
WB R	328		328					12.9			
NB L	739				739					15.2	
NB TH	439		439		864	1,618	13.1		0.6	14.2	
NB R	425		425					13.2			
SB L	500					500					17.4
SB TH	364		364		1,226	717	12.2		13.8	0.5	
SB R	353		353					12.3			
Total	5,594										

Movement	Products				
	Int 1	Int 2	Int 3	Int 4	Int 5
EB L	12,024	0	0	0	0
EB TH	515	6,337	14,061	0	0
EB R	0	6,161	0	0	0
WB L	0	0	8,505	0	0
WB TH	25,006	4,352	334	0	0
WB R	0	4,231	0	0	0
NB L	0	0	0	11,233	0
NB TH	0	5,751	0	518	22,976
NB R	0	5,610	0	0	0
SB L	0	0	0	0	8,700
SB TH	0	4,441	0	16,919	359
SB R	0	4,342	0	0	0
Total	162,373				
Average	29.0				

Notes: EB = eastbound, WB = westbound, NB = northbound, SB = southbound, TH = through, L = left, R = right, Orig. = original (non-DLT) intersection, Int = intersection.

Validity Checks

Chapter 23 cites a number of conditions that would invalidate the DLT analysis method. If any of these conditions are met, the analysis results are unreliable, and alternative tool analysis is recommended:

- Displaced left-turn vehicles are significantly delayed at the main intersection,
- The displaced left-turn approach's through and left-turning movements are not served by exactly the same signal phasing and timing,

Exhibit 34-150
Example Problem 17:
Weighted Average Control
Delays

- Green times at the main intersection are not large enough to serve displaced left-turning vehicle demands fully, or
- Side street green durations do not exceed the sum of (a) main street travel time between supplemental and main intersections and (b) displaced left-turn queue clearance time.

3. OPERATIONAL ANALYSIS FOR INTERCHANGE TYPE SELECTION

INTRODUCTION

The operational analysis for interchange type selection can be used to evaluate the operational performance of various interchange types. It allows the user to compare eight fundamental types of interchanges for a given set of demand flows. The eight signalized interchange types covered by the interchange type selection analysis methodology are as follows:

1. SPUI,
2. Tight urban diamond interchange (TUDI),
3. Compressed urban diamond interchange (CUDI),
4. Conventional diamond interchange (CDI),
5. Parclo A—four quadrants (Parclo A-4Q),
6. Parclo A—two quadrants (Parclo A-2Q),
7. Parclo B—four quadrants (Parclo B-4Q), and
8. Parclo B—two quadrants (Parclo B-2Q).

Other types of signalized interchanges cannot be investigated with this interchange type selection analysis methodology. Also, the operational analysis methodology does not distinguish between the TUDI, CUDI, and CDI types. In general, the interchange type selection analysis methodology categorizes diamond interchanges by the distance between the centerlines of the ramp roadways that form the signalized intersections. This distance is generally between 200 and 400 ft for the TUDI, between 600 and 800 ft for the CUDI, and between 1,000 and 1,200 ft for the CDI.

The method is based on research (4). The research also provides a methodology for selecting unsignalized interchanges. Since unsignalized interchanges are not covered by Chapter 23, users should consult the original source for this information.

The methodology is based on the estimation of the sums of critical flow ratios through the interchange and their use to estimate interchange delay. A combination of simulation and field data was used to develop critical relationships for the methodology.

The sum of critical flow ratios is based on an identification of all flows served during a particular signal phase and the determination of maximum flow ratios among the movements served by that phase. The models are similar to those used in Chapter 19 for signalized intersections; they are modified to take into account the fact that each signal phase involves two signalized intersections. Interchange delay is defined as the total of all control delays experienced by all interchange movements involved in signalized ramp terminal movements divided by the sum of all external movement flows. Additional information is available in the source report (4).

Because signalization is not specified for an interchange type selection analysis, the following interchange types are assumed to be operated by a single signal controller: SPUI, TUDI, and CUDI. All other types are assumed to be operated by separate controllers at each signalized ramp terminal. In all cases, optimal signal timing and phasing are assumed.

INPUTS AND APPLICATIONS

This interchange type selection analysis methodology can be used in several ways:

1. For a given set of O-D interchange movements, eight basic types of signalized interchanges may be compared on the basis of interchange delay.
2. For a given type of interchange, the impact of intersection spacing on interchange delay can be examined (within the range of applicability for each interchange type).
3. For a given type of interchange, the impact of the number of lanes on ramp and surface arterial approaches and the movements assigned to these lanes can be examined, again by using interchange delay as the measure of effectiveness.

For any of these applications, all interchange O-D movements must be specified, generally by using full peak-hour volumes. The interchange type selection methodology is not detailed enough to use flow rates or to consider such factors as the presence of heavy vehicles.

In addition, for any given computation, the number of lanes assigned to each phase movement and the distance between the centerlines of the two ramps, measured along the surface arterial, must be specified.

SATURATION FLOW RATES

Implementation of the interchange type selection methodology requires the adoption of default values for saturation flow rate. Research (3) suggests the use of 1,900 veh/hg/ln for some basic cases. However, this is based on a suggested base saturation flow rate of 2,000 pc/hg/ln, which is higher than the default values suggested in Chapter 19, Signalized Intersections. For consistency with the base saturation flow rate of 1,900 pc/hg/ln specified in Chapter 19 and to recognize the impact of various movements on saturation flow rate, the default values shown in Exhibit 34-151 are recommended for use in conjunction with the interchange type selection methodology. Alternatively, if relevant information is available, the default values provided in Chapter 19 (Exhibit 19-11 and Exhibit 19-12) may be used. Where turning movements are in shared lanes, the “through” saturation flow rates should be used for analysis.

Interchange Type	Default Saturation Flow Rate (veh/hg/ln)		
	Left Turns	Through	Right Turns
SPII	1,800	1,800	1,800
TUDI	1,700	1,800	1,800
CUDI	1,700	1,800	1,800
CDI	1,700	1,800	1,800
Parclo A-4Q	1,700	1,800	1,800
Parclo A-2Q	1,700	1,800	1,800
Parclo B-4Q	1,700	1,800	1,800
Parclo B-2Q	1,700	1,800	1,800

Exhibit 34-151

Default Values of Saturation Flow Rate for Use with the Operational Analysis for Interchange Type Selection

COMPUTATIONAL STEPS

Step 1: Mapping O-D Flows into Interchange Movements

Since the primary objective of an interchange type selection analysis is to compare up to eight interchange types against a given set of design volumes, conversion of a given set of design origin and destination volumes to movement flows through the signalized interchange is necessary first. The methodology identifies volumes by signal phase by using the standard NEMA numbering sequence for interchange phasing. Thus, movements are numbered 1 through 8 on the basis of the signal phase that accommodates the movement. Not all configurations and signalizations include all eight NEMA phases, and for some interchange forms some movements are not signalized and do not, therefore, contribute to interchange delay.

As for the operational analysis methodology, to simplify the mapping process, the freeway is assumed to be oriented north-south and the surface arterial east-west. If the freeway is oriented in the east-west direction, rotate the interchange drawing or diagram clockwise until the freeway is in the north-south direction. In rotating clockwise, the westbound freeway direction becomes northbound and the eastbound freeway direction becomes southbound; the northbound arterial direction becomes eastbound and the southbound arterial direction becomes westbound. The methodology allows for separate consideration of freeway U-turn movements through the interchange. Thus, 14 basic movements must be mapped for each interchange type.

For interchange types using two controllers, phase movements through the left (Intersection I) and right (Intersection II) intersections of the interchange are separately mapped and used in the procedure.

Exhibit 34-152 indicates the appropriate mapping of O-D demand volumes into phase movement volumes for the eight covered interchange types. The designation of the O-D demands is shown in Exhibit 34-162. The mapped phase movement volumes are then used in Step 2 to compute critical flow ratios.

Exhibit 34-152

Mapping of Interchange Origins and Destinations into Phase Movements for Operational Interchange Type Selection Analysis

Interchange Type	NEMA Phase Movement Number							
	1	2	3	4	5	6	7	8
SPUI	H	I+F	A+M	C	E	J+G	D+N	B
TUDI /CUDI	H+M	E+I+F	--	D+C+N	E+N	H+J+G	--	A+M+B
CDI (I)	H+M	E+I+F	--	D+C+N	--	J+A	--	--
CDI (II)	--	I+D	--	--	E+N	H+J+G	--	A+M+B
Parclo A-4Q (I)	--	E+I	--	D+N+C	--	J+A+M+H	--	--
Parclo A-4Q (II)	--	I+D+N+E	--	--	--	J+H	--	A+M+B
Parclo A-2Q (I)	--	E+I	--	D+N+C	F	J+A+H+M	--	--
Parclo A-2Q (II)	G	I+D+E+N	--	--	--	H+J	--	A+M+B
Parclo B-4Q (I)	H+M	I+E+F	--	--	--	J+A	--	--
Parclo B-4Q (II)	--	I+D	--	--	E+N	H+J+G	--	--
Parclo B-2Q (I)	H+M	E+I+F	--	--	--	J+A	--	C
Parclo B-2Q (II)	--	I+D	--	B	E+N	H+J+G	--	--

Notes: -- indicates that phase movement does not exist for this interchange configuration. **Bold** indicates movements not included when they operate from a separate lane with YIELD or STOP control.

Step 2: Computation of Critical Flow Ratios

The subsections that follow detail the computation of the critical flow ratio Y_c for the interchange for the eight basic configurations covered by this methodology.

Single-Point Urban Interchange

The phase movements in a SPUI are illustrated in Exhibit 34-153. The sum of critical flow ratios is estimated as follows:

Equation 34-1

$$Y_c = A + R$$

with

Equation 34-2

$$A = \max \left[\left(\frac{v_1}{s_1 n_1} + \frac{v_2}{s_2 n_2} \right), \left(\frac{v_5}{s_5 n_5} + \frac{v_6}{s_6 n_6} \right) \right]$$

Equation 34-3

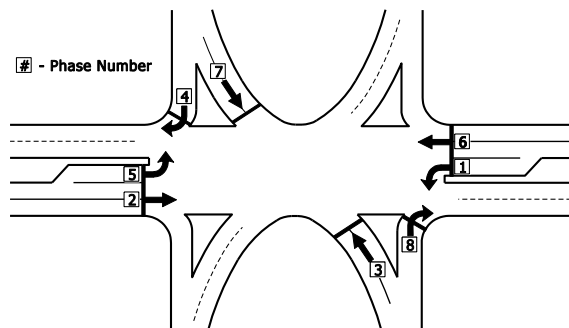
$$R = \max \left[\left(\frac{v_3}{s_3 n_3} + \frac{v_4}{s_4 n_4} \right), \left(\frac{v_7}{s_7 n_7} + \frac{v_8}{s_8 n_8} \right) \right]$$

where

- Y_c = sum of the critical flow ratios,
- v_i = phase movement volume for phase i (veh/h),
- n_i = number of lanes serving phase movement i ,
- s_i = saturation flow rate for phase movement i (veh/hg/ln),
- A = critical flow ratio for the arterial movements, and
- R = critical flow ratio for the exit ramp movements.

Exhibit 34-153

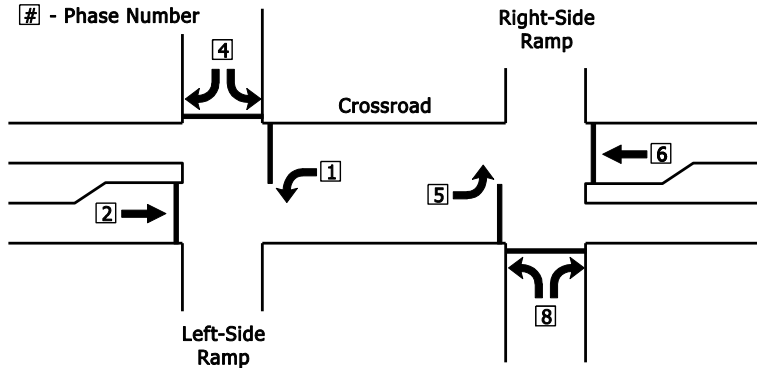
Phase Movements in a SPUI



Source: Bonneson et al. (4).

Tight Urban Diamond Interchange

Phase movements in a TUDI are illustrated in Exhibit 34-154.



Source: Bonneson et al. (4).

The sum of critical flow ratios is computed as follows:

$$Y_c = A + R$$

with

$$A = \max \left[\left(\frac{v_2}{s_2 n_2} + \frac{v_4}{s_4 n_4} \right) - y_3, \left(\frac{v_5}{s_5 n_5} + y_7 \right) \right]$$

$$R = \max \left[\left(\frac{v_1}{s_1 n_1} + y_3 \right), \left(\frac{v_6}{s_6 n_6} + \frac{v_8}{s_8 n_8} - y_7 \right) \right]$$

$$y_3 = \min \left(\frac{v_4}{s_4 n_4}, y_t \right)$$

$$y_7 = \min \left(\frac{v_8}{s_8 n_8}, y_t \right)$$

where y_3 and y_7 are the effective flow ratios for concurrent (or transition) Phases 3 and 7, respectively; and y_t is the effective flow ratio for the concurrent phase when dictated by travel time.

For preliminary design applications, the default values of Exhibit 34-155 are recommended for y_t . The distance between the two intersections is measured from the centerline of the left ramp roadway to the centerline of the right ramp roadway.

Distance Between Intersections D' (ft)	Default Value for y_t
200	0.050
300	0.070
400	0.085

For Phase Movements 2 and 6, the number of assigned lanes (n_2 and n_6) is related to the arterial left-turn bay design. If the left-turn bay extends back to the external approach to the interchange, the number of lanes on these external approaches is the total number of approaching lanes, including the left-turn bay.

Exhibit 34-154

Phase Movements in a Tight Urban or Compressed Urban Diamond Interchange

Equation 34-4

Equation 34-5

Equation 34-6

Equation 34-7

Equation 34-8

Exhibit 34-155

Default Values for y_t

If the left-turn bay is provided only on the internal arterial link, n_2 or n_6 , or both, would not include this lane.

Compressed Urban Diamond Interchange

Exhibit 34-154 illustrates the phase movement volumes for a CUDI. They are the same as for a TUDI. The sum of critical flow ratios is computed as follows:

Equation 34-9

$$Y_c = A + R$$

with

Equation 34-10

$$A = \max \left[\left(\frac{v_1}{s_1 n_1} + y_2 \right), \left(\frac{v_5}{s_5 n_5} + y_6 \right) \right]$$

Equation 34-11

$$R = \max \left(\frac{v_4}{s_4 n_4}, \frac{v_8}{s_8 n_8} \right)$$

Equation 34-12

$$y_2 = \max \left(\frac{v_2}{s_2 n_2}, \frac{v_5}{s_2} \right)$$

Equation 34-13

$$y_6 = \max \left(\frac{v_8}{s_8 n_8}, \frac{v_1}{s_6} \right)$$

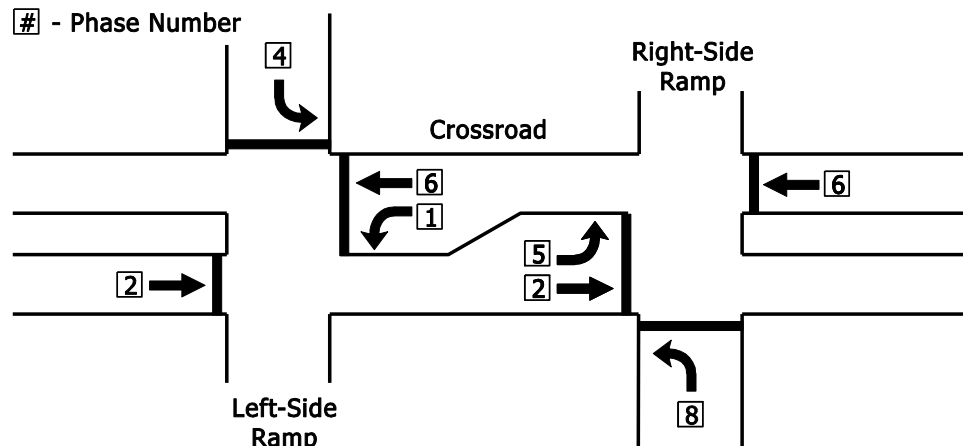
where y_2 and y_6 are the flow ratios for Phases 2 and 6, respectively, with consideration of pre-positioning.

All Interchanges with Two Signalized Intersections and Separate Controllers

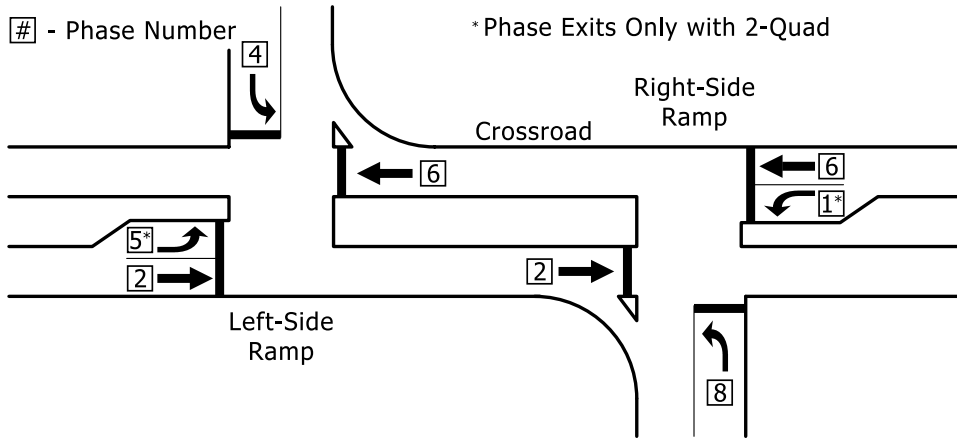
These interchange types include CDI, Parclo A-4Q, Parclo A-2Q, Parclo B-4Q, and Parclo B-2Q. The computation of the maximum sum of critical volumes is the same for each. Each has two signalized intersections, and each is generally operated with two controllers.

While the equations for estimating the maximum sum of critical volumes are the same, the phase movement volumes differ for each type of interchange, as was indicated in Exhibit 34-152. Exhibit 34-156 through Exhibit 34-158 illustrate the phase movements for each of these interchange types.

Exhibit 34-156
Phase Movements in a CDI

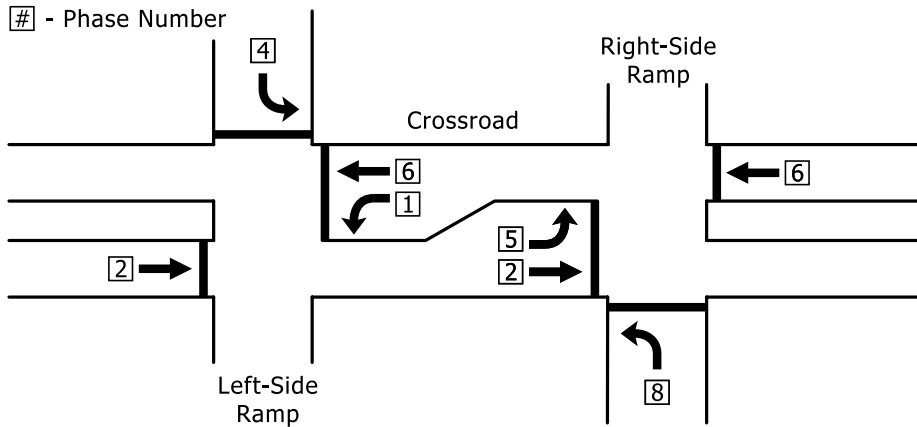


Source: Bonneson et al. (4).



Source: Messer and Bonneson (3).

Exhibit 34-157
Phase Movements in Parclo A-2Q and A-4Q Interchanges



Source: Messer and Bonneson (3).

Exhibit 34-158
Phase Movements in Parclo B-2Q and B-4Q Interchanges

For all conventional diamond, Parclo A, and Parclo B interchanges, the sum of critical flow ratios is computed as follows:

$$Y_{c,max} = \max(Y_{c,I}, Y_{c,II})$$

with

$$Y_{c,I} = A_I + R_I$$

$$Y_{c,II} = A_{II} + R_{II}$$

$$A_{I,II} = \max \left[\left(\frac{v_1}{s_1 n_1} + \frac{v_2}{s_2 n_2} \right), \left(\frac{v_5}{s_5 n_5} + \frac{v_6}{s_6 n_6} \right) \right]$$

$$R_{I,II} = \max \left(\frac{v_4}{s_4 n_4}, \frac{v_8}{s_8 n_8} \right)$$

where

$Y_{c,I}$ = sum of the critical flow ratios for Intersection I,

$Y_{c,II}$ = sum of the critical flow ratios for Intersection II,

$Y_{c,max}$ = sum of the critical flow ratios for the interchange,

A_I = critical flow ratio for the arterial movements for Intersection I,

Equation 34-14

Equation 34-15

Equation 34-16

Equation 34-17

Equation 34-18

- A_{II} = critical flow ratio for the arterial movements for Intersection II,
- $A_{I,II}$ = critical flow ratio for the arterial movements for the interchange,
- R_I = critical flow ratio for the exit-ramp movements for Intersection I,
- R_{II} = critical flow ratio for the exit-ramp movements for Intersection II, and
- $R_{I,II}$ = critical flow ratio for the exit-ramp movements for the interchange.

Note that when values of A_I , A_{II} , R_I , and R_{II} are computed, the movement volumes vary for Intersections I and II, even though the phase movement designations are the same (Exhibit 34-152).

Some of the phase movement volumes do not exist in either Intersection I or II. A value of 0 is used for the volume in each case where this occurs.

Step 3: Estimation of Interchange Delay

Interchange delay for each interchange type or design is estimated by using regression models that were developed primarily from simulation output but validated with a limited amount of field data (4). In each case, two delay estimators are provided on the basis of the control of the off-ramp right-turn movements:

- Case A, used where the right-turn movements from freeway off-ramps are controlled by the signal.
- Case B, used where the right-turn movements from freeway off-ramps have a separate lane or lanes that are either free (uncontrolled) or controlled by a YIELD sign.

For SPUIs, a third condition is added. Where the right turns from the freeway ramps are controlled by a signal and right turn on red is allowed, both cases are used, and the results are weighted by the proportions of right turns made during the red and green indications. Since the signal timing is unknown for an interchange type selection application, the assumption of a 50%/50% split is recommended.

This modification, applied only to SPUIs, is necessary due to difficulties experienced in simulating right turn on red at these interchanges.

Exhibit 34-159 gives the delay equations used to estimate interchange delay for the eight interchange types covered by the interchange type selection procedure. In each case, the variables used are defined as follows:

d = interchange delay (s/veh);

Y_c = critical or controlling flow ratio from Step 1; and

D' = distance between the two intersections, measured between the centerlines of the two ramp roadways along the surface arterial (ft).

Exhibit 34-159 also shows the ranges of D' over which these equations are valid. They generally represent the normal design range for these interchange types. These equations should be used with great caution beyond these ranges.

Interchange Type	Valid Range of D' (ft)	Case A:	Case B:
		Right Turns Signalized	Right Turns Free or YIELD-Controlled
SPUI	150–400	$15.1 + (16.0 + 0.01D) \left(\frac{Y_c}{1 - Y_c} \right)$	$15.1 + (5.9 + 0.008D) \left(\frac{Y_c}{1 - Y_c} \right)$
TUDI	200–400	$13.4 + 14.2 \left(\frac{Y_c}{1 - Y_c} \right)$	$13.4 + 12.8 \left(\frac{Y_c}{1 - Y_c} \right)$
CUDI	600–800	$19.2 + [9.4 - 0.011(D - 700)] \left(\frac{Y_c}{1 - Y_c} \right)$	$19.2 + [8.6 - 0.009(D - 700)] \left(\frac{Y_c}{1 - Y_c} \right)$
CDI	900–1,300	$17.1 + [5.0 - 0.011(D - 1,100)] \left(\frac{Y_c}{1 - Y_c} \right)$	$17.1 + [4.6 - 0.009(D - 1,100)] \left(\frac{Y_c}{1 - Y_c} \right)$
Parclo A-4Q	700–1,000	$11.7 + [7.8 - 0.011(D - 800)] \left(\frac{Y_c}{1 - Y_c} \right)$	$11.7 + [6.6 - 0.009(D - 800)] \left(\frac{Y_c}{1 - Y_c} \right)$
Parclo A-2Q	700–1,000	$19.1 + [8.3 - 0.011(D - 800)] \left(\frac{Y_c}{1 - Y_c} \right)$	$19.1 + [8.3 - 0.009(D - 800)] \left(\frac{Y_c}{1 - Y_c} \right)$
Parclo B-4Q	1,000–1,400	$9.3 + [3.5 - 0.011(D - 1,200)] \left(\frac{Y_c}{1 - Y_c} \right)$	$9.3 + [3.4 - 0.009(D - 1,200)] \left(\frac{Y_c}{1 - Y_c} \right)$
Parclo B-2Q	1,000–1,400	$26.2 + [3.9 - 0.011(D - 1,200)] \left(\frac{Y_c}{1 - Y_c} \right)$	$26.2 + [3.2 - 0.009(D - 1,200)] \left(\frac{Y_c}{1 - Y_c} \right)$

Exhibit 34-159
 Estimation of Interchange Delay d_I for Eight Basic Interchange Types

Delay estimates can be related to LOS. For consistency, the same criteria as used for the operational analysis methodology (4) are applied. Because LOS F is based on a v/c ratio greater than 1.00 or a queue storage ratio greater than 1.00, this interchange type selection methodology will never predict LOS F, because it does not predict these ratios. Users should be exceedingly cautious of results when interchange delay exceeds 85 to 90 s/veh.

In evaluating alternative interchange types, the exact distance, D' , may not be known for each of the alternatives. It is recommended that all lengths be selected at the midpoint of the range shown in Exhibit 34-159 for this level of analysis.

Interpretation of Results

The output of the interchange type selection procedure for signalized interchanges is a set of delay predictions for (a) various interchange types, (b) various distances D' between the two intersections, or (c) various numbers and assignments of lanes on ramps and the surface arterials.

Although a lower interchange delay is generally better, a final choice must consider a number of other criteria that are not part of this methodology, including the following:

- Availability of right-of-way,
- Environmental impacts,
- Social impacts,
- Construction cost, and
- Benefit–cost analysis.

This methodology provides valuable information that can be used, in conjunction with other analyses, in making an appropriate choice of an interchange type and some of the primary design parameters. However, the final design will be based on many other criteria in addition to the output of this methodology.

Users are also cautioned that while the definition of interchange delay is similar for the interchange type selection methodology and the operational analysis methodology, different modeling approaches to delay prediction were taken, and there is no guarantee that the results of the two methodologies will be consistent.

4. O-D AND TURNING MOVEMENTS

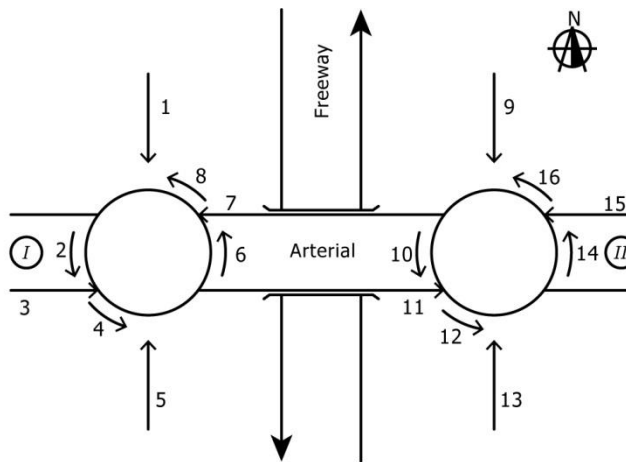
O-D AND TURNING MOVEMENTS FOR INTERCHANGES WITH ROUNDABOUTS

Roundabouts are generally analyzed with the procedures of Chapter 22 of the HCM. This chapter provides guidance for translating O-D demands into movement demands at a roundabout to apply the procedures of Chapter 22.

Exhibit 34-160 defines the movements traveling through an interchange with two roundabouts, while Exhibit 34-161 lists the O-D demands contributing to each of these movements. For example, for diamond interchanges, O-D Movements G, H, and J constitute Movement 15 in Exhibit 34-160.

In analyzing interchanges with roundabouts, Exhibit 34-160 and Exhibit 34-161 should be used to establish the roundabout movements. The procedures of Chapter 22 should then be applied to estimate the capacity and delay for each roundabout approach. Finally, Exhibit 23-14 should be used to determine the LOS for each O-D demand through the interchange.

Exhibit 34-160
Illustration and Notation of
O-D Demands at an
Interchange with
Roundabouts



Movement	Diamond	Parclo A-2Q	Parclo B-2Q	Parclo B-4Q
1	C, D, L, N	C, D, N	--	C
2	D, H, L, M, N	D, N	H, M, N	H, M
3	E, F, I	E, F	E, F, I	E, F, I
4	D, E, F, H, I, L, M, N	D, E, F, I, N	E, F, H, I, M	E, F, H, I, M
5	--	--	C	D, N
6	--	F	C	--
7	A, H, J, M	A, H, J, M	A, H, J, M	A, H, J, M
8	J, M	A, F, H, J, M	A, C, H, J, M	A, H, J, M
9	--	--	A, B, M	A, M
10	--	G	B	-
11	D, E, I, N	D, E, I, N	D, E, I, N	D, E, I, N
12	D, E, I, N	D, E, G, I, N	B, D, E	D, E, I, N
13	A, B, K, M	A, B, M	--	B
14	A, E, K, M, N	A, M	E, N	E, N
15	G, H, J	G, H, J	G, H, J	G, H, J
16	A, E, G, H, J, K, M, N	A, G, H, J, M	E, G, H, J, N	E, G, H, J, N

Movement	SPUI	Parclo AB-4Q	Parclo A-4Q	Parclo AB-2Q
1	C, D, L, N	C	C, D, N	--
2	D, H, L, M, N	H, M	D, N	H, M
3	E, F, I	E, F, I	E, F, I	E, F, I
4	D, E, I, N	E, F, H, I, M	D, E, F, I, N	E, F, H, I, M
5	A, B, K, M	D, N	--	C, D, N
6	A, E, K, M, N	--	--	C
7	G, H, J	A, H, J, M	A, H, J, M	A, H, J, M
8	A, H, J, M	A, H, J, M	A, H, J, M	A, C, H, J, M
9	--	--	--	--
10	--	--	--	G
11	--	D, E, I, N	D, E, I, N	D, E, I, N
12	--	D, E, I, N	D, E, I, N	D, E, G, I, N
13	--	A, B, M	A, B, M	A, B, M
14	--	A, M	A, M	A, M
15	--	G, H, J	G, H, J	G, H, J
16	--	A, G, H, J, M	A, G, H, J, M	A, G, H, J, M

Exhibit 34-161

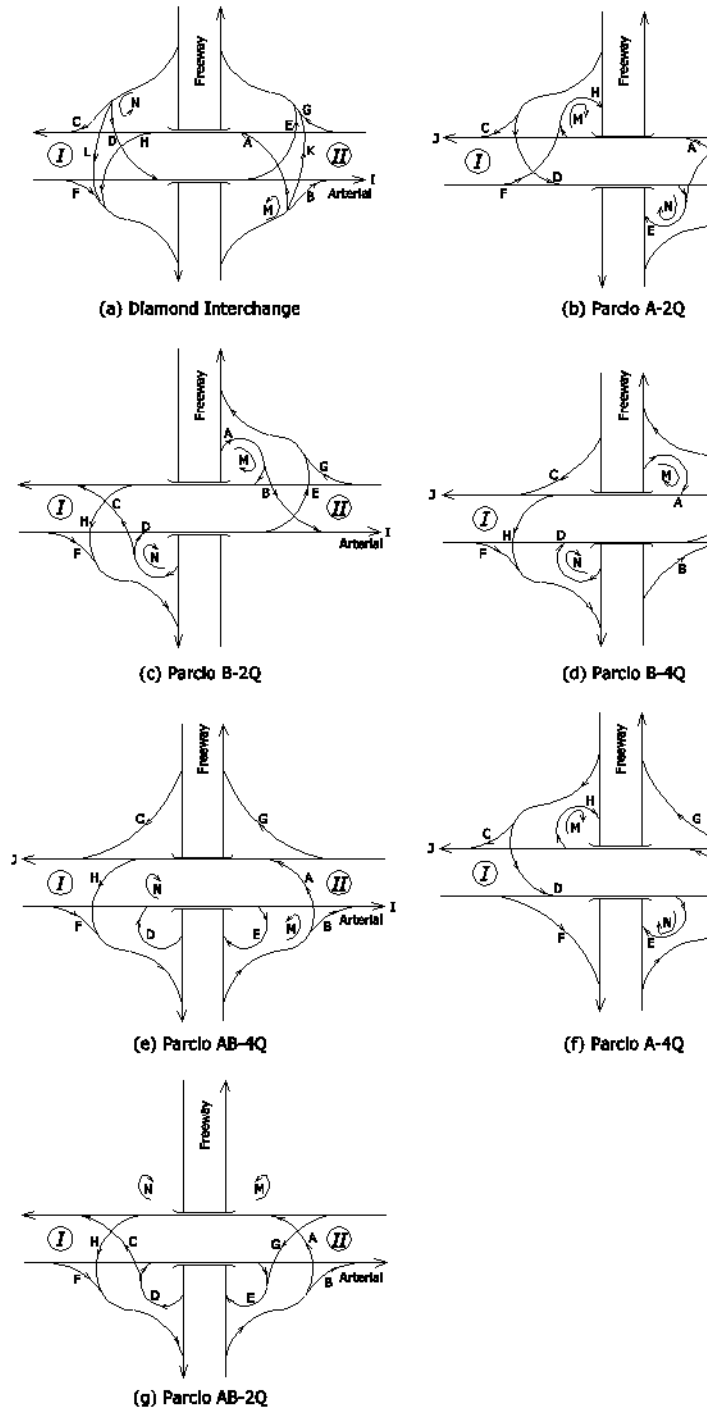
Notation of O-D Demands at Interchanges with Roundabouts

Note: -- indicates movements that do not exist for a given interchange form.

O-D AND TURNING MOVEMENTS FOR CONVENTIONAL INTERCHANGES

Exhibit 34-162 illustrates how O-D movements can be obtained from turning movements for each type of interchange considered in this methodology. Exhibit 34-163 through Exhibit 34-177 provide the corresponding calculations for obtaining turning movements from O-D movements.

Exhibit 34-162
O-D Flows for Each
Interchange Configuration



Input					Output	
Approach	Intersection I		Intersection II		O-D Movement Calculation	Volume (veh/h)
	Turning Move-ment	Volume (veh/h)	Turning Move-ment	Volume (veh/h)		
Eastbound (EB)	EXT-LT		LT		A = (NB LT) - (NB UT)	
	RT		INT-RT		B = NB RT	
	EXT-TH		INT-TH		C = SB RT	
Westbound (WB)	LT		EXT-LT		D = (SB LT) - (SB UT)	
	INT-RT		RT		E = (EB INT-RT) - (SB UT)	
	INT-TH		EXT-TH		F = EB EXT-LT	
Northbound (NB)	LT		LT		G = WB EXT-LT	
	RT		RT		H = (WB INT-RT) - (NB UT)	
	TH		TH		I = (EB INT-TH) - (SB LT) + (SB UT)	
	UT		UT		J = (WB INT-TH) - (NB LT) + (NB UT)	
Southbound (SB)	LT		LT		K	
	RT		RT		L	
	TH		TH		M = NB UT	
	UT		UT		N = SB UT	

Notes: LT = left turn, RT = right turn, UT = U-turn, TH = through, INT = internal, EXT = external.
 The flows of the two U-turn movements from the freeway (SB UT and NB UT) are user-specified.
 Shading indicates movements that do not occur in this interchange form.

Exhibit 34-163

Worksheet for Obtaining O-D Movements from Turning Movements for Parclo A-2Q Interchanges

Input					Output	
Approach	Intersection I		Intersection II		O-D Movement Calculation	Volume (veh/h)
	Turning Move-ment	Volume (veh/h)	Turning Move-ment	Volume (veh/h)		
Eastbound (EB)	LT		LT		A = (NB LT) - (NB UT)	
	EXT-RT		INT-RT		B = NB RT	
	EXT-TH		INT-TH		C = SB RT	
Westbound (WB)	LT		LT		D = (SB LT) - (SB UT)	
	INT-RT		EXT-RT		E = (EB INT-RT) - (SB UT)	
	INT-TH		EXT-TH		F = EB EXT-RT	
Northbound (NB)	LT		LT		G = WB EXT-RT	
	RT		RT		H = (WB INT-RT) - (NB UT)	
	TH		TH		I = (EB INT-TH) - (SB LT) + (SB UT)	
	UT		UT		J = (WB INT-TH) - (NB LT) + (NB UT)	
Southbound (SB)	LT		LT		K	
	RT		RT		L	
	TH		TH		M = NB UT	
	UT		UT		N = SB UT	

Notes: LT = left turn, RT = right turn, UT = U-turn, TH = through, INT = internal, EXT = external.
 The flows of the two U-turn movements from the freeway (SB UT and NB UT) are user-specified.
 Shading indicates movements that do not occur in this interchange form.

Exhibit 34-164

Worksheet for Obtaining O-D Movements from Turning Movements for Parclo A-4Q Interchanges

Input					Output	
Approach	Intersection I		Intersection II		O-D Movement Calculation	Volume (veh/h)
	Turning Move-ment	Volume (veh/h)	Turning Move-ment	Volume (veh/h)		
Eastbound (EB)	LT		LT		A = (NB LT(II)) - (NB UT(II))	
	EXT-RT		INT-RT		B = NB RT(II)	
	EXT-TH		INT-TH		C = NB LT(I)	
Westbound (WB)	INT-LT		EXT-LT		D = (NB RT(I)) - (NB UT(I))	
	RT		RT		E = (EB INT-RT) - (NB UT(I))	
	INT-TH		EXT-TH		F = EB EXT-RT	
Northbound (NB)	LT(I)		LT(II)		G = WB EXT-LT	
	RT(I)		RT(II)		H = (WB INT-LT) - (NB UT(II))	
	TH		TH		I = (EB INT-TH) - (NB RT(I)) + (NB UT(I))	
	UT(I)		UT(II)		J = (WB INT-TH) - (NB LT(II)) + (NB UT(II))	
Southbound (SB)	LT		LT		K	
	RT		RT		L	
	TH		TH		M = NB UT(II)	
	UT		UT		N = NB UT(I)	

Notes: LT = left turn, RT = right turn, UT = U-turn, TH = through, INT = internal, EXT = external.
 The flows of the two U-turn movements from the freeway [NB UT(I) and NB UT(II)] are user-specified.
 Shading indicates movements that do not occur in this interchange form.

Exhibit 34-165

Worksheet for Obtaining O-D Movements from Turning Movements for Parclo AB-2Q Interchanges

Exhibit 34-166

Worksheet for Obtaining O-D Movements from Turning Movements for Parclo AB-4Q Interchanges

Input					Output	
Approach	Intersection I		Intersection II		O-D Movement Calculation	Volume (veh/h)
	Turning Movement	Volume (veh/h)	Turning Movement	Volume (veh/h)		
Eastbound (EB)	LT		LT		$A = (NB\ LT(II)) - (NB\ UT(II))$	
	EXT-RT		INT-RT		$B = NB\ RT(II)$	
	EXT-TH		INT-TH		$C = SB\ RT(I)$	
Westbound (WB)	INT-LT		LT		$D = (NB\ RT(I)) - (NB\ UT(I))$	
	RT		EXT-RT		$E = (EB\ INT-RT) - (NB\ UT(I))$	
	INT-TH		EXT-TH		$F = EB\ EXT-RT$	
Northbound (NB)	LT		LT(II)		$G = WB\ EXT-LT$	
	RT(I)		RT(II)		$H = (WB\ INT-LT) - (NB\ UT(II))$	
	TH		TH		$I = (EB\ INT-TH) - (NB\ RT(I)) + (NB\ UT(I))$	
Southbound (SB)	UT(I)		UT(II)		$J = (WB\ INT-TH) - (NB\ LT(II)) + (NB\ UT(II))$	
	LT		LT		K	
	RT(I)		RT		L	
	TH		TH		$M = NB\ UT(II)$	
	UT		UT		$N = NB\ UT(I)$	

Notes: LT = left turn, RT = right turn, UT = U-turn, TH = through, INT = internal, EXT = external.
The flows of the two U-turn movements from the freeway [NB UT(I) and NB UT(II)] are user-specified.
Shading indicates movements that do not occur in this interchange form.

Exhibit 34-167

Worksheet for Obtaining O-D Movements from Turning Movements for Parclo B-2Q Interchanges

Input					Output	
Approach	Intersection I		Intersection II		O-D Movement Calculation	Volume (veh/h)
	Turning Movement	Volume (veh/h)	Turning Movement	Volume (veh/h)		
Eastbound (EB)	LT		INT-LT		$A = (SB\ RT) - (SB\ UT)$	
	EXT-RT		RT		$B = SB\ LT$	
	EXT-TH		INT-TH		$C = NB\ LT$	
Westbound (WB)	INT-LT		LT		$D = (NB\ RT) - (NB\ UT)$	
	RT		EXT-RT		$E = (EB\ INT-LT) - (NB\ UT)$	
	INT-TH		EXT-TH		$F = (EB\ EXT-RT)$	
Northbound (NB)	LT		LT		$G = (WB\ EXT-RT)$	
	RT		RT		$H = (WB\ INT-LT) - (SB\ UT)$	
	TH		TH		$I = (EB\ INT-TH) - (NB\ RT) + (NB\ UT)$	
Southbound (SB)	UT		UT		$J = (WB\ INT-TH) - (SB\ RT) + (SB\ UT)$	
	LT		LT		K	
	RT		RT		L	
	TH		TH		$M = SB\ UT$	
	UT		UT		$N = NB\ UT$	

Notes: LT = left turn, RT = right turn, UT = U-turn, TH = through, INT = internal, EXT = external.
The flows of the two U-turn movements from the freeway (NB UT and SB UT) are user-specified.
Shading indicates movements that do not occur in this interchange form.

Exhibit 34-168

Worksheet for Obtaining O-D Movements from Turning Movements for Parclo B-4Q Interchanges

Input					Output	
Approach	Intersection I		Intersection II		O-D Movement Calculation	Volume (veh/h)
	Turning Movement	Volume (veh/h)	Turning Movement	Volume (veh/h)		
Eastbound (EB)	LT		INT-LT		$A = (SB\ RT(II)) - (SB\ UT)$	
	EXT-RT		RT		$B = NB\ RT(II)$	
	EXT-TH		INT-TH		$C = SB\ RT(I)$	
Westbound (WB)	INT-LT		LT		$D = (NB\ RT(I)) - (NB\ UT)$	
	RT		EXT-RT		$E = (EB\ INT-LT) - (NB\ UT)$	
	INT-TH		EXT-TH		$F = EB\ EXT-RT$	
Northbound (NB)	LT		LT		$G = WB\ EXT-RT$	
	RT(I)		RT(II)		$H = (WB\ INT-LT) - (SB\ UT)$	
	TH		TH		$I = (EB\ INT-TH) - (NB\ RT(I)) + (NB\ UT)$	
Southbound (SB)	UT		UT		$J = (WB\ INT-TH) - (SB\ RT(II)) + (SB\ UT)$	
	LT		LT		K	
	RT(I)		RT(II)		L	
	TH		TH		$M = SB\ UT$	
	UT		UT		$N = NB\ UT$	

Notes: LT = left turn, RT = right turn, UT = U-turn, TH = through, INT = internal, EXT = external.
The flows of the two U-turn movements from the freeway (NB UT and SB UT) are user-specified.
Shading indicates movements that do not occur in this interchange form.

Input					Output	
Approach	Intersection I		Intersection II		O-D Movement Calculation	Volume (veh/h)
	Turning Movement	Volume (veh/h)	Turning Movement	Volume (veh/h)		
Eastbound (EB)	LT		INT-LT		$A = (NB\ LT) - (NB\ UT)$	
	EXT-RT		RT		$B = NB\ RT$	
	EXT-TH		INT-TH		$C = SB\ RT$	
Westbound (WB)	INT-LT		LT		$D = (SB\ LT) - (SB\ UT)$	
	RT		EXT-RT		$E = (EB\ INT-LT) - (SB\ UT)$	
	INT-TH		EXT-TH		$F = EB\ EXT-RT$	
Northbound (NB)	LT		LT		$G = WB\ EXT-RT$	
	RT		RT		$H = (WB\ INT-LT) - (NB\ UT)$	
	TH		TH		$I = (EB\ INT-TH) - (SB\ LT) + (SB\ UT)$	
	UT		UT		$J = (WB\ INT-TH) - (NB\ LT) + (NB\ UT)$	
Southbound (SB)	LT		LT		$K = NB\ TH$	
	RT		RT		$L = SB\ TH$	
	TH		TH		$M = NB\ UT$	
	UT		UT		$N = SB\ UT$	

Notes: LT = left turn, RT = right turn, UT = U-turn, TH = through, INT = internal, EXT = external.
 The flows of the two U-turn movements from the freeway (NB UT and SB UT) are user-specified.
 Shading indicates movements that do not occur in this interchange form.

Exhibit 34-169
 Worksheet for Obtaining O-D Movements from Turning Movements for Diamond Interchanges

Input			Output	
Approach	Turning Movement	Volume (veh/h)	O-D Movement Calculation	Volume (veh/h)
Eastbound (EB)	LT		$A = NB\ LT$	
	RT		$B = NB\ RT$	
	TH		$C = SB\ RT$	
Westbound (WB)	LT		$D = SB\ LT$	
	RT		$E = EB\ LT$	
	TH		$F = EB\ RT$	
Northbound (NB)	LT		$G = WB\ RT$	
	RT		$H = WB\ LT$	
	TH		$I = EB\ TH$	
	UT		$J = WB\ TH$	
Southbound (SB)	LT		$K = NB\ TH$	
	RT		$L = SB\ TH$	
	TH		M	
	UT		N	

Notes: LT = left turn, RT = right turn, UT = U-turn, TH = through.
 The flow of the two U-turn movements from the freeway (NB UT and SB UT) are user-specified.
 Shading indicates movements that do not occur in this interchange form.

Exhibit 34-170
 Worksheet for Obtaining O-D Movements from Turning Movements for SPUIS

Input		Output				
O-D Movement	Volume (veh/h)	Approach	Intersection I		Intersection II	
			Turning Movement Calculation	Volume (veh/h)	Turning Movement Calculation	Volume (veh/h)
A		Eastbound (EB)	EXT-LT = F		LT	
B			RT		INT-RT = E+N	
C			EXT-TH = I+E		INT-TH = I+D	
D		Westbound (WB)	LT		EXT-LT = G	
E			INT-RT = H+M		RT	
F			INT-TH = J+A		EXT-TH = J+H	
G		Northbound (NB)	LT		LT = A+M	
H			RT		RT = B	
I			TH		TH	
J			UT		UT = M	
K		Southbound (SB)	LT = D+N		LT	
L			RT = C		RT	
M			TH		TH	
N			UT = N		UT	

Notes: LT = left turn, RT = right turn, UT = U-turn, TH = through, INT = internal, EXT = external.
 Shading indicates movements that do not occur in this interchange form.

Exhibit 34-171
 Worksheet for Obtaining Turning Movements from O-D Movements for Parclo A-2Q and Parclo A-4Q Interchanges

Exhibit 34-172

Worksheet for Obtaining Turning Movements from O-D Movements for Parclo AB-2Q Interchanges

Input		Output				
O-D Move-ment (veh/h)	Volume (veh/h)	Approach	Intersection I		Intersection II	
			Turning Movement Calculation	Volume (veh/h)	Turning Movement Calculation	Volume (veh/h)
A		Eastbound (EB)	LT		LT	
B			EXT RT = F		INT-RT = E+N	
C			EXT-TH = I+E		INT-TH = I+D	
D		Westbound (WB)	INT-LT = H+M		EXT-LT = G	
E			RT		RT	
F			INT-TH = J+A		EXT-TH = J+H	
G		Northbound (NB)	LT(I) = C		LT(II) = A+M	
H			RT(I) = D+N		RT(II) = B	
I			TH		TH	
J			UT(I) = N		UT(II) = M	
K		Southbound (SB)	LT		LT	
L			RT		RT	
M			TH		TH	
N			UT		UT	

Notes: LT = left turn, RT = right turn, UT = U-turn, TH = through, INT = internal, EXT = external. Shading indicates movements that do not occur in this interchange form.

Exhibit 34-173

Worksheet for Obtaining Turning Movements from O-D Movements for Parclo AB-4Q Interchanges

Input		Output				
O-D Move-ment (veh/h)	Volume (veh/h)	Approach	Intersection I		Intersection II	
			Turning Movement Calculation	Volume (veh/h)	Turning Movement Calculation	Volume (veh/h)
A		Eastbound (EB)	LT		LT	
B			EXT RT = F		INT-RT = E+N	
C			EXT-TH = I+E		INT-TH = I+D	
D		Westbound (WB)	INT-LT = H+M		LT	
E			RT		EXT-RT = G	
F			INT-TH = J+A		EXT-TH = J+H	
G		Northbound (NB)	LT		LT(II) = A+M	
H			RT(I) = D+N		RT(II) = B	
I			TH		TH	
J			UT(I) = N		UT(II) = M	
K		Southbound (SB)	LT		LT	
L			RT(I) = C		RT	
M			TH		TH	
N			UT		UT	

Notes: LT = left turn, RT = right turn, UT = U-turn, TH = through, INT = internal, EXT = external. Shading indicates movements that do not occur in this interchange form.

Exhibit 34-174

Worksheet for Obtaining Turning Movements from O-D Movements for Parclo B-2Q Interchanges

Input		Output				
O-D Move-ment (veh/h)	Volume (veh/h)	Approach	Intersection I		Intersection II	
			Turning Movement Calculation	Volume (veh/h)	Turning Movement Calculation	Volume (veh/h)
A		Eastbound (EB)	LT		INT-LT = E+N	
B			EXT RT = F		RT	
C			EXT-TH = I+E		INT-TH = I+D	
D		Westbound (WB)	INT-LT = H+M		LT	
E			RT		EXT-RT = G	
F			INT-TH = J+A		EXT-TH = J+H	
G		Northbound (NB)	LT = C		LT	
H			RT = D+N		RT	
I			TH		TH	
J			UT = N		UT	
K		Southbound (SB)	LT		LT = B	
L			RT		RT = A+M	
M			TH		TH	
N			UT		UT = M	

Notes: LT = left turn, RT = right turn, UT = U-turn, TH = through, INT = internal, EXT = external. Shading indicates movements that do not occur in this interchange form.

Input		Output				
O-D Move-ment (veh/h)	Volume (veh/h)	Approach	Intersection I		Intersection II	
			Turning Movement Calculation	Volume (veh/h)	Turning Movement Calculation	Volume (veh/h)
A		Eastbound (EB)	LT		INT-LT = E+N	
B			EXT RT = F		RT	
C			EXT-TH = I+E		INT-TH = I+D	
D		Westbound (WB)	INT-LT = H+M		LT	
E			RT		EXT-RT = G	
F			INT-TH = J+A		EXT-TH = J+H	
G		Northbound (NB)	LT		LT	
H			RT(I) = D+N		RT(II) = B	
I			TH		TH	
J			UT = N		UT	
K		Southbound (SB)	LT		LT	
L			RT(I) = C		RT(II) = A+M	
M			TH		TH	
N			UT		UT = M	

Notes: LT = left turn, RT = right turn, UT = U-turn, TH = through, INT = internal, EXT = external.
Shading indicates movements that do not occur in this interchange form.

Exhibit 34-175

Worksheet for Obtaining Turning Movements from O-D Movements for Parclo B-4Q Interchanges

Input		Output				
O-D Move-ment (veh/h)	Volume (veh/h)	Approach	Intersection I		Intersection II	
			Turning Movement Calculation	Volume (veh/h)	Turning Movement Calculation	Volume (veh/h)
A		Eastbound (EB)	LT		INT-LT = E+N	
B			EXT RT = F		RT	
C			EXT-TH = I+E		INT-TH = I+D	
D		Westbound (WB)	INT-LT = H+M		LT	
E			RT		EXT-RT = G	
F			INT-TH = J+A		EXT-TH = J+H	
G		Northbound (NB)	LT		LT = A+M	
H			RT		RT = B	
I			TH		TH = K	
J			UT		UT = M	
K		Southbound (SB)	LT = D+N		LT	
L			RT = C		RT	
M			TH = L		TH	
N			UT = N		UT	

Notes: LT = left turn, RT = right turn, UT = U-turn, TH = through, INT = internal, EXT = external.
Shading indicates movements that do not occur in this interchange form.

Exhibit 34-176

Worksheet for Obtaining Turning Movements from O-D Movements for Diamond Interchanges

Input		Output		
O-D Movement	Volume (veh/h)	Approach	Turning Movement Calculation	Volume (veh/h)
A		Eastbound (EB)	LT = E	
B			RT = F	
C			TH = I	
D		Westbound (WB)	LT = H	
E			RT = G	
F			TH = J	
G		Northbound (NB)	LT = A	
H			RT = B	
I			TH = K	
J			UT	
K		Southbound (SB)	LT = D	
L			RT = C	
M			TH = L	
N			UT	

Notes: LT = left turn, RT = right turn, UT = U-turn, TH = through.
Shading indicates movements that do not occur in this interchange form.

Exhibit 34-177

Worksheet for Obtaining Turning Movements from O-D Movements for SPUIS

5. REFERENCES

1. Elefteriadou, L., C. Fang, R. P. Roess, E. Prassas, J. Yeon, X. Cui, A. Kondyli, H. Wang, and J. M. Mason. *Capacity and Quality of Service of Interchange Ramp Terminals*. Final Report, National Cooperative Highway Research Program Project 3-60. Pennsylvania State University, University Park, March 2005.
2. Elefteriadou, L., A. Elias, C. Fang, C. Lu, L. Xie, and B. Martin. *Validation and Enhancement of the Highway Capacity Manual's Interchange Ramp Terminal Methodology*. Final Report, National Cooperative Highway Research Program Project 3-60A. University of Florida, Gainesville, 2009.
3. Messer, C. J., and J. A. Bonneson. *Capacity of Interchange Ramp Terminals*. Final Report, National Cooperative Highway Research Program Project 3-47. Texas A&M Research Foundation, College Station, April 1997.
4. Bonneson, J., K. Zimmerman, and M. Jacobson. *Review and Evaluation of Interchange Ramp Design Considerations for Facilities Without Frontage Roads*. Research Report 0-4538-1. Cooperative Research Program, Texas Transportation Institute, Texas A&M University System, College Station, 2004.
5. Federal Highway Administration. EDC2 Intersection and Interchange Geometrics website. <https://www.fhwa.dot.gov/everydaycounts/edctwo/2012/>. Accessed Dec. 30, 2014.
6. *National Transportation Communications for ITS Protocol: Object Definitions for Actuated Traffic Signal Controller (ASC) Units-1202*. National Electrical Manufacturers Association, Rosslyn, Va., Jan. 2005.



HIGHWAY CAPACITY MANUAL

6TH EDITION | A GUIDE FOR MULTIMODAL MOBILITY ANALYSIS

VOLUME 4: APPLICATIONS GUIDE

The National Academies of
SCIENCES • ENGINEERING • MEDICINE

TRANSPORTATION RESEARCH BOARD
WASHINGTON, D.C. | WWW.TRB.ORG

TRANSPORTATION RESEARCH BOARD 2016 EXECUTIVE COMMITTEE *

Chair: James M. Crites, Executive Vice President of Operations,
Dallas–Fort Worth International Airport, Texas

Vice Chair: Paul Trombino III, Director, Iowa Department of
Transportation, Ames

Executive Director: Neil J. Pedersen, Transportation Research Board

Victoria A. Arroyo, Executive Director, Georgetown Climate Center;
Assistant Dean, Centers and Institutes; and Professor and Director,
Environmental Law Program, Georgetown University Law Center,
Washington, D.C.

Scott E. Bennett, Director, Arkansas State Highway and Transportation
Department, Little Rock

Jennifer Cohan, Secretary, Delaware Department of Transportation, Dover

Malcolm Dougherty, Director, California Department of
Transportation, Sacramento

A. Stewart Fotheringham, Professor, School of Geographical Sciences
and Urban Planning, Arizona State University, Tempe

John S. Halikowski, Director, Arizona Department of Transportation,
Phoenix

Susan Hanson, Distinguished University Professor Emerita, Graduate
School of Geography, Clark University, Worcester, Massachusetts

Steve Heminger, Executive Director, Metropolitan Transportation
Commission, Oakland, California

Chris T. Hendrickson, Hamerschlag Professor of Engineering, Carnegie
Mellon University, Pittsburgh, Pennsylvania

Jeffrey D. Holt, Managing Director, Power, Energy, and Infrastructure
Group, BMO Capital Markets Corporation, New York

S. Jack Hu, Vice President for Research and J. Reid and Polly Anderson
Professor of Manufacturing, University of Michigan, Ann Arbor

Roger B. Huff, President, HGLC, LLC, Farmington Hills, Michigan

Geraldine Knatz, Professor, Sol Price School of Public Policy, Viterbi
School of Engineering, University of Southern California, Los Angeles

Ysela Llort, Consultant, Miami, Florida

Melinda McGrath, Executive Director, Mississippi Department of
Transportation, Jackson

James P. Redeker, Commissioner, Connecticut Department of
Transportation, Newington

Mark L. Rosenberg, Executive Director, The Task Force for Global
Health, Inc., Decatur, Georgia

Kumares C. Sinha, Olson Distinguished Professor of Civil Engineering,
Purdue University, West Lafayette, Indiana

Daniel Sperling, Professor of Civil Engineering and Environmental
Science and Policy; Director, Institute of Transportation Studies,
University of California, Davis

Kirk T. Steudle, Director, Michigan Department of Transportation,
Lansing (Past Chair, 2014)

Gary C. Thomas, President and Executive Director, Dallas Area Rapid
Transit, Dallas, Texas

Pat Thomas, Senior Vice President of State Government Affairs, United
Parcel Service, Washington, D.C.

Katherine F. Turnbull, Executive Associate Director and Research
Scientist, Texas A&M Transportation Institute, College Station

Dean Wise, Vice President of Network Strategy, Burlington Northern
Santa Fe Railway, Fort Worth, Texas

Thomas P. Bostick (Lieutenant General, U.S. Army), Chief of Engineers
and Commanding General, U.S. Army Corps of Engineers, Washington,
D.C. (ex officio)

James C. Card (Vice Admiral, U.S. Coast Guard, retired), Maritime
Consultant, The Woodlands, Texas, and Chair, TRB Marine Board
(ex officio)

T. F. Scott Darling III, Acting Administrator and Chief Counsel, Federal
Motor Carrier Safety Administration, U.S. Department of Transportation
(ex officio)

Marie Therese Dominguez, Administrator, Pipeline and Hazardous
Materials Safety Administration, U.S. Department of Transportation
(ex officio)

Sarah Feinberg, Administrator, Federal Railroad Administration,
U.S. Department of Transportation (ex officio)

Carolyn Flowers, Acting Administrator, Federal Transit Administration,
U.S. Department of Transportation (ex officio)

LeRoy Gishi, Chief, Division of Transportation, Bureau of Indian
Affairs, U.S. Department of the Interior, Washington, D.C. (ex officio)

John T. Gray II, Senior Vice President, Policy and Economics,
Association of American Railroads, Washington, D.C. (ex officio)

Michael P. Huerta, Administrator, Federal Aviation Administration,
U.S. Department of Transportation (ex officio)

Paul N. Jaenichen, Sr., Administrator, Maritime Administration,
U.S. Department of Transportation (ex officio)

Bevan B. Kirley, Research Associate, University of North Carolina
Highway Safety Research Center, Chapel Hill, and Chair, TRB Young
Members Council (ex officio)

Gregory G. Nadeau, Administrator, Federal Highway Administration,
U.S. Department of Transportation (ex officio)

Wayne Nastri, Acting Executive Officer, South Coast Air Quality
Management District, Diamond Bar, California (ex officio)

Mark R. Rosekind, Administrator, National Highway Traffic Safety
Administration, U.S. Department of Transportation (ex officio)

Craig A. Rutland, U.S. Air Force Pavement Engineer, U.S. Air Force
Civil Engineer Center, Tyndall Air Force Base, Florida (ex officio)

Reuben Sarkar, Deputy Assistant Secretary for Transportation,
U.S. Department of Energy (ex officio)

Richard A. White, Acting President and CEO, American Public
Transportation Association, Washington, D.C. (ex officio)

Gregory D. Winfree, Assistant Secretary for Research and Technology,
Office of the Secretary, U.S. Department of Transportation (ex officio)

Frederick G. (Bud) Wright, Executive Director, American Association
of State Highway and Transportation Officials, Washington, D.C.
(ex officio)

Paul F. Zukunft (Admiral, U.S. Coast Guard), Commandant, U.S. Coast
Guard, U.S. Department of Homeland Security (ex officio)

Transportation Research Board publications are available by ordering
individual publications directly from the TRB Business Office, through
the Internet at www.TRB.org, or by annual subscription through
organizational or individual affiliation with TRB. Affiliates and library
subscribers are eligible for substantial discounts. For further information,
contact the Transportation Research Board Business Office, 500 Fifth
Street, NW, Washington, DC 20001 (telephone 202-334-3213;
fax 202-334-2519; or e-mail TRBsales@nas.edu).

Copyright 2016 by the National Academy of Sciences.

All rights reserved.

Printed in the United States of America.

ISBN 978-0-309-36997-8 [Slipcased set of three volumes]

ISBN 978-0-309-36998-5 [Volume 1]

ISBN 978-0-309-36999-2 [Volume 2]

ISBN 978-0-309-37000-4 [Volume 3]

ISBN 978-0-309-37001-1 [Volume 4, online only]

The National Academies of
SCIENCES • ENGINEERING • MEDICINE

The **National Academy of Sciences** was established in 1863 by an Act of Congress, signed by President Lincoln, as a private, nongovernmental institution to advise the nation on issues related to science and technology. Members are elected by their peers for outstanding contributions to research. Dr. Ralph J. Cicerone is president.

The **National Academy of Engineering** was established in 1964 under the charter of the National Academy of Sciences to bring the practices of engineering to advising the nation. Members are elected by their peers for extraordinary contributions to engineering. Dr. C. D. Mote, Jr., is president.

The **National Academy of Medicine** (formerly the Institute of Medicine) was established in 1970 under the charter of the National Academy of Sciences to advise the nation on medical and health issues. Members are elected by their peers for distinguished contributions to medicine and health. Dr. Victor J. Dzau is president.

The three Academies work together as the National Academies of Sciences, Engineering, and Medicine to provide independent, objective analysis and advice to the nation and conduct other activities to solve complex problems and inform public policy decisions. The Academies also encourage education and research, recognize outstanding contributions to knowledge, and increase public understanding in matters of science, engineering, and medicine.

Learn more about the National Academies of Sciences, Engineering, and Medicine at **www.national-academies.org**.

The **Transportation Research Board** is one of seven major programs of the National Academies of Sciences, Engineering, and Medicine. The mission of the Transportation Research Board is to increase the benefits that transportation contributes to society by providing leadership in transportation innovation and progress through research and information exchange, conducted within a setting that is objective, interdisciplinary, and multimodal. The Board's varied committees, task forces, and panels annually engage about 7,000 engineers, scientists, and other transportation researchers and practitioners from the public and private sectors and academia, all of whom contribute their expertise in the public interest. The program is supported by state transportation departments, federal agencies including the component administrations of the U.S. Department of Transportation, and other organizations and individuals interested in the development of transportation.

Learn more about the Transportation Research Board at **www.TRB.org**.

CHAPTER 35
PEDESTRIANS AND BICYCLES: SUPPLEMENTAL

CONTENTS

1. INTRODUCTION 35-1

2. EXAMPLE PROBLEMS 35-2

 Example Problem 1: Pedestrian LOS on Shared-Use and Exclusive
 Paths..... 35-2

 Example Problem 2: Bicycle LOS on a Shared-Use Path 35-4

LIST OF EXHIBITS

Exhibit 35-1 List of Example Problems 35-2

1. INTRODUCTION

Chapter 35 is the supplemental chapter for Chapter 24, Off-Street Pedestrian and Bicycle Facilities, which is found in Volume 3 of the *Highway Capacity Manual*. It provides two example problems demonstrating the calculation of pedestrian and bicycle level of service (LOS) for off-street paths.

VOLUME 4: APPLICATIONS
GUIDE

- 25. Freeway Facilities:
Supplemental
- 26. Freeway and Highway
Segments: Supplemental
- 27. Freeway Weaving:
Supplemental
- 28. Freeway Merges and
Diverges: Supplemental
- 29. Urban Street Facilities:
Supplemental
- 30. Urban Street Segments:
Supplemental
- 31. Signalized Intersections:
Supplemental
- 32. STOP-Controlled
Intersections:
Supplemental
- 33. Roundabouts:
Supplemental
- 34. Interchange Ramp
Terminals: Supplemental
- 35. Pedestrians and
Bicycles: Supplemental**
- 36. Concepts: Supplemental
- 37. ATDM: Supplemental

2. EXAMPLE PROBLEMS

Exhibit 35-1
List of Example Problems

Example Problem	Description	Application
1	Pedestrian LOS on shared-use and exclusive paths	Operational analysis
2	Bicycle LOS on a shared-use path	Planning analysis

EXAMPLE PROBLEM 1: PEDESTRIAN LOS ON SHARED-USE AND EXCLUSIVE PATHS

The Facts

The parks and recreation department responsible for an off-street shared-use path has received several complaints from pedestrians that the volume of bicyclists using the path makes walking on the path an uncomfortable experience. The department wishes to quantify path operations and, if necessary, evaluate potential solutions.

The following information was collected in the field for this path:

- Q_{sb} = bicycle volume in same direction = 100 bicycles/h;
- Q_{ob} = bicycle volume in opposing direction = 100 bicycles/h;
- v_{15} = peak 15-min pedestrian volume = 100 pedestrians;
- PHF = peak hour factor = 0.83;
- S_p = average pedestrian speed = 4.0 ft/s (2.7 mi/h);
- S_b = average bicycle speed = 16.0 ft/s (10.9 mi/h); and
- No pedestrian platooning was observed.

Step 1: Gather Input Data

The shared-use path pedestrian LOS methodology requires pedestrian and bicycle speeds and bicycle demand, all of which are available from the field measurements just given.

Step 2: Calculate Number of Bicycle Passing and Meeting Events

The number of passing events F_p is determined from Equation 24-5:

$$F_p = \frac{Q_{sb}}{PHF} \left(1 - \frac{S_p}{S_b} \right)$$

$$F_p = \frac{100 \text{ bicycles/h}}{0.83} \left(1 - \frac{4.0 \text{ ft/s}}{16.0 \text{ ft/s}} \right)$$

$$F_p = 90 \text{ events/h}$$

The number of meeting events F_m is determined from Equation 24-6:

$$F_m = \frac{Q_{ob}}{PHF} \left(1 + \frac{S_p}{S_b} \right)$$

$$F_m = \frac{100 \text{ bicycles/h}}{0.83} \left(1 + \frac{4.0 \text{ ft/s}}{16.0 \text{ ft/s}} \right)$$

$$F_m = 151 \text{ events/h}$$

The total number of events is calculated from Equation 24-7:

$$F = (F_p + 0.5F_m)$$

$$F = (90 + 0.5(151))$$

$$F = 166 \text{ events/h}$$

Step 3: Determine Shared-Use Path Pedestrian LOS

The shared-use path LOS is determined from Exhibit 24-4. The value of F , 166 events/h, falls into the LOS E range. Because this LOS is rather low, what would happen if a parallel, 5-ft-wide, pedestrian-only path were provided?

Step 4: Compare Exclusive-Path Pedestrian LOS

Step 4.1: Determine Effective Walkway Width

Assuming no obstacles exist on or immediately adjacent to the path, the effective width would be the same as the actual width, or 5 ft. If common amenities like trash cans and benches will be located along the path, they should be placed at least 3 ft and 5 ft, respectively, off the path to avoid affecting the effective width. These distances are based on data from Exhibit 24-9.

Step 4.2: Calculate Pedestrian Flow Rate

Because a peak 15-min pedestrian volume was measured in the field, it is not necessary to use Equation 24-2 to determine v_{15} . The unit flow rate for the walkway v_p is determined from Equation 24-3 as follows:

$$v_p = \frac{v_{15}}{15 \times W_E}$$

$$v_p = \frac{100}{15 \times 5}$$

$$v_p = 1.33 \text{ p/ft/min}$$

Step 4.3: Calculate Average Pedestrian Space

Average pedestrian space is determined from Equation 24-4, including applying a conversion from seconds to minutes:

$$A_p = \frac{S_p}{v_p}$$

$$A_p = (4.0 \text{ ft/s})(60 \text{ s/min}) / (1.33 \text{ p/ft/min})$$

$$A_p = 180 \text{ ft}^2/\text{p}$$

Step 4.4: Determine LOS

Because no pedestrian platooning was observed, Exhibit 24-1 should be used to determine LOS. A value of 180 ft²/min corresponds to LOS A.

Discussion

The existing shared-use path operates at LOS E for pedestrians. Pedestrian LOS would increase to LOS A if a parallel, 5-ft-wide pedestrian path were provided.

EXAMPLE PROBLEM 2: BICYCLE LOS ON A SHARED-USE PATH

The Facts

A new shared-use path is being planned. On the basis of data from a similar facility in the region, planners estimate the path will have a peak hour volume of 340 users, a peak hour factor of 0.90, and a 50/50 directional split. The path will be 10 ft wide, without obstacles or a centerline. The segment analyzed here is 3 mi long.

Step 1: Gather Input Data

Facility and overall demand data are available but not the mode split of users or the average mode group speed. Those values will need to be defaulted by using Exhibit 24-6. On the basis of the default mode split and the estimated directional split, the directional flow rate by mode is as follows:

- Directional bicycle flow rate = $(340 \text{ users/h} \times 0.5 \times 0.55)/0.90 = 104$ bicycles/h;
- Directional pedestrian flow rate = $(340 \times 0.5 \times 0.20)/0.90 = 38$ p/h;
- Directional runner flow rate = $(340 \times 0.5 \times 0.10)/0.90 = 19$ runners/h;
- Directional inline skater flow rate = $(340 \times 0.5 \times 0.10)/0.90 = 19$ skaters/h; and
- Directional child bicyclist volume = $(340 \times 0.5 \times 0.05)/0.90 = 9$ child bicyclists/h.

From Exhibit 24-6, average mode group speeds μ and standard deviations σ are as follows:

- Bicycle: $\mu = 12.8$ mi/h, $\sigma = 3.4$ mi/h;
- Pedestrian: $\mu = 3.4$ mi/h, $\sigma = 0.6$ mi/h;
- Runner: $\mu = 6.5$ mi/h, $\sigma = 1.2$ mi/h;
- Inline skater: $\mu = 10.1$ mi/h, $\sigma = 2.7$ mi/h; and
- Child bicyclist: $\mu = 7.9$ mi/h, $\sigma = 1.9$ mi/h.

Step 2: Calculate Active Passings per Minute

Active passings per minute must be calculated separately for each mode by using Equation 24-9 through Equation 24-11. The path segment length L is 3 mi, and the path is considered as broken into 300 pieces, each of which has a length dx of 0.01 mi.

For a given modal user in the path when the average bicyclist enters, the probability of being passed is expressed by Equation 24-9. The average probability of passing within each piece j can be estimated as the average of the probabilities at the start and end of each piece, as expressed by Equation 24-10.

The probability of passing a bicycle at the end of the first 0.01-mi piece of path (i.e., at $x = 0.01$ mi) is derived from a normal distribution of bicycle speeds with a mean speed μ and a standard deviation σ .

$$F(x) = P\left[v_{bicycle} < U\left(1 - \frac{x}{L}\right)\right] = P\left[v_{bicycle} < 12.8\left(1 - \frac{0.01}{3}\right)\right]$$

$$F(x) = P[v_{bicycle} < 12.76] = 0.4950$$

The probability of passing a bicycle at the start of the first 0.01-mi piece of path is

$$F(x - dx) = P\left[v_{bicycle} < U\left(1 - \frac{x - dx}{L}\right)\right] = P\left[v_{bicycle} < 12.8\left(1 - \frac{0.01 - 0.01}{3}\right)\right]$$

$$F(x - dx) = P[v_{bicycle} < 12.8] = 0.5000$$

Next, the average probability of passing in the first piece is

$$P(v_{bicycle}) = 0.5[F(x - dx) + F(x)]$$

$$P(v_{bicycle}) = 0.5[0.5000 + 0.4950] = 0.4975$$

The expected number of times the average bicyclist passes users of mode i over the entire path segment is determined by multiplying $P(v_i)$ by the density of users of mode i and summing over all pieces of the segment. The number of active passings per minute is then obtained by dividing the result by the number of minutes required for the bicyclist to traverse the path segment, as given by Equation 24-11:

$$A_i = \sum_{j=1}^n P(v_i) \times \frac{q_i}{\mu_i} \times \frac{1}{t} dx_j$$

For the first mode, adult bicyclists, for the first piece, the expected active passings per minute is

$$A_{bicycle,1} = 0.4975 \times \frac{104}{12.8} \times \frac{1}{14} (0.01) = 0.0029$$

Repeating this procedure for all pieces from $n = 1$ to $n = 300$ and summing the results yields

$$\text{Active bicycle passings per minute} = 0.0029 + A_{bicycle,2} + \dots + A_{bicycle,n} = 0.18$$

When the same methodology is applied for each mode, the following active passings per minute are found for the other modes:

- Pedestrians, 1.74;
- Runners, 0.31;
- Inline skaters, 0.09; and
- Child bicyclists, 0.10.

Total active passings are then determined by using Equation 24-12:

$$A_T = \sum_i A_i$$

$$\text{Total passings per minute} = 0.18 + 1.74 + 0.31 + 0.09 + 0.10 = 2.42$$

Step 3: Calculate Meetings per Minute

Meetings per minute of users already on the path segment M_1 are calculated for each mode i with Equation 24-13:

$$M_1 = \frac{U}{60} \sum_i \frac{q_i}{\mu_i}$$

$$M_1 = (12.8/60) \times [(104/12.8) + (38/3.4) + (19/6.6) + (19/10.1) + (9/7.9)]$$

$$M_1 = 5.36$$

Meetings per minute of users in the opposing direction not yet on the path segment at the time the average bicyclist enters must be calculated separately for each mode. For the number of bicycles passed per minute, the section of path beyond the study segment is considered as broken into n pieces, each of which has length $dx = 0.01$ mi, and a total segment length equivalent to L (3 mi). For the first piece ending at $x = 0.01$ mi, Equation 24-14 gives

$$F(X) = P\left(v_{bike} > X \frac{U}{L}\right) = P\left(v_{bike} > 0.01 \times \frac{12.8}{3}\right)$$

$$F(X) = P(v_{bike} > 0.4267) = 0.99992$$

$$F(X - dx) = P\left(v_{bike} > (X - dx) \frac{U}{L}\right) = P\left(v_{bike} > 0 \times \frac{12.8}{3}\right)$$

$$F(X - dx) = P(v_{bike} > 0) = 1.00000$$

Applying Equation 24-10 and Equation 24-15 then gives the probability of passing in the first piece:

$$P(v_{bike}) = 0.5[F(X - dx) + F(x)]$$

$$P(v_{bike}) = 0.5[0.99992 + 1.00000] = 0.99996$$

$$M_{2,bike,j} = \sum_{j=1}^n P(v_{o,bike}) \times \frac{q_{bike}}{\mu_{bike}} \times \frac{1}{t} dx_j$$

$$M_{2,bike,1} = 0.99996 \times (104/12.8) \times (1/14) \times 0.01 = 0.0058$$

Repeating this procedure for all pieces from $n = 1$ to $n = 300$ and summing the results yields

$$M_{2,bike} = \text{meetings of bicycles per minute} = 0.0058 + M_{2,bike,2} + \dots + M_{2,bike,n}$$

$$M_{2,bike} = 1.55$$

When the foregoing procedure is repeated for the other modes, the following meetings per minute are found for each mode:

- Pedestrians, 0.63;
- Runners, 0.32;
- Inline skaters, 0.31; and
- Child bicyclists, 0.16.

Total meetings are then determined by using Equation 24-16:

$$M_T = \left(M_1 + \sum_i M_{2,i} \right)$$

$$\text{Total meetings per minute} = 5.36 + 1.55 + 0.63 + 0.32 + 0.31 + 0.16 = 8.33$$

Step 4: Determine the Number of Effective Lanes

From Exhibit 24-14, a 10-ft-wide path has two effective lanes.

Step 5: Calculate the Probability of Delayed Passing

From Step 4, it is clear that a path with a width of 10 ft will operate as two lanes. Therefore, delayed passings per minute must be calculated separately for each of the 25 modal pairs by using Equation 24-17 and Equation 24-20. For instance, considering the probability of a delayed passing of a bicyclist as a result of an opposing bicyclist overtaking a pedestrian gives the following:

$$P_{n,i} = 1 - e^{-p_i k_i}$$

$$P_{n,bike} = 1 - e^{-\left(\frac{100}{5,280}\right) \times \left(\frac{104}{12.8}\right)} = 1 - 0.8574 = 0.1426$$

$$P_{n,ped} = 1 - e^{-\left(\frac{100}{5,280}\right) \times \left(\frac{38}{3.4}\right)} = 1 - 0.8092 = 0.1908$$

Substituting into Equation 24-20 yields $P_{bike-ped,ds}$:

$$P_{bike-ped,ds} = \frac{P_{n,ped}P_{n,bike} + P_{n,ped}(1 - P_{n,bike})^2}{1 - P_{n,ped}P_{n,bike}(1 - P_{n,ped})(1 - P_{n,bike})}$$

$$P_{bike-ped,ds} = \frac{0.1908 \times 0.1426 + 0.1908(1 - 0.1426)^2}{1 - (0.1908 \times 0.1426)(1 - 0.1908)(1 - 0.1426)} = 0.1707$$

Step 6: Determine Delayed Passings per Minute

Step 5 is performed for each of the 25 modal pairs. Equation 24-33 is used to determine the total probability of delayed passing:

$$P_{Tds} = 1 - \prod_m (1 - P_{m,ds})$$

$$P_{Tds} = 1 - (1 - 0.1707) \times (1 - P_{bike-runner,ds}) \times \dots \times (1 - P_{m,ds}) = 0.8334$$

Thus, the probability of delayed passing is 83.34%.

Equation 24-34 is used to determine the total number of delayed passings per minute:

$$DP_m = A_T \times P_{Tds} \times PHF$$

$$DP_m = 2.42 \times 0.8334 \times 0.90 = 1.82$$

Step 7: Calculate LOS

Equation 24-35 is used to determine the bicycle LOS (BLOS) score for the path:

$$BLOS = 5.446 - 0.00809E - 15.86RW - 0.287CL - DP$$

$$BLOS = 5.446 - 0.00809[8.33 + (10 \times 2.42)] - 15.86\left(\frac{1}{10}\right) - 0.287(0) \\ - (\min [DP_m \times 0.5, 1.5]) = 2.69$$

Because the bicyclist perception index is between 2.5 and 3.0, the path operates at LOS D according to Exhibit 24-5.

Results

The results indicate that the path would operate close to its functional capacity. A slightly wider path would provide three effective lanes and a better LOS.



HIGHWAY CAPACITY MANUAL

6TH EDITION | A GUIDE FOR MULTIMODAL MOBILITY ANALYSIS

VOLUME 4: APPLICATIONS GUIDE

The National Academies of
SCIENCES • ENGINEERING • MEDICINE

TRANSPORTATION RESEARCH BOARD
WASHINGTON, D.C. | WWW.TRB.ORG

TRANSPORTATION RESEARCH BOARD 2016 EXECUTIVE COMMITTEE *

Chair: James M. Crites, Executive Vice President of Operations,
Dallas–Fort Worth International Airport, Texas

Vice Chair: Paul Trombino III, Director, Iowa Department of
Transportation, Ames

Executive Director: Neil J. Pedersen, Transportation Research Board

Victoria A. Arroyo, Executive Director, Georgetown Climate Center;
Assistant Dean, Centers and Institutes; and Professor and Director,
Environmental Law Program, Georgetown University Law Center,
Washington, D.C.

Scott E. Bennett, Director, Arkansas State Highway and Transportation
Department, Little Rock

Jennifer Cohan, Secretary, Delaware Department of Transportation, Dover

Malcolm Dougherty, Director, California Department of
Transportation, Sacramento

A. Stewart Fotheringham, Professor, School of Geographical Sciences
and Urban Planning, Arizona State University, Tempe

John S. Halikowski, Director, Arizona Department of Transportation,
Phoenix

Susan Hanson, Distinguished University Professor Emerita, Graduate
School of Geography, Clark University, Worcester, Massachusetts

Steve Heminger, Executive Director, Metropolitan Transportation
Commission, Oakland, California

Chris T. Hendrickson, Hamerschlag Professor of Engineering, Carnegie
Mellon University, Pittsburgh, Pennsylvania

Jeffrey D. Holt, Managing Director, Power, Energy, and Infrastructure
Group, BMO Capital Markets Corporation, New York

S. Jack Hu, Vice President for Research and J. Reid and Polly Anderson
Professor of Manufacturing, University of Michigan, Ann Arbor

Roger B. Huff, President, HGLC, LLC, Farmington Hills, Michigan

Geraldine Knatz, Professor, Sol Price School of Public Policy, Viterbi
School of Engineering, University of Southern California, Los Angeles

Ysela Llorca, Consultant, Miami, Florida

Melinda McGrath, Executive Director, Mississippi Department of
Transportation, Jackson

James P. Redeker, Commissioner, Connecticut Department of
Transportation, Newington

Mark L. Rosenberg, Executive Director, The Task Force for Global
Health, Inc., Decatur, Georgia

Kumares C. Sinha, Olson Distinguished Professor of Civil Engineering,
Purdue University, West Lafayette, Indiana

Daniel Sperling, Professor of Civil Engineering and Environmental
Science and Policy; Director, Institute of Transportation Studies,
University of California, Davis

Kirk T. Steudle, Director, Michigan Department of Transportation,
Lansing (Past Chair, 2014)

Gary C. Thomas, President and Executive Director, Dallas Area Rapid
Transit, Dallas, Texas

Pat Thomas, Senior Vice President of State Government Affairs, United
Parcel Service, Washington, D.C.

Katherine F. Turnbull, Executive Associate Director and Research
Scientist, Texas A&M Transportation Institute, College Station

Dean Wise, Vice President of Network Strategy, Burlington Northern
Santa Fe Railway, Fort Worth, Texas

Thomas P. Bostick (Lieutenant General, U.S. Army), Chief of Engineers
and Commanding General, U.S. Army Corps of Engineers, Washington,
D.C. (ex officio)

James C. Card (Vice Admiral, U.S. Coast Guard, retired), Maritime
Consultant, The Woodlands, Texas, and Chair, TRB Marine Board
(ex officio)

T. F. Scott Darling III, Acting Administrator and Chief Counsel, Federal
Motor Carrier Safety Administration, U.S. Department of Transportation
(ex officio)

Marie Therese Dominguez, Administrator, Pipeline and Hazardous
Materials Safety Administration, U.S. Department of Transportation
(ex officio)

Sarah Feinberg, Administrator, Federal Railroad Administration,
U.S. Department of Transportation (ex officio)

Carolyn Flowers, Acting Administrator, Federal Transit Administration,
U.S. Department of Transportation (ex officio)

LeRoy Gishi, Chief, Division of Transportation, Bureau of Indian
Affairs, U.S. Department of the Interior, Washington, D.C. (ex officio)

John T. Gray II, Senior Vice President, Policy and Economics,
Association of American Railroads, Washington, D.C. (ex officio)

Michael P. Huerta, Administrator, Federal Aviation Administration,
U.S. Department of Transportation (ex officio)

Paul N. Jaenichen, Sr., Administrator, Maritime Administration,
U.S. Department of Transportation (ex officio)

Bevan B. Kirley, Research Associate, University of North Carolina
Highway Safety Research Center, Chapel Hill, and Chair, TRB Young
Members Council (ex officio)

Gregory G. Nadeau, Administrator, Federal Highway Administration,
U.S. Department of Transportation (ex officio)

Wayne Nastri, Acting Executive Officer, South Coast Air Quality
Management District, Diamond Bar, California (ex officio)

Mark R. Rosekind, Administrator, National Highway Traffic Safety
Administration, U.S. Department of Transportation (ex officio)

Craig A. Rutland, U.S. Air Force Pavement Engineer, U.S. Air Force
Civil Engineer Center, Tyndall Air Force Base, Florida (ex officio)

Reuben Sarkar, Deputy Assistant Secretary for Transportation,
U.S. Department of Energy (ex officio)

Richard A. White, Acting President and CEO, American Public
Transportation Association, Washington, D.C. (ex officio)

Gregory D. Winfree, Assistant Secretary for Research and Technology,
Office of the Secretary, U.S. Department of Transportation (ex officio)

Frederick G. (Bud) Wright, Executive Director, American Association
of State Highway and Transportation Officials, Washington, D.C.
(ex officio)

Paul F. Zukunft (Admiral, U.S. Coast Guard), Commandant, U.S. Coast
Guard, U.S. Department of Homeland Security (ex officio)

Transportation Research Board publications are available by ordering
individual publications directly from the TRB Business Office, through
the Internet at www.TRB.org, or by annual subscription through
organizational or individual affiliation with TRB. Affiliates and library
subscribers are eligible for substantial discounts. For further information,
contact the Transportation Research Board Business Office, 500 Fifth
Street, NW, Washington, DC 20001 (telephone 202-334-3213;
fax 202-334-2519; or e-mail TRBsales@nas.edu).

Copyright 2016 by the National Academy of Sciences.

All rights reserved.

Printed in the United States of America.

ISBN 978-0-309-36997-8 [Slipcased set of three volumes]

ISBN 978-0-309-36998-5 [Volume 1]

ISBN 978-0-309-36999-2 [Volume 2]

ISBN 978-0-309-37000-4 [Volume 3]

ISBN 978-0-309-37001-1 [Volume 4, online only]

* Membership as of June 2016.

The National Academies of
SCIENCES • ENGINEERING • MEDICINE

The **National Academy of Sciences** was established in 1863 by an Act of Congress, signed by President Lincoln, as a private, nongovernmental institution to advise the nation on issues related to science and technology. Members are elected by their peers for outstanding contributions to research. Dr. Ralph J. Cicerone is president.

The **National Academy of Engineering** was established in 1964 under the charter of the National Academy of Sciences to bring the practices of engineering to advising the nation. Members are elected by their peers for extraordinary contributions to engineering. Dr. C. D. Mote, Jr., is president.

The **National Academy of Medicine** (formerly the Institute of Medicine) was established in 1970 under the charter of the National Academy of Sciences to advise the nation on medical and health issues. Members are elected by their peers for distinguished contributions to medicine and health. Dr. Victor J. Dzau is president.

The three Academies work together as the National Academies of Sciences, Engineering, and Medicine to provide independent, objective analysis and advice to the nation and conduct other activities to solve complex problems and inform public policy decisions. The Academies also encourage education and research, recognize outstanding contributions to knowledge, and increase public understanding in matters of science, engineering, and medicine.

Learn more about the National Academies of Sciences, Engineering, and Medicine at **www.national-academies.org**.

The **Transportation Research Board** is one of seven major programs of the National Academies of Sciences, Engineering, and Medicine. The mission of the Transportation Research Board is to increase the benefits that transportation contributes to society by providing leadership in transportation innovation and progress through research and information exchange, conducted within a setting that is objective, interdisciplinary, and multimodal. The Board's varied committees, task forces, and panels annually engage about 7,000 engineers, scientists, and other transportation researchers and practitioners from the public and private sectors and academia, all of whom contribute their expertise in the public interest. The program is supported by state transportation departments, federal agencies including the component administrations of the U.S. Department of Transportation, and other organizations and individuals interested in the development of transportation.

Learn more about the Transportation Research Board at **www.TRB.org**.

CHAPTER 36
CONCEPTS: SUPPLEMENTAL

CONTENTS

1. INTRODUCTION..... 36-1

2. PRESENTATION OF RESULTS..... 36-2

 Guidance on the Display of HCM Results 36-2

 Presenting Results to Facilitate Interpretation..... 36-3

 Graphic Representation of Results 36-4

3. MEASURING TRAVEL TIME RELIABILITY IN THE FIELD..... 36-7

 Measurement of Travel Time Reliability 36-7

 Data Sources for Travel Time Reliability..... 36-7

 Recommended Method for Computing Reliability by Using
 Roadway-Based Spot Measurement Detectors..... 36-11

 Recommended Method for Computing Reliability by Using Probe
 Vehicles..... 36-13

4. RELIABILITY VALUES FOR SELECTED U.S. FACILITIES..... 36-15

 Data Sources 36-15

 Reliability Statistics for a Cross Section of U.S. Facilities..... 36-15

 Reliability Statistics for Florida Freeways 36-20

5. VEHICLE TRAJECTORY ANALYSIS..... 36-22

 Introduction 36-22

 Trajectory Analysis Examples 36-24

 Estimating Performance Measures from Vehicle Trajectory Data..... 36-37

6. SUMMARY OF CHANGES FROM HCM2000 TO HCM 2010..... 36-52

 Introduction 36-52

 Overview 36-52

 Methodological Changes by System Element..... 36-54

7. REFERENCES..... 36-58

LIST OF EXHIBITS

Exhibit 36-1 Example of a Graphic Display of LOS	36-4
Exhibit 36-2 Example of a Thematic Graphic Display of LOS.....	36-5
Exhibit 36-3 Example Presentation of Planning Analysis Results	36-5
Exhibit 36-4 Three-Dimensional Reliability Box.....	36-7
Exhibit 36-5 Spot Speed (Vertical) Sampling of Loop Detectors	36-9
Exhibit 36-6 Time–Space (Diagonal) Sampling of Probe Vehicle Detectors.....	36-10
Exhibit 36-7 Comparison of Loop Detector and Probe Cumulative Travel Time Distributions	36-10
Exhibit 36-8 Rankings of U.S. Facilities by Mean TTI and PTI (A.M. Peak, Midday, and P.M. Peak Combined).....	36-16
Exhibit 36-9 Rankings of U.S. Facilities by Mean TTI and PTI (A.M. Peak).....	36-16
Exhibit 36-10 Rankings of U.S. Facilities by Mean TTI and PTI (Midday)	36-17
Exhibit 36-11 Rankings of U.S. Facilities by Mean TTI and PTI (P.M. Peak)	36-17
Exhibit 36-12 Freeway Reliability Values: Weekday A.M. Peak Period	36-18
Exhibit 36-13 Freeway Reliability Values: Weekday Midday Periods.....	36-18
Exhibit 36-14 Freeway Reliability Values: Weekday P.M. Peak Period	36-19
Exhibit 36-15 Urban Street Reliability Values: Weekday A.M. Peak Period	36-19
Exhibit 36-16 Urban Street Reliability Values: Weekday Midday Periods.....	36-20
Exhibit 36-17 Urban Street Reliability Values: Weekday P.M. Peak Period	36-20
Exhibit 36-18 Florida Freeway Reliability Statistics.....	36-21
Exhibit 36-19 Vehicle Data Stored for Each Time Step	36-23
Exhibit 36-20 Basic Signalized Intersection Example.....	36-25
Exhibit 36-21 Trajectory Plots for Uniform Arrivals and Departures	36-25
Exhibit 36-22 Introducing Randomness into the Simulation.....	36-26
Exhibit 36-23 Cycle Failure Example.....	36-27
Exhibit 36-24 Oversaturated Signal Approach	36-28
Exhibit 36-25 Queue Backup from a Downstream Signal	36-29
Exhibit 36-26 Trajectory Plot for More Complex Signal Phasing.....	36-30
Exhibit 36-27 Weaving Segment Description and Animated Graphics View	36-31
Exhibit 36-28 Trajectory Plot for Freeway Links	36-32
Exhibit 36-29 Trajectory Plot for Entrance and Exit Ramp Links	36-33
Exhibit 36-30 Entrance Ramp Merging Segment Graphics View	36-34
Exhibit 36-31 Trajectory Plot for All Freeway Lanes in the Merge Area	36-34

Exhibit 36-32 Trajectory Plot for Freeway Lane 1 (Rightmost) in the Merge Area.....	36-35
Exhibit 36-33 Trajectory Plot for Freeway Lane 2 (Center) in the Merge Area	36-35
Exhibit 36-34 Trajectory Plot for Freeway Lane 3 (Leftmost) in the Merge Area.....	36-35
Exhibit 36-35 Trajectory Plot for Acceleration and Deceleration Lanes	36-36
Exhibit 36-36 Addition of Intermediate Nodes for Continuous Trajectory Plots.....	36-37
Exhibit 36-37 Trajectory Plot for Acceleration Lane and Freeway Lane 1	36-37
Exhibit 36-38 Trajectories for Several Cycles on a Signalized Approach	36-45
Exhibit 36-39 Example Trajectory Analysis Plots	36-45
Exhibit 36-40 Analysis of a Full and a Partial Stop	36-46
Exhibit 36-41 BOQ Analysis by Time Step	36-47
Exhibit 36-42 BOQ Histogram	36-48
Exhibit 36-43 Accumulated Delay by Various Definitions	36-49
Exhibit 36-44 Delay Analysis for All Vehicles on a Segment.....	36-50
Exhibit 36-45 Longitudinal Analysis of Delay for a Selected Vehicle in a Weaving Area	36-50
Exhibit 36-46 Example Spatial Analysis by Lane.....	36-51
Exhibit 36-47 Major Research Projects Contributing to the Preupdate HCM 2010.....	36-53

1. INTRODUCTION

Chapter 36 is the supplemental chapter for Volume 1, Concepts, of the *Highway Capacity Manual* (HCM).

Section 2 supplements material in Chapter 7, Interpreting HCM and Alternative Tool Results. It provides information on the recommended number of significant digits to use in presenting results and guidance on presenting analysis results to decision makers, the public, and practitioners.

Sections 3 and 4 supplement material in Chapter 4, Traffic Operations and Capacity Concepts. Section 3 provides guidance on measuring travel time reliability in the field, and Section 4 presents travel time reliability values for selected freeway and arterial facilities as an aid to analysts in interpreting travel time reliability performance measures.

Section 5 supplements Chapters 4 and 7. It provides expanded guidance on the use of vehicle trajectory analysis as a means by which performance measures can be consistently estimated by various alternative analysis tools.

Section 6 supplements Chapter 1, HCM User's Guide. Section 5 of Chapter 1 presented the changes to the HCM made in the Sixth Edition, along with the research basis for those changes. Section 6 of this chapter identifies the new material in the HCM 2010 that was not changed in the Sixth Edition, along with the research basis for that material.

VOLUME 4: APPLICATIONS GUIDE

- 25. Freeway Facilities:
Supplemental
- 26. Freeway and Highway
Segments: Supplemental
- 27. Freeway Weaving:
Supplemental
- 28. Freeway Merges and
Diverges: Supplemental
- 29. Urban Street Facilities:
Supplemental
- 30. Urban Street Segments:
Supplemental
- 31. Signalized Intersections:
Supplemental
- 32. STOP-Controlled
Intersections:
Supplemental
- 33. Roundabouts:
Supplemental
- 34. Interchange Ramp
Terminals: Supplemental
- 35. Pedestrians and Bicycles:
Supplemental
- 36. Concepts:
Supplemental**
- 37. ATDM: Supplemental

2. PRESENTATION OF RESULTS

GUIDANCE ON THE DISPLAY OF HCM RESULTS

Tabular values and calculated results are displayed in a consistent manner throughout the HCM. Analyst adherence to these conventions is suggested. A key objective is to use the number of significant digits that is reasonable, to indicate to users, decision makers, and other viewers that the results are not extremely precise but take on the precision and accuracy associated with the input variables used. This guidance applies primarily to inputs and final outputs; intermediate results in a series of calculations should not be rounded unless specifically indicated by a particular methodology.

Input Values

Following is a list of representative (not exhaustive) input variables and the suggested number of digits for each.

- Volume (whole number);
- Grade (whole number);
- Lane width (one decimal place);
- Percentage of heavy vehicles (whole number);
- Peak hour factor (two decimal places);
- Pedestrian volume (whole number);
- Bicycle volume (whole number);
- Parking maneuvers (whole number);
- Bus stopping (whole number);
- Green, yellow, all-red, and cycle times (one decimal place);
- Lost time/phase (whole number); and
- Minimum pedestrian time (one decimal place).

Adjustment Factors

Factors interpolated from tabular material can use one more decimal place than is presented in the table. Factors generated from equations can be taken to three decimal places.

Service Volume Tables

When volumes for service volume tables are rounded, the precision used should be no greater than the nearest 10 vehicles or passenger cars for hourly tables and no greater than the nearest 100 vehicles or passenger cars for daily tables.

Free-Flow Speed

For a base free-flow speed (FFS), show the value to the nearest 1 mi/h. If the FFS has been adjusted for various conditions and is considered an intermediate calculation, show speed to the nearest 0.1 mi/h.

Speeds

For threshold values that define level of service (LOS), show speed to the nearest 1 mi/h. For intermediate calculations of speed, use one decimal place.

Volume-to-Capacity and Demand-to-Capacity Ratios

Show volume-to-capacity and demand-to-capacity ratios with two decimal places.

Delay

In computing delay, show results with one decimal place. In presenting delay as a threshold value in LOS tables, show a whole number.

Density

Show density results with one decimal place.

Pedestrian Space

Show pedestrian space values with one decimal place.

Occurrences and Events

For all event-based items, use values to a whole number. These items include parking maneuvers, buses stopping, and passing and meeting events along a pedestrian or bicycle path.

General Factors

In performing all calculations on a computer, the full precision available should be used. Intermediate calculation outputs should be displayed to three significant digits throughout. For the measure that defines LOS, the number of significant digits presented should exceed by one the number of significant digits shown in the LOS table.

PRESENTING RESULTS TO FACILITATE INTERPRETATION

Several performance measures can result from HCM analyses. Determination of the appropriate measures will depend on the transportation need being studied. However, decision-making situations generally can be divided into those involving the public (e.g., city councils and community groups) and those involving technicians (e.g., state and local engineering and planning staff).

The HCM is highly technical and complex. The results of the analyses can be difficult for people to interpret for decision making unless the data are carefully organized and presented. In general, the results should be presented as simply as possible. The presentation might use a small set of performance measures and provide the data in an aggregate form without losing the ability to relate to the underlying variations and factors that generated the results.

The LOS concept was created, in part, to make presentation of results easier than if numerical values of service measures were reported directly. In many cases, analysts and decision makers prefer to see one service measure rather than multiple performance measures. At the same time, relying solely on LOS results

Performance measures selected should be related to the problem being addressed.

in making recommendations or decisions can lead to important information available from other performance measures being overlooked. Despite the limitations to its usefulness, the LOS concept remains a part of the HCM because of its acceptance by the public and decision makers.

Decision makers who represent the public usually prefer measures that their constituents can understand. The public can relate to LOS results, which describe relative differences in highway operations. Unit delay (e.g., seconds per vehicle) and travel speed are also readily understood. However, volume-to-capacity ratio, density, percent time-spent-following, and vehicle hours of travel are not measures to which the public easily relates. In the selection of measures to present, recognition by the analyst of the orientation of the decision maker and the context in which the decision will be made is important. In general, these measures can be differentiated as system user or system manager oriented.

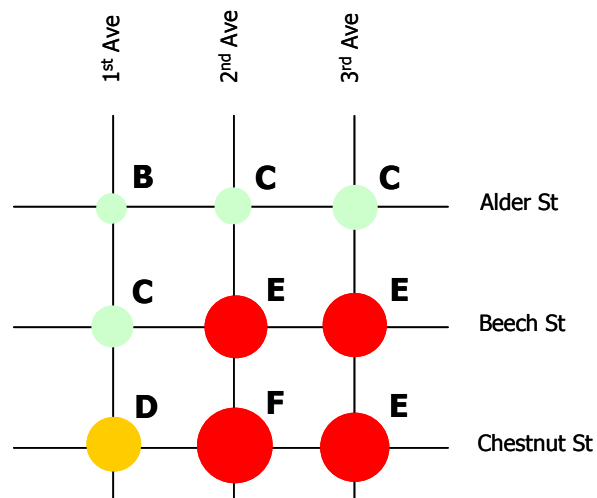
GRAPHIC REPRESENTATION OF RESULTS

Historically, data and analysis results have been presented primarily in tables. However, results may be best presented as pictures and supplemented only as necessary with the underlying numbers in some situations. Graphs and charts should be conceived and fashioned to aid in interpretation of the meaning behind the numbers (1).

Most performance measures in the HCM are quantitative, continuous variables. However, LOS values result from step functions and do not lend themselves to graphing. When they are placed on a scale, LOS results must be given an equivalent numeric value, as shown in Exhibit 36-1, which presents the LOS for a group of intersections. The LOS letter is indicated, and shaded (or colored) areas indicate intersections that are below, at, or above the analysis objective of LOS D. The size of the indicator at each intersection shows the relative control delay value for the indicated LOS.

Present results to make them very plain (obvious) to the audience.

Exhibit 36-1
Example of a Graphic Display of LOS



The issue is whether the change in value between successive LOS values (i.e., the interval) should be equal. For example, is conversion of LOS A to F to a scale of 0 through 5 appropriate? Should the numerical equivalent assigned to the

difference of the thresholds between LOS A and B be the same as the difference between LOS E and F? These questions have not been addressed in research, except in the area of traveler perception models. Furthermore, LOS F is not given an upper bound. Therefore, a graph of LOS should be considered ordinal, not interval, because the numeric differences between the levels would not appear significant.

However, it is difficult to refrain from comparing the differences. A scale representing the relative values of the LOS letters would have to incorporate the judgment of the analyst and the opinions of the public or decision makers—a difficult task. A thematic graphic presentation avoids this issue. In Exhibit 36-2, for example, shading is used to highlight time periods and basic freeway segments that do not meet the objective LOS (in this case, D).

Start Time	Segment 1	Segment 2	Segment 3	Segment 4
5:00 p.m.	A	B	B	A
5:15 p.m.	B	B	D	A
5:30 p.m.	B	B	F	A
5:45 p.m.	B	D	F	A
6:00 p.m.	B	F	F	A
6:15 p.m.	D	F	E	A
6:30 p.m.	D	E	C	A
6:45 p.m.	B	B	B	A

Exhibit 36-2
Example of a Thematic Graphic Display of LOS

Further simplification of the presentation can be achieved by converting LOS letters into general descriptors of conditions. For example, Exhibit 36-3 shows a map of a portion of a downtown area, where street segments have been labeled by the analyst as “not congested” (e.g., LOS A, B, or C), “becoming congested” (e.g., LOS D or E), or “congested” (e.g., LOS F). (Note that these represent the analyst’s choice of how to interpret and present the results; the HCM does not define specific levels of congestion.) This type of presentation is particularly useful for planning applications where many inputs into the HCM method have been defaulted and therefore the results may be less precise.

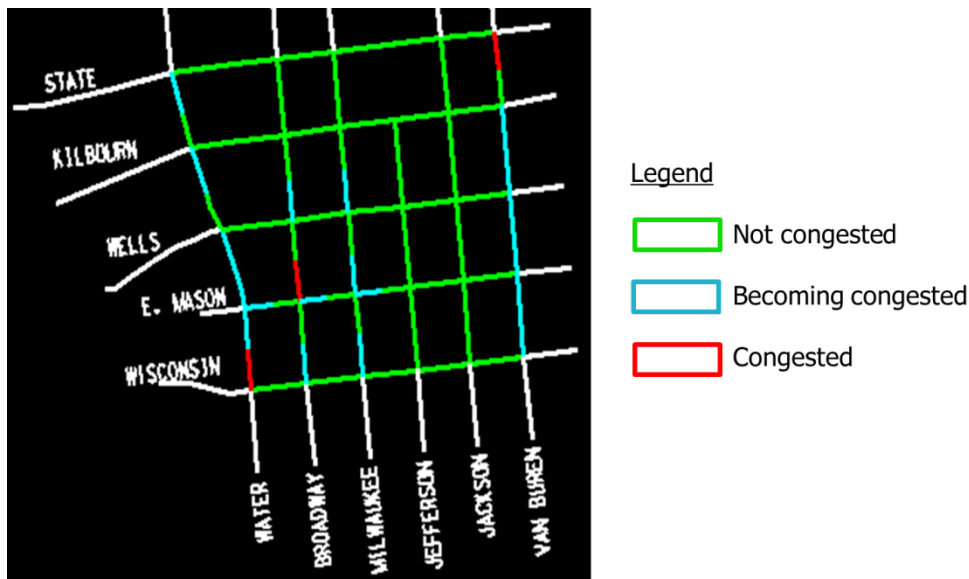


Exhibit 36-3
Example Presentation of Planning Analysis Results

Source: City of Milwaukee.

The HCM provides valuable assistance in making transportation management decisions in a wide range of situations. It offers the user a selection of performance measures to meet a variety of needs. The analyst should recognize that using the HCM involves mixing art with science. Sound judgment is needed not only for interpreting the values produced but also for summarizing and presenting the results.

3. MEASURING TRAVEL TIME RELIABILITY IN THE FIELD

This section provides a recommended method for measuring travel time reliability in the field. The intent is to provide a standardized method for gathering and reporting travel time reliability for freeways and arterials directly from field sensors, which can be used for validating estimates of reliability produced by the HCM method and for consistently comparing reliability across facilities.

MEASUREMENT OF TRAVEL TIME RELIABILITY

Measuring travel time reliability in the field involves the development of the three-dimensional reliability box. The three dimensions of reliability are the study section of the facility, the daily study period, and the reliability reporting period (Exhibit 36-4). For example, travel time reliability can be computed for a 1-mi length of freeway during the afternoon peak hour for all nonholiday weekdays in a year.

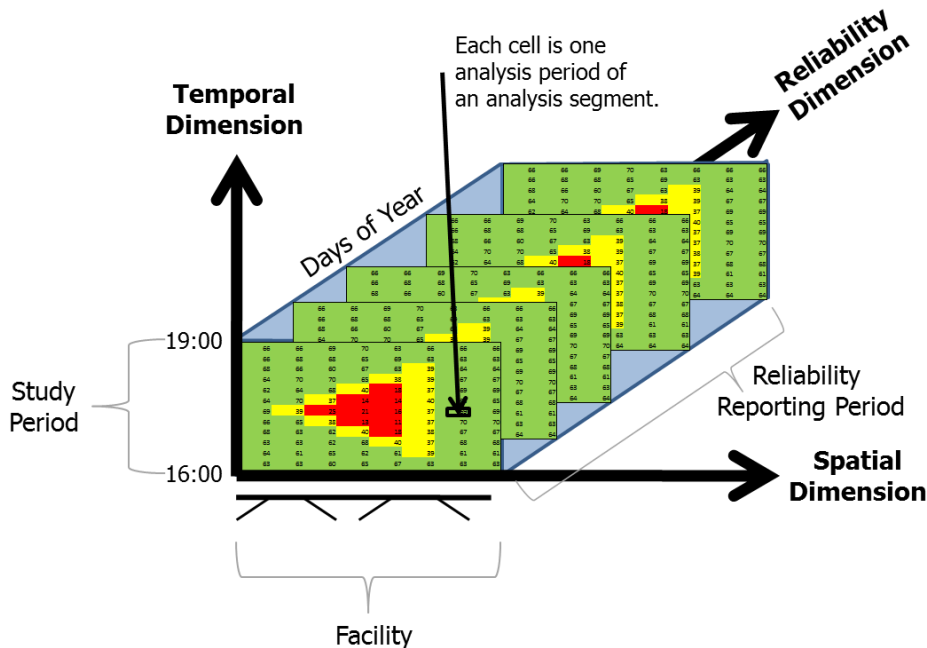


Exhibit 36-4
Three-Dimensional Reliability Box

Source: Zegeer et al. (2).

DATA SOURCES FOR TRAVEL TIME RELIABILITY

Travel time reliability (and travel times generally) may be measured by recording a sample of the vehicle travel times over a fixed length of facility (probe vehicle method) or by recording the spot speeds of all vehicles as they pass over a set of stationary detectors. The latter method will be called for convenience the “spot measurement detector method”; many technologies are available (loops, radar, video, etc.) for measuring spot speeds.

Measuring reliability is all about measuring variability, so the larger the sample (in terms of number of vehicles and hours of the year), the more confidence one can have in the result.

Travel time, like demand, exhibits strong daily and weekly cyclic patterns. There may also be strong seasonal patterns to both demand and travel time. To obtain a useful estimate of the travel time distribution for any given hour of the day or day of the week, a sufficient sample of that hour and that day (and that season, if seasonality is significant) must be obtained to estimate the mean and the standard deviation of the travel time for that hour (and day of the week) within an acceptable range of accuracy. A reference provides details and examples of computing the required sample size to estimate the mean of the travel time distribution for the hour (3).

Estimating the standard deviation of the travel time distribution generally requires a much larger sample than estimating the mean to the same precision. To estimate the standard deviation of a normal distribution to within 10% of its true value at the 95% confidence level will require on the order of 200 samples of travel time for the hour (close to a year's worth of nonholiday, weekday data). Only 50 samples are needed to estimate the standard deviation to within 20% of its true value at a 95% confidence level (4).

Note that travel time is not normally distributed, so the minimum sample sizes described here should be considered as providing lower confidence levels than the 95% confidence level cited from the literature for the normal distribution.

Roadway-Based Spot Measurement Detectors

Spot measurement detectors can be as close as $\frac{1}{3}$ to $\frac{1}{2}$ mi apart, but they can be much farther apart. However, as detector spacing increases, the assumption that speeds are constant over the entire distance becomes more problematic. While an upper limit on spacing has not been established by research, detector spacing of $\frac{1}{2}$ mi or less is greatly preferred.

Single detectors will measure the time a vehicle spends within the detector's detection zone and will divide this time by the estimated average vehicle length (supplied by the operator) to arrive at the estimated speed of the vehicle.

Pairs of detectors will measure the lag between the time the leading edge of the vehicle arrives at the first detector and the time the leading edge arrives at the second detector. The distance between the two detectors is divided by the time difference between the arrival of the leading edge of the vehicle at the upstream detector and its arrival at the downstream detector to obtain the vehicle speed for the short distance between the two detectors.

Probe Vehicles

Electronic toll tag or Bluetooth readers can be deployed at certain segments of freeway so that time stamps of vehicles crossing at these locations can be tracked. When a vehicle with a toll tag or a discoverable Bluetooth device crosses locations with readers, identification of the same vehicle can be matched with

different time stamps and corresponding locations. Then the travel time between a pair of toll tag reader locations can be obtained.

In addition, “crowd-sourced” data may be available. To obtain such data, the movements of vehicles and people carrying various GPS-equipped telecommunication devices are monitored anonymously. The observed point speed data or the point-to-point travel times are filtered, converted into average travel times, and archived for later retrieval. The Federal Highway Administration’s (FHWA’s) National Performance Management Research Data Set is one example of a crowd-sourced database of travel times (5).

For point-to-point measurements of travel time, the analyst will need to develop and apply a filtering algorithm that removes vehicles from the sample that take an excessive amount of time to appear at the downstream detector because they have left the facility to stop for errands between the two detectors. The closer together the two readers, the tighter the filtering criterion can be.

Comparison of Sampling Methods

Spot detectors (e.g., loops) take a vertical sample of the facility time-space diagram, while probe vehicle (e.g., electronic toll collection) detectors take a diagonal sample of the facility time-space diagram (compare Exhibit 36-5 and Exhibit 36-6).

At the time of writing, the probe data available from vendors resemble detector data more closely than true probe data. The data may have started out as recorded positions of selected vehicles traveling on a facility, but the processed data that analysts receive are speeds on a link. Consequently, vendor-supplied data at present do not look at all like the Bluetooth or toll tag data collected by agencies.

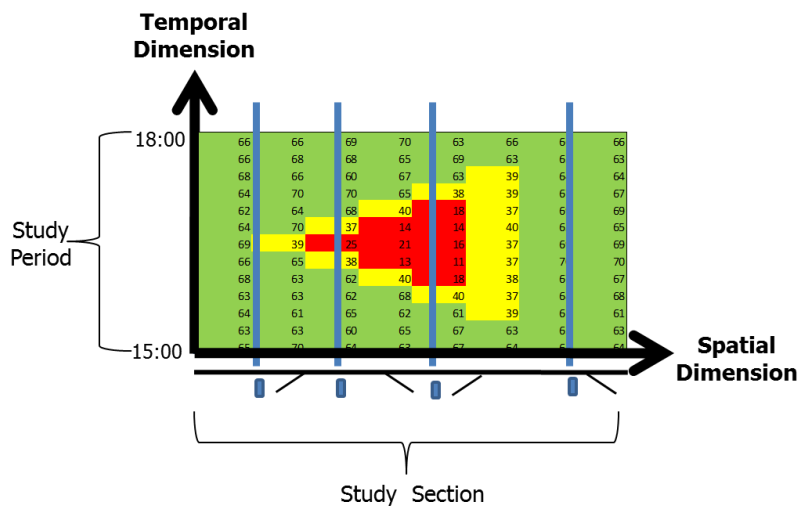
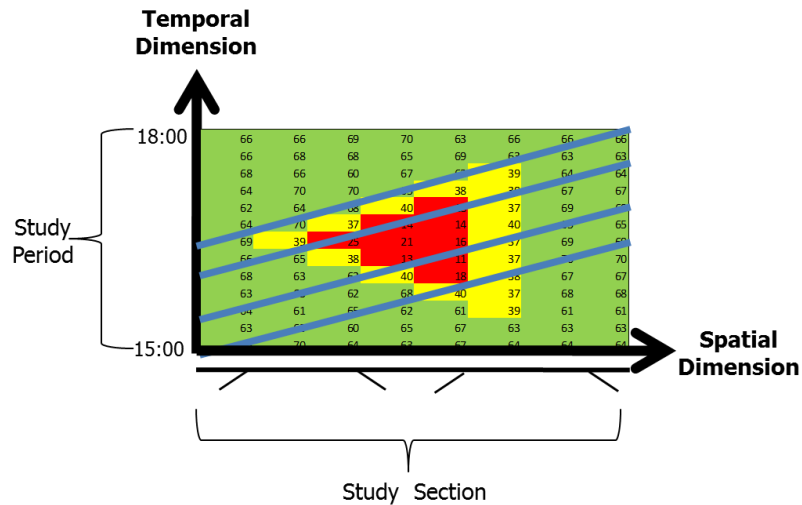


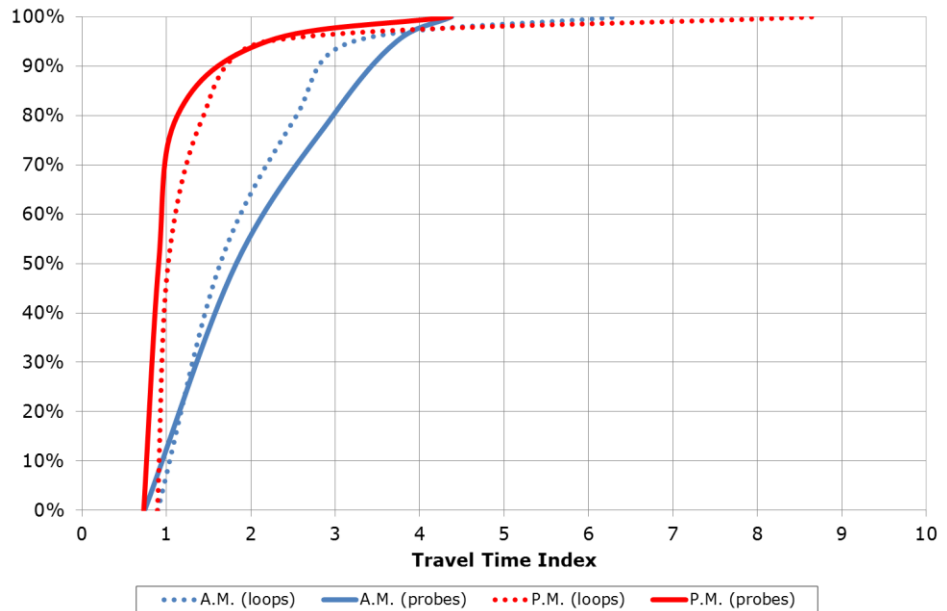
Exhibit 36-5
Spot Speed (Vertical)
Sampling of Loop Detectors

Exhibit 36-6
Time-Space (Diagonal)
Sampling of Probe Vehicle
Detectors



Since the two measurement methods sample the three-dimensional reliability space differently, they will produce slightly different estimates of the travel time reliability distribution, as illustrated for one freeway in Exhibit 36-7. However, the differences between the methods will generally be less than the differences in reliability between different peak periods.

Exhibit 36-7
Comparison of Loop Detector
and Probe Cumulative
Travel Time Distributions



Source: Kittelson & Associates, Inc.
Note: I-80 westbound, Contra Costa County, California.

Each method has its strengths and weaknesses, and neither method is always the best. A dense network of loop detectors may produce better estimates than a sparse network of toll tag readers. The reverse may also be true. Thus the choice of method is contingent on the density of the detection available for each method.

Similarly, crowd-sourced data may be superior or inferior to field detector-based measuring methods, depending on the sample size and the gaps in the crowd-sourced data and the density and reliability of the field detectors.

RECOMMENDED METHOD FOR COMPUTING RELIABILITY BY USING ROADWAY-BASED SPOT MEASUREMENT DETECTORS

The recommended method for computing travel time reliability statistics for freeways by using stationary sensors of spot speeds and volumes is described below. Because of the highly varying nature of speeds by distance from signal on urban streets, this method is *not* recommended for urban streets.

1. *Define reliability study bounds.* Select facility direction, length, study period, and reliability reporting period. The analyst should select the reliability reporting period appropriate for the purposes of the analysis. This may be all the nonholiday weekdays of a year (approximately 250 days out of the year) if the analyst is evaluating the reliability of a facility that has regular recurring weekday congestion. It may be the summer or winter weekends of a year if the analyst is evaluating a facility with regular recreational travel congestion.
2. *Download data.* Download lane-by-lane vehicle speeds and volumes aggregated or averaged to 5-min periods for all mainline speed detectors for the selected study direction, within the selected facility length and study period, and for all days included in the reliability reporting period.
3. *Quality check data.*
 - a. If the system fills gaps in detector data (e.g., detectors down) with estimates, remove data with less than 70% observed rating.
 - b. Remove unrealistic speeds from the data set. Analysts will need to review the data and use local knowledge to determine what is unreasonable. In addition, FHWA provides guidance on quality control for detector data (6).
 - c. Gaps in data are treated as nonobservations.
4. *Compute 5-min vehicle miles traveled (VMT).*
 - a. For each detector station, identify the length of facility represented by the detector. This is usually half the distance to the upstream detector station plus half the distance to the downstream detector, but it can be a different value based on local knowledge of the facility.
 - b. Sum volumes across all lanes at the detector station for 5-min time periods.
 - c. Neglect periods when the detector is not functioning.
 - d. $VMT(t, d) = V(t, d) \times L(d)$, where $VMT(t, d)$ = vehicle miles traveled during time period t measured at detector station d ; $L(d)$ = length represented by detector station d (mi), and $V(t, d)$ = sum of lane volumes (veh) measured at detector station d during time period t .
5. *Compute 5-min vehicle hours traveled (VHT).*
 - a. $VHT(t, d) = VMT(t, d) / S(t, d)$, where $VHT(t, d)$ = vehicle hours traveled during time period t measured at lane detector station d

and $S(t, d)$ = arithmetic average speed of vehicles (mi/h) measured during time period t at lane detector station d .

- b. Neglect periods when the detector is not functioning.
6. *Compute the FFS for the facility.* For a facility analysis, the use of data from continuously operating devices (roadway detectors or probe vehicles) is the preferred method, as described below. However, the analyst should be satisfied with the quality of the data from the suggested time periods before proceeding. For performance monitoring of multiple facilities or complete roadway systems, the analyst may wish to establish FFS in other ways, mainly to establish a consistent base from which to track trends. For example, if monitoring is performed on an annual basis, calculation of FFS every year on a facility may lead to different values for each year. One way to address this problem is to use the empirical method given below in the first year of the monitoring program to set the FFS for all years. Other methods include picking a constant FFS on the basis of agency policy for that facility type or speed limit. The “agency policy” FFS reflects in some way the agency’s performance objectives for the facility. Whatever method is used, the analyst should clearly specify it.
- a. Select a nonholiday weekend (or other period known to the analyst to be a light-flow period without congestion).
 - b. For each detector, obtain 5-min speeds for 7 to 9 a.m. on a typical *weekend* morning (or other uncongested, light-flow period).
 - c. Neglect periods when the detector is not functioning.
 - d. Quality control for excessively high speeds or excessively low volumes as discussed earlier.
 - e. Identify the average (mean) speed during the observed light-flow period. That is the FFS for the detector.
 - f. Convert speed to segment travel times.
 - g. Sum segment times to obtain facility free-flow travel times.

7. *Compute the VMT and VHT for each time period.*

$$VMT_t = \sum_d VMT_{t,d}$$

$$VHT_t = \sum_d VHT_{t,d}$$

8. *Compute the travel time index (TTI) for the facility for each time period.*

$$TTI_t = \frac{VHT_t}{VHTFF_t}$$

where $VHTFF_t$ is the VHT that would occur during time period t if all vehicles traveled at the FFS:

$$VHTFF_t = \frac{VMT_t}{FFS}$$

9. *Develop a distribution of the TTI_t values for the facility for the entire analysis period.* Each TTI_t value becomes an observation in the distribution. All performance measures are derived from this distribution. The statistics and percentiles are calculated by using VMT_t as a weight; this is done to account for the fact that the TTIs in each time period are based on a different number of vehicles.

RECOMMENDED METHOD FOR COMPUTING RELIABILITY BY USING PROBE VEHICLES

The recommended method for computing travel time reliability statistics for freeways and arterials by using probe vehicles and Bluetooth, toll tag, or license plate readers is described below. The instructions assume that the data are obtained from a commercial vendor of historical traffic message channel (TMC) segment speed data.

1. *Define reliability study bounds.* Select the facility direction, length, study period, and reliability reporting period. The analyst should select the reliability reporting period appropriate for the purposes of the analysis. This may be all the nonholiday weekdays of a year (approximately 250 days out of the year) if the analyst is evaluating the reliability of a facility that has regular recurring weekday congestion. It may be the summer or winter weekends of a year if the analyst is evaluating a facility with regular recreational travel congestion.
2. *Download data.* Download TMC segment speeds (or travel times if Bluetooth or toll tag reader data are being used) aggregated or averaged to 5-min (or similar) periods for all mainline segments for the selected study direction and selected facility length, for all study periods and days included in the reliability reporting period.
3. *Quality check data.*
 - a. If travel time data (e.g., Bluetooth or toll tag reader data) are being used, convert data to speeds for error-checking purposes.
 - b. Remove unrealistic speeds from the data set. Analysts will need to review the data and use local knowledge to determine what is unreasonable.
4. *Compute facility travel times for each analysis period.*
 - a. For each TMC (or Bluetooth or toll tag reader) segment, identify its length in miles (to the nearest 0.01 mi).
 - b. Divide the segment length by speed to obtain the segment travel time for each analysis period (skip this step if Bluetooth or toll tag travel time data are being used).
 - c. Sum the segment travel times to obtain the facility travel time for each time period.

TMC segments are industry-standard roadway sections used in communicating traffic information to drivers (for example, via a vehicle's navigation system).

Vendor-supplied urban street reference speeds may include traffic signal delays not included in the HCM definition of FFS.

5. Compute FFS for the facility. Steps 5a to 5g below are only applicable to freeway facilities, as urban street segment reference speeds or probe vehicle speeds under low-volume conditions may include traffic signal delays not included in the HCM definition of FFS. For urban street facilities, FFS can be established by use of an alternate method, including (a) picking a constant FFS on the basis of agency policy for a given facility type or speed limit; (b) establishing FFS on the basis of the actual speed limit (e.g., speed limit plus a constant); and (c) measuring speeds at locations not influenced by traffic control or junctions (e.g., midsegment on urban streets).
 - a. If the segment reference speed provided by the commercial vendor is reliable, that can be used for the FFS. If it is not reliable, perform the following steps.
 - b. Select a nonholiday weekend (or other period known to the analyst to be a light-flow period without congestion).
 - c. For each segment, obtain speeds for 5-min time periods for 7 to 9 a.m. on a typical *weekend* morning (or other uncongested, light-flow period).
 - d. Quality control for excessively high speeds or travel times as explained earlier.
 - e. Identify the average (mean) speed. That is the FFS for the segment.
 - f. Convert the segment speed to segment travel times (segment length divided by segment speed).
 - g. Sum the segment times to obtain facility free-flow travel times.
6. Compute the VMT and VHT for each time period.

$$VMT_t = \sum_d VMT_{t,d}$$

$$VHT_t = \sum_d VHT_{t,d}$$

7. Compute the TTI for the facility for each time period.

$$TTI_t = \frac{VHT_t}{VHTFF_t}$$

where $VHTFF_t$ is the VHT that would occur during time period t if all vehicles traveled at the FFS:

$$VHTFF_t = \frac{VMT_t}{FFS}$$

8. Develop a distribution of the TTI_t values for the facility for the entire analysis period. Each TTI_t value becomes an observation in the distribution. All performance measures are derived from this distribution. The statistics and percentiles are calculated by using VMT_t as a weight; this is done to account for the fact that the TTIs in each time period are based on a different number of vehicles.

4. RELIABILITY VALUES FOR SELECTED U.S. FACILITIES

DATA SOURCES

Reliability data for 1 year of nonholiday weekday travel time were obtained from the following sources:

- 2-min traffic speed data in the I-95 corridor for 2010 (7), and
- 5-min traffic speed data in California for 2010 (8).

The first data set includes freeway and urban street reliability data for states and metropolitan areas in the I-95 corridor (i.e., U.S. East Coast). The average speed of traffic was measured every 2 min for each TMC road segment (9). Road segments vary but generally terminate at a decision point for the driver (e.g., intersection, start of left-turn pocket, ramp merge or diverge). Traffic speeds are obtained by monitoring the positions of GPS units in participating vehicles. A “free-flow reference speed” is established for each TMC segment on the basis of empirical observations. It may not correspond exactly to the FFS that would be estimated by the HCM’s analytical or field-measurement methods.

The California data include freeway reliability data for the state’s major metropolitan areas, plus reliability data for one urban street in Chula Vista. The data come from two sources: toll tag readers and loop detectors. California’s system provides a function for stringing together a series of loop detector station speeds into an estimate of the overall average speed for the facility. The loop detector data used to compute an average speed for each segment of the facility are offset by the time taken by the average vehicle to traverse the upstream segment. Thus for a selected direction of travel, the average speed of vehicles in Segment 1 is used to compute the average travel time t for the selected time period (e.g., 5 min) for that segment starting at time $T = 0$. The mean speed is computed for the next downstream segment for the 5-min period starting at $T = 0 + t$. The resulting mean travel times are then added together to get the average travel time of vehicles for the 5-min period starting their trip at $0 < T < 5$ min.

RELIABILITY STATISTICS FOR A CROSS SECTION OF U.S. FACILITIES

Exhibit 36-8 through Exhibit 36-11 show the distribution of 50th percentile travel time index (TTI_{50}), mean travel time index (TTI_{mean}), and planning time index (PTI or TTI_{95}) observed in the data set of U.S. freeways and urban streets described above, for all time periods combined, the 2-h a.m. peak period, the 2-h midday period, and the 2-h p.m. peak period, respectively. Exhibit 36-11 is an expanded version of Exhibit 11-3 in Chapter 11, Freeway Reliability and Strategy Assessment. The exhibits provide values in 5 percentile increments and include a combined set of values.

Because the free-flow reference speeds used in these data sets do not exactly correspond to the FFS estimates that an HCM analytical method or field-measurement technique would produce, the TTI values presented in these exhibits should be interpreted as being relative to the stated reference speed.

The base travel time for freeways was an empirically measured free-flow travel time. For urban streets, the base travel time corresponded to the 85th percentile highest speed observed during off-peak hours. Therefore, the free-flow reference speeds used in these data sets do not correspond exactly to the FFS that an HCM method would produce.

TTIs calculated by using the HCM definition of FFS could be different, but the general patterns observed would be similar.

Exhibit 36-8

Rankings of U.S. Facilities by Mean TTI and PTI (A.M. Peak, Midday, and P.M. Peak Combined)

Percentile Rank	Freeways			Urban Streets		
	TTI ₅₀	TTI _{mean}	PTI	TTI ₅₀	TTI _{mean}	PTI
Minimum	1.01	1.02	1.07	1.03	1.06	1.23
Worst 95%	1.02	1.05	1.09	1.09	1.12	1.27
Worst 90%	1.02	1.06	1.13	1.13	1.15	1.29
Worst 85%	1.04	1.06	1.14	1.15	1.16	1.32
Worst 80%	1.05	1.08	1.17	1.17	1.20	1.33
Worst 75%	1.05	1.08	1.22	1.19	1.20	1.35
Worst 70%	1.05	1.09	1.25	1.19	1.22	1.36
Worst 65%	1.06	1.10	1.30	1.20	1.22	1.39
Worst 60%	1.07	1.12	1.34	1.20	1.23	1.41
Worst 55%	1.08	1.15	1.39	1.21	1.23	1.42
Worst 50%	1.10	1.16	1.47	1.23	1.26	1.44
Worst 45%	1.11	1.19	1.57	1.24	1.27	1.47
Worst 40%	1.13	1.23	1.73	1.25	1.28	1.49
Worst 35%	1.14	1.30	1.84	1.25	1.29	1.52
Worst 30%	1.17	1.33	1.97	1.26	1.30	1.54
Worst 25%	1.20	1.39	2.24	1.30	1.34	1.60
Worst 20%	1.26	1.43	2.71	1.33	1.36	1.63
Worst 15%	1.31	1.51	2.90	1.35	1.38	1.70
Worst 10%	1.59	1.78	3.34	1.39	1.47	1.84
Worst 5%	1.75	1.97	3.60	1.45	1.54	1.98
Maximum	2.55	2.73	4.73	1.60	1.66	2.55

Source: Derived from directional values in Exhibit 36-12 through Exhibit 36-17. Entries are the lowest value for a category.

Note: TTI₅₀ = 50th percentile travel time index (50th percentile travel time divided by base travel time).

TTI_{mean} = mean travel time index (mean travel time divided by base travel time).

PTI = planning time index (95th percentile travel time divided by base travel time).

For freeways, the base travel time is the free-flow travel time. For urban streets, the base travel time corresponds to the 85th percentile highest speed observed during off-peak hours.

Exhibit 36-9

Rankings of U.S. Facilities by Mean TTI and PTI (A.M. Peak)

Percentile Rank	Freeways			Urban Streets		
	TTI ₅₀	TTI _{mean}	PTI	TTI ₅₀	TTI _{mean}	PTI
Minimum	1.01	1.02	1.07	1.03	1.06	1.24
Worst 95%	1.01	1.03	1.08	1.08	1.12	1.24
Worst 90%	1.03	1.05	1.12	1.12	1.13	1.27
Worst 85%	1.04	1.06	1.14	1.13	1.15	1.29
Worst 80%	1.04	1.08	1.14	1.14	1.16	1.29
Worst 75%	1.05	1.08	1.17	1.15	1.16	1.31
Worst 70%	1.06	1.09	1.24	1.16	1.17	1.33
Worst 65%	1.07	1.10	1.36	1.18	1.20	1.35
Worst 60%	1.08	1.11	1.40	1.19	1.20	1.37
Worst 55%	1.08	1.16	1.47	1.19	1.21	1.39
Worst 50%	1.09	1.17	1.53	1.20	1.23	1.41
Worst 45%	1.11	1.19	1.58	1.20	1.24	1.42
Worst 40%	1.12	1.21	1.70	1.22	1.26	1.44
Worst 35%	1.13	1.21	1.78	1.24	1.27	1.50
Worst 30%	1.15	1.25	1.89	1.24	1.28	1.52
Worst 25%	1.20	1.42	2.13	1.25	1.29	1.54
Worst 20%	1.28	1.48	2.61	1.26	1.29	1.57
Worst 15%	1.54	1.83	3.17	1.26	1.29	1.66
Worst 10%	1.72	1.93	3.55	1.28	1.31	1.71
Worst 5%	1.95	2.08	3.92	1.35	1.36	1.84
Maximum	2.17	2.73	4.66	1.38	1.49	2.13

Source: Derived from directional values in Exhibit 36-12 through Exhibit 36-17. Entries are the lowest value for a category.

Note: TTI₅₀ = 50th percentile travel time index (50th percentile travel time divided by base travel time).

TTI_{mean} = mean travel time index (mean travel time divided by base travel time).

PTI = planning time index (95th percentile travel time divided by base travel time).

For freeways, the base travel time is the free-flow travel time. For urban streets, the base travel time corresponds to the 85th percentile highest speed observed during off-peak hours.

Percentile Rank	Freeways			Urban Streets		
	TTI ₅₀	TTI _{mean}	PTI	TTI ₅₀	TTI _{mean}	PTI
Minimum	1.02	1.03	1.07	1.05	1.07	1.23
Worst 95%	1.02	1.04	1.08	1.08	1.10	1.27
Worst 90%	1.02	1.05	1.11	1.15	1.18	1.28
Worst 85%	1.02	1.06	1.14	1.16	1.18	1.30
Worst 80%	1.03	1.06	1.15	1.18	1.20	1.33
Worst 75%	1.04	1.08	1.17	1.19	1.21	1.34
Worst 70%	1.05	1.08	1.20	1.19	1.22	1.37
Worst 65%	1.05	1.09	1.21	1.20	1.22	1.39
Worst 60%	1.05	1.09	1.24	1.20	1.23	1.41
Worst 55%	1.06	1.11	1.26	1.21	1.23	1.42
Worst 50%	1.06	1.12	1.32	1.22	1.24	1.45
Worst 45%	1.07	1.13	1.34	1.24	1.27	1.47
Worst 40%	1.09	1.15	1.37	1.25	1.29	1.48
Worst 35%	1.09	1.15	1.43	1.25	1.30	1.51
Worst 30%	1.10	1.17	1.51	1.27	1.32	1.53
Worst 25%	1.12	1.26	1.65	1.30	1.34	1.57
Worst 20%	1.14	1.30	1.92	1.31	1.34	1.60
Worst 15%	1.16	1.32	2.41	1.32	1.35	1.63
Worst 10%	1.17	1.42	2.85	1.33	1.38	1.63
Worst 5%	1.21	1.46	3.16	1.35	1.42	1.86
Maximum	1.31	1.76	3.96	1.47	1.55	2.01

Source: Derived from directional values in Exhibit 36-12 through Exhibit 36-17. Entries are the lowest value for a category.

Note: TTI₅₀ = 50th percentile travel time index (50th percentile travel time divided by base travel time).
 TTI_{mean} = mean travel time index (mean travel time divided by base travel time).
 PTI = planning time index (95th percentile travel time divided by base travel time).
 For freeways, the base travel time is the free-flow travel time. For urban streets, the base travel time corresponds to the 85th percentile highest speed observed during off-peak hours.

Exhibit 36-10
 Rankings of U.S. Facilities by Mean TTI and PTI (Midday)

Percentile Rank	Freeways			Urban Streets		
	TTI ₅₀	TTI _{mean}	PTI	TTI ₅₀	TTI _{mean}	PTI
Minimum	1.01	1.05	1.10	1.13	1.14	1.32
Worst 95%	1.03	1.06	1.14	1.13	1.15	1.35
Worst 90%	1.04	1.06	1.22	1.18	1.21	1.35
Worst 85%	1.05	1.08	1.24	1.20	1.22	1.36
Worst 80%	1.05	1.09	1.28	1.20	1.22	1.37
Worst 75%	1.06	1.10	1.31	1.21	1.23	1.40
Worst 70%	1.07	1.14	1.32	1.22	1.23	1.41
Worst 65%	1.11	1.16	1.38	1.23	1.25	1.42
Worst 60%	1.14	1.23	1.59	1.24	1.26	1.44
Worst 55%	1.14	1.30	1.72	1.24	1.27	1.47
Worst 50%	1.17	1.31	1.85	1.25	1.28	1.49
Worst 45%	1.20	1.34	1.94	1.25	1.29	1.50
Worst 40%	1.21	1.36	2.06	1.31	1.33	1.52
Worst 35%	1.23	1.38	2.25	1.34	1.36	1.59
Worst 30%	1.26	1.41	2.46	1.35	1.38	1.64
Worst 25%	1.29	1.48	2.62	1.39	1.44	1.68
Worst 20%	1.35	1.57	2.77	1.41	1.49	1.78
Worst 15%	1.61	1.71	2.93	1.41	1.52	1.83
Worst 10%	1.70	1.86	3.26	1.49	1.56	1.88
Worst 5%	1.76	1.99	3.54	1.56	1.60	2.10
Maximum	2.55	2.73	4.73	1.60	1.66	2.55

Source: Derived from directional values in Exhibit 36-12 through Exhibit 36-17. Entries are the lowest value for a category.

Note: TTI₅₀ = 50th percentile travel time index (50th percentile travel time divided by base travel time).
 TTI_{mean} = mean travel time index (mean travel time divided by base travel time).
 PTI = planning time index (95th percentile travel time divided by base travel time).
 For freeways, the base travel time is the free-flow travel time. For urban streets, the base travel time corresponds to the 85th percentile highest speed observed during off-peak hours.

Exhibit 36-11
 Rankings of U.S. Facilities by Mean TTI and PTI (P.M. Peak)

Exhibit 36-12 through Exhibit 36-14 present the source freeway data for the a.m. peak, midday, and p.m. peak periods, respectively. Exhibit 36-15 through

Exhibit 36-17 present the source urban street data for the a.m. peak, midday, and p.m. peak periods, respectively.

Exhibit 36-12

Freeway Reliability Values:
Weekday A.M. Peak Period

Location	Freeway	Length (mi)	FFRS (mi/h)	Direction	Avg. Travel Time (min)	TTI _{mean}	PTI
Delaware	I-495	11.5	65	NB	11.0	1.03	1.08
Delaware	I-495	11.6	65	SB	11.1	1.03	1.07
Delaware	I-95	13.4	60	NB	14.6	1.10	1.37
Delaware	I-95	13.1	61	SB	13.5	1.05	1.13
Los Angeles	I-10	4.6	64	EB	4.5	1.06	1.12
Los Angeles	I-10	4.6	65	WB	4.5	1.08	1.14
Los Angeles	I-210	4.6	66	EB	4.9	1.17	1.57
Los Angeles	I-210	4.6	69	WB	4.6	1.16	1.57
Maryland	I-495 ES	26.5	63	SB	28.0	1.10	1.42
Maryland	I-495 ES	26.7	62	NB	31.1	1.20	1.71
Maryland	I-495 WS	15.4	60	NB	18.3	1.19	1.68
Maryland	I-495 WS	15.3	61	SB	26.9	1.78	2.71
Pennsylvania	I-76	3.7	51	EB	4.7	1.08	1.22
Pennsylvania	I-76	3.6	49	WB	6.5	1.49	3.06
Philadelphia	I-76	3.7	51	EB	4.7	1.08	1.22
Philadelphia	I-76	3.6	49	WB	6.5	1.79	3.06
Sacramento	US-50	6.0	69	EB	5.7	1.10	1.27
Sacramento	US-50	6.0	71	WB	6.2	1.21	1.78
Sacramento	I-80	12.4	68	EB	11.5	1.06	1.14
Sacramento	I-80	12.4	67	WB	12.0	1.09	1.17
San Diego	I-5	10.6	71	NB	11.1	1.23	1.81
San Diego	I-5	10.6	72	SB	9.1	1.02	1.07
San Diego	I-15	3.9	70	NB	4.7	1.41	2.10
San Diego	I-15	3.9	69	SB	7.3	1.58	3.38
San Francisco	I-880	4.6	71	NB	4.6	1.17	1.47
San Francisco	I-880	4.8	67	SB	8.2	1.92	3.57
San Francisco	I-680	4.2	66	NB	4.8	1.26	1.92
San Francisco	I-680	4.7	65	SB	5.2	1.21	1.49

Notes: FFRS = free-flow reference speed, calculated empirically; may not exactly match the HCM-defined FFS.
 TTI_{mean} = mean travel time index (mean travel time divided by free-flow travel time).
 PTI = planning time index (95th percentile travel time divided by free-flow travel time).
 NB = northbound, SB = southbound, EB = eastbound, WB = westbound, ES = east side, WS = west side.

Exhibit 36-13

Freeway Reliability Values:
Weekday Midday Periods

Location	Roadway	Length (mi)	FFRS (mi/h)	Direction	Avg. Travel Time (min)	TTI _{mean}	PTI
Delaware	I-495	11.5	65	NB	11.0	1.03	1.07
Delaware	I-495	11.6	65	SB	11.3	1.05	1.11
Delaware	I-95	13.4	60	NB	13.9	1.05	1.20
Delaware	I-95	13.1	61	SB	13.8	1.08	1.34
Los Angeles	I-10	4.6	64	EB	4.5	1.06	1.15
Los Angeles	I-10	4.6	65	WB	4.5	1.08	1.14
Los Angeles	I-210	4.6	66	EB	4.8	1.16	1.32
Los Angeles	I-210	4.6	69	WB	4.4	1.10	1.18
Maryland	I-495 ES	26.5	63	SB	27.2	1.07	1.31
Maryland	I-495 ES	26.7	62	NB	28.2	1.09	1.42
Maryland	I-495 WS	15.4	60	NB	20.5	1.34	2.69
Maryland	I-495 WS	15.3	61	SB	19.8	1.30	2.26
Pennsylvania	I-76	3.7	51	EB	5.0	1.13	1.39
Pennsylvania	I-76	3.6	49	WB	6.2	1.43	2.95
Philadelphia	I-76	3.7	51	EB	5.0	1.13	1.39
Philadelphia	I-76	3.6	49	WB	6.2	1.72	2.95
Sacramento	US-50	6.0	69	EB	5.8	1.11	1.20
Sacramento	US-50	6.0	71	WB	5.9	1.15	1.47
Sacramento	I-80	12.4	68	EB	11.8	1.09	1.25
Sacramento	I-80	12.4	67	WB	11.9	1.08	1.14
San Diego	I-5	10.6	71	NB	9.3	1.03	1.07
San Diego	I-5	10.6	72	SB	9.5	1.06	1.21
San Diego	I-15	3.9	70	NB	3.8	1.13	1.23
San Diego	I-15	3.9	69	SB	4.1	1.24	1.61
San Francisco	I-880	4.6	71	NB	4.5	1.17	1.53
San Francisco	I-880	4.8	67	SB	5.6	1.31	1.96
San Francisco	I-680	4.2	66	NB	4.4	1.15	1.34
San Francisco	I-680	4.7	65	SB	5.0	1.15	1.26

Notes: FFRS = free-flow reference speed, calculated empirically; may not exactly match the HCM-defined FFS.
 TTI_{mean} = mean travel time index (mean travel time divided by free-flow travel time).
 PTI = planning time index (95th percentile travel time divided by free-flow travel time).
 NB = northbound, SB = southbound, EB = eastbound, WB = westbound, ES = east side, WS = west side.

Location	Roadway	Length (mi)	FFRS (mi/h)	Direction	Avg. Travel Time (min)	TTI _{mean}	PTI
Delaware	I-495	11.5	65	NB	11.4	1.06	1.23
Delaware	I-495	11.6	65	SB	12.0	1.10	1.39
Delaware	I-95	13.4	60	NB	14.6	1.10	1.29
Delaware	I-95	13.1	61	SB	16.8	1.30	1.83
Los Angeles	I-10	4.6	64	EB	5.1	1.20	1.31
Los Angeles	I-10	4.6	65	WB	4.9	1.16	1.28
Los Angeles	I-210	4.6	66	EB	4.5	1.08	1.35
Los Angeles	I-210	4.6	69	WB	4.2	1.06	1.15
Maryland	I-495 ES	26.5	63	SB	33.3	1.31	1.85
Maryland	I-495 ES	26.7	62	NB	33.7	1.31	1.98
Maryland	I-495 WS	15.4	60	NB	41.8	2.73	4.73
Maryland	I-495 WS	15.3	61	SB	30.6	2.02	3.67
Pennsylvania	I-76	3.7	51	EB	6.0	1.36	1.94
Pennsylvania	I-76	3.6	49	WB	7.7	1.78	3.29
Philadelphia	I-76	3.7	51	EB	6.0	1.36	1.94
Philadelphia	I-76	3.6	49	WB	7.7	1.78	3.29
Sacramento	US-50	6.0	69	EB	7.0	1.35	2.12
Sacramento	US-50	6.0	71	WB	7.7	1.51	2.74
Sacramento	I-80	12.4	68	EB	13.9	1.28	1.84
Sacramento	I-80	12.4	67	WB	12.1	1.09	1.31
San Diego	I-5	10.6	71	NB	9.4	1.05	1.22
San Diego	I-5	10.6	72	SB	13.1	1.47	2.45
San Diego	I-15	3.9	70	NB	4.7	1.18	2.97
San Diego	I-15	3.9	69	SB	3.8	1.14	1.50
San Francisco	I-880	4.6	71	NB	7.7	1.96	3.43
San Francisco	I-880	4.8	67	SB	5.8	1.34	1.73
San Francisco	I-680	4.2	66	NB	6.1	1.59	2.74
San Francisco	I-680	4.7	65	SB	5.0	1.15	1.25

Notes: FFRS = free-flow reference speed, calculated empirically; may not exactly match the HCM-defined FFS.
 TTI_{mean} = mean travel time index (mean travel time divided by free-flow travel time).
 PTI = planning time index (95th percentile travel time divided by free-flow travel time).
 NB = northbound, SB = southbound, EB = eastbound, WB = westbound, ES = east side, WS = west side.

Exhibit 36-14
 Freeway Reliability Values:
 Weekday P.M. Peak Period

Location	Roadway	Length (mi)	FFRS (mi/h)	Direction	Avg. Travel Time (min)	TTI _{mean}	PTI
California	Telegraph Canyon Rd.	4.4	45	EB	6.19	1.06	1.24
California	Telegraph Canyon Rd.	4.4	45	WB	6.57	1.12	1.42
Delaware	US-202	3.8	42	NB	6.97	1.28	1.55
Delaware	US-202	3.9	44	SB	6.52	1.20	1.41
Maryland	Hwy 175	7.4	38	NB	13.92	1.20	1.32
Maryland	Hwy 175	7.4	38	SB	14.00	1.21	1.35
Maryland	Hwy 193	5.9	33	EB	13.75	1.26	1.45
Maryland	Hwy 193	5.9	33	WB	13.72	1.27	1.52
Maryland	Hwy 198	10.1	42	EB	16.51	1.13	1.24
Maryland	Hwy 198	10.2	41	WB	16.95	1.15	1.27
Maryland	Hwy 355	4.2	30	NB	10.37	1.23	1.38
Maryland	Hwy 355	4.2	30	SB	12.57	1.49	2.13
Maryland	Randolph Rd.	6.7	35	EB	14.13	1.22	1.36
Maryland	Randolph Rd.	6.7	35	WB	15.28	1.31	1.71
Maryland	US-40	4.1	41	EB	7.00	1.16	1.29
Maryland	US-40	4.2	39	WB	8.50	1.29	1.85
Pennsylvania	US-1	8.0	33	NB	19.68	1.36	1.67
Pennsylvania	US-1	7.6	32	SB	18.18	1.29	1.52
Philadelphia	Hwy 611	3.4	20	NB	13.26	1.29	1.58
Philadelphia	Hwy 611	3.3	19	SB	12.89	1.25	1.41
South Carolina	US-378	5.5	44	EB	8.61	1.16	1.29
South Carolina	US-378	5.4	45	WB	8.37	1.16	1.31

Notes: FFRS = free-flow reference speed, calculated empirically; may not exactly match the HCM-defined FFS.
 TTI_{mean} = mean travel time index (mean travel time divided by free-flow travel time).
 PTI = planning time index (95th percentile travel time divided by base travel time).
 NB = northbound, SB = southbound, EB = eastbound, WB = westbound.
 The base travel time corresponds to the 85th percentile highest speed observed during off-peak hours.

Exhibit 36-15
 Urban Street Reliability
 Values: Weekday A.M. Peak
 Period

Exhibit 36-16

Urban Street Reliability
Values: Weekday Midday
Periods

Location	Roadway	Length (mi)	FFRS (mi/h)	Direction	Avg. Travel Time (min)	TTI _{mean}	PTI
California	Telegraph Canyon Rd.	4.4	45	EB	6.27	1.07	1.23
California	Telegraph Canyon Rd.	4.4	45	WB	6.46	1.10	1.28
Delaware	US-202	3.8	42	NB	7.28	1.34	1.63
Delaware	US-202	3.9	44	SB	6.93	1.28	1.47
Maryland	Hwy 175	7.4	38	NB	13.93	1.20	1.33
Maryland	Hwy 175	7.4	38	SB	14.17	1.23	1.38
Maryland	Hwy 193	5.9	33	EB	14.29	1.31	1.52
Maryland	Hwy 193	5.9	33	WB	13.99	1.29	1.49
Maryland	Hwy 198	10.1	42	EB	17.13	1.18	1.29
Maryland	Hwy 198	10.2	41	WB	17.47	1.18	1.27
Maryland	Hwy 355	4.2	30	NB	12.02	1.42	1.87
Maryland	Hwy 355	4.2	30	SB	13.07	1.55	2.01
Maryland	Randolph Rd.	6.7	35	EB	14.22	1.23	1.36
Maryland	Randolph Rd.	6.7	35	WB	14.62	1.25	1.42
Maryland	US-40	4.1	41	EB	7.44	1.23	1.47
Maryland	US-40	4.2	39	WB	8.01	1.22	1.42
Pennsylvania	US-1	8.0	33	NB	19.23	1.33	1.53
Pennsylvania	US-1	7.6	32	SB	19.02	1.35	1.58
Philadelphia	Hwy 611	3.4	20	NB	14.12	1.38	1.61
Philadelphia	Hwy 611	3.3	19	SB	13.78	1.34	1.63
South Carolina	US-378	5.5	44	EB	8.88	1.20	1.33
South Carolina	US-378	5.4	45	WB	8.78	1.22	1.40

Notes: FFRS = free-flow reference speed, calculated empirically; may not exactly match the HCM-defined FFS.
TTI_{mean} = mean travel time index (mean travel time divided by free-flow travel time).
PTI = planning time index (95th percentile travel time divided by base travel time).
NB = northbound, SB = southbound, EB = eastbound, WB = westbound.
The base travel time corresponds to the 85th percentile highest speed observed during off-peak hours.

Exhibit 36-17

Urban Street Reliability
Values: Weekday P.M. Peak
Period

Location	Roadway	Length (mi)	FFRS (mi/h)	Direction	Avg. Travel Time (min)	TTI _{mean}	PTI
California	Telegraph Canyon Rd.	4.4	45	EB	6.71	1.14	1.35
California	Telegraph Canyon Rd.	4.4	45	WB	6.73	1.15	1.35
Delaware	US-202	3.8	42	NB	7.42	1.36	1.62
Delaware	US-202	3.9	44	SB	6.84	1.26	1.43
Maryland	Hwy 175	7.4	38	NB	14.20	1.23	1.36
Maryland	Hwy 175	7.4	38	SB	14.81	1.28	1.49
Maryland	Hwy 193	5.9	33	EB	16.39	1.50	1.83
Maryland	Hwy 193	5.9	33	WB	15.67	1.45	1.69
Maryland	Hwy 198	10.1	42	EB	18.53	1.27	1.50
Maryland	Hwy 198	10.2	41	WB	17.81	1.21	1.32
Maryland	Hwy 355	4.2	30	NB	14.03	1.66	2.11
Maryland	Hwy 355	4.2	30	SB	13.47	1.60	1.89
Maryland	Randolph Rd.	6.7	35	EB	16.11	1.39	1.65
Maryland	Randolph Rd.	6.7	35	WB	14.33	1.23	1.36
Maryland	US-40	4.1	41	EB	9.40	1.56	2.55
Maryland	US-40	4.2	39	WB	8.04	1.22	1.41
Pennsylvania	US-1	8.0	33	NB	19.63	1.36	1.53
Pennsylvania	US-1	7.6	32	SB	21.31	1.52	1.80
Philadelphia	Hwy 611	3.4	20	NB	13.22	1.29	1.48
Philadelphia	Hwy 611	3.3	19	SB	13.19	1.28	1.46
South Carolina	US-378	5.5	44	EB	9.22	1.24	1.41
South Carolina	US-378	5.4	45	WB	8.81	1.22	1.39

Notes: FFRS = free-flow reference speed, calculated empirically; may not exactly match the HCM-defined FFS.
TTI_{mean} = mean travel time index (mean travel time divided by free-flow travel time).
PTI = planning time index (95th percentile travel time divided by base travel time).
NB = northbound, SB = southbound, EB = eastbound, WB = westbound.
The base travel time corresponds to the 85th percentile highest speed observed during off-peak hours.

RELIABILITY STATISTICS FOR FLORIDA FREEWAYS

Exhibit 36-18 presents reliability statistics for a cross section of Florida freeways (10). The data were gathered and reported for the p.m. peak period (4:30 to 6:00 p.m.) and are *not* aggregated over the length of the facility. The data consist of spot speeds that have been inverted into travel time rates (min/mi).

The reliability statistics for Florida are reported separately from the rest of the United States because Florida was testing a variety of definitions of FFS in the

research from which these data were obtained (10). Florida usually sets the FFS for its freeways as the posted speed limit plus 5 mi/h. However, a speed of 5 mi/h less than the posted speed limit and a policy speed of 40 mi/h were also being tested for reliability computation purposes. The following statistics are presented:

- Four different TTIs (50th, 80th, 90th, and 95th percentile TTIs) based on a definition of FFS of the posted speed plus 5 mi/h;
- Two policy indices, one based on the 50th percentile speed and a target speed of the posted speed minus 5 mi/h, the other based on the 50th percentile speed and a speed of 40 mi/h;
- A buffer time index based on the 95th percentile speed and the mean speed; and
- A misery index based on the average of the highest 5% of travel times and a free-flow travel time derived from the posted speed plus 5 mi/h.

Location	TTI ₅₀	TTI ₈₀	TTI ₉₀	TTI ₉₅ (PTI)	Policy Index Alt. 1	Policy Index Alt. 2	Buffer Time Index	Misery Index
I-95 NB at NW 19th St.	1.00	1.36	1.69	2.01	1.27	1.75	2.02	2.22
I-95 SB at NW 19th St.	1.08	1.19	1.58	2.01	1.27	1.75	1.86	2.48
I-95 NB, S of Atlantic Blvd.	1.03	1.28	1.73	2.23	1.27	1.75	2.16	2.74
I-95 SB, S of Atlantic Blvd.	1.10	1.36	1.89	2.37	1.27	1.75	2.15	2.93
SR 826 NB at NW 66th St.	2.40	2.82	3.07	3.35	1.33	1.50	1.39	3.69
SR 826 SB at NW 66th St.	1.01	1.28	2.63	4.06	1.33	1.50	4.02	4.62
SR 826 WB, W of NW 67th Ave.	1.04	1.08	1.21	1.77	1.33	1.50	1.70	2.10
SR 826 EB, W of NW 67th Ave.	0.98	1.00	1.02	1.04	1.33	1.50	1.07	1.10
I-4 EB, W of World Dr.	0.97	1.04	1.06	1.08	1.27	1.75	1.12	1.12
I-4 WB, W of World Dr.	1.02	1.09	1.49	1.90	1.27	1.75	1.86	2.22
I-4 EB, W of Central Florida Pkwy.	1.06	1.13	1.18	1.31	1.27	1.75	1.24	1.56
I-4 WB, W of Central Florida Pkwy.	1.05	1.36	1.63	1.81	1.27	1.75	1.72	2.03
I-275 NB, N of MLK Jr Blvd.	1.45	1.71	1.91	2.16	1.33	1.50	1.49	2.58
I-275 SB, N of MLK Jr Blvd.	0.97	1.01	1.04	1.12	1.33	1.50	1.15	1.28
I-275 NB, N of Fletcher Blvd.	1.05	1.07	1.11	1.21	1.33	1.50	1.16	1.35
I-275 SB, N of Fletcher Blvd.	0.96	0.98	0.99	1.00	1.33	1.50	1.04	1.01
I-10 EB, E of Lane Ave.	0.93	0.96	0.98	0.99	1.33	1.50	1.07	1.01
I-10 WB, E of Lane Ave.	0.97	1.10	1.24	1.46	1.33	1.50	1.51	1.87
I-95 NB, S of Spring Glen Rd.	1.04	1.09	1.26	1.77	1.27	1.75	1.70	2.00
I-95 SB, S of Spring Glen Rd.	1.16	1.30	1.42	1.60	1.27	1.75	1.38	1.88
Minimum	0.93	0.96	0.98	0.99	1.27	1.50	1.04	1.01
Average	1.11	1.26	1.51	1.81	1.30	1.63	1.64	2.09
Maximum	2.40	2.82	3.07	4.06	1.33	1.75	4.02	4.62

Exhibit 36-18
Florida Freeway Reliability Statistics

Source: Adapted from Kittelson & Associates, Inc. (10).

Notes: TTI_{xx} = travel time index based on the percentile speed indicated in the subscript and a free-flow speed defined as the posted speed plus 5 mi/h.

PTI = planning time index.

Policy Index Alternative 1 = index based on the 50th percentile speed and a target speed of the posted speed minus 10 mi/h.

Policy Index Alternative 2 = index based on the 50th percentile speed and a target speed of 40 mi/h.

Buffer time index = index based on the ratio of the 95th percentile and mean travel speeds.

Misery index = index based on the ratio of (a) the average of the highest 5% of travel times and (b) a free-flow travel time defined as the posted speed plus 5 mi/h.

N = north, S = south, E = east, W = west, NB = northbound, SB = southbound, EB = eastbound, WB = westbound.

5. VEHICLE TRAJECTORY ANALYSIS

INTRODUCTION

Overview

This section contains expanded guidance for the use of alternative traffic analysis tools (mostly microsimulation tools) in assessing the performance of highway facilities. An important part of the guidance deals with the use of vehicle trajectory analysis as the “lowest common denominator” for comparing performance measures from different tools. Material on vehicle trajectory analysis is also included in the following chapters:

- *Chapter 4, Traffic Operations and Capacity Concepts*, introduces the concept of individual vehicle trajectory analysis. A growing school of thought suggests that comparing results between traffic analysis tools and methods is possible only through analyzing vehicle trajectories as the “lowest common denominator.” Vehicle trajectories can be used to develop performance measures that are consistent with HCM definitions, with field measurement techniques, and with each other. Examples of vehicle trajectory plots were shown that illustrate the visual properties of vehicle trajectories.
- *Chapter 7, Interpreting HCM and Alternative Tool Results*, explores the use of vehicle trajectory analysis in defining and estimating consistent performance measures. First, it introduces the mathematical properties of trajectories as an extension of the visual properties. Next, it identifies the performance measures that can be computed from trajectories and explores their compatibility with the performance measures estimated by the computational procedures presented throughout the HCM.

Chapter 7 presents general guidelines for defining and comparing measures from different traffic analysis tools. Those guidelines are expanded in this section through presentation of more specific trajectory analysis procedures by which consistent performance measures can be estimated. The trajectory analysis procedures described in this section were developed and tested by postprocessing the external trajectory files produced by a typical simulation tool. The postprocessor features and the process by which the procedures were developed are described elsewhere (11).

Several examples of the analysis of vehicle trajectories on both interrupted- and uninterrupted-flow facilities are presented here. These examples demonstrate the complexities that can arise, for example, in multilane situations, multiphase operations, situations in which the demand exceeds the capacity, and situations in which vehicles are unable to access a desired lane because of congestion. Specific procedures are then proposed and demonstrated with additional examples.

Mathematical Properties of Vehicle Trajectories

As was pointed out in Chapter 7, an analysis of vehicle trajectories requires a mathematical representation that includes a set of properties associated with each vehicle at specific points in time and space. Some of the material on mathematical properties of vehicle trajectories presented in this section is also included in Chapter 7. It is repeated here to provide a convenient introduction to the topic of vehicle trajectory analysis. A graphic representation of the path of an individual vehicle in space and time is also repeated here as Exhibit 36-19.

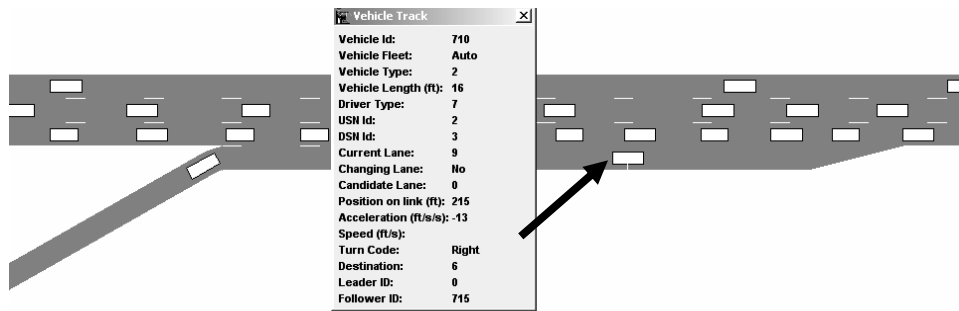


Exhibit 36-19
Vehicle Data Stored for Each
Time Step

Many properties can be associated with a specific vehicle at a point in time. Some properties are required for the accurate determination of performance measures from trajectories. Others are used for different purposes, such as safety analysis.

Basic Trajectory Properties

The basic trajectory properties from which all the required performance measures can be estimated include the following information for each vehicle within the facility boundaries and for each time step within the analysis period:

- *Vehicle identification:* Vehicle identification is required to distinguish a specific vehicle from all other vehicles within the facility boundaries.
- *Position:* This property is the most basic of all, and many other properties may be derived from it. A one-dimensional position is sufficient to produce performance measures. Some question remains about a universal representation of position, because different tools specify the position in different ways. A common reference point for position needs to be established. A reference point that indicates the relative position of the vehicle in the link would be desirable to enable developers to produce uniform measures.
- *Link or segment:* A link or segment is required to associate performance measures with a specific link or analysis segment for reporting purposes.
- *Lane:* In multilane facilities, knowledge of the lane in which the vehicle is traveling is important because headways, densities, and other measures must be estimated by lane. It is also necessary for identifying lane changes.

Static Vehicle and Facility Parameters

Some required properties can be derived from the basic properties with knowledge of certain parameters that are constant with respect to time:

- *Vehicle length*: Required to convert headways to gaps, and
- *Link end positions*: Required to determine the position of the vehicle with respect to the upstream or downstream end of the link.

Some simulation tools repeat this static information in each record to avoid the need for an external parameter file.

Derived Trajectory Properties

The remainder of the required trajectory properties can be derived from the basic properties as follows:

- *Instantaneous speed*: This property can be determined from the relative positions of the vehicle at time t and time $t - \Delta t$ on the assumption of a constant acceleration during Δt . However, since most tools update vehicle positions from the speeds, speed is commonly included as a basic trajectory property.
- *Instantaneous acceleration*: This property can be determined from the relative speeds of the vehicle at time t and time $t - \Delta t$ on the assumption of a constant acceleration during Δt . However, since most tools update vehicle speeds from the acceleration, acceleration is commonly included as a basic trajectory property.

TRAJECTORY ANALYSIS EXAMPLES

This section demonstrates the ability of alternative analysis tools to quantify trajectory properties. Several examples are presented for both uninterrupted- and interrupted-flow facilities.

Basic Signalized Intersection

The first example is very basic. The intersection configuration involves two single-lane, one-way streets as shown in Exhibit 36-20. To simplify the situation even more, the simulation parameters are adjusted to enforce a uniform operation. Essentially, all the randomness inherent in simulation is removed. A simulation of uniform conditions would not normally produce useful results, but this example provides a good starting point for illustrating the nature of vehicle trajectory plots.

A trajectory plot showing two cycles of simulated operation for this example is presented in Exhibit 36-21(a). This form is the classic one that appears often in the literature to support discussion related to queue accumulation and discharge. A copy of the exhibit used in Chapter 31, Signalized Intersections: Supplemental, to illustrate the basic traffic signal principles is also included as Exhibit 36-21(b). The two figures are different in that the first was produced directly from the vehicle trajectory data while the second was drawn by hand. The ability to reproduce the classic representation from controlled conditions will provide a measure of confidence in the validity of future examples involving much more complicated situations.

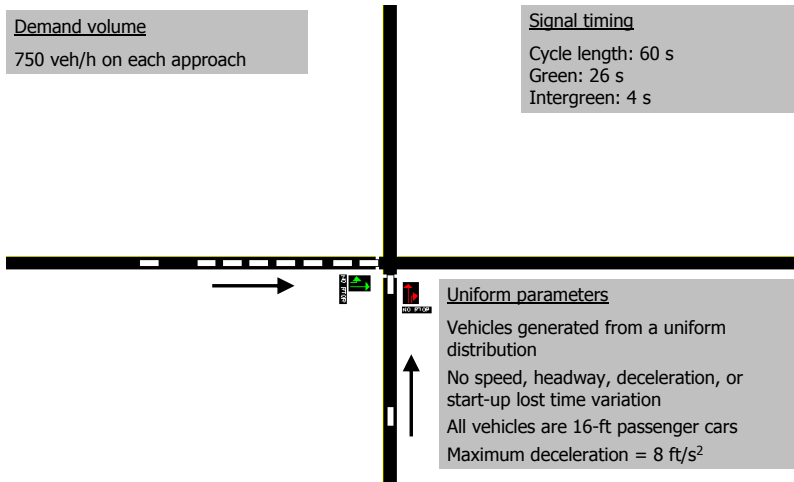
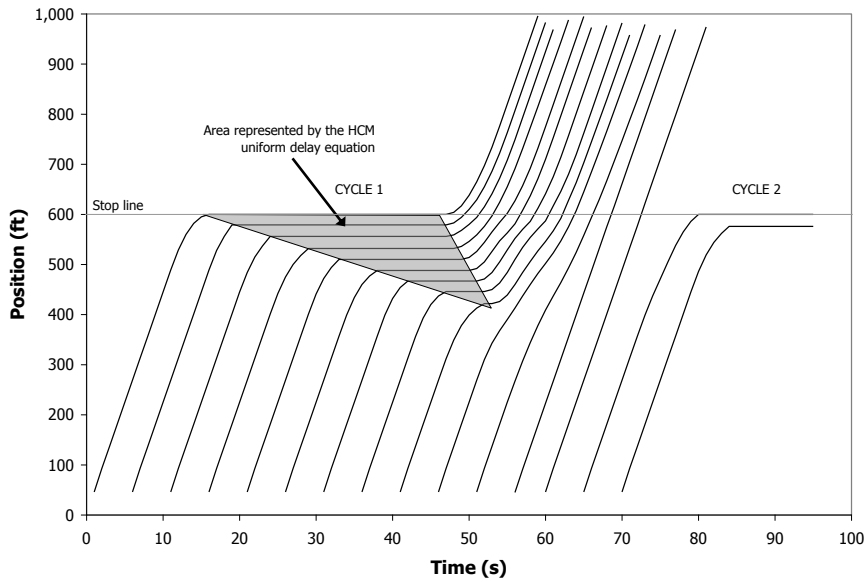
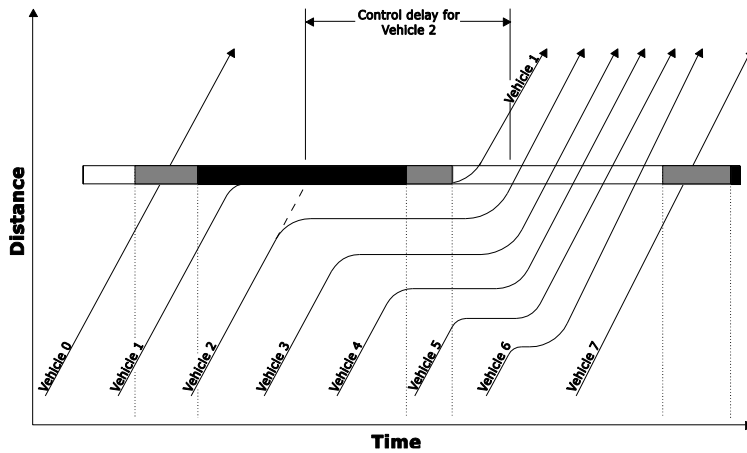


Exhibit 36-20
Basic Signalized Intersection Example



(a) Plot Produced from Simulation



(b) Plot Produced by Hand

Exhibit 36-21
Trajectory Plots for Uniform Arrivals and Departures

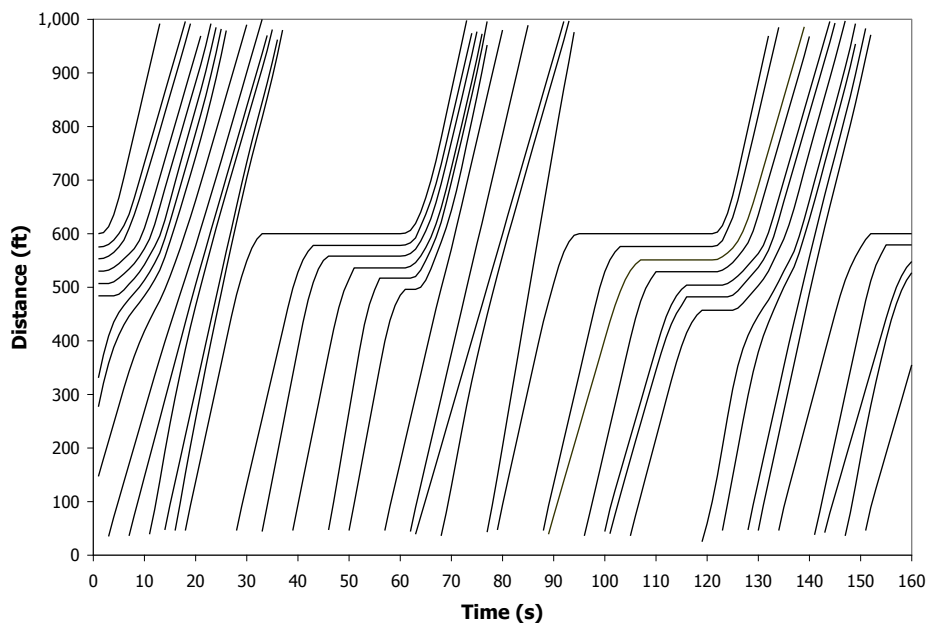
Note the similarity between the trajectories obtained from the file (above) and those developed manually in Chapter 31 (below) to illustrate the basic principles of signalized intersection operation.

Restoring Randomness to the Simulation

To simplify the discussion, the first example was presented with all randomness removed from the operation. Subsequent examples are more realistic in their treatment of traffic flow. Vehicles are generated at entry points from a Poisson distribution, and the simulation tool's default parameters for randomizing driver behavior are applied.

Exhibit 36-22 shows a sample trajectory plot for the same operation depicted in Exhibit 36-21. As expected, the individual trajectories follow the same pattern as the uniform case, except that some spacings and speeds are not as consistent. The trajectory lines do not cross each other in this example because the example uses a single-lane approach and overtaking is not possible.

Exhibit 36-22
Introducing Randomness into the Simulation



Vehicle Trajectories for Oversaturated Operation

Up to this point, the examples have involved volume-to-capacity ratios less than 1.0, in which all vehicles arriving on a given cycle were able to clear on the same cycle. Saturation levels close to and above 1.0 present a different picture. Three cases are presented here:

1. *Cycle failure*, occurring when saturation approaches 1.0 and residual queues build on one cycle but are resolved on the next cycle;
2. *Oversaturated operation*, a situation in which the link has a demand volume exceeding the link's capacity and queues extend throughout the approach link; and
3. *Undersaturated operation*, in which queues extend to an upstream link for a part of a cycle because of closely spaced intersections.

Cycle Failure

A cycle failure example is presented in Exhibit 36-23. This trajectory plot shows a situation in which some vehicles arriving in Cycle 1 were unable to clear until Cycle 2. This condition is identified from the trajectory plot for four stopped vehicles (i.e., horizontal trajectory lines) that were forced to stop again before reaching the stop line. These vehicles became the first four vehicles in the queue for Cycle 2. Fortunately, the arrivals during Cycle 2 were few enough that all stopped vehicles were able to clear the intersection before the beginning of the red phase. A closer inspection of Exhibit 36-23 shows that one more vehicle, which was not stopped, was also able to clear.

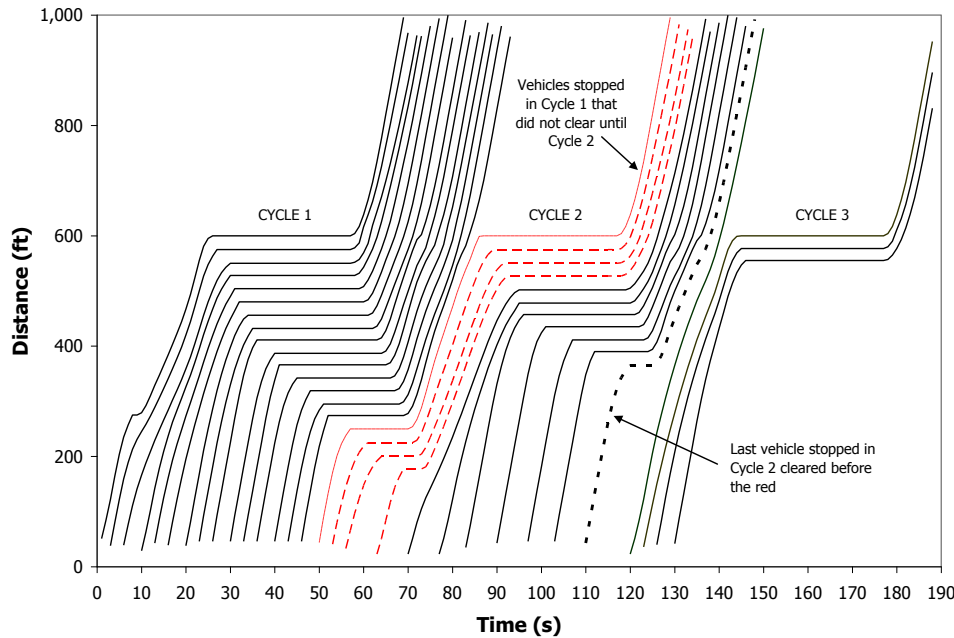


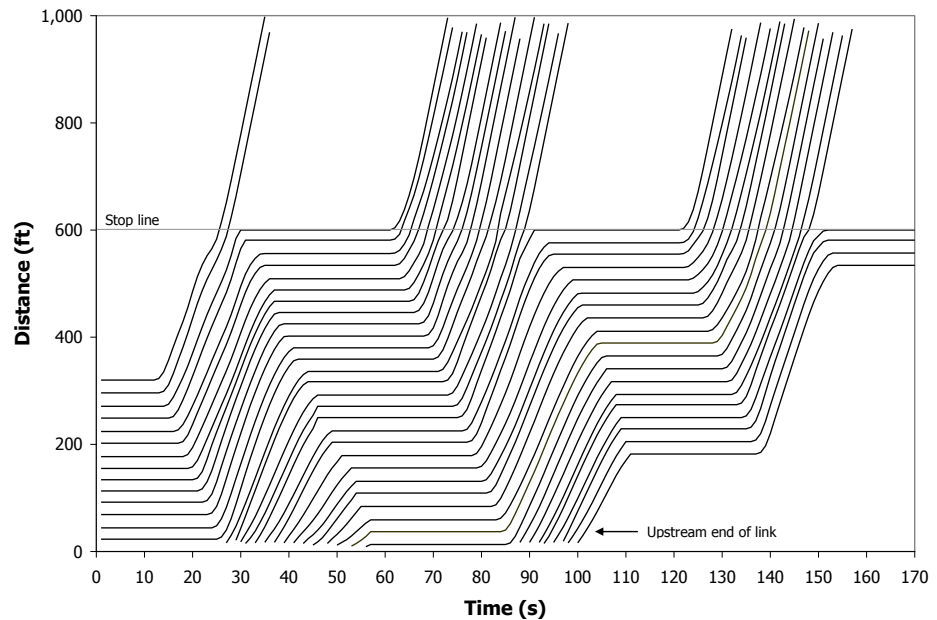
Exhibit 36-23
Cycle Failure Example

Severely Oversaturated Operation

Oversaturated operation was produced by increasing the demand volume to the point where it exceeded the capacity of the approach. The increased demand produced a queue that extended the length of the link. Inspection of the animated graphics showed that the queue did, in fact, back up beyond the link entry point.

The vehicle trajectory plot for this operation is presented in Exhibit 36-24. The move-up process is represented in the trajectories. Vehicles entering the link require up to three cycles to clear the intersection. The implications for control delay computations when the queue occupies a substantial proportion of the link are discussed in Chapter 7.

Exhibit 36-24
Oversaturated Signal Approach



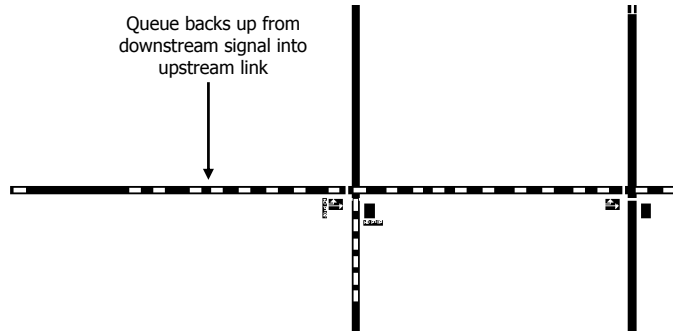
A larger question is what to do with the vehicles denied entry during the analysis period. The answer is that, as indicated in Chapter 19, Signalized Intersections, the analysis period must be long enough to include a period of uncongested operation at each end. The delay to vehicles denied entry to this link will be accounted for in upstream links during the period. The upstream links must include a holding area outside the system. Some tools include the delay to vehicles denied entry and some do not. If a tool is used that does not include denied-entry delay, fictitious links must be built into the network structure for that purpose.

Queue Backup from a Downstream Signal

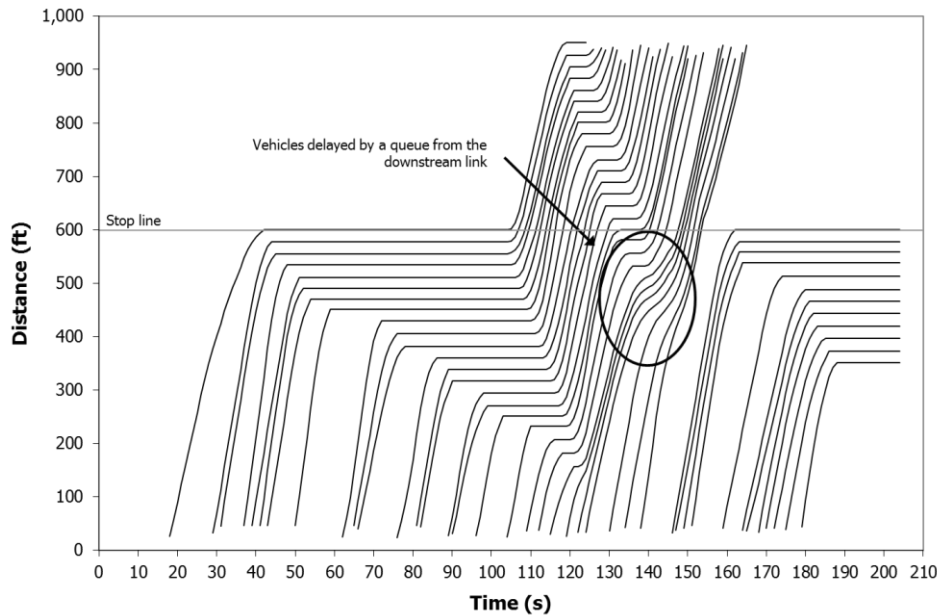
Even when an approach is not fully saturated, queues might back up from a downstream signal for a portion of the cycle. This happens when intersections are closely spaced. An example of queue backup within a cycle is shown in Exhibit 36-25.

The two-intersection configuration for this example is shown in Exhibit 36-25(a). The graphics screen capture shows that vehicles that would normally pass through the upstream link are prevented from doing so by queues that extend beyond the end of the downstream link for a portion of the cycle. The question is how to treat the resulting delay.

By the definitions given to this point, the delay in the upstream link would be assigned to the upstream link, even though the signal on the downstream link was the primary cause. The important thing is not to overlook any delay and to assign all delay somewhere and in a consistent manner. With simulation modeling, the only practical place to assign delay consistently is the link on which the delay occurred. Subtle complexities make it impractical to do otherwise. For example, the root cause of a specific backup might not be the immediate downstream link. The backup might be secondary to a problem at some distant location in the network at some other point in time.



(a) Simulation Graphics Representation



(b) Vehicle Trajectory Representation

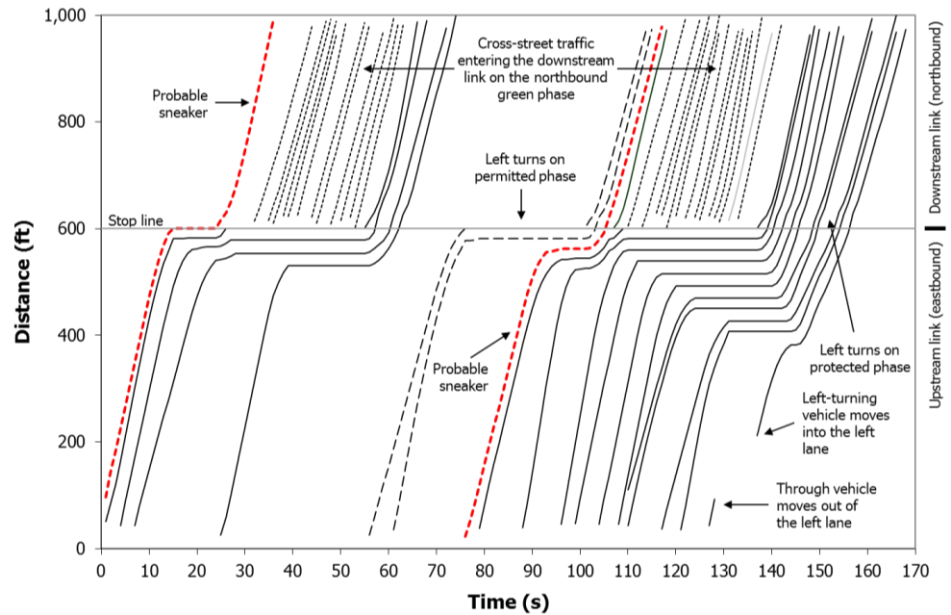
Exhibit 36-25
Queue Backup from a Downstream Signal

More Complex Signal Phasing

Up to this point only simple signal phasing has been considered. Many applications involve simulating more complex phasing on urban streets. As an example of a more complex situation, a left turn moving on both a protected and a permitted phase is examined.

Exhibit 36-26 shows the trajectory plot for an eastbound left-turn movement from an exclusive lane controlled by a signal with both protected and permitted phases. In this case, the upstream link is the eastbound approach to the intersection and the downstream link is the northbound approach to the next intersection. Because the distance on a trajectory plot is one-dimensional, the distance scale is linear, even though the actual route takes a right-angle bend.

Exhibit 36-26
Trajectory Plot for More
Complex Signal Phasing



Even with an undersaturated operation, this trajectory plot is substantially more involved than the previous ones. Several phenomena are identified in the exhibit, including the following:

1. Cross-street traffic entering the downstream link on the northbound phase: These vehicles do not appear on the upstream link because they are on a different link. They enter the downstream link at the stop line on the red phase for the left-turn movement of interest.
2. Left turns on the protected phase, shown as solid lines on the trajectory plot: The protected left-turn phase takes place immediately after the red phase. The left-turning vehicles begin to cross the stop line at that point.
3. Left turns on the permitted phase, shown as broken lines on the trajectory plot: The permitted left-turn phase takes place immediately after the protected phase. There is a gap in the trajectory plot because the left-turning vehicles must wait for oncoming traffic to clear.
4. Left-turn “sneakers”: Explicit identification of a sneaker on the trajectory plot is not possible; however, the last left turn to clear the intersection on the permitted phase is probably a sneaker if it enters at the end of the permitted phase.
5. Left-turn vehicles that enter the link in the through lane and change into the left lane somewhere along the link: These vehicles are identified by trajectories that begin in the middle of the link.
6. Through vehicles that enter the link in the left-turn lane and change into the through lane somewhere along the link: These vehicles are identified by trajectories that end abruptly in the middle of the link.

The trajectory plot shown for this example is more complex than the previous plots; however, performance can be analyzed in the same way.

Freeway Examples

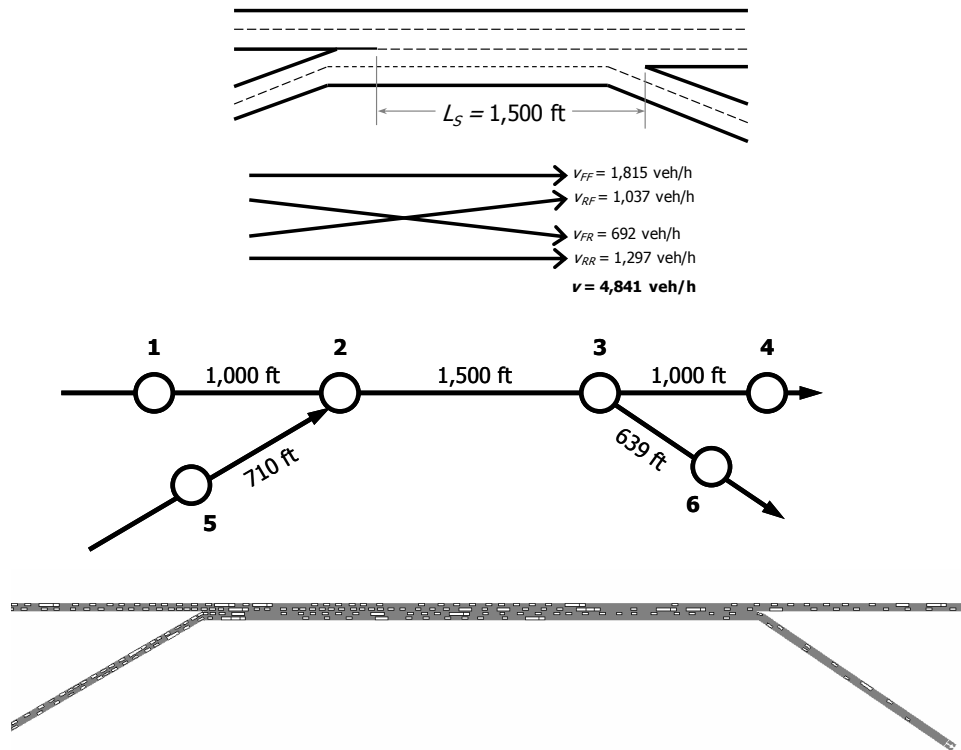
Freeway trajectories follow the same definitions as surface street trajectories, but the queuing patterns differ because they are created by car-following phenomena and not by traffic signals. The performance measures of interest also differ. There is no notion of control delay on freeways because there is no control. The level of service on uninterrupted-flow facilities is based on traffic density expressed in units of vehicles per mile per lane. In some cases, such as merging segments, the density in specific lanes is of interest.

Two cases are examined. The first deals with a weaving segment, and the second deals with merging at an entrance ramp.

Weaving Segment Example

Simulation Network Structure

The problem description, link-node structure, and animated graphics view for the weaving segment example are shown in Exhibit 36-27. The scenario is the same as that used in Example Problem 1 in Chapter 27, Freeway Weaving: Supplemental. There are two lanes on the freeway and on each ramp. The two ramp lanes are connected by full auxiliary lanes.



Note: L_S = length of segment, V_{FF} = vehicles entering from freeway and leaving to freeway, V_{RF} = vehicles entering from ramp and leaving to freeway, V_{FR} = vehicles entering from freeway and leaving to ramp, V_{RR} = vehicles entering from ramp and leaving to ramp, veh/h = vehicles per hour.

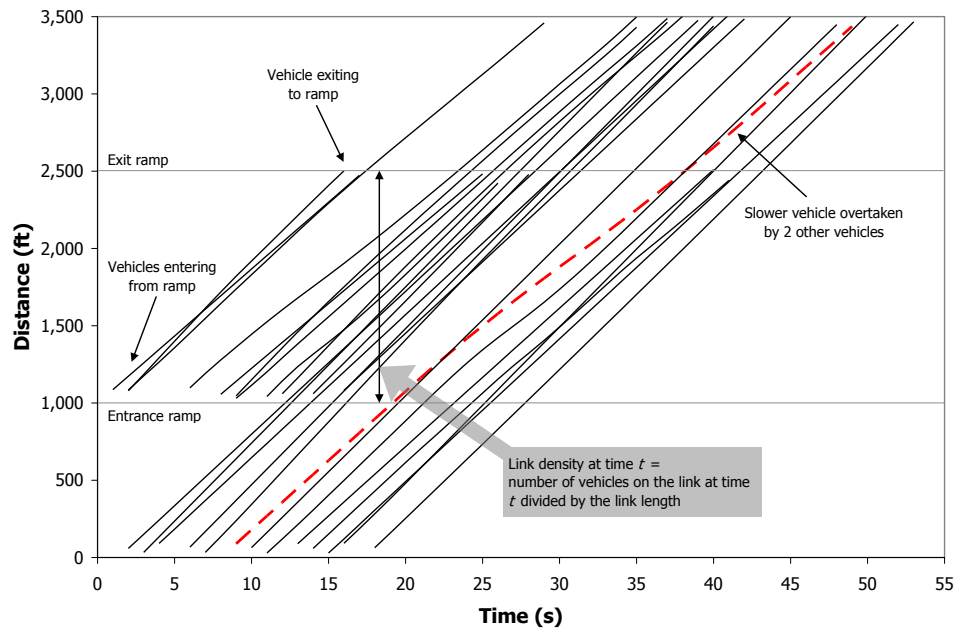
Exhibit 36-27
Weaving Segment Description
and Animated Graphics View

Vehicle Trajectories for the Freeway Lanes

The vertical (i.e., distance) axis of the trajectory plot provides a linear one-dimensional representation of a series of connected links. The links can follow any pattern as long as some of the vehicles leaving one link flow into the next link. The analysis tool accommodates a maximum of eight connected links. When multiple links are connected to a node (as is usually the case), different combinations of links may be used to construct a multilink trajectory analysis. The route configuration must be designed with the end product in mind. Sometimes multiple routes must be examined to obtain a complete picture of the operation.

There are two entry links and two exit links to the weaving segment, giving four possible routes for analysis. Two routes are examined in this example. The first route, which is represented in Exhibit 36-28, shows the traffic entering the weaving segment from the freeway and leaving to the freeway (V_{FF} in Exhibit 36-27), represented by Links 1-2-3-4. The second route will be examined in the next subsection.

Exhibit 36-28
Trajectory Plot for Freeway Links



In this multilane plot, in contrast to previous plots, some of the trajectory lines might cross each other because of different speeds in different lanes. One such instance is highlighted in Exhibit 36-28. This figure also shows vehicles that enter and leave the weaving segment on the ramps. Because the ramps are not part of the selected route, the ramp vehicles appear on the trajectory plot only on the link that represents the weaving segment. Examples of ramp vehicles are identified in the figure.

The definition of link density (vehicles per mile) is also indicated in Exhibit 36-28. Density as a function of time t is expressed in vehicles per mile and is determined by counting the number of vehicles within the link and dividing by the link length in miles. Average lane density (vehicles per mile per lane) on the

link may then be determined by dividing the link density by the number of lanes. To obtain individual lane densities, the trajectory analysis must be performed on each lane. The analysis must also be performed on a per lane basis to examine individual vehicle headways.

Vehicle Trajectories for the Entrance and Exit Ramps

By specifying the links on the route as 5-2-3-6 instead of 1-2-3-4, the trajectories for vehicles entering and leaving the weaving segment on the ramps (V_{RR} in Exhibit 36-27) can be examined. This trajectory plot is shown in Exhibit 36-29. This figure is similar to Exhibit 36-28, except that the vehicles that do not appear outside the weaving segment are those on the freeway links instead of the ramp links.

Two other routes can also be constructed, one for vehicles entering from the freeway and leaving to the exit ramp, V_{FR} as 1-2-3-6, and one for those entering from the ramp and leaving to the freeway, V_{RF} , as 5-2-3-4. These plots are not included here.

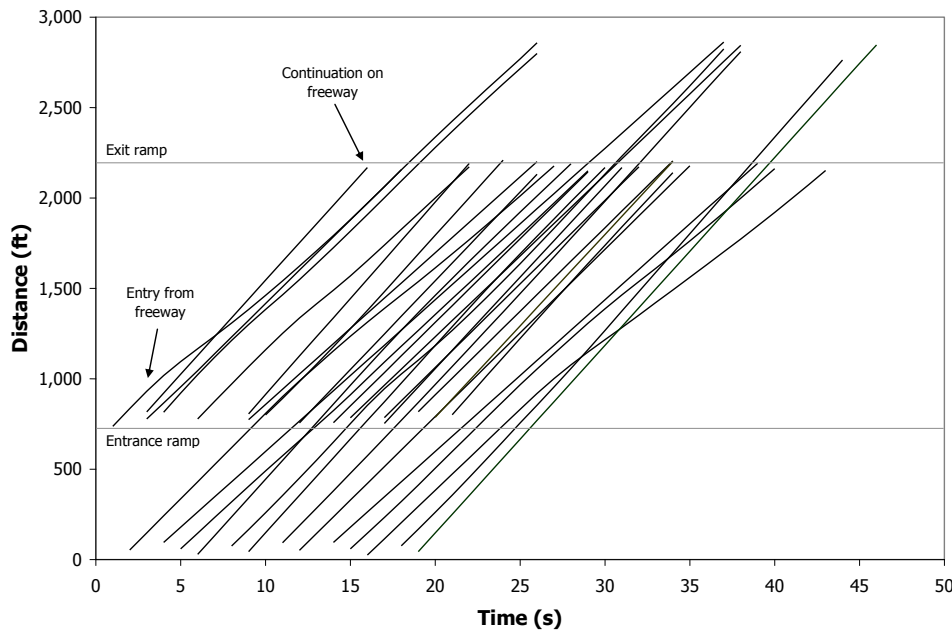


Exhibit 36-29
Trajectory Plot for Entrance and Exit Ramp Links

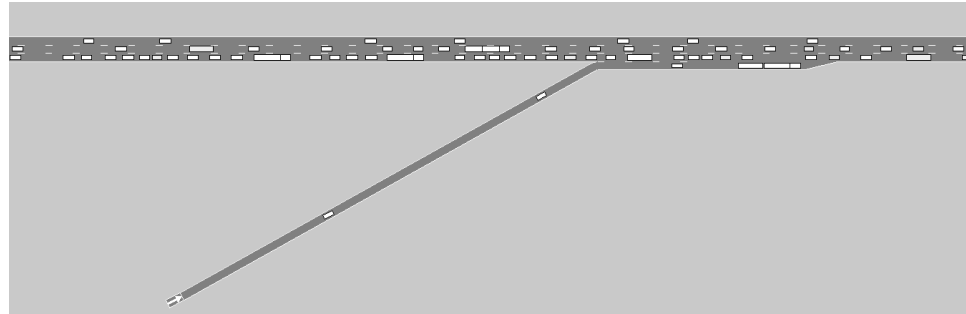
Entrance Ramp Merging Example

Merging segments provide another good example of vehicle trajectory analysis on a freeway. The merging vehicles affect freeway operation differently in each lane, so each lane must be examined independently.

Simulation Network Structure

The same node structure used in the weaving segment example is used here. The lane configuration has been changed to be more representative of a merge operation. Three lanes have been assigned to the freeway and one lane to the entrance ramp. The demand volumes have been specified to provide a near-saturated operation to observe the effects of merging under these conditions. A graphic view of the operation is presented in Exhibit 36-30.

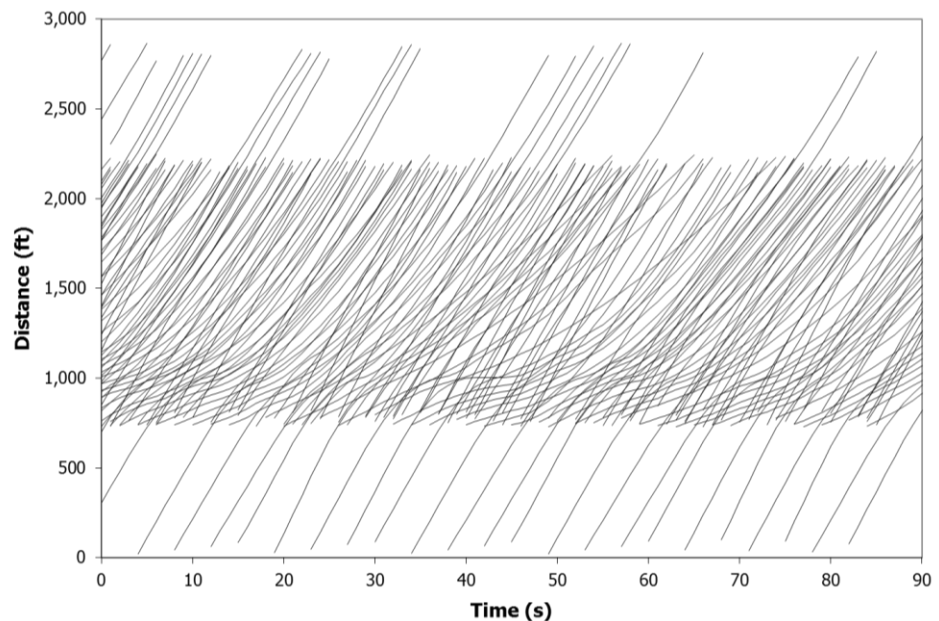
Exhibit 36-30
Entrance Ramp Merging
Segment Graphics View



Trajectory Plots for All Lanes

Exhibit 36-31 shows a trajectory plot for all freeway lanes combined within the merge area. The operation is clearly heterogeneous, with a mixture of fast and slow speeds. Many trajectory lines cross each other, and not much can be done in the way of analysis with these data.

Exhibit 36-31
Trajectory Plot for All Freeway
Lanes in the Merge Area



Trajectory Plots for Individual Lanes

Clearly, each lane must be examined individually. Exhibit 36-32, Exhibit 36-33, and Exhibit 36-34 show selected trajectories for Lanes 1, 2, and 3, respectively, from a later point in time in the simulation. Because these plots represent individual lanes, the trajectory lines do not cross each other. The effect of the merging operation is observable (and predictable) in these three figures.

In Lane 1, freeway speeds are low upstream of the merge point. Merging vehicles enter the freeway slowly but pick up speed rapidly downstream of the merge point bottleneck. The merging vehicles enter the freeway from the acceleration lane, which begins at 1,000 ft on the distance scale. The merging vehicle trajectories before entry onto the freeway are not shown in Exhibit 36-32 because those vehicles are either on a different link or in a different lane.

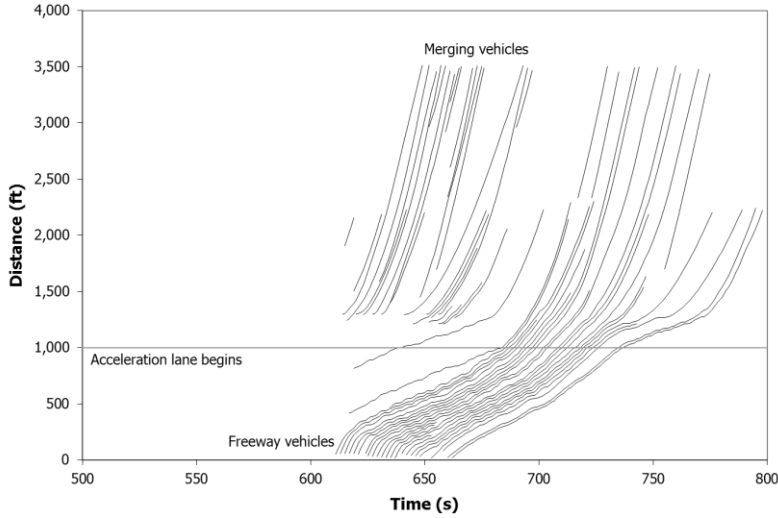


Exhibit 36-32
Trajectory Plot for Freeway Lane 1 (Rightmost) in the Merge Area

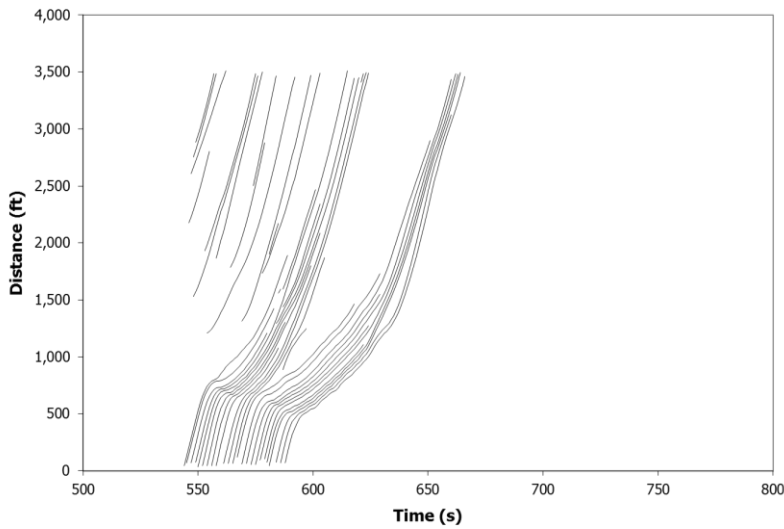


Exhibit 36-33
Trajectory Plot for Freeway Lane 2 (Center) in the Merge Area

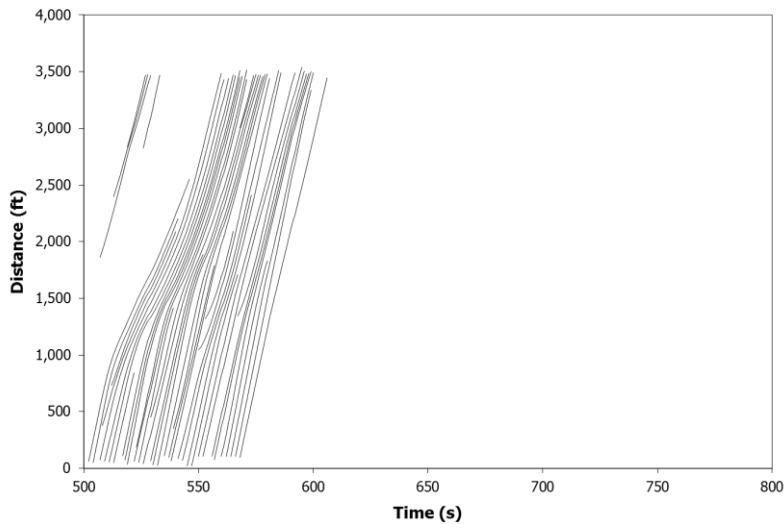


Exhibit 36-34
Trajectory Plot for Freeway Lane 3 (Leftmost) in the Merge Area

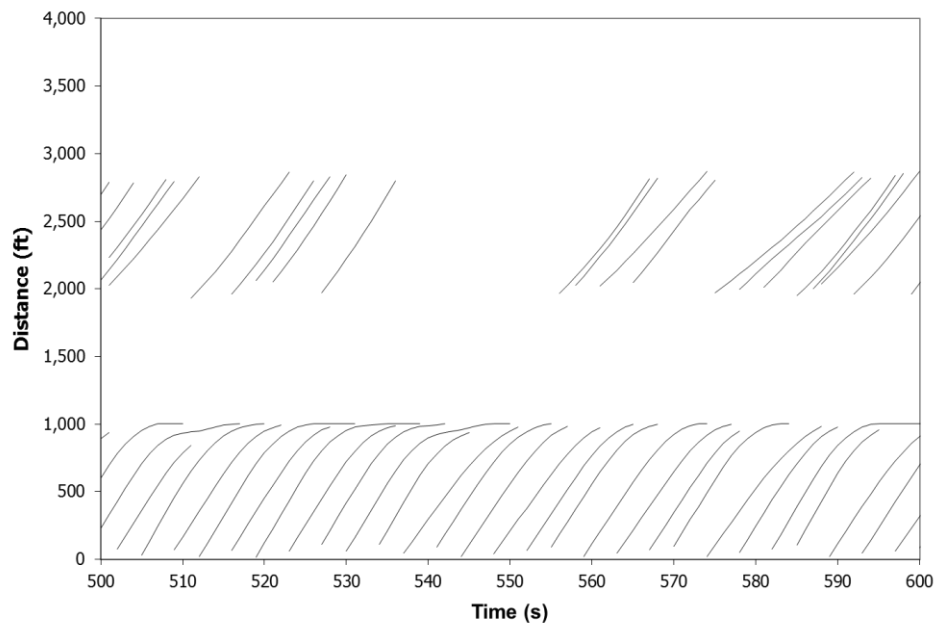
In Lane 2, the freeway speeds are higher but still well below the FFS, indicating that the merge operation affects the second lane as well. Some vehicles enter Lane 2 in the vicinity of the acceleration lane, but they are generally vehicles that have left Lane 1 to avoid the friction. Both Lane 1 and Lane 2 show several discontinuous trajectories that indicate lane changes. The Lane 3 operation is much more homogeneous and speeds are higher, indicating a much smaller effect of the merging operation.

Trajectory Plots for Ramp Vehicles

To configure a trajectory route covering the entrance ramp vehicles, the ramp and acceleration lane, which were not represented in Exhibit 36-32 through Exhibit 36-34, must be selected in place of the upstream freeway link. The acceleration lane number must first be identified from the simulation tool’s output. Because of the selected tool’s unique and somewhat creative lane numbering scheme, the acceleration lane will be Lane 9. To cover both the ramp and the acceleration lane, Lane 9 must be selected on the freeway link (2–3).

The trajectory plot for this route is shown in Exhibit 36-35. The results are not what might be anticipated. Vehicles are observed on the ramp and in the acceleration lane, but they disappear as soon as they enter the freeway. More vehicles eventually appear toward the end of the freeway link. The vehicles disappear because Lane 9 was selected for the freeway link, so vehicles in Lane 1 do not show up on the plot. The vehicles that reappear at the end of the link are those leaving the freeway at the downstream exit. They reappear at that point because the deceleration lane at the end of the link is also assigned as Lane 9. This plot is not particularly useful, except that it illustrates the complexities of trajectory analysis.

Exhibit 36-35
Trajectory Plot for
Acceleration and Deceleration
Lanes



To obtain a continuous plot of ramp vehicles, nodes must be added to the network at the points where the acceleration and deceleration lanes join the freeway. These nodes are shown as Nodes 7 and 8 in Exhibit 36-36. A continuous route may then be configured as 5–2–7–8–3–4. Selected trajectories from the trajectory plot for this route are shown in Exhibit 36-37. This plot shows the entering vehicles on the ramp as they pass through the acceleration lane onto the freeway. There are some discontinuities in the trajectories because of the different point at which vehicles leave the acceleration lane.

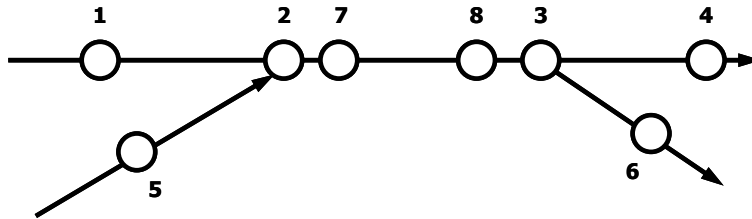


Exhibit 36-36
Addition of Intermediate Nodes for Continuous Trajectory Plots

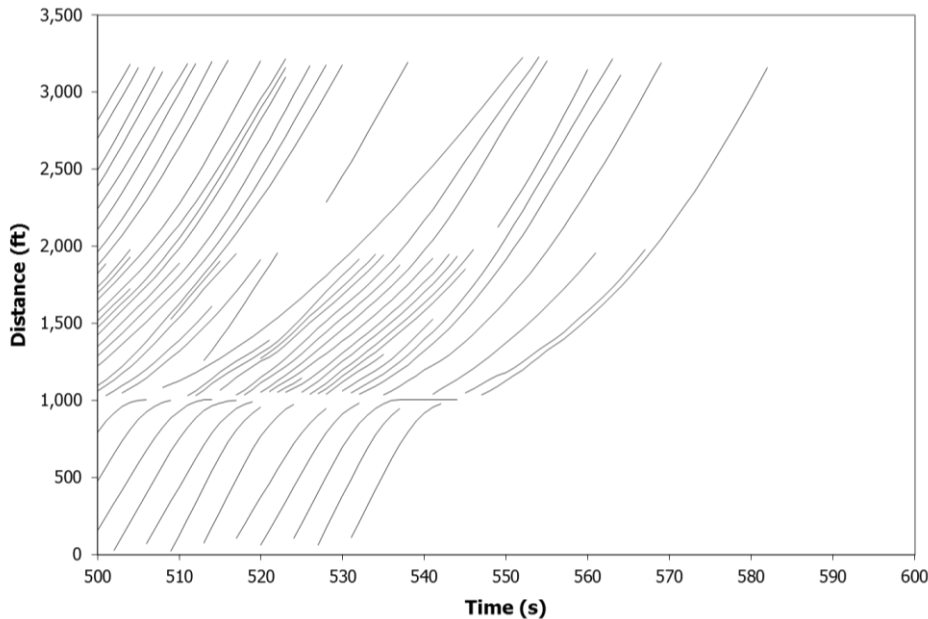


Exhibit 36-37
Trajectory Plot for Acceleration Lane and Freeway Lane 1

ESTIMATING PERFORMANCE MEASURES FROM VEHICLE TRAJECTORY DATA

The preceding subsections demonstrated that the production of vehicle trajectory plots that can be interpreted and analyzed is possible. This subsection focuses on computation of the performance measures from a mathematical analysis of the data represented in these plots.

Trajectory Analysis Procedures Overview

One development goal for the HCM 2010 was the creation of a set of computational procedures by which developers of simulation tools could produce performance measures that are consistent among different tools and, to the extent possible, compatible with the HCM's deterministic procedures. The procedures presented here were designed to be implemented easily by using the

common trajectory properties described previously and illustrated by examples. Developers of simulation tools are encouraged to implement these procedures, and users of simulation tools are encouraged to consider the extent to which the procedures have been implemented in the traffic analysis tool selection process described in Chapter 6, HCM and Alternative Analysis Tools.

Requirements for Trajectory Analysis Algorithm Development

A basic set of guidelines for computing uniform performance measures from vehicle trajectory analysis was introduced in Chapter 7, Interpreting HCM and Alternative Tool Results. Since these requirements are also incorporated into the specific computational procedures proposed in this chapter, they are repeated here to promote a better understanding of the procedures. The general guidelines suggested in Chapter 7 include the following:

1. The trajectory analysis procedures are limited to analysis of trajectories produced by the traffic flow model of each simulation tool. The nature of the procedures must not suggest the need for developers to change their driver behavior or traffic flow modeling logic.
2. If the procedures for estimating a particular measure cannot be satisfactorily defined to permit a valid comparison between the HCM and other modeling approaches, such comparisons should not be made.
3. All performance measures that accrue over time and space should be assigned to the link and time interval in which they occur. Subtle complexities make it impractical to do otherwise. For example, the root cause of a specific delay might not be within the link or the immediate downstream link. The delay might be secondary to a problem at some distant location in the network and in a different time interval.
4. The spatial and temporal boundaries of the analysis domain must include a period that is free of congestion on all sides. This principle is also stated in Chapter 10, Freeway Facilities Core Methodology, and in Chapter 19, Signalized Intersections, for multiperiod signalized intersection analysis. To ensure that delays to vehicles denied entry to the system during a given period are properly recognized, creation of fictitious links outside the physical network to hold such vehicles might be necessary. A more detailed discussion of spatial and temporal boundaries is provided in Chapter 7.
5. It is important to ensure that the network has been properly initialized or “seeded” before trajectory analysis is performed. When the warm-up periods are set and applied, simulation tools typically start with an empty network and introduce vehicles until the vehicular content of the network stabilizes. Trajectory analysis should not begin until stability has been achieved. If the simulation period begins with oversaturated conditions, stability may never be achieved. See the discussion in Chapter 7 on temporal and spatial boundaries.

In addition to the general guidelines, some requirements must be addressed here to promote the development of trajectory analysis procedures that can be

applied in a practical manner by the developers of simulation tools. The following requirements are suggested:

1. The algorithms must be suitable for computation “on the fly.” They must not require information from a future time step that would complicate the data handling within the simulation process.
2. Arbitrary thresholds for determining parameters should be kept to a minimum because of the difficulty of obtaining acceptance throughout the user community for specific thresholds. When arbitrary thresholds cannot be avoided, they should be justified to the extent possible by definitions in the literature, and above all, they should be applied consistently for different types of analysis.
3. Computationally complex and time-consuming methods should be avoided to minimize the additional load on the model. Methods should be developed to simplify situations with many special cases because of the difficulty of enumerating all special cases.
4. The same definitions, thresholds, and logic should be used for determination of similar parameters in different computational algorithms for longitudinal and spatial analysis.

Summary of Computational Procedures

Several performance measures were examined in Chapter 7, and general guidelines for comparing measures produced by different tools were presented. Previous material in this section has demonstrated the potential for development of uniform measures by individual vehicle trajectory analysis and has proposed some requirements for development of the analysis procedures. Specific procedures for analyzing vehicle trajectories are now presented and demonstrated with additional examples.

Thresholds for Computation of Performance Measures

Elimination of arbitrary and user-specified values is an important element of standardization. Avoidance of arbitrary thresholds was identified earlier as a requirement for the development of trajectory analysis procedures. Avoidance of all arbitrary thresholds is desirable. If thresholds cannot be avoided, they should be justified in terms of the literature. When no such justification exists, they should at least be established on the basis of consensus and applied consistently. The following thresholds cannot be avoided in vehicle trajectory analysis.

Car Length

The following is stated in Chapter 31, Signalized Intersections:
Supplemental:

A vehicle is considered as having joined the queue when it approaches within one car length of a stopped vehicle and is itself about to stop. This definition is used because of the difficulty of keeping track of the moment when a vehicle comes to a stop.

So, for estimation of queue-related measures, a value that represents one car length must be chosen. For the purposes of this section, a value of 20 ft is used.

Stopped-Vehicle State

One example of an arbitrary threshold is the speed at which a vehicle is considered to have come to a stop. Several arbitrary thresholds have been applied for this purpose. To maintain consistency with the definition of the stopped state applied in other chapters of the HCM, a speed less than 5 mi/h is used here for determining when a vehicle has stopped.

Moving-Vehicle States

Other states in addition to the stopped state that must be defined consistently for vehicle trajectory analysis include the following:

- The uncongested state, in which a vehicle is moving in a traffic stream that is operating below its capacity;
- The congested state, in which the traffic stream has reached a point that is at or slightly above its capacity, but no queuing from downstream bottlenecks is present; and
- The severely constrained state, in which downstream bottlenecks have affected the operation.

These states apply primarily to uninterrupted flow. A precise definition would require complex modeling algorithms involving capacity computations or “look ahead” features, both of which would create a computational burden. Therefore, an easily applied approximation must be sought. Threshold speeds are a good candidate for such an approximation.

These states can be thought of conveniently in terms of speed ranges. To avoid specifying arbitrary speeds as absolute values, use of the target speed of each vehicle as a reference is preferable. The target speed is the speed at which the driver prefers to travel. It differs from the FFS in the sense that most simulation tools apply a “driver aggressiveness” factor to the FFS to determine the target speed. In the absence of accepted criteria, three equal speed ranges are applied for the purposes of this section. Thus, the operation is defined as uncongested if the speed is above two-thirds of the target speed. It is defined as severely constrained when the speed is below one-third of the target speed, and it is considered congested in the middle speed range. This stratification is used to produce performance measures directly (e.g., percent of time severely constrained). It is also used in computing other performance measures (e.g., release from a queue).

Computational Procedures for Stop-Related Measures

The two main stop-related measures are number of stops and stopped delay. The beginning of a stop is defined in the same way for both measures. The end of a stop is treated differently for stopped delay and number of stops. For stopped delay, the end of a stop is established as soon as the vehicle starts to move (i.e., its speed reaches 5 mi/h or greater). For determining the number of stops, some hysteresis is required. For purposes of this section, after a vehicle is stopped a

subsequent stop is not recognized until it leaves the severely constrained state (i.e., its speed reaches one-third of the target speed).

Because subsequent stops are generally made from a lower speed, they can be expected to have a smaller impact on driver perception, operating costs, and safety. Recognizing this fact, the National Cooperative Highway Research Program (NCHRP) 03-85 project proposed a “proportional stop” concept (11), in which the proportion of a subsequent stop is based on the relative kinetic energy loss and is therefore proportional to the square of the speed from which the stop was made. Thus, each time a vehicle speed drops below 5 mi/h, the number of stops is incremented by $(S_{max}/S_{target})^2$, where S_{max} is the maximum speed attained since the last stop and S_{target} is the target speed.

This procedure has not been applied in practice. It is mentioned here because it offers an interesting possibility for the use of simulation to produce measures that could be obtained in the field but could not be estimated by the macroscopic deterministic models described in the HCM. The procedure is illustrated by an example later in this section.

Computational Procedures for Delay-Related Measures

The procedures for computing delay from vehicle trajectories involve aggregating all delay measures over each time step. Therefore, the results take the form of aggregated delay and not unit delay, as defined in Chapter 7. To determine unit delays, the aggregated delays must be divided by the number of vehicles involved in the aggregation. Partial trips made over a segment during the time period add some complexity to the unit delay computations.

The following procedures should be used to compute the various delay-related measures from vehicle trajectories:

- *Time step delay*: The delay on any time step is, by definition, the length of the time step minus the time the vehicle would have taken to cover the distance traveled in the step at the target speed. This value is easily determined and is the basis for the remainder of the delay computations.
- *Segment delay*: Segment delay is the time actually taken to traverse a segment minus the time that would have been taken to traverse the segment at the target speed. The segment delay on any step is equal to the time step delay. Segment delays accumulated over all time steps in which a vehicle is present on the segment represent the segment delay for that vehicle.
- *Queue delay*: Queue delay is equal to the time step delay on any step in which the vehicle is in a queued state; otherwise, it is zero. Queue delays are accumulated over all time steps while the vehicle is in a queue.
- *Stopped delay*: Stopped delay is equal to the time step delay on any step in which the vehicle is in a stopped state; otherwise, it is zero. Because a vehicle is considered to be “stopped” if it is traveling at less than a threshold speed, a consistent definition of stopped delay requires that the travel time at the target speed be subtracted. Time step delays

Queue delay computed from trajectory analysis provides the most appropriate representation of control delay.

accumulated over all time steps in which the vehicle was in the stopped state represent the stopped delay.

- *Control delay:* Control delay is the additional travel time caused by operation of a traffic control device. It cannot be computed directly from the vehicle trajectories in a manner consistent with the procedures given in Chapters 19 and 31 for signalized intersection analysis. However, it is an important measure because it is the basis for determining the level of service on a signalized approach.

The queue delay computed from vehicle trajectories provides a reasonable approximation of control delay when the following conditions are met:

1. The queue delay is caused by a traffic control device, and
2. The identification of the queued state is consistent with the definitions provided in this section.

Computational Procedures for Queue-Related Measures

Procedures for computing queue-related measures begin with determining whether each vehicle in a segment is in a queued state. A vehicle is in a queued state if it has entered a queue and has not yet left it. The beginning of a queued state occurs when

- The gap between a vehicle and its leader is less than or equal to 20 ft,
- The vehicle speed is greater than or equal to the leader speed, and
- The vehicle speed is less than or equal to one-third of the target speed (i.e., the speed is severely constrained).

A separate case must be created to accommodate the first vehicle to arrive at the stop line. If the link is controlled (interrupted-flow case), the beginning of the queued state also occurs when

- No leader is present on the link,
- The vehicle is within 50 ft of the stop line, and
- The vehicle is decelerating or has stopped.

These rules have been found to cover all the conditions encountered.

The ending of the queued state also requires some rules. For most purposes, the vehicle should be considered to remain in the queue until it leaves the link. The analysis is done on a link-by-link basis. In the case of queues that extend over multiple links, a vehicle leaving a link immediately enters the queue on the next link. Experience with trajectory analysis has shown that other conditions need to be applied to supplement this rule. Thus, the end of the queued state also occurs when

- The vehicle has reached two-thirds of the target speed (i.e., uncongested operation), and
- The leader speed is greater than or equal to the vehicle speed or the vehicle has no leader in the same link.

The additional conditions cover situations in which, for example, a vehicle escapes a queue by changing lanes into an uncongested lane (e.g., through vehicle caught temporarily in a turn bay overflow).

Chapters 19 and 31 offer the following guidance on estimating queue length:

1. The maximum queue reach (i.e., back of queue, or BOQ) is a more useful measure than the number of vehicles in the queue, because the BOQ causes blockage of lanes. The maximum BOQ is reached when the queue has almost dissipated (i.e., has zero vehicles remaining).
2. A procedure is prescribed to estimate average maximum BOQ on a signalized approach.

Because of its macroscopic nature, the HCM queue estimation procedure cannot be applied directly to simulation. On the other hand, simulation can produce additional useful measures because of its higher level of detail. The first step in queue length determination has already been dealt with by setting up the rules for determining the conditions that indicate when a vehicle is in a queue. The next step is to determine the position of the last vehicle in the queue.

The BOQ on any step is a relatively simple thing to determine. The trick is to figure out how to accumulate the individual BOQ measures over the entire period. Several measures can be produced.

1. The maximum BOQ at some percentile value—for example, 95%;
2. The maximum BOQ on any cycle at some percentile value—for example, 95%;
3. The historical maximum BOQ (i.e., the longest queue recorded during the period);
4. The probability that a queue will back up beyond a specified point; and
5. The proportion of time that the queue will be backed up beyond a specified point.

Some of these measures are illustrated later in an example.

Computational Procedures for Density-Related Measures

The uninterrupted-flow procedures described in the HCM base their LOS estimates on the density of traffic in terms of passenger cars per mile per lane (pc/mi/ln). In one case (freeway merges and diverges), the density is estimated only for the two lanes adjacent to the ramp.

Density computations do not require a detailed analysis of the trajectory of each vehicle. They are best made by simply counting the number of vehicles in each lane on a given segment, recognizing that the results represent actual vehicles and not passenger cars.

For comparable results, the simulated densities must be converted to pc/mi/ln, especially if simulation tools are used to evaluate the LOS on a segment. Because the effect of heavy vehicles on the flow of traffic is treated microscopically, there is no notion of passenger car equivalence in simulation modeling. In addition, traffic flow models may differ among the various simulation tools in their detailed treatment of heavy vehicles. Therefore, a simple

The BOQ at any time step will be determined by the position of the last queued vehicle on the link plus the length of that vehicle.

conversion process that will ensure full compatibility with the HCM's LOS estimation procedures cannot be prescribed. One possible method for developing passenger car equivalence conversion factors involves multiple simulation runs:

1. Use the known demand flow rates, v , and truck proportions to obtain the resulting segment density in vehicles per mile per lane (veh/mi/ln), d_1 .
2. Use the known demand flow rates, v , with passenger cars only to obtain the resulting segment density in veh/mi/ln, d_2 .
3. Determine the heavy vehicle equivalence factor as $f_{HV} = d_2/d_1$.
4. Set the demand flow rates to v/f_{HV} with passenger cars only to obtain the resulting segment density in pc/mi/ln.

This process is more precise because it adheres to the definition of passenger car equivalence. Unfortunately, it is too complicated to be of much practical value. However, two methods could produce a more practical approximation. Both require determining the heavy vehicle adjustment factor, f_{HV} , by the method prescribed in Chapter 12 for basic freeway segments. This method is also referenced and used in the procedural chapters covering other types of freeway segments. The simplest approximation may be obtained by running the simulation with known demand flow rates and truck proportions and then dividing the simulated density by f_{HV} . Another approximation involves dividing the demand flow rates by f_{HV} before running the simulation with passenger cars only. The resulting densities are then expressed in pc/mi/ln. The second method conforms better to the procedures prescribed in Chapters 11 to 13, but the first method is probably easier to apply.

Follower density is an emerging density-based measure for two-lane highways (12, 13). It is defined as the number of followers per mile per lane. A vehicle can be classified as following when

- The gap between the rear and the front ends of the leading and following vehicles, respectively, are shorter than or equal to 3 s; and
- The speed of the following vehicle is not more than 12 mi/h lower than that of the preceding vehicle.

The follower density can be derived from point measurements by means of the following formula:

$$\text{Follower density} = \% \text{ followers} \times \text{flow rate} / \text{time mean speed}$$

Although this performance measure is not computed by the procedures in the HCM, it is mentioned because it has attracted significant international interest and can easily be computed by vehicle trajectory analysis.

Equation 36-1

Analysis of a Signalized Approach

The simple approach to a signalized intersection (Exhibit 36-20) is now converted to a two-lane approach with a length of 2,000 ft. A 10-min (600-s) analysis period is used. The cycle length is 60 s, giving 10 cycles for inspection. The analysis period would normally be longer, but 10 min is adequate for demonstration purposes.

Trajectory Plots

The trajectory plot for the first few cycles is shown in Exhibit 36-38. The vehicle track selected for later analysis is also shown in this exhibit.

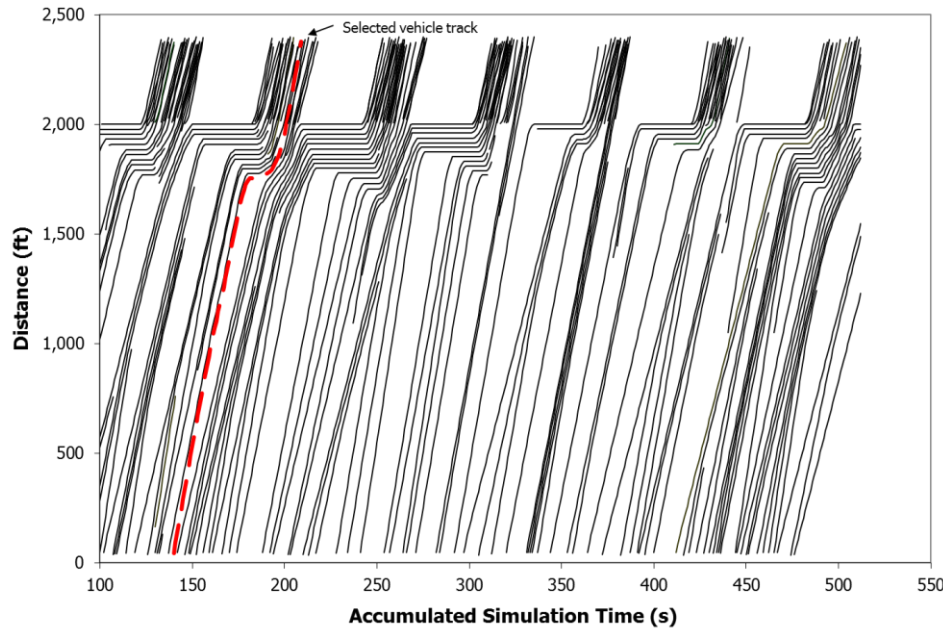
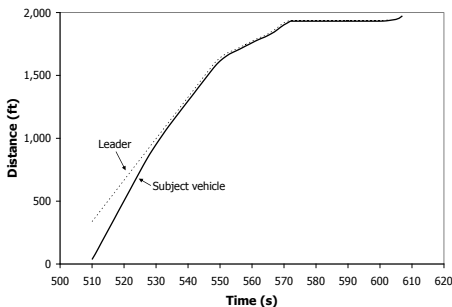
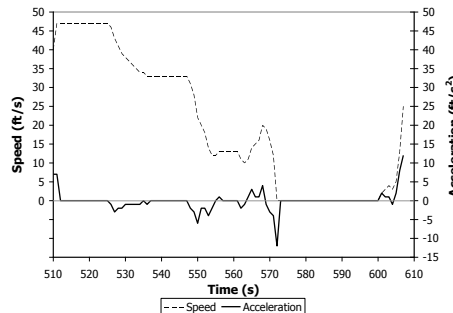


Exhibit 36-38
Trajectories for Several Cycles on a Signalized Approach

Two individual trajectory analysis plots are shown in Exhibit 36-39. The first plot shows the trajectories of two vehicles where the progress of the subject vehicle is constrained by its leader. The second plot shows the speed and acceleration profiles for the subject vehicle.



(a) Subject Vehicle and Leader Vehicle Trajectories



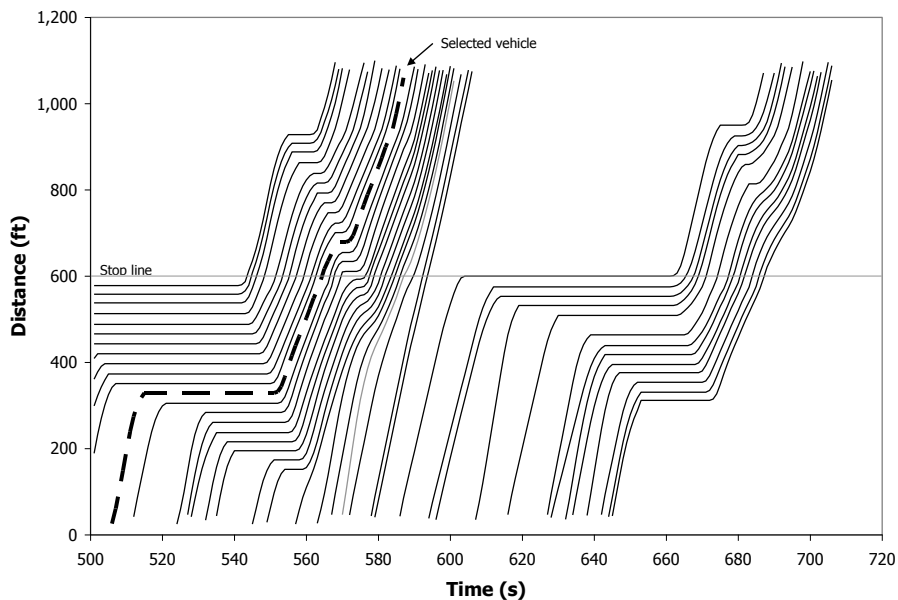
(b) Speed and Acceleration Profile of Subject Vehicle

Exhibit 36-39
Example Trajectory Analysis Plots

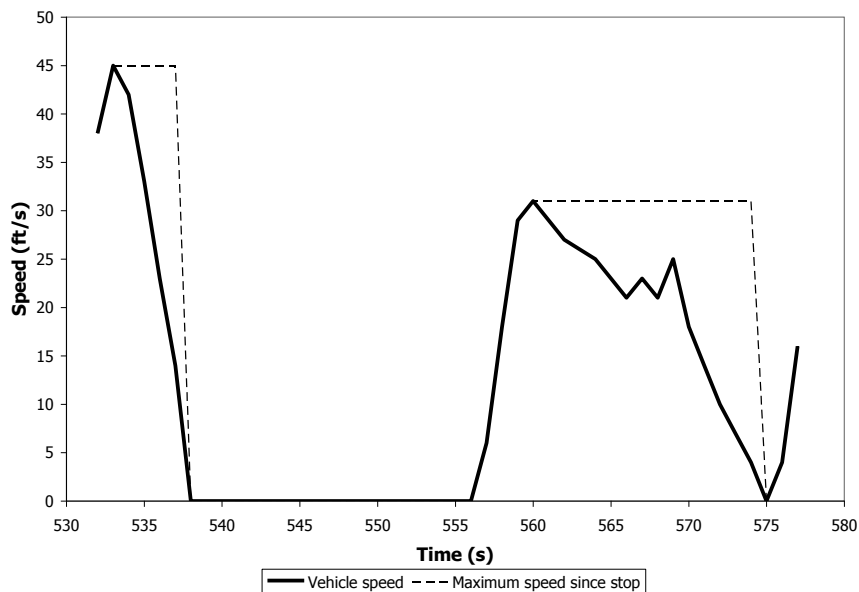
Exhibit 36-40
Analysis of a Full and a Partial Stop

Analysis of Stops

An example of the analysis of a single vehicle selected from the entire trajectory plot is shown in Exhibit 36-40. With the definition of a partial stop based on the NCHRP 03-85 kinetic energy loss concept, the total stop value was 1.81 because the second stop was made from a lower speed.



(a) Vehicle Trajectories



(b) Selected Vehicle Speed

Segment delay	Queue delay	Stop delay	Number of stops
34.64 s	33.23 s	20 s	1.81

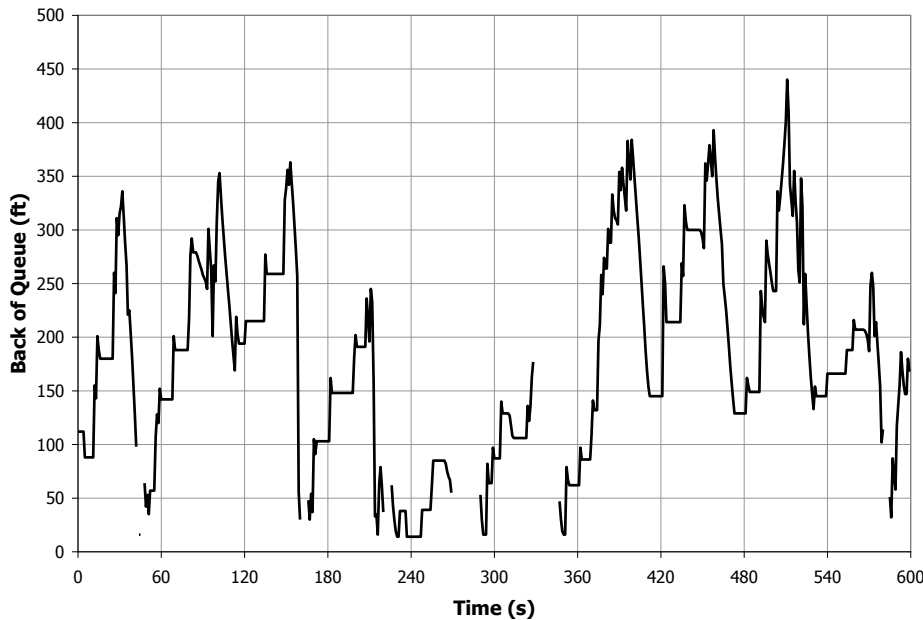
(c) Performance Measures for Selected Vehicle

Queuing Analysis

Exhibit 36-41(a) illustrates the queue length (BOQ) per step for one lane of the signalized approach over all the time steps in the period. The 10 cycles are discernible in this figure. Also, a considerable variation in the cyclical maximum BOQ is evident.

The percentile instantaneous BOQ and the percentile maximum BOQ per cycle should be distinguished. For the instantaneous BOQ, the individual observation is the BOQ on any step, so the sample size is the number of steps covered (600 in this case). For cyclical maximum BOQ, the individual observation is the maximum BOQ in any cycle, so the sample size is the number of cycles (10 in this case). The maximum BOQ in any cycle can be determined only by inspecting the plotted instantaneous values. No procedure is proposed here for automatic extraction of the maximum cyclical BOQ from the instantaneous BOQ data.

A statistical analysis showing the average BOQ, the 95th percentile BOQ (based on 2 standard deviations past the average value), and the historical maximum BOQ is presented in Exhibit 36-41(b). One important question is whether the 95% BOQ can be represented statistically on the basis of the standard deviation, assuming a normal distribution. The BOQ histogram showing the distribution of instantaneous BOQ for the 600 observations is shown in Exhibit 36-42. The appearance of this histogram does not suggest any analytical distribution; however, the relationship between the 95% BOQ and the historical maximum appears to be reasonable for this example.



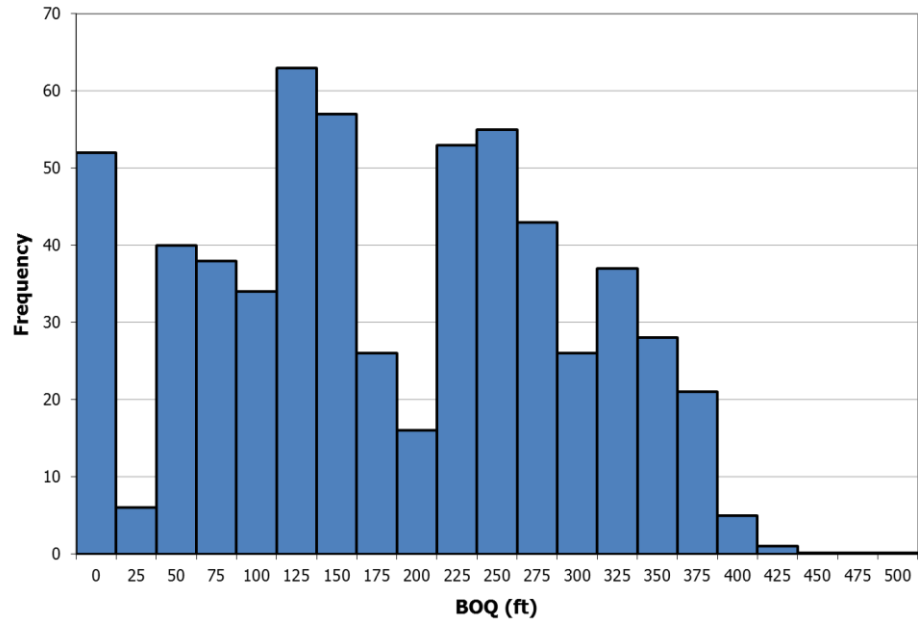
(a) BOQ Plot

Average queue 174 ft	Standard deviation 110 ft	95th percentile queue 395 ft	Maximum queue 440 ft
-------------------------	------------------------------	---------------------------------	-------------------------

(b) Queue-Related Performance Measures

Exhibit 36-41
BOQ Analysis by Time Step

Exhibit 36-42
BOQ Histogram

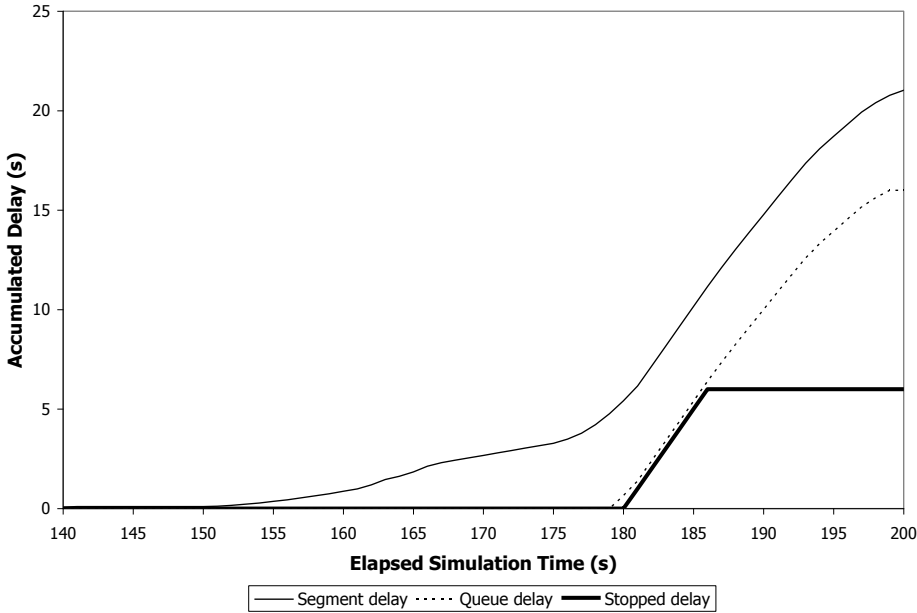


The queue length on an isolated approach that is close to saturation will have a near uniform distribution (i.e., equal probability of all lengths between zero and the maximum). The standard deviation of a uniform distribution is greater than one-half of the mean, so the 95th percentile estimator (mean value plus 2 standard deviations) will be greater than the maximum value. This situation raises some doubt about the validity of basing the 95th percentile BOQ on the standard deviation, especially with cyclical queuing.

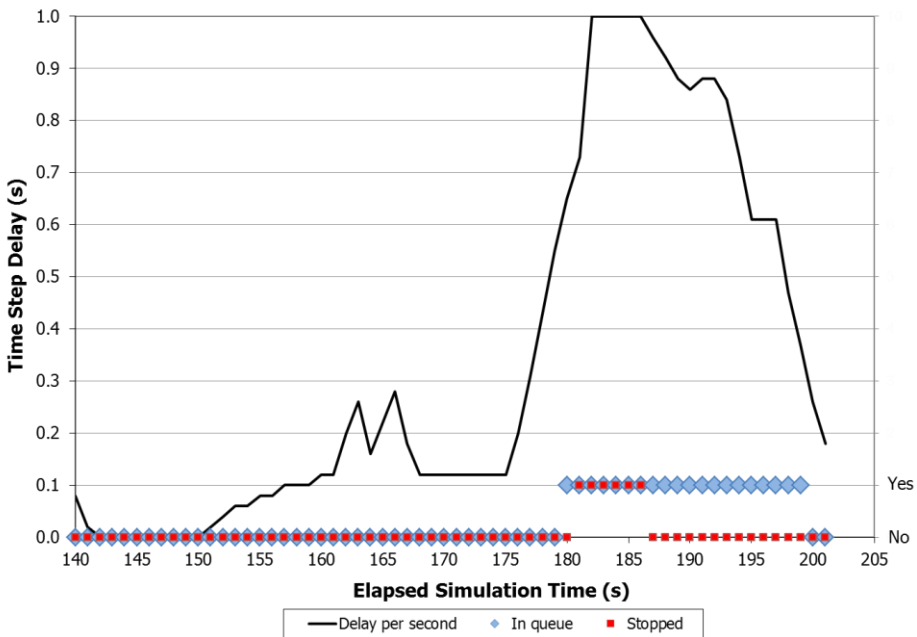
Delay Analysis for a Single Trajectory

A comparison of the accumulated delay by all definitions for the selected vehicle track indicated in Exhibit 36-38 is presented in Exhibit 36-43(a). The relationships between segment delay, queue delay, and stopped delay are evident in this figure. The segment delay begins to accumulate before the vehicle approaches the intersection because of midsegment interactions that reduce the speed below the target speed. The queue delay begins to accumulate as the vehicle enters the queue, and the stopped delay begins to accumulate a few seconds later. The stopped delay ceases to accumulate as soon as the vehicle starts to move, but the queue delay continues to accumulate until the vehicle leaves the link.

The time step delay analysis plots shown in Exhibit 36-43(b), based on 1-s time steps, provide additional insight into the operation. The time step delay is close to zero as the vehicle enters the segment, indicating that the speed is close to the target speed. Small delays begin to accumulate in advance of the intersection. The accumulation becomes more rapid when the vehicle enters the queue. The periods when the vehicle is in the stopped and the queued state are also shown in this figure.



(a) Accumulated Delay



(b) Time Step Delay

Exhibit 36-43
Accumulated Delay by Various Definitions

As was indicated previously, the value of control delay cannot be determined by simulation in a manner that is comparable with the procedures prescribed in Chapters 19 and 31. Because this segment terminates at a signal, it is suggested that the queue delay would provide a reasonable estimate of control delay because the queue delay offers a close approximation to the delay that would be measured in the field.

Delay Analysis for All Vehicles on the Segment

The preceding example dealt with accumulated delay of a single vehicle traversing the segment. A useful delay measure requires the accumulation of delay to all vehicles traversing the segment during the period. An example is shown in Exhibit 36-44. In keeping with the recommendations offered elsewhere (14), only vehicles that traversed the entire link during the period are included in this analysis. Therefore, the number of vehicles analyzed (210) is lower than the number of vehicles that were actually on the link during the period (286).

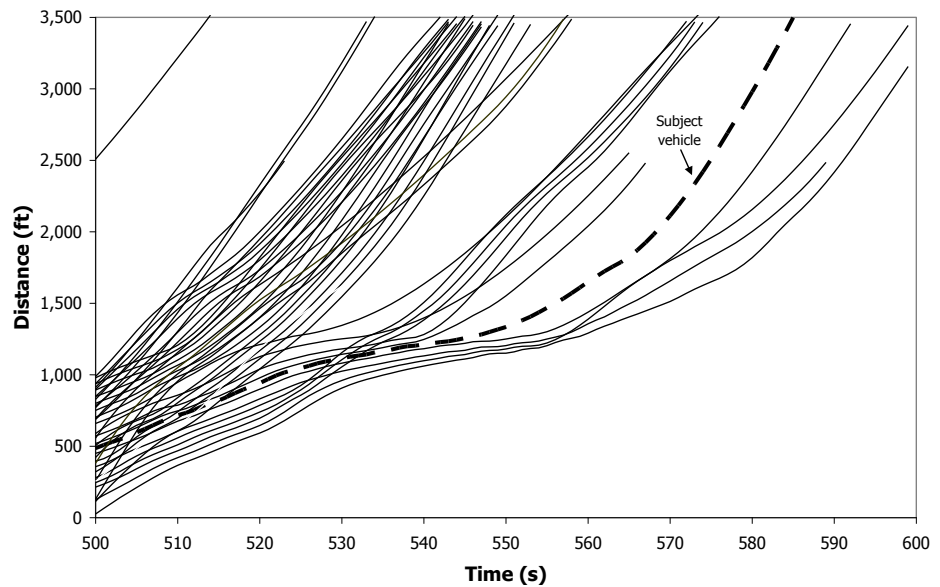
Exhibit 36-44
Delay Analysis for All Vehicles on a Segment

	Segment Delay (s)	Queue Delay (s)	Stop Delay (s)	No. of Stops
Lane 1	3,128	2,562	1,957	95.4
Lane 2	3,400	2,793	2,047	96.2
Total	6,529	5,355	4,004	191.6
Average per vehicle	31.09	25.50	19.07	0.91

Analysis of a Freeway Segment

A performance analysis of the freeway weaving area originally shown in Exhibit 36-27 is presented here. A single vehicle is selected from the trajectory plot and its trajectory is analyzed. The results are shown in Exhibit 36-45. The analysis produced segment delay and queue delay. This segment was very congested, as indicated by the trajectory plot. No stopped delay was produced because the vehicle never actually came to a stop (i.e., its speed stayed above 5 mi/h).

Exhibit 36-45
Longitudinal Analysis of Delay for a Selected Vehicle in a Weaving Area



(a) Vehicle Trajectories

Segment delay Queue delay Stopped delay
39.58 s 37.01 s 0 s

(b) Delay-Related Performance Measures for Subject Vehicle

A spatial analysis of the entire segment can also be performed to produce the following measures by lane:

- Average density over the segment,
- Percent slow vehicles (i.e., traveling at less than two-thirds the target speed),
- Percent queued vehicles,
- Average queue length (measured from front of queue to BOQ),
- Average BOQ position,
- Maximum BOQ position, and
- Percent of time steps when the queue overflowed the segment.

The results are presented in tabular form in Exhibit 36-46. The values are presented by lane, and the exhibit note presents combined density values for Lanes 1 and 2 for compatibility with the HCM definition of merge area density.

	Lane 1	Lane 2	Lane 3	Acceleration Lane
Average density (veh/mi/ln)	73.4	51.0	43.6	9.9
Percent slow vehicles (%)	88.4	68.5	41.5	65.7
Percent queued vehicles (%)	63.4	22.0	2.4	26.7
Average queue length (ft)	600	215	15	40
Average back of queue (ft)	1,471	1,119	135	562
Maximum back of queue (ft)	1,497	1,497	1,492	1,474
Percent overflow	66.1	29.6	0.5	0.17

Note: Average Lane 1 and Lane 2 density is 62.2 veh/mi/ln.

Exhibit 36-46
Example Spatial Analysis by Lane

6. SUMMARY OF CHANGES FROM HCM2000 TO HCM 2010

INTRODUCTION

This section documents the major research projects that contributed to the previous edition of the manual, the HCM 2010. The What's New in the HCM Sixth Edition section of Chapter 1, HCM User's Guide, describes the new research incorporated into the present edition of the HCM.

OVERVIEW

Research Basis for the Preupdate HCM 2010

Exhibit 36-47 lists the major research projects that contributed to the HCM 2010. The impacts of these and other projects on individual HCM chapters are described later in this section.

Focus Groups

After the publication of the HCM2000, the Transportation Research Board's Committee on Highway Capacity and Quality of Service sponsored a series of focus groups at various locations around the United States to obtain feedback and to identify desired improvements for the next edition. Committee and subcommittee members also prepared an audit of the HCM in the areas of planning, design and operations, and educational needs (15). After the HCM 2010 was funded, the Institute of Transportation Engineers sponsored a web-based survey on HCM usage and desired improvements, and NCHRP Project 03-92 organized several focus groups on those topics. The feedback from these and other sources was considered when decisions were made on the format, content, and organization of the HCM 2010.

Reorganization from the HCM2000

The HCM 2010 consisted of four volumes: (a) Volume 1: Concepts, (b) Volume 2: Uninterrupted Flow, (c) Volume 3: Interrupted Flow, and (d) Volume 4: Applications Guide. Material from Parts I to V of the HCM2000 was distributed into Volumes 1 to 4 of the HCM 2010 as follows:

- *Part I: Overview* material appeared in Volume 1.
- *Part II: Concepts* material appeared in Volumes 2 and 3 if used directly in an analysis (e.g., default values and LOS tables) and in Volume 1 otherwise.
- *Part III: Methodologies* material appeared in Volume 2 for uninterrupted-flow chapters and Volume 3 for interrupted-flow chapters. Worksheets and highly detailed descriptions of methodological steps appeared in the Volume 4 chapters.
- *Part IV: Corridor and Area-wide* material that is conceptual in nature appeared in Volume 1. More detailed analytical material was removed in favor of guidance in the use of alternative tools for corridor and area-wide analyses.

- *Part V: Simulation and Other Models* material was distributed throughout the HCM 2010. Volume 1 contained an overview of alternative tools (Chapter 6) and general guidance on comparing HCM and alternative results (Chapter 7). Specific guidance on when to consider alternative tools was presented in each chapter in Volumes 2 and 3. Selected Volume 4 chapters provided examples of applying alternative tools to situations that cannot be addressed by HCM methodologies.

Project	Project Title	Project Objective(s)
NCHRP 03-60	Capacity and Quality of Service of Interchange Ramp Terminals	Develop improved methods for capacity and quality-of-service analysis of interchange ramp terminals for a full range of interchange types.
NCHRP 03-64	<i>Highway Capacity Manual Applications Guide</i>	Develop an HCM Applications Guide that shows how to apply HCM methodologies to real-world problems and indicates when other methods may be more appropriate.
NCHRP 03-65	Applying Roundabouts in the United States	Develop methods for estimating the safety and operational impacts of U.S. roundabouts and refine the design criteria used for them.
NCHRP 03-70	Multimodal Level of Service Analysis for Urban Streets	Develop a framework and enhanced methods for determining levels of service for automobile, transit, bicycle, and pedestrian modes on urban streets, in particular with respect to the interaction among the modes.
NCHRP 03-75	Analysis of Freeway Weaving Sections	Develop improved methods for capacity and LOS analysis of freeway weaving sections.
NCHRP 03-79	Measuring and Predicting the Performance of Automobile Traffic on Urban Streets	Develop techniques for measuring the performance of automobile traffic on urban streets for real-time applications; develop procedures for predicting the performance of automobile traffic on urban streets.
NCHRP 03-82	Default Values for Capacity and Quality of Service Analyses	Determine appropriate default values for inputs to HCM analyses; develop a guide to select default values for various applications.
NCHRP 03-85	Guidance for the Use of Alternative Traffic Analysis Tools in Highway Capacity Analyses	Enhance the guidance in the HCM for the selection and use of alternative traffic analysis tools.
NCHRP 03-92	Production of the Year 2010 <i>Highway Capacity Manual</i>	Develop the 2010 edition of the HCM.
Federal Highway Administration	Evaluation of Safety, Design, and Operation of Shared-Use Paths (DTFH61-00-R-00070)	Develop an LOS estimation method for shared-use paths to assist path designers and operators in determining how wide to make new or rebuilt paths and whether to separate the different types of users.
Federal Highway Administration	Active Traffic Management Measures for Increasing Capacity and Improving Performance (DTFH61-06-D-00004)	Describe active traffic management techniques and available information and analysis methods for evaluating their effectiveness in increasing highway facility capacity and improving operational performance.

Exhibit 36-47
Major Research Projects Contributing to the Preupdate HCM 2010

Multimodal Approach

To encourage HCM users to consider all travelers on a facility when they perform analyses and make decisions, the HCM 2010 integrated material on nonautomobile and automobile modes. Thus, there were no stand-alone Pedestrian, Bicycle, and Transit chapters in this edition. Instead, users were referred to the Urban Streets chapter for analysis procedures for pedestrians, bicyclists, and transit users on urban streets; to the Signalized Intersections chapter for procedures relating to signalized intersections; and so on.

In recognition of the companion *Transit Capacity and Quality of Service Manual* (TCQSM) (16) and of the difficulty in keeping the two manuals in synch, users were referred to the TCQSM for transit-specific capacity and quality-of-service procedures. However, transit quality of service in a multimodal context continued to be addressed in the HCM.

Traveler Perception Models

Since the 1985 HCM, LOS was defined in terms of measures of operational conditions within a traffic stream (17, 18). HCM methodologies have generally presented a single LOS measure per system element that can be (a) directly measured in the field, (b) perceived by travelers, and (c) affected by facility owners. However, since the publication of the HCM2000, a number of research projects studied whether a single operational factor is sufficient to describe LOS, as well as whether nonoperational factors should also be used (19). These projects proposed models that (a) incorporated multiple factors of traveler satisfaction and (b) set LOS thresholds based on traveler perceptions of service quality. Traveler perception models from two of these studies (20, 21) were incorporated into the Multilane Highways, Two-Lane Highways, Urban Street Facilities, Urban Street Segments, and Off-Street Pedestrian and Bicycle Facilities chapters.

Generalized Service Volume Tables

The HCM2000 provided “example service volume tables” for 10 system elements. The service volume tables were developed by using a single set of default values and were accompanied by cautionary notes that they were illustrative only. The HCM 2010 provided “generalized service volume tables” for facilities that incorporate a range of national default values. These tables could be considered for such applications as statewide performance reporting, areawide (i.e., regional) modeling, and future-year analyses as part of a long-range transportation planning process.

METHODOLOGICAL CHANGES BY SYSTEM ELEMENT

Freeway Facilities

The basic methodology was similar to the one given in the HCM2000 but incorporated a new weaving-segment analysis procedure. A significant change was the addition of LOS thresholds for freeway facilities based on density. Other changes included updates to the material on the impact of weather and work zones on freeway facility capacity, along with new information on the impact of active traffic management measures on freeway operations.

Basic Freeway Segments

The basic methodology was similar to the one given in the HCM2000. The FFS prediction model was improved, and a speed-flow curve for segments with a 75-mi/h FFS was added.

Freeway Weaving Segments

This chapter was completely updated and incorporated the methodology developed by NCHRP Project 03-75. Although the general process for analyzing weaving segments was similar to that given in the HCM2000, the HCM 2010 models was based on an up-to-date set of weaving data. The following are the two major differences in how the methodology is applied: (a) a single algorithm for predicting weaving speeds and a single algorithm for predicting nonweaving speeds were provided, regardless of the weaving configuration, and (b) the LOS F threshold was changed.

Ramps and Ramp Junctions

The following revisions were made to the HCM2000 methodology:

- Procedures were added to check for unreasonable lane distributions that overload the left or right lane(s) (or both) of the freeway.
- A revision was made to correct an illogical trend involving on-ramps on eight-lane freeways in which density increases as the length of the acceleration lane increases.

Multilane Highways

The multilane highways automobile methodology was essentially the same as that given in the HCM2000. A methodology for calculating bicycle LOS for multilane highways was added.

Two-Lane Highways

The following revisions were made to the HCM2000 automobile methodology:

- The two-direction analysis was dropped: the one-direction methodology is the only one used, with two-direction results obtained by appropriate weighted averaging of the one-direction results.
- Several key curves and tables used in one-direction analyses were adjusted and incorporated into the chapter.

A bicycle LOS methodology for two-lane highways was added.

Urban Street Facilities

This was a new chapter containing guidance to help analysts determine the scope of their analysis (i.e., isolated intersection versus coordinated signal system) and the relevant travel modes (i.e., automobile, pedestrian, bicycle, transit, or a combination). The methodology section described how to aggregate results from the segment and point levels of analysis into an overall facility assessment. Information on the impact of active traffic management measures on urban street performance was added.

Urban Street Segments

This chapter was completely rewritten. The work of NCHRP Project 03-79 was incorporated into the chapter, providing improved methods for estimating urban street FFS and running times, along with a new method for estimating the stop rate along an urban street. In addition, the work of NCHRP Project 03-70 was incorporated, providing a multimodal LOS methodology that could be used to evaluate trade-offs in how urban street right-of-way is allocated among the modes using the street.

Signalized Intersections

The following revisions were made to the HCM2000 methodology:

- A new incremental queue accumulation method was added to calculate the d_1 delay term and the Q_1 length term. It was equivalent to the HCM2000 method for the idealized case but was more flexible to accommodate nonideal cases, including coordinated arrivals and multiple green periods with differing saturation flow rates (i.e., protected-plus-permitted left turns and sneakers).
- An actuated controller operation modeling procedure was added.
- A left-turn lane overflow check procedure was added.
- Pedestrian and bicycle LOS methodologies relating to signalized intersections were moved into this chapter.

Unsignalized Intersections

The HCM2000's Unsignalized Intersections chapter was split into three chapters: two-way STOP-controlled intersections, all-way STOP-controlled intersections, and roundabouts.

Two-Way STOP-Controlled Intersections

The two-way STOP-controlled intersection methodology for the automobile mode was essentially the same as the one given in the HCM2000, except gap-acceptance parameters for six-lane streets were added. Furthermore, pedestrian and bicycle LOS methodologies relating to two-way STOP-controlled intersections were moved into this chapter.

All-Way STOP-Controlled Intersections

The all-way STOP-controlled intersection methodology was essentially the same as the one given in the HCM2000. A queue-estimation model was added.

Roundabouts

This chapter replaced the HCM2000 roundabout content. It was based on the work of NCHRP Project 03-65, which developed a comprehensive database of U.S. roundabout operations and new methodologies for evaluating roundabout performance. A LOS table for roundabouts was added.

Interchange Ramp Terminals

Material on interchange ramp terminals was completely updated on the basis of NCHRP Project 03-60.

Off-Street Pedestrian and Bicycle Facilities

The pedestrian path procedures were essentially the same as those of the HCM2000, but guidance was provided on how to apply the procedures to a wider variety of facility types. The bicycle path procedures, which were based on Dutch research in the HCM2000, were updated on the basis of results of an FHWA study to calibrate the Dutch model for U.S. conditions and increase the number of path user groups (e.g., inline skaters and runners) addressed by the procedures.

7. REFERENCES

Some of these references can be found in the Technical Reference Library in Volume 4.

1. Tufte, E. R. *The Visual Display of Quantitative Information*. Graphics Press, Cheshire, Conn., 1983.
2. Zegeer, J., J. Bonneson, R. Dowling, P. Ryus, M. Vandehey, W. Kittelson, N. Roupail, B. Schroeder, A. Hajbabaie, B. Aghdashi, T. Chase, S. Sajjadi, R. Margiotta, and L. Elefteriadou. *Incorporating Travel Time Reliability into the Highway Capacity Manual*. SHRP 2 Report S2-L08-RW-1. Transportation Research Board of the National Academies, Washington, D.C., 2014.
3. National Institute of Statistics and Sematech. *E-Handbook of Statistical Methods*. <http://www.itl.nist.gov/div898/handbook/index.htm>. Accessed March 9, 2015.
4. Greenwood, J., and M. Sandomire. Sample Size Required for Estimating the Standard Deviation as a Percent of Its True Value. *Journal of the American Statistical Association*, Vol. 45, No. 250, June 1950, pp. 257–260.
5. Federal Highway Administration. National Performance Management Research Data Set (NPMRDS) Technical Frequently Asked Questions. http://www.ops.fhwa.dot.gov/freight/freight_analysis/perform_meas/vpds/npmrdsfaqs.htm. Accessed April 24, 2015.
6. Turner, S. *Quality Control Procedures for Archived Operations Traffic Data: Synthesis of Practice and Recommendations*. Final Report, Contract DTFH61-97-C-00010. Federal Highway Administration, Washington, D.C., March 2007.
7. INRIX and I-95 Corridor Coalition. I-95 Vehicle Probe Data website. <http://www.i95coalition.org/i95/VehicleProbe/tabid/219/Default.aspx>. Accessed Aug. 10, 2012.
8. California Department of Transportation. California Performance Measurement System (PeMS) website. <http://pems.dot.ca.gov/>. Accessed Aug. 10, 2012.
9. INRIX. Traffic Scorecard Methodology website. <http://www.inrix.com/scorecard/methodology.asp>. Accessed Aug. 10, 2012.
10. Kittelson & Associates, Inc. *Comparison of Freeway Travel Time Index and Other Travel Time Reliability Measures*. Florida Department of Transportation, Tallahassee, May 2012.
11. Courage, K. G., S. Washburn, L. Elefteriadou, and D. Nam. *Guidance for the Use of Alternative Traffic Analysis Tools in Highway Capacity Analyses*. National Cooperative Highway Research Program Project 03-85 Final Report. University of Florida, Gainesville, 2010.
12. Van As, S. C., and A. Van Niekerk. The Operational Analysis of Two-Lane Rural Highways. Presented at 23rd Annual Southern African Transport Conference, Pretoria, South Africa, July 2004.
13. Catbagan, J. L., and H. Nakamura. Probability-Based Follower Identification in Two-Lane Highways. Presented at 88th Annual Meeting of the Transportation Research Board, Washington, D.C., 2009.

14. Dowling, R. *Traffic Analysis Toolbox Volume VI: Definition, Interpretation, and Calculation of Traffic Analysis Tools Measures of Effectiveness*. Report FHWA-HOP-08-054. Federal Highway Administration, Washington, D.C., Jan. 2007.
15. *Transportation Research Circular E-C081: A Research Program for Improvement of the Highway Capacity Manual*. Transportation Research Board of the National Academies, Washington, D.C., Dec. 2005.
<http://onlinepubs.trb.org/onlinepubs/circulars/ec081.pdf>.
16. Kittelson & Associates, Inc.; Parsons Brinckerhoff, Inc.; KFH Group, Inc.; Texas A&M Transportation Institute; and Arup. *TCRP Report 165: Transit Capacity and Quality of Service Manual*, 3rd ed. Transportation Research Board of the National Academies, Washington, D.C., 2013.
17. *Special Report 209: Highway Capacity Manual*. Transportation Research Board, National Research Council, Washington, D.C., 1985.
18. *Highway Capacity Manual*. Transportation Research Board, National Research Council, Washington, D.C., 2000.
19. Flannery, A., D. McLeod, and N. J. Pedersen. Customer-Based Measures of Level of Service. *ITE Journal*, Vol. 76, No. 5, May 2006, pp. 17–21.
20. Dowling, R. G., D. B. Reinke, A. Flannery, P. Ryus, M. Vandehey, T. A. Petritsch, B. W. Landis, N. M. Roupail, and J. A. Bonneson. *NCHRP Report 616: Multimodal Level of Service Analysis for Urban Streets*. Transportation Research Board of the National Academies, Washington, D.C., 2008.
21. Hummer, J. E., N. M. Roupail, J. L. Toole, R. S. Patten, R. J. Schneider, J. S. Green, R. G. Hughes, and S. J. Fain. *Evaluation of Safety, Design, and Operation of Shared-Use Paths—Final Report*. Report FHWA-HRT-05-137. Federal Highway Administration, U.S. Department of Transportation, Washington, D.C., July 2006.



HIGHWAY CAPACITY MANUAL

6TH EDITION | A GUIDE FOR MULTIMODAL MOBILITY ANALYSIS

VOLUME 4: APPLICATIONS GUIDE

The National Academies of
SCIENCES • ENGINEERING • MEDICINE

TRANSPORTATION RESEARCH BOARD
WASHINGTON, D.C. | WWW.TRB.ORG

TRANSPORTATION RESEARCH BOARD 2016 EXECUTIVE COMMITTEE *

Chair: James M. Crites, Executive Vice President of Operations,
Dallas–Fort Worth International Airport, Texas

Vice Chair: Paul Trombino III, Director, Iowa Department of
Transportation, Ames

Executive Director: Neil J. Pedersen, Transportation Research Board

Victoria A. Arroyo, Executive Director, Georgetown Climate Center;
Assistant Dean, Centers and Institutes; and Professor and Director,
Environmental Law Program, Georgetown University Law Center,
Washington, D.C.

Scott E. Bennett, Director, Arkansas State Highway and Transportation
Department, Little Rock

Jennifer Cohan, Secretary, Delaware Department of Transportation, Dover

Malcolm Dougherty, Director, California Department of
Transportation, Sacramento

A. Stewart Fotheringham, Professor, School of Geographical Sciences
and Urban Planning, Arizona State University, Tempe

John S. Halikowski, Director, Arizona Department of Transportation,
Phoenix

Susan Hanson, Distinguished University Professor Emerita, Graduate
School of Geography, Clark University, Worcester, Massachusetts

Steve Heminger, Executive Director, Metropolitan Transportation
Commission, Oakland, California

Chris T. Hendrickson, Hamerschlag Professor of Engineering, Carnegie
Mellon University, Pittsburgh, Pennsylvania

Jeffrey D. Holt, Managing Director, Power, Energy, and Infrastructure
Group, BMO Capital Markets Corporation, New York

S. Jack Hu, Vice President for Research and J. Reid and Polly Anderson
Professor of Manufacturing, University of Michigan, Ann Arbor

Roger B. Huff, President, HGLC, LLC, Farmington Hills, Michigan

Geraldine Knatz, Professor, Sol Price School of Public Policy, Viterbi
School of Engineering, University of Southern California, Los Angeles

Ysela Llort, Consultant, Miami, Florida

Melinda McGrath, Executive Director, Mississippi Department of
Transportation, Jackson

James P. Redeker, Commissioner, Connecticut Department of
Transportation, Newington

Mark L. Rosenberg, Executive Director, The Task Force for Global
Health, Inc., Decatur, Georgia

Kumares C. Sinha, Olson Distinguished Professor of Civil Engineering,
Purdue University, West Lafayette, Indiana

Daniel Sperling, Professor of Civil Engineering and Environmental
Science and Policy; Director, Institute of Transportation Studies,
University of California, Davis

Kirk T. Steudle, Director, Michigan Department of Transportation,
Lansing (Past Chair, 2014)

Gary C. Thomas, President and Executive Director, Dallas Area Rapid
Transit, Dallas, Texas

Pat Thomas, Senior Vice President of State Government Affairs, United
Parcel Service, Washington, D.C.

Katherine F. Turnbull, Executive Associate Director and Research
Scientist, Texas A&M Transportation Institute, College Station

Dean Wise, Vice President of Network Strategy, Burlington Northern
Santa Fe Railway, Fort Worth, Texas

Thomas P. Bostick (Lieutenant General, U.S. Army), Chief of Engineers
and Commanding General, U.S. Army Corps of Engineers, Washington,
D.C. (ex officio)

James C. Card (Vice Admiral, U.S. Coast Guard, retired), Maritime
Consultant, The Woodlands, Texas, and Chair, TRB Marine Board
(ex officio)

T. F. Scott Darling III, Acting Administrator and Chief Counsel, Federal
Motor Carrier Safety Administration, U.S. Department of Transportation
(ex officio)

Marie Therese Dominguez, Administrator, Pipeline and Hazardous
Materials Safety Administration, U.S. Department of Transportation
(ex officio)

Sarah Feinberg, Administrator, Federal Railroad Administration,
U.S. Department of Transportation (ex officio)

Carolyn Flowers, Acting Administrator, Federal Transit Administration,
U.S. Department of Transportation (ex officio)

LeRoy Gishi, Chief, Division of Transportation, Bureau of Indian
Affairs, U.S. Department of the Interior, Washington, D.C. (ex officio)

John T. Gray II, Senior Vice President, Policy and Economics,
Association of American Railroads, Washington, D.C. (ex officio)

Michael P. Huerta, Administrator, Federal Aviation Administration,
U.S. Department of Transportation (ex officio)

Paul N. Jaenichen, Sr., Administrator, Maritime Administration,
U.S. Department of Transportation (ex officio)

Bevan B. Kirley, Research Associate, University of North Carolina
Highway Safety Research Center, Chapel Hill, and Chair, TRB Young
Members Council (ex officio)

Gregory G. Nadeau, Administrator, Federal Highway Administration,
U.S. Department of Transportation (ex officio)

Wayne Nastri, Acting Executive Officer, South Coast Air Quality
Management District, Diamond Bar, California (ex officio)

Mark R. Rosekind, Administrator, National Highway Traffic Safety
Administration, U.S. Department of Transportation (ex officio)

Craig A. Rutland, U.S. Air Force Pavement Engineer, U.S. Air Force
Civil Engineer Center, Tyndall Air Force Base, Florida (ex officio)

Reuben Sarkar, Deputy Assistant Secretary for Transportation,
U.S. Department of Energy (ex officio)

Richard A. White, Acting President and CEO, American Public
Transportation Association, Washington, D.C. (ex officio)

Gregory D. Winfree, Assistant Secretary for Research and Technology,
Office of the Secretary, U.S. Department of Transportation (ex officio)

Frederick G. (Bud) Wright, Executive Director, American Association
of State Highway and Transportation Officials, Washington, D.C.
(ex officio)

Paul F. Zukunft (Admiral, U.S. Coast Guard), Commandant, U.S. Coast
Guard, U.S. Department of Homeland Security (ex officio)

Transportation Research Board publications are available by ordering
individual publications directly from the TRB Business Office, through
the Internet at www.TRB.org, or by annual subscription through
organizational or individual affiliation with TRB. Affiliates and library
subscribers are eligible for substantial discounts. For further information,
contact the Transportation Research Board Business Office, 500 Fifth
Street, NW, Washington, DC 20001 (telephone 202-334-3213;
fax 202-334-2519; or e-mail TRBsales@nas.edu).

Copyright 2016 by the National Academy of Sciences.

All rights reserved.

Printed in the United States of America.

ISBN 978-0-309-36997-8 [Slipcased set of three volumes]

ISBN 978-0-309-36998-5 [Volume 1]

ISBN 978-0-309-36999-2 [Volume 2]

ISBN 978-0-309-37000-4 [Volume 3]

ISBN 978-0-309-37001-1 [Volume 4, online only]

The National Academies of
SCIENCES • ENGINEERING • MEDICINE

The **National Academy of Sciences** was established in 1863 by an Act of Congress, signed by President Lincoln, as a private, nongovernmental institution to advise the nation on issues related to science and technology. Members are elected by their peers for outstanding contributions to research. Dr. Ralph J. Cicerone is president.

The **National Academy of Engineering** was established in 1964 under the charter of the National Academy of Sciences to bring the practices of engineering to advising the nation. Members are elected by their peers for extraordinary contributions to engineering. Dr. C. D. Mote, Jr., is president.

The **National Academy of Medicine** (formerly the Institute of Medicine) was established in 1970 under the charter of the National Academy of Sciences to advise the nation on medical and health issues. Members are elected by their peers for distinguished contributions to medicine and health. Dr. Victor J. Dzau is president.

The three Academies work together as the National Academies of Sciences, Engineering, and Medicine to provide independent, objective analysis and advice to the nation and conduct other activities to solve complex problems and inform public policy decisions. The Academies also encourage education and research, recognize outstanding contributions to knowledge, and increase public understanding in matters of science, engineering, and medicine.

Learn more about the National Academies of Sciences, Engineering, and Medicine at **www.national-academies.org**.

The **Transportation Research Board** is one of seven major programs of the National Academies of Sciences, Engineering, and Medicine. The mission of the Transportation Research Board is to increase the benefits that transportation contributes to society by providing leadership in transportation innovation and progress through research and information exchange, conducted within a setting that is objective, interdisciplinary, and multimodal. The Board's varied committees, task forces, and panels annually engage about 7,000 engineers, scientists, and other transportation researchers and practitioners from the public and private sectors and academia, all of whom contribute their expertise in the public interest. The program is supported by state transportation departments, federal agencies including the component administrations of the U.S. Department of Transportation, and other organizations and individuals interested in the development of transportation.

Learn more about the Transportation Research Board at **www.TRB.org**.

CHAPTER 37
ATDM: SUPPLEMENTAL

CONTENTS

1. INTRODUCTION 37-1

2. TYPES OF ATDM STRATEGIES 37-2

 Overview 37-2

 Roadway Metering 37-2

 Congestion Pricing 37-3

 Traveler Information Systems 37-4

 Managed Lanes 37-5

 Speed Harmonization 37-6

 Traffic Signal Control 37-7

 Specialized Applications of ATDM Strategies 37-7

3. EFFECTS OF SHOULDER AND MEDIAN LANE STRATEGIES 37-9

 Open Shoulders as Auxiliary Lanes Between Adjacent On- and Off-
 Ramps 37-9

 Open Shoulders to Buses Only 37-9

 Open Shoulders to HOVs Only 37-10

 Open Right Shoulders to All Traffic 37-10

 Open Median Shoulder to Buses Only 37-10

 Open Median Shoulder to HOVs Only 37-10

 Open Median Shoulder to All Traffic 37-10

4. EFFECTS OF RAMP-METERING STRATEGIES 37-11

 Capacity of Ramp-Metered Merge Sections 37-11

 Locally Dynamic Ramp Metering 37-11

5. PLANNING AN ATDM PROGRAM 37-12

 Travel Demand Management Plans 37-12

 Weather-Responsive Traffic Management Plans 37-13

 Traffic Incident Management Plans 37-14

 Work Zone Transportation Management Plans 37-16

 Special Event Management Plans 37-19

6. REFERENCES 37-20

LIST OF EXHIBITS

Exhibit 37-1 Freeway Ramp Metering, SR-94, Lemon Grove, California 37-2
Exhibit 37-2 Minnesota Dynamic Pricing for HOT Lanes..... 37-3
Exhibit 37-3 San Francisco Bay Area Traffic Map 37-4
Exhibit 37-4 HOV Lane 37-5
Exhibit 37-5 Variable Speed Limit Signs, Rotterdam, The Netherlands 37-6
Exhibit 37-6 Possible Incident Management Strategies 37-16

1. INTRODUCTION

Chapter 37 presents additional information about the following aspects of active traffic and demand management (ATDM):

- An overview of typical ATDM strategies for managing demand, capacity, and the performance of the highway and street system;
- Guidance on analyzing shoulder lane, median lane, and ramp metering strategies using the *Highway Capacity Manual* (HCM); and
- Guidance on designing an ATDM program.

Chapter 11, Freeway Reliability Analysis, and Chapter 17, Urban Street Reliability and ATDM, provide methods for analyzing the effects of ATDM strategies on freeway and urban street operations, respectively.

VOLUME 4: APPLICATIONS
GUIDE

- 25. Freeway Facilities:
Supplemental
- 26. Freeway and Highway
Segments: Supplemental
- 27. Freeway Weaving:
Supplemental
- 28. Freeway Merges and
Diverges: Supplemental
- 29. Urban Street Facilities:
Supplemental
- 30. Urban Street Segments:
Supplemental
- 31. Signalized Intersections:
Supplemental
- 32. STOP-Controlled
Intersections:
Supplemental
- 33. Roundabouts:
Supplemental
- 34. Interchange Ramp
Terminals: Supplemental
- 35. Pedestrians and Bicycles:
Supplemental
- 36. Concepts: Supplemental
- 37. ATDM: Supplemental**

2. TYPES OF ATDM STRATEGIES

OVERVIEW

This section provides brief overviews of typical ATDM strategies for managing demand, capacity, and the performance of the highway and street system. The strategies described here are intended to be illustrative rather than definitive. ATDM strategies constantly evolve as technology advances.

ROADWAY METERING

Roadway metering treatments store surges in demand at various points in the transportation network. Typical examples of roadway metering include freeway on-ramp metering, freeway-to-freeway ramp metering, freeway mainline metering, peak period freeway ramp closures, and arterial signal metering. Exhibit 37-1 illustrates a freeway ramp-metering application.

More in-depth and up-to-date information on ATDM strategies is available at the Federal Highway Administration's website: <http://www.ops.fhwa.dot.gov/atdm>.

Exhibit 37-1
Freeway Ramp Metering,
SR-94, Lemon Grove,
California



Source: FHWA (1).

Roadway metering may be highly dynamic or comparatively static. A comparatively static roadway metering system would establish some preset metering rates on the basis of historical demand data, periodically monitor system performance, and adjust the rates to obtain satisfactory facility performance. A static metering system, unlike a dynamic system, would not generally be considered an ATDM strategy. A highly dynamic system may monitor system performance on a real-time basis and automatically adjust metering rates by using a predetermined algorithm in response to changes in observed facility conditions. Preferential treatment of high-occupancy vehicles (HOVs) may be part of a roadway metering strategy.

Roadway metering may be applied on freeways or arterials. On arterials, metering might be accomplished through "gating," in which an upstream signal is used to control the number of vehicles reaching downstream signals. Surges in

demand are temporarily stored at the upstream signal and released later when the downstream signals can better serve the vehicles.

CONGESTION PRICING

Congestion or value pricing is the practice of charging tolls for the use of all or part of a facility or a central area according to the severity of congestion. The tolls may vary by distance traveled, vehicle class, and estimated time savings. The objective of congestion pricing is to preserve reliable operating speeds on the tolled facility with a tolling system that encourages drivers to switch to other times of the day, other modes, or other facilities when demand starts to approach facility capacity. Exhibit 37-2 shows an example of congestion pricing in Minnesota.

The objective of congestion pricing is to preserve reliable operating speeds on the tolled facility.



Exhibit 37-2
Minnesota Dynamic Pricing for HOT Lanes

Source: FHWA (2) (courtesy of Minnesota Department of Transportation).

Congestion pricing may use different degrees of responsiveness and automation. Some implementations may use a preset schedule under which the toll varies by the same amount for preset times during the day and week. The implementation may be monitored on a regular schedule and the pricing adjusted to achieve or maintain desired facility performance. An ATDM-based implementation of congestion pricing may monitor facility performance much more frequently and use automatic or semiautomatic dynamic pricing to vary the toll on the basis of a predetermined algorithm according to the observed performance of the facility.

High-occupancy toll (HOT) lanes (also called express lanes) are tolled lanes adjacent to general purpose lanes. HOT lanes allow motorists to pay tolls to enter

Central area pricing is an areawide implementation of congestion pricing.

the lanes to avoid congested nontoll lanes. HOVs may be allowed to enter the lanes for free or at a reduced toll rate.

Central area pricing and dynamic parking pricing are examples of an areawide implementation of congestion pricing. Central area pricing imposes tolls on vehicles entering or traveling within a central area street network during certain hours of certain days. The fee varies by time of day and day of week or according to real-time measurements of congestion within the central area. The toll may be reduced or waived for certain vehicle types, such as HOVs, or for residents of the zone.

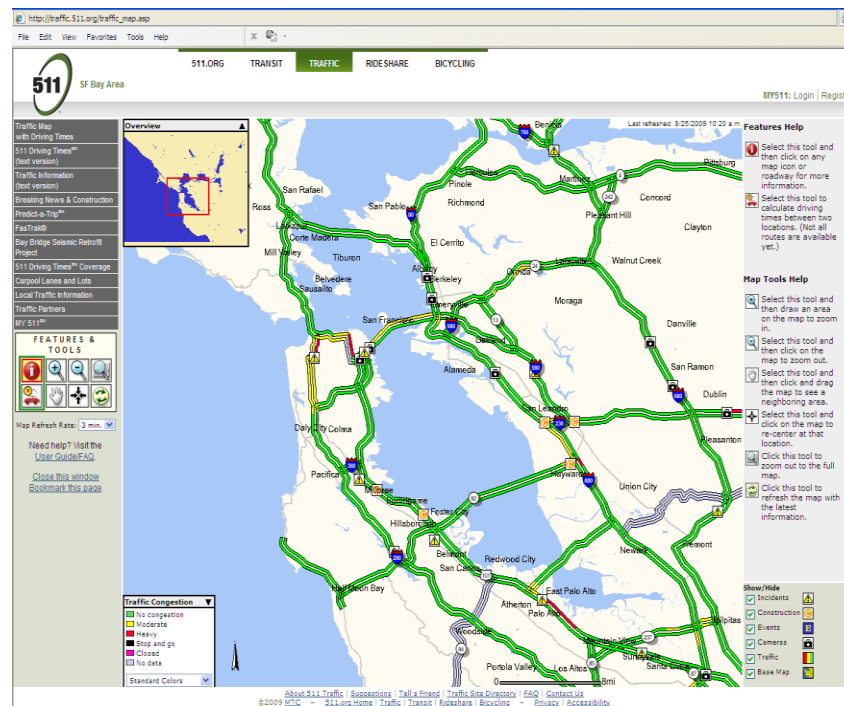
TRAVELER INFORMATION SYSTEMS

Traveler information is an integration of technologies allowing the general public to access real-time or near-real-time data on incident conditions, travel time, speed, and possibly other information. Traveler information enhances awareness of current and anticipated traffic conditions on the transportation system. Traveler information may be tailored to one or more specific modes of travel, such as auto, truck, bus, bicycle, or pedestrian.

Traveler information can be grouped into three types (pretrip, in vehicle, and roadside) according to when the information is made available and how it is delivered to the driver.

Pretrip information is obtained from various sources and transmitted to motorists before the start of their trip through various means. Exhibit 37-3 illustrates Internet-based dissemination of travel information.

Exhibit 37-3
San Francisco Bay Area
Traffic Map



Source: © 2009 Metropolitan Transportation Commission (<http://traffic.511.org>).

In-vehicle information may involve route guidance or dissemination of incident and travel time conditions to the en route vehicle. Route guidance involves Global Positioning System–based real-time data acquisition to calculate the most efficient routes for drivers. This technology allows individual vehicles and their occupants to receive optimal route guidance via various telecommunications devices and provides a method for the transportation network operator to make direct and reliable control decisions to stabilize network flow.

Roadside messages consist of dynamic message signs (also called changeable or variable message signs) and highway advisory radio (also called traveler advisory radio) that display or transmit information on road conditions for travelers while they are en route.

MANAGED LANES

Managed lanes include reversible lanes, HOV lanes, HOT lanes, truck lanes, bus lanes, speed harmonization, temporary closures for incidents or maintenance, and temporary use of shoulders during peak periods (see Exhibit 37-4). HOT lanes are described above under congestion pricing, and speed harmonization is described in the next section.

HOV lanes assign a portion of the roadway capacity to vehicles that carry the most people on the facility or that in some other way meet societal objectives for reducing the environmental impacts of vehicular travel. HOV lanes may operate 24 hours a day, 7 days a week, or they may be limited to the peak periods when demand is greatest. The minimum vehicle-occupancy requirement for the HOV lanes may be adjusted in response to operating conditions to preserve uncongested HOV lane operation.



Source: FHWA (3).

Exhibit 37-4
HOV Lane

Reversible lanes provide additional capacity for directional peak flows depending on the time of the day. Reversible lanes on freeways may be located in the center of a freeway with gate control on both ends. On interrupted-flow facilities, reversible lanes may be implemented through lane-use control signals and signs that open and close lanes by direction.

The temporary use of shoulders during peak periods by all or a subset of vehicle types can provide additional capacity in a bottleneck section and improve overall facility performance. Part-time shoulder use by buses in queuing locations can substantially reduce bus delays by enabling them to proceed along the roadway without having to wait in the mainline queue.

SPEED HARMONIZATION

The objective of speed harmonization is to improve safety and facility operations by reducing the shock waves that typically occur when traffic abruptly slows upstream of a bottleneck or for an incident. The reduction of shock waves decreases the probability of secondary incidents and reduces the loss of capacity associated with incident-related and recurring traffic congestion.

Changeable speed limit or speed advisory signs are typically used to implement speed harmonization. Exhibit 37-5 shows an example of variable speed limit signs used for speed harmonization in the Netherlands. The speed restrictions may apply uniformly across all lanes or may vary by lane. The same lane signs may be used to close individual lanes upstream of an incident until the incident is cleared (this practice is not strictly speed harmonization).

The variable speed limit may be advisory or regulatory. Advisory speeds indicate a recommended speed, which drivers may exceed if they believe doing so is safe under prevailing conditions. Regulatory speed limits may not be exceeded under any conditions.

Exhibit 37-5
Variable Speed Limit Signs,
Rotterdam, The Netherlands



Source: FHWA Active Traffic Management Scan, Jessie Yung.

TRAFFIC SIGNAL CONTROL

Signal timing optimization is the single most cost-effective action that can be taken to improve a roadway corridor's capacity and performance (4). Signal timing is as important as the number of lanes in determining the capacity and performance of an urban street.

Traffic signal timing optimization and coordination minimize the stops, delay, and queues for vehicles at individual and multiple signalized intersections.

Traffic signal preemption and priority provide special timing for certain classes of vehicles (e.g., buses, light rail vehicles, emergency response vehicles, and railroad trains) using the intersection. Preemption interrupts the regular signal operation. Priority either extends or advances the time when a priority vehicle obtains the green phase, but generally the priority is within the constraints of the regular signal-operating scheme.

Traffic-responsive operation and adaptive control provide for different levels of automation in the adjustment of signal timing due to variations in demand. Traffic-responsive operation selects from a prepared set of timing plans on the basis of the observed level of traffic in the system. Adaptive traffic signal control involves advanced detection of traffic, prediction of its arrival at the downstream signal, and adjustment of the downstream signal operation based on that prediction.

SPECIALIZED APPLICATIONS OF ATDM STRATEGIES

ATDM strategies are often applied to the day-to-day operation of a facility. Incident management and work zone management are example applications of one or more ATDM strategies to address specific facility conditions. Employer-based demand management is an example of private-sector applications in which traveler information systems may be an important component.

Incident Management

Traffic incident management (TIM) is "the coordinated, preplanned use of technology, processes, and procedures to reduce the duration and impact of incidents, and to improve the safety of motorists, crash victims and incident responders" (4). An incident is "any non-recurring event that causes a reduction in capacity or an abnormal increase in traffic demand that disrupts the normal operation of the transportation system" (4). Such events include traffic crashes, disabled vehicles, spilled cargo, severe weather, and special events such as sporting events and concerts. ATDM strategies may be included as part of an overall incident management plan to improve facility operations during and after incidents.

Work Zone Management

Work zone management has the objective of moving traffic through the working area with as little delay as possible consistent with the safety of the workers, the safety of the traveling public, and the requirements of the work being performed. Transportation management plans are a collection of

administrative, procedural, and operational strategies used to manage and mitigate the impacts of a work zone project. The plan may have three components: a temporary traffic control plan, a transportation operations plan, and a public information plan. The temporary traffic control plan describes the control strategies, traffic control devices, and project coordination. The transportation operations plan identifies the demand management, corridor management, work zone safety management, and the traffic or incident management and enforcement strategies. The public information plan describes the public awareness and motorist information strategies (4). ATDM strategies can be important components of a transportation management plan.

Employer-Based Demand Management

Employer-based demand management consists of cooperative actions taken by employers to reduce the impacts of recurring or nonrecurring traffic congestion on employee productivity. For example, a large employer may implement work-at-home or stay-at-home days in response to announced snow days; “spare the air” days; or traffic alerts concerning major construction projects, incidents, and highway facility closures. Another company may contract for or directly provide regular shuttle van service to and from transit stations. Flexible or staggered work hours may be implemented to enable employees to avoid peak commute hours. Rideshare-matching services and incentives may be implemented by the employer to facilitate employee ridesharing.

Employers may use components of a traveler information system to determine appropriate responses to changing traffic conditions. Employees can use traveler information systems in their daily commuting choices.

3. EFFECTS OF SHOULDER AND MEDIAN LANE STRATEGIES

This section provides details on the free-flow speed and capacity adjustments associated with temporary shoulder and median lane strategies.

OPEN SHOULDERS AS AUXILIARY LANES BETWEEN ADJACENT ON- AND OFF-RAMPS

This strategy involves opening a shoulder lane for use by all vehicles entering at the upstream on-ramp or exiting at the downstream off-ramp. Some through vehicles may temporarily use the auxiliary lane to try to jump ahead of the queue.

The capacity of an auxiliary lane is assumed by the Chapter 10 freeway facilities method to be the same as that of a regular lane; however, utilization of the auxiliary lane may be lower than that of a through lane. In addition, the freeway method does not provide a capacity for shoulder lanes. Until the HCM has specific information on the capacities of auxiliary shoulder lanes, this procedure assumes that the capacity of an auxiliary shoulder lane is one-half that of a normal freeway through lane.

Because the freeway facilities method does not recognize individual lane capacities, computation of an average capacity for freeway sections with auxiliary shoulder lanes across all lanes is necessary.

$$AveCap(s) = \frac{CapShldr(s) + CapMFlanes(s) \times MFlanes(s)}{1 + MFlanes(s)}$$

Equation 37-1

where

$AveCap(s)$ = average capacity per lane for section s (veh/h/ln),

$CapShldr(s)$ = capacity per shoulder lane for section s (veh/h/ln),

$CapMFlanes(s)$ = capacity per mixed-flow lane in section s (veh/h/ln), and

$MFlanes(s)$ = number of mixed-flow lanes in section s (integer).

The number of lanes on the freeway segments between adjacent on- and off-ramps is increased by one for the shoulder lane.

Until the HCM has more specific information for shoulder lanes, free-flow speeds on auxiliary shoulder lanes are assumed in this procedure to be the same as for regular through lanes.

OPEN SHOULDERS TO BUSES ONLY

This strategy involves opening a shoulder lane to buses only. The same procedure and assumptions as described above for auxiliary shoulder lanes are used to compute freeway section capacities, lanes, and free-flow speeds where buses are allowed on shoulders, with the following exception: the capacity of the shoulder lane is the number of buses per hour using the shoulder lane or the user-specified capacity, whichever is less (the user can override the default capacity).

OPEN SHOULDERS TO HOVs ONLY

This strategy involves opening a shoulder lane to buses, vanpools, and carpools (HOVs) only. The same procedure and assumptions as described above for auxiliary shoulder lanes are used to compute freeway section capacities, lanes, and free-flow speeds where HOVs are allowed on shoulders, with the following exception: the capacity of the shoulder lane is the number of HOVs per hour using the shoulder lane or the user-specified capacity, whichever is less.

OPEN RIGHT SHOULDERS TO ALL TRAFFIC

This strategy involves opening a shoulder lane to all vehicles. The same procedure and assumptions as described above for auxiliary shoulder lanes are used to compute freeway section capacities, lanes, and free-flow speeds where all vehicles are allowed on shoulders, with the following exception: the capacity of the shoulder lane is as specified by the user.

OPEN MEDIAN SHOULDER TO BUSES ONLY

This strategy involves opening a median lane to buses only. The same procedure and assumptions as described above for auxiliary shoulder lanes are used to compute freeway section capacities, lanes, and free-flow speeds, with the following exception: the capacity of the median lane is the number of buses per hour using the shoulder lane or the user-designated capacity, whichever is less.

OPEN MEDIAN SHOULDER TO HOVs ONLY

This strategy involves opening a median lane to HOVs (buses, vanpools, carpools) only. The same procedure and assumptions as described above for auxiliary shoulder lanes are used to compute freeway section capacities, lanes, and free-flow speeds, with the following exception: the capacity of the median lane is the number of HOVs per hour using the shoulder lane or the user-designated capacity, whichever is less.

OPEN MEDIAN SHOULDER TO ALL TRAFFIC

This strategy involves opening a median lane to all traffic. The same procedure and assumptions as described above for auxiliary shoulder lanes are used to compute freeway section capacities, lanes, and free-flow speeds, with the following exception: the capacity of the median lane is as designated by the user.

4. EFFECTS OF RAMP-METERING STRATEGIES

This section provides details on the capacity adjustments associated with ramp-metering strategies.

CAPACITY OF RAMP-METERED MERGE SECTIONS

A capacity adjustment factor of 1.03 is recommended to be applied to freeway merge segments in the Chapter 10 freeway facilities method for those times when ramp metering is in operation (5).

LOCALLY DYNAMIC RAMP METERING

For locally dynamic ramp metering, an adaptation of the ALINEA algorithm (6) is used to estimate the ramp-metering rate for each analysis period for each scenario:

$$R(t) = \frac{(CM - VM(t))}{NR}$$

Equation 37-2

subject to

$$\begin{aligned} &MinRate < R(t) < MaxRate \\ R(t) > &\frac{VR(t) + QR(t - 1) - QRS}{NR} \end{aligned}$$

where

$R(t)$ = ramp-metering rate for analysis period t (veh/h/ln),

NR = number of metered lanes on ramp (integer),

CM = capacity of downstream section (veh/h),

$VM(t)$ = volume on upstream section for analysis period t (veh/h),

$VR(t)$ = volume on ramp during analysis period t (veh/h),

$QR(t - 1)$ = queue on ramp at end of previous analysis period $t - 1$ (veh),

QRS = queue storage capacity of ramp (veh),

$MinRate$ = user-defined minimum ramp-metering rate (veh/h/ln) (default value is 240 veh/h/ln), and

$MaxRate$ = user-defined maximum ramp-metering rate (veh/h/ln) (default value is 900 veh/h/ln).

5. PLANNING AN ATDM PROGRAM

ATDM strategies are combined into an overall ATDM program to address challenges to the efficient operation of the highway system. The ATDM program will have different plan elements to address specific challenges to the system:

- The travel demand management (TDM) plan element will address how demand management will be used to address recurring congestion on the facility.
- The weather traffic management plan element will identify the ATDM strategies to be used during weather events. The weather traffic management plan will have a TDM component targeted to special weather events.
- The TIM plan element will identify the ATDM strategies to be used for incidents. The TIM will have a TDM component for managing demand on the facility during incidents.
- The work zone traffic management plan element will identify the ATDM strategies to be used for work zones. The work zone traffic management plan will have a TDM component for managing demand while work zones are present.
- Facilities located next to major sporting and entertainment venues may also have a special event management plan with ATDM strategies identified to support management of traffic before and after major events.

TRAVEL DEMAND MANAGEMENT PLANS

The Federal Highway Administration's (FHWA) Travel Demand Management Toolbox website provides resources to help manage traffic congestion by better managing demand. These resources include publications, web links, and training offerings. Demand management strategies include the following (7):

- Technology accelerators:
 - Real-time traveler information,
 - National 511 phone number, and
 - Electronic payment systems;
- Financial incentives:
 - Tax incentives,
 - Parking cash-out,
 - Parking pricing,
 - Variable pricing,
 - Distance-based pricing, and
 - Incentive reward programs;
- Travel time incentives:
 - HOT lanes,

FHWA's Travel Demand Management Toolbox is available at <http://ops.fhwa.dot.gov/tdm/toolbox.htm>.

- Signal priority systems, and
- Preferential parking;
- Marketing and education:
 - Social marketing and
 - Individualized marketing;
- Mode-targeted strategies:
 - Guaranteed ride home,
 - Transit pass programs, and
 - Shared vehicles;
- Departure time–targeted strategies:
 - Worksite flextime and
 - Coordinated event or shift scheduling;
- Route-targeted strategies:
 - Real-time route information,
 - In-vehicle navigation, and
 - Web-based route-planning tools;
- Trip reduction–targeted strategies:
 - Employer telework programs and policies and
 - Compressed workweek programs; and
- Location- and design-targeted strategies:
 - Transit-oriented development,
 - Live near your work, and
 - Proximate commute.

FHWA’s guide on this topic (7) should be consulted for more information on designing the TDM element of an ATDM program.

WEATHER-RESPONSIVE TRAFFIC MANAGEMENT PLANS

Weather-responsive traffic management involves the implementation of traffic advisory, control, and treatment strategies in direct response to or in anticipation of developing roadway and visibility issues that result from deteriorating or forecast weather conditions (8).

Weather-responsive traffic management strategies include the following:

- Motorist advisory, alert, and warning systems;
- Speed management strategies;
- Vehicle restriction strategies;
- Road restriction strategies;
- Traffic-signal control strategies;
- Traffic incident management;

- Personnel and asset management; and
- Agency coordination and integration.

FHWA's report on this topic (8) should be consulted for additional information on the design and selection of weather-responsive traffic management strategies.

TRAFFIC INCIDENT MANAGEMENT PLANS

An FHWA handbook (9) provides information on the design of TIM plans.

TIM is "the coordinated, preplanned use of technology, processes, and procedures to reduce the duration and impact of incidents, and to improve the safety of motorists, crash victims and incident responders." An incident is "any non-recurring event that causes a reduction in capacity or an abnormal increase in traffic demand that disrupts the normal operation of the transportation system" (10). Such events include traffic crashes, disabled vehicles, spilled cargo, severe weather, and special events such as sporting events and concerts. ATDM strategies may be included as part of an overall TIM plan to improve facility operations during and after incidents.

An agency's incident management plan documents the agency's strategy for dealing with incidents. It is, in essence, a maintenance of traffic plan (MOTP) for incidents and unplanned work zones. The responses available to the agency are more limited for incident management and by definition must be real-time, dynamic responses to each incident as it presents itself. The agency's incident MOTP ensures that adequate resources are prepositioned and interagency communications are established to respond rapidly and effectively to an incident. The TIM plan may include measures in effect 24 hours a day and 7 days a week, weekdays only, weekday peak periods, or any other periods of time or days of the week that are the focus of the TIM plan.

Incidents Defined and Classified

An incident is an unplanned disruption to the capacity of the facility. Incidents do not need to block a travel lane to disrupt the capacity of the facility. They can be a simple distraction within the vehicle (e.g., spilling coffee), on the side of the road, or in the opposite direction of the facility.

Incidents can be classified according to the response resources and procedures required to clear the incident. This classification helps in identifying strategic options for improving incident management.

Section 6I.01 of the 2009 *Manual on Uniform Traffic Control Devices* (MUTCD) (11) classifies incidents according to their expected duration:

- *Extended-duration* incidents are those expected to persist for more than 24 h and should be treated like work zones.
- *Major* incidents have expected durations of more than 2 h.
- *Intermediate* incidents have expected durations of 0.5 h up to and including 2 h.
- *Minor* incidents are expected to persist for less than 30 min.

Stages of Incident Management

Incident management is the systematic, planned, and coordinated use of human, institutional, mechanical, and technical resources to reduce the duration and impact of incidents. Incident management has several stages:

- Detection;
- Verification;
- Response;
- Motorist information; and
- Site management, consisting of
 - Traffic management,
 - Investigation, and
 - Clearance.

Detection is the first notice the agency receives that there may be an incident on the facility. Detection may occur via 911 calls, closed-circuit TV cameras, or detector feeds to a transportation management center or to maintenance or enforcement personnel monitoring the facility.

Verification confirms an incident has occurred; collects additional information on the nature of the incident; and refines the operating agency's understanding of the nature, extent, and location of the incident for an effective response.

A *response* is selected after an incident is verified, and the appropriate resources are dispatched to the incident. A decision is also made as to the dissemination of information about the incident to the motoring public.

Motorist information informs drivers not at the site about the location and severity of the incident to enable them to anticipate conditions at the site and give them the opportunity to divert and avoid the site.

Site management refers to the management of resources to remove the incident and reduce the impact on traffic flow and safety. This stage involves the following three major tasks:

- *Traffic management*, which is the control and safe movement of traffic through the incident zone;
- *Investigation*, which documents the causes of traffic incidents for safety evaluation and legal and insurance purposes; and
- *Clearance*, which refers to the safe and timely removal of any wreckage or spilled material from the roadway.

An incident management plan has the following strategic and tactical program elements (9):

- Management objectives and performance measurement;
- Designated interagency teams' membership, roles, and responsibilities;
- Response and clearance policies and procedures; and
- Responder and motorist safety laws and equipment.

Incident Response and Clearance Strategies

The incident management plan will designate the responder roles and responsibilities, establish an incident command system with a unified command across agencies, identify who is responsible for bringing which equipment and resources to the incident site, establish response and clearance procedures by responding agency and by incident type, and identify state and local laws that apply to incident clearance procedures.

Exhibit 37-6 presents a menu of possible incident management strategy improvements that an agency may wish to evaluate by using the ATDM analysis procedure (12). The expected effect of each class of strategies on highway capacities and speeds is included in this exhibit.

Exhibit 37-6
Possible Incident Management Strategies

Strategy	Description
Improved detection and verification	Closed-circuit TV, routine service patrol, or other continuously monitored incident detection system to spot incidents more quickly and verify the required resources to clear the incident. Enhanced 911, automated positioning systems, motorist aid call boxes, and automated collision notification systems are included.
Traveler information system	511 systems, traveler information websites, media partnerships, dynamic message signs, standardized dynamic message sign message sets, and usage protocols to improve the information available to travelers.
Response	Personnel and equipment resource lists, towing and recovery vehicle identification guide, instant tow dispatch procedures, towing and recovery zone-based contracts, enhanced computer-aided dispatch, dual or optimized dispatch procedures, motorcycle patrols, equipment staging areas or prepositioned equipment.
Scene management and traffic control	Incident command system, response vehicle parking plans, high-visibility safety apparel and vehicle markings, on-scene emergency lighting procedures, safe and quick clearance laws, effective traffic control through on-site traffic management teams, overhead lane-closure signs, variable speed limits, end-of-queue advance warning systems, alternate route plans.
Quick clearance and recovery	Abandoned-vehicle laws, safe and quick clearance laws, service patrols, vehicle-mounted push bumpers, incident investigation sites, noncargo vehicle fluid-discharge policy, fatality certification and removal policy, expedited crash investigation, quick clearance using fire apparatus, towing and recovery quick clearance incentives, major incident response teams.

Source: Adapted from Carson (12).

WORK ZONE TRANSPORTATION MANAGEMENT PLANS

Work zone management has the objective of moving traffic through the working area with as little delay as possible, consistent with the safety of the workers, the safety of the traveling public, and the requirements of the work being performed. Transportation management plans are a collection of administrative, procedural, and operational strategies used to manage and mitigate the impacts of a work zone project.

The work zone MOTP may have three components: a temporary traffic control plan, a transportation operations plan, and a public information plan. The temporary traffic control plan describes the control strategies, traffic control devices, and project coordination. The transportation operations plan identifies the demand management, corridor management, work zone safety management, and the traffic and incident management and enforcement strategies. The public

information plan describes the public awareness and motorist information strategies (10). ATDM strategies can be important components of a transportation management plan (13).

The work zone MOTP codifies the agency's management strategy. It has the following elements:

- *Construction approach*: staging, sequencing, lane and ramp closure alternatives, alternative work schedules (e.g., night, weekend).
- *Traffic control operations*: a mix of dynamic (ATDM) and static measures consisting of speed limit reductions, truck restrictions, signal timing (coordination and phasing), reversible lanes, and physical barriers.
- *Public information*: a mix of dynamic (ATDM) and static pretrip and en route information (e.g., 511, newspapers, meetings, websites, closed-circuit television over the Internet), plus on-site information signing such as static signs, changeable or variable message signs, and highway advisory radio.
- *TDM*: employer-based and other incentives (in addition to public information) for use of alternative modes of travel, including park-and-ride.
- *Incident management and enforcement*: generally, ATDM measures specified in an incident management plan (i.e., an incident MOTP), such as traffic management centers, intelligent transportation systems, emergency service patrols, hazardous materials teams, and enhanced police enforcement. A particularly aggressive incident MOTP may be put in place for work zones.

Construction Approach

The work zone MOTP must consider several alternative construction approaches (including traffic maintenance) and recommend the construction approach that best meets the agency's objectives for the construction project.

Traffic maintenance approaches to be considered in the work zone MOTP include the following:

1. Complete closure of the work area for a short time versus partial closure for a longer time,
2. Nighttime versus daytime lane closures, and
3. Off-peak versus peak hour lane closures.

Traffic Control Operations

The traffic control element of the MOTP specifies work zone speed-limit reductions, signal timing changes (if needed), reversible lanes (e.g., flagging), and the locations of physical barriers and cones. The traffic control elements may be dynamic, responding in real time to changing conditions, or they may be more static, operating at prespecified times of the day.

MUTCD Section 6G.02 defines work zone types according to duration and time of day (11):

- *Duration Type A*: long-term stationary work that occupies a location more than 3 days;
- *Duration Type B*: intermediate-term stationary work that occupies a location more than one daylight period up to 3 days, or nighttime work lasting more than 1 h;
- *Duration Type C*: short-term stationary daytime work that occupies a location for more than 1 h within a single daylight period;
- *Duration Type D*: short-duration work that occupies a location up to 1 h; and
- *Duration Type E*: mobile work that moves intermittently or continuously.

Work zones are further categorized by MUTCD Section 6G.03 according to their location on the facility. Work zones within the traveled way (Location Type E) are further subdivided by facility type (11):

- *Location Type A*: outside the shoulder (Section G6.06);
- *Location Type B*: on the shoulder with no encroachment (Section G6.07);
- *Location Type C*: on the shoulder with minor encroachment, leaving at least a 10-ft lane (Section G6.08);
- *Location Type D*: within the median (Section G6.09); and
- *Location Type E*: within the traveled way of
 - A two-lane highway (Section 6G.10),
 - An urban street (Section 6G.11),
 - A multilane non-access-controlled highway (Section 6G.12),
 - An intersection (Section 6G.13), or
 - A freeway or an expressway (Section 6G.14).

Each work zone type has an associated typical application of temporary traffic controls. They are described in MUTCD Section 6H-1 (11).

Public Information Element

The public information element is intended to provide the public with pretrip and en route information and with preconstruction and during-construction information on the work zone so the public can plan accordingly. The intent is to encourage travelers who can to reschedule or reroute their trip to avoid the work zone during periods of peak closures. Public information includes 511 alerts; press interviews; public information meetings; project update websites; and on-site web-accessible closed-circuit cameras, variable message signs, and highway advisory radio.

Travel Demand Management Element

In coordination with the public information element, the TDM element identifies incentives, such as park-and-ride lots, that will be provided for travelers using alternative modes. The public information element and the TDM element differ in that the public information is neutral, leaving it to the traveler to choose how to respond. The TDM element provides monetary and service incentives to encourage a particular subset of choices.

Incident Management and Enforcement Element

Incident management includes the development of incident management plans for the work zone. The plans describe coordination with traffic management centers, the use of intelligent transportation systems devices, deployment of emergency service patrols in the work zone, and enhanced police enforcement. Enforcement may be strengthened with speed limit feedback signs and other devices.

SPECIAL EVENT MANAGEMENT PLANS

Special event management deals with moving people and traffic to and from special event locations, such as a sports stadium, concert hall, or arena. The objective is to get people and traffic onto and off of the site with minimal backups onto the public transportation system and in a reasonable time. Traffic control officers, temporary cones and signs, reversible lanes, and special signal control plans are often part of a special event management plan (14).

A special event management plan typically has the following components:

- Preevent ingress control,
- During-event access control, and
- Postevent egress control.

The special event management plan will deploy a combination of temporary signing, lane controls, signal timing plans, and personnel to move traffic into and out of the event venue, much like a short-term work zone.

Many of these references are available in the Technical Reference Library in Volume 4.

6. REFERENCES

1. *Ramp Management and Control: A Primer*. Report FHWA-HOP-06-080. Federal Highway Administration, Washington, D.C., Jan. 2006.
2. *Technologies That Complement Congestion Pricing: A Primer*. Report FHWA-HOP-08-043. Federal Highway Administration, Washington, D.C., Oct. 2008.
3. *Managed Lanes: A Primer*. Report FHWA-HOP-05-031. Federal Highway Administration, Washington, D.C., 2005.
4. *National Signal Timing Optimization Project: Summary Evaluation Report*. Federal Highway Administration, Washington, D.C., and University of Florida, Gainesville, May 1982.
5. Zhang, L., and D. Levinson. Ramp Metering and Freeway Bottleneck Capacity. In *Transportation Research Part A*, Vol. 44, 2010, pp. 218–235.
6. Papageorgiou, M., H. Hadj-Salem, and J.-M. Blosseville. ALINEA: A Local Feedback Control Law for On-Ramp Metering. In *Transportation Research Record 1320*, Transportation Research Board, National Research Council, Washington, D.C., 1991, pp. 58–64.
7. Association for Commuter Transportation, UrbanTrans Consultants, Parsons Brinckerhoff, and ESTC. *Mitigating Traffic Congestion: The Role of Demand-Side Strategies*. Report FHWA-HOP-05-001. Federal Highway Administration, Washington, D.C., Oct. 2004.
8. Gopalakrishna, D., F. Kitchener, and K. Blake. *Developments in Weather Responsive Traffic Management Strategies*. Report FHWA-JPO-11-086. Federal Highway Administration, Washington, D.C., June 2011.
9. Owens, N., A. Armstrong, P. Sullivan, C. Mitchell, D. Newton, R. Brewster, and T. Trego. *Traffic Incident Management Handbook*. Report FHWA-HOP-10-013. Federal Highway Administration, Washington, D.C., Jan. 2010.
10. Balke, K. N. *Traffic Incident Management in Construction and Maintenance Work Zones*. Report FHWA-HOP-08-056. Federal Highway Administration, Washington, D.C., Jan. 2009.
11. *Manual on Uniform Traffic Control Devices for Streets and Highways*. Federal Highway Administration, Washington, D.C., 2009. <http://mutcd.fhwa.dot.gov>. Accessed Feb. 1, 2010.
12. Carson, J. L. *Best Practices in Traffic Incident Management*. Report FHWA-HOP-10-050. Federal Highway Administration, Washington, D.C., Sept. 2010.
13. Jeannotte, K., and A. Chandra. *Developing and Implementing Transportation Management Plans for Work Zones*. Report FHWA-HOP-05-066. Federal Highway Administration, Washington, D.C., Dec. 2005.
14. Carson, J. L., and R. G. Bylsma. *NCHRP Synthesis of Highway Practice 309: Transportation Planning and Management for Special Events*. Transportation Research Board of the National Academies, Washington, D.C., 2003.